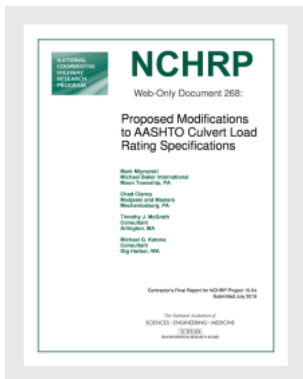


This PDF is available at <http://nap.edu/25673>

SHARE



Proposed Modifications to AASHTO Culvert Load Rating Specifications (2019)

DETAILS

601 pages | 8.5 x 11 | PAPERBACK

ISBN 978-0-309-67150-7 | DOI 10.17226/25673

GET THIS BOOK

FIND RELATED TITLES

CONTRIBUTORS

National Cooperative Highway Research Program; Transportation Research Board; National Academies of Sciences, Engineering, and Medicine

SUGGESTED CITATION

National Academies of Sciences, Engineering, and Medicine 2019. *Proposed Modifications to AASHTO Culvert Load Rating Specifications*. Washington, DC: The National Academies Press. <https://doi.org/10.17226/25673>.

Visit the National Academies Press at NAP.edu and login or register to get:

- Access to free PDF downloads of thousands of scientific reports
- 10% off the price of print titles
- Email or social media notifications of new titles related to your interests
- Special offers and discounts



Distribution, posting, or copying of this PDF is strictly prohibited without written permission of the National Academies Press. (Request Permission) Unless otherwise indicated, all materials in this PDF are copyrighted by the National Academy of Sciences.

Copyright © National Academy of Sciences. All rights reserved.

NCHRP

Web-Only Document 268:

Proposed Modifications to AASHTO Culvert Load Rating Specifications

Mark Mlynarski
Michael Baker International
Moon Township, PA

Chad Clancy
Modjeski and Masters
Mechanicsburg, PA

Timothy J. McGrath
Consultant
Arlington, MA

Michael G. Katona
Consultant
Gig Harbor, WA

Contractor's Final Report for NCHRP Project 15-54
Submitted July 2019

ACKNOWLEDGMENT

This work was sponsored by the American Association of State Highway and Transportation Officials (AASHTO), in cooperation with the Federal Highway Administration, and was conducted in the National Cooperative Highway Research Program (NCHRP), which is administered by the Transportation Research Board (TRB) of the National Academies of Sciences, Engineering, and Medicine.

COPYRIGHT INFORMATION

Authors herein are responsible for the authenticity of their materials and for obtaining written permissions from publishers or persons who own the copyright to any previously published or copyrighted material used herein.

Cooperative Research Programs (CRP) grants permission to reproduce material in this publication for classroom and not-for-profit purposes. Permission is given with the understanding that none of the material will be used to imply TRB, AASHTO, FAA, FHWA, FMCSA, FRA, FTA, Office of the Assistant Secretary for Research and Technology, PHMSA, or TDC endorsement of a particular product, method, or practice. It is expected that those reproducing the material in this document for educational and not-for-profit uses will give appropriate acknowledgment of the source of any reprinted or reproduced material. For other uses of the material, request permission from CRP.

DISCLAIMER

The opinions and conclusions expressed or implied in this report are those of the researchers who performed the research. They are not necessarily those of the Transportation Research Board; the National Academies of Sciences, Engineering, and Medicine; or the program sponsors.

The information contained in this document was taken directly from the submission of the author(s). This material has not been edited by TRB.

The National Academies of
SCIENCES • ENGINEERING • MEDICINE



TRANSPORTATION RESEARCH BOARD

The National Academies of **SCIENCES • ENGINEERING • MEDICINE**

The **National Academy of Sciences** was established in 1863 by an Act of Congress, signed by President Lincoln, as a private, non-governmental institution to advise the nation on issues related to science and technology. Members are elected by their peers for outstanding contributions to research. Dr. Marcia McNutt is president.

The **National Academy of Engineering** was established in 1964 under the charter of the National Academy of Sciences to bring the practices of engineering to advising the nation. Members are elected by their peers for extraordinary contributions to engineering. Dr. John L. Anderson is president.

The **National Academy of Medicine** (formerly the Institute of Medicine) was established in 1970 under the charter of the National Academy of Sciences to advise the nation on medical and health issues. Members are elected by their peers for distinguished contributions to medicine and health. Dr. Victor J. Dzau is president.

The three Academies work together as the **National Academies of Sciences, Engineering, and Medicine** to provide independent, objective analysis and advice to the nation and conduct other activities to solve complex problems and inform public policy decisions. The National Academies also encourage education and research, recognize outstanding contributions to knowledge, and increase public understanding in matters of science, engineering, and medicine.

Learn more about the National Academies of Sciences, Engineering, and Medicine at www.national-academies.org.

The **Transportation Research Board** is one of seven major programs of the National Academies of Sciences, Engineering, and Medicine. The mission of the Transportation Research Board is to increase the benefits that transportation contributes to society by providing leadership in transportation innovation and progress through research and information exchange, conducted within a setting that is objective, interdisciplinary, and multimodal. The Board's varied committees, task forces, and panels annually engage about 7,000 engineers, scientists, and other transportation researchers and practitioners from the public and private sectors and academia, all of whom contribute their expertise in the public interest. The program is supported by state transportation departments, federal agencies including the component administrations of the U.S. Department of Transportation, and other organizations and individuals interested in the development of transportation.

Learn more about the Transportation Research Board at www.TRB.org.

COOPERATIVE RESEARCH PROGRAMS

CRP STAFF FOR NCHRP Web-Only Document 268

Christopher J. Hedges, *Director, Cooperative Research Programs*
Lori L. Sundstrom, *Deputy Director, Cooperative Research Programs*
Waseem Dekelbab, *Senior Program Officer*
Megan A. Chamberlain, *Senior Program Assistant*
Eileen P. Delaney, *Director of Publications*
Natalie Barnes, *Associate Director of Publications*
Kathleen Mion, *Senior Editorial Assistant*

NCHRP PROJECT 15-54 PANEL

Field of Design—General Design

Timothy A. Armbrecht, *Illinois DOT, Springfield, IL (Chair)*
Thomas Kevin Koch, *Garner, NC*
Yi Qiu, *Texas DOT, Austin, TX*
Holly O'Neal Thomas, *St. Tammany Parish Government, Covington, LA*
Bradley M. Wagner, *Michigan DOT, Lansing, MI*
James L. Withiam, *D'Appolonia Engineering Division of Ground Technology, Inc., Monroeville, PA*
Lubin Gao, *FHWA Liaison*
Stephen F. Maher, *TRB Liaison*

Author Acknowledgements

The research reported herein was performed under NCHRP 15-54 by Michael Baker International, Modjeski & Masters, Inc., Timothy McGrath (consultant), and Michael Katona (consultant). Michael Baker International was the contractor for this study. The work undertaken by Modjeski & Masters, Inc, Timothy McGrath, and Michael Katona was under a subcontract with Michael Baker Jr., Inc.

Mark Mlynarski, P.E, Project Manager, Michael Baker Jr., Inc., and Chad M. Clancy, P.E., Modjeski & Masters, Inc. were the Co-principal investigators. The other authors of this report and significant contributors to this research were Timothy J. McGrath, Ph.D., and Michael G. Katona, Ph.D.

The work was performed under the general supervision of Mr. Mlynarski and Mr. Clancy. The software development and data extraction work at Michael Baker International was performed under the supervision of Mr. Mlynarski with the assistance of Krisha Kennelly, P.E., Technical Manager-Bridge Software. Field assistance, Michael Pichura, P.E., Aaron Colorito, P.E., and Jerry Jones P.E. The work at Modjeski & Masters was performed under the supervision of Mr. Clancy with the instrumentation assistance of Dave Barrett, P.E., the technical guidance of Tom Murphy, P.E. Ph.D., and the 3D modeling assistance of Reza Baie and Jesus M. Villanueva.

Special thanks to the states of Massachusetts, Maryland, Ohio, and Pennsylvania for their willingness to provide structures to be tested, staff to assist in the field testing, traffic control and loaded trucks for use in the field testing. Also, thanks to the State Police of those states for their efforts in weighing to loaded vehicles. While no culverts were selected for their state, thanks also the state of Illinois for volunteering to offer the field testing of their culverts.

Also, a special thanks to Jerry Silagyi, P.E. of Lane Enterprises, Joel Hahm, P.E from Big R Bridge, and Kevin Grant of Contech for assisting in locating culverts, models, and plans for this research.

CONTENTS

SUMMARY.....	VII
CHAPTER 1.....	1
Background.....	1
Surveying / Soliciting Data.....	1
CHAPTER 2.....	3
Research Approach	3
Development of Field Test Program	4
Culverts Selected	4
Review and Selection Process.....	4
Selection Criteria.....	4
Vendors	4
Pennsylvania (DOT and County).....	5
Maryland DOT	5
Ohio DOT.....	5
Massachusetts DOT.....	5
Illinois DOT	5
Executing the Field Testing Program	7
Culvert Instrumentation	7
Model 1 – Field Test - Reinforced Concrete Box – Single Cell (M1C1).....	10
Model 2 – Field Test - Reinforced Concrete Box –Twin Cell (M2C1)	13
Model 3 – Field Test - Reinforced Concrete Box – Single Cell – Precast (M3C1)	16
Model 4 – Field Test - Reinforced Concrete Arch (M4C1)	19
Model 5 – Field Test - Metal Arch (M5C1).....	23
Model 6 – Field Test - Metal Box Arch (M6C2)	27
Model 7 – Field Test - Metal Box Arch (M7C1)	31
Development of Analysis Testing Plan	35
Software Used for the Analysis/ Data Gathering.....	35
CANDE Toolbox/Development of the 2D CANDE Models.....	35
Changes to the CANDE GUI and Steps for Creating CANDE Models	36
BrDR Regression Testing and Data Mining.....	40
Development of the 3D Models.....	42

CHAPTER 3.....	43
Findings and Applications	43
Calibration of the 3D Models.....	43
Summary of Areas of Specification to Review	44
Effects of Subgrade on Rating.....	45
Design-Analysis	55
Culvert Load Distribution.....	63
Non-Rectangular Culverts	66
Pavement.....	66
Model 7 3D Analysis Review	67
Culvert Loading and Instrumentation	67
Results Before and After Paving.....	70
CANDE Models with and Without Pavement.....	78
Model 7	78
Recommendations	79
Shear Capacity	80
Economic Impact.....	81
Live Load Surcharge vs. Approaching Wheel Load	86
Background/Spec Change Proposal	86
Economic Impact.....	89
CHAPTER 4.....	92
Conclusions and Suggested Research	92
Proposed Revisions to the LRFD Specifications and the MBE.....	93
Suggested Research	110
Data Archiving	110
Changes to the CANDE Software	110
CANDE Input Files	110
AASHTOWare BrDR Export Files (XML).....	111
AASHTOWare BrDR Regression Data/Report ID Descriptions	111
3D FEM Files.....	111
Field Testing Data	112
List of Appendices	113

Summary

This report highlights the work accomplished under the AASHTO-sponsored project entitled “Proposed Modifications to AASHTO Culvert Load Rating Specifications.” Administered by NCHRP as Project 15-54, the research has provided proposals for changes to the AASHTO Manual for Bridge Evaluation (MBE) through the load testing of seven culverts and the review and data analysis of culvert models of varying types. The culverts were analyzed using 3D analysis, 2D analysis using Culvert ANalysis and Design (CANDE) (Mlynarski, M., M. G. Katona, and T. J. McGrath. *NCHRP Report 619: Modernize and Upgrade CANDE for Analysis and LRFD Design of Buried Structures*. Transportation Research Board of the National Academies, Washington, D.C., 2008.), AASHTOWare Bridge® Design and Rating (BrDR), and BOXCAR (FHWA).

Over the past decade, significant state and federal resources have been expended to develop a state-of-the-art set of reliability-based bridge design and load rating specifications, the LRFD and LRFR. In addition, states continue to load rate using the load factor (LFR) and allowable stress (ASR) rating methods according to the MBE. However, these design and rating methods were developed for larger bridge structures and can result in overly conservative ratings when applied to buried culverts. Of the 600,000+ records in the National Bridge Inventory (NBI), over 130,000 represent culverts, thus constituting a significant proportion of the nation’s bridge infrastructure and, since the NBI only records culverts spanning more than 20 feet, and most culverts have spans of less than 20 feet, the actual number of culverts is vastly higher. As stated in the Request for Proposals document, the choice of, or change in the load rating method may affect the transportation of goods and services over the nation’s highways by imposing load limits on routes that were previously unrestricted. Determining effective revisions to the existing specifications for culverts and the potential economic impact for possible changes in ratings due to the changes and/or rating method was critical to the success of this project.

The objective of this research was to propose modifications to the culvert load rating specifications in the MBE and revise the AASHTO LRFD Bridge Design Specifications accordingly.

The objective was accomplished by

- Surveying the DOTs for current culvert practices and issues related to culvert rating.
- Contacting states via telephone who agreed to talk to us.
- Developing and executing full scale field tests on seven culverts with the aid of four different state agencies (Maryland, Massachusetts, Ohio, and Pennsylvania).
- Developing and executing a full analysis of the subject culverts in both 3D and 2D analysis.
- Identifying areas of the (MBE) and LRFD Specifications for improvement and recommendations for updates to those specifications based on the field testing and analysis results.

The literature survey was conducted in the first phase of the project to ascertain the current state of the culvert rating specifications. This survey included an online survey with an optional follow-up interview at the agency’s request. Some of the results yielded by the survey and interviews were:

- Concrete culverts are used extensively, followed by steel corrugated culverts. Only one state indicated that they rated thermoplastic culverts and they are not reporting rating issues for those types of structures.
- Reinforced concrete culverts are not rating well but don’t show physical signs of distress.
- Studies that included input files for culvert analysis that could be utilized by this study.
- Other research efforts including those from California, Ohio, and Pennsylvania which were utilized in this research.

Based on the literature survey and subsequent interaction with the project panel, a sample testing plan and target field testing matrix was developed. Upon approval by the project panel, the effort to locate target culverts was conducted by contacting the state DOTs. This process yielded a field testing plan that was developed in tandem with an analytical plan that would be used to evaluate the current processes and

specifications used for culvert rating and evaluation. In all, seven culverts were field tested and analyzed in 3D using a FEM software package and in 2D using the CANDE software updated under NCHRP Project 15-28. The seven culverts analyzed and their location were:

Model 1 – Reinforced Concrete Box (Single Cell)	Pennsylvania
Model 2 – Reinforced Concrete Box (Twin Cell)	Maryland
Model 3 – Reinforced Concrete Box – (Single Cell-Precast)	Pennsylvania
Model 4 – Reinforced Concrete Arch	Ohio
Model 5 – Metal Arch	Pennsylvania
Model 6 – Metal Arch	Pennsylvania
Model 7 – Metal Arch (Long span) – Deep Corrugation	Massachusetts

In addition to the load testing, each of these models was analyzed in 3D and CANDE. In some cases, software was developed for this project (CANDE Tool Box and revisions to the CANDE analysis engine) to facilitate the research. These tools are delivered with this project so that others may use them as well. The reinforced concrete box models were also analyzed in BrDR.

Upon review of the existing specifications, modifications were proposed and, where possible, testing the changes using the BrDR software through a process of regression testing by analytically comparing the current specification with the suggested changes. The results of those recommendations are provided as part of this research and include modifications to the MBE and LRFD Specifications including:

- Recommendations for culvert live load distribution.
- Recommendations for non-rectangular culverts.
- A study on the effects of pavement in culvert rating and recommendations for the use of an analytical tool developed on this project (CANDE Tool Box and CANDE) for analyzing culverts with pavement elements. Recommendations were also made for implementing the effects of pavement in other culvert programs.
- Changes to the shear capacity calculations for reinforced concrete box culverts.
- Changes to the live load surcharge loads (now described as approaching wheel load).
- The effects of fill depth on live load.
- The effects of haunches on reinforced concrete culvert analysis.
- Sections for concrete, metal, and plastic culverts.

CHAPTER 1

Background

Load rating bridges and culverts is a key step in assessing the condition of structures that go under and over our highways and roads. The *Manual for Bridge Evaluation, 3rd Edition* (MBE) provides detailed guidance for the rating process for bridges but has only limited guidance for the treatment of culverts. This is a significant issue as culverts constitute about 130,000 of the structures listed in the National Bridge Inventory which includes spans of 20 ft and greater, but also includes millions more culverts with spans less than 20ft.

In recent years, the Federal Highway Administration (FHWA) and the American Association of Highway and Transportation Officials (AASHTO) has begun to focus on the issue of rating culverts. This effort has shown significant issues in rating concrete box sections which have been providing good service but are being rated as deficient when analyzed by current codes. Further, there is little guidance provided to rate concrete culverts of other shapes or of other materials. Corrugated structural plate structures have spans of 25 feet and larger, but little guidance is offered for rating. Deep corrugated metal structures, which are relatively new to the AASHTO specifications, also have long spans and are not addressed in the MBE at all. Thermoplastic and fiberglass culverts have smaller diameters and are not considered in the NBI, but rating is required in some states, thus these structures too should be addressed in the MBE.

Surveying / Soliciting Data

The objective of the survey for this project was to determine the overall impressions of the states regarding the specifications related to culverts and to solicit data for building a suite of culvert bridges for use in later regression testing of the specification recommendations.

To begin the review, a survey related to culvert rating was compiled using the web software SurveyMonkey® and distributed. The survey content is listed in Appendix A. The survey distribution was compiled from a list provided by AASHTO and included the AASHTO SCOBS (Subcommittee on Bridges and Structures) email list along with the RADBUD (Rating and Design Bridge User Group-AASHTOWare BrDR) email list.

In all, 42 respondents provided complete survey responses; incomplete survey responses (those that only answered the first one or two questions) were discarded. In all, 37 states completed the survey, plus the District of Columbia, and the U.S. Army Corp of Engineers. Three states had two responses from different individuals. Of those 42 respondents, 19 requested follow-up interviews. The additional interviews were conducted by phone, with the exception of 1, which was conducted via email. Four states that requested follow-up interviews did not respond in time to set up interviews for this report. The detailed results of the survey are provided in Appendix B. A summary discussion of the survey and follow-up interviews are provided in the following sections.

A cursory review of the survey results and the follow-up interviews indicate the following:

- Concrete culverts are used extensively, followed by steel corrugated culverts. Only one state indicated that they rated thermoplastic culverts and they are not reporting rating issues for those types of structures. Reinforced concrete culverts are not rating well but don't show physical signs of distress.
- Seven of the states surveyed are using Ohio DOT's metal corrugated spreadsheet in some form for the rating of metal culverts. (Ohio, Iowa, Idaho, Louisiana, California, Oregon, Michigan).
- There seems to be a severe rating penalty for metal corrugated culverts when moving from the just above the 12" fill height to just below that height.
- Large fill heights often present a problem, causing the rating for culvert structures to fail under dead load conditions.

- AASHTOWare BrDR™ is used by many states for reinforced concrete box culvert analysis. Several states use BRASS.
- A variety of research efforts were described in the survey results.

The survey and the literature have provided a number of studies that were pertinent to this project including the following:

Caltrans Culvert Study – Caltrans instituted a study of reinforced concrete box sections (RCBs) to investigate how they might be rated to meet current FHWA requirements. As part of this study, Caltrans created BrDR input files for RCBs designed under both current and historical standards. Caltrans provided us with about 140 such files representing a variety of sizes (single and double boxes), depths of fill, and date of construction (1922-2010). Many of these input files were used in subsequent project phases to evaluate (regression testing) current and proposed design and rating practices.

Ohio DOT and Michigan DOT Metal Culvert Spreadsheets and Supporting Research - Ohio DOT has developed a series of three spreadsheets for rating metal culverts:

- Standard metal culverts
- Low cover metal culverts
- Metal box culverts

The spreadsheets are based on Design Data Sheet No. 19 which was produced by the National Corrugated Steel Pipe Association in 1995. Despite their age, the data sheet and the Ohio DOT spreadsheets provide good guidance for rating metal culverts. At least seven states use the spreadsheets and Michigan has modified it for their own purposes.

PennDOT Box Culvert Live Load Distribution Study – PennDOT initiated a study of live load distribution on RCBs to investigate the differences between the distributions in the AASHTO Standard and the initial edition of the AASHTO LRFD Specifications. The study was completed by Dr. McGrath. The study provided a recommendation that the AASHTO Standard Specification distribution is more appropriate for RCBs and AASHTO subsequently adopted this recommendation. The study also developed insights into load distribution that are pertinent to this project.

CHAPTER 2

Research Approach

The objective was accomplished by

- Surveying the DOTs for current culvert practices and issues related to culvert rating.
- Contacting states via telephone who agreed to talk to us.
- Developing and executing full scale field tests on seven culverts with the aid of four different state agencies (Maryland, Massachusetts, Ohio, and Pennsylvania).
- Developing and executing a full analysis of the subject culverts in both 3D and 2D analysis.
- Identifying areas of the MBE and LRFD Specifications for improvement and recommendations for updates to those specifications based on the field testing and analysis results.

The literature survey was conducted in the first phase of the project to ascertain the current state of the culvert rating specifications. This survey included an online survey with an optional follow-up interview at the agency's request. Some of the results yielded by the survey and interviews were:

- Concrete culverts are used extensively, followed by steel corrugated culverts. Only one state indicated that they rated thermoplastic culverts and they are not reporting rating issues for those types of structures.
- Reinforced concrete culverts are not rating well but don't show physical signs of distress.
- Studies that included input files for culvert analysis that could be utilized by this study.
- Other research efforts including those from California, Ohio, and Pennsylvania which were utilized in this research.

Based on the literature survey and subsequent interaction with the project panel, a sample testing plan and target field testing matrix was developed. Upon approval by the project panel, the effort to locate target culverts was conducted by contacting the state DOTs. This process yielded a field testing plan that was developed in tandem with an analytical plan that would be used to evaluate the current processes and specifications used for culvert rating and evaluation. In all, seven culverts were field tested and analyzed in 3D using a FEM software package and in 2D using the CANDE (Culvert ANalysis and Design) software updated under NCRHP Project 15-28 (Mlynarski, M., M. G. Katona, and T. J. McGrath. *NCHRP Report 619: Modernize and Upgrade CANDE for Analysis and LRFD Design of Buried Structures*. Transportation Research Board of the National Academies, Washington, D.C., 2008.). The culverts selected and the process for selection are described in subsequent sections of this chapter.

In addition to the field testing plan, an analysis testing plan was developed to model the selected field testing results and to review the current specifications to determine where improvements could be made to the rating process. This process for the analysis and the tools used is described in detail in later sections of this chapter. The results of those recommendations are part of this research and include modifications to the MBE and LRFD Specifications. The process for the specification review and recommendations is provided in more detail in Chapter 3. The recommendations for the specification changes are provided in Chapter 4 and include:

- Recommendations for culvert live load distribution.
- Recommendations for non-rectangular culverts.
- A study on the effects of pavement in culvert rating and recommendations for the use of an analytical tool developed on this project (CANDE Tool Box and CANDE) for analyzing culverts with pavement elements. Recommendations were also made for implementing the effects of pavement in other culvert programs.
- Changes to the shear capacity calculations for reinforced concrete box culverts.
- Changes to the live load surcharge loads (now described as approaching wheel load).

- The effects of fill depth on live load.
- The effects of haunches on reinforced concrete culvert analysis.
- Sections for concrete, metal, and plastic culverts.

Development of Field Test Program

The process for selecting the field tested culverts is described in this section. It includes:

- The culverts selected.
- The selection process.
- A description of the culverts selected.

Culverts Selected

This section provides a description of the culvert selection process, some information about the culverts selected, and a description of the models that were prepared (both 3D and 2D). The culverts were selected from four states: Pennsylvania, Ohio, Massachusetts, and Maryland. The matrix of culvert types was developed early in the process and presented to the panel for review with each culvert type having multiple candidates. The final list of models for analysis and field testing is provided in Table 1. A more detailed description of the culverts is provided in subsequent sections of this document. The detailed field testing data is provided in Appendix F. The following sections provide a brief description of the selection process.

Review and Selection Process

Several states agreed to cooperate with the field testing portion of the research effort. These are Pennsylvania, Maryland, Illinois, Ohio, and Massachusetts. Ultimately, seven culverts were chosen for field testing from Pennsylvania (2 state, 2 county), Ohio (1), Maryland (1), and Massachusetts (1).

Selection Criteria

During the selection process of the culverts that would ultimately be used for field testing and analysis, the following criteria was considered:

- Relatively low ADT to minimize disruption to traffic and to simplify access and instrumentation.
- Close proximity to the members of the research team that are performing the instrumentation. This reduced some of the travel cost and set up for the testing.
- Availability of detailed drawings – unlike with non-culvert structures, DOTs tend to retain less detailed plan information on culverts. Furthermore, DOT design plans tend to be less detailed for culvert structures than for other types of bridges because some of the design and detail development is left for the fabrication stage. As such, for most structure types included in this research effort, both design and shop drawings of the candidate structures was required to have sufficient detail for analytical modeling and field testing. This was a significant limiting factor on the availability of suitable candidates for the research.
- Review of potential paving schedules (if available) for reviewing the effects of existing pavement versus new pavement.

Vendors

Representatives from the vendors BigR Bridge and CONTECH were contacted to assist in the identification of suitable candidate structures. This was important particularly because of the previously mentioned requirement that shop drawings of the candidate structures be obtained and in many cases these drawings were found to be absent from the DOT files. Furthermore, for some of the selected structures,

CONTECH and BigR Bridge were able to provide design calculation and structure modeling information helpful to the research effort.

Pennsylvania (DOT and County)

PennDOT provided an inventory of all culverts in the state, which was then reviewed for culverts that meet the criteria of the matrix provided in Table 1 and the selection criteria provided in the previous section. The culverts selected from Pennsylvania were:

- Model 1-Candidate 1, Single Cell Reinforced Concrete Box Culvert – longer span
- Model 3-Candidate 1, Precast Single Cell Reinforced Concrete Box Culvert – shorter span
- Model 5- Candidate 1, Metal Corrugated Arch
- Model 6-Candidate 2, Metal Corrugated Box Arch

Maryland DOT

Multiple structure types were solicited in Maryland including concrete arch and box structures. However, after reviewing the availability of structures provided by the DOT and with consideration of the structures already identified in other states, only concrete boxes in Maryland were selected as test candidates. The culvert selected from Maryland was:

- Model 2-Candidate 1 – Twin Cell Reinforced Concrete Box Culvert

Ohio DOT

For Ohio, CONTECH helped the research team identify several suitable test candidates within the state of Ohio. Ultimately one field test was scheduled for a concrete arch culvert in Ohio

- Model 4-Candidate 1-Reinforced concrete arch culvert

Massachusetts DOT

MASSDOT and BigR Bridge provided information that led to the effort of being able to field test a longer span metal corrugated culvert. This structure, in Attleboro, Massachusetts, was selected to broaden the range of structure types being included in analytical and field testing and being new construction, allowed for load testing both before and after paving. The model selected was:

- Model 7-Candidate 1 – Deep Corrugate Metal Arch Culvert

Illinois DOT

While Illinois DOT offered to provide support for field testing culverts, the above states provided a good selection of culverts that met the criteria of the developed testing matrix but were closer geographically and thus more economical for the research team.

Table 1 – Field Testing Matrix (Selected culverts are highlighted)

Model	Structure Type	Desired Features	Span (ft)	Depth (ft)	Candidate 1/ State/	Candidate 2/ State
1	Reinforced concrete box - single cell	Precast	16-20	Field Test Depth + 2 additional	PA BRKEY: 20274, 25'x7'-6" Juniata County PA	PA BRKEY 46704, 18' Span
2	Reinforced concrete box - multiple cell	Cast-in-place	10-12/cell	Field Test Depth + 2 additional	MD 329500: 10x7 2-cell 15degree skew, 40' width, 1' cover	MD 301700: 12'x12' 2-cell 29 degree skew, 40' width, min cover
3	Reinforced concrete box	New – precast	>10	Field Test Depth + 2 additional	PA BRKEY 48389 Single 14'-cell, 80 degree skew	PA BRKEY 9649 2-16' cells 90 degree skew
4	Three-sided arch top concrete	CONSPAN type	24-36	0-2	36'x12' (2'-6 cover) Perry County OH	24'x10' (2' cover) New Albany, OH
5	Metal arch	6x2 corrugation	30 -35	AASHTO min. or less	31'-7x10' (3' min cover) Willshire Estates Dauphin Co, PA	Toledo OH Arch 30'x9'-6 (3' cover)
6	Metal box culvert		25	1.4	Kiwanas Rd, 20'-1"x6'-6" (1'-4"cover) Orange Twp, Dauphin Co, PA	Sleepy Hollow (Shermans' Dale Perry County PA), 19'0x6'-1 (2'-6"cover)
7	Deep corrugated metal culvert	5.5 to 6 in. deep corrugation	40	Minimum available	56'6" or 40' New Constr Box, Attleboro, MA	

Executing the Field Testing Program

The field testing program drafted in the first phase and finalized in the second phase of this project was implemented. The following sections provide details of the field testing program. The detailed testing plans are presented in Appendix F of this report. Table 2 provides a summary table of the structures that were tested, the dates tested, the state, and the geographical latitude and longitude. Subsequent sections provide information regarding the loading, load lines, and general information regarding the testing.

Table 2 – Field Testing Table

Culvert Model	Date Tested	State/Agency	Latitude, Longitude (click on link to open in a browser)
Model 1 – Reinforced Concrete Box (Single Cell)	8/30/2017	Pennsylvania DOT, District 2-0	40.3538, -77.6488
Model 2 – Reinforced Concrete Box (Twin Cell)	12/14/2017	Maryland, MDOT	39.411056, -76.409278
Model 3 – Reinforced Concrete Box – (Single Cell-Precast)	11/7/20017	Pennsylvania DOT, District 9-0	40.0513, -78.9943
Model 4 – Reinforced Concreted Arch	4/17/2018	Ohio DOT, District 6	39.79083, -82.25111
Model 5 – Metal Arch	6/12/2018	Pennsylvania, Lower Paxton Township	40.300437, -76.8018666
Model 6 – Metal Arch	5/3/2018	Pennsylvania, Carroll Township	40.359593, -77.142020
Model 7 – Metal Arch (Long span) – Deep Corrugation	5/1/2017 (no pavement) 6/1/2017 (with pavement)	Massachusetts, Mass DOT	41.962574, -71.299294

Culvert Instrumentation

The research team worked with state DOTs and municipalities to facilitate the instrumentation and load testing of the selected candidate culverts. In general, the cooperating agencies provided access to the culverts, loaded trucks for testing and traffic control during the load tests. The agencies and/or the research team also coordinated with the state police who weighed the load trucks with mobile scales. The research team developed the customized testing plans (see Appendix F) to perform the tests, installed the instrumentation gauges tied to a data acquisition system, set up the test loading positions and executed the tests. Typically, the instrumentation was set up a day or two before the load test took place and measures were taken to protect the installed gauges from the elements. A sample of the instrumentation for Model 1

is shown in Figure 1. In the case of Model 7 where testing was performed in two phases (before and after paving), there was a significant gap between the two phases as roadway construction above the culvert was completed. All load tests were performed without any other traffic on the culvert. Typically, multiple strain gauges were installed at each point of interest for redundancy. Details on the test procedures including instrumentation locations, loading positions and data collected can be found in Appendix F.

Load lines were painted on the roadway surface to correspond to the gage locations. See Figure 2 for a sample used on Model 1 (M1C1). Following the load testing, a cursory review of the collected data was performed prior to releasing the loaded truck driver and traffic control. The collected data strain and deflection data was then brought into the office for post processing to prepare it for comparison to the FEM models and calibration.



Figure 1 – M1C1 Culvert Instrumentation

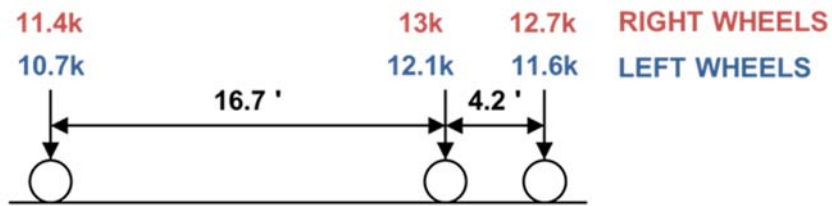


Figure 2 – M1C1 Load Line on Roadway

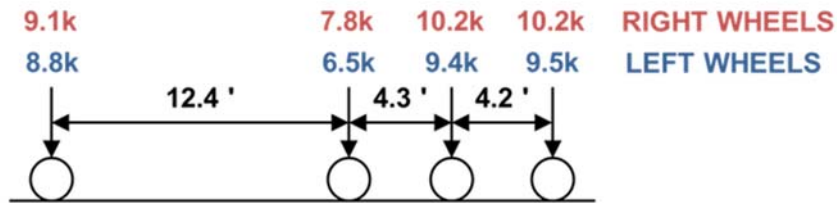
Model 1 – Field Test - Reinforced Concrete Box – Single Cell (M1C1)

This section summarizes general information related to the field testing for Model 1, a 25 foot single cell reinforced concrete box culvert with less than 1 foot of cover. The truck axle weight and configuration are shown in Figure 3. The culvert plan and typical section are provided in Figure 4. A sample load testing photograph is shown in Figure 5. Additional information regarding the testing such as the overall test plan and data regarding the loading are provided in Appendix F.

Location: State: Pennsylvania
 Route: 3020
 Latitude-Longitude: [40.3538, -77.6488](#)



**M1C1 Test Truck - Lift Axle Up
 (Tandem Config)**



**M1C1 Test Truck - Lift Axle
 Down (Tridem Config)**



Figure 3 – Wheel Loads/Configurations for Model 1-Candidate 1 (M1C1)

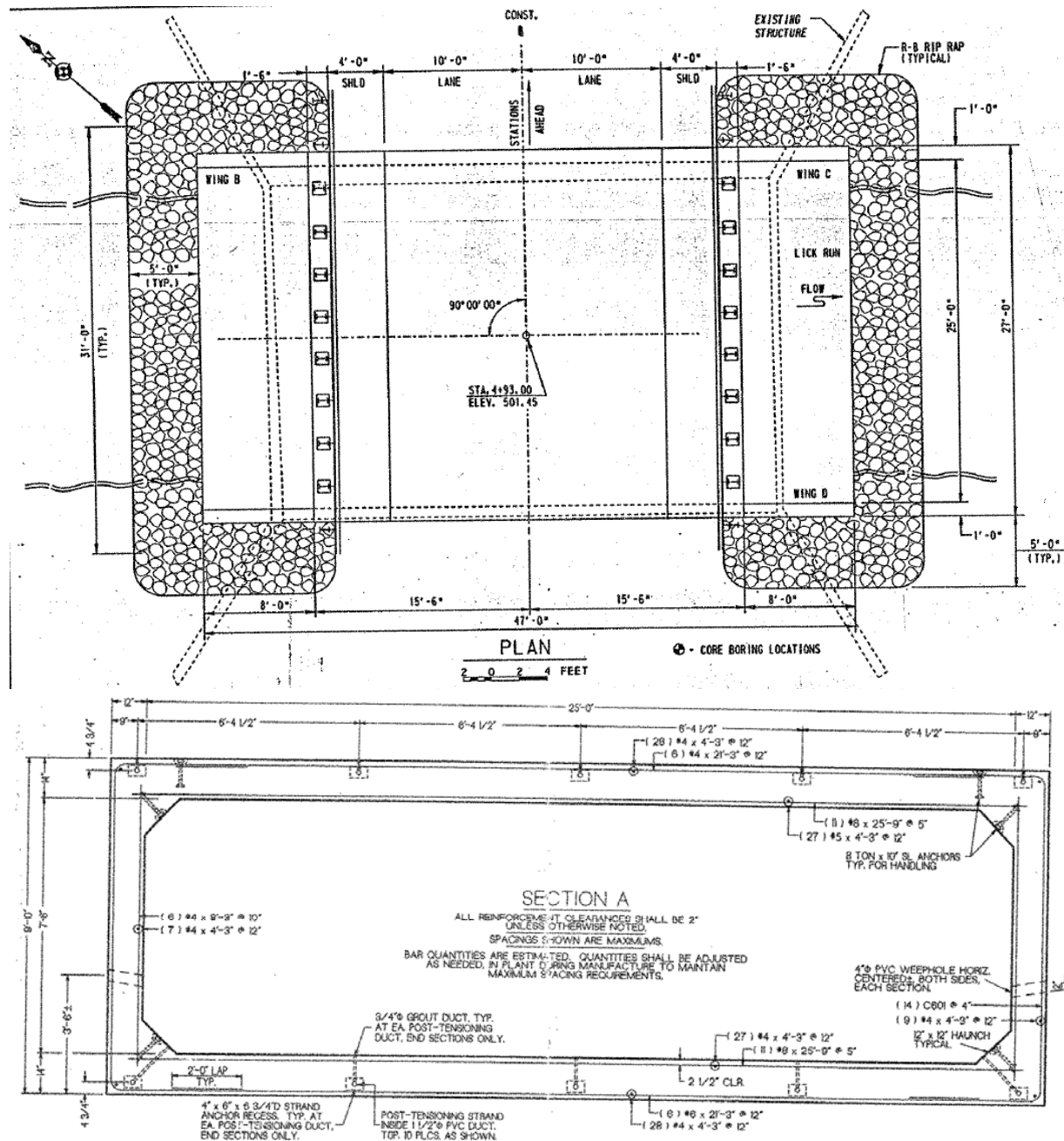


Figure 4 – Model 1, Candidate 1 (M1C1) – Plan and Typical Section

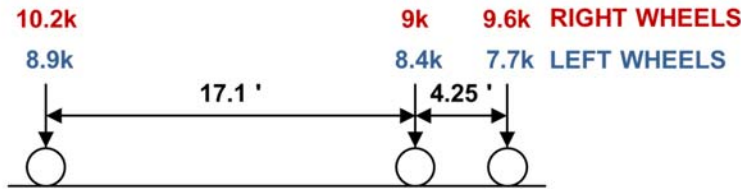


Figure 5 – M1C1 Load Testing

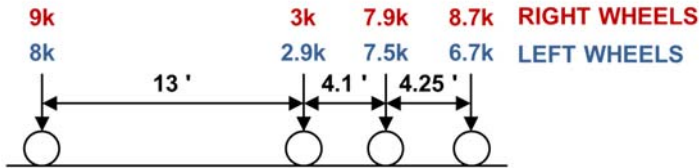
Model 2 – Field Test - Reinforced Concrete Box –Twin Cell (M2C1)

This section summarizes general information related to the field testing for Model 2, a twin cell (10 foot each) reinforced concrete box culvert with 1 foot of fill. The truck axle weight and configuration are shown in Figure 6. The culvert plan and typical section are provided in Figure 7 and instrumentation and load testing photographs are shown in Figure 8 and Figure 9. Additional information regarding the testing such as the overall test plan and data regarding the loading are provided in Appendix F.

Location: State: Maryland DOT
 Route: SR 7 (Philadelphia RD)
 Latitude-Longitude: [39.411056, -76.409278](#)



**M2C1 Test Truck - Lift Axle Up
 (Tandem Configuration)**



**M2C1 Test Truck - Lift Axle Down
 (Tridem Configuration)**



Figure 6 – Wheel Loads/Configurations/Testing Times for Model 2-Candidate 1 (M2C1)



Figure 8 – M2C1 Culvert Instrumentation

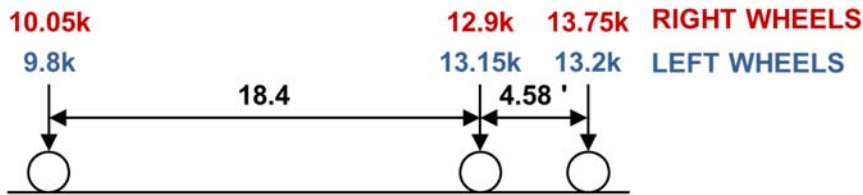


Figure 9 – M2C1 Load Testing

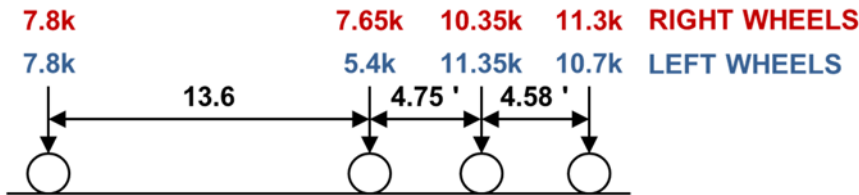
Model 3 – Field Test - Reinforced Concrete Box – Single Cell – Precast (M3C1)

This section summarizes general information related to the field testing for Model 3, a 12' single cell, precast reinforced concrete box culvert with 1' of fill. The truck axle weight and configuration are shown in Figure 10. The culvert plan and typical section are provided in Figure 11 and instrumentation and load testing photographs are shown in Figure 12 and Figure 13. Additional information regarding the testing such as the overall test plan and data regarding the loading are provided in Appendix F.

Location: State: Pennsylvania
 Route: SR 281
 Latitude-Longitude: [40.0513, -78.9943](#)



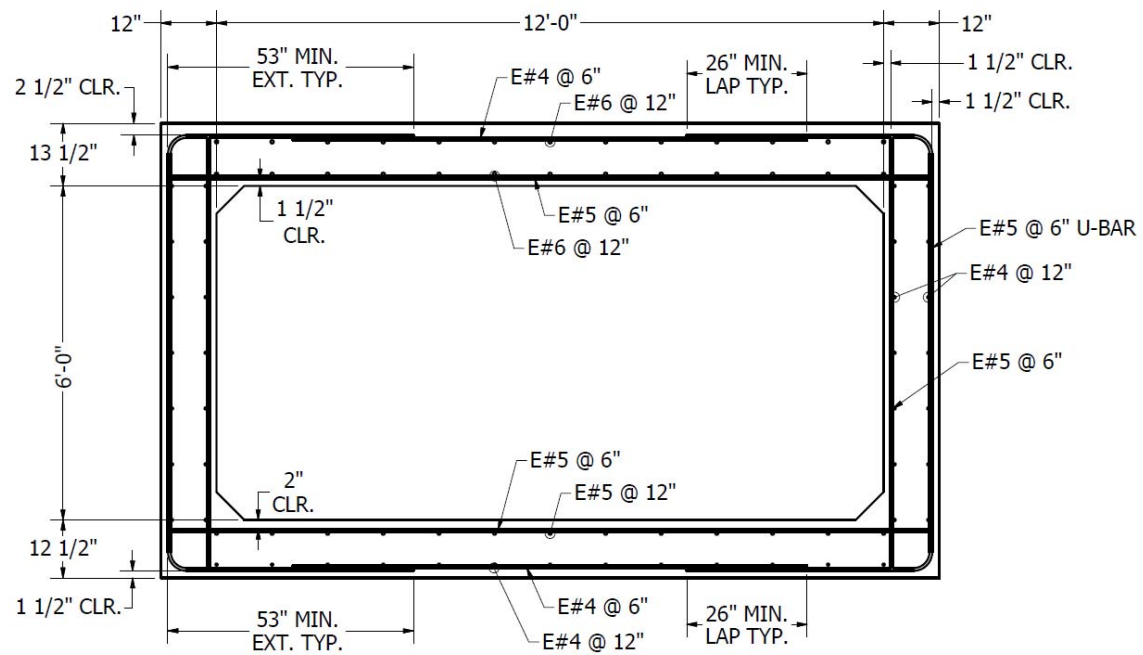
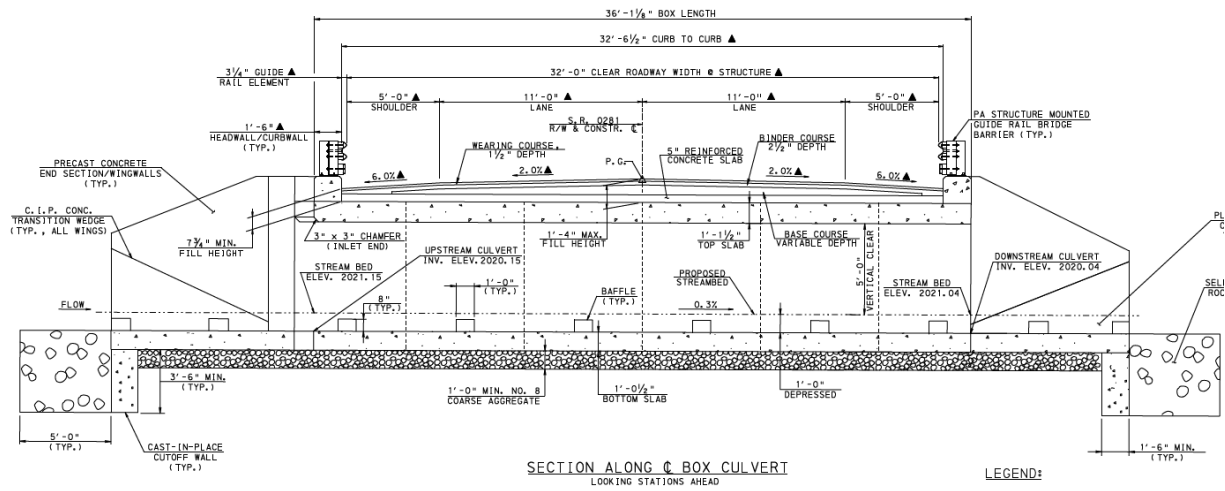
**M3C1 Test Truck - Lift Axle Up
 (Tandem Configuration)**



**M3C1 Test Truck - Lift Axle
 Down (Tridem Configuration)**



Figure 10 – Wheel Loads/Configurations/Testing Times for Model 3-Candidate 1 (M3C1)



TYPICAL SECTION VIEW - BOX

Figure 11 – Model 3, Candidate 1 (M3C1) – Plan and Typical Section



Figure 12 – M3C1 Culvert Instrumentation

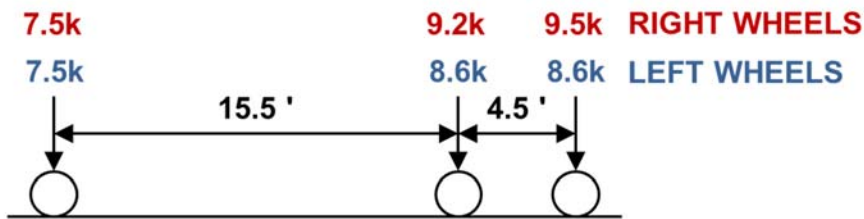


Figure 13 – M3C1 Load Testing

Model 4 – Field Test - Reinforced Concrete Arch (M4C1)

This section summarizes general information related to the field testing for Model 4, a 36 foot precast reinforced concrete arch with 1 foot of fill. The truck axle weight and configuration are shown in Figure 14. The culvert plan and typical section are provided in Figure 15 and instrumentation and load testing photographs are shown in Figure 16 and Figure 17. Additional information regarding the testing such as the overall test plan and data regarding the loading are provided in Appendix F.

Location: State: Ohio DOT
 Route: SR 669
 Latitude-Longitude: [39.79083, -82.25111](#)



**M4C1 Test Truck
 (Tandem Truck)**



Figure 14 – Wheel Loads/Configurations/Testing Times for Model 4-Candidate 1 (M4C1)

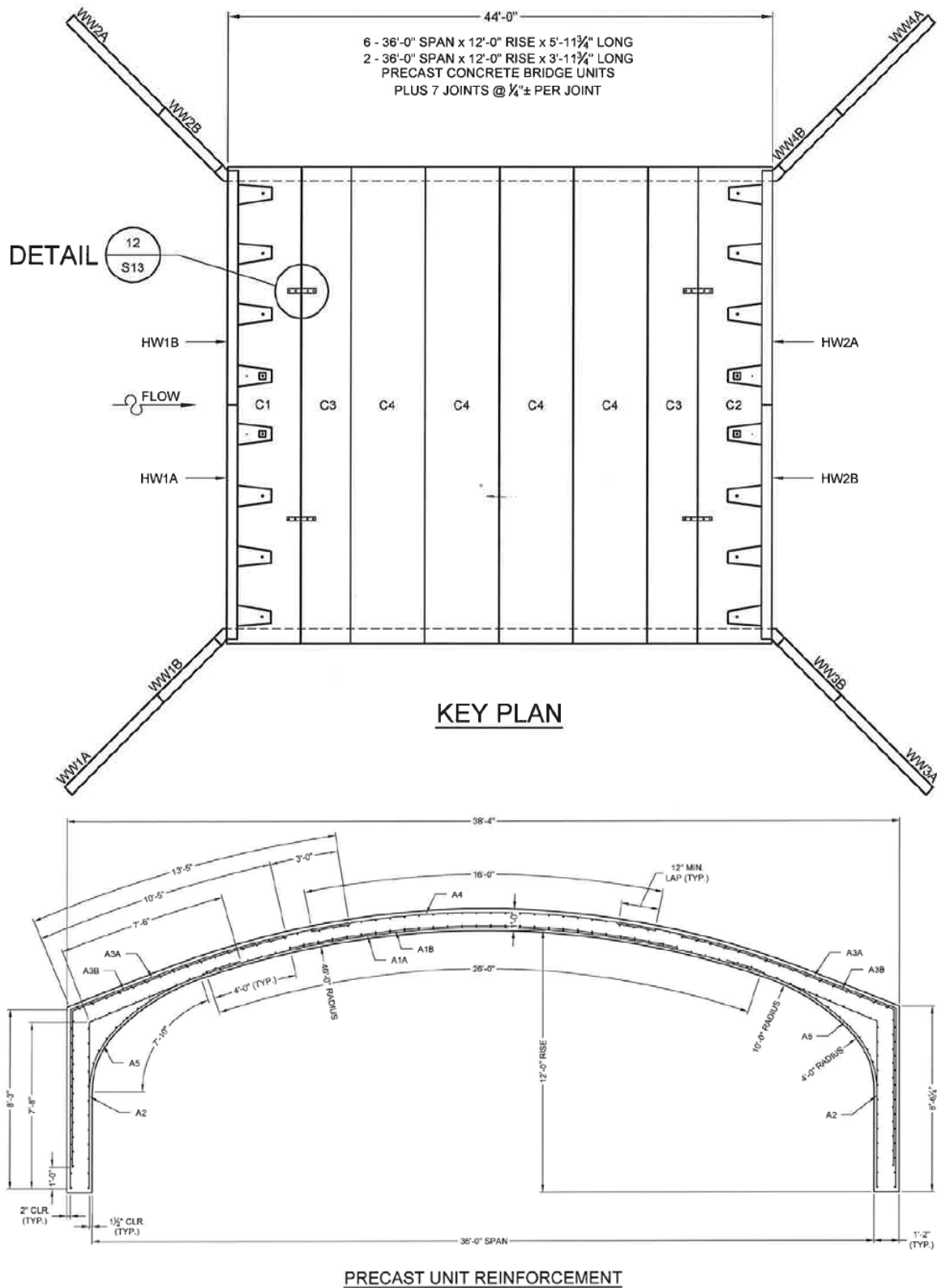


Figure 15 – Model 4, Candidate 1 (M4C1) – Plan and Typical Section



Figure 16 – M4C1 Culvert Instrumentation/ Load Line

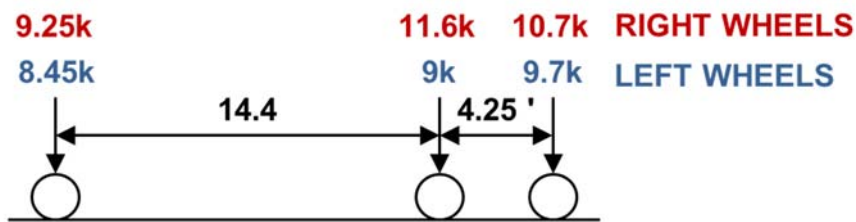


Figure 17 – M4C1 Load Testing

Model 5 – Field Test - Metal Arch (M5C1)

This section summarizes general information related to the field testing for Model 5, a 23 foot metal corrugated arch. The truck axle weight and configuration are shown in Figure 18. The culvert plan and typical section are provided in Figure 19 and instrumentation and load testing photographs are shown in Figure 20 and Figure 21. Additional information regarding the testing such as the overall test plan and data regarding the loading are provided in Appendix F.

Location: State: Pennsylvania
 Route:
 Latitude-Longitude: [40.300437, -76.8018666](#)



**M5C1 Test Truck
(Tandem Truck)**



Figure 18 – Wheel Loads/Configurations for Model 5-Candidate 1 (M5C1)

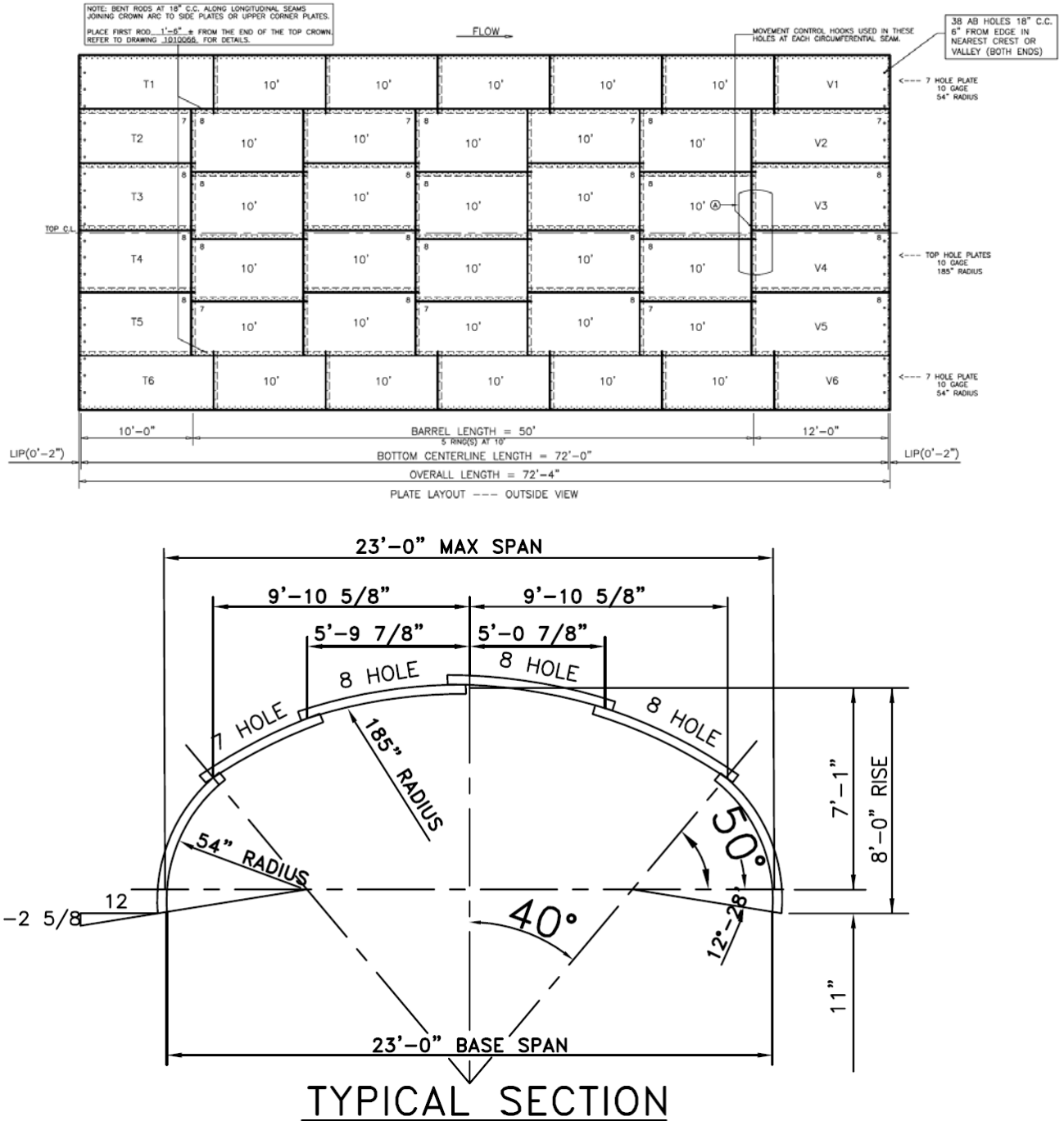


Figure 19 – Model 5, Candidate 1 (M5C1) – Plan and Typical Section



Figure 20 – M5C1 Culvert Instrumentation/ Load Line

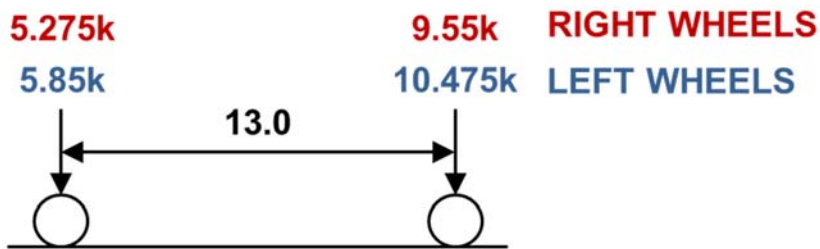


Figure 21 – M5C1 Load Testing

Model 6 – Field Test - Metal Box Arch (M6C2)

This section summarizes general information related to the field testing for Model 6, a 19 foot metal corrugated box arch. The truck axle weight and configuration are shown in Figure 22. The culvert plan and typical section are provided in Figure 23 and instrumentation and load testing photographs are shown in Figure 24 and Figure 25. Additional information regarding the testing such as the overall test plan and data regarding the loading are provided in Appendix F.

Location: State: Pennsylvania, Carroll Twp
 Route: Sleepy Hollow Rd.
 Latitude-Longitude: [40.359593, -77.142020](#)



**M6C2 Test Truck
 (Two Axle Dump)**



Figure 22 – Wheel Loads/Configurations for Model 6-Candidate 1 (M6C2)

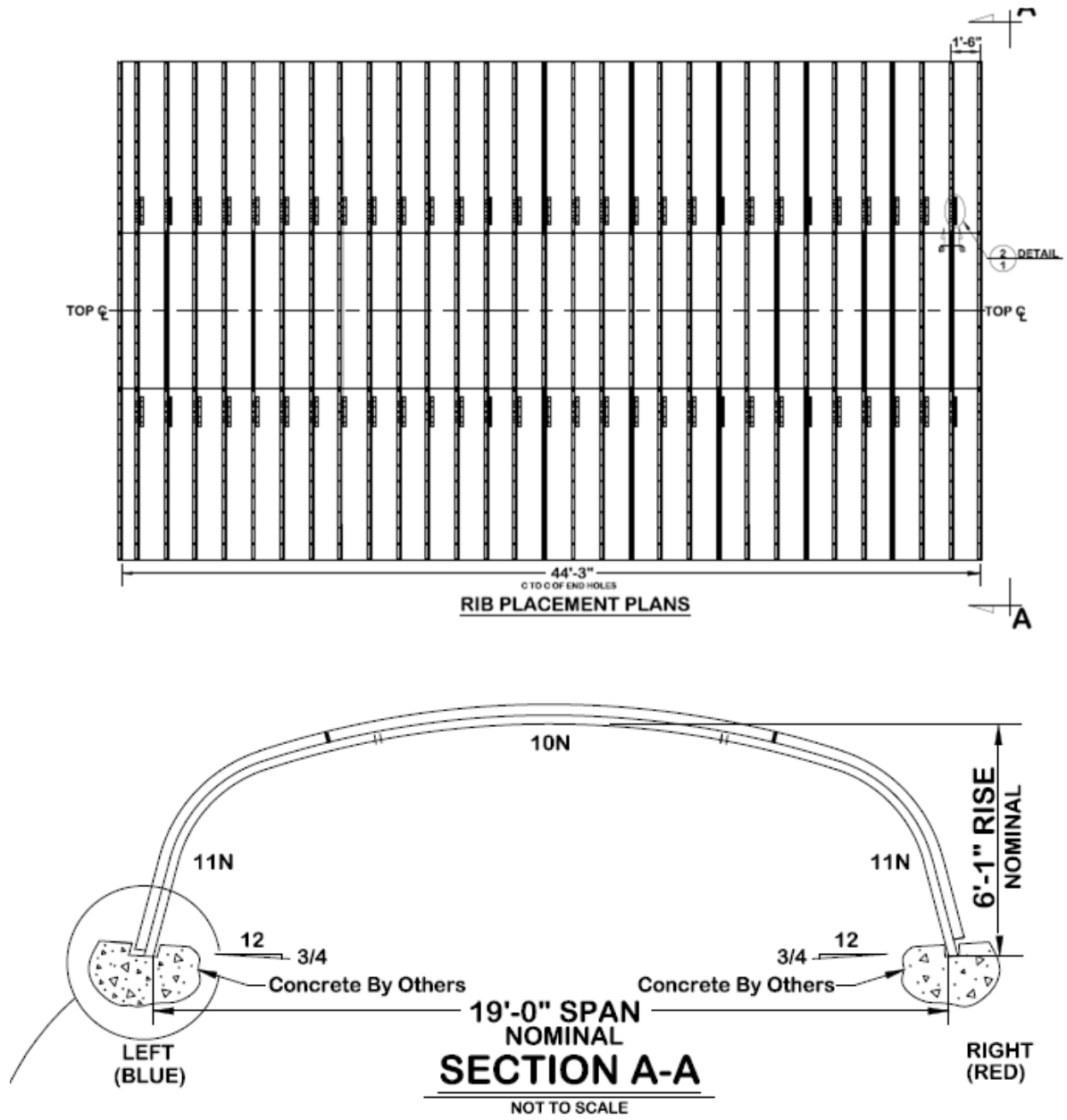


Figure 23 – Model 6, Candidate 1 (M6C1) – Plan and Typical Section

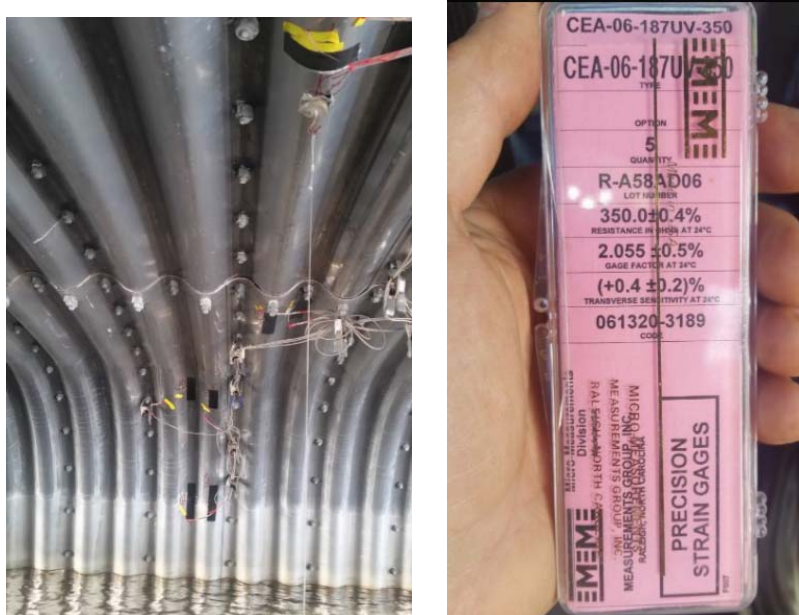


Figure 24 – M6C2 Culvert Instrumentation





Figure 25 – M6C2 Load Testing/Load Line

Model 7 – Field Test - Metal Box Arch (M7C1)

This section summarizes general information related to the field testing for Model 7, a 56.5 foot long span metal corrugated box arch with 2 foot of fill. The truck axle weight and configuration are shown in Figure 26. The culvert plan and typical section are provided in Figure 27 and instrumentation and load testing photographs are shown in Figure 28 and Figure 29. Additional information regarding the testing such as the overall test plan and data regarding the loading are provided in Appendix F. Since this culvert was under construction, it was tested in two phases; once without pavement and once with pavement.

Location: State: Massachusetts
 Route: I-95 over North Avenue
 Latitude-Longitude: [41.962574, -71.299294](#)

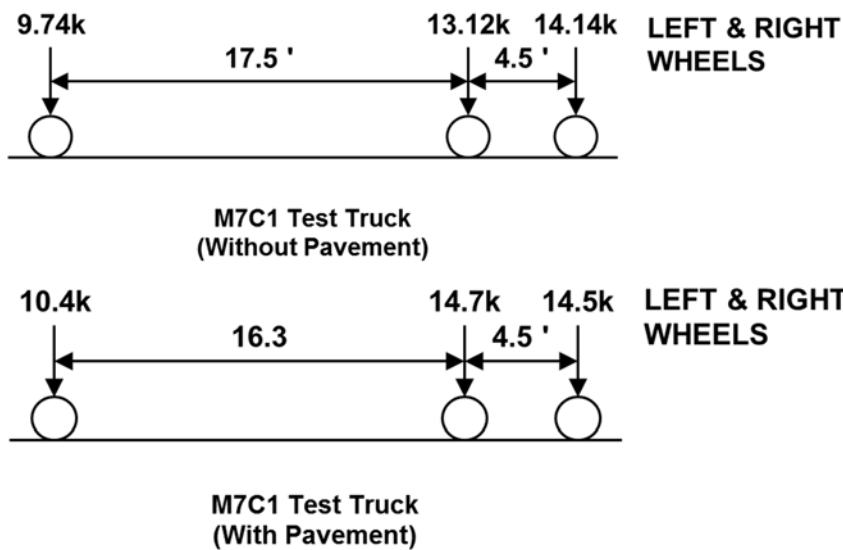
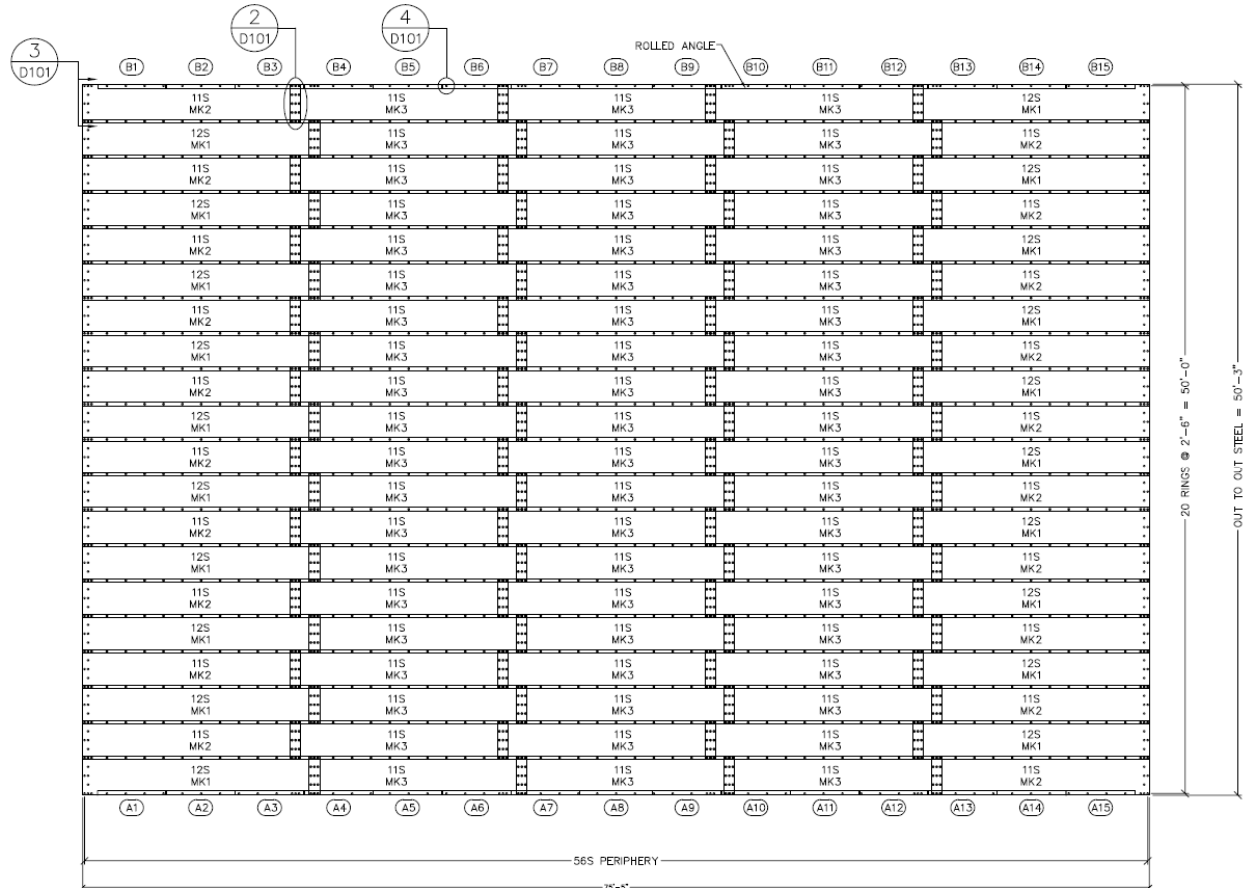


Figure 26 – Wheel Loads/Configurations for Model 7-Candidate 1 (M7C1)



STRUCTURE LAYOUT - OUTSIDE FLAT VIEW

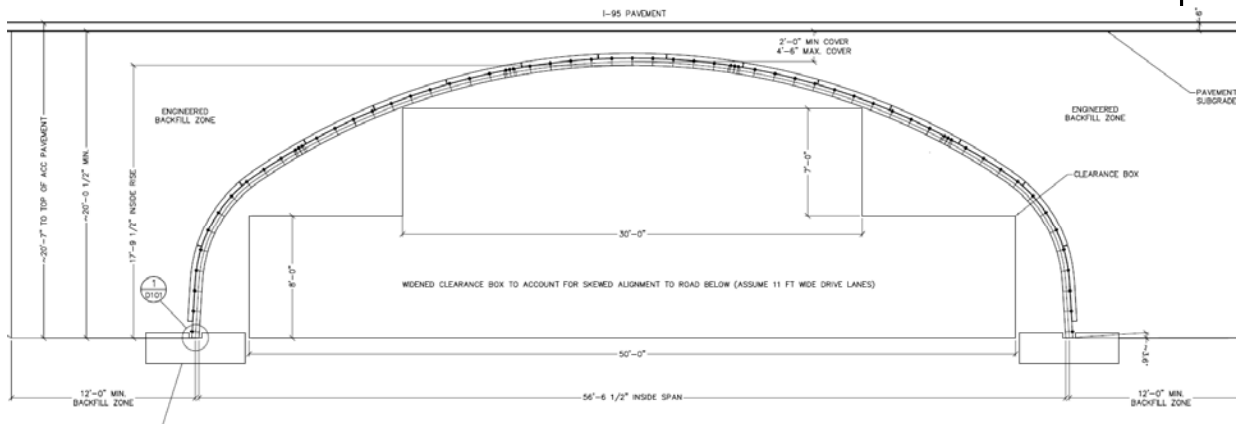


Figure 27 – Model 7, Candidate 1 (M7C1) – Plan and Typical Section

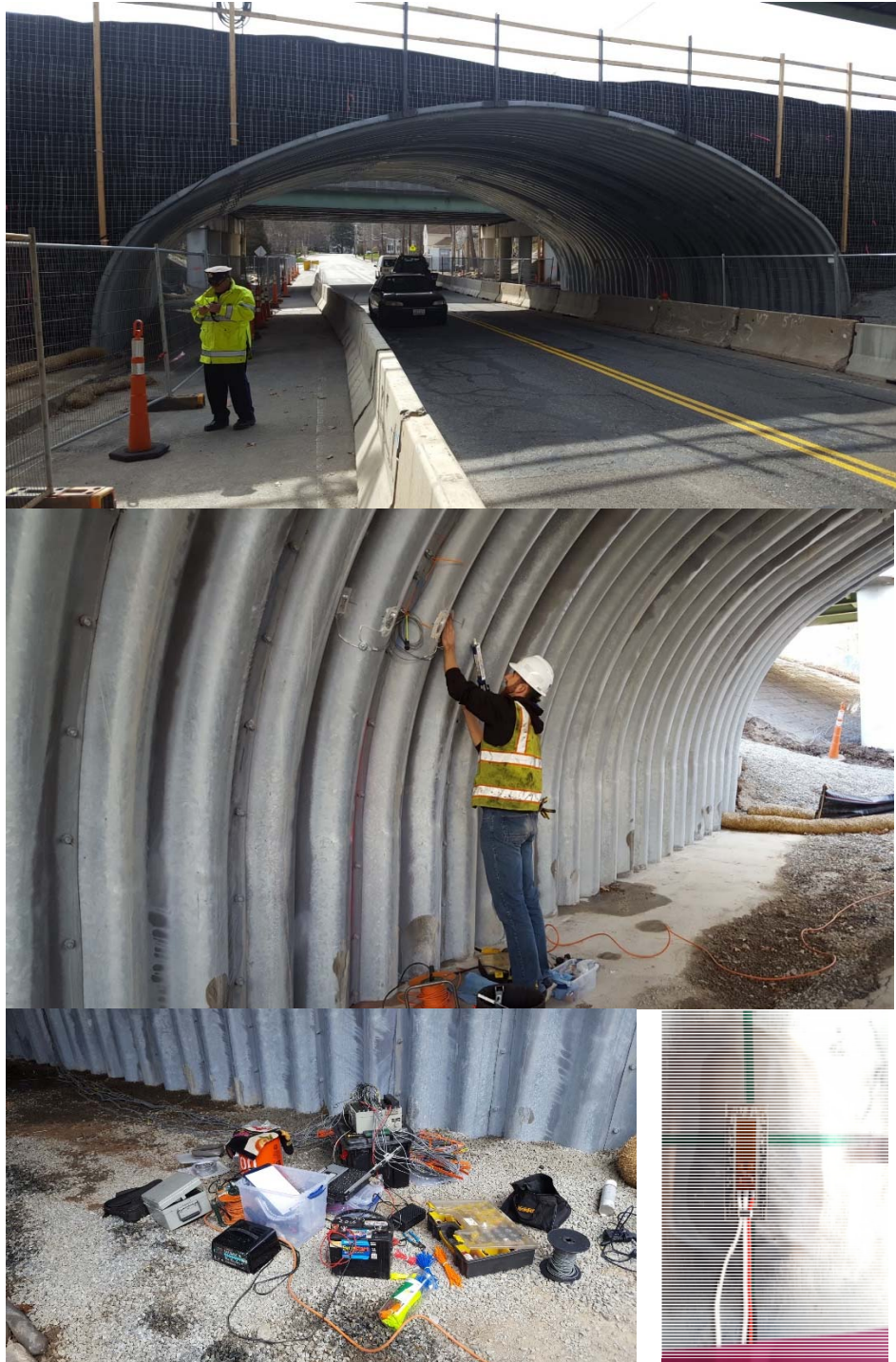


Figure 28 – M7C1 Culvert Instrumentation



Figure 29 – M7C1 Load Testing/Load Line

Development of Analysis Testing Plan

The analysis testing plan for this research project was developed concurrently with the field testing plan for this project. As mentioned in the field testing section, the ability to analyze the proposed structures was necessary to compare the analytical results with those of the field testing. As such, choosing structures with available plans, shop drawings, and/or existing models was a criteria for choosing the models.

Software Used for the Analysis/Data Gathering

Changes to software tools were performed on this research project to enable help with the analysis of the selected culverts, to refine models, and to determine the effects of proposed changes to the specifications. The CANDE software was originally developed in the 1980's and was updated to include new analytical capabilities and a modern user interface under NCHRP Project 15-28 (Mlynarski, M., M. G. Katona, and T. J. McGrath. *NCHRP Report 619: Modernize and Upgrade CANDE for Analysis and LRFD Design of Buried Structures*. Transportation Research Board of the National Academies, Washington, D.C., 2008.).

The AASHTOWare Bridge® Design and Rating (BrDR) software contains a reinforced concrete culvert component that was utilized to not only test how the current rating specifications perform but also to compare those results with the proposed specifications that were a result of this research.

This section provides a description of the software modifications and the functions of the changes with respect to this research project and the use for engineers beyond this project. These revisions include:

- The CANDE Tool Box – This utility provides options to modify CANDE models and includes items as creating a refined model, modeling pavement elements, and rating culverts. A full description of the CANDE Tool Box Manual is provided in Appendix C. The revised source code will be a delivery with this project.
- CANDE interface – changes were made to the CANDE interface to apply some rudimentary features to refine existing CANDE models. The revised source code will be a delivery with this project.
- BrDR changes – regression data mining – with AASHTO's permission, changes to BrDR regression tool were made to allow for additional data mining of the regression data produced by the software. Changes to the specification articles were also made to compare the current specifications to the proposed specification revisions. This source code will be available for future releases of the BrDR software.

CANDE Tool Box/Development of the 2D CANDE Models

A pre/post processor tool (CANDE Tool Box) was created for this project and includes the options listed below that helped build and analyze the models need for this project. A user manual for this software is included in Appendix C of this report. The five available options for the CANDE Tool Box are:

Option 1 – This option will develop a full level 3 mesh from a level 2 input file. Currently level 2 models in CANDE only produce a half mesh. The advantage of using a level 2 model is that minimal input is required to generate the model (e.g. basic model geometry). The full level 3 mesh (full finite element model) facilitates the live loading of the model.

Option 2 – This option provides the automated insertion of a surface pavement on any FEM mesh. This is applicable to any existing level 3 input file that has a continuous horizontal soil surface. The added pavement layer is characterized by linear-elastic beam elements whose thickness and material properties are input by the user. The following is the input that is provided by the user. The input required is:

- Pavement uniform thickness (default = 8.0 inches)
- Young's modulus (default = 200,000 psi)
- Poisson ratio (default = 0.3)
- Weight density (default = 140 lbs/ft³)

Option 3 – This option creates the boundary conditions to simulate a moving live load. It is applicable to any existing level 3 input file that has a continuous horizontal soil surface above the culvert wherein the soil surface may be paved or unpaved. Live loads are simulated by point-like strip forces applied as boundary conditions specified for specific nodes and load steps. An option is provided to proportionately distribute the live load to adjacent nodes when a live load axle falls between two nodes. The user specifies the desired truck type: HL93-design, HL93-tandem, or User-defined with up to ten axles and provides yes/no answers to a series of sub-options as well as information on the vehicle travel path. The final output of option 3 is a completely new input file with the same name as the original input file except with the preface “live”. The live load is distributed through RSL (Reduce Surface Load) or CLS (Continuous Load Spreading). These are defined in the CANDE Tool Box User Manual (See Appendix C).

Option 4 – This option provides a permanent bandwidth minimization and is applicable to any existing level 3 input file wherein node numbering is not optimum, thereby creating long solution times or exceeding system storage capacity. The procedure to permanently minimize bandwidth is to redefine the nodal numbering, starting with node "1" in lower left corner of element located in the lower left corner of the mesh.

Option 5 – This option automatically computes the load ratings factor (RF) from an existing CANDE output file and writes the final RF values along with all supporting information at the end of the CANDE output report. This option is applicable to any existing level 2 or level 3 output file dealing with live load analysis based on LRFD methodology.

The above options are described in detail in the CANDE Tool Box Manual described in Appendix C of this report.

Changes to the CANDE GUI and Steps for Creating CANDE Models

The changes described in the CANDE Tool Box, along with some additional mesh generating capabilities, were used to generate more complex CANDE models from simple level 2 input. A brief description of the process is provided below for Model 1 – Candidate 1. A similar process was performed on other models with the results for pavement vs. no pavement discussed in Chapter 3 of this report.

Step 1– Generate the level 2 model

Level 2 models in CANDE can be generated with minimal input. For a full definition of level 2 models, refer to the CANDE User Manual. In general, level 2 models in CANDE are a mirrored image of the model (i.e., only half the mesh is generated). They are models that can be easily generated with relatively few input commands by the user. See Figure 30.

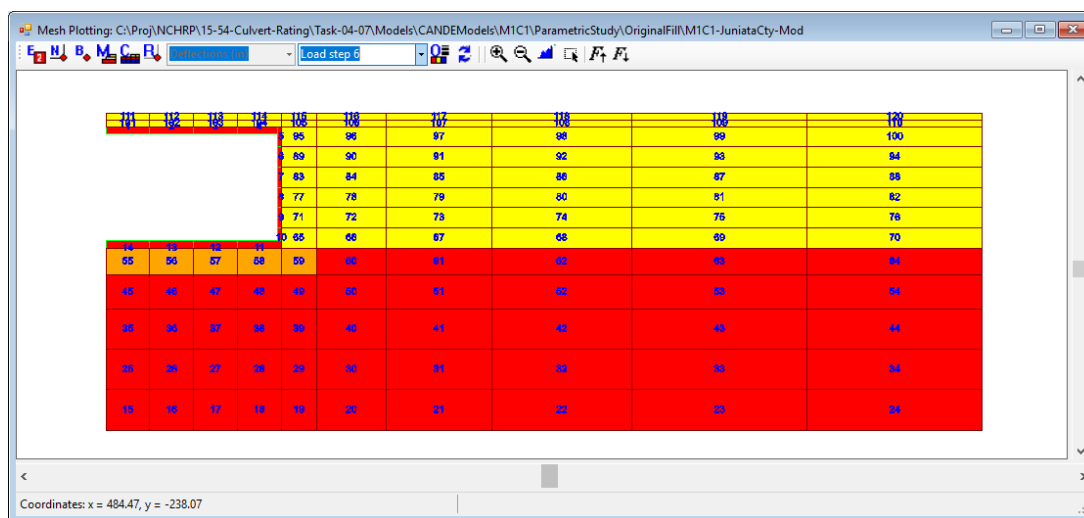


Figure 30 – Level 2 Plot of Model 1 - Candidate 1

Step 2 – Generate the level 3 model from the level 2 model

To facilitate a useful model for this project, the CANDE Tool Box converts a level 2 model into a level 3 model so that it can be analyzed for live load. For a full definition of level 3 models, refer to the CANDE User Manual. In general, level 3 models in CANDE are more complex, fully defined FEM models. They are more difficult to generate (many often with an external mesh generator), so providing an option to generate them from a simpler level 2 input is a helpful enhancement for the user. The level 3 model generated can then be used for non-symmetrical loading (such as live loading). See Figure 31 below.

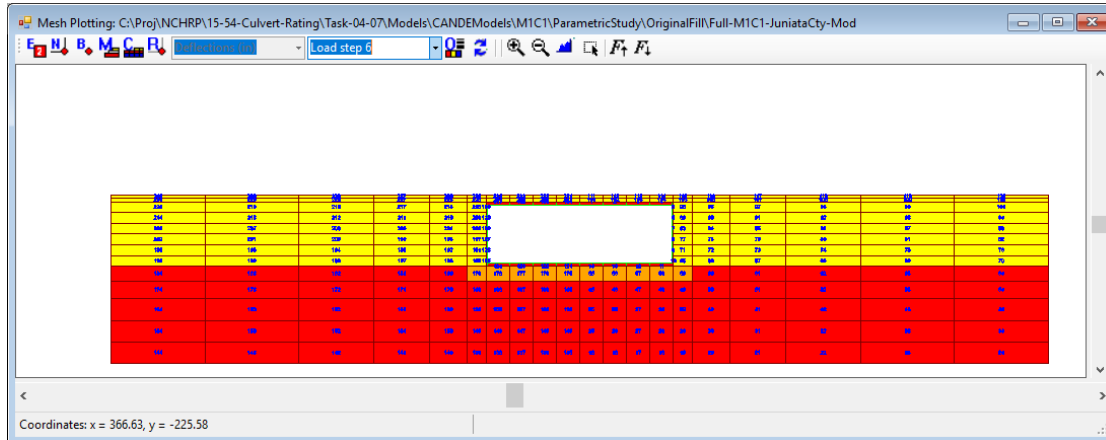


Figure 31 – CANDE Level 2 Model After Conversion to a Level 3 Model

Step 3 – Create a more refined mesh using the CANDE UI tools

Some tools have been added to the CANDE UI that facilitate the generation of CANDE mesh elements for dividing the generated CANDE mesh from Step 2, into a less-coarse mesh. The new options are shown in Figure 32. These options along with the CANDE Tool Box are project deliverables.

model. Once the analysis is performed, the results can be post-processed using the CANDE Tool Box to produce a rating factor. A sample of the CANDE rating factor table output is shown in Figure 35. Full rating tables for each member of the culvert are also available.

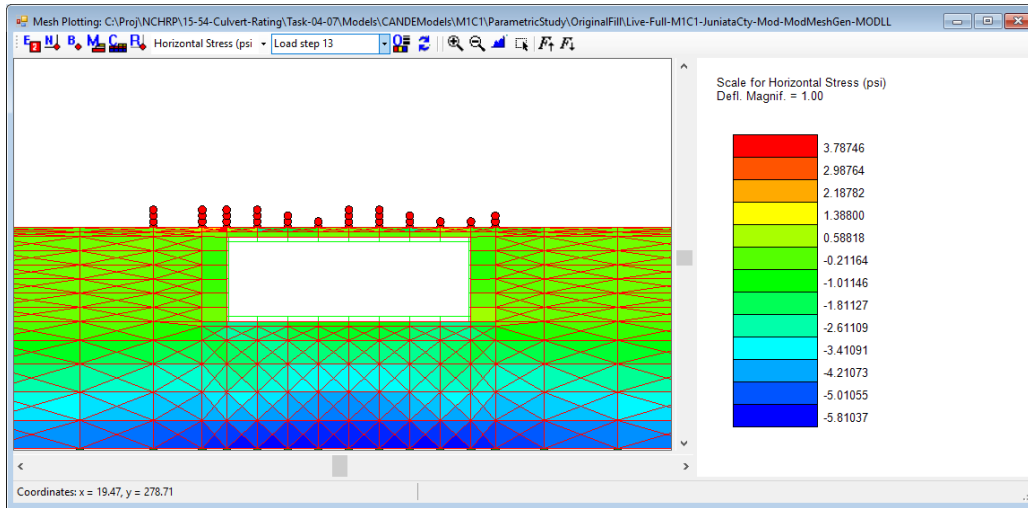


Figure 34 – Simulating a Live Load Vehicle in CANDE

LOWEST RATING FACTORS PER DESIGN CRITERION AT CONTROLLING LOAD STEP AND NODE:

DESIGN-CRITERION (Strength)	LOAD STEP	LOCAL NODE	DEAD-LOAD DEMAND	LIVE-LOAD DEMAND	EFFECTIVE CAPACITY	*RATING FACTOR
*STEEL YIELDING (psi)	15	24	9363.94	31754.14	54000.00	1.41
*CONCRETE CRUSHING (psi)	15	24	1037.81	1790.06	3750.00	1.52
*SHEAR FAILURE (lbs/in)	19	4	301.22	714.65	1330.70	1.44
*RADIAL-TENSION FAIL (psi)	18	2	0.00	0.05	61.10	1222.00

Figure 35 – Sample CANDE Tool Box Rating Output

Step 5 – Check the same model for varying fill depths

The same model can be used with varying fill depths. The current model has a fill depth of 0.97 feet. Additional models of 2', 5', and 10' were also generated. A model with the 5' fill depth is shown in Figure 36.

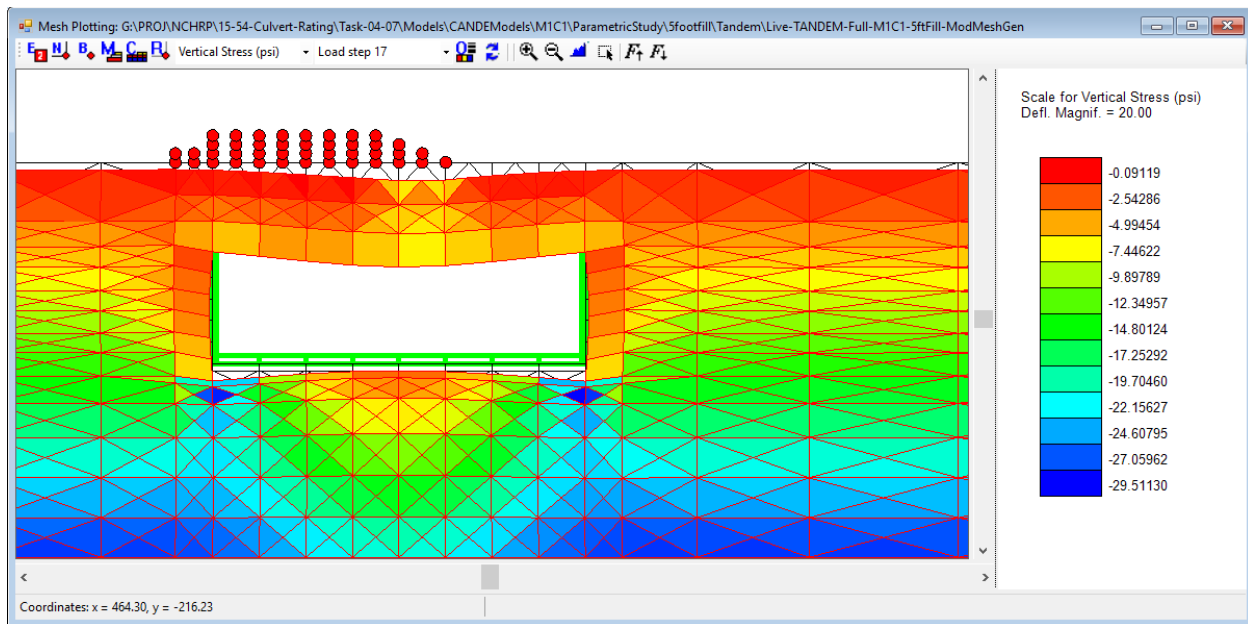


Figure 36 – Model with 5' Fill Depth

Step 6 – Modify the model to include pavement elements

The CANDE Tool Box has the capability to add pavement elements to the model, so that the same model can be analyzed with and without the effects of the pavement. Each model was tested using this option.

In general, this process was used to help develop the CANDE models that represent the culverts that were field tested for this project. A more detailed description of the models and the backup for the development is provided in Chapter 3 and Appendix D of this report.

BrDR Regression Testing and Data Mining

The BrDR software provides the capability to produce data in a form that can be used for regression testing. For the purposes of this research, that regression testing was used primarily to view data for the same culvert with respect to fill depth changes and with respect to changes in the specification. Each regression test utility file (RTU) produced by BrDR contains data in a form that can be imported in a relational database and analyzed with respect to a revised subsequent version of the software. This allowed the RT to compare the current specification articles with the articles proposed as a result of this research.

In the BrDR RTU files, report IDs are used to identify each piece of output produced by the BrDR engine (spec output and analysis output). This is based on the NCHRP 12-50 process (Michael Baker Jr., Inc., Bridgetech, Inc., Modjeski and Masters, Inc., and Paul D. Thompson. *NCHRP Report 485: Bridge Software—Validation Guidelines and Examples*. Transportation Research Board of the National Academies, Washington, D.C., 2003.). BrDR report IDs used in the BrDR RTU were examined and additional report IDs were added. In addition, some inconsistencies in labeling the RTU records for culverts were discovered and reported. These were addressed for the next release of BrDR (6.8.3).

The regression database was reviewed and a data mining option was added to the regression testing tool (see Figure 37). Using the regression database, critical rating factors for shear and moment were queried and results for other report IDs (capacity, loads, spec results, etc.) can be obtained at the same locations. This enabled the RT to extract critical data for multiple culverts at varying fill depths at critical moment and shear rating locations. The results of the data mining are depicted graphically in Figure 38.

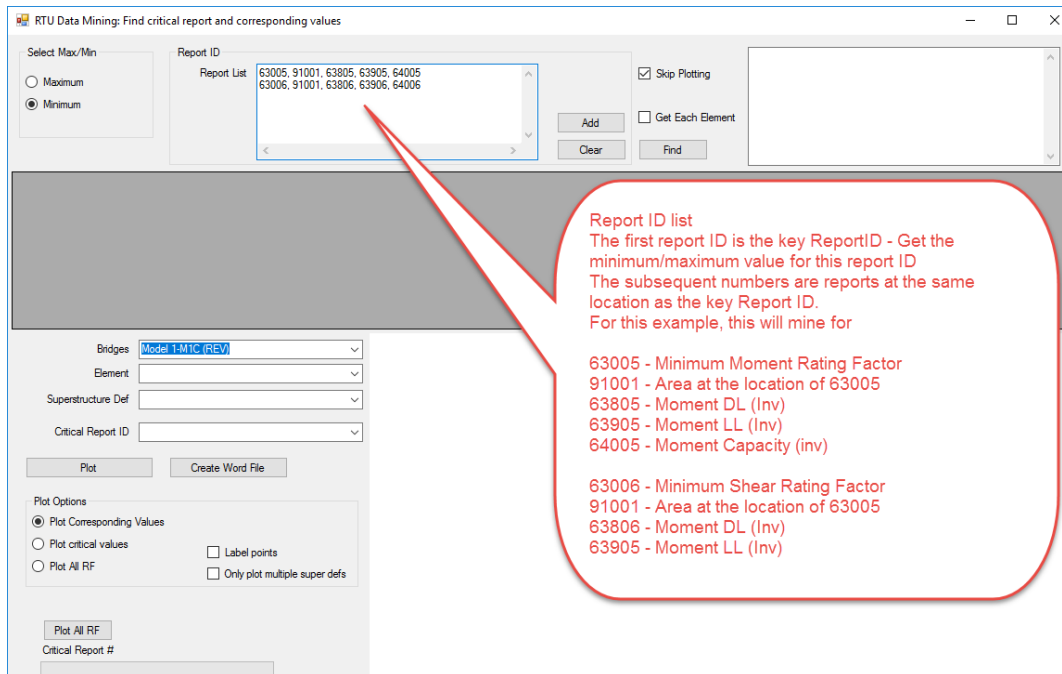


Figure 37 – Getting Critical Rating Information from the BrDR Regression Data

In addition, extraction of the RTU data allowed for the review of the effects on specifications before and after recommendations. A simple data mining function was added to the regression test utility that allows for data to be presented in different forms (e.g. find the minimum rating factor and corresponding values related to that factor; DL, LL, Capacity). A rudimentary interface for the data mining tool is shown in. An example of the graphs that can be produced with the tool is provided in Figure 38. The figure displays the rating results of one of the Caltrans culvert models at different fill depths (right vertical axis), against the rating parameters (Capacity, DL, LL) on the left vertical axis. The bottom axis is the fill depth. Using the regression test utility and the regression data generated by BrDR, these graphs can be generated and exported to a Word document for quick review.

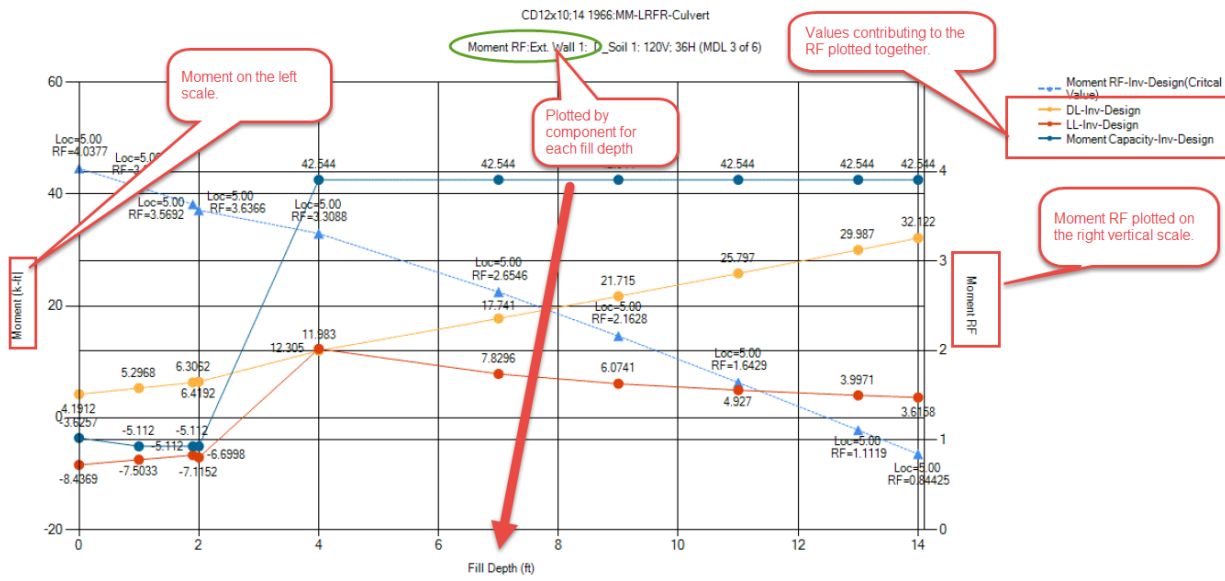


Figure 38 – Data Mining Using the BrDR Regression Tool – Getting Critical Data and Corresponding Values

The RT used BrR models provided by Caltrans during the survey portion of this research and obtained a final set of the culvert models that were used to regression test the specification changes described in Chapters 3 and 4. The regression tool with the data mining option was during this research for helping to identify areas of the specification for potential review. Samples for data mining performed on the Caltrans Double Box culverts are provided in Appendix J.

Development of the 3D Models

A document was developed to establish the parameters and approach to the 3D modeling effort and to achieve agreement among the research team on key aspects of the 3D modeling (See Appendix M). This document was used to develop each of the 3D culvert models summarized in Appendix E. Also included in Appendix E is sample output for the completed 3D models.

CHAPTER 3

Findings and Applications

This chapter summarizes the findings from the literature review, field testing, analysis, and the experiences of the research team and discusses application to practice. The summary of the outcomes of this chapter (specification recommendations) are provided in Chapter 4.

Calibration of the 3D Models

The field testing and portions of the analytical program are closely linked in that the FEA models are an analytical representation of what is being tested in the field.

The models create during phase II were constructed using available information from the contract plans of the structures with consideration of the type of installation and backfill material specified in the contract documents. The initial models developed in phase II were used as a starting point. Any other pertinent information available in the field was included where possible in the modeling effort including pavement type and condition, actual test loading and installed sensor positions, environmental conditions, etc., with the objective of matching the analytical model as closely as possible to the field test conditions.

Summaries of each of the seven field tests are presented in Appendix K. Additional details on the modeling approach taken in the development of Model 7 are also provided in that appendix due to the complexities involved in the modeling of the corrugations of a metal culvert. Model 7 is also unique in that this was the only culvert where the RT was able to model the culvert both before and after paving as this model was under construction during these tests.

In reviewing the results presented in Appendix K, it should be noted that deflection measurements capture the total response of the soil-structure system, while strains measurements capture thrusts and moments. Deflection and strain measurements were compared to computer model predictions to assess the accuracy of the model. The research team adjusted the models based on this comparison. A complete match of model to field data is often difficult with buried structures as many material properties cannot be as accurately characterized as in the case of above ground bridges. As such, the research team looked for significant deviations from expected results that indicate unanticipated behavior.

The calibration effort involved the development of the 3D models in LUSAS and applying loading conditions to match the applied experimental loads used in the field testing of each of the culverts. The strains and deflection data obtained in the field is offloaded from the data acquisition system and imported into spreadsheet form for further processing. This processing involves a review of the data, averaging raw strain and deflection values to remove “noise” and formatting the data to appear in a more readily understood form (labeling, etc.) This data is then combined with the recorded time data taken in the field that represents the time window for each loading condition. Stresses and deflections within each of those time windows are then averaged to generate values to be compared to analytical results from the 3D models.

The first step of the calibration consists of an initial review of the output to see that the deflected shape of the culvert conforms to the expected shape under the applied loading and is also in line with the field-obtained data. If good agreement between the field and analytical data is not observed at the onset, adjustments are made to the models to attempt to achieve better agreement. This includes adjustments to the geometric stiffness which must be approximated in particular for the corrugated metal structures,

material stiffness for concrete structures where the compressive strength may differ from the target design strength and can also be impacted by cracking. Soil properties are also considered in the adjustments to the model as necessary to complete the calibration. The modeling effort and the calibration methods used for Model 7 (the long span corrugated steel culvert) was documented and details of that calibration are provided in Appendix K. The RT documented notable aspects of the calibration effort for each of the models included in the summary reports of these calibrations.

Summary of Areas of Specification to Review

This section provides a summary and background for the proposed specifications and any background data for the expected effect that those revisions will have. Chapter 4 of the report contains the recommended specification changes based on this research. Appendix H contains the draft specification agenda items –

Effects of Subgrade on Rating

The effects of using the modulus of subgrade reaction to model the foundation support under box culverts are discussed in this section. Three different subgrade soils will be used for comparison purpose. The culverts were analyzed using AASHTOWare BrDR using a variety of fill depths. The models used were the field tested RC box models and a couple of the models provided by Caltrans. Each model was analyzed in BrDR; once without considering spring support and additional runs considering spring supports with different subgrade moduli (see Figure 39).

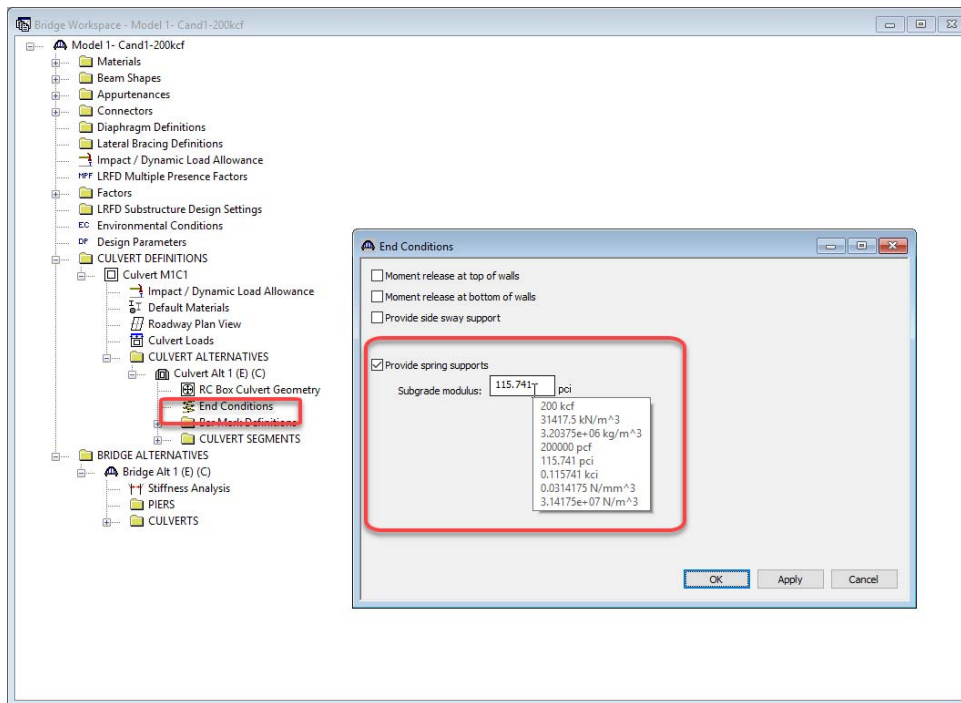


Figure 39 – BrDR Input Window for Spring Constants

Design of box culverts in BrDR typically applies vertical loads as uniform pressures. This approach ignores the effects of soil-culvert interaction which produces a beneficial redistribution of load with pressure peak over the sidewalls and reduced pressure at midspan. This is demonstrated in Figure 40 taken from the CANDE program.

The higher soil strains near midspan produce shear stresses in the soil that transfer load toward the corners of the box section. This reduces the moments. BrDR can reproduce this effect by the use of springs under the bottom slab that simulate soil-culvert interaction. The effect is significant in the bottom slab at all depths of fill and in the top slab at deep fills. The moments in the top slab of shallow culverts is dominated by moving vehicle loads and load redistribution cannot be modeled with BrDR. This redistribution suggests areas for improvement in culvert rating:

- Providing guidance for spring stiffnesses when rating with BrDR or other box culvert programs that support spring stiffeners. Stiffer foundation soils will result in greater redistribution of soil pressure and a more significant reduction in moments and shears.
- For deep culverts, where the top and bottom slabs are subject to the same vertical forces, the bottom slab shear and moment forces, which benefit from the load redistribution, can be considered as governing the top slab as well if the geometry and reinforcement are the same in the top and bottom of the culvert.

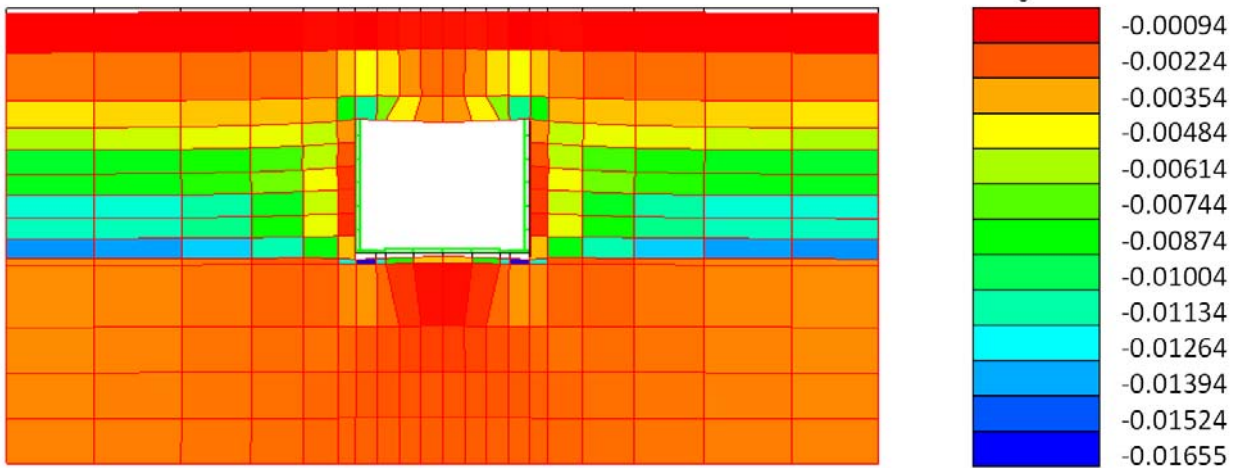


Figure 40 – Vertical Soil Strain (in./in.) on Concrete Box Section

The benefits of using springs is demonstrated in the form of rating factors from BrDR based on the analyses listed in Table 3.

Table 3 – Description of Models Analyzed in BrDR Along with Soil Models for Spring Constants

Model	Description	Modulus of Subgrade Re
Model 1 – NCHRP 15-54 field tested model	Single Cell Culvert: 25' span 7.5' height Various Fill Depths	100 kcf (Clayey soil $q_u < 4$ ksf) 200 kcf (Medium Dense Sand) 400 kcf (Clayey Soil, $q_u > 8$ ksf)
Model 2 – NCHRP 15-54 field tested model	Twin Cell Culvert 2-10' spans 7' height Various fill depths	100 kcf (Clayey soil $q_u < 4$ ksf) 200 kcf (Medium Dense Sand) 400 kcf (Clayey Soil, $q_u > 8$ ksf)
Model 3 – NCHRP 15-54 field tested model	Single Cell Culvert 12' span 6' height	100 kcf (Clayey soil $q_u < 4$ ksf) 200 kcf (Medium Dense Sand) 400 kcf (Clayey Soil, $q_u > 8$ ksf)
CS16x12;0 1922 EAE-200kcf Caltrans Model (y. 1922)	Single Cell Culvert 16' span 12' height	200 kcf (Medium Dense Sand)
CS12x8;10 1952-Rev-200KCF Caltrans Model (y. 1952)	Single Cell Culvert 12' span 8' height	200 kcf (Medium Dense Sand)

The rating factors for varying fill depths are provided in the following tables and figures. Table 4 provides an inventory/operating rating factor comparison for LRFR with an HL93 vehicle in a model with no foundation springs and a model with a 100 kcf subgrade modulus. Table 5 provides a similar comparison for 200 kcf subgrade modulus and Table 6 with a 400 kcf subgrade modulus. Figure 42 through Figure 46

provide comparative plots of the HL93 inventory ratings for 200 kcf springs/no-springs. As expected, the benefit of the springs is minimal for depths of cover less than 2 ft and increasingly more significant as the depth increases and is greater with stiffer subgrade soils. The benefit due to the use of springs is not as evident in Model 2, a two-cell culvert, due to the presence of the center wall which reduces deflection of the slab and the subsequent redistribution of load. The recommendations for the agenda item related to this are provided in Chapter 4 of this report. The agenda item is provided in Appendix H.

It should be noted that a decrease in the rating factor occurs as the fill depth increases for some of the culvert models. An example is the Model 1 RF in Table 4 (highlighted) which for inventory (with 100 kcf springs) decreases from 1.376 to 0.816 when the fill depth changes from 5 feet to 7 feet. The operating rating factor also decreases in the same range from 1.793 to 1.058.

Looking closely at the rating differences between the 5' and 7' layer for the 100 kcf springs indicates that the DL is increasing at a faster rate than the LL is decreasing. The plot in Figure 41 below shows the plot of the regression data produced by BrDR where the DL, LL, and Capacity changes as the fill increases for the Model 1 culvert with springs. A similar plot occurs (not pictured) for the case without springs. The rating factor (RF) is also plotted. From this graph, the rating factors are calculated as follows (all units in kip-feet).

$$\begin{aligned} \text{At 5' fill} & \quad \text{RF} = (56.593 - 35.31)/15.472 = 1.376 \\ \text{At 7' fill} & \quad \text{RF} = (56.855 - 47.037)/12.029 = 0.816 \end{aligned}$$

As the graph illustrates, the dead load is about 62% of the capacity at 5 feet of fill and about 84% of the capacity at 7 feet of fill. At the same time the live load is about 27% of the capacity at 5 feet of fill and only decreases to 21% at 7 feet of fill.

It should also be noted that for Model 2, the springs will have little effect. This is a shallow culvert where live load effects dominate the rating factor in the upper half of the culvert.

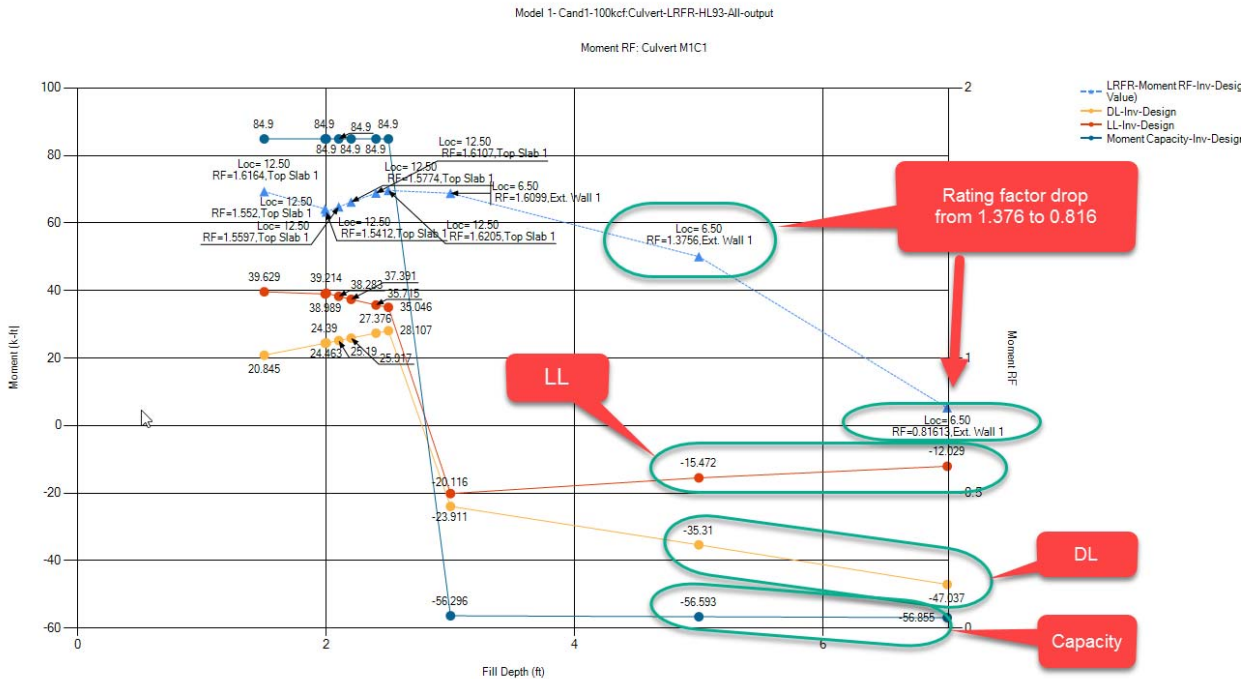


Figure 41 – Rating Results Moment (left vertical axis), Rating (right vertical axis) vs. Fill Depth

Table 4 – Rating Factors – Models 1,2,3 – No Springs vs. 100 kcf

Fill Depth (ft)	Vehicle	HL93-Inv-NoSprings	HL93-Op-NoSprings	HL93-Inv-100 kcf Springs	HL93-Op-100kcf Springs	Inv-Ratio*	Op-Ratio*
Model 1							
1.5	HL-93 (US)	0.8	1.038	0.802	1.04	0.998	0.998
1.99	HL-93 (US)	0.733	0.95	0.739	0.957	0.992	0.993
2	HL-93 (US)	1.47	1.905	1.541	1.998	0.954	0.953
2.1	HL-93 (US)	1.486	1.927	1.56	2.022	0.953	0.953
2.2	HL-93 (US)	1.502	1.947	1.577	2.045	0.952	0.952
2.4	HL-93 (US)	1.531	1.984	1.611	2.088	0.950	0.950
2.5	HL-93 (US)	1.538	1.994	1.621	2.101	0.949	0.949
3	HL-93 (US)	1.509	1.956	1.61	2.087	0.937	0.937
5	HL-93 (US)	1.147	1.487	1.376	1.783	0.834	0.834
7	HL-93 (US)	0.395	0.512	0.816	1.058	0.484	0.484
Model 2							
1.5	HL-93 (US)	0.791	1.026	0.782	1.014	1.012	1.012
1.9	HL-93 (US)	0.8	1.037	0.783	1.015	1.022	1.022
2	HL-93 (US)	1.524	1.976	1.541	1.998	0.989	0.989
2.5	HL-93 (US)	1.712	2.22	1.717	2.225	0.997	0.998
3	HL-93 (US)	1.92	2.489	1.925	2.495	0.997	0.998
3.5	HL-93 (US)	2.148	2.784	2.152	2.789	0.998	0.998
4	HL-93 (US)	2.335	3.027	2.339	3.032	0.998	0.998
7	HL-93 (US)	3.271	4.24	3.19	4.136	1.025	1.025
10	HL-93 (US)	2.738	3.55	2.671	3.462	1.025	1.025
Model 3							
1.5	HL-93 (US)	1.452	1.882	1.461	1.894	0.994	0.994
1.9	HL-93 (US)	1.452	1.882	1.461	1.894	0.994	0.994
2	HL-93 (US)	1.414	1.833	1.423	1.845	0.994	0.993
2.5	HL-93 (US)	1.547	2.006	1.558	2.019	0.993	0.994
3	HL-93 (US)	1.7	2.204	1.713	2.22	0.992	0.993
3.5	HL-93 (US)	1.811	2.347	1.841	2.386	0.984	0.984
4	HL-93 (US)	1.823	2.363	1.943	2.519	0.938	0.938
7	HL-93 (US)	1.627	2.11	1.859	2.41	0.875	0.876
10	HL-93 (US)	0.841	1.09	1.206	1.564	0.697	0.697

*the ratios indicate the no spring model RF divided by the spring model rating factor. A value less than 1.0 indicates a higher RF for the spring model.

Table 5 – Rating Factors – Models 1,2,3 – Caltrans Models – No Springs vs. 200 kcf

Fill Depth (ft)	Vehicle	HL93-Inv-NoSprings	HL93-Op-NoSprings	HL93-Inv-200 kcf Springs	HL93-Op-200 kcf Springs	Inv-Ratio*	Op-Ratio*
Model 1							
1.5	HL-93 (US)	0.8	1.038	0.803	1.041	0.996	0.997
1.99	HL-93 (US)	0.733	0.95	0.739	0.958	0.992	0.992
2	HL-93 (US)	1.47	1.905	1.573	2.039	0.935	0.934
2.1	HL-93 (US)	1.486	1.927	1.593	2.064	0.933	0.934
2.2	HL-93 (US)	1.502	1.947	1.611	2.089	0.932	0.932
2.4	HL-93 (US)	1.531	1.984	1.646	2.134	0.930	0.930
2.5	HL-93 (US)	1.538	1.994	1.657	2.148	0.928	0.928
3	HL-93 (US)	1.509	1.956	1.655	2.146	0.912	0.911
5	HL-93 (US)	1.147	1.487	1.438	1.864	0.798	0.798
7	HL-93 (US)	0.395	0.512	0.9	1.167	0.439	0.439
Model 2							
1.5	HL-93 (US)	0.791	1.026	0.783	1.015	1.010	1.011
1.9	HL-93 (US)	0.8	1.037	0.785	1.017	1.019	1.020
2	HL-93 (US)	1.524	1.976	1.54	1.996	0.990	0.990
2.5	HL-93 (US)	1.712	2.22	1.729	2.241	0.990	0.991
3	HL-93 (US)	1.92	2.489	1.939	2.514	0.990	0.990
3.5	HL-93 (US)	2.148	2.784	2.169	2.811	0.990	0.990
4	HL-93 (US)	2.335	3.027	2.357	3.055	0.991	0.991
7	HL-93 (US)	3.271	4.24	3.288	4.263	0.995	0.995
10	HL-93 (US)	2.738	3.55	2.861	3.708	0.957	0.957
Model 3							
1.5	HL-93 (US)	1.452	1.882	1.469	1.904	0.988	0.988
1.9	HL-93 (US)	1.452	1.882	1.469	1.904	0.988	0.988
2	HL-93 (US)	1.414	1.833	1.431	1.855	0.988	0.988
2.5	HL-93 (US)	1.547	2.006	1.567	2.031	0.987	0.987
3	HL-93 (US)	1.7	2.204	1.723	2.233	0.986	0.987
3.5	HL-93 (US)	1.811	2.347	1.852	2.401	0.977	0.977
4	HL-93 (US)	1.823	2.363	1.956	2.535	0.932	0.932
7	HL-93 (US)	1.627	2.11	2.128	2.758	0.764	0.765
10	HL-93 (US)	0.841	1.09	1.631	2.114	0.515	0.515
CS16x12;0 1922 EAE-200kcf							
1.5	HL-93 (US)	0.559	0.725	0.695	0.901	0.804	0.805
1.9	HL-93 (US)	0.512	0.664	0.662	0.858	0.773	0.774
2	HL-93 (US)	0.496	0.643	0.649	0.841	0.764	0.765
2.5	HL-93 (US)	0.52	0.674	0.675	0.874	0.770	0.771

Fill Depth (ft)	Vehicle	HL93-Inv-NoSprings	HL93-Op-NoSprings	HL93-Inv-200 kcf Springs	HL93-Op-200 kcf Springs	Inv-Ratio*	Op-Ratio*
3	HL-93 (US)	0.514	0.666	0.693	0.898	0.742	0.742
3.5	HL-93 (US)	0.439	0.569	0.682	0.884	0.644	0.644
4	HL-93 (US)	0.35	0.454	0.661	0.857	0.529	0.529
CS12x8;10 1952-Rev-200KCF							
1.5	HL-93 (US)	0.923	1.197	0.911	1.18	1.013	1.014
1.9	HL-93 (US)	0.905	1.173	0.899	1.165	1.006	1.007
2	HL-93 (US)	1.027	1.332	1.08	1.401	0.951	0.951
3	HL-93 (US)	1.243	1.611	1.267	1.643	0.981	0.981
4	HL-93 (US)	1.315	1.705	1.396	1.809	0.942	0.942
7	HL-93 (US)	1.204	1.56	1.481	1.92	0.813	0.813
10	HL-93 (US)	0.363	0.471	0.609	0.789	0.596	0.597

*the ratios indicate the no spring model RF divided by the spring model rating factor. A value less than 1.0 indicates a higher RF for the spring model.

Table 6 – Rating Factors – Models 1,2,3 – No Springs vs. 400 kcf

Fill Depth (ft)	Vehicle	HL93-Inv No Springs	HL93-Op-No Springs	HL93-Inv 400 kcf Springs	HL93-Op 400 kcf Springs	Inv-Ratio*	Op-Ratio*
Model 1							
1.5	HL-93 (US)	0.8	1.038	0.804	1.042	0.995025	0.996161
1.99	HL-93 (US)	0.733	0.95	0.74	0.959	0.990541	0.990615
2	HL-93 (US)	1.47	1.905	1.604	2.08	0.916459	0.915865
2.1	HL-93 (US)	1.486	1.927	1.625	2.106	0.914462	0.915005
2.2	HL-93 (US)	1.502	1.947	1.644	2.131	0.913625	0.913656
2.4	HL-93 (US)	1.531	1.984	1.681	2.179	0.910767	0.910509
2.5	HL-93 (US)	1.538	1.994	1.693	2.194	0.908447	0.908842
3	HL-93 (US)	1.509	1.956	1.701	2.205	0.887125	0.887075
5	HL-93 (US)	1.147	1.487	1.5	1.944	0.764667	0.764918
7	HL-93 (US)	0.395	0.512	0.983	1.274	0.401831	0.401884
Model 2							
1.5	HL-93 (US)	0.791	1.026	0.784	1.016	1.008929	1.009843
1.9	HL-93 (US)	0.8	1.037	0.787	1.021	1.016518	1.015671
2	HL-93 (US)	1.524	1.976	1.551	2.011	0.982592	0.982596
2.5	HL-93 (US)	1.712	2.22	1.745	2.262	0.981089	0.981432
3	HL-93 (US)	1.92	2.489	1.958	2.538	0.980592	0.980693
3.5	HL-93 (US)	2.148	2.784	2.19	2.839	0.980822	0.980627
4	HL-93 (US)	2.335	3.027	2.384	3.09	0.979446	0.979612
7	HL-93 (US)	3.271	4.24	3.419	4.433	0.956712	0.956463
10	HL-93 (US)	2.738	3.55	3.241	4.201	0.844801	0.845037
Model 3							
1.5	HL-93 (US)	1.452	1.882	1.482	1.921	0.979757	0.979698
1.9	HL-93 (US)	1.452	1.882	1.482	1.921	0.979757	0.979698
2	HL-93 (US)	1.414	1.833	1.444	1.872	0.979224	0.979167
2.5	HL-93 (US)	1.547	2.006	1.582	2.05	0.977876	0.978537
3	HL-93 (US)	1.7	2.204	1.74	2.256	0.977011	0.97695
3.5	HL-93 (US)	1.811	2.347	1.872	2.427	0.967415	0.967037
4	HL-93 (US)	1.823	2.363	1.979	2.565	0.921172	0.921248
7	HL-93 (US)	1.627	2.11	2.51	3.254	0.648207	0.648433
10	HL-93 (US)	0.841	1.09	2.254	2.922	0.373114	0.373032

*the ratios indicate the no spring model RF divided by the spring model rating factor. A value less than 1.0 indicates a higher RF for the spring model.

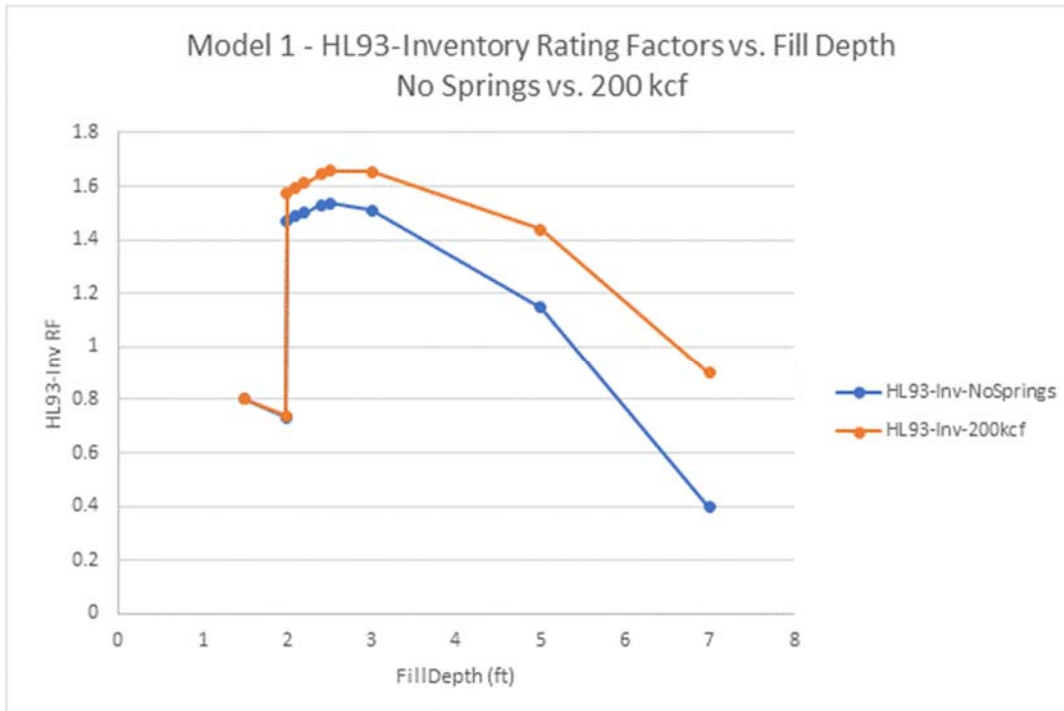


Figure 42 – Model 1 – HL93-Inventory Rating Factors vs. Fill Depth – No Spring vs. 200 kcf

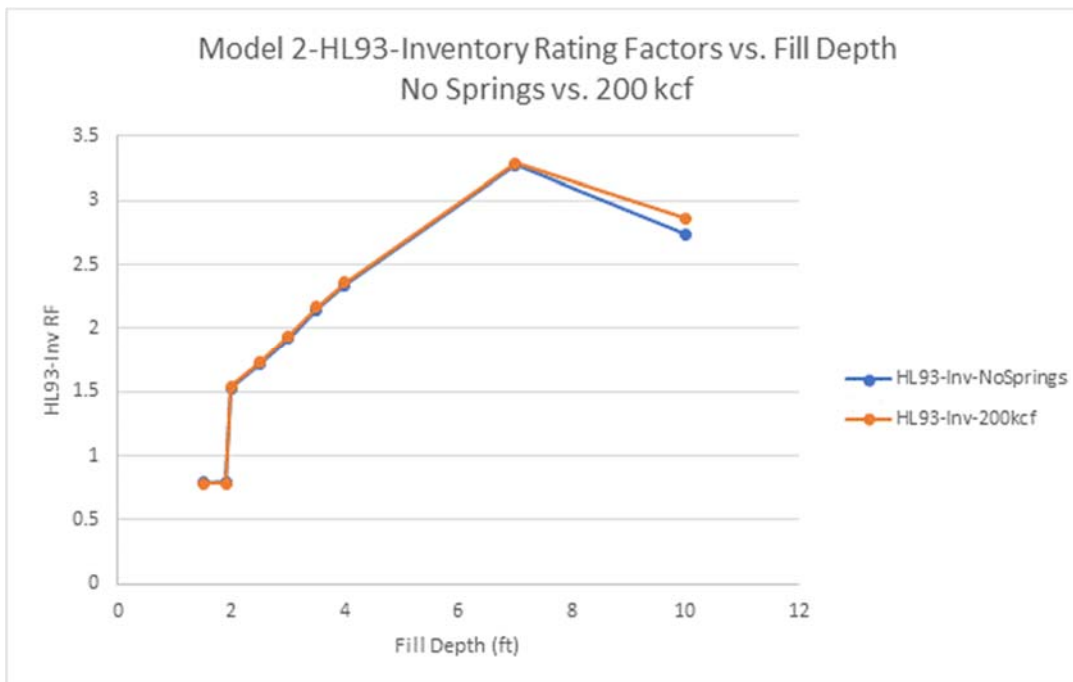


Figure 43 – Model 2 – HL93-Inventory Rating Factors vs. Fill Depth – No Spring vs. 200 kcf

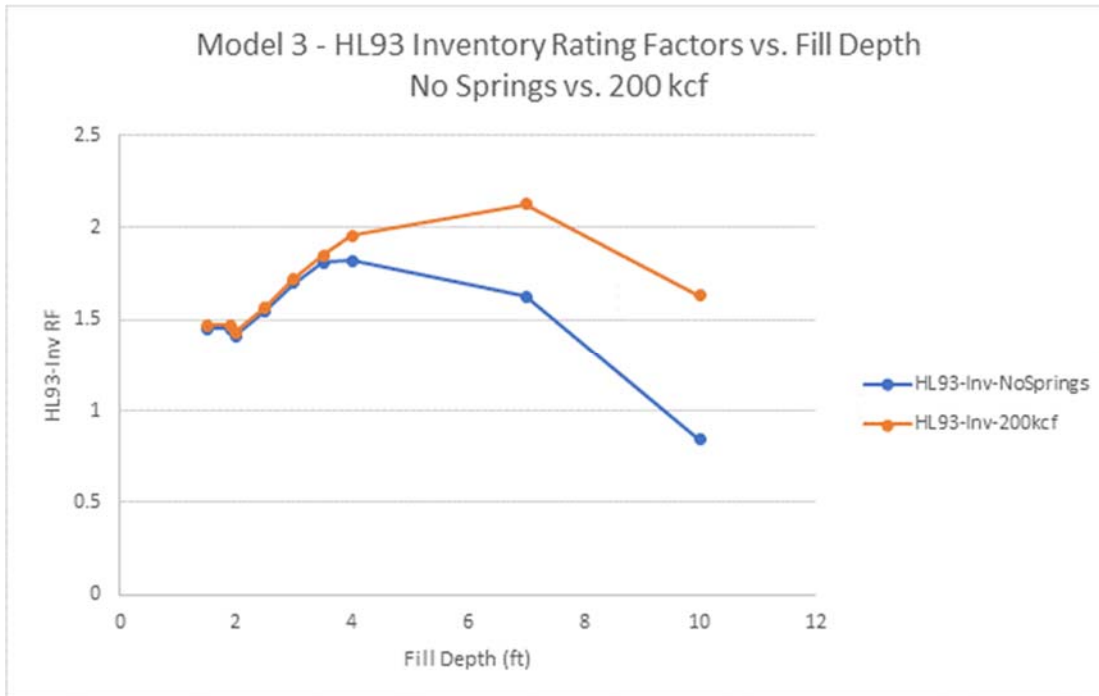


Figure 44 – Model 3 – HL93-Inventory Rating Factors vs. Fill Depth – No Spring vs. 200 kcf

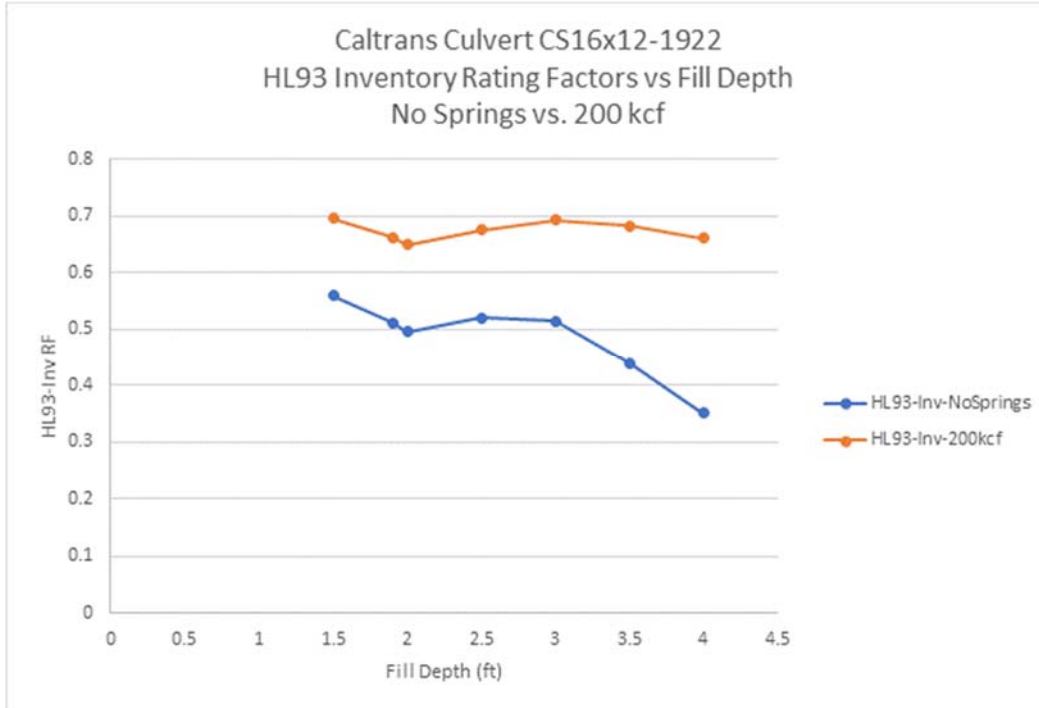


Figure 45–Caltrans-CS16x12-1922 – HL93-Inventory Rating Factors vs. Fill Depth – No Spring vs. 200 kcf

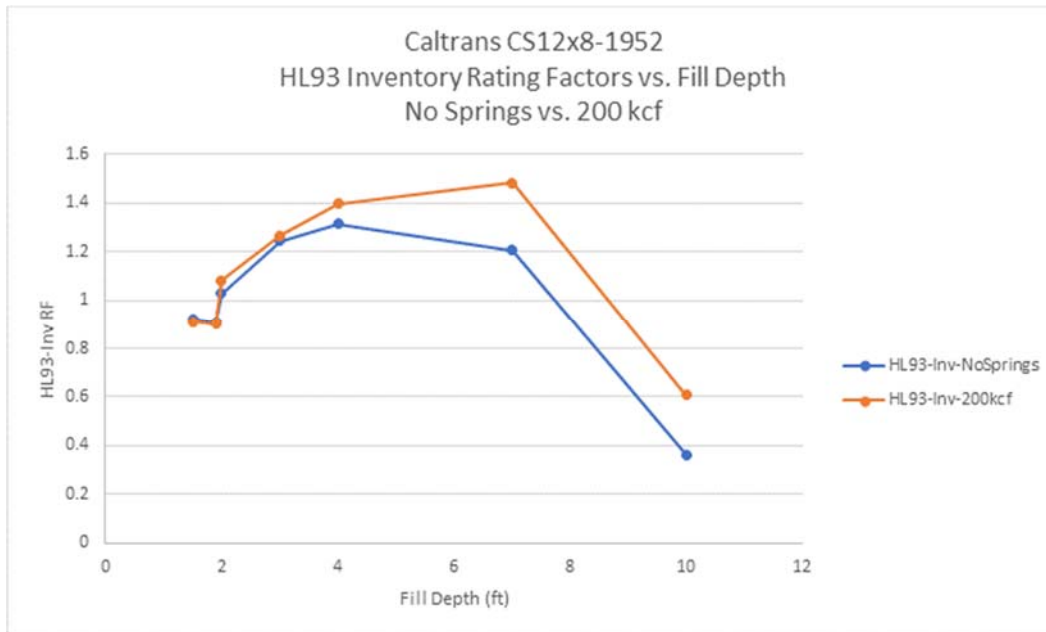


Figure 46 – Caltrans CS12x8-1952– HL93-Inventory Rating Factors vs. Fill Depth – No Spring vs. 200 kcf

Design-Analysis

Much of the Design-Analysis guidance was based on results presented in the following paragraphs. The conclusion from that study are presented as an agenda item in Appendix H of this report.

In the RT's experience, box culvert computer design programs often make different assumptions in modeling and designing box sections. This can result in unnecessarily conservative designs/ratings if the assumptions do not address actual behavior and in varying rating strengths relative to design strengths if different programs are used for design and rating. If a less conservative program is used for rating, the capacity will be underestimated and could result in rating factors less than one for good culverts.

Analysis/Design decisions that can affect load rating include:

- the stiffness effect of haunches,
- the change in critical design locations resulting from haunches,
- reduction of reinforcement tension by compressive thrust, and
- load redistribution due to culvert and soil stiffness.

This review evaluates design and analysis options in three computer programs and how those options can affect box culvert load ratings.

- **BOXCAR** – BOXCAR V3.2 designs box sections in accordance with current AASHTO LRFD Specifications. BOXCAR, or its predecessors has been used to develop all of the standard designs for precast concrete box sections in ASTM and AASHTO product specifications. Analysis in BOXCAR is completed with an elastic frame model. BOXCAR does not rate culverts but produces output that is sufficient for rating.
- **CANDE** – CANDE is a finite element program developed to analyze and design all types of culverts. CANDE was developed by FHWA for the purpose of completing soil-structure interaction models of culverts. CANDE incorporates non-linear models for steel, reinforced concrete and embedment soils.
- **BrDR** – BrDR is the AASHTO software for designing and rating bridges. BrDR includes a module for the design and analysis of buried culverts.

An analysis was performed on a 10 ft span by 10 ft rise culvert with geometry based on a 1962 Caltrans design, as presented in Table 7. This geometry demonstrates the features of concern in comparing programs.

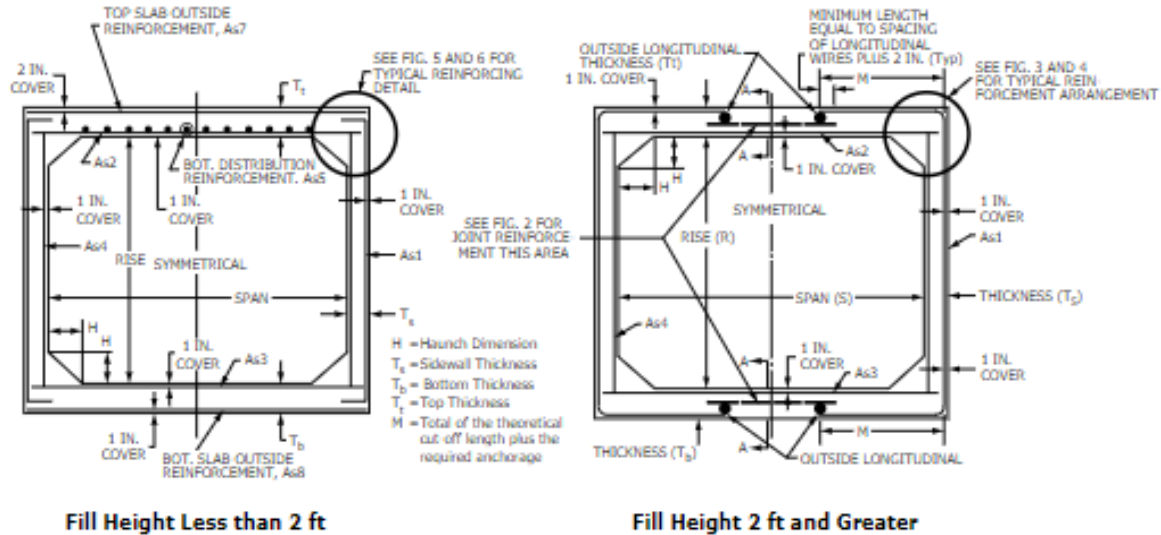
Table 7 - Box Study Culvert Geometry

Parameter		Cover over reinforcement	
Span (ft)	10	All inside reinforcement (in)	1.5
Rise (ft)	10	Top outside (in)	2.0
Top slab thickness (in)	9.5	Side outside (in)	1.5
Bottom slab thickness (in)	10	Bottom outside ((in)	3.0
Wall thickness (in)	11	Material strengths	
Vertical haunch (in)	0, 10	Reinforcement yield stress (ksi)	60.0
Horizontal haunch (in)	0, 10	Concrete design strength (ksi)	4.0

Some evaluations were conducted in design mode to generate required reinforcing areas (BOXCAR) while others were conducted in evaluation mode to determine design forces and/or ratings. In all cases, the

reinforcing layouts consisted of u-shaped outside reinforcement extending into and lapping at the center of the top and bottom slabs and straight bars for inside reinforcement.

The culvert was subjected to earth loads using a soil density of 120 pcf. Live load was HL-93 for BOXCAR and BrDr, but just the design tandem for CANDE (i.e. 2-25kip axles spaced at 4'). Figure 47 shown below is taken from ASTM C1433 for precast reinforced concrete box sections. The diagram for Fill Height 2 ft and Greater shows the reinforcement layout, except for our modeling we extended the U bars to the center of the slab to avoid numerical issues in CANDE.



BOXCAR - The culvert was analyzed at depths of 0.0, 2.0, 8.0, and 12.0 feet. Reinforcement and shear capacities are presented in Table 8 and Table 9.

Table 8 – BOXCAR Reinforcement (in²/ft)

Depth (ft)	0.0	2.00	8.0	8.0 No LL	12.0	12.0 No LL	12.0 No Thrust
With Haunches							
Outside	0.264	0.264	0.264	0.264	0.280	0.264	0.420
Top inside	0.427	0.411	0.352	0.253	0.450	0.389	0.493
Bottom inside	0.355	0.389	0.379	0.278	0.478	0.416	0.538
Without Haunches							
Outside	0.323	0.486	0.637	-	-	-	-
Top inside	0.459	0.450	0.389	-	-	-	-
Bottom inside	0.397	0.440	0.447	-	-	-	-

Notes:

- Outside reinforcement in the section with haunches is always controlled in the sidewall and is minimum required reinforcement to depths through 8 ft.
- Outside reinforcement in the box without haunches is always controlled in the top slab.
- At a depth of 8.0 ft the outside reinforcement in the section without haunches is controlled by cracking which is not a required check for rating.

Table 9 – BOXCAR Shear Loads (Fraction of capacity)

Depth (ft)	0.0	2.00	8.0	8.0 No LL	12.0	12.0 No LL
With Haunches						
Top slab	1.01	0.91	0.52	0.40	0.66	0.60
Bottom slab	0.77	0.84	0.66	0.54	0.82	0.75
Without Haunches						
Top slab	1.13	0.99	0.63	0.49		
Bottom slab	1.04	0.94	0.80	0.66		

Effect of Haunches - The inclusion of haunches results in significantly reduced reinforcement due to the following effects:

- The stiffness effect of haunches increases the negative corner moments and decreases the positive moments.
- Haunches reduce inside and outside reinforcement. The outside reinforcement decreases even though the corner moments increase since the critical design location moves from top slab face of wall to sidewall tip of haunch.

- Design shear forces are reduced as the location of the critical sections moves to a distance “d” from the tip of the haunch.

Design for Shear Capacity -

- Exceeding the shear capacity at zero cover was expected based on the culvert geometry and the concrete strength. At the time this culvert was designed the code allowed slabs that met flexural design requirements to be assumed adequate in shear.
- The change in shear design criteria in the LRFD Specifications results in a significant increase in shear capacity as the fill depth becomes greater than 2.0 ft. At depths less than 2 ft shear is evaluated using the general design method in LRFD Article 5.7.3 while at depths greater than 2 ft the shear strength need is evaluated according to LRFD Article 5.7.12.3, where the β factor need not be taken less than 3.

Live Load Attenuation with Depth

It is common among designers to read the LRFD Specifications as not requiring consideration of live loads for depths greater than 8 ft, although the specifications state “Live load may be neglected when the depth of fill is more than the span length and exceeds the span length; for multiple span culverts the effects may be neglected where the depth of fill exceeds the distance between the inside faces of the end walls.” This requires that as the span increases above 8 ft the depth of fill for live load design increases at the same rate.

- At a depth of 8 ft earth load reinforcement accounts for about 70% of the total reinforcement.
- At a depth of 12 ft earth load reinforcement accounts for about 86% of total reinforcement.

For the box culvert considered above, with 12 ft of cover, the live load would not be considered in design according to the current LRFD Specifications (Depth greater than 8 ft and greater than the span). If considered, the factored live load moment is 15% of the total factored earth moment under typical frame analysis assumptions (i.e. BOXCAR type analysis). The factored dead load moment is 20% greater than the service earth plus live load moments, suggesting a net load factor of about 1.2. While this is less than commonly assumed target values, the project team is unaware of performance issues related to the current design specifications. This is in part due to the small overall live load relative to earth load, but there is additional safety due to the assumption of uniform pressure distribution, as shown elsewhere in this report.

Consideration of Thrust -

- At a depth of 8 ft, required outside reinforcement increases about 10% if the calculation does not include the effect of compressive thrust. The project team recommends that thrust always be considered in design and rating. This produces economy in design without reducing overall safety. We included the analysis with and without thrust as we have seen some computer programs in the past that did not include thrust. We wished to demonstrate the shortcomings of that approach.
- At a depth of 12 ft required outside reinforcement increases about 50% if the calculation does not include the effect of compressive thrust.

CANDE

CANDE is a culvert-soil interaction program. As such, it does not apply loads directly to the culvert, rather it allows the soil and culvert to interact as governed by the material properties and calculates the internal structural forces that result. There are many levels of sophistication in how finite element analyses are conducted. CANDE incorporates non-linear soil and non-linear culvert behavior to allow matching actual in situ behavior as closely as possible.

In this study, CANDE was operated in an analysis mode where reinforcement areas are provided, and the output is the culvert response. For this comparison, the CANDE model incorporated reinforcement that approximated the BOXCAR analysis for 8 ft of fill without live load (see Table 10).

Table 10 – Reinforcement Areas in CANDE Models (in²/ft)

Outside	Top inside	Bottom inside
0.26	0.35	0.35

In situ soil was modeled as a linear elastic soil with a modulus of 5,000 psi while the bedding and backfill were modeled as with non-linear properties representing a sandy gravel without fines compacted to 90% of maximum standard Proctor density.

A key feature of culvert-soil interaction analysis is that the soil pressures on the culvert are not uniform. The culvert slabs deflect at midspan which results in a shift of load toward the corners. This is demonstrated in Figure 48 which shows the soil vertical strains at a depth of 8 ft. The deflection at midspan allows more vertical strain and thus the transfer of load to the corners. This effect varies with the stiffness (soil type and compaction level) of the materials around the culvert and is generally more pronounced in the bottom slab as in situ soils are often quite stiff.

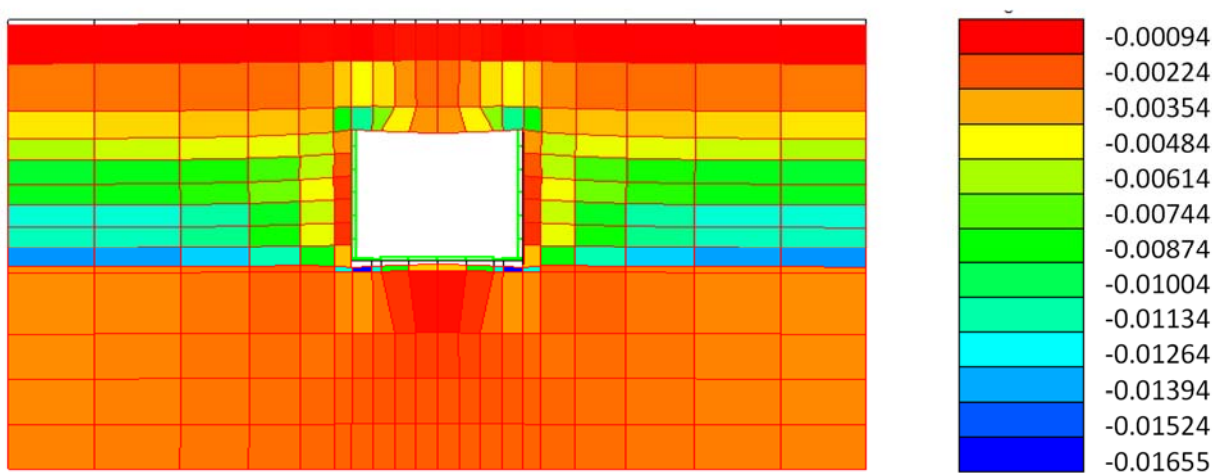


Figure 48 – CANDE Typical Vertical Strain Around Box Section

A first comparison is the design forces calculated in CANDE versus those calculated in BOXCAR (see Table 11).

Table 11 – Comparison of Factored Moments – CANDE vs BOXCAR, 8 Ft Fill (ft-k/ft)

	No Haunch – No LL		No Haunch – LL		Haunch	
	CANDE	BOXCAR	CANDE	BOXCAR	CANDE	BOXCAR
Negative	-12.9	-11.8	-13.9	-14.8	-7.6	-11.9
Top positive	10.0	11.6	12.7	14.0	9.2	10.5
Bottom positive	10.9	14.9	10.8	16.6	10.6	12.8

Note: The controlling moment for negative reinforcement occurs in the slabs for sections without haunches and in the walls for sections with haunches

For the section without haunches, Table 11 shows comparable moments for the negative and top positive moments and substantially lower moment for the bottom positive moment which is a result of the load redistribution discussed above. The positive moments are lower when haunches are added, particularly the negative moments in CANDE due to the load redistribution. BOXCAR shows about the same negative moment with and without haunches; however, the shift of the critical section from the top slab to the sidewall means more compressive thrust and more favorable geometry as the wall is thicker than the top slab and the reinforcing cover is reduced in the sidewall, hence the reduction in reinforcement with haunches shown in Table 7 for BOXCAR. CANDE shows the bottom slab moments to be relatively unchanged with or without haunches and live loading. This is because the soil-structure interaction results in high vertical pressures under the culvert walls and low vertical pressure at midspan.

We recommend that rectangular box section continue to be designed using frame models and uniform pressure assumptions. This offers simplicity of design and has a long history of successful application. For special cases, where rating proves difficult with this approach, finite element analysis offers more accurate modeling of soil-culvert interaction and can reduce the moment and shear forces with the resulting pressure redistributions. Structures designed with finite element analysis should be rated with finite element modeling. CANDE is only one such finite element program but it was developed specifically for culverts and has a load rating function in the latest version developed under this project.

BrDr

AASHTOWare BrDR was used to rate the culvert at depths of 0 ft, 2 ft, and 8 ft. At 0 and 2 ft the standard distributed load assumption was used while at 8 ft the standard distribution was compared to spring supports with stiffnesses of 100 and 400 pci. In all cases the reinforcement provided was based on the BOXCAR evaluations at 8 ft of fill. Results are presented in Table 12.

Table 12 – BrDr Inventory Rating Factors

Depth (ft)	Load application	No Haunch	Loc./Limit	With Haunch	Loc./Limit
0	Distributed	0.93	Top/shear	1.14	Top/shear
2	Distributed	1.10	Top/flexure	1.19	Top/flexure
8	Distributed	1.81	Top/flexure	1.88	Bot/flexure
8	Bedding springs, 100 pci	1.86	Top/flexure	2.10	Bot/flexure
8	Bedding springs, 400 pci	1.99	Top/flexure	2.42	Top/flexure

Review of Table 12 in light of the BOXCAR analyses and reinforcement level indicates the following:

- The rating factor at 0.0 ft cover and no haunches of less than 1.0 was expected.
- The rating factors at 2.0 ft cover of just over 1.0 were expected given the reinforcement was based on BOXCAR analysis at 8 ft.
- Introducing haunches improves the rating factor.
- The introduction of spring support for the bedding reaction increases the rating factor as a function of the spring stiffness. At 400 pci in the section with haunches the limiting location shifts back to the top slab. This is consistent with the low forces in the bottom slab in CANDE.

Discussion and Findings

The results presented above confirm some prior knowledge about box section capacity and demonstrates several areas where changes to current design and rating procedures may be made.

Known analysis/design features that should be clearly delineated in the MBE include:

- Haunches should be included in the analysis if present in the actual box section. This includes the stiffness effect of haunches and the change in design locations.
- The effect of compressive thrust in reducing reinforcing requirements can be significant, especially for deeper culverts. This should be considered in design and rating.

A change in live load distribution at 2 ft of fill is a long-standing feature of the AASHTO design specifications related to the change in treatment of the top slab from a bridge deck to a buried slab. While this was mitigated with revisions to the AASHTO Design Specifications in 2000, there is still a slight change. The bridge deck treatment takes advantage of the longitudinal stiffness of the top slab to increase the load distribution provided by the soil. The research team looked at two options for providing a uniform change in load:

- The simple approach of using the deck strip width at depths greater than 2 ft until the distribution width calculated using the soil distribution width is greater.
- Dr. Katona developed another approach based on engineering mechanics (See Appendix I). While the research team found this approach to offer little benefit for new design which requires design only for a single loaded lane with multiple presence factor of 1.2. This approach provides adequate designs for multiple lane conditions. The method proposed by Dr. Katona provides greater distribution widths for single lane loadings but would not result in significant savings or increased ratings as the multiple lane conditions would limit the width that could be used. The method has applications for low volume roads where a rating engineer might consider only a single lane loading as appropriate.

The consideration of culvert-soil interaction in CANDE or spring supports in BrDr improves culvert design and rating. Based on this limited study the effect is greater in CANDE where load redistribution

occurs in both the top and bottom slab. The difficulty in this approach for design is uncertainty about the foundation and backfill stiffness that will be achieved in the field. However, for rating culverts, where construction records and inspection findings can provide guidance on the stiffness of the bedding and backfill, this should be a good tool to help improve ratings.

The BOXCAR models show that the factored live load is about 36% of the total factored load (factored vertical earth plus live load) at a depth of 8 feet, controlled by the design tandem. This percentage continues to decrease with increasing depth of cover. This raises the question of whether rating should be required for culverts under deep fills and if not, at what depths it could be dispensed with. Again, there are two possibilities:

- AASHTO LRFD Specifications do not require consideration of live load if the depth is greater than 8 ft and greater than the span of the culvert. One approach is to accept the current limit not require rating for live load if consideration in design was not required. However, this approach would require longer span culverts to be designed for live load at considerable depths, such as the model 1 culvert in this program, with a 25 ft span.
- This provision requires consideration of live load until the depth exceeds the span; however, in the experience of some members of the research team the provision is often interpreted as ignoring live loads at depths of 8 ft and greater. At a depth of 8 ft, the live load (design tandem) is 36% of the total load and if dropped from design consideration, the net load factor (factored earth load/(service earth plus live load, in psf) is only 1.03. This low factor of safety likely occurred in part because the provision was developed under the Standard Specifications which used $LLDF = 1.75$ resulting in a factored live load of 26% of the factored earth load and a net load factor of 1.14. The proposed provision changes the depth of fill for dropping live load consideration to about 13 ft for the design tandem. At this depth the net load factor when not considering live load is 1.20 and is insensitive to overloaded live load vehicles.

Shear strength of slabs in concrete box culverts is problematic in that many culverts were designed at a time when slabs were assumed adequate in shear if properly designed for flexure yet do not meet current standards for shear strength capacity. In general, these culverts are providing good service. We recommend that rating engineers investigate these culverts and how they are analyzed to determine if a refined approach such as discussed here will show that these culverts can be rated. If that is not possible, we will include a provision in the MBE recommendations that the culvert may be rated at 1.0 for shear strength if inspections show it to be in good condition.

Culvert Load Distribution

The proposed culvert load distribution modifications are shown in Appendix H Agenda Item (Subject: Live Load Distribution for Culverts). The changes are to Article 3.6.1.2.6a and various parts of Article 4.6.2.10. The changes were incorporated into a debug version of BrDR and regression test to determine the overall effects of the change. Since the tire dimensions used for the test were 20" x 10", the primary effects occur at the 2' fill mark where there was a slight increase in the rating factor for the revised change. The results using several of the Caltrans culverts (modified) are shown in Table 13. Culverts with 2 foot of cover show a slight improvement in rating factor and no change at other depths.

Table 13 – Effects on Rating Factors for Changes to LRFR Live Load Distribution in BrDR

Caltrans Culvert Name, Year Built	Fill Depth	Vehicle	Inv Rating Before Change	Op Rating Before Change	Inv Rating After Change	Op Rating After Change	Inv Ratio Before/ After*	Op Ratio Before/ After
CD8x8;10 1924-Rev	1.9 ft Cover	HL-93 (US)	0.579	0.751	0.579	0.751	1	1
CD8x8;10 1924-Rev	2 ft Cover	HL-93 (US)	0.596	0.773	0.602	0.781	0.990	0.990
CD8x8;10 1924-Rev	3 ft Cover	HL-93 (US)	1.27	1.646	1.27	1.646	1	1
CD8x8;10 1933-Rev	1.9 ft Cover	HL-93 (US)	0.657	0.851	0.657	0.851	1	1
CD8x8;10 1933-Rev	2 ft Cover	HL-93 (US)	0.676	0.876	0.684	0.886	0.988	0.989
CD8x8;10 1933-Rev	3 ft Cover	HL-93 (US)	1.388	1.8	1.388	1.8	1	1
CD10x8;3 1952-Rev	1.9 ft Cover	HL-93 (US)	0.578	0.75	0.578	0.75	1	1
CD10x8;3 1952-Rev	2 ft Cover	HL-93 (US)	0.594	0.77	0.6	0.778	0.990	0.990
CD10x8;3 1952-Rev	3 ft Cover	HL-93 (US)	0.706	0.915	0.706	0.915	1	1
CD10x8;16 1966-Rev	1.9 ft Cover	HL-93 (US)	0.736	0.954	0.736	0.954	1	1
CD10x8;16 1966-Rev	2 ft Cover	HL-93 (US)	0.753	0.976	0.762	0.987	0.988	0.989
CD10x8;16 1966-Rev	2.5 ft Cover	HL-93 (US)	1.125	1.459	1.125	1.459	1	1
CD10x8;16 1966-Rev	3 ft Cover	HL-93 (US)	1.449	1.879	1.449	1.879	1	1
CS10x8;5 1922-Rev	1.9 ft Cover	HL-93 (US)	0.932	1.208	0.932	1.208	1	1
CS10x8;5 1922-Rev	2 ft Cover	HL-93 (US)	0.917	1.189	0.924	1.197	0.992	0.993
CS10x8;5 1922-Rev	2.5 ft Cover	HL-93 (US)	0.985	1.277	0.985	1.277	1	1
CS10x8;5 1922-Rev	3 ft Cover	HL-93 (US)	1.041	1.35	1.041	1.35	1	1
CS10x8;5 1933-Rev	1.9 ft Cover	HL-93 (US)	0.748	0.97	0.748	0.97	1	1
CS10x8;5 1933-Rev	2 ft Cover	HL-93 (US)	0.735	0.952	0.74	0.959	0.993	0.993
CS10x8;5 1933-Rev	2.5 ft Cover	HL-93 (US)	0.768	0.996	0.768	0.996	1	1
CS10x8;5 1933-Rev	3 ft Cover	HL-93 (US)	0.786	1.018	0.786	1.018	1	1

Caltrans Culvert Name, Year Built	Fill Depth	Vehicle	Inv Rating Before Change	Op Rating Before Change	Inv Rating After Change	Op Rating After Change	Inv Ratio Before/After*	Op Ratio Before/After
CS10x8;10 1933-Rev	1.9 ft Cover	HL-93 (US)	1.297	1.681	1.297	1.681	1	1
CS10x8;10 1933-Rev	2 ft Cover	HL-93 (US)	1.282	1.661	1.291	1.674	0.993	0.992
CS10x8;10 1933-Rev	2.5 ft Cover	HL-93 (US)	1.409	1.827	1.409	1.827	1	1
CS10x8;10 1933-Rev	3 ft Cover	HL-93 (US)	1.559	2.021	1.559	2.021	1	1
CD12x8;9 1948-Rev	1.9 ft Cover	HL-93 (US)	0.569	0.737	0.569	0.737	1	1
CD12x8;9 1948-Rev	2 ft Cover	HL-93 (US)	0.553	0.717	0.606	0.785	0.912	0.913
CD12x8;9 1948-Rev	4 ft Cover	HL-93 (US)	0.811	1.052	0.811	1.052	1	1
CD12x8;9 1952-Rev	1.9 ft Cover	HL-93 (US)	0.834	1.081	0.834	1.081	1	1
CD12x8;9 1952-Rev	2 ft Cover	HL-93 (US)	0.855	1.108	0.865	1.121	0.988	0.988
CD12x8;9 1952-Rev	3 ft Cover	HL-93 (US)	1.501	1.945	1.501	1.945	1	1
CD12x12;2 1966-Rev	1.9 ft Cover	HL-93 (US)	0.545	0.706	0.545	0.706	1	1
CD12x12;2 1966-Rev	2 ft Cover	HL-93 (US)	0.516	0.67	0.517	0.67	0.998	1
CD12x12;2 1966-Rev	2.5 ft Cover	HL-93 (US)	0.383	0.496	0.383	0.496	1	1
CD12x12;2 1966-Rev	3 ft Cover	HL-93 (US)	0.244	0.316	0.244	0.316	1	1
CD12x12;20 2010-Rev	1.9 ft Cover	HL-93 (US)	1.553	2.013	1.553	2.013	1	1
CD12x12;20 2010-Rev	2 ft Cover	HL-93 (US)	2.435	3.157	2.452	3.179	0.993	0.993
CD12x12;20 2010-Rev	2.5 ft Cover	HL-93 (US)	2.435	3.157	2.452	3.179	0.993	0.993
CD12x12;20 2010-Rev	3 ft Cover	HL-93 (US)	3.359	4.355	3.359	4.355	1	1
CS12x8;5 1922-Rev	1.9 ft Cover	HL-93 (US)	0.98	1.27	0.98	1.27	1	1
CS12x8;5 1922-Rev	2 ft Cover	HL-93 (US)	0.965	1.251	0.972	1.26	0.993	0.993
CS12x8;5 1922-Rev	3 ft Cover	HL-93 (US)	1.098	1.423	1.098	1.423	1	1
CS12x8;10 1952-Rev	1.9 ft Cover	HL-93 (US)	0.905	1.173	0.905	1.173	1	1
CS12x8;10 1952-Rev	2 ft Cover	HL-93 (US)	1.027	1.332	1.035	1.341	0.992	0.993
CS12x8;10 1952-Rev	3 ft Cover	HL-93 (US)	1.243	1.611	1.243	1.611	1	1
CS12x8;10 2010-Rev	1.9 ft Cover	HL-93 (US)	0.748	0.97	0.748	0.97	1	1
CS12x8;10 2010-Rev	2 ft Cover	HL-93 (US)	1.576	2.043	1.587	2.058	0.993	0.992
CS12x8;10 2010-Rev	2.5 ft Cover	HL-93 (US)	1.733	2.246	1.733	2.246	1	1
CS12x8;10 2010-Rev	3 ft Cover	HL-93 (US)	1.913	2.48	1.913	2.48	1	1

Caltrans Culvert Name, Year Built	Fill Depth	Vehicle	Inv Rating Before Change	Op Rating Before Change	Inv Rating After Change	Op Rating After Change	Inv Ratio Before/After*	Op Ratio Before/After
CS12x12;10 2002-Rev	1.9 ft Cover	HL-93 (US)	0.569	0.738	0.569	0.738	1	1
CS12x12;10 2002-Rev	2 ft Cover	HL-93 (US)	1.339	1.736	1.349	1.749	0.992	0.992
CS12x12;10 2002-Rev	2.5 ft Cover	HL-93 (US)	1.465	1.899	1.465	1.899	1	1
CS12x12;10 2002-Rev	3 ft Cover	HL-93 (US)	1.584	2.053	1.584	2.053	1	1

*Ratios are of the Before Rating Factor / After Rating Factor. If this ratio is less than 1.0 the rating factor improved.

Non-Rectangular Culverts

Culverts other than box sections incorporate a range of shapes and sizes and are designed by a variety of methods, most developed by manufacturer's trade associations and then adopted by AASHTO. While design procedures for concrete box culverts have evolved, procedures for other types of culverts have remained largely unchanged since first added to the AASHTO Specifications. Thus, providing methods to deal with changes, e.g. early box sections were assumed adequate in shear if designed properly to meet flexure requirements, is not necessary for these other types of culverts.

Culverts carry loads through their own structure and through soil support. This is particularly true for the non-rectangular shapes. The nature of soil support is a key factor in rating the non-rectangular shapes and this must be evaluated through inspections. Inspections should document culvert shape, cracks in culvert walls, and any other field conditions that indicate potential distress. Design methods for flexible pipe in particular must consider the effect of shape change in the rating calculation.

Concrete pipes have long been designed with an indirect design procedure based on the three-edge bearing test. In the 1980's the concrete pipe industry developed a direct design method based on finite element analyses. Both methods are incorporated into the LRFD Specifications. Concrete pipes can be rated by either method, but should be completed by the same method used for design as the methods produce different results. In the experience of the research team, the direct design method is quite conservative when applied to small diameter pipes.

There are a number of different corrugated metal structures and each has its own design method – empirical (pipe and long-span structures), semi-empirical (box culverts) and rigorous (deep corrugated). These structures must be rated by the same method by which they were designed. The National Corrugated Steel Pipe Association (NCSPA) issued Design Data No. 19 *Load Rating and Structural Evaluation of In-Service Corrugated Steel Structures* (NCSPA DD 19) in 1995 which provides useful guidance that is still applicable to most metal culvert types today. Deep corrugated structures were added to AASHTO Specifications after the publication of NCSPA DD 19. These structures are designed and should be rated by finite element analysis. The Ohio DOT has developed a series of spreadsheets to conduct rating calculations for metal culverts based on NCSPA DD 19. They have also developed a procedure to rate metal pipe installed at less than the AASHTO prescribed minimum depth of fill. Other states are using these methods and are satisfied with the findings.

Thermoplastic pipe design procedures have evolved some since first incorporated in the LRFD Specifications, but the current procedure is applicable to all thermoplastic pipes. The method is semi-empirical in nature but addresses all key limit states.

Fiberglass pipe, the most recent addition to the LRFD Specifications, are designed and should be rated in accordance with the procedures in American Water Works Association Manual of Practice 54 (AWWA M54). This method was developed in the 1980's by the AWWA and has served as a national and international standard for fiberglass pipe design since that time.

Pavement

This section provides the background for the effects of pavement on the ratings of culverts. The first section provides a review of the Model 7 culvert that was load tested with and without pavement. The next section provides a review of the CANDE models created using the CANDE Tool Box developed for this project and reviewed/rated for pavement and no pavement.

Model 7 3D Analysis Review

Model 7 is a corrugated metal box culvert located in Attleboro, Massachusetts. The research team was able to coordinate with MASSDOT and the culvert contractor to instrument and test this culvert under construction with the intent that the effects of paving on the response of the culvert could be captured.

The following sections present the LUSAS results (3-D finite element analysis) of Model 7, Candidate 1 under the truck load that was used in the experimental program. For this culvert, the experimental program consisted of two main phases: Phase 1 loading the culvert prior to placement of the pavement; and Phase 2, loading the culvert after the pavement is placed. The results herein show the force effects obtained both prior to and after paving.

The calibration and the approach to the 3-D modeling of this culvert in LUSAS is documented in detail in Appendix K and Appendix M.

Culvert Loading and Instrumentation

Each phase included three main sets of loading (Figure 49): N1, with the center of truck over the center of the culvert (and gages); N2, with the left wheel line of the truck centered over the centerline of the culvert; and N3, with the right wheel line of the truck centered over the centerline of the culvert. The truck dimensions for each phase is provided in Figure 50.

Five clusters of four gages (20 gages total) were mounted on the lower face of the culvert as shown in Figure 51. For each test, one of the axles of the truck (3 axles) is placed over one of the gage clusters, producing 15 loading configurations for each set of loading (see Figure 52).

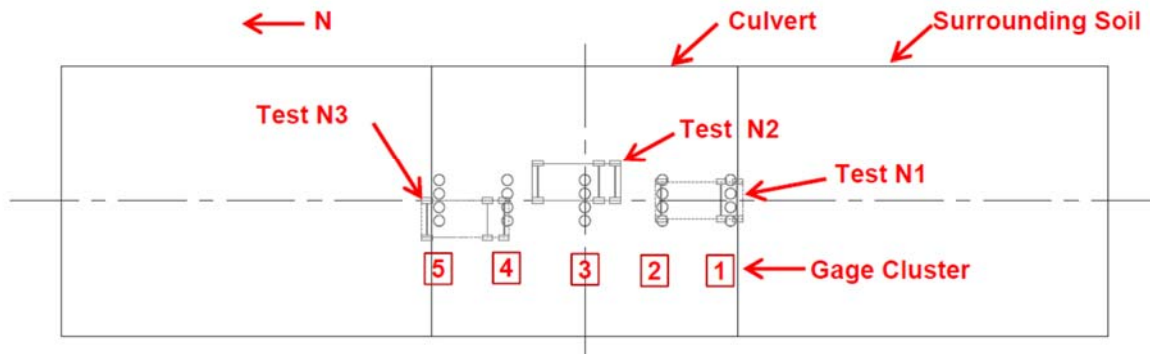


Figure 49 M7C1 Plan View: Showing Location of Gages and Truck Positioning for Each Set of Test

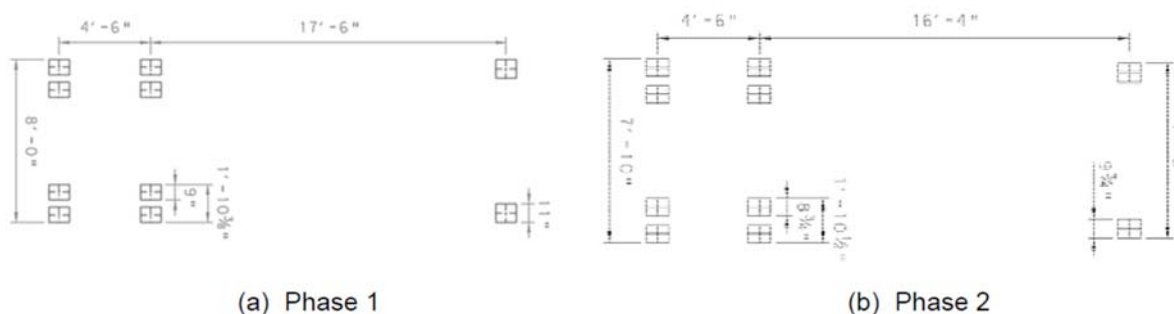


Figure 50 - Truck Dimensions for Each Phase of Testing

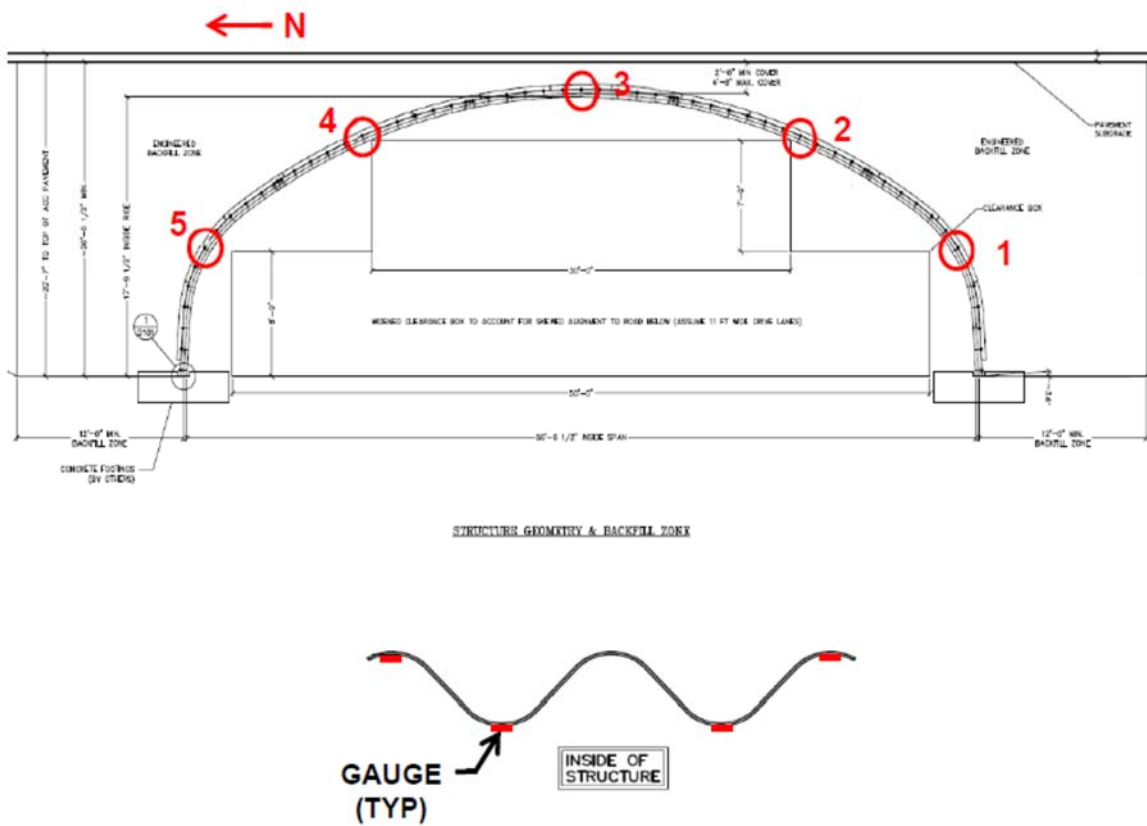
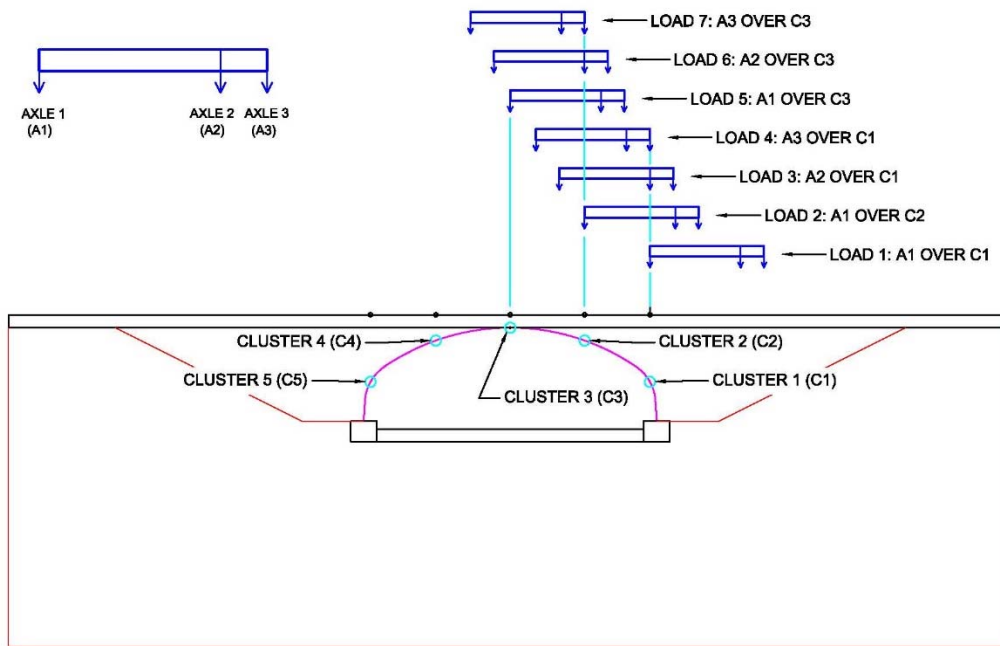
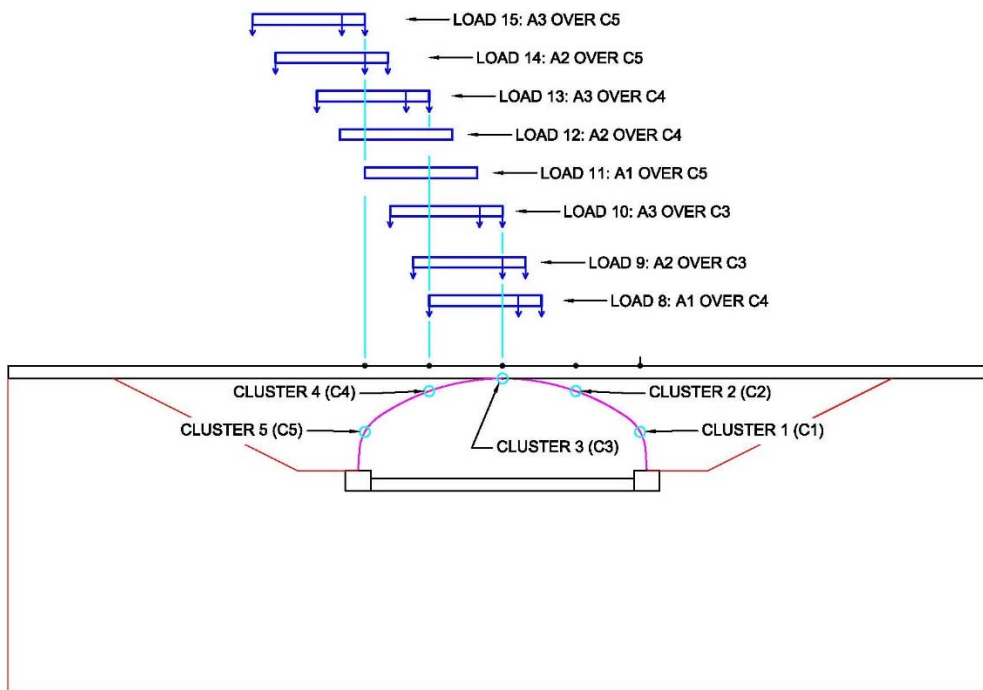


Figure 51 - Instrumentation Locations



Load Set 1 thru 7.



Load Set 8 thru 15.

Figure 52 - Schematics of Loading for Each Load Case for Culvert 7

Results Before and After Paving

While the results presented in Appendix K and Appendix M document the selection of a 3-D modeling scheme and the corresponding results from Test 1 (prior to paving), the results herein illustrate the differences in the stresses at each of the strain gauge locations as measured in the field. Similar comparisons were made between the stresses at each location as obtained in the 3-D LUSAS models.

In the figures below (Figure 53 to Figure 67), Test 1 results are shown in dashed lines and represent the condition without pavement and Test 2 results are shown in solid lines and represent the culvert after paving. The results show a significant reduction in measured strains. Gage Cluster 3 at midspan shows a 33% reduction in peak stress under the live load. Gage Cluster 4 at the shoulder, the other critical location, shows a 50% reduction. These reductions are also notable as the pavement was placed on high quality, highly compacted fill being prepared for interstate traffic. Pavements over softer soils will show a more significant benefit with the same paving.

Stress Comparison (Gage Cluster 5)

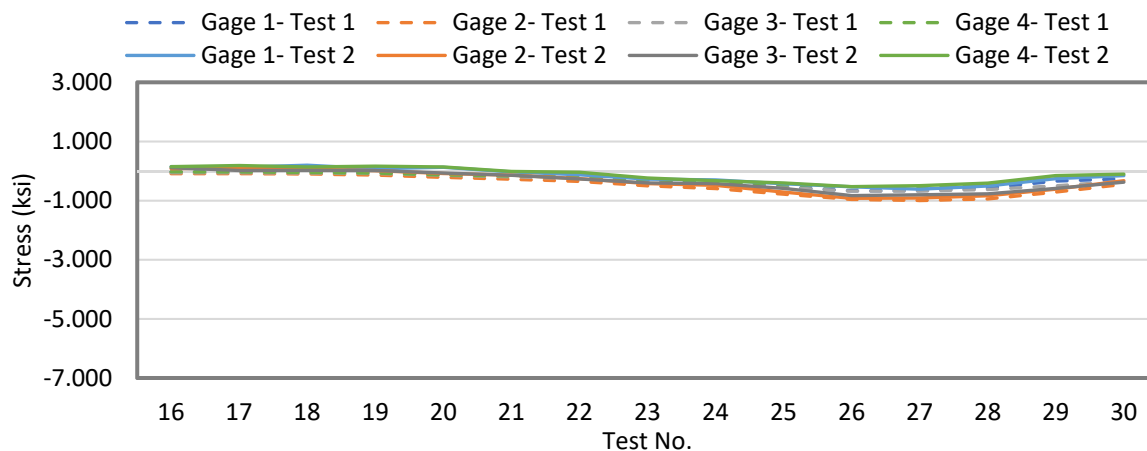


Figure 53 - Model 7 Before and After Paving: Test N1, Gauges 1-4 (Cluster 5)

Stress Comparison (Gage Cluster 4)

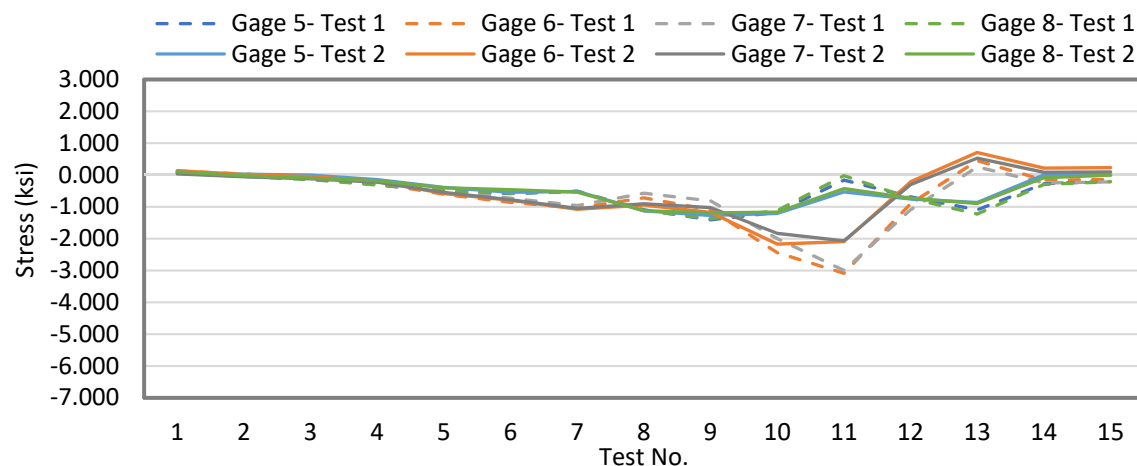


Figure 54 - Model 7 Before and After Paving: Test N1, Gauges 5-8 (Cluster 4)

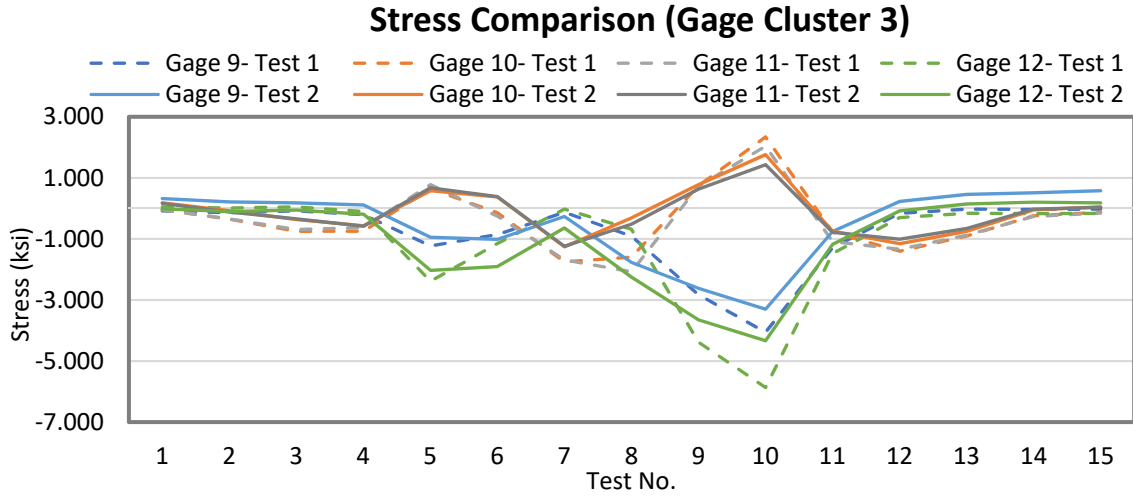


Figure 55 - Model 7 Before and After Paving: Test N1, Gauges 9-12 (Cluster 3)

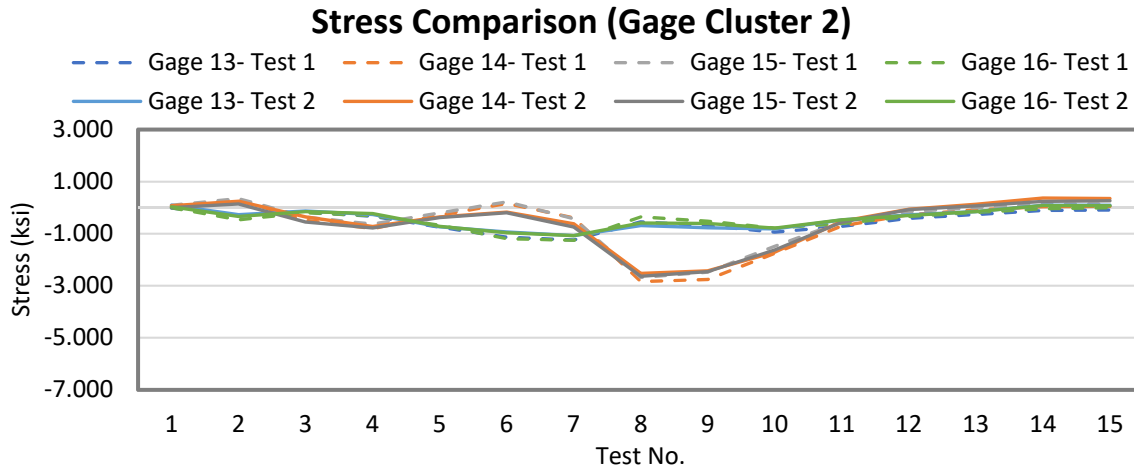


Figure 56 - Model 7 Before and After Paving: Test N1, Gauges 13-16 (Cluster 2)

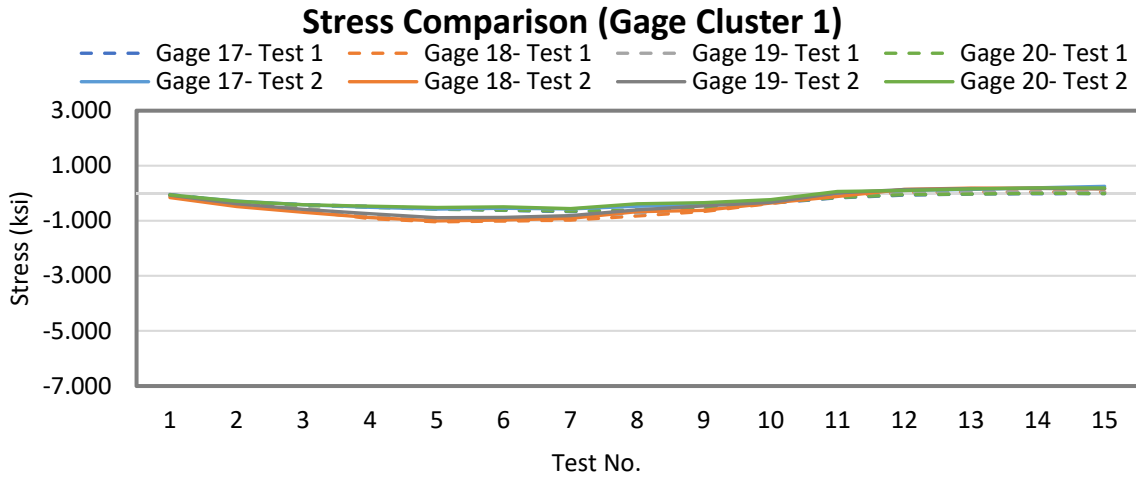


Figure 57 - Model 7 Before and After Paving: Test N1, Gauges 17-20 (Cluster 1)

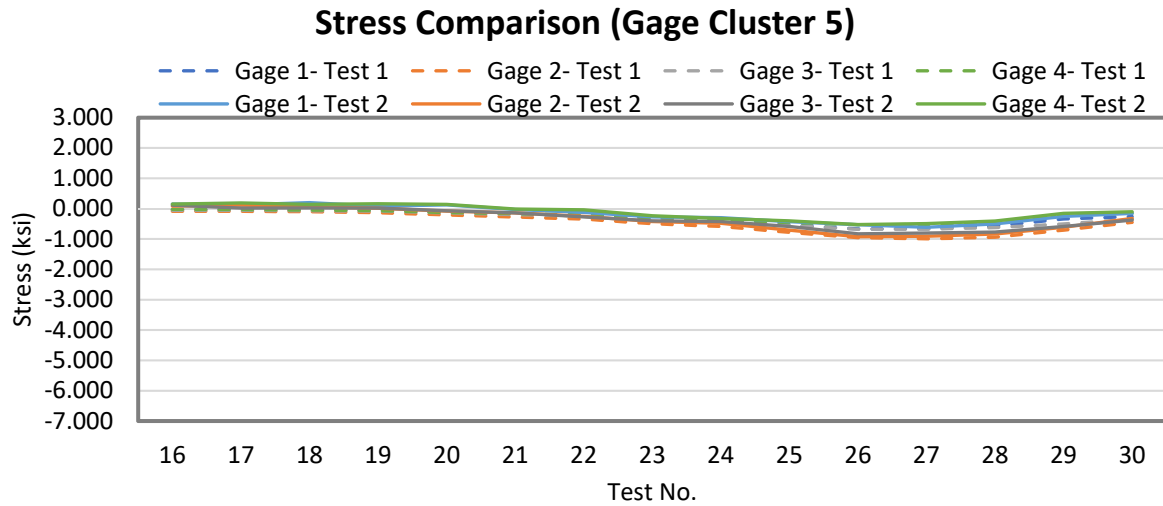


Figure 58 - Model 7 Before and After Paving: Test N2, Gauges 1-4 (Cluster 5)

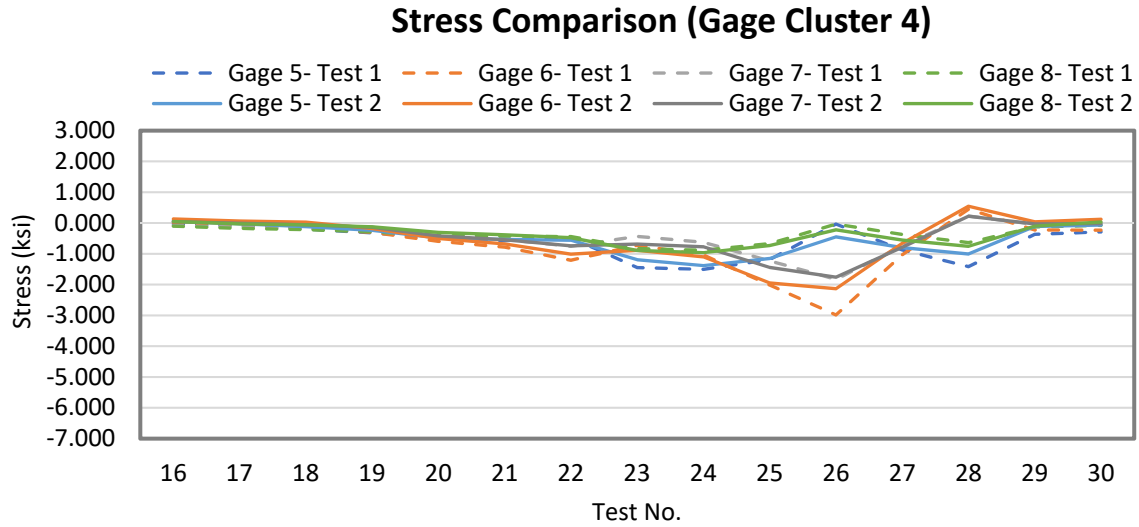


Figure 59 - Model 7 Before and After Paving: Test N2, Gauges 5-8 (Cluster 4)

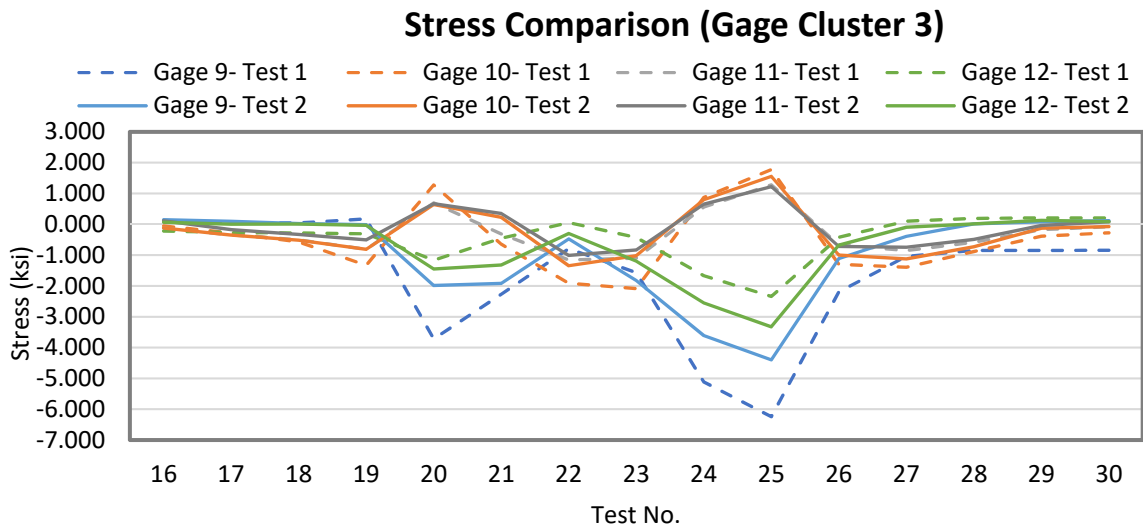


Figure 60 - Model 7 Before and After Paving: Test N2, Gauges 9-2 (Cluster 3)

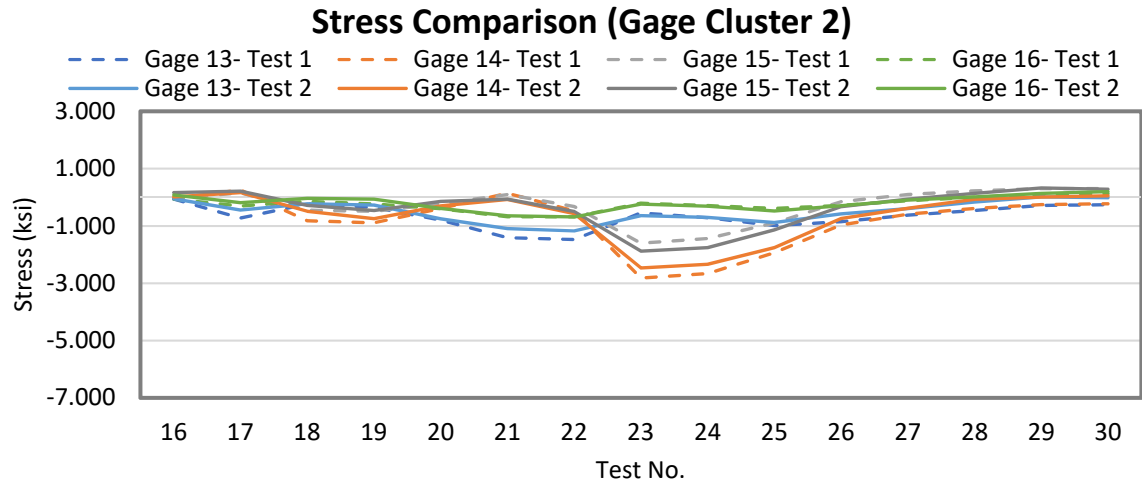


Figure 61 - Model 7 Before and After Paving: Test N2, Gauges 13-16 (Cluster 1)

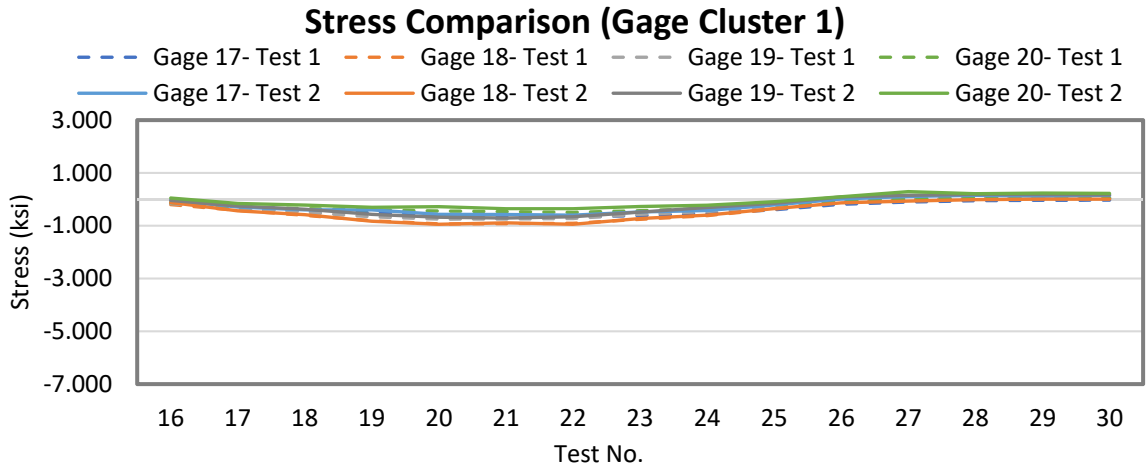


Figure 62 - Model 7 Before and After Paving: Test N2, Gauges 17-20 (Cluster 1)

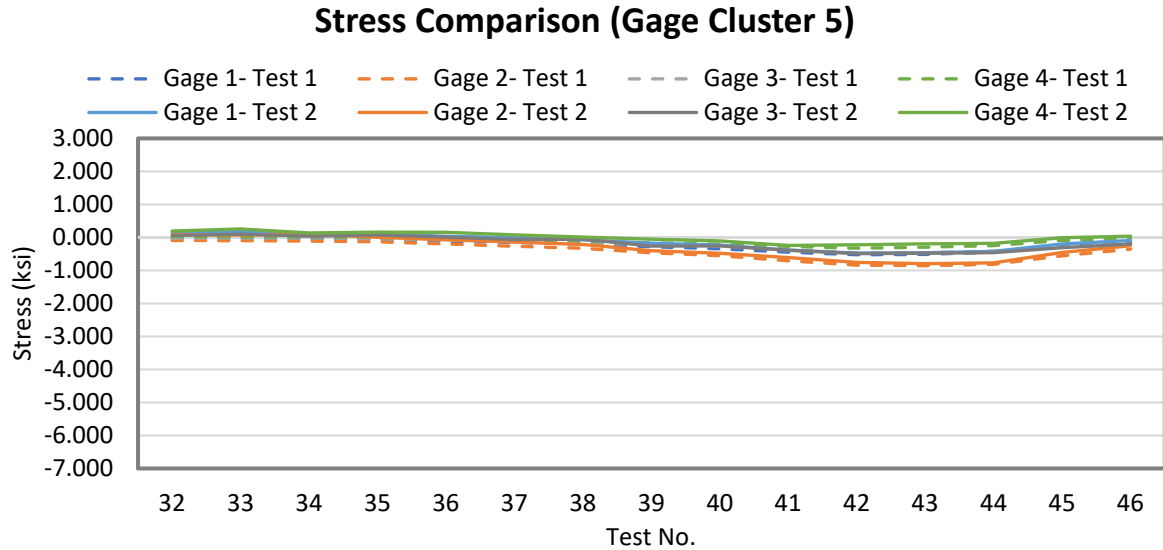


Figure 63 – Model 7 Before and After Paving: Test N3, Gauges 1-4 (Cluster 5)

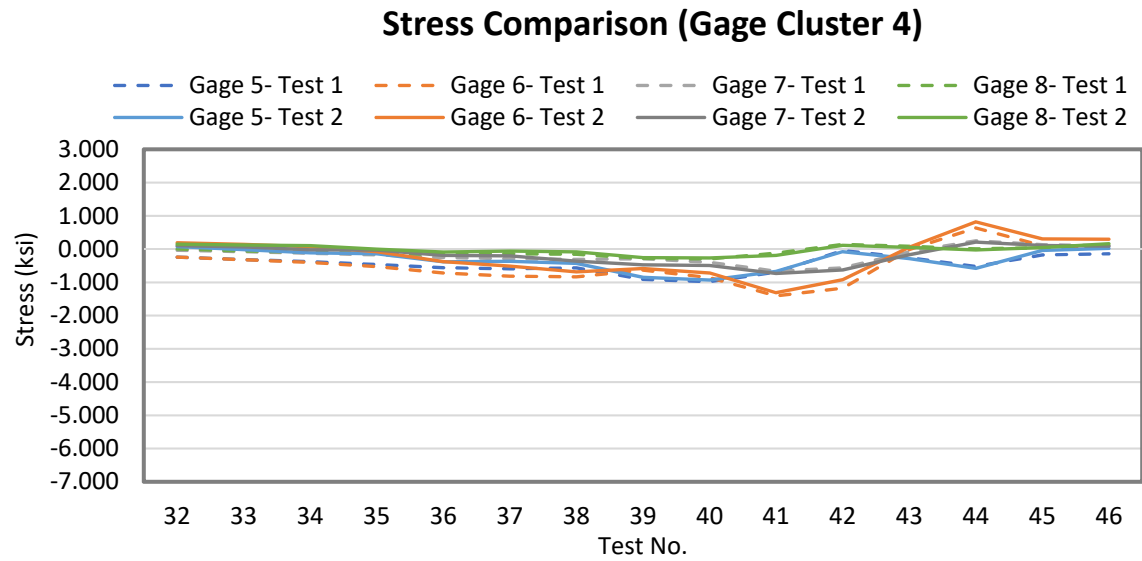


Figure 64 – Model 7 Before and After Paving: Test N3, Gauges 5-8 (Cluster 4)

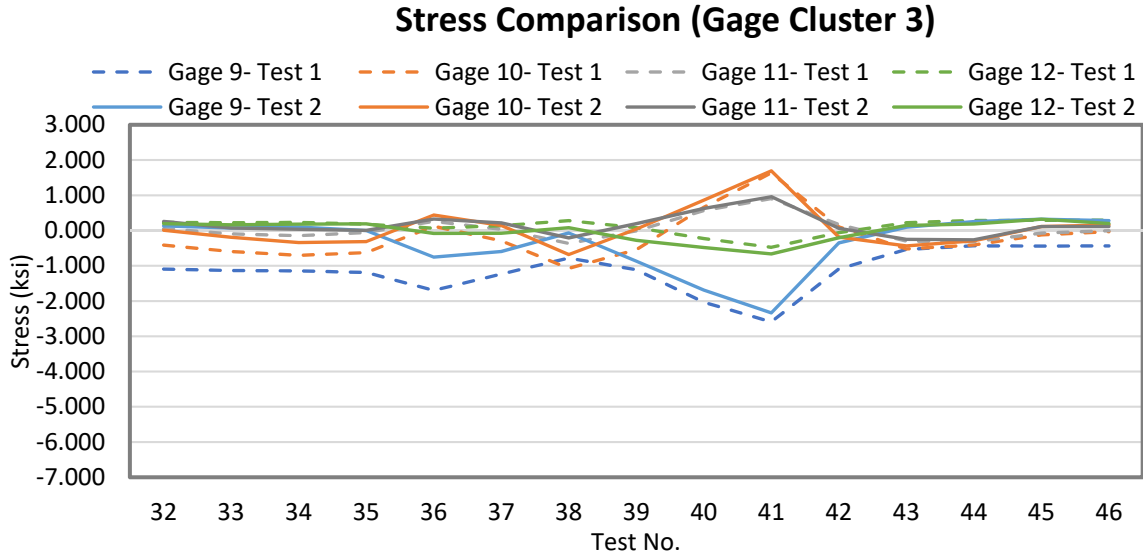


Figure 65 – Model 7 Before and After Paving: Test N3, Gauges 9-12 (Cluster 3)

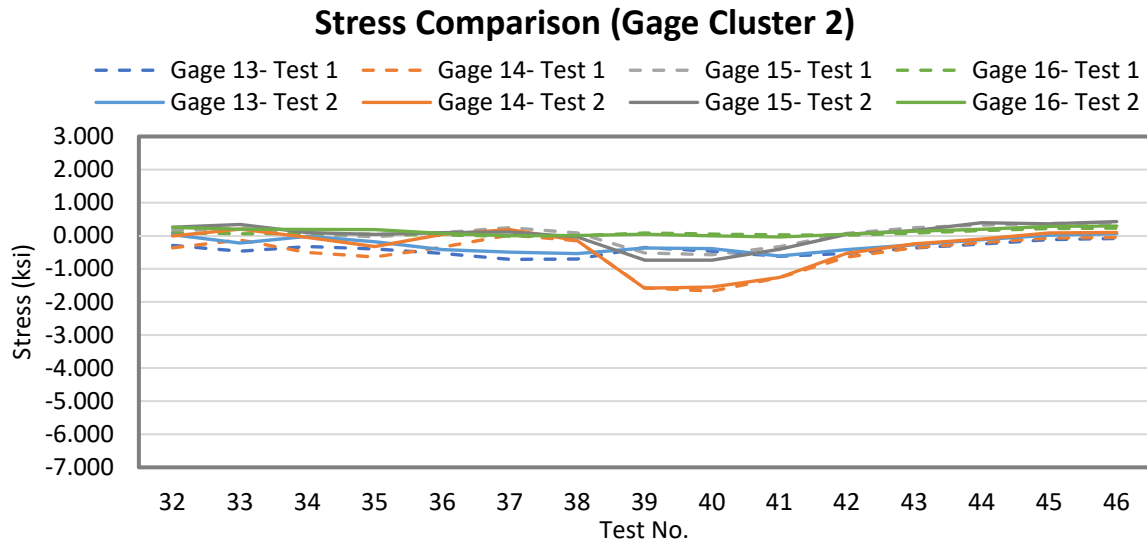


Figure 66 – Model 7 Before and After Paving: Test N3, Gauges 13-16 (Cluster 2)

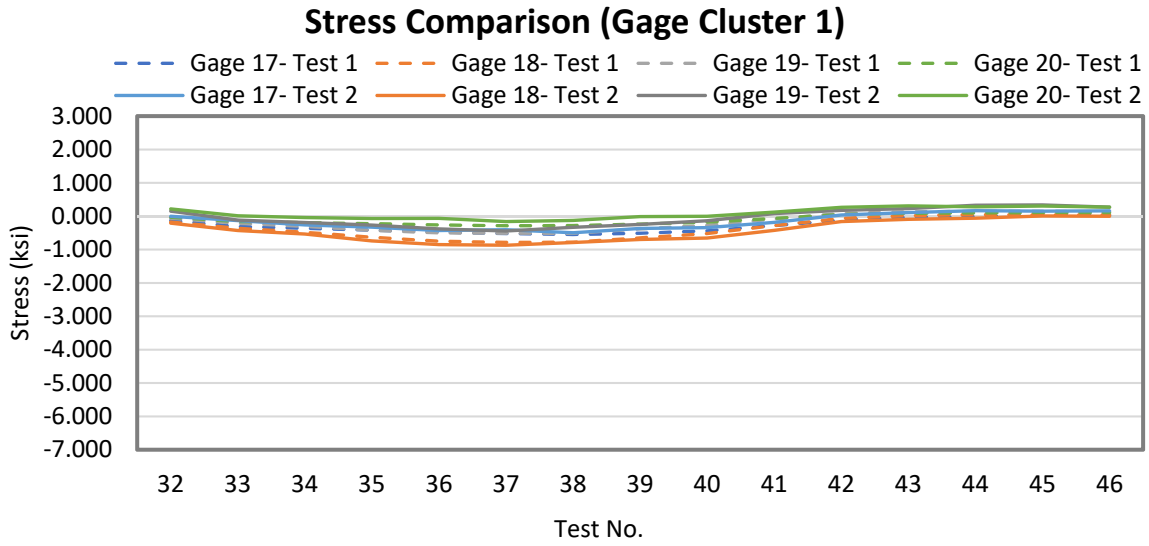


Figure 67 – Model 7 Before and After Paving: Test N3, Gauges 17-20 (Cluster 1)

CANDE Models with and Without Pavement

Several of the models in this study were analyzed in CANDE with varying fill heights and with and without pavement elements. These were analyzed using CANDE and the new features provided in the CANDE Tool Box. Each of the models were reviewed and the rating results compared. For discussion purposes, Model 7 results are shown here while the analysis for the remaining models are provided in Appendix D of this report.

Model 7

The original CANDE mesh for this model was provided by CONTECH. The general process for modifying the model is described in an earlier section of this report. A sample mesh of the model is provided in Figure 68 below. The model was modified to include the moving tandem load and was analyzed with and without pavement.

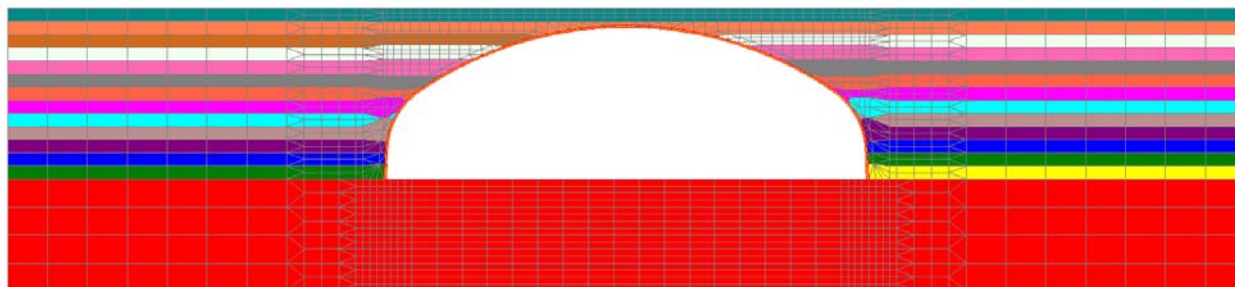


Figure 68 – M7C1 Sample CANDE Mesh Without Pavement

The rating analysis for the culvert with and without pavement using a two axle tandem load and excluding lane load is provided in Table 14. A schematic showing the beam nodes referenced in the table are provided in Figure 69. The results for this model and those presented in Appendix D for the other models indicate that the pavement provides a benefit for increasing the rating factor.

Table 14 – M7C1 Rating Results

Rating	No pavement	E = 200,000 psi v = 0.33 Pavement (6")
1.5 ft fill		
Material Thrust	14.64 (Node 16)	15.61 (Node 14)
Buckling Thrust	8.56 (Node 16)	4.57 (Node 9)
Seam Thrust	14.64 (Node 16)	15.61 (Node 14)
Plastic-Penatrate	10000 (Node 1)	10000 (Node 1)
Combined T&M Ratio	2.13 (Node 23)	3.75 (Node 23)

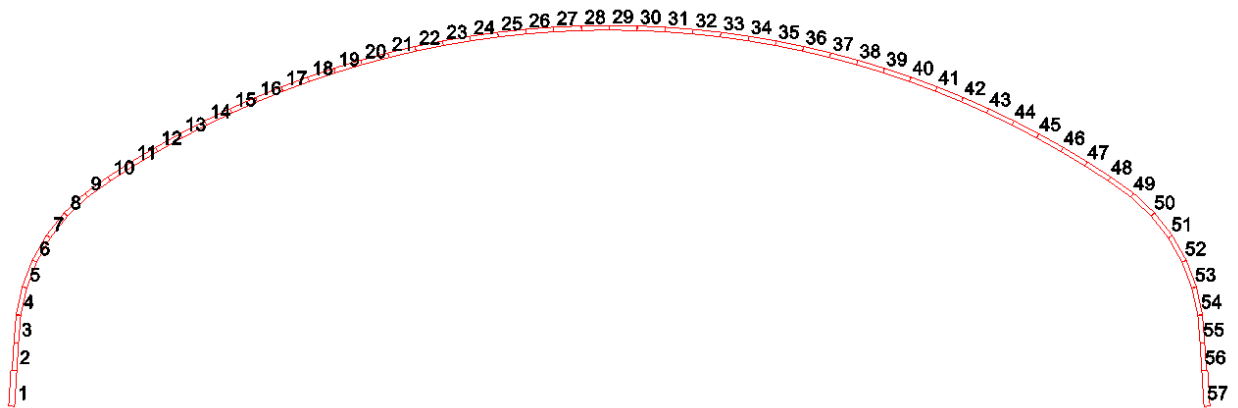


Figure 69 – Node Numbering for M7C1

Recommendations

We conclude that live load ratings can be improved by including the effects of pavement. A 3-D model is not required to analyze live load response associated with a paved surface. As discussed and detailed in the previous section, the 2-D CANDE software has been modified to allow the user to specify a paved surface (See Chapter 2 of this report and Appendix C-CANDE Tool Box Manual for Load Rating). Recommendations for using pavement for rating is provided in the form of recommend specification changes and are provided in Chapter 4 and in Appendix H. A parametric study of the 2D models tested for this project using CANDE and the CANDE Tool Box is provided in Appendix D.

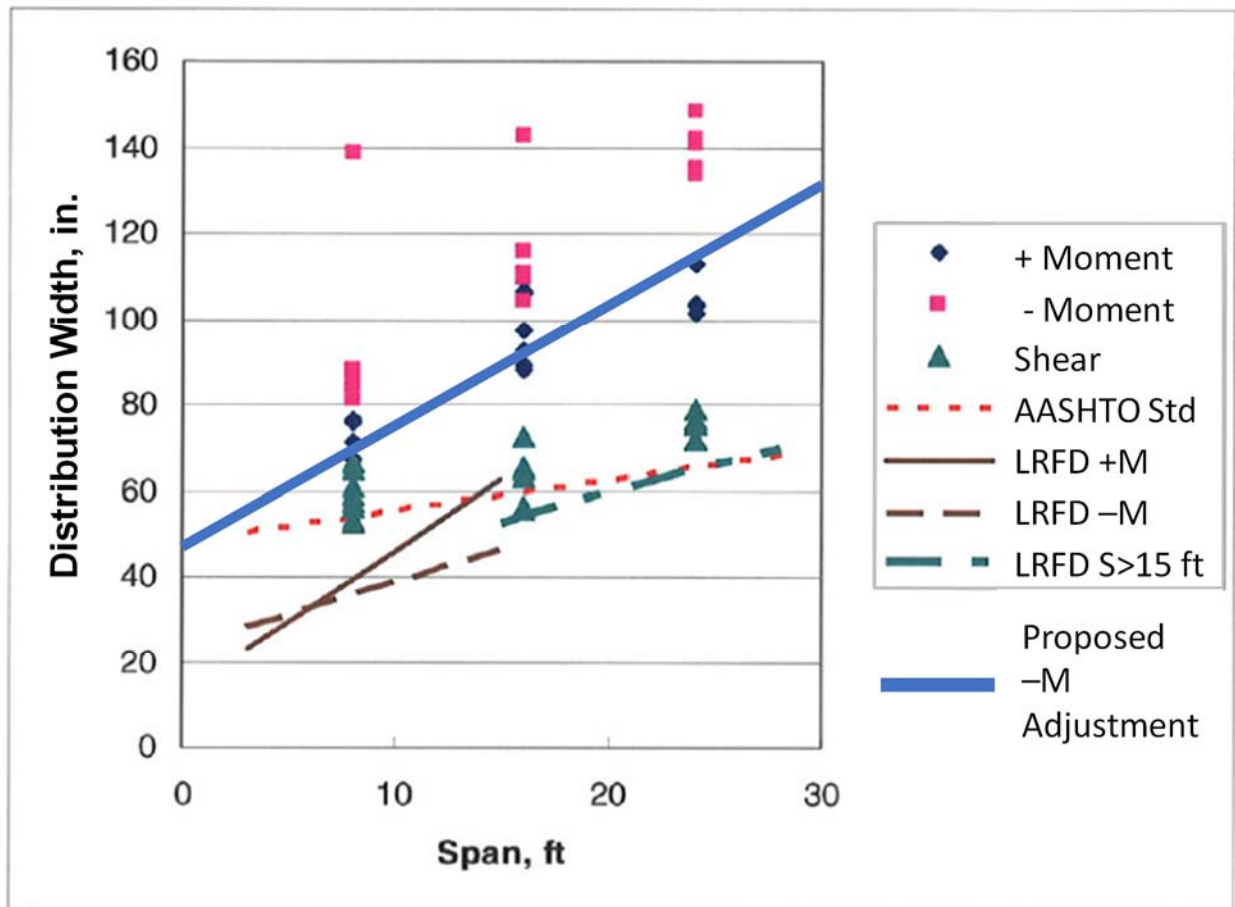
The recommendations for reducing loads on culverts from the effects of pavement are provided in Chapter 4 and in the Appendix H ballot items (Subject: Rating and Condition Evaluation of Culverts).

Shear Capacity

The shear capacity of reinforced concrete culverts was reviewed as part of this research. The following sections provide the reasoning for the changes recommend in Chapter 4 of this report related to the AASHTO MBE Article 6A.5.13.1. The final agenda item for Shear Capacity is provided in Appendix H (Ballot MBE-1) and is also highlighted in Chapter 4

The culvert set described in this section was analyzed and ratings were saved for the existing 3rd Edition MBE using the AASHTOWare BrR program (version 6.8.3). The Inventory HL93 shear ratings were compared with the same ratings after the proposed modifications were made for BrDR. The comparative results for the shear rating are provided in a table later in this section.

The PennDOT study (modified from McGrath et al., 2004, 2005) investigated longitudinal live load distribution (i.e., distribution perpendicular to the span) for the purpose of investigating the suitability of the distribution incorporated into the 2nd Edition of the LRFD Specifications relative to the provision from the AASHTO Standard Specifications. Figure 70 presents the distribution of forces at critical design sections from that study.



Note: LRFD refers to AASHTO LRFD Bridge Design Specifications, 2nd Edition

Figure 70 – Distribution Width vs. Span (PennDOT Study, McGrath et al, 2004, 2005)

The PennDOT study concluded that the distribution from the AASHTO Standard Specifications (red dotted line) matched the distribution width for shear forces and was the most conservative. Based on this, the provisions of the AASHTO Standard Specification were adopted into the LRFD Specifications. However, the positive and negative moments distribute over broader widths. The proposed fix to the shear equation is to reduce the negative moments at dv from the tip of the haunch to take advantage of that broader distribution. The solid blue line represents a curve proposed to reduce negative moments at critical shear design locations as discussed below. Reducing the negative moments increases the shear strength as described here.

In the LRFD general procedure, the reinforcement strain is computed as:

$$\epsilon_s = \frac{\left(\frac{|M_u|}{d_v} + 0.5N_u + |V_u - V_f| - A_{ps}f_{po} \right)}{E_s A_s + E_p A_{ps}} \quad (5.7.3.4.2-4)$$

The term M_u/dv is significant in this equation and reducing the moment to reflect the PennDOT report figure effectively reduces the reinforcement strain. However, the LRFD definitions state that M_u shall not be taken less than $V_u * d$, a limitation that prevents a significant increase in capacity. Therefore, two steps are required to improve ratings based on shear.

1. Reduce the negative moments at the controlling shear design sections (not at all locations).
2. Eliminate the requirement that $M_u > V_u * d$.

This change is suggested only for the rating top slabs of box culverts under less than 2 ft of fill and showing good performance in the field. Box culverts with more than two feet of fill are designed by Article 5.12.7.3 which allows using a minimum β factor of 3.0.

The modification is based on relating the LRFD Load distribution width Equation 4.6.2.10-1:

$$\text{Axle Distribution} = 96 + 1.44 * \text{Span}$$

to the solid blue line shown in Figure 70:

$$\text{Modified Axle Distribution} = 96 + 5.47 * \text{Span}$$

Assuming the greater distribution width produces a proportional reduction in the live load moment at critical shear sections, we can compute a reduction factor for the live load moments to be used in Eq. 5.7.3.4.2-4):

$$\text{Moment Modification Factor} = \text{Axle Distribution} / \text{Modified Axle Distribution}$$

Economic Impact

Overall the change provided an improvement in shear rating factors for many culverts with a fill depth below 2'. Cases where no improvement was shown are when the value for M_u is greater than zero at the d_{critical} location.

Table 15 provides a comparison of differences in the shear rating factor with the revised specification vs. the existing specification. The values displayed are for covers below 2 feet. As expected, no changes were detected above 2 feet of cover. The full table showing all of the culvert runs for the shear capacity changes

is provided in Appendix G. These were run using AASHTOWare BrR using a revision to 6.8.3 of the software. The ratio in the final column is of the existing shear capacity calculation to the revised shear capacity calculation. A value below 1.0 indicates an improvement in the rating factor for HL93. Many of the culverts were obtained from Caltrans and show a variety of culvert sizes and years built. The Models 1, 2, and 3 were culverts that were load tested for the NCHRP 15-54 project. Improvements for this change were shown below 2' of fill.

The average shear rating factor improvement for fills below 2' is about 8.5% with a maximum improvement of about 20% (Culvert Model1 with 1.5 foot of fill -1.8193 vs a previous value of 1.4574).

Table 15 – Comparisons of Shear Rating Factors for Change in the Shear Capacity Calculation

Bridge ID	Fill Depth	Critical Element (Before)	Location (Before)	Critical Element (After)	Location (After)	Shear Inv Rating Factor HL93 (Before)	Shear Inv Rating Factor HL93 (After)	Ratio (Before/After)
CD10x8;10 2002-Rev	1.5	Top Slab 2	0.6025	Top Slab 2	0.6025	1.1099	1.1789	0.9415
CD10x8;10 2002-Rev	1.9	Top Slab 2	0.6025	Top Slab 2	0.6025	1.1066	1.1835	0.9350
CD10x8;10 2010-Rev	1.5	Top Slab 2	0.6925	Top Slab 2	0.6925	1.4619	1.557	0.9389
CD10x8;10 2010-Rev	1.9	Top Slab 2	0.6925	Top Slab 2	0.6925	1.5025	1.5806	0.9506
CD10x8;16 1966-Rev	1.9	Top Slab 1	9.0893	Top Slab 1	9.0893	1.601	1.8908	0.8467
CD10x8;2 1966-Rev	0.5	Top Slab 1	9.3866	Top Slab 1	0.6354	1.0071	1.0407	0.9677
CD10x8;2 1966-Rev	1	Top Slab 1	9.3866	Top Slab 1	0.6354	1.0185	1.1017	0.9245
CD10x8;2 1966-Rev	1.5	Top Slab 1	9.3866	Top Slab 1	9.3866	1.0306	1.0946	0.9415
CD10x8;2 1966-Rev	1.9	Top Slab 1	9.3866	Top Slab 1	9.3866	1.0314	1.0873	0.9486
CD10x8;3 1952-Rev	1.5	Top Slab 1	8.8819	Top Slab 1	8	1.0699	1.3251	0.8074
CD10x8;3 1952-Rev	1.9	Top Slab 1	8.8819	Top Slab 1	8.8819	1.0888	1.3459	0.8090
CD10x8;5 1948-Rev	1	Top Slab 1	8.9271	Top Slab 1	1.1034	1.1191	1.2936	0.8651
CD10x8;5 1948-Rev	1.5	Top Slab 1	8.9271	Top Slab 1	8.9271	1.1443	1.3417	0.8529
CD10x8;5 1948-Rev	1.9	Top Slab 1	8.9271	Top Slab 1	8.9271	1.1661	1.3478	0.8652
CD10x8;9 1948-Rev	1.5	Top Slab 1	8.8924	Top Slab 1	8.8924	1.3002	1.5054	0.8637
CD10x8;9 1948-Rev	1.9	Top Slab 1	8.8924	Top Slab 1	8.8924	1.3303	1.5218	0.8742
CD12x12;20 2010-Rev	1.9	Top Slab 2	1.227	Top Slab 2	1.227	3.1552	3.5462	0.8897
CD12x12;2 1966-Rev	1.5	Top Slab 1	11.252	Top Slab 1	11.252	1.3301	1.435	0.9269
CD12x12;2 1966-Rev	1.9	Top Slab 1	11.252	Top Slab 1	11.252	1.3323	1.4171	0.9402
CD12x8;9 1948-Rev	0	Top Slab 1	1.2486	Top Slab 1	1.2486	1.2529	1.2529	1.0000
CD12x8;9 1948-Rev	0.5	Top Slab 1	1.2486	Top Slab 1	1.2486	1.3022	1.3022	1.0000
CD12x8;9 1948-Rev	1	Top Slab 1	10.79	Top Slab 1	1.2486	1.2176	1.3535	0.8996
CD12x8;9 1948-Rev	1.5	Top Slab 1	10.79	Top Slab 1	10.79	1.2164	1.381	0.8808
CD12x8;9 1948-Rev	1.9	Top Slab 1	10.79	Top Slab 1	10.79	1.2148	1.364	0.8906
CD12x8;9 1952-Rev	1.5	Top Slab 1	9.6	Top Slab 1	9.6	2.0712	2.1877	0.9467
CD12x8;9 1952-Rev	1.9	Top Slab 1	10.465	Top Slab 1	10.465	1.8899	2.2891	0.8256
CD14x13;10 2002-Rev	1.5	Top Slab 2	0.7525	Top Slab 2	0.7525	1.2995	1.3937	0.9324
CD14x13;10 2002-Rev	1.9	Top Slab 2	0.7525	Top Slab 2	0.7525	1.2622	1.3677	0.9229
CD14x9;10 2002-Rev	1.5	Top Slab 2	0.7525	Top Slab 2	0.7525	1.2781	1.3776	0.9278
CD14x9;10 2002-Rev	1.9	Top Slab 2	0.7525	Top Slab 2	0.7525	1.2383	1.3488	0.9181
CD14x9;10 2010-Rev	1.5	Top Slab 2	0.852	Top Slab 2	0.852	1.6473	1.7383	0.9477
CD14x9;10 2010-Rev	1.9	Top Slab 2	0.852	Top Slab 2	0.852	1.6197	1.7224	0.9404
CD8x8;10 1924-Rev	1	Top Slab 1	7.0713	Top Slab 1	7.0713	2.2342	2.4854	0.8989
CD8x8;10 1924-Rev	1.9	Top Slab 1	7.0713	Top Slab 1	7.0713	2.5273	2.8542	0.8855
CD8x8;10 1933-Rev	1	Top Slab 1	7.0937	Top Slab 1	7.0937	2.0784	2.3505	0.8842

Bridge ID	Fill Depth	Critical Element (Before)	Location (Before)	Critical Element (After)	Location (After)	Shear Inv Rating Factor HL93 (Before)	Shear Inv Rating Factor HL93 (After)	Ratio (Before/After)
CD8x8;10 1933-Rev	1.9	Top Slab 1	7.0937	Top Slab 1	7.0937	2.3552	2.7004	0.8722
CD8x8;5 1924-Rev	1	Top Slab 1	7.2356	Top Slab 1	0.7722	1.6345	1.7773	0.9197
CD8x8;5 1924-Rev	1.5	Top Slab 1	7.2356	Top Slab 1	0.7722	1.7321	1.9571	0.8850
CD8x8;5 1924-Rev	1.9	Top Slab 1	7.2356	Bottom Slab 1	0.6055	1.821	2.0376	0.8937
CS10x8;10 1933-Rev	1.9	Top Slab 1	1.1503	Top Slab 1	1.1503	2.4883	2.4883	1.0000
CS10x8;10 1981-Rev	1.5	Top Slab 1	0.5425	Top Slab 1	0.5425	1.1412	1.2482	0.9143
CS10x8;10 1981-Rev	1.9	Bottom Slab 1	0.48	Top Slab 1	0.5425	1.1637	1.2681	0.9177
CS10x8;10 2002-Rev	1.5	Top Slab 1	0.5425	Top Slab 1	0.5425	1.2232	1.3337	0.9171
CS10x8;10 2002-Rev	1.9	Bottom Slab 1	0.48	Top Slab 1	0.5425	1.2561	1.3578	0.9251
CS10x8;10 2010-Rev	1.5	Top Slab 1	0.6325	Top Slab 1	0.6325	1.5199	1.7165	0.8855
CS10x8;10 2010-Rev	1.9	Top Slab 1	0.6325	Top Slab 1	0.6325	1.5698	1.7605	0.8917
CS10x8;12 1952-Rev	1.9	Top Slab 1	1.116	Top Slab 1	1.116	1.6469	1.8724	0.8796
CS10x8;5 1922-Rev	1.5	Top Slab 1	1.6879	Top Slab 1	1.6879	2.5801	2.6162	0.9862
CS10x8;5 1922-Rev	1.9	Top Slab 1	1.6879	Top Slab 1	1.6879	2.7172	2.7663	0.9823
CS10x8;5 1933-Rev	1.5	Bottom Slab 1	0.7389	Bottom Slab 1	0.7389	1.4995	1.4995	1.0000
CS10x8;5 1933-Rev	1.9	Bottom Slab 1	0.7389	Bottom Slab 1	0.7389	1.5042	1.5042	1.0000
CS10x8;5 1952-Rev	1.5	Bottom Slab 1	0.51	Bottom Slab 1	0.51	0.96278	1.1542	0.8342
CS10x8;5 1952-Rev	1.9	Bottom Slab 1	0.51	Bottom Slab 1	0.51	0.95991	1.1504	0.8344
CS10x8;6 1948-Rev	1.5	Bottom Slab 1	0.576	Bottom Slab 1	0.576	1.3847	1.5789	0.8770
CS10x8;6 1948-Rev	1.9	Bottom Slab 1	0.576	Bottom Slab 1	0.576	1.3951	1.5891	0.8779
CS10x8;8 1966-Rev	1.5	Top Slab 1	0.62	Top Slab 1	2	1.0366	1.2219	0.8484
CS10x8;8 1966-Rev	1.9	Top Slab 1	0.62	Top Slab 1	2	1.0618	1.291	0.8225
CS12x12;10 2002-Rev	1.5	Top Slab 1	0.6325	Top Slab 1	0.6325	1.2302	1.3203	0.9318
CS12x12;10 2002-Rev	1.9	Top Slab 1	0.6325	Top Slab 1	0.6325	1.2444	1.3195	0.9431
CS12x8;10 1952-Rev	1.5	Top Slab 1	1.3398	Top Slab 1	1.3398	1.7957	1.9911	0.9019
CS12x8;10 1952-Rev	1.9	Bottom Slab 1	0.7834	Top Slab 1	1.3398	1.8349	2.0668	0.8878
CS12x8;10 2010-Rev	1.5	Top Slab 1	0.6925	Top Slab 1	0.6925	1.5694	1.7585	0.8925
CS12x8;10 2010-Rev	1.9	Top Slab 1	0.6925	Top Slab 1	0.6925	1.5984	1.781	0.8975
CS12x8;5 1922-Rev	1.5	Top Slab 1	2.0204	Top Slab 1	2.0204	2.8244	2.8715	0.9836
CS12x8;5 1922-Rev	1.9	Top Slab 1	2.0204	Top Slab 1	2.0204	2.934	2.996	0.9793
CS14x14;10 2002-Rev	1.5	Bottom Slab 1	0.69	Bottom Slab 1	0.69	1.3813	1.4832	0.9313
CS14x14;10 2002-Rev	1.9	Bottom Slab 1	0.69	Bottom Slab 1	0.69	1.3527	1.46	0.9265
CS14x9;10 2002-Rev	1.5	Top Slab 1	0.6325	Top Slab 1	0.6325	1.1166	1.2179	0.9168
CS14x9;10 2002-Rev	1.9	Top Slab 1	0.6325	Top Slab 1	0.6325	1.111	1.1973	0.9279
CS14x9;10 2010-Rev	1.5	Top Slab 1	0.7825	Top Slab 1	1.4	1.4648	1.7391	0.8423
CS14x9;10 2010-Rev	1.9	Top Slab 1	0.7825	Top Slab 1	0.7825	1.4714	1.7734	0.8297

Bridge ID	Fill Depth	Critical Element (Before)	Location (Before)	Critical Element (After)	Location (After)	Shear Inv Rating Factor HL93 (Before)	Shear Inv Rating Factor HL93 (After)	Ratio (Before/After)
CS16x12;0 1922 EAE-Rev	1.5	Top Slab 1	2.3528	Top Slab 1	2.3528	2.1968	2.2408	0.9804
CS16x12;0 1922 EAE-Rev	1.9	Top Slab 1	2.3528	Top Slab 1	2.3528	2.2376	2.3038	0.9713
CS16x8;5 1922 EAE-Rev	1.5	Top Slab 1	2.6645	Top Slab 1	2.6645	2.4898	2.5762	0.9665
CS16x8;5 1922 EAE-Rev	1.9	Top Slab 1	2.6645	Top Slab 1	2.6645	2.5454	2.6561	0.9583
CS7x7;10 2010-Rev	1.5	Bottom Slab 1	0.51	Bottom Slab 1	0.51	1.5433	1.5433	1.0000
CS7x7;10 2010-Rev	1.9	Bottom Slab 1	0.51	Bottom Slab 1	0.51	1.5855	1.5855	1.0000
CS8x8;10 2010-Rev	1.5	Bottom Slab 1	0.51	Bottom Slab 1	0.51	1.3655	1.3655	1.0000
CS8x8;10 2010-Rev	1.9	Bottom Slab 1	0.51	Bottom Slab 1	0.51	1.3896	1.3896	1.0000
Model 1- Candidate 1-Rev	1.5	Top Slab 1	1.8759	Top Slab 1	1.8759	1.4574	1.8193	0.8011
Model 1- Candidate 1-Rev	1.99	Top Slab 1	1.8759	Top Slab 1	1.8759	1.3847	1.726	0.8023
Model 2- Candidate 1-Rev	1.5	Top Slab 2	1.13	Top Slab 2	1.13	1.5227	1.698	0.8968
Model 2- Candidate 1-Rev	1.9	Top Slab 2	1.13	Top Slab 2	1.13	1.579	1.743	0.9059
Model 3- Candidate 1-Rev	1.5	Top Slab 1	1.4337	Top Slab 1	1.4337	3.1686	3.4535	0.9175
Model 3- Candidate 1-Rev	1.9	Top Slab 1	1.4337	Top Slab 1	1.4337	3.1686	3.4535	0.9175

References:

McGrath, T.J., Liepins, A.A., and Beaver, J.L., (2005), Live Load Distribution Widths for Reinforced Concrete Box Sections, *Transportation Research Record: Journal of the Transportation Research Board, CD 11-S*, Transportation Research Board of the National Academies, Washington, DC, pp 99-108.

McGrath, T.J., Liepins, A.A., Beaver, J.L., Strohmman, B.P., (2004), *Live Load Distributions for Design of Box Culverts, A Study for the Pennsylvania Department of Transportation*.

Live Load Surcharge vs. Approaching Wheel Load

This section summarizes the change related to the proposed culvert section in the LRFD 3.11.6.4.

The culvert set described in this section was run and ratings were saved for the existing 8th Edition LRFD. The overall HL93 inventory and operating ratings were compared with the same ratings after the proposed modifications were made for BrDR. The comparative results for the LL surcharge rating are provided in a table later in this section.

Background/Spec Change Proposal

The current LRFD Specifications and the MBE define a live load surcharge (LS) in Article 3.11.6.4 to account for vehicles located adjacent to retaining walls. The loading is also applied to culverts to represent the effect of a vehicle approaching a culvert. This is not an appropriate representation of an approaching wheel load (AW) because:

- Unlike retaining walls where a vehicle load near the wall increases the overturning moment, a vehicle approaching a culvert produces a small lateral pressure that is resisted by the soil on the far side of the culvert.
- The lateral pressure on a culvert produced by an approaching wheel reduces rapidly with increasing depth of fill.
- The point of highest lateral pressure from an approaching vehicle on a culvert is near the top. This pressure is transmitted directly through the top slab and does not create bending moments.

ASTM standards for precast reinforced concrete box sections with depths of fill less than two feet have always been designed for a lateral pressure resulting from an approaching vehicle using the formula:

$$p\text{-lat}(H) = 700/H < 800 \text{ psf}$$

where:

p-lat = lateral soil pressure resulting from an approaching wheel load at depth H, psf
 H = depth of fill to depth where pressure is calculated, ft

The basis for this change is shown in Figure 71 below. In the figure, the culvert is shown schematically in green. The other plotted lines show the lateral pressures based on the AASHTO LRFD Specifications with a 2 ft surcharge and lateral pressure coefficient of 0.5, ASTM box section specifications, and FEM calculated pressures for three axle positions approaching the culvert from Model 1 of this project.

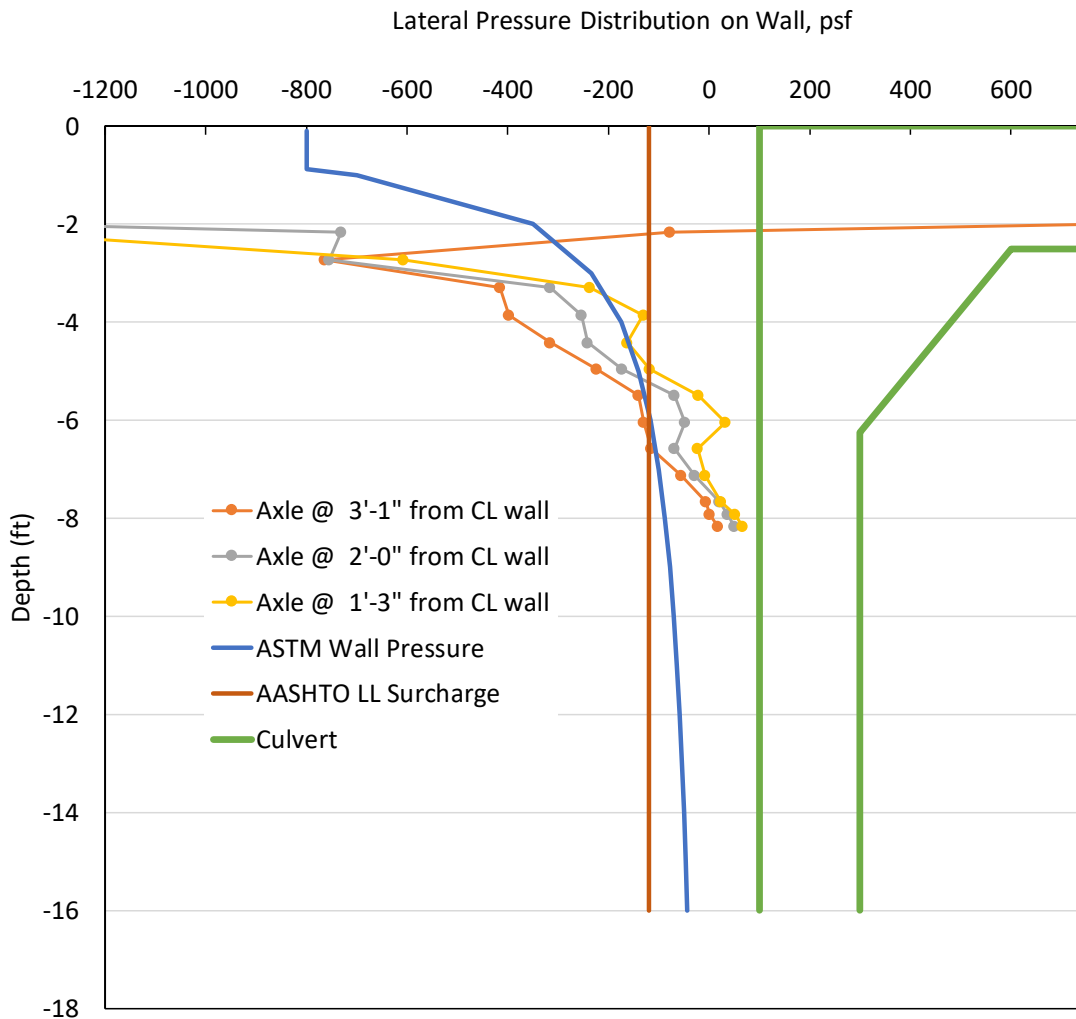


Figure 71 – Approaching Vehicle Lateral Pressure on Culvert Wall vs. Depth

The FEM models show high pressure near the surface that reduces quickly with increasing depth of fill. The ASTM design pressure shows a similar trend, while the LRFD pressure is constant with depth based on the assumption of an additional depth of fill. While the FEM pressures exceed both the ASTM and LRFD pressures at the surface, this is likely not a design issue for several reasons.

- The pressure, shown in the figure are the peak pressures and decrease away from the wheel location.
- The load is primarily transmitted as a thrust through the top slab, reacting with the soil on the far side of the culvert. The moments resulting from this pressure are small. Also, the compression load spreads longitudinally through the slab and the reaction pressure is much smaller than the applied pressure.
- The research team is unaware of any structural issues in a box culvert due to lateral load.

As the load pressure decreases rapidly with increasing depth of fill, it is proposed to require the ASTM approaching wheel load for culverts with depths of fill less than 2 ft and no lateral surcharge for deeper culverts. For the BrDR runs described in the following section, the distributed vertical load was applied at all depths (i.e. even at depths below 2' of top fill), based on the $700/H$ calculation.

For the existing specifications, the following values were input that are used in the calculation of the LS load in BrDR

- Lateral Earth Pressure Coefficient = 0.5
- Surcharge Height = 2.0'
- Unit weight of Soil = 120.0 Pcf

Note: The change made in BrDR was applying a revised LS (now referred to as AW) at all fill depths. The change was applied as shown in Table 16 and Figure 72.

Table 16 – Proposed Lateral Pressure p-lat(H) vs. Current Lateral Pressure qls

Fill Depth (ft)	Proposed-p-lat(H) (ksf)	Current-qls (ksf)
0	0.8000	0.120
0.5	0.8000	0.120
1	0.7000	0.120
1.5	0.4667	0.120
2	0.3500	0.120
2.5	0.2800	0.120
3	0.2333	0.120
3.5	0.2000	0.120
4	0.1750	0.120
4.5	0.1556	0.120
5	0.1400	0.120
5.5	0.1273	0.120
6	0.1167	0.120
6.5	0.1077	0.120
7	0.1000	0.120
7.5	0.0933	0.120
8	0.0875	0.120
8.5	0.0824	0.120
9	0.0778	0.120
9.5	0.0737	0.120
10	0.0700	0.120
10.5	0.0667	0.120
11	0.0636	0.120
11.5	0.0609	0.120

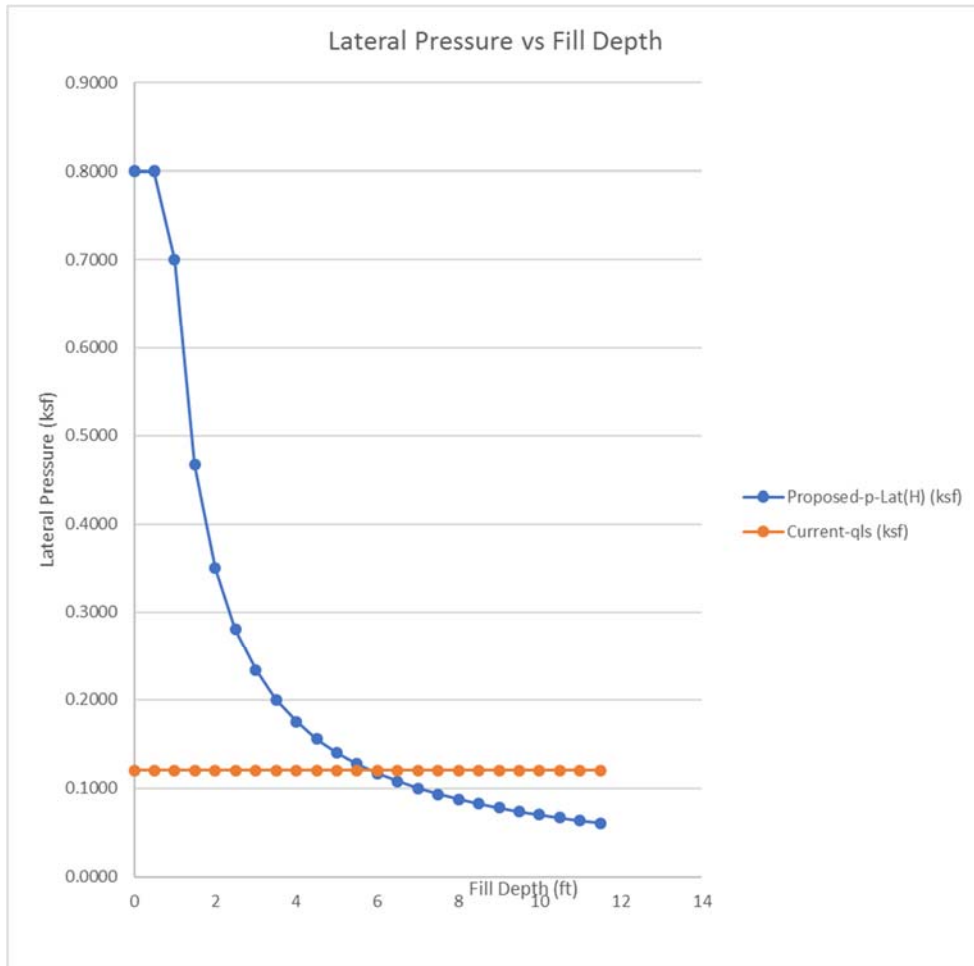


Figure 72 – Lateral Pressure vs. Fill Depth (Proposed/Current)

Economic Impact

Overall the change provided an improvement in the controlling rating factors for many culverts. In many cases, improvement is shown for both less than 2’ of fill and for greater than 2’ of fill. A few cases show a very slight decrease in the overall rating factor (3rd decimal place of the RF). These are all for fill depths less than 2 feet.

Table 17 below represents the culverts that had changes in the controlling HL93 inventory ratings for a randomly selected set of culverts from the Caltrans set and the 3 RC box culverts field tested for this research. A full table showing all of the culverts run and the depths of cover are provided in Appendix G.

For the table below, the average increase in rating factor is about 6.5%, while the maximum increase in rating factor is about 36% - Culvert LS-CD8x8;10 1924-Rev at 5 feet of cover (Inventory 1.453 vs. 0.919).

Table 17 – HL93 Inventory Controlling Rating Comparisons for the Change in LL Surcharge

Culvert	Cover	Inv Rating HL93 (Before)	Oper Rating Factor HL93 (Before)	Inv Rating HL93 (After)	Oper Rating Factor HL93 (After)	Inventory Ratio	Operating Ratio
LS-CD8x8;10 1924-Rev	5 ft Cover	0.919	1.191	1.453	1.883	0.632485	0.632501
LS-CD8x8;10 1933-Rev	3.5 ft Cover	1.625	2.106	1.739	2.254	0.934445	0.934339
LS-CD8x8;10 1933-Rev	4 ft Cover	1.496	1.939	2.119	2.746	0.705993	0.706118
LS-CD10x8;16 1966-Rev	1.9 ft Cover	0.723	0.937	0.736	0.954	0.982337	0.98218
LS-CD10x8;16 1966-Rev	2 ft Cover	0.692	0.897	0.753	0.976	0.918991	0.919057
LS-CD10x8;16 1966-Rev	2.5 ft Cover	0.549	0.712	0.652	0.845	0.842025	0.842604
LS-CD10x8;16 1966-Rev	3 ft Cover	0.401	0.52	0.51	0.661	0.786275	0.786687
LS-CD10x8;16 1966-Rev	3.5 ft Cover	0.249	0.323	0.337	0.437	0.738872	0.73913
LS-CD10x8;16 1966-Rev	4 ft Cover	0.093	0.121	0.134	0.174	0.69403	0.695402
LS-CS10x8;5 1933-Rev	1.5 ft Cover	0.566	0.734	0.569	0.738	0.994728	0.99458
LS-CS10x8;5 1933-Rev	1.9 ft Cover	0.456	0.591	0.494	0.64	0.923077	0.923438
LS-CS10x8;5 1933-Rev	2 ft Cover	0.429	0.556	0.473	0.613	0.906977	0.907015
LS-CS10x8;5 1933-Rev	2.5 ft Cover	0.293	0.379	0.35	0.454	0.837143	0.834802
LS-CS10x8;5 1933-Rev	3 ft Cover	0.157	0.204	0.203	0.263	0.773399	0.775665
LS-CS10x8;5 1933-Rev	3.5 ft Cover	0.023	0.03	0.032	0.041	0.71875	0.731707
LS-CS10x8;10 1933-Rev	7 ft Cover	1.525	1.977	1.758	2.279	0.867463	0.867486
LS-CD12x8;9 1948-Rev	1.9 ft Cover	0.427	0.553	0.448	0.58	0.953125	0.953448
LS-CD12x8;9 1948-Rev	2 ft Cover	0.399	0.517	0.425	0.551	0.938824	0.938294
LS-CD12x8;9 1952-Rev	1.5 ft Cover	0.591	0.766	0.61	0.791	0.968852	0.968394
LS-CD12x8;9 1952-Rev	1.9 ft Cover	0.481	0.624	0.528	0.685	0.910985	0.910949
LS-CD12x8;9 1952-Rev	2 ft Cover	0.453	0.588	0.505	0.655	0.89703	0.89771
LS-CD12x8;9 1952-Rev	3 ft Cover	0.182	0.236	0.233	0.302	0.781116	0.781457
LS-CD12x8;9 1952-Rev	3.5 ft Cover	0.04	0.052	0.054	0.071	0.740741	0.732394
LS-CD12x12;20 2010-Rev	1.9 ft Cover	2.352	3.048	2.369	3.071	0.992824	0.992511
LS-CD12x12;20 2010-Rev	2 ft Cover	2.36	3.059	2.378	3.083	0.992431	0.992215
LS-CD12x12;20 2010-Rev	2.5 ft Cover	2.36	3.059	2.378	3.083	0.992431	0.992215
LS-CD12x12;20 2010-Rev	3 ft Cover	3.232	4.19	3.282	4.254	0.984765	0.984955
LS-CD12x12;20 2010-Rev	3.5 ft Cover	3.651	4.733	3.722	4.825	0.980924	0.980933
LS-CD12x12;20 2010-Rev	4 ft Cover	4.064	5.268	4.161	5.393	0.976688	0.976822
LS-CD12x12;20 2010-Rev	5 ft Cover	4.999	6.48	5.168	6.699	0.967299	0.967309
LS-CS12x8;10 2010-Rev	1.5 ft Cover	1.56	2.022	1.556	2.017	1.002571	1.002479
LS-CS12x8;10 2010-Rev	1.9 ft Cover	1.588	2.059	1.585	2.055	1.001893	1.001946
LS-CS12x12;10 2002-Rev	1.5 ft Cover	1.191	1.544	1.192	1.545	0.999161	0.999353

Culvert	Cover	Inv Rating HL93 (Before)	Oper Rating Factor HL93 (Before)	Inv Rating HL93 (After)	Oper Rating Factor HL93 (After)	Inventory Ratio	Operating Ratio
LS-CS12x12;10 2002-Rev	1.9 ft Cover	1.17	1.516	1.183	1.533	0.989011	0.988911
LS-CS12x12;10 2002-Rev	2 ft Cover	1.238	1.605	1.249	1.619	0.991193	0.991353
LS-CS12x12;10 2002-Rev	2.5 ft Cover	1.334	1.73	1.349	1.749	0.988881	0.989137
LS-CS12x12;10 2002-Rev	3 ft Cover	1.49	1.932	1.505	1.951	0.990033	0.990261
LS-CS14x14;10 2002-Rev	1.5 ft Cover	1.261	1.634	1.281	1.66	0.984387	0.984337
LS-CS14x14;10 2002-Rev	1.9 ft Cover	1.227	1.591	1.249	1.619	0.982386	0.982705
LS-CS14x14;10 2002-Rev	2.5 ft Cover	1.5	1.944	1.504	1.95	0.99734	0.996923
LS-Model 1- Candidate 1-R	1.5 ft Cover	1.458	1.891	1.454	1.885	1.002751	1.003183
LS-Model 1- Candidate 1-R	1.99 ft Cover	1.386	1.796	1.383	1.793	1.002169	1.001673
LS-Model 2- Candidate 1-R	1.5 ft cover	1.475	1.912	1.471	1.907	1.002719	1.002622
LS-CD10x8;9 1948-Rev	1.5 ft Cover	0.331	0.43	0.323	0.419	1.024768	1.026253
LS-CD10x8;9 1948-Rev	1.9 ft Cover	0.215	0.279	0.224	0.291	0.959821	0.958763
LS-CD10x8;9 1948-Rev	2 ft Cover	0.186	0.241	0.197	0.255	0.944162	0.945098
LS-CD10x8;10 2002-Rev	1.5 ft Cover	1.077	1.396	1.072	1.39	1.004664	1.004317
LS-CS7x7;10 2010-Rev	1.5 ft Cover	1.528	1.981	1.529	1.982	0.999346	0.999495
LS-CS10x8;10 1981-Rev	1.5 ft Cover	1.133	1.469	1.129	1.464	1.003543	1.003415
LS-CS10x8;10 1981-Rev	1.9 ft Cover	1.15	1.491	1.152	1.493	0.998264	0.99866
LS-CS10x8;10 1981-Rev	7 ft Cover	1.814	2.351	1.865	2.417	0.972654	0.972693
LS-CS10x8;10 2002-Rev	1.5 ft Cover	1.215	1.575	1.211	1.57	1.003303	1.003185
LS-CS10x8;10 2002-Rev	1.9 ft Cover	1.242	1.61	1.244	1.612	0.998392	0.998759
LS-CS10x8;10 2002-Rev	7 ft Cover	2.106	2.729	2.156	2.795	0.976809	0.976386
LS-CS10x8;10 2010-Rev	1.5 ft Cover	1.51	1.957	1.505	1.951	1.003322	1.003075
LS-CS10x8;10 2010-Rev	1.9 ft Cover	1.558	2.02	1.555	2.016	1.001929	1.001984
LS-CS14x9;10 2002-Rev	1.5 ft Cover	1.106	1.434	1.103	1.429	1.00272	1.003499
LS-CS14x9;10 2002-Rev	1.9 ft Cover	1.084	1.406	1.083	1.403	1.000923	1.002138
LS-CS14x9;10 2002-Rev	2 ft Cover	1.188	1.539	1.19	1.542	0.998319	0.998054
LS-CS14x9;10 2002-Rev	4 ft Cover	1.355	1.756	1.366	1.771	0.991947	0.99153
LS-CS14x9;10 2002-Rev	7 ft Cover	1.28	1.659	1.294	1.677	0.989181	0.989267

CHAPTER 4

Conclusions and Suggested Research

Following are the conclusions and recommendations that can be drawn based on the review of the analysis results shown in this report and in the appendices:

Recommendations – AASHTO LRFD Bridge Design Specifications

- Depth of live load, Article 3.6.1.2a

Currently the AASHTO LRFD Specifications state:

“For single span culverts the effects of live load may be neglected where the depth of fill is more than 8.0 ft and exceeds the span length; for multiple span culverts the effects may be neglected where the depth of fill exceeds the distance between inside faces of end walls.”

This provision requires consideration of live load until the depth exceeds the span; however, in the experience of some members of the research team the provision is often interpreted as ignoring live loads at depths of 8 ft and greater. At a depth of 8 ft, the live load (design tandem) is 36% of the total load and if dropped from design consideration, the net load factor (factored earth load/(service earth plus live load, in psf) is only 1.03. This low factor of safety likely occurred in part because the provision was developed under the Standard Specifications which used $LLDF = 1.75$ resulting in a factored live load of 26% of the factored earth load and a net load factor of 1.14. The proposed provision changes the depth of fill for dropping live load consideration to about 13 ft for the design tandem. At this depth the net load factor when not considering live load is 1.20 and is insensitive to overloaded live load vehicles.

- Live load distribution, Articles 3.6.1.2a, Article 4.6.2.10.2 –

The current specifications for live load distribution through earth fill are discontinuous at a depth of 2 feet of fill due to change from a slab bridge distribution procedure (Article 4.6.2.10) to a distribution through earth fill procedure (Article 3.6.1.2.6). The suggested revision is based on an investigation of this research of this discontinuity in live load distribution and provides a rational alternative to eliminate it. Further, the load distribution for traffic at depths less than 2.0 ft so that distributions in Articles 3.6.2.6 and 4.6.2.10 are both expressed in terms of wheel loads. The new equations in 4.6.2.10.3 provide the expressions necessary to address the interaction of adjacent axles for multi-axle configurations such as tandems and tridem.

- Lateral Pressure Coefficient, Article 3.11.5.1

The proposed addition is intended to achieve consistency between the design and rating specifications. The existing provision for lateral earth pressure in the LRFD Bridge Design Specifications results in a higher pressure than what is specified in the MBE. The proposed revision is also based on successful past practice for the design of reinforced concrete box culverts that are performing well in the field.

- Approaching wheel load, Article 3.11.6.4.1

ASTM standards for precast reinforced concrete box sections (ASTM C1577) with depths of fill less than two feet have been designed for the proposed lateral pressure resulting from an approaching vehicle since the standards were first developed and the loading is also used in AASHTO Standard M273.

Figure 71 (previous chapter) includes results from FEM models of culverts analyzed during NCHRP Project 15-54 which show high pressure near the surface that reduce quickly with increasing depth of fill. The design pressure used for precast box sections (ASTM C1577, identical to AASHTO M273) show a similar trend, while the LRFD live load surcharge pressure is constant with depth based on the assumption of an additional depth of fill. While the FEM pressures exceed both the ASTM and LRFD pressures at the surface, this is not a design issue for several reasons.

- The pressures, are the peak pressures and decrease away from the wheel location.

- The load is primarily transmitted as a thrust through the top slab, reacting with the soil on the far side of the culvert. The moments resulting from this pressure are small.
- The research team is unaware of any structural issues in a box culvert due to lateral load from vehicles.

As the load pressure decreases rapidly with increasing depth of fill, it is proposed to require the ASTM approaching wheel load for culverts with depths of fill less than 2 ft and no lateral surcharge for deeper culverts.

Recommendations – AASHTO Manual for Bridge Evaluation (MBE)

- LRFR Culverts, New Article 6A.10

A new section for rating of culverts in LRFR has been added. This touches on rating issues such as use of spring constants, finite element modeling, use of pavements, shear capacity, and approaching wheel load (live load surcharge). It also includes sections on metal, thermoplastic and fiberglass culverts.

- ASD/LFD Culverts, New Article 6B.10

This section provides guidance for rating culverts that were designed using ASD or LFD.

These recommend changes are presented in the following section. The changes in ballot item format are provided in Appendix H.

Proposed Revisions to the LRFD Specifications and the MBE

Based on the conclusions and proposals presented, the following revisions to the LRFD Specifications and to the MBE are suggested. Deletions and additions are noted. The full background of each proposed revision (in ballot item format) is provided in Appendix H of this report.

The proposed revisions on the following pages are modified from the *AASHTO Manual for Bridge Evaluation, 3rd Edition* and the *AASHTO LRFD Bridge Design Specifications, 8th Edition*, by the American Association of State Highway and Transportation Officials, Washington, DC. Used by permission.

Article 3.6.1.2.6a

Revise the first paragraph of Article 3.6.1.2.6a-General in the Design Specifications as follows:

The effects of live load may be neglected when the factored live load pressure at the surface of the culvert is less than 10% of the sum of the factored earth load plus factored live load pressure.

Article 3.6.1.2.6a**Revise 2nd paragraph**

Live load shall be distributed to the top slabs of flat top three- or four-sided concrete culverts, three-sided arch top concrete culverts or concrete arch culverts over the area calculated in this article, but not less than the dimensions calculated using the procedure specified in Article 4.6.2.10. Live load shall be distributed to concrete pipe culverts with 1.0 ft or more but less than 2.0 ft of cover in accordance with Article 4.6.2.10. Culverts other than concrete with 1.0 ft or more but less than 2.0 ft of cover shall be designed for a depth of 1.0 ft. Culverts with curved tops and less than 1.0 ft of cover shall be analyzed with more comprehensive methods.

Delete 5th Paragraph**Revise Article 4.6.2.10.2****Modify 2nd paragraph and Equations**

Wheel loads shall be distributed to the top slab for determining moment, thrust, and shear as follows:

Perpendicular to the span:

$$E = 28 + t_{d1} + 1.44 S \quad (4.6.2.10.2-1)$$

Parallel to the span:

$$E_{span} = t_{d2} + LLDF(H) \quad (4.6.2.10.2-2)$$

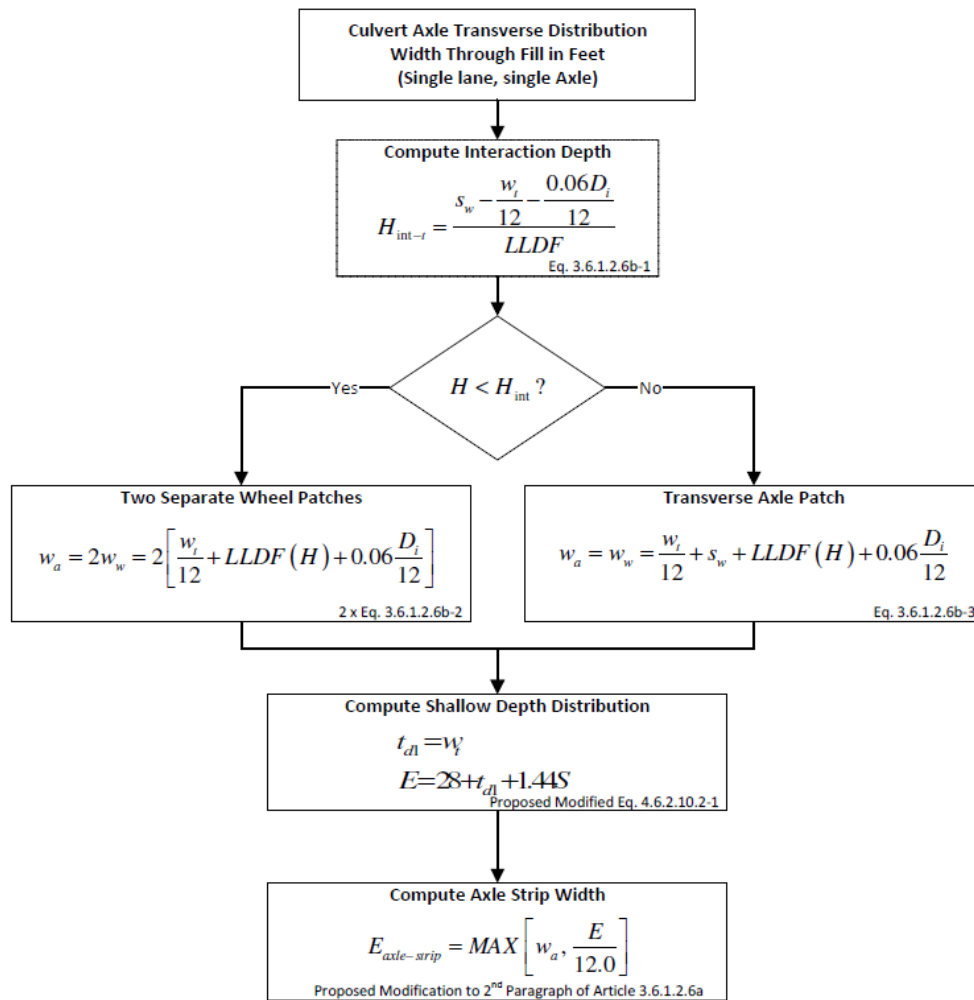
Add to notation

t_{d1} = tire dimension (l_t or w_t , see 3.6.1.2.6) perpendicular to the span

t_{d2} = tire dimension (l_t or w_t , see 3.6.1.2.6) parallel to the span

Revise Article C4.6.2.10.2**Add new paragraph**

Strip widths for culverts are expressed in terms of wheel loads. Culvert spans are typically small and design forces are controlled by single wheel effects. A flowchart illustrating the determination of the transverse distribution (strip width) for a single-axle load through fill is shown in Figure C4.6.2.10.2-1.



Note: This determines the culvert strip width for a single lane, single axle loading in the direction perpendicular to the flow of traffic. The effects of multiple presence, dynamic load allowance and distribution in the direction parallel to the flow of traffic must also be considered as well as the effects of multiple adjacent axles. Equation 4.6.2.10.2-3 can be used to evaluate groups of axles.

Figure C4.6.2.10.2-1 – Single-Axle Transverse Distribution Through Fill

Revise Article 4.6.2.10.3

Traffic traveling perpendicular to the span shall consider multiple lane loadings with the appropriate multiple presence factor. When traffic travels perpendicular to the span, wheel loads shall be distributed to the top slab as specified here:

Perpendicular to the span:

$$E = ((Ax - 1) * 48 + Ax_{sp} + t_{d1} + 1.44 S) / Ax \tag{4.6.2.10.2-3}$$

Parallel to the span:

$$E_{span} = t_{d2} + LLDF(H) \tag{4.6.2.10.2-4}$$

where:

- Ax = No. of axles in axle group
- Ax_{sp} = Spacing of axles in axle group

Revise Article C4.6.2.10.3

Add new paragraph:

When vehicles travel perpendicular to the span, the wheel loads from adjacent axles (e.g. typical tandem and tridem axle configurations) interact. The equations in this section address this.

Article 3.11.5.1

Addition to Article 3.11.5.1

3.11.5.1-Lateral Earth Pressure: *EH*

Add to existing article:

For the design of rectangular reinforced concrete culverts, the lateral pressure coefficient, k_o , need not be taken greater than 0.5 for culverts embedded in granular soils.

Add to existing commentary:

C3.11.5.1

The lateral pressure on culverts is the same on both sides of the structure and produces small culvert forces relative to the forces due to vertical loads. The value of $k_o = 0.5$ has long been used and produces safe designs.

Article 3.11.6.4.1

Add new title to Article 3.11.6.4.1

Article 3.11.6.4.1 Walls

(Section otherwise unchanged)

Add new article:

Article 3.11.6.4.2 Culverts

Concrete box culverts and three-sided flat-topped culverts with a depth of fill less than 2 ft shall be subjected to an approaching wheel load in the form of a lateral soil pressure representing a vehicle approaching the culvert. The pressure shall decrease with increasing depth of fill in accordance with Eq. 3.11.6.4.2-1:

$$\Delta_p(h_d) = 700/h_d \leq 800 \text{ psf} \qquad \text{Eq. 3.11.6.4.2-1}$$

Where:

$\Delta_p(h_d)$ = lateral soil pressure at depth h_d , psf

h_d = depth of fill at which pressure is calculated, ft

The calculated pressure shall be applied to both sides of the culvert model.

This load need not be applied to culverts with a depth of fill over the top slab greater than 2 ft nor to concrete culverts with round tops or metal, thermoplastic or fiberglass culverts.

Add new commentary:

Article C3.11.6.4.1

Retaining walls have historically been designed considering a lateral live load surcharge pressure to represent the additional load applied by a vehicle located near the wall. This loading was historically applied to culverts as well. However, while a lateral load on a wall increases the overturning moment, such a load on a culvert is transmitted through the culvert, largely through compressive thrust and minimal bending moments. The approaching wheel load, Figure C3.11.6.4.1-1, replaces the live load surcharge as more appropriate for culverts.

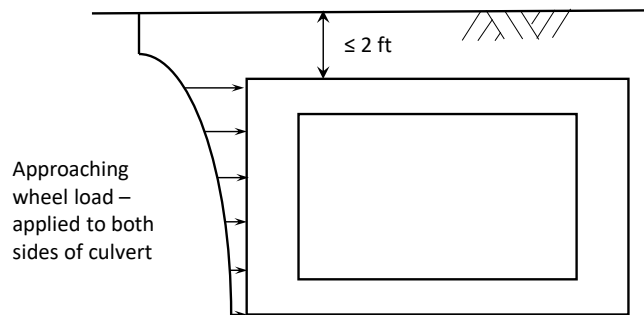


Figure C3.11.6.4.1-1 – Approaching Wheel Load Pressure Condition for Culverts

Delete Article 6A.5.12

As noted, portions of this Article are incorporated into the proposed new Article 6A.10

Add new Article 6A.10 Rating of Culverts

6A.10.1-Scope

This article incorporates provisions specific to the load rating culvert of types designed using the AASHTO LRFD methodology and it provides a load rating that is consistent with that approach. This article assumes culverts have been inspected prior to rating and that the current condition of the culvert can be properly accounted for.

C6A.10.1

Good structural performance of culverts results from interaction of the culvert and the soil it is embedded in. Further, culverts are often designed by product specific methods developed by industry and adopted by AASHTO. This article addresses the issues specific to culverts.

Metal and concrete culverts are often constructed in sizes where rating is mandatory. Thermoplastic, fiberglass, and many metal and concrete culverts are typically not rated; however, brief guidance is provided here for those organizations that rate all culvert types. Older culverts designed using ASD and LFD can also be load rated using these provisions. In cases where the resulting ratings show deficiencies, consideration may be given to rating the culvert using the specifications for which it was designed.

It is common practice for most of the culvert specific variables to be taken directly from the construction documents or standard plans. These include culvert dimensions, materials and material properties, and

installation methods. The data from construction documents, including culvert dimensions, materials and material properties, and installation methods should be confirmed during a visual inspection of the culvert and any discrepancies from the construction documents should be addressed.

6A.10.2-General Rating Requirements

Culvert ratings should recognize that these structures experience several loadings that are not applicable to most bridge superstructures, including vertical and horizontal soil loads and approaching wheel load. Culverts shall be evaluated for the limit states required in design in Article 12 of the AASHTO LRFD Specifications as modified for specific structures herein. Load ratings shall be calculated at critical sections for each load effect to establish the controlling load rating.

6A.10.3-Structural Analysis of Culverts

The analysis of culverts may be based on any rational method acceptable to the owner and consistent with the methods used for design in the AASHTO LRFD Specifications.

C6A.10.3

Analysis procedures for culverts in the AASHTO LRFD Specifications vary widely depending on the culvert shape and material. Concrete box culverts and three-sided culverts are primarily analyzed and designed with computer programs such as simple frame or finite element models. Other shapes and materials are often analyzed through simple empirical procedures, often developed independently by manufacturer's trade associations, and adopted by AASHTO into the LRFD Design Specifications.

6A.10.3.1 Rectangular Concrete Culverts

Rectangular concrete culverts include box culverts and three-sided, flat-top culverts. Structural analysis for rectangular concrete culverts is most often completed with frame models subjected to uniform pressures, but finite element modeling is acceptable.

For box culverts analyzed with frame models, culvert-soil interaction can be mimicked in part by supporting the bottom slab with springs that simulate actual soil support and allowing the soil load to redistribute, much like a beam on elastic foundation. This redistribution of pressure typically reduces the moment and shear forces in the bottom slab as compared to traditional uniformly applied bedding pressure. Spring constants, in the form of moduli of subgrade reaction values, must be selected by a qualified geotechnical engineer based on available site information. General values are presented in Table 6A.10.3.1-1 for consideration. For conditions where a bedding layer is placed over undisturbed native soils, the design value should represent the combined stiffness of the two layers. The native soil layer may have more effect on the combined stiffness than the bedding soil.

Table 6A.10.3.1-1 Modulus of Subgrade Reaction for Bedding Support of Rectangular Concrete Culverts

Soil	Range ² (pci)	Rating Values ³ (pci)
Loose sand	15-60	30
Medium dense sand	35-290	115
Dense sand	230-460	290
Clayey medium dense sand	115-290	200
Silty medium dense sand	85-170	145
Clayey Soils ¹		
$q_u \leq 4$ ksf	40-85	60
$8 \text{ ksf} \leq q_u \leq 4$ ksf	85-170	155
$q_u > 8$ ksf	170	> 230

1. q_u = unconfined compression strength
2. Values for undisturbed native soils can be much higher.
3. Suggested values. Rating engineers must use field data to make a final determination for analysis.

Based on: Bowles, J.E. (1996) *Foundation Analysis and Design, 5th Ed.*, McGraw Hill, New York.

C6A.10.3.1

For cases where springs are modeled, there should be at least 10 support points for springs. Analysis and computations required to rate concrete box culverts is completed with the use of computer programs written for that purpose. A number of programs have been developed over the years; however, these programs often make different assumptions for the analysis model and design. Further, some programs used for design of box sections do not have the features necessary to rate them. Thus, it is possible that a box culvert could be designed with one set of assumptions and rated with another. If the rating program makes more conservative assumptions than the design program, unnecessarily conservative rating factors will result. This section provides guidance for analysis and design features that engineers should evaluate when selecting rating software.

Analysis methods used in these programs fall into two and perhaps three categories:

- Two-dimensional frame (2-D Frame) models – In these programs, a two-dimensional frame model is created and subjected to uniform or linearly varying pressure distributions representing the applied earth, live, and, water (external only for rating) loads. Some programs allow the use of springs to model bottom soil support which mimics culvert-soil interaction and produces some of the benefits of FE modeling discussed next.
- Two-dimensional finite element models – Finite element analysis programs model the box culvert and soil as a continuum of discrete elements each assigned appropriate properties. The inclusion of soil in the model allows a realistic evaluation of culvert-soil interaction. These models often result in pressure distributions that peak at the corners and are reduced at midspan, thus reducing moment and shear forces relative to frame models. Rating with finite element models should only be conducted by engineers experienced with this type of analysis. See discussion of the CANDE finite element model in C6A10.3.3.
- Three-dimensional finite element (3-D FE) models – Currently, full three-dimensional modeling of box culverts is used almost exclusively for research studies as the modeling takes considerable time, expertise, and computer capacity. It is included here as it provides the most complete and accurate model currently possibly of soil-culvert interaction and does not require external decisions

on how to apply and distribute live loads to account for the three-dimensional load spreading that occurs as load is transmitted through the soil.

Specific modeling and design assumptions that engineers should evaluate include the following.

- 2-D Frame vs 3-D FE – 2-D frame models distribute loads as uniform pressures while 3-D FE models include the soil in the model and allow the soil and live loads on the culvert to redistribute due to the flexibility of the culvert and shear strength of the soil. This redistribution results in higher pressures at the corners and lower pressures at midspan which reduces design moment and shear forces.
- 45° Haunches – The use of haunches in the corners of box culverts has varied over time. Older culverts were primarily constructed with cast-in-place methods and used small or no haunches. Newer culverts, and, in particular, precast box culvert sections, almost always use 45° haunches with dimensions often equivalent to the thickness of the culvert slabs. The structural effect of haunches should be considered in analysis. A haunch stiffens the corner of the model resulting in higher moments at the corners and lower moments at midspan. The higher corner moments do not increase the design moment as discussed below.
- Non-45° haunches – Some box sections include haunches that extend further out into the slabs than down the sidewalls. These haunches produce the beneficial stiffening effect noted above, but the critical design section may occur at the tip of the haunch or at the face of the wall. Some 3-sided box sections (no bottom slab) include non-45° haunches.
- Critical design locations – As noted above, the presence of haunches shifts critical design locations. Reinforcement for box culvert corners should be determined based on the moment and thrust at the tip of the haunch. Shear capacity should be based on the moment, thrust, and shear forces at the location d , or d_v from the tip of the haunch.
- Thrust forces – It is common to think of culvert elements as flexural members to be designed considering only the applied moment. However, thrust forces in culverts can be considerable, particularly in the sidewall of deeper box culverts as about 50% of compressive thrust reduces the tension in the reinforcement. Consideration of this thrust produces more economical designs and higher rating factors.

6A.10.3.2 Concrete Arches, Metal, Thermoplastic, and Fiberglass Pipe and Other Metal Culvert Types

Most metal and all thermoplastic, and fiberglass pipe are typically analyzed and rated by the empirical procedures embodied in the LRFD Specifications or by rigorous methods such as finite element models.

6A.10.3.3 – Finite Element Modeling

Finite element-based computer modeling is used routinely for analysis of concrete arch culverts and deep corrugated metal culverts. It may be used for any culvert. Finite element modeling should only be undertaken by engineers experienced in the use of such programs for culvert analysis.

Finite element analysis should consider loadings to mimic reduced lateral pressure as is done for rectangular concrete culverts in frame models. This can be accomplished by adjusting the soil properties, such as by reducing the backfill density.

C6A.10.3.3

The most commonly used program for finite element analysis of culverts is CANDE. Originally developed by the FHWA and upgraded through NCHRP Projects, CANDE offers many features that aid in analyzing and rating culverts, and some that improve rating but are not allowed in the LRFD Design Specifications, including:

- Continuous load scaling (CLS) – this feature permits a live load to spread longitudinally as it is transferred from the top of the culvert to the bottom slab. This feature is appropriate and useful for single lane loadings and not typically available in two-dimensional finite element programs. For multiple lane loadings the LRFD Design Specifications require that the same live load pressure applied to the top slab be applied as reaction on the bottom slab with a multiple presence factor, $m = 1.2$. This approach has been shown to be controlling over multiple lane loadings with $m = 1.0$. Thus, for multiple lane designs, analyze for a single lane without using the CLS feature.
- Soil models – CANDE includes options for several soil models. It is most common to use linear properties for in situ soils, but soft in situ soils may require using a non-linear model. While there is no “correct” non-linear model, most AASHTO culvert specifications are based on the Duncan soil model with the Selig hyperbolic bulk modulus.

Engineers should understand the implications of any finite element program feature prior to applying it to culvert rating.

6A.10.4 Load Rating Equation for Culverts

Load rating of culverts shall be carried out for each load effect using the following rating factor expression with the lowest value determining the controlling rating factor. Limit states and load factors for load rating shall be selected from Table 6A.10.5-1.

$$RF = \frac{C \pm \gamma_{DC} DC \pm \gamma_{DW} DW \pm \gamma_{EV} EV \pm \gamma_{EH} EH \pm \gamma_{ES} ES}{(\gamma_{LL})(LL + IM) \pm (\gamma_{AW})(AW)} \quad (6A.1-4-1)$$

In which, for the strength limit states:

$$C = \varphi_c \varphi_s \varphi R_n \quad (6A.1-4-2)$$

Where:

RF	=	rating factor
C	=	capacity
R_n	=	nominal member resistance (as inspected)
DC	=	dead load effect due to structural components and attachments
DW	=	dead load effect due to wearing surface and utilities
EV	=	vertical earth pressure
EH	=	horizontal earth pressure
ES	=	uniform earth surcharge
LL	=	live load effect
IM	=	dynamic load allowance
AW	=	approaching wheel load
γ_{DC}	=	LRFD load factor for structural components and attachments
γ_{DW}	=	LRFD load factor for wearing surfaces and utilities
γ_{EV}	=	LRFD load factor for vertical earth pressure
γ_{EH}	=	LRFD load factor for horizontal earth pressure
γ_{ES}	=	LRFD load factor for earth surcharge
γ_{LL}	=	evaluation live load factor
γ_{AW}	=	Live load factor for approaching wheel load
φ_c	=	condition factor
φ_s	=	system factor
φ	=	LRFD resistance factor

The product of φ_c and φ_s shall not be taken less than 0.85.

Components subject to combined load effects shall be load rated considering the interaction of load effects.

C6A.10.4

The approaching wheel load replaces the live load surcharge as more appropriate for culverts.

6A.10.5 – Limit States

Culverts shall be load rated for the Strength I load combination for the design and legal loads and the Strength II load combination for permit loads.

The applicable loads and their combinations for evaluation are specified in Table 6A.10.5-1 and in Articles 6A.10.6 through 6A.10.10.

Service limit state for crack width control need not be checked when load rating concrete culverts if internal inspection does not indicate reinforcement corrosion.

C6A.10.5

Maximum and minimum load factors for different loads should be combined to produce the largest load effect. The load cases should be selected to generate the critical combinations of moment, shear, and thrust demands at all critical sections for each load case.

It is prudent to also perform an evaluation of the culvert under permanent loads only if the depth of earth fill over the culvert has changed since the original construction.

Table 6A.10.5-1 Limit States and Load Factors for Culvert Load Rating (Modified from current MBE Table 6A.5.12.5-1)

Bridge Type	Limit State	DC		DW		Design Load ^a		Legal Load ^b	Permit ^b Load	AW AW		EH ^c		EV		ES ^d		
		Max	Min	Max	Min	Inv.	Opr.			Max	Min	Max	Min	Max	Min	Max	Min	
		γ_{DC}	γ_{DC}	γ_{DW}	γ_{DW}	γ_{LL}	γ_{LL}			γ_{LL}	γ_{LL}	γ_{AW}	γ_{AW}	γ_{EH}	γ_{EH}	γ_{EV}	γ_{EV}	γ_{ES}
Reinforced Concrete Box Culvert	Strength I	1.25	0.90	1.50	0.65	1.75	1.35	2.00	—	Same as LF for Design/ Legal Loads	0.00	1.35	0.90 1.0	1.50 1.0	1.50	0.75		
	Strength II	1.25	0.90	1.50	0.65	—	—	—	Table 6A.4.5.4.2a-1	Same as LF for Permit Loads	0.00	1.35	0.90 1.0	1.50 1.0	1.50	0.75		

Notes:

- ^a In addition to the load factor, use the 1.2 multiple presence factor for single-lane loading
- ^b Multiple presence factor is not included and is not required for single-lane loading for permit load vehicles
- ^c Use a 50 percent reduction to *EH* for rating positive moment in top slabs; need not be combined with the minimum load factor
- ^d Use a 50 percent reduction to *ES* for rating positive moment in top slabs; need not be combined with the minimum load factor. Water loads on interior walls are neglected.
- *EH* and *AW* apply only to rectangular concrete culverts.
- *EH* load factor for the minimum condition is taken as 1.0 as this condition is accounted for with a reduced lateral pressure
- If the depth of fill and backfill density are known, maximum load factor for *EV* may be taken as the average of 1.0 and appropriate load factor from AASHTO LRFD Specifications Table 3.4.1-2 culverts.

6A.10.6-Resistance Factors

Resistance factors for culverts shall be taken as specified in LRFD Design Article 12.5.5.

6A.10.7-Condition Factors

Use of condition factors as presented in Table 6A.4.2.3-1 may be considered optional based on an agency's load rating practice.

6A.10.8-System Factor: ϕ_s

The system factor for strength limit states for culverts shall be taken as 1.0

6A.10.9-Materials

No change from current Article 6A.5.12.9

C6A.10.9

No change from current Article C6A.5.12.9

6A.5.12.10-Loads for Evaluation*6A.5.12.10.1-Dead Loads*

No change from current Article 6A.5.12.9

*6A.5.12.10.2- Earth Pressure**6A.5.12.10.2a-Vertical Earth Pressure: EV*

The unit weight of the soil may be taken as shown in LRFD Design Table 3.5.1-1 or in accordance with agency design practice. Weight of earth shall be modified for culvert-soil interaction in accordance with the LRFD Design Specifications for the culvert material being analyzed.

6A.5.12.10.2b-Horizontal Earth Pressure: EH

Lateral earth pressure is only explicitly applied to rectangular concrete culverts analyzed with frame models. It shall be assumed linearly proportional to the depth of soil based on the at rest pressure coefficient as shown in LRFD Design Article 3.11.5.2. The coefficient for the maximum condition need not be taken greater than 0.5 and the coefficient for the minimum condition need not be taken less than 0.25.

Lateral pressure for non-rectangular culverts is embedded in the material specific LRFD Design methods and no additional evaluation is required.

Culverts rated with finite element programs automatically consider lateral soil pressures as part of the culvert-soil interaction. If inspection of flexible culverts shows high deflections, the backfill conditions must be modeled to match those deflections during rating analysis.

6A.5.12.10.2c-Uniform Surcharge Loads: ES

Typically, uniform surcharge loads are not considered in culvert design or rating unless temporary fill will be added over the culvert during or after construction. If applied, the culvert shall be evaluated both with and without the surcharge load.

6A.10.10.3-Live Loads

No change from current Article 6A.5.12.10.3

C6A.5.12.10.3

No change from current Article C6A.5.12.10.3

C6A.5.12.10.3a-Live Load Distribution

Current specification Article 6A.5.12.10.3a with proposed changes listed below.

6A.5.12.10.3a—Live Load Distribution

Distribution of wheel loads for culverts with less than 2.0 ft of fill shall be taken as specified in LRFD Design Article 4.6.2.10. Distribution of wheel loads to culverts with 2.0 ft or more of cover shall be as specified in LRFD Design Article 3.6.1.2.6. ~~Single-span culverts with depth of fill more than 8 ft need not be load rated for live loads as the live load effects are negligible; for multiple span culverts, the effects of live load may be neglected where the depth of fill exceeds the distance between faces of end walls.~~ The vertical live load should be applied as a moving load across the top of the culvert structure.

Culverts with deep fills should be evaluated for the effects of permanent loads only.

C6A.5.12.10.3a

~~For culverts with depth of fill greater than 8 ft, the live loads will constitute a negligible portion of the overall loading.~~ The capacity of the culvert should be checked for permanent loads only for the possible ultimate demand obtained by the maximum and minimum load factors.

Box culverts are normally analyzed as two-dimensional frames. Equivalent strip widths defined in LRFD Design Article 4.6.2.10 for box culverts with depth of fill less than 2 ft are used to simplify the analysis. ~~Distribution length parallel to the span may be conservatively selected in most load ratings.~~

For earth fills of 2 ft or more, the tire contact area for distribution purposes may be taken as 20 in. wide × 10 in. long, for a wheel of one or two tires (LRFD Design Article A3.6.1.2.5). For other truck loads, the tire area may be calculated following the provisions of LRFD Design ~~Article C3.6.1.2.5.~~ Lane loads are distributed ~~only transversely.~~

~~LRFD Design Article 3.6.1.2.6 states that wheel loads may be considered to be uniformly distributed over a rectangular area with sides equal to the dimensions of the tire contact area and increased by 1.15 times the depth of fill in select granular backfill. Where such areas from multiple wheels overlap, the total load should be uniformly distributed over the area but the total width of distribution shall not~~

Change 1 - Replace deleted sentence with:

Culverts where design for live load is not required per the LRFD Design Specifications Article 3.6.1.2.6a do not require rating for live loads.

Change 2 – Deleted sentence. No replacement.

Change 3 – Replace deleted sentence with:

Distribution parallel to the span with increasing depth is accomplished by adding LLDF * Depth of fill to the tire dimension. Per LRFD Design Specifications Article 4.6.2.10.

Change 4 – Replace deleted sentence with:

Lane loads are only considered for culverts with spans greater than 20 ft.

Change 5 - Delete entire paragraph (only a portion of the deleted paragraph is shown above). No replacement.

6A.10.10.3b-Dynamic Load Allowance: IM
No change from current Article 6A.5.12.10.3b

C6A.5.12.10.3b

No change from current Article C6A.5.12.10.3b

6A.10.10.3c – Approaching Wheel Load

Rectangular concrete culverts with less than or equal to 2 ft of cover shall be loaded with a lateral pressure distribution to produce the effects of a truck axle just before going over the culvert. This pressure shall be computed using Eq. 6A.10.10.3c-1 and shall be applied to both sides of the culvert.

$$p\text{-lat}(h_d) = 700/h_d \leq 800 \text{ psf} \qquad \text{Eq. 6A.10.10.3c-1}$$

where:

$p\text{-lat}(h_d)$ = lateral soil pressure resulting from an approaching wheel load at depth h_d , psf
 h_d = depth of fill to depth where pressure is calculated, ft

The approaching wheel load need not be considered for culverts with more than 2 ft of fill from top of culvert to top of pavement.

C6A.10.10.3c

Culverts have traditionally been evaluated for a live load surcharge that is appropriate for earth retaining structures. The live load surcharge is not appropriate for rectangular culverts for the following reasons:

- Unlike retaining walls, where a vehicle load near a wall increases the overturning moment, a vehicle approaching a culvert produces a small lateral pressure that is resisted by the soil on the far side of the culvert.
- Lateral pressure near the mid-height of the wall will result in an increase in positive moments in the sidewall and negative moments at the corners and a decrease in positive moments in the slabs. Lateral pressure near the top of a shallow culvert primarily results in a thrust in the top slab which has almost no effect on the moments, and hence the reinforcement requirements.

This approaching wheel load has been used in AASHTO and ASTM standards for precast concrete box culverts for over 40 years. It was first proposed by Heger, F.J. and Long, K.N. (1976) *Structural Design of Precast Concrete Box Sections for Zero to Deep Cover Earth Cover Conditions and Surface Wheel Loads, Concrete Pipe and the Soil-Structure System*, ASTM STP 630.

6A.10.10.3d - Pavements

Pavements are used to spread the effects of wheel loads over a greater area and thus reduce soil stresses below the pavement. Rating engineers may consider the effects of asphalt or concrete pavements in reducing the loads applied to culverts. This can be completed using finite element soil-structure interaction analyses which can directly model the pavement layer, or with elasticity based or empirical procedures. Such analyses must consider the current and expected future condition of the pavement. Analysis of asphalt pavements must consider anticipated temperature effects on properties.

C6A.10.10.3d

Most culverts are designed without consideration of the improved load distribution resulting from pavements over the culvert. The only exception to this is some metal box section designs as detailed in LRFD Article 12.9.4.6. The effect of pavements is ignored primarily to allow for construction loads prior to placement of pavement. The finite element analysis culvert program most commonly used for analysis, design, and rating of culverts is CANDE, originally developed by FHWA and later updated by AASHTO through the NCHRP Program. Empirical procedures for considering pavements include elasticity theory procedures for layered systems and the Westergaard procedure for distributing live loads through concrete pavements as embodied in the American Concrete Pipe Association's *Concrete Pipe Handbook*.

Table C6A.10.10.3d-1 presents guidance on the conditions and locations where pavements are effective in reducing loads on culverts.

**Table C6A.10.10.3d-1
Pavement Effect in Distributing Live Load on Culverts**

Pavement thickness, in.	Asphalt stiff subgrade	Asphalt soft subgrade Concrete stiff subgrade	Concrete soft subgrade
	E1/E2 ~3	E1/E2 ~ 35	E1/E2 ~ 400
4	NB	NB	0.50 / 5 ft
8	NB	0.60 / 6 ft	0.25 / 6 ft
16	0.75 / 6 ft	0.50 / 7 ft	0.15 / 8 ft

Where:

- E1 = modulus of pavement layer
- E2 = modulus of soil subgrade
- NB = no benefit
- The data lines, such as 0.50 / 5 ft indicate the reduction that may be applied to the live load at the surface of the pavement and the depth at which no benefit is derived in reducing pavement load.

Table C6A.10.10.3d-1 is derived from an elastic solution derived by Fox and presented in Poulos, H.G., and Davis, E.H. (1991) Elastic Solutions for Soil and Rock Mechanics, which is available at <http://research.engr.oregonstate.edu/usucger/PandD/PandD.htm>, and uses the following assumptions:

- E-concrete pavement = 4,000 ksi
- E-asphalt pavement = 0.3 ksi
- E-soft subgrade approximately 8 ksi
- E-stiff subgrade approximately 100 ksi

One relationship between the soil modulus and the common parameters, as recommended by the Federal Aviation Administration Advisory Circular 150/5320-6E, 2016, are:

$$E = 1,500 \text{ CBR} \quad \text{Eq. C6A.10.10.3d-1}$$

$$E = 20.15 k^{1.284} \quad \text{Eq. C6A.10.10.3d-2}$$

Where:

- E = modulus of elasticity of subgrade, psi
- CBR = California bearing ratio
- k = modulus of subgrade reaction, pci

Note that Eqs. C 6A.10.10.3d-1 and C6A.10.10.3d-2 provide values of subgrade modulus considerably higher than typically used in culvert backfill design.

As an example, for an 8 in. concrete pavement with a soft subgrade, the live load could be reduced to 25% of the applied load for a culvert directly under the pavement and there would be no reduction if the culvert is more than 5 ft below the pavement. Linear extrapolation can be used to determine the reduction for intermediate depths.

6A.10.11 - Concrete Culverts

6A.10.11.1 Design for Shear

The shear strength of culverts without prestressing and with less than 2.0 ft of cover that are performing well based on inspection can be evaluated with a modified approach to shear capacity. Use the General Procedure for shear strength in LRFD Design Specifications Article 5.7.3.4.2, substituting the following procedure to compute the strain in the reinforcement:

$$\varepsilon_s = \frac{|M_{u-mod}| + 0.5 N_u + V_u}{E_s A_s d_v} \quad \text{Eq. 6A.10.11.1-1}$$

Where M_{u-mod} is the factored moment at the critical shear design location, which may be modified as follows if it is a negative moment:

$$M_{u-mod} = M_u \frac{96 + 1.44 S}{96 + 5.47 S} \quad \text{Eq. 6A.10.11.1-2}$$

where:

S = clear span of the culvert (ft) – (same value as used in 4.6.2.10.2-1)

Use the unmodified M_u if the controlling factored moment is positive. Further, the limitation that the minimum value of $M_u = V_u d_v$ does not apply.

This expression can be applied to box sections analyzed and designed with two-dimensional frame or finite element models.

The use of springs to represent bedding pressure noted in Article 6A.10.3.1 results in reduced shear and moments. The rating factors for the lower half of box culverts analyzed in this manner may be applied to the locations in the upper half of the culvert provided the following conditions are met:

- The culvert is installed at a depth where live load is not considered.
- The reinforcing in the upper half of the culvert matches that in the lower half.

C6A.10.11.1

Many concrete culverts that have been in service and performed well for many years have rating values less than 1.0 due to computing shear strength by current procedures. There are two primary reasons for this:

- Past editions of AASHTO Specifications have allowed designers to assume shear strength is adequate if the section is properly designed for flexure.
- Frame models of box sections are inherently conservative due to the assumption of uniform pressures to model vertical loads.

The equations in this section provide a moderately increased shear capacity to reflect this history. The reduction in negative moment at the critical section is based on:

McGrath, T.J., A.A. Liepins, and J.L Beaver, "Live Load Distribution Widths for Reinforced Concrete Box Sections", *Transportation Research Record: Journal of the Transportation Research Board, CD 11-S*, Transportation Research Board of the National Academies, Washington, DC, 2005, pp 99-108.

Culvert inspections should evaluate flexural cracking or concrete crushing which could indicate the culvert is carrying more load than considered in design.

C6A.10.12 - Metal Culverts

Metal culverts should only be rated after a field inspection has documented the culvert shape and condition. Metal Culverts should be analyzed for service and factored forces in accordance with the LRFD Design Specifications and appropriate provisions of this manual. Suitable adjustments should be included to consider the current condition of the culvert.

Metal culverts that are designed using finite element modeling must be rated with the same analysis method. Modeling must consider installation conditions that produce the culvert shape observed in the field.

C6.A.10.12

The long-term performance of these culverts is dependent on the performance of the backfill soil around the culvert. The culvert shape is a key indicator of backfill quality and careful measurements in the field are warranted.

National Corrugate Steel Pipe Association (NCSPA) Design Data Sheet No. 19 provides recommended procedures for rating metal culverts and suggested adjustments based on existing conditions. Rating engineers should note that the design methods and load factors for the several types of metal culverts are quite different as they are often empirical or semi-empirical. In addition to loss of section due to corrosion, the field inspection should document the shape of the culvert.

6.A.10.13 -Thermoplastic and Fiberglass Culverts

Thermoplastic and fiberglass culverts should only be rated after a field inspection has documented the culvert shape and condition. Such culverts should be analyzed for service and factored forces in accordance with the LRFD Design Specifications and appropriate provisions of this manual. Suitable adjustments should be included to consider the current condition of the culvert. The effect of the observed deflected shape on culvert forces must be considered.

C6A.10.13

Thermoplastic and fiberglass culverts are both considered flexible. The long-term performance of these culverts is dependent on the performance of the backfill soil around the culvert. The culvert shape is generally a key indicator of backfill quality and careful measurements in the field are required.

Add New Article 6B.9**Article 6.B.9**

Culverts may be load rated in accordance with the current LRFD Specifications or with the specifications under which they were originally design. Culvert ratings based on older specifications must be inspected prior to rating and the current conditions must be considered.

C6.B.9

Concrete pipe, metal, thermoplastic, and fiberglass pipe are essentially designed by the same methods as were incorporated into prior bridge design specifications and, thus, most should rate in accordance with the current LRFD Specifications. Reinforced concrete box sections have been designed under AASHTO Specifications for many years and the provisions have changed such that many do not meet current standards. This is particularly true for shear strength, as some editions of AASHTO Specifications did not require design for shear in slabs, such as the top and bottom slab of box culverts. This article allows rating engineers to take advantage of the less demanding older specifications provided the culvert has demonstrated good performance and the loading has not changed since prior ratings.

Article 6A.10 provides several provisions for analysis and rating that will assist engineers using older specifications for rating.

Suggested Research

In addition to the results of the research and recommendations provided in the previous section, the following are recommended follow-ups to the research of this project:

- Updates to CANDE – The CANDE software was updated for this project and is included as part of the deliverable. While in some cases the analysis engine was updated, time and budget constraints prevented the CANDE graphical user interface from being updated. The software is not unusable in its current form but should be updated so that the GUI input matches the formatted text input of the analysis engine.
- Updates to the CANDE Tool Box – while this was not a software development project, the CANDE Tool Box was developed for this research to facilitate the investigation. Currently the CANDE Tool Box runs as a separate pre-processor and post-processor to the CANDE software. While the software worked well for this research and can continued to be used, the integration of these tools into the CANDE software would be beneficial to future users.
- CANDE import – An export file from BrR to CANDE could be developed to allow for box culverts developed in BrR be exported to CANDE input files for further analysis. Conversely, an export file from CANDE to a BrDR could also be created so that CANDE models could be imported into BrDR. This would need to be discussed under the AASHTOWare contract.
- LFRD-LFD comparison – and initial comparison of the LFRD/LFD ratings for a set of reinforced concrete box culverts were made for this project using BrR. A full review of these results was not completed for this project and perhaps this comparison could be made with the culverts gathered for this research. (See Appendix L).

Data Archiving

Upon completion of the analysis and testing program phases, many data are available that could aid future researchers. This section provides a description of the data that is delivered this project These include but are not necessarily limited to:

- Any changes in the CANDE software that are used for this project
- CANDE input files used for this research project
- AASHTOWare BrDR export files (XML) of all culverts analyzed for this project
- AASHTOWare regression data with newly created report ID's defined
- 3D FEM model files used during the analysis phase
- Field testing data

The files described above are documented and included as a final delivery for the research project. The full documentation of the files is provided on the media on which it is delivered. The following sections provide a brief description of the anticipated data included for each item.

Changes to the CANDE Software

The revised CANDE software, both program source code and compiled installation versions of the software is provided. This code is documented and new features of the software are documented within the programs User Manuals. A new manual is provided for the CANDE Tool Box software is provided on the media (see Appendix C of this report as well). A revised installation of the software is also provided.

CANDE Input Files

The CANDE input files used for this project are documented and included on the media delivered with the final report. The documentation includes descriptions of each file or groups of files along with a summary description of the contents.

AASHTOWare BrDR Export Files (XML)

The AASHTOWare BrDR software has the intrinsic capability to export bridge files (in this case culvert files) to an XML format that can then be reimported into future versions of the software. The BrDR export files for each culvert used in this research are included on the media delivered with this project. This includes the test suite provided by Caltrans and revised for this project along with additional BrDR culvert files created for this project. The files are documented in a summary form and are included with the delivered research data.

AASHTOWare BrDR Regression Data/Report ID Descriptions

AASHTOWare BrDR has the ability to produce output data in a format similar to that developed for NCHRP 12-50. The data for each of the culverts run in the current version of BrDR will be saved for use in comparison with BrDR data after specification changes have been implemented. This type of comparison is referred to as regression testing. The regression testing data for culverts in AASHTOWare BrDR was recently updated and can be useful for this type of testing. The regression test files from both original version of BrDR with unchanged specs along with the regression data from the revised specs are included in the data delivery. The data includes a summary document of each file or groups of files.

In addition, a document providing a description of the report IDs is provided. For a description of 'report IDs, see *NCHRP Report 485: Bridge Software–Validation Guidelines and Examples*.

3D FEM Files

The research team used the LUSAS finite element modeling software to perform all of the 3D analyses required as part of the analytical work performed for NCHRP 15-54. In an effort to preserve the data for future use, the archival of the native LUSAS command (data input) files will be supplemented by also saving the model data in one of the various neutral and/or third party formats available as export options within the current version of LUSAS. Below is a summary of the various file formats supported in LUSAS for importing and exporting model data.

Interface file name and extension	Import file into LUSAS?	Export file from LUSAS?
CMD (.cmd)	YES	YES
SOLVER Data File (.dat)	YES	NO
DXF (.dxf)	YES	YES
IGES (.igs)	YES	YES
LMS CADA-X (.nf)	YES	YES
NASTRAN Bulk Data Files (.bdf, .dat)	YES	NO
ANSYS (cdb)	YES	NO
ABAQUS (.input)	YES	NO
PATRAN (.def)	YES	NO
STEP (.step, .stp)	YES	YES
STL (.stl)	YES	YES

Interface files are used to transfer external modeling or material data into and out of LUSAS Modeller. The full model or a selected portion of a model can, dependent upon the file format chosen, be exported to a chosen interface file.

The currently supported list of interface file formats is:

- **CMD (.cmd)** Format for import of LUSAS Modeller model files saved as command (CMD) files in previous versions of LUSAS.
- **Solver Data Files (.dat)** LUSAS Solver data files (used to import or node and element data).
- **DXF (.dxf)** AutoCAD Drawing eXchange Format.
- **IGES (.igs)** Initial Graphics Exchange Specification. Format for import and export of geometry data.
- **LMS CADA-X (.nf)** Model description and modal data exported to a file that can be read by the LMS software.
- **NASTRAN Bulk Data files (.bdf, .dat)** (used to import node and element data).
- **ANSYS cdb files (.cdb)** (used to import node and element data).
- **Abaqus input files (.inp)** (used to import node and element data).
- **PATRAN (.def)** Neutral file format for inputting phase I geometry information and outputting phase II mesh information.
- **STEP (.stp)** Standard for the Exchange of Product data.
- **STL (.stl)** Stereolithography data files.

Field Testing Data

The raw data files arising out of the field testing effort is include along with the post-processed data that is also be archived in a readily accessible format, e.g., Microsoft Excel spreadsheets or ASCII text files. The content of the files is documented for content and format.

List of Appendices

Appendix A	Survey	Electronic media
Appendix B	Survey Results	Electronic media
Appendix C	CANDE Tool Box User Manual	Electronic media
Appendix D	2D Analysis Backup	Electronic media
Appendix E	3D Modeling backup	Electronic media
Appendix F	Field Testing Plans	Electronic media
Appendix G	Specification Backup	Electronic media
Appendix H	Proposed Agenda Items	Electronic media
Appendix I	Live Load Improvements	Electronic media
Appendix J	Regression Data Mined	Electronic media
Appendix K	3D Model Calibrations	Electronic media
Appendix L	Caltrans Models	Electronic media
Appendix M	3D Culvert Approach	Electronic media

Appendix A – Survey Questions

Appendix A – Survey Questions / Follow-up Questions

The following pages are is a list of questions provided in the survey. The survey was developed using the SurveyMonkey® web site and was distributed to a list of emails for AASHTO SCOBS and for the AASHTOWare BrDR User group.

At the end of this Appendix is a list of questions asked to those participants requesting a follow-up phone calls.

Appendix A – Survey Questions

On-line Survey Questions

NCHRP 15-54 Survey: Proposed Modifications to AASHTO Culvert Load Rating Specifications

1. NCHRP 15-54 Survey: Proposed Modifications to AASHTO Culvert Load Rating Specifications

As Co-Principal Investigators for NCHRP project 15-54 “Proposed Modifications to AASHTO Culvert Load Rating Specifications” we seek your input regarding your states culvert rating via the attached survey. A synopsis of this project can be viewed directly at the following URL:

<http://apps.trb.org/cmsfeed/TRBNetProjectDisplay.asp?ProjectID=3869>

This survey of information will ultimately help us with the development of a field testing and analysis program for the purposes of modifying the AASHTO Manual for Bridge Evaluation for culvert load rating.

If your state participates in the AASHTOWare™ BrDR software development, we also ask that you consider providing data from your AASHTOWare database related to culvert rating, particularly if you have issues with culverts that do not rate successfully.

If you have input for other commercially available software, we would also be interested in those input files as well.

Thank you for your participation.

Mark Mlynarski, P.E.	Michael Baker International	Co-principal Investigator	412-269-7933
Chad Clancy, P.E.	Modjeski and Masters	Co-principal Investigator	717-790-9565

You may call one of the above numbers to discuss this survey.

Michael Baker
INTERNATIONAL



Appendix A – Survey Questions

NCHRP 15-54 Survey: Proposed Modifications to AASHTO Culvert Load Rating Specifications

2. Enter location information

1. For which state or U.S. territory DOT/Organization do you work?

<input type="radio"/> Alabama <input type="radio"/> Alaska <input type="radio"/> American Samoa <input type="radio"/> Arizona <input type="radio"/> Arkansas <input type="radio"/> California <input type="radio"/> Colorado <input type="radio"/> Connecticut <input type="radio"/> Delaware <input type="radio"/> District of Columbia (DC) <input type="radio"/> Florida <input type="radio"/> Georgia <input type="radio"/> Guam <input type="radio"/> Hawaii <input type="radio"/> Idaho <input type="radio"/> Illinois <input type="radio"/> Indiana <input type="radio"/> Iowa <input type="radio"/> Kansas <input type="radio"/> Kentucky <input type="radio"/> Louisiana <input type="radio"/> Maine <input type="radio"/> Maryland <input type="radio"/> Massachusetts <input type="radio"/> Michigan	<input type="radio"/> Minnesota <input type="radio"/> Mississippi <input type="radio"/> Missouri <input type="radio"/> Montana <input type="radio"/> Nebraska <input type="radio"/> Nevada <input type="radio"/> New Hampshire <input type="radio"/> New Jersey <input type="radio"/> New Mexico <input type="radio"/> New York <input type="radio"/> North Carolina <input type="radio"/> North Dakota <input type="radio"/> Northern Marianas Islands <input type="radio"/> Ohio <input type="radio"/> Oklahoma <input type="radio"/> Oregon <input type="radio"/> Pennsylvania <input type="radio"/> Puerto Rico <input type="radio"/> Rhode Island <input type="radio"/> South Carolina <input type="radio"/> South Dakota <input type="radio"/> Tennessee <input type="radio"/> Texas <input type="radio"/> Utah <input type="radio"/> Vermont <input type="radio"/> Virginia <input type="radio"/> Virgin Islands <input type="radio"/> Washington <input type="radio"/> West Virginia <input type="radio"/> Wisconsin <input type="radio"/> Wyoming
---	--

Other (please specify)

Appendix A – Survey Questions

NCHRP 15-54 Survey: Proposed Modifications to AASHTO Culvert Load Rating Specifications

3. Culvert Types

2. Are you currently using LRFR to load rate existing Culverts?

- Yes
- No

If the answer to the question above is "Yes", what types of culverts are you rating using LRFR and what types using alternate methods?

3. What types of culverts (material) does your state currently rate?(In the comment box, please provide the name of any software packages used for rating for each culvert type)

- Steel/ Metal corrugated
- Concrete Box
- Concrete Pipe
- Thermoplastic

Other (please list) Also list any software used to rate a specific culvert type

Appendix A – Survey Questions

NCHRP 15-54 Survey: Proposed Modifications to AASHTO Culvert Load Rating Specifications

4. Culvert issues and studies

4. Does your state have issues with rating culverts? (e.g. culverts that do not rate, but do not appear to be in distress)

Yes

No

5. If your answer to Question 3 above is "Yes", provide a brief description next to any specific type of culvert for which you experience an issue, i.e. project failure mode and location. Also note which of the following culvert types are most prone to failing load rating.

Steel/ Metal corrugated

Concrete Box

Concrete Pipe

Thermoplastic

Other (please list)

6. With respect to the previous question above, please describe any workaround procedures your agency has used to modify load ratings for culverts that show deficient load ratings but are performing well in service (to avoid posting or closure).

7. Has your state performed any studies or research related to the rating of culverts that you would be willing to share with the research team?

Yes

No

If 'Yes' please describe below and if possible, please provide contact information for the lead researcher.

Appendix A – Survey Questions

NCHRP 15-54 Survey: Proposed Modifications to AASHTO Culvert Load Rating Specifications

5. Culvert software

8. What software do you use for analysis/rating? (check any that apply)

- CANDE
- AASHTOWare BrR
- BOXCAR
- BRASS

Other (provide description)

9. Would you be willing to provide input files for culverts rated by your state agency?

- Yes
- No

If 'Yes' which software program(s)? How many input files would you be able to provide?

Appendix A – Survey Questions

NCHRP 15-54 Survey: Proposed Modifications to AASHTO Culvert Load Rating Specifications

6. Contact information/ further discussion

10. Do you wish to discuss over the phone your state's practices and issues related to culvert rating?

Yes

No

If 'Yes' please provide contact information.

11. Do you have any other concerns related to culvert rating that you think would be beneficial to this research (i.e. shortcomings of the culvert load rating specifications that need to be addressed)?

Appendix A – Survey Questions

Follow-up Interview Questions

The following is a list of questions asked during the follow-up phone interviews:

Q: Do you have any issues with the current MBE/FHWA requirements for load rating of culverts? *If so, please also note the type(s) of culverts that are having issues, describe what is controlling (low) ratings, design method used, age of culverts with issues, etc.*

Q: Is the currently available software adequate for performing required load ratings?

Q: Have you used refined methods to rate culverts (such as CANDE) when issues arise?

Q: Are you aware of any culvert-related research performed by your agency that would be helpful in our investigation?

Q: Do you have any other concerns related to load rating of culverts?

Q: If you have any culvert input data (for AASHTO BrR or CANDE), particularly for problem culverts, we would be interested in making use of this for our research so please indicate whether you would be able to contribute any input files.

Appendix B- Complete Survey Results

Appendix B – Complete Survey Results

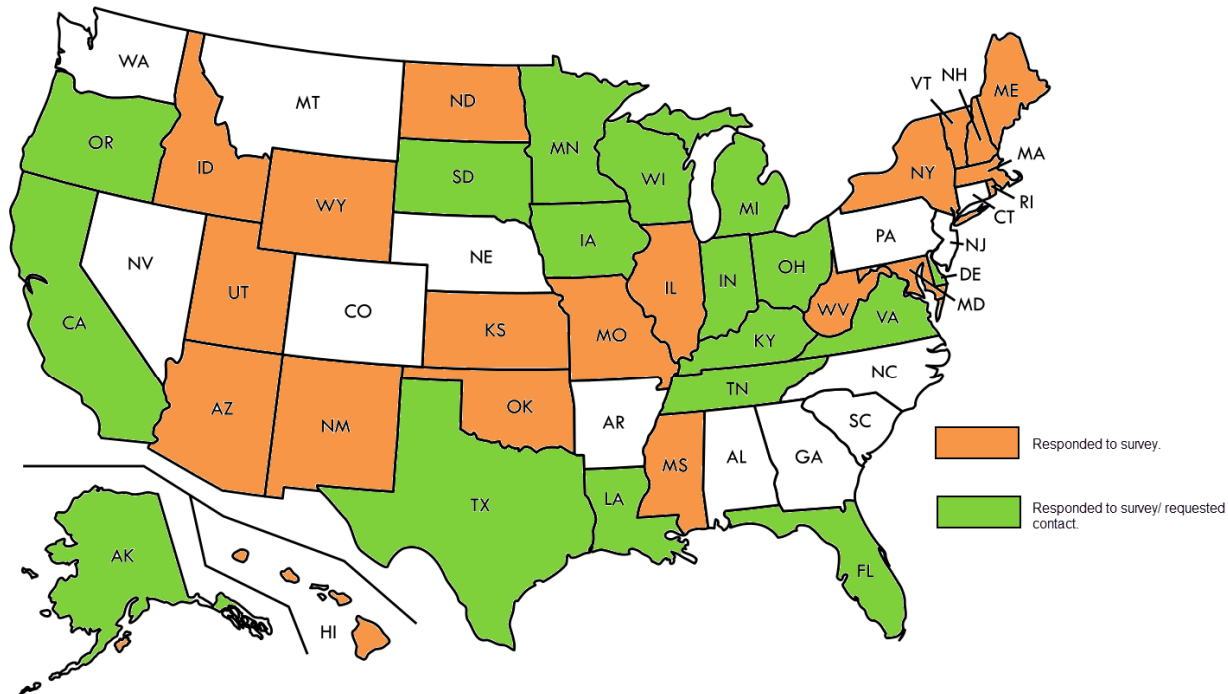
The following pages provide the complete survey results with state and email information removed. This appendix also includes survey questions asked during the follow-up phone interviews.

Appendix B- Complete Survey Results

On-line survey questions/responses

Q1: For which state or U.S. territory DOT/Organization do you work?

- Answered: 41
- Skipped: 1



Also included:

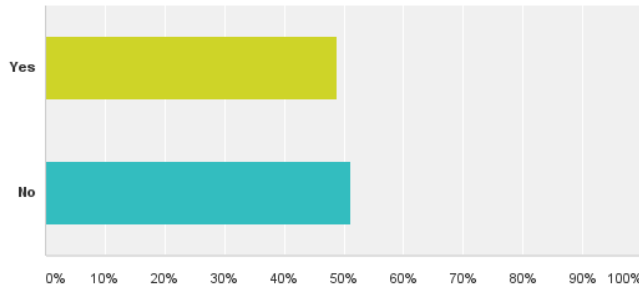
- Army Corp of Engineers
- District of Columbia

Appendix B- Complete Survey Results

Q2: Are you currently using LRFR to load rate existing Culverts?

Q2 Are you currently using LRFR to load rate existing Culverts?

Answered: 41 Skipped: 1



If the answer to the question above is “Yes”, what types of culverts are you rating using LRFR and what types using alternate methods?

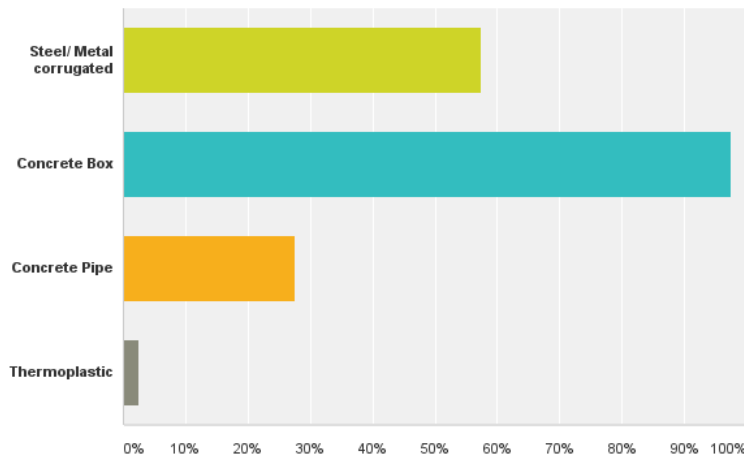
Only culverts that were designed per LRFD.
We have only rated concrete box culverts using LRFR but for all culverts qualifying as "bridges" we intend to rate all types of culverts based on LRFR if LRFR specifications exist.
Existing culverts would use the same specification used in the design of the culvert to load rate the culvert whether it be ASD, LFD or LRFD. Just to clarify, New York State only load rates "bridge size" culverts and three-sided frames, implying a clear span in excess of 20 feet when measured horizontally along the center line of roadway.
I exclusively use the MBE LRFR procedures for precast and cast-in-place arch and box culverts. I have used ASTM C 76 for RCP and ASTM A 796 for CMP.
Only new culverts designed by LRFD for the HL-93 loading are rated by LRFR. All older culverts are rated by LFR.
Metal and Concrete Box.
concrete box culverts, CMPs, structural steel box culverts using LRFR.
We are planning to start using LRFR to load rate NBI length reinforced concrete box culverts and metal pipe culverts. We will begin this task this fall/winter.
We use BrR to rate three-sided culverts an box culverts. We use Smartculvert to rate conspan type structures.
Our initial load rating of RC Box culverts using AASHTOWare BrR software yielded zero rating factor. As a result, we have initiated an investigate study to find out the reason for zero rating factor. Initial findings are (1) software were mis-coded whenever axial and moment interaction occurs (2) rating factor equations are not coded properly (3) load factors and earth pressure given within MBE seems to be too high.
Concrete box/frame culverts using BRASS-LRFR.
Culverts designed after October 1, 2010 are load rated using LRFR. All culverts designed previous to Oct. 1, 2010 are load rated using LFR.
There are a few instances where design plans for culverts are not available, in which case, the culvert is rated using an engineering judgment procedure.
RC Box Culverts - LFR & LRFR RC 3-sided frames - LFR & LRFR CMP - LFR & LRFR.
Reinforced Concrete Box culverts.
LRFR is used for those culverts designed by LRFD. We use LFR and ASR for those designed as such.
we rate all culverts with LRFR first. if the LRFR results lead to load posting or load restriction, the results will be compared with LFR results and favorable ratings are used. According to Iowa DOT design manual, LFR has two different earth load definitions. One is the same as AASHTO specification and called AASHTO load; the other one is called office load, with which, the lateral earth pressure applied on the exterior walls is taken as an equivalent fluid pressure of 36 psf foer foot.
Existing culverts designed LRFD are rated LRFR. All other culverts are LFD rated.

Appendix B- Complete Survey Results

Q3: What types of culverts (material) does your state currently rate? (In the comment box, please provide the name of any software packages used for rating for each culvert type.)

Q3 What types of culverts (material) does your state currently rate? (In the comment box, please provide the name of any software packages used for rating for each culvert type)

Answered: 40 Skipped: 2



Other (please list). Also list any software used to rate a specific culvert type.

AASHTOWare BrR used to rate concrete boxes
BRASS
Concrete Three-Sided Frames
New York State currently uses ETCulvert by Eriksson Technologies Inc.
I do all of my ratings by hands and typically use STAAD or other frame programs for box and arch culverts
BRASS Culvert, AASHTOWare Bridge Rating
In-house program in combination with an older PennDOT box culvert program has been used for the past 15+ years. We are now using AASHTOWare BrR for LRFR culverts.
BRASS Culvert and AASHTOWare BrR for concrete culverts
We used to rate concrete culverts, but none of the available programs, or the analytical methods, resulted in realistic, consistent results. Therefore we have stopped rating these structures until reliable methods (AASHTO guidelines) or programs have been developed.
We are considering the use of BRASS Culvert for reinforced concrete box culverts. We may end up using Midas Civil in conjunction with Excel or Mathcad to rate structures that require soil-structure interaction. We are also considering using the Ohio DOT Excel tools for rating metal pipe culverts in LRFR.
We use CANDE with LFR to rate culverts that cannot be rated using BrR. Purdue University is working on a research for us to rate bridges with no plans that includes culverts. Purdue uses ABACUS for FE and pre and post processing. Arch type structures may be analyzed using MIDAS
BRASS Culvert
We have attempted to load rate Steel/Metal corrugated culverts. However, these culverts provide many challenges such as establishing curvature, actual thickness when rust exist and etc. We have used the OHIO DOT's guidance material to load rate the steel corrugated arches. We are using AASHTOWare BrR for Concrete Box culverts.
Load ratings for bridge-length culverts have been determined primarily using the method of field evaluation and documented engineering judgment.

Appendix B- Complete Survey Results

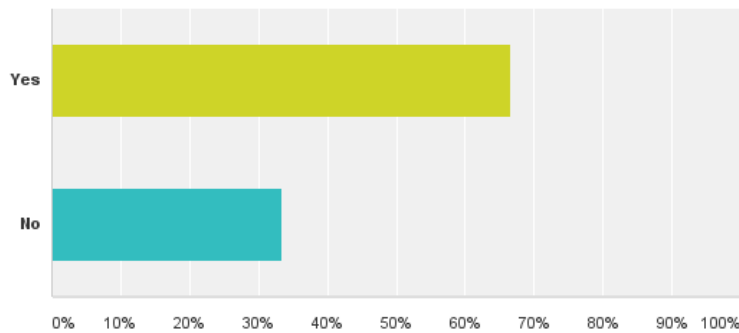
AASHTOWARE Software BrR
BRASS
AASHTO BRDR
Ohio DOT CMP-Excel
AASHTOWare Bridge Rating for Concrete Box
Require the fabricator to provide ratings for Concrete Pipe and Metal Corrugated
Culv5, CulvLR - both developed for TxDOT through research projects.
Steel/Metal corrugated culverts are load rated using the Ohio DOT cmp spreadsheets, which were modified for the Idaho legal trucks.
Concrete boxes are load rated using AASHTOWare BrR software. The BrR Culvert module is used for most new box culvert ratings, but occasionally only the top slab of the box is rated using a line girder method.
Steel/Metal Corrugated - Internally developed spreadsheets
RC Box - BRASS Culvert and AASHTO BrR
AASHTOWare BrR
BRASS/BrR/CANDE
BRASS and LARS Bridge for concrete. We have a study with KTC at the University of Kentucky to do these ratings.
In-house developed software (CulvertCalc) is used for concrete box rating
For Steel/Metal corrugated structures, in most cases, ratings are provided by manufactures. If not a spreadsheet twisted from Ohio spreadsheet is used
Metal Corrugated: In-house templates
Concrete Box: BoxCar
Concrete Pipes and Thermoplastic Pipes: Assigned ratings based on design loads or based on field evaluation and engineering judgment.
spreadsheets for metal and AASHTOWare Bridge Rating (BrR)
AASHTOWare Br R for concrete boxes. Other finite-element software for pipes and corrugated as the need arises.
We use BrR to rate Concrete Boxes.
Steel - Mathcad/Excel worksheets
Concrete Box - primarily FDOT Mathcad worksheets, also BRASS Culvert, ETCulvert by Eriksson, and CANDE Culvert
Concrete Pipe - Mathcad worksheets
Virtis/Lars Supplemented with Spreadsheets

Appendix B- Complete Survey Results

Q4: Does your state have issues with rating culverts (e.g., culverts that do not rate, but do not appear to be in distress)?

Q4 Does your state have issues with rating culverts? (e.g. culverts that do not rate, but do not appear to be in distress)

Answered: 42 Skipped: 0



Q5: If your answer to Question 3 above is "Yes", provide a brief description next to any specific type of culvert for which you experience an issue, i.e. project failure mode and location. Also note which of the following culvert types are most prone to failing load rating.

Steel/ Metal Corrugated	Concrete Box	Concrete Pipe	Thermoplastic	Other (please list)
We have a spreadsheet adapted from ODOT's spreadsheet. It is helpful, but often fails well performing culverts, especially under shallow fills.	Older culvers lack the proper reinforcement in the bottom slab and corners.			
	Does not rate / shear and code changes - we use inspection to determine rating needs.			
No issues.	Exterior walls can control from horizontal earth loading. Under higher fills, they can fail (RF < 0). Slabs will rate low and can result in posting due to live loads under smaller fill heights.			
Culverts with insufficient cover due per NCSPA Design Data Sheet No. 19				
	Some older box culverts will not rate well for shear.			
	Do not rate, but it's not always for the same reason. Most often is excessive fill and the culvert will fail under dead load.			
Most issues are self-inflicted. Original installed shape was not recorded	The analysis show failures however no corresponding distress can be found with the concrete box.			
	Exterior walls are failing in flexure at wall mid-height.			

Appendix B- Complete Survey Results

Steel/ Metal Corrugated	Concrete Box	Concrete Pipe	Thermoplastic	Other (please list)
	the analysis often shows that these fail in any one of the four walls, oftentimes the sidewalls or bottom slab.			
when the AASHTO minimum cover requirements do not meet, the rating factors are very low, but most of the times culverts are in good conditions				
	Sidewalls typically fail rating, but show no signs of distress.			
	(refer to "Other" below for fill).			R/C Slab & Frame Culverts under fill and R/C Frame/Box Culverts with insufficient rebar around the corners
RF seems too high for cases where arch is already buckled	Axial-Moment interaction region; Shear in walls though they are in good condition.			
Metal with perforations have limited or no capacity in the steel, but most of the load is carried through soil-structure interaction and pavement above is not distressed	Shear failure in slabs per calculations, but no signs of distress.			
failure mode	older box with only one layer of rebars.			
Unknown original culvert shapes - large deformation calculated reduced the load carrying capacity of the culverts that actually performed quite well	Legacy designs do not rate. Yet they have been placed for several decades.			
	Old Concrete Box Structures.			
	negative bending in top slab over interior supports, axial capacity of interior walls, positive bending in bottom slabs - the culverts most prone to this are the direct traffic culverts.			
CMP's not meeting minimum fill depths	High fill depths create high dead loads which reduces the numerator of the rating equation.			
Culvert under shallow fill fail in calculations but perform well in the field as long as the retaining material is there	Some of the RC boxes culverts designed by ASTM design tables fail in calculations but perform well in the field. We also had problems with RC culverts failing in shear calculations,	N/A	N/A	
	We have load rating "failures" at the 1.3-1.4 mark in the negative moment region for multi barrel culverts that were designed using AS. However, these culverts do not show distress in the field.			

Appendix B- Complete Survey Results

Steel/ Metal Corrugated	Concrete Box	Concrete Pipe	Thermoplastic	Other (please list)
	DESIGNED AS PINNED STRUCTURES, RATE AS FRAME.			
	Flexural/axial interaction at mid-height of exterior wall; slab shear.			
Heavy section losses result in zero calculated capacity, but the culverts are often retaining their shape and stability.	Often knee and leg moment capacities for boxes or 3-sided frame culverts do not rate well, but appear to be performing adequately.	n/a	n/a	Metal pipes are most prone to failing load ratings.
Shallow fill depths.	Tall exterior walls.			The quality of analysis is uneven.
	They typically rate lower than design load because of the differences between the rating analysis and the design process.			

Appendix B- Complete Survey Results

Q6: With respect to the previous question above, please describe any workaround procedures your agency has used to modify load ratings for culverts that show deficient load ratings but are performing well in service (to avoid posting or closure).

Answered: 29 Skipped: 13

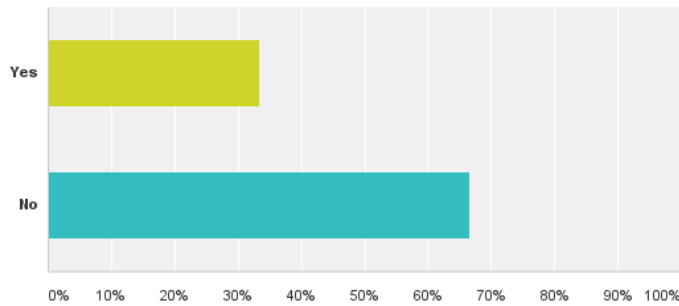
Response Text
Judgment ratings are often used for deeper cover culverts as permitted by AASHTO.
Most of our culverts have not been load rated. If they appear to be performing well through routine inspections, we assume they can support legal loads to avoid posting.
We will not post culverts - use inspection results and monitor on state wide bases.
We have done 3D modeling and get some benefit, but typically I will ignore exterior wall loads if results are restrictive.
None.
If the box culvert has been in service for many years and does not show any signs of shear damage, we will ignore the shear values and rate for moment only.
We will sometimes try a different method from ASD to LFD. We will use the old spec on older culverts that allows the fill weight to be reduced to 70%.
Refine analysis and various assumptions to enhance the capacity.
We resort to engineering judgment. AASHTO MBE allows engineering judgment for concrete structures with no available structural details. We apply this practice to concrete culverts even if we do have plans.
Field measurements including fill heights, load testing per MBE.
Rate only top and bottom slabs - ignore sidewalls.
The majority of ratings for culverts/buried structures are considered unrated or rated based on engineering judgment. Having a software that would rate different types of culverts/buried structures (metal, concrete boxes, frames, etc.) in all rating methods (ASR, LFR, LRFR) would be beneficial.
N/A; Postponing load posting bridges until research has been completed - refer to questions below.
We increase the shear capacity equation to $3\sqrt{f'c}$ instead of $2\sqrt{f'c}$ on wall considering the fact that the wall is under compression at all time.
We use documented engineering judgment and field evaluations, including consideration of where deterioration has occurred, amount of overburden, progression of deterioration through past inspections, and history of live loads regularly travelling over them.
N/A
we use original design load for the ratings and with inspection condition to adjust the rating values.
Assigned rating on concrete culverts that have condition rating of 5 or better with at least 2 feet of fill.
Review the inspection reports and pictures, if no distress is present we assign the rating for the truck it was designed with.
Our policy is still being developed for these cases.
In some cases where the rating results are deficient using analysis methods, the culvert is rating using the engineering judgment procedure, which bases the rating results on bridge condition.
We have modified our spreadsheets to incorporate alternate methods to load rate CMP culverts under shallow fill.
Invoke MBE clause provided it does not show any signs of distress.
Using the caveat in the MBE that says if a concrete structure shows no sign of distress, then we don't have to worry about load rating.
Two different load rating runs in BrR.
Rate culvert with design specifications; allow assigned load ratings for culverts performing well for sufficient service time.
For the 3-sided frame legs and knees that fail load ratings, we often assign the capacity to meet legal loads since they have been in service for decades carrying legal loads without distress.
Neglect existing exterior walls (1) in good condition, and (2) not part of a widening/extension project.
We don't rate anything that has more than 6 feet of fill on it. For ones less than 6 feet of fill, we go thru a process to modify the live load distribution factors. This process is based on researched that was completed at the university.

Appendix B- Complete Survey Results

Q7: Has your state performed any studies or research related to the rating of culverts that you would be willing to share with the research team?

Q7 Has your state performed any studies or research related to the rating of culverts that you would be willing to share with the research team?

Answered: 42 Skipped: 0



If “Yes” please describe below and if possible, please provide contact information for the lead researcher.

<p>Maybe. Our Engineering and Research Development Center conducted load testing on several culverts but never finished the report. I will see if I can get the draft.</p>
<p>Yes, TDOT funded an extensive research project with TN Technology University to investigate methods to load rate concrete box culverts. The vast majority of TN culverts are of concrete box design. The lead researcher was Dr. Sharon Huo (xhuo@tntech.edu). This research project produced load rating software tools and an extensive final report. I can email you the report upon request.</p>
<p>For a selected group of culverts slated to be closed or severely load posted, LADOTD tasked M&M to evaluate the culverts using any reasonable analysis method in hoping it would produce results showing a more favorable load capacity.</p>
<p>Ohio DOT developed Excel files to load rate existing short span CMPs with low covers, the AASHTO required minimum covers are modified in the spreadsheets based on ODOT research.</p>
<p>Currently in progress.</p>
<p>Completed research through the University of Delaware on frame culverts/slab bridges that had insufficient rebar around the corner. Research has showed that these bridges can have the load ratings improved significantly.</p> <p>Currently working on research through the University of Delaware that is looking at the dynamic impact versus fill for our buried frame/box culverts and slab bridges.</p> <p>Ping Jiang, PhD. DeIDOT Load Rating Engineer</p> <p>302-760-2297 ping.jiang@state.de.us</p>
<p>Our investigative work towards improving the rating factor revolves around BrR software. We are trying to find work around that provides a rating factor that matches the field observation. Please note that our field inspectors are finding that the culverts (even those built in 1930s) are functioning without distress.</p> <p>As a result, we are trying to find the earth pressure that provides a RF of 1.0 and use that pressure as 'operating pressure' for rating bridges.</p>

Appendix B- Complete Survey Results

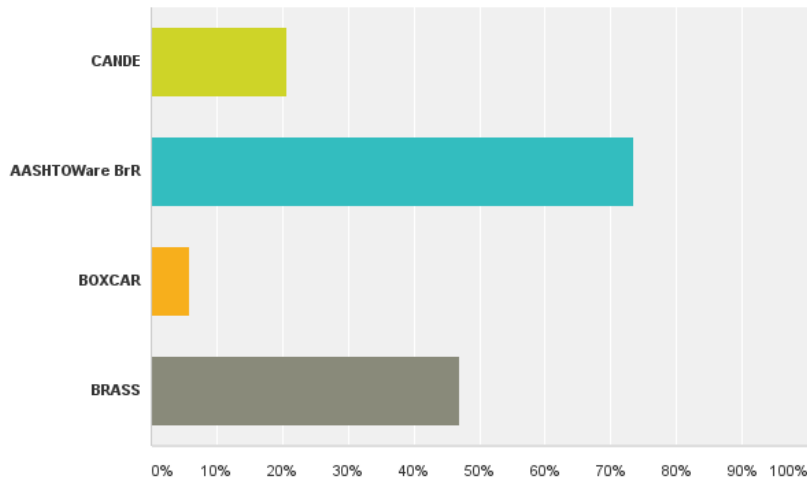
murugesu.vinayagamoorthy@dot.ca.gov
We have surveyed policies from other states and also considered the recent MBE modification for culvert load ratings with unknown construction details.
For new design culverts by LRFR, we did comparison between HL 93 and MN overweight permit vehicles and develop the standard concrete culvert plan sheets meeting both HL 93 and MN overweight permit load requirements.
The research report is available on the Center for Transportation Research library. Project No. 0-5849: "Evaluating Existing Culverts for Load Capacity Allowing for Soil Structure Interaction".
There are some older research reports, which we are aware of but we do not have a complete report. We had load tested several CMPs under 2 meter or more fill. We also tested a few CMPs under very shallow fill (less than 2 feet). Their research reports are available on our research website.
Dr. Issam Harik and Dr. Abheeta Peiris at the University of Kentucky.
we did some culvert load testing. Results show that the live load effect is very limited even with minimum top soil. The pavement can distribute live load a lot and this is ignored in analysis.
It's a little dated, and too simple, but
http://www.dot.state.fl.us/structures/structuresresearchcenter/Final%20Reports/BC354_47_pt2.pdf
We did some live load testing to show that the live load effects on culverts are minimal as the fill depth increases. The AASHTO codes are ridiculous when it comes to the live load effects on culverts for load rating purposes. FHWA required us to load rate all of our culverts regardless of the amount of fill just because of how things are stated in the manuals. They wouldn't listen to common sense on the issue. We did the research project with MU to justify using different live load distribution methods on culverts, when needed for ones that had low load ratings using normal procedures. Send me an email request at David.Koenig@modot.mo.gov and I will send you a copy of the research report.

Appendix B- Complete Survey Results

Q8: What software do you use for analysis/rating? (Check any that apply.)

Q8 What software do you use for analysis/rating? (check any that apply)

Answered: 34 Skipped: 8



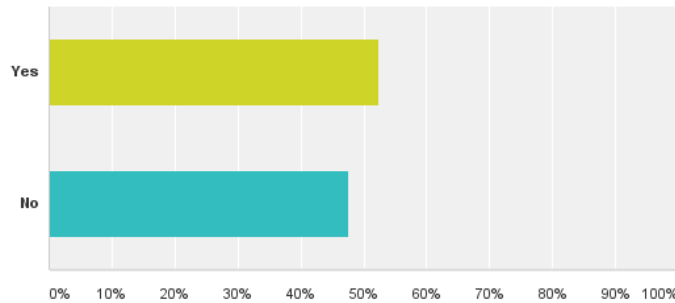
Other (provide description)
For the design of a new culvert, one consultant used cande to make sure it supported the traffic load. DDOT has not rated any existing culverts.
spreadsheets and MathCAD
CANDE has been used for non-prismatic 3-sided frames.
ETCulvert by Eriksson Technologies Inc. is used primarily for 4-sided box culverts and prismatic 3-sided frames.
Internal program
MathCad
Excel sheet from MDOT and check via hand computations.
RISA 3D with supplemental Excel sheet for concrete box culverts.
We've used BOX5, a PennDOT program. BRASS has also been used, with the same unreliable results. It's not so much the programs, perhaps, that have the problem. It's more so the AASHTO code, at least that's the prevailing theory in our office.
Ohio DOT in-house Excel files
STAAD (as needed)
Wisconsin's in-house program. Similar to AASHTOWare BrR. These are for concrete box culverts only.
ETCulvert
CulvLR - uses Culv5 as an engine for lower level analyses, then Risa-3D for higher level
Culv5
In-house developed spreadsheets
LARS Bridge
CulvertCalc developed by Iowa DOT and Consultant company
In-house Spreadsheets and Mathcad Templates.
ET culvert
LARS
Mathcad worksheets

Appendix B- Complete Survey Results

Q9: Would you be willing to provide input files for culverts rated by your state agency?

Q9 Would you be willing to provide input files for culverts rated by your state agency?

Answered: 40 Skipped: 2



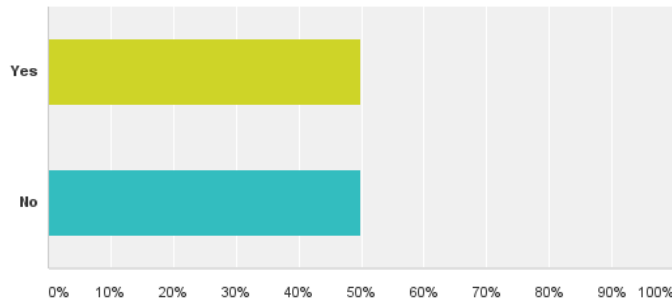
If 'Yes' which software program(s)? How many input files would you be able to provide?
BrR models, unsure of exactly how many we have available.
We suggest Eriksson Technologies be contacted for ETCulvert input files.
Eriksson Technologies Inc. Software Company Address: 9385 N 56th St #201, Temple Terrace, FL 33617 Phone:(813) 989-3317
Would for a few in BrR if team would like them.
Several
Excel sheets we have on file (around 70).
3
We have the models for 2,493 of our standard culvert drawings (1920's to 1990's). Each drawing generates a number of variations depending upon cell depth, skew, fill depth, etc. In all, we have about 45,000 models. These models are all done in BRASS Culvert so there are about 45,000 BRASS Culvert data files.
AASHTOWare or BRASS. Dozens in BRASS, several in AASHTOWare
We do not have any as of yet.
BrR, CANDE- a few bridges
BRASS - However many you would like to obtain.
BrR software. We have shared 104 RC Box culvert models. We will share any models we create from hereafter, if requested.
Most of our files are in our in-house program, which would be of little use to others without the program.
CulVLR - we would be willing to provide 10 input files.
AASHTOWare BrR software, using both the AASHTO and BRASS engines. Up to 100 input files could be provided.
>10
BRASS when we get the files (see research project comment) and LARS bridge.
The input files are developed for our in-house software Culvertcalc
We would rate culverts in BrR as the need arose. However, we do not have any input files at present.
We could provide some Virtis files. I am not sure how many, or if they include the live load modifications that we do with a spreadsheet. We should be able to provide several hundred without much of a problem.

Appendix B- Complete Survey Results

Q10: Do you wish to discuss over the phone your state's practices and issues related to culvert rating?

Q10 Do you wish to discuss over the phone your state's practices and issues related to culvert rating?

Answered: 40 Skipped: 2



Q11: Do you have any other concerns related to culvert rating that you think would be beneficial to this research (i.e. shortcomings of the culvert load rating specifications that need to be addressed)?

Answered: 31 Skipped: 11

Response Text
A potential issue with ASTM designed precast culvert was recently brought up by our design unit. ASTM supposedly uses the circumferential reinforcement equations in box culverts. We haven't looked into this further.
No
See commentary above in Question #10.
Will Interim Reports be made available for viewing?
We need to use risk based approach - we cannot resource or prioritize rating culverts.
Expanded guidelines on horizontal loads (ES, EH, LS), distribution of vertical loads, it has to be better than we are assuming.
How to address culverts with no bottom but no load induced damage, section loss other than NCSPA, include thrust beam effects, local/global pipe reversals due to rail posts, adequately field measure culverts, soil densities to use other than 120pcf, missing bolts in seams, and interaction between closely spaces culverts (2-10ft pipes 3ft apart).
Need more accurate load to be applied Concrete culverts with pinned connection evaluation method.
The current analysis method is too focused on simplicity such as used on 2d analysis and also does not take advantage of soil-member interaction.
No
We are highly concerned about this issue, but we have just gotten started looking at it. This is the reason I answered no to questions 9 and 10. I don't really have enough information to speak intelligently about the issue. However, I have ran a few of our Interstate box culverts through BrR, and the results show they should be posted. This is not correct, as these bridge have been in service for 40+ years and show no signs of distress from overloading.
If new rating specifications are put out, an effort should be made to make the equations/methods as brief, simple and quickly executable as possible. The new LRFR bridge rating specifications are a little out of hand, and without a computer program to run all the sets and subsets of equations, are not that easy to deal with.
Most of the guidance for culvert rating in the MBE is for reinforced concrete culverts. There is not much for metal pipe culverts.
I would like a tabular result sheet with help tabs for making the right assumptions and linking the effect of live loads with fill heights for various spans and span combinations for AASHTO live loads and Certain SHV's.

Appendix B- Complete Survey Results

-Simplified methods for rating steel and concrete pipes/arches/etc.
-More accurate soil interaction models with no special soil/backfill parameters.
The lack of information, i.e. as-built plans and specifications, materials, thicknesses, depth and type of fill, etc. can be an issue.
Not at this time.
1. Whenever DL/LL ratio exceeds a threshold (say 5 or 10), RF approach makes no sense. C/D ratio would be a better approach.
2. In many situation, amount of compaction, fill material used are not available and therefore, rating engineer need to use approximate values for EH and EV. Use of operating and inventory load factor/pressure should be made available
3. Shear capacity expressions are very sensitive (especially MCFT).
Through research, empirical load ratings may be able to be developed based on construction type, year of construction, overburden, and condition. Culverts which have successfully carried legal loads without any signs of distress do not warrant strenuous finite-element soil-structure interaction analysis to determine load ratings.
No.
The method shall be simple and clear, not involve a lot of modeling or time consuming analysis because the numbers of culverts in our state are large and majority are on local agencies which have limited resources.
One big factor in rating culvert is the assumption of soil pressures. The pressure distribution is much more complicated than just using active, passive and at rest pressures in the current methodology. For concrete culverts with little or no fill, the top slab provides the bracing effect that will change the soil pressure distribution. For culverts with large amount of fill, the arching effect can be significant. The bottom slab design using one subgrade modulus is flawed. The culvert walls are much stiffer than the bottom slab, the soils beneath the slab would respond accordingly. The soil reaction will be concentrated under the culvert walls making the bottom slab design and rating unreasonable by over-estimating the soil pressure under the bottom slab. One possible solution is to change the load factor for buried structures based on structural type and embedment ratios. A study on this effect will greatly benefit the evaluation of the true behavior of the culverts.
Another study will be very beneficial is to study of the structural reliability of the currently installed culverts. It is my personal belief that most culverts failed because of hydraulic inadequacy, not structural deficiency.
Culvert ratings should take advantage of the redistribution of LL due to type of pavement.
Based on our experience with these analyses, the guidance for lateral distribution for live load is nowhere near the actual live load distribution for direct traffic culverts or through fill.
Corrugated steel 5x1 seam strength is not listed in specifications.
current MBE only include LRFR method. LFR approach should be included because LFR is still valid. EH, EV, live load distribution through earth fill, live load surcharge, and dynamic load impact factor should be studied and more realistic/representative analysis model shall be provided.
none that haven't already been discussed.
Culvert ratings appear to be more of an exercise in academia than providing meaningful data.
N/A
The failure mode of "culverts" is totally different than for "Bridges" the load rating requirement is just an exercise in futility as the probably of posting a culvert for load is highly remote. we'd use engineering judgment based on the condition, height of fill and culvert spans to determine if posting would be warranted rather than the theoretical results.
(1) At 1.99ft-to-2.01ft D.fill, shear capacity increases stepwise. (2) The MBE ought to include an easy-to-follow example, with classic hinged-ends. (3) For lateral distribution, LRFD's "interaction depth" hides meaning; an E vs D.fill plot would better explain distribution width "E." (3) Include provisions for routine permits, by considering adjacent trucks and multiple presence factors. (4) AASHTO longitudinal axle overlapping can distribute a light axle to a heavy axle; say whether Boussinesq is better, and easier to program. (5) A slick culvert analysis tool would be nice.
There should be an emphasis placed on communicating the effects of the 2.0 live load factor for culverts when used to try to manipulate software to rate structures that are similar in nature to culverts but are not designed as culverts. This larger number in the denominator of the general rating equation has a significant effect on the final answer from the equation.
There needs to be some common sense put back into the specifications. We don't need some load rating method or process that takes a PHD to understand. Once you get above 6' or so on culverts, the live load effects are very negligible. I am not saying that we shouldn't design for live load above that fill depth, but we should not have to load rate them once you get above that point.

Appendix B- Complete Survey Results

Follow-up interview questions/responses

The following questions were asked in the 14 follow-up interviews. The table below shows the states/organizations that were interviewed and the date of the interview.

Organization	Date Interviewed
Army Corp	9/4/15
California	8/26/15
Delaware	*
Florida	9/10/15
Indiana	*
Iowa	8/26/15
Kentucky	*
Louisiana	9/4/15
Michigan	9/28/15
Minnesota	8/27/15
Missouri	*
Ohio	9/3/15
Oregon	9/3/15
South Dakota	9/10/15
Tennessee	**
Texas	9/8/15
Virginia	9/11/15
Wisconsin	8/25/15

* Note: Interview requests were made for these states, they were contacted via email to set up the interview, but as of this writing of this report, a date had not been set up to conduct the interview.

** No phone interview was held, but post-survey emails were exchanged to obtain additional information.

Q1: Do you have any issues with the current MBE/FHWA requirements for load rating of culverts? If so, please also note the type(s) of culverts that are having issues, describe what is controlling (low) ratings, design method used, age of culverts with issues, etc.

Alaska rates 77 culverts of which 8 are concrete box culverts. The remainder are metal corrugated culverts. The steel types of culverts are CMP(circular), pipe arch, low profile arches, horizontal ellipses, and inverted pairs. An inverted pair is a subset of long-span culverts and can be found in Figure 12.8.1-1 of the LRFD. This shape is used mainly for railroad to road conflicts as the railroad has specific requirements for clearances.

They are currently rating the steel culverts utilizing a spreadsheet from Michigan DOT (which is a modification of a spreadsheet developed by Ohio DOT).

For the concrete culverts, they have used RISA 3D with some spreadsheets for post processing. For the concrete culverts, the models have springs in the bottom slabs but the sides do not take into account soil pressure. They are not seeing distress in their concrete culverts. One was constructed in 1904 and is not reinforcement, but is still in good operating condition.

The LRFR spec is telling us to use a density of 120, but the specs we are getting are 130-140. The 120 is helping the rating because it is lighter-less dead load.

Appendix B- Complete Survey Results

Q1: Do you have any issues with the current MBE/FHWA requirements for load rating of culverts? If so, please also note the type(s) of culverts that are having issues, describe what is controlling (low) ratings, design method used, age of culverts with issues, etc.

We have rated culverts that are failing the rating, sometimes a less than zero rating (i.e. failing under earth loads) and the physical inspection of the culvert is good- no distress. The Army has rated culverts with a span length as low as 6', but typically shorter span culverts are reviewed for physical condition.

The Air Force on rates culverts over 20' (NBI length).

: Almost all of Florida's culverts are reinforced concrete. For concrete culverts, some of the problems they are seeing are often with exterior walls; particularly where the wall heights are 8-10' or more. They typically fail and it is mainly due to factored DL. Some of the problem he believes are related to the specification. Culverts that appear in good shape physically, are failing in rating. They are using both LFR and LRFR to rate their culverts.

When rating analyses are performed more rigorously (closer adherence to the spec):

- Take shear at d_v away from face, and consider provisions for haunches
- Use the appropriate shear capacity equations (5.14.5.3-1 for deep fills, or 5.8.3.3 for shallow fills), rather than the simplified $2\sqrt{f_c}$
- Use truly coincident loading for shear assessment
- Use area-distributed loading, rather than point-distributed load, or point emulations (BRASS)
- Consider lateral live load distribution to the bottom slab (Std.Spec. 17th Ed. 16.6.4.3)
- Include axial effects

Results improve. Commercial culvert programs include many of these considerations. However bespoke MathCAD/Excel worksheets, which frequently perform assessments for older culverts, are necessarily more crude, per time limitations on worksheet development.

Other issues related to the specs:

- Culvert specs jump around from section-to-section; it's confusing.
- For shallow fills, the shear strength reduction/resistance factor is 0.90 (5.5.4.2.1), or 0.85 (12.5.5-1)?
- When longitudinal axle distributions through soil overlap, (1) "...the total load shall be uniformly distributed over the area" (Std.Spec. and LRFD 6th Ed.), (2) the distribution triangles overlap, per BRASS method, or (3) the loads are confined to the length of the footprint at the depth of first overlap, per MBE A10.7.4-1. Which method does LRFD endorse? Is a better method available?
- For lateral distribution in shallow fills, LRFD 6th Ed 2012 at 3.6.1.2.6 called for 4.6.2.10 (Std.Spec. slab distribution with $mpf=1.20$), MBE 2013 Interims at C6A.5.12.10.3a says likewise, but LRFD 7th Ed. 2014 at 3.6.1.2.6a calls for 4.6.2.1, which is actually deck distribution. Was the later a typo?
- MBE 6A.5.12.5-1 applies a single-lane multiple presence factor of 1.20 to the HL93 lateral distribution; however $mpf=1.00$ for the legal loads. This appears inconsistent with other areas of the MBE, which applies $mpf=1.20$ to both design and legal loads.
- It would be helpful to clarify that the longitudinal distribution takes no multiple presence factor.
- Some E vs D.fill charts would be useful.
- Does E.lateral consider two trucks? It's a pretty big difference, one trucks vs two trucks, especially where single-lane $mpf=1.00$.

Appendix B- Complete Survey Results

Q1: Do you have any issues with the current MBE/FHWA requirements for load rating of culverts? If so, please also note the type(s) of culverts that are having issues, describe what is controlling (low) ratings, design method used, age of culverts with issues, etc.

tire_length := 10in lane_w := 12ft L_ClearSpan = 10.00ft tire_width := 20in + 0.06·L_ClearSpan = 2.27ft DF_earth := 1.15 gage := 6ft

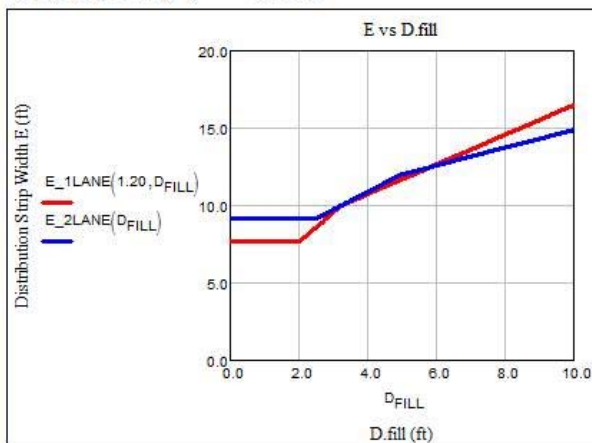
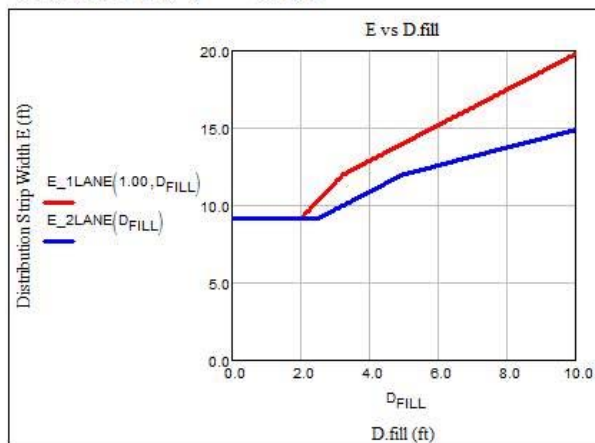
$$E_{\text{slab}}(\text{mpf}, D) := \frac{8\text{ft} + 0.12 \cdot L_{\text{ClearSpan}}}{\text{mpf}}$$

$$E_{\text{earth_1truck}}(\text{mpf}, D) := \min\left(2 \cdot \frac{\text{tire_width} + D \cdot DF_{\text{earth}}}{\text{mpf}}, 1 \cdot \frac{\text{tire_width} + DF_{\text{earth}} \cdot D + \text{gage}}{\text{mpf}}\right)$$

$$E_{\text{earth_2trucks}}(D) := \min\left[1 \cdot (\text{tire_width} + D \cdot DF_{\text{earth}} + 4\text{ft}), 0.5 \cdot (\text{tire_width} + D \cdot DF_{\text{earth}} + 2 \cdot \text{gage} + 4\text{ft})\right]$$

$$E_{\text{1LANE}}(\text{mpf}, D) := \max(E_{\text{slab}}(\text{mpf}, D), E_{\text{earth_1truck}}(\text{mpf}, D))$$

$$E_{\text{2LANE}}(D) := \max(E_{\text{slab}}(1.00, D), E_{\text{earth_2trucks}}(D))$$

1-LANE MPF = 1.20**1-LANE MPF = 1.00**

LADOT is having a lot of issues with cast-in-place reinforced concrete culverts failing in rating for LRFR. Many of the culverts are older. The oldest culverts have one layer of design steel and pretty much everything is failing in LRFR. The culverts are not showing any signs of distress under physical inspection. Louisiana uses the NBI span length and only rates culverts that are greater than 20' in span length.

Modjeski & Masters is currently working with LA DOT on load rating of their culverts.

Michigan has had issues with RC Box culverts appear to be good upon physical inspection but are not rating well. In some cases, culverts are failing under dead load; this is particularly the case for culverts with deep fill heights. In one case, Michigan reduced the soil density to 70% of its actual weight of 120pcf per the AASHTO edition 6th. This allowed the culvert to rate well, otherwise Michigan would've posted the bridge or closed it due to deep fill height ~ 16.5 ft.

Without the reduction, presumably the culvert can NOT support fill and its weight giving a RF of 0.0. Again this a culvert that does not show any physical signs of distress.

Michigan's rating policy for culverts is to rate structures that were built 2010 and prior using LFR. Structures built beyond 2010 and designed with LRF, are rated using LRFR.

The 12" minimum fill criteria effects both sides of the rating equation. From the AASHTO code, the LL impact factor goes up when the fill is below 12" thus effecting the load portion of the rating. The NCSA (National Corrugate Steel Pipe Association) spec has criteria that effects the capacity side when the fill is below 12".

MnDOT asked if the project involved both precast and CIP box culverts noting that most of their new R/C box culverts are precast although they have both CIP and precast in their inventory. Mr. Clancy responded that a

Appendix B- Complete Survey Results

<p>Q1: Do you have any issues with the current MBE/FHWA requirements for load rating of culverts? If so, please also note the type(s) of culverts that are having issues, describe what is controlling (low) ratings, design method used, age of culverts with issues, etc.</p>
<p>number of different types of culvert construction are being considered but the types of culverts that are to be part of the field testing program are yet to be determined and this is somewhat dependent upon what the participating DOTs offer up to be tested. Furthermore we are looking to include one or more culverts under construction to allow for more flexibility in instrumentation.</p> <p>From MnDOT's perspective, there are three primary ways to perform culvert analysis: 1) FEA, 2) Beam on Elastic Foundation and 3) "Brute Force" i.e., using a method such as BRASS Culvert or BOXCAR. Each of these methods provides different answers and differences can also be attributed to the specifics of the modeling such as the treatment of the haunch with respect to stiffness, location of critical sections, etc. MnDOT would like to see more unification of the methods used to load rate culverts such that it is being done on a more consistent basis. This might also include some guidance on rating based on what is required for various fill-height ranges.</p>
<p>ODOT has had issues with rating CMP (Metal culverts) in the past and the AASHTO Specs are lacking for metal culverts which prompted ODOT about 6 years ago to create a spreadsheet for rating CMP culverts. Ohio law requires them to rate culverts that are 10' in span length and above.</p> <p>The creation of the spreadsheet, which can be used for really low covers (as low as 3"), prompted research to be performed by the Ohio State University. This research looked at 3D FEM models of several culverts, and Ms. Wang believes that at least one of those models took into account pavement. The research has gone on for the past year and was used to help validate assumptions that were made in the spreadsheet calculations. Ms. Wang was the manager for ODOT for that research.</p> <p>The spreadsheet will take into account deterioration by entering a percentage loss of the CMP. If deflection is more than 5% a more refined analysis is used (e.g. CANDE).</p> <p>As a follow-up, ODOT said that Michigan has performed some research that has tagged on to the work that ODOT has performed.</p>
<p>In the past, Oregon did not rate culverts. Currently, Oregon has 300 NBI culverts (>20') in their inventory. About half are reinforced concrete and half are steel corrugated. The culverts are currently not rated, but Oregon is looking into the best way to provide load rating for these structures. They have had a consultant do some limited work on 1 or 2 rigid frames (with fill) using BRASS Culvert.</p> <p>They are looking at the new ballot item (which was approved/passed during the last SCOBS), which will be included within the next interim revision of the MBE for RC culverts that are in good condition that perhaps do not need rated. Jon forwarded a copy of the ballot item to me. The ballot items allows for assigning inventory ratings of 1.0 and operating ratings of 1.3 for HL-93 design loads for culverts that have been carrying normal traffic for an appreciable period of time and shows no distress as determined by a physical inspection of the culvert by a qualified inspector and documented in the inspection report.</p> <p>Oregon DOT is currently Working with a consultant to rate the RC and metal culverts in LRFR.</p>
<p>South Dakota really hasn't had any large issues with the rating of their culverts. Most of their culverts are reinforced concrete box culverts and about 98% were designed using ASD. This method was used until October, 2010 when the culvert design method was switched to LRFD. South Dakota has approximately 550 NBI records (state-owned) that are culverts out of a total of about 1800 NBI records. South Dakota follows the NBI criteria for span length for NBI records.</p> <p>For culverts designed from 2010 on, ETCulvert (Eriksson) was used for design. These culverts have some minor rating issues in BrR where the inventory rating of the bottom slab can be around 0.95 in some cases. Current design procedures for culverts include designing the culverts in ETCulvert and then checking them in BrR. Prior to the 1970's culverts were designed using standard culvert detailing drawings. These drawings are available in hard copy format (they have not yet been scanned in). Asked for how many of the culverts in the current inventory were designed using the 1930's & 1950's standards, South Dakota estimated that number to be about 40-50% of the culvert inventory. Some of the culverts in the inventory are up to 80+ years old.</p> <p>They agreed to scan and send sample pages of the culvert standards for our review.</p>
<p>Texas DOT is rating using LFR. They feel that the distribution of the loads (even on direct traffic culverts) does not provide a true representation of actual loading conditions. They are OK with capacity side of the equation, but think that the demand side may be too conservative. They have some reinforced concrete culverts that are not showing signs of distress but do not pass for rating.</p>

Appendix B- Complete Survey Results

Q1: Do you have any issues with the current MBE/FHWA requirements for load rating of culverts? If so, please also note the type(s) of culverts that are having issues, describe what is controlling (low) ratings, design method used, age of culverts with issues, etc.
They don't have many metal culverts in their system and currently don't have an easy way to rate them. I told him of the spreadsheet that Ohio DOT is using for metal culverts.
Virginia hasn't really had any issues with rating culverts. The procedure they use for older culverts is described in the response to the following question.
A new ballot item has been approved related to the load rating of reinforced concrete culverts in cases where no plans are available. However, there is nothing similar for other culvert types.
***** <i>Are you having problems rating other culvert types or are they not rating them yet?</i> We have load rated all types of bridge-length culverts using approximate methods which include a combination of calculations, field evaluation and documented engineering judgment. The new AASHTO ballot item provides explicit guidance for using approximate load ratings for concrete culverts, but does not apply this same criteria to flexible buried culverts. The only explicit guidance via national publication on load rating flexible culverts I am aware of is NCSA Design Data Sheet No. 19, which requires knowledge of seam construction, corrugation pattern, gage thickness, % pipe crown deflection, steel strength, and assumed soil-structure interaction. Many of these parameters are unknown for old buried flexible culverts. These structures are at relatively low risk of immediate failure, so it would make sense to extend the same economical methods of assigning load ratings for these types of culverts as has been defined for reinforced concrete box culverts.

Q2: Is the currently available software adequate for performing required load ratings?
Alaska is using an Excel spreadsheet from Michigan DOT (that is a modification from an Ohio DOT spreadsheet) along with hand calculations to aid in the load rating of the steel corrugated culverts. They are using RISA 3D with supplemental Excel spreadsheets for concrete box culverts.
They mostly use STAAD for analysis and MathCADD spreadsheet to perform the rating. I told Phil about CANDE and will send him the URL to download.
Florida is using a combination of both in-house and external software for Culvert rating as shown below: <ul style="list-style-type: none"> - PSBeam (by Erikson). - BRASS (use most frequently). - AASHTOWare BrDR (have played around with this a bit). - MathCAD (developed in-house). The primary worksheet, for frames, was developed by Design in the 90's, and most recently updated in 2015. A newer worksheet, for older hinged-end culverts, is under development in Maintenance. Both sheets generate forces internally (stiffness matrix, and area-moment influence matrices).
Louisiana uses AASHTOWare BrDR for rating precast reinforced concrete culverts. Many of these are not rating well. He is willing to share input files from BrDR with the research team. (Note that that most precast culverts (ASTM D1433) easily pass LRFR ratings.) LA DOT also uses Midas (2D) for arch type reinforced concrete structures. Midas supports simple soil models. They have not used CANDE in-house, but he used it many years ago. I told him I would send him the link to the latest CANDE software on the NCHRP web site. For metal corrugated culverts, Louisiana is using the Ohio DOT spreadsheet for rating.
Michigan currently uses AASHTOWare BrDR and BRASS. When culverts have failed using BrDR they have on occasion been rated with BRASS and provide comparable results. So it appears that the rating issues may be related to the specification.
MnDOT is just starting to use AASHTO BrR so they are not able to give any detailed feedback on that software. CANDE is good but it would be better if it had better functionality with respect to load rating. The available software does not have the capability to perform ratings after lining type rehabilitations. Shotcrete and lined/grouted repairs are done by vendors and they have their own way of determining the as-repaired

Appendix B- Complete Survey Results

Q2: Is the currently available software adequate for performing required load ratings?
strength of the system but MnDOT does not have any means of independently verifying the vendor's claims. A means to quantitatively determine the strength of a rehabbed culvert is needed.
The spreadsheet helps to address rating issues related to CMPs. Long span CMP might use CANDE for more complicated cases. For RCBox culverts, ODOT doesn't really have any load rating issues but ODOT does make exceptions to the LRFR specifications for concrete box culverts. They will send a list of the ODOT specs where exceptions are made.
Oregon DOT is just starting to rate culverts. Of the 300 NBI culverts (>20' span length) in Oregon's inventory, about half are metal corrugated and half are reinforced concrete. Oregon will try to use the Ohio DOT spreadsheet for rating the metal culverts and have not yet selected the RC rating method. They are looking at BRASS and perhaps AASHTOWare (they are not currently an AASHTOWare licensee).
ETCulvert – Eriksson software – used for design and BrDR is used to do a rating check for each new design. BrDR is used for rating of the culvert inventory.
Culv5 was a program developed in the 1970's in FORTRAN and is for the analysis of reinforced concrete box culverts. The CulvLR software was developed more recently (2009) and utilizes the Culv5 engine to perform the analysis. If the culvert fails using the Culv5 engine, CulvLR generates a Risa model (2D) which uses plates to model the soil. Both programs were developed for TxDOT through research projects. I asked if this software was available to the research team along with input files that could be utilized by the research team. I also said it would be preferable to have input for culverts that appear to be performing well physically but do not rate well. TxDOT will check to see if the programs are available for use by the research team.
For Virginia DOT, newer culverts 2014-15 on are rated with BrR. Culverts designed prior to that use a design table and an accompanying tonnage chart. The designs are for specific size culverts. The ratings are obtained by using the tonnage information in those charts. VDOT agreed to send me the URL information for those design procedures/charts.
Yes, in general. However, WisDOT has experienced shear failures in concrete boxes using BrR software in cases where the culvert is performing well in service. In such cases, these failures are neglected (based on condition and performance). <i>**** Where is the software predicting failures (top slab, sidewalls, etc.), What sizes of culverts are they having problems with? What is the age and design method for culverts having this problem. Can they send us an input file?</i> We have only rated a few in BrR but we did see shear ratings coming out lower than the original design for both top and bottom slab, however the sample size is small. BrR has actually added options to "ignore shear" and "exclude bottom slab" in ratings for box culverts. Their tech support informed us this came at the request of three other agencies. For the most part we have preferred to use our in-house software for concrete box culvert ratings, and have only tested out BrR with a few trial culverts.

Q3: Have you used refined methods to rate culverts (such as CANDE) when issues arise?
They have not used CANDE. I will send them a link to the software.
They have performed some 3D modeling for some benefit, but it was used mostly to compare the 2D results with and 3D results.
Have used CANDE but it is a bit too complicated for their needs.
From previous response: LA DOT uses Midas (2D). Have not used CANDE.
Have access to BOXCAR but haven't used it. Michigan has not used CANDE. Some special culverts like arch culverts which cannot be analyzed using BrDR or BRASS have been analyzed/rated by consultants using FEM software.

Appendix B- Complete Survey Results

MnDOT uses CANDE for metal culverts. It was noted that even with CANDE various levels of analysis are available. It was also noted that CANDE is not very user friendly when used as a tool for load rating. Mr. Clancy noted that with Mike Katona on the team it is anticipated that some enhancements to the CANDE software will be implemented to make the software more useful in the research effort and that some of these enhancements will likely make their way into the released product. These enhancements will benefit those who are using the software for load rating.
Yes. Long span CMP might use CANDE for complicated cases.
Oregon DOT hasn't started using refined methods yet. If needed will most likely use Midas Civil with post processing in Excel.
No. Not typically.
They have not used CANDE, but CulvLR generates a Risa model (2D) where plates are used to model soil elements. They looked into CANDE but would be too cumbersome to use for the number of culverts that Texas has in its inventory.
He (VDOT) thinks that CANDE has been used for cons pan-type arches. Some other non-NBI culverts have used BRASS.
No.

Q4: Are you aware of any culvert-related research performed by your agency that would be helpful in our investigation?
No. Up to 2011 Alaska was not in compliance for rating culverts. Load rating for culverts began in 2013-2014. They now have rated all of the culverts that are owned by the state (77 total culverts).
Phil was aware of some culvert field testing that was performed out of the Vicksburg office and will try to locate the research paper. The work was performed around 2006-2007 and involved the instrumentation of culverts for live loading. The paper was not formally published and he asked that keep it within our research team. Since it is unpublished work, if we include it as part of the research, we should let the Army Corps know.
Some older research (http://www.dot.state.fl.us/structures/structuresresearchcenter/Final%20Reports/BC354_47_pt2.pdf and http://www.dot.state.fl.us/structures/structuresresearchcenter/CompletedResearch.shtm#evaluations), but not nearly as good as Texas in 2010 http://texashistory.unt.edu/ark:/67531/metaph326775/
Louisiana is preparing to do some field testing (possibly as early as next year). Ching is willing to share that information with the research team. When we are preparing the field testing document, he is interested in talking to our research team regarding our methods for instrumentation. He may be willing to adjust his instrumentation to benefit our research. I told him we would contact him when are preparing our field testing plan and he agreed that we could contact him directly.
For metal corrugated culverts, Michigan modified the ODOT spreadsheet to include Michigan's 28 legal vehicles. Michigan has recently updated the spreadsheet and is willing to provide the research team a copy once they have been reviewed.
Primarily changed the way that the live load was distributed through the soil. For Ohio DOT's version, the assumption was made that the maximum axle for the HL-93 was controlling. Michigan has a lot of different vehicles to rate (28) and developed a spreadsheet to calculate the effect of each of those vehicles on varying fill heights. Vehicles with closer axle spacing begin to have overlapping loads at around 5'-6' of fill. The spreadsheet took this into account and determined the critical vehicle at different fill heights (every 6"). The values were then ported back into the ODOT spreadsheet.
They provided the URL for the Michigan version of spreadsheet (along with the spreadsheet to calculate the LL distribution through fill). http://www.michigan.gov/mdot/0,4616,7-151-9625_24768_24773-201633--,00.html

Appendix B- Complete Survey Results

Q4: Are you aware of any culvert-related research performed by your agency that would be helpful in our investigation?
Michigan is currently working on version 2.0 of the CMP spreadsheet and they will provide that to the research team when it is available. The spreadsheet works for both LFD and LRFD
MnDOT has some internal research on PE Pipes and just started some research on looking at various methods of repairing pipes and the structural evaluation of such. MnDOT provided the following links: http://www.dot.state.mn.us/research/TS/2012/2012-27.pdf http://www.dot.state.mn.us/research/TS/2005/200522.pdf http://www.dot.state.mn.us/research/pdf/1992-02.pdf other reports can be found at: http://www.dot.state.mn.us/research/reports-2014.html
Yes. ODOT forwarded their most recent research with Ohio University and the Ohio State University.
The Michigan report which utilizes the Ohio DOT CMP spreadsheet. Oregon forwarded the URL address. http://www.michigan.gov/mdot/0,4616,7-151-9622_11045_24249_24251-322991--,00.html
No.
Tennessee DOT provided the following: The only thing that I would add is that TN Tech developed a couple of spreadsheets that act to look up the LFR ratings that they developed for our standard culverts. So, we have all the files that supplement this report. These files included: <ol style="list-style-type: none"> 1) Two spreadsheets. One for concrete box designs (with a bottom slab) and one for concrete slab designs (without a bottom slab – with footings keyed into rock). 2) Approximately 45,000 BRASS Culvert data files with resulting output files. 3) The standard drawings for the culverts and slabs that were analyzed (over 1,000 standard drawings). Would you be interested any of this other information? It is too much data to send by email but I could probably upload it to you if you have a public folder for such things. Or I could just save it on a thumb drive and mail it to you. All the files total about 5.2 GB on disk. They are mailing the information
The research report is available on the Center for Transportation Research library. Project No. 0-5849: "Evaluating Existing Culverts for Load Capacity Allowing for Soil Structure Interaction".
Just the VDOT design tables described for the previous question. Links are below: Our load rating page is here: http://www.virginiadot.org/business/bridge_load_rating.asp The tables mentioned are in the back portion of the I&IM 86 linked here: http://www.virginiadot.org/business/resources/Load_Rating_Data/IIM-SB-86.pdf
No.

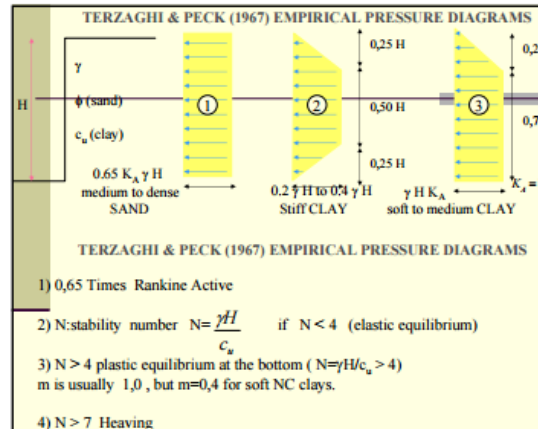
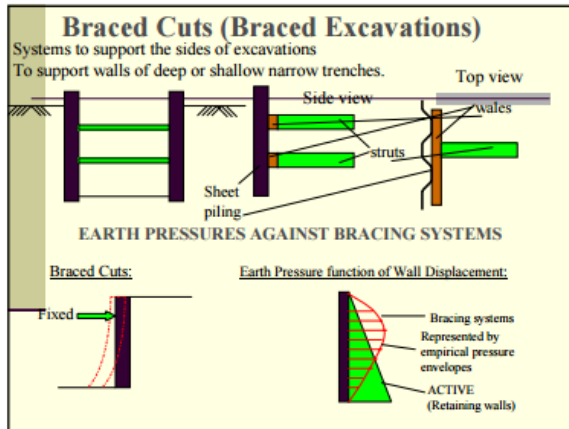
Q5: Do you have any other concerns related to load rating of culverts?
Some of the DOT's concern for culvert rating were expressed in their survey responses and include: How to address culverts with no bottom but no load induced damage, section loss other than NCSPA, include thrust beam effects, local/global pipe reversals due to rail posts, adequately field measure culverts, soil densities to use other than 120pcf, missing bolts in seams, and interaction between closely spaces culverts (2-10ft pipes 3ft apart). Alaska DOT is very interested in this research and wanted to know if they could know of the culvert areas that are being reviewed as the project proceeds.
The procedures seem to be conservative on loads. Both the earth loads and live loads, especially on distribution of live loads and earth loads. He believes that for culverts with eight or more feet of fill the horizontal loads on the walls are too conservative.

Appendix B- Complete Survey Results

Q5: Do you have any other concerns related to load rating of culverts?

Concerned with the way the spec interprets the triangular distribution. Perhaps too conservative.

For unbraced walls, the wall is rotating about an axis near the bottom, the triangular load distribution assumption used by BrDR is reasonable. However, since the culverts are braced both at the top and bottom of the walls (even more lateral supports for multilevel culverts), the lateral earth pressure distribution become either rectangular or trapezoidal depending upon the soil conditions (see Peck 1967).



I copied the above presentation slides from a web site. There are many other studies on the distribution of lateral earth pressure for braced or anchored walls. Even though the above presentation is about braced excavation, the concept is the same – the earth pressure distributions are not triangular. If we cannot model the loads correctly, any effort in improving structural model is futile.

There are two issues that Michigan is concerned about:

1. The issue with large fill height causing 0.0 ratings for culverts that don't appear under distressed. This is described in a previous answer.
2. For CMP's (metal culverts), the issue of the minimum height requirement (12" minimum). Under 12" minimum fill height, the code takes a different path which causes the ratings to fail. Using the equation/criteria for fills less than 12" causes a failure, whereas fills just greater than 12" pass with room to spare.

MnDOT would like to see an evaluation of AASHTO BrR in terms of its usability

MnDOT has seen differences in the load combinations used to rate culverts in various software tools so further guidance on the correct LCs to consider should be given.

The different load factors for vertical and horizontal earth pressure can be difficult to apply when performing a refined analysis such as FEA.

No.

Metal culvert specification is not as defined as the concrete culvert specification.

Mentioned that there seems to be a big change in LRFR at around the 2' fill line. Fills that are 1.9' provide very different results that fills that are 2.1'. They are interested to see if our research would investigate this. He said that this was also an issue in ASD but appears to be more pronounced in LRFR. Being under 2' of fill seems to come with a severe penalty. Current SD procedure is to design at different fill depths (e.g. 1'-5') and use the critical design.

Didn't want the project to be so broad that loses site of improving the specification while keeping it simple. The lateral distribution seems to be way off. The demand side (loads) don't seem to correlate well with the capacities.

No.

Based on talking to other state DOTs about what they are doing, there seem to be mixed messages from FHWA as to what is required as different agencies are taking different approaches to meet the FHWA requirements.

Also, given the number of culverts in the DOT inventories, there does not seem to be a significant benefit to load rating all of these structures given the amount of effort and cost to do so for little benefit given the low risk of failure of these structures.

Appendix B- Complete Survey Results

Q6: If you have any culvert input data (for AASHTO BrR or CANDE), particularly for problem culverts, we would be interested in making use of this for our research so please indicate whether you would be able to contribute any input files.
The spreadsheet they use is just a copy from MDOT.
Has mostly MathCADD spreadsheets.
No (from survey). Very little CANDE and BrR. Wouldn't likely be useful.
LADOT is willing to share AASHTOWare BrDR input files.
Michigan provided 4 AASHTOWare culvert files with rating issues with the following descriptions. <ul style="list-style-type: none"> • 70170025000C020 / M-6/WILDLIFE CROSSING : gives 0.0 RF due to depth fill height, extremely deep culvert ~ 29 ft buried • 77177011000C030 / M-19/COWHY DRAIN : it fails for overload class A but we scale down the axle weights for those routine permit trucks presumably will have gage width more 6 ft • 77177023000C030 / I-69 WB/ BURT DRAIN : we reduced the soil density and taken it as 70% of its actual weight 120pcf per AASHTO edition 6th otherwise we would've posted the bridge or closing it due to deep fill height ~ 16.5ft (presumably the culvert can NOT support fill and its weight, RF=0.0) • 46146041000C010 / M-34 Over BEAR CREEK : this is similar to C03 of 77011 <p>Most of our problems with culvert not rating is /was due to mainly fill heights, extremely deep buried culvert that according to BrR can't stand fill weight. Also we'd few problems with overload class A vehicles mainly to 60 kips truck. I couldn't find any structure that was done in-house that we ignored shear, there are couple instances that we only analyzed the top slab and ignored the walls.</p>
ODOT provided their spreadsheet they developed for CMPs.
Just starting to rate culverts.
Yes, South Dakota will share a few BrDR input files.
TxDOT will check to see if we can use CulvLR/Culv5.
I asked VDOT to elaborate on the following comment provided in his survey: <i>“There should be an emphasis placed on communicating the effects of the 2.0 live load factor for culverts when used to try to manipulate software to rate structures that are similar in nature to culverts but are not designed as culverts. This larger number in the denominator of the general rating equation has a significant effect on the final answer from the equation.”</i> <p>In some cases, BrR is used for culverts that don't quite fit the mold for BrR culverts. For example a three-sided culvert with an elliptical or oval shape (BrR only works with rectangular shaped culverts). VDOT will try to use Bridgeware (BrR) to approximate the loading. This is correct Conceptually, if you use the general equation (6A.4.2.1-1) from the MBE, when 2.0 is substituted for the live load factors given in Table 6A.4.2.2-1, the mathematical effect is to lower the rating factor.</p>

CANDE Tool Box Manual

For Load Rating

1 EXECUTIVE SUMMARY

The CANDE Tool Box greatly enhances the user friendliness of the CANDE finite element program to compute load rating factors (RF) for existing culvert-soil systems for any truck or live load configuration. The CANDE Tool Box is a standalone computer program that offers the user several options to ease the pain of developing CANDE input files and computing rating factors. Currently there are five options, which are briefly described below and explained in much greater detail within this manual.

1. Convert any Level-2 input file with half-mesh symmetry into an equivalent Level-3 file with full mesh topology. Useful for applying non-symmetric loading, alternate layering, and void zones.
2. Modify any Level-3 input file to include a pavement layer over the soil surface and/or convert top soil layer to an elastic wearing course. Useful for Load Rating existing culverts to include the load-spreading benefits inherent in pavements and prevent failure of nonlinear soil models.
3. Extend any Level-3 input file to include boundary conditions to simulate live loads moving over the mesh surface. Choose HL93 design or tandem truck or define any truck up to 10 axles. Useful for load rating existing culverts as well as designing new culverts.
4. Permanently revise the node numbering of any Level-3 input file to minimize the bandwidth of mesh topology. Useful for circumventing the time-consuming need to employ CANDE's built-in bandwidth minimizer that must be activated every time the input file is executed.
5. Compute load-ratings factors RF from CANDE output files including the controlling RF values for each design criteria along with all supporting information printed out at end of the CANDE Output Report.

This manual is organized in three major parts called Overview, Getting Started and Option Details. It is not necessary to read the entire manual before using CANDE Tool Box Program because the screen instructions and dialogue lead the user through executing each option and sub option. The user is encouraged to experiment with CANDE Tool Box by clicking on the executable icon contained in the same folder as this user manual.

CANDE Tool Box Manual For Load Rating

Table of Contents

1	EXECUTIVE SUMMARY.....	1
2	OVERVIEW	3
2.1	Tool Box Purpose.	3
2.2	Tool Box Options (user choices).	3
2.3	Input File Requirements.	3
2.4	File Names and Manipulations.	3
3	GETTING STARTED	5
3.1	Initial Screen Views.	5
3.2	Intermediate Screen Views.	8
3.3	Final Screen View.	8
4	OPTION DETAILS	9
4.1	OPTION 1: Level-2 half mesh to Level 3 full mesh.	9
4.2	OPTION 2: Add pavement and/or elastic wearing course.	10
4.3	OPTION 3: Add live loads on upper surface.	11
4.4	OPTION 4: Minimize Bandwidth.	17
4.5	OPTION 5: Calculate Load Rating Factor RF.	18

Appendix C – CANDE Tool Box Manual

2 OVERVIEW

2.1 Tool Box Purpose.

CANDE Tool Box (CTB) is a stand-alone computer program that operates on existing CANDE input and output files to generate new executable CANDE input files with enhanced capabilities or to compute load rating factors from previous CANDE solutions with live loads. All generated files and calculations are saved in the originating folder for easy access. Currently there are five options, which are briefly described below and subsequently explained in greater detail.

2.2 Tool Box Options (user choices).

1. Convert any Level-2 input file with half-mesh symmetry into an equivalent Level-3 file with full mesh topology. Useful for applying non-symmetric loading, alternate layering, and void zones.
2. Modify any Level-3 input file to include a pavement layer over the soil surface and/or convert top soil layer to an elastic wearing course. Useful for Load Rating existing culverts to include the load-spreading benefits inherent in pavements and prevent failure of nonlinear soil models.
3. Extend any Level-3 input file to include boundary conditions to simulate live loads moving over the mesh surface. Choose HL93 design or tandem truck or define any truck up to 10 axles. Useful for load rating existing culverts as well as designing new culverts.
4. Permanently revise the node numbering of any Level-3 input file to minimize the bandwidth of mesh topology. Useful for circumventing the time-consuming need to activate CANDE's built-in bandwidth minimizer that must be activated every time the input file is executed.
5. Compute load-ratings factors RF from CANDE output files that represent LRFR analysis and printout the final RF values with supporting information at the end of the CANDE output report.

2.3 Input File Requirements.

To exercise any of the options, the existing input file (CID) must have been successfully executed by the CANDE program, and the associated CANDE Output file (OUT) is resident in the same folder as the input file, which is the normal case unless the user rearranged the file locations. Taken together, the original input file and output files supply the basic information for creating new CID files with Options 1 to 4. For Option 5, the output file provides the data source to compute load-rating RF values as well as the permanent file to record the results.

2.4 File Names and Manipulations.

For purposes of discussion, assume that the originating CANDE input file is named "MyCulvert.cid", and as always, the associated CANDE output file is automatically named "MyCulvert.out". The table below shows the final result of applying any Tool Box option on an existing file, MyCulvert.cid. The last column shows the new file name generated by the Tool Box and stored in the original folder. The four-letter prefixes (Full-, Pave-, Live- and Bmin-) remind the user how this file has been modified from the

Appendix C – CANDE Tool Box Manual

originating file. For example, Full-MyCulvert.cid implies a full mesh input file has been created from the Level-2 half mesh file called MyCulvert.cid.

Table 1. Overview of Tool Box options and file creation and modifications.

Tool Box User Options	Originating file identified by user via a browser	Additional data Supplied by user via screen prompts	New file generated by Tool Box
(1) Create Level-3 Full mesh from Level-2 Half mesh	MyCulvert.cid (Any Level-2 File)	None	Full-MyCulvert.cid (Level-3 file)
(2) Add Pavement layer or elastic wearing course to surface of soil	MyCulvert.cid (Any Level-3 File)	Pavement and/or wearing course data: Elastic properties.	Pave-MyCulvert.cid (Level-3 file)
(3) Add live loads over mesh surface	MyCulvert.cid (Any Level-3 File)	Vehicle data: Axles, loads, footprints, locations, adjustments, etc.	Live-MyCulvert.cid (Level-3 file)
(4) Minimize bandwidth by permanently renumbering nodes	MyCulvert.cid (Any Level-3 File)	None	Bmin-MyCulvert.cid (Level-3 file)
(5) Compute load-rating values and add to Output Report.	MyCulvert.cid (Any Level-3 File) (Or Level-2 File)	Load-step data: End of Construction, Start of Live load, End of Live load.	MyCulvert.out (Same file as original output file with additional RF data)

Appendix C – CANDE Tool Box Manual

If desired, the Tool Box options may be applied in succession, i.e., one option after another. For example, to add a Pavement overlay to the newly generated full mesh file, select Option 2 and identify the originating file as Full-MyCulvert.cid. The final output from the Tool Box is called Pave-Full-MyCulvert.cid. If all four options are selected in succession, then the final file is named, Bmin-Live-Pave-Full-MyCulvert.cid.

Option 1 works on any Level 2 input file including all modifications with Level-2 Extended. For Options 2, 3 and 4 the originating file may be any valid Level 3 cid file, perhaps developed manually or generated by third-party software packages such as NASTRAN or Cande-Cad-Pro. It is not necessary that the originating input file have line tags like those created by the CANDE GUI. If line tags do not exist on the originating file, they will not be inserted on the generated file. Conversely, if line tags are used in the originating file, they will also be inserted in the generated file.

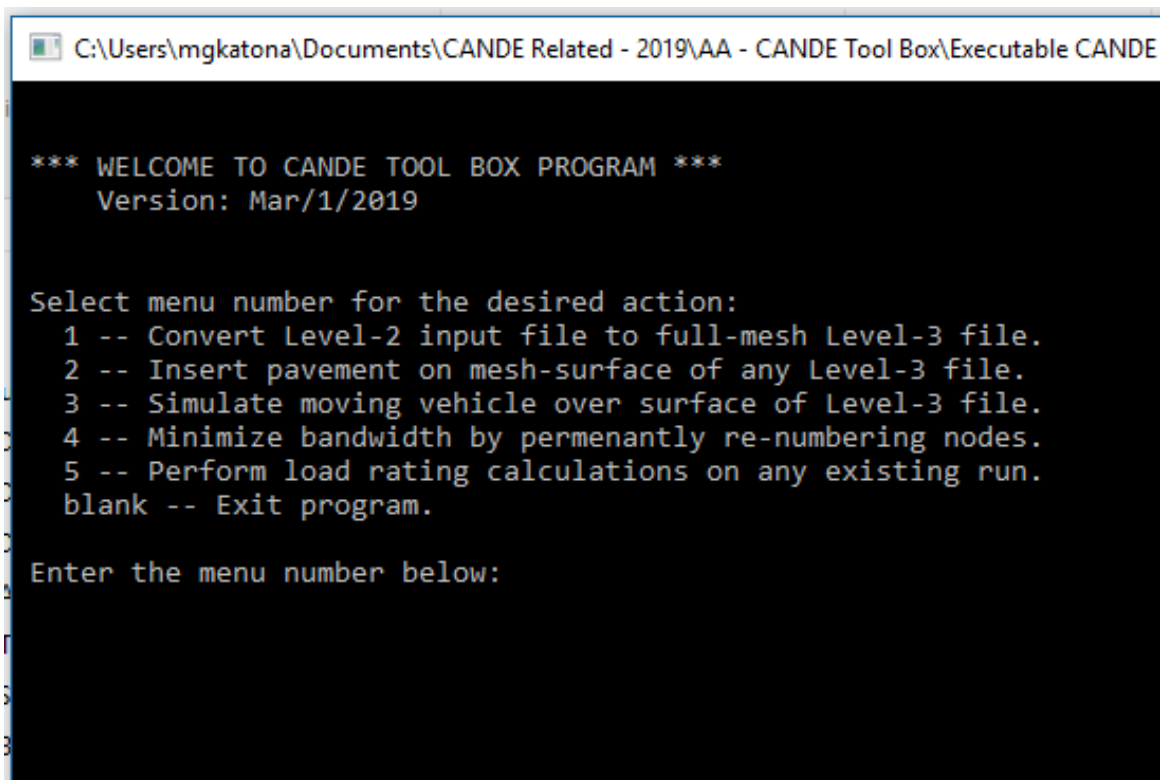
Option 5 works on any output file. It does not create a new file, but rather, reads and processes the originating output file to compute the load rating factor RF and then prints the results at the end of the originating output file. Detailed explanations about option 5 as well as the other options are presented in the last section of this document.

3 GETTING STARTED

3.1 Initial Screen Views.

After the CANDE Tool Box (CTB) executable program is downloaded and stored in the computer, the user need only double click the application icon to open the welcoming screen shown below. As shown, the first query requests the user to select the desired option by entering the number 1, 2, 3, 4, or 5. Entering a blank value is the signal to exit the program. The welcoming screen reappears after each option is completed so multiple options can be executed in one session.

Appendix C – CANDE Tool Box Manual



```
C:\Users\mgkatona\Documents\CANDE Related - 2019\AA - CANDE Tool Box\Executable CANDE

*** WELCOME TO CANDE TOOL BOX PROGRAM ***
Version: Mar/1/2019

Select menu number for the desired action:
 1 -- Convert Level-2 input file to full-mesh Level-3 file.
 2 -- Insert pavement on mesh-surface of any Level-3 file.
 3 -- Simulate moving vehicle over surface of Level-3 file.
 4 -- Minimize bandwidth by permanently re-numbering nodes.
 5 -- Perform load rating calculations on any existing run.
blank -- Exit program.

Enter the menu number below:
```

After any option number is entered, the screen shows the number and description of the selected option along with a request for the user to identify the associated CANDE CID file. The example shown below is the view screen when Option 1 is selected. Remember, the selected originating file must have been executed with CANDE before selecting it.

Appendix C – CANDE Tool Box Manual

```

C:\Users\vmgkatona\Documents\CANDE Related - 2019\AA - CANDE Tool Box\Executable CANDE T
*** WELCOME TO CANDE TOOL BOX PROGRAM ***
Version: Mar/1/2019

Select menu number for the desired action:
 1 -- Convert Level-2 input file to full-mesh Level-3 file.
 2 -- Insert pavement on mesh-surface of any Level-3 file.
 3 -- Simulate moving vehicle over surface of Level-3 file.
 4 -- Minimize bandwidth by permanently re-numbering nodes.
 5 -- Perform load rating calculations on any existing run.
blank -- Exit program.

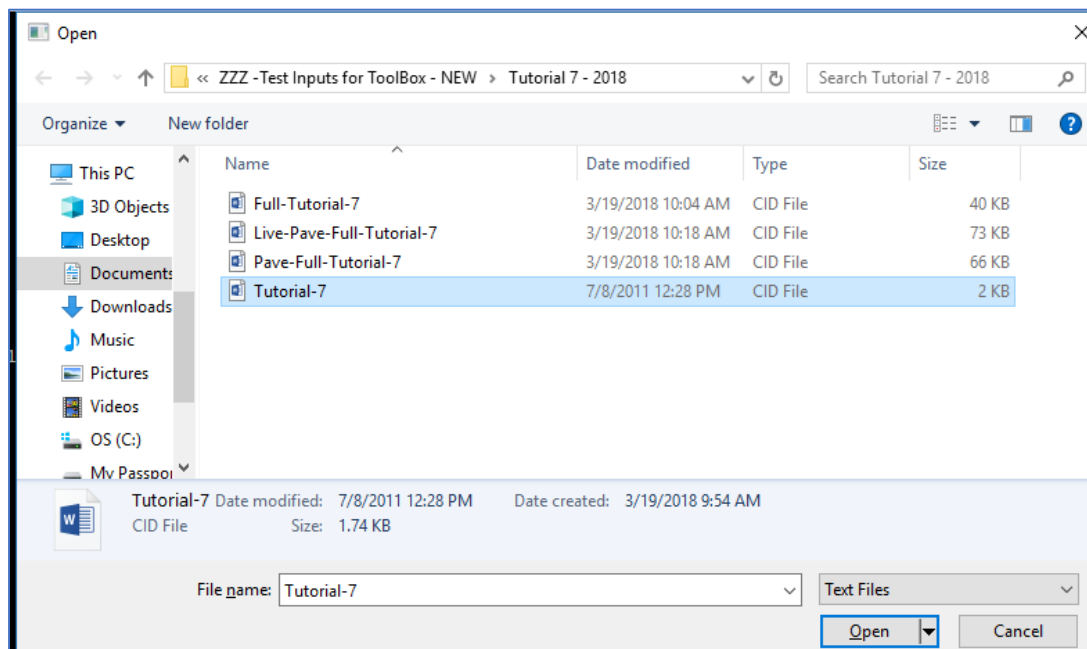
Enter the menu number below:
1
Menu number = 1

MENU OPTION #1: LEVEL 2 to LEVEL 3 FULL MESH CONVERTER.
Using the following browser screen, select the Level 2 cid
file to be processed for creating a new Level 3 cid file.

Press enter to see browser screen.

```

As indicated by the last sentence in the above screen, the user is required to press “Enter” on the key board to open a browser to the computer directory in order to select the desired CID file by double clicking. An example browser screen is shown below wherein “Tutorial-7.cid” is the chosen CID file.



Appendix C – CANDE Tool Box Manual

3.2 Intermediate Screen Views.

The above three screen views are similar for all options; however, the subsequent screen views are dependent on the selected option number. Options 1 and 4 require no additional user input, whereas Options 2, 3, and 5 require additional user input as directed by individual queries appearing on the screen. The third column in Table 2 indicates the type of data that is requested from the user; and the last section of this document provides greater detail on the data requested for each option along with default values. The screen views offer reasonable default options that the user may select to answer the queries.

3.3 Final Screen View.

The last screen view is similar for all options. First, a message to the user states that the option was successfully completed. If it had not been successful, the user would have been previously notified of the cause of the problem such as the Output file could not be found in the specified directory. Second, the user is informed of the name of the new CID file generated by options 1, 2, 3 or 4; or for option 5, the user is provided with a summary of the load rating calculations. An example of the final screen view is shown below for option 1.

```

MENU OPTION #1: LEVEL 2 to LEVEL 3 FULL MESH CONVERTER.
Using the following browser screen, select the Level 2 cid
file to be processed for creating a new Level 3 cid file.

Press enter to see browser screen.

Selected CID File Name = Tutorial-7.cid

Good Start! Level-2 first input line A-1 reads:
Heading = New Input file

Success!
Full level-3 cid file is located in same folder
New file name = Full-Tutorial-7
Information is printed at botton of file after STOP

Press Enter for next options.

```

As shown, the new CID file is named “Full-Tutorial-7”, and as indicated by the 2nd to last line, a description of the new CID file is written at the bottom of the input file for future reference. Indeed, all five options provide a written record of user selections and key calculations for future reference.

Appendix C – CANDE Tool Box Manual

4 OPTION DETAILS

4.1 OPTION 1: Level-2 half mesh to Level 3 full mesh.

This option is applicable to any existing Level-2 input file including all Level-2-Extended modifications. To develop the new Level-3 input file with full mesh topology, information is taken from the originating Level-2 input file and also from the Level-2 output file. The output file contains generated data from the CANDE pre-processing subroutines including the complete set of nodal coordinates, element properties and boundary conditions that define the right half of the full Level-3 input file.

The Option-1 algorithm generates the left-half side of the full mesh as a mirror image of the right-side mesh so that original number of nodes (N_{half}), elements (M_{half}), and boundary conditions (BC_{half}) become approximately doubled for the full mesh; i.e., $N_{\text{full}} \approx 2 N_{\text{half}}$, $M_{\text{full}} \approx 2 M_{\text{half}}$, and $BC_{\text{full}} \approx 2 BC_{\text{half}}$. Note the relationships are “approximately” doubled due to the vertical centerline ($x = 0$) wherein nodes, interface elements and boundary conditions are not counted twice because the centerline does not have a separate mirror image.

Specifically, the left-side mesh topology is generated from the right side by assigning each left-side node number n_L equal to the corresponding right-side node n_R plus the total number of half-mesh nodes, and then expressing the x and y coordinates as the mirror image as shown below.

- $n_L = n_R + N_{\text{half}}$ for $n_R = 1, 2, 3 \dots N_{\text{half}}$
- $x(n_L) = -x(n_R)$
- $y(n_L) = y(n_R)$

In a similar manner, the left side elements m_L and boundary conditions bc_L are generated from the corresponding right side numbering as shown below.

- $m_L = m_R + M_{\text{half}}$ for $m_R = 1, 2, 3 \dots M_{\text{half}}$
- $bc_L = bc_R + BC_{\text{half}}$ for $bc_R = 1, 2, 3 \dots BC_{\text{half}}$

As already indicated, the above assignments are not performed whenever a node, interface element, or boundary condition is on the centerline ($x=0$). Special modifications are required for the original boundary conditions on the centerline, i.e., all lateral displacement constraints are removed and the magnitude of vertical forces are doubled to correctly represent the original half- symmetric conditions. Other special treatments include revising the beam element numbering for arch meshes so that the beam elements are in ascending order in traveling from the left footing to the right footing.

The new Full-mesh input file as created by Option 1 is theoretically equivalent to the original Level-2 input file so, without further changes, both solutions give essentially the same results. Slight differences in solutions are observed due to truncation of coordinate values recorded in the output report, round-off error in equation solving, and extrapolation approximations for beam-element nodes at the start and end of a pipe group.

Of course, the whole purpose of creating the Full-mesh input file is to modify it in order to apply non-symmetric loads and/or material zones to the new mesh. To this end, it is recommended to first execute

Appendix C – CANDE Tool Box Manual

the Full-mesh input file and utilize the GUI Mesh Plot to visualize the nodes, elements and boundary conditions you wish to add or change.

4.2 OPTION 2: Add pavement and/or elastic wearing course.

This option is applicable to any existing Level-3 input file that has a continuous horizontal soil surface. Three sub-options are available: (1) Add pavement layer, (2) Change top layer to an elastic wearing course, and (3) Perform both operations. Each sub-option is explained below.

1. **Pavement.** Add a pavement layer to the soil surface to take advantage of the real beneficial effects on load-rating analysis. Pavement is modeled with elastic beam elements whose properties are defined by the user in response to screen prompts. Default values represent modest asphalt.
 - Pavement uniform thickness (default = 8.0 inches)
 - Young's modulus (default = 200,000 psi)
 - Poisson ratio (default = 0.2)
 - Weight density (default = 140 lbs./ft³)

The beam elements are placed over the highest layer of soil elements. Each beam element coincides with the top face of a surface soil element so that the beam-element length matches the soil element's surface length. Since beam elements share the same nodes as the soil elements, no new nodes are added to the system, only beam elements. The pavement extends over the entire surface except for the soil elements at the extreme left and extreme right so that pavement does not receive any boundary support from the sides of the mesh. The pavement is formed with BASIC beam elements, which are assigned a group number one digit higher than the highest existing beam group number in the originating input file.

2. **Elastic Wearing Course.** Change the top row of soil elements from a nonlinear model such as Duncan/Selig or Mohr/Coulomb to an elastic wearing course in order to avoid local failure due to concentrated live loads. Elastic wearing course properties are input by the user in response to screen prompts wherein the default values represent properties of an average soil.
 - Young's modulus (default = 1,800 psi)
 - Poisson ratio (default = 0.33)

If pavement is not included in the CANDE model, then sub-option 2 is generally required in order to avoid surface failure of nonlinear soil models from concentrated live loads. Engineers do not usually include pavements when designing new installations because construction vehicles operate over soil surface prior to being paved. In such cases, the elastic wearing course is recommended.

3. **Pavement plus Wearing Course.** Add a pavement layer and change top soil layer to an elastic wearing course. This sub-option is useful when nonconvergence occurs due to sub-pavement soil failure that may occur if the pavement is too flexible.

For any of the three sub-options, the new input file is uniquely named by adding the prefix "Pave-" to the name of the originating file, and a permanent record of the pavement details and/or wearing course is printed at the end of input file for future reference.

Appendix C – CANDE Tool Box Manual

4.3 OPTION 3: Add live loads on upper surface.

This option is applicable to any existing Level-3 input file that has a continuous horizontal soil surface above the culvert wherein the soil surface may be paved or unpaved. Live loads are simulated by point-like strip forces applied as boundary conditions at specific nodes and load steps. Moving loads are simulated by applying the strip force to a particular node at load-step k and then applying the force to the neighboring node at step $k+1$ while at the same time removing the strip force from the previous node. This process may be repeated to generate long travel paths and can be generalized for multiple axle loads to simulate truck travel.

To make this option as general as possible, the user is required to input a variety of data; however, the default values provided by the program make this task relative easy. The series of data entries and default values are presented below.

1. **Identify the pipe-group number of structure subject to live loading** . (Default = 1)

Often there is only 1 pipe group defined in the input file so that default value often applies.

However if multiple pipe groups are defined in the input file, then user selects the group number of the current target structure (Option 3 can repeated for other target group numbers). Once the target structure is identified, the program determines the soil cover height and key node information relative to the target structure and prints the information on the screen for reference.

2. **Specify desired truck type – Enter 1, 2 or 3:** (Default = 1)

- Enter 1 for HL93 3-axle Design Truck (as defined by AASHTO)
- Enter 2 for HL93 2-axle Tandem Truck (as defined by AASHTO)
- Enter 3 for User-defined truck (N-axles specified by user)

If the user enters 1 or 2 no additional truck data is required, and the AASHTO defined truck properties are printed on the screen. If the user enters 3, the following additional data must be supplied:

- Number of axles (from 1 to 10)
- Weight of each axle in kips
- Spacing between axles in feet
- Wheel footprint dimensions L x W in inches. (Default 10" x 20" for all wheels)
- Centerline spacing between wheels in feet. (Default 6' for all axles)

3. **Answer yes or no to a series of questions on live-load modifications.** If the answer is yes, then additional information must be provided, or accept the default value.

a) Do you wish to remove previous live loads the input file?

If yes, enter the beginning load step numbers of the old live loads. Or accept default. Default = load-step number following the last soil-construction load step.

This is a quick way of clearing all previous live-loads in the originating CID file; otherwise, the old live loads will be applied in addition to the new live loads.

Appendix C – CANDE Tool Box Manual

- b) Do you wish to add a lane-loading pressure on top surface?
If yes, enter the lane pressure in psi units. Or accept default value.
Default = 0.444 psi per AASHTO.
- c) Do you wish to apply a dynamic impact factor to vehicle loads?
If yes, enter the impact factor as a fraction of total load. Or accept default calculation.
Default = $0.33(1 - H/8)$, where H is cover height in feet per AASHTO.
- d) Do you wish to invoke a multi-lane presence factor to increase loads?
If yes, enter multi-lane presence factor as a fraction of total load. Or accept default value.
Default = 0.2 per AASHTO.

Comment on load modifications. The load modifications described in items c and d produce the AASHTO service load value that increases static truck weight. Modifications for longitudinal effects and LRFD load factors are discussed in items 4 and 5, respectively.

4. Do you wish to account for longitudinal load-spreading and 3D stiffness effects?

If yes, select the desired method of accounting for longitudinal load spreading and 3D stiffness effects. Whereas longitudinal load spreading is inherent in all culvert installations, the phenomenon of 3D stiffness effects (3DSE) is currently only documented for reinforced concrete boxes and arches under shallow fill, AASHTO Article 4.6.2.10. (For full discussion, see latest version of CANDE Solution Methods and Formulations Manual, Chap. 8.1).

- (1) Enter 1 for the AASHTO Reduced Surface Load (RSL) procedure using AASHTO load-spreading Equations 3.6.1.2.6, (i.e., $W(H) = W_0 + 1.15H + 0.06*\text{Span}/12$, where all variables are expressed in inches). RSL reduces the surface load to account for longitudinal load spreading through the soil for 1-wheel or 2-wheel axle loads depending on culvert depth. If requested, 3D stiffness effects (3DSE) re-adjust the distribution width as required. Note that the term “ $0.06*\text{Span}/12$ ” is relatively new in the AASHTO specifications, and it implies the the reference depth for correcting the surface load is deeper than just the cover depth H, which was the old reference depth used in legacy AASHTO specifications.
- (2) Enter 2 for the new Continuous Load Spreading (CLS) procedure, which automatically spreads 1- and 2-wheel axle loads by increasing element thickness as a continuous function of soil depth using the Elasticity-Based-Method for load-spreading. If requested, 3D stiffness effects are also applied to the culvert in a continuous and mechanically consistent manner. CLS is considered the most accurate procedure to account for longitudinal load-spreading and 3DSE. See latest version of CANDE Solution Methods and Formulations Manual, Chap. 8.1.3 for a complete understanding of this revolutionary new procedure.

Appendix C – CANDE Tool Box Manual

- (3) Enter -1 for the legacy AASHTO Reduced Surface Load (RSL) procedure using the old AASHTO load-spreading Equation $W(H) = W_0 + 1.15H$ (without the “Span” term). Otherwise, this choice is identical to (1). AASHTO’s legacy specification is more conservative than AASHTO’s current specification. See latest version of CANDE Solution Methods and Formulations Manual, Chap. 8.1.2 for a complete understanding of the current AASHTO specifications.

If RSL is selected by either 1 or -1, choose a sub-option . Two RSL sub-options are available: (a) constant reduction factor based on minimum soil cover over entire structure, or (b) variable reduction factor based on soil cover between each live-load surface node and the vertical distance to the structure’s periphery.

- (a) Enter 1 for RSL constant reduction factor for all live-load locations. This is considered the traditional conservative approach
- (b) Enter 2 for RSL variable reduction factor dependent on live-load location. This is considered a more realistic approach.

For either RSL sub-option, the user has the choice to include 3D stiffness effects (3DSE) to further reduce the surface load in accordance AASHTO LRFD Specifications 4.6.2.10 for r/c boxes and arches. This choice is activated by entering a non-zero value for the culvert length in response to the following screen request:

- Enter lay length of precast r/c culvert (feet) → 3DSE is on.
- Or, enter full length of cast-in-place culvert (feet) → 3DSE is on.
- Or, enter blank to ignore special 3D effects. → 3DSE is off.

The CANDE Tool Box (CTB) computes the RSL reduction factor(s) in two-steps, first load spreading through the soil and then consideration for 3DSE if requested.

For load spreading through the soil, the AASHTO Ad Hoc Method (AAM) is employed, which assumes a 30-degree spread beneath the wheel length (W_0) as a function of soil depth H . Thus, depending on the user’s choice of the RSL sub-option, H is defined in one of two ways.

- For RSL-suboption (a), H = cover height over crown, a constant value for all live-load locations.
- For RSL-suboption (b), H = variable cover height, i.e., vertical distance between load location on surface and the culvert periphery directly below the loaded node.

With the above understanding, CTB calculates the load-spreading reduction factor for each live-load location in accordance with AASHTO 1-wheel and 2-wheel interaction rules, which are dependent on H and the 2-wheel interaction depth H_{int} , i.e.;

$$H_{int} = (S - W_0 - D_6)/1.15$$

Where, S = spacing between wheels on axle (inches)

W_0 = wheel width, typically 20 inches

Appendix C – CANDE Tool Box Manual

$$D_6 = \begin{cases} 0.06 * \text{Span} / 12, & \text{additional span term for current AASHTO} \\ 0.0, & \text{no span term for legacy AASHTO approach} \end{cases}$$

$$\text{Spreading reduction factor} = \begin{cases} W_0 / (W_0 + 1.15H + D_6) & \text{for } H < H_{\text{int}} \\ 2W_0 / (W_0 + S + 1.15H + D_6) & \text{for } H \geq H_{\text{int}} \end{cases}$$

If 3D stiffness effects are activated (3DSE on), enter the culvert 3DSE parameters, W_{min} and W_{critical} , which are the minimum and critical 3DSE distribution widths, respectively. Or, accept the AASHTO 4.6.2.10 values for r/c box and arch culverts, dependent on the culvert's span and length. Currently, AASHTO assumes a constant 3DSE distribution width so that $W_{\text{min}} = W_{\text{critical}}$ as shown below (all units are inches).

$$W_{\text{min}} = W_{\text{critical}} = \frac{1}{2}(96.0 + 0.12 * \text{Span}), \text{ but } W_{\text{min}} \ \& \ W_{\text{critical}} \leq \text{Culvert length.}$$

Thus, the reduction factor as controlled by 3DSE is given by;

$$\text{3DSE reduction factor} = W_0 / \left(W_{\text{min}} + \frac{H_n}{H_{\text{trans}}} (W_{\text{critical}} - W_{\text{min}}) \right)$$

H_{trans} is the transition soil depth wherein the load spreading width is equal to W_{critical} , and H_n is the minimum cover for sub-option (a) or the vertical cover beneath the loaded surface node for sub-option (b).

Finally, the controlling RSL reduction factor applied to a particular surface load location is given by the minimum value from load spreading and 3DSE calculations. That is,

$$\text{Controlling reduction factor} = \text{Minimum of: (load spreading, 3DSE)}$$

Comment on RSL methods. RSL sub-option (a) with constant H (soil cover over crown) is the older traditional RSL method that some investigators still prefer. RSL sub-option (b) with variable H (dependent on location of live load) is a newer approach preferred by various practitioners. Clearly for a single live load located directly over the crown both sub-options produce the same results. For multiple axle trucks, sub-option (a) tends to be slightly more conservative, but this is not always the case.

If CLS is selected. The CLS method does not require any additional input from the user to simulate load spreading through soil and structure. This is because the CANDE program automatically amplifies the stiffness of each element as a continuous function of soil depth based on the EBM theory of longitudinal load spreading denoted as $W(y)$.

Appendix C – CANDE Tool Box Manual

If it is also desired to consider 3D stiffness effects (3DSE) for reinforced concrete boxes and arches (AASHTO LRFD Section 4.6.2.10.), then enter a non-zero value to the following screen prompt:

- Enter lay length of precast r/c culvert (feet) → 3DSE is on.
- Or, enter full length of cast-in-place culvert (feet) → 3DSE is on.
- Or, enter blank to ignore special 3D effects. → 3DSE is off.

If 3DSE is on, enter the culvert 3DSE parameters, W_{\min} and W_{critical} , which are the minimum and critical 3DSE distribution widths, respectively. Or, accept the AASHTO 4.6.2.10 values for r/c box and arch culverts, dependent on the culvert's span and length where all units are inches.

$$W_{\min} = W_{\text{critical}} = \frac{1}{2}(96.0 + 0.12 * \text{Span}), \text{ but } W_{\min}, W_{\text{critical}} \text{ upper limit is Culvert length.}$$

With the above information, the CLS algorithm in the CANDE program applies the controlling amplification factor to each soil and structure element to simultaneously account for load spreading and 3DSE. For a detailed discussion see latest version of CANDE Solution Methods and Formulations Manual, Chapter 8.1.5.

Comment on CLS Method. The CLS method is more accurate than the RSL methods and is easier to use because the CLS method automatically applies the appropriate amplification to each element as a function the element depth beneath the travel surface. No reduction factors are calculated or used; rather, the truck's service line-load is applied directly to the surface nodes. Thus, the soil beneath the wheel experiences the actual transmitted state of stress, not a reduced stress state like RSL. Although the current AASHTO specifications imply $W_{\min} = W_{\text{critical}}$ (one effective parameter), the two parameter methodology is in anticipation of future changes to the AASHTO LRFD Specifications.

5. Do you wish to apply an LRFD or LRFR load factor to all live-loading steps?

If yes, enter load factor applied to all live loads. Or accept default value.

Default = 1.75 for ASSHTO LRFD analysis.

LRFD (or LRFR) load factors are stored separately at the end of the CANDE input file (E-lines) as a function of load step. Load factors are applied to the service loads generated above prior to each incremental solution obtained at each load step. The beauty of this arrangement is that the user may execute solutions with new load factors without having to regenerate the service loads.

6. Identify load-step number to initiate the first vehicle loading.

Enter load-step number to begin vehicle loading. Or accept default load step

Default = first load step after construction is complete & lane load is applied.

7. Identify key axle number for positioning vehicle relative to structure.

Enter key axle number of vehicle for positioning. Or accept default axle number.

Default = axle number of heaviest axle (first axle number for same weight axles)

Appendix C – CANDE Tool Box Manual

For example, the key axle number for HL93 Design trucks = 2 (2nd axle)

8. Identify the surface node number for the initial key-axle position.

Enter surface node number for starting position of key axle. Or accept default node number.

Default = the surface node located directly above the left periphery of the structure.

9. Identify the surface node number for the final key-axle position.

Enter surface node number for final position of key axle. Or accept default node number.

Default = the surface node located directly above the right periphery of the structure.

10. Select node-loading method for axles other than the key axle. Non-key axles are invariably positioned between two adjacent surface nodes, rather than positioned on a single node like the key axle.

- Enter 1 to apply non-key axle loads at only one node, i.e., the node closest to key-axle position (conservative approach). Default method
- Enter 2 to apply load to both nodes in proportion to the node's proximity to the non-key axle load. Thus if the axle is located midway between the nodes, each node would receive 50% of the non-key axle load (reasonable approach).

Comment on vehicle travel path. Vehicle travel is from left to right wherein the key-axle is placed at the starting node for the initial live-load step and then advances to the next adjacent node on the next load and so on until the key axle is advanced to the final node position. Thus the number of load-steps associated with vehicle travel is equal to the number of nodes along the key-axle path. All other axles (if any) track in lock-step fashion as dictated by their fixed distances from the key axle. These non-key axle loads are applied to either one node (worst case) or distributed to two nodes (reasonable case) per user's selection in item 10. The one-node method uses that node of the node pair that is closest to the key-axle load and thereby localizing load contributions, a conservative method. Alternatively, the two-node method may be selected if the one-node appears too conservative.

All of the above input data and selections made by the user are permanently recorded at the end of the new input file. For example, the result of applying Option 3 to a full mesh version of CANDE Tutorial-7 for passage of a tandem truck is copied below.

Appendix C – CANDE Tool Box Manual

USER-SELECTED LIVE LOAD PARAMETERS:

- * Initially applied lane pressure (psi) = 0.4444
- * Number of axles on vehicle = 2
- * Key axle number for tracking = 1
- * Starting node for key axle = 262
- * Ending node for key axle = 128
- * Beginning vehicle load step # = 8
- * Ending vehicle load step # = 16
- * Number of nodes loaded for Non-key axles = 2

VEHICLE CHARACTERISTICS PER AXLE:

Axle number	Axle load, lbs	Axle Distance to key-axle, ft	Wheel LxW print, in	Wheel tire spacing, ft	Wheel line load, lbs/in
1	25000.00	0.00	10 x 20	6.00	625.00
2	25000.00	-4.00	10 x 20	6.00	625.00

MULTIPLIERS ON WHEEL LINE-LOAD DEFINING SERVICE LOAD.

CANDE BOUNDARY CONDITIONS SHOW THE FINAL SERVICE LOAD.

- * Multilane presence factor (multiplier) = 1.200
- * Dynamic impact factor (multiplier) = 1.248

LONGITUDINAL LOAD SPREADING AND 3D STIFFNESS EFFECTS

- * User selected RSL-constant-reduction factor procedure.
- * $W_{critical} = 55.80$, therefore, 3DSE is considered.
- * Default AASHTO reduction factor is controlled by Special 3DSE width controls
- * Value of the default AASHTO reduction factor = 0.358
- * User chosen value for constant reduction factor = 0.358

LIVE-LOAD FACTORS FOR LRFD or LRFR ANALYSIS ARE SHOWN IN THE LAST SEGMENT OF THE ABOVE CANDE INPUT FILE AND ARE AUTOMATICALLY APPLIED TO THE SERVICE LOADS SHOWN IN THE BCs

4.4 OPTION 4: Minimize Bandwidth.

This option is applicable to any existing Level-3 input file wherein node numbering is not optimum and is alternative to using CANDE's internal bandwidth minimizer. The downside of CANDE's internal bandwidth minimizer is that it is time consuming and must be repeated every time the input file is executed. In contrast, the Tool Box bandwidth minimizer creates a permanent change in the nodal numbering scheme within the new input file so that input file may be executed multiple times without the need of any further bandwidth minimization. No additional data is required for Option 4.

Bandwidth is proportional to the maximum difference in the nodal numbers assigned to any element. A prime cause of large bandwidths comes from adding nodes and elements into an existing finite model such as introducing an interface or link element between existing elements thereby causing a large mismatch in the element's nodal numbers. Another example is a result of Tool Box Option 1 wherein the first row of elements on the mirror side of the centerline contains a fusion of low-numbered and high-numbered node numbers. Thus, applying Option 4 to full Level-3 meshes created from Option 1 is generally a good idea to reduce the time for each CANDE solution.

The procedure to minimize bandwidth is to permanently redefine the nodal numbering, not the coordinate values, but just the node number assigned to the coordinates. This is achieved by starting with node "1"

Appendix C – CANDE Tool Box Manual

in lower left corner of element located in the lower left corner of the mesh. Node numbers are sequentially increased for the next upward element and so on up to the top surface. Next shifting to the bottom of the mesh, the process is repeated again and again until the entire mesh has been processed. During the process an “is/was” vector is developed that correlates the old node number to the new node number. The is/was vector is used to assign the new node numbers to the element connectivity array and to update the boundary conditions with the new node numbers.

The originating CID file and the new CID file should produce the same results except for round-off error which is less for the new file with the Bmin prefix because there are less calculations in solving the global system of equations.

4.5 OPTION 5: Calculate Load Rating Factor RF.

This option is applicable to any existing Level-2 or Level-3 output file that contains live loads. Ideally the CANDE analysis should use LRFD methodology, which is directly related to LRFR load rating analysis. Working Stress methodology may be used; however, the user must adjust the applied loads and capacities to represent factored values. The basic assumption is that the associated CANDE input file is developed especially for the particular culvert installation and vehicle being load rated. That is, the load factors, resistance factors, and system parameters are in accordance with the governing LRFR specifications such as *ASSHTO Manual for Bridge Evaluation*.

As defined below, the AASHTO load rating factor RF_n must be greater or equal to 1 for all strength-related design criteria in order for a particular vehicle to safely passover the culvert installation.

$$RF_n = \frac{C_n - D_n^{\text{dead}}}{D_n^{\text{live}}} \geq 1 \quad \text{for } n = 1, 2, 3 \dots \quad \text{Equation 5a}$$

where, C_n = factored capacity (resistance) for design criterion n.

D_n^{dead} = factored dead-load demand for dead and earth loads for design criterion n

D_n^{live} = factored live-load demand for vehicle and lane loads for design criterion n

n = index number for design criterion, which is dependent on culvert material.

Said another way, if $RF_n \geq 1.0$ for all design criterions $n = 1, 2, 3 \dots$, then the culvert safely passes the load-rating test for the particular live load analyzed. The minimum RF_n value (simply referred to as RF) is the controlling value, and its value is a multiple of the live-load safety. For example, if $RF = 1.80$, the culvert system is capable of safely carrying a live-load approximately 1.8 times greater than the magnitude of live-load analyzed.

It is important to understand that Equation 5a is exactly equivalent to the LRFD design requirement that the ratio of the total factored demand to factored capacity is less than 1 for all design criteria. That is,

$$\text{Ratio}_n = \frac{D_n^{\text{total}}}{C_n} \leq 1 \quad \text{for } n = 1, 2, 3 \dots \quad \text{Equation 5b}$$

where, $D_n^{\text{total}} = D_n^{\text{dead}} + D_n^{\text{live}} =$ total factored demand for design criterion n.

Appendix C – CANDE Tool Box Manual

To prove that the inequality in Equation 5b is exactly equivalent to the inequality in Equation 5a, multiply both sides of inequality 5b by the factored capacity C_n , then replace D_n^{total} with the above component definition and subtract D_n^{dead} from both sides, and finally divide by D_n^{live} to get the same inequality shown in 5a.

Since CANDE automatically computes Equation 5b in the “assessment summary” at the end of each load step, the equivalence of the inequalities expressed in Equations 5a and 5b has the following useful benefit. If the CANDE solution shows that the assessment summaries satisfy, $\text{Ratio}_n < 1.0$, for all load steps and all design criteria, then it is guaranteed that all $\text{RF}_n > 1$, meaning the live-load safely passes the load rating test. The opposite is also true, if $\text{Ratio}_n > 1.0$ at any load step and for any design criterion, then it is guaranteed that $\text{RF}_n < 1$, meaning the live-load did not safely pass the load rating test.

Thus, if an engineer only wants to know if a particular vehicle passes the load rating test ($\text{RF} \geq 1$), then it is only necessary to scan the CANDE assessment summaries to verify that all Ratios are ≤ 1 for all load steps. On the other hand, if an engineer wants to know the controlling RF_n values, then a much more extensive search through the CANDE output report is required, not just the assessment summaries. This is because the load step and node where Ratio_n is maximum is not necessarily the same load step and node where RF_n is minimum. Only in the case $\text{Ratio}_n = \text{RF}_n = 1$, can it be guaranteed that controlling demand-to-capacity ratio and the controlling load-rating factor occur at the same node and load step.

To initiate load-rating process (Option 5), the user is requested to identify the pipe group number under investigation, the load-step number that completes dead loads, and the live-load step numbers that define the start and end of the vehicle path whether it be 1 step or many. As noted below the CTB program provides reasonable default values that may be accepted in lieu of entering data.

1. Enter pipe-group number of structure to be load rated. Or, accept default value = 1. Often there is only 1 pipe group in the input file so that the default value usually applies. However if multiple pipe groups are defined, then choose the group number of the desired structure to be load rated. Other structures (groups) may be load rated on repeated applications of Option 5.
2. Enter load-step number, $\text{Step}_{\text{dead}}$, demarking the completion of dead loads.
Or accept default, $\text{Step}_{\text{dead}} =$ highest load-step number found in the element property array.
3. Enter load-step number for start of live loads, $\text{Step}_{\text{LL-start}}$.
Or accept default, $\text{Step}_{\text{LL-start}} = \text{Step}_{\text{dead}} + 1$, (i.e., begin live-load steps following last dead load)
4. Enter load-step number for end of live loads, $\text{Step}_{\text{LL-end}}$.
Or accept default, $\text{Step}_{\text{LL-end}} =$ Last load step, (i.e., input value NINC).

The CANDE Tool Box (CTB) program undertakes a brute force search through the CANDE output file to collect all the relevant data needed to ultimately determine the controlling RF value (minimum), along with the associated load-step number (vehicle location), design criterion (failure mode), and node number (location in structure). The CTB step-by-step search and data collection procedure is described below:

- a) From the assessment summaries at the end of each load step, the controlling demand and capacity values are collected for each design criterion at the controlling node with highest demand-to-capacity ratio. From this set of data, CTB verifies the demands of the dead-load step ($\text{Step}_{\text{dead}}$) do not exceed the corresponding capacities for all design criteria, i.e., $\text{Ratio}_n \leq 1$. If this is not true,

Appendix C – CANDE Tool Box Manual

USER-DEFINED KEY LOAD STEPS FOR LOAD RATING ANALYSIS:

- * Load step used for dead/earth load RF reference = 6
- * Load step beginning live-load search range = 7
- * Load step terminating live-load search range = 16

BOTTOM LINE FINDINGS FOR LOAD RATING OF CULVERT

- * Controlling design criterion = STEEL YIELDING (psi)
- * Controlling load-rating factor RF = 1.17
- * Controlling local-node number = 20
- * Controlling live-load step number = 10
- * Safety assessment of culvert = SAFE

LOWEST RATING FACTORS PER DESIGN CRITERION AT CONTROLLING LOAD STEP AND NODE:

DESIGN-CRITERION (Strength)	LOAD STEP	LOCAL NODE	DEAD-LOAD DEMAND	LIVE-LOAD DEMAND	EFFECTIVE CAPACITY	*RATING FACTOR
*STEEL YIELDING (psi)	10	20	1972.64	48410.19	58500.00	1.17
*CONCRETE CRUSHING (psi)	10	20	539.34	1427.05	3750.00	2.25
*SHEAR FAILURE (lbs/in)	13	26	175.66	318.76	973.00	2.50
*RADIAL-TENSION FAIL (psi)	16	1	0.00	0.03	61.10	2036.67

DEFINITIONS AND RELATIONS FOR EACH CRITERION "n":

- * Rating Factor(n) = (Capacity(n) - Dead(n))/Live(n)
- * Total Demand(n) = Dead(n) + Live(n) at specified node
- * Dead(n) = Dead load demand for criterion n (factored)
- * Live(n) = Live load demand for criterion n (factored)
- * Capacity(n) = Capacity for criterion n (factored)

- - - - - ADDITIONAL DIAGNOSTICS FOR ALL NODES - - - - -

DIAGNOSTICS FOR 4 STRENGTH DESIGN CRITERIA FOR CONCRETE RATING FACTORS LISTED FOR ALL NODES AT CONTROLLING STEP

DESIGN CRITERION # 1 = STEEL YIELDING (psi)

LOCAL NODE#	LOAD STEP#	DEAD-LOAD DEMAND	LIVE-LOAD DEMAND	EFFECTIVE CAPACITY	RATING FACTOR
1	14	1528.27	24656.69	58500.00	2.31
2	15	1401.07	23155.68	58500.00	2.47
3	16	1016.92	1057.20	58500.00	54.37
4	11	370.16	539.96	58500.00	107.66
5	13	172.30	704.42	58500.00	82.80
6	13	788.82	45162.98	58500.00	1.28
7	13	1067.77	1626.28	58500.00	35.32
8	14	1293.09	757.28	58500.00	75.54
9	15	1589.47	28003.94	58500.00	2.03
10	16	1972.64	45471.52	58500.00	1.24
11	16	786.17	248.49	58500.00	232.26
12	16	416.10	349.57	58500.00	166.16
13	11	1013.71	285.38	58500.00	201.44
14	12	2018.81	38057.50	58500.00	1.48
15	14	40422.08	6462.12	58500.00	2.80
16	15	2018.81	37939.91	58500.00	1.49
17	15	1013.71	287.47	58500.00	199.97
18	9	416.10	481.38	58500.00	120.66

Appendix C – CANDE Tool Box Manual

19	9	786.17	299.37	58500.00	192.78
20	10	1972.64	48410.19	58500.00	1.17
21	12	1589.47	1097.79	58500.00	51.84
22	13	1293.09	705.88	58500.00	81.04
23	14	1067.77	27718.34	58500.00	2.07
24	14	788.82	42166.68	58500.00	1.37
25	14	172.30	717.39	58500.00	81.31
26	9	370.16	827.84	58500.00	70.22
27	10	1016.92	1145.57	58500.00	50.18
28	12	1401.07	23032.95	58500.00	2.48
29	14	1528.27	24677.12	58500.00	2.31

DESIGN CRITERION # 2 = CONCRETE CRUSHING (psi)

LOCAL NODE#	LOAD STEP#	DEAD-LOAD DEMAND	LIVE-LOAD DEMAND	EFFECTIVE CAPACITY	RATING FACTOR
1	14	283.43	1078.51	3750.00	3.21
2	15	257.64	1009.40	3750.00	3.46
3	16	179.61	216.93	3750.00	16.46
4	12	48.46	122.22	3750.00	30.29
5	13	38.62	136.53	3750.00	27.18
6	13	239.03	1506.76	3750.00	2.33
7	14	311.35	334.50	3750.00	10.28
8	14	373.05	213.05	3750.00	15.85
9	15	448.44	1153.06	3750.00	2.86
10	16	539.34	1337.56	3750.00	2.40
11	16	174.28	51.85	3750.00	68.96
12	16	130.99	71.68	3750.00	50.49
13	10	251.49	53.76	3750.00	65.08
14	11	451.31	950.92	3750.00	3.47
15	15	1421.24	204.02	3750.00	11.41
16	15	451.31	950.35	3750.00	3.47
17	16	251.49	53.91	3750.00	64.90
18	8	130.99	105.93	3750.00	34.16
19	9	174.28	61.58	3750.00	58.07
20	10	539.34	1427.05	3750.00	2.25
21	11	448.44	216.18	3750.00	15.27
22	13	373.05	200.43	3750.00	16.85
23	14	311.35	1203.96	3750.00	2.86
24	14	239.03	1392.18	3750.00	2.52
25	14	38.62	137.93	3750.00	26.91
26	9	48.46	165.21	3750.00	22.41
27	10	179.61	234.53	3750.00	15.22
28	12	257.64	1010.24	3750.00	3.46
29	14	283.43	1079.04	3750.00	3.21

DESIGN CRITERION # 3 = SHEAR FAILURE (lbs/in)

LOCAL NODE#	LOAD STEP#	DEAD-LOAD DEMAND	LIVE-LOAD DEMAND	EFFECTIVE CAPACITY	RATING FACTOR
1	16	0.32	113.98	973.00	8.53
2	12	56.39	153.78	973.00	5.96
3	13	113.63	228.34	973.00	3.76
4	14	175.66	311.20	973.00	2.56
5	15	143.20	143.63	2117.71	13.75
6	16	75.04	0.00	973.00	10000.00
7	16	66.56	0.00	973.00	10000.00
8	16	68.33	10.44	973.00	86.65
9	16	85.02	24.20	973.00	36.69
10	16	118.35	34.40	973.00	24.84
11	14	193.57	46.56	2117.71	41.33
12	16	448.40	97.60	973.00	5.37
13	16	290.65	62.28	973.00	10.96

Appendix C – CANDE Tool Box Manual

14	16	142.38	35.47	973.00	23.42
15	9	0.00	17.63	973.00	55.19
16	9	142.38	39.59	973.00	20.98
17	9	290.65	67.63	973.00	10.09
18	10	448.40	103.50	973.00	5.07
19	13	193.57	44.23	2117.71	43.50
20	8	118.35	72.27	973.00	11.83
21	8	85.02	65.20	973.00	13.62
22	8	68.33	58.37	973.00	15.50
23	8	66.56	51.40	973.00	17.64
24	8	75.04	43.08	973.00	20.84
25	12	143.20	147.14	2117.71	13.42
26	13	175.66	318.76	973.00	2.50
27	14	113.63	234.25	973.00	3.67
28	15	56.39	158.74	973.00	5.77
29	10	0.32	117.44	973.00	8.28

DESIGN CRITERION # 4 = RADIAL-TENSION FAIL (psi)

LOCAL NODE#	LOAD STEP#	DEAD-LOAD DEMAND	LIVE-LOAD DEMAND	EFFECTIVE CAPACITY	RATING FACTOR
1	16	0.00	0.03	61.10	2036.67
2	16	0.00	0.03	61.10	2036.67
3	16	0.00	0.00	61.10	10000.00
4	16	0.00	0.00	61.10	10000.00
5	16	0.00	0.00	61.10	10000.00
6	16	0.00	0.00	61.10	10000.00
7	16	0.00	0.00	61.10	10000.00
8	16	0.00	0.00	61.10	10000.00
9	16	0.00	0.00	61.10	10000.00
10	16	0.00	0.00	61.10	10000.00
11	16	0.00	0.00	61.10	10000.00
12	16	0.00	0.00	61.10	10000.00
13	16	0.00	0.00	61.10	10000.00
14	16	0.00	0.02	61.10	3055.00
15	16	0.02	0.01	61.10	6108.00
16	16	0.00	0.02	61.10	3055.00
17	16	0.00	0.00	61.10	10000.00
18	16	0.00	0.00	61.10	10000.00
19	16	0.00	0.00	61.10	10000.00
20	16	0.00	0.00	61.10	10000.00
21	16	0.00	0.00	61.10	10000.00
22	16	0.00	0.00	61.10	10000.00
23	16	0.00	0.00	61.10	10000.00
24	16	0.00	0.00	61.10	10000.00
25	16	0.00	0.00	61.10	10000.00
26	16	0.00	0.00	61.10	10000.00
27	16	0.00	0.00	61.10	10000.00
28	13	0.00	0.03	61.10	2036.67
29	16	0.00	0.03	61.10	2036.67

Appendix D – 2D Analysis Backup

Appendix D – 2D Analysis Backup

Appendix D – 2D Analysis Backup

Model 1 Analysis Backup

Input Information

Meshes for Model 1 were generated for fills of 0.97', 2', 5' and 10'. Using the CANDE ToolBox, different fill depth meshes can be generated if needed for Phase III.

M1C1 – Juniata County SR 3020 PennDOT, 25' 0" span box section – Site/Structure Information

Depth of Fill (road centerline):

Invert elevation: 491.98 ft
 Top of pavement: 501.45 ft
 Top of box to top of pavement: 0.97 ft
 Bedding depth: 18 in.

Precast Box Geometry:

Span x Rise x Length: 25 ft x 7.5 ft x 4.458 ft
 Top/Bottom/Sidewall: 14 in., 14 in., 12 in.
 Haunches: 12 in. x 12 in. top & bottom

Reinforcement (Sections 2 thru 6):	in.²/ft	in.²/in.	Clear cover
AS1 – outside: C601@ 4 in.	1.320	0.110	2 in.
AS2 – top inside: #8@ 5 in.	1.896	0.158	2 in.
AS3 – bottom inside: #8@ 5 in.	1.896	0.158	2.5 in. (run with 2 in. – CANDE only accepts one value – change in level 3)
AS4 – side inside #4@ 10 in.	0.240	0.020	2 in.
AS5 – top outside #4@ 12 in.	0.200	0.017	2 in.
AS6 – bottom outside #6@ 12 in.	0.440	0.037	2 in.

Note: Box is post-tensioned longitudinally

Materials:

Reinforcement yield stress: 60 ksi
 Concrete f'_c : 5 ksi

CANDE Model notes:

Concrete tensile rupture strain: 0.0001 in./in. (typically neglected in design, but used for analysis)
 $\sim 7 f'_c{}^{0.5}$

In situ – linear elastic E = 5,000 psi, Poisson = 0.3 – both assumed

Appendix D – 2D Analysis Backup

Bedding – 18 in. structure backfill, 6 in. No. 8 stone

Duncan Selig – SW100 (assume well compacted)

Backfill – Assumed

Duncan/Selig – SW95

Input for level 3 CANDE model for concrete area clear/ center to bar

Node Number	Thickness	AS (inner cage) In ² /in	AS (outer cage) in ² /in	Clear Cover (inner) (in)	Clear Cover (outer) (in)
1	14	0.158	0.0167	2.5	2.25
2	14	0.158	0.0167	2.5	2.25
3	14	0.158	0.0167	2.5	2.25
4	14	0.158	0.11	2.5	2.375
5	25	0.158	0.11	2.5	2.375
6	12	0.02	0.11	2.25	2.375
7	12	0.02	0.11	2.25	2.375
8	12	0.02	0.11	2.25	2.375
9	12	0.02	0.11	2.25	2.375
10	12	0.02	0.11	2.25	2.375
11	25	0.158	0.11	3	2.875
12	14	0.158	0.11	3	2.875
13	14	0.158	0.037	3	2.875
14	14	0.158	0.037	3	2.875
15	14	0.158	0.037	3	2.875
16	14	0.158	0.037	3	2.875
17	14	0.158	0.11	3	2.875
18	14	0.158	0.11	3	2.875
19	25	0.158	0.11	3	2.875
20	12	0.02	0.11	2.25	2.375
21	12	0.02	0.11	2.25	2.375
22	12	0.02	0.11	2.25	2.375
23	12	0.02	0.11	2.25	2.375
24	12	0.02	0.11	2.25	2.375
25	25	0.158	0.11	2.5	2.375
26	14	0.158	0.11	2.5	2.375
27	14	0.158	0.0167	2.5	2.25
28	14	0.158	0.0167	2.5	2.25
29	14	0.158	0.0167	2.5	2.25

Appendix D – 2D Analysis Backup

The live load distributions (see Table 1 below) for CANDE are in accordance with AASHTO, and were computed through a spreadsheet from Dr. McGrath. Briefly:

- Concrete culverts and arches, $H < 2$ ft: Strip width from 4.6.2.10
- Concrete culverts and arches, $H \geq 2$ ft: Section 3.6.1.2.6 (note that the LLDF for concrete pipe is variable with diameter).
- Concrete pipe and flexible pipe, $H < 1$ ft: Special analysis
- Concrete pipe and flexible pipe, $H \geq 1$ ft: Section 3.6.1.2.6

Table 1 – Reduction of surface load for varying fills for Model 1

Fill Depth (ft)	RSL
0.97	0.303
2	.177
5	0.142
10	0.070

Sample Spreadsheet Calculation for Model 1 for a fill depth of 2'.

Live Load Calculations - Tandem Axle

TJM

23-Apr-17

DepthC3:H37	24.00 in.	2.00 ft
Span	25 ft	
Wheel load	12.5 k	50% of axle load
Axle width, c-c	72 in.	
Axle spacing, c-c	48 in.	
Tire		
	width	20 in.
	length	10 in.
Factors		
	Multiple presence	1.2
	Dynamic load allowance	1.25
	LLDF	1.15
	Live load factor	1.75
Calculations		
	Wheel strip width ($H < 2$ ft)	66 in. 50% of AASHTO axle strip, no change with depth
	Wheel/axle width at surface ($H > 2$ ft)	20.00 in. Increases when load areas interact longitudinally
	Load width at top of box ($H > 2$ ft)	47.60 in.
	Load length at top of box	10.00
	Length at top of box	37.60 in.

"AASHTO"

Loads applied at mesh surface - reduced for longitudinal distribution to top of box
Wheels on axle considered as one load once load areas overlap at top of box
Each axle treated separately

Total Service Wheel Load	18713 lb		
Service Load on mesh	165 lb/in.	RLS	0.177
Factored Load on mesh	289 lb/in.		

Appendix D – 2D Analysis Backup

CANDE output results

Figure 1 displays a typical CANDE plot of model 1 with the Tandem vehicle near midspan. CANDE models the vehicle by using load steps. Each load step removes the subsequent vehicle and places it at its new locations. Figure 2 displays the dead load moment diagrams for the first 6 load steps (incremental fill levels), while Figure 3 displays the live load envelope for the tandem vehicle for all of the live load steps (7-23). Figure 4 displays the deflection (magnified by 40) and shear stress as the tandem vehicle steps across the culvert.

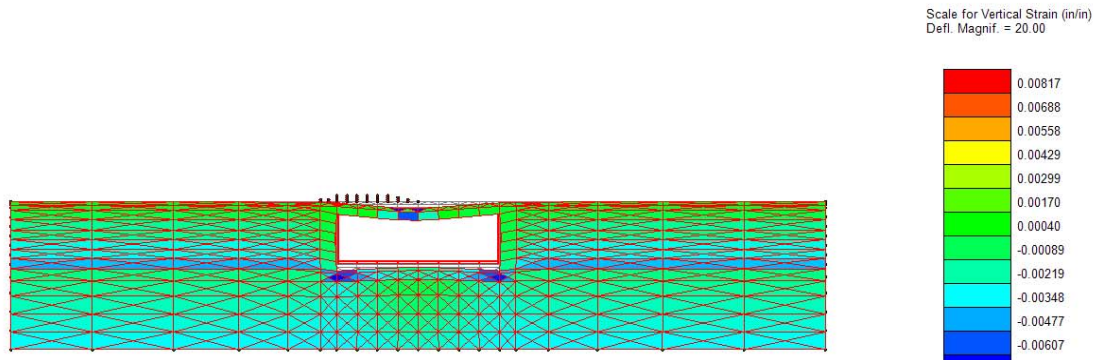


Figure 1 – M1C1 Vertical strain with Tandem Vehicle near midspan (no pavement)

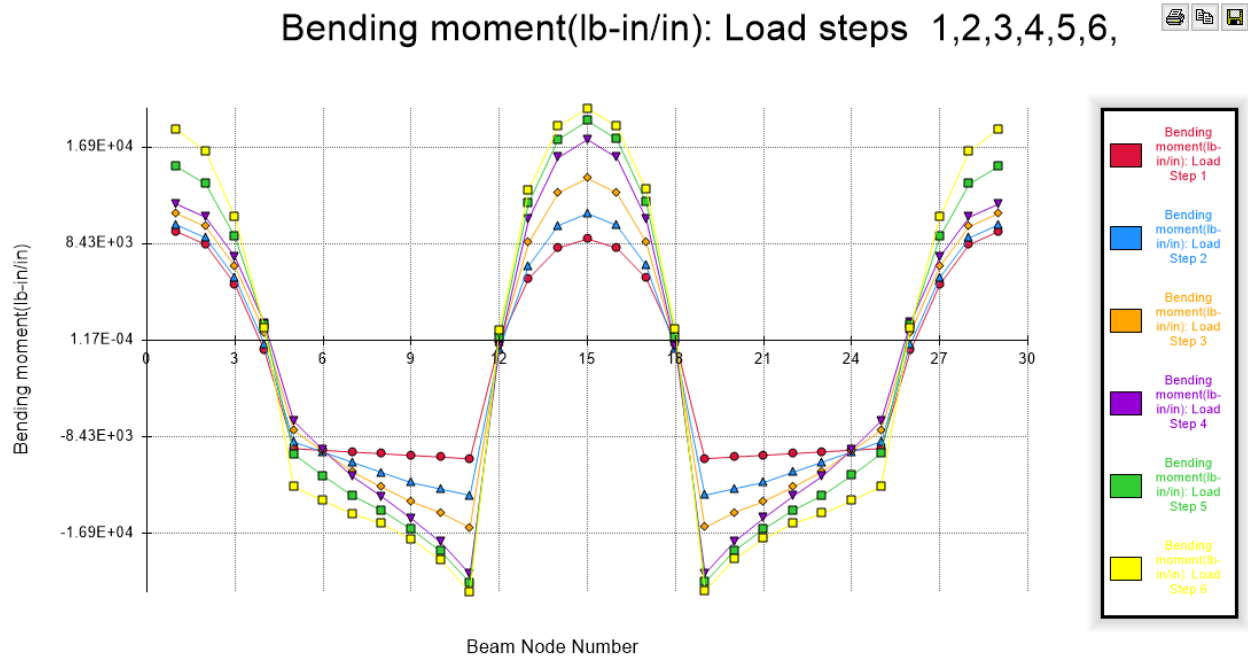


Figure 2 – M1C1- CANDE Bending Moment - Dead load envelope – Load steps 1-6

Appendix D – 2D Analysis Backup

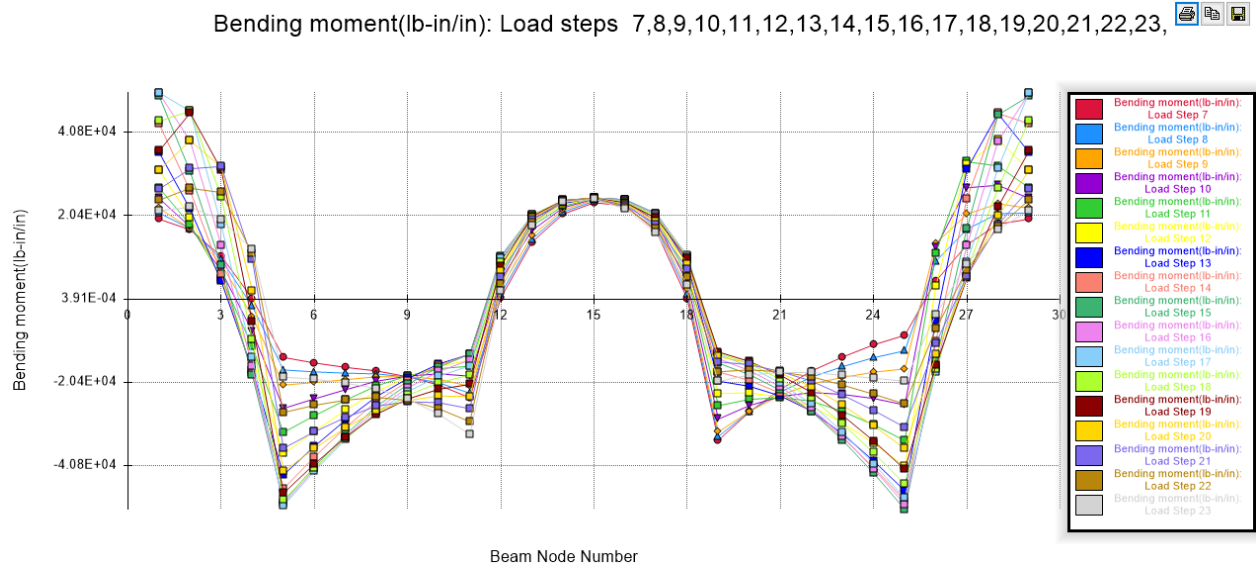


Figure 3 - M2C1 – CANDE bending moment envelope - live load steps – load steps 7-23 (2 axle Tandem ,25 kip/axle) (without pavement)

Appendix D – 2D Analysis Backup

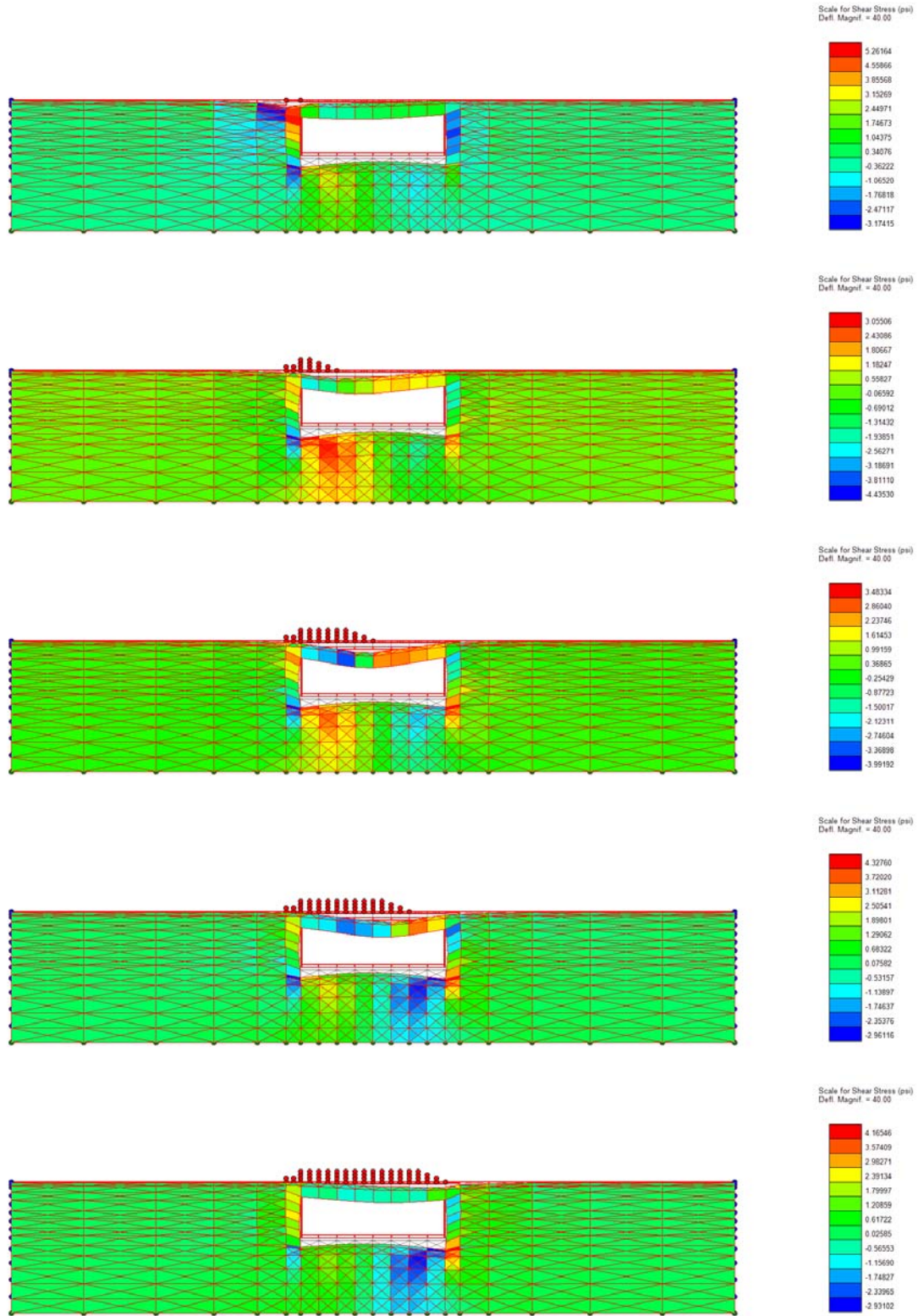


Figure 4 – M1C1 showing shear stress as Tandem vehicle moves across culvert (0.97' fill, no pavement)

Appendix D – 2D Analysis Backup

Figure 5 below provides a sample of the CANDE output load rating report for the no pavement and 0.97' fill.

```

* * * * *
          CANDE TOOL BOX -- LOAD RATING REPORT.
* * * * *

LOAD RATING SUMMARY FOR PIPE-GROUP = 1, PIPE TYPE = CONCRETE
CANDE FILE NAME: Live-TANDEM-Full-M1C1-1ftFill-ModMeshGen.out

User-defined key load steps for Load Rating Analysis:
* Load step used for dead/earth load RF reference = 6
* Load step beginning live-load search range = 7
* Load step terminating live-load search range = 23

LOAD-STEP NUMBER CAUSING LARGEST STRUCTURAL DISTRESS = 19
DEMANDS & CAPACITIES FOR EACH STRENGTH CRITERION ARE BELOW.

      DESIGN-CRITERION      GROUP   DEAD-LOAD   LIVE-LOAD      TOTAL      *RATING
      (Strength)           NODE #   DEMAND      DEMAND      CAPACITY      FACTOR
STEEL YIELDING (psi)       6       9370.09     29567.11     54000.00      1.51
CONCRETE CRUSHING (psi)    6       1038.72     1679.48      3750.00       1.61
SHEAR FAILURE (lbs/in)    4        301.22      714.68      1330.70       1.44
RADIAL-TENSION FAIL (psi) 2          0.00        0.00         61.10     10000.00

DEFINITIONS AND RELATIONS FOR EACH CRITERION "n":
* Rating Factor(n) = (Capacity(n) - Dead(n))/Live(n)
* Total Demand(n) = Dead(n) + Live(n) at specified node
* Dead(n) = Dead load demand for criterion n (factored)
* Live(n) = Live load demand for criterion n (factored)
* Capacity(n) = Capacity for criterion n (factored)

BOTTOM LINE FINDINGS FOR LOAD RATING OF CULVERT
* Controlling design criterion = SHEAR FAILURE (lbs/in)
* Controlling load-rating factor RF = 1.44
* Controlling group-node number = 4
* Controlling live-load step number = 19
* Safety assessment of culvert = SAFE

```

Figure 5 – CANDE load rating report Model 1 (Tandem Vehicle, no pavement, 0.97' fill)

Appendix D – 2D Analysis Backup

Pavement Rating Results

A parametric study was performed on the model by varying the fill height in increments. Models were built for fill heights of 0.97', 2', 5', and 10'. The CANDE model with 5' of fill is shown in Figure 6. Note that while the pavement elements are SHOWN at different thicknesses, they are actually this same thickness. This is a glitch in the CANDE graphics software. For fill models of 2' and over, the CANDE shear option for LRFD for fills over 2' was selected. Each model was also reviewed for no pavement and 3 varying pavements. The rating results produced by the CANDE toolbox are provide in Table 2. The vehicle used for loading is the LRFD Tandem vehicle (2-25kip axles spaced at 4'). The node numbering referenced in the table is shown in Figure 7.

There is a noticeable jump in the shear ratings when moving from 0.97' to 2' of fill. The 2' fill takes advantage of the LRFD increase in capacity over the 2' fill level. This is discussed in more in detail under Task 5. For fill levels of 10', this culvert fails under dead load.

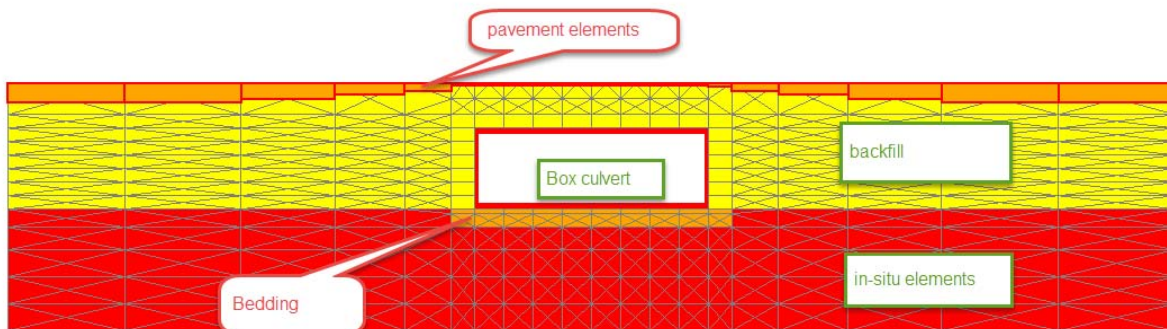


Figure 6 – CANDE model M1C1 with 5' of backfill and pavement

Appendix D – 2D Analysis Backup

Table 2 – Model 1 -CANDE Rating Factors (from CANDE Toolbox) Tandem vehicle, without and with pavement (varying fill depths)

Rating	No pavement	E = 200,000 psi ν = 0.33 Pavement (6")	E = 400,000 psi ν = 0.33 Pavement (6")	E = 600,000 psi ν = 0.33 Pavement (6")
0.97 ft fill				
Steel Yielding	1.41(Node 6)	1.47 (Node 6)	1.48 (Node 6)	1.49 (Node 6)
Concrete Crushing	1.52(Node 6)	1.55 (Node 6)	1.56 (Node 6)	1.56 (Node 6)
Shear Failure*	1.44 (Node 4)	1.84 (Node 4)	1.84 (Node 4)	1.85 (Node 4)
Radial-Tension Fail	1222.0(Node 1)	1527.25 (Node 29)	1527.25 (Node 29)	1527.25 (Node 29)
*Note	Uses the < 2' fill shear option in CANDE			
2.0 ft fill				
Steel Yielding	2.18 (Node 24)	2.42 (Node 6)	2.46 (Node 6)	2.49 (Node 6)
Concrete Crushing	2.06 (Node 24)	2.15 (Node 6)	2.17 (Node 6)	2.18 (Node 6)
Shear Failure	4.86 (Node 26)	5.33 (Node 4)	5.39 (Node 4)	5.43 (Node 4)
Radial-Tension Fail	3054 (Node 1)	3054 (Node 29)	3054 (Node 29)	3054 (Node 29)
5.0 ft fill				
Steel Yielding	2.22 (Node 6)	2.26 (Node 6)	2.32 (Node 6)	2.36 (Node 6)
Concrete Crushing	3.81 (Node 6)	3.74 (Node 6)	3.86 (Node 6)	3.91 (Node 6)
Shear Failure	7.22 (Node 4)	6.97 (Node 4)	7.86 (Node 4)	7.63 (Node 4)
Radial-Tension Fail	3055 (Node 27)	6107 (Node 29)	6107 (Node 29)	6107 (Node 29)
10.0 ft fill				
Steel Yielding	-0.74** (Node 6)	0.61** (Node 6)	0.61** (Node 6)	0.61** (Node 6)
Concrete Crushing	1.55 (Node 24)	2.14 (Node 6)	2.19 (Node 6)	2.22 (Node 6)
Shear Failure	11.67 (Node 26)	14.39 (Node 4)	14.61 (Node 4)	14.75 (Node 4)
Radial-Tension Fail	1526 (Node 27)	1526 (Node 1)	1526 (Node 1)	1526 (Node 1)

**Fails under dead load

Appendix D – 2D Analysis Backup

* - Note: These were transcription errors in Interim Report #2 that have been corrected.

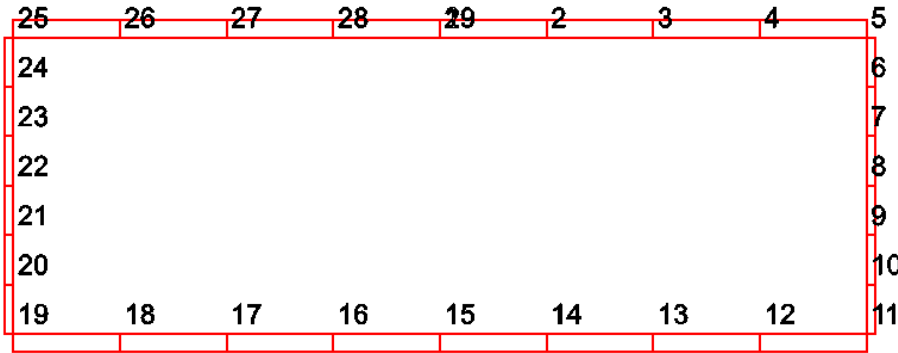


Figure 7 – Beam node numbering for M1C1

Generated BrDR Model

Model 1 was also input into the AASHTOWare BrDR software and run for varying fill heights (1.99', 2.00', 5', 7', 8', and 10'). The reinforcement schematic from BrDR is shown in Figure 8. The LRFR ratings (HL93) are shown in Table 3. The ratings are provided at each fill height. For comparison purposes, the LFR rating was performed with the HS25 vehicle. The ratings for LFR are provided as well.

Model 1- Candidate 1
 Mod1-Cand1-NCHRP - Culvert M1C1-(1.99' fill) -
 05/15/17

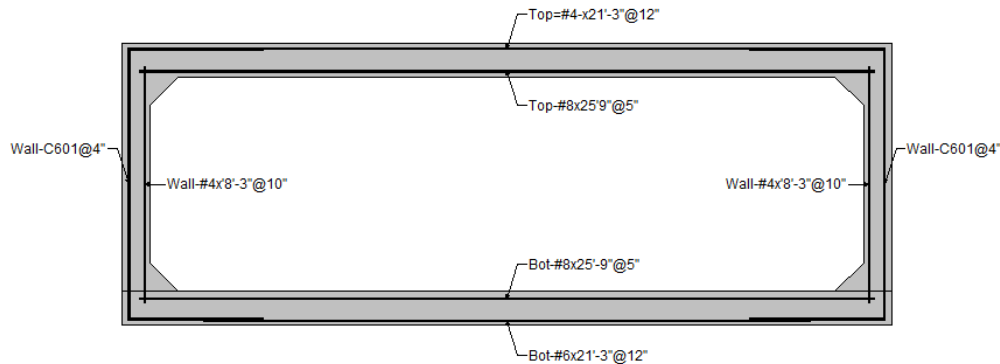


Figure 8 - BrDR Model M1C1 reinforcement schematic

Table 3 – BrDR Model M1C1 ratings – LFR/LRFR

Fill	LRFR Ratings			LFR (Ratings)		
Culvert M1C1 (1.99' fill)	HL-93 (US)	0.727	0.943	HS-25	0.675	1.127
Culvert M1C1 (2.00' fill)	HL-93 (US)	1.063	1.378	HS-25	0.783	1.308
Culvert M1C1 (5.00' fill)	HL-93 (US)	1.025	1.329	HS-25	0.723	1.207
Culvert M1C1 (7.00' fill)	HL-93 (US)	0.353	0.458	HS-25	0	0
Culvert M1C1 (8.00' fill)	HL-93 (US)	0	0	HS-25	0	0
Culvert M1C1 (10.00' fill)	HL-93 (US)	0	0	HS-25	0	0

Appendix D – 2D Analysis Backup

For the LRFR ratings, a noticeable step can be seen from a fill of 1.99' to 2.00'. For 1.99' the controlling inventory rating of 0.727 is governed by shear in the top slab near the support at the critical shear distance. For the fill of 2', the controlling inventory rating of 1.063 is governed by flexure in the center of the top slab. This difference is due primarily to the difference in the calculation of concrete shear capacity at the 2' fill level. For fills under 2' of fill the concrete shear capacity V_c is calculated using equation 5.8.3.3-3 (7th Edition, AASHTO LRFD specification) 5.7.3.3-3 (8th Edition). For fills over 2', V_c is calculated using equation 5.14.5.3-1 (7th Edition, AASHTO LRFD specification) 5.12.7.3-1 (8th Edition) (see Figure 9).

5.8.3.3—Nominal Shear Resistance

The nominal shear resistance, V_n , shall be determined as the lesser of:

$$V_n = V_c + V_s + V_p \quad (5.8.3.3-1)$$

$$V_n = 0.25f'_c b_v d_v + V_p \quad (5.8.3.3-2)$$

in which:

$$V_c = 0.0316\beta\sqrt{f'_c} b_v d_v, \text{ if the procedures of Articles 5.8.3.4.1 or 5.8.3.4.2 are used} \quad (5.8.3.3-3)$$

V_c = the lesser of V_{ci} and V_{cw} , if the procedures of Article 5.8.3.4.3 are used

5.14.5.3—Design for Shear in Slabs of Box Culverts

The provisions of Article 5.8 apply unless modified herein. For slabs of box culverts under 2.0 ft or more fill, shear strength V_c may be computed by:

$$V_c = \left(0.0676\sqrt{f'_c} + 4.6\frac{A_s}{bd_e} \frac{V_u d_e}{M_u} \right) bd_e \quad (5.14.5.3-1)$$

but V_c shall not exceed $0.126\sqrt{f'_c} bd_e$

Figure 9 – LRFD Spec Comparison of concrete shear resistance at 2' fill level

For model 1 the calculations of the concrete shear capacity and overall shear resistance are presented in Table 4. This jump in shear capacity is discussed more under Task 5.

Table 4 - BrDR Model M1C1 shear capacity comparison at 1.99' fill and 2.00' fill

Fill depth		Inv Rating	Oper Rating	Concrete	Steel Shear	Shear
				Resistance V_c (kips)	Resistance V_s (kips)	Resistance V_r (kips)
Culvert M1C1 (1.99' fill)	HL-93 (US)	0.727	0.943	14.9*	0	12.7
Culvert M1C1 (2.00' fill)	HL-93 (US)	1.063	1.378	24.7	0	21.0

*Note: This uses the AASHTO LRFD Simplified for shear and not the iterative shear method provided in Appendix B of AASHTO. The Appendix B option is not available for culverts in BrDR.

Appendix D – 2D Analysis Backup

Model 2 Analysis Backup

Input Information

Meshes for Model 2 were generated for fills of 2' and 5'. Using the CANDE ToolBox, different fill depth meshes can be generated if needed for Phase III. The reduction of surface load factor for Model 2 is shown in Table 5 for each fill height.

Table 5 – Reduction of surface load for varying fills for Model 2

Fill Depth (ft)	RSL
2	0.177
5	0.142

The live load distributions for CANDE are in accordance with AASHTO, and were computed through a spreadsheet from Dr. McGrath. A sample of the spreadsheet is provided in this appendix under 'Model 1 Analysis Backup'. Briefly:

- Concrete culverts and arches, $H < 2$ ft: Strip width from 4.6.2.10
- Concrete culverts and arches, $H \geq 2$ ft: Section 3.6.1.2.6 (note that the LLDF for concrete pipe is variable with diameter).
- Concrete pipe and flexible pipe, $H < 1$ ft: Special analysis
- Concrete pipe and flexible pipe, $H \geq 1$ ft: Section 3.6.1.2.6

Reinforcement Input for BrDR (Based on labeling in Figure 10)

Bar Mark	Type	Bar Number	Spacing (in)	A	B	C	H	area	area/in
A1	Corner	7	24	5.25	6.83			0.6	0.025
A2	C Bar	7	24	8.5	4	4		0.6	0.025
A3	Straight	8	24	13				0.79	0.032917
A4	Hook	8	24		8			0.79	0.032917
A5	Bent	6	24	8.25	6.167	8.25	0.5417	0.44	0.018333
A6	Straight	4	12	8.5				0.2	0.016667
A7	Straight	4	18	8.5				0.2	0.011111
A8	Straight	8	24	22.667				0.79	0.032917

Reinforcement Input for CANDE (based on node numbering in Figure 10)

Node	Bar 1	Bar 2	Bar 3	Area 1	Area 2	Area 3	CANDE input	Node
Inner Cage								
1	a8			0.032917	0	0	0.033	1
2	a8			0.032917	0	0	0.033	2
3	a8	a5		0.032917	0.018333	0	0.051	3
4	a8	a5		0.032917	0.018333	0	0.051	4
5	a8	a5		0.032917	0.018333	0	0.051	5

Appendix D – 2D Analysis Backup

Node	Bar 1	Bar 2	Bar 3	Area 1	Area 2	Area 3	CANDE input	Node
6	a6			0.016667	0	0	0.017	6
7	a6			0.016667	0	0	0.017	7
8	a6			0.016667	0	0	0.017	8
9	a6			0.016667	0	0	0.017	9
10	a6			0.016667	0	0	0.017	10
11	a6			0.016667	0	0	0.017	11
12	a8	a5		0.032917	0.018333	0	0.051	12
13	a8	a5		0.032917	0.018333	0	0.051	13
14	a8			0.032917	0	0	0.033	14
15	a8			0.032917	0	0	0.033	15
16	a8			0.032917	0	0	0.033	16
17	a8	a5		0.032917	0.018333	0	0.051	17
18	a8	a5		0.032917	0.018333	0	0.051	18
19	a8	a5		0.032917	0.018333	0	0.051	19
20	a6			0.016667	0	0	0.017	20
21	a6			0.016667	0	0	0.017	21
22	a6			0.016667	0	0	0.017	22
23	a6			0.016667	0	0	0.017	23
24	a6			0.016667	0	0	0.017	24
25	a8	a5		0.032917	0.018333	0	0.051	25
26	a8	a5		0.032917	0.018333	0	0.051	26
27	a8	a5		0.032917	0.018333	0	0.051	27
28	a8			0.032917	0	0	0.033	28
29	a8			0.032917	0	0	0.033	29
Outer cage								
1	a3	a4	a5	0.032917	0.032917	0.018333	0.084	1
2	a3	a4	a5	0.032917	0.032917	0.018333	0.084	2
3	a3	a1		0.032917	0.025	0	0.058	3
4	a1	a2		0.025	0.025	0	0.050	4
5	a1	a2		0.025	0.025	0	0.050	5
6	a1	a2		0.025	0.025	0	0.050	6
7	a1	a2		0.025	0.025	0	0.050	7
8	a1	a2		0.025	0.025	0	0.050	8
9	a1	a2		0.025	0.025	0	0.050	9
10	a1	a2		0.025	0.025	0	0.050	10
11	a1	a2		0.025	0.025	0	0.050	11
12	a1	a2		0.025	0.025	0	0.050	12
13	a1	a3		0.025	0.032917	0	0.058	13
14	a3	a4	a5	0.032917	0.032917	0.018333	0.084	14
15	a3	a4	a5	0.032917	0.032917	0.018333	0.084	15

Appendix D – 2D Analysis Backup

Node	Bar 1	Bar 2	Bar 3	Area 1	Area 2	Area 3	CANDE input	Node
16	a3	a4	a5	0.032917	0.032917	0.018333	0.084	16
17	a1	a3		0.025	0.032917	0	0.058	17
18	a1	a2		0.025	0.025	0	0.050	18
19	a1	a2		0.025	0.025	0	0.050	19
20	a1	a2		0.025	0.025	0	0.050	20
21	a1	a2		0.025	0.025	0	0.050	21
22	a1	a2		0.025	0.025	0	0.050	22
23	a1	a2		0.025	0.025	0	0.050	23
24	a1	a2		0.025	0.025	0	0.050	24
25	a1	a2		0.025	0.025	0	0.050	25
26	a1	a2		0.025	0.025	0	0.050	26
27	a3	a1		0.032917	0.025	0	0.058	27
28	a3	a4	a5	0.032917	0.032917	0.018333	0.084	28
29	a3	a4	a5	0.032917	0.032917	0.018333	0.084	29

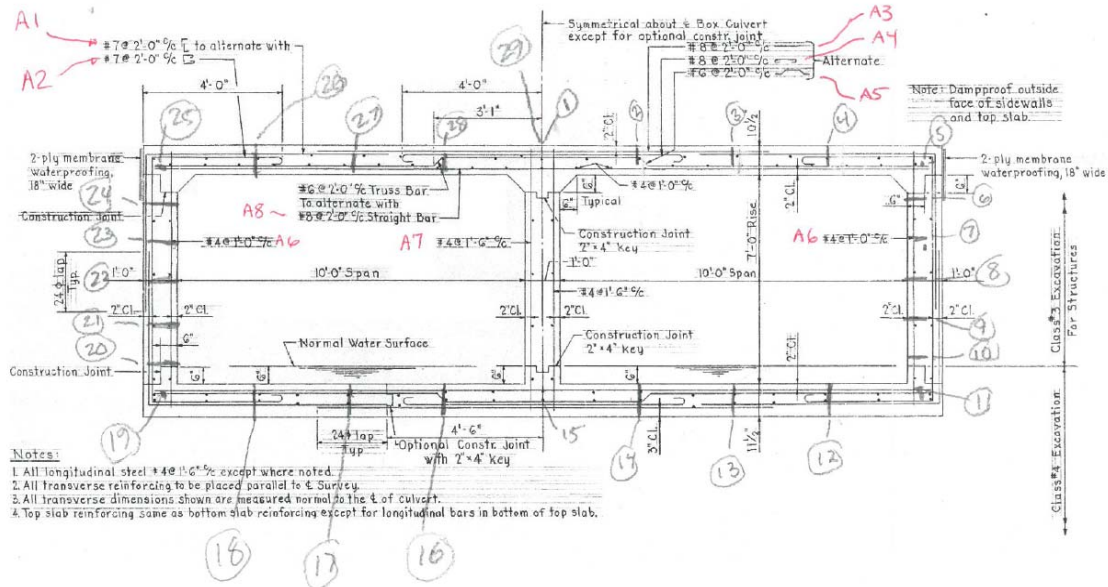


Figure 10 – M2C1 reinforcement labeling

CANDE output results

Figure 11 displays a typical CANDE plot of model 2 with the Tandem vehicle near midspan. CANDE models the vehicle by using load steps. Each load step removes the subsequent vehicle and places it at its new locations. Figure 12 displays the dead load moment diagrams for the first 6 load steps (incremental fill levels), while Figure 13 displays the live load envelope for the tandem vehicle for all of the live load steps (7-23). Figure 14 displays the deflection (magnified by 30) and shear stress as the tandem vehicle steps across the culvert.

Appendix D – 2D Analysis Backup

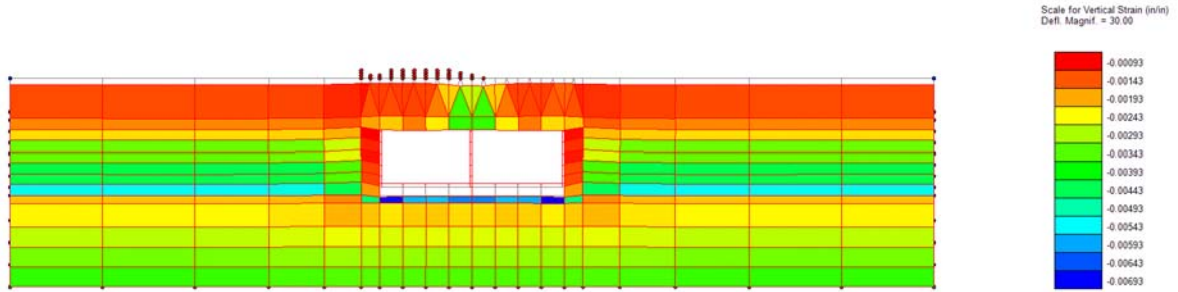


Figure 11 – M2C1 Vertical strain with Tandem Vehicle near midspan (no pavement)

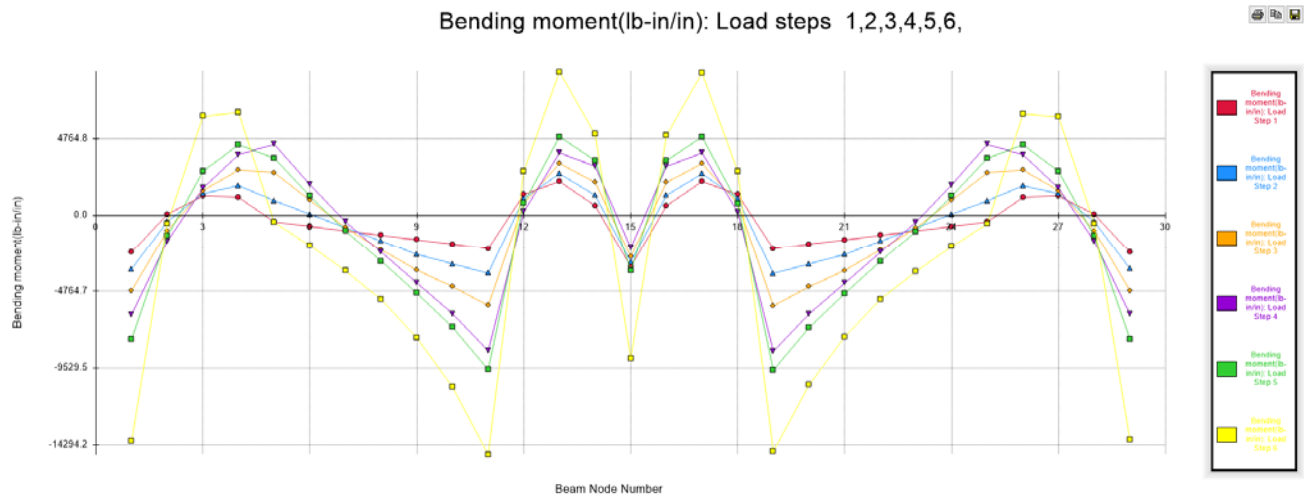


Figure 12 – M2C1- CANDE Bending Moment - Dead load envelope – Load steps 1-6

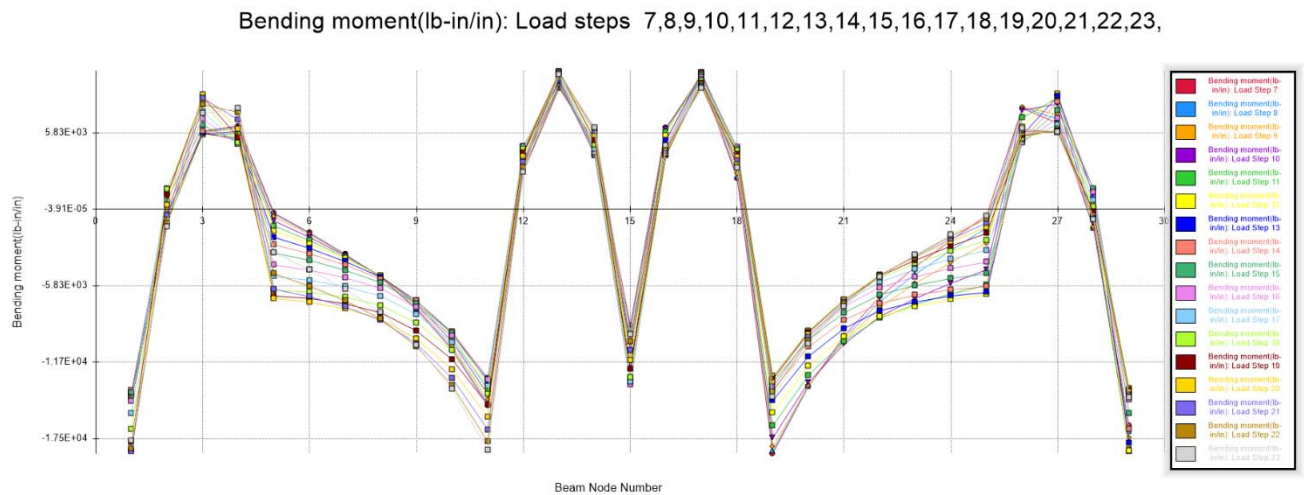


Figure 13 - M2C1 – CANDE bending moment envelope - live load steps – load steps 7-23 (2 axle Tandem ,25 kip/axle) (without pavement)

Appendix D – 2D Analysis Backup

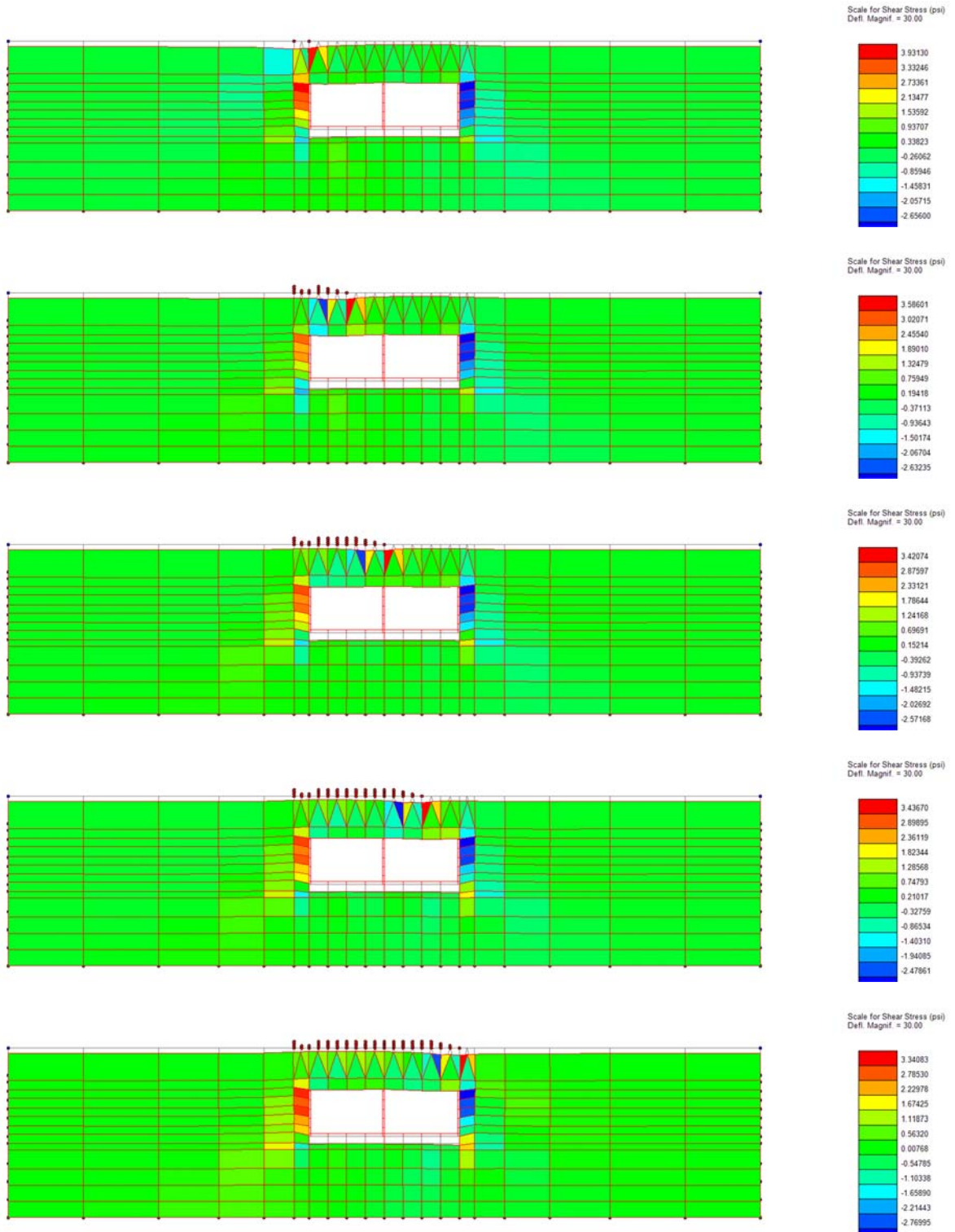


Figure 14 – M2C1 showing shear stress as Tandem vehicle moves across culvert (5' fill, no pavement)

Appendix D – 2D Analysis Backup

Figure 15 below provides a sample of the CANDE output load rating report for the no pavement and 0.97' fill.

```

* * * * *
          CANDE TOOL BOX -- LOAD RATING REPORT.
* * * * *

LOAD RATING SUMMARY FOR PIPE-GROUP = 1, PIPE TYPE = CONCRETE
CANDE FILE NAME: Live-Full-M2C1-5ftFill-ModMesh.out

User-defined key load steps for Load Rating Analysis:
* Load step used for dead/earth load RF reference = 6
* Load step beginning live-load search range = 7
* Load step terminating live-load search range = 23

LOAD-STEP NUMBER CAUSING LARGEST STRUCTURAL DISTRESS = 11
DEMANDS & CAPACITIES FOR EACH STRENGTH CRITERION ARE BELOW.

      DESIGN-CRITERION      GROUP   DEAD-LOAD   LIVE-LOAD      TOTAL      *RATING
      (Strength)           NODE #   DEMAND      DEMAND      CAPACITY      FACTOR
STEEL YIELDING (psi)       29      24071.08    7601.92    36000.00      1.57
CONCRETE CRUSHING (psi)    29      1432.90     197.70     2250.00       4.13
SHEAR FAILURE (lbs/in)     29      511.95      169.85     986.40        2.79
RADIAL-TENSION FAIL (psi) 27        0.00        0.00       47.30      10000.00

DEFINITIONS AND RELATIONS FOR EACH CRITERION "n":
* Rating Factor(n) = (Capacity(n) - Dead(n))/Live(n)
* Total Demand(n) = Dead(n) + Live(n) at specified node
* Dead(n) = Dead load demand for criterion n (factored)
* Live(n) = Live load demand for criterion n (factored)
* Capacity(n) = Capacity for criterion n (factored)

BOTTOM LINE FINDINGS FOR LOAD RATING OF CULVERT
* Controlling design criterion = STEEL YIELDING (psi)
* Controlling load-rating factor RF = 1.57
* Controlling group-node number = 29
* Controlling live-load step number = 11
* Safety assessment of culvert = SAFE

```

Figure 15 – CANDE load rating report Model 2 (Tandem Vehicle, no pavement, 5.0' fill)

Appendix D – 2D Analysis Backup

Pavement Rating Results

The CANDE mesh for this model was generated using the tools in the CANDE Toolbox and the information provided on the design drawings. The general process for generating the model is described in the main body of this report. The CANDE Toolbox will not automatically generate the interior vertical wall. The outside of the box was generated first using the toolbox and the interior vertical was added manually. The rating factors produced by the CANDE Toolbox are summarized in Table 6. The CANDE model local beam node configuration referenced in the table is shown in Figure 16.

Table 6 – Model 2 -CANDE Rating Factors (from CANDE Toolbox) Tandem vehicle, without and with pavement (varying fill depths)

Rating	No pavement	E = 200,000 psi ν = 0.33 Pavement (6")	E = 400,000 psi ν = 0.33 Pavement (6")	E = 600,000 psi ν = 0.33 Pavement (6")
2.0 ft fill				
Steel Yielding	1.47 (Node 27)	1.46 (Node 26)	1.57 (Node 29)	1.61 (Node 27)
Concrete Crushing	1.98 (Node 27)	1.97 (Node 27)	2.14 (Node 27)	2.16 (Node 29)
Shear Failure	2.87 (Node 29)	1.99 (Node 29)	2.63 (Node 29)	2.62 (Node 29)
Radial-Tension Fail	2365 (Node 27)	2365 (Node 27)	4730 (Node 27)	4730 (Node 27)
5.0 ft fill				
Steel Yielding	1.57 (Node 29)	1.62 (Node 29)	1.65 (Node 29)	1.67 (Node 29)
Concrete Crushing	2.52 (Node 27)	2.60 (Node 27)	2.64 (Node 27)	2.66 (Node 27)
Shear Failure	2.79 (Node 29)	2.80 (Node 29)	2.81 (Node 29)	2.84 (Node 29)
Radial-Tension Fail	4730 (Node 17)	4730 (Node 17)	4730 (Node 17)	4730 (Node 17)

Appendix D – 2D Analysis Backup

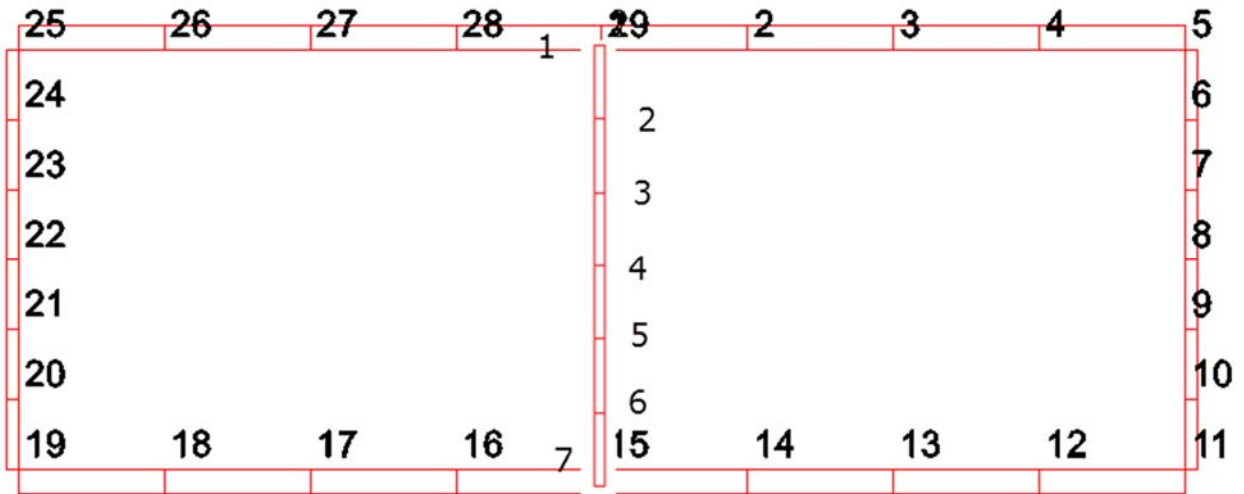


Figure 16 – Beam node numbering for M2C1

The rating factors for the 5' fill for the CANDE model do not appreciably increase as is seen in the BrDR model (see next section).

Appendix D – 2D Analysis Backup

Generated BrDR Model

Model 2 was also input into the AASHTOWare BrDR software and run for varying fill heights (1.99', 2.00', 5', 7', 8', and 10'). The reinforcement schematic from BrDR is shown in Figure 17. The LRFR ratings (HL93) are shown in Table 7. The ratings are provided at each fill height. For comparison purposes, the LFR rating was performed with the HS25 vehicle. The ratings for LFR are provided as well.

Model 2- Candidate 1
Mod2-Cand1-NCHRP - Culvert M2C1 1 (2' fill) -
05/09/17

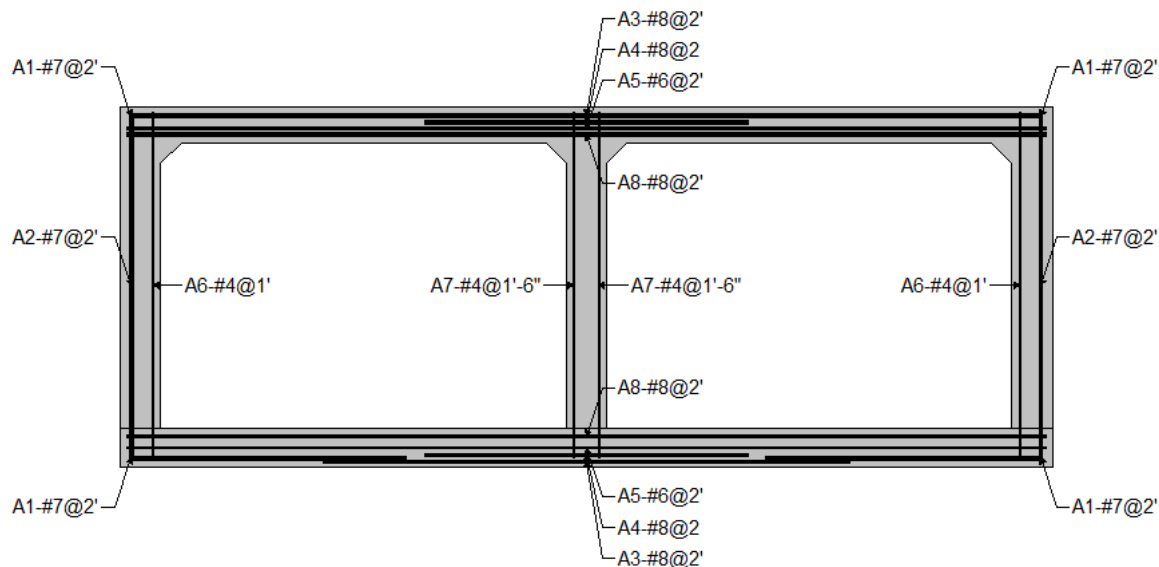


Figure 17 - BrDR Model M2C1 reinforcement schematic*

*Note: There is currently a bug in the BrDR software that prevents hooked and bent bars from displaying properly. The reinforcement was checked to match the drawings.

Table 7 – BrDR Model M2C1 ratings – LFR/LRFR

Fill	LRFR Ratings			LFR (Ratings)		
Culvert M2C1 (1.99' fill)	HL-93 (US)	0.799	1.036	HS-25	0.665	1.111
Culvert M2C1 (2.00' fill)	HL-93 (US)	1.322	1.714	HS-25	1.201	2.005
Culvert M2C1 (5.00' fill)	HL-93 (US)	2.615	3.39	HS-25	3.343	5.582
Culvert M2C1 (7.00' fill)	HL-93 (US)	3.149	4.082	HS-25	4.357	7.289
Culvert M2C1 (8.00' fill)	HL-93 (US)	3.154	4.089	HS-25	5.492	9.037
Culvert M2C1 (10.00' fill)	HL-93 (US)	2.651	3.437	HS-25	5.804	9.656

Similar to Model 1, for the LRFR ratings, a noticeable step can be seen from a fill of 1.99' to 2.00'. For 1.99' the controlling inventory rating of 0.799 is governed by shear in the top slab near the support at the critical shear distance. For the fill of 2', the controlling inventory rating of 1.322 is governed by flexure in the center of the top slab. This difference is due primarily to the difference in the calculation of concrete shear capacity at the 2' fill level. See the discussion under Model 1.

Appendix D – 2D Analysis Backup

For model 2 the calculations of the concrete shear capacity and overall shear resistance are presented in Table 8. This jump in shear capacity is discussed more under Task 5.

Table 8 - BrDR Model M2C1 shear capacity comparison at 1.99' fill and 2.00' fill

Fill depth		Inv Rating	Oper Rating	Concrete Shear Resistance	Steel Shear Resistance	Shear Resistance
				V_c (kips)	V_s (kips)	V_r (kips)
Culvert M1C1 (1.99' fill)	HL-93 (US)	0.799	1.036	9.93*	0	8.44
Culvert M1C1 (2.00' fill)	HL-93 (US)	1.322	1.714	16.83	0	14.3

*Note: This uses the AASHTO LRFD Simplified for shear and not the iterative shear method provided in Appendix B of AASHTO. The Appendix B option is not available for culverts in BrDR.

Appendix D – 2D Analysis Backup

Model 3 Analysis Backup

Input Information

Meshes for Model 2 were generated for a fill of 1.5'. Using the CANDE ToolBox, different fill depth meshes can be generated if needed for Phase III. The reduction of surface load factor for Model 3 is shown in Table 9 for each fill height.

Table 9 – Reduction of surface load for varying fills for Model 3

Fill Depth (ft)	RSL
1.5	0.353

Depth of Fill (max - road centerline):

Top of box to top of pavement: 16 in. (5 in. reinf. concrete slab, variable depth (2% slope) base course, 2.5 in. binder course, 1.5 in. wearing course)

Bedding depth: 12 in. No. 8 coarse aggregate

Precast Box Geometry:

Span x Rise x Length: 12 ft x 6 ft x 6.46 ft

Top/Bottom/Sidewall: 13.5 in./12.5 in./12 in.

Haunches: 6 in. x 6 in. top & bottom

Reinforcement CANDE (Sections 2 thru 6):		in.²/ft	in.²/in.	Clear cover
AS1 – outside: #5@ 6 in.	0.620	0.052	2.5 in. to top, 1.5 in.	
AS2 – top inside: #5@ 6 in.	0.620	0.052	1.5 in.	
AS3 – bottom inside: #5@ 6 in.	0.620	0.052	2.0 in.	
AS4 – side inside #5@ 6 in.	0.620	0.052	1.5 in.	
AS5 – top outside #4@ 6 in.	0.400	0.033	2.5 in.	
AS6 – bottom outside #4@ 6 in.	0.400	0.033	1.5 in.	

Note: Top slab has inserts for anchors to 5 in. slab.

Materials:

Reinforcement yield stress: 60 ksi – epoxy coated

Concrete f'_c : 6 ksi

CANDE Model notes:

Concrete tensile rupture strain: 0.0001 in./in. (typically neglected in design, but used for analysis)
 $\sim 7 f'_c{}^{0.5}$

In situ – linear elastic $E = 5,000$ psi, Poisson = 0.3 – both assumed

Bedding – 18 in. structure backfill, 6 in. No. 8 stone

Duncan Selig – SW100 (assume well compacted)

Backfill – Assumed

Duncan/Selig – SW95

Appendix D – 2D Analysis Backup

Reinforcement for BrDR

Bar Mark	Type	Bar Number	Spacing (in)	A	B	C
A1	Straight	4	6	9.25		
A2	Straight	5	6	13.75		
A3	Bent	5	6	7.833333	4.416667	4.416667
A4	Straight	5	6	7.833333		

CANDE output results

Figure 18 displays a typical CANDE plot of vertical strain of model 3 with the Tandem vehicle near midspan. Figure 25 displays the dead load moment diagrams for the first 6 load steps (incremental fill levels), while Figure 20 displays the live load envelope for the tandem vehicle for all of the live load steps (7-23). Figure 21 displays the deflection (magnified by 30) and shear stress as the tandem vehicle steps across the culvert.

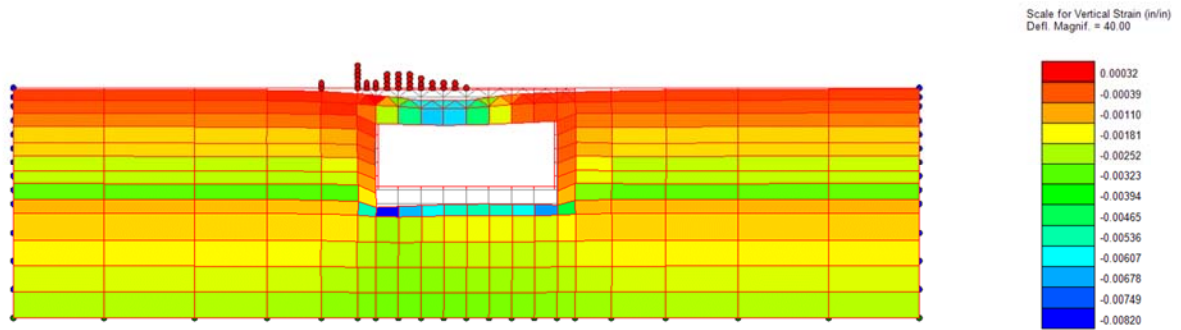


Figure 18 – M3C1 Vertical strain with Tandem Vehicle near midspan (with pavement)

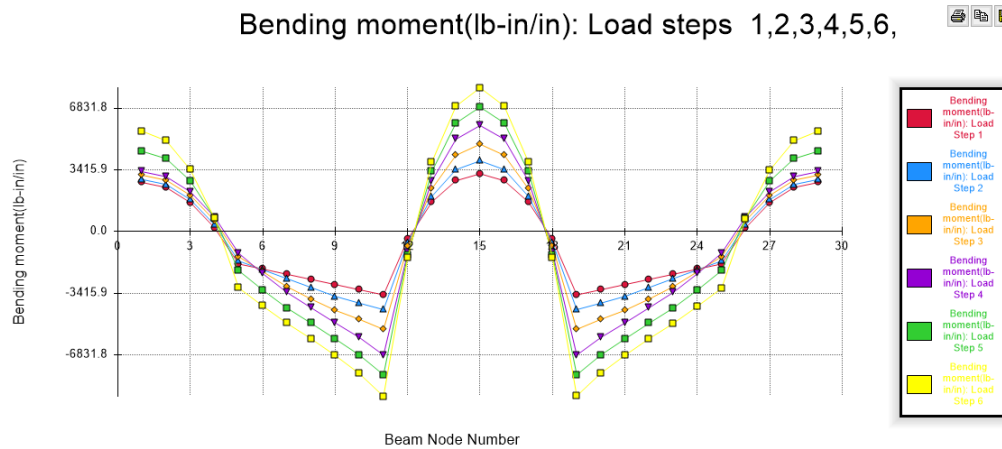


Figure 19 – M3C1- CANDE Bending Moment - Dead load envelope – Load steps 1-6

Appendix D – 2D Analysis Backup

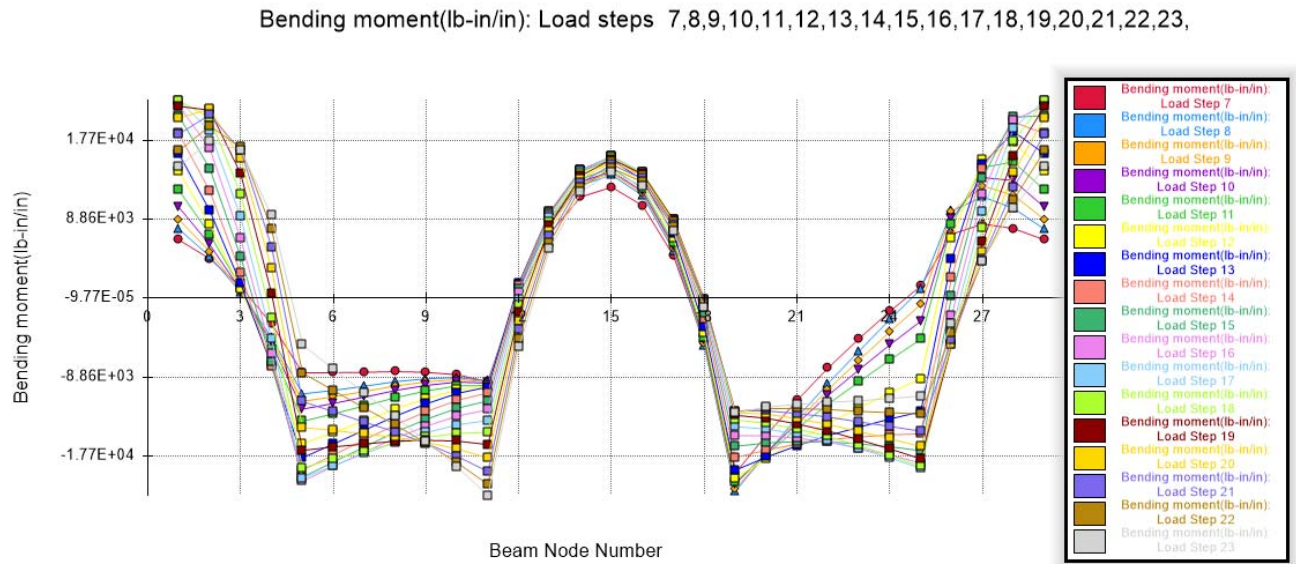


Figure 20 – M3C1 – CANDE bending moment envelope - live load steps – load steps 7-23 (2 axle Tandem ,25 kip/axle) (with pavement)

Appendix D – 2D Analysis Backup

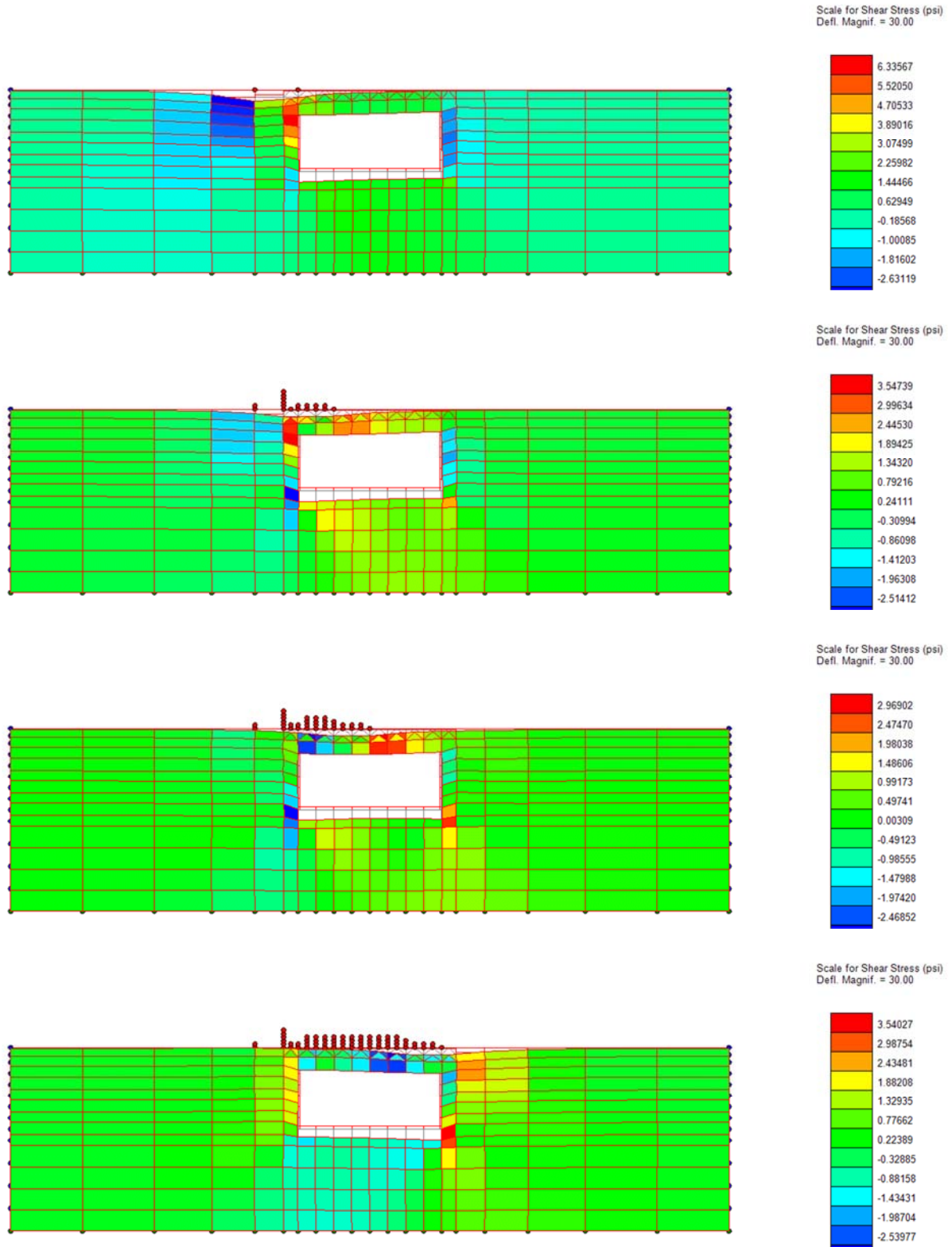


Figure 21 – M3C1 showing shear stress as Tandem vehicle moves across culvert (5' fill, no pavement)

Appendix D – 2D Analysis Backup

Pavement Rating Results

An analysis of the CANDE model 3 was performed using the following options:

- Solution for tandem-truck load traveling over surface no pavement.
- Solution with pavement with modulus of Elasticity = 200,000 psi
- Solution with pavement with modulus of Elasticity = 400,000 psi
- Solution with pavement with modulus of Elasticity = 600,000 psi

Base Model 3 differs from the original Contech model in the following ways:

- The top row of SW95 soil elements changed to elastic wearing course using default Tool Box values. This is necessary to avoid failure of the shear failure of one element.
- Changed load factor for earth load steps 2 thru 6 to 1.37 (= 1,3 * 1.05).
- Soil Material #3 (Duncan/Selig SW95) upgraded to include Katona Modification for unloading.

Live-Base Model 3 simulates a tandem truck moving over the soil surface (no pavement): The live loading includes the following

- Lane loading
- Dynamic impact factor.
- Multilane presence factor.
- Standard live-load factor (1.75) specified in E-lines.
- RSL longitudinal modification including 3DSE assuming lay-length = 6 feet.
- Details of the live-load assumptions are at bottom of the CANDE input file (CID extension) as printed by the tool box.

The three pavement models with E = 200,000, 400,000 and 600,000 psi were created by the Tool Box wherein pavement thickness = 6", Poisson ratio = 0.33 and the pavement density = 0 pcf in each case. Density was set to zero to offset not reducing the dynamic impact factor and RSL from the added 6".

Table 10 – Model 3 -CANDE Rating Factors (from CANDE Toolbox) Tandem vehicle, without and with pavement (varying fill depths)

Rating Factors per Design Criterion	No pavement	E = 200,000 psi v = 0.33 Pavement (6")	E = 400,000 psi v = 0.33 Pavement (6")	E = 600,000 psi v = 0.33 Pavement (6")
1.33 ft fill				
Steel yielding	1.61 (Node 29)	1.62 (Node 29)	1.64 (Node 29)	1.65 (Node 29)
Concrete crushing	3.72 (Node 6)	3.74 (Node 6)	3.75 (Node 6)	3.79 (Node 6)
Shear failure	1.98 (Node 4)	2.12 (Node 26)	2.15 (Node 26)	2.18 (Node 26)
Radial tension	531.00 (Node 5)	1858.00 (Node 1)	1858.00 (Node 1)	1858.00 (Node 1)

The new results show an improvement in rating as the pavement is added and the elasticity modulus increased.

Appendix D – 2D Analysis Backup

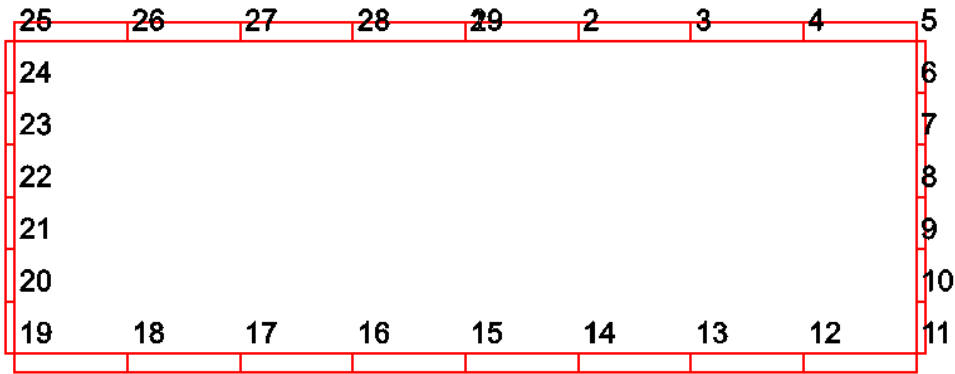
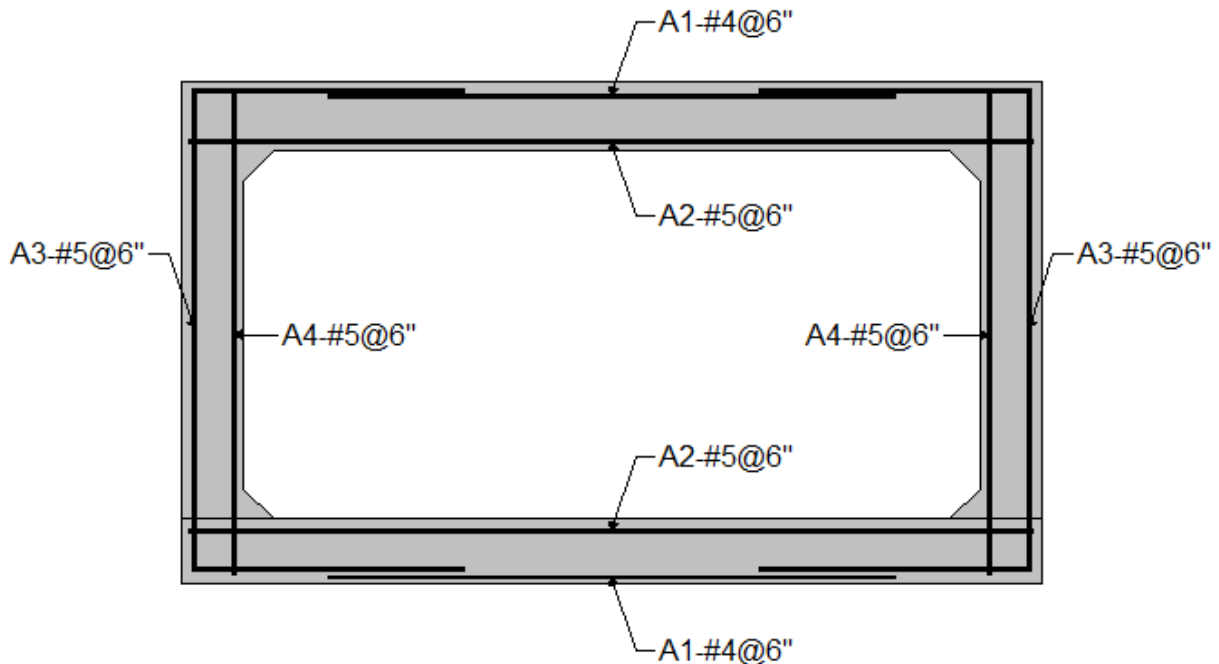


Figure 22 – Beam node numbering for M3C1

Generated BrDR Model

Model 3 was also input into the AASHTOWare BrDR software and run for varying fill heights (1.99', 2.00', 5', 7', 8', and 10'). The reinforcement schematic from BrDR is shown in Figure 23. The LRFR ratings (HL93) are shown in Table 11. The ratings are provided at each fill height. For comparison purposes, the LFR rating was performed with the HS25 vehicle. The ratings for LFR are provided as well.

Model 3- Candidate 1
 Mod1-Cand1-NCHRP - Culvert (1.99' fill) -
 05/16/17



Appendix D – 2D Analysis Backup

Figure 23 - BrDR Model M3C1 reinforcement schematic

Table 11 – BrDR Model M3C1 ratings – LFR/LRFR

Fill	LRFR Ratings			LFR (Ratings)		
Culvert M3C1 (1.99' fill)	HL-93 (US)	1.401	1.816	HS-25	1.111	1.855
Culvert M3C1 (2.00' fill)	HL-93 (US)	1.177	1.525	HS-25	1.176	1.965
Culvert M3C1 (5.00' fill)	HL-93 (US)	1.688	2.188	HS-25	2.677	4.47
Culvert M3C1 (7.00' fill)	HL-93 (US)	1.528	1.981	HS-25	3.267	5.455
Culvert M3C1 (8.00' fill)	HL-93 (US)	1.441	1.869	HS-25	3.476	5.805
Culvert M3C1 (10.00' fill)	HL-93 (US)	0.799	1.036	HS-25	2.636	4.403

Similar to Model 1, for the LRFR ratings, a noticeable step can be seen from a fill of 1.99' to 2.00'. In this case the step is downward and the governing rating is flexure. The culvert, built in 2013, was designed with the LRFD shear specifications accounting for the change at the 2' fill. For model 3 the difference in live load moment is shown in Table 12. The difference in the live loads is likely due to the distribution of live load from LRFD articles 3.6.1.2.6 (greater or equal to 2') and 4.6.2.10.

Table 12 - BrDR Model M3C1 live load moment at 1.99' fill and 2.00' fill

Fill depth		Inv Rating	Oper Rating	Live Load at critical rating
				M _{LL} (kip-ft)
Culvert M3C1 (1.99' fill)	HL-93 (US)	1.401	1.816	11.28
Culvert M3C1 (2.00' fill)	HL-93 (US)	1.177	1.525	13.42

*Note: Even though this table is for moment, a panel member asked which shear procedure was used. This model uses the AASHTO LRFD Simplified for shear and not the iterative shear method provided in Appendix B of AASHTO. The Appendix B option is not available for culverts in BrDR.

Appendix D – 2D Analysis Backup

Figure 25 – Model 4 area of steel for CANDE model

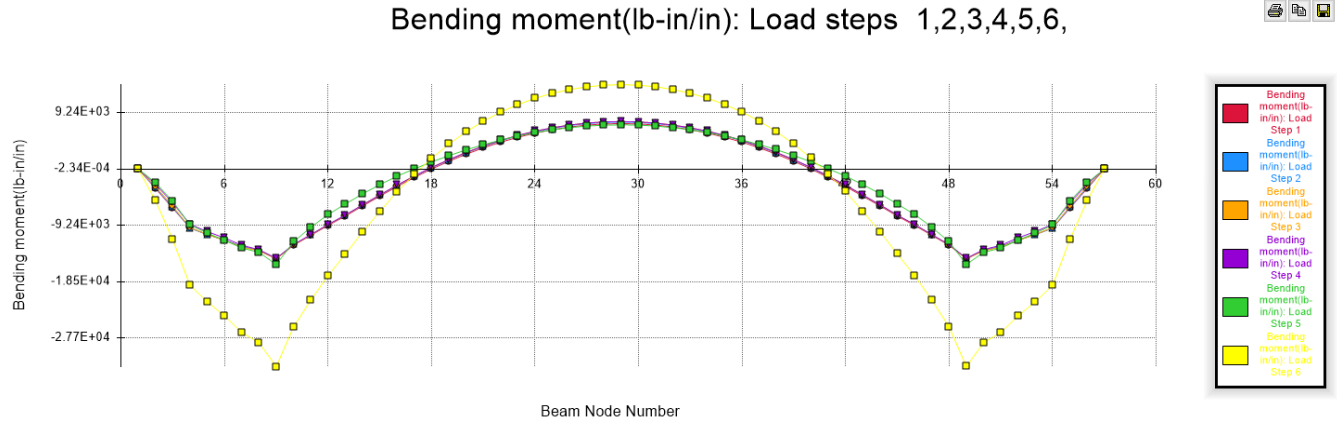


Figure 26 – M4C1- CANDE Bending Moment - Dead load envelope – Load steps 1-6

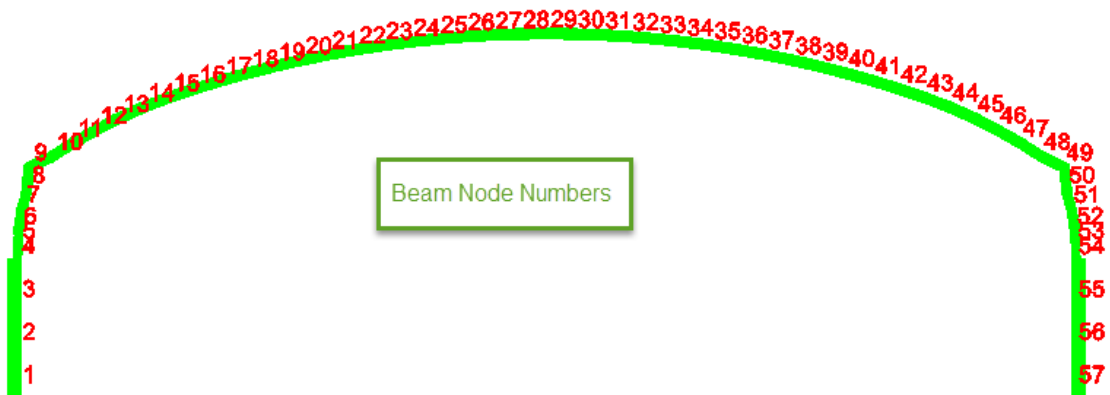
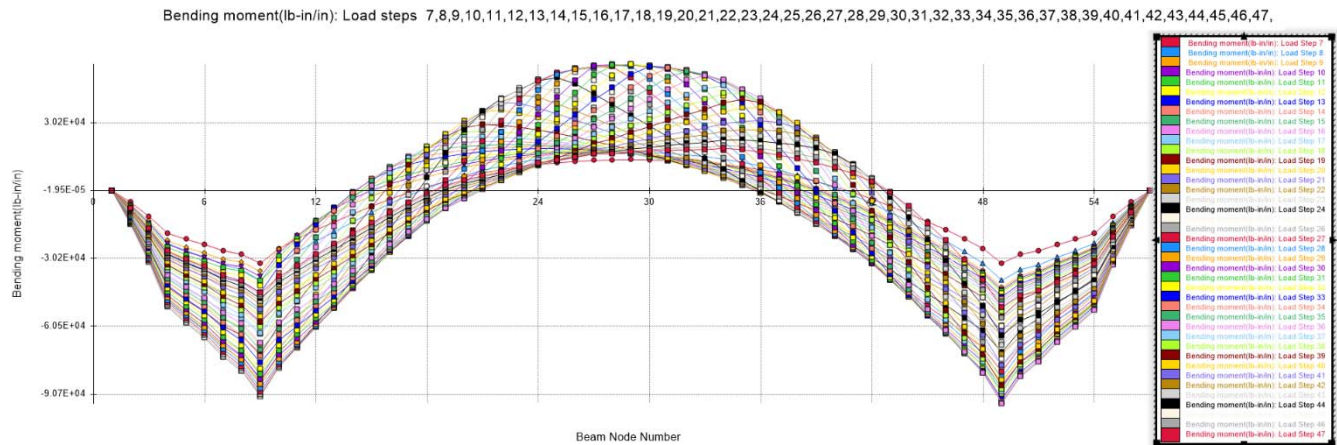


Figure 27 – M4C1 – CANDE bending moment envelope - live load steps – load steps 7-47 (2 axle Tandem ,25 kip/axle + Lane loading) (with pavement)

Appendix D – 2D Analysis Backup

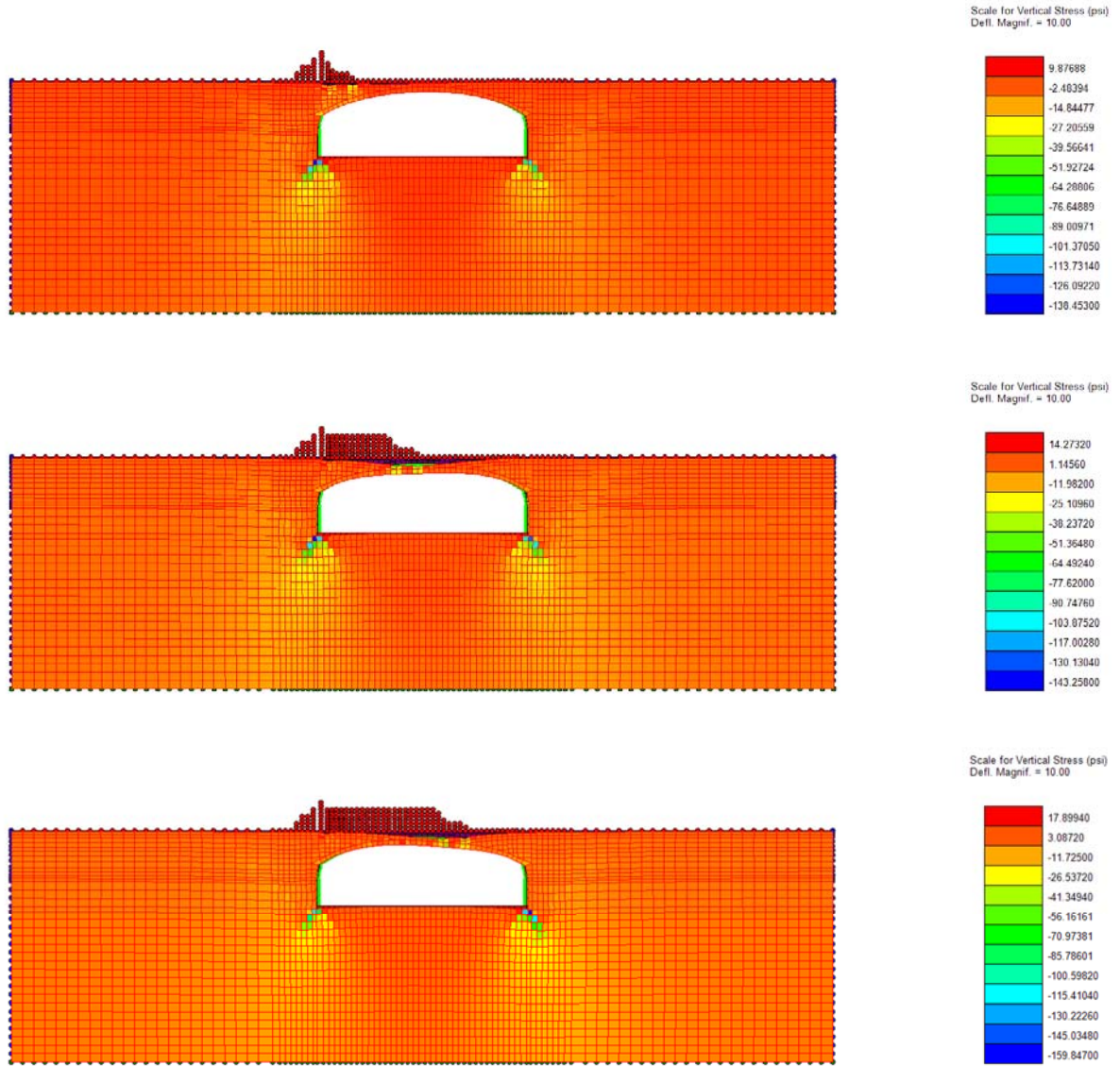


Figure 28 – M4C1 showing vertical stress as Tandem vehicle moves across culvert (1' fill, no pavement)

Appendix D – 2D Analysis Backup

Pavement Rating Results

An analysis of the CANDE model 4 (see Figure 29) was performed using the following options:

- Solution for tandem-truck load traveling over surface no pavement.
- Solution with pavement with modulus of Elasticity = 200,000 psi
- Solution with pavement with modulus of Elasticity = 400,000 psi
- Solution with pavement with modulus of Elasticity = 600,000 psi

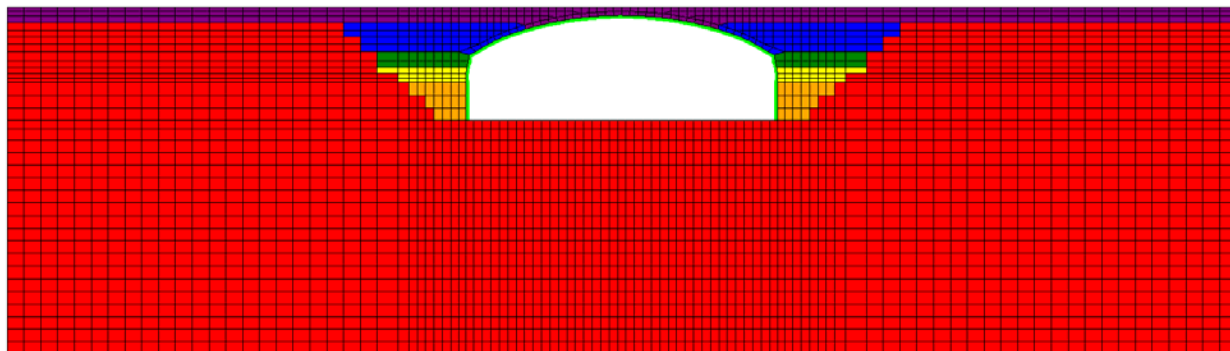


Figure 29 – CANDE Model 4 (M4C1)

Base Model 4 differs from the original Contech model in the following ways:

- Contech's deep burial elements that enter into the system at load step 9, were reset to come into the system at system at step 99 (i.e., never appear).
- Contech's working stress methodology (LRFD=0) was changed to LRFD = 1. Dead and earth load factors were set accordingly and soil densities changed to realistic values. (See CANDE User Manual)
- The soil fill above the crown was changed from Duncan SM90 to Duncan/Selig SW90 as the latter is more realistic and less prone to nonconvergence. (See CANDE User Manual)
- A wearing course (linear elastic soil with $E = 1800$ psi) was inserted on the top row elements.

Live-Base Model 4 simulates a tandem truck moving over the surface. Included with live load are:

- HL93 lane loading.
- dynamic impact factor.
- Multilane presence factor.
- And the standard live-load factor (1.75) specified in E-lines.
- Details of the live-load assumptions may be observed at the bottom of the CANDE input file as printed out by the CANDE tool box.

The three pavement models with $E = 200,000$, $400,000$ and $600,000$ psi were created by the CANDE Tool Box wherein the pavement thickness = 6 inches, Poisson ratio = 0.2 and the pavement density = 140 pcf in each case.

The CANDE solutions for all live load cases were processed by Option 5 in the CANDE tool box and the bottom line load-rating factors are shown in the Table 13 below.

Appendix D – 2D Analysis Backup

Table 13 – Model 4 (M4C1) load ratings for a Tandem Vehicle with lane load

Rating Factors per Design Criterion	No pavement	E = 200,000 psi $\nu = 0.20$ Pavement (6")	E = 400,000 psi $\nu = 0.20$ Pavement (6")	E = 600,000 psi $\nu = 0.20$ Pavement (6")
1.0 ft fill				
Steel yielding	1.00 (Node 29)	1.07 (Node 52)	1.07 (Node 52)	1.08 (Node 52)
Concrete crushing	1.15 (Node 29)	1.27 (Node 29)	1.27 (Node 29)	1.29 (Node 29)
Shear failure	1.27 (Node 43)	1.35 (Node 43)	1.37 (Node 43)	1.38 (Node 43)
Radial tension	5.14 (Node 32)	5.82 (Node 32)	5.90 (Node 29)	5.99 (Node 29)

Appendix D – 2D Analysis Backup

Model 5 Analysis Backup

Input Information

A request has been made of CONTECH for the CANDE input file for this culvert. If we are not able to obtain the file, the CANDE model will be created from the shop drawings provided.

Note: The backup for the CANDE analysis of Model is provided for Interim Report #3.

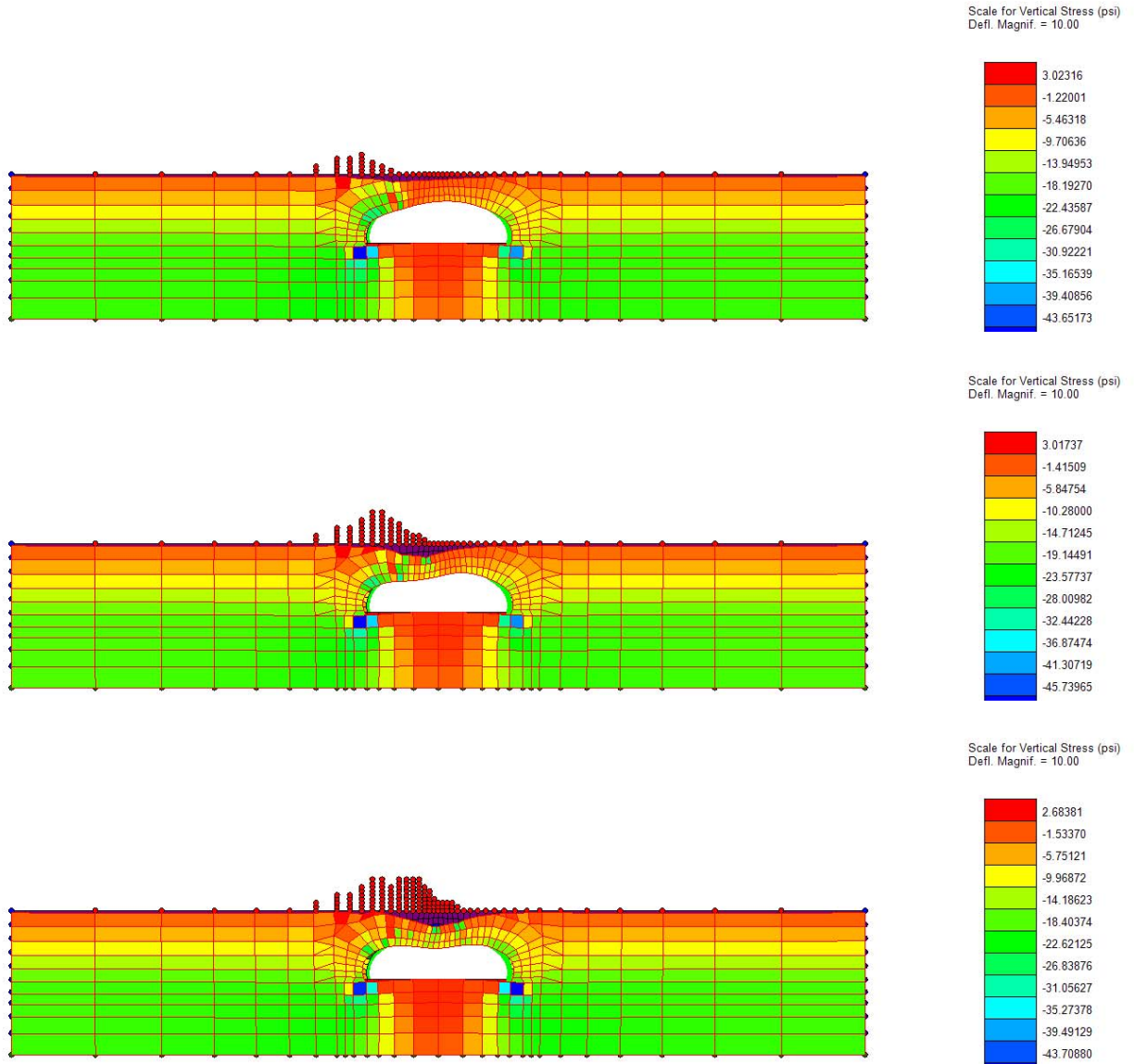


Figure 30 – M5C1 showing vertical stress as Tandem vehicle moves across culvert (no pavement)

Appendix D – 2D Analysis Backup

Pavement Rating Results

An analysis of the CANDE model 5 (see Figure 31) was performed using the following options:

- Solution for tandem-truck load traveling over surface no pavement.
- Solution with pavement with modulus of Elasticity = 200,000 psi
- Solution with pavement with modulus of Elasticity = 400,000 psi
- Solution with pavement with modulus of Elasticity = 600,000 psi

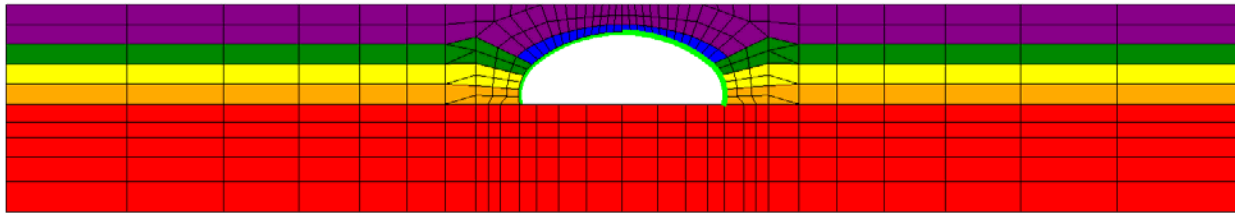


Figure 31 – CANDE Model 5 (M5C1)

Base Model 5, which is a corrugated steel arch under 3 feet of soil cover, remains essentially the same as originally constructed. The only change is replacing the top row of Mohr-Coulomb soil elements over the arch with an elastic wearing course whose elastic properties match the Mohr-Coulomb model. This is necessary to avoid failure of the Mohr Coulomb elements from the excessive shear forces caused by point loads representing the traveling tandem truck. (see CANDE User Manual).

Live-Base Model 5 simulates a tandem truck moving over the surface. Included with live load are:

- HL93 lane loading.
- dynamic impact factor.
- Multilane presence factor.
- And the standard live-load factor (1.75) specified in E-lines.
- RSL reduction for longitudinal load spreading is used based on variable cover height.
- Details of the live-load assumptions may be observed at the bottom of the cid file as printed out by the CANDE tool box.

The three pavement models with $E = 200,000$, $400,000$ and $600,000$ psi were created by the CANDE Tool Box wherein the pavement thickness = 6 inches, Poisson ratio = 0.2 and the pavement density = 140 pcf in each case.

The CANDE solutions for all live load cases were processed by Option 5 in the CANDE tool box and the bottom line load-rating factors are shown in the Table 14 below.

Table 14 – Model 5 (M5C1) load ratings for a Tandem Vehicle with lane load

Rating Factors per Design Criterion	No pavement	E = 200,000 psi $\nu = 0.20$ Pavement (6")	E = 400,000 psi $\nu = 0.20$ Pavement (6")	E = 600,000 psi $\nu = 0.20$ Pavement (6")
3.0 ft fill				
Material thrust yield	3.69 (Node 7)	4.20 (Node 33)	4.27 (Node 33)	4.21 (Node 18)
Buckling thrust failure	3.77	4.30	4.37	4.29

Appendix D – 2D Analysis Backup

	(Node 7)	(Node 33)	(Node 33)	(Node 18)
Seam thrust failure	3.39 (Node 7)	3.87 (Node 33)	3.93 (Node 33)	3.90 (Node 18)
Plastic penetration	3.14 (Node 3)	3.82 (Node 37)	3.91 (Node 37)	3.90 (Node 37)

Figure 32 provides a copy of the load-rating summaries from CANDE Tool Box that are summarized in Table 14.

(1) No Pavement

DESIGN-CRITERION (Strength)	LOAD STEP	LOCAL NODE	DEAD-LOAD DEMAND	LIVE-LOAD DEMAND	EFFECTIVE CAPACITY	*RATING FACTOR
*MATERIAL THRUST (psi)	20	7	7480.00	6920.00	33000.00	3.69
*BUCKLING THRUST (psi)	20	7	7480.00	6920.00	33575.00	3.77
*SEAM THRUST (psi)	20	7	7480.00	6920.00	30957.00	3.39
*PLASTIC-PENETRATE (%)	16	3	0.00	28.68	90.00	3.14

(2) Pavement E = 200,000 psi

DESIGN-CRITERION (Strength)	LOAD STEP	LOCAL NODE	DEAD-LOAD DEMAND	LIVE-LOAD DEMAND	EFFECTIVE CAPACITY	*RATING FACTOR
*MATERIAL THRUST (psi)	24	33	7280.00	6120.00	33000.00	4.20
*BUCKLING THRUST (psi)	24	33	7280.00	6120.00	33575.00	4.30
*SEAM THRUST (psi)	24	33	7280.00	6120.00	30957.00	3.87
*PLASTIC-PENETRATE (%)	26	37	0.00	23.55	90.00	3.82

(3) Pavement E = 400,000 psi

DESIGN-CRITERION (Strength)	LOAD STEP	LOCAL NODE	DEAD-LOAD DEMAND	LIVE-LOAD DEMAND	EFFECTIVE CAPACITY	*RATING FACTOR
*MATERIAL THRUST (psi)	24	33	7280.00	6020.00	33000.00	4.27
*BUCKLING THRUST (psi)	24	33	7280.00	6020.00	33575.00	4.37
*SEAM THRUST (psi)	24	33	7280.00	6020.00	30957.00	3.93
*PLASTIC-PENETRATE (%)	26	37	0.00	23.04	90.00	3.91

(4) Pavement E = 600,000 psi

DESIGN-CRITERION (Strength)	LOAD STEP	LOCAL NODE	DEAD-LOAD DEMAND	LIVE-LOAD DEMAND	EFFECTIVE CAPACITY	*RATING FACTOR
*MATERIAL THRUST (psi)	27	18	4930.00	6670.00	33000.00	4.21
*BUCKLING THRUST (psi)	27	18	4930.00	6670.00	33575.00	4.29
*SEAM THRUST (psi)	27	18	4930.00	6670.00	30957.00	3.90
*PLASTIC-PENETRATE (%)	26	37	0.00	23.09	90.00	3.90

Figure 32 – Model 5 (M5C1) – CANDE Toolbox rating output

Appendix D – 2D Analysis Backup

Model 6 Analysis Backup

Input Information

Meshes for Model 6 were created for CANDE for 1.5' and 2' of fill. The reduction for surface load for the fills used in the CANDE models is shown in Table 15.

Table 15 – Reduction of surface load for varying fills for Model 6

Fill Depth (ft)	RSL
1.5	0.324
2	0.177

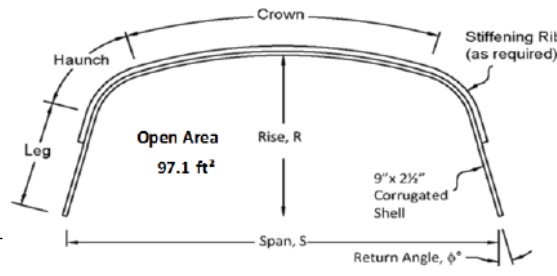
The following was provided by Lane Enterprises.



Vehicle Loading
HL-93 Truck
kips per axle 32
wheels/axle group 4

Cover Height, H
Minimum Cover 1.4 ft
Maximum Cover 5.0 ft
H = height of cover from box culvert rise to top of pavement

AASHTO LRFD Bridge Design Specifications, Seventh Edition, 2014, Section 12.9, Structural Plate Box Culverts



Aluminum Box Culvert Data

Shell Designation	BC-A-43
Span x Rise	19'-0" x 6'-1"
Crown Plate	0.225"
Haunch Plate	0.125"
Crown Stiffening Rib	Type VI @ 18"
Haunch Stiffening Rib	Type VI @ 18"
φ°	14.9

Crown Plastic Moment Capacity, M_{PC} (k-ft/ft) = 21.74
Haunch Plastic Moment Capacity, M_{PH} (k-ft/ft) = 20.09

Cover Height Investigated, H = 1.4 ft

(1) Calculate the unfactored sum of the nominal crown and haunch dead load moments, M_{dl} [k-ft/ft]

For $S \leq 25'-5"$ $M_{dl} = \gamma_S \{ S^3 [0.0053 - 0.00024 (S-12)] + 0.053 (H - 1.4) S^2 \}$ $\gamma_S = 0.120$ kcf
 For $S \geq 25'-6"$ $M_{dl} = \gamma_S \{ S^3 [0.00194 - 0.0002 (S - 26) (H - 1.1)] + (H - 1.4) [0.053 S^2 + 0.6 (S - 26)^2] \}$

Factored sum of nominal crown and haunch dead load moments, $M_{dlu} = \eta_{EV} \gamma_{DL} M_{dl} = 4.69$ k-ft/ft Earth load modifier, $\eta_{EV} = 1.05$
Earth load factor, $\gamma_{DL} = 1.5$

(2) Calculate the unfactored sum of the nominal crown and haunch live load moments, M_{ll} [k-ft/ft]

$M_{ll} = C_{ll} K_1 S / K_2 = C_1 C_2 A_L K_1 S / K_2$

Where:

C_{ll} = adjusted live load = $C_1 C_2 A_L$ (kips)

$C_1 = 1.0$ for single axles and $0.5 + S/50 \leq 1.0$ for tandem axles $C_1 = 1.000$

C_2 = adjustment factor for number of wheels on a design axle $C_2 = 1.00$

A_L = sum of all axle loads in an axle group (kips) $A_L = 32$

K_1 For $S < 20'$, $K_1 = 0.08 / (H/S)^{0.2}$
 For $S \geq 20'$, $K_1 = [0.08 - 0.002 (S - 20)] / (H/S)^{0.2}$ $K_1 = 0.13$

K_2 For $1.4 \leq H < 3$, $K_2 = 0.54 H^2 - 0.4 H + 5.05$
 For $3.0 \leq H \leq 5.0$, $K_2 = 1.90 H + 3$ $K_2 = 5.55$

Factored sum of nominal crown and haunch live load moments, $M_{llu} = \eta_{LL} \gamma_{LL} M_{ll} = 29.54$ k-ft/ft

H (ft)	C ₂ Values		
	2	4	8
1.4	1.18	1.00	0.63
2.0	1.21	1.00	0.70
3.0	1.24	1.00	0.82
4.0	1.13	1.00	0.88
5.0	1.02	1.00	0.93

Intermediate values interpolated

Live load modifier, $\eta_{LL} = 1.00$

Live load factor, $\gamma_{LL} = 2.0$

Appendix D – 2D Analysis Backup

(3) Calculate the proportioned sum of the adjusted dead and live load moments for the crown and the haunch

$$M_{PC} \geq C_H P_C (M_{du} + M_{lu}) \quad [Eq. 3.1]$$

$$M_{PH} \geq C_H (1.0 - P_C) (M_{du} + R_H M_{lu}) \quad [Eq. 3.2]$$

The plastic moment resistance of the crown (M_{PC}) and the plastic moment resistance of the haunch (M_{PH}) shall not be less than the proportioned sum of adjusted dead and live load moments.

Where:

C_H = crown soil cover factor

P_C = crown moment proportioning factor

R_H = haunch moment reduction factor

Design moments shall be increased where the cover is less than 3.5 ft.

Ratio of total moment carried by the crown.

The haunch moment may be reduced for spans less than 25'-5".

For $1.4 \leq H < 3.5$, $C_H = 1.15 - (H - 1.4)/14$

For $H \geq 3.5$, $C_H = 1.0$

$C_H = 1.15$

$R_H = 0.66$

P_C (Allowable Range)

Spans $\leq 25'-5"$	
$S < 10.0$	$0.55 \leq P_C \leq 0.70$
$10.0 \leq S \leq 15.0$	$0.50 \leq P_C \leq 0.70$
$15.0 \leq S \leq 20.0$	$0.45 \leq P_C \leq 0.70$
$20.0 \leq S \leq 25.4$	$0.45 \leq P_C \leq 0.60$
Spans $> 25'-5"$	
$1.4 \leq H \leq 2.5$	$0.55 \leq P_C \leq 0.65$
$2.5 < H \leq 4.0$	$0.45 \leq P_C \leq 0.55$
$4.0 < H \leq 5.0$	$0.35 \leq P_C \leq 0.55$

R_H Factors

H	$S \leq 25'-5"$	$S > 25'-5"$
1.4	0.66	1.00
2.0	0.74	1.00
3.0	0.87	1.00
4.0	1.00	1.00
5.0	1.00	1.00

Interpolated for intermediate values

Method

Solve Eq. 3.1 for P_C using the actual crown flexural capacity. With P_C known, solve Eq. 3.2 for M_{PH} . If Eq. 3.1 yields a value of P_C above the allowable range, the actual crown is over-designed, which is acceptable. However, the upper range value of P_C should be used to calculate the required M_{PH} from Eq. 3.2.

$$P_C = \frac{M_{PC}}{C_H (M_{du} + M_{lu})} = 0.55$$

allowable range
 $0.45 \leq P_C \leq 0.70$

The crown moment proportioning factor is within the range, therefore use the calculated value to determine the haunch moment.

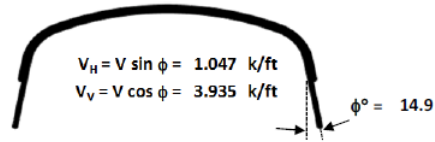
Using Eq. 3.2, $M_{PH} \geq 12.45$ k-ft/ft

Actual $M_{PH} = 20.09$ k-ft/ft

Therefore okay

(4) Calculate the unfactored footing reaction, V [k/ft]

$$V = \gamma_s \left(\frac{HS}{2.0} + \frac{S^2}{40.0} \right) + \frac{A_L}{8 + 2(H + R)} = 4.07 \text{ k/ft}$$



Appendix D – 2D Analysis Backup

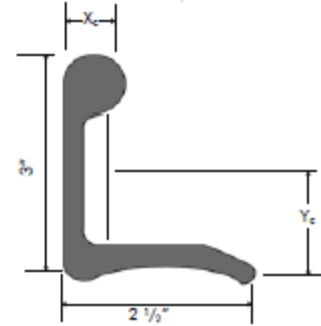
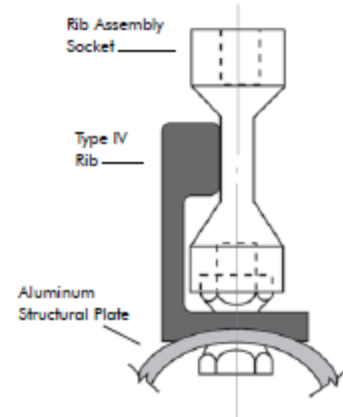
Aluminum Structural Plate Rib Design

TABLE 30A. SECTION PROPERTIES OF PLATES ONLY 9" X 2-1/2" CORRUGATION					
Thickness Inches	Moment of Inertia In. ⁴ /Ft.	Section Modulus In. ³ /Ft.	Radius of Gyration Inches	Area of Section In. ² /Ft.	Ultimate Seam Strength kip./ft.
0.100	0.997	0.767	0.844	1.404	28.0
0.125	1.248	0.951	0.844	1.750	41.0
0.150	1.499	1.131	0.845	2.100	54.1
0.175	1.751	1.309	0.845	2.449	63.7
0.200	2.004	1.484	0.846	2.799	73.4
0.225	2.258	1.657	0.847	3.149	83.2
0.250	2.513	1.828	0.847	3.501	93.1

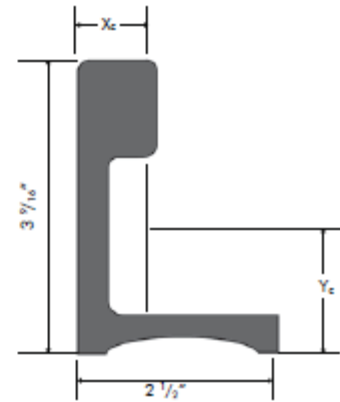
Notes:
1. Design Yield Stress is 24 ksi.
2. 0.100" Thickness can not be curved.

Rib Type	Metal Thickness, Inches						
	0.125	0.150	0.175	0.200	0.225	0.250	
No Rib	2.65	3.18	3.71	4.24	4.77	5.30	
Type II	Plastic Moment Capacity, M_p (kip-ft./ft.)						
@ 54	4.62	5.46	6.04	6.61	7.17	7.74	
@ 27	6.18	7.25	7.94	8.60	9.25	9.87	
@ 18	7.41	8.66	9.48	10.26	11.00	11.71	
@ 9	10.63	12.13	13.08	14.05	15.03	16.02	
Type IV	@ 54	5.87	6.82	7.43	8.04	8.63	9.21
@ 27	8.32	9.59	10.39	11.14	11.85	12.55	
@ 18	10.42	11.90	12.84	13.72	14.57	15.39	
@ 9	16.45	18.46	19.41	20.38	21.37	22.37	
Type VI	@ 54	8.74	9.51	10.24	10.95	11.64	12.32
@ 27	13.76	14.33	15.16	16.19	17.36	17.48	
@ 18	20.09	20.56	20.79	21.30	21.74	22.58	
@ 9	32.24	34.35	36.46	38.54	39.88	40.63	

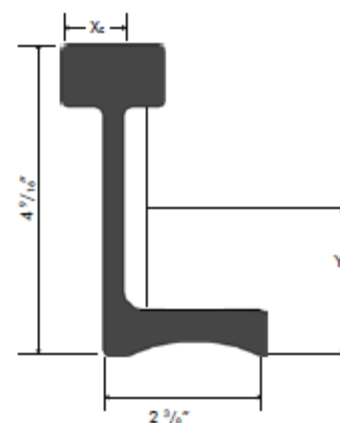
TABLE 32. SECTION PROPERTIES OF ALSP REINFORCING RIB			
	Type VI Rib	Type IV Rib	Type II Rib
Alloy	6061-T6	6061-T6	6061-T6
Area	3.62 in. ²	2.27 in. ²	1.71 in. ²
Center of Mass	$X_c = 0.91$ inches $Y_c = 2.27$ inches	$X_c = 0.652$ inches $Y_c = 1.76$ inches	$X_c = 0.645$ inches $Y_c = 1.02$ inches
Moment of Inertia	$I_x = 9.700$ in. ⁴ $I_y = 1.014$ in. ⁴	$I_x = 3.555$ in. ⁴ $I_y = 1.050$ in. ⁴	$I_x = 1.802$ in. ⁴ $I_y = 0.787$ in. ⁴
Radius of Gyration	$R_{x_c} = 1.636$ inches $R_{y_c} = 0.529$ inches	$R_{x_c} = 1.251$ inches $R_{y_c} = 0.680$ inches	$R_{x_c} = 1.026$ inches $R_{y_c} = 0.678$ inches
Section Modulus	$S_x = 4.38$ in. ³	$S_x = 1.90$ in. ³	$S_x = 1.046$ in. ³
Plastic Modulus	$Z_x = 5.66$ in. ³	$Z_x = 2.68$ in. ³	$Z_x = 1.705$ in. ³
Plastic Moment	$M_p = 16.52$ kip-ft.	$M_p = 7.81$ kip-ft.	$M_p = 4.97$ kip-ft.
Yield Strength	$F_y = 35$ ksi	$F_y = 35$ ksi	$F_y = 35$ ksi
Tensile Strength	$F_u = 38$ ksi	$F_u = 38$ ksi	$F_u = 38$ ksi
Minimum Curving Radius	104 in.	104 in.	60 in.



Type II Rib



Type IV Rib



Type VI Rib

Appendix D – 2D Analysis Backup

The following figures are output from the CANDE software. Figure 33 represents the bending moment for dead load and the soil load. Figure 34 provides and envelope of the tandem load that is provided in load steps 9-27. Figure 35 provides the deflection and the shear stress as the TANDEM vehicle moves across the structure (with pavement).

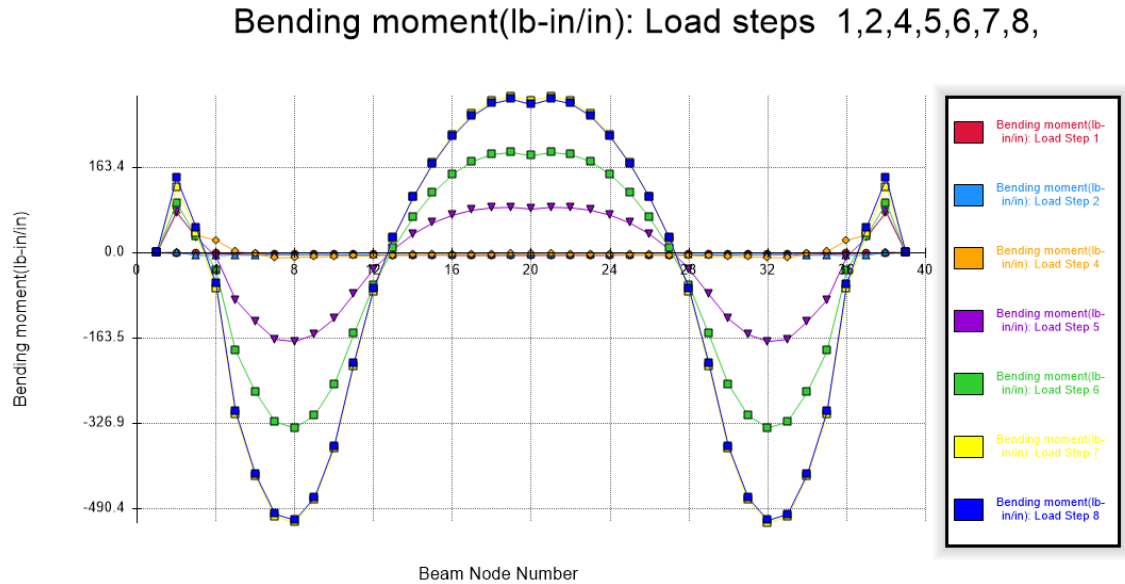


Figure 33 – M6C2- CANDE Bending Moment - Dead load envelope – Load steps 1-8

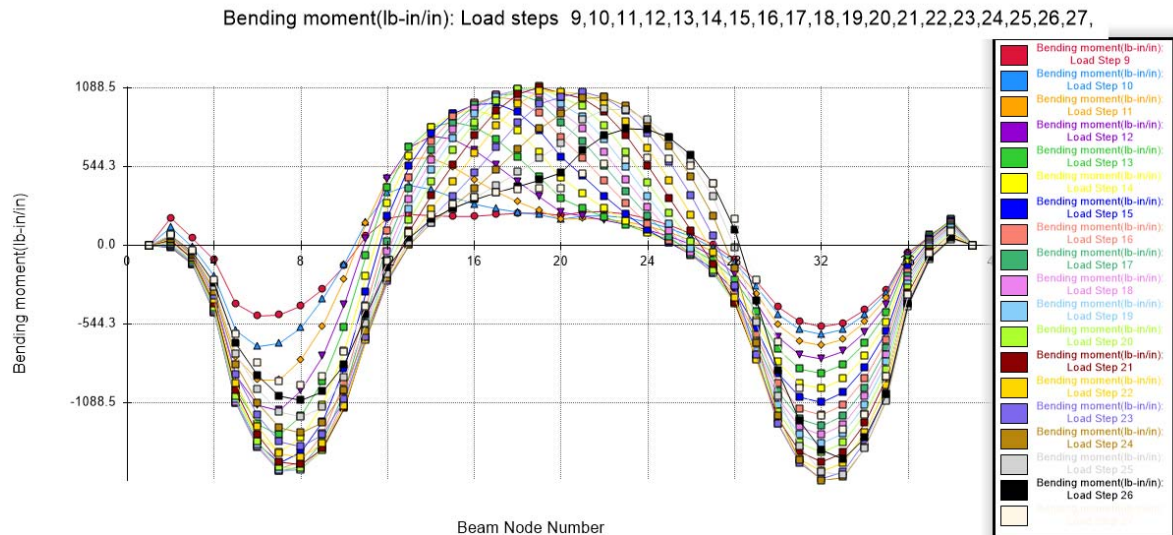


Figure 34 – M6C2 – CANDE bending moment envelope - live load steps – load steps 9-27 (2 axle Tandem ,25 kip/axle) (with pavement)

Appendix D – 2D Analysis Backup

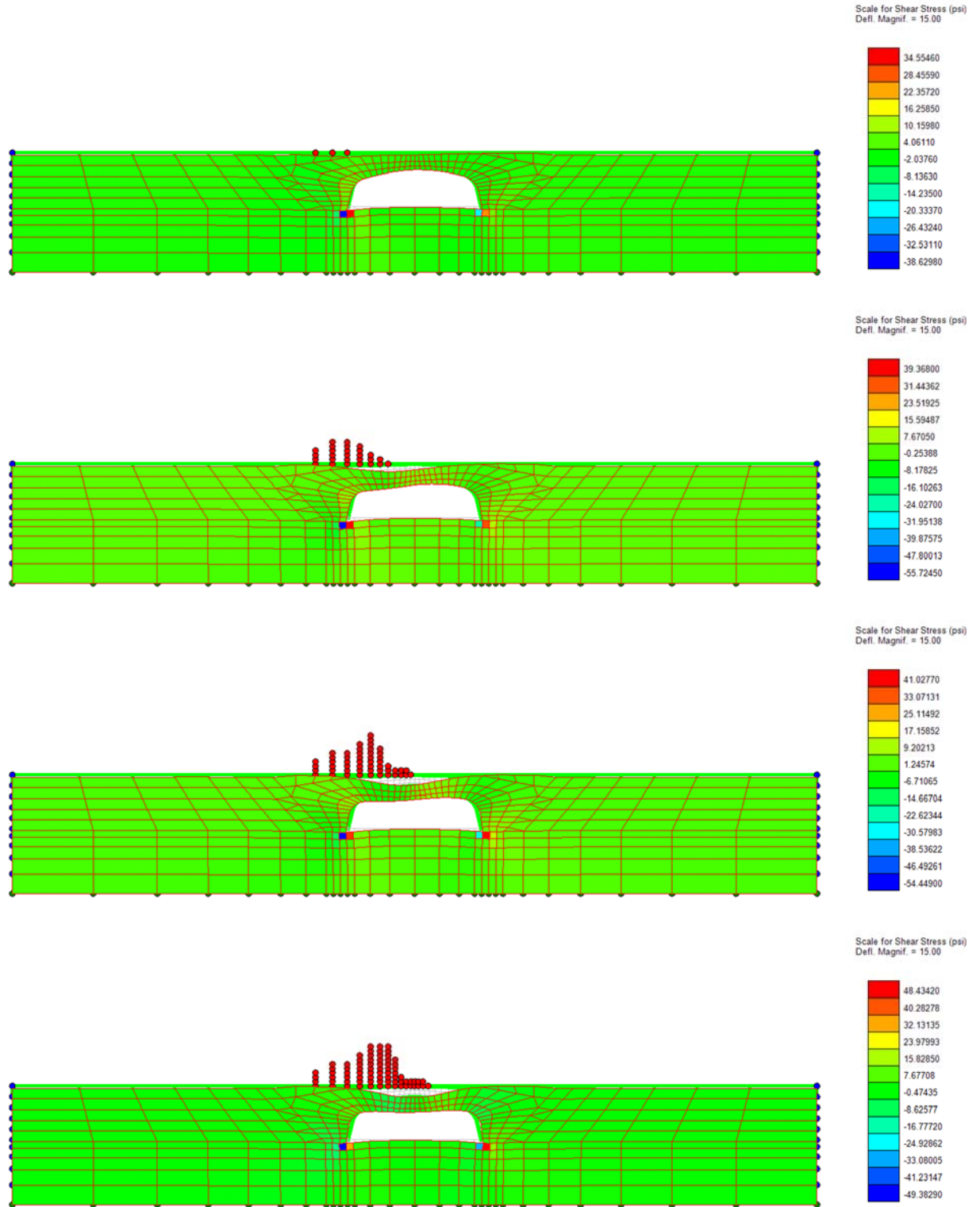


Figure 35 – M6C2 – CANDE Shear stress and deflection as Tandem vehicle moves across the structure (with pavement, E=600,000 psi)

Appendix D – 2D Analysis Backup

Model 7 Analysis Backup

Input Information

Meshes for Model 7 were created for CANDE for 2' of fill and were generated with pavement and without pavement. The original model was provided by CONTECH. The reduction for surface load for the fills used in the CANDE models is shown in Table 16.

Table 16 – Reduction of surface load for varying fills for Model 7

Fill Depth (ft)	RSL
2	0.177

The following figures are output from the CANDE software. Figure 36 represents the bending moment for dead load and the soil load. Figure 37 provides an envelope of the tandem load that is provided in load steps 9-27. Figure 38 provides the deflection and the shear stress as the TANDEM vehicle moves across the structure (with pavement).

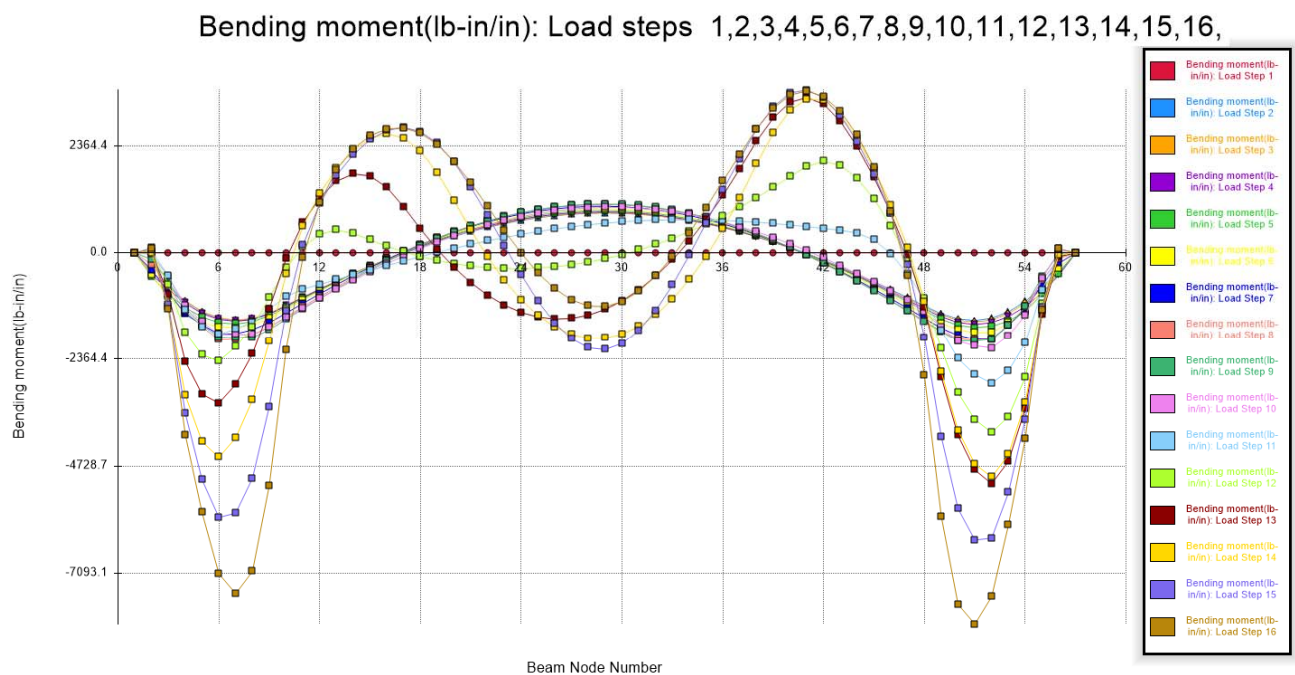


Figure 36 – M7C1- CANDE Bending Moment - Dead load envelope – Load steps 1-16

Appendix D – 2D Analysis Backup

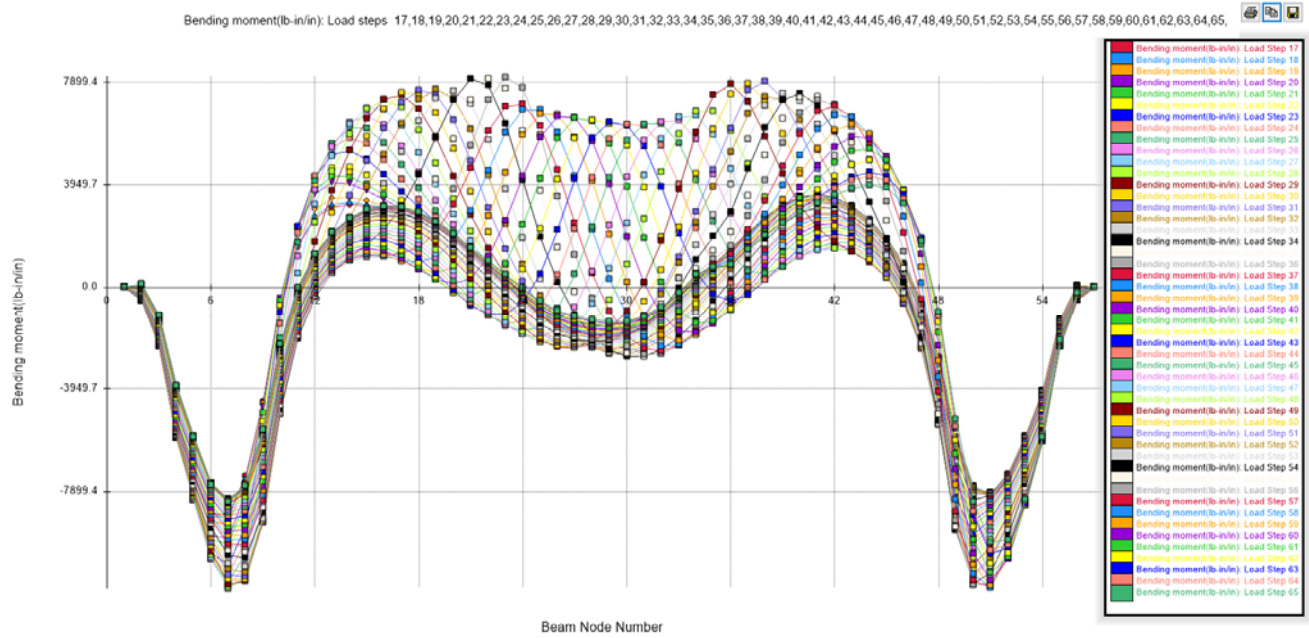


Figure 37 – M7C1 – CANDE bending moment envelope - live load steps – load steps 17-65 (2 axle Tandem ,25 kip/axle) (with pavement)

Appendix D – 2D Analysis Backup

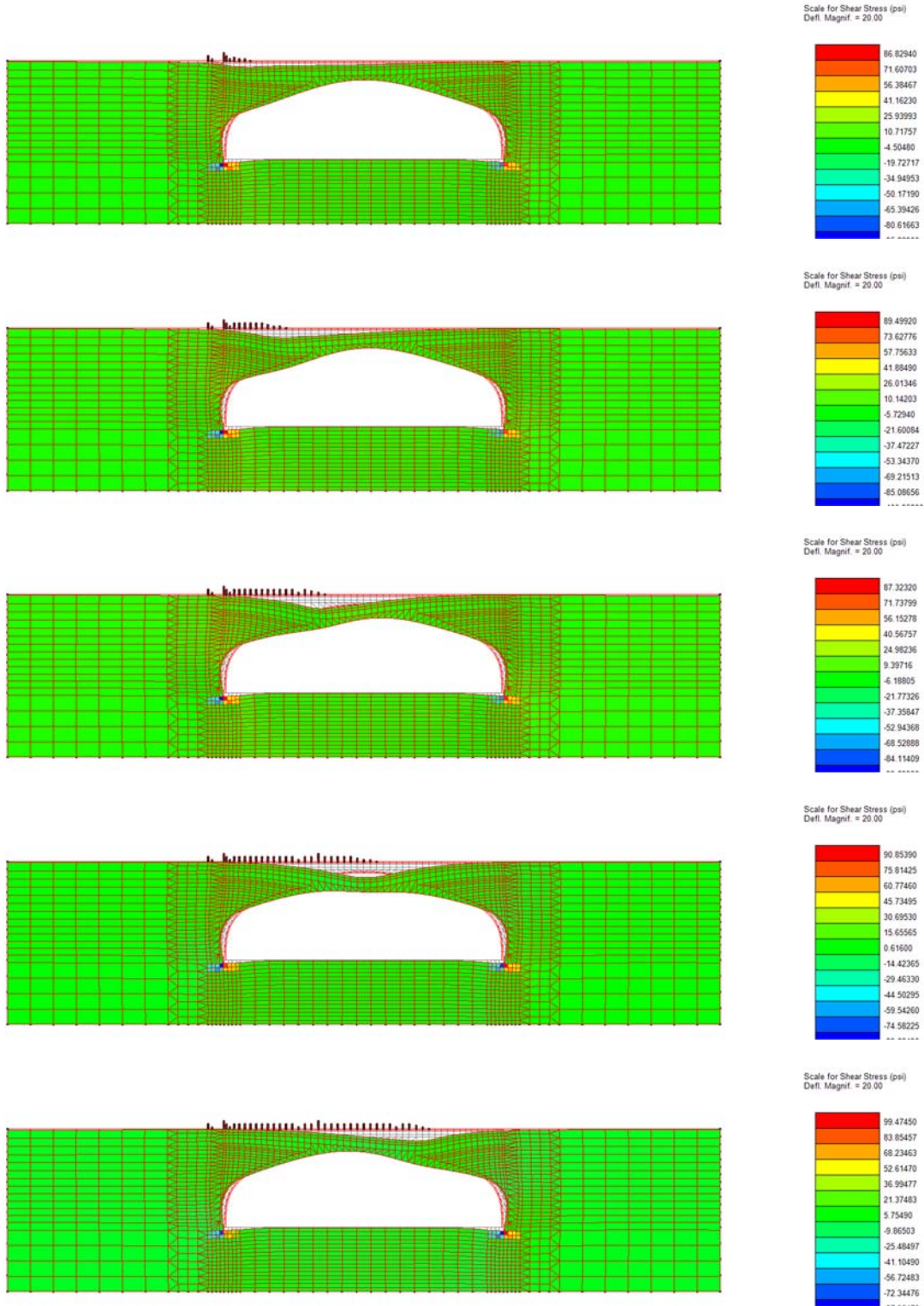


Figure 38 – M7C1 – CANDE Shear stress and deflection as Tandem vehicle moves across the structure (with pavement, E=200,000 psi) (20X magnified)

MEMORANDUM

To: Chad Clancy & Tom Murphy, Modjeski and Masters, Mechanicsburg, PA

From: Reza Baie, Summit Engineering Group, Littleton, CO

RE: Project: NHCRP 15-54
Update on Lusas Modeling Progress

Progress on numerical modeling of culverts using LUSAS software is reported herein. This progress report includes a general description of each culvert, geometry, and material properties. Assumptions are listed and analysis method is described. Finally, results of nonlinear analysis under live load is presented.

MODEL 1- CANDIDATE 1 (M1C1)

Model 1 represents a prototype of reinforced concrete box single-cell culverts. Of three proposed candidates for Model 1 (per Quarterly Progress Report submitted on April 1, 2016), Candidate 1 is selected for this category.

Geometry

Geometry and layout of Model 1 Candidate 1 (M1C1) is presented in the Quarterly Progress Report and is presented here as Appendix A. Figure 1 (a) presents the section of the culvert and the equivalent geometry that is modeled in Lusas. The thickness of the top flange and side wall elements is set to the actual thickness of the members. Figure 1 (b) depicts the assigned thickness of the corner elements at the chamfered sections of the concrete box culvert.

The Lusas model includes the entire length of the culvert. As shown in Figure 1 (a), the depth of model extends to 28'-11". Laterally, the geometry extends to 45' on each side. Therefore, the cross section of model is 90'x28'-11" and the length is 31'.

Material Properties

The linear material properties of the culvert are generated based on AASHTO LRFD Bridge Design Specifications for compressive strength of $f'_c = 5$ ksi; modulus of elasticity (E) = 4074 ksi, Poisson's ratio (ν) = 0.2, unit weight = 150 pcf, and coefficient of thermal expansion (α) = 10.8×10^{-6} 1/C.

Overlay and pavement is defined as a linear material with modulus of elasticity (E) = 4000 ksi, Poisson's ratio (ν) = 0.35, and unit weight = 140 pcf.

Table 1 presents the material properties of in-situ soil and backfill. The in-situ soil is defined as an elastic material, while the nonlinear material properties are considered for backfill, varying with depth. The values in Table 1 are adopted from previous study by McGrath et al. (2005).

Mesh

Quadrilateral quadratic thick shell elements are used to model the culvert. The thick shell elements are used for the culvert to incorporate the shear and bending of the culvert.

Hexahedral quadratic solid elements are used to model the pavement (overlay), in-situ soil, and backfill. The mesh size around the culverts and in backfill is 1'-6" and expands to 6' at the boundaries. The mesh size along the length of culvert varies between 6' at the edges to 1'-6" at the center.

Boundary Condition

At the end of the in-situ soil medium, perpendicular restraints are used for each boundary surface, i.e. lateral restraints at vertical faces and vertical restraints at the bottom of the in-situ soil.

“Tied Mesh Constraints” are assigned between the culvert and soil as well as the culvert and overlay to assure deformation compatibility. This option assures compatible deformation of adjacent shell elements and solid elements. No contact element or interaction properties are assigned.

Load Cases

Gravity is applied as a body force. Soil pressure is considered using vertical and lateral pressure (to provide in-situ conditions with close to zero deflections under soil self-weight).

Live Load: “Wheel load” is modeled as a discrete patch load over a 10”x20” area. A load case with single axle load, and a load case with standard HL-93 truck moving load is applied to model. The truck load is moved across the culvert to capture the critical loading condition. The live load will be updated when the wheel load of the actual truck that is used in the experiment is determined.

Results

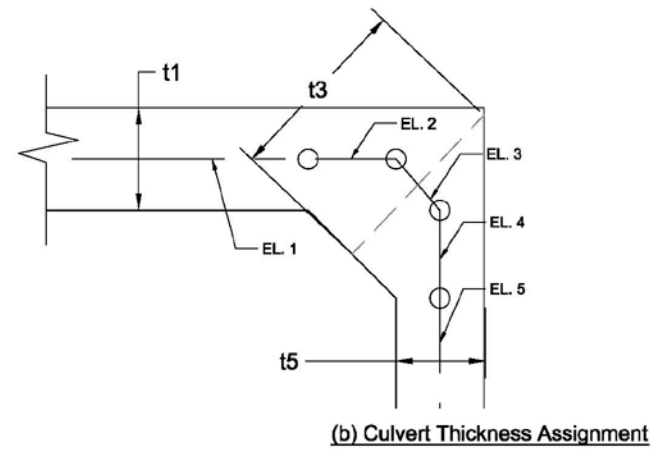
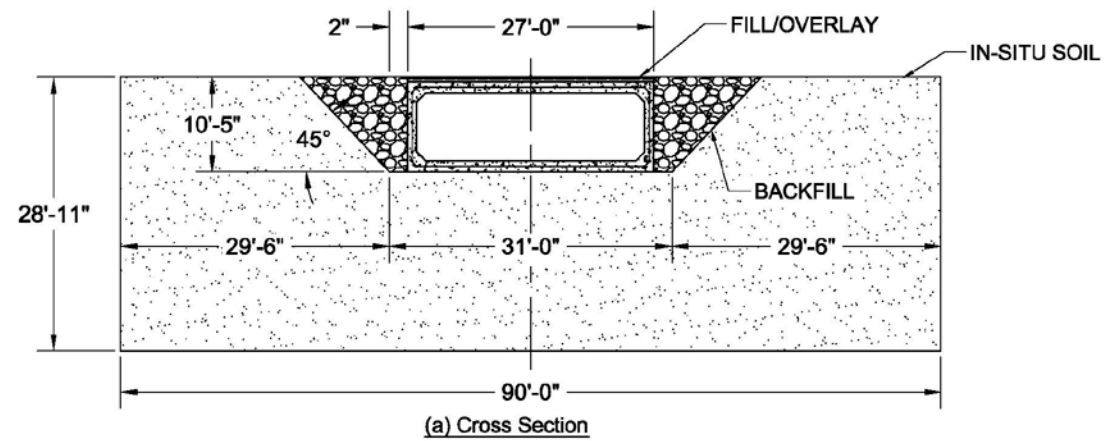
Figures 2 to 18 present the behavior of M1C1 in terms of displacement, strains and stresses under axle load at center of the culvert. Because for nonlinear analysis, all loads must be applied sequentially, gravity and dead loads are applied first, then live load is applied and the final results are under both dead load and live load. Given that for experimental study, only the effect of live load is measured, a load combination is defined in Lusas that removes the effect of dead load by subtracting the results of “dead load analysis” from the results after application of live load.

It should be noted that maximum and minimum envelopes of results under moving loads are available, however, given that Lusas develops two separate envelopes for maximum and minimum, contour presentation may become misleading, unless both envelopes are compared side by side. This is especially important when the dead load effects (constant) are being deduced from the total “dead + live load” results. Results of envelop results of moving loads will be presented later where a specific entity or stage of loading is determined.

Table 1. M1C1- Material Properties of Backfill and In-Situ Soil

Properties	Backfill: 0-1 ft	Backfill: 1-6 ft	Backfill: 6-11 ft	In-Situ Soil
Modulus of Elasticity, E (ksf)	230.4	576.0	864.0	864.0
Poisson's Ratio (v)	0.4	0.29	0.24	0.25
Unit Weight (pcf)	121	121	121	127
Initial Cohesion (psf)	0.000144	0.000144	0.000144	-
Initial Friction Angle	40	40	40	-
Final Friction Angle	40	40	40	-
Dilation Angle	10	10	10	-
Cohesion Hardening (psf)	0	0	0	-
Limiting Plastic Strain	0.001	0.001	0.001	-

Appendix E - 3D Modeling Backup

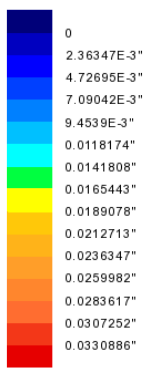


Thickness of Culvert Shell Elements	
Element #	Thickness
EL. 1	t_1 (1'-2")
EL. 2	$\frac{1}{2}[t_1+t_3]$ (1'-8")
EL. 3	t_3 (2'-2")
EL. 4	$\frac{1}{2}[t_3+t_5]$ (1'-7")
EL. 5	t_5 (1'-0")

Figure 1. M1C1- Geometry and Culvert Thickness Assignment

Appendix E - 3D Modeling Backup

Axle 32-32
Entity: Displacement
Component: RSLT (Units: ft)



Maximum 0.0354521" at node 10429
Minimum 0 at node 1

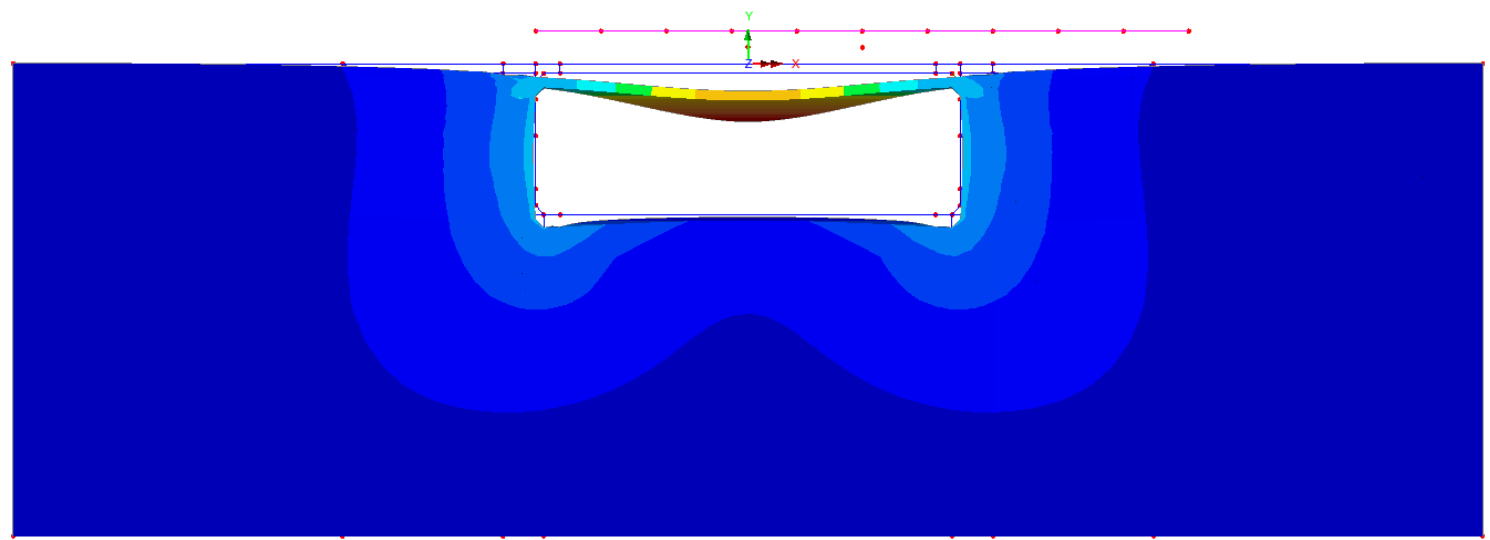


Figure 2. M1C1- Resultant Displacement of Solid Elements – 32 k Axle at Center of Culvert

Appendix E - 3D Modeling Backup

Axle 32-32
Entity: Displacement
Component: DY (Units: ft)

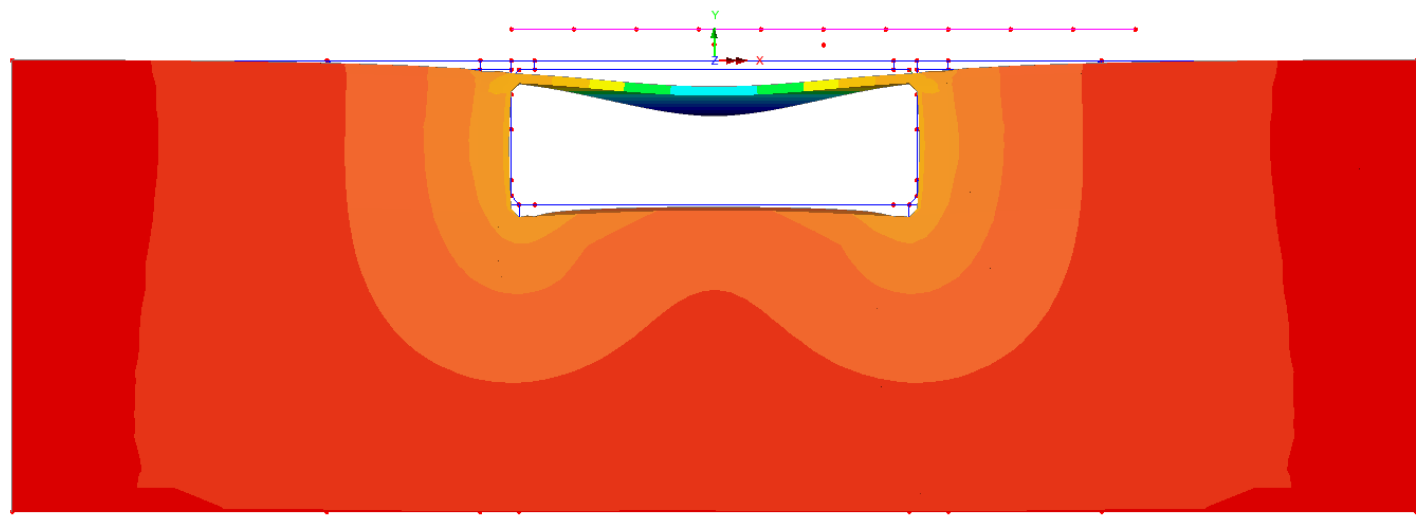
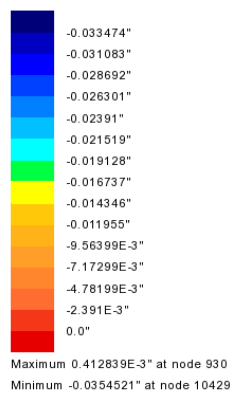
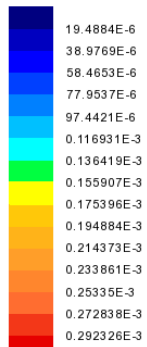


Figure 3. M1C1- Vertical Displacement of Solid Elements - 32 k Axle at Center of Culvert

Appendix E - 3D Modeling Backup

Axle 32-32
Entity: Strain - Solids
Component: EE



Maximum 0.292446E-3 at node 1742
Minimum 0.119457E-6 at node 19469

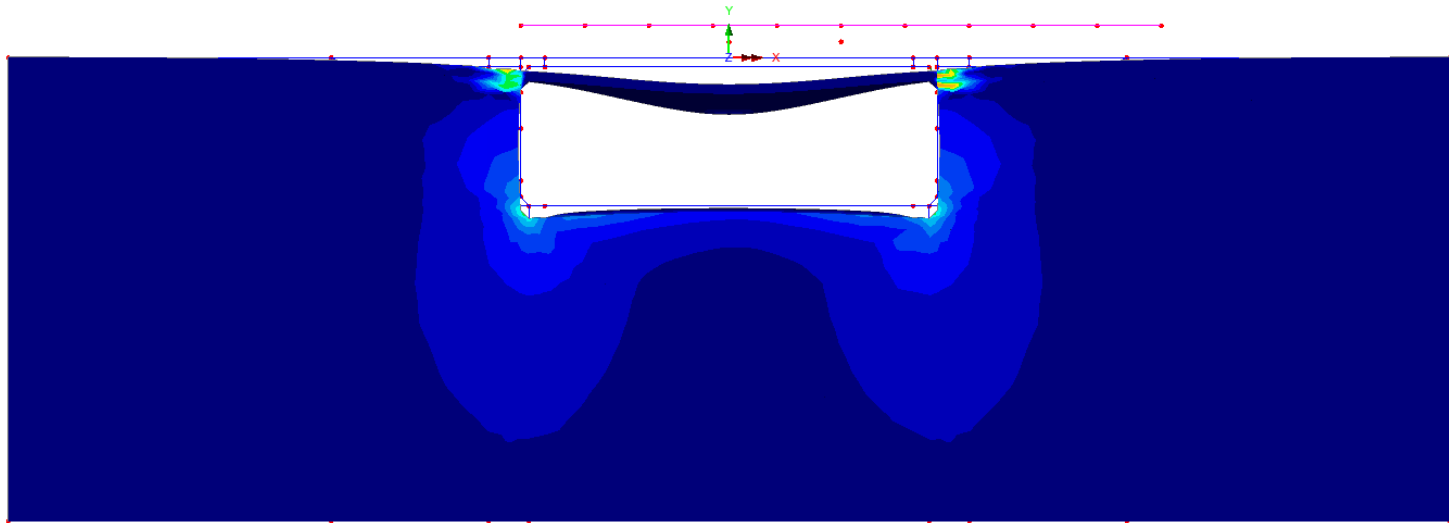


Figure 4. M1C1- Von Mises Strain of Solid Elements- 32 k Axle at Center of Culvert

Appendix E - 3D Modeling Backup

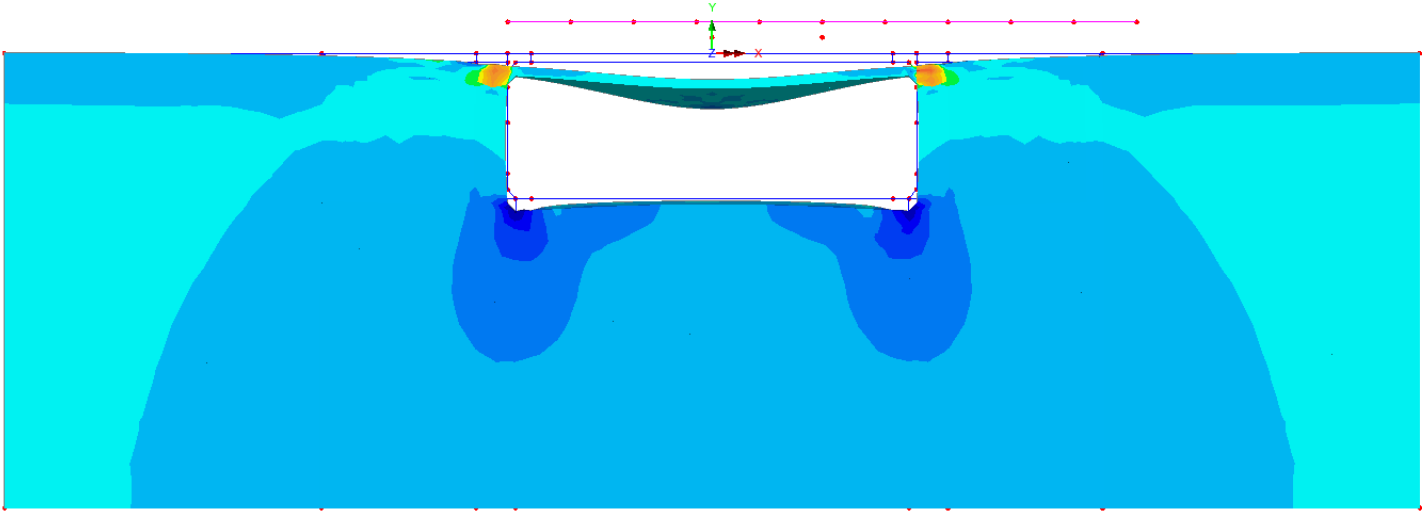
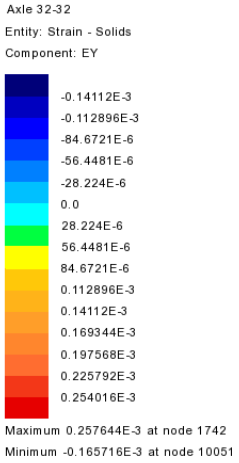


Figure 5. M1C1- Vertical Strain (EV) of Solid Elements- 32 k Axle at Center of Culvert

Appendix E - 3D Modeling Backup

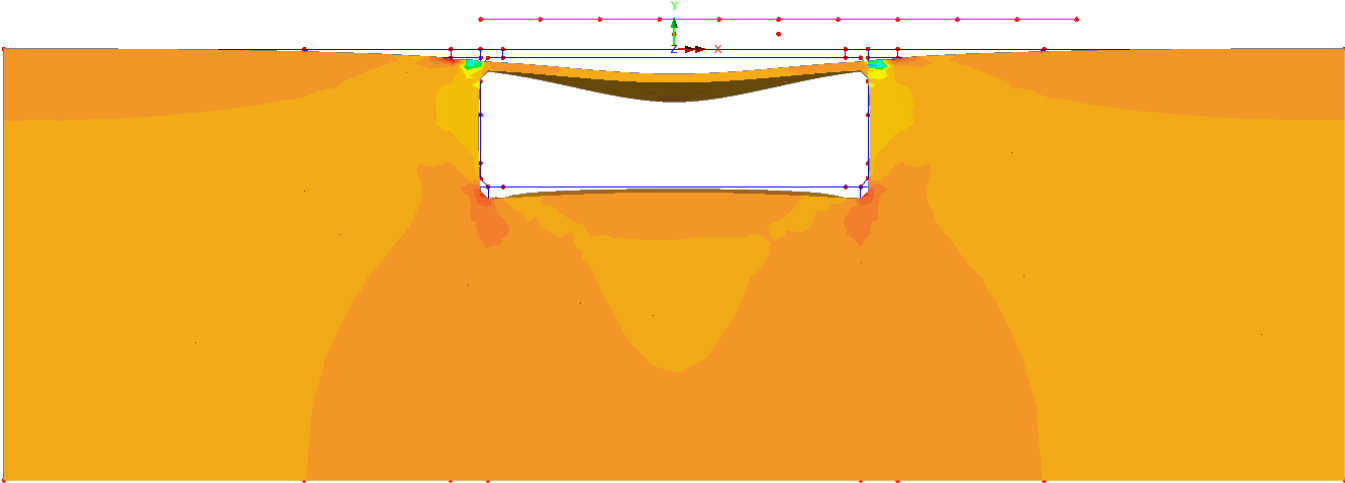


Figure 6. M1C1- Horizontal Strain (EX) of Solid Elements- 32 k Axle at Center of Culvert

Appendix E - 3D Modeling Backup

Axle 32-32
Entity: Stress - Solids
Component: SE (Units: kip/ft²)

0.179931
0.359863
0.539794
0.719726
0.899657
1.07959
1.25952
1.43945
1.61938
1.79931
1.97925
2.15918
2.33911
2.51904
2.69897

Maximum 2.6991 at node 6712
Minimum 0.123853E-3 at node 19469

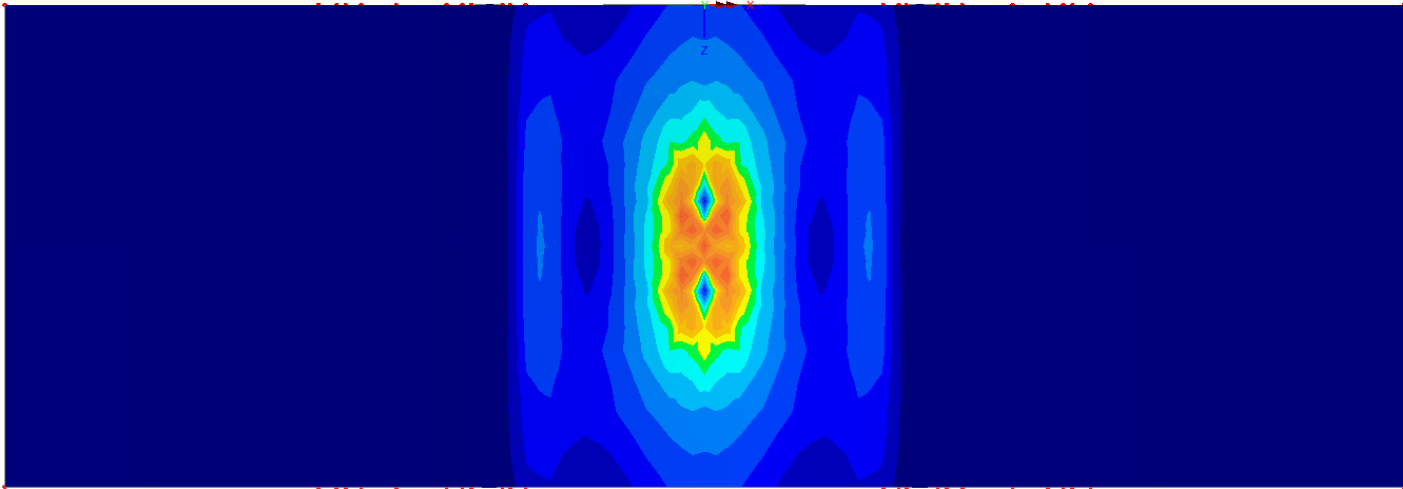
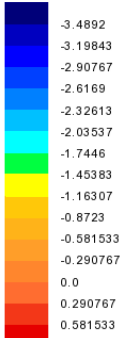


Figure 7. M1C1- Von Mises Stress of Solid Elements- 32 k Axle at Center of Culvert

Appendix E - 3D Modeling Backup

Axle 32-32
Entity: Stress - Solids
Component: SY (Units: kip/ft²)



Maximum 0.724568 at node 10554
Minimum -3.63693 at node 6834

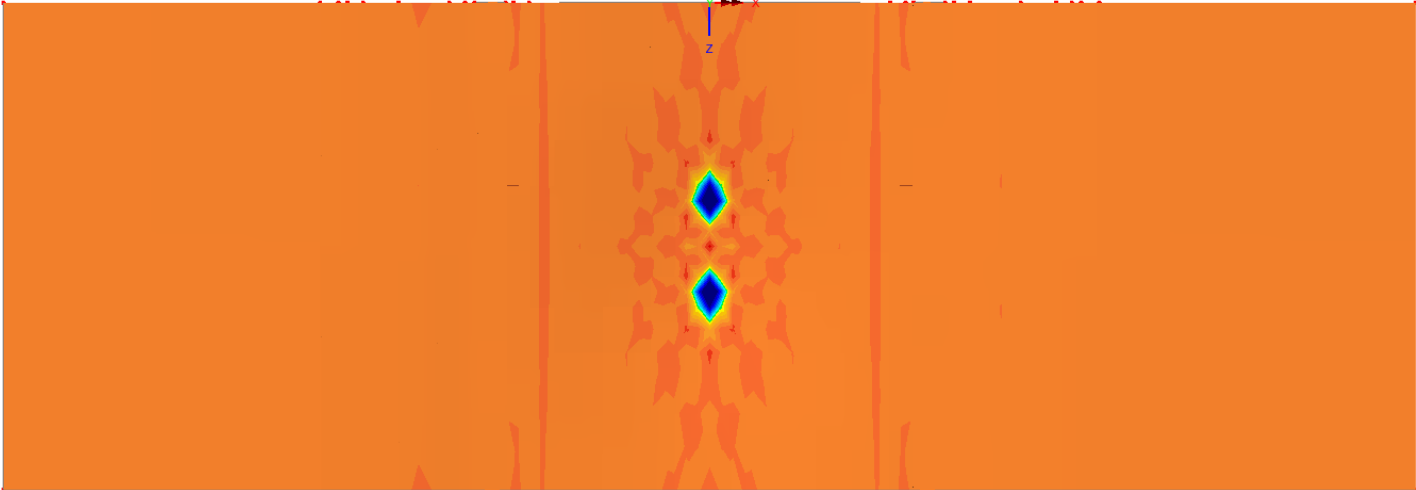


Figure 8. M1C1- Vertical Stress (SY) of Solid Elements- 32 k Axle at Center of Culvert

Appendix E - 3D Modeling Backup

Axle 32-32
Entity: Stress - Solids
Component: SX (Units: kip/ft²)

Color	Value
Dark Blue	-3.92425
Blue	-3.59723
Light Blue	-3.27021
Cyan	-2.94319
Green	-2.61617
Yellow-Green	-2.28914
Yellow	-1.96212
Orange	-1.6351
Light Orange	-1.30808
Light Yellow	-0.981062
Yellow-Orange	-0.654041
Orange	-0.327021
Light Orange	0.0
Red-Orange	0.327021
Red	0.654041

Maximum 0.824653 at node 10568
Minimum -4.08066 at node 7330

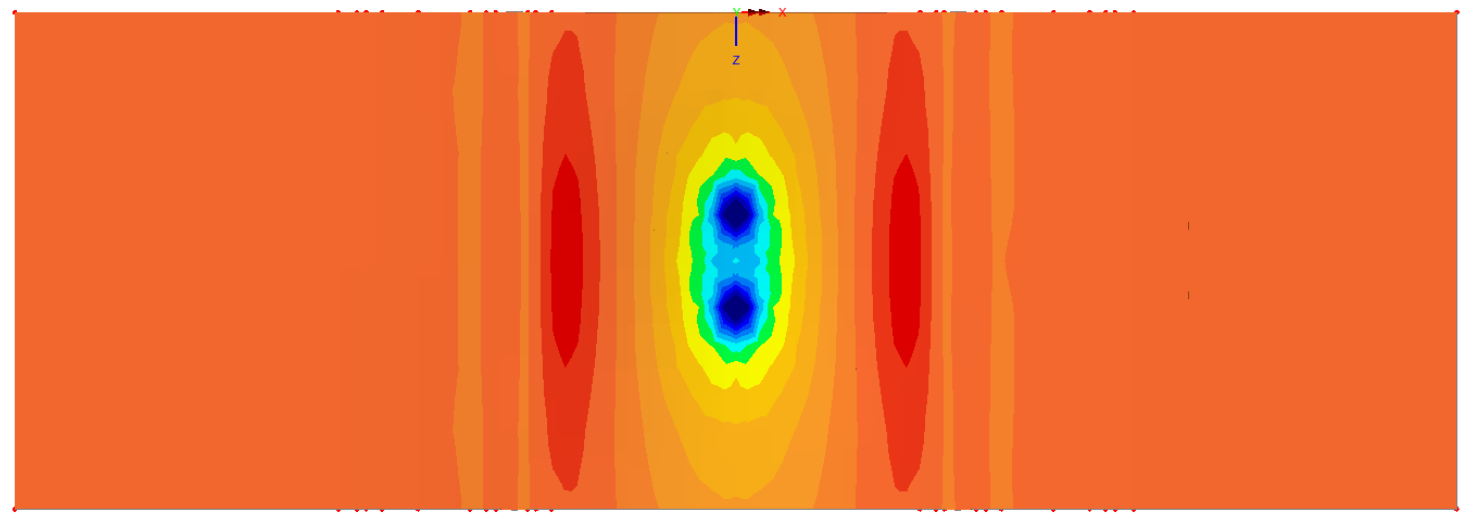


Figure 9. M1C1- Horizontal Stress (SX) of Solid Elements- 32 k Axle at Center of Culvert

Appendix E - 3D Modeling Backup

Axle 32-32
Entity: Displacement
Component: DY (Units: ft)

Dark Blue	-0.0353834"
Blue	-0.0333021"
Light Blue	-0.0312207"
Cyan	-0.0291393"
Green	-0.0270579"
Yellow-Green	-0.0249765"
Yellow	-0.0228952"
Orange	-0.0208138"
Light Orange	-0.0187324"
Orange	-0.016651"
Light Orange	-0.0145697"
Orange	-0.0124883"
Light Orange	-0.0104069"
Red-Orange	-8.32551E-3"
Red	-6.24414E-3"

Maximum -4.23143E-3" at node 766
Minimum -0.0354521" at node 10429

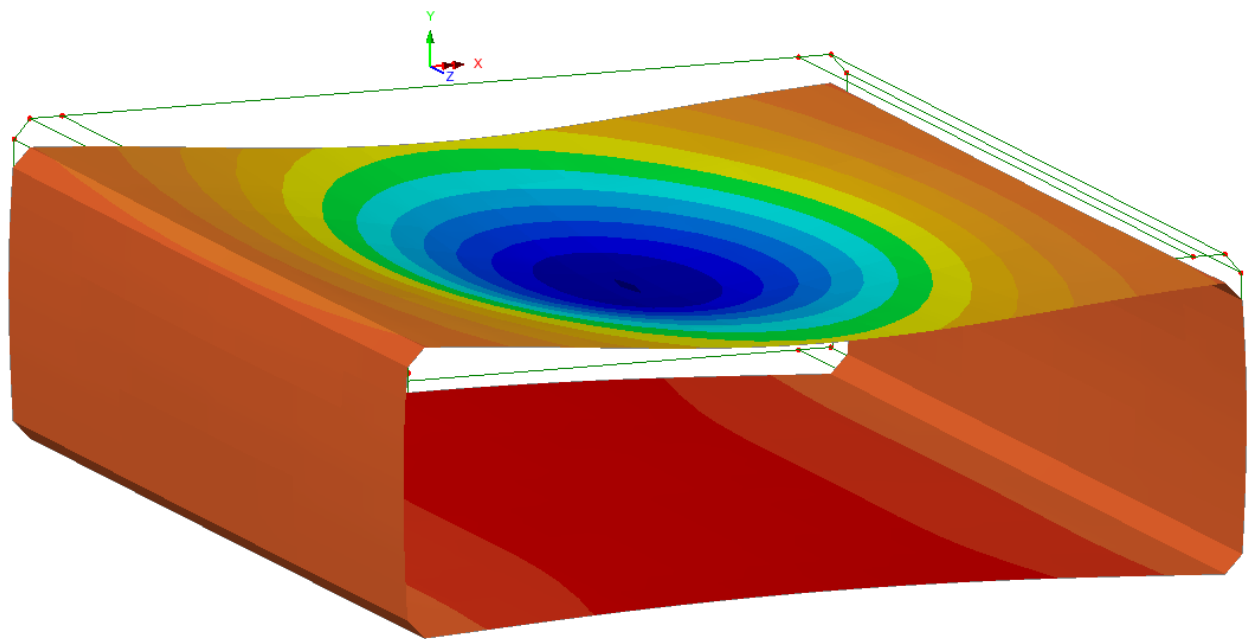


Figure 10. M1C1- Vertical Displacement of Culvert- 32 k Axle at Center of Culvert

Appendix E - 3D Modeling Backup

Axle 32-32
Entity: Strain (top) - Thick Shell
Component: EE

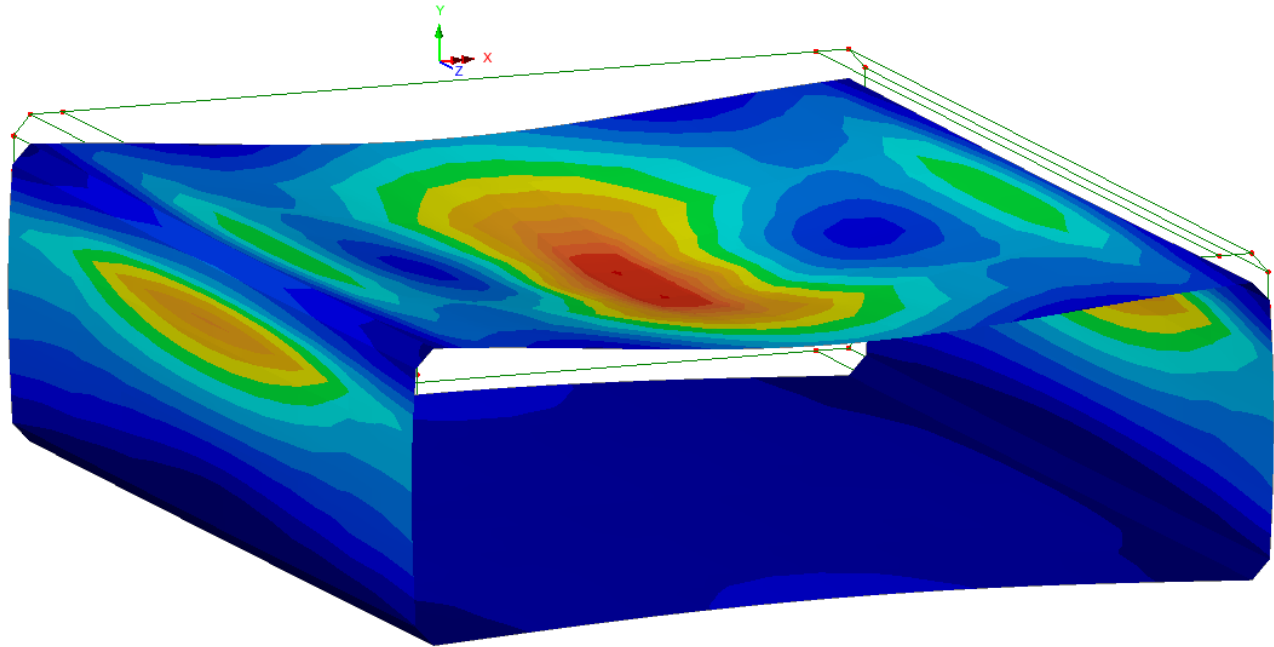
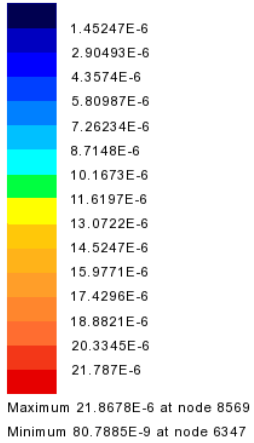
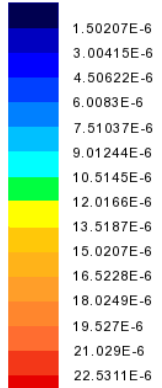


Figure 11. M1C1- Von Mises Strain at Top Fiber in Culvert- 32 k Axle at Center of Culvert

Appendix E - 3D Modeling Backup

Axle 32-32
Entity: Strain (bottom) - Thick Shell
Component: EE



Maximum 22.6139E-6 at node 8569
Minimum 82.7403E-9 at node 6346

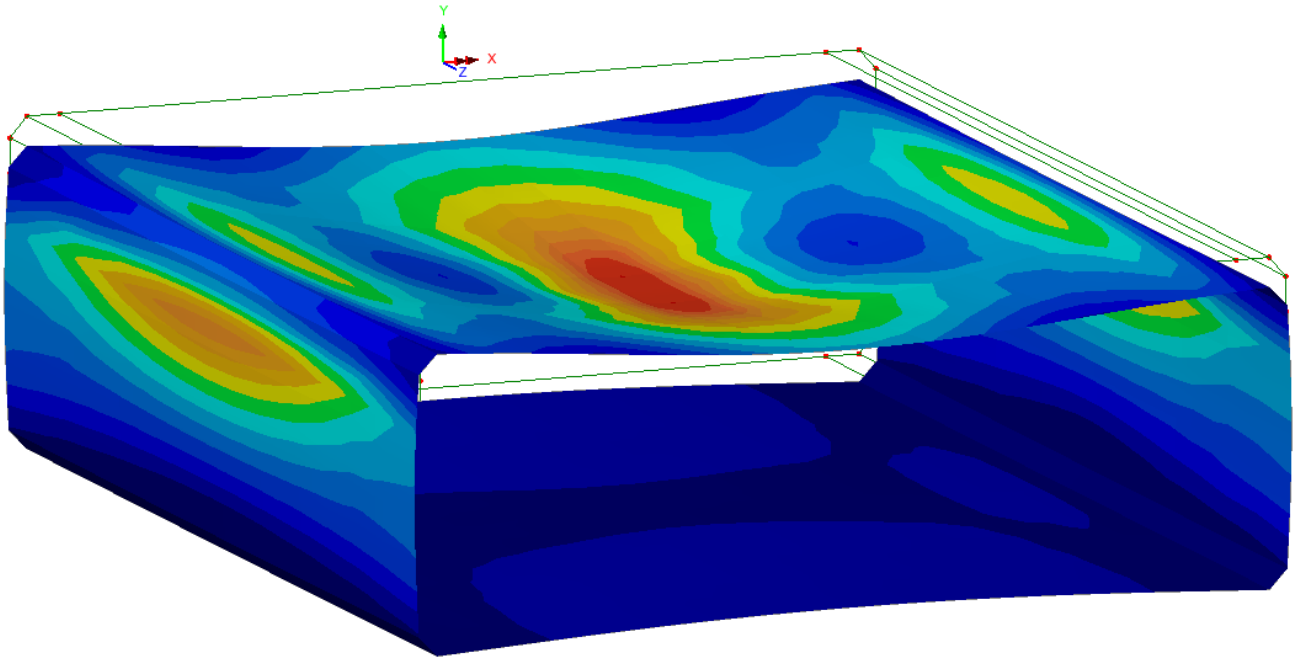


Figure 12. M1C1- Von Mises Strain at Bottom Fiber in Culvert- 32 k Axle at Center of Culvert

Appendix E - 3D Modeling Backup

Axle 32-32
Entity: Strain (top) - Thick Shell
Component: EX

Dark Blue	-35.9292E-6
Blue	-32.3362E-6
Light Blue	-28.7433E-6
Cyan	-25.1504E-6
Green	-21.5575E-6
Yellow-Green	-17.9646E-6
Yellow	-14.3717E-6
Orange	-10.7787E-6
Light Orange	-7.18583E-6
Dark Orange	-3.59292E-6
Red-Orange	0.0
Red	3.59292E-6
Dark Red	7.18583E-6
Light Red	10.7787E-6
Dark Red	14.3717E-6

Maximum 16.3317E-6 at node 10458
Minimum -37.562E-6 at node 8569

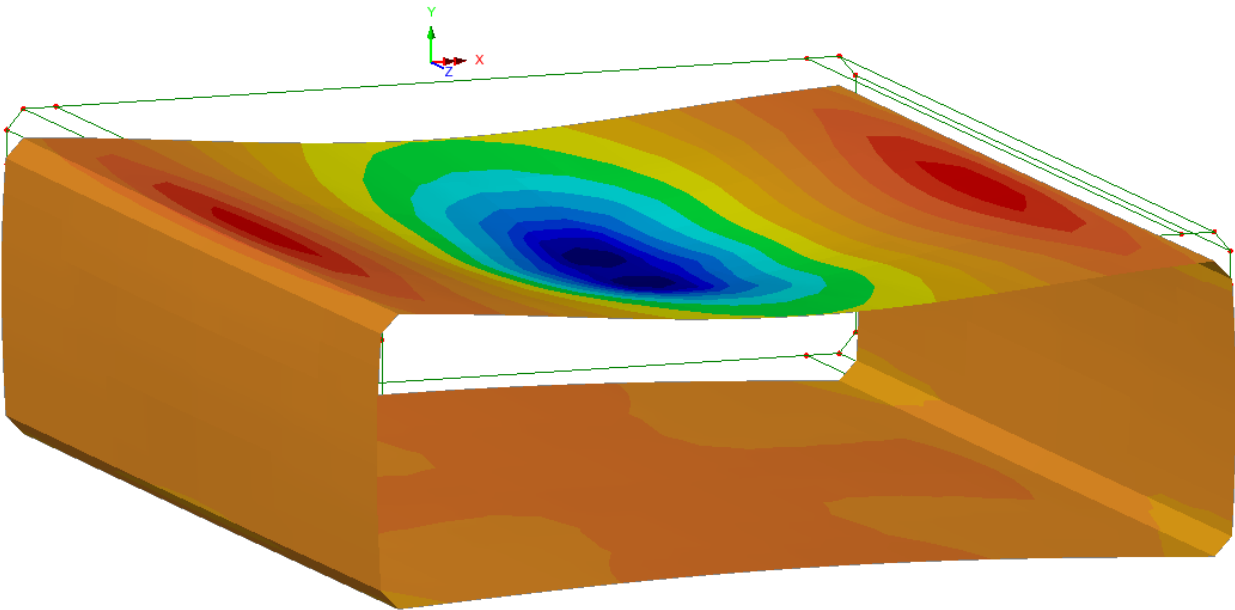


Figure 13. M1C1- Bending Strain at Top Fiber in Culvert- 32 k Axle at Center of Culvert

Appendix E - 3D Modeling Backup

Axle 32-32
Entity: Strain (bottom) - Thick Shell
Component: EX

Dark Blue	-15.4449E-6
Blue	-11.5837E-6
Light Blue	-7.72244E-6
Cyan	-3.86122E-6
Green	0.0
Yellow-Green	3.86122E-6
Yellow	7.72244E-6
Orange	11.5837E-6
Light Orange	15.4449E-6
Orange	19.3061E-6
Red-Orange	23.1673E-6
Red	27.0285E-6
Dark Red	30.8898E-6
Red	34.751E-6
Dark Red	38.6122E-6

Maximum 38.9834E-6 at node 8569
Minimum -18.9349E-6 at node 10458

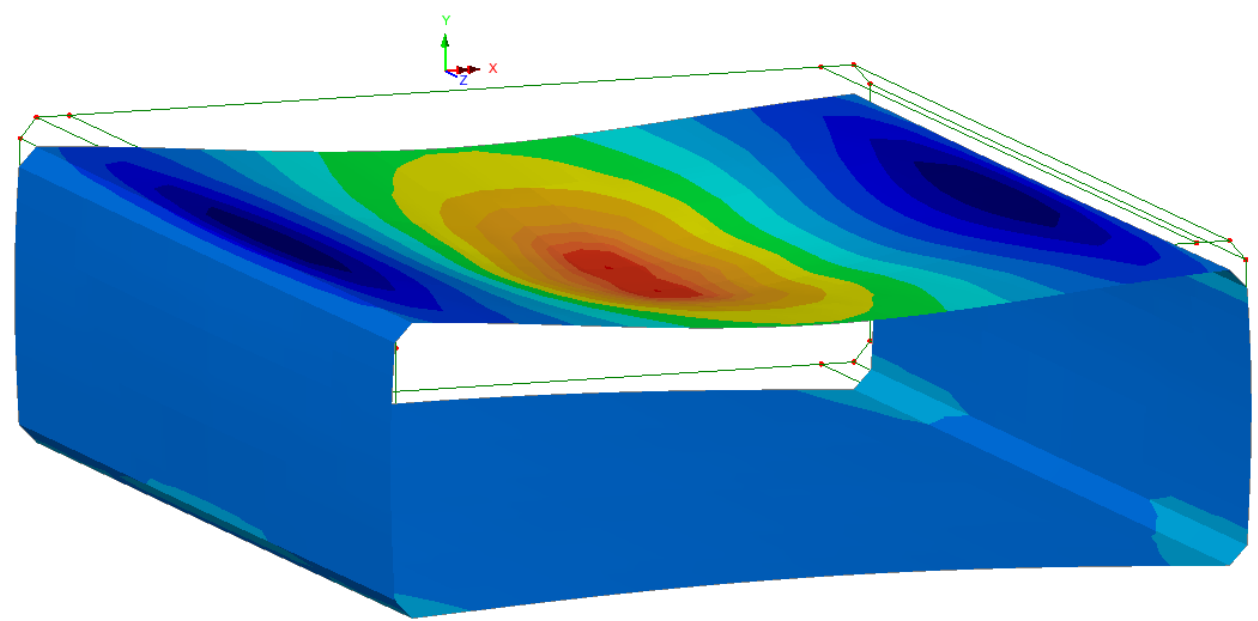


Figure 14. M1C1- Bending Strain at Bottom Fiber in Culvert- 32 k Axle at Center of Culvert

Appendix E - 3D Modeling Backup

Axle 32-32
Entity: Stress (top) - Thick Shell
Component: SE (Units: kip/ft²)

1.42491
2.84982
4.27473
5.69964
7.12456
8.54947
9.97438
11.3993
12.8242
14.2491
15.674
17.0989
18.5238
19.9488
21.3737

Maximum 21.4509 at node 8569
Minimum 0.0772148 at node 5307

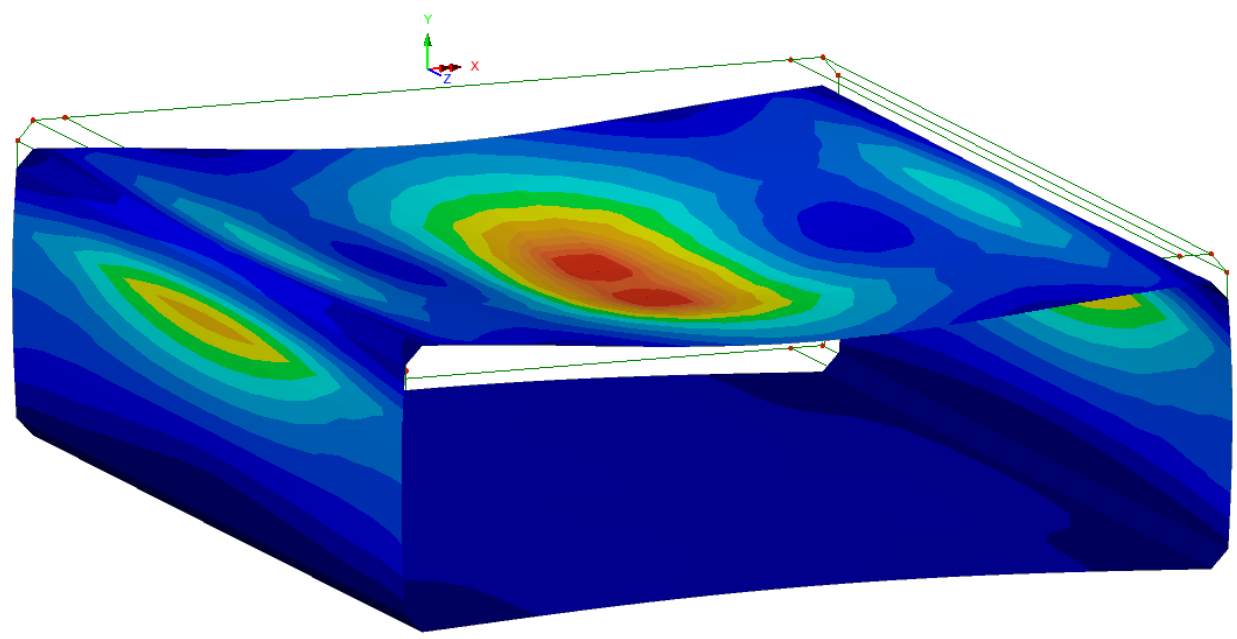


Figure 15. M1C1- Von Mises Stress at Top Fiber in Culvert- 32 k Axle at Center of Culvert

Appendix E - 3D Modeling Backup

Axle 32-32
Entity: Stress (bottom) - Thick Shell
Component: SE (Units: kip/ft²)

1.48934
2.97867
4.46801
5.95735
7.44668
8.93602
10.4254
11.9147
13.404
14.8934
16.3827
17.872
19.3614
20.8507
22.34

Maximum 22.416 at node 8569
Minimum 0.0759751 at node 5306

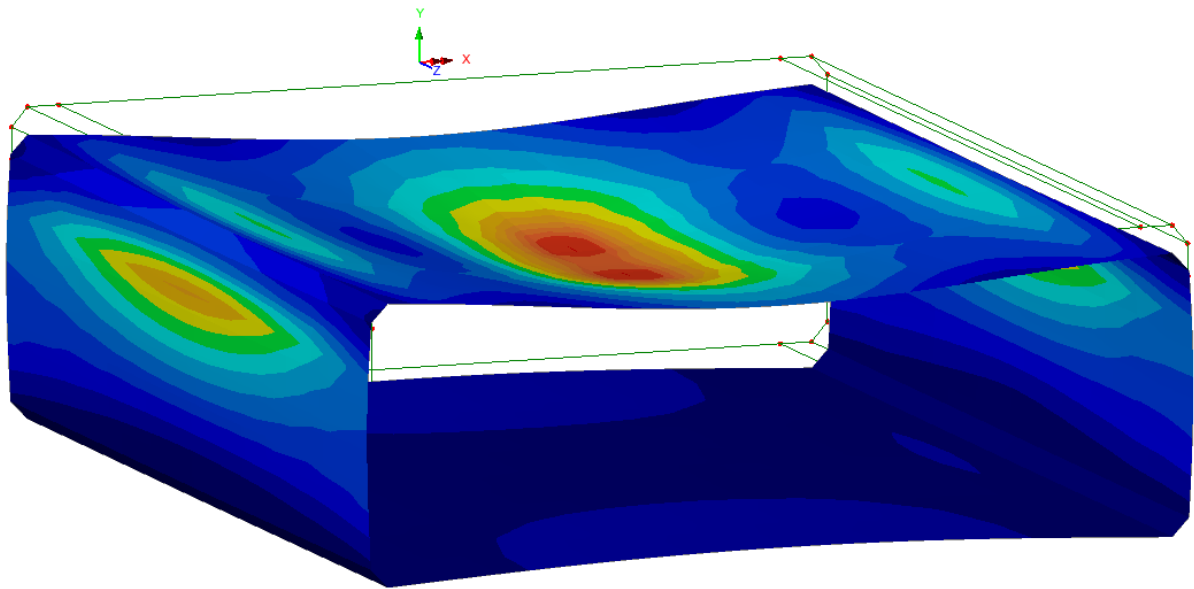


Figure 16. M1C1- Von Mises Stress at Bottom Fiber in Culvert- 32 k Axle at Center of Culvert

Appendix E - 3D Modeling Backup

Axle 32-32
Entity: Stress (top) - Thick Shell
Component: SX (Units: kip/ft²)

Dark Blue	-22.9863
Blue	-20.6877
Light Blue	-18.3891
Cyan	-16.0904
Green	-13.7918
Yellow-Green	-11.4932
Yellow	-9.19454
Orange	-6.8959
Light Orange	-4.59727
Orange	-2.29863
Yellow	0.0
Light Orange	2.29863
Orange	4.59727
Red-Orange	6.8959
Red	9.19454

Maximum 9.74422 at node 10458
Minimum -24.7353 at node 8569

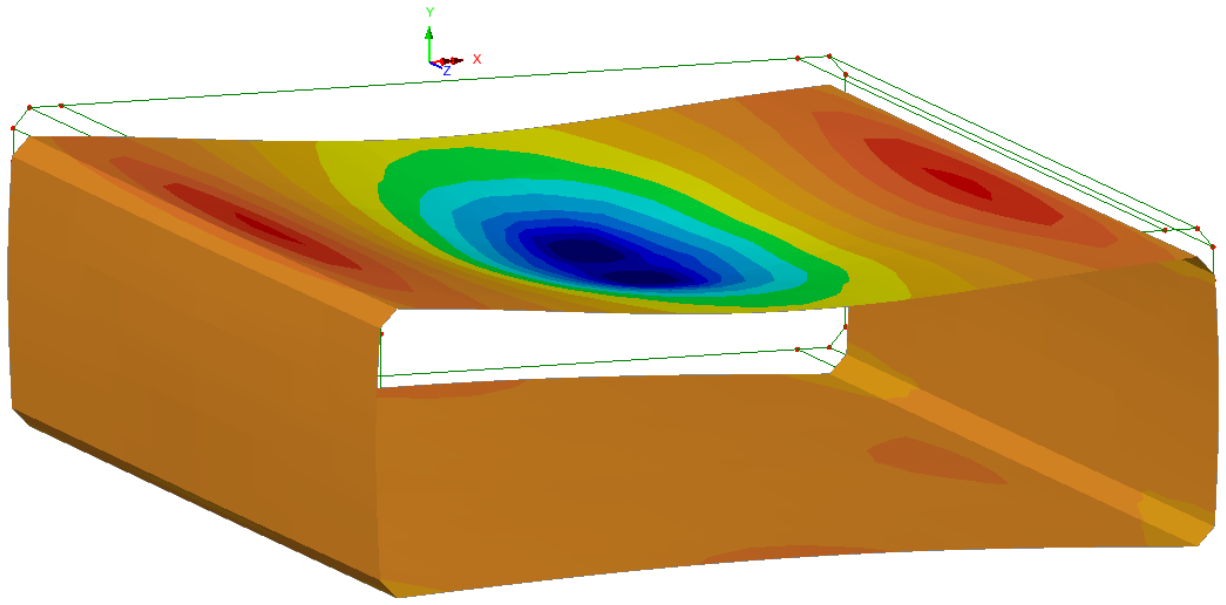


Figure 17. M1C1- Bending Stress at Top Fiber in Culvert- 32 k Axle at Center of Culvert

Appendix E - 3D Modeling Backup

Axle 32-32
Entity: Stress (bottom) - Thick Shell
Component: SX (Units: kip/ft²)

Color	Value
Dark Blue	-9.91578
Blue	-7.43684
Light Blue	-4.95789
Cyan	-2.47895
Green	0.0
Yellow-Green	2.47895
Yellow	4.95789
Orange	7.43684
Red-Orange	9.91578
Red	12.3947
Dark Red	14.8737
Dark Red	17.3526
Dark Red	19.8316
Dark Red	22.3105
Dark Red	24.7895

Maximum 25.8036 at node 8569
Minimum -11.3805 at node 10458

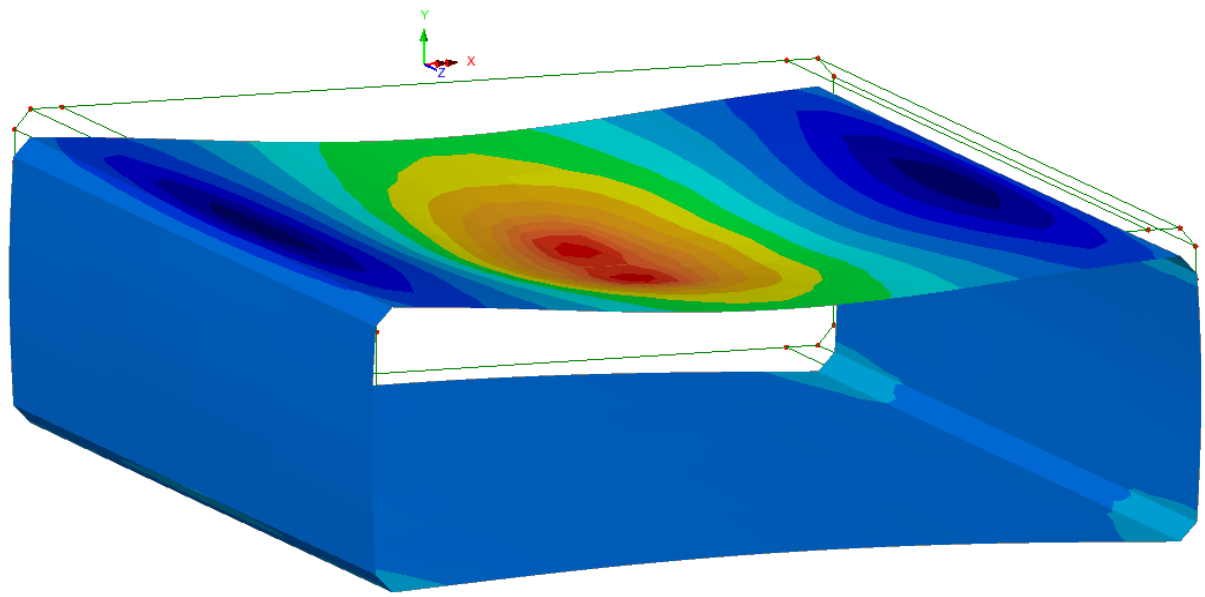


Figure 18. M1C1- Bending Stress at Bottom Fiber in Culvert- 32 k Axle at Center of Culvert

MODEL 2- CANDIDATE 1 (M2C1)

Model 2 represents a prototype of reinforced concrete box multi-cell culverts. Of three proposed candidates for Model 2 (per Quarterly Progress Report submitted on April 1, 2016), Candidate 1 is selected for this category.

Geometry

Geometry and layout of Model 2 Candidate 1 (M2C1) is presented in the Quarterly Progress Report and is presented here as Appendix B. Figure 19 (a) presents the section of the culvert and the equivalent geometry that is modeled in Lusas. The thickness of the top flange and side wall elements is set to the actual thickness of the members. Figure 19 (b) depicts the assigned thickness of the corner elements at the chamfered sections of the concrete box culvert.

The Lusas model includes the entire length of the culvert. As shown in Figure 19 (a), the depth of model extends to 25'-6". Laterally, the geometry extends to 39' on each side. Therefore, the cross section of model is 78'x25'-6" and the length is 31'. Also, the culvert has a 15° skew which is incorporated in the model.

Material Properties

The linear material properties of culvert are generated based on AASHTO LRFD Bridge Design Specifications for compressive strength of $f'_c = 5$ ksi: modulus of elasticity (E) = 4074 ksi, Poisson's ratio (ν) = 0.2, unit weight = 150 pcf, and coefficient of thermal expansion (α) = 10.8×10^{-6} 1/C.

Overlay and pavement is defined as a linear material with modulus of elasticity (E) = 4000 ksi, Poisson's ratio (ν) = 0.35, and unit weight = 140 pcf.

Table 2 presents the material properties of in-situ soil and backfill. In-situ soil is defined as an elastic material, while nonlinear material properties are considered for backfill, varying with depth. The values in Table 2 are adopted from previous study by McGrath et al. (2005).

Mesh

Quadrilateral quadratic thick shell elements are used to model the culvert. The thick shell elements are used for the culvert to incorporate the shear and bending of the culvert.

Hexahedral quadratic solid elements are used to model the pavement (overlay), in-situ soil, and backfill. The mesh size around the culverts and in backfill is 1'-6" and expands to 6' at the boundaries. The mesh along the length of culvert varies between 6' at edges to 1'-6" at center.

Boundary Condition

At the end of the in-situ soil medium, perpendicular restraints are used for each boundary surface, i.e. lateral restraints at vertical faces and vertical restraints at the bottom of the in-situ soil.

"Tied Mesh Constraints" are assigned between the culvert and soil as well as the culvert and overlay to assure deformation compatibility. This option assures compatible deformation of adjacent shell elements and solid elements. No contact element or interaction properties are assigned.

Load Cases

Gravity is applied as a body force. Soil pressure is considered using vertical and lateral pressure (to provide in-situ conditions with close to zero deflections under soil self-weight).

Live Load: Wheel load is modeled as a discrete patch load over a 10"x20" area. A load case with single axle load, and a load case with standard HL-93 truck moving load is applied to model. The truck load is moved across the culvert to capture the critical loading condition. The live load will be updated when the wheel load of the actual truck that is used in the experiment is determined.

Results

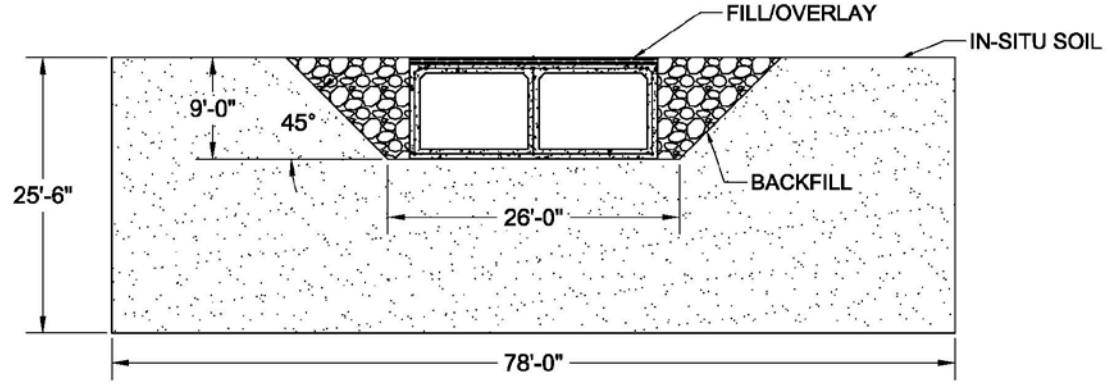
Figures 20 to 36 present the behavior of M2C1 in terms of displacement, strains and stresses under axle load at center of the culvert. Due to the skew, the axle loads are positioned so that the center of each axle passes through the centerline of culvert. Figures 37 to 53 presents the behavior of M2C1 when axle loads are applied at center of the left cell only. Because for nonlinear analysis, all loads must be applied sequentially, gravity and dead loads are applied first, then live load is applied and the final results are under both dead load and live load. Given that for experimental study, only the effect of live load is measured, a load combination is defined in Lusas that removes the effect of dead load by subtracting the results of “dead load analysis” from the results after application of live load.

It should be noted that maximum and minimum envelopes of results under moving loads are available, however, given that Lusas develops two separate envelopes for maximum and minimum, contour presentation may become misleading, unless both envelopes are compared side by side. This is especially important when the dead load effects (constant) are being deduced from the total “dead + live load” results. Results of envelop results of moving loads will be presented later where a specific entity or stage of loading is determined.

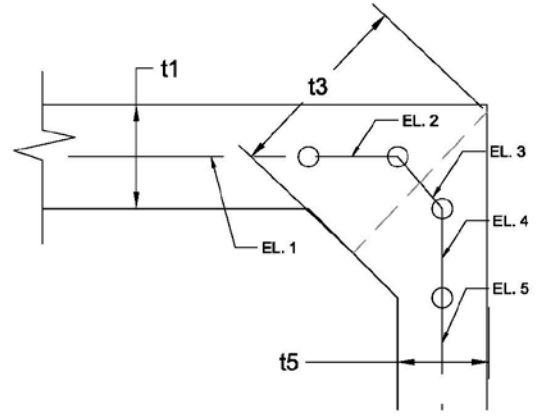
Table 2. M2C1- Material Properties of Backfill and In-Situ Soil

Properties	Backfill: 0-1 ft	Backfill: 1-6 ft	Backfill: 6-11 ft	In-Situ Soil
Modulus of Elasticity, E (ksf)	230.4	576.0	864.0	864.0
Poisson's Ratio (ν)	0.4	0.29	0.24	0.25
Unit Weight (pcf)	121	121	121	127
Initial Cohesion (psf)	0.000144	0.000144	0.000144	-
Initial Friction Angle	40	40	40	-
Final Friction Angle	40	40	40	-
Dilation Angle	10	10	10	-
Cohesion Hardening (psf)	0	0	0	-
Limiting Plastic Strain	0.001	0.001	0.001	-

Appendix E - 3D Modeling Backup



(a) Cross Section



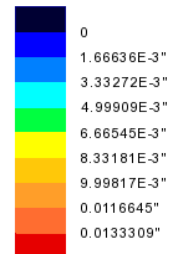
(b) Culvert Thickness Assignment

Thickness of Culvert Shell Elements	
Element #	Thickness
EL. 1	t1 (10½")
EL. 2	½[t1+t3] (1'-2¾")
EL. 3	t3 (1'-7")
EL. 4	½[t3+t5] (1'-3½")
EL. 5	t5 (1'-0")

Figure 19. M2C1- Geometry and Culvert Thickness Assignment

Appendix E - 3D Modeling Backup

Axle over center
Entity: Displacement
Component: RSLT (Units: ft)



Maximum 0.0149973" at node 22682
Minimum 0 at node 1

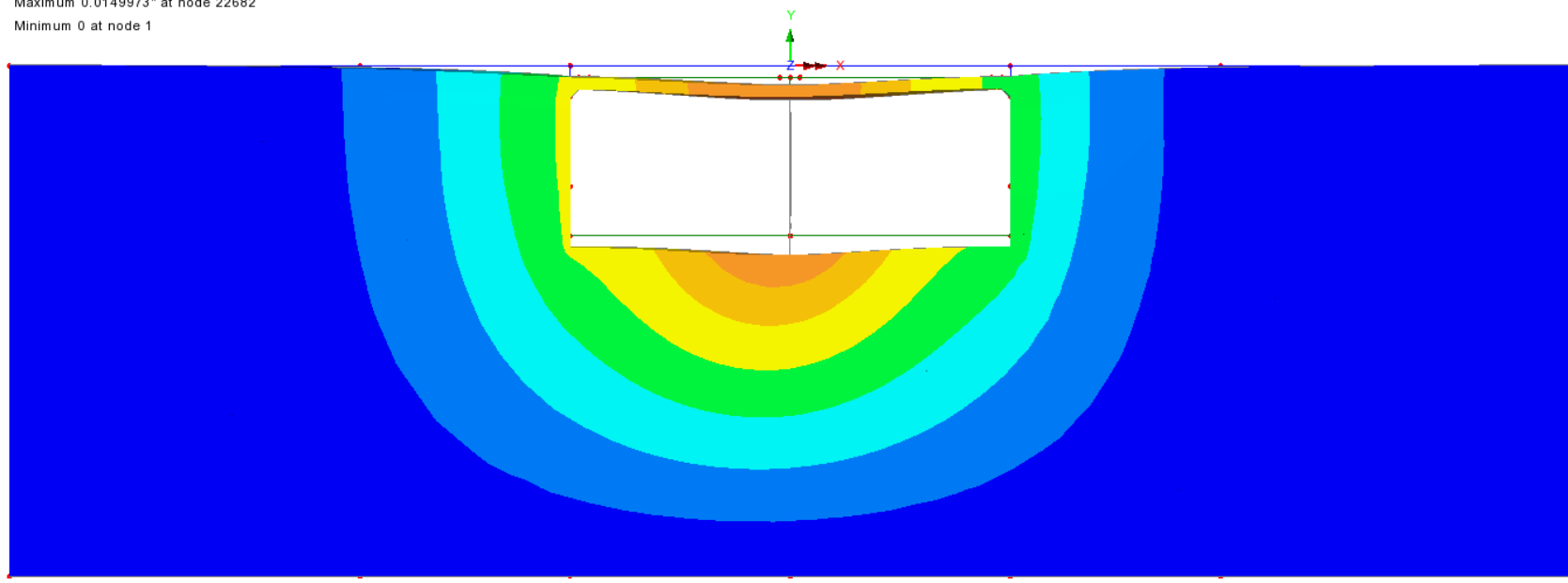


Figure 20. M2C1- Resultant Displacement of Solid Elements – 2 Lane 32 k Axle at Center of Culvert

Appendix E - 3D Modeling Backup

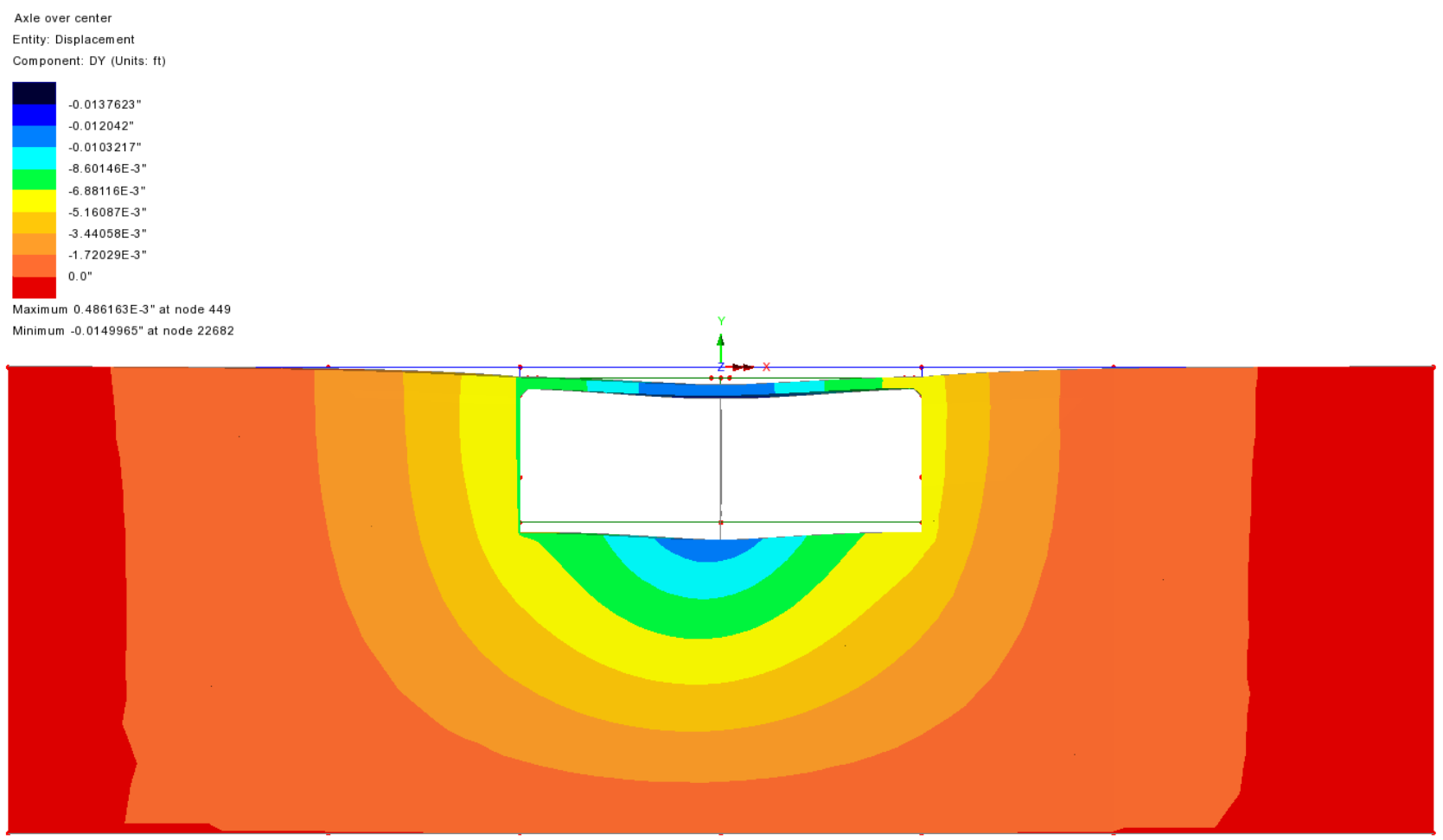
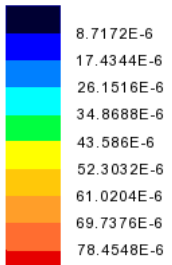


Figure 21. M2C1- Vertical Displacement of Solid Elements - 2 Lane 32 k Axle at Center of Culvert

Appendix E - 3D Modeling Backup

Axle over center
Entity: Strain - Solids
Component: EE



Maximum 78.6354E-6 at node 24058
Minimum 0.18052E-6 at node 503

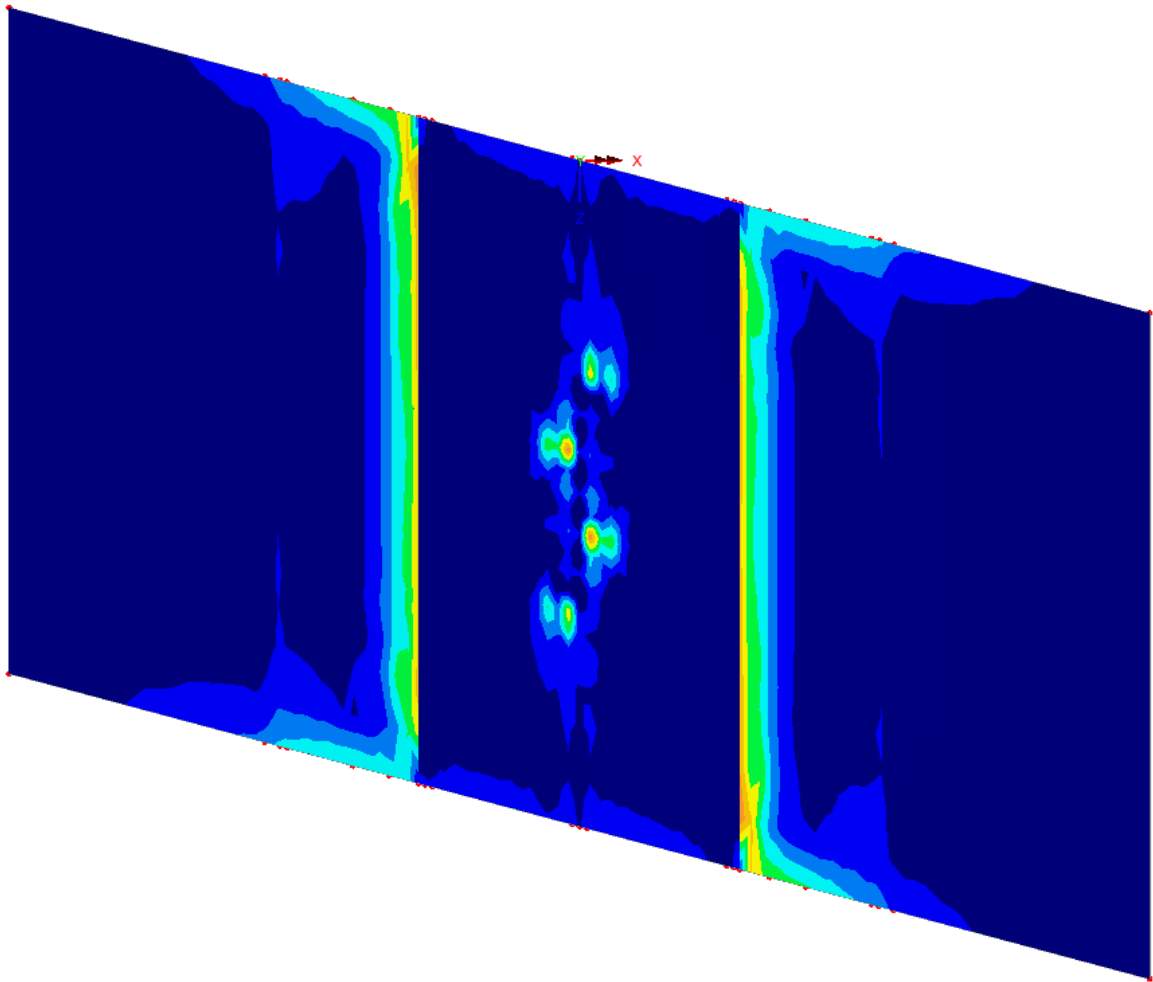


Figure 22. M2C1- Von Mises Strain of Solid Elements- 2 Lane 32 k Axle at Center of Culvert

Appendix E - 3D Modeling Backup

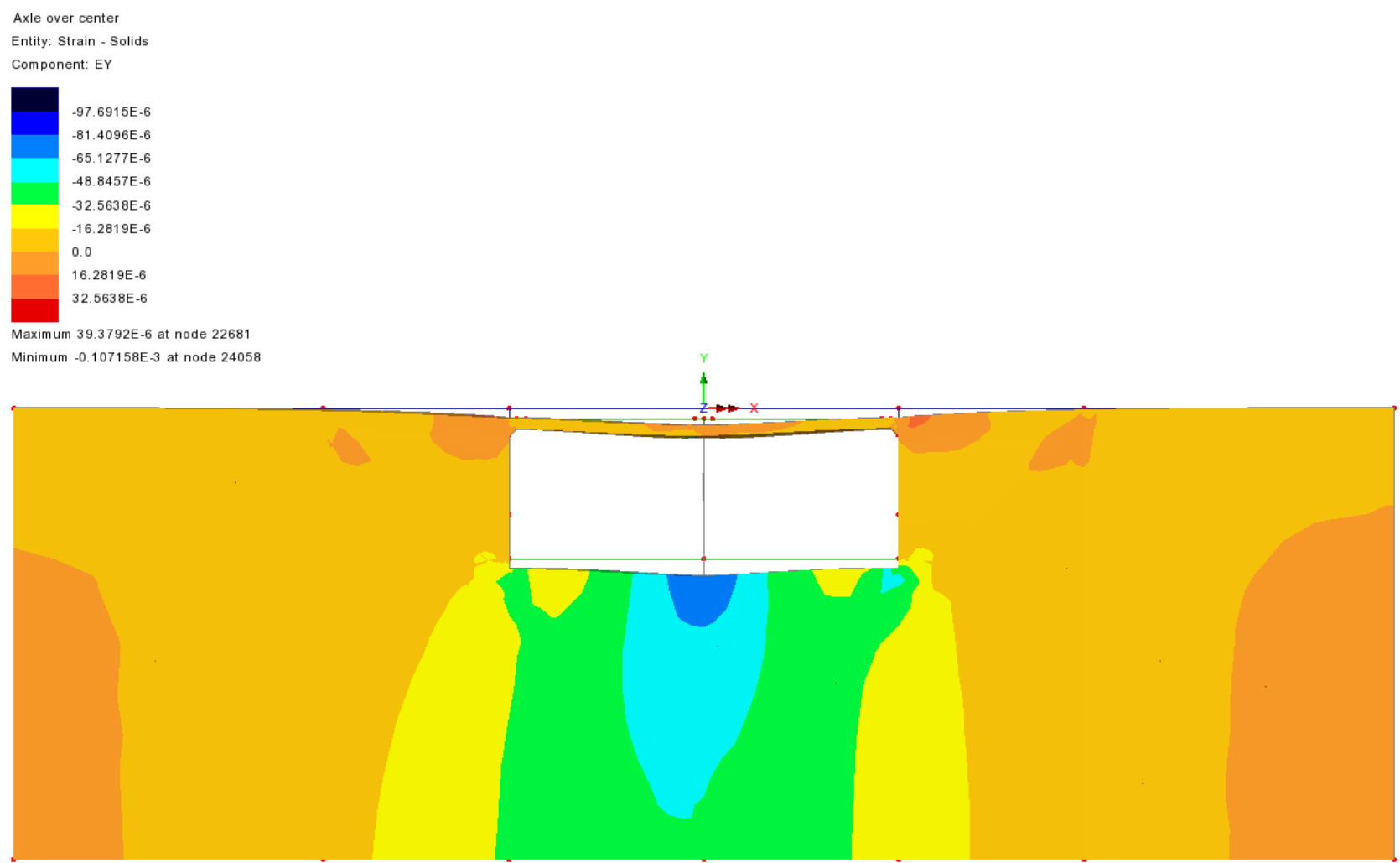
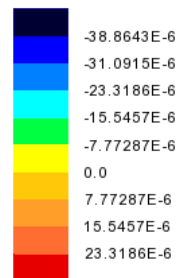


Figure 23. M2C1- Vertical Strain (EV) of Solid Elements- 2 Lane 32 k Axle at Center of Culvert

Appendix E - 3D Modeling Backup

Axle over center
Entity: Strain - Solids
Component: EX



Maximum 24.1784E-6 at node 4594
Minimum -45.7774E-6 at node 6407

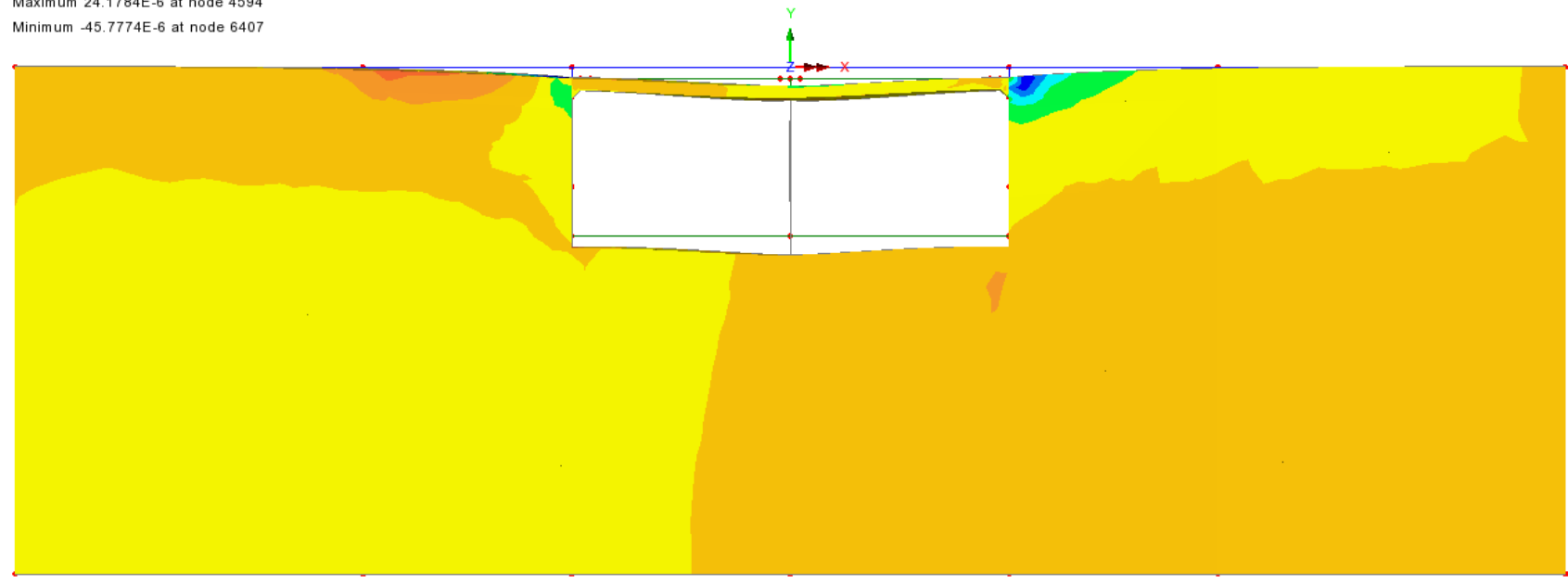


Figure 24. M2C1- Horizontal Strain (EX) of Solid Elements- 2 Lane 32 k Axle at Center of Culvert

Appendix E - 3D Modeling Backup

Axle over center
Entity: Stress - Solids
Component: SE (Units: kip/ft²)



Maximum 5.03266 at node 24058
Minimum 0.187163E-3 at node 503

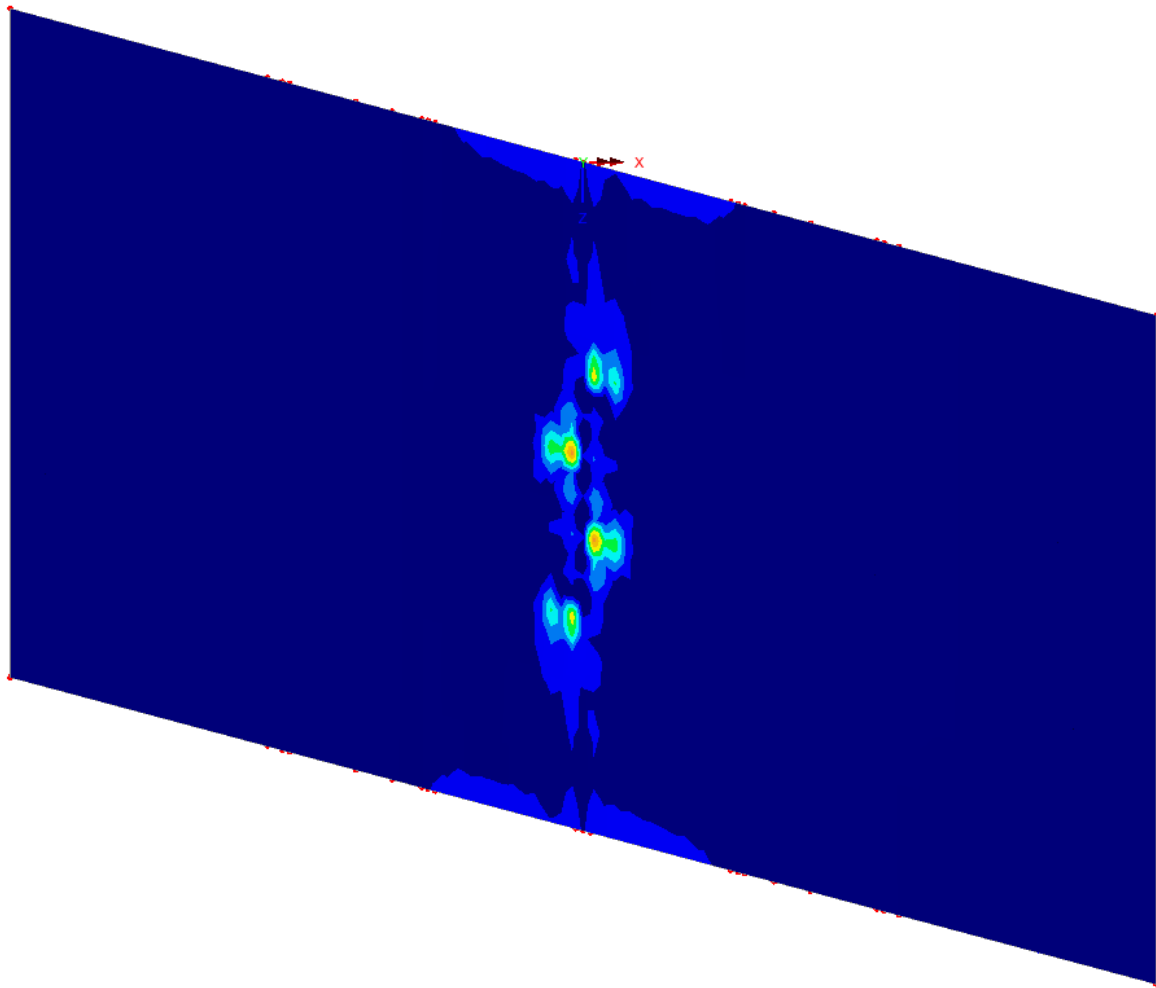
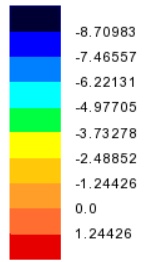


Figure 25. M2C1- Von Mises Stress of Solid Elements- 2 Lane 32 k Axle at Center of Culvert

Appendix E - 3D Modeling Backup

Axle over center
Entity: Stress - Solids
Component: SY (Units: kip/ft²)



Maximum 1.90569 at node 22681
Minimum -9.29266 at node 24058

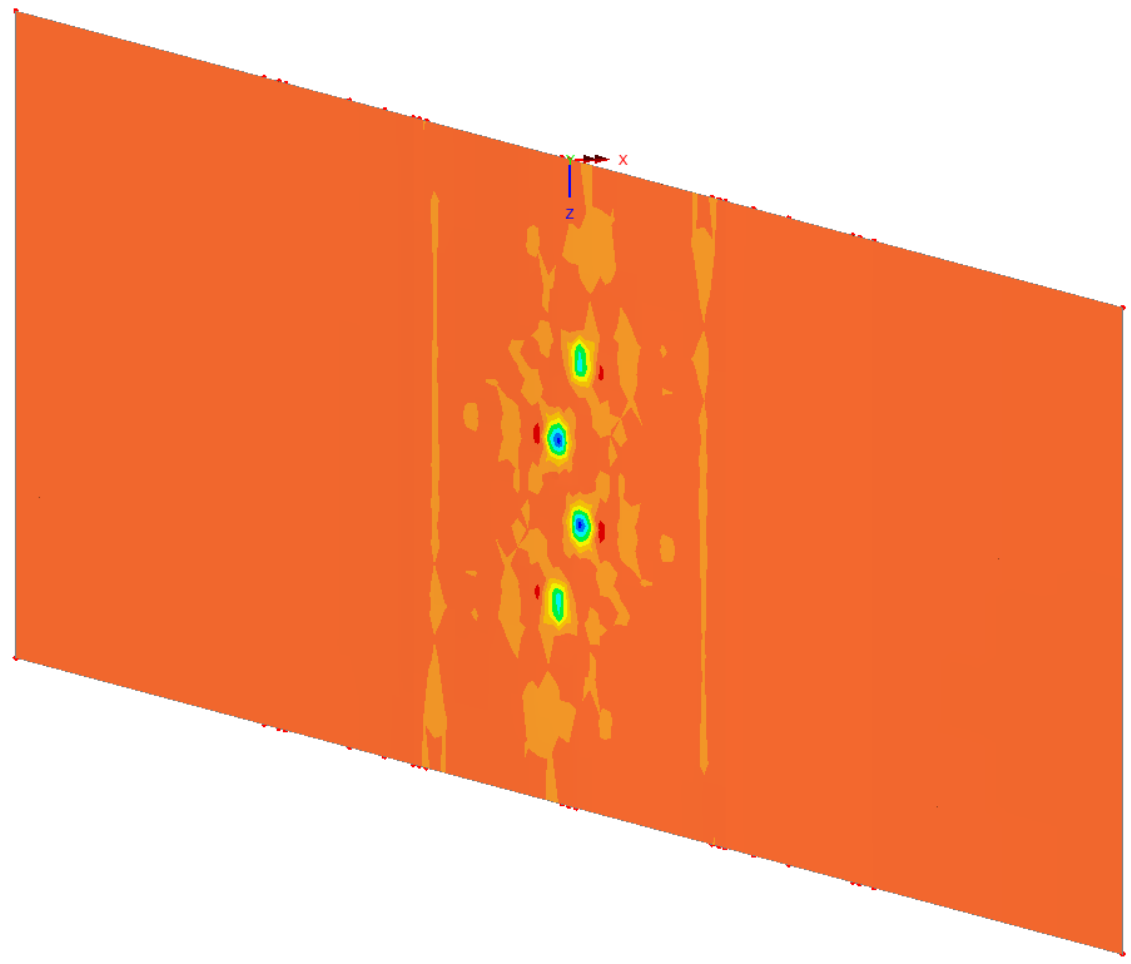


Figure 26. M2C1- Vertical Stress (SY) of Solid Elements- 2 Lane 32 k Axle at Center of Culvert

Appendix E - 3D Modeling Backup

Axle over center
Entity: Stress - Solids
Component: SX (Units: kip/ft²)

Dark Blue	-4.03631
Blue	-3.45969
Cyan	-2.88308
Green	-2.30646
Yellow	-1.72985
Orange	-1.15323
Light Orange	-0.576615
Red	0.0
Dark Red	0.576615

Maximum 0.701465 at node 23218
Minimum -4.48807 at node 22682

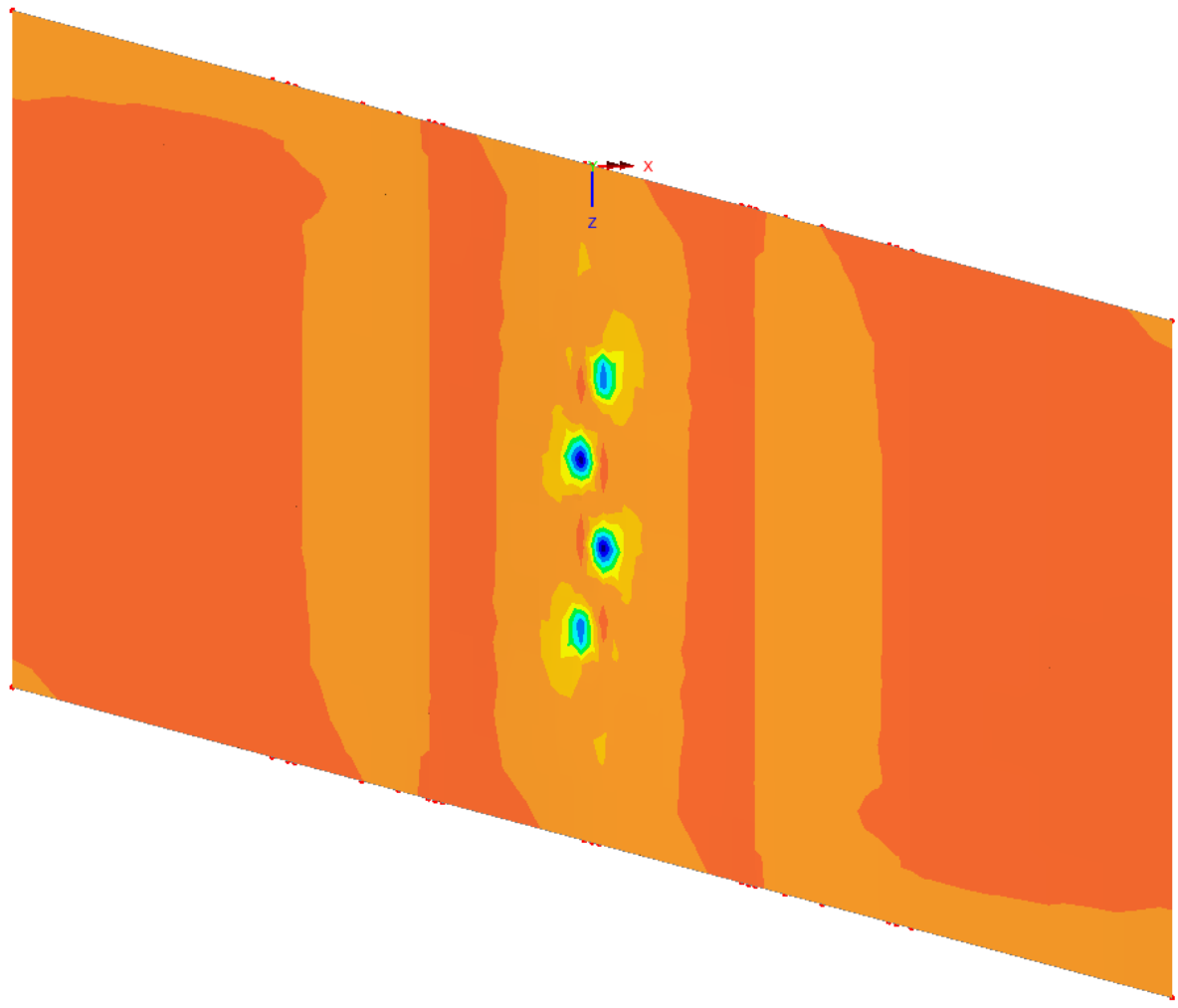
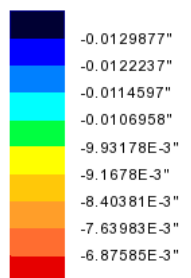


Figure 27. M2C1- Horizontal Stress (SX) of Solid Elements- 2 Lane 32 k Axle at Center of Culvert

Appendix E - 3D Modeling Backup

Axle over center
Entity: Displacement
Component: DY (Units: ft)



Maximum -6.44016E-3" at node 2303
Minimum -0.013316" at node 25633

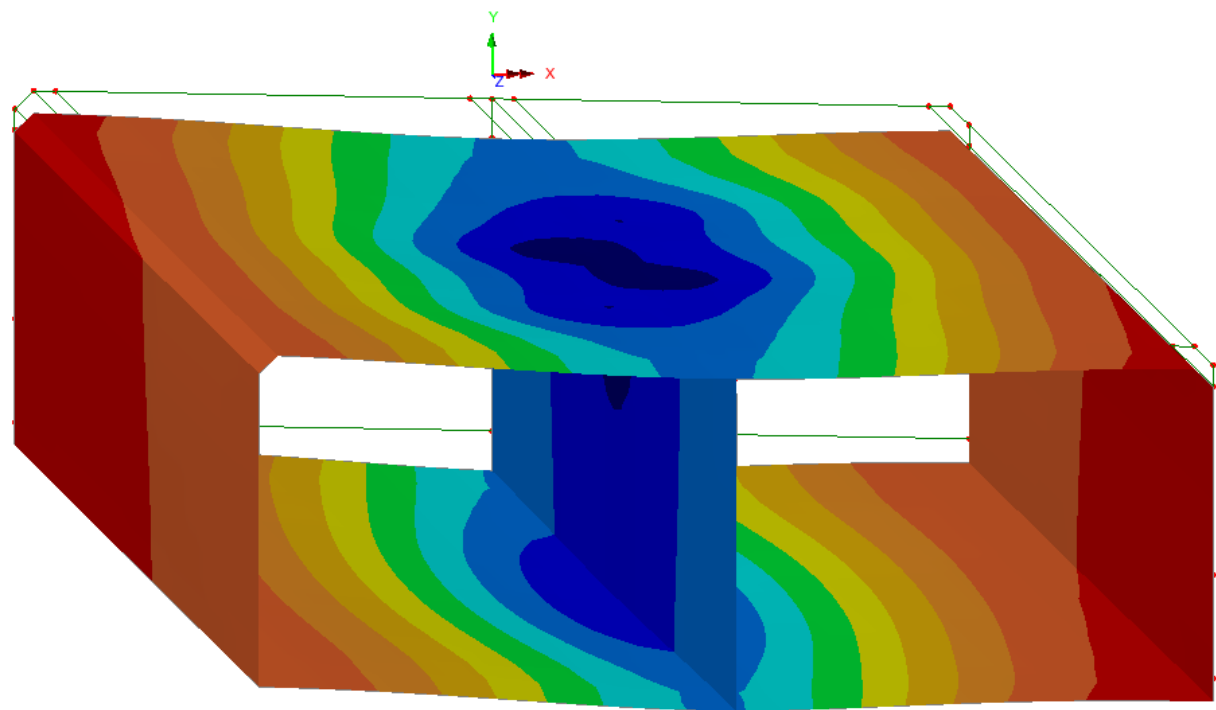


Figure 28. M2C1- Vertical Displacement of Culvert- 2 Lane 32 k Axle at Center of Culvert

Appendix E - 3D Modeling Backup

Axle over center
Entity: Strain (top) - Thick Shell
Component: EE

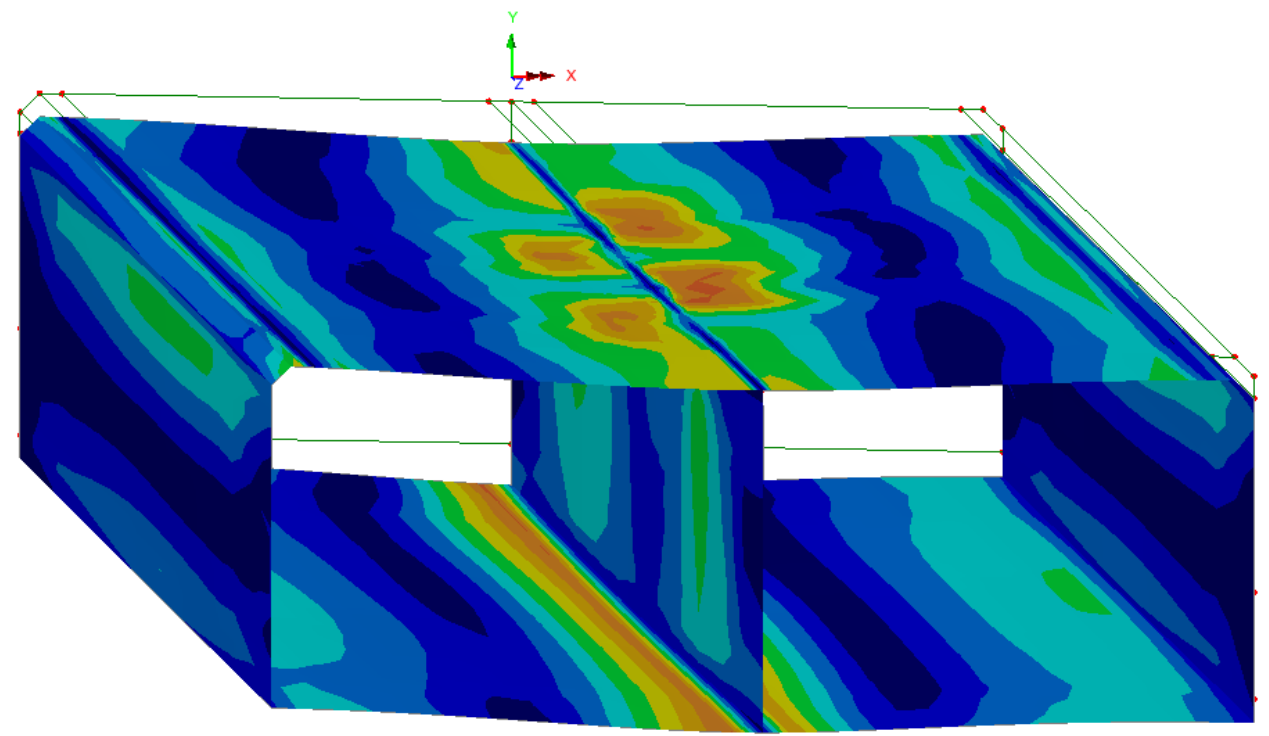
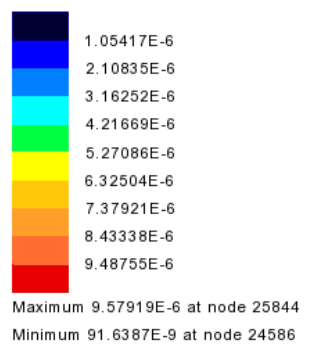
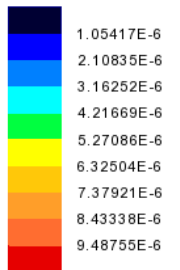


Figure 29. M2C1- Von Mises Strain at Top Fiber in Culvert- 2 Lane 32 k Axle at Center of Culvert

Appendix E - 3D Modeling Backup

Axle over center
Entity: Strain (bottom) - Thick Shell
Component: EE



Maximum 9.57919E-6 at node 25633
Minimum 91.6387E-9 at node 24226

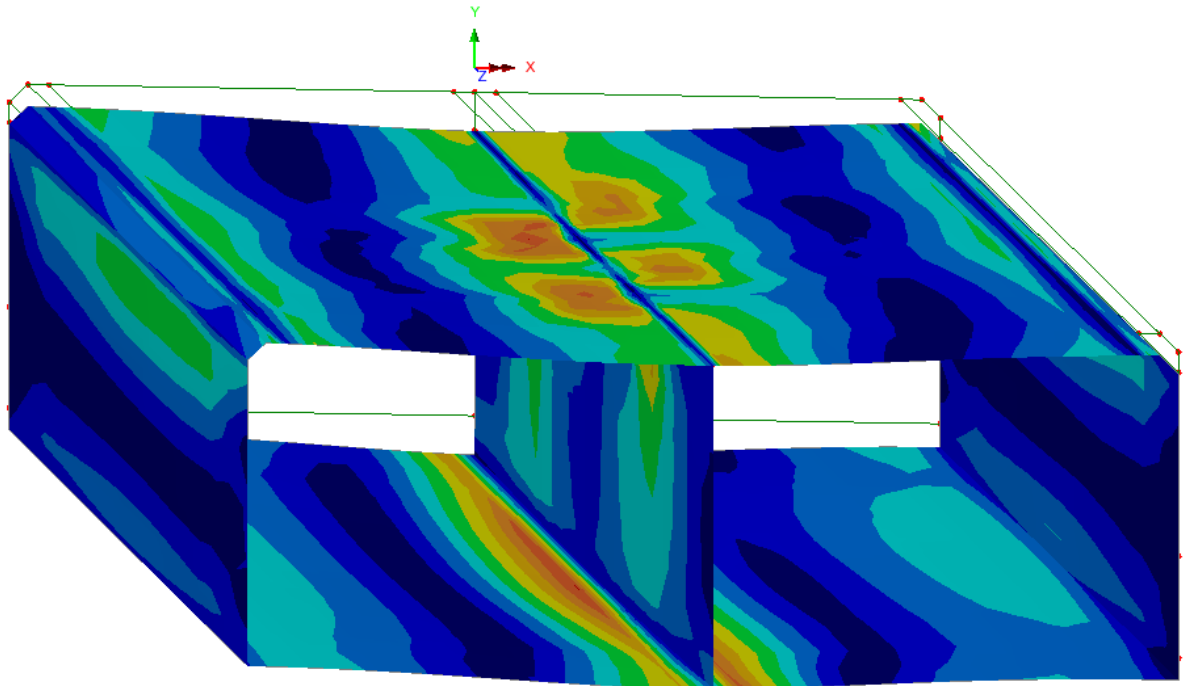
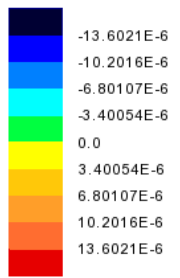


Figure 30. M2C1- Von Mises Strain at Bottom Fiber in Culvert- 2 Lane 32 k Axle at Center of Culvert

Appendix E - 3D Modeling Backup

Axle over center
Entity: Strain (top) - Thick Shell
Component: EX



Maximum 16.4164E-6 at node 25844
Minimum -14.1884E-6 at node 25633

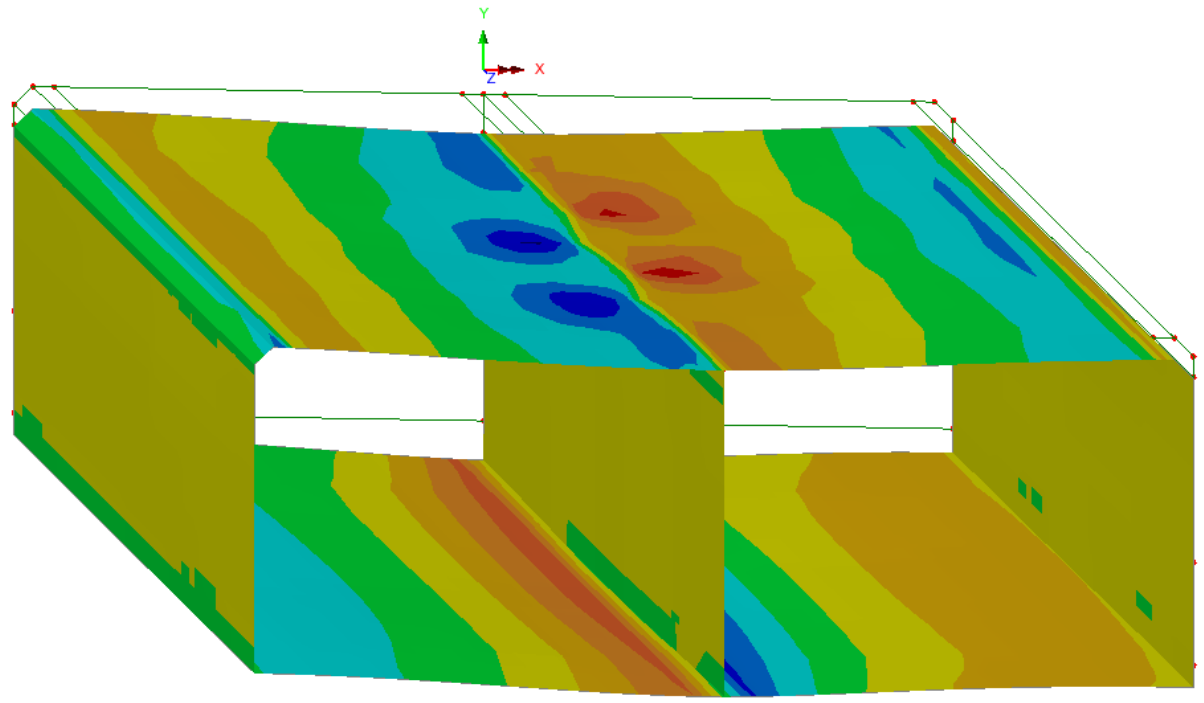
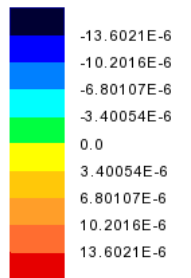


Figure 31. M2C1- Bending Strain at Top Fiber in Culvert- 2 Lane 32 k Axle at Center of Culvert

Appendix E - 3D Modeling Backup

Axle over center
Entity: Strain (bottom) - Thick Shell
Component: EX



Maximum 16.4164E-6 at node 25633
Minimum -14.1884E-6 at node 25844

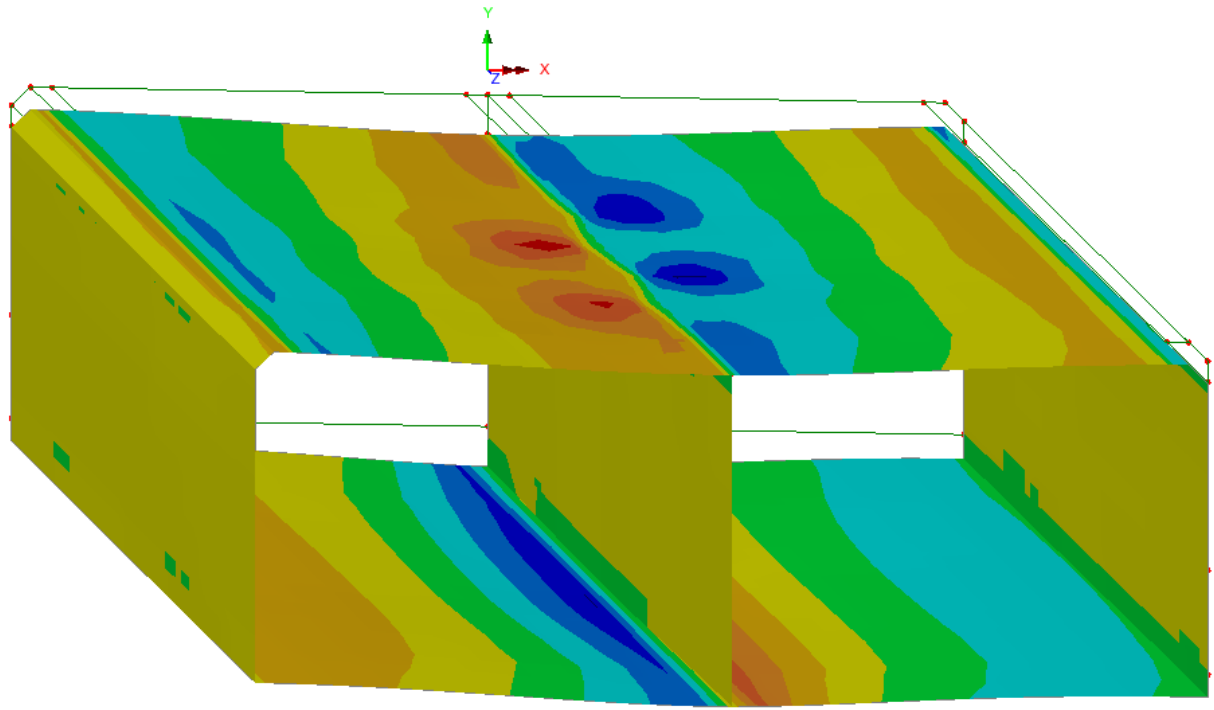


Figure 32. M2C1- Bending Strain at Bottom Fiber in Culvert- 2 Lane 32 k Axle at Center of Culvert

Appendix E - 3D Modeling Backup

Axle over center
Entity: Stress (top) - Thick Shell
Component: SE (Units: kip/ft²)

1.03049
2.06099
3.09148
4.12198
5.15247
6.18297
7.21346
8.24395
9.27445

Maximum 9.34383 at node 25844
Minimum 0.0693865 at node 24586

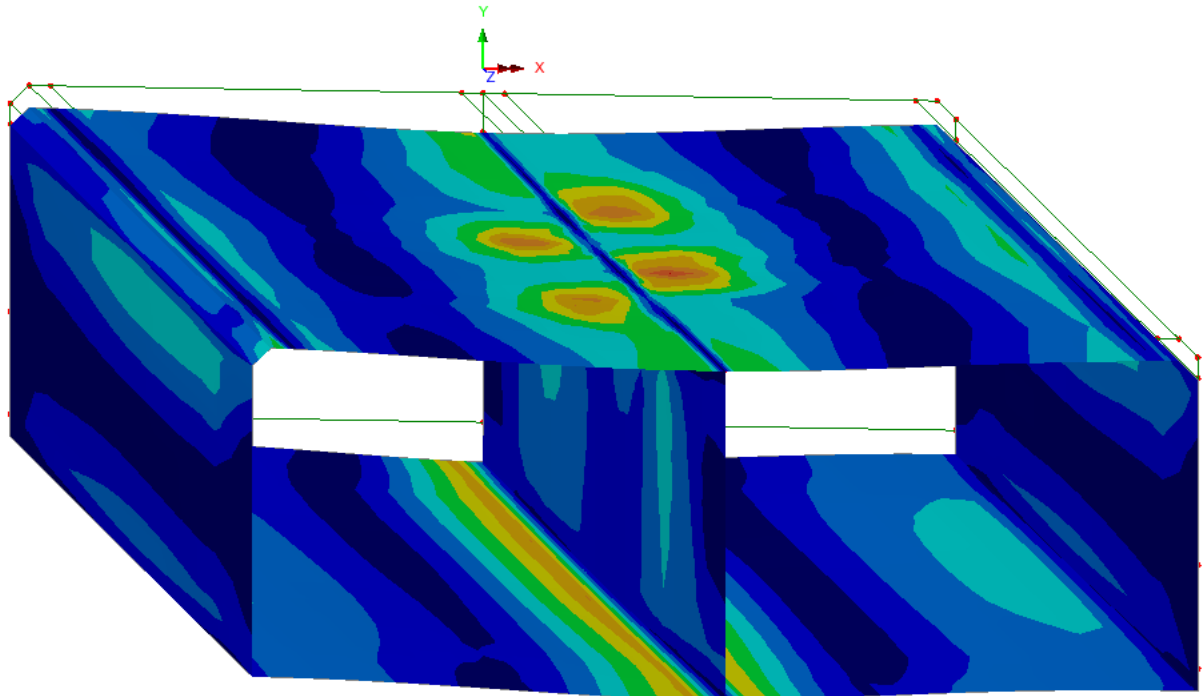
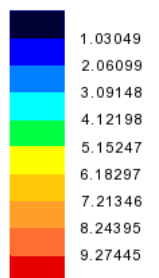


Figure 33. M2C1- Von Mises Stress at Top Fiber in Culvert- 2 Lane 32 k Axle at Center of Culvert

Appendix E - 3D Modeling Backup

Axle over center
Entity: Stress (bottom) - Thick Shell
Component: SE (Units: kip/ft²)



Maximum 9.34383 at node 25633
Minimum 0.0693865 at node 24226

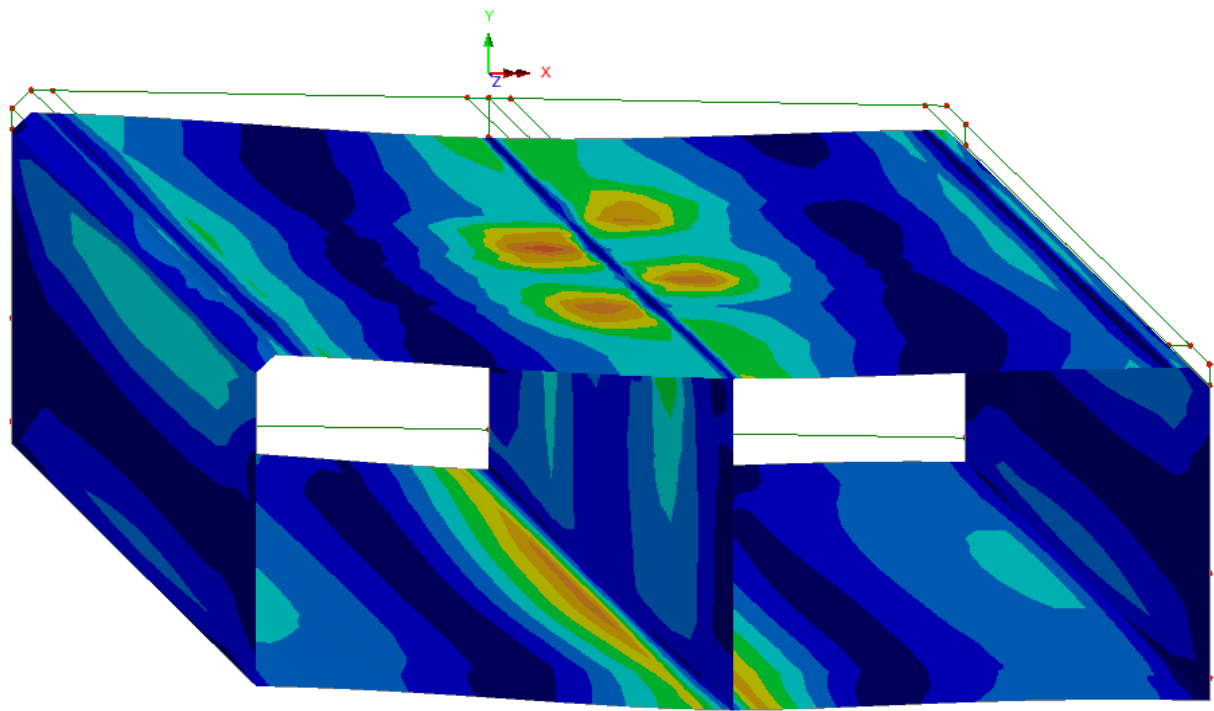
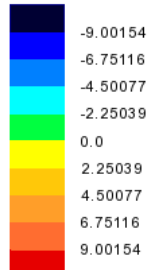


Figure 34. M2C1- Von Mises Stress at Bottom Fiber in Culvert- 2 Lane 32 k Axle at Center of Culvert

Appendix E - 3D Modeling Backup

Axle over center
Entity: Stress (top) - Thick Shell
Component: SX (Units: kip/ft²)



Maximum 10.7813 at node 25844
Minimum -9.47221 at node 25633

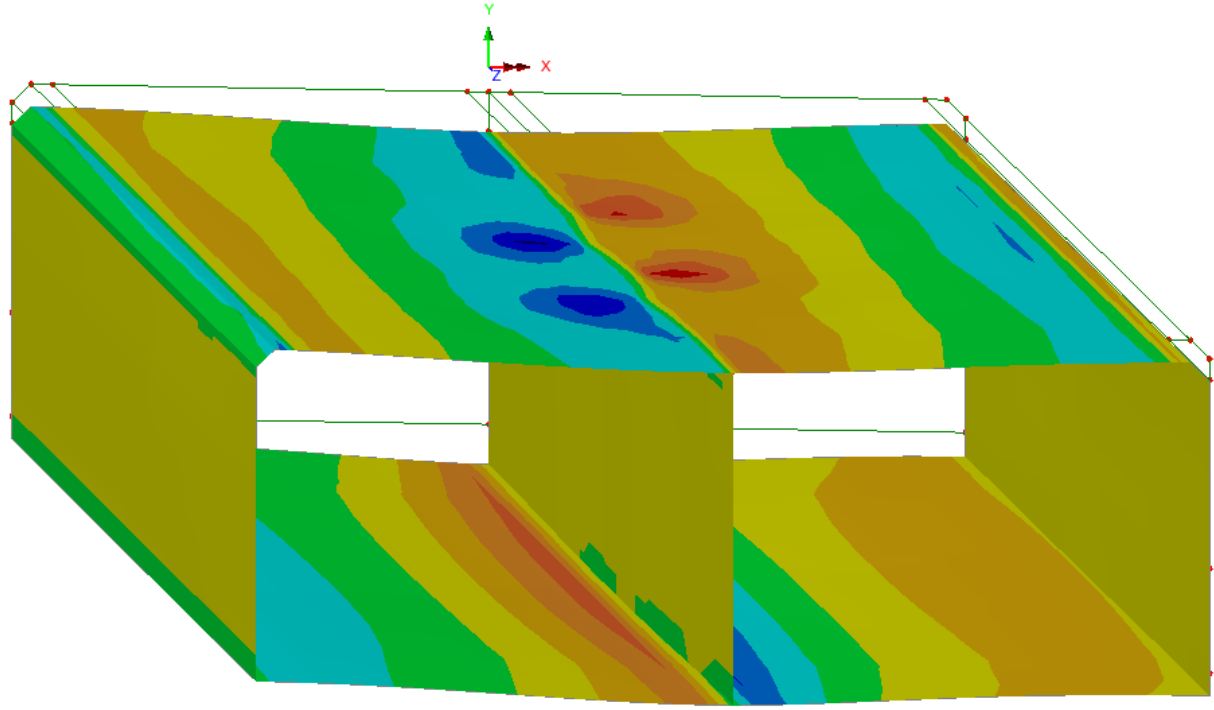
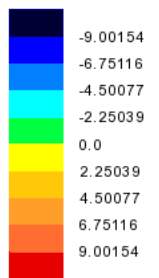


Figure 35. M2C1- Bending Stress at Top Fiber in Culvert- 2 Lane 32 k Axle at Center of Culvert

Appendix E - 3D Modeling Backup

Axle over center
Entity: Stress (bottom) - Thick Shell
Component: SX (Units: kip/ft²)



Maximum 10.7813 at node 25633
Minimum -9.47221 at node 25844

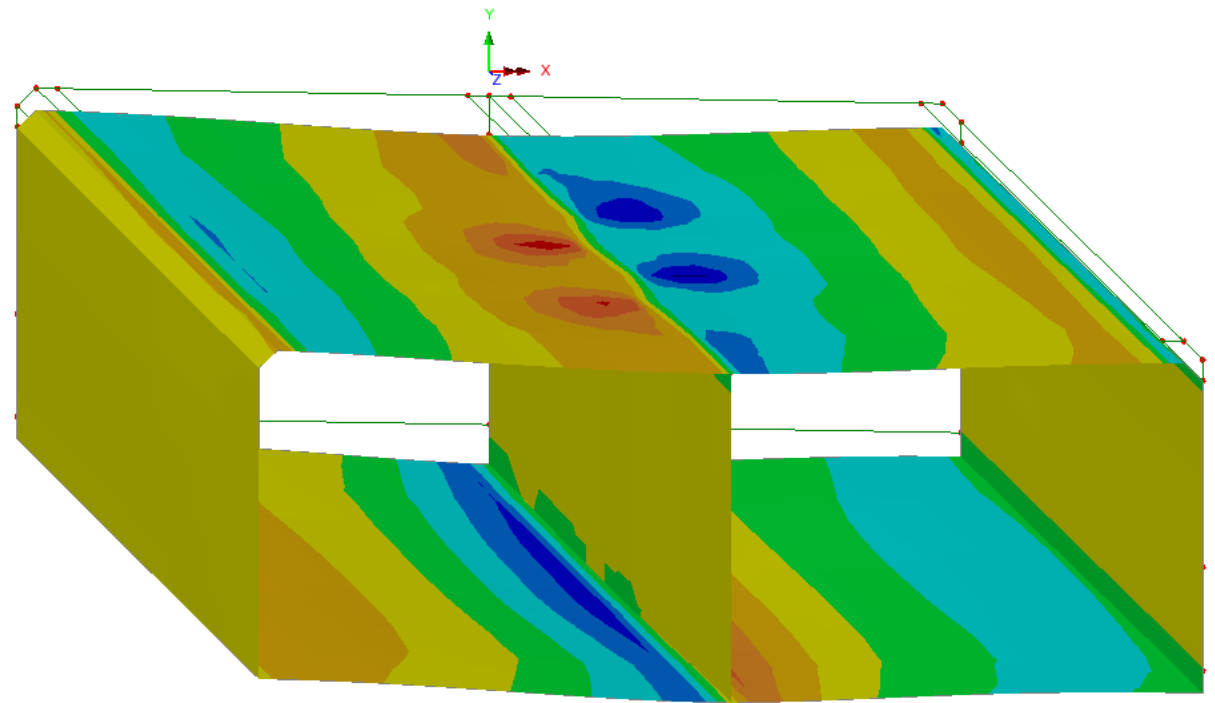
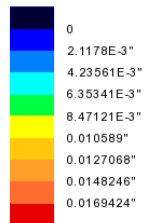


Figure 36. M2C1- Bending Stress at Bottom Fiber in Culvert- 2 Lane 32 k Axle at Center of Culvert

Appendix E - 3D Modeling Backup

Axle over mid left cell
Entity: Displacement
Component: RSLT (Units: ft)



Maximum 0.0190602" at node 22677
Minimum 0 at node 1

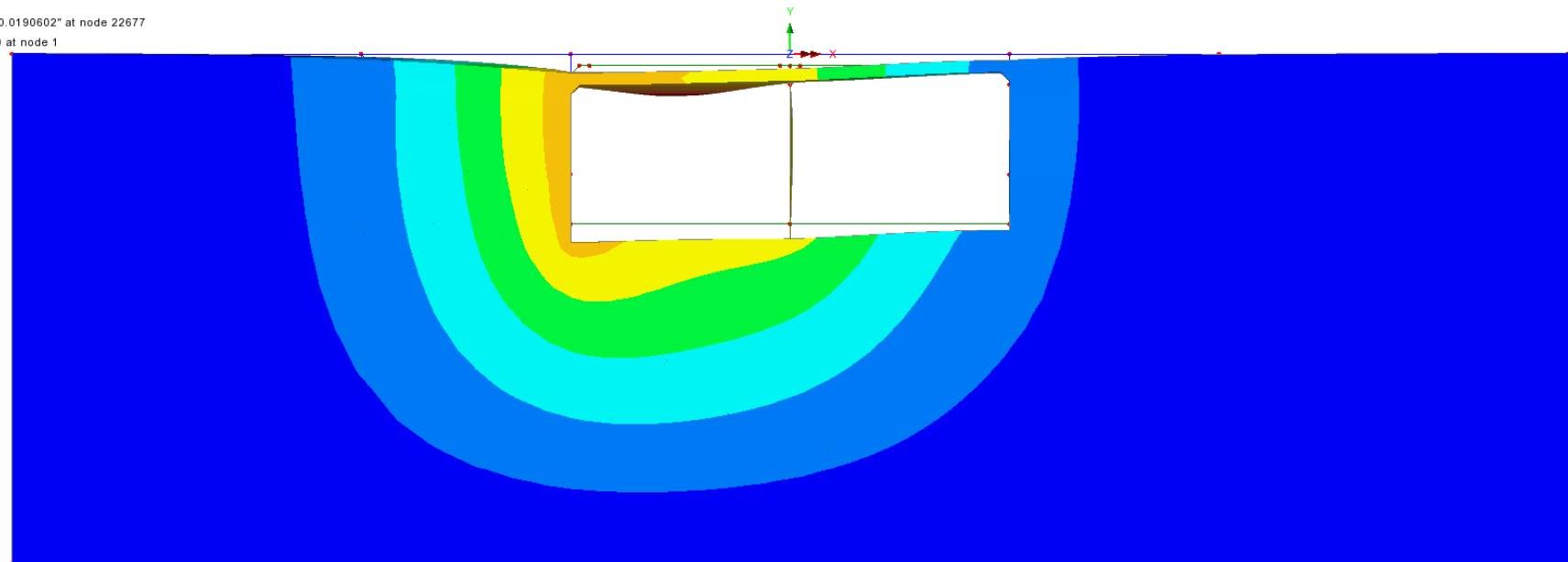
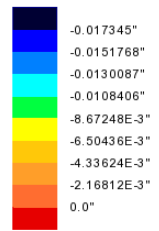


Figure 37. M2C1- Resultant Displacement of Solid Elements – 2 Lane 32 k Axle at Mid-Span of Left Cell

Appendix E - 3D Modeling Backup

Axle over mid left cell
Entity: Displacement
Component: DY (Units: ft)



Maximum 0.456952E-3" at node 16360
Minimum -0.0190561" at node 22677

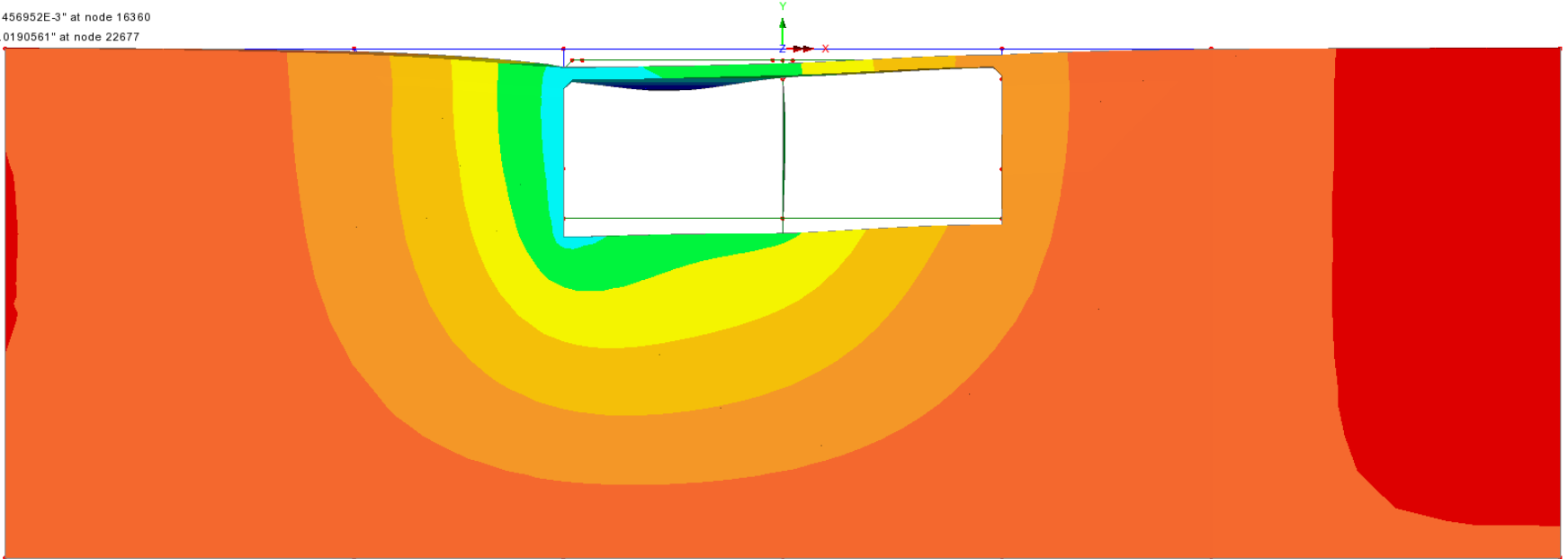
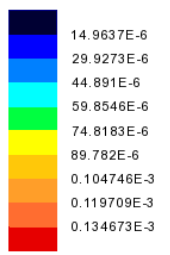


Figure 38. M2C1- Vertical Displacement of Solid Elements - 2 Lane 32 k Axle at Mid-Span of Left Cell

Appendix E - 3D Modeling Backup

Axle over mid left cell
Entity: Strain - Solids
Component: EE



Maximum 0.134884E-3 at node 6407
Minimum 0.211528E-6 at node 8078

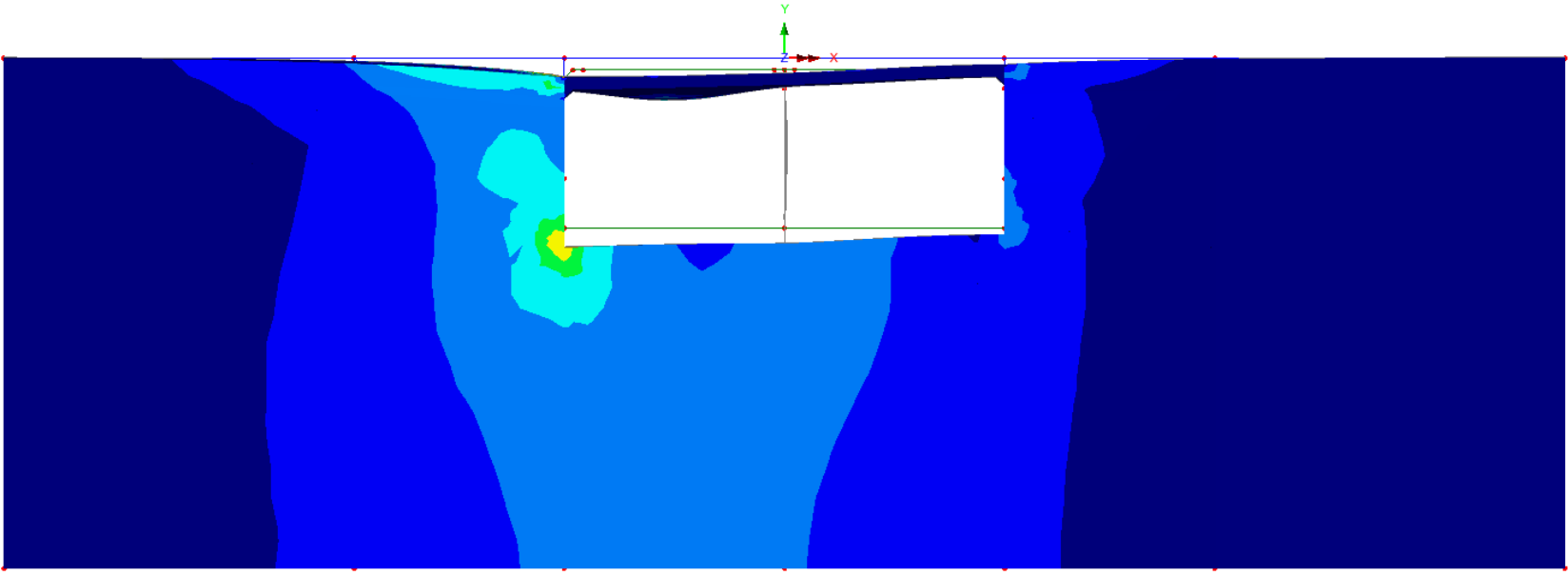


Figure 39. M2C1- Von Mises Strain of Solid Elements- 2 Lane 32 k Axle at Mid-Span of Left Cell

Appendix E - 3D Modeling Backup

Axle over mid left cell
Entity: Strain - Solids
Component: EY

Black	-0.124869E-3
Dark Blue	-0.104057E-3
Blue	-83.2458E-6
Cyan	-62.4344E-6
Green	-41.6229E-6
Yellow	-20.8115E-6
Orange	0.0
Light Orange	20.8115E-6
Red	41.6229E-6

Maximum 56.4394E-6 at node 4315
Minimum -0.130864E-3 at node 2826

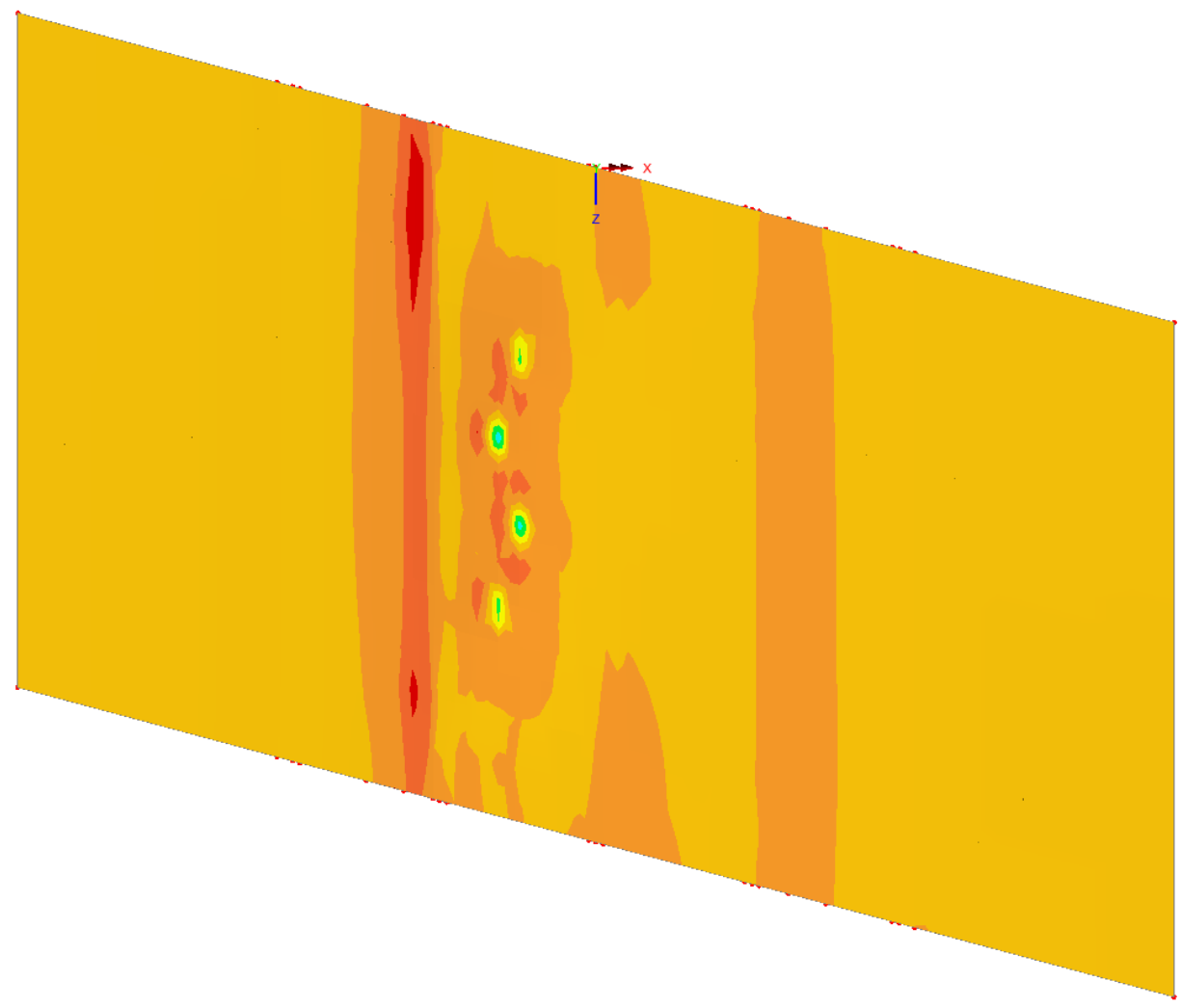


Figure 40. M2C1- Vertical Strain (EV) of Solid Elements- 2 Lane 32 k Axle at Mid-Span of Left Cell

Appendix E - 3D Modeling Backup

Axle over mid left cell
Entity: Strain - Solids
Component: EX

Dark Blue	-86.9475E-6
Blue	-69.558E-6
Cyan	-52.1685E-6
Green	-34.779E-6
Yellow	-17.3895E-6
Orange	0.0
Light Orange	17.3895E-6
Red-Orange	34.779E-6
Red	52.1685E-6

Maximum 54.2679E-6 at node 4594
Minimum -0.102238E-3 at node 6407

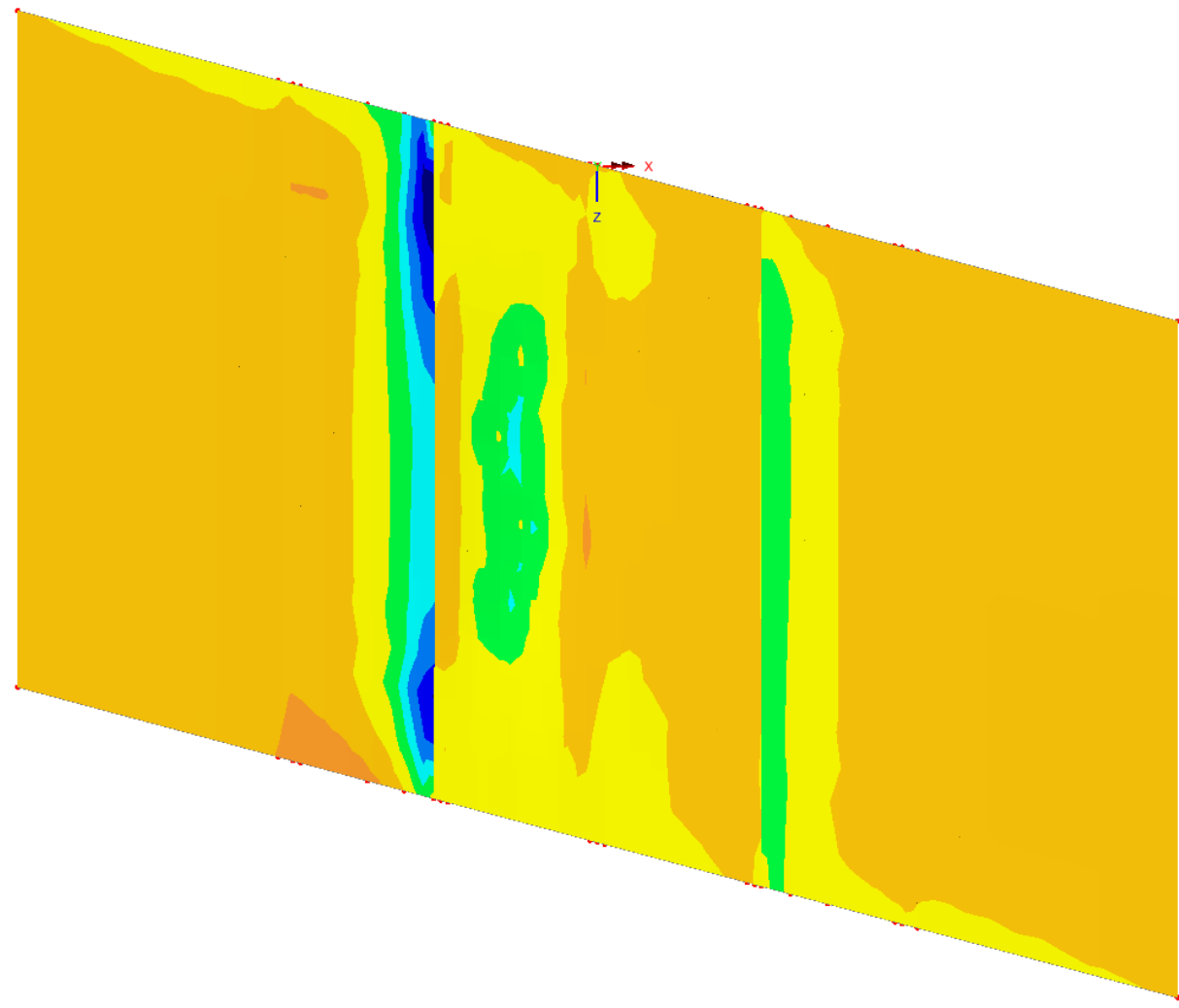
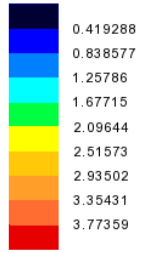


Figure 41. M2C1- Horizontal Strain (EX) of Solid Elements- 2 Lane 32 k Axle at Mid-Span of Left Cell

Appendix E - 3D Modeling Backup

Axle over mid left cell
Entity: Stress - Solids
Component: SE (Units: kip/ft²)



Maximum 3.77366 at node 23578
Minimum 68.234E-6 at node 15296

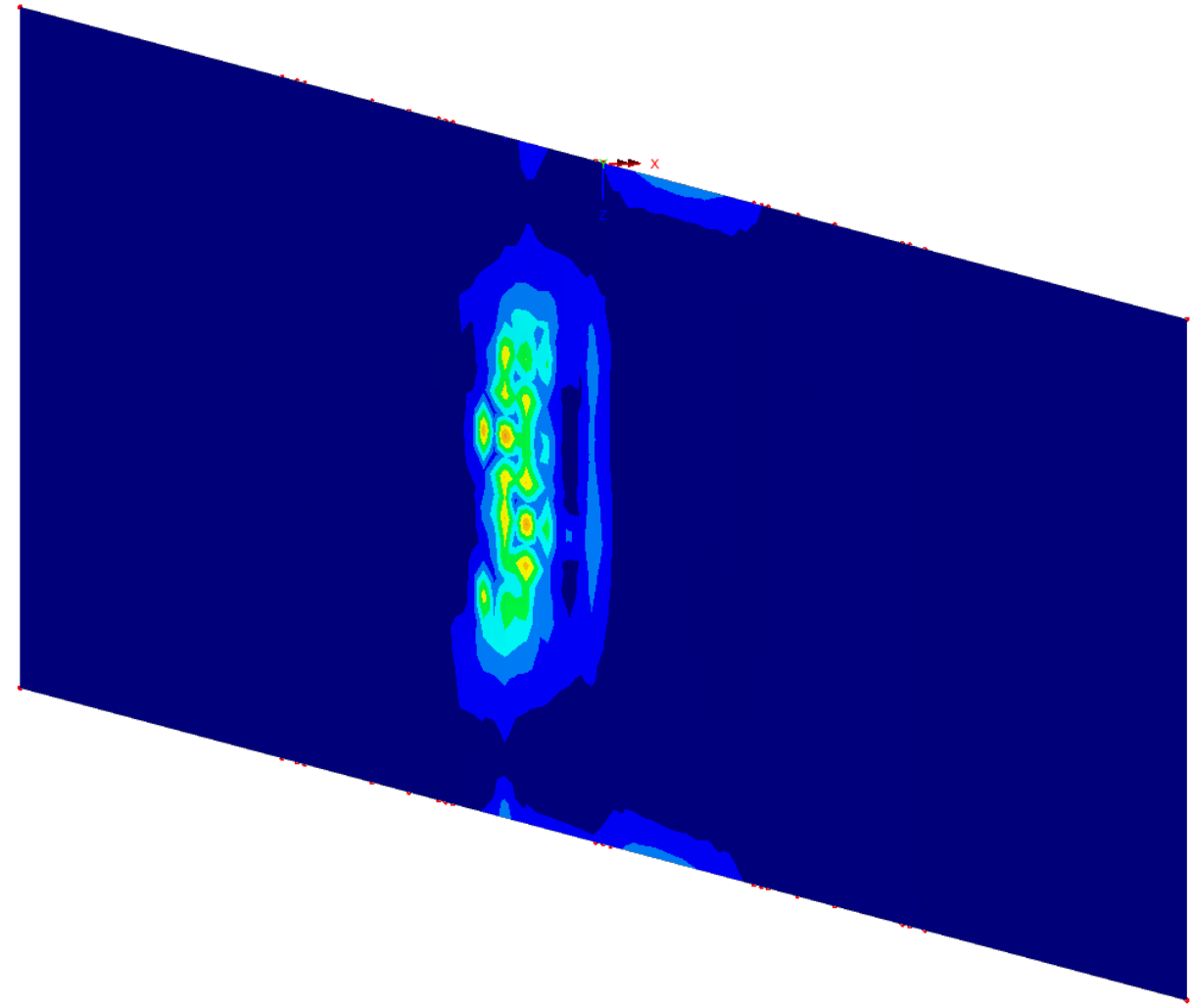


Figure 42. M2C1- Von Mises Stress of Solid Elements- 2 Lane 32 k Axle at Mid-Span of Left Cell

Appendix E - 3D Modeling Backup

Axle over mid left cell
Entity: Stress - Solids
Component: SY (Units: kip/ft²)

Black	-8.11194
Blue	-6.95309
Cyan	-5.79424
Green	-4.63539
Yellow	-3.47654
Orange	-2.3177
Light Orange	-1.15885
Red	0.0
Dark Red	1.15885

Maximum 2.0634 at node 22676
Minimum -8.36623 at node 22677

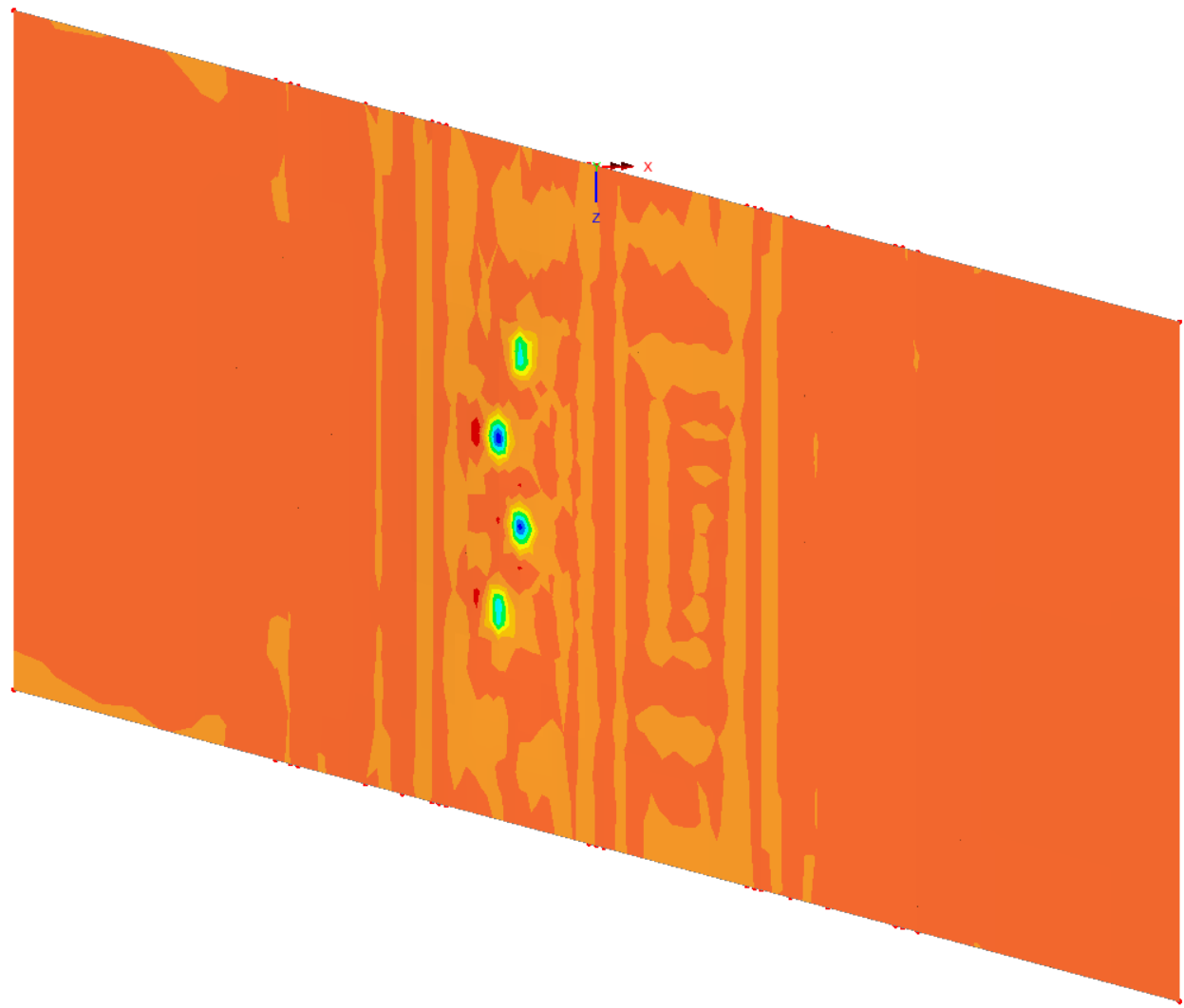
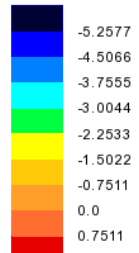


Figure 43. M2C1- Vertical Stress (SY) of Solid Elements- 2 Lane 32 k Axle at Mid-Span of Left Cell

Appendix E - 3D Modeling Backup

Axle over mid left cell
Entity: Stress - Solids
Component: SX (Units: kip/ft²)



Maximum 1.21551 at node 22652
Minimum -5.54439 at node 22677

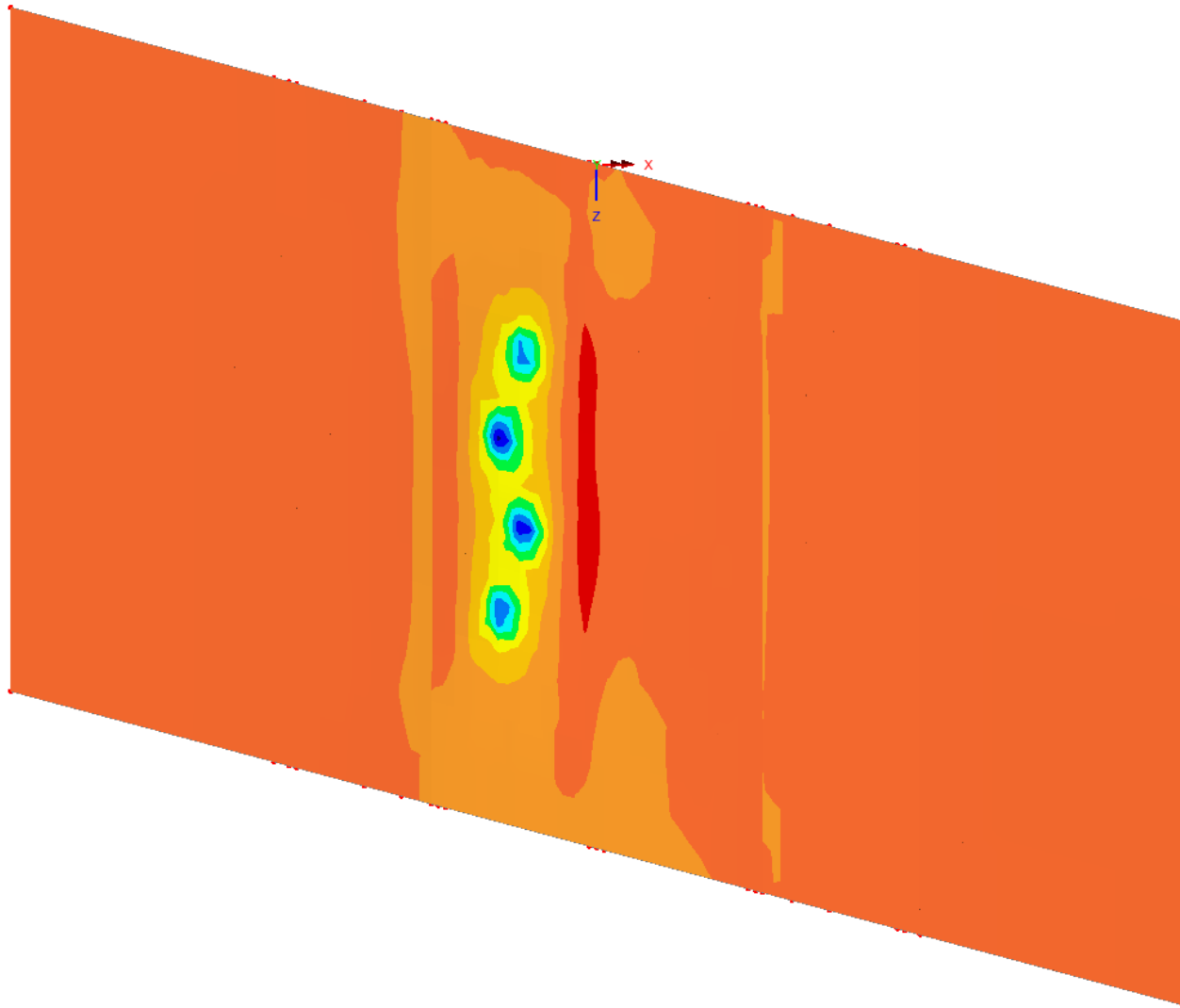


Figure 44. M2C1- Horizontal Stress (SX) of Solid Elements- 2 Lane 32 k Axle at Mid-Span of Left Cell

Appendix E - 3D Modeling Backup

Axle over mid left cell
Entity: Displacement
Component: DY (Units: ft)

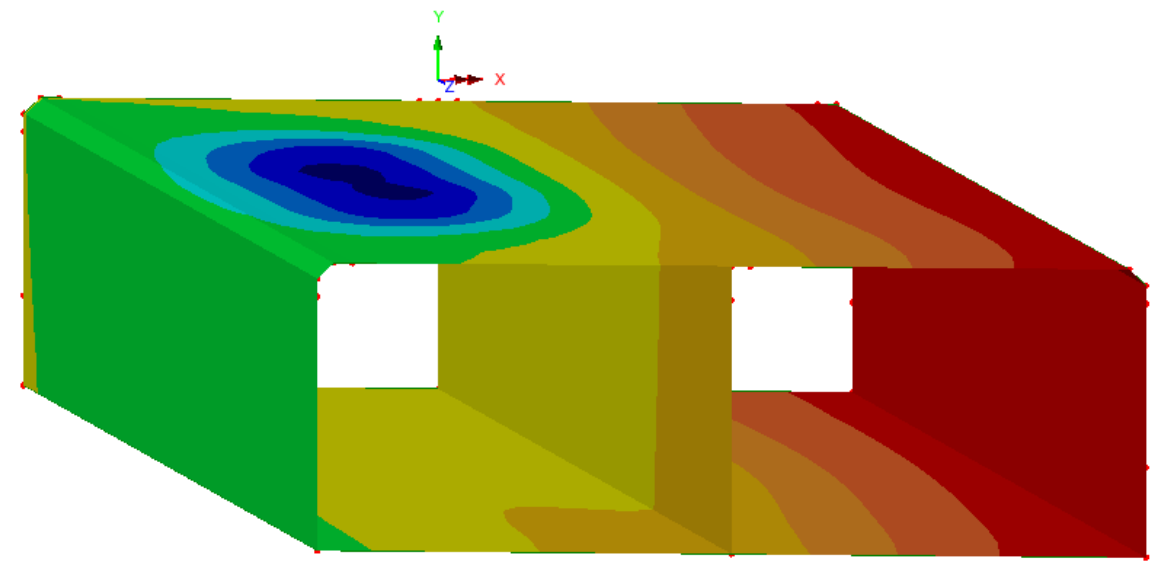
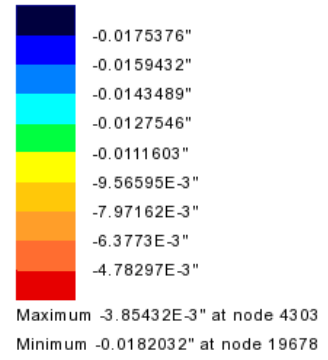


Figure 45. M2C1- Vertical Displacement of Culvert- 2 Lane 32 k Axle at Mid-Span of Left Cell

Appendix E - 3D Modeling Backup

Axle over mid left cell
Entity: Strain (top) - Thick Shell
Component: EE

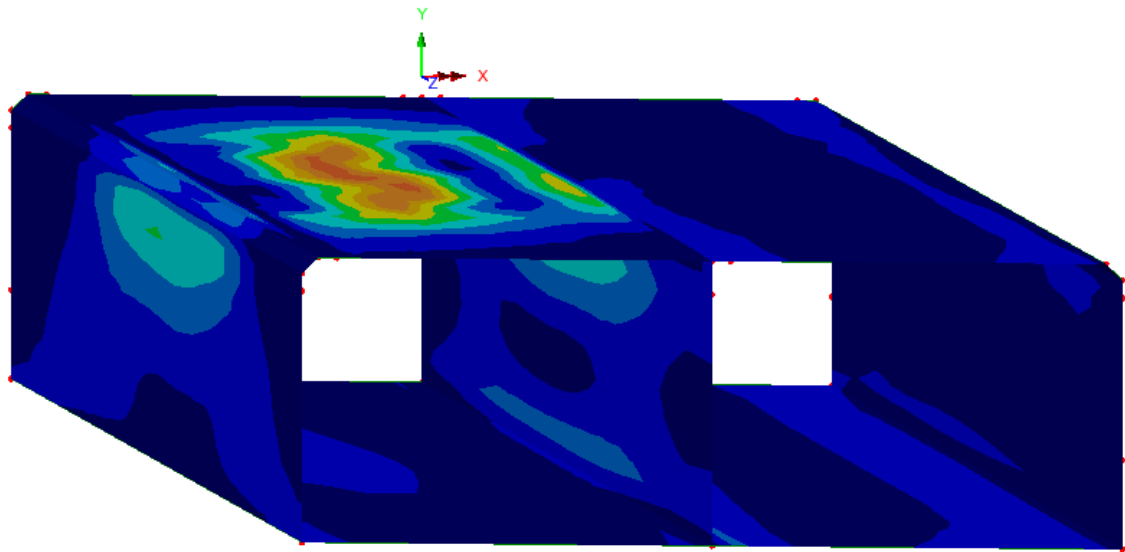


Figure 46. M2C1- Von Mises Strain at Top Fiber in Culvert- 2 Lane 32 k Axle at Mid-Span of Left Cell

Appendix E - 3D Modeling Backup

Axle over mid left cell
Entity: Strain (bottom) - Thick Shell
Component: EE

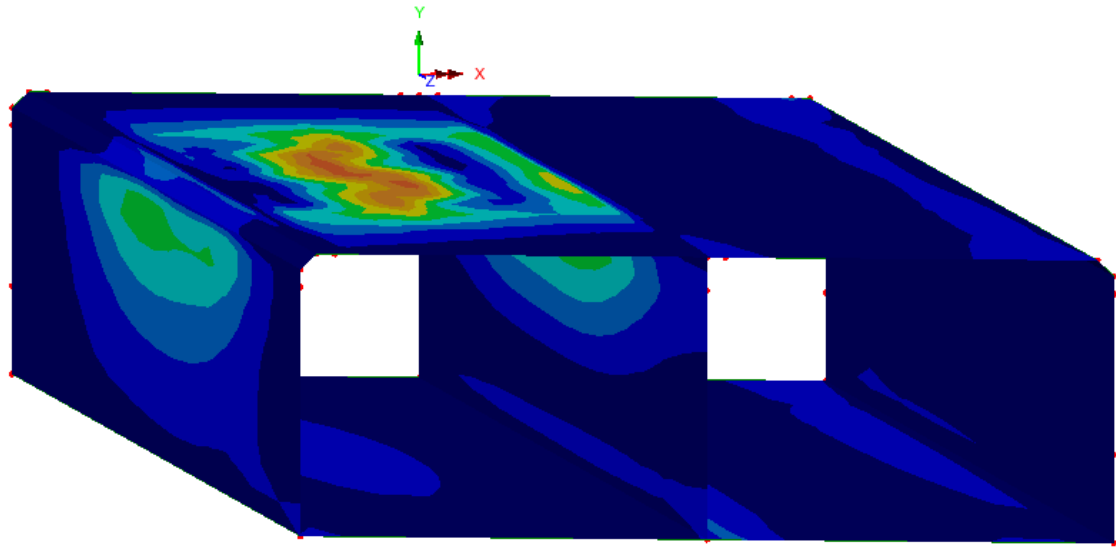


Figure 47. M2C1- Von Mises Strain at Bottom Fiber in Culvert- 2 Lane 32 k Axle at Mid-Span of Left Cell

Appendix E - 3D Modeling Backup

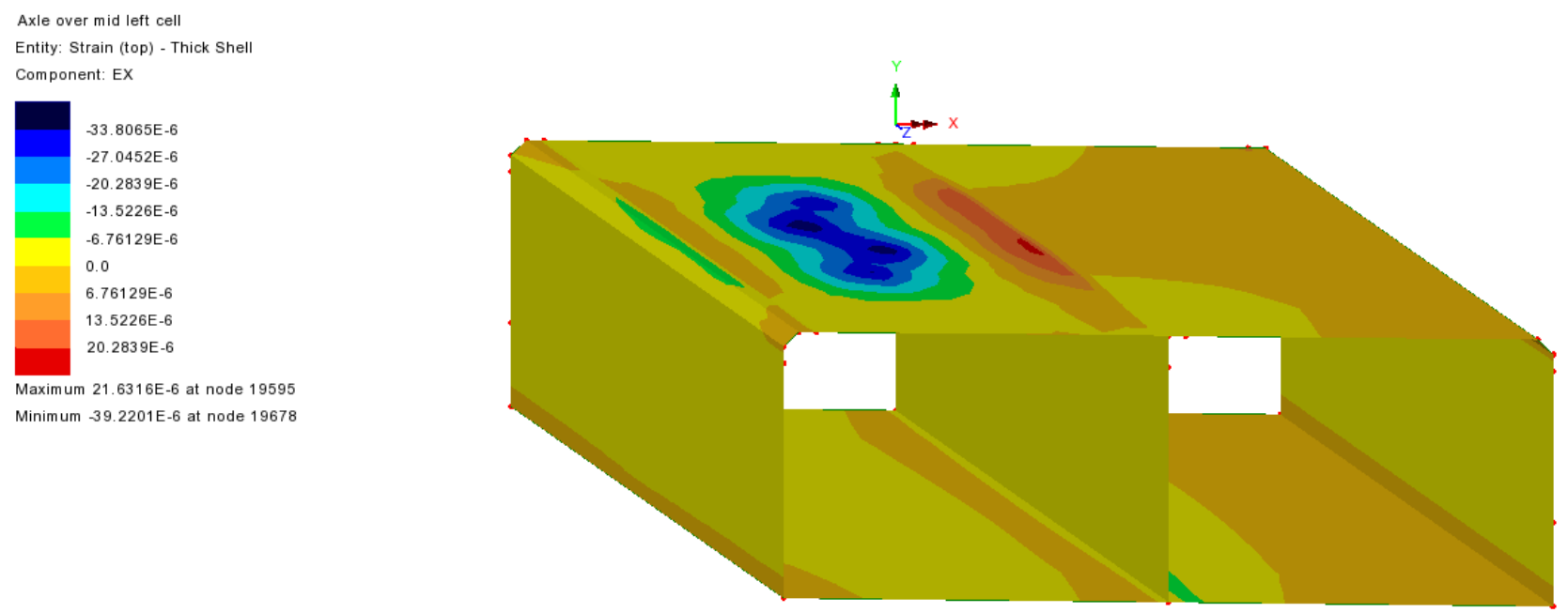


Figure 48. M2C1- Bending Strain at Top Fiber in Culvert- 2 Lane 32 k Axle at Mid-Span of Left Cell

Appendix E - 3D Modeling Backup

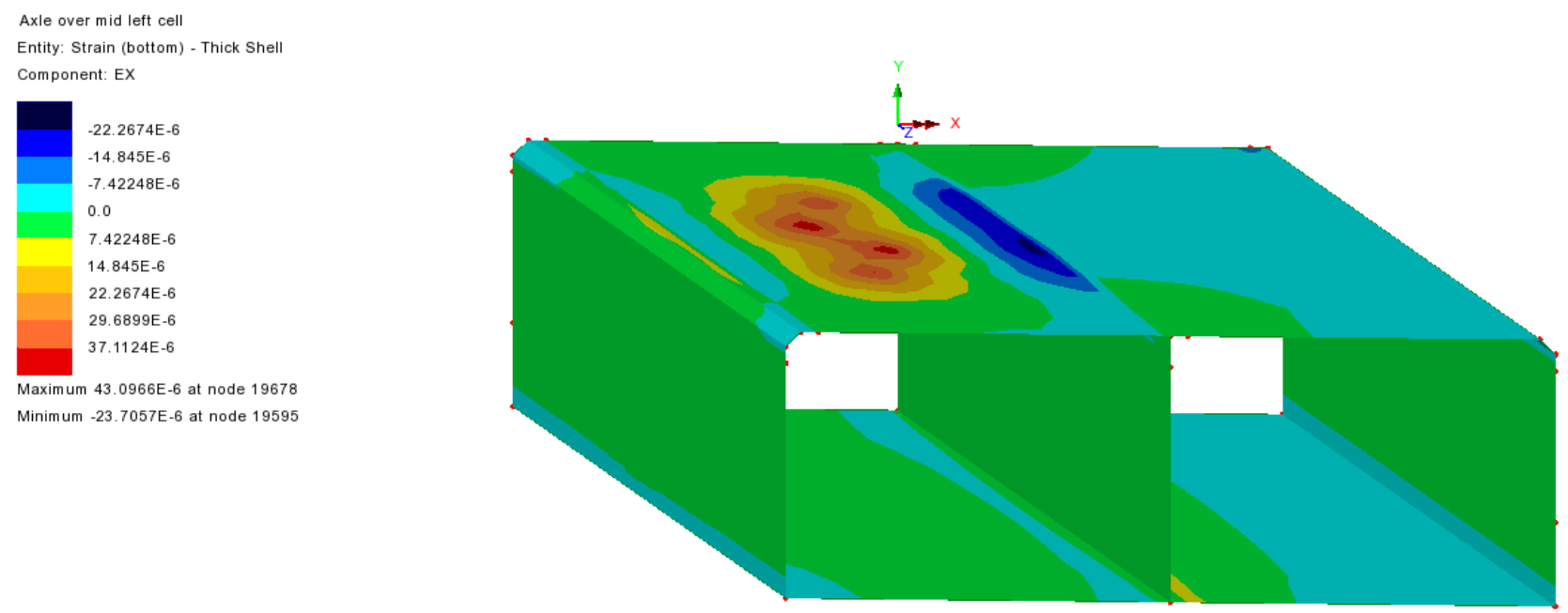


Figure 49. M2C1- Bending Strain at Bottom Fiber in Culvert- 2 Lane 32 k Axle at Mid-Span of Left Cell

Appendix E - 3D Modeling Backup

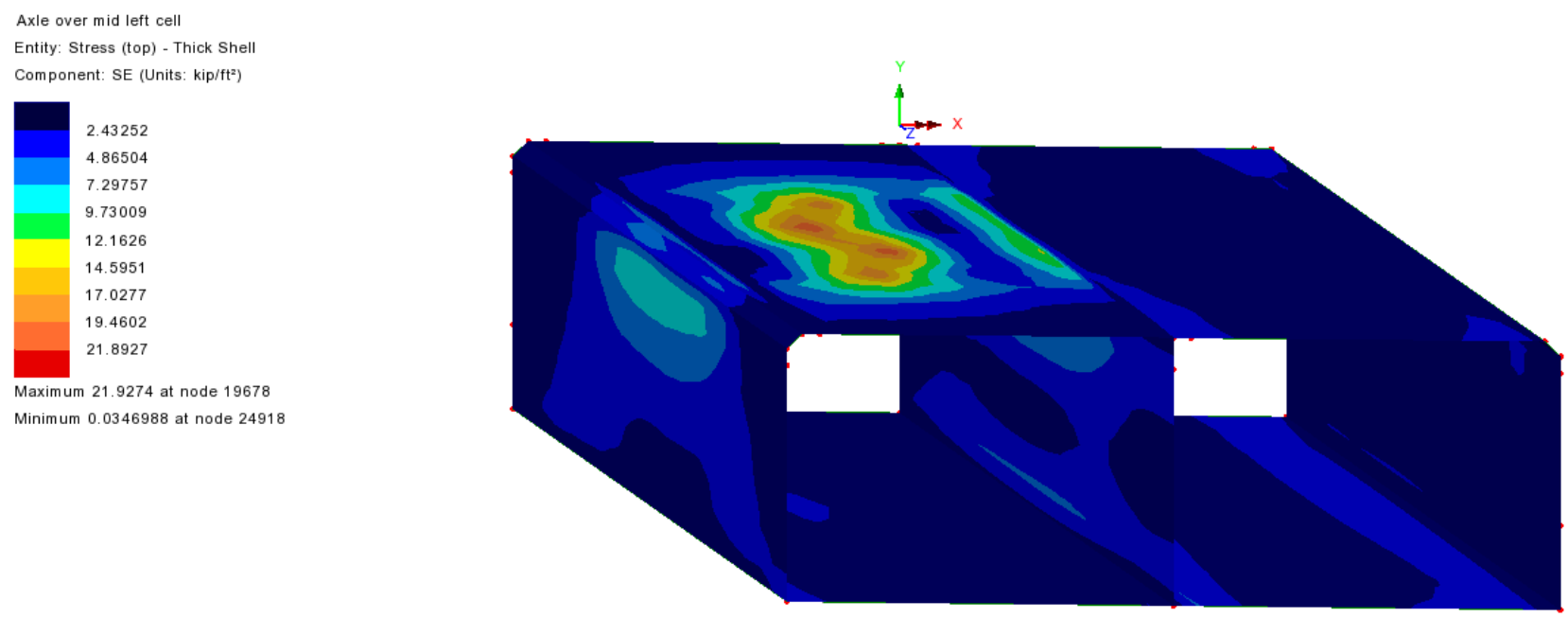
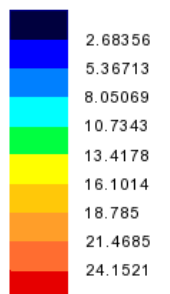


Figure 50. M2C1- Von Mises Stress at Top Fiber in Culvert- 2 Lane 32 k Axle at Mid-Span of Left Cell

Appendix E - 3D Modeling Backup

Axle over mid left cell
Entity: Stress (bottom) - Thick Shell
Component: SE (Units: kip/ft²)



Maximum 24.1748 at node 19678
Minimum 0.0227261 at node 24882

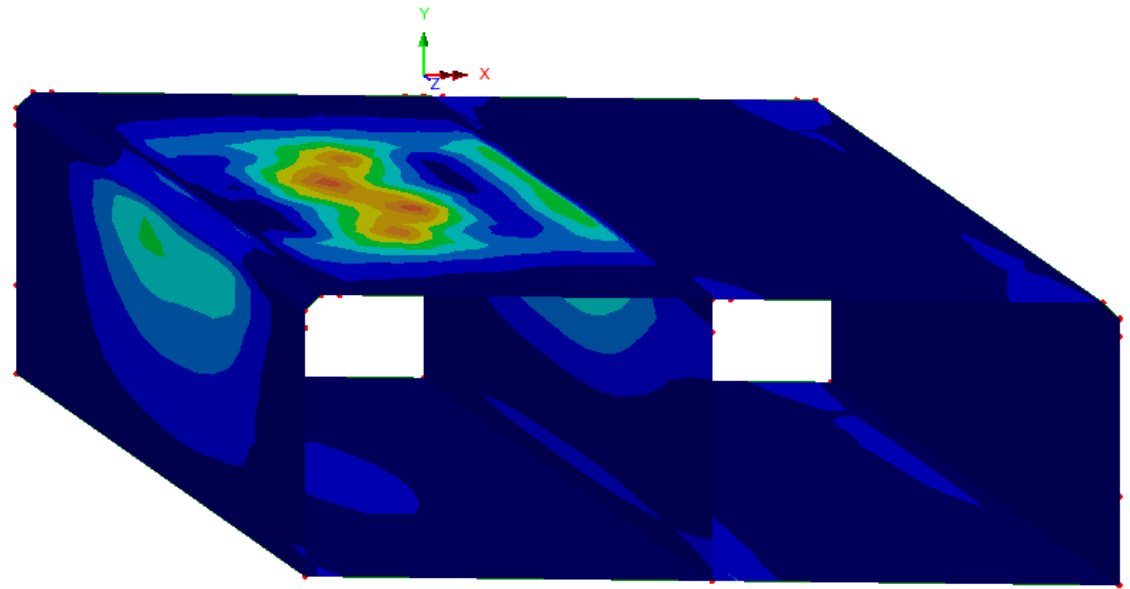


Figure 51. M2C1- Von Mises Stress at Bottom Fiber in Culvert- 2 Lane 32 k Axle at Mid-Span of Left Cell

Appendix E - 3D Modeling Backup

Axle over mid left cell
Entity: Stress (top) - Thick Shell
Component: SX (Units: kip/ft²)

Dark Blue	-21.276
Blue	-17.0208
Light Blue	-12.7656
Cyan	-8.51038
Green	-4.25519
Yellow	0.0
Orange	4.25519
Red-Orange	8.51038
Red	12.7656

Maximum 13.0228 at node 19595
Minimum -25.2739 at node 19678

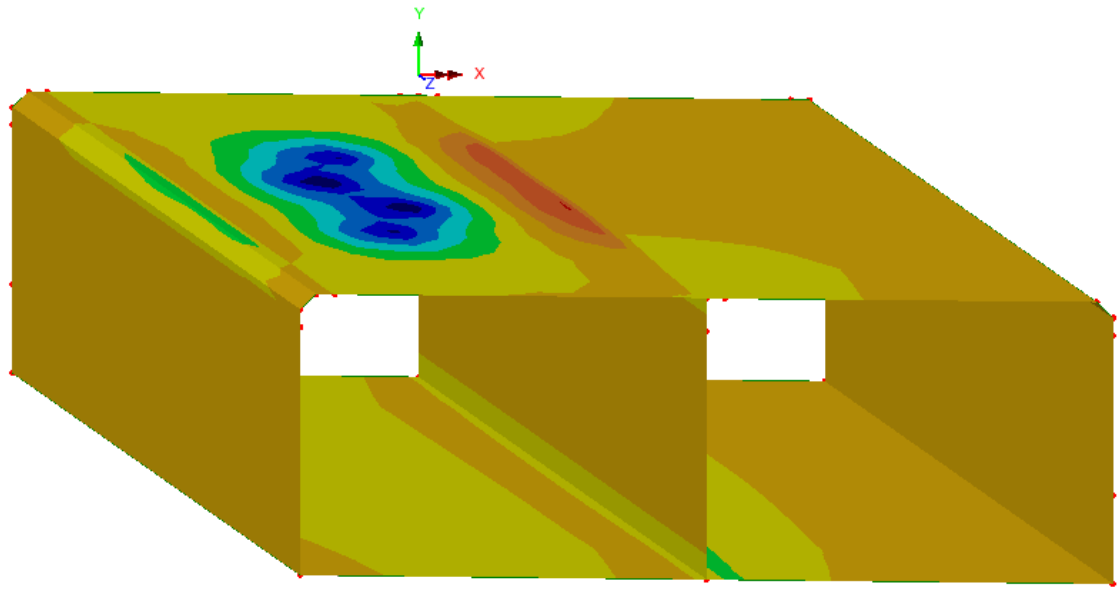
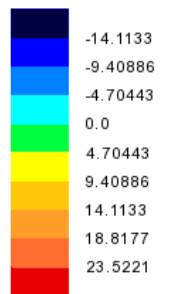


Figure 52. M2C1- Bending Stress at Top Fiber in Culvert- 2 Lane 32 k Axle at Mid-Span of Left Cell

Appendix E - 3D Modeling Backup

Axle over mid left cell
Entity: Stress (bottom) - Thick Shell
Component: SX (Units: kip/ft²)



Maximum 27.8681 at node 19678
Minimum -14.4717 at node 19595

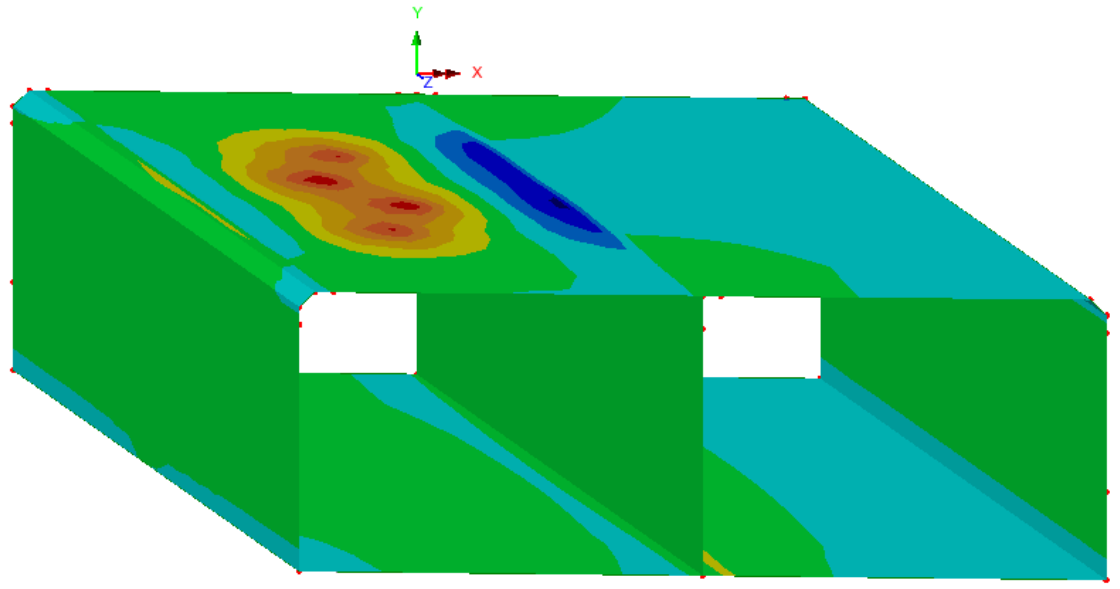


Figure 53. M2C1- Bending Stress at Bottom Fiber in Culvert- 2 Lane 32 k Axle at Mid-Span of Left Cell

MODEL 3- CANDIDATE 1 (M3C1)

Model 3 represents a prototype of new precast concrete box culverts. Of three proposed candidates for Model 3 (per Quarterly Progress Report submitted on April 1, 2016), Candidate 1 is selected for this category.

Geometry

Geometry and layout of Model 3 Candidate 1 (M3C1) is presented in the Quarterly Progress Report and is presented here as Appendix C. Figure 54 (a) presents the section of the culvert and the equivalent geometry that is modeled in Lusas. The thickness of the top flange and side wall elements is set to the actual thickness of the members. Figure 54 (b) depicts the assigned thickness of the corner elements at the chamfered sections of the concrete box culvert.

The Lusas model includes the entire length of the culvert. As shown in Figure 54 (a), the depth of model extends to 22'-9". Laterally, the geometry extends to 24' on each side. Therefore, the cross section of model is 48'x22'-9" and the length is 36'. Also, the culvert has a 10° skew which is incorporated in the model. A one-foot bedding of coarse gravel is modeled under the culvert, per contract drawings. Also, the slope of backfill is assumed 1:1/2 vertical to horizontal.

Material Properties

The linear material properties of culvert are generated based on AASHTO LRFD Bridge Design Specifications for compressive strength of $f'_c = 5$ ksi: modulus of elasticity (E) = 4074 ksi, Poisson's ratio (ν) = 0.2, unit weight = 150 pcf, and coefficient of thermal expansion (α) = 10.8 e-6 1/C.

Overlay and pavement is defined as a linear material with modulus of elasticity (E) = 4000 ksi, Poisson's ratio (ν) = 0.35, and unit weight = 140 pcf.

Table 3 presents the material properties of in-situ soil and backfill. In-situ soil is defined as an elastic material, while nonlinear material properties are considered for backfill, varying with depth. The values in Table 3 are adopted from previous study by McGrath et al. (2005).

Mesh

Quadrilateral quadratic thick shell elements are used to model the culvert. Thick shell elements are used for the culvert to incorporate the shear and bending of the culvert.

Hexahedral quadratic solid elements are used to model the pavement (overlay), in-situ soil, and backfill. The mesh size is 1' around the culverts and in backfill and 4' at the boundaries. The mesh size along the length of culvert varies between 8' at edges to 2'" at center.

Boundary Condition

At the end of the in-situ soil medium, perpendicular restraints are used for each boundary surface, i.e. lateral restraints at vertical faces and vertical restraints at the bottom of the in-situ soil.

"Tied Mesh Constraints" are assigned between the culvert and soil as well as the culvert and overlay to assure deformation compatibility. This option assures compatible deformation of adjacent shell elements and solid elements. No contact element or interaction properties are assigned.

Load Cases

Gravity is applied as a body force. Soil pressure is considered using vertical and lateral pressure (to provide in-situ conditions with close to zero deflections under soil self-weight).

Live Load: Wheel load is modeled as a discrete patch load over a 10"x20" area. A load case with single axle load in two lanes and a load case with standard HL-93 truck moving load is applied to the model. The

truck load is moved across the culvert to capture the critical loading condition. The live load will be updated when the wheel load of the actual truck that is used in the experiment is determined.

Results

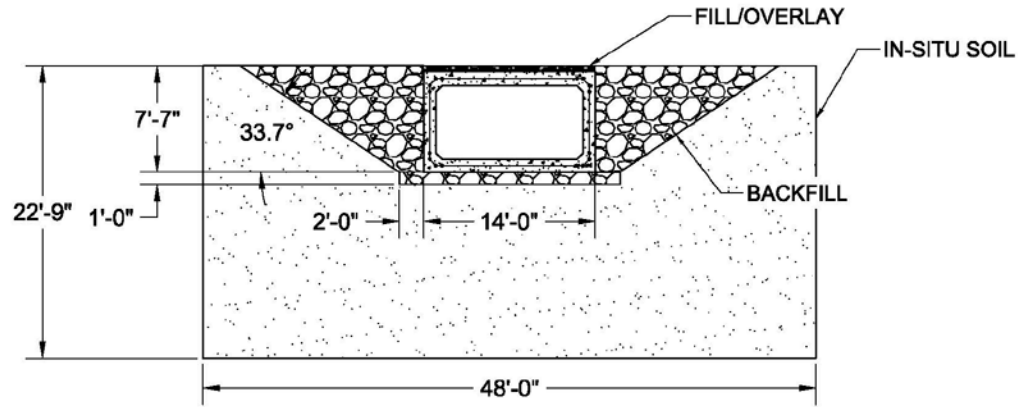
Figures 55 to 71 present the behavior of M3C1 in terms of displacement, strains and stresses under axle load at center of the culvert. Due to the skew, the axle loads are positioned so that the center of each axle passes through the centerline of culvert. Because for nonlinear analysis, all loads must be applied sequentially, gravity and dead loads are applied first, then live load is applied and the final results are under both dead load and live load. Given that for experimental study, only the effect of live load is measured, a load combination is defined in Lusas that removes the effect of dead load by subtracting the results of “dead load analysis” from the results after application of live load.

It should be noted that maximum and minimum envelopes of results under moving loads are available, however, given that Lusas develops two separate envelopes for maximum and minimum, contour presentation may become misleading, unless both envelopes are compared side by side. This is especially important when the dead load effects (constant) are being deduced from the total “dead + live load” results. Results of envelop results of moving loads will be presented later where a specific entity or stage of loading is determined.

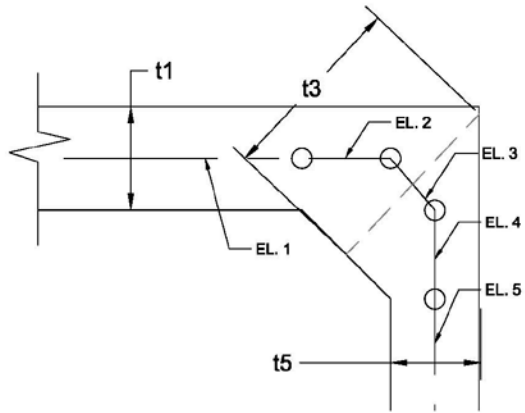
Table 3. M3C1- Material Properties of Backfill and In-Situ Soil

Properties	Backfill: 0-1 ft	Backfill: 1-6 ft	Backfill: 6-11 ft	In-Situ Soil
Modulus of Elasticity, E (ksf)	230.4	576.0	864.0	864.0
Poisson's Ratio (v)	0.4	0.29	0.24	0.25
Unit Weight (pcf)	121	121	121	127
Initial Cohesion (psf)	0.000144	0.000144	0.000144	-
Initial Friction Angle	40	40	40	-
Final Friction Angle	40	40	40	-
Dilation Angle	10	10	10	-
Cohesion Hardening (psf)	0	0	0	-
Limiting Plastic Strain	0.001	0.001	0.001	-

Appendix E - 3D Modeling Backup



(a) Cross Section



(b) Culvert Thickness Assignment

Thickness of Culvert Shell Elements	
Element #	Thickness
EL. 1	t1 (1'-1½")
EL. 2	½[t1+t3] (1'-5⅝")
EL. 3	t3 (1'-9¼")
EL. 4	½[t3+t5] (1'-4⅝")
EL. 5	t5 (1'-0")

Figure 54. M3C1- Geometry and Culvert Thickness Assignment

Appendix E - 3D Modeling Backup

2Lane Axle at Center
Entity: Displacement
Component: RSLT (Units: ft)

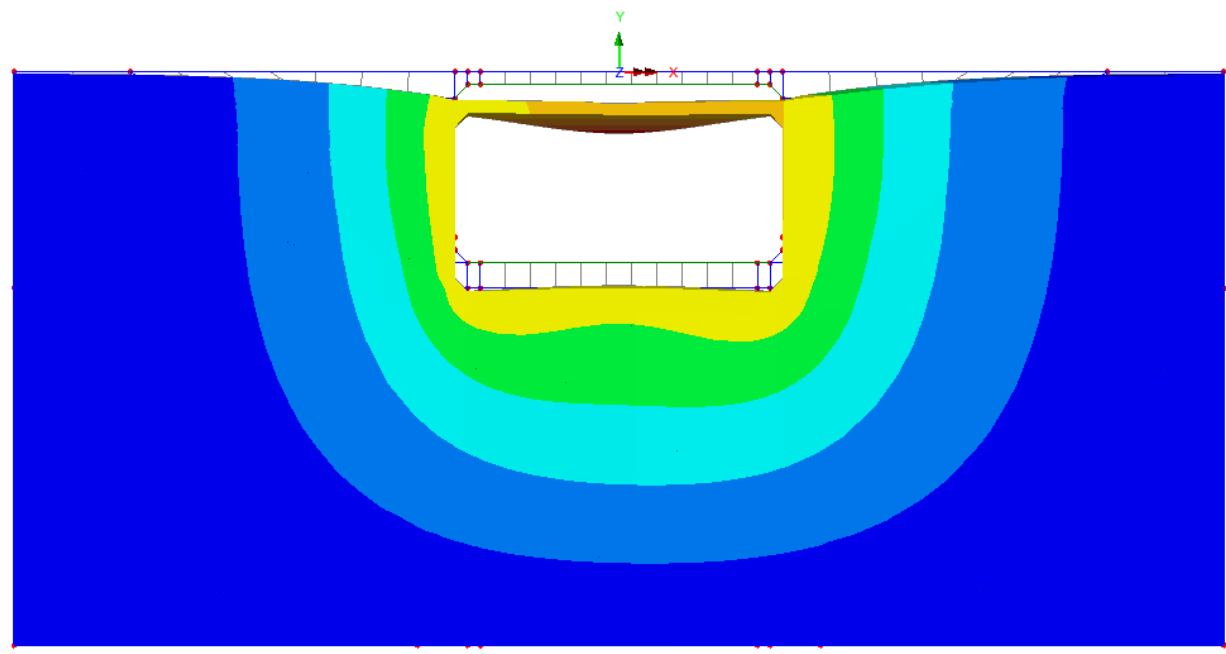
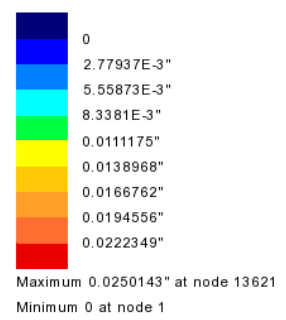


Figure 55. M3C1- Resultant Displacement of Solid Elements – 2 Lane 32 k Axle at Center of Culvert

Appendix E - 3D Modeling Backup

2Lane Axle at Center
Entity: Displacement
Component: DY (Units: ft)

Dark Blue	-0.0250141"
Blue	-0.0222348"
Cyan	-0.0194554"
Light Blue	-0.0166761"
Green	-0.0138967"
Yellow-Green	-0.0111174"
Yellow	-8.33804E-3"
Orange	-5.55869E-3"
Red	-2.77935E-3"

Maximum 0 at node 1
Minimum -0.0250141" at node 13621

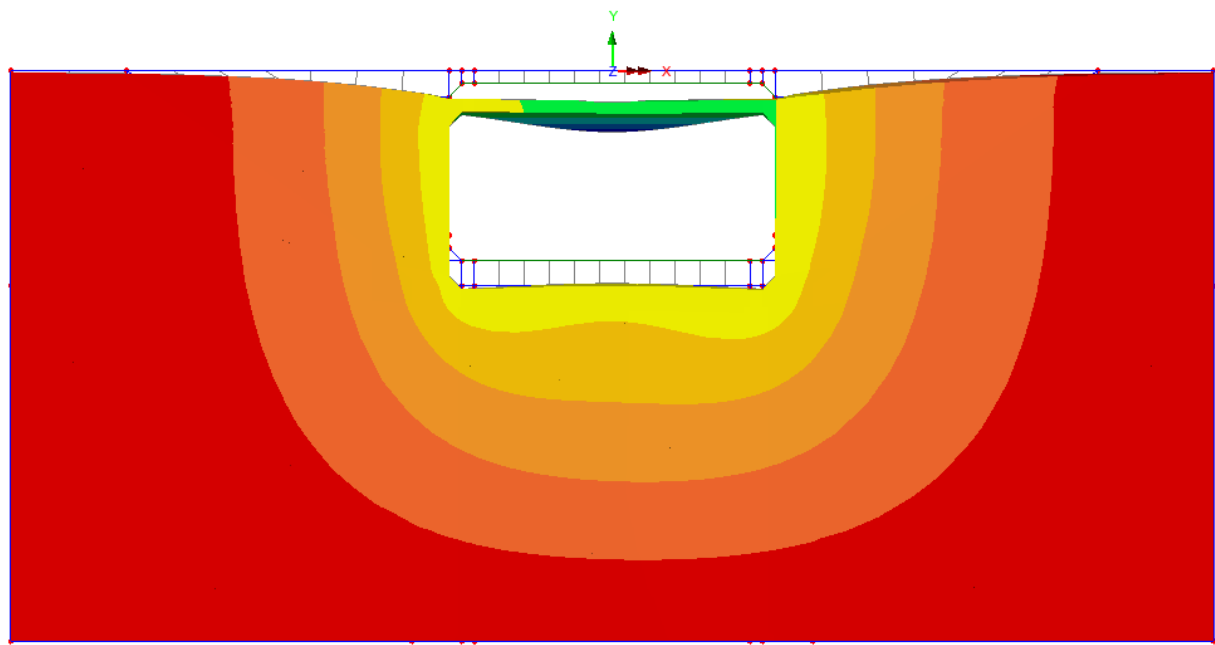
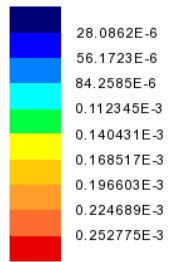


Figure 56. M3C1- Vertical Displacement of Solid Elements - 2 Lane 32 k Axle at Center of Culvert

Appendix E - 3D Modeling Backup

2Lane Axle at Center
Entity: Strain - Solids
Component: EE



Maximum 0.253133E-3 at node 18594
Minimum 0.357342E-6 at node 6717

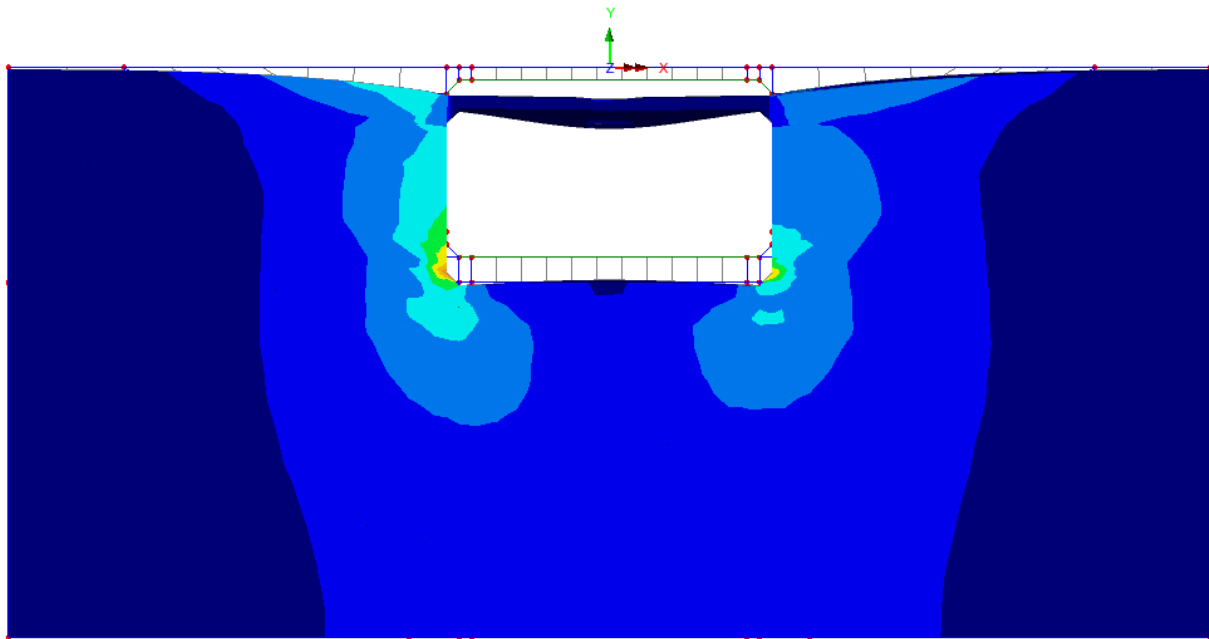
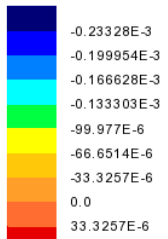


Figure 57. M3C1- Von Mises Strain of Solid Elements- 2 Lane 32 k Axle at Center of Culvert

Appendix E - 3D Modeling Backup

2Lane Axle at Center
Entity: Strain - Solids
Component: EY



Maximum 59.367E-6 at node 13642
Minimum -0.240564E-3 at node 10843

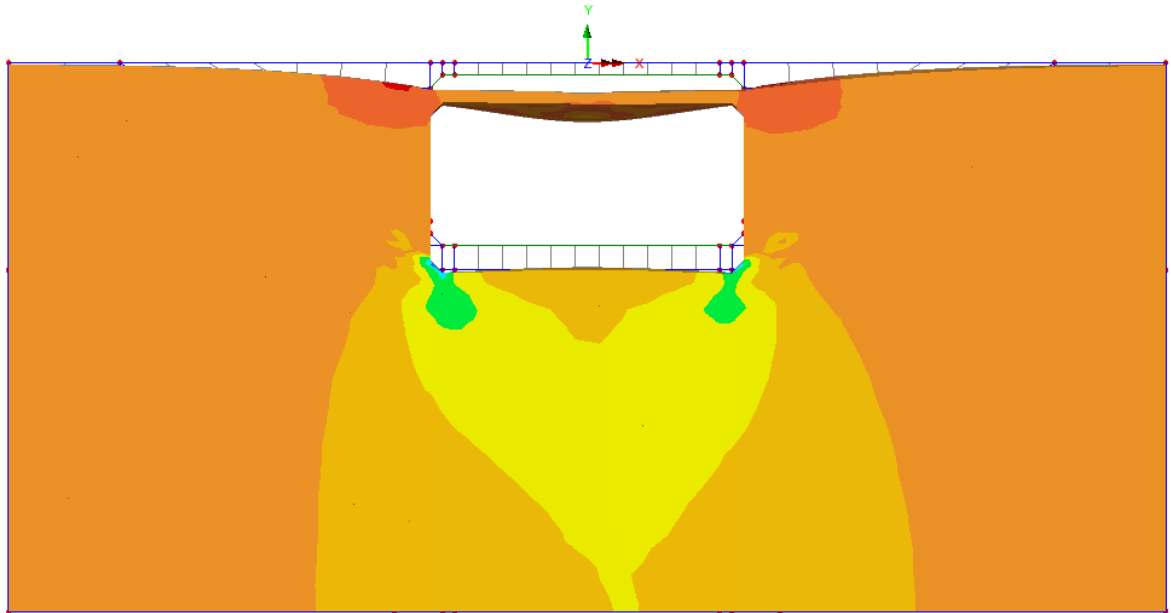
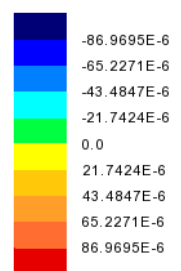


Figure 58. M3C1- Vertical Strain (EV) of Solid Elements- 2 Lane 32 k Axle at Center of Culvert

Appendix E - 3D Modeling Backup

2Lane Axle at Center
Entity: Strain - Solids
Component: EX



Maximum 0.105734E-3 at node 18280
Minimum -89.9472E-6 at node 12541

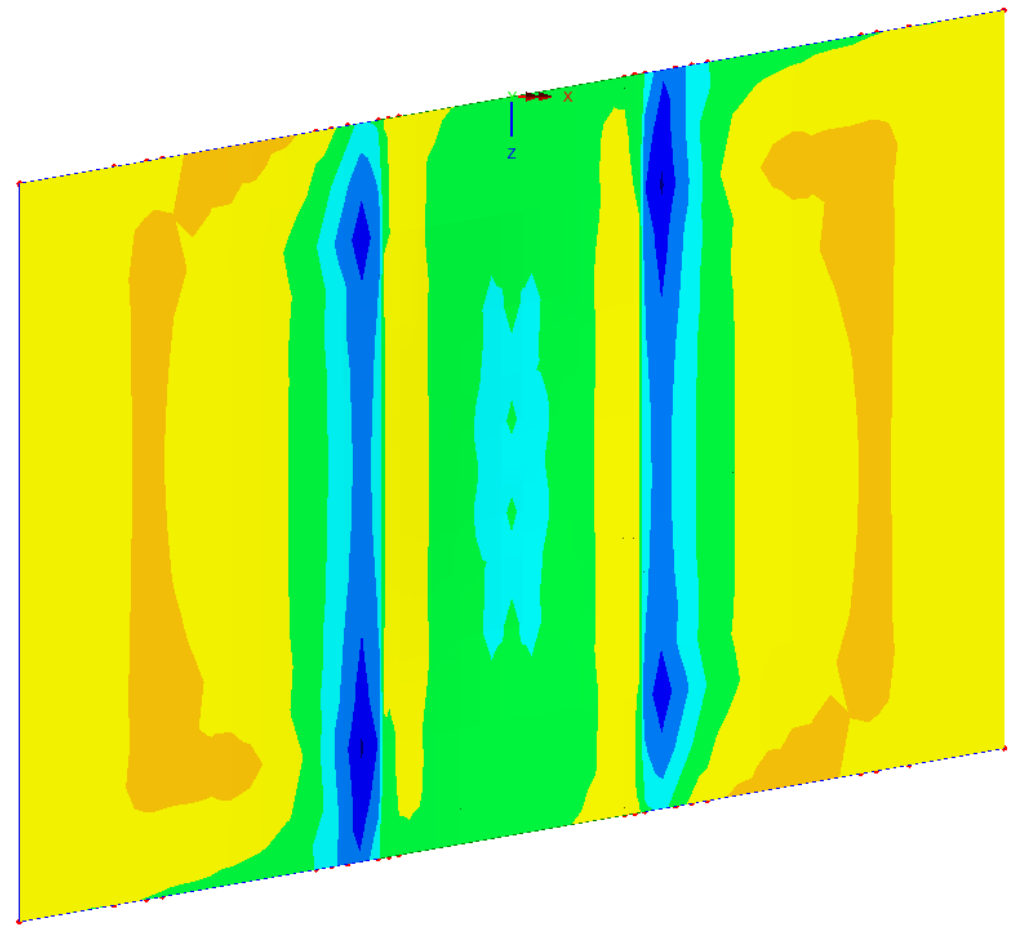
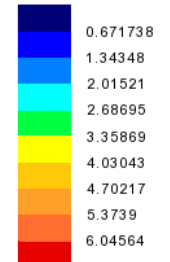


Figure 59. M3C1- Horizontal Strain (EX) of Solid Elements- 2 Lane 32 k Axle at Center of Culvert

Appendix E - 3D Modeling Backup

2Lane Axle at Center
Entity: Stress - Solids
Component: SE (Units: kip/ft²)



Maximum 6.04601 at node 12982
Minimum 0.370492E-3 at node 6717

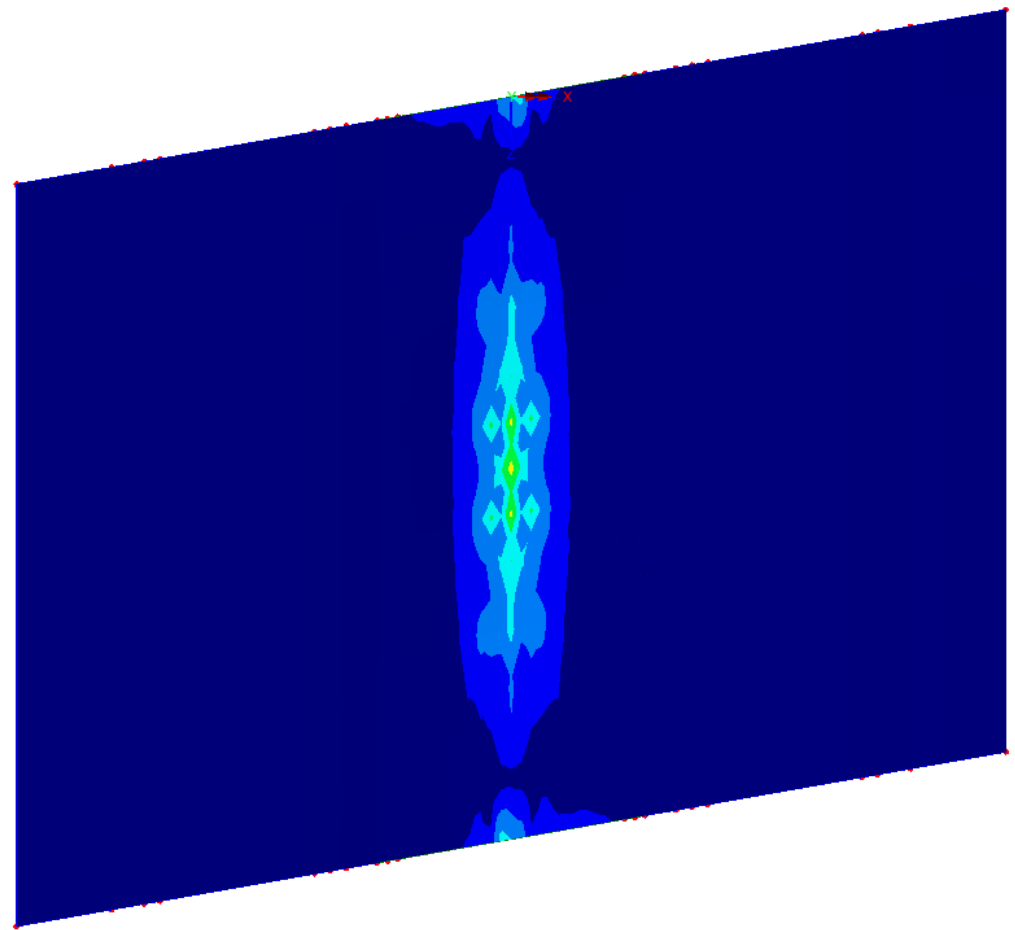
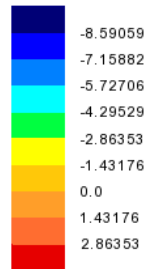


Figure 60. M3C1- Von Mises Stress of Solid Elements- 2 Lane 32 k Axle at Center of Culvert

Appendix E - 3D Modeling Backup

2Lane Axle at Center
Entity: Stress - Solids
Component: SY (Units: kip/ft²)



Maximum 3.39911 at node 13642
Minimum -9.48677 at node 13621

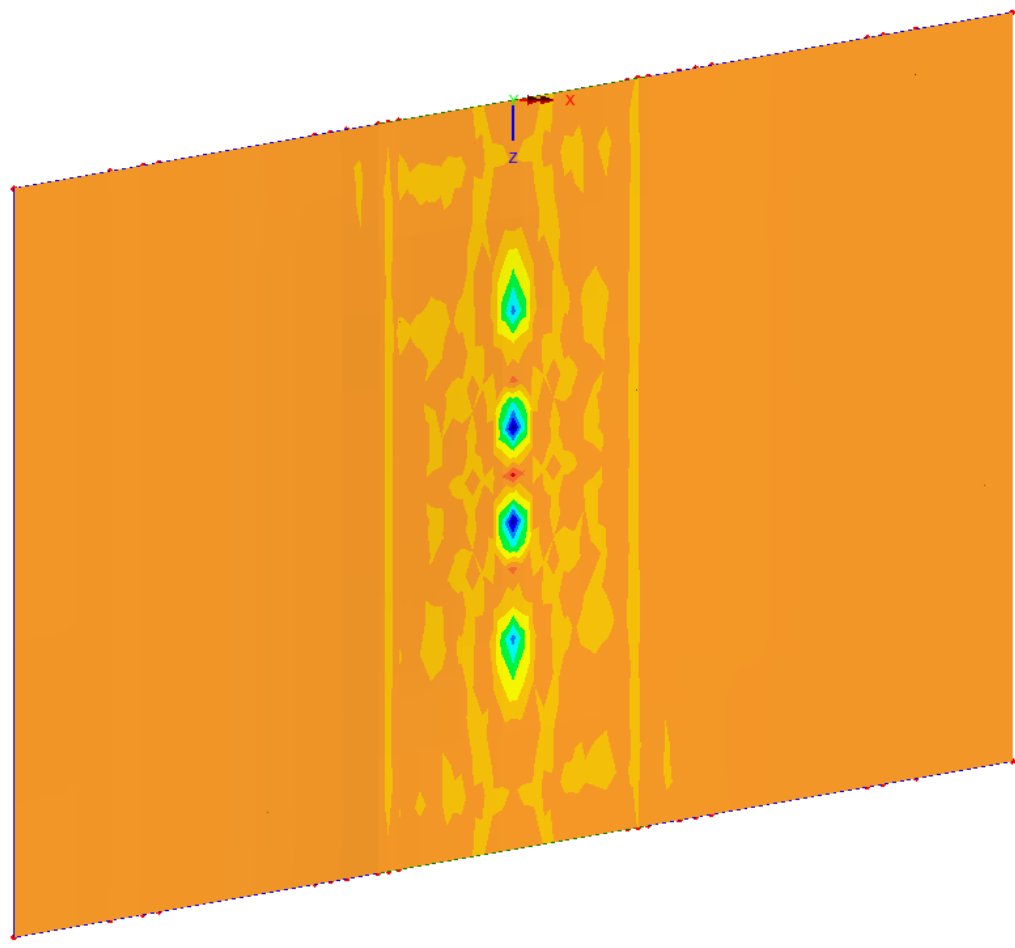
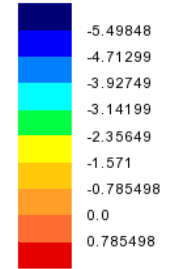


Figure 61. M3C1- Vertical Stress (SY) of Solid Elements- 2 Lane 32 k Axle at Center of Culvert

Appendix E - 3D Modeling Backup

2Lane Axle at Center
Entity: Stress - Solids
Component: SX (Units: kip/ft²)



Maximum 0.950522 at node 13114
Minimum -6.11896 at node 13621

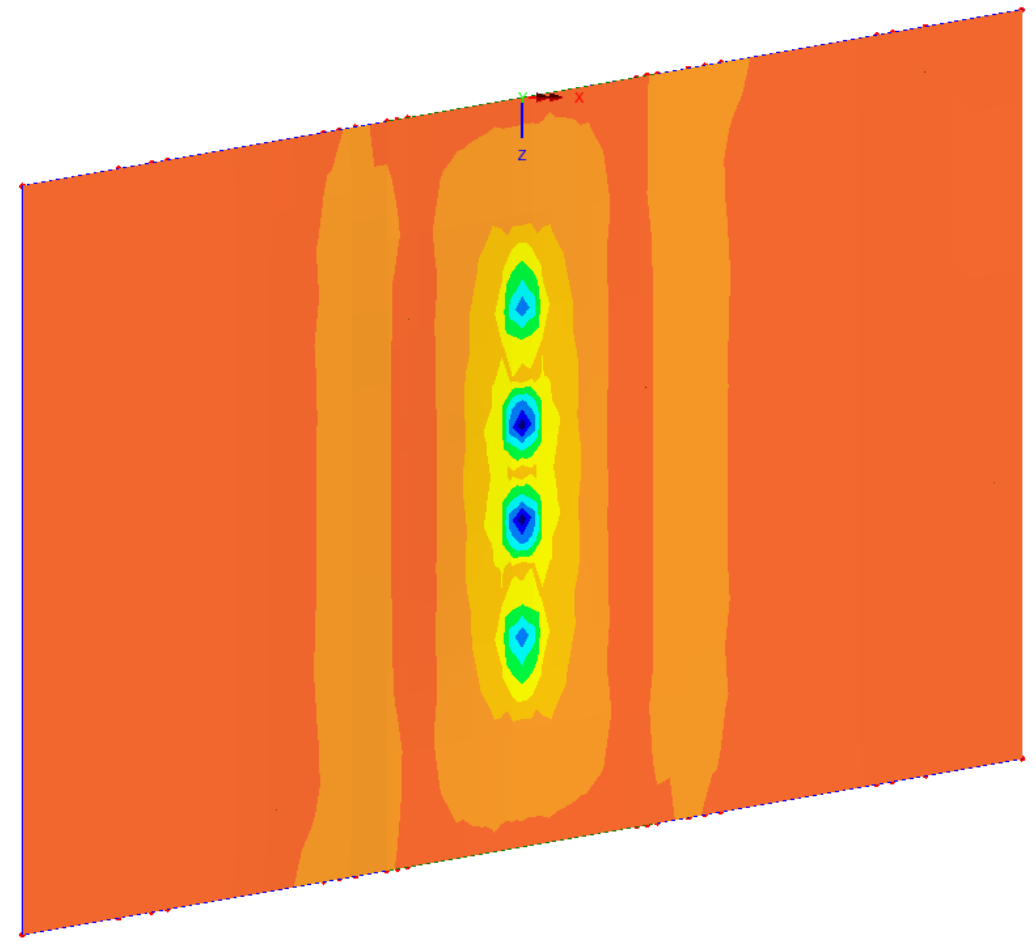
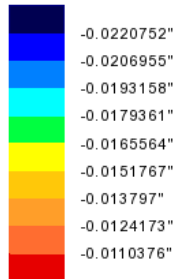


Figure 62. M3C1- Horizontal Stress (SX) of Solid Elements- 2 Lane 32 k Axle at Center of Culvert

Appendix E - 3D Modeling Backup

2Lane Axle at Center
Entity: Displacement
Component: DY (Units: ft)



Maximum -0.0108927" at node 19423
Minimum -0.02331" at node 19755

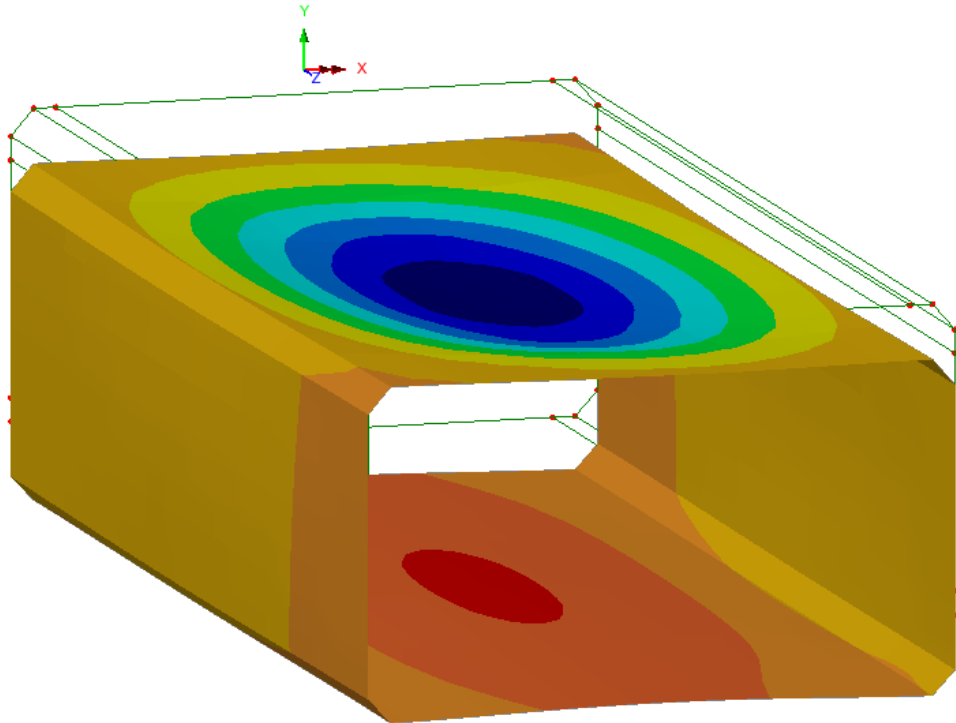
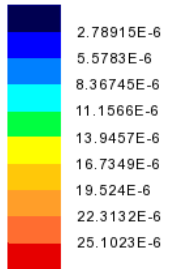


Figure 63. M3C1- Vertical Displacement of Culvert- 2 Lane 32 k Axle at Center of Culvert

Appendix E - 3D Modeling Backup

2Lane Axle at Center
Entity: Strain (top) - Thick Shell
Component: EE



Maximum 25.2321E-6 at node 19755
Minimum 0.129706E-6 at node 19169

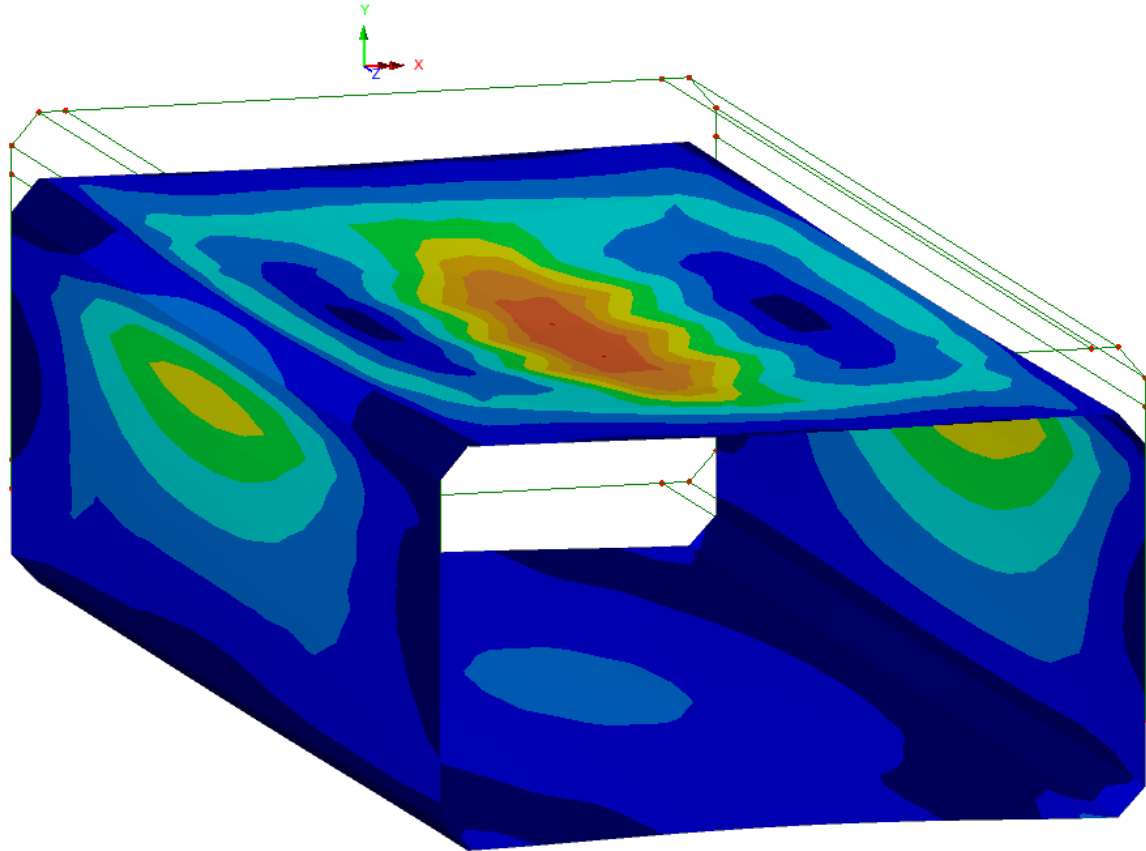


Figure 64. M3C1- Von Mises Strain at Top Fiber in Culvert- 2 Lane 32 k Axle at Center of Culvert

Appendix E - 3D Modeling Backup

2Lane Axle at Center
Entity: Strain (bottom) - Thick Shell
Component: EE

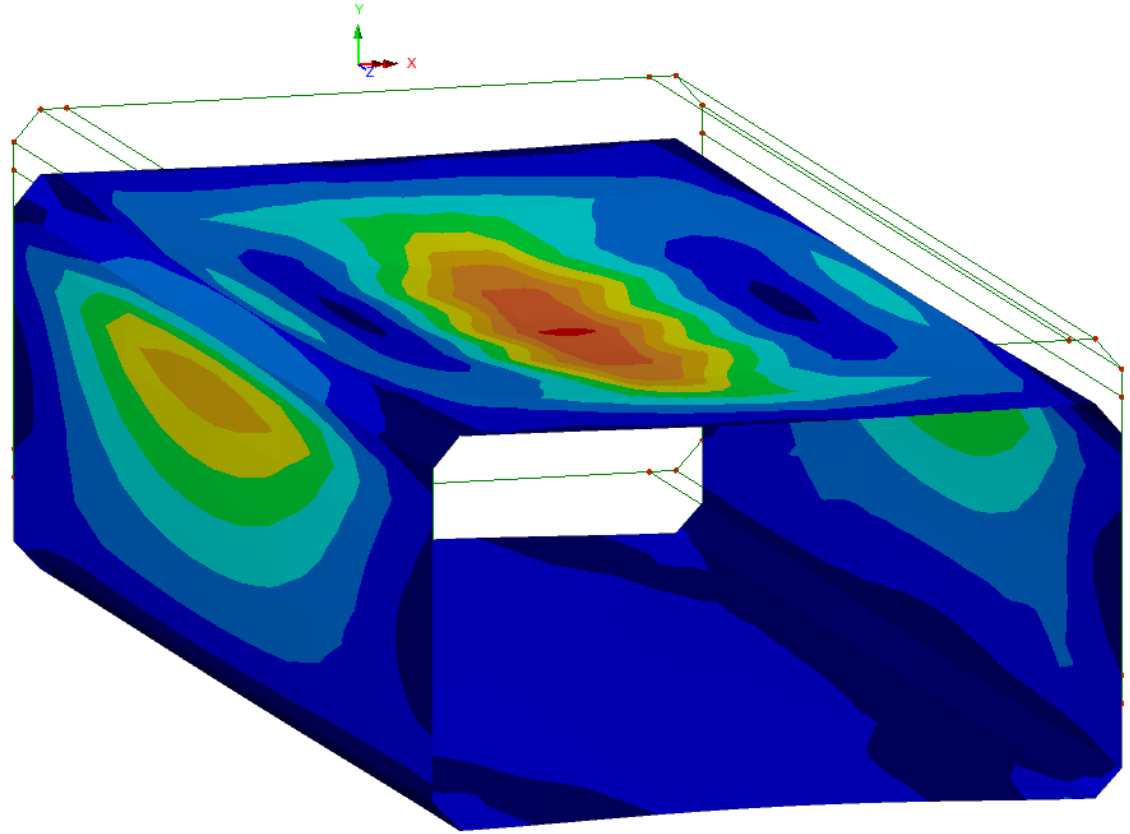
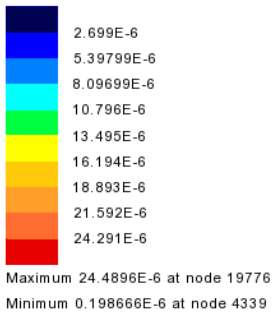


Figure 65. M3C1- Von Mises Strain at Bottom Fiber in Culvert- 2 Lane 32 k Axle at Center of Culvert

Appendix E - 3D Modeling Backup

2Lane Axle at Center
Entity: Strain (top) - Thick Shell
Component: EX

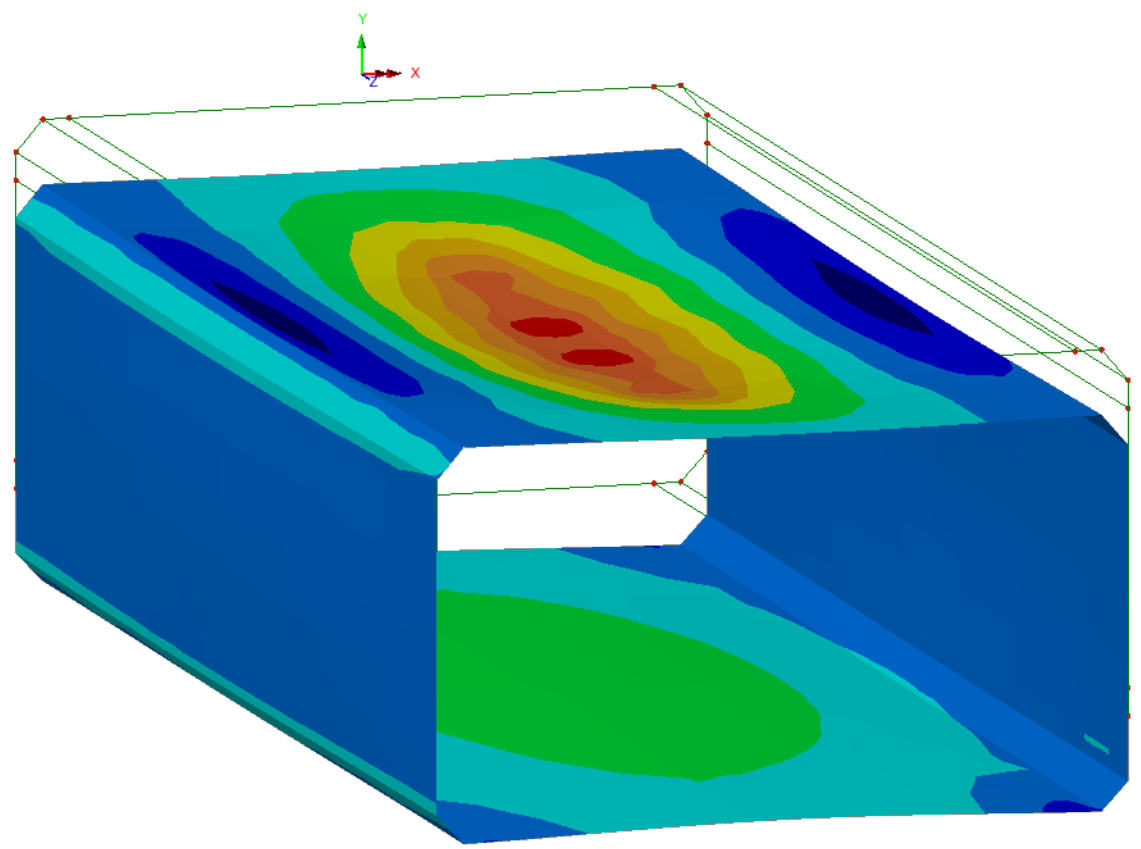
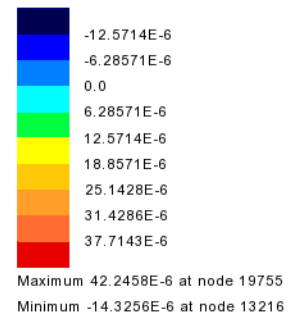
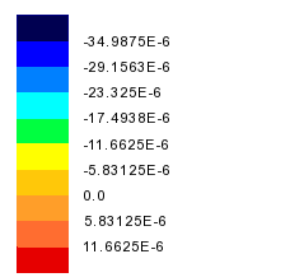


Figure 66. M3C1- Bending Strain at Top Fiber in Culvert- 2 Lane 32 k Axle at Center of Culvert

Appendix E - 3D Modeling Backup

2Lane Axle at Center
Entity: Strain (bottom) - Thick Shell
Component: EX



Maximum 12.5932E-6 at node 13216
Minimum -39.8881E-6 at node 19797

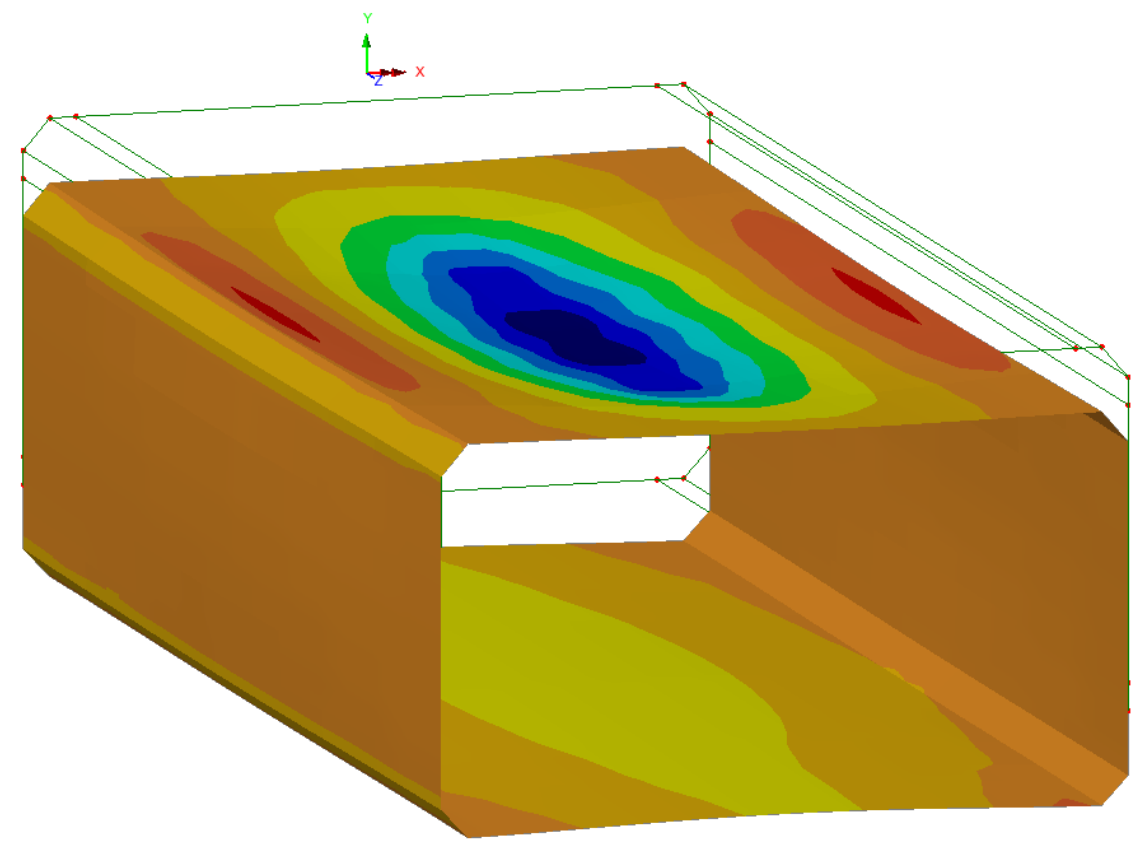


Figure 67. M3C1- Bending Strain at Bottom Fiber in Culvert- 2 Lane 32 k Axle at Center of Culvert

Appendix E - 3D Modeling Backup

2Lane Axle at Center
Entity: Stress (top) - Thick Shell
Component: SE (Units: kip/ft²)

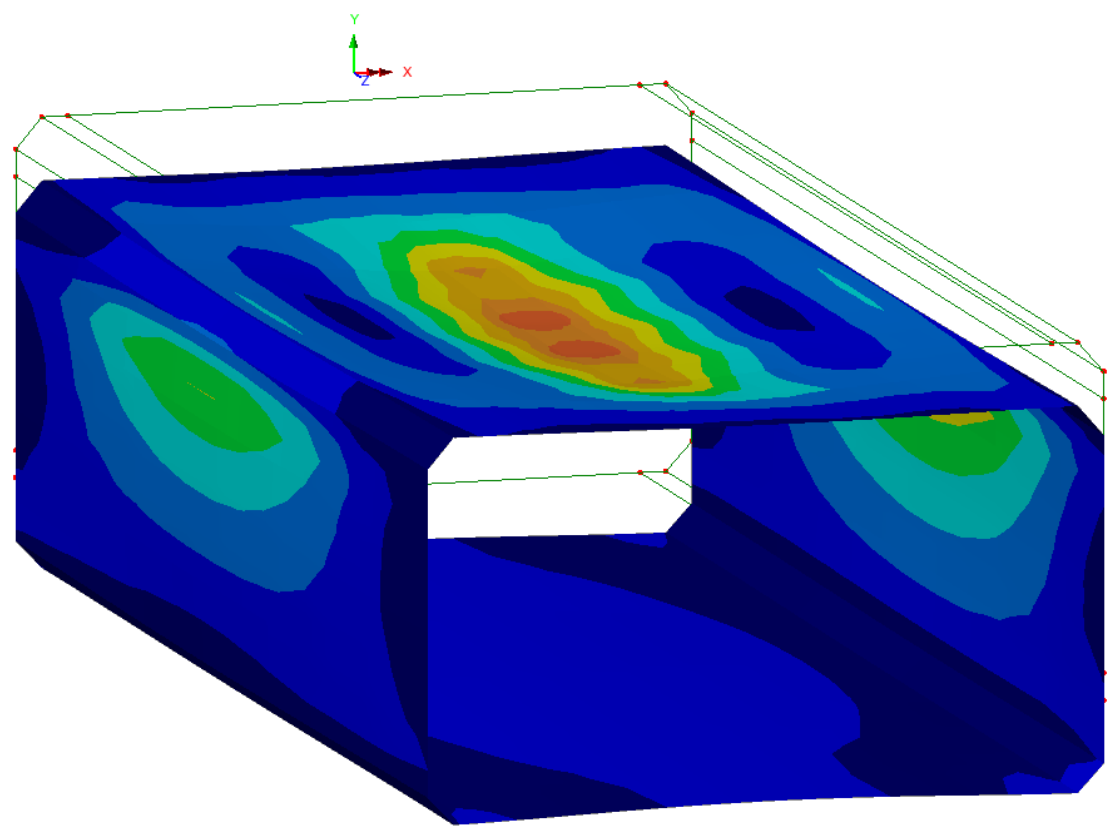
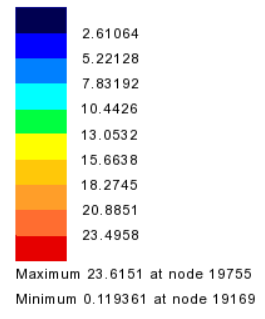


Figure 68. M3C1- Von Mises Stress at Top Fiber in Culvert- 2 Lane 32 k Axle at Center of Culvert

Appendix E - 3D Modeling Backup

2Lane Axle at Center
Entity: Stress (bottom) - Thick Shell
Component: SE (Units: kip/ft²)

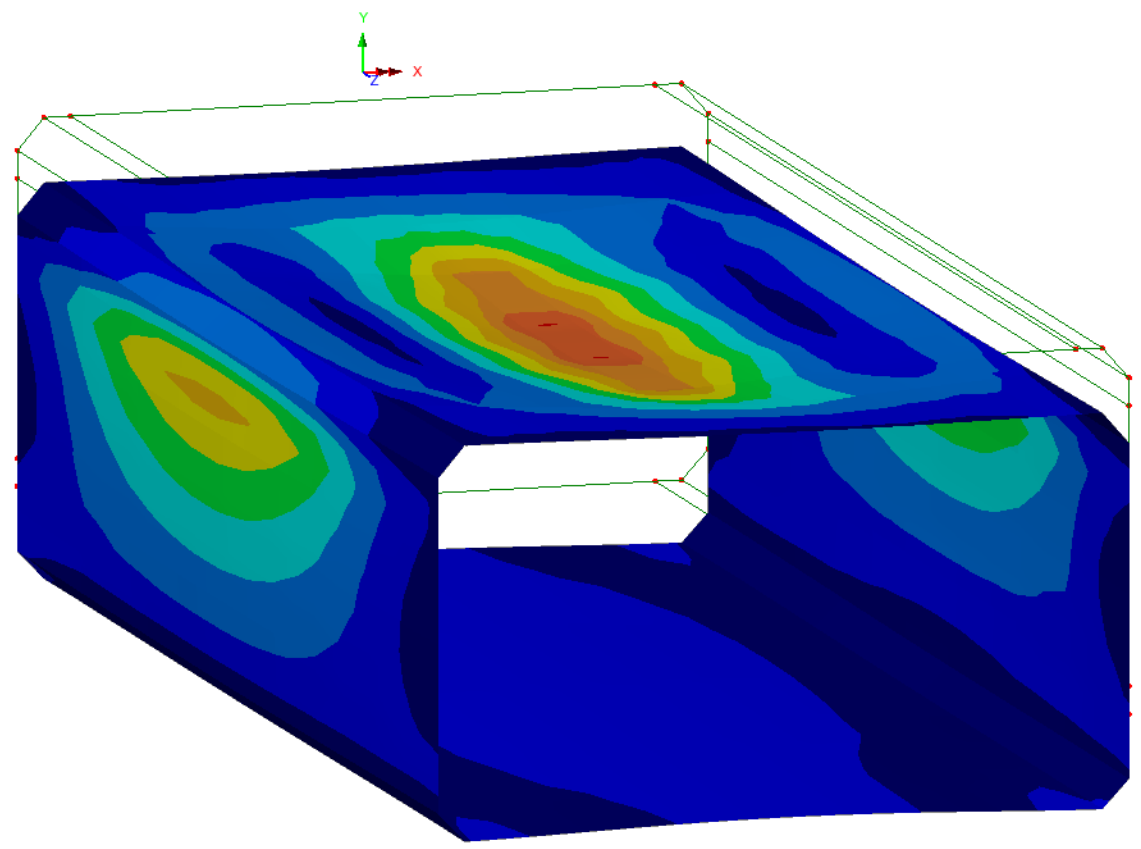
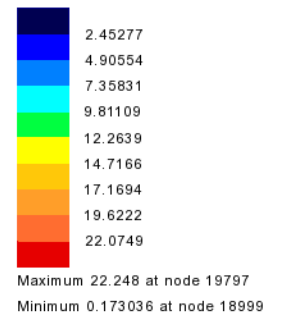


Figure 69. M3C1- Von Mises Stress at Bottom Fiber in Culvert- 2 Lane 32 k Axle at Center of Culvert

Appendix E - 3D Modeling Backup

2Lane Axle at Center
Entity: Stress (top) - Thick Shell
Component: SX (Units: kip/ft²)

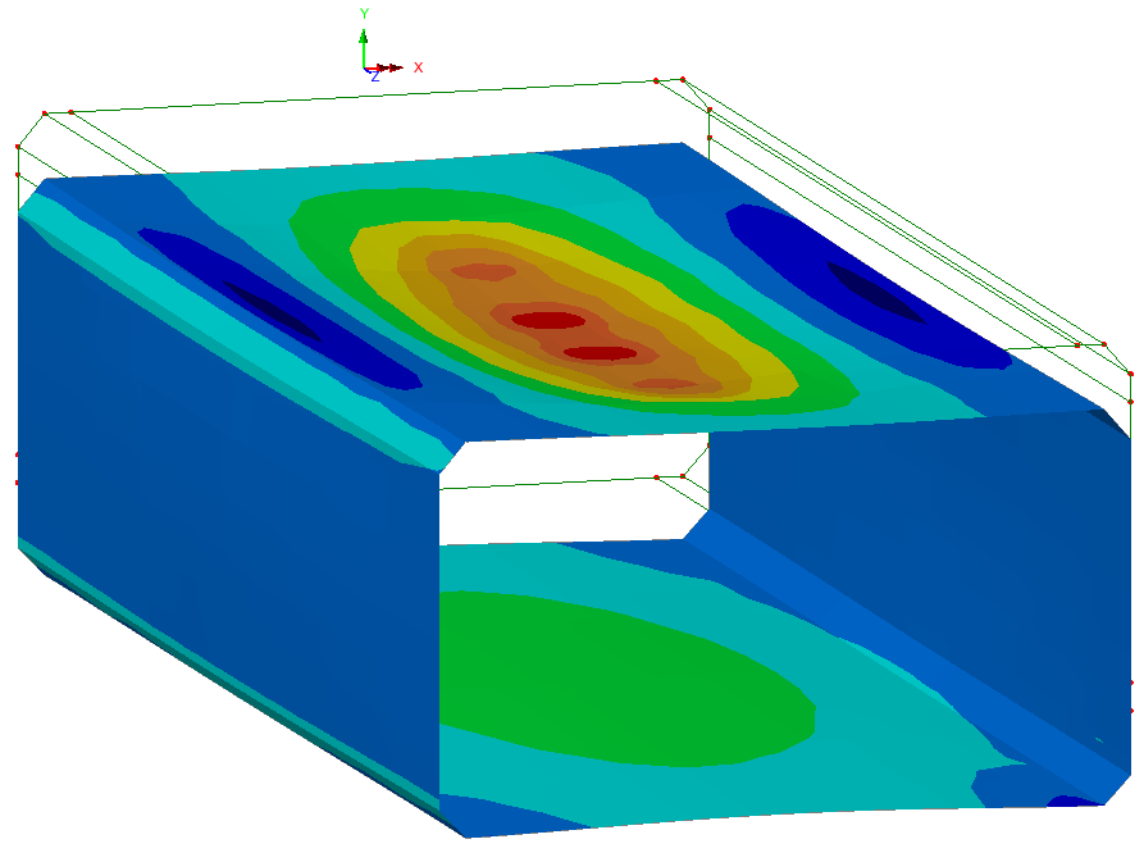
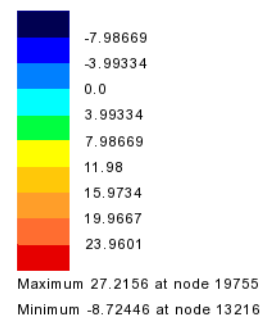
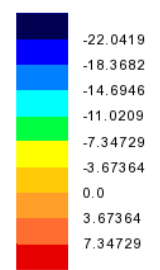


Figure 70. M3C1- Bending Stress at Top Fiber in Culvert- 2 Lane 32 k Axle at Center of Culvert

Appendix E - 3D Modeling Backup

2Lane Axle at Center
Entity: Stress (bottom) - Thick Shell
Component: SX (Units: kip/ft²)



Maximum 7.45468 at node 13216
Minimum -25.6081 at node 19797

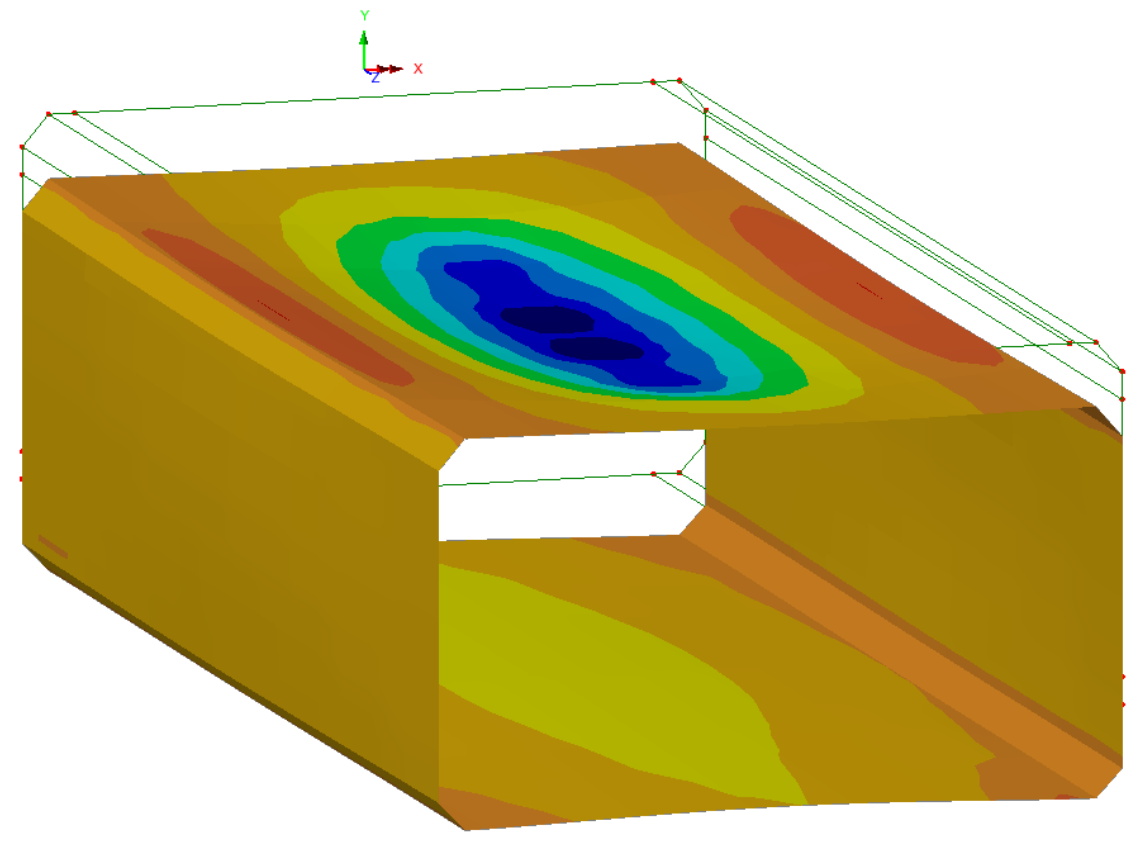


Figure 71. M3C1- Bending Stress at Bottom Fiber in Culvert- 2 Lane 32 k Axle at Center of Culvert

MODEL 6- CANDIDATE 2 (M6C2)

Model 6 represents a prototype of corrugated metal box culverts. Candidate 2 is selected for this category.

Geometry

Geometry and layout of Model 6 Candidate 2 (M6C2) is presented in Appendix D. Figure 72 presents the section of the culvert and the equivalent geometry that is modeled in Lusas. Thickness of the corrugated metal sheet and modulus of elasticity are adjusted to capture the behavior of the corrugated metal sheet.

The Lusas model includes the entire length of the culvert. As shown in Figure 72, the span of culvert is 19' and the depth of the model extends to 23'-7.5". Laterally, the geometry extends to 37'-6" on each side. Therefore, the cross section of model is 23'-7.5"x75' and the length is 44'-3". A concrete 2'Wx1.5'D footing is modeled at each end of the arch culvert. A 1'-6" deep pavement is assumed over the culvert, where the live load is applied to the structure. The slope of backfill is assumed 45°.

Material Properties

Given that corrugated metal sheets have different axial and flexural behavior in two directions, orthotropic material properties are used to define the behavior of the culvert. For Model 6, a Lusas model using the appropriate corrugated aluminum sheet sections and type IV ribs was generated and a point load was applied at the center of the section. Using the model with the corrugations, a model with thin shell sections was generated and its material properties adjusted until deflections on both models were similar (Figure 74). Corrugated cross sections and simulated plate cross sections for top and bottom part of the culvert are shown in Figure 73. The following steps were taken to generate thin shell sections that will produce similar deflections:

- 1- Elastic modulus in the x direction was set as 9,940 ksi, which is the elastic modulus of aluminum.
- 2- Thickness of the thin shell element was adjusted until vertical deflections match vertical deflections of the corrugated sheet section model. The thickness values that would provide similar results were 3" for top sheets and 2.25" for side sheets.
- 3- Elastic modulus in the y direction was modified until deflections in this direction match deflections obtained from the corrugated sheet section model. The elastic modulus in the y direction was selected as 1/100,000 of the elastic modulus in the x direction.

Overlay and pavement is defined as a linear material with modulus of elasticity (E) = 4000 ksi, Poisson's ratio (ν) = 0.35, and unit weight = 140 pcf.

The linear material properties of concrete footings are generated based on AASHTO LRFD Bridge Design Specifications for compressive strength of $f'_c = 5$ ksi: modulus of elasticity (E) = 4074 ksi, Poisson's ratio (ν) = 0.2, unit weight = 150 pcf, and coefficient of thermal expansion (α) = 10.8 e-6 1/C.

Table 4 presents the material properties of in-situ soil and backfill. In-situ soil is defined as an elastic material, while nonlinear material properties are considered for backfill, varying with depth. The values in Table 4 are adopted from previous study by McGrath et al. (2005).

Mesh

Quadrilateral quadratic thin shell elements are used to model the culvert. Given that the corrugated metal sheet is quite thin, transferred shear through the section is minimal, hence thin shell element may effectively capture the behavior of the culvert.

Hexahedral quadratic solid elements are used to model the pavement (overlay), footings, in-situ soil, and backfill. Due to limitation of number of elements and large dimensions for M7C1, the mesh size is set to 1' around the culverts and in backfill and 4' at the boundaries. The mesh size along the length of culvert is 5'-6".

Boundary Condition

At the end of the in-situ soil medium, perpendicular restraints are used for each boundary surface, i.e. lateral restraints at vertical faces and vertical restraints at the bottom of the in-situ soil.

"Tied Mesh Constraints" are assigned between the culvert and soil as well as the culvert and overlay to assure deformation compatibility. This option assures compatible deformation of adjacent shell elements and solid elements. No contact element or interaction properties are assigned.

Load Cases

Gravity is applied as a body force. Soil pressure is considered using vertical and lateral pressure (to provide in-situ conditions with close to zero deflections under soil self-weight).

Live Load: Wheel load is modeled as a discrete patch load over a 10"x20" area. A load case with single axle load in three lanes and a load case with standard HL-93 truck moving load is applied to the model. The truck load is moved across the culvert to capture the critical loading condition. The live load will be updated when the wheel load of the actual truck that is used in the experiment is determined.

Results

Figures 77 to 93 present the behavior of M6C2 in terms of displacement, strains and stresses under axle load at center of the culvert. Due to the skew, the axle loads are positioned so that the center of each axle passes through the centerline of culvert, as shown in Figure 76. Because for nonlinear analysis, all loads must be applied sequentially, gravity and dead loads are applied first, then live load is applied and the final results are under both dead load and live load. Given that for experimental study, only the effect of live load is measured, a load combination is defined in Lusas that removes the effect of dead load by subtracting the results of "dead load analysis" from the results after application of live load.

It should be noted that maximum and minimum envelopes of results under moving loads are available, however, given that Lusas develops two separate envelopes for maximum and minimum, contour presentation may become misleading, unless both envelopes are compared side by side. This is especially important when the dead load effects (constant) are being deduced from the total "dead + live load" results. Results of envelop results of moving loads will be presented later where a specific entity or stage of loading is determined.

Table 4. M6C2- Material Properties of Backfill and In-Situ Soil

Properties	Backfill: 0-1 ft	Backfill: 1-6 ft	Backfill: 6-11 ft	In-Situ Soil
Modulus of Elasticity, E (ksf)	230.4	576.0	864.0	864.0
Poisson's Ratio (ν)	0.4	0.29	0.24	0.25
Unit Weight (pcf)	121	121	121	127
Initial Cohesion (psf)	0.000144	0.000144	0.000144	-
Initial Friction Angle	40	40	40	-
Final Friction Angle	40	40	40	-
Dilation Angle	10	10	10	-
Cohesion Hardening (psf)	0	0	0	-
Limiting Plastic Strain	0.001	0.001	0.001	-

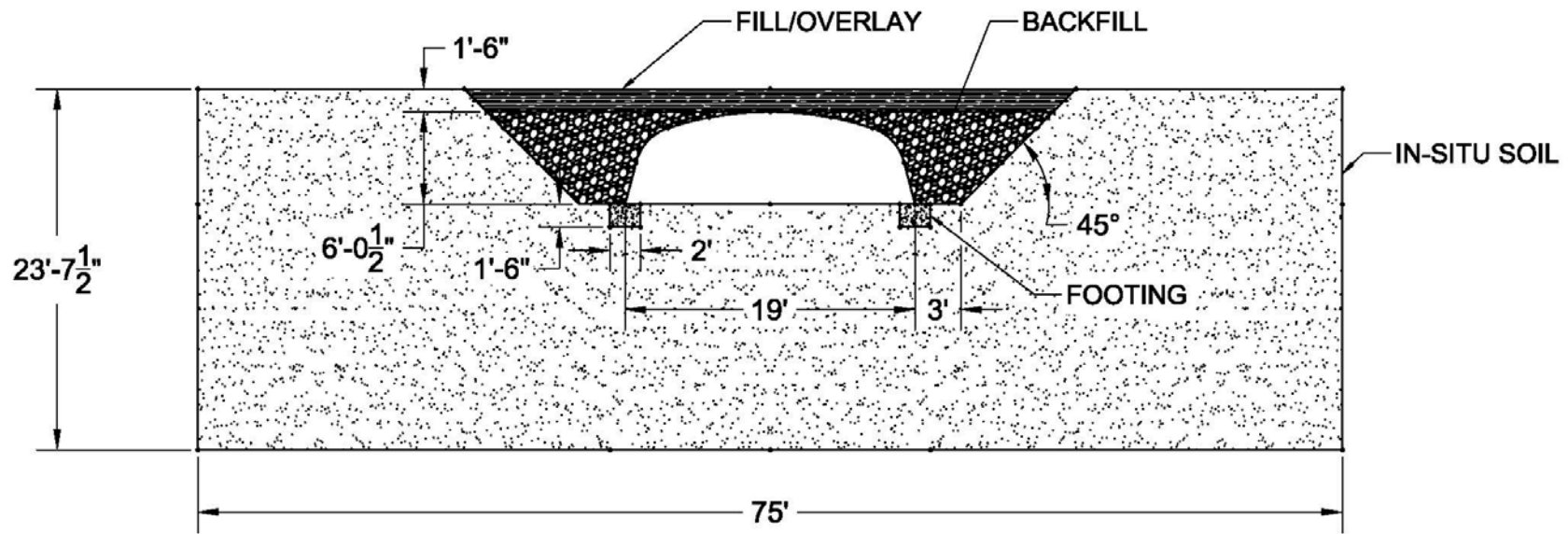


Figure 72. M6C2- Cross Section

Appendix E - 3D Modeling Backup

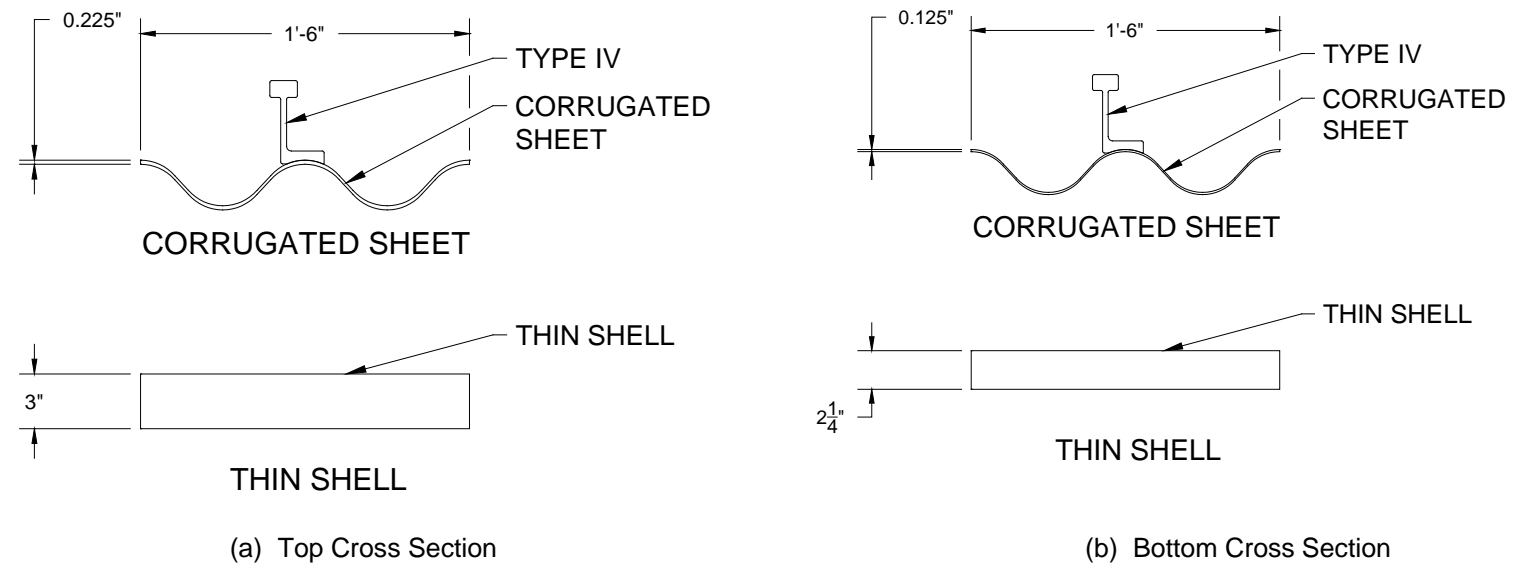


Figure 73. M6C2- Corrugated Cross Section and Simulated Plate Cross Section

Appendix E - 3D Modeling Backup

Analysis: Analysis 1
Loadcase: 1: Loadcase 1
Results file: Model 6 Candidate 2 (2a)-Analysis 1.mys
Entity: Displacement
Component: RSLT (Units: ft)

0
6.63087E-3"
0.0132617"
0.0198926"
0.0265235"
0.0331543"
0.0397852"
0.0464161"
0.053047"

Maximum 0.0596778" at node 32116
Minimum 0 at node 1

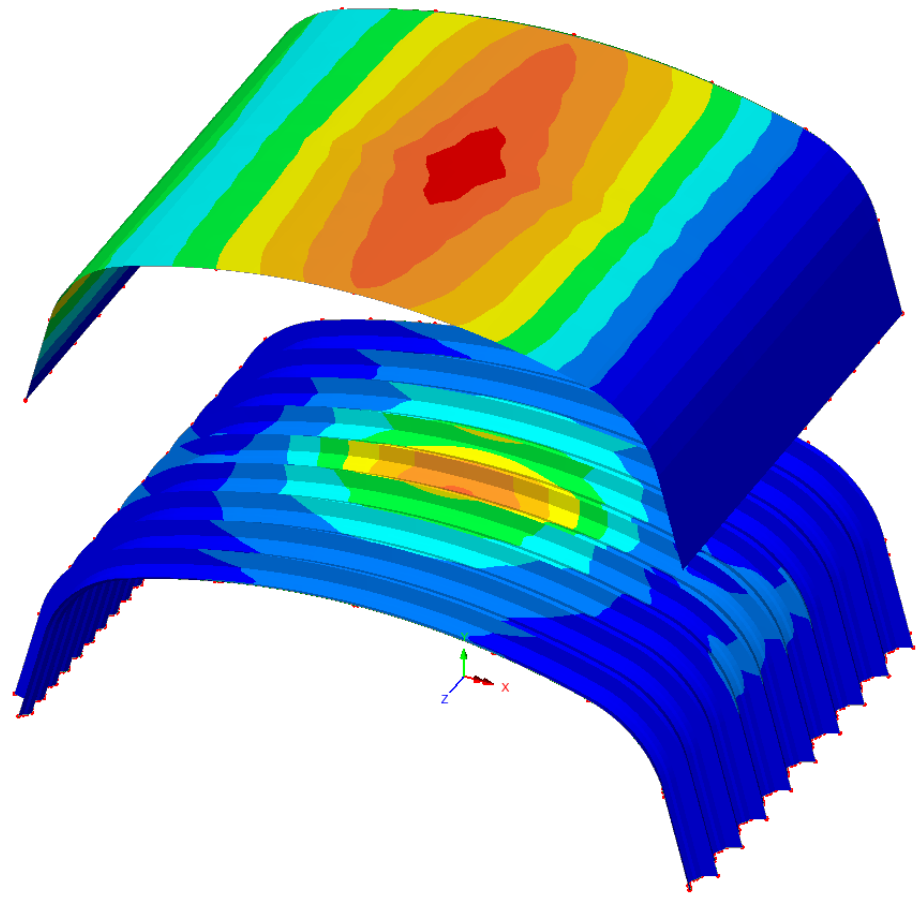


Figure 74. M6C2- Corrugation Simulation: Resultant Displacements – 1 kip Load at Center.

Appendix E - 3D Modeling Backup

Analysis: Analysis 1
Loadcase: 1: Loadcase 1
Results file: Model 6 Candidate 2 (2a)-Analysis 1.mys
Entity: Stress (top) - Thin Shell
Component: SE (Units: kip/ft²)

30.0987
60.1975
90.2962
120.395
150.494
180.592
210.691
240.79
270.889

Maximum 270.941 at node 32048
Minimum 0.0521381 at node 1692

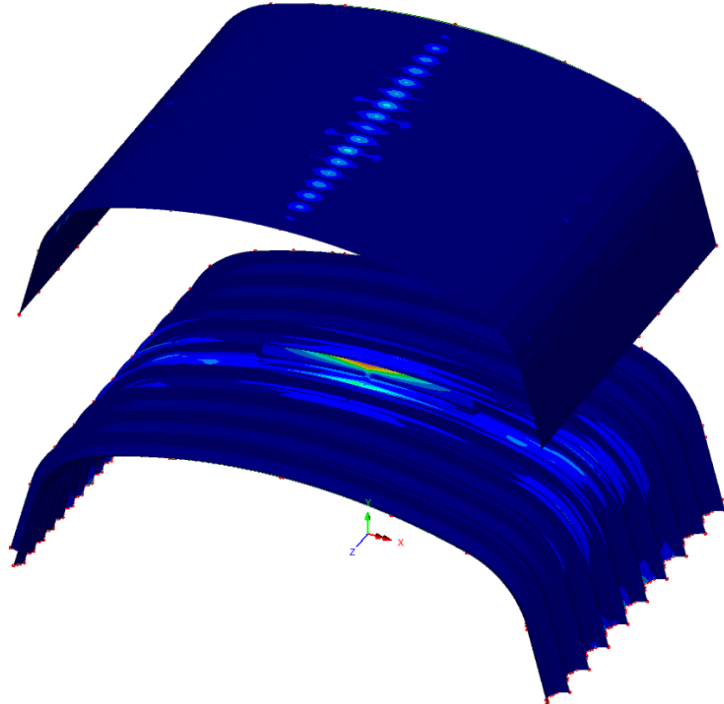


Figure 75. M6C2- Corrugation Simulation: Von Mises Stress at Top Fiber – 1 kip Load at Center.

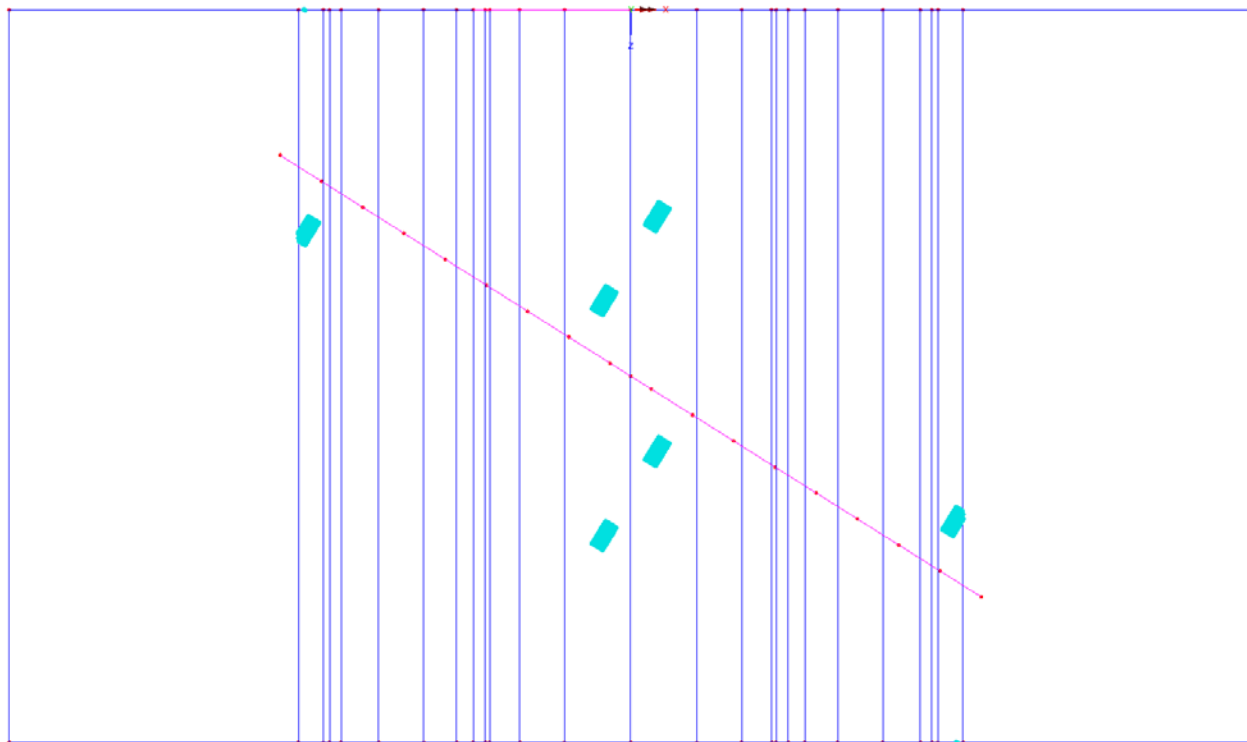


Figure 76. M6C2- Positioning of Truck Axles in Two Lanes for Maximum Mid-span Deflection

Appendix E - 3D Modeling Backup

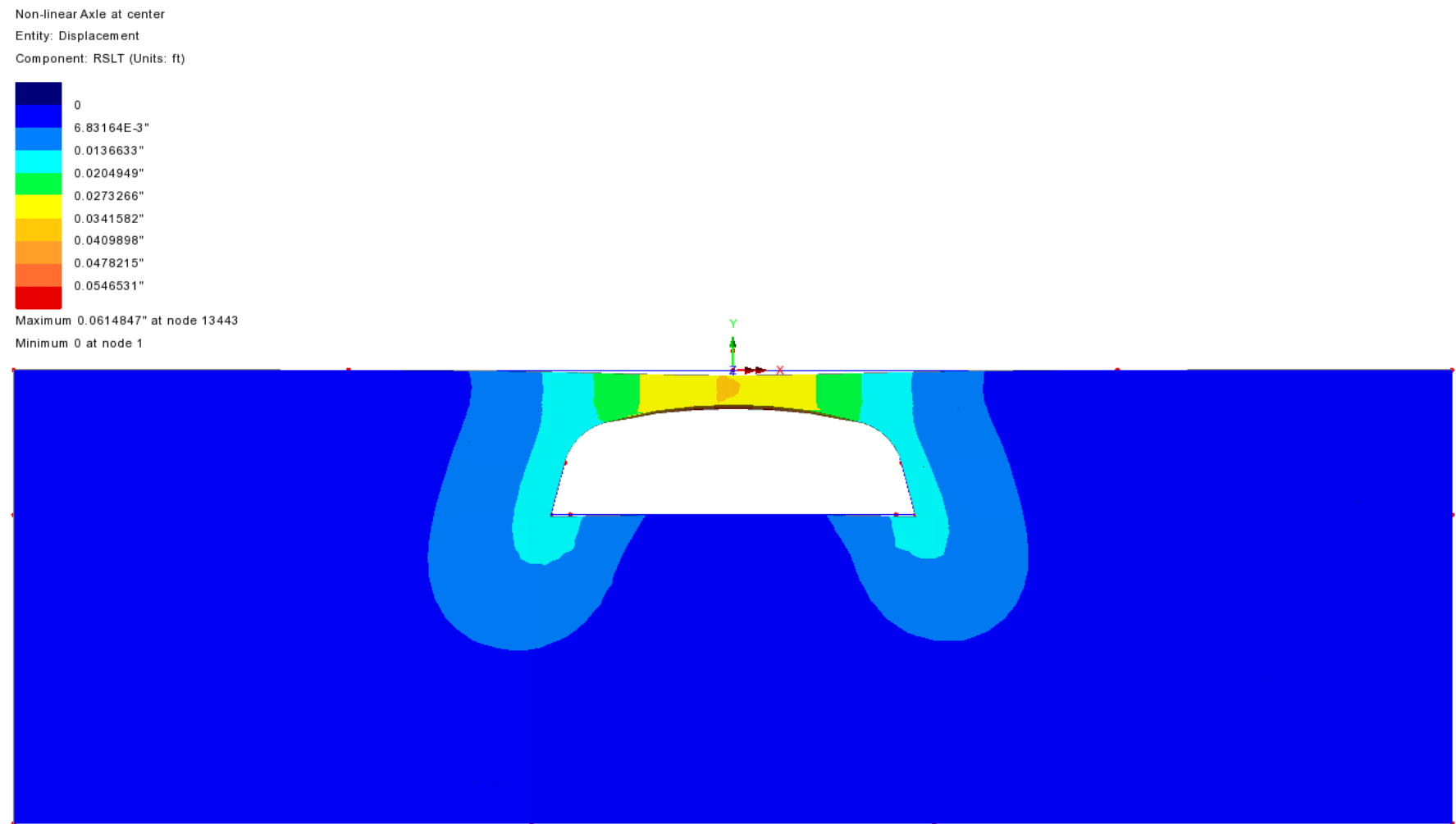


Figure 77. Resultant Displacement of Solid Elements – 2 Lane 32 k Axle at Center of Culvert

Appendix E - 3D Modeling Backup

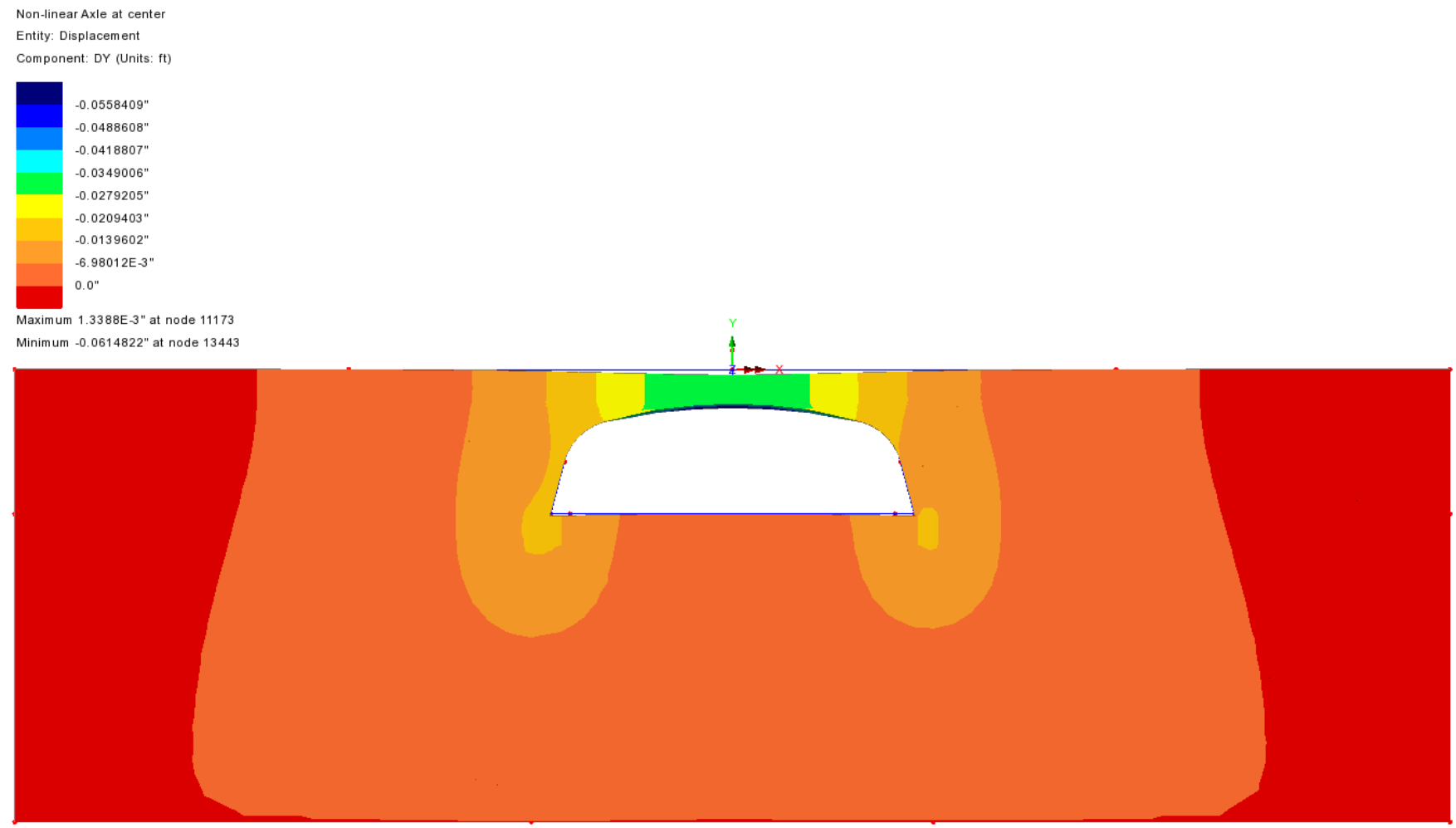


Figure 78. Vertical Displacement of Solid Elements - 2 Lane 32 k Axle at Center of Culvert

Appendix E - 3D Modeling Backup

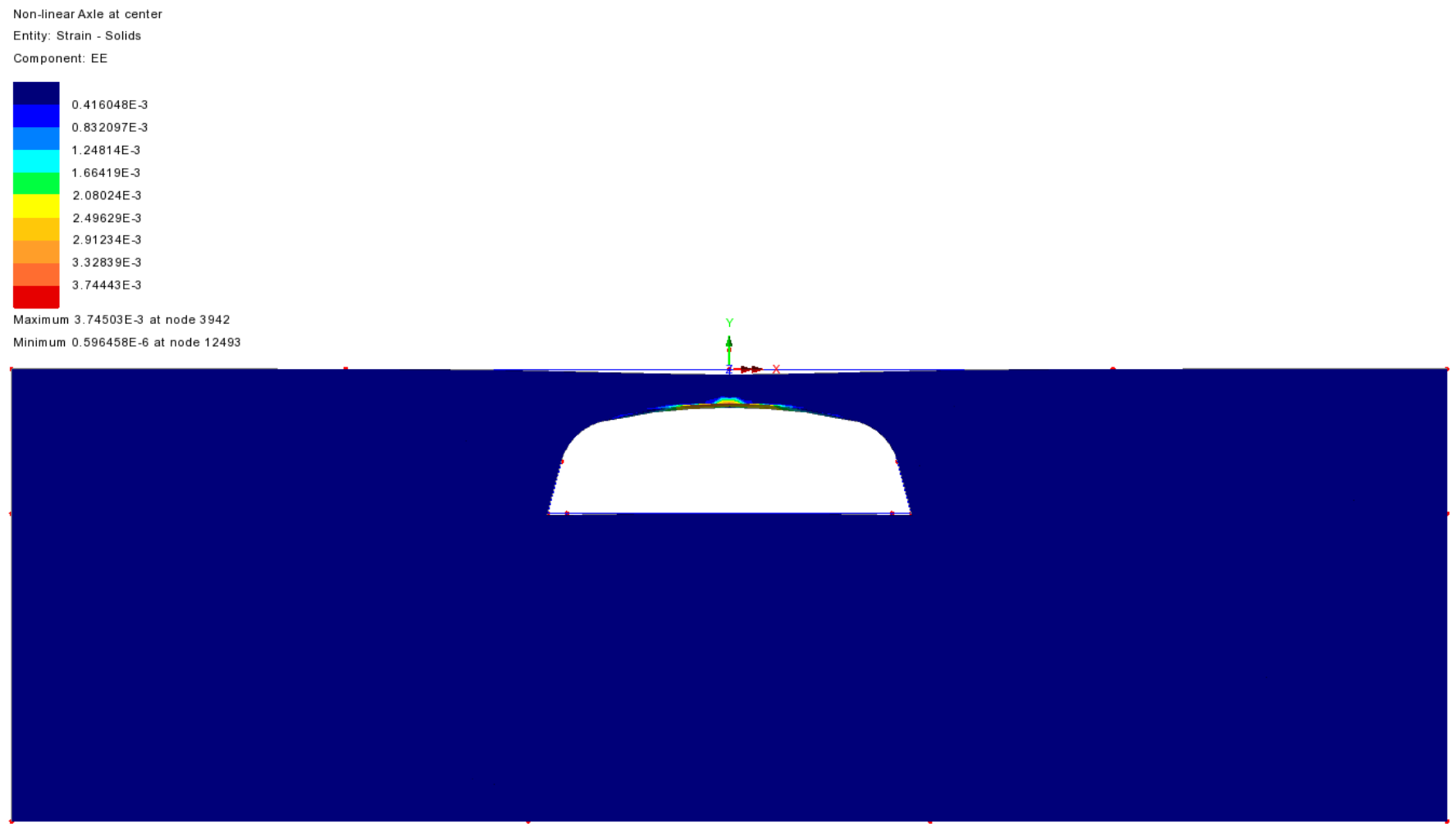


Figure 79. Von Mises Strain of Solid Elements- 2 Lane 32 k Axle at Center of Culvert

Appendix E - 3D Modeling Backup

Non-linear Axle at center
Entity: Strain - Solids
Component: EY

Dark Blue	-0.693972E-3
Blue	0.0
Cyan	0.693972E-3
Green	1.38794E-3
Yellow	2.08192E-3
Orange	2.77589E-3
Red-Orange	3.46986E-3
Red	4.16383E-3
Dark Red	4.85781E-3

Maximum 5.30948E-3 at node 3942
Minimum -0.936272E-3 at node 8440

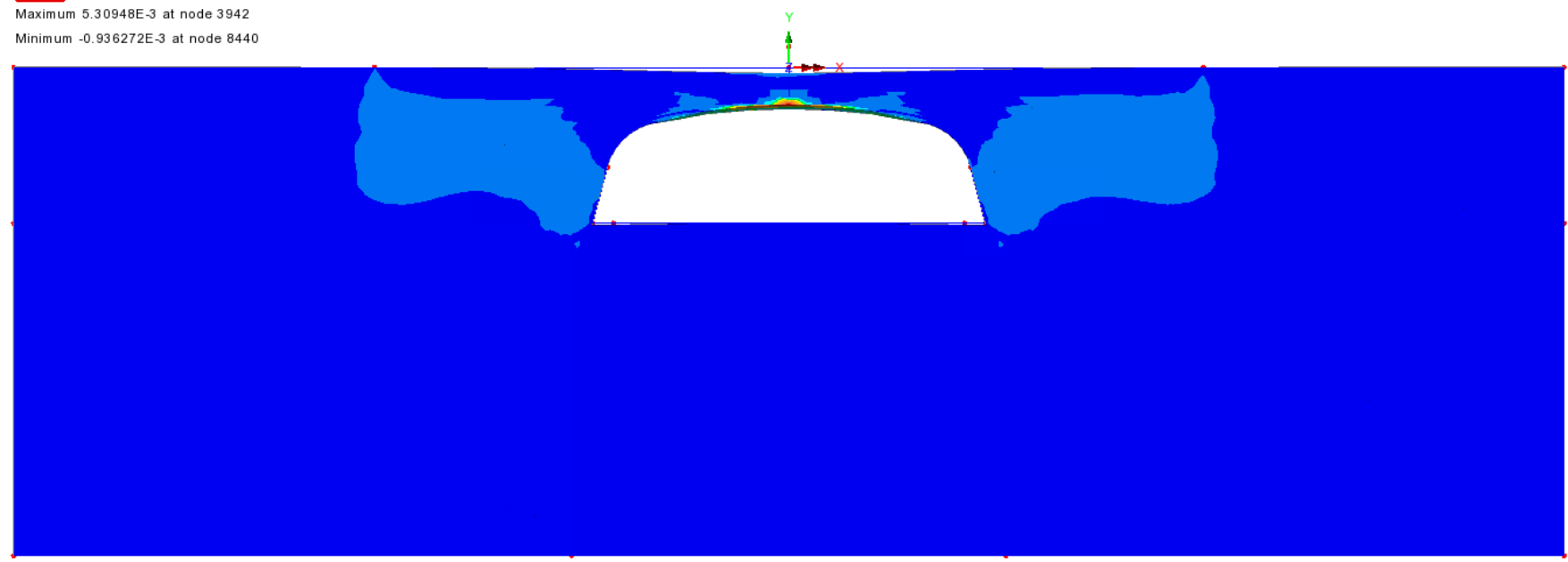
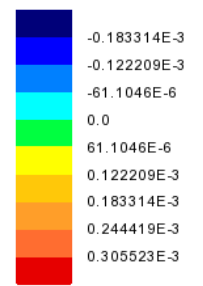


Figure 80. Vertical Strain (EY) of Solid Elements- 2 Lane 32 k Axle at Center of Culvert

Appendix E - 3D Modeling Backup

Non-linear Axle at center
Entity: Strain - Solids
Component: EX



Maximum 0.341939E-3 at node 15517
Minimum -0.208003E-3 at node 8211

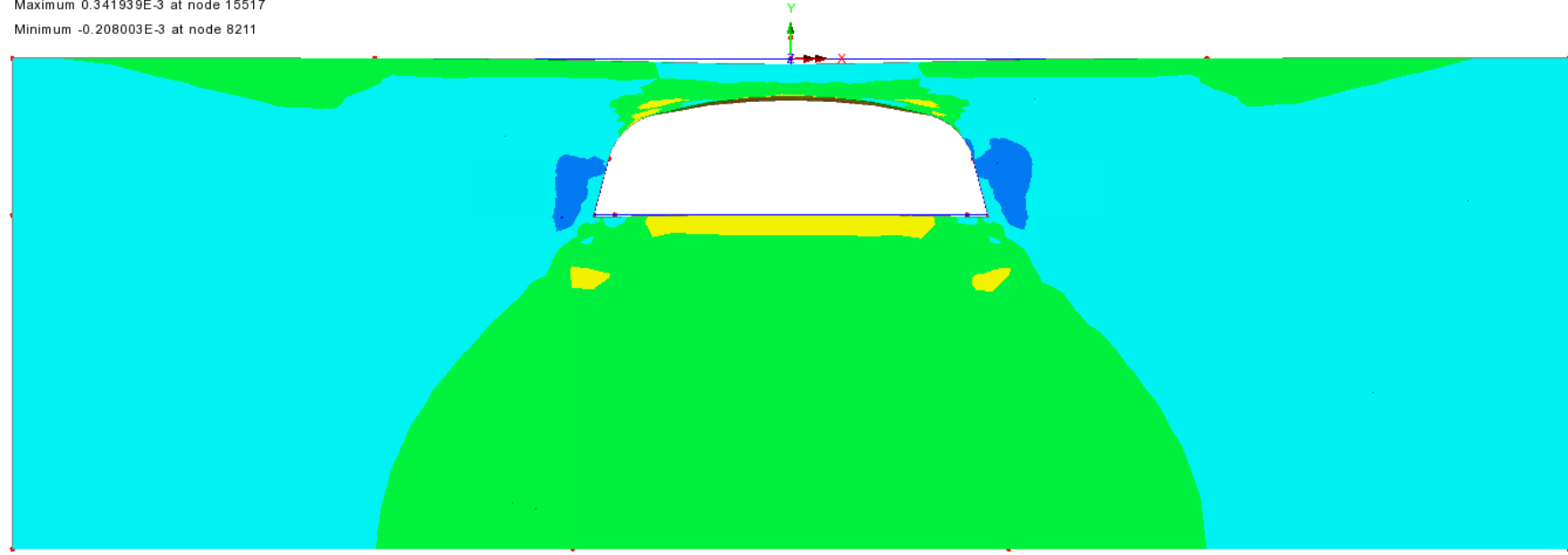
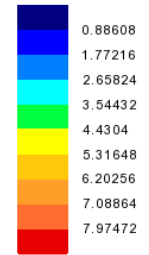


Figure 81. Horizontal Strain (EX) of Solid Elements- 2 Lane 32 k Axle at Center of Culvert

Appendix E - 3D Modeling Backup

Non-linear Axle at center
Entity: Stress - Solids
Component: SE (Units: kip/ft²)



Maximum 7.97559 at node 8784
Minimum 0.862436E-3 at node 1736

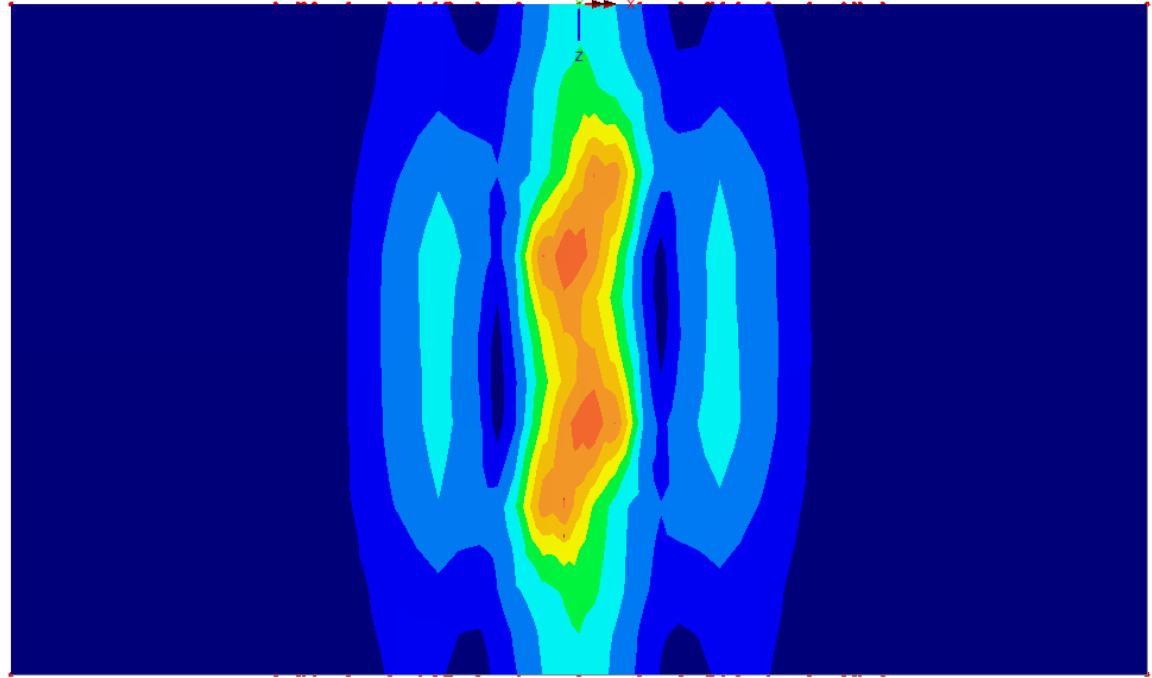


Figure 82. Von Mises Stress of Solid Elements- 2 Lane 32 k Axle at Center of Culvert

Appendix E - 3D Modeling Backup

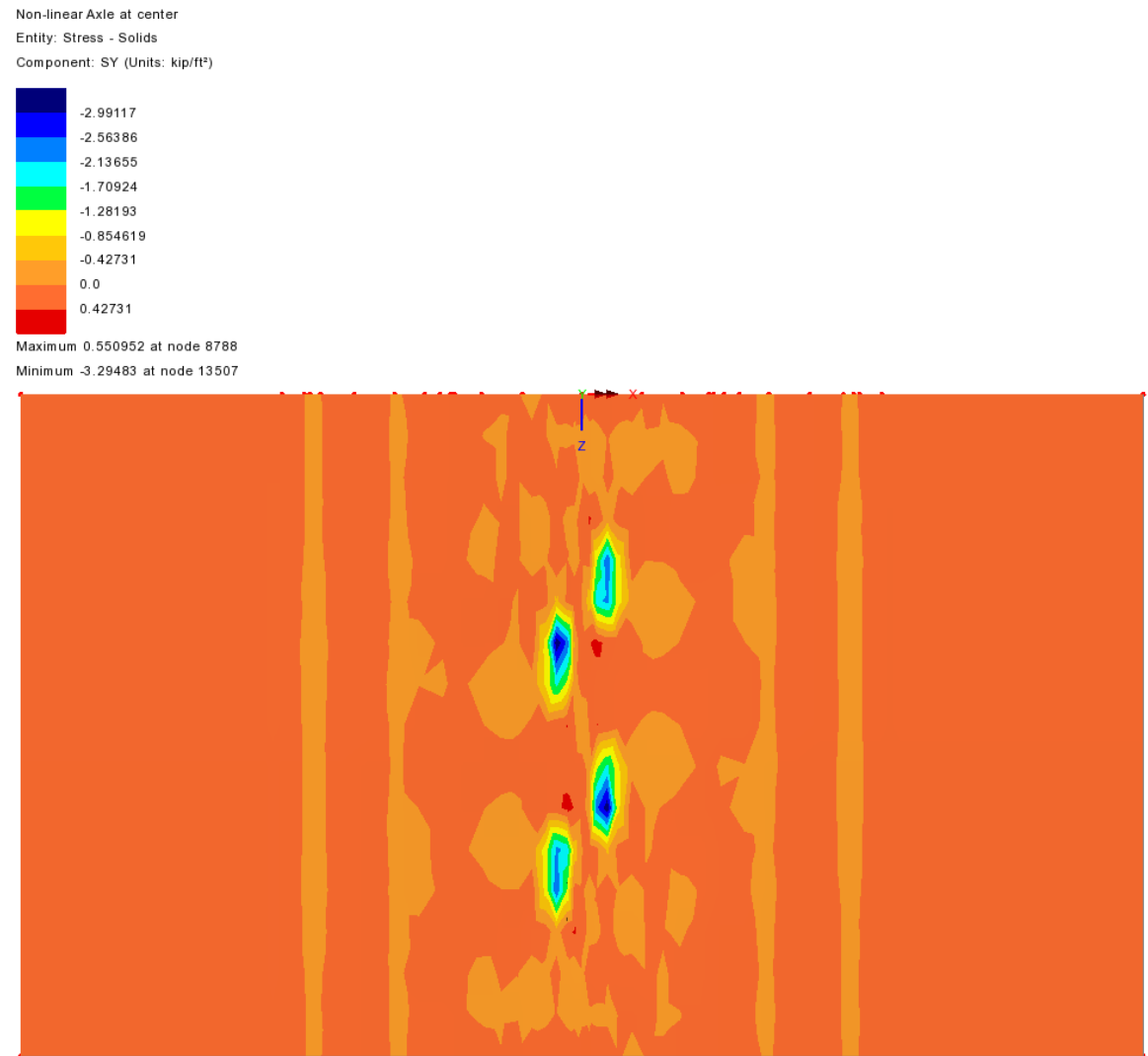


Figure 83. Vertical Stress (SY) of Solid Elements- 2 Lane 32 k Axle at Center of Culvert

Appendix E - 3D Modeling Backup

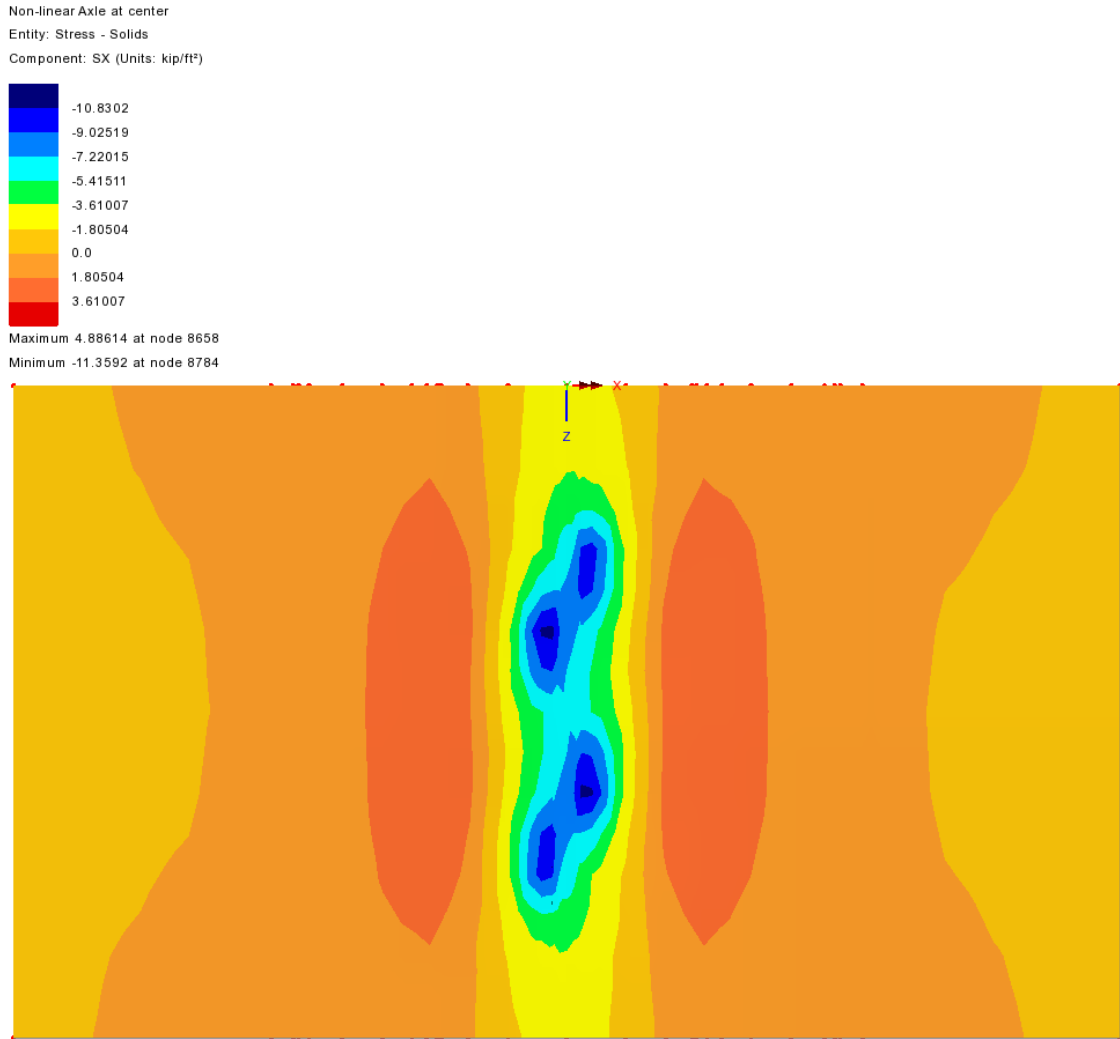


Figure 84. Horizontal Stress (SX) of Solid Elements- 2 Lane 32 k Axle at Center of Culvert

Appendix E - 3D Modeling Backup

Non-linear Axle at center
Entity: Displacement
Component: DY (Units: ft)

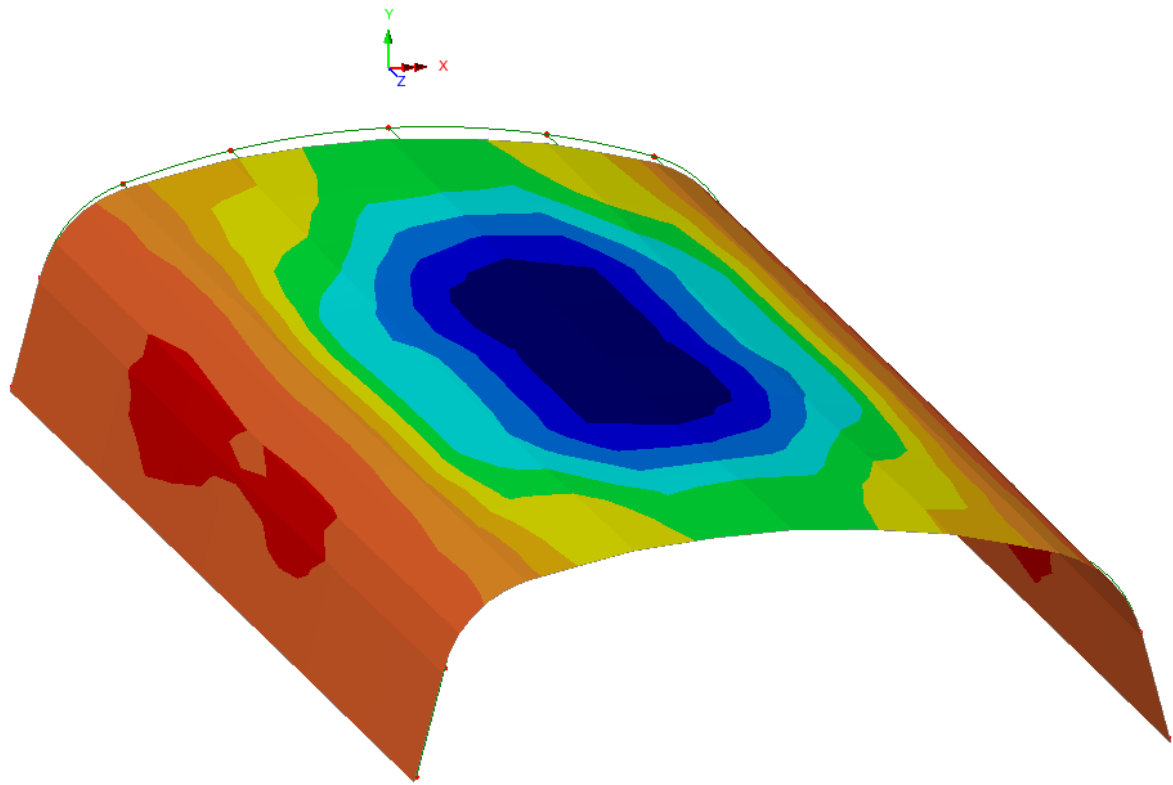
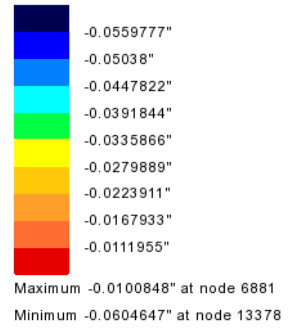


Figure 85. Vertical Displacement of Culvert- 2 Lane 32 k Axle at Center of Culvert

Appendix E - 3D Modeling Backup

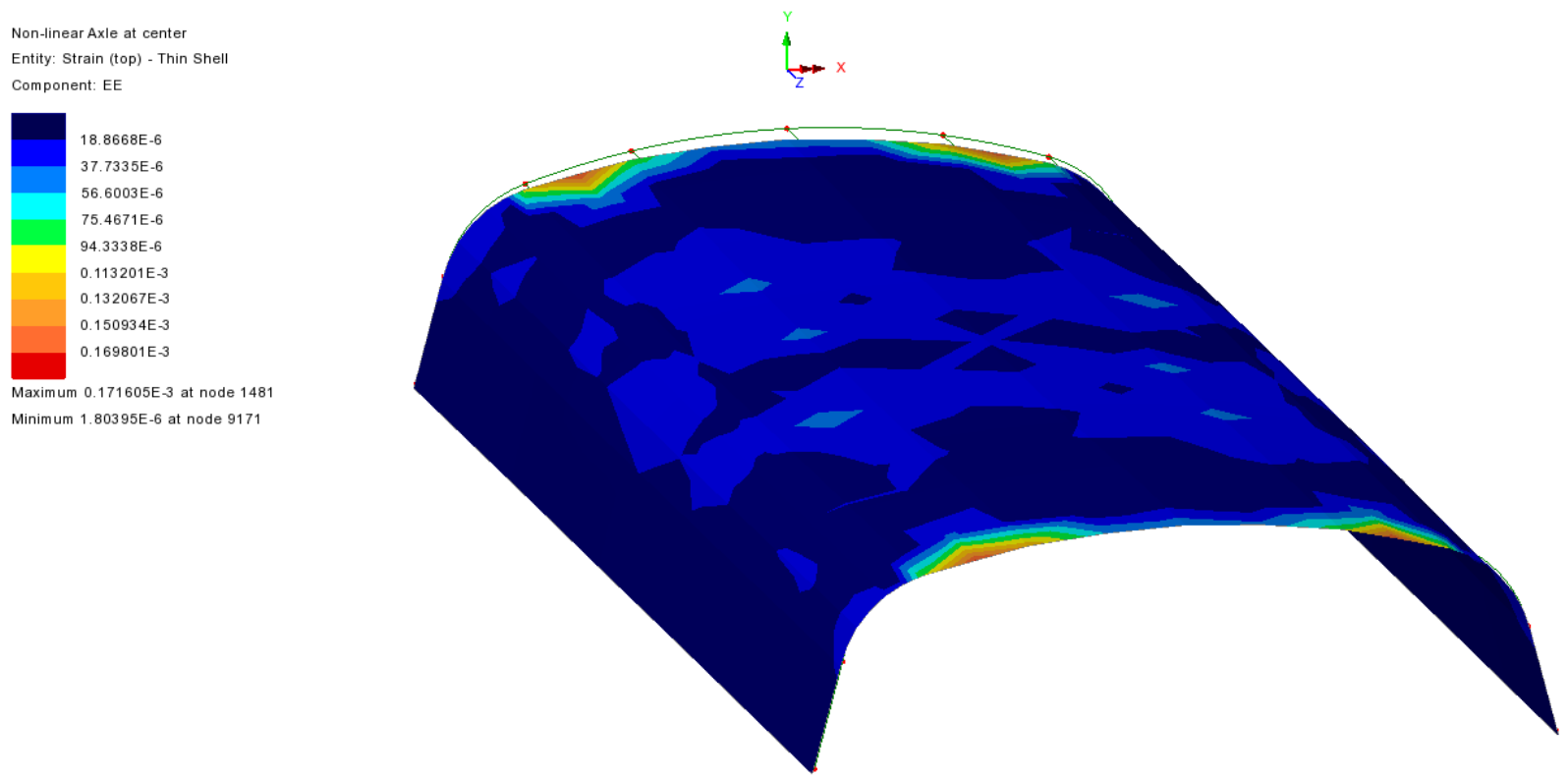


Figure 86. Von Mises Strain at Top Fiber in Culvert- 2 Lane 32 k Axle at Center of Culvert

Appendix E - 3D Modeling Backup

Non-linear Axle at center
Entity: Strain (bottom) - Thin Shell
Component: EE

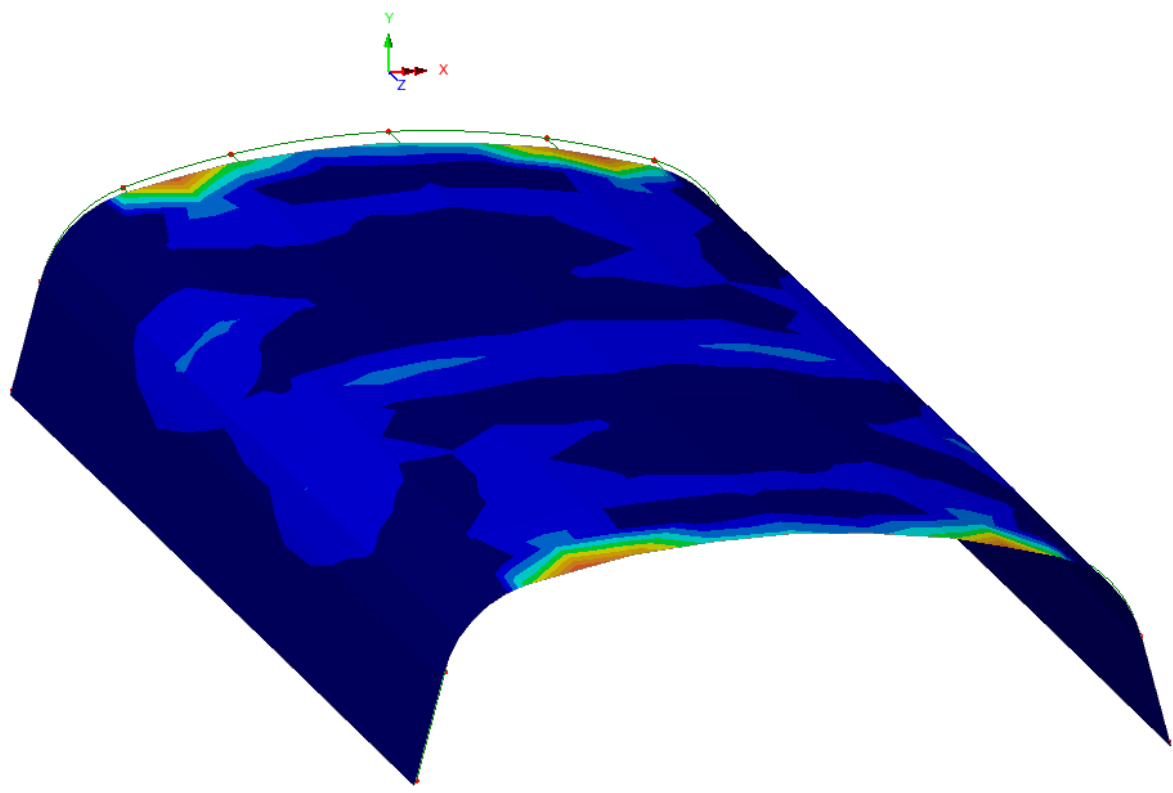
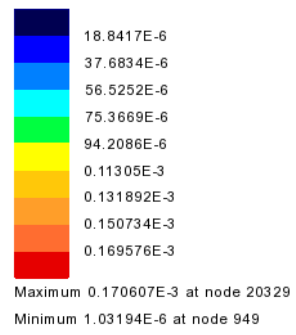


Figure 87. Von Mises Strain at Bottom Fiber in Culvert- 2 Lane 32 k Axle at Center of Culvert

Appendix E - 3D Modeling Backup

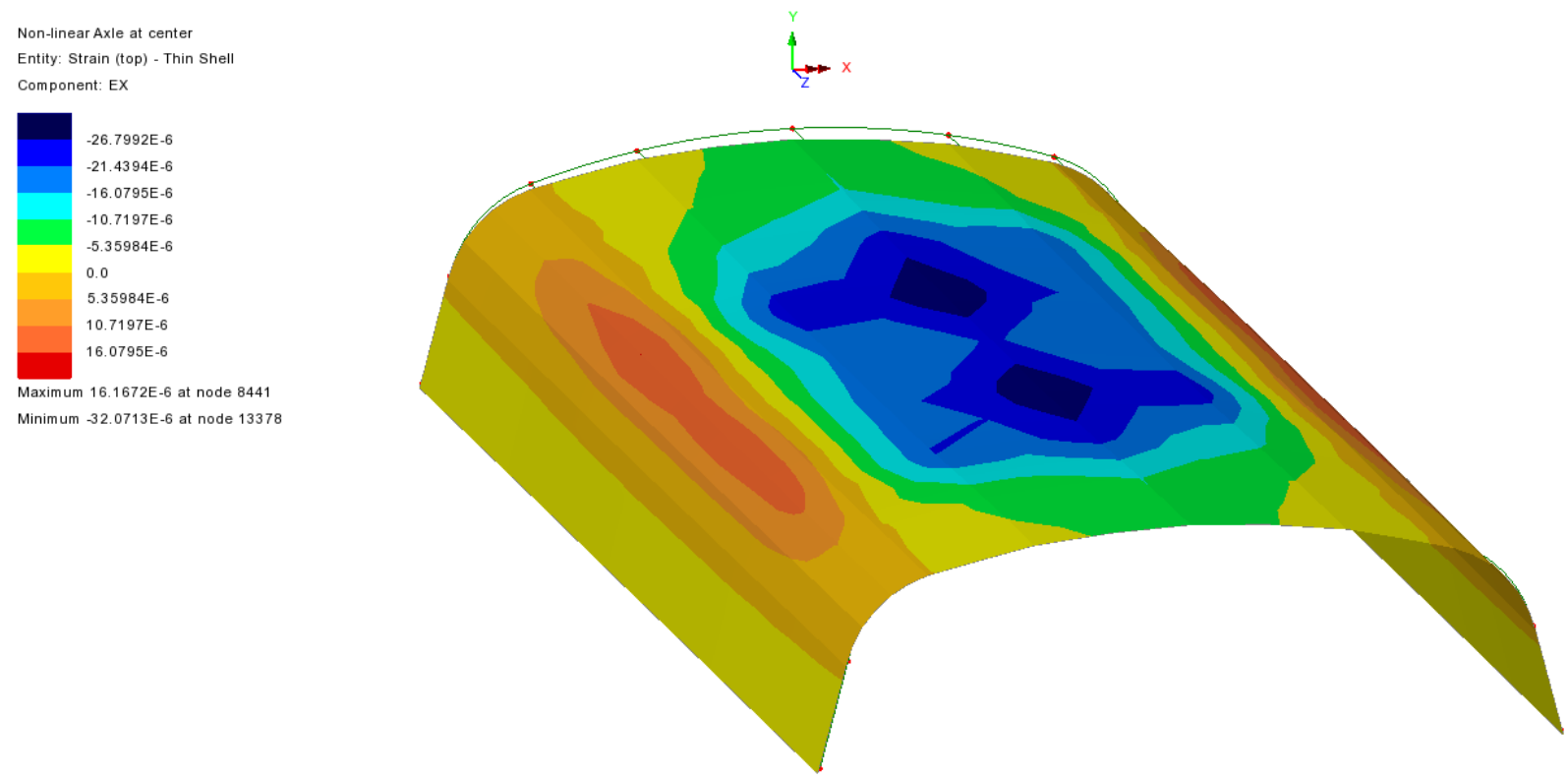


Figure 88. Bending Strain at Top Fiber in Culvert- 2 Lane 32 k Axle at Center of Culvert

Appendix E - 3D Modeling Backup

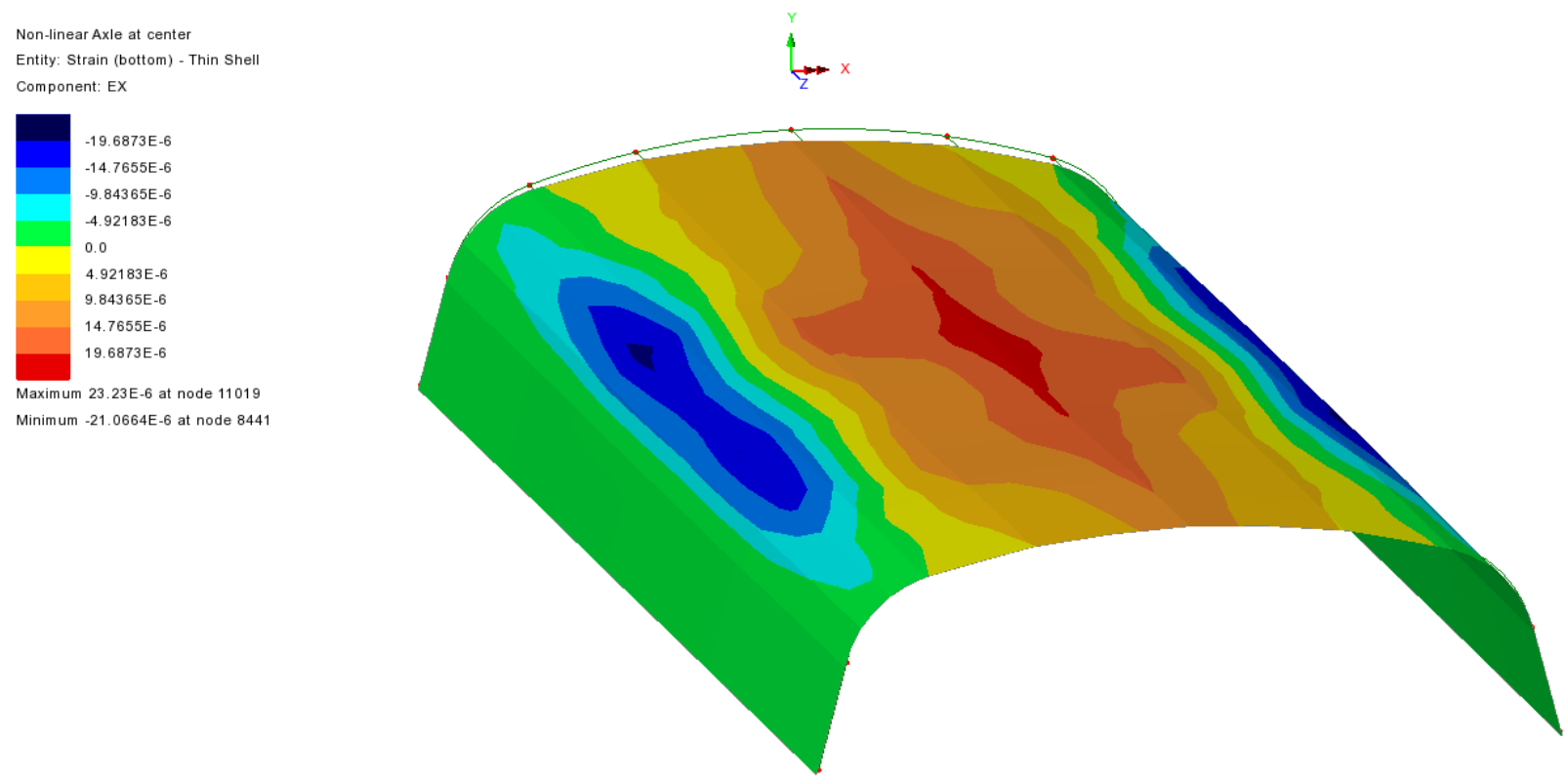


Figure 89. Bending Strain at Bottom Fiber in Culvert- 2 Lane 32 k Axle at Center of Culvert

Appendix E - 3D Modeling Backup

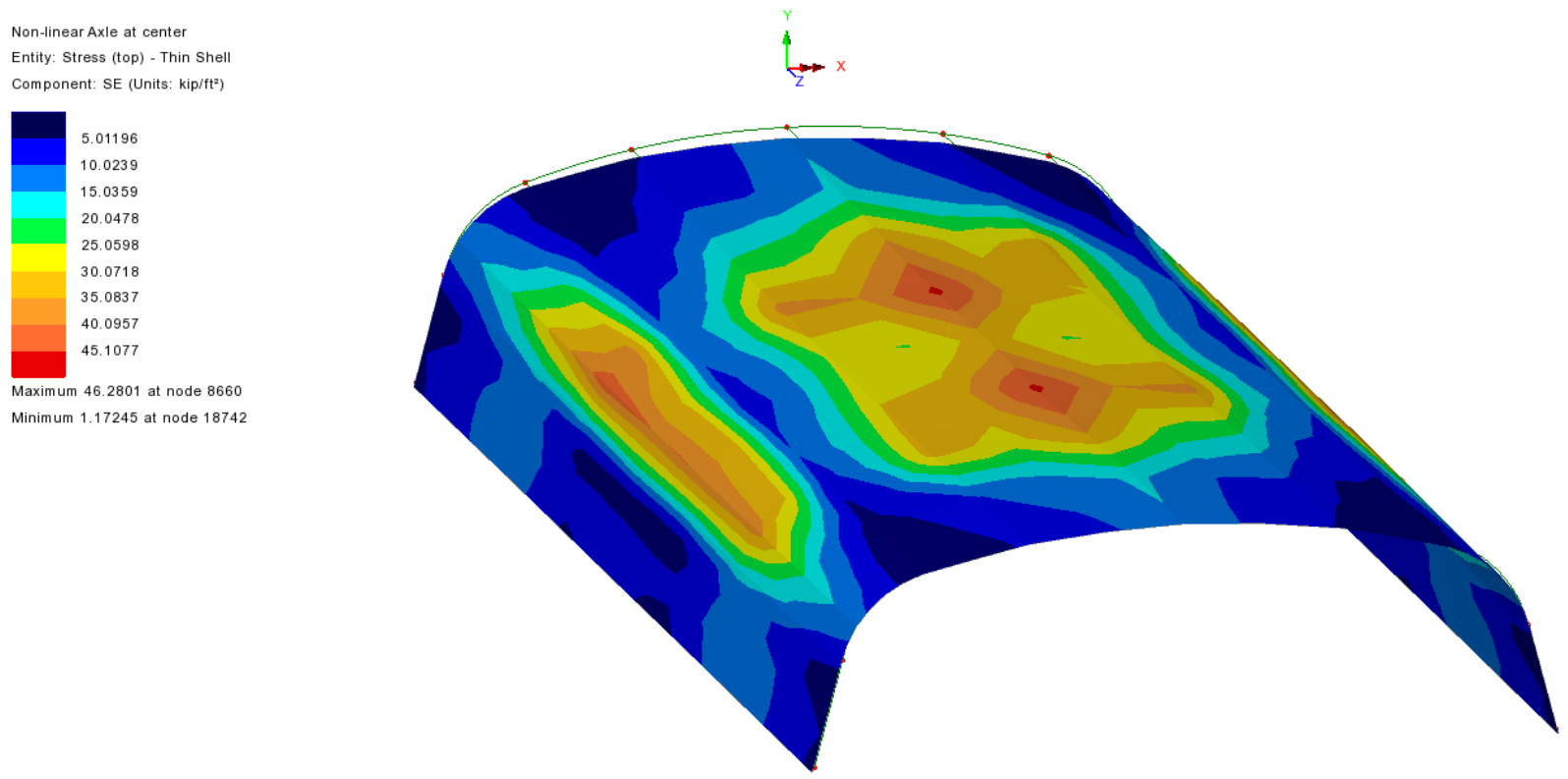


Figure 90. Von Mises Stress at Top Fiber in Culvert- 2 Lane 32 k Axle at Center of Culvert

Appendix E - 3D Modeling Backup

Non-linear Axle at center
Entity: Stress (bottom) - Thin Shell
Component: SE (Units: kip/ft²)

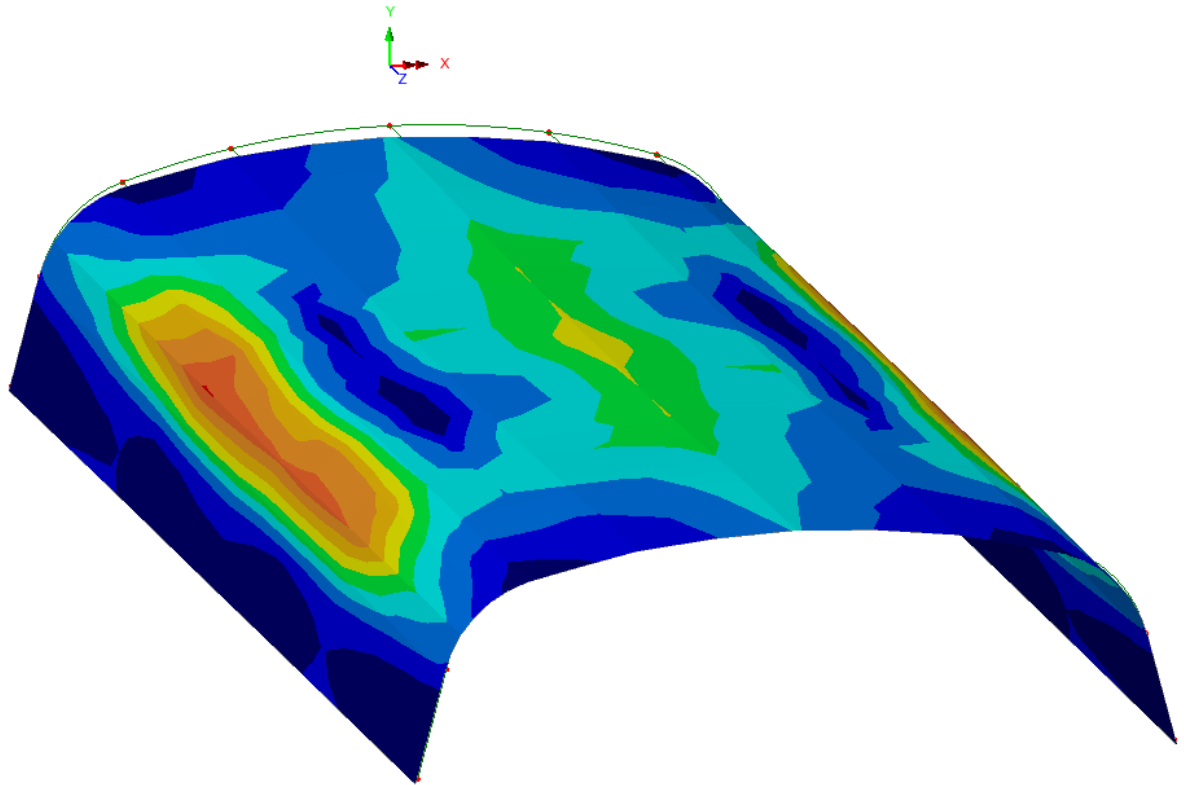
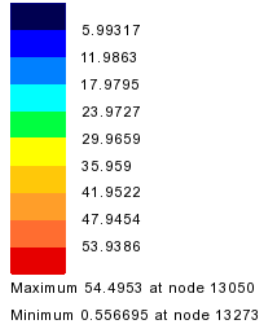


Figure 91. Von Mises Stress at Bottom Fiber in Culvert- 2 Lane 32 k Axle at Center of Culvert

Appendix E - 3D Modeling Backup

Non-linear Axle at center
Entity: Stress (top) - Thin Shell
Component: SX (Units: kip/ft²)

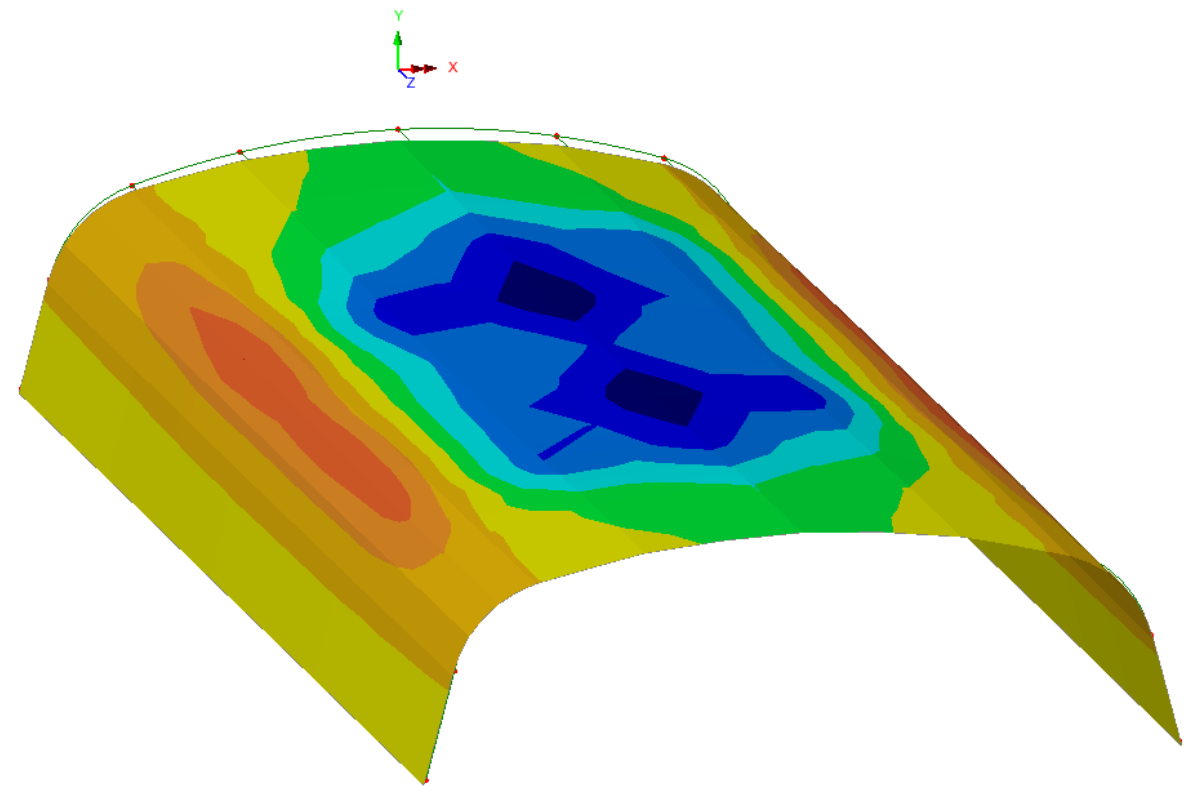
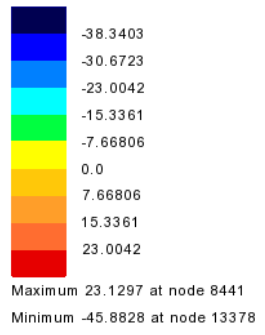


Figure 92. Bending Stress at Top Fiber in Culvert- 2 Lane 32 k Axle at Center of Culvert

Appendix E - 3D Modeling Backup

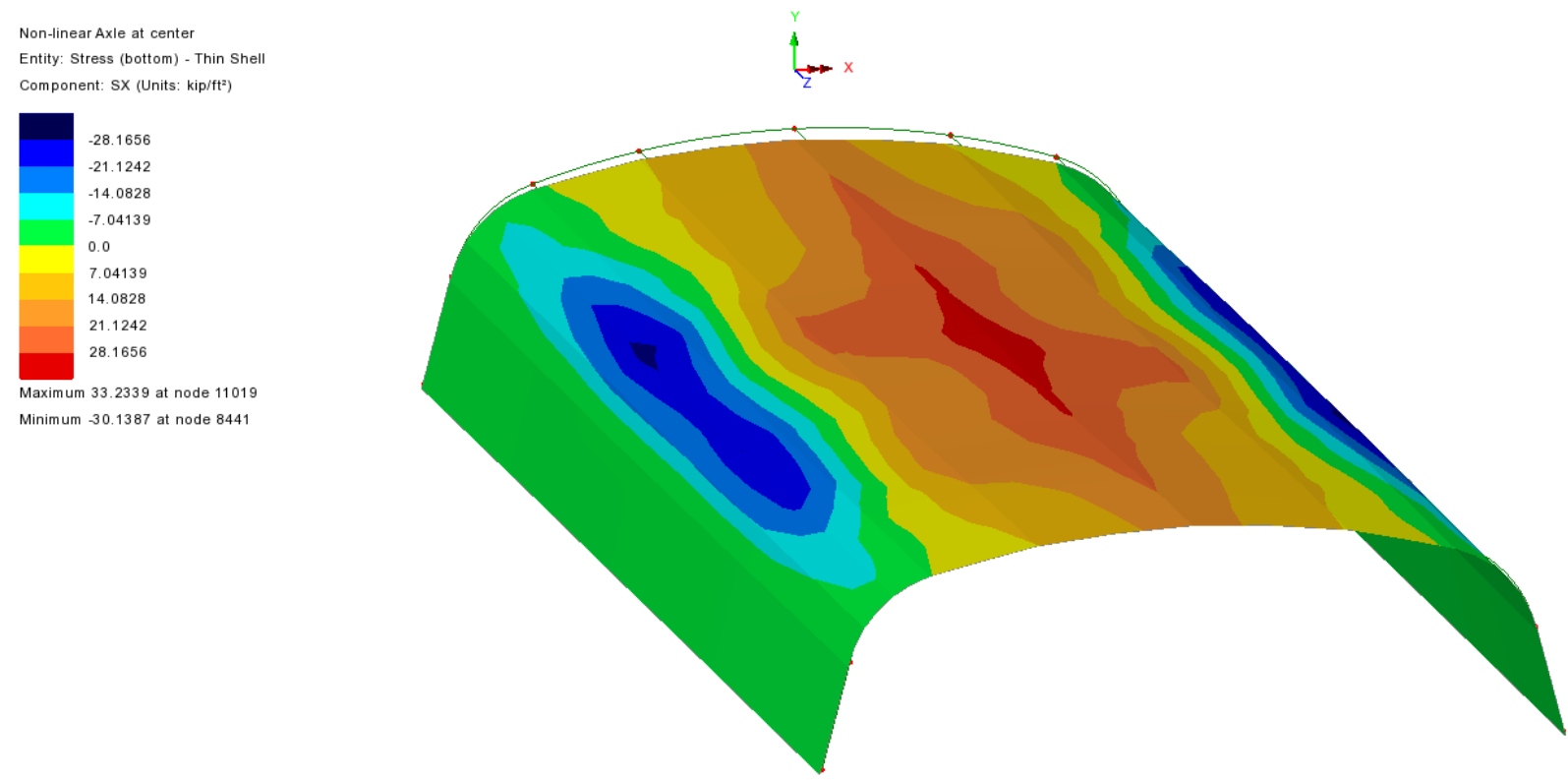


Figure 93. Bending Stress at Bottom Fiber in Culvert- 2 Lane 32 k Axle at Center of Culvert

MODEL 7- CANDIDATE 1 (M7C1)

Model 7 represents a prototype of deep corrugated metal culverts. Candidate 1 is selected for this category.

Geometry

Geometry and layout of Model 7 Candidate 1 (M7C1) is presented in Appendix E. Figure 94 presents the section of the culvert and the equivalent geometry that is modeled in Lusas. Thickness of the corrugated metal sheet and moduli of elasticity are adjusted to capture the behavior of the corrugated metal sheet.

The Lusas model includes the entire length of the culvert. As shown in Figure 94, the span of culvert is 57' and the depth of the model extends to 64'. Laterally, the geometry extends to 97' on each side. Therefore, the cross section of model is 194'x64' and the length is 50'. A concrete 5Wx4D footing is modeled at each end of the arch culvert. A 2.5 ft deep pavement is assumed between the footings providing temporary road access through the culvert. Another 2.5 ft deep pavement is assumed over the culvert, where the live load is applied to culvert. The slope of backfill is assumed 1:2 vertical to horizontal.

Material Properties

Given that corrugated metal sheets have different axial and flexural behavior in two directions, orthotropic material properties are used to define the behavior of the culvert. However, according to Samanta and Mukhopadhyay (1997), Wennberg, et al. (2011), and Briassoulis (1985), both flexural and axial properties of the corrugated sheets are different, and by defining an orthotropic material, only one of the axial or flexural behavior may be adjusted. Given that the ratio of correction factors, for the existing model, material is defined so that the modulus of elasticity in weak axis (E_x) is adjusted for axial behavior, and in strong axis it is adjusted for flexural behavior. Other combinations of material properties are formulated and by using experimental data, the appropriate behavior may be selected. Formulation and adjustment factors are adopted from Samanta and Mukhopadhyay (1997).

Originally, the thickness of the culvert elements was set to the actual value (0.2391") and the moduli of elasticity were set accordingly. The corrugation effects and orthotropic behavior were captured perfectly. However, due to the very small thickness, the culvert showed localized deformations at the footing. Therefore, the thickness of the corrugation was increased to avoid the localized deformation and stress concentration issue. Finally, the moduli of elasticity were adjusted accordingly to represent the same behavior according to formulation of Samanta and Mukhopadhyay (1997).

Overlay and pavement is defined as a linear material with modulus of elasticity (E) = 4000 ksi, Poisson's ratio (ν) = 0.35, and unit weight = 140 pcf.

The linear material properties of concrete footings are generated based on AASHTO LRFD Bridge Design Specifications for compressive strength of $f'_c = 5$ ksi: modulus of elasticity (E) = 4074 ksi, Poisson's ratio (ν) = 0.2, unit weight = 150 pcf, and coefficient of thermal expansion (α) = 10.8×10^{-6} 1/C.

Table 5 presents the material properties of in-situ soil and backfill. In-situ soil is defined as an elastic material, while nonlinear material properties are considered for backfill, varying with depth. The values in Table 5 are adopted from previous study by McGrath et al. (2005).

Mesh

Quadrilateral quadratic thin shell elements are used to model the culvert. Given that thickness of the corrugated metal sheet very small, transferred shear through the section is minimal, hence the thin shell element may effectively capture the behavior of the culvert.

Hexahedral quadratic solid elements are used to model the pavement (overlay), footings, in-situ soil, and backfill. Due to limitation of number of elements and large dimensions for M7C1, the mesh size is set to 3' around the culverts and in backfill and 15' at the boundaries. The mesh along the length of culvert varies

between 8' at edges to 2" at center. A sensitivity analysis in linear mode showed that the current mesh size provides comparable results with finer mesh.

Boundary Condition

At the end of the in-situ soil medium, perpendicular restraints are used for each boundary surface, i.e. lateral restraints at vertical faces and vertical restraints at the bottom of the in-situ soil.

"Tied Mesh Constraints" are assigned between the culvert and soil as well as the culvert and overlay to assure deformation compatibility. This option assures compatible deformation of adjacent shell elements and solid elements. No contact element or interaction properties are assigned.

Load Cases

Gravity is applied as a body force. Soil pressure is considered using vertical and lateral pressure (to provide in-situ conditions with close to zero deflections under soil self-weight).

Live Load: Wheel load is modeled as a discrete patch load over a 10"x20" area. A load case with single axle load in three lanes and a load case with standard HL-93 truck moving load is applied to the model. The truck load is moved across the culvert to capture the critical loading condition. The live load will be updated when the wheel load of the actual truck that is used in the experiment is determined.

Results

Figures 95 to 111 present the behavior of M7C1 in terms of displacement, strains and stresses under axle load at center of the culvert. Because for nonlinear analysis, all loads must be applied sequentially, gravity and dead loads are applied first, then live load is applied and the final results are under both dead load and live load. Given that for experimental study, only the effect of live load is measured, a load combination is defined in Lusas that removes the effect of dead load by subtracting the results of "dead load analysis" from the results after application of live load.

It should be noted that maximum and minimum envelopes of results under moving loads are available, however, given that Lusas develops two separate envelopes for maximum and minimum, contour presentation may become misleading, unless both envelopes are compared side by side. This is especially important when the dead load effects (constant) are being deduced from the total "dead + live load" results. Results of envelop results of moving loads will be presented later where a specific entity or stage of loading is determined.

Table 5. M7C1- Material Properties of Backfill and In-Situ Soil

Properties	Backfill: 0-1 ft	Backfill: 1-6 ft	Backfill: 6-11 ft	In-Situ Soil
Modulus of Elasticity, E (ksf)	230.4	576.0	864.0	864.0
Poisson's Ratio (ν)	0.4	0.29	0.24	0.25
Unit Weight (pcf)	121	121	121	127
Initial Cohesion (psf)	0.000144	0.000144	0.000144	-
Initial Friction Angle	40	40	40	-
Final Friction Angle	40	40	40	-
Dilation Angle	10	10	10	-
Cohesion Hardening (psf)	0	0	0	-
Limiting Plastic Strain	0.001	0.001	0.001	-

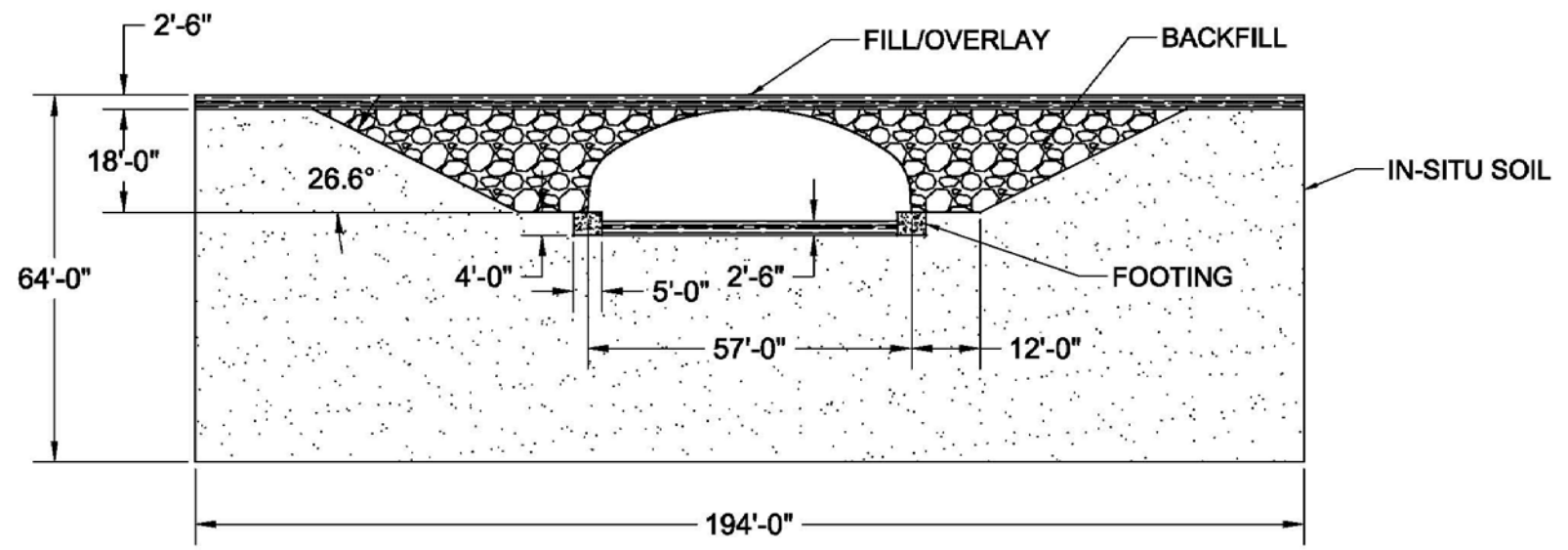


Figure 94. M7C1- Cross Section

Appendix E - 3D Modeling Backup

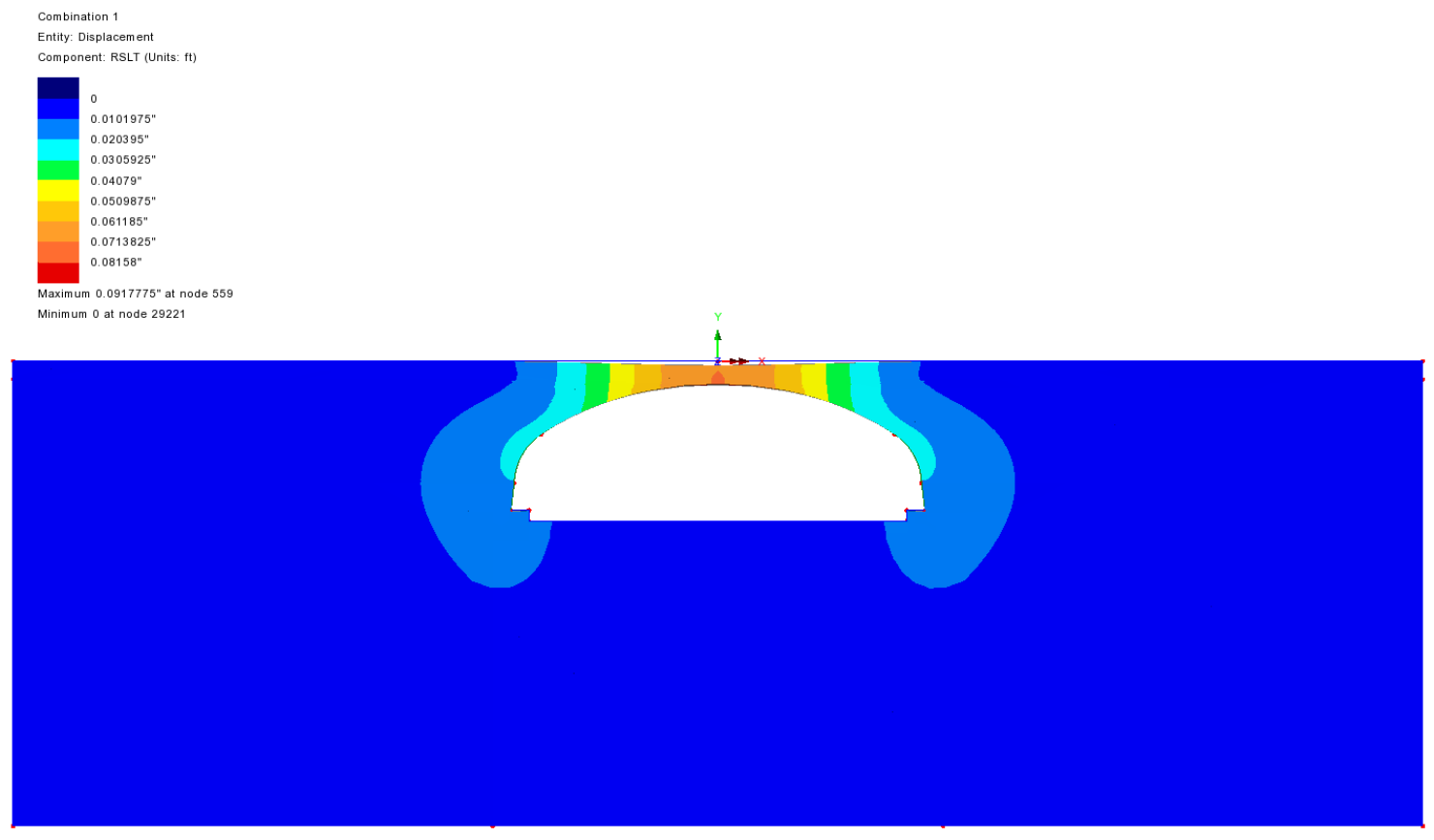


Figure 95. Resultant Displacement of Solid Elements – 2 Lane 32 k Axle at Center of Culvert

Appendix E - 3D Modeling Backup

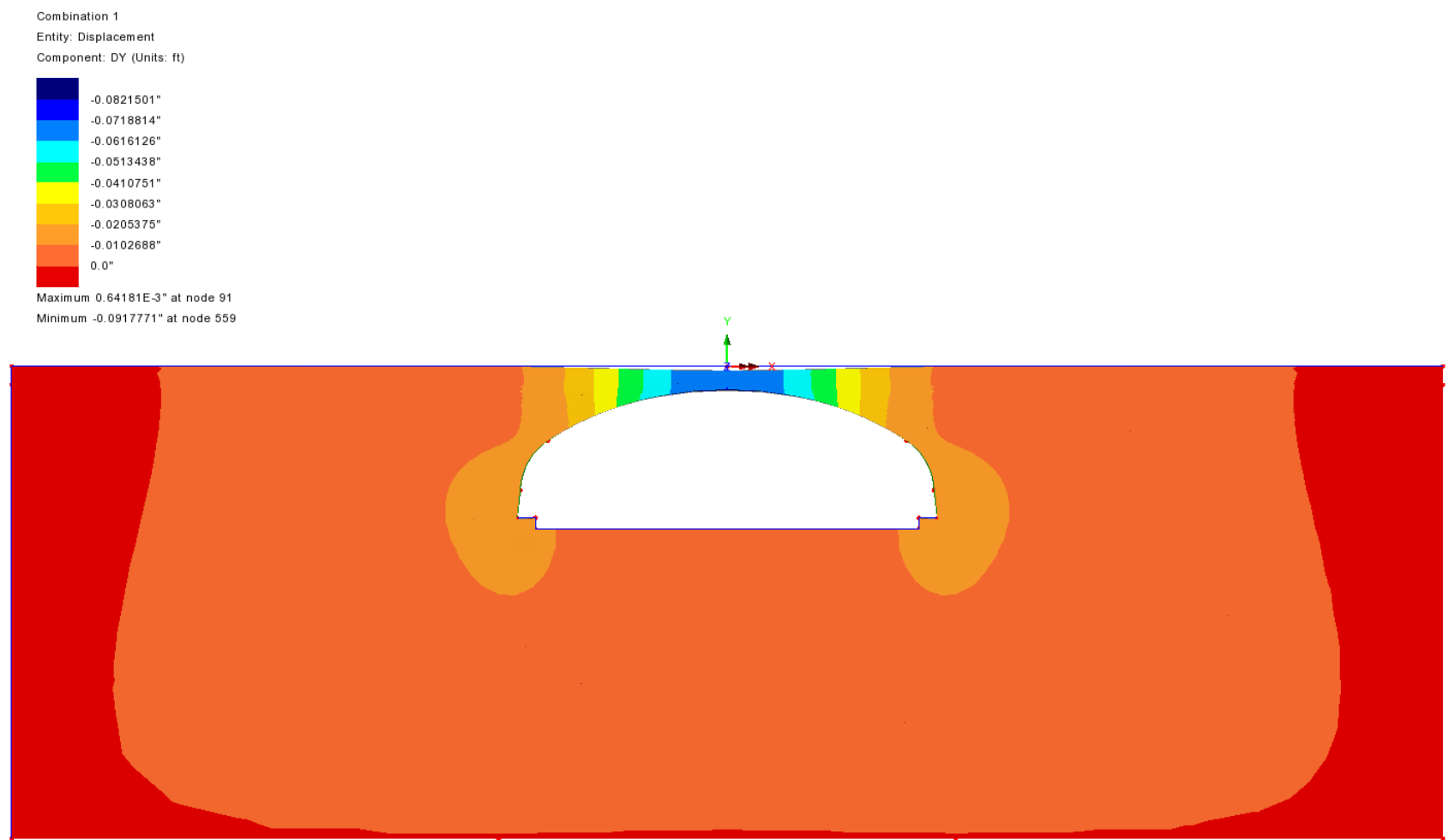
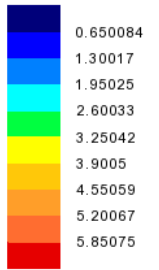


Figure 96. Vertical Displacement of Solid Elements - 2 Lane 32 k Axle at Center of Culvert

Appendix E - 3D Modeling Backup

Combination 1
Entity: Stress - Solids
Component: SE (Units: kip/ft²)



Maximum 5.85104 at node 561
Minimum 0.286846E-3 at node 29715

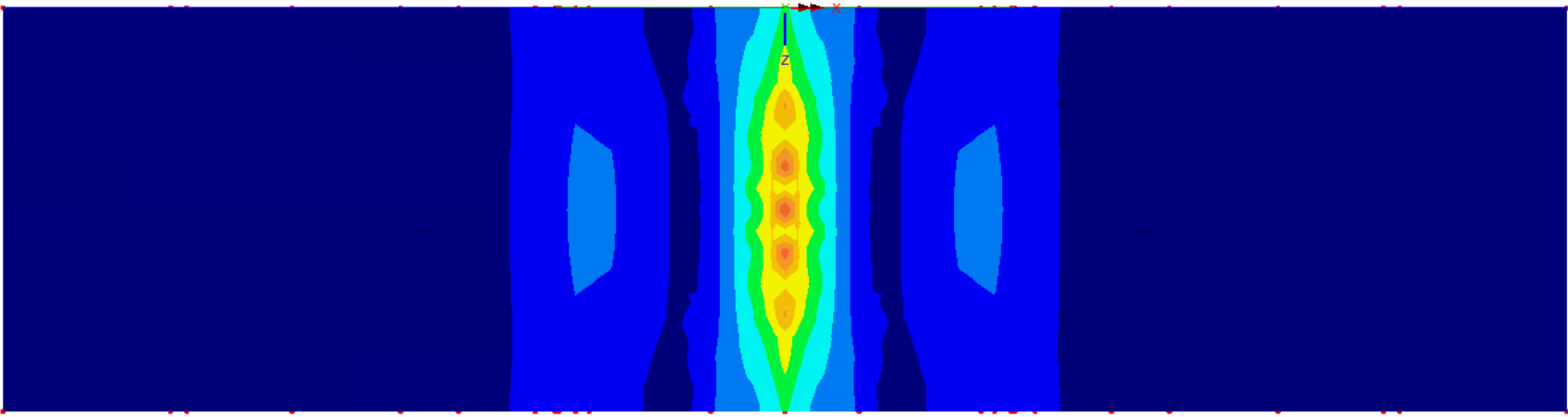


Figure 97. Von Mises Strain of Solid Elements- 2 Lane 32 k Axle at Center of Culvert

Appendix E - 3D Modeling Backup

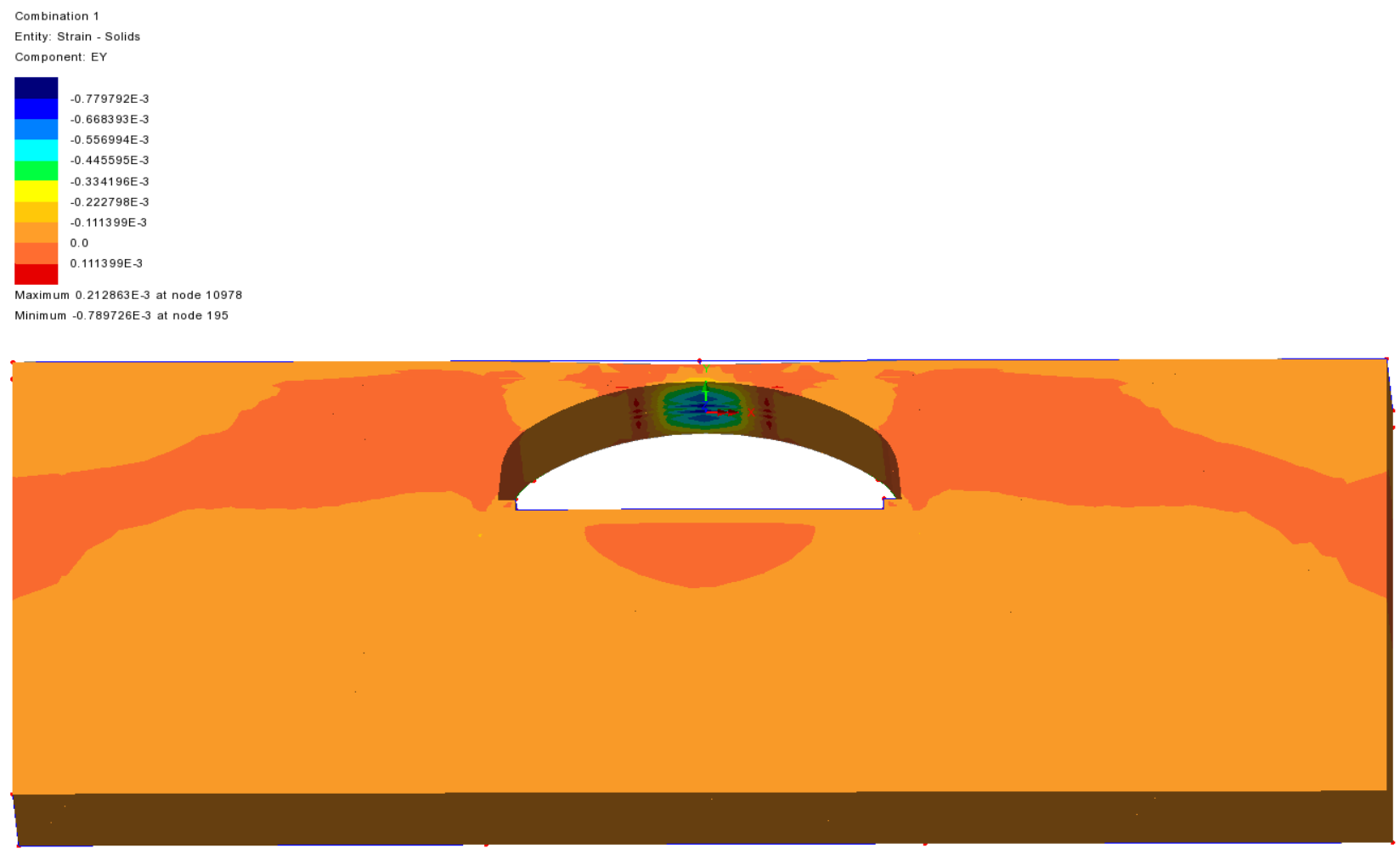


Figure 98. Vertical Strain (EY) of Solid Elements- 2 Lane 32 k Axle at Center of Culvert

Appendix E - 3D Modeling Backup

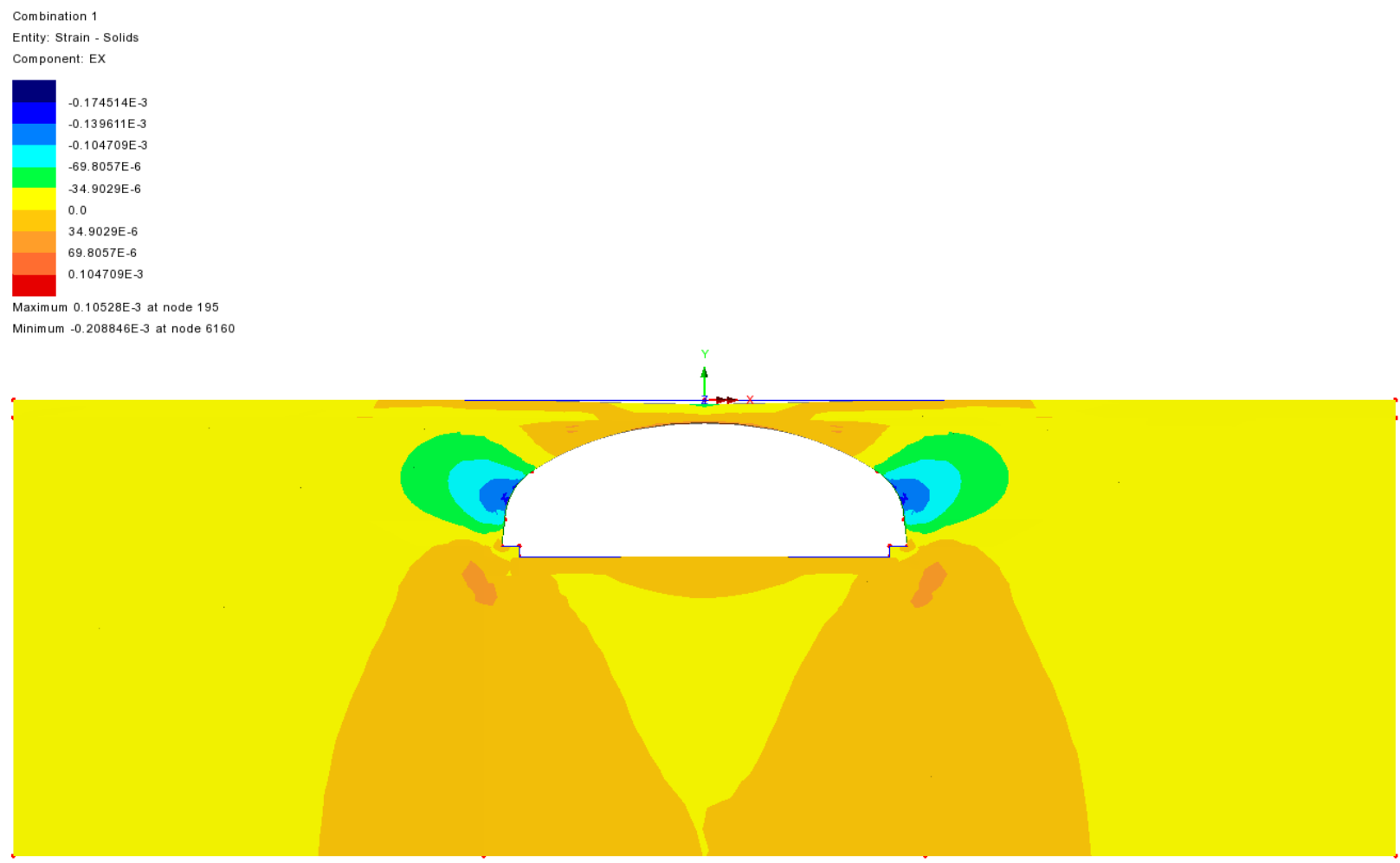


Figure 99. Horizontal Strain (EX) of Solid Elements- 2 Lane 32 k Axle at Center of Culvert

Appendix E - 3D Modeling Backup

Combination 1
Entity: Stress - Solids
Component: SE (Units: kip/ft²)



Maximum 5.85104 at node 561
Minimum 0.286846E-3 at node 29715

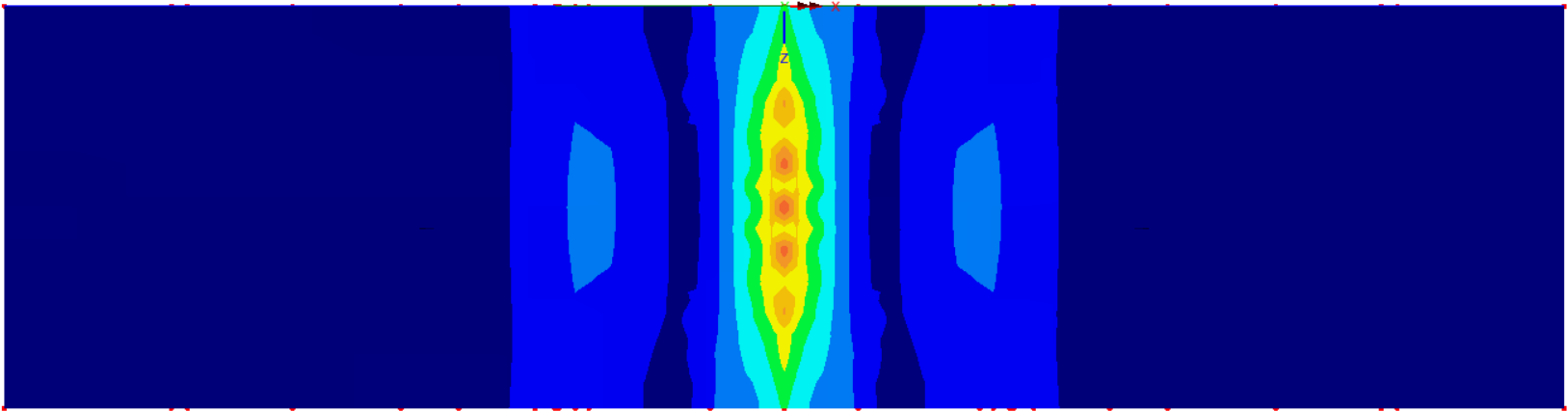
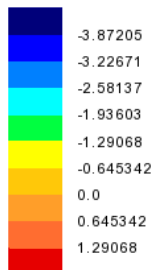


Figure 100. Von Mises Stress of Solid Elements- 2 Lane 32 k Axle at Center of Culvert

Appendix E - 3D Modeling Backup

Combination 1
Entity: Stress - Solids
Component: SY (Units: kip/ft²)



Maximum 1.63773 at node 561
Minimum -4.17035 at node 559

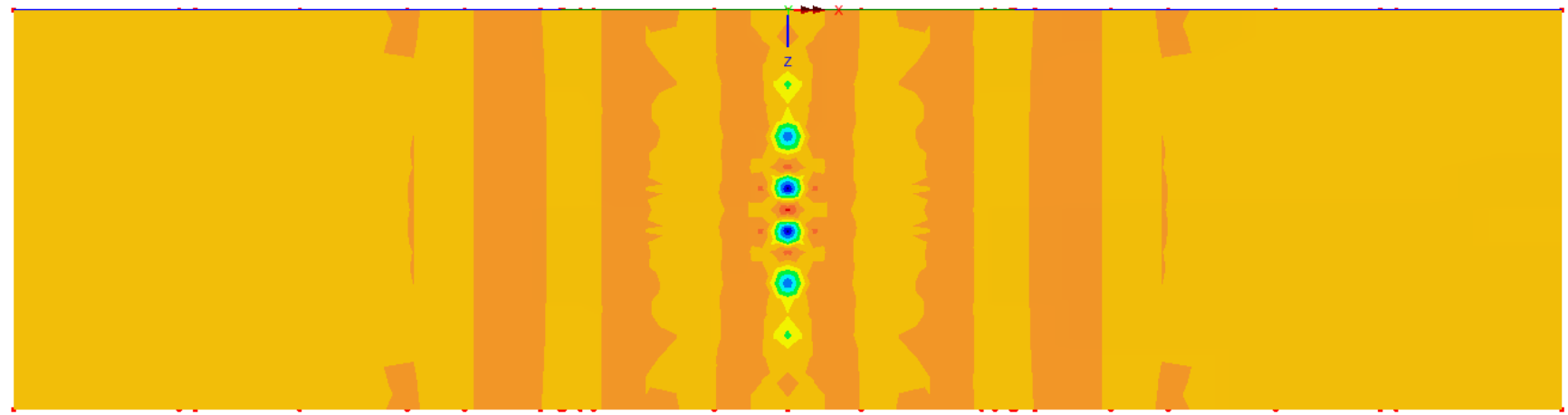
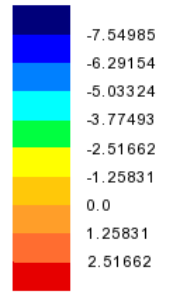


Figure 101. Vertical Stress (SY) of Solid Elements- 2 Lane 32 k Axle at Center of Culvert

Appendix E - 3D Modeling Backup

Combination 1
Entity: Stress - Solids
Component: SX (Units: kip/ft²)



Maximum 3.23721 at node 195
Minimum -8.08757 at node 559

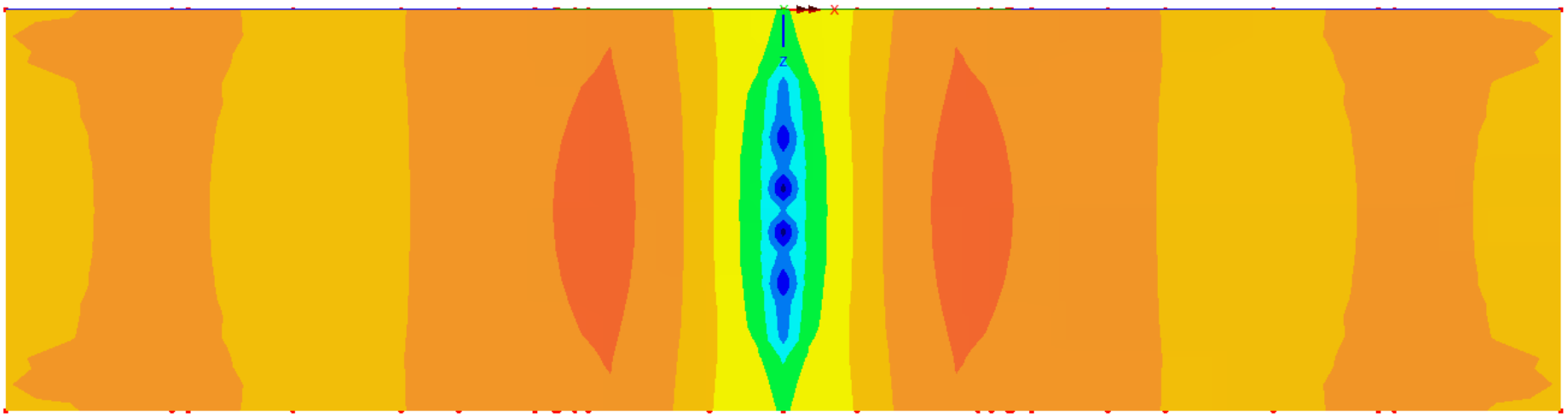


Figure 102. Horizontal Stress (SX) of Solid Elements- 2 Lane 32 k Axle at Center of Culvert

Appendix E - 3D Modeling Backup

Combination 1
Entity: Displacement
Component: DY (Units: ft)

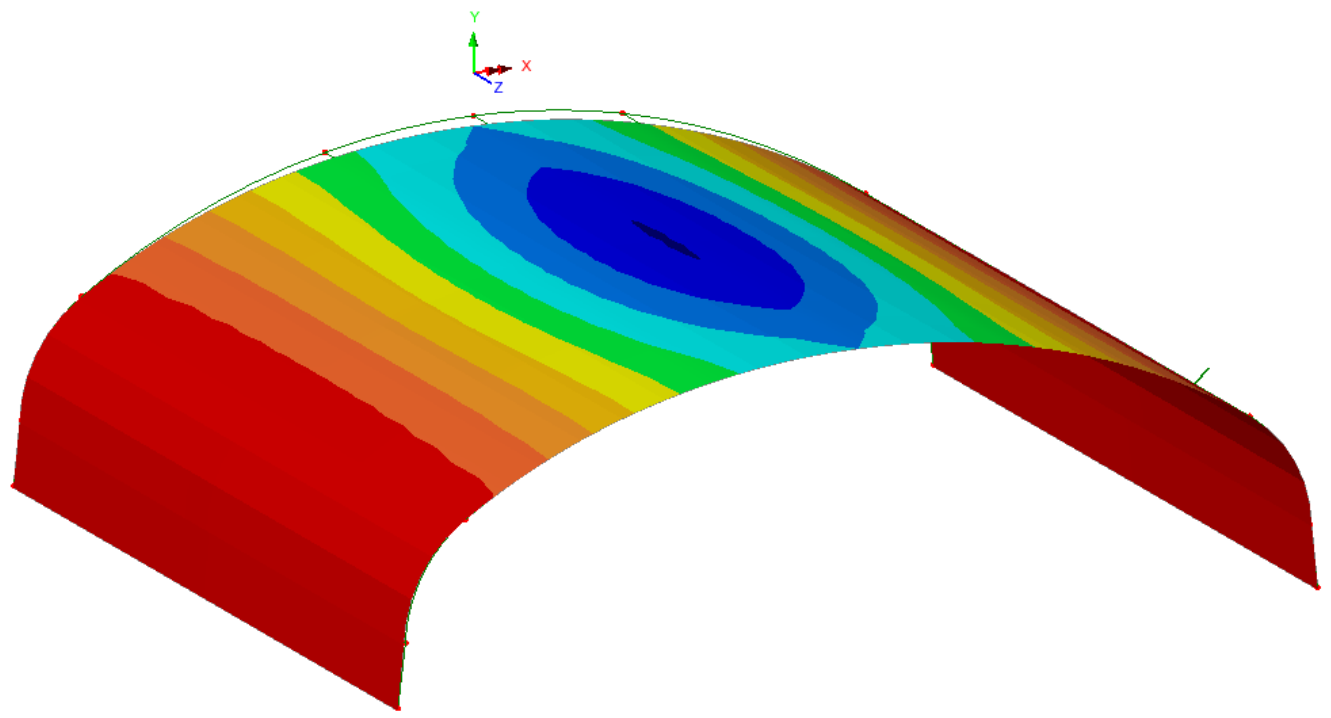
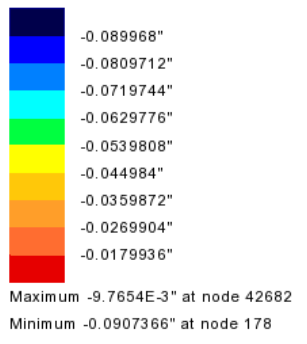


Figure 103. Vertical Displacement of Culvert- 2 Lane 32 k Axle at Center of Culvert

Appendix E - 3D Modeling Backup

Combination 1
Entity: Strain (top) - Thin Shell
Component: EE

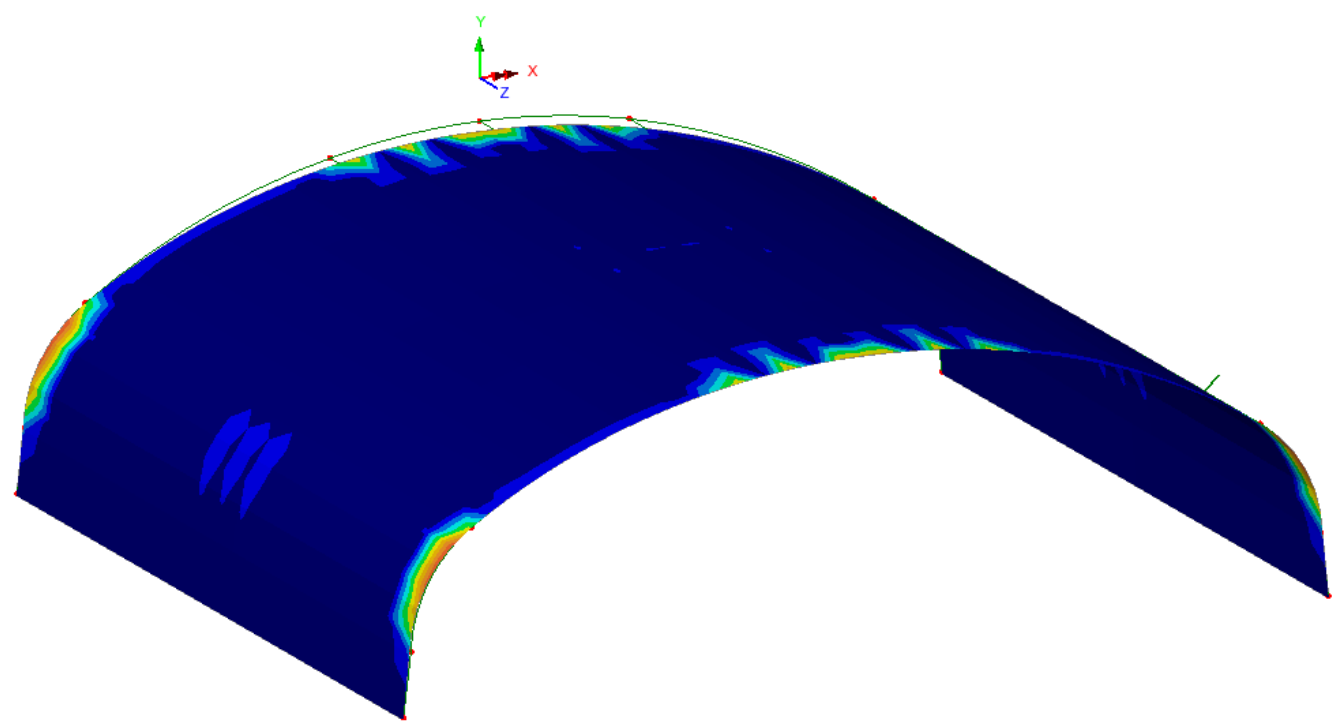
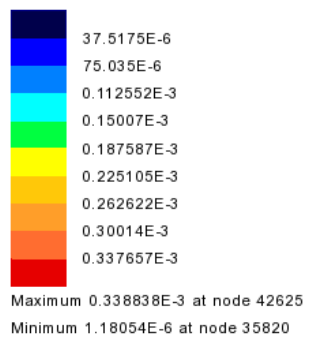


Figure 104. Von Mises Strain at Top Fiber in Culvert- 2 Lane 32 k Axle at Center of Culvert

Appendix E - 3D Modeling Backup

Combination 1
Entity: Strain (bottom) - Thin Shell
Component: EE

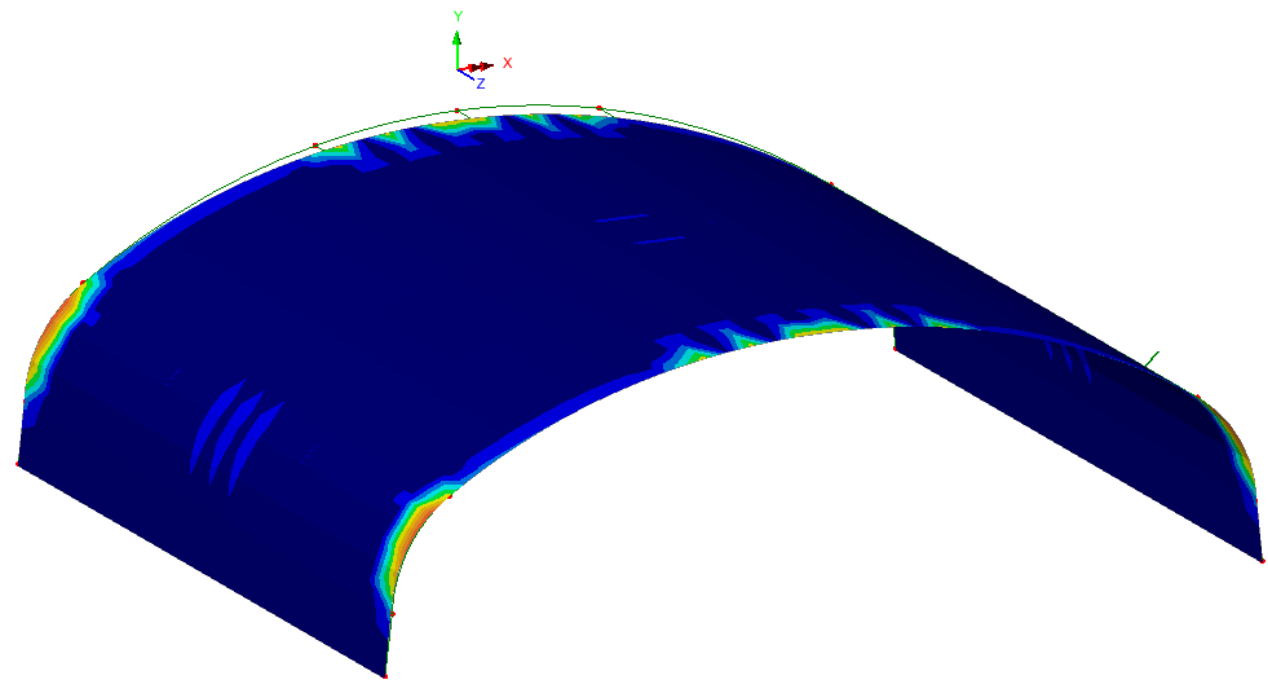
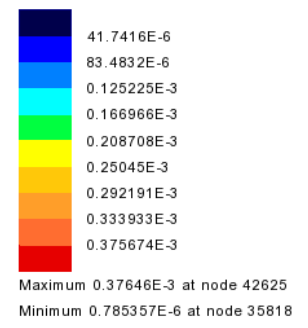


Figure 105. Von Mises Strain at Bottom Fiber in Culvert- 2 Lane 32 k Axle at Center of Culvert

Appendix E - 3D Modeling Backup

Combination 1
Entity: Strain (top) - Thin Shell
Component: EX

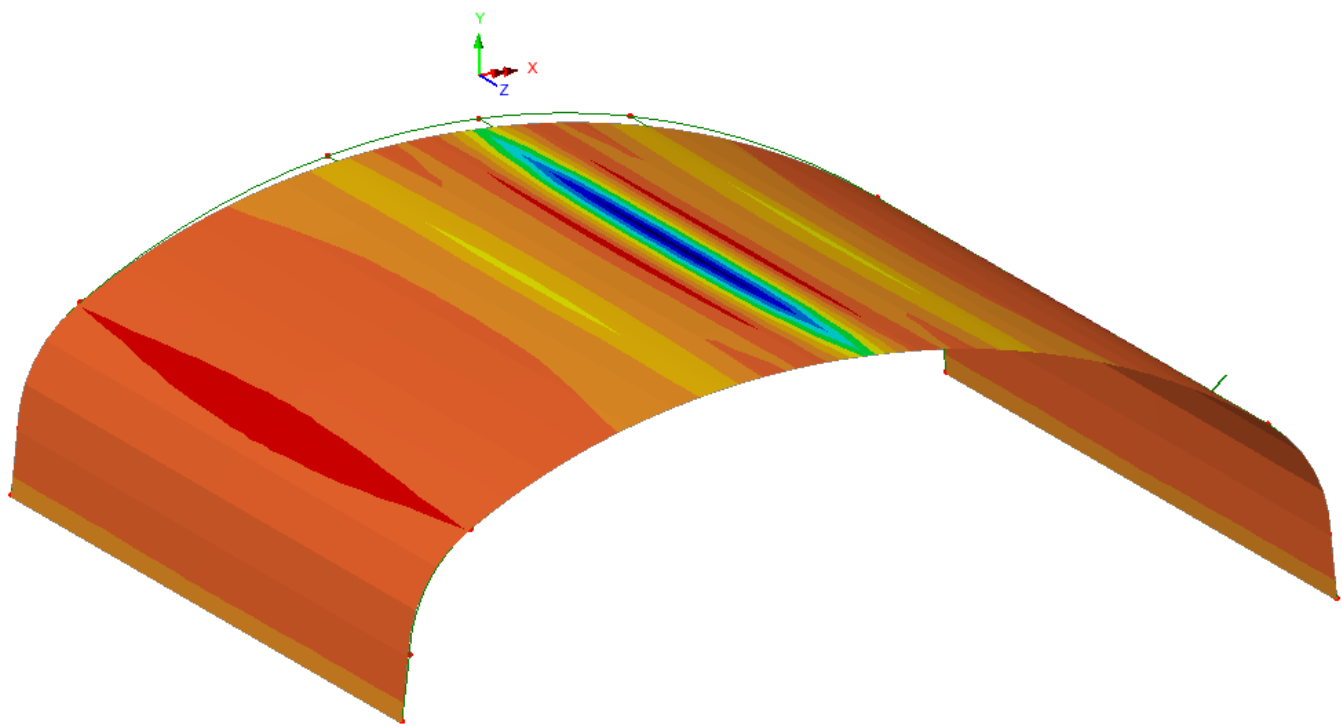
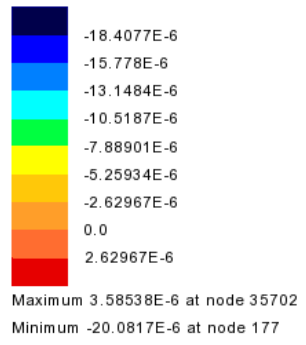
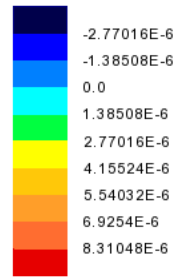


Figure 106. Bending Strain at Top Fiber in Culvert- 2 Lane 32 k Axle at Center of Culvert

Appendix E - 3D Modeling Backup

Combination 1
Entity: Strain (bottom) - Thin Shell
Component: EX



Maximum 8.96828E-6 at node 177
Minimum -3.49744E-6 at node 1819

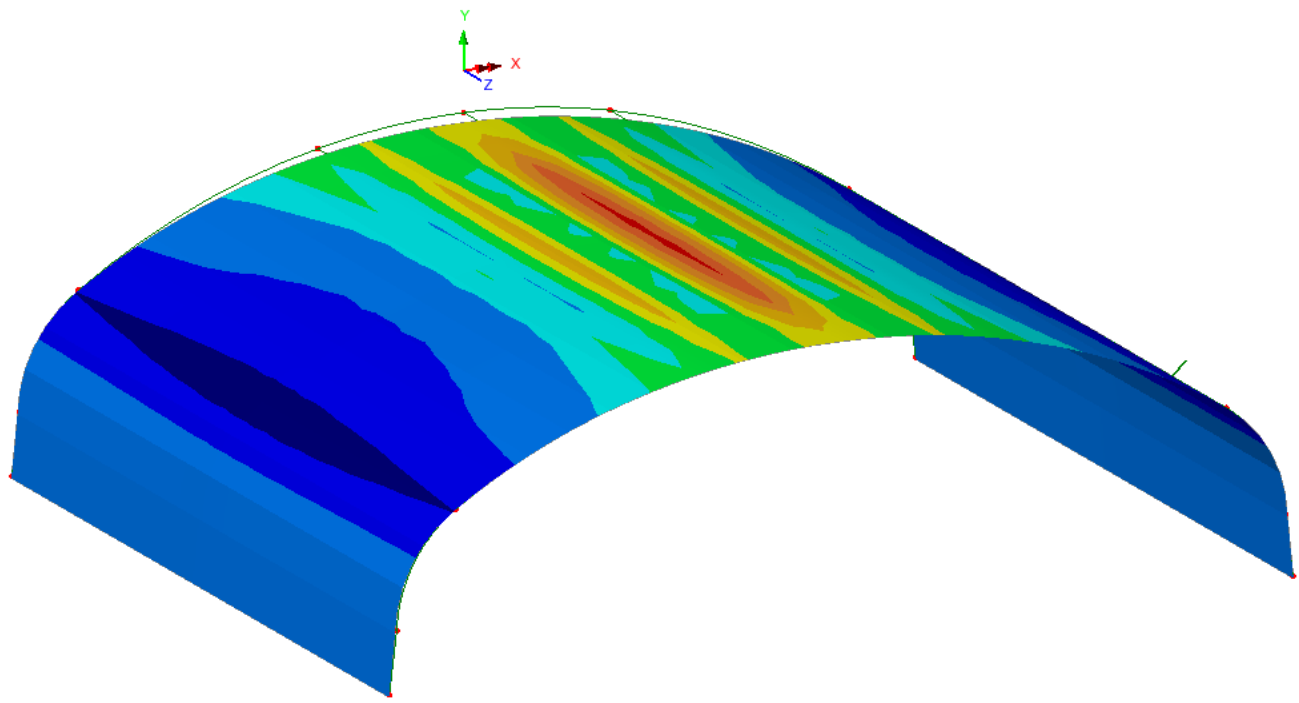
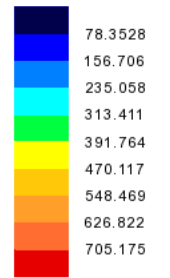


Figure 107. Bending Strain at Bottom Fiber in Culvert- 2 Lane 32 k Axle at Center of Culvert

Appendix E - 3D Modeling Backup

Combination 1
Entity: Stress (top) - Thin Shell
Component: SE (Units: kip/ft²)



Maximum 707.758 at node 177
Minimum 2.58278 at node 42546

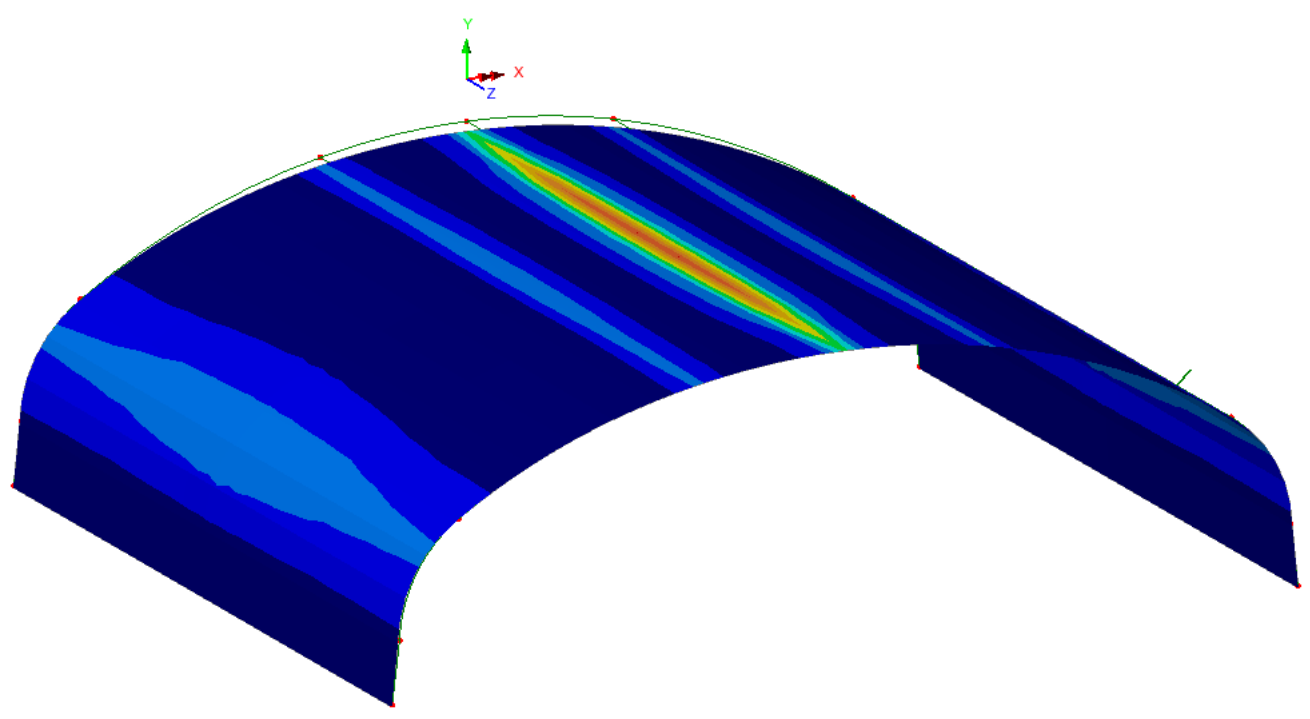
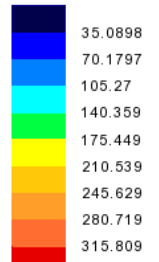


Figure 108. Von Mises Stress at Top Fiber in Culvert- 2 Lane 32 k Axle at Center of Culvert

Appendix E - 3D Modeling Backup

Combination 1
Entity: Stress (bottom) - Thin Shell
Component: SE (Units: kip/ft²)



Maximum 316.071 at node 177
Minimum 0.262106 at node 2390

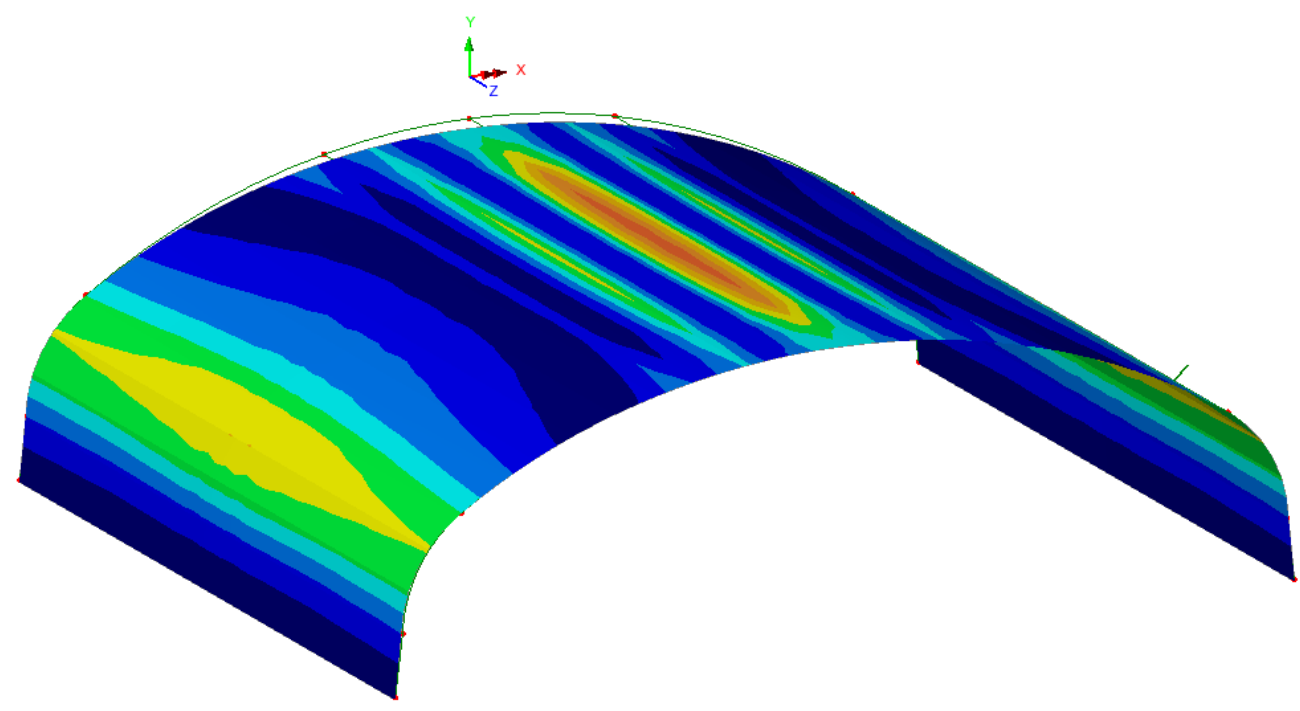
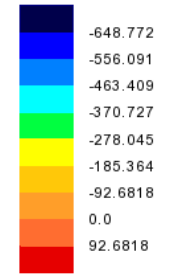


Figure 109. Von Mises Stress at Bottom Fiber in Culvert- 2 Lane 32 k Axle at Center of Culvert

Appendix E - 3D Modeling Backup

Combination 1
Entity: Stress (top) - Thin Shell
Component: SX (Units: kip/ft²)



Maximum 126.363 at node 35702
Minimum -707.773 at node 177

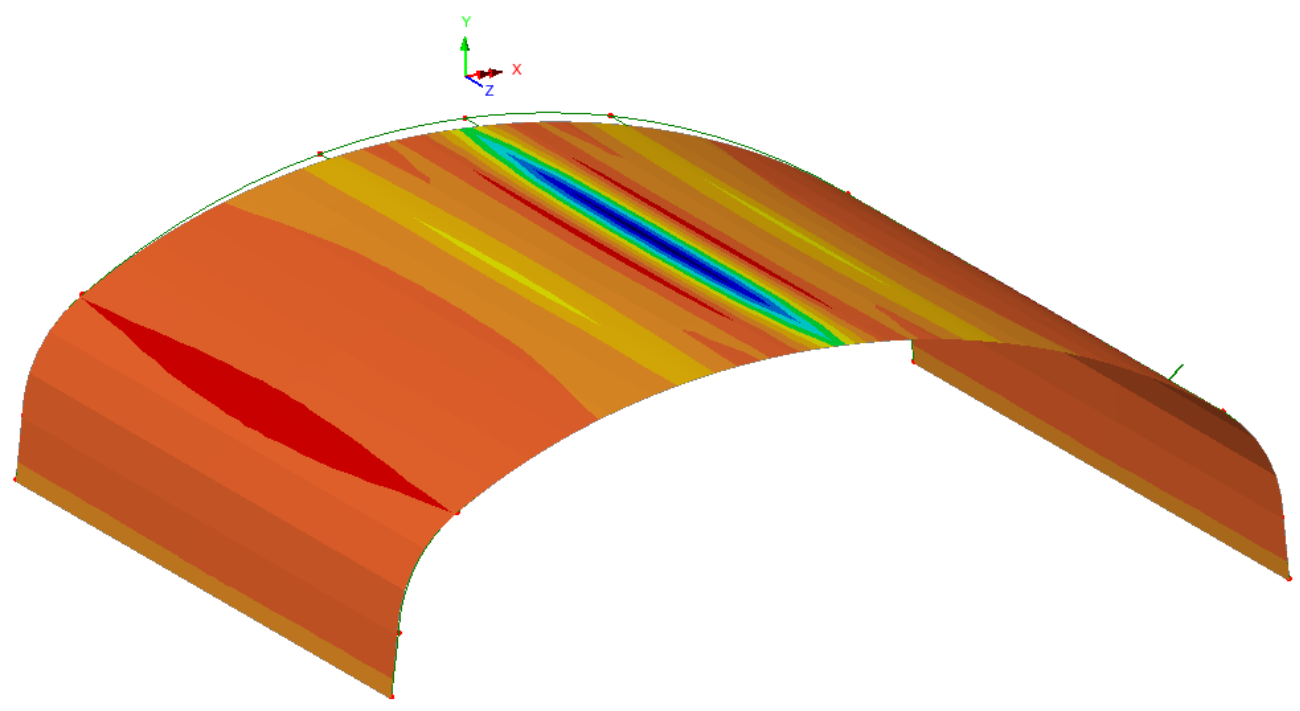
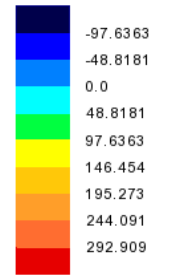


Figure 110. Bending Stress at Top Fiber in Culvert- 2 Lane 32 k Axle at Center of Culvert

Appendix E - 3D Modeling Backup

Combination 1
Entity: Stress (bottom) - Thin Shell
Component: SX (Units: kip/ft²)



Maximum 316.096 at node 177
Minimum -123.267 at node 1819

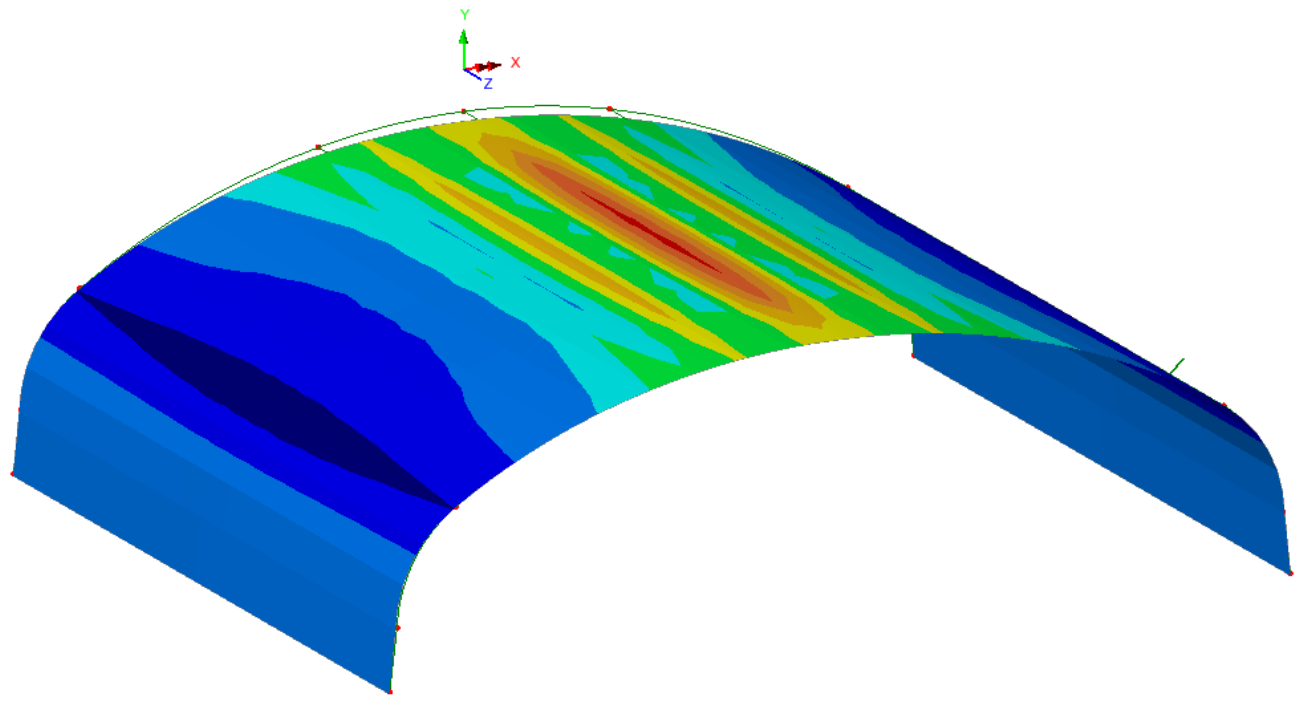


Figure 111. Bending Stress at Bottom Fiber in Culvert- 2 Lane 32 k Axle at Center of Culvert

Appendix F – Field Testing Plans

Appendix F – Field Testing Plans

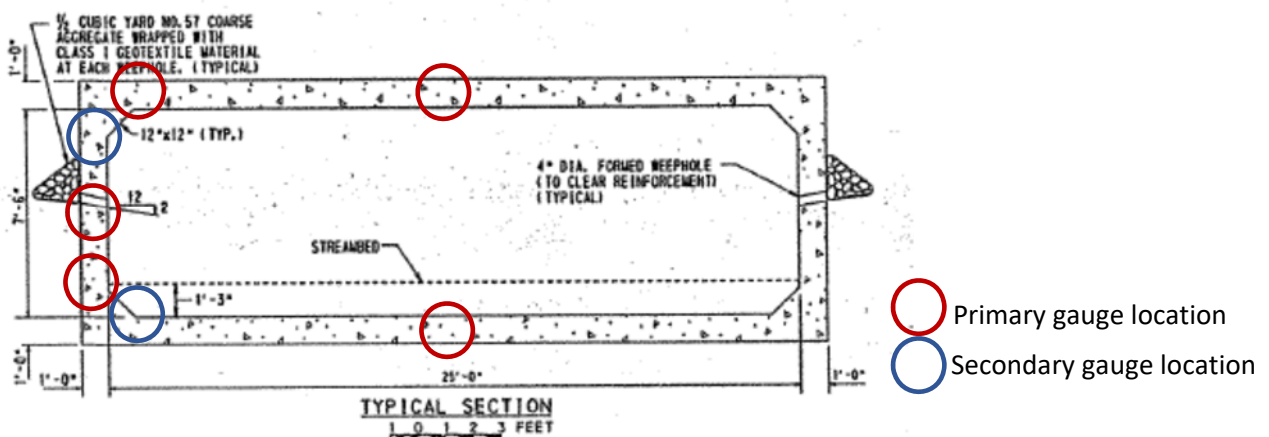
This appendix provides the field testing plans developed for the seven culverts that were field tested for this project.

Appendix F – Field Testing Plans

Model 1 – Testing Plan - Reinforced Concrete Box – Single Cell Site/General

- Single will be conducted – Instrumentation will be installed week of Aug 21, 2017 and load tested the following week. Gauges operation will be verified after installation and prior to test.
- Test vehicles – Weighed test vehicle (Triaxle dump with raised axle) will be provided by PennDOT District forces. Each wheel of truck to be weighed.
- PennDOT District will also provide traffic control during the test phase. No traffic control during gauge installation will be required.

Instrumentation



- Instrumentation locations – strain gauges will be mounted at each of the primary gauge locations indicated in the figure above along a single line near the center of the travelway the culvert. If time permits, additional gauges will be placed at the secondary locations. Where possible, string pot gauges will be mounted to capture deflections at the slab midspan locations.
- Strain- 5 locations minimum as shown above, midspan of top and bottom slabs and at corners as close as possible to the edge of the haunch (measure actual distance). If time permits, mount backup redundant gauges. The strain gauges require small gauge electric wire cables to be run to a central location to be connected to the data acquisition device. Modjeski will perform this work, assisted by Baker.
- String pot gauges, where possible, will be mounted to collect deflection data at slab midspan by mounting to a reference frame supported at locations unaffected by the truck loading.

Pre-test

- Install instruments and test proper operation

Trucks

- Trucks to be provided by PennDOT per cooperative letter. All trucks shall be consistent with design loadings. District indicated they can provide a dump truck with 3 rear axles
- During the test, at times when gauge readings are being taken, no other traffic can be on the culvert structure. Readings taken are for static loading so if it is necessary for a vehicle to traverse the structure, accommodations can be made. However, the structure will have to be closed to traffic during testing.

Appendix F – Field Testing Plans

Test

- Measure axle loads (see above)
- Record air and pavement temperature (if still warm)
- Read instruments pre-test
- Truck positions for readings (as truck moves across span). Three vehicle paths will be established – one with a wheel line directly over the gauges, the second with the wheel line 3 feet transverse to the line of gauges (such that the truck is centered over the line of gauges) and the third with the wheel line 3 feet from the line of gauges and the second wheel line is 9 feet from the gauge line. Two passes will be made along each of these passes of the truck, stopping as each wheel/axle passes directly over a gauge

Time

- Gauge/Target/Wiring installation and setup – approx 1 day
- Load testing – approx ½ day

Results

- Per NCHRP policy, test results cannot be shared with the PennDOT prior to publication

Schedule

- Schedule is subject to change. Current preliminary schedule for setup and testing is as follows:

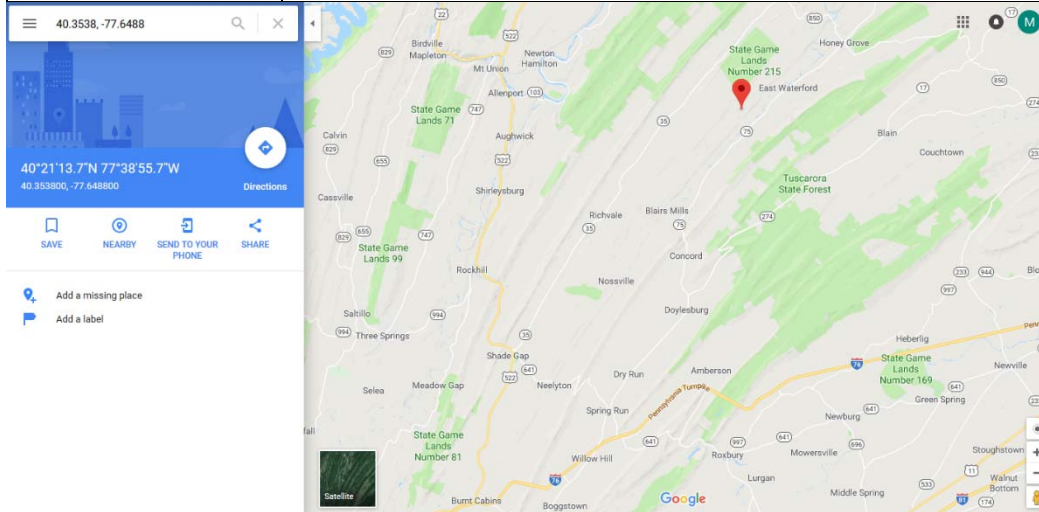
Operation	Dates
Install instruments	Week of Aug 21, 2017
Load Test	Week of Aug 28, 2017

Appendix F – Field Testing Plans

Testing Data

General

Location:	State: Pennsylvania Route: 3020 Latitude-Longitude: 40.3538, -77.6488 (click link to open in browser)
------------------	---



Actual Instrumentation Date:	August 28-29, 2017
Actual Testing date:	August 30, 2017
Weather/Other Test conditions:	61 F, Sunny
Contractor Personnel:	Dave Barrett, Chad Clancy (Modjeski & Masters) Mike Pichura, Mark Mlynarski (Michael Baker International)
State Personnel/Contacts:	George Helsey Pennsylvania Department of Transportation District 2-0 George Prestash III, P.E. District Bridge Engineer Pennsylvania Department of Transportation Engineering District 2-0 70 PennDOT Drive Clearfield, PA 16830

Appendix F – Field Testing Plans

Truck Wheel Load and Spacing Data/ Truck Positioning Data

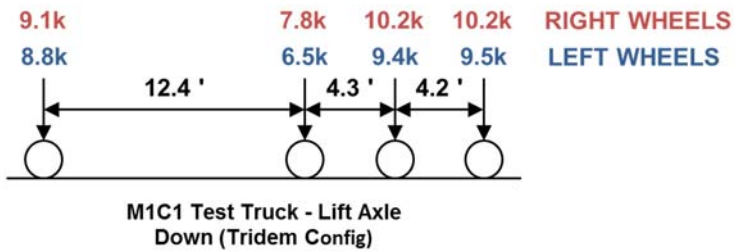
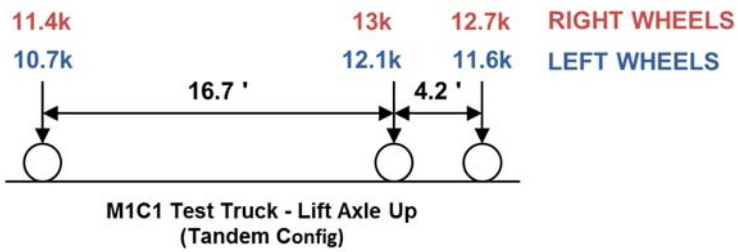


Figure 1 – Wheel loads/configurations for Model 1-Candidate 1 (M1C1)

Appendix F – Field Testing Plans

Lift axle up runs		
CL of left <u>wheel</u> running on gauge line		
Wheel	Position	Time
1	1	10:21
1	2	10:22
1	3	10:23
1	4	10:24
1	5	10:24
2	1	10:27
2	2	10:27
2	3	10:28
2	4	10:29
2	5	10:30
3	1	10:33
3	2	10:34
3	3	10:35
3	4	10:36
3	5	10:36

CL of <u>truck</u> running on gauge line		
Wheel	Position	Time
1	3	10:40
2	3	10:41
3	3	10:42

Lift Axle Down runs		
CL of left wheel over CL gauge line		
Wheel	Position	Time
1	1	10:45
1	2	10:46
1	3	10:47
1	4	10:47
1	5	10:48
L	1	10:50
L	2	10:50
L	3	10:51
L	4	10:52

Appendix F – Field Testing Plans

	5	10:52
2	1	10:54
2	2	10:54
2	3	10:55
2	4	10:56
2	5	10:56
3	1	10:59
3	2	10:59
3	3	11:00
3	4	11:01
3	5	11:01

CL of truck running on gauge line		
Wheel	Position	Time
1	3	11:03
L	3	11:04
2	3	11:05
3	3	11:06
Left wheel on CL gauge line		
Lift axle down		
5 mph speed going across culvert		
Time:	11:08	

Wheel Position Descriptions (typ)

- 1 Wheel centered over inside face of culvert vertical wall
- 2 Wheel at first quarter point on top slab
- 3 Wheel centered over midspan (2nd quarter point)
- 4 Wheel at third quarter point on top of slab
- 5 Wheel centered over inside face of far culvert vertical wall

All wheels were spaced at 6'-2" center-center of wheel on each axle

The front wheel was 13 inches wide

The Lift axle wheels were 2@8.5" wide with an out-out width of 22"

The #2 axle (2nd from rear) wheels were 2@9" wide with an out-out width of 22.5"

The #3 axle (rear) wheels were 2@9" wide with an out-out width of 22.5"

Appendix F – Field Testing Plans

Culvert Plans

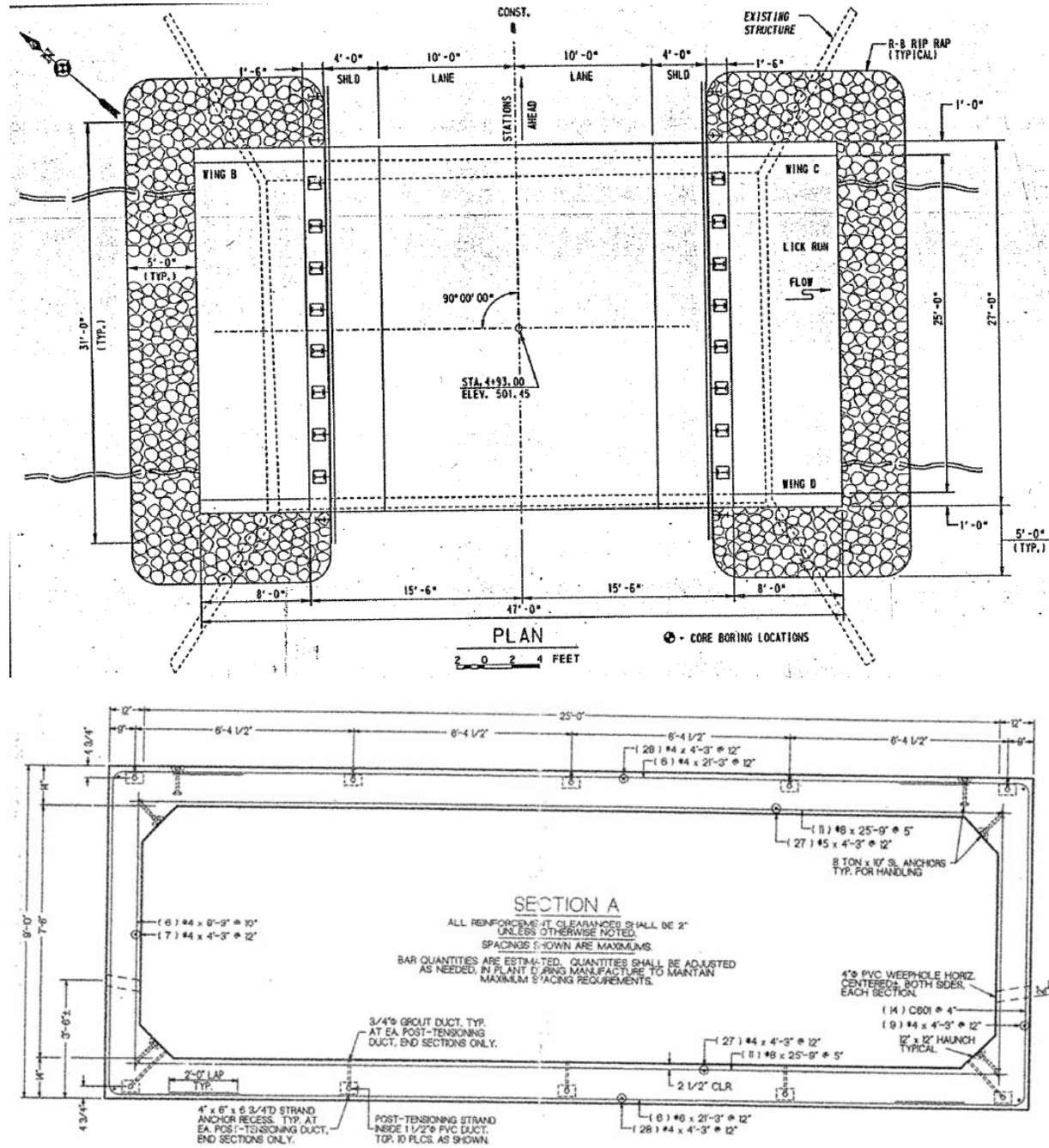


Figure 2 – Model 1, Candidate 1 (M1C1) – Plan and Typical Section

Appendix F – Field Testing Plans

Model 2 – Testing Plan - Reinforced Concrete Box – Twin Cell
 Site/General

- Instrumentation will be installed week of Dec 11, 2017 and load tested the same week. Gauges operation will be verified after installation and prior to test.
- Test truck to be on site at 10am, traffic control needed starting at 9am
- Test vehicles – Weighed test vehicle will be provided by Maryland DOT forces. Each wheel of truck to be weighed.
- Maryland DOT will also provide traffic control during the test phase. No traffic control during gauge installation will be required, however, traffic control will be required 1 hour prior to testing to lay out load path line.

Instrumentation

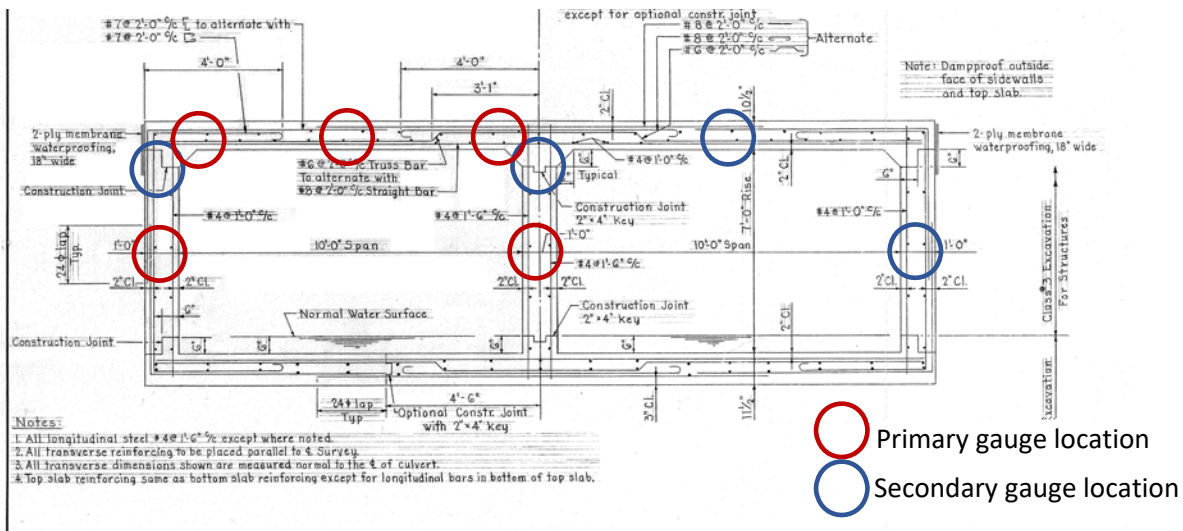


Figure 3 - Instrumentation locations

Appendix F – Field Testing Plans

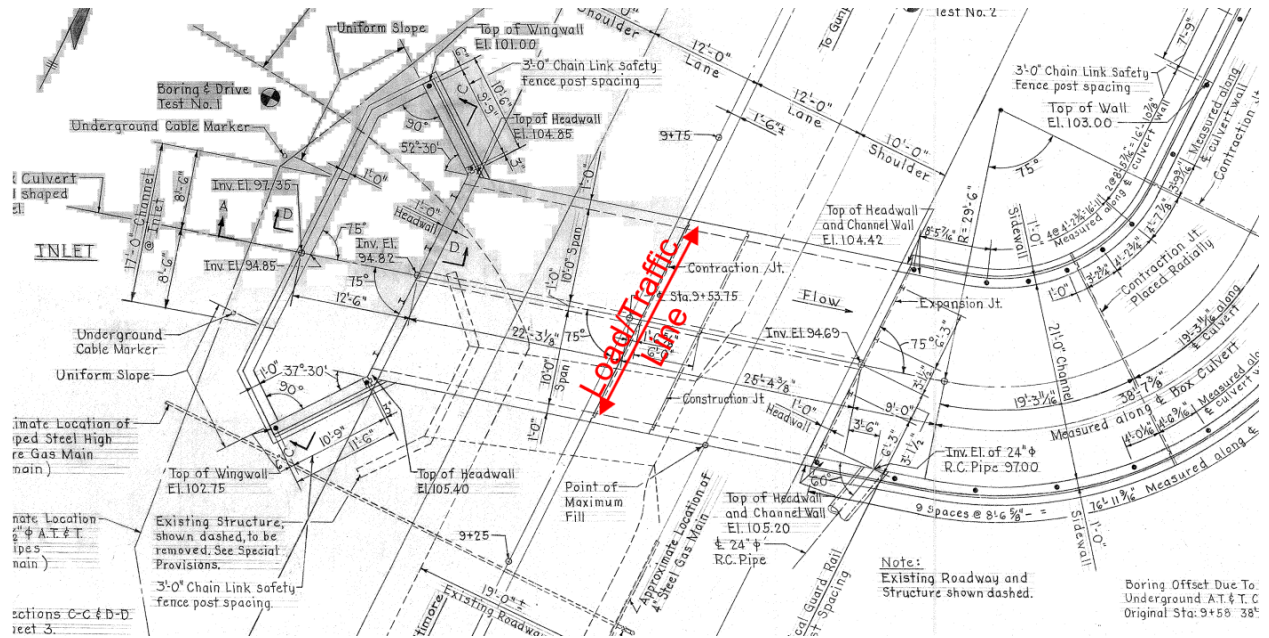


Figure 4 - Plan View

- Instrumentation locations – strain gauges will be mounted at each of the primary gauge locations indicated in the figure above along the “load line” near the center of the culvert segment (based on the orientation of the reinforcing, the line of sensors are to be installed along a line parallel to the traffic/outside edges of the culvert). If time permits, additional gauges will be placed at the secondary locations. Where possible, string pot gauges will be mounted to capture deflections at the slab midspan locations.
- Strain- locations minimum as shown above, midspan of top and bottom slabs and at corners as close as possible to the edge of the haunches (measure actual distance). If time permits, mount backup redundant gauges (redundant gauge at midspan is required). The strain gauges require small gauge electric wire cables to be run to a central location to be connected to the data acquisition device. Modjeski will perform this work, assisted by Baker.
- String pot gauges, where possible, will be mounted to collect deflection data at slab midspans by mounting to a reference frame supported at locations unaffected by the truck loading.

Pre-test

- Install instruments and test proper operation

Trucks

- A loaded truck to be provided by Maryland DOT per cooperative letter. All trucks shall be consistent with design loadings. District indicated they can provide a dump truck
- During the test, at times when gauge readings are being taken, no other traffic can be on the culvert structure. Readings taken are for static loading so if it is necessary for a vehicle to traverse the structure, accommodations can be made. However, the structure will have to be closed to traffic during testing.

Test

- Measure individual wheel loads (Maryland DOT to work with State Police to obtain, see above)
- Record air and pavement temperature

Appendix F – Field Testing Plans

- Read instruments pre-test
- Truck positions for readings (as truck moves across span). Vehicle paths will be established as shown in layout diagram—with a wheel line directly over the gauges, the second with the wheel line 3 feet transverse to the line of gauges (such that the truck is centered over the line of gauges) Each wheel will be stopped over the vertical culvert wall, ¼ point and at midspan of the culvert top slab. In the event gauges are placed at the midspan locations of the second span, a wheel stop location will be placed at midspan of that cell.

Time

- Gauge/Target/Wiring installation and setup – approx 1 day
- Load testing – approx ½ day

Results

- Per NCHRP policy, test results cannot be shared with the DOT prior to publication

Schedule

- Schedule is subject to change. Current preliminary schedule for setup and testing is as follows:

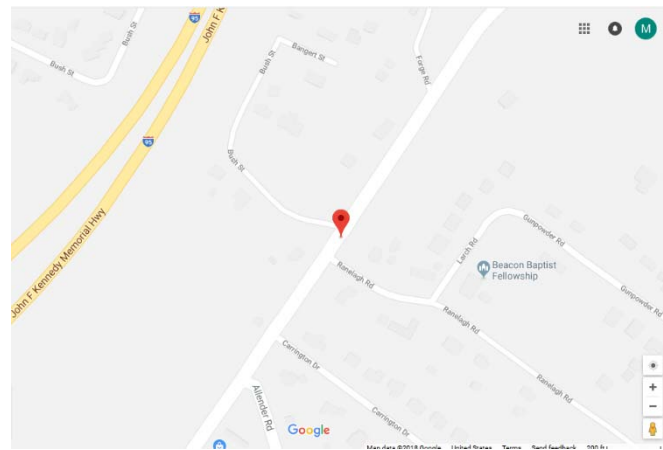
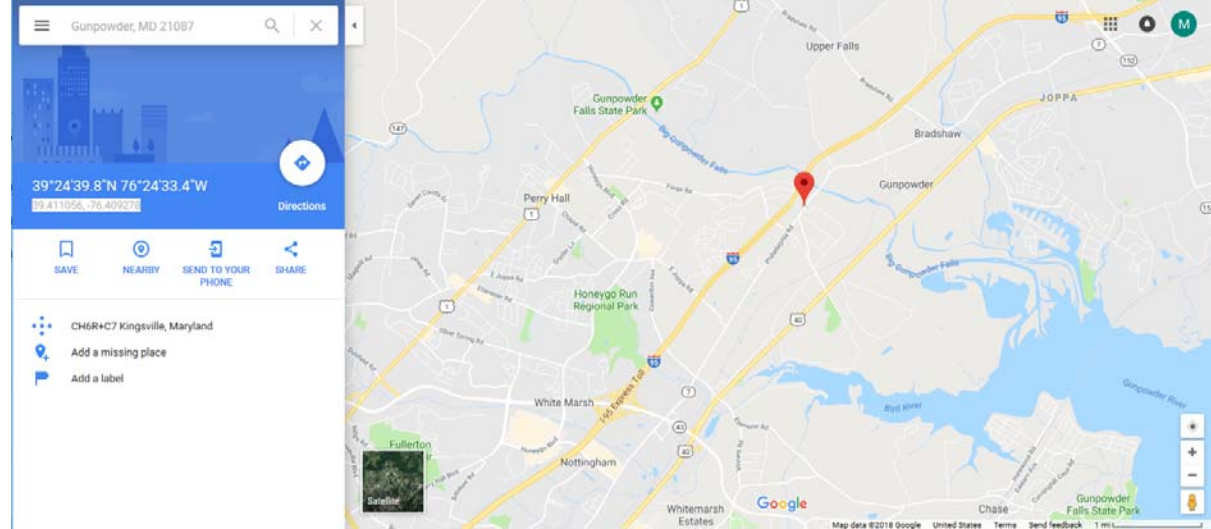
Operation	Dates
Install instruments	Week of Dec 11, 2017
Load Test	Dec 14 th (Rain date Dec 13 th), 2017

Appendix F – Field Testing Plans

Testing Data

General

Location:	State: Maryland DOT Route: SR 7 (Philadelphia RD) Latitude-Longitude: 39.411056, -76.409278 (click link to open in browser)
------------------	--



Actual Instrumentation Date:	December 12, 2017
Actual Testing date:	December 13, 2017
Weather/Other Test conditions:	25 F, Sunny
Contractor Personnel:	Dave Barrett (Modjeski & Masters) Mike Pichura, Aaron Colorito (Michael Baker International)
State Personnel/Contacts:	Justin Mohr, P.E. MDOT Maryland State Highway Administration – Office of Structures 707 N. Calvert Street, MS – 203 Baltimore, MD 21202 410.545.8365 jmohr@sha.state.md.us

Appendix F – Field Testing Plans

Culvert Plans

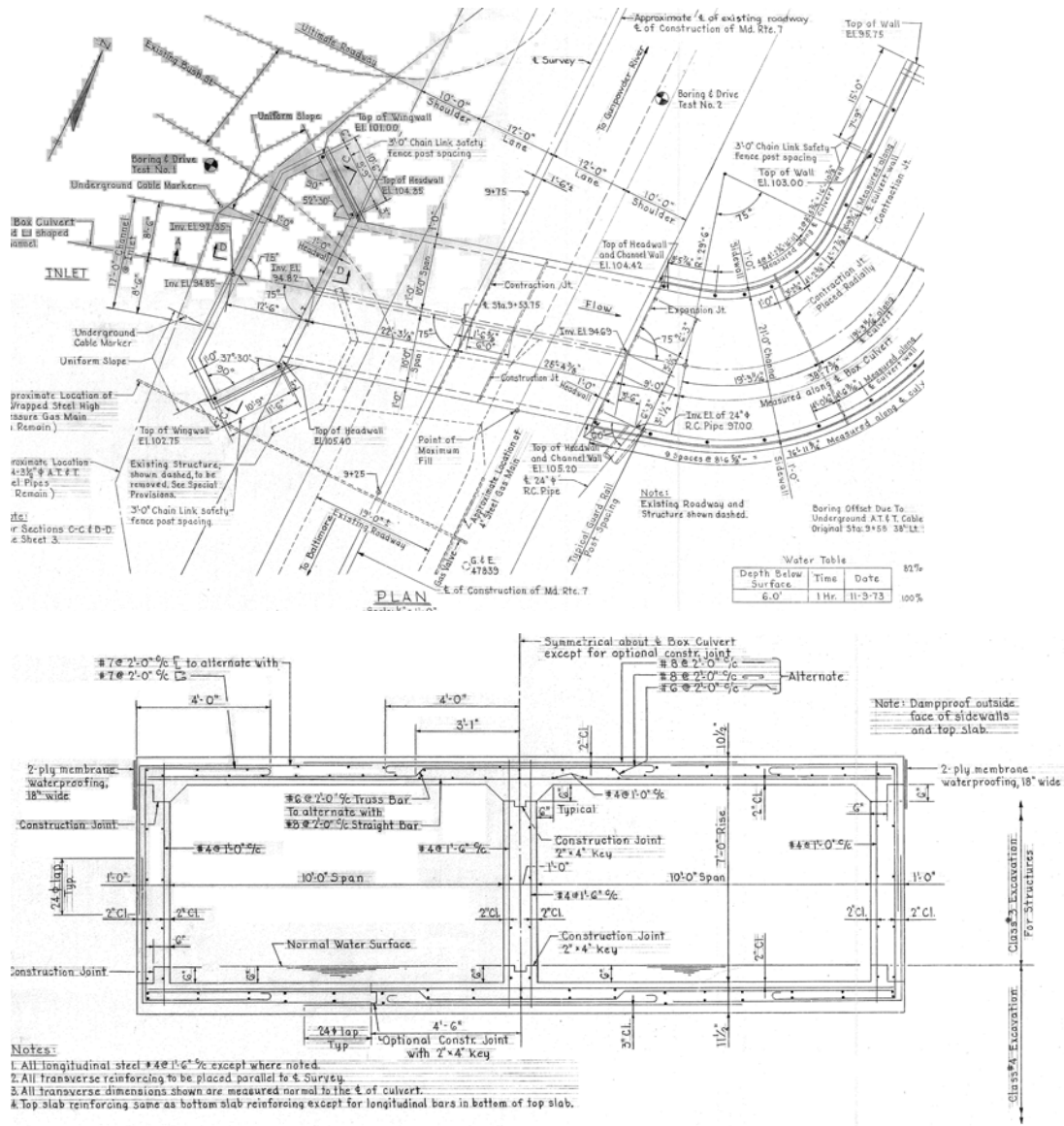


Figure 6 – Model 2, Candidate 1 (M2C1) – Plan and Typical Section

Appendix F – Field Testing Plans

Model 3 – Testing Plan - Reinforced Concrete Box – Single Cell Precast

Site/General

- Instrumentation will be installed week of Nov 6, 2017 and load tested the same week. Gauges operation will be verified after installation and prior to test.
- Test truck to be on site at 10am, traffic control needed starting at 9am
- Test vehicles – Weighed test vehicle will be provided by PennDOT District forces. Each wheel of truck to be weighed.
- PennDOT District will also provide traffic control during the test phase. No traffic control during gauge installation will be required, however, traffic control will be required 1 hour prior to testing to lay out load path line.

Instrumentation

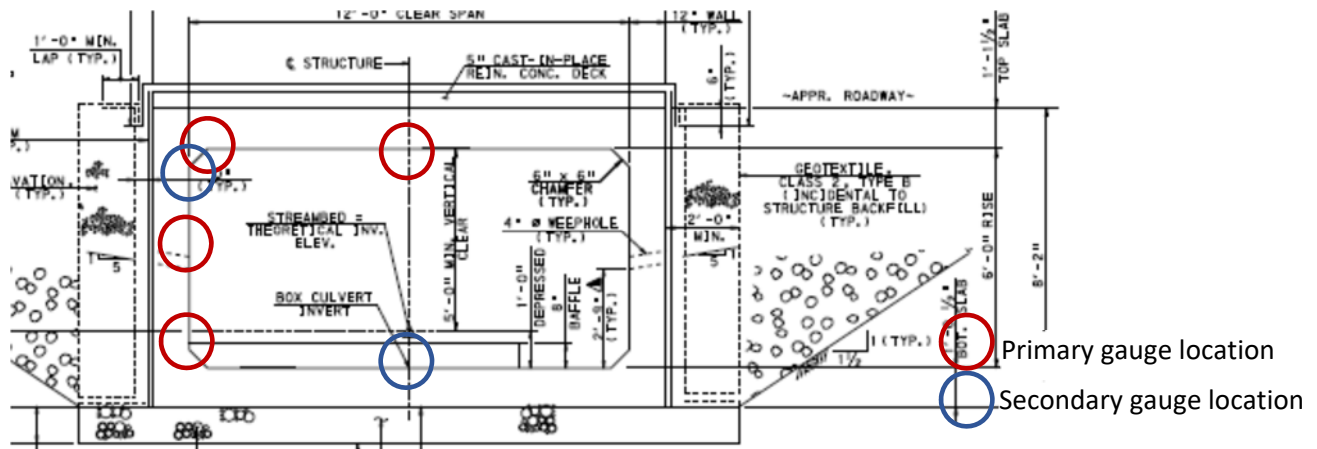


Figure 7 - Instrumentation locations

- Instrumentation locations – strain gauges will be mounted at each of the primary gauge locations indicated in the figure above along the “load line” near the center of the the culvert segment (see figure above and layout figure at the end of the testing plan). If time permits, additional gauges will be placed at the secondary locations. Where possible, string pot gauges will be mounted to capture deflections at the slab midspan locations.
- Strain- locations minimum as shown above, midspan of top and bottom slabs and at corners as close as possible to the edge of the haunch (measure actual distance). If time permits, mount backup redundant gauges (redundant gauge at midspan is required). The strain gauges require small gauge electric wire cables to be run to a central location to be connected to the data acquisition device. Modjeski & Masters will perform this work, assisted by Baker.
- String pot gauges, where possible, will be mounted to collect deflection data at slab midspan by mounting to a reference frame supported at locations unaffected by the truck loading.

Pre-test

- Install instruments and test proper operation

Appendix F – Field Testing Plans

Trucks

- A loaded truck to be provided by PennDOT per cooperative letter. All trucks shall be consistent with design loadings. District indicated they can provide a dump truck
- During the test, at times when gauge readings are being taken, no other traffic can be on the culvert structure. Readings taken are for static loading so if it is necessary for a vehicle to traverse the structure, accommodations can be made. However, the structure will have to be closed to traffic during testing.

Test

- Measure individual wheel loads (PennDOT to work with State Police to obtain, see above)
- Record air and pavement temperature
- Read instruments pre-test
- Truck positions for readings (as truck moves across span). Vehicle paths will be established as shown in layout diagram—with a wheel line directly over the gauges, the second with the wheel line 3 feet transverse to the line of gauges (such that the truck is centered over the line of gauges) Each wheel will be stopped over the vertical culvert wall, ¼ point and at midspan of the culvert top slab.

Time

- Gauge/Target/Wiring installation and setup – approximately 1 day
- Load testing – approximately ½ day

Results

- Per NCHP policy, test results cannot be shared with the PennDOT prior to publication

Schedule

- Schedule is subject to change. Current preliminary schedule for setup and testing is as follows:

Operation	Dates
Install instruments	Week of Nov 6, 2017
Load Test	Nov 7 th (Rain date Nov 8 th), 2017

Appendix F – Field Testing Plans

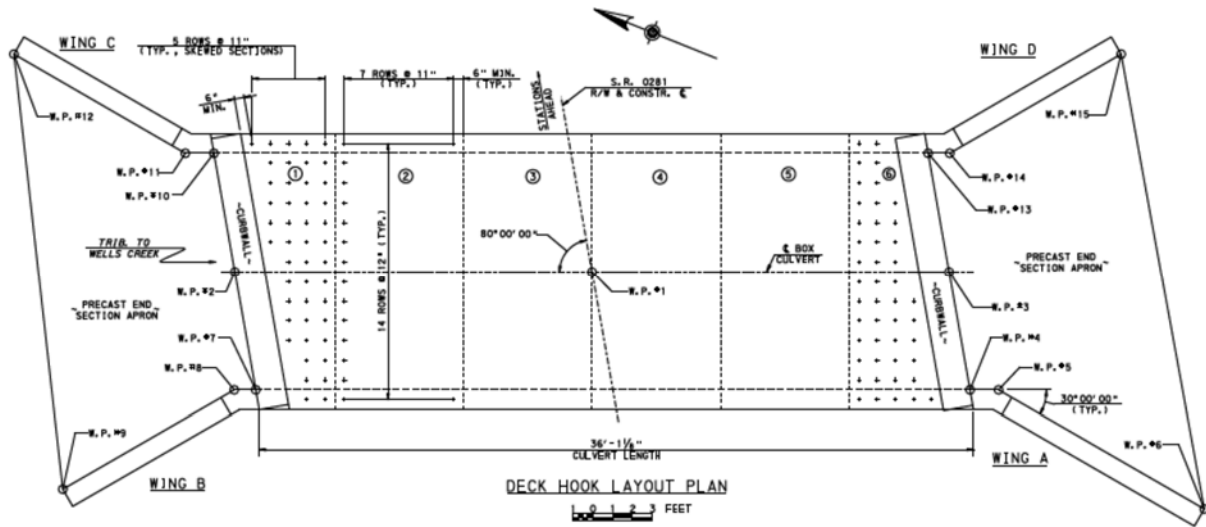


Figure 10 - Culvert Segments

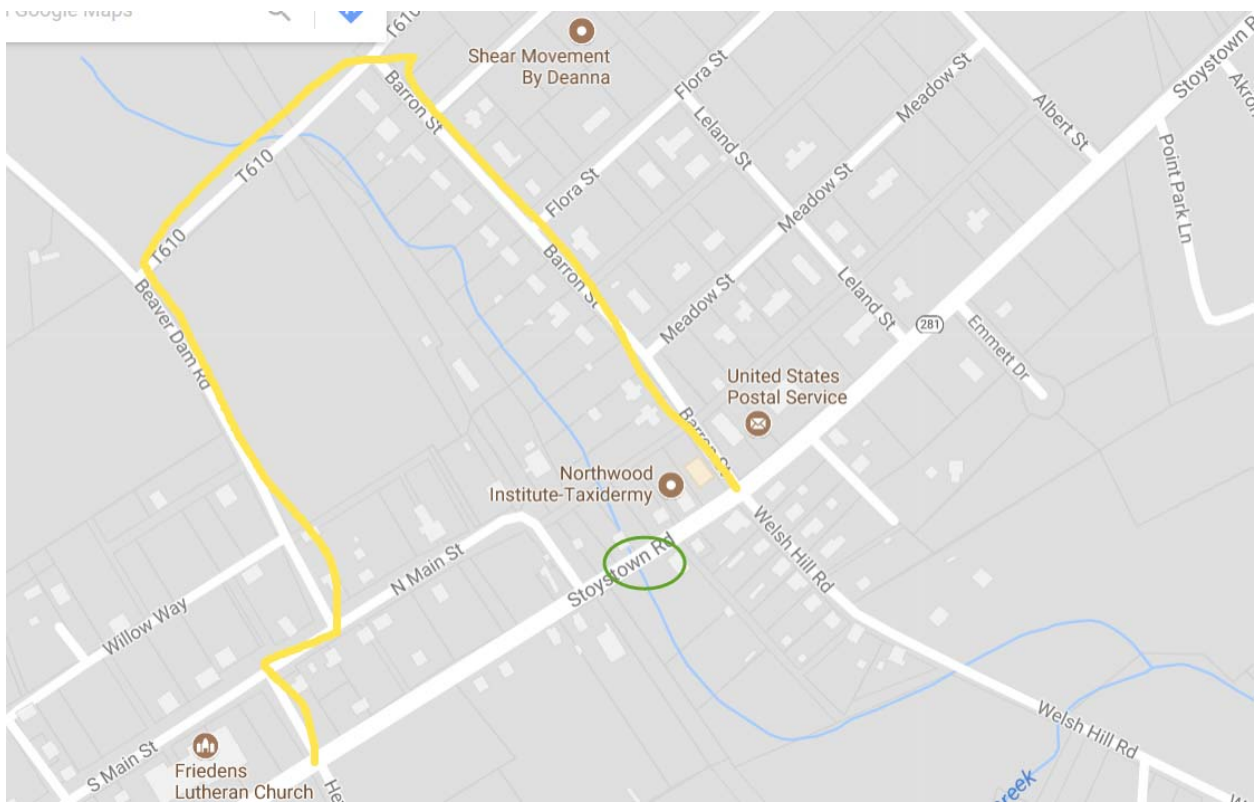


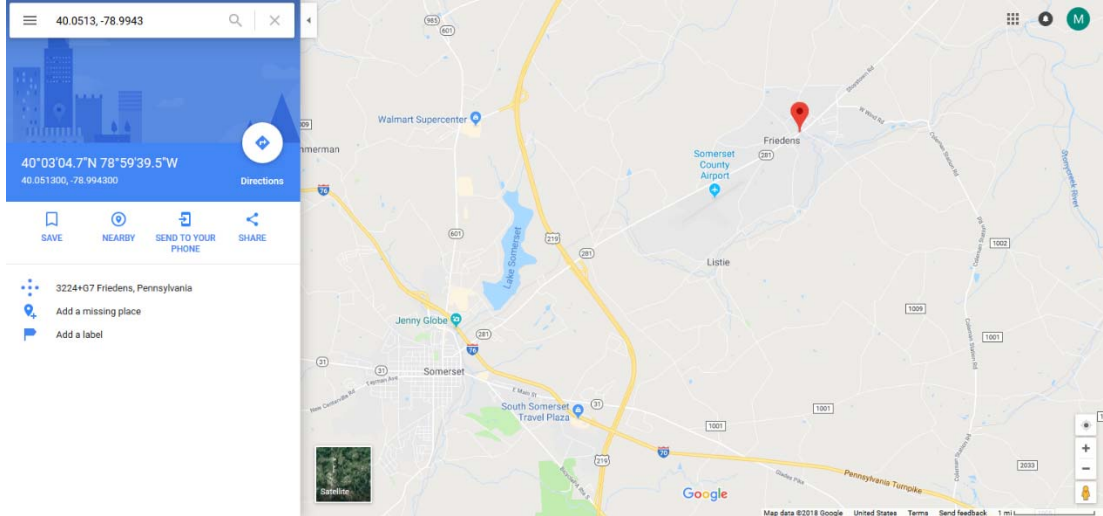
Figure 11 - Possible Truck Detour, if Required

Appendix F – Field Testing Plans

Testing Data

General

Location:	State: Pennsylvania Route: SR 281 Latitude-Longitude: 40.0513, -78.9943 (click link to open in browser)
------------------	--



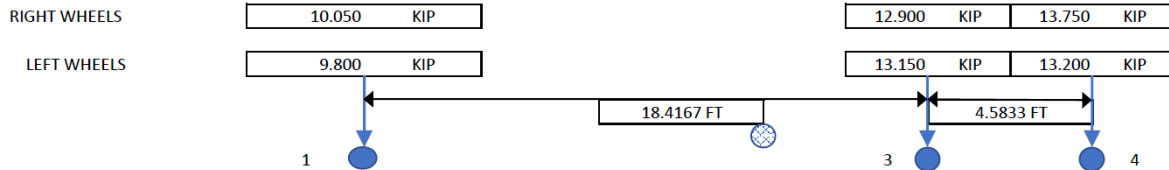
Actual Instrumentation Date:	11/5/2017-11/6/2017
Actual Testing date:	11/7/2017
Weather/Other Test conditions:	36 F, Sunny
Contractor Personnel:	Dave Barrett (Modjeski & Masters) Mike Pichura, (Michael Baker International) Aaron Colorito (Michael Baker International)
State Personnel/Contacts:	Ralph DeStefano, P.E. District 9-0 Bridge Engineer William D. Oleksak, P.E. District Maintenance Manager Engineering District 9-0 1620 North Juniata Street Hollidaysburg, PA 16648 (814) 696-7129

Appendix F – Field Testing Plans

Truck Wheel Load and Spacing Data/ Truck Positioning Data

TEST TRUCK - LIFT AXLE UP - WHEEL ON LOAD LINE				
QUARTER POINT	WHEEL			
	1	2	3	4
0.00 L	10:56:30 AM		11:03:18 AM	11:10:04 AM
0.25 L	10:56:58 AM		11:03:47 AM	11:10:51 AM
0.50 L	10:57:28 AM		11:04:26 AM	11:11:38 AM
0.75 L	10:57:52 AM		11:05:00 AM	11:12:08 AM
1.00 L	10:58:19 AM		11:05:35 AM	11:12:38 AM

CULVERT NAME:	STOYSTOWN ROAD OVER WELLS CREEK
DISTRICT/COUNTY:	D9/SOMERSET
BMS NO.:	55-0281-0590-2521
BR KEY:	48389
DATE:	11/7/2017



TEST TRUCK - LIFT AXLE DOWN - WHEEL ON LOAD LINE*				
QUARTER POINT	WHEEL			
	1	2	3	4
0.00 L	10:11:00 AM	10:20:00 AM	10:31:00 AM	10:39:00 AM
0.25 L	10:12:00 AM	10:21:00 AM	10:32:00 AM	10:40:00 AM
0.50 L	10:13:00 AM	10:22:00 AM	10:32:00 AM	10:40:00 AM
0.75 L	10:13:00 AM	10:23:00 AM	10:33:00 AM	10:41:00 AM
1.00 L	10:14:00 AM	10:24:00 AM	10:33:00 AM	10:41:00 AM

WHEEL LINE 1	7.25
WHEEL LINE 2	6.0000
WHEEL LINE 3	6.0000
WHEEL LINE 4	6.0000

* SECONDS NOT RECORDED

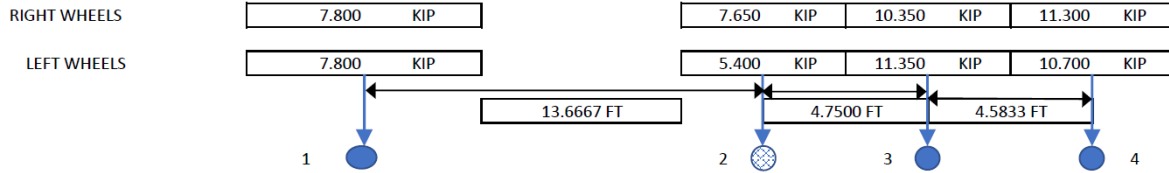


Figure 12 – Wheel loads/configurations/testing times for Model 3-Candidate 1 (M3C1)

Appendix F – Field Testing Plans

Culvert Plans

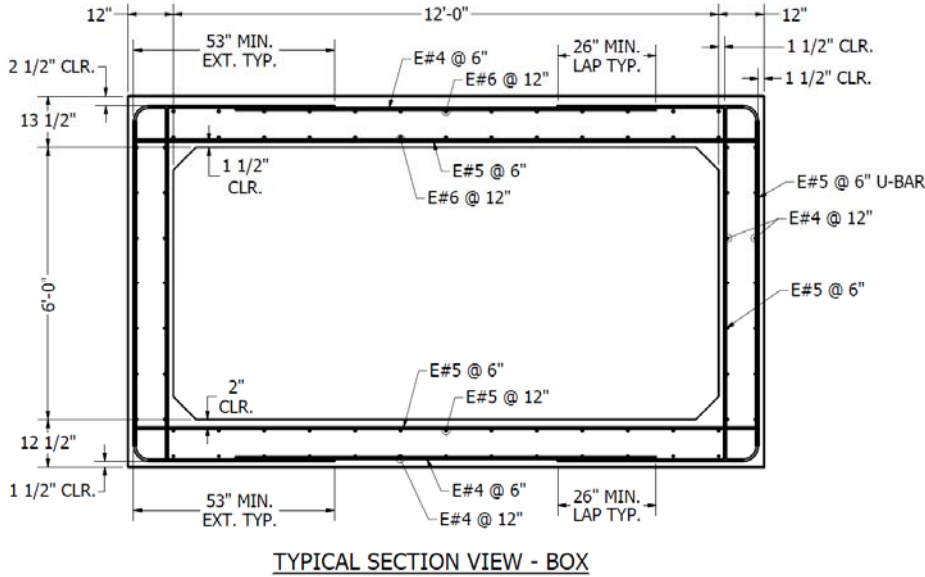
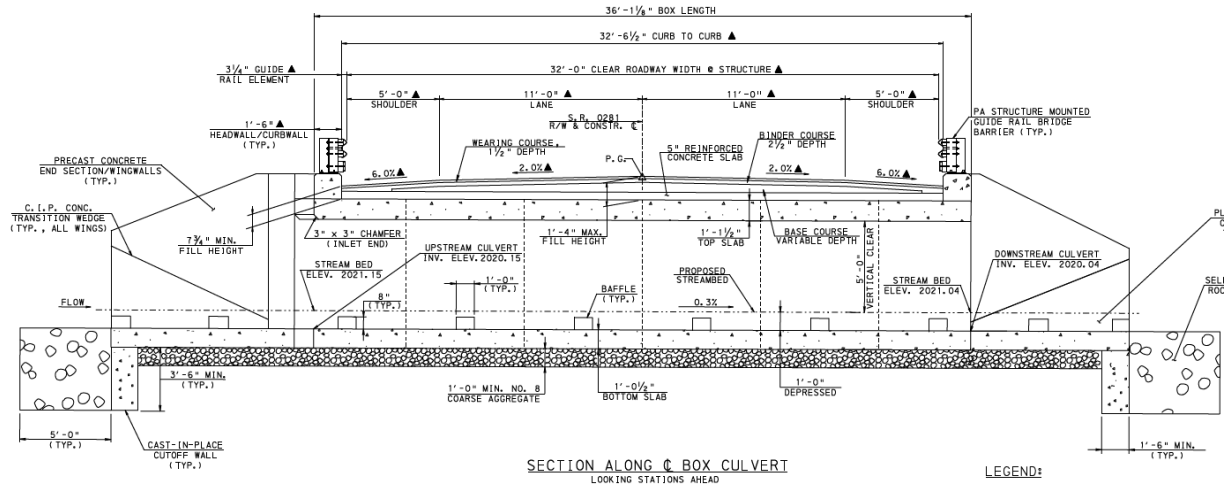


Figure 13 – Model 3, Candidate 1 (M3C1) – Plan and Typical Section

Appendix F – Field Testing Plans

Model 4 – Testing Plan – Reinforced Concrete Arch

Site/General

- Instrumentation will be installed week of April 16, 2018 and load tested the same week. Gauges operation will be verified after installation and prior to test.
- Test truck to be on site at 10am, traffic control needed starting at 9am
- Test vehicles – Weighed test vehicle will be provided by Ohio DOT forces. Each wheel of truck to be weighed. Contact info:

Shawn Rostorfer
Highway Management Administrator
District 6
400 E. William St., Delaware, OH 43015
740.833.8069

- Ohio DOT will also provide traffic control during the test phase. No traffic control during gauge installation will be required, however, traffic control will be required 1 hour prior to testing to lay out load path line.

Instrumentation

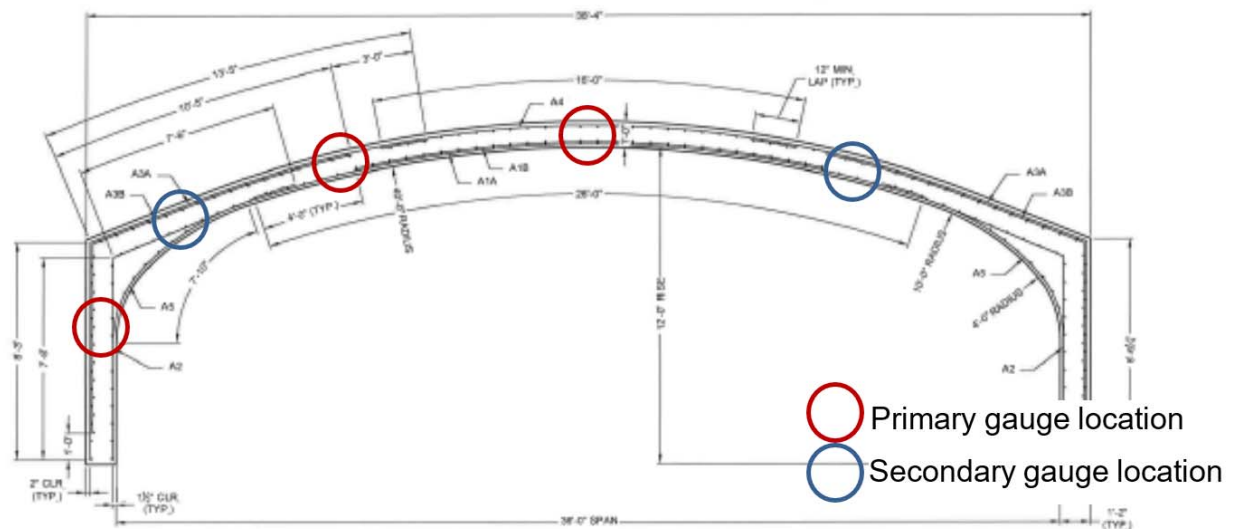


Figure 14 – M4C1 Instrumentation locations

Appendix F – Field Testing Plans

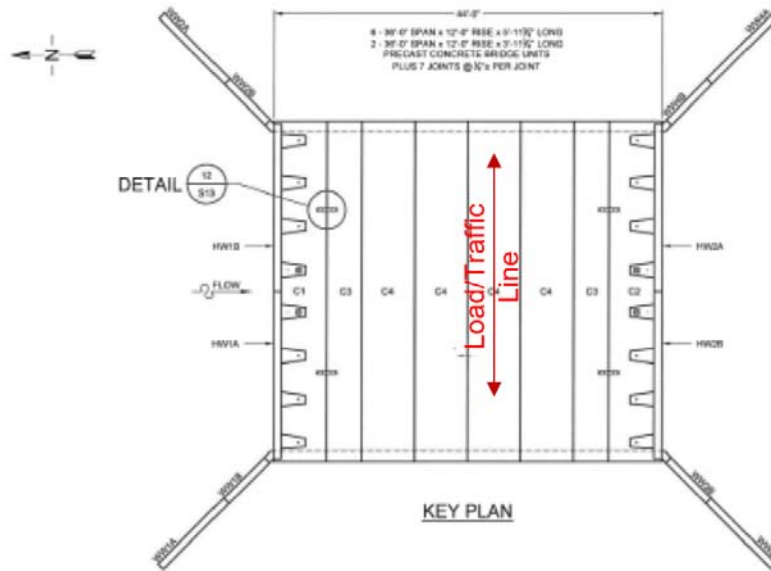


Figure 15 – M4C1 Load Traffic Line

- Instrumentation locations – strain gauges will be mounted at each of the primary gauge locations indicated in the figure above along the “load line” near the center of the culvert segment (based on the orientation of the reinforcing, the line of sensors are to be installed along a line parallel to the traffic/outside edges of the culvert). If time permits, additional gauges will be placed at the secondary locations. Where possible, string pot gauges will be mounted to capture deflections at the slab midspan locations.
- Strain- locations minimum as shown above, midspan of top slabs and at corners as close as possible to the specified locations and measurements taken to record their exact position. If time permits, mount backup redundant gauges (redundant gauge at midspan is required). The strain gauges require small gauge electric wire cables to be run to a central location to be connected to the data acquisition device. Modjeski will perform this work, assisted by Baker.
- String pot gauges, where possible, will be mounted to collect deflection data at slab midspans by mounting to a reference frame supported at locations unaffected by the truck loading.

Pre-test

- Install instruments and test proper operation

Trucks

- A loaded truck to be provided by Ohio DOT per cooperative letter. All trucks shall be consistent with design loadings.
- During the test, at times when gauge readings are being taken, no other traffic can be on the culvert structure. Readings taken are for static loading so if it is necessary for a vehicle to traverse the structure, accommodations can be made. However, the structure will have to be closed to traffic during testing.

Test

- Measure individual wheel loads (Ohio DOT to work with State Police to obtain, see above)
- Record air and pavement temperature

Appendix F – Field Testing Plans

- Read instruments pre-test
- Truck positions for readings (as truck moves across span). Vehicle paths will be established as shown in layout diagram—with a wheel line directly over the gauges, the second with the wheel line 3 feet transverse to the line of gauges (such that the truck is centered over the line of gauges) Each wheel will be stopped over the vertical culvert wall, ¼ point and at midspan of the culvert top slab. In the event gauges are placed at the midspan locations of the second span, a wheel stop location will be placed at midspan of that cell.

Time

- Gauge/Target/Wiring installation and setup – approx 1 day
- Load testing – approx ½ day

Results

- Per NCHRP policy, test results cannot be shared with the DOT prior to publication

Schedule

- Schedule is subject to change. Current preliminary schedule for setup and testing is as follows:

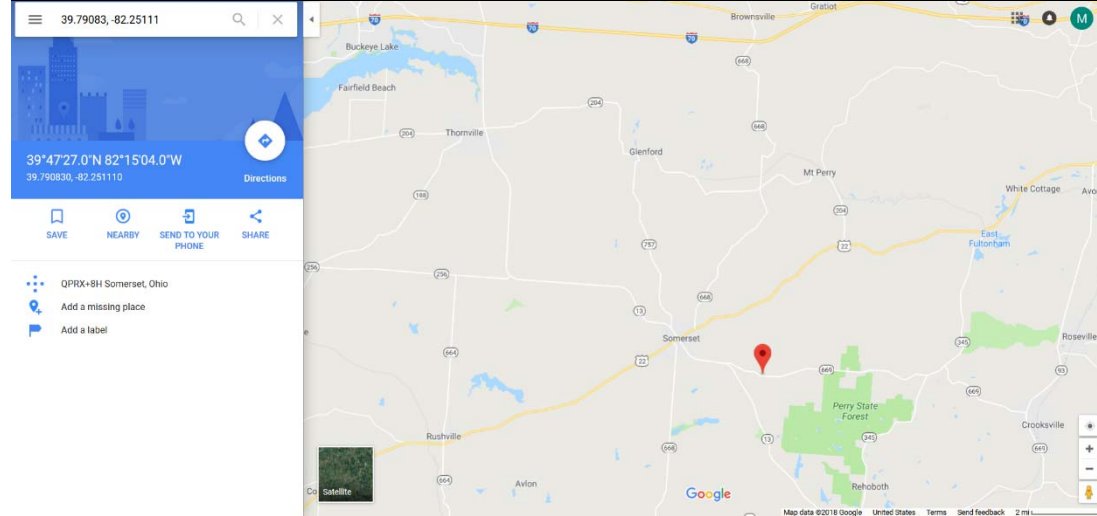
Operation	Dates
Install instruments	Week of April 16, 2018
Load Test	April 16, 2018

Appendix F – Field Testing Plans

Testing Data

General

Location:	State: Ohio DOT Route: SR 669 Latitude-Longitude: 39.79083, -82.25111 (click link to open in browser)
------------------	--



Actual Instrumentation Date:	4/16/2018
Actual Testing date:	4/17/2018
Weather/Other Test conditions:	31 F, Snow
Contractor Personnel:	Dave Barrett (Modjeski & Masters) Mike Pichura, (Michael Baker International) Gerry Jones (Michael Baker International)
State Personnel/Contacts:	Shawn Rostorfer Highway Management Administrator District 6 400 E. William St., Delaware, OH 43015 740.833.8069

Appendix F – Field Testing Plans

Truck Wheel Load and Spacing Data

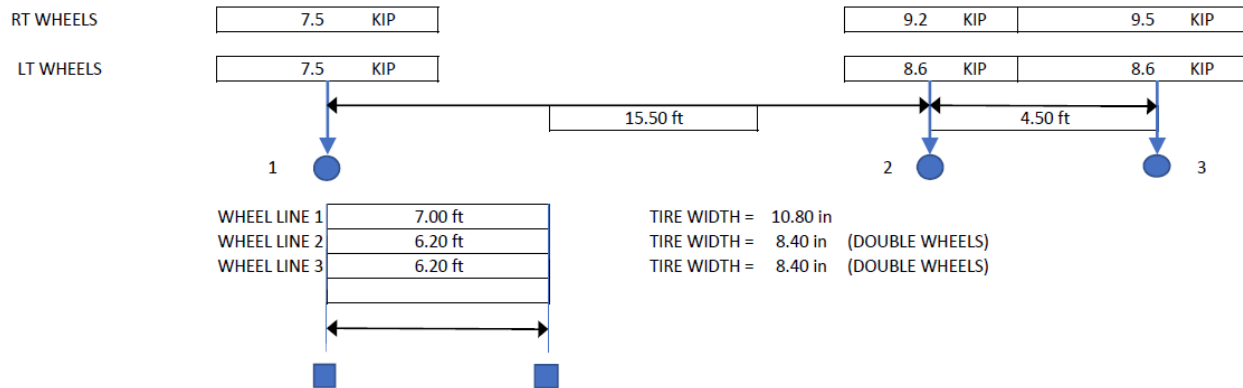


Figure 16 – Wheel loads/configurations/testing times for Model 4-Candidate 1 (M4C1)

Appendix F – Field Testing Plans

Truck Positioning Data

MODEL 4			
CULVERT NAME:	SR 669 OVER CENTER BRANCH RUSH CREEK		
DISTRICT/COUNTY :	DISTRICT 5/ PERRY COUNTY		
BMS NO.:			
BR KEY:			
DATE:	4/17/2018		

SNOW - 31 °F
NO LIFT AXLE ON
TRUCK

0.00L = East end

TEST TRUCK - ON LOAD LINE				
QUARTER POINT	WHEEL			
	1	2	3	
0.00 L	9:53:55 AM	9:58:13 AM	10:01:45 AM	
0.25 L	9:54:21 AM	9:58:48 AM	10:02:11 AM	
0.50 L	9:54:46 AM	9:59:24 AM	10:02:35 AM	
0.75 L	9:55:12 AM	9:59:53 AM	10:03:00 AM	
1.00 L	9:55:40 AM	10:00:26 AM	10:03:28 AM	

TEST TRUCK - CENTERED ABOUT LOAD LINE				
QUARTER POINT	WHEEL			
	1	2	3	
0.00 L	10:10:46 AM	10:14:33 AM	10:17:47 AM	
0.25 L	10:11:16 AM	10:14:55 AM	10:18:12 AM	
0.50 L	10:11:40 AM	10:15:20 AM	10:18:39 AM	
0.75 L	10:12:11 AM	10:15:47 AM	10:19:05 AM	
1.00 L	10:12:35 AM	10:16:19 AM	10:19:30 AM	

Appendix F – Field Testing Plans

Model 5 – Testing Plan – Metal Arch

Site/General

- Instrumentation will be installed week of June 11, 2018 and load tested the same week. Gauges operation will be verified after installation and prior to test.
- Test truck to be on site at 9am, traffic control needed starting at 8:30am
- Test vehicles – Weighed test vehicle will be provided the township and weighed by PA State Police forces. Each wheel of truck to be weighed. Contact info:

Greg Fisher – PA State Police
717-346-7330

Lower Paxton will also provide traffic control during the test phase. No traffic control during gauge installation will be required.

Instrumentation

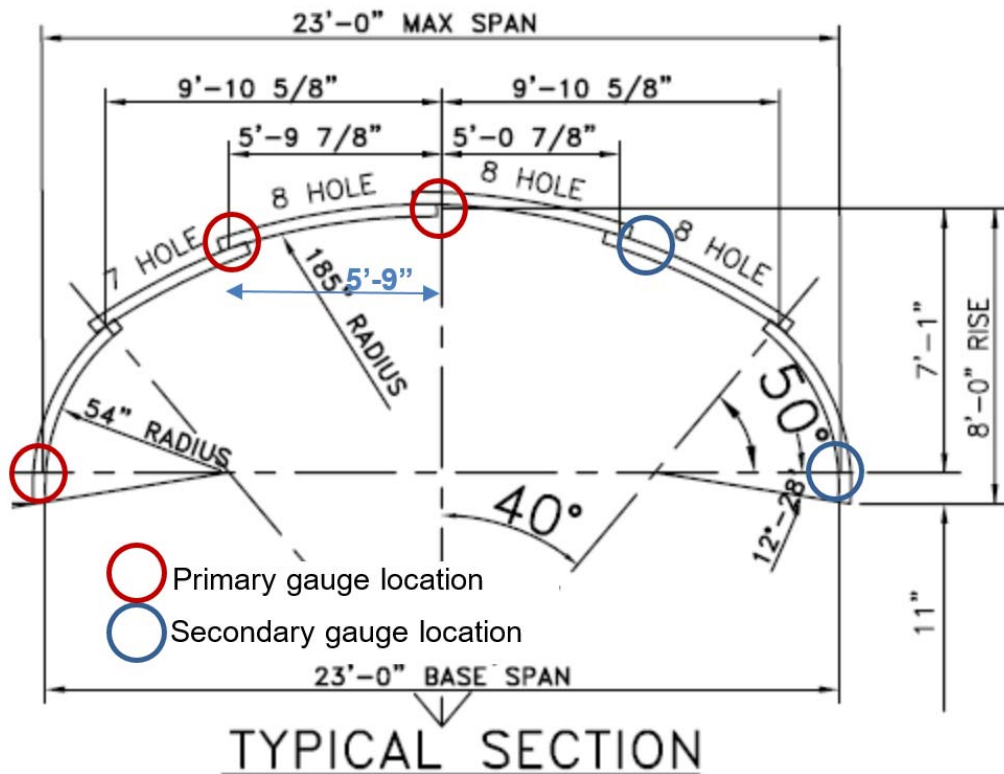


Figure 18 – M5C1 Instrumentation locations

Appendix F – Field Testing Plans

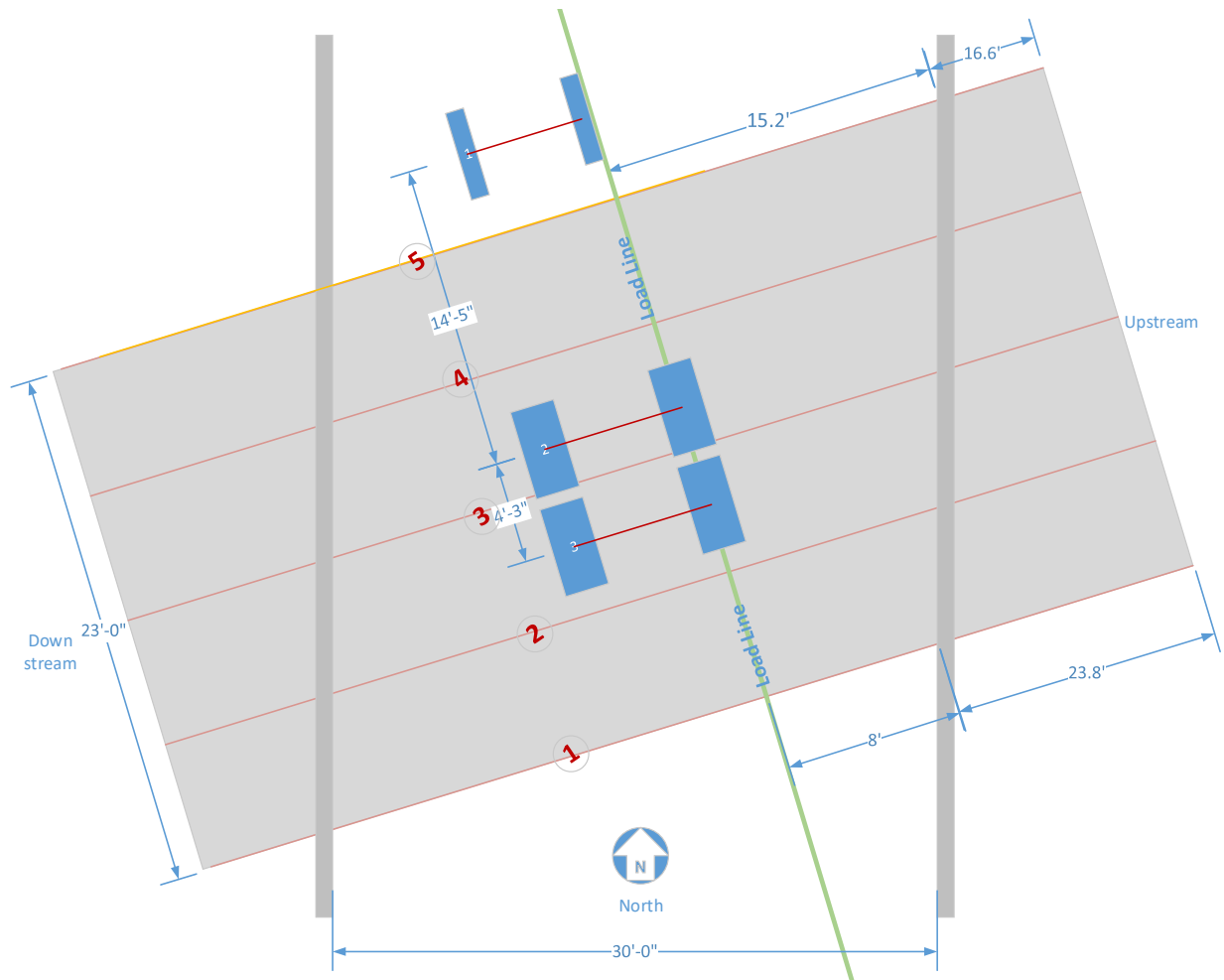


Figure 19 – M5C1 Load Traffic Line

- Instrumentation locations – strain gauges will be mounted at each of the primary gauge locations indicated in the figure above along the “load line” near the center of the culvert segment (based on the orientation of the culvert span/ribs, the line of sensors are to be installed along a line parallel to the traffic/outside edges of the culvert). If time permits, additional gauges will be placed at the secondary locations. Where possible, string pot gauges will be mounted to capture deflections at the culvert midspan locations.
- Strain- locations minimum as shown above, midspan of top of the metal culvert and at corners as close as possible to the specified locations and measurements taken to record their exact position. If time permits, mount backup redundant gauges (redundant gauge at midspan is required). The strain gauges require small gauge electric wire cables to be run to a central location to be connected to the data acquisition device. Modjeski will perform this work. See photos and time/data spreadsheet for arc length to gauges relative to the centerline of culvert gauge.
- String pot gauges, where possible, will be mounted to collect deflection data at midspan by mounting to a reference frame supported at locations unaffected by the truck loading.

Pre-test

- Install instruments and test proper operation

Appendix F – Field Testing Plans

Trucks

- A loaded truck to be provided by Lower Paxton Township per coordination Jeff Kline (717-364-9983). All trucks shall be consistent with design loadings.
- During the test, at times when gauge readings are being taken, no other traffic can be on the culvert structure. Readings taken are for static loading so if it is necessary for a vehicle to traverse the structure, accommodations can be made. However, the structure will have to be closed to traffic during testing.

Test

- Measure individual wheel loads (State Police to obtain, see above)
- Record air and pavement temperature
- Read instruments pre-test
- Truck positions for readings (as truck moves across span). Vehicle paths will be established as shown in layout diagram—with a wheel line directly over the gauges, if feasible, the second with the wheel line 3 feet transverse to the line of gauges (such that the truck is centered over the line of gauges) Each wheel will be stopped over the vertical culvert wall, ¼ point and at midspan of the culvert top.

Time

- Gauge/Target/Wiring installation and setup – approx 1 day

Load testing – approx ½ day

Results

- Per NCHRP policy, test results cannot be shared with the DOT prior to publication

Schedule

- Schedule is subject to change. Current preliminary schedule for setup and testing is as follows:

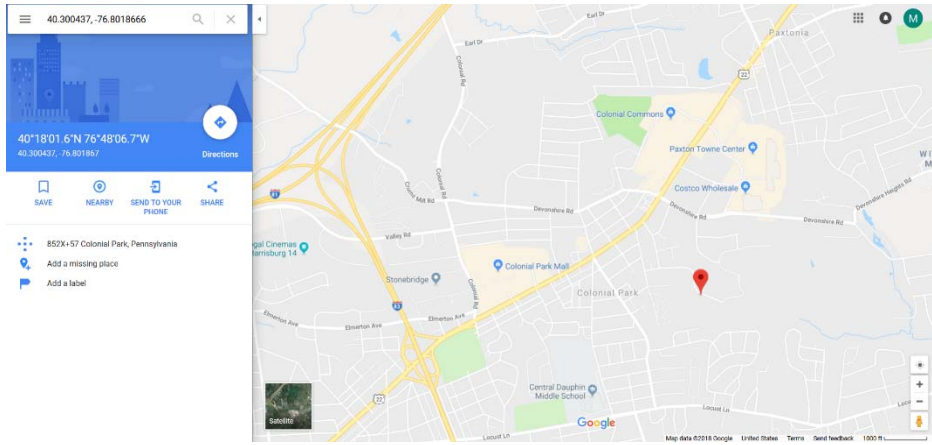
Operation	Dates
Install instruments	June 11, 2018
Load Test	June 12, 2018, Rain Date June 13

Appendix F – Field Testing Plans

Testing Data

General

<p>Location:</p>	<p>State: Pennsylvania Route: Latitude-Longitude: 40.300437, -76.8018666 (click link to open in browser)</p>
-------------------------	---



Actual Instrumentation Date:	6/11/2018
Actual Testing date:	6/12/2018
Weather/Other Test conditions:	82 F at 10:15 AM
Contractor Personnel:	Dave Barrett (Modjeski & Masters) Chad Clancy (Modjeski & Masters)
State Personnel/Contacts:	Jeff Kline Lower Paxton Township (717-364-9983) Greg Fisher – PA State Police 717-346-7330

Appendix F – Field Testing Plans

Truck Wheel Load and Spacing Data

Wheel Loads

Axle	Left	Right
1 (Front)	8450 lb	9250 lb
2	9000 lb	11,600 lb
3 (Rear)	9700 lb	10,700 lb

Tire widths	Axle widths
10.5"	90" out-out
9" each and 22" out-out	95" out-out
9" each and 22" out-out	95" out-out

Axle Spacings	
14'-5"	Axle 1 - Axle 2
4'-3"	Axle 2 - Axle 3

Culvert Data

Curb height: 9.5 inches

Top of curb to top of headwall distance at south corners of headwall

Upstream

Side 27"

Downstream

Side 23"

Curb-Curb Roadway distance = 30'

Load Line description

Load line 1 is centered over line of gauges and is parallel to the culvert ends (follows rib of corrugation). Right wheel of truck is centered on load line.

Load line 2 is parallel to load line 1 and offset 3 feet to the right. This places approx center of truck centered over the centerline of gauges when right wheel is on this line.

Load Points	Description	
1	South edge of culvert	
2	First quarter point	
3	Midspan of culvert	
4	Quarter point between midspan and north edge	
5	North Edge of culvert	

Arc distances to gauges:

1/2 -> 3/4	83.5 inches
3/4 -> 5/6	71 inches
5/6 -> 7/8	67.5 inches
7/8 -> 9/10	87 inches

Appendix F – Field Testing Plans



Figure 20 – Wheel loads/configurations for Model 5-Candidate 1 (M5C1)

Truck Positioning Data

Pass #1: Load Line 1 (Note: Passes 1 and 2 were repeated as 3 and 4 after removing charger that was causing extraneous signal noise)

Load Point	Axle No	Time
1	1	9:29:40
2	1	9:30:20
3	1	9:30:55
4	1	9:31:28
5	1	9:31:58
1	2	9:33:25
2	2	9:33:50
3	2	9:34:15
4	2	9:34:48
5	2	9:35:22
1	3	9:38:38
2	3	9:39:43
3	3	9:40:09
4	3	9:40:34

Appendix F – Field Testing Plans

5	3	9:40:57
---	---	---------

Pass #2: Load Line 2 (Note: Passes 1 and 2 were repeated as 3 and 4 after removing charger that was causing extraneous signal noise)

Load Point	Axle No	Time
1	1	9:42:16
2	1	9:42:36
3	1	9:42:53
4	1	9:43:16
5	1	9:43:41
1	2	9:44:49
2	2	9:45:13
3	2	9:45:35
4	2	9:45:59
5	2	9:46:24
1	3	9:47:20
2	3	9:47:55
3	3	9:48:10
4	3	9:48:35
5	3	9:49:15
1	3	9:51:30
2	3	9:51:45
3	3	9:52:05
4	3	9:52:46
5	3	9:53:07

Appendix F – Field Testing Plans

Pass #3: Load Line 1 (Note: Passes 1 and 2 were repeated as 3 and 4 after removing charger that was causing extraneous signal noise)

Load Point	Axle No	Time
1	1	10:01:00
2	1	10:01:25
3	1	10:01:50
4	1	10:02:20
5	1	10:02:45
1	2	10:03:57
2	2	10:04:23
3	2	10:04:45
4	2	10:05:08
5	2	10:05:30
1	3	10:06:30
2	3	10:06:52
3	3	10:07:10
4	3	10:07:30
5	3	10:07:50

Appendix F – Field Testing Plans

Pass #4: Load Line 2 (Note: Passes 1 and 2 were repeated as 3 and 4 after removing charger that was causing extraneous signal noise)

Load Point	Axle No	Time
1	1	10:09:15
2	1	10:09:35
3	1	10:09:55
4	1	10:10:10
5	1	10:10:33
1	2	10:11:30
2	2	10:11:44
3	2	10:12:11
4	2	10:12:30
5	2	10:12:48
1	3	10:11:30
2	3	10:11:44
3	3	10:12:11
4	3	10:12:30
5	3	10:12:48

Appendix F – Field Testing Plans

Culvert Plans

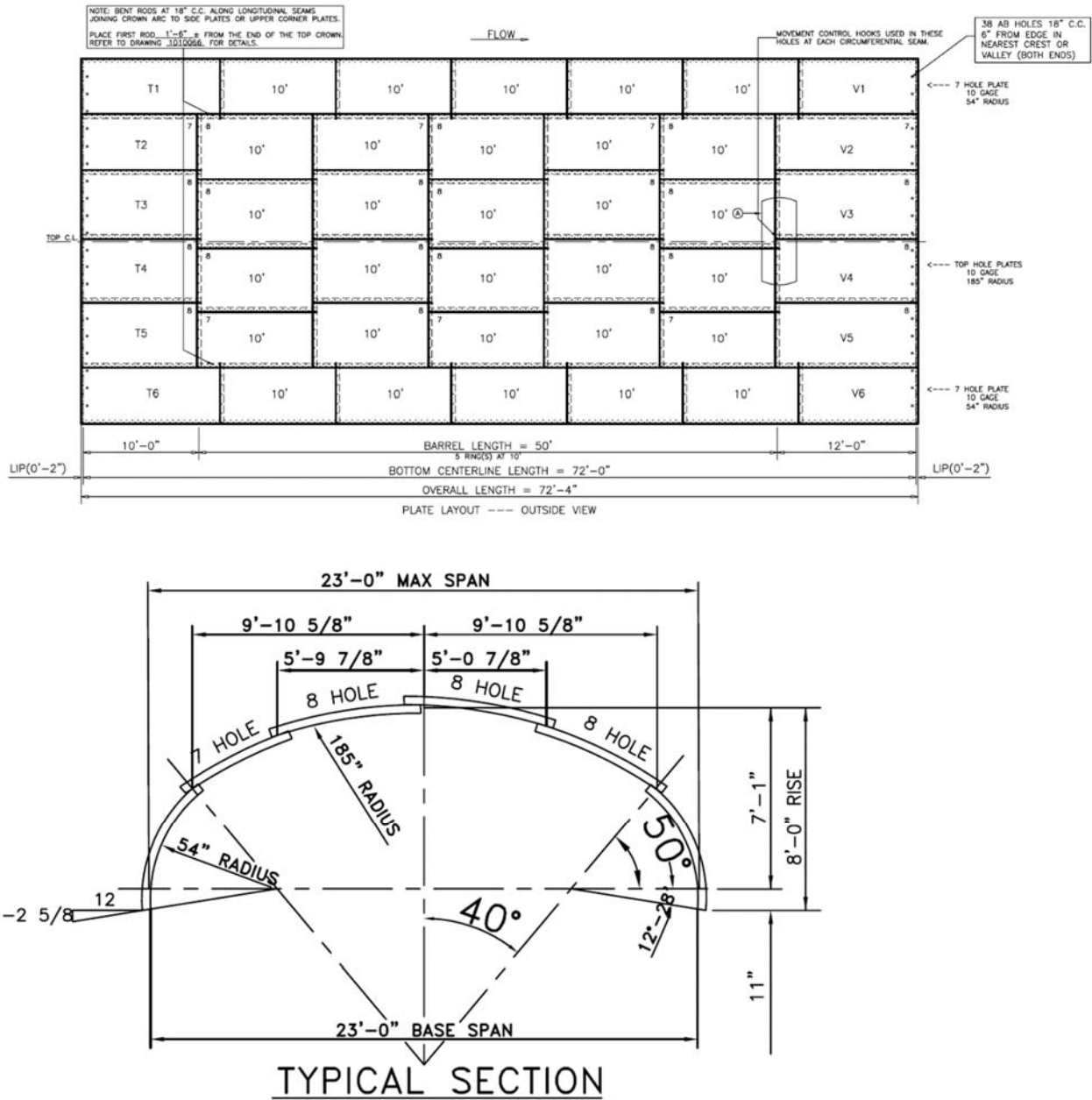


Figure 21- Model 5, Candidate 1 (M5C1) – Plan and Typical Section

Appendix F – Field Testing Plans

Model 6 – Testing Plan – Metal Arch

Site/General

- Instrumentation will be installed week of May 2, 2018 and load tested the same week. Gauges operation will be verified after installation and prior to test.
- Test truck to be on site at 10am, traffic control needed starting at 9am
- Test vehicles – Weighed test vehicle will be provided by PA State Police forces. Each wheel of truck to be weighed. Contact info:

Greg Fisher – PA State Police
717-346-7330

- Carroll Township will also provide traffic control during the test phase. No traffic control during gauge installation will be required, however, traffic control will be required 1 hour prior to testing to lay out load path line.

Instrumentation

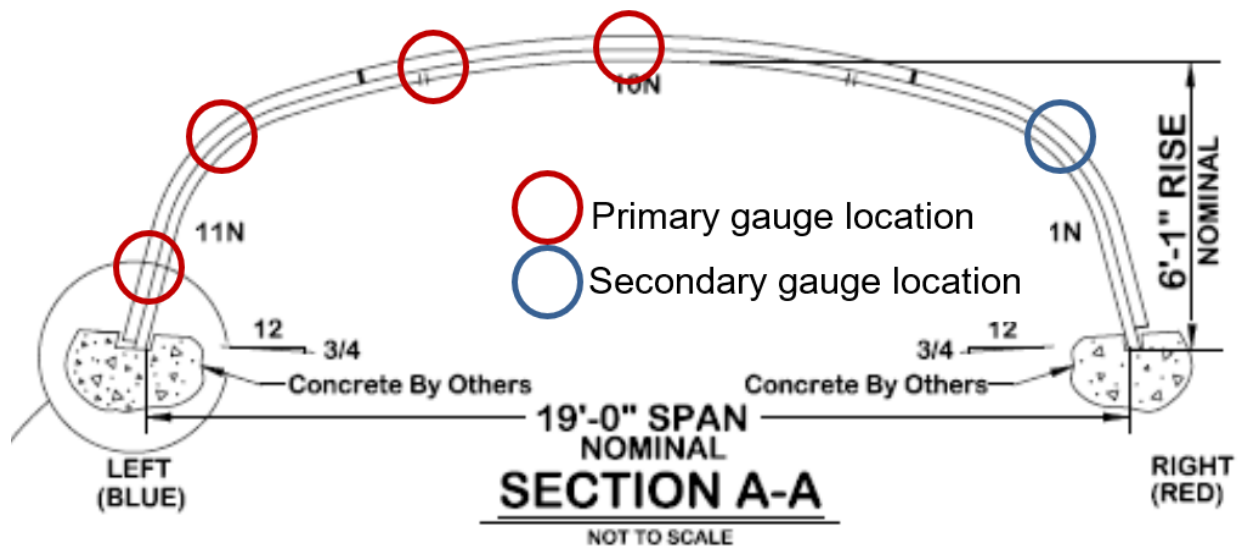


Figure 22 – M6C2 Instrumentation locations

Appendix F – Field Testing Plans

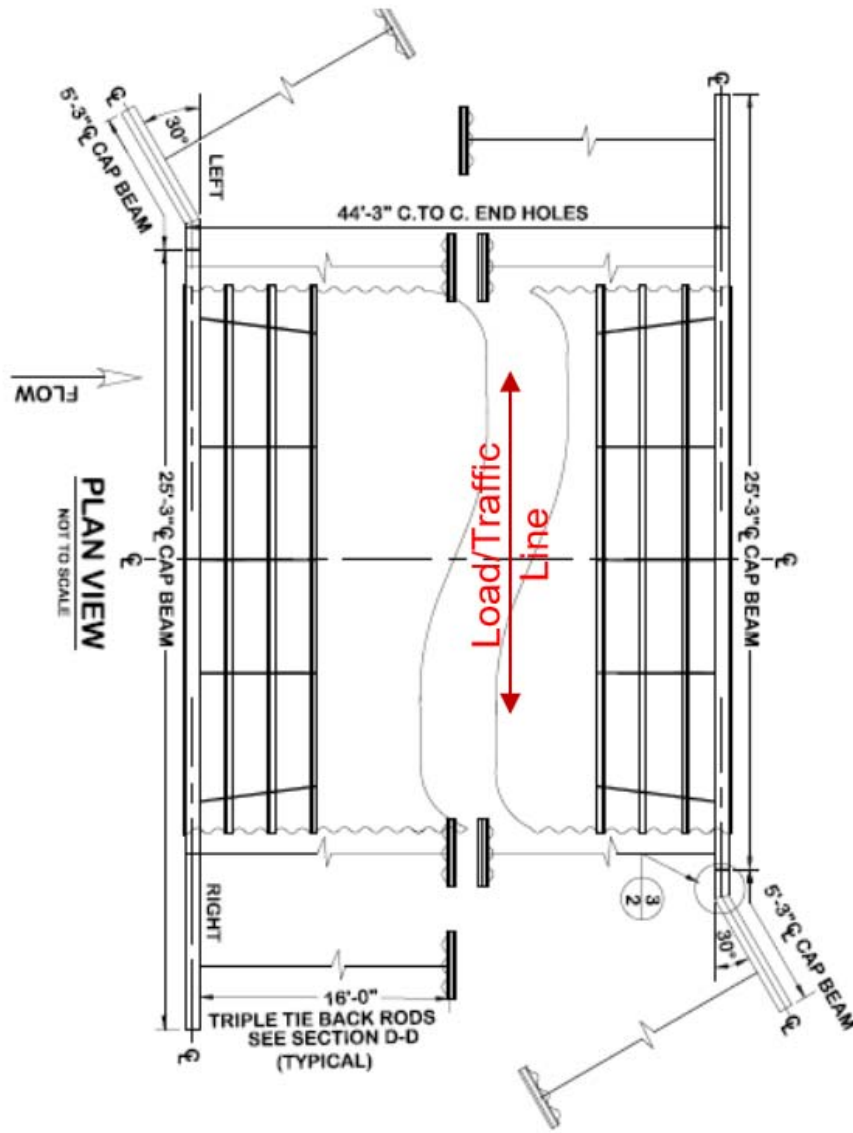


Figure 23 – M6C2 Load Traffic Line

- Instrumentation locations – strain gauges will be mounted at each of the primary gauge locations indicated in the figure above along the “load line” near the center of the culvert segment (based on the orientation of the culvert span/ribs, the line of sensors are to be installed along a line parallel to the traffic/outside edges of the culvert). If time permits, additional gauges will be placed at the secondary locations. Where possible, string pot gauges will be mounted to capture deflections at the culvert midspan locations.
- Strain- locations minimum as shown above, midspan of top of the metal culvert and at corners as close as possible to the specified locations and measurements taken to record their exact position. If time permits, mount backup redundant gauges (redundant gauge at midspan is required). The strain gauges require small gauge electric wire cables to be run to a central location to be connected to the data acquisition device. Modjeski will perform this work.
- String pot gauges, where possible, will be mounted to collect deflection data at midspan by mounting to a reference frame supported at locations unaffected by the truck loading.

Appendix F – Field Testing Plans

Pre-test

- Install instruments and test proper operation

Trucks

- A loaded truck to be provided by Carroll Township per coordination with Bryon Cramer. All trucks shall be consistent with design loadings.
- During the test, at times when gauge readings are being taken, no other traffic can be on the culvert structure. Readings taken are for static loading so if it is necessary for a vehicle to traverse the structure, accommodations can be made. However, the structure will have to be closed to traffic during testing.

Test

- Measure individual wheel loads (State Police to obtain, see above)
- Record air and pavement temperature
- Read instruments pre-test
- Truck positions for readings (as truck moves across span). Vehicle paths will be established as shown in layout diagram—with a wheel line directly over the gauges, the second with the wheel line 3 feet transverse to the line of gauges (such that the truck is centered over the line of gauges) Each wheel will be stopped over the vertical culvert wall, $\frac{1}{4}$ point and at midspan of the culvert top.

Time

- Gauge/Target/Wiring installation and setup – approx 1 day

Load testing – approx $\frac{1}{2}$ day

Results

- Per NCHRP policy, test results cannot be shared with the DOT prior to publication

Schedule

- Schedule is subject to change. Current preliminary schedule for setup and testing is as follows:

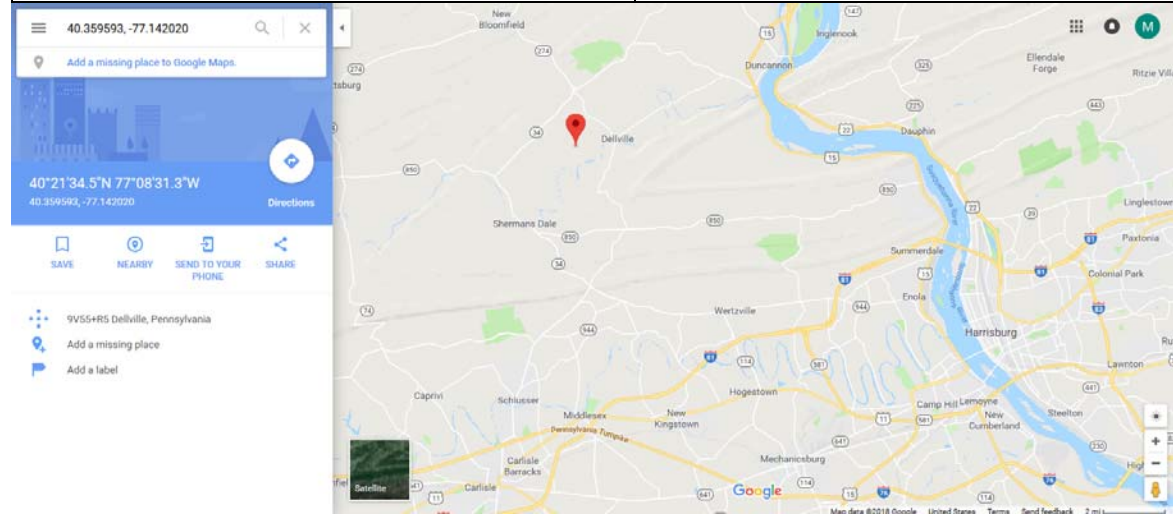
Operation	Dates
Install instruments	May 2, 2018
Load Test	May 3, 2018

Appendix F – Field Testing Plans

Testing Data

General

Location:	State: Pennsylvania, Carroll Twp Route: Sleepy Hollow Rd. Latitude-Longitude: 40.359593, -77.142020 (click link to open in browser)
------------------	--



Actual Instrumentation Date:	5/2/2018
Actual Testing date:	5/3/2018
Weather/Other Test conditions:	80 F at 9:30 AM
Contractor Personnel:	Dave Barrett (Modjeski & Masters) Chad Clancy (Modjeski & Masters)
State Personnel/Contacts:	Bryon Cramer Carroll Township Greg Fisher – PA State Police 717-346-7330

Appendix F – Field Testing Plans

Truck Wheel Load and Spacing Data

Axle Loads (lb)	Left	Right	Axle spacing c-c Front to rear
Front	5850	5275	13'-1"
Rear	10475	9550	



Figure 24 – Wheel loads/configurations for Model 6-Candidate 1 (M6C2)

Appendix F – Field Testing Plans

Truck Positioning Data

Points

1 = Edge/Wall

2 = 1/4 Point

3 = Midspan

Axles (2-axle Dump truck)

1 = Front

2 = Rear

Axle No	Point No	Time
2	1	9:30:00
2	2	9:30:30
2	3	9:31:27
2	1	9:32:40
2	2	9:33:20
2	3	9:33:55
2	1	9:37:00
2	2	9:37:32
2	3	9:38:14

Test No.	Truck Position	Axle No.	Gauge Location	Start Time (time format)	End Time (time format)	Start Time (integer format)	End Time (integer format)
1	1	2	1	9:30:00	9:30:15	9.500	9.504
2	2	2	2	9:30:30	9:30:45	9.508	9.513
3	3	2	3	9:31:27	9:31:42	9.524	9.528
4	1	2	1	9:32:40	9:32:55	9.544	9.549
5	2	2	2	9:33:20	9:33:35	9.556	9.560
6	3	2	3	9:33:55	9:34:10	9.565	9.569
7	1	2	1	9:37:00	9:37:15	9.617	9.621
8	2	2	2	9:37:32	9:37:47	9.626	9.630
9	3	2	3	9:38:14	9:38:29	9.637	9.641

Time each location = 15 seconds

Appendix F – Field Testing Plans

Culvert Plans

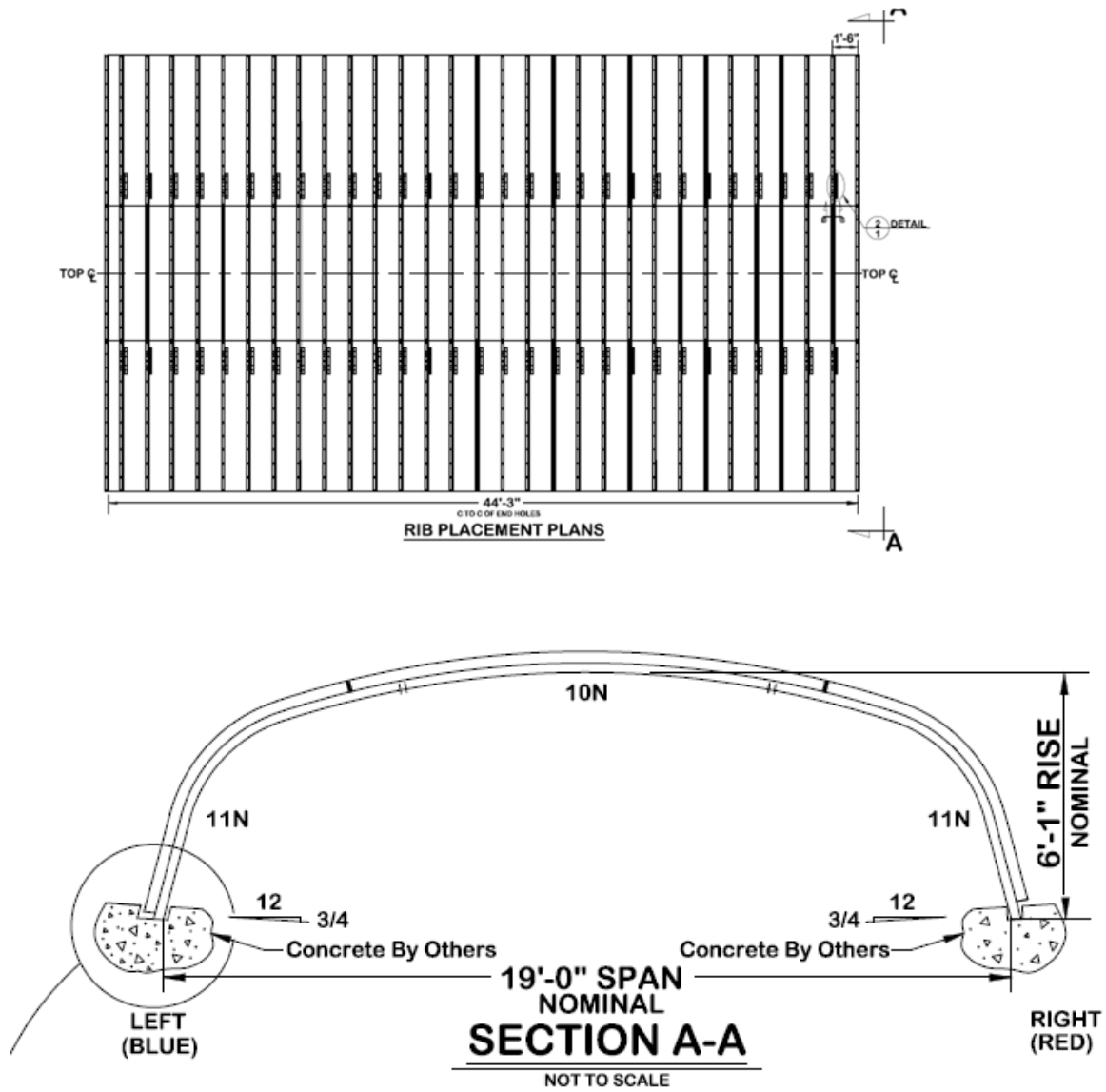


Figure 25- Model 6, Candidate 1 (M6C2) – Plan and Typical Section

Appendix F – Field Testing Plans

Model 7 – Testing Plan – Metal Arch

Site/General

- Two tests will be conducted – One test prior to paving with the trucks being run over the compacted pavement subgrade material and another test to be run after pavement is in place. It would be ideal if these tests could be conducted on the same day and or trip to the site but this is not necessary.
- Sidfill/Backfill/Subgrade – sample materials – Dr. McGrath will obtain soil data from contractor/fabricator
- Test vehicles (Provided by MassDOT – will need to coordinate with district, axle configurations, axle loads. Wheel loads will have to be weighed – coordinate with state police to weigh if possible. Alternatively use quarry scales to obtain individual axle loads). JF White will coordinate with MassDOT, MassDOT will coordinate with State Police for axle weighing
- Surveying for actual depths of fill – obtain from contractor if possible

Instrumentation

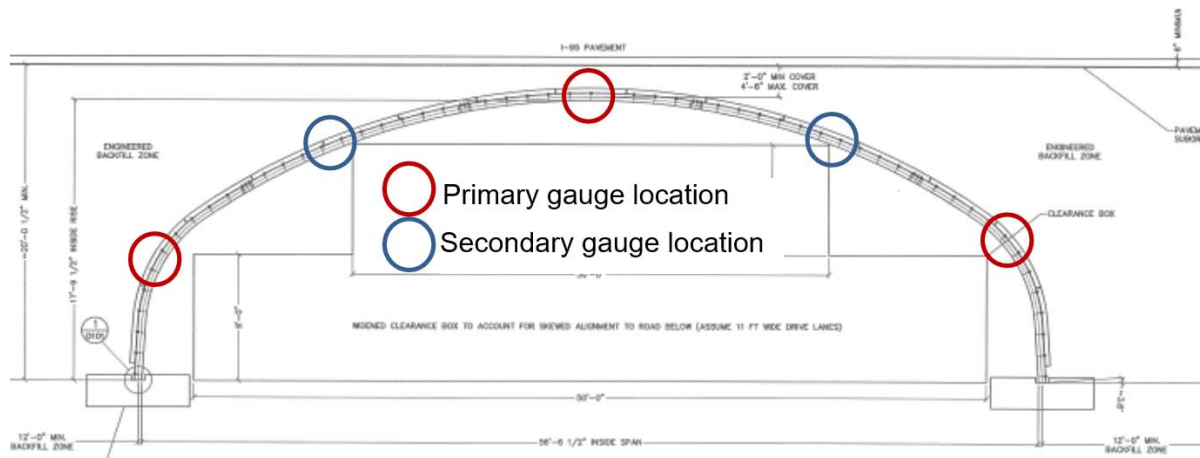
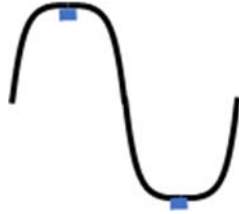


Figure 26 – M6C2 Instrumentation locations

- Instrumentation locations – strain gauges and deflection targets will be mounted at each of the primary gauge locations indicated in the figure above along a single line near the middle of the culvert. If time permits, additional gauges will be placed at the secondary locations.
- Deflection – survey targets to be attached to culvert during assembly if possible. If feasible and time permits, string potentiometer gauges will be placed to back up the deflection data being obtained via surveying equipment. Note that the primary direction of deflections to be captured are vertical at the midspan location and horizontal at the corners. Modjeski will perform this work with surveying by CME.
- Strain- 6 gauges minimum: 2 at each location (1 at outer crest of corrugation, 1 at trough – see figure below), 2 at each corner and 2 at midspan. If time permits, mount backup redundant gauges particularly in areas difficult to reach. The strain gauges require small gauge electric wire cables to be run to a central location to be connected to the data acquisition device. Modjeski will perform this work

Appendix F – Field Testing Plans



If gauges are to be mounted when culvert panel is in its final position a lift or ladders will be needed to mount the gauges. Modjeski will supply ladders or will use contractor's on-site lifts if available.

- Instrumentation locations – strain gauges will be mounted at each of the primary gauge locations indicated in the figure above along the “load line” near the center of the culvert segment (based on the orientation of the culvert span/ribs, the line of sensors are to be installed along a line parallel to the traffic/outside edges of the culvert). If time permits, additional gauges will be placed at the secondary locations. Where possible, string pot gauges will be mounted to capture deflections at the culvert midspan locations.
- Strain- locations minimum as shown above, midspan of top of the metal culvert and at corners as close as possible to the specified locations and measurements taken to record their exact position. If time permits, mount backup redundant gauges (redundant gauge at midspan is required). The strain gauges require small gauge electric wire cables to be run to a central location to be connected to the data acquisition device. Modjeski will perform this work.
- String pot gauges, where possible, will be mounted to collect deflection data at midspan by mounting to a reference frame supported at locations unaffected by the truck loading.

Pre-test

- Monitor sidefill/backfill (or collect records)
- Install instruments

Trucks

- Trucks to be provided by MassDOT per cooperative letter. All trucks shall be consistent with design loadings. Desired vehicles include a HS-20 truck (preferable) or alternatively a design tandem and a dump truck with 3 rear axles
- During the test, at times when gauge readings are being taken, no other traffic can be on the culvert structure. Readings taken are for static loading so if it is necessary for a vehicle to traverse the structure, accommodations can be made. However, the structure will have to be closed to traffic in the paved condition during that phase of the testing.

Test

- Measure axle loads (see above)
- Record air and pavement temperature (if still warm)
- Read instruments pre-test
- Modjeski sub CME will provide surveying services to measure deflections
- Truck positions for readings (as truck moves across span). Three vehicle paths will be established – one with a wheel line directly over the gauges, the second with the wheel line 3 feet transverse to the line of gauges (such that the truck is centered over the line of gauges) and the third with the wheel line 3 feet from the line of

Appendix F – Field Testing Plans

gauges and the second wheel line is 9 feet from the gauge line. Two passes will be made along each of these passes of the truck, stopping as each wheel/axle passes directly over a gauge.

Time

- Gauge/Target/Wiring installation and setup – approx 1 day to occur after backfill and compacting, if possible.
- Load testing – approx ½ day pre each of the two tests (with pavement and without pavement)

Results

- Per NCHRP policy, test results cannot be shared with the contractor or MassDOT prior to publication in the final report.

Schedule

- Schedule is subject to change. Current preliminary schedule for setup and testing is as follows:
- Schedule is subject to change to coincide with construction operations. Current preliminary schedule for setup and testing is as follows:

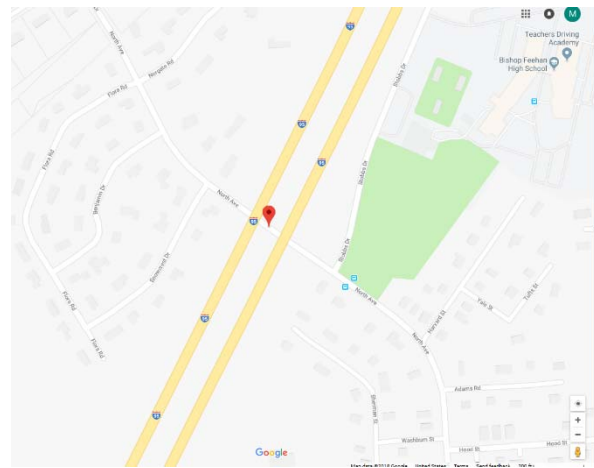
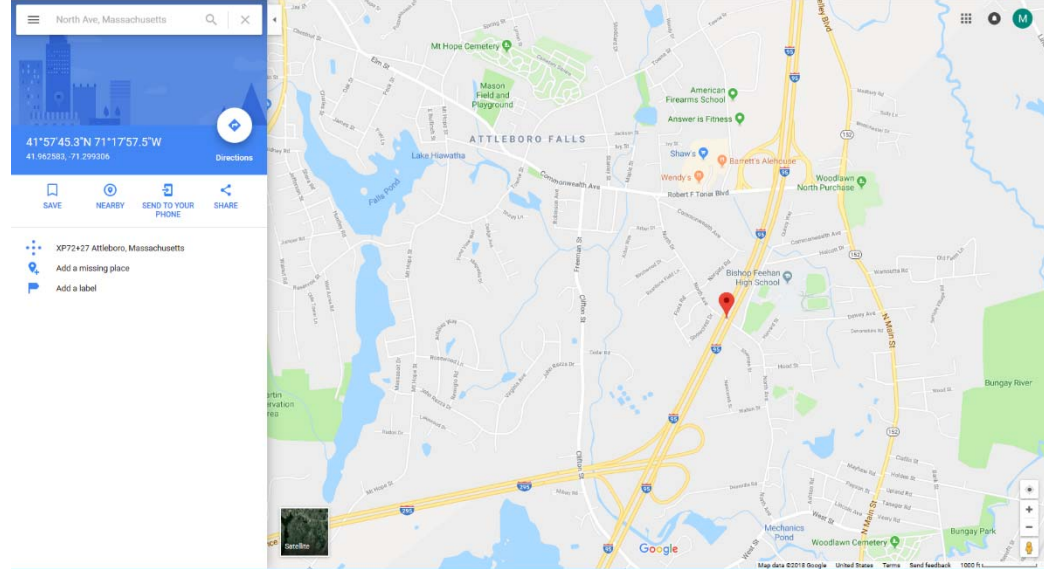
Install instruments	on/about 13 April 2017 to be confirmed by JFW 3 days in advance
Load Test on subgrade	on/about 14 April 2017 to be confirmed by JFW 3 days in advance
Load Test on pavement	on/about 27 April 2017 to be confirmed by JFW 3 days in advance

Appendix F – Field Testing Plans

Testing Data

General

Location:	State: Massachusetts Route: I-95 over North Avenue Latitude-Longitude: 41.962574, -71.299294 (click link to open in browser)
------------------	---



Actual Instrumentation Date:	May 1, 2017 (Stage A) June 1, 2017 (Stage B)
Actual Testing date:	May 3, 2017 (Stage A) June 2, 2017 (Stage B)
Weather/Other Test conditions:	
Contractor Personnel:	Dave Barrett (Modjeski & Masters) Travis Hopper (Modjeski & Masters)
State Personnel/Contacts:	Jim Cahill – JF White Dan Viera – Mass DOT 508-884-4223

Appendix F – Field Testing Plans

Truck Wheel Load and Spacing Data

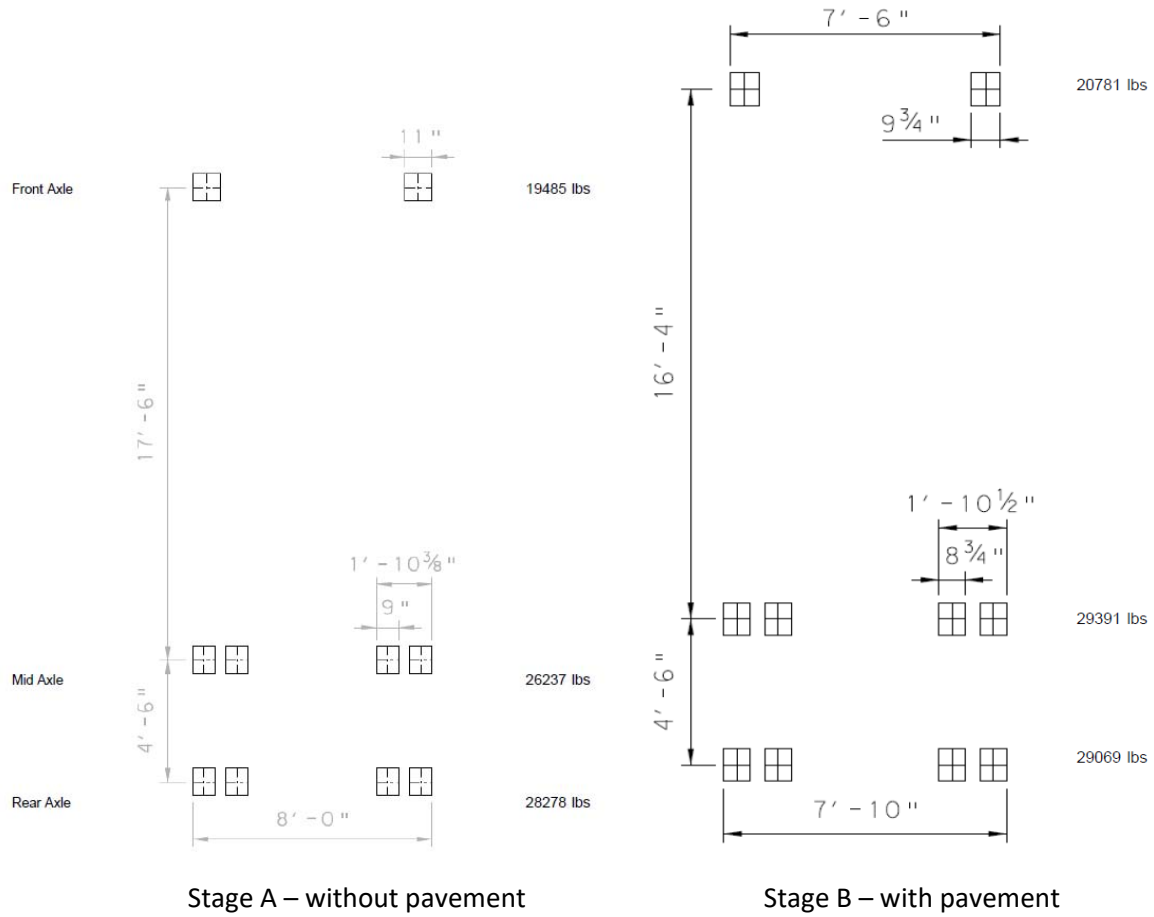


Figure 30 – Wheel loads/configurations for Model 7-Candidate 1 (M7C1)

Appendix F – Field Testing Plans

Truck Positioning Data (Stage A – Without pavement)

Truck Positions

Notation	Description
1	Truck centered over centerline of culvert
2	Left wheel line centered on centerline of culvert
3	left wheel line offset 3 ft from centerline of culvert, right wheel line offset (3 ft + axle width) from centerline of culvert
N/S	truck facing North or South

Axle Numbering

- Each axle was centered over each gauge line. Notation is as follows.

Notation	Description
1	Front Axle
2	Mid Axle
3	Rear Axle

Gauge Locations

- Each cluster of gauges was assigned a number.

- Numbering was from South to North, numbers 1 through 5 as shown below.

Test No.	CME Survey Shot No.	Truck Position	Axle No.	Gauge Location	Start Time	End Time	Start Time	End Time	Notes
0	500								zero
1	502	1N	1	1	13:12:15	13:12:30	1:12:15 PM	1:12:30 PM	
2	503	1N	1	2	13:13:35	13:13:51	1:13:35 PM	1:13:51 PM	
3	504	1N	2	1	13:14:55	13:15:06	1:14:55 PM	1:15:06 PM	
4	505	1N	3	1	13:17:53	13:18:07	1:17:53 PM	1:18:07 PM	
5	506	1N	1	3	13:19:20	13:19:42	1:19:20 PM	1:19:42 PM	
6	507	1N	2	2	13:20:20	13:21:02	1:20:20 PM	1:21:02 PM	
7	508	1N	3	2	13:21:33	13:21:53	1:21:33 PM	1:21:53 PM	
8	509	1N	1	4	13:22:43	13:23:00	1:22:43 PM	1:23:00 PM	
9	510	1N	2	3	13:23:30	13:23:47	1:23:30 PM	1:23:47 PM	
10	511	1N	3	3	13:24:22	13:24:37	1:24:22 PM	1:24:37 PM	
11	512	1N	1	5	13:25:12	13:25:28	1:25:12 PM	1:25:28 PM	
12	513	1N	2	4	13:26:03	13:26:19	1:26:03 PM	1:26:19 PM	
13	514	1N	3	4	13:26:55	13:27:11	1:26:55 PM	1:27:11 PM	
14	515	1N	2	5	13:27:52	13:28:07	1:27:52 PM	1:28:07 PM	
15	516	1N	3	5	13:28:40	13:28:55	1:28:40 PM	1:28:55 PM	
16	517	2N	1	1	13:31:22	13:31:45	1:31:22 PM	1:31:45 PM	
17	518	2N	1	2	13:32:28	13:32:45	1:32:28 PM	1:32:45 PM	

Appendix F – Field Testing Plans

Test No.	CME Survey Shot No.	Truck Position	Axle No.	Gauge Location	Start Time	End Time	Start Time	End Time	Notes
18	519	2N	2	1	13:33:20	13:33:35	1:33:20 PM	1:33:35 PM	
19	520	2N	3	1	13:34:11	13:34:30	1:34:11 PM	1:34:30 PM	
20	521	2N	1	3	13:35:13	13:35:33	1:35:13 PM	1:35:33 PM	
21	522	2N	2	2	13:36:06	13:36:22	1:36:06 PM	1:36:22 PM	
22	523	2N	3	2	13:37:30	13:37:51	1:37:30 PM	1:37:51 PM	
23	524	2N	1	4	13:38:35	13:38:57	1:38:35 PM	1:38:57 PM	
24	525	2N	2	3	13:39:29	13:39:50	1:39:29 PM	1:39:50 PM	
25	526	2N	3	3	13:40:30	13:40:55	1:40:30 PM	1:40:55 PM	
26	527	2N	1	5	13:41:44	13:42:00	1:41:44 PM	1:42:00 PM	
27	528	2N	2	4	13:42:30	13:42:48	1:42:30 PM	1:42:48 PM	
28	529	2N	3	4	13:43:14	13:43:31	1:43:14 PM	1:43:31 PM	
29	530	2N	2	5	13:44:07	13:44:24	1:44:07 PM	1:44:24 PM	
30	531	2N	3	5	13:44:52	13:45:09	1:44:52 PM	1:45:09 PM	
31	532				13:46:35	13:47:09	1:46:35 PM	1:47:09 PM	zero
32	533	3N	1	1	13:48:12	13:48:30	1:48:12 PM	1:48:30 PM	
33	534	3N	1	2	13:49:14	13:49:33	1:49:14 PM	1:49:33 PM	
34	535	3N	2	1	13:50:01	13:50:19	1:50:01 PM	1:50:19 PM	
35	536	3N	3	1	13:50:53	13:51:11	1:50:53 PM	1:51:11 PM	
36	537	3N	1	3	13:51:49	13:52:32	1:51:49 PM	1:52:32 PM	
37	538	3N	2	2	13:54:05	13:54:16	1:54:05 PM	1:54:16 PM	
38	539	3N	3	2	13:54:41	13:54:54	1:54:41 PM	1:54:54 PM	
39	540	3N	1	4	13:55:29	13:55:44	1:55:29 PM	1:55:44 PM	hand written notes have 13:55:00 (not possible), assume start +15 sec
40	541	3N	2	3	13:56:07	13:56:26	1:56:07 PM	1:56:26 PM	
41	542	3N	3	3	13:56:49	13:57:07	1:56:49 PM	1:57:07 PM	
42	543	3N	1	5	13:57:42	13:58:03	1:57:42 PM	1:58:03 PM	
43	544	3N	2	4	13:58:29	13:58:50	1:58:29 PM	1:58:50 PM	
44	545	3N	3	4	13:59:15	13:59:32	1:59:15 PM	1:59:32 PM	
45	546	3N	2	5	14:00:13	14:00:28	2:00:13 PM	2:00:28 PM	
46	547	3N	3	5	14:01:35	14:01:52	2:01:35 PM	2:01:52 PM	
47	548				14:02:57	14:03:17	2:02:57 PM	2:03:17 PM	zero
48	549	1S	1	5	14:04:43	14:05:07	2:04:43 PM	2:05:07 PM	
49	550	1S	1	4	14:05:41	14:05:54	2:05:41 PM	2:05:54 PM	
50	551	1S	2	5	14:06:25	14:06:36	2:06:25 PM	2:06:36 PM	
51	552	1S	3	5	14:07:14	14:07:33	2:07:14 PM	2:07:33 PM	
52	553	1S	1	3	14:08:51	14:09:09	2:08:51 PM	2:09:09 PM	
53	554	1S	2	4	14:09:45	14:10:03	2:09:45 PM	2:10:03 PM	
54	555	1S	3	4	14:10:28	14:10:49	2:10:28 PM	2:10:49 PM	

Appendix F – Field Testing Plans

Test No.	CME Survey Shot No.	Truck Position	Axle No.	Gauge Location	Start Time	End Time	Start Time	End Time	Notes
55	556	1S	1	2	14:11:23	14:11:41	2:11:23 PM	2:11:41 PM	
56	557	1S	2	3	14:12:06	14:12:23	2:12:06 PM	2:12:23 PM	
57	558	1S	3	3	14:12:50	14:13:05	2:12:50 PM	2:13:05 PM	
58	559	1S	1	1	14:13:36	14:13:49	2:13:36 PM	2:13:49 PM	
59	560	1S	2	2	14:14:15	14:14:32	2:14:15 PM	2:14:32 PM	
60	561	1S	3	2	14:14:57	14:15:12	2:14:57 PM	2:15:12 PM	
61	562	1S	2	1	14:15:42	14:15:56	2:15:42 PM	2:15:56 PM	
62	563	1S	3	1	14:16:21	14:16:38	2:16:21 PM	2:16:38 PM	
63	564	1S			14:17:23	14:17:37	2:17:23 PM	2:17:37 PM	zero

Truck Positioning Data (Stage B – With pavement)

Truck Positions

Notation	Description
1	Truck centered over centerline of culvert
2	Left wheel line centered on centerline of culvert
3	left wheel line offset 3 ft from centerline of culvert, right wheel line offset (3 ft + axle width) from centerline of culvert
N/S	truck facing North or South

Axle Numbering

- Each axle was centered over each gauge line. Notation is as follows.

Notation	Description
1	Front Axle
2	Mid Axle
3	Rear Axle

Gauge Locations

- Each cluster of gauges was assigned a number.

- Numbering was from South to North, numbers 1 through 5 as shown below.

Test No.	CME Survey Shot No.	Truck Position	Axle No.	Gauge Location	Start Time	End Time	Start Time	End Time	Notes
0									test
1	600	1N	1	1	12:06:25	12:06:46	12:06:25 PM	12:06:46 PM	
2	601	1N	1	2	12:07:40	12:08:00	12:07:40 PM	12:08:00 PM	
3	602	1N	2	1	12:08:56	12:09:13	12:08:56 PM	12:09:13 PM	
4	603	1N	3	1	12:09:50	12:10:08	12:09:50 PM	12:10:08 PM	

Appendix F – Field Testing Plans

Test No.	CME Survey Shot No.	Truck Position	Axle No.	Gauge Location	Start Time	End Time	Start Time	End Time	Notes
5	604	1N	1	3	12:11:27	12:11:44	12:11:27 PM	12:11:44 PM	
6	605	1N	2	2	12:12:21	12:12:39	12:12:21 PM	12:12:39 PM	
7	606	1N	3	2	12:13:24	12:13:42	12:13:24 PM	12:13:42 PM	
8	607	1N	1	4	12:14:38	12:14:57	12:14:38 PM	12:14:57 PM	
9	608	1N	2	3	12:15:35	12:15:56	12:15:35 PM	12:15:56 PM	
10	609	1N	3	3	12:16:38	12:16:57	12:16:38 PM	12:16:57 PM	
11	610	1N	1	5	12:17:42	12:17:59	12:17:42 PM	12:17:59 PM	
12	611	1N	2	4	12:19:59	12:20:19	12:19:59 PM	12:20:19 PM	
13	612	1N	3	4	12:21:10	12:21:29	12:21:10 PM	12:21:29 PM	
14	613	1N	2	5	12:22:32	12:23:04	12:22:32 PM	12:23:04 PM	
15	614	1N	3	5	12:24:03	12:24:25	12:24:03 PM	12:24:25 PM	
16	615	2N	1	1	12:29:05	12:29:25	12:29:05 PM	12:29:25 PM	
17	616	2N	1	2	12:30:10	12:30:28	12:30:10 PM	12:30:28 PM	
18	617	2N	2	1	12:31:04	12:31:21	12:31:04 PM	12:31:21 PM	
19	618	2N	3	1	12:31:56	12:32:14	12:31:56 PM	12:32:14 PM	
20	619	2N	1	3	12:32:56	12:33:14	12:32:56 PM	12:33:14 PM	
21	620	2N	2	2	12:33:46	12:34:05	12:33:46 PM	12:34:05 PM	
22	621	2N	3	2	12:34:36	12:34:52	12:34:36 PM	12:34:52 PM	
23	622	2N	1	4	12:35:35	12:35:54	12:35:35 PM	12:35:54 PM	
24	623	2N	2	3	12:36:37	12:36:54	12:36:37 PM	12:36:54 PM	
25	624	2N	3	3	12:37:27	12:37:43	12:37:27 PM	12:37:43 PM	
26	625	2N	1	5	12:38:22	12:38:40	12:38:22 PM	12:38:40 PM	
27	626	2N	2	4	12:40:18	12:40:36	12:40:18 PM	12:40:36 PM	
28	627	2N	3	4	12:41:14	12:41:31	12:41:14 PM	12:41:31 PM	
29	628	2N	2	5	12:42:07	12:42:24	12:42:07 PM	12:42:24 PM	
30	629	2N	3	5	12:42:54	12:43:12	12:42:54 PM	12:43:12 PM	
31	630	3N	1	1	12:46:36	12:46:55	12:46:36 PM	12:46:55 PM	
32	631	3N	1	2	12:47:36	12:47:57	12:47:36 PM	12:47:57 PM	
33	632	3N	2	1	12:48:27	12:48:43	12:48:27 PM	12:48:43 PM	
34	633	3N	3	1	12:49:21	12:49:38	12:49:21 PM	12:49:38 PM	
35	634	3N	1	3	12:50:32	12:50:49	12:50:32 PM	12:50:49 PM	
36	635	3N	2	2	12:51:14	12:51:38	12:51:14 PM	12:51:38 PM	
37	636	3N	3	2	12:52:16	12:52:34	12:52:16 PM	12:52:34 PM	
38	637	3N	1	4	12:53:14	12:53:32	12:53:14 PM	12:53:32 PM	
39	638	3N	2	3	12:54:01	12:54:19	12:54:01 PM	12:54:19 PM	
40	639	3N	3	3	12:54:49	12:55:05	12:54:49 PM	12:55:05 PM	
41	640	3N	1	5	12:55:48	12:56:05	12:55:48 PM	12:56:05 PM	
42	641	3N	2	4	12:56:45	12:57:02	12:56:45 PM	12:57:02 PM	
43	642	3N	3	4	12:57:39	12:57:57	12:57:39 PM	12:57:57 PM	
44	643	3N	2	5	12:58:33	12:58:51	12:58:33 PM	12:58:51 PM	
45	644	3N	3	5	12:59:27	12:59:44	12:59:27 PM	12:59:44 PM	

Appendix F – Field Testing Plans

Test No.	CME Survey Shot No.	Truck Position	Axle No.	Gauge Location	Start Time	End Time	Start Time	End Time	Notes
46	645	1S	1	5	13:04:23	13:04:38	1:04:23 PM	1:04:38 PM	originally recorded end time was 12:04:38
47	646	1S	1	4	13:05:47	13:06:12	1:05:47 PM	1:06:12 PM	
48	647	1S	2	5	13:06:52	13:07:10	1:06:52 PM	1:07:10 PM	
49	648	1S	3	5	13:07:51	13:08:14	1:07:51 PM	1:08:14 PM	
50	649	1S	1	3	13:09:02	13:09:19	1:09:02 PM	1:09:19 PM	
51	650	1S	2	4	13:09:59	13:10:18	1:09:59 PM	1:10:18 PM	
52	651	1S	3	4	13:10:47	13:11:02	1:10:47 PM	1:11:02 PM	
53	652	1S	1	2	13:11:40	13:11:56	1:11:40 PM	1:11:56 PM	
54	653	1S	2	3	13:13:28	13:13:46	1:13:28 PM	1:13:46 PM	
55	654	1S	3	3	13:14:20	13:14:37	1:14:20 PM	1:14:37 PM	
56	655	1S	1	1	13:15:18	13:15:37	1:15:18 PM	1:15:37 PM	
57	656	1S	2	2	13:16:10	13:16:33	1:16:10 PM	1:16:33 PM	
58	657	1S	3	2	13:17:19	13:17:35	1:17:19 PM	1:17:35 PM	
59	658	1S	2	1	13:18:14	13:18:31	1:18:14 PM	1:18:31 PM	
60	659	1S	3	1	13:18:59	13:19:18	1:18:59 PM	1:19:18 PM	
61	660	2S	1	5	13:22:17	13:22:36	1:22:17 PM	1:22:36 PM	
62	661	2S	1	4	13:23:12	13:23:29	1:23:12 PM	1:23:29 PM	
63	662	2S	2	5	13:24:02	13:24:19	1:24:02 PM	1:24:19 PM	
64	663	2S	3	5	13:24:55	13:25:09	1:24:55 PM	1:25:09 PM	
65	664	2S	1	3	13:25:45	13:26:03	1:25:45 PM	1:26:03 PM	
66	665	2S	2	4	13:26:36	13:26:53	1:26:36 PM	1:26:53 PM	
67	666	2S	3	4	13:27:21	13:27:39	1:27:21 PM	1:27:39 PM	
68	667	2S	1	2	13:28:22	13:28:38	1:28:22 PM	1:28:38 PM	
69	668	2S	2	3	13:29:13	13:29:32	1:29:13 PM	1:29:32 PM	
70	669	2S	3	3	13:30:09	13:30:28	1:30:09 PM	1:30:28 PM	
71	670	2S	1	1	13:31:05	13:31:22	1:31:05 PM	1:31:22 PM	
72	671	2S	2	2	13:31:59	13:32:17	1:31:59 PM	1:32:17 PM	
73	672	2S	3	2	13:32:55	13:33:13	1:32:55 PM	1:33:13 PM	
74	673	2S	2	1	13:33:54	13:34:11	1:33:54 PM	1:34:11 PM	
75	674	2S	3	1	13:34:47	13:35:07	1:34:47 PM	1:35:07 PM	
76	675	3S	1	5	13:38:59	13:39:09	1:38:59 PM	1:39:09 PM	
77	676	3S	1	4	13:40:15	13:40:53	1:40:15 PM	1:40:53 PM	
78	677	3S	2	5	13:41:44	13:42:07	1:41:44 PM	1:42:07 PM	
79	678	3S	3	5	13:42:44	13:43:03	1:42:44 PM	1:43:03 PM	
80	679	3S	1	3	13:43:49	13:44:07	1:43:49 PM	1:44:07 PM	
81	680	3S	2	4	13:45:45	13:46:09	1:45:45 PM	1:46:09 PM	
82	681	3S	3	4	13:47:03	13:47:21	1:47:03 PM	1:47:21 PM	
83	682	3S	1	2	13:48:07	13:48:24	1:48:07 PM	1:48:24 PM	
84	683	3S	2	3	13:49:16	13:49:35	1:49:16 PM	1:49:35 PM	
85	684	3S	3	3	13:50:07	13:50:22	1:50:07 PM	1:50:22 PM	
86	685	3S	1	1	13:51:46	13:52:02	1:51:46 PM	1:52:02 PM	

Appendix F – Field Testing Plans

Test No.	CME Survey Shot No.	Truck Position	Axle No.	Gauge Location	Start Time	End Time	Start Time	End Time	Notes
87	686	3S	2	2	13:52:42	13:52:59	1:52:42 PM	1:52:59 PM	
88	687	3S	3	2	13:53:32	13:53:49	1:53:32 PM	1:53:49 PM	
89	688	3S	2	1	13:54:45	13:55:06	1:54:45 PM	1:55:06 PM	
90	689	3S	3	1	13:55:45	13:56:04	1:55:45 PM	1:56:04 PM	

Appendix F – Field Testing Plans

Culvert Plans

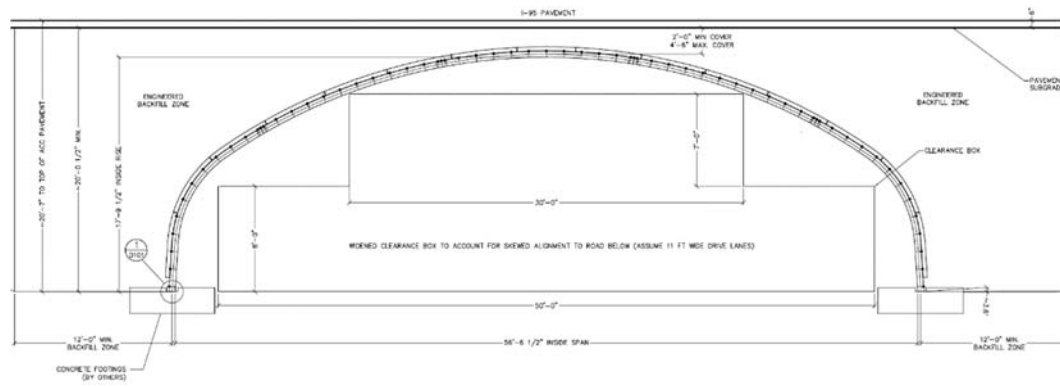
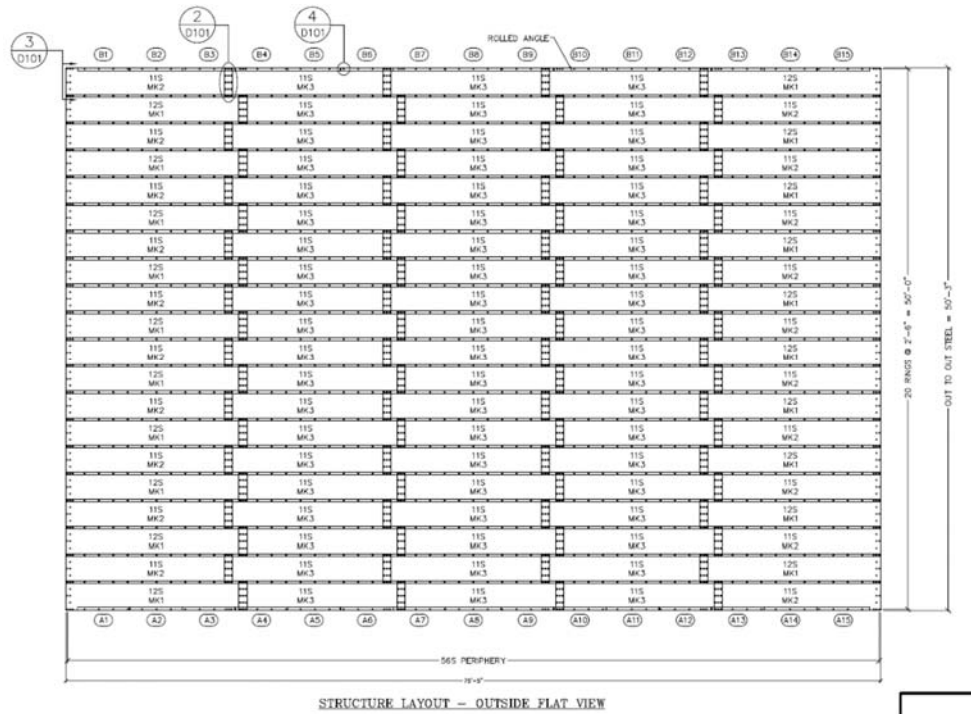


Figure 31- Model 7, Candidate 1 (M7C1) – Plan and Typical Section

Appendix G – Specification Backup

Full Table of BrDR runs for Shear Capacity changes.

The following table represents the AASHTOWare BrDR analysis runs for a select set of the Caltrans culverts for the change in the shear capacity.

Bridge ID	Fill Depth	Critical Element (Before)	Location (Before)	Critical Element (After)	Location (After)	Shear Inv Rating Factor HL93 (Before)	Shear Op Rating Factor HL93 (After)	Ratio (before/after)
CD10x8;10 2002-Rev	1.5	Top Slab 2	0.6025	Top Slab 2	0.6025	1.1099	1.1789	0.9415
CD10x8;10 2002-Rev	1.9	Top Slab 2	0.6025	Top Slab 2	0.6025	1.1066	1.1835	0.9350
CD10x8;10 2002-Rev	2	Top Slab 2	0.6025	Top Slab 2	0.6025	1.1051	1.1051	1.0000
CD10x8;10 2002-Rev	4	Top Slab 2	0.6025	Top Slab 2	0.6025	1.7365	1.7365	1.0000
CD10x8;10 2002-Rev	7	Bottom Slab 1	9.46	Bottom Slab 1	9.46	1.5147	1.5147	1.0000
CD10x8;10 2010-Rev	1.5	Top Slab 2	0.6925	Top Slab 2	0.6925	1.4619	1.557	0.9389
CD10x8;10 2010-Rev	1.9	Top Slab 2	0.6925	Top Slab 2	0.6925	1.5025	1.5806	0.9506
CD10x8;10 2010-Rev	2	Top Slab 2	0.6925	Top Slab 2	0.6925	1.5521	1.5521	1.0000
CD10x8;10 2010-Rev	4	Top Slab 2	0.6925	Top Slab 2	0.6925	2.4874	2.4874	1.0000
CD10x8;10 2010-Rev	7	Bottom Slab 1	9.37	Bottom Slab 1	9.37	2.911	2.911	1.0000
CD10x8;16 1966-Rev	1.9	Top Slab 1	9.0893	Top Slab 1	9.0893	1.601	1.8908	0.8467
CD10x8;16 1966-Rev	2	Top Slab 1	9.0893	Top Slab 1	9.0893	1.5982	1.5982	1.0000
CD10x8;16 1966-Rev	2.5	Top Slab 1	9.0893	Top Slab 1	9.0893	1.9313	1.9313	1.0000
CD10x8;16 1966-Rev	3	Top Slab 1	9.0893	Top Slab 1	9.0893	2.2948	2.2948	1.0000
CD10x8;16 1966-Rev	3.5	Top Slab 1	9.0893	Top Slab 1	9.0893	2.6131	2.6131	1.0000
CD10x8;16 1966-Rev	4	Top Slab 1	9.0893	Top Slab 1	9.0893	2.8796	2.8796	1.0000
CD10x8;16 1966-Rev	7	Top Slab 1	9.0893	Top Slab 1	9.0893	4.0435	4.0435	1.0000
CD10x8;16 1966-Rev	9	Top Slab 1	9.0893	Top Slab 1	9.0893	3.7745	3.7745	1.0000
CD10x8;2 1966-Rev	0.5	Top Slab 1	9.3866	Top Slab 1	0.6354	1.0071	1.0407	0.9677
CD10x8;2 1966-Rev	1	Top Slab 1	9.3866	Top Slab 1	0.6354	1.0185	1.1017	0.9245
CD10x8;2 1966-Rev	1.5	Top Slab 1	9.3866	Top Slab 1	9.3866	1.0306	1.0946	0.9415
CD10x8;2 1966-Rev	1.9	Top Slab 1	9.3866	Top Slab 1	9.3866	1.0314	1.0873	0.9486
CD10x8;2 1966-Rev	2	Bottom Slab 1	9.475	Bottom Slab 1	9.475	1.2291	1.2291	1.0000
CD10x8;2 1966-Rev	3	Bottom Slab 1	9.475	Bottom Slab 1	9.475	1.2291	1.2291	1.0000
CD10x8;3 1952-Rev	1.5	Top Slab 1	8.8819	Top Slab 1	8	1.0699	1.3251	0.8074
CD10x8;3 1952-Rev	1.9	Top Slab 1	8.8819	Top Slab 1	8.8819	1.0888	1.3459	0.8090
CD10x8;3 1952-Rev	2	Top Slab 1	8.8819	Top Slab 1	8.8819	1.2148	1.2148	1.0000
CD10x8;3 1952-Rev	3	Bottom Slab 1	9.4	Bottom Slab 1	9.4	1.4473	1.4473	1.0000
CD10x8;3 1952-Rev	3.5	Bottom Slab 1	9.4	Bottom Slab 1	9.4	1.4692	1.4692	1.0000
CD10x8;3 1952-Rev	4	Bottom Slab 1	9.4	Bottom Slab 1	9.4	1.4456	1.4456	1.0000

Appendix G – Specification Backup

Bridge ID	Fill Depth	Critical Element (Before)	Location (Before)	Critical Element (After)	Location (After)	Shear Inv Rating Factor HL93 (Before)	Shear Op Rating Factor HL93 (After)	Ratio (before/after)
CD10x8;5 1948-Rev	1	Top Slab 1	8.9271	Top Slab 1	1.1034	1.1191	1.2936	0.8651
CD10x8;5 1948-Rev	1.5	Top Slab 1	8.9271	Top Slab 1	8.9271	1.1443	1.3417	0.8529
CD10x8;5 1948-Rev	1.9	Top Slab 1	8.9271	Top Slab 1	8.9271	1.1661	1.3478	0.8652
CD10x8;5 1948-Rev	2	Top Slab 1	8.9271	Top Slab 1	8.9271	1.3326	1.3326	1.0000
CD10x8;5 1948-Rev	3	Bottom Slab 1	9.1319	Bottom Slab 1	9.1319	1.5773	1.5773	1.0000
CD10x8;5 1948-Rev	4	Bottom Slab 1	9.1319	Bottom Slab 1	9.1319	1.5516	1.5516	1.0000
CD10x8;5 1948-Rev	5	Bottom Slab 1	9.1319	Bottom Slab 1	9.1319	1.4464	1.4464	1.0000
CD10x8;9 1948-Rev	1.5	Top Slab 1	8.8924	Top Slab 1	8.8924	1.3002	1.5054	0.8637
CD10x8;9 1948-Rev	1.9	Top Slab 1	8.8924	Top Slab 1	8.8924	1.3303	1.5218	0.8742
CD10x8;9 1948-Rev	2	Top Slab 1	8.8924	Top Slab 1	8.8924	1.5024	1.5024	1.0000
CD10x8;9 1948-Rev	4	Bottom Slab 1	8.9736	Bottom Slab 1	8.9736	2.415	2.415	1.0000
CD10x8;9 1948-Rev	6	Bottom Slab 1	8.9736	Bottom Slab 1	8.9736	2.3231	2.3231	1.0000
CD10x8;9 1948-Rev	8	Bottom Slab 1	8.9736	Bottom Slab 1	8.9736	2.0001	2.0001	1.0000
CD12x12;20 2010-Rev	1.9	Top Slab 2	1.227	Top Slab 2	1.227	3.1552	3.5462	0.8897
CD12x12;20 2010-Rev	2	Top Slab 2	1.227	Top Slab 2	1.227	3.1521	3.1521	1.0000
CD12x12;20 2010-Rev	2.5	Top Slab 2	1.227	Top Slab 2	1.227	3.1521	3.1521	1.0000
CD12x12;20 2010-Rev	3	Top Slab 2	1.227	Top Slab 2	1.227	4.395	4.395	1.0000
CD12x12;20 2010-Rev	3.5	Top Slab 2	1.227	Top Slab 2	1.227	4.9055	4.9055	1.0000
CD12x12;20 2010-Rev	4	Top Slab 2	1.227	Top Slab 2	1.227	5.3773	5.3773	1.0000
CD12x12;20 2010-Rev	5	Top Slab 2	1.227	Top Slab 2	1.227	6.426	6.426	1.0000
CD12x12;2 1966-Rev	1.5	Top Slab 1	11.252	Top Slab 1	11.252	1.3301	1.435	0.9269
CD12x12;2 1966-Rev	1.9	Top Slab 1	11.252	Top Slab 1	11.252	1.3323	1.4171	0.9402
CD12x12;2 1966-Rev	2	Bottom Slab 1	11.37	Bottom Slab 1	11.37	1.398	1.398	1.0000
CD12x12;2 1966-Rev	2.5	Bottom Slab 1	11.37	Bottom Slab 1	11.37	1.5088	1.5088	1.0000
CD12x12;2 1966-Rev	3	Bottom Slab 1	11.37	Bottom Slab 1	11.37	1.5887	1.5887	1.0000
CD12x12;2 1966-Rev	3.5	Bottom Slab 1	11.37	Bottom Slab 1	11.37	1.5659	1.5659	1.0000
CD12x12;2 1966-Rev	4	Bottom Slab 1	11.37	Bottom Slab 1	11.37	1.5203	1.5203	1.0000
CD12x8;9 1948-Rev	0	Top Slab 1	1.2486	Top Slab 1	1.2486	1.2529	1.2529	1.0000
CD12x8;9 1948-Rev	0.5	Top Slab 1	1.2486	Top Slab 1	1.2486	1.3022	1.3022	1.0000
CD12x8;9 1948-Rev	1	Top Slab 1	10.79	Top Slab 1	1.2486	1.2176	1.3535	0.8996
CD12x8;9 1948-Rev	1.5	Top Slab 1	10.79	Top Slab 1	10.79	1.2164	1.381	0.8808

Appendix G – Specification Backup

Bridge ID	Fill Depth	Critical Element (Before)	Location (Before)	Critical Element (After)	Location (After)	Shear Inv Rating Factor HL93 (Before)	Shear Op Rating Factor HL93 (After)	Ratio (before/after)
CD12x8;9 1948-Rev	1.9	Top Slab 1	10.79	Top Slab 1	10.79	1.2148	1.364	0.8906
CD12x8;9 1948-Rev	2	Top Slab 1	10.79	Top Slab 1	10.79	1.3333	1.3333	1.0000
CD12x8;9 1948-Rev	4	Top Slab 1	10.79	Top Slab 1	10.79	1.943	1.943	1.0000
CD12x8;9 1948-Rev	6	Top Slab 1	10.79	Top Slab 1	10.79	1.9194	1.9194	1.0000
CD12x8;9 1948-Rev	8	Bottom Slab 1	10.79	Bottom Slab 1	10.79	1.5434	1.5434	1.0000
CD12x8;9 1948-Rev	9	Bottom Slab 1	10.79	Bottom Slab 1	10.79	1.1156	1.1156	1.0000
CD12x8;9 1952-Rev	1.5	Top Slab 1	9.6	Top Slab 1	9.6	2.0712	2.1877	0.9467
CD12x8;9 1952-Rev	1.9	Top Slab 1	10.465	Top Slab 1	10.465	1.8899	2.2891	0.8256
CD12x8;9 1952-Rev	2	Top Slab 1	10.465	Top Slab 1	10.465	1.8811	1.8811	1.0000
CD12x8;9 1952-Rev	3.5	Top Slab 1	10.465	Top Slab 1	10.465	2.8637	2.8637	1.0000
CD12x8;9 1952-Rev	3	Top Slab 1	10.465	Top Slab 1	10.465	2.5928	2.5928	1.0000
CD12x8;9 1952-Rev	4	Top Slab 1	10.465	Top Slab 1	10.465	3.1016	3.1016	1.0000
CD14x13;10 2002-Rev	1.5	Top Slab 2	0.7525	Top Slab 2	0.7525	1.2995	1.3937	0.9324
CD14x13;10 2002-Rev	1.9	Top Slab 2	0.7525	Top Slab 2	0.7525	1.2622	1.3677	0.9229
CD14x13;10 2002-Rev	2	Top Slab 2	0.7525	Top Slab 2	0.7525	1.3325	1.3325	1.0000
CD14x13;10 2002-Rev	2.5	Top Slab 2	0.7525	Top Slab 2	0.7525	1.4176	1.4176	1.0000
CD14x13;10 2002-Rev	3	Top Slab 2	0.7525	Top Slab 2	0.7525	1.5063	1.5063	1.0000
CD14x13;10 2002-Rev	3.5	Top Slab 2	0.7525	Top Slab 2	0.7525	1.5443	1.5443	1.0000
CD14x13;10 2002-Rev	4	Top Slab 2	0.7525	Top Slab 2	0.7525	1.5649	1.5649	1.0000
CD14x9;10 2002-Rev	1.5	Top Slab 2	0.7525	Top Slab 2	0.7525	1.2781	1.3776	0.9278
CD14x9;10 2002-Rev	1.9	Top Slab 2	0.7525	Top Slab 2	0.7525	1.2383	1.3488	0.9181
CD14x9;10 2002-Rev	2	Top Slab 2	0.7525	Top Slab 2	0.7525	1.2947	1.2947	1.0000
CD14x9;10 2002-Rev	4	Top Slab 2	0.7525	Top Slab 2	0.7525	1.512	1.512	1.0000
CD14x9;10 2002-Rev	7	Bottom Slab 1	13.31	Bottom Slab 1	13.31	1.282	1.282	1.0000
CD14x9;10 2010-Rev	1.5	Top Slab 2	0.852	Top Slab 2	0.852	1.6473	1.7383	0.9477
CD14x9;10 2010-Rev	1.9	Top Slab 2	0.852	Top Slab 2	0.852	1.6197	1.7224	0.9404
CD14x9;10 2010-Rev	2	Top Slab 2	0.852	Top Slab 2	0.852	1.7144	1.7144	1.0000
CD14x9;10 2010-Rev	4	Top Slab 2	0.852	Top Slab 2	0.852	2.1355	2.1355	1.0000
CD14x9;10 2010-Rev	7	Top Slab 2	0.852	Top Slab 2	0.852	2.2762	2.2762	1.0000
CD8x8;10 1924-Rev	1	Top Slab 1	7.0713	Top Slab 1	7.0713	2.2342	2.4854	0.8989
CD8x8;10 1924-Rev	1.9	Top Slab 1	7.0713	Top Slab 1	7.0713	2.5273	2.8542	0.8855
CD8x8;10 1924-Rev	2	Top Slab 1	7.0713	Top Slab 1	7.0713	2.5427	2.5427	1.0000
CD8x8;10 1924-Rev	3	Top Slab 1	7.0713	Top Slab 1	7.0713	3.8408	3.8408	1.0000
CD8x8;10 1924-Rev	5	Bottom Slab 1	7.1546	Bottom Slab 1	7.1546	5.7973	5.7973	1.0000

Appendix G – Specification Backup

Bridge ID	Fill Depth	Critical Element (Before)	Location (Before)	Critical Element (After)	Location (After)	Shear Inv Rating Factor HL93 (Before)	Shear Op Rating Factor HL93 (After)	Ratio (before/after)
CD8x8;10 1933-Rev	1	Top Slab 1	7.0937	Top Slab 1	7.0937	2.0784	2.3505	0.8842
CD8x8;10 1933-Rev	1.9	Top Slab 1	7.0937	Top Slab 1	7.0937	2.3552	2.7004	0.8722
CD8x8;10 1933-Rev	2	Top Slab 1	7.0937	Top Slab 1	7.0937	2.3678	2.3678	1.0000
CD8x8;10 1933-Rev	3	Top Slab 1	7.0937	Top Slab 1	7.0937	3.5884	3.5884	1.0000
CD8x8;10 1933-Rev	3.5	Top Slab 1	7.0937	Top Slab 1	7.0937	4.1518	4.1518	1.0000
CD8x8;10 1933-Rev	4	Top Slab 1	7.0937	Top Slab 1	7.0937	4.565	4.565	1.0000
CD8x8;5 1924-Rev	1	Top Slab 1	7.2356	Top Slab 1	0.7722	1.6345	1.7773	0.9197
CD8x8;5 1924-Rev	1.5	Top Slab 1	7.2356	Top Slab 1	0.7722	1.7321	1.9571	0.8850
CD8x8;5 1924-Rev	1.9	Top Slab 1	7.2356	Bottom Slab 1	0.6055	1.821	2.0376	0.8937
CD8x8;5 1924-Rev	2	Top Slab 1	7.2356	Top Slab 1	7.2356	1.8472	1.8472	1.0000
CD8x8;5 1924-Rev	3	Bottom Slab 1	7.4023	Bottom Slab 1	7.4023	2.5361	2.5361	1.0000
CD8x8;5 1924-Rev	4	Bottom Slab 1	7.4023	Bottom Slab 1	7.4023	2.7612	2.7612	1.0000
CS10x8;10 1933-Rev	1.9	Top Slab 1	1.1503	Top Slab 1	1.1503	2.4883	2.4883	1.0000
CS10x8;10 1933-Rev	2	Top Slab 1	1.1503	Top Slab 1	1.1503	2.4912	2.4912	1.0000
CS10x8;10 1933-Rev	2.5	Top Slab 1	1.1503	Top Slab 1	1.1503	3.0667	3.0667	1.0000
CS10x8;10 1933-Rev	3	Top Slab 1	1.1503	Top Slab 1	1.1503	3.6997	3.6997	1.0000
CS10x8;10 1933-Rev	3.5	Top Slab 1	1.1503	Top Slab 1	1.1503	4.2713	4.2713	1.0000
CS10x8;10 1933-Rev	4	Bottom Slab 1	1.067	Bottom Slab 1	1.067	4.625	4.625	1.0000
CS10x8;10 1933-Rev	7	Bottom Slab 1	1.067	Bottom Slab 1	1.067	6.7502	6.7502	1.0000
CS10x8;10 1981-Rev	1.5	Top Slab 1	0.5425	Top Slab 1	0.5425	1.1412	1.2482	0.9143
CS10x8;10 1981-Rev	1.9	Bottom Slab 1	0.48	Top Slab 1	0.5425	1.1637	1.2681	0.9177
CS10x8;10 1981-Rev	2	Top Slab 1	0.5425	Top Slab 1	0.5425	1.322	1.322	1.0000
CS10x8;10 1981-Rev	4	Bottom Slab 1	0.48	Bottom Slab 1	0.48	1.9619	1.9619	1.0000
CS10x8;10 1981-Rev	7	Bottom Slab 1	0.48	Bottom Slab 1	0.48	2.2522	2.2522	1.0000
CS10x8;10 2002-Rev	1.5	Top Slab 1	0.5425	Top Slab 1	0.5425	1.2232	1.3337	0.9171
CS10x8;10 2002-Rev	1.9	Bottom Slab 1	0.48	Top Slab 1	0.5425	1.2561	1.3578	0.9251
CS10x8;10 2002-Rev	2	Top Slab 1	0.5425	Top Slab 1	0.5425	1.391	1.391	1.0000
CS10x8;10 2002-Rev	4	Bottom Slab 1	0.48	Bottom Slab 1	0.48	2.0835	2.0835	1.0000
CS10x8;10 2002-Rev	7	Bottom Slab 1	0.48	Bottom Slab 1	0.48	2.4697	2.4697	1.0000
CS10x8;10 2010-Rev	1.5	Top Slab 1	0.6325	Top Slab 1	0.6325	1.5199	1.7165	0.8855
CS10x8;10 2010-Rev	1.9	Top Slab 1	0.6325	Top Slab 1	0.6325	1.5698	1.7605	0.8917
CS10x8;10 2010-Rev	2	Top Slab 1	0.6325	Top Slab 1	0.6325	1.668	1.668	1.0000
CS10x8;10 2010-Rev	4	Top Slab 1	0.6325	Top Slab 1	0.6325	2.7829	2.7829	1.0000
CS10x8;10 2010-Rev	7	Bottom Slab 1	0.6	Bottom Slab 1	0.6	4.124	4.124	1.0000

Appendix G – Specification Backup

Bridge ID	Fill Depth	Critical Element (Before)	Location (Before)	Critical Element (After)	Location (After)	Shear Inv Rating Factor HL93 (Before)	Shear Op Rating Factor HL93 (After)	Ratio (before/after)
CS10x8;12 1952-Rev	1.9	Top Slab 1	1.116	Top Slab 1	1.116	1.6469	1.8724	0.8796
CS10x8;12 1952-Rev	2	Top Slab 1	1.116	Top Slab 1	1.116	1.6908	1.6908	1.0000
CS10x8;12 1952-Rev	4	Bottom Slab 1	0.6483	Bottom Slab 1	0.6483	2.4756	2.4756	1.0000
CS10x8;12 1952-Rev	7	Bottom Slab 1	0.6483	Bottom Slab 1	0.6483	3.4233	3.4233	1.0000
CS10x8;5 1922-Rev	1.5	Top Slab 1	1.6879	Top Slab 1	1.6879	2.5801	2.6162	0.9862
CS10x8;5 1922-Rev	1.9	Top Slab 1	1.6879	Top Slab 1	1.6879	2.7172	2.7663	0.9823
CS10x8;5 1922-Rev	2	Top Slab 1	1.6879	Top Slab 1	1.6879	2.7291	2.7291	1.0000
CS10x8;5 1922-Rev	2.5	Top Slab 1	8.327	Top Slab 1	8.327	3.3489	3.3489	1.0000
CS10x8;5 1922-Rev	3	Top Slab 1	1.673	Top Slab 1	1.673	4.0583	4.0583	1.0000
CS10x8;5 1922-Rev	3.5	Top Slab 1	1.673	Top Slab 1	1.673	4.7156	4.7156	1.0000
CS10x8;5 1922-Rev	4	Top Slab 1	1.673	Top Slab 1	1.673	5.2913	5.2913	1.0000
CS10x8;5 1933-Rev	1.5	Bottom Slab 1	0.7389	Bottom Slab 1	0.7389	1.4995	1.4995	1.0000
CS10x8;5 1933-Rev	1.9	Bottom Slab 1	0.7389	Bottom Slab 1	0.7389	1.5042	1.5042	1.0000
CS10x8;5 1933-Rev	2	Bottom Slab 1	0.7389	Bottom Slab 1	0.7389	1.5314	1.5314	1.0000
CS10x8;5 1933-Rev	2.5	Bottom Slab 1	0.7389	Bottom Slab 1	0.7389	1.754	1.754	1.0000
CS10x8;5 1933-Rev	3	Bottom Slab 1	0.7389	Bottom Slab 1	0.7389	2.0166	2.0166	1.0000
CS10x8;5 1933-Rev	3.5	Bottom Slab 1	0.7389	Bottom Slab 1	0.7389	2.207	2.207	1.0000
CS10x8;5 1933-Rev	4	Bottom Slab 1	0.7389	Bottom Slab 1	0.7389	2.3248	2.3248	1.0000
CS10x8;5 1952-Rev	1.5	Bottom Slab 1	0.51	Bottom Slab 1	0.51	0.96278	1.1542	0.8342
CS10x8;5 1952-Rev	1.9	Bottom Slab 1	0.51	Bottom Slab 1	0.51	0.95991	1.1504	0.8344
CS10x8;5 1952-Rev	2	Bottom Slab 1	0.51	Bottom Slab 1	0.51	1.0579	1.0579	1.0000
CS10x8;5 1952-Rev	3	Bottom Slab 1	0.51	Bottom Slab 1	0.51	1.3237	1.3237	1.0000
CS10x8;5 1952-Rev	4	Bottom Slab 1	0.51	Bottom Slab 1	0.51	1.4756	1.4756	1.0000
CS10x8;5 1952-Rev	5	Bottom Slab 1	0.51	Bottom Slab 1	0.51	1.5688	1.5688	1.0000
CS10x8;6 1948-Rev	1.5	Bottom Slab 1	0.576	Bottom Slab 1	0.576	1.3847	1.5789	0.8770
CS10x8;6 1948-Rev	1.9	Bottom Slab 1	0.576	Bottom Slab 1	0.576	1.3951	1.5891	0.8779
CS10x8;6 1948-Rev	2	Bottom Slab 1	0.576	Bottom Slab 1	0.576	1.5684	1.5684	1.0000
CS10x8;6 1948-Rev	3	Bottom Slab 1	0.576	Bottom Slab 1	0.576	2.0211	2.0211	1.0000
CS10x8;6 1948-Rev	4	Bottom Slab 1	0.576	Bottom Slab 1	0.576	2.3376	2.3376	1.0000
CS10x8;6 1948-Rev	5	Bottom Slab 1	0.576	Bottom Slab 1	0.576	2.6057	2.6057	1.0000

Appendix G – Specification Backup

Bridge ID	Fill Depth	Critical Element (Before)	Location (Before)	Critical Element (After)	Location (After)	Shear Inv Rating Factor HL93 (Before)	Shear Op Rating Factor HL93 (After)	Ratio (before/after)
CS10x8;8 1966-Rev	1.5	Top Slab 1	0.62	Top Slab 1	2	1.0366	1.2219	0.8484
CS10x8;8 1966-Rev	1.9	Top Slab 1	0.62	Top Slab 1	2	1.0618	1.291	0.8225
CS10x8;8 1966-Rev	2	Top Slab 1	0.62	Top Slab 1	0.62	1.2081	1.2081	1.0000
CS10x8;8 1966-Rev	4	Bottom Slab 1	0.555	Bottom Slab 1	0.555	1.7073	1.7073	1.0000
CS10x8;8 1966-Rev	6	Bottom Slab 1	0.555	Bottom Slab 1	0.555	2.0076	2.0076	1.0000
CS12x12;10 2002-Rev	1.5	Top Slab 1	0.6325	Top Slab 1	0.6325	1.2302	1.3203	0.9318
CS12x12;10 2002-Rev	1.9	Top Slab 1	0.6325	Top Slab 1	0.6325	1.2444	1.3195	0.9431
CS12x12;10 2002-Rev	2	Top Slab 1	0.6325	Top Slab 1	0.6325	1.3395	1.3395	1.0000
CS12x12;10 2002-Rev	2.5	Top Slab 1	0.6325	Top Slab 1	0.6325	1.4653	1.4653	1.0000
CS12x12;10 2002-Rev	3	Top Slab 1	0.6325	Top Slab 1	0.6325	1.6013	1.6013	1.0000
CS12x12;10 2002-Rev	3.5	Top Slab 1	0.6325	Top Slab 1	0.6325	1.7225	1.7225	1.0000
CS12x12;10 2002-Rev	4	Bottom Slab 1	0.6	Bottom Slab 1	0.6	1.8007	1.8007	1.0000
CS12x8;10 1952-Rev	10	Bottom Slab 1	0.7834	Bottom Slab 1	0.7834	3.4034	3.4034	1.0000
CS12x8;10 1952-Rev	1.5	Top Slab 1	1.3398	Top Slab 1	1.3398	1.7957	1.9911	0.9019
CS12x8;10 1952-Rev	1.9	Bottom Slab 1	0.7834	Top Slab 1	1.3398	1.8349	2.0668	0.8878
CS12x8;10 1952-Rev	2	Bottom Slab 1	0.7834	Bottom Slab 1	0.7834	1.8218	1.8218	1.0000
CS12x8;10 1952-Rev	3	Bottom Slab 1	0.7834	Bottom Slab 1	0.7834	2.3807	2.3807	1.0000
CS12x8;10 1952-Rev	4	Bottom Slab 1	0.7834	Bottom Slab 1	0.7834	2.6871	2.6871	1.0000
CS12x8;10 1952-Rev	7	Bottom Slab 1	0.7834	Bottom Slab 1	0.7834	3.2658	3.2658	1.0000
CS12x8;10 2010-Rev	1.5	Top Slab 1	0.6925	Top Slab 1	0.6925	1.5694	1.7585	0.8925
CS12x8;10 2010-Rev	1.9	Top Slab 1	0.6925	Top Slab 1	0.6925	1.5984	1.781	0.8975
CS12x8;10 2010-Rev	2	Top Slab 1	0.6925	Top Slab 1	0.6925	1.759	1.759	1.0000
CS12x8;10 2010-Rev	2.5	Top Slab 1	0.6925	Top Slab 1	0.6925	2.0268	2.0268	1.0000
CS12x8;10 2010-Rev	3	Top Slab 1	0.6925	Top Slab 1	0.6925	2.3093	2.3093	1.0000
CS12x8;10 2010-Rev	3.5	Top Slab 1	0.6925	Top Slab 1	0.6925	2.5235	2.5235	1.0000
CS12x8;10 2010-Rev	4	Top Slab 1	0.6925	Top Slab 1	0.6925	2.7149	2.7149	1.0000
CS12x8;5 1922-Rev	1.5	Top Slab 1	2.0204	Top Slab 1	2.0204	2.8244	2.8715	0.9836
CS12x8;5 1922-Rev	1.9	Top Slab 1	2.0204	Top Slab 1	2.0204	2.934	2.996	0.9793
CS12x8;5 1922-Rev	2	Top Slab 1	2.0204	Top Slab 1	2.0204	2.937	2.937	1.0000
CS12x8;5 1922-Rev	3	Top Slab 1	2.0204	Top Slab 1	2.0204	4.2056	4.2056	1.0000
CS12x8;5 1922-Rev	4	Top Slab 1	2.0027	Top Slab 1	2.0027	5.2324	5.2324	1.0000
CS12x8;5 1922-Rev	5	Top Slab 1	2.0027	Top Slab 1	2.0027	6.3741	6.3741	1.0000
CS14x14;10 2002-Rev	1.5	Bottom Slab 1	0.69	Bottom Slab 1	0.69	1.3813	1.4832	0.9313
CS14x14;10 2002-Rev	1.9	Bottom Slab 1	0.69	Bottom Slab 1	0.69	1.3527	1.46	0.9265

Appendix G – Specification Backup

Bridge ID	Fill Depth	Critical Element (Before)	Location (Before)	Critical Element (After)	Location (After)	Shear Inv Rating Factor HL93 (Before)	Shear Op Rating Factor HL93 (After)	Ratio (before/after)
CS14x14;10 2002-Rev	2	Top Slab 1	0.7225	Top Slab 1	0.7225	1.5401	1.5401	1.0000
CS14x14;10 2002-Rev	2.5	Top Slab 1	0.7225	Top Slab 1	0.7225	1.7043	1.7043	1.0000
CS14x14;10 2002-Rev	3	Top Slab 1	0.7225	Top Slab 1	0.7225	1.8188	1.8188	1.0000
CS14x14;10 2002-Rev	3.5	Bottom Slab 1	0.69	Bottom Slab 1	0.69	1.8584	1.8584	1.0000
CS14x14;10 2002-Rev	4	Bottom Slab 1	0.69	Bottom Slab 1	0.69	1.8852	1.8852	1.0000
CS14x9;10 2002-Rev	1.5	Top Slab 1	0.6325	Top Slab 1	0.6325	1.1166	1.2179	0.9168
CS14x9;10 2002-Rev	1.9	Top Slab 1	0.6325	Top Slab 1	0.6325	1.111	1.1973	0.9279
CS14x9;10 2002-Rev	2	Top Slab 1	0.6325	Top Slab 1	0.6325	1.2211	1.2211	1.0000
CS14x9;10 2002-Rev	4	Top Slab 1	0.6325	Top Slab 1	0.6325	1.4358	1.4358	1.0000
CS14x9;10 2002-Rev	7	Top Slab 1	0.6325	Top Slab 1	0.6325	1.3875	1.3875	1.0000
CS14x9;10 2010-Rev	1.5	Top Slab 1	0.7825	Top Slab 1	1.4	1.4648	1.7391	0.8423
CS14x9;10 2010-Rev	1.9	Top Slab 1	0.7825	Top Slab 1	0.7825	1.4714	1.7734	0.8297
CS14x9;10 2010-Rev	2	Top Slab 1	0.7825	Top Slab 1	0.7825	1.5539	1.5539	1.0000
CS14x9;10 2010-Rev	2.5	Top Slab 1	0.7825	Top Slab 1	0.7825	1.7586	1.7586	1.0000
CS14x9;10 2010-Rev	3	Top Slab 1	0.7825	Top Slab 1	0.7825	1.9669	1.9669	1.0000
CS14x9;10 2010-Rev	3.5	Top Slab 1	0.7825	Top Slab 1	0.7825	2.0896	2.0896	1.0000
CS14x9;10 2010-Rev	4	Top Slab 1	0.7825	Top Slab 1	0.7825	2.2055	2.2055	1.0000
CS16x12;0 1922 EAE-Rev	1.5	Top Slab 1	2.3528	Top Slab 1	2.3528	2.1968	2.2408	0.9804
CS16x12;0 1922 EAE-Rev	1.9	Top Slab 1	2.3528	Top Slab 1	2.3528	2.2376	2.3038	0.9713
CS16x12;0 1922 EAE-Rev	2	Top Slab 1	2.3528	Top Slab 1	2.3528	2.2285	2.2285	1.0000
CS16x12;0 1922 EAE-Rev	2.5	Top Slab 1	2.3528	Top Slab 1	2.3528	2.6235	2.6235	1.0000
CS16x12;0 1922 EAE-Rev	3	Top Slab 1	2.3315	Top Slab 1	2.3315	3.0002	3.0002	1.0000
CS16x12;0 1922 EAE-Rev	3.5	Top Slab 1	2.3315	Top Slab 1	2.3315	3.2459	3.2459	1.0000
CS16x12;0 1922 EAE-Rev	4	Top Slab 1	2.3315	Top Slab 1	2.3315	3.4994	3.4994	1.0000
CS16x8;5 1922 EAE-Rev	1.5	Top Slab 1	2.6645	Top Slab 1	2.6645	2.4898	2.5762	0.9665
CS16x8;5 1922 EAE-Rev	1.9	Top Slab 1	2.6645	Top Slab 1	2.6645	2.5454	2.6561	0.9583
CS16x8;5 1922 EAE-Rev	2	Top Slab 1	2.6645	Top Slab 1	2.6645	3.0398	3.0398	1.0000
CS16x8;5 1922 EAE-Rev	2.5	Top Slab 1	2.6645	Top Slab 1	2.6645	3.5048	3.5048	1.0000
CS16x8;5 1922 EAE-Rev	3	Top Slab 1	2.6645	Top Slab 1	2.6645	3.9755	3.9755	1.0000
CS16x8;5 1922 EAE-Rev	4	Top Slab 1	2.676	Top Slab 1	2.676	5.0277	5.0277	1.0000
CS7x7;10 2010-Rev	1.5	Bottom Slab 1	0.51	Bottom Slab 1	0.51	1.5433	1.5433	1.0000
CS7x7;10 2010-Rev	1.9	Bottom Slab 1	0.51	Bottom Slab 1	0.51	1.5855	1.5855	1.0000

Appendix G – Specification Backup

Bridge ID	Fill Depth	Critical Element (Before)	Location (Before)	Critical Element (After)	Location (After)	Shear Inv Rating Factor HL93 (Before)	Shear Op Rating Factor HL93 (After)	Ratio (before/after)
CS7x7;10 2010-Rev	2	Bottom Slab 1	0.51	Bottom Slab 1	0.51	1.5806	1.5806	1.0000
CS7x7;10 2010-Rev	4	Bottom Slab 1	0.51	Bottom Slab 1	0.51	3.0855	3.0855	1.0000
CS7x7;10 2010-Rev	7	Bottom Slab 1	0.51	Bottom Slab 1	0.51	4.7945	4.7945	1.0000
CS8x8;10 2010-Rev	1.5	Bottom Slab 1	0.51	Bottom Slab 1	0.51	1.3655	1.3655	1.0000
CS8x8;10 2010-Rev	1.9	Bottom Slab 1	0.51	Bottom Slab 1	0.51	1.3896	1.3896	1.0000
CS8x8;10 2010-Rev	2	Bottom Slab 1	0.51	Bottom Slab 1	0.51	1.382	1.382	1.0000
CS8x8;10 2010-Rev	4	Bottom Slab 1	0.51	Bottom Slab 1	0.51	2.4193	2.4193	1.0000
CS8x8;10 2010-Rev	7	Bottom Slab 1	0.51	Bottom Slab 1	0.51	3.4916	3.4916	1.0000
Model 1- Candidate 1-Rev	1.5	Top Slab 1	1.8759	Top Slab 1	1.8759	1.4574	1.8193	0.8011
Model 1- Candidate 1-Rev	1.99	Top Slab 1	1.8759	Top Slab 1	1.8759	1.3847	1.726	0.8023
Model 1- Candidate 1-Rev	2	Top Slab 1	1.8759	Top Slab 1	1.8759	1.6066	1.6066	1.0000
Model 1- Candidate 1-Rev	2.1	Top Slab 1	1.8759	Top Slab 1	1.8759	1.6323	1.6323	1.0000
Model 1- Candidate 1-Rev	2.2	Top Slab 1	1.8759	Top Slab 1	1.8759	1.6575	1.6575	1.0000
Model 1- Candidate 1-Rev	2.4	Top Slab 1	1.8759	Top Slab 1	1.8759	1.7064	1.7064	1.0000
Model 1- Candidate 1-Rev	2.5	Top Slab 1	1.8759	Top Slab 1	1.8759	1.7241	1.7241	1.0000
Model 1- Candidate 1-Rev	3	Top Slab 1	1.8759	Top Slab 1	1.8759	1.7543	1.7543	1.0000
Model 1- Candidate 1-Rev	5	Top Slab 1	1.8759	Top Slab 1	1.8759	1.7624	1.7624	1.0000
Model 1- Candidate 1-Rev	7	Top Slab 1	1.8759	Top Slab 1	1.8759	1.5137	1.5137	1.0000
Model 2- Candidate 1-Rev	1.5	Top Slab 2	1.13	Top Slab 2	1.13	1.5227	1.698	0.8968
Model 2- Candidate 1-Rev	1.9	Top Slab 2	1.13	Top Slab 2	1.13	1.579	1.743	0.9059
Model 2- Candidate 1-Rev	2	Top Slab 2	1.13	Top Slab 2	1.13	1.634	1.634	1.0000
Model 2- Candidate 1-Rev	2.5	Top Slab 1	1.13	Top Slab 1	1.13	1.822	1.822	1.0000
Model 2- Candidate 1-Rev	3	Top Slab 1	1.13	Top Slab 1	1.13	2.2039	2.2039	1.0000
Model 2- Candidate 1-Rev	3.5	Top Slab 1	1.13	Top Slab 1	1.13	2.5422	2.5422	1.0000
Model 2- Candidate 1-Rev	4	Top Slab 1	1.13	Top Slab 1	1.13	2.8282	2.8282	1.0000
Model 2- Candidate 1-Rev	10	Bottom Slab 1	9.31	Bottom Slab 1	9.31	2.7384	2.7384	1.0000
Model 2- Candidate 1-Rev	7	Bottom Slab 1	9.31	Bottom Slab 1	9.31	3.4624	3.4624	1.0000
Model 3- Candidate 1-Rev	1.5	Top Slab 1	1.4337	Top Slab 1	1.4337	3.1686	3.4535	0.9175

Appendix G – Specification Backup

Bridge ID	Fill Depth	Critical Element (Before)	Location (Before)	Critical Element (After)	Location (After)	Shear Inv Rating Factor HL93 (Before)	Shear Op Rating Factor HL93 (After)	Ratio (before/after)
Model 3- Candidate 1-Rev	1.9	Top Slab 1	1.4337	Top Slab 1	1.4337	3.1686	3.4535	0.9175
Model 3- Candidate 1-Rev	2	Top Slab 1	1.4337	Top Slab 1	1.4337	3.2834	3.2834	1.0000
Model 3- Candidate 1-Rev	2.5	Top Slab 1	1.4337	Top Slab 1	1.4337	3.9636	3.9636	1.0000
Model 3- Candidate 1-Rev	3	Bottom Slab 1	1.2608	Bottom Slab 1	1.2608	4.5826	4.5826	1.0000
Model 3- Candidate 1-Rev	3.5	Bottom Slab 1	1.2608	Bottom Slab 1	1.2608	4.9611	4.9611	1.0000
Model 3- Candidate 1-Rev	4	Bottom Slab 1	1.2608	Bottom Slab 1	1.2608	5.2644	5.2644	1.0000
Model 3- Candidate 1-Rev	10	Bottom Slab 1	1.2608	Bottom Slab 1	1.2608	8.9506	8.9506	1.0000
Model 3- Candidate 1-Rev	7	Bottom Slab 1	1.2608	Bottom Slab 1	1.2608	6.9788	6.9788	1.0000

Appendix G – Specification Backup

Full Table of BrDR runs for LL Surcharge vs Approaching Wheel Load changes.

The following table represents the AASHTOWare BrDR analysis runs for a select set of the Caltrans culverts and project culverts for the change in the LL Surcharge vs. Approaching Wheel Load.

Culvert	Cover	Inv Rating HL93 (Before)	Oper Rating Factor HL93 (After)	Inv Rating HL93 (After)	Oper Rating Factor HL93 (After)	Inventory Ratio	Operating Ratio
LS-CD8x8;10 1924-Rev	1.0 ft Cover	0.41	0.531	0.41	0.531	1	1
LS-CD8x8;10 1924-Rev	1.9 ft Cover	0.579	0.751	0.579	0.751	1	1
LS-CD8x8;10 1924-Rev	2 ft Cover	0.596	0.773	0.596	0.773	1	1
LS-CD8x8;10 1924-Rev	3 ft Cover	1.27	1.646	1.27	1.646	1	1
LS-CD8x8;10 1924-Rev	5 ft Cover	0.919	1.191	1.453	1.883	0.632485	0.632501
LS-CD8x8;10 1933-Rev	1.0 ft Cover	0.466	0.605	0.466	0.605	1	1
LS-CD8x8;10 1933-Rev	1.9 ft Cover	0.657	0.851	0.657	0.851	1	1
LS-CD8x8;10 1933-Rev	2 ft Cover	0.676	0.876	0.676	0.876	1	1
LS-CD8x8;10 1933-Rev	3 ft Cover	1.388	1.8	1.388	1.8	1	1
LS-CD8x8;10 1933-Rev	3.5 ft Cover	1.625	2.106	1.739	2.254	0.934445	0.934339
LS-CD8x8;10 1933-Rev	4 ft Cover	1.496	1.939	2.119	2.746	0.705993	0.706118
LS-CD10x8;16 1966-Rev	1.9 ft Cover	0.723	0.937	0.736	0.954	0.982337	0.98218
LS-CD10x8;16 1966-Rev	2 ft Cover	0.692	0.897	0.753	0.976	0.918991	0.919057
LS-CD10x8;16 1966-Rev	2.5 ft Cover	0.549	0.712	0.652	0.845	0.842025	0.842604
LS-CD10x8;16 1966-Rev	3 ft Cover	0.401	0.52	0.51	0.661	0.786275	0.786687
LS-CD10x8;16 1966-Rev	3.5 ft Cover	0.249	0.323	0.337	0.437	0.738872	0.73913
LS-CD10x8;16 1966-Rev	4 ft Cover	0.093	0.121	0.134	0.174	0.69403	0.695402
LS-CS10x8;5 1922-Rev	1.5 ft Cover	1.001	1.298	1.001	1.298	1	1
LS-CS10x8;5 1922-Rev	1.9 ft Cover	0.973	1.261	0.973	1.261	1	1
LS-CS10x8;5 1922-Rev	2 ft Cover	0.958	1.242	0.958	1.242	1	1
LS-CS10x8;5 1922-Rev	2.5 ft Cover	1.036	1.343	1.036	1.343	1	1
LS-CS10x8;5 1922-Rev	3 ft Cover	1.102	1.429	1.102	1.429	1	1
LS-CS10x8;5 1922-Rev	3.5 ft Cover	1.13	1.465	1.13	1.465	1	1
LS-CS10x8;5 1922-Rev	4 ft Cover	1.122	1.454	1.122	1.454	1	1
LS-CS10x8;5 1933-Rev	1.5 ft Cover	0.566	0.734	0.569	0.738	0.994728	0.99458
LS-CS10x8;5 1933-Rev	1.9 ft Cover	0.456	0.591	0.494	0.64	0.923077	0.923438
LS-CS10x8;5 1933-Rev	2 ft Cover	0.429	0.556	0.473	0.613	0.906977	0.907015
LS-CS10x8;5 1933-Rev	2.5 ft Cover	0.293	0.379	0.35	0.454	0.837143	0.834802
LS-CS10x8;5 1933-Rev	3 ft Cover	0.157	0.204	0.203	0.263	0.773399	0.775665
LS-CS10x8;5 1933-Rev	3.5 ft Cover	0.023	0.03	0.032	0.041	0.71875	0.731707
LS-CS10x8;10 1933-Rev	1.9 ft Cover	1.297	1.681	1.297	1.681	1	1
LS-CS10x8;10 1933-Rev	2 ft Cover	1.282	1.661	1.282	1.661	1	1
LS-CS10x8;10 1933-Rev	2.5 ft Cover	1.409	1.827	1.409	1.827	1	1
LS-CS10x8;10 1933-Rev	3 ft Cover	1.559	2.021	1.559	2.021	1	1
LS-CS10x8;10 1933-Rev	3.5 ft Cover	1.69	2.191	1.69	2.191	1	1

Appendix G – Specification Backup

Culvert	Cover	Inv Rating HL93 (Before)	Oper Rating Factor HL93 (After)	Inv Rating HL93 (After)	Oper Rating Factor HL93 (After)	Inventory Ratio	Operating Ratio
LS-CS10x8;10 1933-Rev	4 ft Cover	1.699	2.202	1.699	2.202	1	1
LS-CS10x8;10 1933-Rev	7 ft Cover	1.525	1.977	1.758	2.279	0.867463	0.867486
LS-CD12x8;9 1948-Rev	0.0 ft Cover	0.255	0.33	0.255	0.33	1	1
LS-CD12x8;9 1948-Rev	0.5 ft Cover	0.33	0.428	0.33	0.428	1	1
LS-CD12x8;9 1948-Rev	1.0 ft Cover	0.412	0.534	0.412	0.534	1	1
LS-CD12x8;9 1948-Rev	1.5 ft Cover	0.506	0.656	0.506	0.656	1	1
LS-CD12x8;9 1948-Rev	1.9 ft Cover	0.427	0.553	0.448	0.58	0.953125	0.953448
LS-CD12x8;9 1948-Rev	2 ft Cover	0.399	0.517	0.425	0.551	0.938824	0.938294
LS-CD12x8;9 1952-Rev	1.5 ft Cover	0.591	0.766	0.61	0.791	0.968852	0.968394
LS-CD12x8;9 1952-Rev	1.9 ft Cover	0.481	0.624	0.528	0.685	0.910985	0.910949
LS-CD12x8;9 1952-Rev	2 ft Cover	0.453	0.588	0.505	0.655	0.89703	0.89771
LS-CD12x8;9 1952-Rev	3 ft Cover	0.182	0.236	0.233	0.302	0.781116	0.781457
LS-CD12x8;9 1952-Rev	3.5 ft Cover	0.04	0.052	0.054	0.071	0.740741	0.732394
LS-CD12x12;20 2010-Rev	1.9 ft Cover	2.352	3.048	2.369	3.071	0.992824	0.992511
LS-CD12x12;20 2010-Rev	2 ft Cover	2.36	3.059	2.378	3.083	0.992431	0.992215
LS-CD12x12;20 2010-Rev	2.5 ft Cover	2.36	3.059	2.378	3.083	0.992431	0.992215
LS-CD12x12;20 2010-Rev	3 ft Cover	3.232	4.19	3.282	4.254	0.984765	0.984955
LS-CD12x12;20 2010-Rev	3.5 ft Cover	3.651	4.733	3.722	4.825	0.980924	0.980933
LS-CD12x12;20 2010-Rev	4 ft Cover	4.064	5.268	4.161	5.393	0.976688	0.976822
LS-CD12x12;20 2010-Rev	5 ft Cover	4.999	6.48	5.168	6.699	0.967299	0.967309
LS-CS12x8;5 1922-Rev	1.5 ft Cover	1.018	1.32	1.018	1.32	1	1
LS-CS12x8;5 1922-Rev	1.9 ft Cover	0.991	1.285	0.991	1.285	1	1
LS-CS12x8;5 1922-Rev	2 ft Cover	0.977	1.266	0.977	1.266	1	1
LS-CS12x8;5 1922-Rev	3 ft Cover	1.134	1.471	1.134	1.471	1	1
LS-CS12x8;5 1922-Rev	4 ft Cover	1.119	1.45	1.119	1.45	1	1
LS-CS12x8;5 1922-Rev	5 ft Cover	1.022	1.325	1.022	1.325	1	1
LS-CS12x8;10 1952-Rev	1.5 ft Cover	1.112	1.441	1.112	1.441	1	1
LS-CS12x8;10 1952-Rev	1.9 ft Cover	1.087	1.409	1.087	1.409	1	1
LS-CS12x8;10 1952-Rev	2 ft Cover	1.072	1.39	1.072	1.39	1	1
LS-CS12x8;10 1952-Rev	3 ft Cover	1.259	1.632	1.259	1.632	1	1
LS-CS12x8;10 1952-Rev	4 ft Cover	1.387	1.798	1.387	1.798	1	1
LS-CS12x8;10 1952-Rev	7 ft Cover	1.442	1.869	1.442	1.869	1	1
LS-CS12x8;10 1952-Rev	10 ft Cover	0.608	0.788	0.608	0.788	1	1
LS-CS12x8;10 2010-Rev	1.5 ft Cover	1.56	2.022	1.556	2.017	1.002571	1.002479
LS-CS12x8;10 2010-Rev	1.9 ft Cover	1.588	2.059	1.585	2.055	1.001893	1.001946
LS-CS12x8;10 2010-Rev	2 ft Cover	1.588	2.059	1.588	2.059	1	1
LS-CS12x8;10 2010-Rev	2.5 ft Cover	1.748	2.265	1.748	2.265	1	1
LS-CS12x8;10 2010-Rev	3 ft Cover	1.932	2.504	1.932	2.504	1	1

Appendix G – Specification Backup

Culvert	Cover	Inv Rating HL93 (Before)	Oper Rating Factor HL93 (After)	Inv Rating HL93 (After)	Oper Rating Factor HL93 (After)	Inventory Ratio	Operating Ratio
LS-CS12x8;10 2010-Rev	3.5 ft Cover	2.088	2.707	2.088	2.707	1	1
LS-CS12x8;10 2010-Rev	4 ft Cover	2.219	2.876	2.219	2.876	1	1
LS-CS12x12;10 2002-Rev	1.5 ft Cover	1.191	1.544	1.192	1.545	0.999161	0.999353
LS-CS12x12;10 2002-Rev	1.9 ft Cover	1.17	1.516	1.183	1.533	0.989011	0.988911
LS-CS12x12;10 2002-Rev	2 ft Cover	1.238	1.605	1.249	1.619	0.991193	0.991353
LS-CS12x12;10 2002-Rev	2.5 ft Cover	1.334	1.73	1.349	1.749	0.988881	0.989137
LS-CS12x12;10 2002-Rev	3 ft Cover	1.49	1.932	1.505	1.951	0.990033	0.990261
LS-CS12x12;10 2002-Rev	3.5 ft Cover	1.563	2.026	1.571	2.037	0.994908	0.9946
LS-CS12x12;10 2002-Rev	4 ft Cover	1.613	2.091	1.613	2.091	1	1
LS-CS14x14;10 2002-Rev	1.5 ft Cover	1.261	1.634	1.281	1.66	0.984387	0.984337
LS-CS14x14;10 2002-Rev	1.9 ft Cover	1.227	1.591	1.249	1.619	0.982386	0.982705
LS-CS14x14;10 2002-Rev	2 ft Cover	1.381	1.79	1.381	1.79	1	1
LS-CS14x14;10 2002-Rev	2.5 ft Cover	1.5	1.944	1.504	1.95	0.99734	0.996923
LS-CS14x14;10 2002-Rev	3 ft Cover	1.636	2.121	1.636	2.121	1	1
LS-CS14x14;10 2002-Rev	3.5 ft Cover	1.693	2.194	1.693	2.194	1	1
LS-CS14x14;10 2002-Rev	4 ft Cover	1.736	2.251	1.736	2.251	1	1
LS-CD14x13;10 2002-Rev	1.5 ft Cover	1.28	1.659	1.28	1.659	1	1
LS-CD14x13;10 2002-Rev	1.9 ft Cover	1.265	1.64	1.265	1.64	1	1
LS-CD14x13;10 2002-Rev	2 ft Cover	1.255	1.627	1.255	1.627	1	1
LS-CD14x13;10 2002-Rev	2.5 ft Cover	1.381	1.79	1.381	1.79	1	1
LS-CD14x13;10 2002-Rev	3 ft Cover	1.525	1.976	1.525	1.976	1	1
LS-CD14x13;10 2002-Rev	3.5 ft Cover	1.581	2.049	1.581	2.049	1	1
LS-CD14x13;10 2002-Rev	4 ft Cover	1.606	2.082	1.606	2.082	1	1
LS-CS16x12;0 1922 EAE-Rev	1.5 ft cover	0.596	0.773	0.596	0.773	1	1
LS-CS16x12;0 1922 EAE-Rev	1.9 ft cover	0.541	0.701	0.541	0.701	1	1
LS-CS16x12;0 1922 EAE-Rev	2 ft cover	0.523	0.678	0.523	0.678	1	1
LS-CS16x12;0 1922 EAE-Rev	2.5 ft cover	0.54	0.7	0.54	0.7	1	1
LS-CS16x12;0 1922 EAE-Rev	3 ft cover	0.522	0.677	0.522	0.677	1	1
LS-CS16x12;0 1922 EAE-Rev	3.5 ft cover	0.432	0.56	0.432	0.56	1	1
LS-CS16x12;0 1922 EAE-Rev	4 ft cover	0.325	0.421	0.325	0.421	1	1
LS-CS16x8;5 1922 EAE-Rev	1.5 ft cover	0.112	0.145	0.112	0.145	1	1
LS-CS16x8;5 1922 EAE-Rev	1.9 ft cover	0.057	0.073	0.057	0.073	1	1
LS-CS16x8;5 1922 EAE-Rev	2 ft cover	0.042	0.054	0.042	0.054	1	1
LS-Model 1- Candidate 1-R	1.5 ft Cover	1.458	1.891	1.454	1.885	1.002751	1.003183
LS-Model 1- Candidate 1-R	1.99 ft Cover	1.386	1.796	1.383	1.793	1.002169	1.001673
LS-Model 1- Candidate 1-R	2.0 ft Cover	1.47	1.905	1.47	1.905	1	1
LS-Model 1- Candidate 1-R	2.1 ft Cover	1.486	1.927	1.486	1.927	1	1
LS-Model 1- Candidate 1-R	2.2 ft Cover	1.502	1.947	1.502	1.947	1	1

Appendix G – Specification Backup

Culvert	Cover	Inv Rating HL93 (Before)	Oper Rating Factor HL93 (After)	Inv Rating HL93 (After)	Oper Rating Factor HL93 (After)	Inventory Ratio	Operating Ratio
LS-Model 1- Candidate 1-R	2.4 ft Cover	1.531	1.984	1.531	1.984	1	1
LS-Model 1- Candidate 1-R	2.5 ft Cover	1.538	1.994	1.538	1.994	1	1
LS-Model 1- Candidate 1-R	3.0 ft Cover	1.509	1.956	1.509	1.956	1	1
LS-Model 1- Candidate 1-R	5.0 ft Cover	1.147	1.487	1.147	1.487	1	1
LS-Model 1- Candidate 1-R	7.0 ft Cover	0.395	0.512	0.395	0.512	1	1
LS-Model 2- Candidate 1-R	1.5 ft cover	1.475	1.912	1.471	1.907	1.002719	1.002622
LS-Model 2- Candidate 1-R	1.9 ft cover	1.535	1.989	1.535	1.989	1	1
LS-Model 2- Candidate 1-R	2.0 ft cover	1.524	1.976	1.524	1.976	1	1
LS-Model 2- Candidate 1-R	2.5 ft cover	1.712	2.22	1.712	2.22	1	1
LS-Model 2- Candidate 1-R	3.0 ft cover	1.92	2.489	1.92	2.489	1	1
LS-Model 2- Candidate 1-R	3.5 ft cover	2.148	2.784	2.148	2.784	1	1
LS-Model 2- Candidate 1-R	4.0 ft cover	2.335	3.027	2.335	3.027	1	1
LS-Model 2- Candidate 1-R	7.0 ft cover	3.462	4.488	3.462	4.488	1	1
LS-Model 2- Candidate 1-R	10.0 ft cover	2.738	3.55	2.738	3.55	1	1
LS-Model 3- Candidate 1-R	1.5 ft cover	1.452	1.882	1.452	1.882	1	1
LS-Model 3- Candidate 1-R	1.9 ft cover	1.452	1.882	1.452	1.882	1	1
LS-Model 3- Candidate 1-R	2.0 ft cover	1.414	1.833	1.414	1.833	1	1
LS-Model 3- Candidate 1-R	2.5 ft cover	1.547	2.006	1.547	2.006	1	1
LS-Model 3- Candidate 1-R	3.0 ft cover	1.7	2.204	1.7	2.204	1	1
LS-Model 3- Candidate 1-R	3.5 ft cover	1.811	2.347	1.811	2.347	1	1
LS-Model 3- Candidate 1-R	4.0 ft cover	1.823	2.363	1.823	2.363	1	1
LS-Model 3- Candidate 1-R	7.0 ft cover	1.627	2.11	1.627	2.11	1	1
LS-Model 3- Candidate 1-R	10.0 ft cover	0.841	1.09	0.841	1.09	1	1
LS-TJM-10x10	1.5 ft Cover	0.639	0.828	0.639	0.828	1	1
LS-TJM-10x10	2.0 ft Cover	0.597	0.774	0.597	0.774	1	1
LS-CD8x8;5 1924-Rev	1.0 ft Cover	0.359	0.465	0.359	0.465	1	1
LS-CD8x8;5 1924-Rev	1.5 ft Cover	0.441	0.572	0.441	0.572	1	1
LS-CD8x8;5 1924-Rev	1.9 ft Cover	0.516	0.669	0.516	0.669	1	1
LS-CD8x8;5 1924-Rev	2 ft Cover	0.532	0.69	0.532	0.69	1	1
LS-CD8x8;5 1924-Rev	3 ft Cover	1.085	1.406	1.085	1.406	1	1
LS-CD8x8;5 1924-Rev	4 ft Cover	1.245	1.613	1.245	1.613	1	1
LS-CD10x8;9 1948-Rev	1.5 ft Cover	0.331	0.43	0.323	0.419	1.024768	1.026253
LS-CD10x8;9 1948-Rev	1.9 ft Cover	0.215	0.279	0.224	0.291	0.959821	0.958763
LS-CD10x8;9 1948-Rev	2 ft Cover	0.186	0.241	0.197	0.255	0.944162	0.945098
LS-CD10x8;10 2002-Rev	1.5 ft Cover	1.077	1.396	1.072	1.39	1.004664	1.004317
LS-CD10x8;10 2002-Rev	1.9 ft Cover	1.116	1.447	1.116	1.447	1	1
LS-CD10x8;10 2002-Rev	2 ft Cover	1.118	1.45	1.118	1.45	1	1
LS-CD10x8;10 2002-Rev	4 ft Cover	1.76	2.282	1.76	2.282	1	1

Appendix G – Specification Backup

Culvert	Cover	Inv Rating HL93 (Before)	Oper Rating Factor HL93 (After)	Inv Rating HL93 (After)	Oper Rating Factor HL93 (After)	Inventory Ratio	Operating Ratio
LS-CD10x8;10 2002-Rev	7 ft Cover	1.609	2.086	1.609	2.086	1	1
LS-CD10x8;10 2010-Rev	1.5 ft Cover	1.466	1.9	1.466	1.9	1	1
LS-CD10x8;10 2010-Rev	1.9 ft Cover	1.506	1.953	1.506	1.953	1	1
LS-CD10x8;10 2010-Rev	2 ft Cover	1.558	2.019	1.558	2.019	1	1
LS-CD10x8;10 2010-Rev	4 ft Cover	2.512	3.256	2.512	3.256	1	1
LS-CD10x8;10 2010-Rev	7 ft Cover	3.01	3.902	3.01	3.902	1	1
LS-CD14x9;10 2002-Rev	1.5 ft Cover	1.283	1.663	1.283	1.663	1	1
LS-CD14x9;10 2002-Rev	1.9 ft Cover	1.248	1.618	1.248	1.618	1	1
LS-CD14x9;10 2002-Rev	2 ft Cover	1.259	1.632	1.259	1.632	1	1
LS-CD14x9;10 2002-Rev	4 ft Cover	1.531	1.985	1.531	1.985	1	1
LS-CD14x9;10 2002-Rev	7 ft Cover	1.36	1.763	1.36	1.763	1	1
LS-CD14x9;10 2010-Rev	1.5 ft Cover	1.656	2.147	1.656	2.147	1	1
LS-CD14x9;10 2010-Rev	1.9 ft Cover	1.629	2.112	1.629	2.112	1	1
LS-CD14x9;10 2010-Rev	2 ft Cover	1.735	2.249	1.735	2.249	1	1
LS-CD14x9;10 2010-Rev	4 ft Cover	2.155	2.793	2.155	2.793	1	1
LS-CD14x9;10 2010-Rev	7 ft Cover	2.318	3.005	2.318	3.005	1	1
LS-CS7x7;10 2010-Rev	1.5 ft Cover	1.528	1.981	1.529	1.982	0.999346	0.999495
LS-CS7x7;10 2010-Rev	1.9 ft Cover	1.536	1.992	1.536	1.992	1	1
LS-CS7x7;10 2010-Rev	2 ft Cover	1.521	1.972	1.521	1.972	1	1
LS-CS7x7;10 2010-Rev	4 ft Cover	2.533	3.284	2.533	3.284	1	1
LS-CS7x7;10 2010-Rev	7 ft Cover	3.835	4.972	3.835	4.972	1	1
LS-CS8x8;10 2010-Rev	1.5 ft Cover	1.345	1.744	1.345	1.744	1	1
LS-CS8x8;10 2010-Rev	1.9 ft Cover	1.325	1.717	1.325	1.717	1	1
LS-CS8x8;10 2010-Rev	2 ft Cover	1.309	1.697	1.309	1.697	1	1
LS-CS8x8;10 2010-Rev	4 ft Cover	1.821	2.36	1.821	2.36	1	1
LS-CS8x8;10 2010-Rev	7 ft Cover	2.435	3.156	2.435	3.156	1	1
LS-CS10x8;5 1952-Rev	1.5 ft Cover	0.691	0.896	0.691	0.896	1	1
LS-CS10x8;5 1952-Rev	1.9 ft Cover	0.663	0.859	0.663	0.859	1	1
LS-CS10x8;5 1952-Rev	2 ft Cover	0.65	0.842	0.65	0.842	1	1
LS-CS10x8;5 1952-Rev	3 ft Cover	0.729	0.945	0.729	0.945	1	1
LS-CS10x8;5 1952-Rev	4 ft Cover	0.762	0.988	0.762	0.988	1	1
LS-CS10x8;5 1952-Rev	5 ft Cover	0.731	0.948	0.731	0.948	1	1
LS-CS10x8;6 1948-Rev	1.5 ft Cover	0.912	1.182	0.912	1.182	1	1
LS-CS10x8;6 1948-Rev	1.9 ft Cover	0.89	1.153	0.89	1.153	1	1
LS-CS10x8;6 1948-Rev	2 ft Cover	0.877	1.136	0.877	1.136	1	1
LS-CS10x8;6 1948-Rev	3 ft Cover	1.024	1.327	1.024	1.327	1	1
LS-CS10x8;6 1948-Rev	4 ft Cover	1.1	1.425	1.1	1.425	1	1
LS-CS10x8;6 1948-Rev	5 ft Cover	1.047	1.357	1.047	1.357	1	1

Appendix G – Specification Backup

Culvert	Cover	Inv Rating HL93 (Before)	Oper Rating Factor HL93 (After)	Inv Rating HL93 (After)	Oper Rating Factor HL93 (After)	Inventory Ratio	Operating Ratio
LS-CS10x8;8 1966-Rev	1.5 ft Cover	0.91	1.18	0.91	1.18	1	1
LS-CS10x8;8 1966-Rev	1.9 ft Cover	0.886	1.149	0.886	1.149	1	1
LS-CS10x8;8 1966-Rev	2 ft Cover	0.873	1.132	0.873	1.132	1	1
LS-CS10x8;8 1966-Rev	4 ft Cover	1.137	1.474	1.137	1.474	1	1
LS-CS10x8;8 1966-Rev	6 ft Cover	1.219	1.58	1.219	1.58	1	1
LS-CS10x8;10 1981-Rev	1.5 ft Cover	1.133	1.469	1.129	1.464	1.003543	1.003415
LS-CS10x8;10 1981-Rev	1.9 ft Cover	1.15	1.491	1.152	1.493	0.998264	0.99866
LS-CS10x8;10 1981-Rev	2 ft Cover	1.179	1.528	1.179	1.528	1	1
LS-CS10x8;10 1981-Rev	4 ft Cover	1.648	2.136	1.648	2.136	1	1
LS-CS10x8;10 1981-Rev	7 ft Cover	1.814	2.351	1.865	2.417	0.972654	0.972693
LS-CS10x8;10 2002-Rev	1.5 ft Cover	1.215	1.575	1.211	1.57	1.003303	1.003185
LS-CS10x8;10 2002-Rev	1.9 ft Cover	1.242	1.61	1.244	1.612	0.998392	0.998759
LS-CS10x8;10 2002-Rev	2 ft Cover	1.246	1.615	1.246	1.615	1	1
LS-CS10x8;10 2002-Rev	4 ft Cover	1.761	2.283	1.761	2.283	1	1
LS-CS10x8;10 2002-Rev	7 ft Cover	2.106	2.729	2.156	2.795	0.976809	0.976386
LS-CS10x8;10 2010-Rev	1.5 ft Cover	1.51	1.957	1.505	1.951	1.003322	1.003075
LS-CS10x8;10 2010-Rev	1.9 ft Cover	1.558	2.02	1.555	2.016	1.001929	1.001984
LS-CS10x8;10 2010-Rev	2 ft Cover	1.655	2.146	1.655	2.146	1	1
LS-CS10x8;10 2010-Rev	4 ft Cover	2.442	3.166	2.442	3.166	1	1
LS-CS10x8;10 2010-Rev	7 ft Cover	3.611	4.681	3.611	4.681	1	1
LS-CS10x8;12 1952-Rev	1.9 ft Cover	1.1	1.426	1.1	1.426	1	1
LS-CS10x8;12 1952-Rev	2 ft Cover	1.086	1.407	1.086	1.407	1	1
LS-CS10x8;12 1952-Rev	4 ft Cover	1.489	1.931	1.489	1.931	1	1
LS-CS10x8;12 1952-Rev	7 ft Cover	1.806	2.341	1.806	2.341	1	1
LS-CS14x9;10 2002-Rev	1.5 ft Cover	1.106	1.434	1.103	1.429	1.00272	1.003499
LS-CS14x9;10 2002-Rev	1.9 ft Cover	1.084	1.406	1.083	1.403	1.000923	1.002138
LS-CS14x9;10 2002-Rev	2 ft Cover	1.188	1.539	1.19	1.542	0.998319	0.998054
LS-CS14x9;10 2002-Rev	4 ft Cover	1.355	1.756	1.366	1.771	0.991947	0.99153
LS-CS14x9;10 2002-Rev	7 ft Cover	1.28	1.659	1.294	1.677	0.989181	0.989267

Appendix H – Proposed AASHTO Ballot Items

Proposed ballot items for AASHTO LRFD Bridge Design Specifications

1. Depth of live load, Article 3.6.1.2a
2. Live load distribution, Articles 3.6.1.2a, Article 4.6.2.10.2
3. Lateral Pressure Coefficient, Article 3.11.5.1
4. Approaching wheel load, Article 3.11.6.4.1

Proposed ballot items for AASHTO Manual for Bridge Evaluation:

1. LRFD Culverts, New Article 6A.10
2. ASD/LFD Culverts, New Article 6B.10

Appendix H – Proposed Ballot Items

Ballot LRFD-1**2019 AASHTO BRIDGE COMMITTEE AGENDA ITEM:** [Click here to enter text](#)**SUBJECT:** Culverts – Depth of Fill and Consideration of Live Load**TECHNICAL COMMITTEE:** T-5 Loads and Load Distribution, T-13 Culverts, T-18 Bridge Management Evaluation and Rehabilitation

<input checked="" type="checkbox"/> REVISION	<input type="checkbox"/> ADDITION	<input type="checkbox"/> NEW DOCUMENT
<input checked="" type="checkbox"/> DESIGN SPEC	<input type="checkbox"/> CONSTRUCTION SPEC	<input type="checkbox"/> MOVABLE SPEC
<input type="checkbox"/> MANUAL FOR BRIDGE EVALUATION	<input type="checkbox"/> SEISMIC GUIDE SPEC	<input type="checkbox"/> MANUAL BRIDGE ELEMENT INSP
	<input type="checkbox"/> OTHER Research	

DATE PREPARED: 7/3/2019**DATE REVISED:** [Click here to enter a date](#)**AGENDA ITEM:**

Revise the first paragraph of Article 3.6.1.2.6a-General in the Design Specifications as follows:

The effects of live load may be neglected when the factored live load pressure at the surface of the culvert is less than 10% of the sum of the factored earth load plus factored live load pressure.

OTHER AFFECTED ARTICLES:

None

BACKGROUND:

Currently the AASHTO LRFD Specifications state:

“For single span culverts the effects of live load may be neglected where the depth of fill is more than 8.0 ft and exceeds the span length; for multiple span culverts the effects may be neglected where the depth of fill exceeds the distance between inside faces of end walls.”

This provision requires consideration of live load until the depth exceeds the span; however, in the experience of some members of the research team the provision is often interpreted as ignoring live loads at depths of 8 ft and greater. At a depth of 8 ft, the live load is 36% of the total load and if dropped from design consideration, the net load factor (factored earth load/(service earth plus live load, in psf) is only 1.03. This low factor of safety likely occurred in part because the provision was developed under the Standard Specifications which used LLDF = 1.75. The proposed provision changes the depth of fill for dropping live load consideration to about 13 ft for the design tandem. At this depth the net load factor when not considering live load is 1.20 and is insensitive to overloaded live load vehicles.

Appendix H – Proposed Ballot Items

Also, the proposed revision provides a clear method for engineers to consider the depths at which permit vehicles and other non-standard loadings need not be considered in design or rating.

REFERENCES:

NCHRP Project 15-54, “Proposed Modifications to AASHTO Culvert Load Rating Specifications”.

Appendix H – Proposed Ballot Items

Ballot LRFD-2**2019 AASHTO BRIDGE COMMITTEE AGENDA ITEM:** [Click here to enter text](#)**SUBJECT:** Live Load Distribution for Culverts**TECHNICAL COMMITTEE:** T-5 Loads and Load Distribution, T-13 Culverts, T-18 Bridge Management and Evaluation

<input checked="" type="checkbox"/> REVISION	<input type="checkbox"/> ADDITION	<input type="checkbox"/> NEW DOCUMENT
<input checked="" type="checkbox"/> DESIGN SPEC	<input type="checkbox"/> CONSTRUCTION SPEC	<input type="checkbox"/> MOVABLE SPEC
<input type="checkbox"/> MANUAL FOR BRIDGE EVALUATION	<input type="checkbox"/> SEISMIC GUIDE SPEC	<input type="checkbox"/> MANUAL BRIDGE ELEMENT INSP
	<input type="checkbox"/> OTHER Research	

DATE PREPARED: 7/3/2019**DATE REVISED:** [Click here to enter a date](#)**AGENDA ITEM:****Item #1****Article 3.6.1.2.6a****Revise 2nd paragraph**

Live load shall be distributed to the top slabs of flat top three- or four-sided concrete culverts, three-sided arch top concrete culverts or concrete arch culverts over the area calculated in this Article, but not less than the dimensions calculated using the procedure specified in Article 4.6.2.10. Live load shall be distributed to concrete pipe culverts with 1.0 ft or more but less than 2.0 ft of cover in accordance with Article 4.6.2.10. Culverts other than concrete with 1.0 ft or more but less than 2.0 ft of cover shall be designed for a depth of 1.0 ft. Culverts with curved tops and less than 1.0 ft of cover shall be analyzed with more comprehensive methods.

Delete 5th Paragraph**Item #2****Revise Article 4.6.2.10.2****Modify 2nd paragraph and Equations**

Wheel loads shall be distributed to the top slab for determining moment, thrust, and shear as follows:

Perpendicular to the span:

$$E = 28 + t_{d1} + 1.44 S \quad (4.6.2.10.2-1)$$

Parallel to the span:

$$E_{span} = t_{d2} + LLDF(H) \quad (4.6.2.10.2-2)$$

Appendix H – Proposed Ballot Items

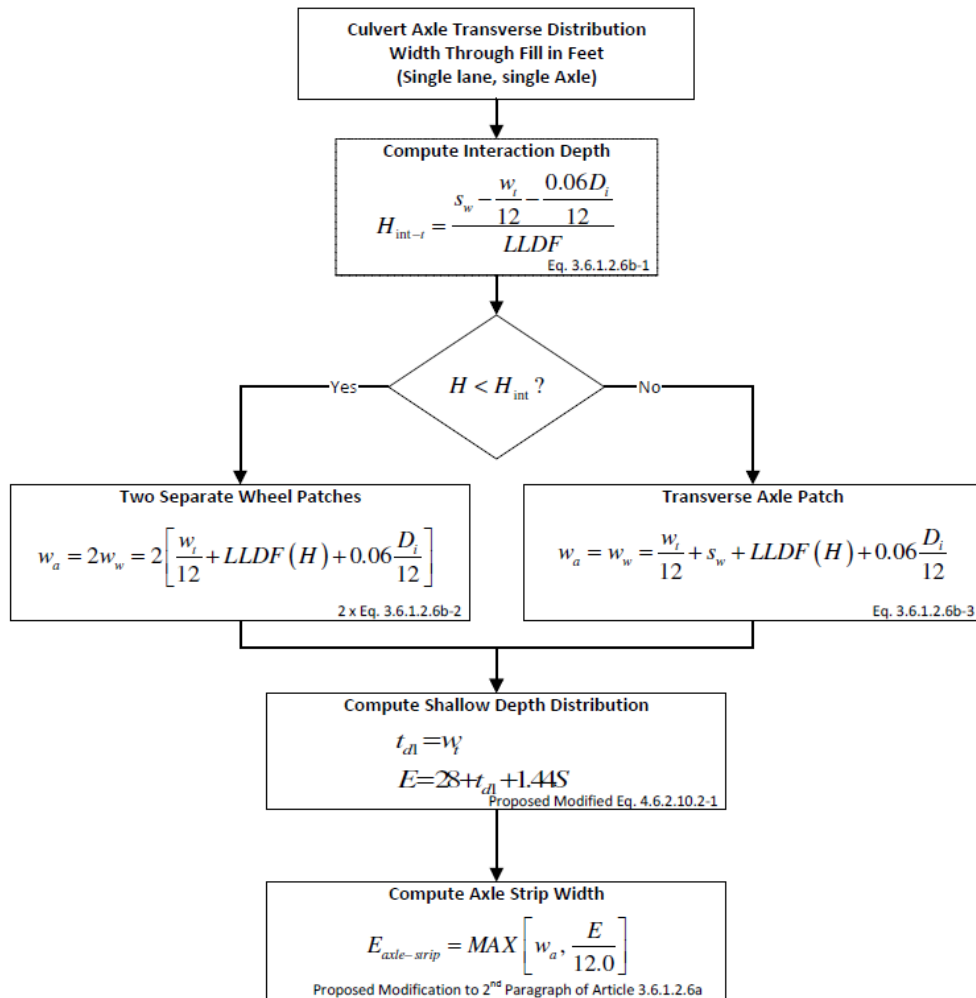
Add to notation

t_{d1} = tire dimension (l_t or w_t , see 3.6.1.2.6) perpendicular to the span

t_{d2} = tire dimension (l_t or w_t , see 3.6.1.2.6) parallel to the span

Revise Article C4.6.2.10.2**Add new paragraph**

Strip widths for culverts are expressed in terms of wheel loads. Culvert spans are typically small and design forces are controlled by single wheel effects. A flowchart illustrating the determination of the transverse distribution (strip width) for a single-axle load through fill is shown in Figure C4.6.2.10.2-1.



Note: This determines the culvert strip width for a single lane, single axle loading in the direction perpendicular to the flow of traffic. The effects of multiple presence, dynamic load allowance and distribution in the direction parallel to the flow of traffic must also be considered as well as the effects of multiple adjacent axles. Equation 4.6.2.10.2-3 can be used to evaluate groups of axles.

Figure C4.6.2.10.2-1 - Single-Axle Transverse Distribution Through Fill

 Appendix H – Proposed Ballot Items

Item #3**Revise Article 4.6.2.10.3**

Traffic traveling perpendicular to the span shall consider multiple lane loadings with the appropriate multiple presence factor. When traffic travels perpendicular to the span, wheel loads shall be distributed to the top slab as specified here:

Perpendicular to the span:

$$E = ((Ax - 1) * 48 + Ax_{sp} + t_{dl} + 1.44 S) / Ax \quad (4.6.2.10.2-3)$$

Parallel to the span:

$$E_{span} = t_{d2} + LLDF(H) \quad (4.6.2.10.2-4)$$

where:

Ax = No. of axles in axle group
 Ax_{sp} = Spacing of axles in axle group

Revise Article C4.6.2.10.3

Add new paragraph:

When vehicles travel perpendicular to the span, the wheel loads from adjacent axles (e.g. typical tandem and tridem axle configurations) interact. The equations in this section address this.

OTHER AFFECTED ARTICLES:

BACKGROUND:

This revision is based on recommendations made in the research report for NCHRP Project 15-54, “Proposed Modifications to AASHTO Culvert Load Rating Specifications”

The current specifications for live load distribution through earth fill are discontinuous at a depth of 2 feet of fill due to the change from a slab bridge distribution procedure (Article 4.6.2.10) to a distribution through earth fill procedure (Article 3.6.1.2.6). The attached material investigates this discontinuity in live load distribution and provides a rational alternative to eliminate it.

Further, the load distribution for traffic at depths less than 2.0 ft so that distributions in Articles 3.6.2.6 and 4.6.2.10 are both expressed in terms of wheel loads. The new equations in 4.6.2.10.3 provide the expressions necessary to address the interaction of adjacent axles for multi-axle configurations such as tandems and tridems.

The NCHRP 15-54 report provides the rationale for this proposed change in further detail.

ANTICIPATED EFFECT ON BRIDGES:

Appendix H – Proposed Ballot Items

This change will increase the distribution width for some culverts in some cases and in those cases will increase the load ratings due to the resulting increase in the capacity of the structure.

REFERENCES:

Project 15-54, “Proposed Modifications to AASHTO Culvert Load Rating Specifications”

OTHER:

Appendix H – Proposed Ballot Items

Ballot LRFD-3**2019 AASHTO BRIDGE COMMITTEE AGENDA ITEM:** [Click here to enter text](#)**SUBJECT:** Use of At-Rest Pressure Coefficient for Reinforced Concrete Box Culverts**TECHNICAL COMMITTEE:** T-5 Loads and Load Distribution, T-18 Bridge Management Evaluation and Rehabilitation, T-13 Culverts REVISION ADDITION NEW DOCUMENT DESIGN SPEC CONSTRUCTION SPEC MOVABLE SPEC MANUAL FOR BRIDGE
EVALUATION SEISMIC GUIDE SPEC MANUAL BRIDGE ELEMENT INSP OTHER Research**DATE PREPARED:** 7/3/2019**DATE REVISED:** [Click here to enter a date](#)**AGENDA ITEM:**

Addition to Article 3.11.5.1

3.11.5.1-Lateral Earth Pressure: *EH*

Add to existing Article:

For the design of rectangular reinforced concrete culverts, the lateral pressure coefficient, k_o , need not be taken greater than 0.5 for culverts embedded in granular soils.

Add to existing commentary:

C3.11.5.1

The lateral pressure on culverts is the same on both sides of the structure and produces small culvert forces relative to the forces due to vertical loads. The value of $k_o = 0.5$ has long been used and produces safe designs.

OTHER AFFECTED ARTICLES:

None

BACKGROUND:

This revision is based on recommendations made in the research report for NCHRP Project 15-54, “Proposed Modifications to AASHTO Culvert Load Rating Specifications”.

Appendix H – Proposed Ballot Items

The proposed addition is intended to achieve consistency between the design and rating specifications. The existing provision for lateral earth pressure in the LRFD Bridge Design Specifications results in a higher pressure than what is specified in the Manual for Bridge Evaluation. The proposed revision is also based on successful past practice for the design of reinforced concrete box culverts that are performing well in the field.

ANTICIPATED EFFECT ON BRIDGES:

The proposed provision will reduce the lateral earth pressure for some culverts to a level consistent with what many of them were designed for. Without such a change culverts designed for this level of earth pressure but rated for the higher at-rest earth pressure may have been deficient.

REFERENCES:

NCHRP Project 15-54, “Proposed Modifications to AASHTO Culvert Load Rating Specifications”.

OTHER:

Appendix H – Proposed Ballot Items

Ballot LRFD-4**2019 AASHTO BRIDGE COMMITTEE AGENDA ITEM:** [Click here to enter text](#)**SUBJECT:** Use of At-Rest Pressure Coefficient for Reinforced Concrete Box Culverts**TECHNICAL COMMITTEE:** T-5 Loads and Load Distribution, T-13 Culverts, T-18 Bridge Management, Evaluation and Rehabilitation

<input type="checkbox"/> REVISION	<input checked="" type="checkbox"/> ADDITION	<input type="checkbox"/> NEW DOCUMENT
<input checked="" type="checkbox"/> DESIGN SPEC	<input type="checkbox"/> CONSTRUCTION SPEC	<input type="checkbox"/> MOVABLE SPEC
<input type="checkbox"/> MANUAL FOR BRIDGE EVALUATION	<input type="checkbox"/> SEISMIC GUIDE SPEC	<input type="checkbox"/> MANUAL BRIDGE ELEMENT INSP
	<input type="checkbox"/> OTHER Research	

DATE PREPARED: 7/3/2019**DATE REVISED:** [Click here to enter a date](#)**AGENDA ITEM:**

Add new title to Article 3.11.6.4.1

Article 3.11.6.4.1 Walls

(section otherwise unchanged)

Add new article:

Article 3.11.6.4.2 Culverts

Concrete box culverts and three-sided flat-topped culverts with a depth of fill less than 2 ft shall be subjected to an approaching wheel load in the form of a lateral soil pressure representing a vehicle approaching the culvert. The pressure shall decrease with increasing depth of fill in accordance with Eq. 3.11.6.4.2-1:

$$\Delta_p(h_d) = 700/h_d \leq 800 \text{ psf} \qquad \text{Eq. 3.11.6.4.2-1}$$

Where

$$\begin{aligned} \Delta_p(h_d) &= \text{lateral soil pressure at depth } h_d, \text{ psf} \\ h_d &= \text{depth of fill at which pressure is calculated, ft} \end{aligned}$$

The calculated pressure shall be applied to both sides of the culvert model.

This load need not be applied to culverts with a depth of fill over the top slab greater than 2 ft nor to concrete culverts with round tops or metal, thermoplastic or fiberglass culverts.

Add new commentary:

Article C3.11.6.4.1

Appendix H – Proposed Ballot Items

Retaining walls have historically been designed considering a lateral live load surcharge pressure to represent the additional load applied by a vehicle located near the wall. This loading was historically applied to culverts as well. However, while a lateral load on a wall increases the overturning moment, such a load on a culvert is transmitted through the culvert, largely through compressive thrust and minimal bending moments. The approaching wheel load replaces the live load surcharge for culverts.

OTHER AFFECTED ARTICLES:

None

BACKGROUND:

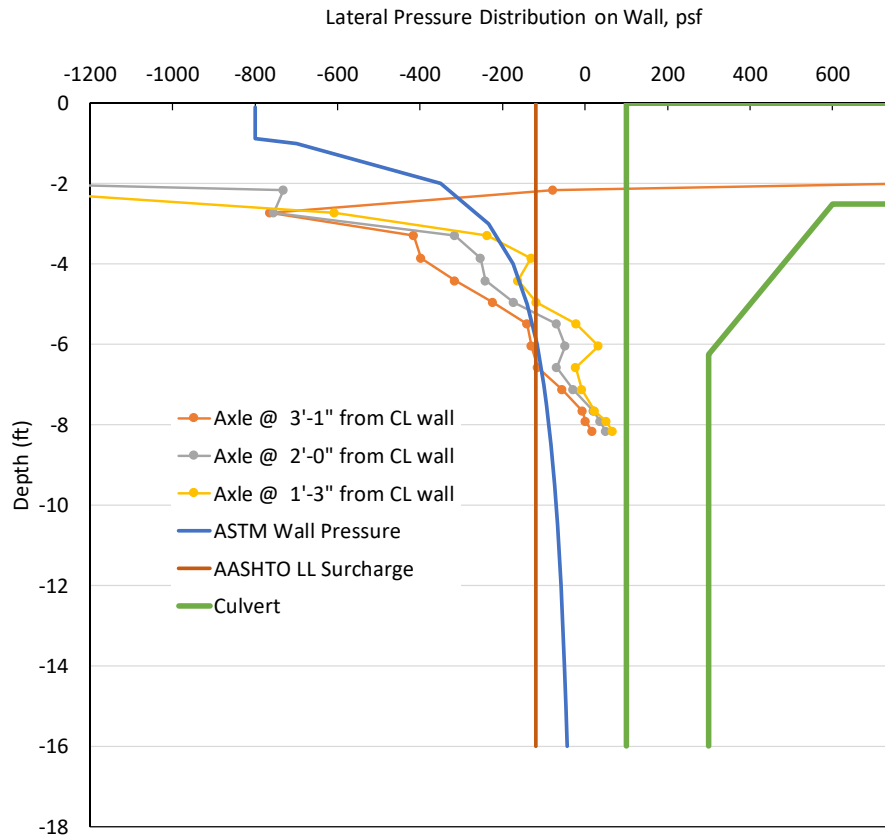
This revision is based on recommendations made in the research report for NCHRP Project 15-54, “Proposed Modifications to AASHTO Culvert Load Rating Specifications”. ASTM standards for precast reinforced concrete box sections (ASTM C1577) with depths of fill less than two feet have been designed for the proposed lateral pressure resulting from an approaching vehicle since the standards were first developed and the loading is also used in AASHTO Standard M273.

The figure below includes results from FEM models of culverts analyzed during NCHRP Project 15-54 which show high pressure near the surface that reduce quickly with increasing depth of fill. The design pressure used for precast box sections (ASTM C1577, identical to AASHTO M273) show a similar trend, while the LRFD live load surcharge pressure is constant with depth based on the assumption of an additional depth of fill. While the FEM pressures exceed both the ASTM and LRFD pressures at the surface, this is not a design issue for several reasons.

- The pressure, shown in the figure are the peak pressures and decrease away from the wheel location.
- The load is primarily transmitted as a thrust through the top slab, reacting with the soil on the far side of the culvert. The moments resulting from this pressure are small.
- The research team is unaware of any structural issues in a box culvert due to lateral load from vehicles.

As the load pressure decreases rapidly with increasing depth of fill, it is proposed to require the ASTM approaching wheel load for culverts with depths of fill less than 2 ft and no lateral surcharge for deeper culverts.

Appendix H – Proposed Ballot Items

**ANTICIPATED EFFECT ON BRIDGES:**

The current LRFD specifications do not explicitly exclude the use of LS for culverts under large fill depths so there is inconsistency in the application of the current provisions while it is known that the effects of LS decrease quickly as the depth of fill increases. The proposed change provides for a more rationally based application of LS to the design and analysis of box culverts. While this amounts to a reduction or elimination of LS for culverts under fill, the effects of LS become negligible under such conditions.

REFERENCES:

NCHRP Project 15-54, "Proposed Modifications to AASHTO Culvert Load Rating Specifications".

ASTM C1577-19 Standard Specification for Precast Reinforced Concrete Monolithic Box Sections for Culverts, Storm Drains, and Sewers Designed According to AASHTO LRFD

AASHTO M 273, Standard Specification for Precast Reinforced Concrete Box Sections for Culverts, Storm Drains, and Sewers with Less Than 2 ft of Cover Subjected to Highway Loadings

OTHER:

Appendix H – Proposed Ballot Items

Ballot MBE-1**2019 AASHTO BRIDGE COMMITTEE AGENDA ITEM:** [Click here to enter text](#)**SUBJECT:** Rating and Condition Evaluation of Culverts**TECHNICAL COMMITTEE:** T-18 Bridge Management, Evaluation and Rehabilitation, T-13 Culverts

<input checked="" type="checkbox"/> REVISION	<input checked="" type="checkbox"/> ADDITION	<input type="checkbox"/> NEW DOCUMENT
<input type="checkbox"/> DESIGN SPEC	<input type="checkbox"/> CONSTRUCTION SPEC	<input type="checkbox"/> MOVABLE SPEC
<input checked="" type="checkbox"/> MANUAL FOR BRIDGE EVALUATION	<input type="checkbox"/> SEISMIC GUIDE SPEC <input type="checkbox"/> OTHER Research	<input type="checkbox"/> MANUAL BRIDGE ELEMENT INSP

DATE PREPARED: 7/3/2019**DATE REVISED:** [Click here to enter a date](#)**AGENDA ITEM:****Item #1****Delete Article 6A.5.12**

As noted, portions of this Article are incorporated into the proposed new Article 6A.10

Item #2**Add new Article 6A.10 Rating of Culverts****6A.10.1-Scope**

This Article incorporates provisions specific to the load rating culvert of types designed using the AASHTO LRFD methodology and it provides a load rating that is consistent with that approach. This Article assumes culverts have been inspected prior to rating and that the current condition of the culvert can be properly accounted for.

C6A.10.1

Good structural performance of culverts results from interaction of the culvert and the soil it is embedded in. Further, culverts are often designed by product specific methods developed by industry and adopted by AASHTO. This Article addresses the issues specific to culverts.

Metal and concrete culverts are often constructed in sizes where rating is mandatory. Thermoplastic, fiberglass, and many metal and concrete culverts are typically not rated; however, brief guidance is provided here for those organizations that rate all culvert types. Older culverts designed using ASD and LFD can also be load rated using these provisions. In cases where the resulting ratings show deficiencies, consideration may be given to rating the culvert using the specifications for which it was designed.

It is common practice for most of the culvert specific variables to be taken directly from the construction documents or standard plans. They include culvert dimensions, materials and material properties, and installation methods. The data from construction documents, including culvert dimensions, materials and

Appendix H – Proposed Ballot Items

material properties, and installation methods should be confirmed during a visual inspection of the culvert and any discrepancies from the construction documents should be addressed.

6A.10.2-General Rating Requirements

Culvert ratings should recognize that these structures experience several loadings that are not applicable to most bridge superstructures, including vertical and horizontal soil loads and approaching wheel load.

Culverts shall be evaluated for the Limit States required in design in Article 12 of the AASHTO LRFD Specifications as modified for specific structures herein. Load ratings shall be calculated at critical sections for each load effect to establish the controlling load rating.

6A.10.3-Structural Analysis of Culverts

The analysis of culverts may be based on any rational method acceptable to the owner and consistent with the methods used for design in the AASHTO LRFD Specifications.

C6A.10.3

Analysis procedures for culverts in the AASHTO LRFD Specifications vary widely depending on the culvert shape and material. Concrete box culverts and three-sided culverts are primarily analyzed and designed with computer programs such as simple frame or finite element models. Other shapes and materials are often analyzed through simple empirical procedures, often developed independently by manufacturer's trade associations, and adopted by AASHTO into the LRFD Design Specifications.

6A.10.3.1 Rectangular Concrete Culverts

Rectangular concrete culverts include box culverts and three-sided, flat-top culverts. Structural analysis for rectangular concrete culverts is most often completed with frame models subjected to uniform pressures, but finite element modeling is acceptable.

For box culverts analyzed with frame models, culvert-soil interaction can be mimicked in part by supporting the bottom slab with springs that simulate actual soil support and allowing the soil load to redistribute, much like a beam on elastic foundation. This redistribution of pressure typically reduces the moment and shear forces in the bottom slab as compared to traditional uniformly applied bedding pressure. Spring constants, in the form of moduli of subgrade reaction values, must be selected by a qualified geotechnical engineer based on available site information. General values are presented in Table 6A.10.3.1-1 for consideration. For conditions where a bedding layer is placed over undisturbed native soils, the design value should represent the combined stiffness of the two layers. The native soil layer may have more effect on the combined stiffness than the bedding soil.

Appendix H – Proposed Ballot Items

Table 6A.10.3.1-1 Modulus of Subgrade Reaction for Bedding Support of Rectangular Concrete Culverts

Soil	Range ² (pci)	Rating Value ³ (pci)
Loose sand	15-60	30
Medium dense sand	35-290	115
Dense sand	230-460	290
Clayey medium dense sand	115-290	200
Silty medium dense sand	85-170	145
Clayey Soils ¹		
$q_u \leq 4$ ksf	40-85	60
$8 \text{ ksf} \leq q_u \leq 4$ ksf	85-170	155
$q_u > 8$ ksf	170	> 230

1. q_u = unconfined compression strength
2. Values for undisturbed native soils can be much higher.
3. Suggested values. Rating engineers must use field data to make a final determination for analysis.

Based on: Bowles, J.E. (1996) *Foundation Analysis and Design, 5th Ed.*, McGraw Hill, New York.

C6A.10.3.1

For cases where springs are modeled, there should be at least 10 support points for springs. Analysis and computations required to rate concrete box culverts is completed with the use of computer programs written for that purpose. A number of programs have been developed over the years; however, these programs often make different assumptions for the analysis model and design. Further, some programs used for design of box sections do not have the features necessary to rate them. Thus, it is possible that a box culvert could be designed with one set of assumptions and rated with another. If the rating program makes more conservative assumptions than the design program, unnecessarily conservative rating factors will result. This section provides guidance for analysis and design features that engineers should evaluate when selecting rating software.

Analysis methods used in these programs fall into two and perhaps three categories:

- Two-dimensional frame (2-D Frame) models – In these programs, a two-dimensional frame model is created and subjected to uniform or linearly varying pressure distributions representing the applied earth, live, and, water (external only for rating) loads. Some programs allow the use of springs to model bottom soil support which mimics culvert-soil interaction and produces some of the benefits of FE modeling discussed next.
- Two-dimensional finite element models – Finite element analysis programs model the box culvert and soil as a continuum of discrete elements each assigned appropriate properties. The inclusion of soil in the model allows a realistic evaluation of culvert-soil interaction. These models often result in pressure distributions that peak at the corners and are reduced at mid-span, thus reducing moment and shear forces relative to frame models. Rating with finite element models should only be conducted by engineers experienced with this type of analysis. See discussion of the CANDE finite element model in C6A10.3.3.
- Three-dimensional finite element (3-D FE) models – Currently, full three-dimensional modeling of box culverts is used almost exclusively for research studies as the modeling takes considerable

Appendix H – Proposed Ballot Items

time, expertise, and computer capacity. It is included here as it provides the most complete and accurate model currently possibly of soil-culvert interaction and does not require external decisions on how to apply and distribute live loads to account for the three-dimensional load spreading that occurs as load is transmitted through the soil.

Specific modeling and design assumptions that engineers should evaluate include the following.

- 2-D Frame vs 3-D FE – 2-D frame models distribute loads as uniform pressures while 3-D FE models include the soil in the model and allow the soil and live loads on the culvert to redistribute due to the flexibility of the culvert and shear strength of the soil. This redistribution results in higher pressures at the corners and lower pressures at midspan which reduces design moment and shear forces.
- 45° Haunches – The use of haunches in the corners of box culverts has varied over time. Older culverts were primarily constructed with cast-in-place methods and used small or no haunches. Newer culverts, and, in particular, precast box culvert sections, almost always use 45° haunches with dimensions often equivalent to the thickness of the culvert slabs. The structural effect of haunches should be considered in analysis. A haunch stiffens the corner of the model resulting in higher moments at the corners and lower moments at midspan. The higher corner moments do not increase the design moment as discussed below.
- Non-45° haunches – Some box sections include haunches that extend further out into the slabs than down the sidewalls. These haunches produce the beneficial stiffening effect noted above, but the critical design section may occur at the tip of the haunch or at the face of the wall. Some 3-sided box sections (no bottom slab) include non-45° haunches.
- Critical design locations – As noted above, the presence of haunches shifts critical design locations. Reinforcement for box culvert corners should be determined based on the moment and thrust at the tip of the haunch. Shear capacity should be based on the moment, thrust, and shear forces at the location d , or d_v from the tip of the haunch.
- Thrust forces – It is common to think of culvert elements as flexural members to be designed considering only the applied moment. However, thrust forces in culverts can be considerable, particularly in the sidewall of deeper box culverts as about 50% of compressive thrust reduces the tension in the reinforcement. Consideration of this thrust produces more economical designs and higher rating factors.

6A.10.3.2 Concrete Arches, Metal, Thermoplastic, and Fiberglass Pipe and Other Metal Culvert Types

Most metal and all thermoplastic, and fiberglass pipe are typically analyzed and rated by the empirical procedures embodied in the LRFD Specifications or by rigorous methods such as finite element models.

6A.10.3.3 – Finite Element Modeling

Finite element-based computer modeling is used routinely for analysis of concrete arch culverts and deep corrugated metal culverts. It may be used for any culvert. Finite element modeling should only be undertaken by engineers experienced in the use of such programs for culvert analysis.

Appendix H – Proposed Ballot Items

Finite element analysis should consider loadings to mimic reduced lateral pressure as is done for rectangular concrete culverts in frame models. This can be accomplished by adjusting the soil properties, such as by reducing the backfill density.

C6A.10.3.3

The most commonly used program for finite element analysis of culverts is CANDE. Originally developed by the FHWA and upgraded through NCHRP Projects, CANDE offers many features that aid in analyzing and rating culverts, and some that improve rating but are not allowed in the LRFD Design specifications, including:

- Continuous load scaling (CLS) – this feature permits a live load to spread longitudinally as it is transferred from the top of the culvert to the bottom slab. This feature is appropriate and useful for single lane loadings and not typically available in two-dimensional finite element programs. For multiple lane loadings the LRFD Design specifications require that the same live load pressure applied to the top slab be applied as reaction on the bottom slab with a multiple presence factor, $m = 1.2$. This approach has been shown to be controlling over multiple lane loadings with $m = 1.0$. Thus, for multiple lane designs, analyze for a single lane without using the CLS feature.
- Soil models – CANDE includes options for several soil models. It is most common to use linear properties for in situ soils, but soft in situ soils may require using a non-linear model. While there is no “correct” non-linear model, most AASHTO culvert specifications are based on the Duncan soil model with the Selig hyperbolic bulk modulus

Engineers should understand the implications of any finite element program feature prior to applying it to culvert rating.

6A.10.4 Load Rating Equation for Culverts

Load rating of culverts shall be carried out for each load effect using the following rating factor expression with the lowest value determining the controlling rating factor. Limit states and load factors for load rating shall be selected from Table 6A.10.5-1.

$$RF = \frac{C \pm \gamma_{dc} DC \pm \gamma_{DW} DW \pm \gamma_{EV} EV \pm \gamma_{EH} EH \pm \gamma_{ES} ES}{(\gamma_{LL})(LL+IM) \pm (\gamma_{AW})(AW)} \quad (6A.10.4-1)$$

In which, for the strength limit states:

$$C = \phi_c \phi_s \phi R_n \quad (6A.10.4-2)$$

Where:

Appendix H – Proposed Ballot Items

RF	=	rating factor
C	=	capacity
R_n	=	nominal member resistance (as inspected)
DC	=	dead load effect due to structural components and attachments
DW	=	dead load effect due to wearing surface and utilities
EV	=	vertical earth pressure
EH	=	horizontal earth pressure
ES	=	uniform earth surcharge
LL	=	live load effect
IM	=	dynamic load allowance
AW	=	approaching wheel load
γ_{DC}	=	LRFD load factor for structural components and attachments
γ_{DW}	=	LRFD load factor for wearing surfaces and utilities
γ_{EV}	=	LRFD load factor for vertical earth pressure
γ_{EH}	=	LRFD load factor for horizontal earth pressure
γ_{ES}	=	LRFD load factor for earth surcharge
γ_{LL}	=	evaluation live load factor
γ_{AW}	=	LRFD load factor for approaching wheel load
ϕ_c	=	condition factor
ϕ_s	=	system factor
ϕ	=	LRFD resistance factor

The product of ϕ_c and ϕ_s shall not be taken less than 0.85.

Components subject to combined load effects shall be load rated considering the interaction of load effects.

C6A.10.4

The approaching wheel load replaces the live load surcharge as more appropriate for culverts.

6A.10.5 – Limit States

Culverts shall be load rated for the Strength I load combination for the design and legal loads and the Strength II load combination for permit loads.

The applicable loads and their combinations for evaluation are specified in Table 6A.10.5-1 and in Articles 6A.10.6 through 6A.10.10.

Service limit state for crack width control need not be checked when load rating concrete culverts if internal inspection does not indicate reinforcement corrosion.

C6A.10.5

Maximum and minimum load factors for different loads should be combined to produce the largest load effect. The load cases should be selected to generate the critical combinations of moment, shear, and thrust demands at all critical sections for each load case.

It is prudent to also perform an evaluation of the culvert under permanent loads only if the depth of earth fill over the culvert has changed since the original construction.

Table 6A.10.5-1 Limit States and Load Factors for Culvert Load Rating (Modified from current MBE Table 6A.5.12.5-1)

Bridge Type	Limit State	DC		DW		Design Load ^a		Legal Load ^b	Permit ^b Load	1.5 AW		EH ^c		EV		ES ^d	
		Max	Min	Max	Min	Inv.	Opr.			Max	Min	Max	Min	Max	Min	Max	Min
		γ_{DC}	γ_{DC}	γ_{DW}	γ_{DW}	γ_{LL}	γ_{LL}			γ_{LL}	γ_{LL}	γ_{AW}	γ_{AW}	γ_{EH}	γ_{EH}	γ_{EV}	γ_{EV}
Culverts Reinforced Concrete Box Culvert	Strength I	1.25	0.90	1.50	0.65	1.75	1.35	2.00	—	Same as LF for Design/ Legal Loads	0.00	1.35	0.90	1.50	0.90	1.50	0.75
	Strength II	1.25	0.90	1.50	0.65	—	—	—	Table 6A.4.5.4.2a-1	Same as LF for Permit Loads	0.00	1.35	0.90	1.20	0.90	1.50	0.75

Notes:

- ^a In addition to the load factor, use the 1.2 multiple presence factor for single-lane loading
- ^b Multiple presence factor is not included and is not required for single-lane loading for permit load vehicles
- ^c Use a 50 percent reduction to *EH* for rating positive moment in top slabs; need not be combined with the minimum load factor
- ^d Use a 50 percent reduction to *ES* for rating positive moment in top slabs; need not be combined with the minimum load factor. Water loads on interior walls are neglected.
- *EH* and *AW* apply only to rectangular concrete culverts.
- *EH* load factor for the minimum condition is taken as 1.0 as this condition is accounted for with a reduced lateral pressure
- If the depth of fill and backfill density are known, maximum load factor for *EV* may be taken as the average of 1.0 and appropriate load factor from AASHTO LRFD Specifications Table 3.4.1-2 culverts.

Appendix H – Proposed Ballot Items

6A.10.6-Resistance Factors

Resistance factors for culverts shall be taken as specified in LRFD Design Article 12.5.5.

6A.10.7-Condition Factors

Use of condition factors as presented in Table 6A.4.2.3-1 may be considered optional based on an agency's load rating practice.

6A.10.8-System Factor: ϕ_s

The system factor for strength limit states for culverts shall be taken as 1.0

6A.10.9-Materials

No change from current Article 6A.5.12.9

C6A.10.9

No change from current Article C6A.5.12.9

6A.5.12.10-Loads for Evaluation

6A.5.12.10.1-Dead Loads

No change from current Article 6A.5.12.9

6A.5.12.10.2- Earth Pressure

6A.5.12.10.2a-Vertical Earth Pressure: EV

The unit weight of the soil may be taken as shown in LRFD Design Table 3.5.1-1 or in accordance with agency design practice. Weight of earth shall be modified for culvert-soil interaction in accordance with the LRFD Design Specifications for the culvert material being analyzed.

6A.5.12.10.2b-Horizontal Earth Pressure: EH

Lateral earth pressure is only explicitly applied to rectangular concrete culverts analyzed with frame models. It shall be assumed linearly proportional to the depth of soil based on the at rest pressure coefficient as shown in LRFD Design Article 3.11.5.2. The coefficient for the maximum condition need not be taken greater than 0.5 and the coefficient for the minimum condition need not be taken less than 0.25.

Lateral pressure for non-rectangular culverts is embedded in the material specific LRFD design methods and no additional evaluation is required.

Culverts rated with finite element programs automatically consider lateral soil pressures as part of the culvert-soil interaction. If inspection of flexible culverts shows high deflections, the backfill conditions must be modeled to match those deflections during rating analysis.

6A.5.12.10.2c-Uniform Surcharge Loads: ES

Typically, uniform surcharge loads are not considered in culvert design or rating unless temporary fill will be added over the culvert during or after construction. If applied, the culvert shall be evaluated both with and without the surcharge load.

Appendix H – Proposed Ballot Items

*6A.10.10.3-Live Loads**No change from current Article 6A.5.12.10.3**C6A.10.10.3**No change from current Article C6A.5.12.10.3**C6A.5.10.10.3a-Live Load Distribution****Current specification Article 6A.5.12.10.3a with proposed changes listed below.****6A.5.12.10.3a—Live Load Distribution*

Distribution of wheel loads for culverts with less than 2.0 ft of fill shall be taken as specified in LRFD Design Article 4.6.2.10. Distribution of wheel loads to culverts with 2.0 ft or more of cover shall be as specified in LRFD Design Article 3.6.1.2.6. ~~Single-span culverts with depth of fill more than 8 ft need not be load rated for live loads as the live load effects are negligible; for multiple-span culverts, the effects of live load may be neglected where the depth of fill exceeds the distance between faces of end walls.~~ The vertical live load should be applied as a moving load across the top of the culvert structure.

Culverts with deep fills should be evaluated for the effects of permanent loads only.

C6A.5.12.10.3a

~~For culverts with depth of fill greater than 8 ft, the live loads will constitute a negligible portion of the overall loading. The capacity of the culvert should be checked for permanent loads only for the possible ultimate demand obtained by the maximum and minimum load factors.~~

Box culverts are normally analyzed as two-dimensional frames. Equivalent strip widths defined in LRFD Design Article 4.6.2.10 for box culverts with depth of fill less than 2 ft are used to simplify the analysis. ~~Distribution length parallel to the span may be conservatively neglected in most load ratings.~~

For earth fills of 2 ft or more, the tire contact area for distribution purposes may be taken as 20 in. wide × 10 in. long, for a wheel of one or two tires (LRFD Design Article A3.6.1.2.5). For other truck loads, the tire area may be calculated following the provisions of LRFD Design Article ~~C3.6.1.2.5. Lane loads are distributed only transversely.~~

~~LRFD Design Article 3.6.1.2.6 states that wheel loads may be considered to be uniformly distributed over a rectangular area with sides equal to the dimensions of the tire contact area and increased by 1.15 times the depth of fill in select granular backfill. Where such areas from multiple wheels overlap, the total load should be uniformly distributed over the area but the total width of distribution shall not~~

Change 1- Replace deleted sentence with:

Culverts where design for live load is not required per the LRFD Design Specifications Article 3.6.1.2.6a do not require rating for live loads.

Change 2 – Deleted sentence. No replacement.

Change 3 – Replace deleted sentence with:

Appendix H – Proposed Ballot Items

Distribution parallel to the span with increasing depth is accomplished by adding LLDF * Depth of fill to the tire dimension. Per LRFD Design Specifications Article 4.6.2.10.

Change 4 – Replace deleted sentence with:

Lane loads are only considered for culverts with spans greater than 20 ft.

Change 5 - Delete entire paragraph (only a portion of the deleted paragraph is shown above). No replacement.

6A.10.10.3b-Dynamic Load Allowance: IM

No change from current Article 6A.5.12.10.3b

C6A.5.12.10.3b

No change from current Article C6A.5.12.10.3b

6A.10.10.3c – Approaching Wheel Load

Rectangular concrete culverts with less than or equal to 2 ft of cover shall be loaded with a lateral pressure distribution to produce the effects of a truck axle just before going over the culvert. This pressure shall be computed using Eq. 6A.10.10.3c-1 and shall be applied to both sides of the culvert.

$$p\text{-lat}(h_d) = 700/h_d \leq 800 \text{ psf} \quad \text{Eq. 6A.10.10.3c-1}$$

where:

- $p\text{-lat}(h_d)$ = lateral soil pressure resulting from an approaching wheel load at depth h_d , psf
 h_d = depth of fill to depth where pressure is calculated, ft

The approaching wheel load need not be considered for culverts with more than 2 ft of fill from top of culvert to top of pavement.

C6A.10.10.3c

Culverts have traditionally been evaluated for a live load surcharge that is appropriate for earth retaining structures. The live load surcharge is not appropriate for rectangular culverts for the following reasons:

- Unlike retaining walls, where a vehicle load near a wall increases the overturning moment, a vehicle approaching a culvert produces a small lateral pressure that is resisted by the soil on the far side of the culvert.
- Lateral pressure near the mid-height of the wall will result in an increase in positive moments in the sidewall and negative moments at the corners and a decrease in positive moments in the slabs. Lateral pressure near the top of a shallow culvert primarily results in a thrust in the top slab which has almost no effect on the moments, and hence the reinforcement requirements.

This approaching wheel load has been used in AASHTO and ASTM standards for precast concrete box culverts for over 40 years. It was first proposed by Heger, F.J. and Long, K.N. (1976) *Structural Design*

Appendix H – Proposed Ballot Items

of Precast Concrete Box Sections for Zero to Deep Cover Earth Cover Conditions and Surface Wheel Loads, Concrete Pipe and the Soil-Structure System, ASTM STP 630.

6A.10.10.3d - Pavements

Pavements are used to spread the effects of wheel loads over a greater area and thus reduce soil stresses below the pavement. Rating engineers may consider the effects of asphalt or concrete pavements in reducing the loads applied to culverts. This can be completed using finite element soil structure interaction analyses which can directly model the pavement layer, or with elasticity based or empirical procedures. Such analyses must consider the current and expected future condition of the pavement. Analysis of asphalt pavements must consider anticipated temperature effects on properties.

C6A.10.10.3d

Most culverts are designed without consideration of the improved load distribution resulting from pavements over the culvert. The only exception to this is some metal box section designs as detailed in LRFD Article 12.9.4.6. The effect of pavements is ignored primarily to allow for construction loads prior to placement of pavement. The finite element analysis culvert program most commonly used for analysis, design, and rating of culverts is CANDE, originally developed by FHWA and later updated by AASHTO through the NCHRP Program. Empirical procedures for considering pavements include elasticity theory procedures for layered systems and the Westergaard procedure for distributing live loads through concrete pavements as embodied in the American Concrete Pipe Association's *Concrete Pipe Handbook*.

Table C6A.10.10.3d-1 presents guidance on the conditions and locations where pavements are effective in reducing loads on culverts.

**Table C6A.10.10.3d-1
Pavement Effect in Distributing Live Load on Culverts**

Pavement thickness, in.	Asphalt stiff subgrade	Asphalt soft subgrade Concrete stiff subgrade	Concrete soft subgrade
	E1/E2 ~3	E1/E2 ~ 35	E1/E2 ~ 400
4	NB	NB	0.50 / 5 ft
8	NB	0.60 / 6 ft	0.25 / 6 ft
16	0.75 / 6 ft	0.50 / 7 ft	0.15 / 8 ft

Where:

- E1 = modulus of pavement layer
- E2 = modulus of soil subgrade
- NB = no benefit
- The data lines, such as 0.50 / 5 ft indicate the reduction that may be applied to the live load at the surface of the pavement and the depth at which no benefit is derived in reducing pavement load.

Table C6A.10.10.3d-1 is derived from an elastic solution derived by Fox and presented in Poulos, H.G., and Davis, E.H. (1991) Elastic Solutions for Soil and Rock Mechanics, which is available at <http://research.engr.oregonstate.edu/usucger/PandD/PandD.htm>, and uses the following assumptions:

Appendix H – Proposed Ballot Items

- E-concrete pavement = 4,000 ksi
- E-asphalt pavement = 0.3 ksi
- E-soft subgrade approximately 8 ksi
- E-stiff subgrade approximately 100 ksi

One relationship between the soil modulus and the common parameters, as recommended by the Federal Aviation Administration Advisory Circular 150/5320-6F, 2016, are:

$$E = 1,500 \text{ CBR} \quad \text{Eq. C6A.10.10.3d-1}$$

$$E = 20.15 k^{1.284} \quad \text{Eq. C6A.10.10.3d-2}$$

Where:

- E = modulus of elasticity of subgrade, psi
 CBR = California bearing ratio
 k = modulus of subgrade reaction, pci

Note that Eqs. C 6A.10.10.3d-1 and C6A.10.10.3d-2 provide values of subgrade modulus considerably higher than typically used in culvert backfill design.

As an example, for an 8 in. concrete pavement with a soft subgrade, the live load could be reduced to 25% of the applied load for a culvert directly under the pavement and there would be no reduction if the culvert is more than 5 ft below the pavement. Linear extrapolation can be used to determine the reduction for intermediate depths.

6A.10.11 - Concrete Culverts

6A.10.11.1 Design for Shear

The shear strength of culverts without prestressing and with less than 2.0 ft of cover that are performing well based on inspection can be evaluated with a modified approach to shear capacity. Use the General Procedure for shear strength in LRFD Design Specifications Article 5.7.3.4.2, substituting the following procedure to compute the strain in the reinforcement:

$$\epsilon_s = \frac{|M_{u-mod}| + 0.5 N_u + |V_u|}{E_s A_s} \quad \text{Eq. 6A.10.11.1-1}$$

Where M_{u-mod} is the factored moment at the critical shear design location, which may be modified as follows if it is a negative moment:

$$M_{u-mod} = M_u \frac{96 + 1.44 S}{96 + 5.47 S} \quad \text{Eq. 6A.10.11.1-2}$$

where:

- S = clear span of the culvert (ft) – (same value as used in 4.6.2.10.2-1)

Use the unmodified M_u if the controlling moment is positive. Further, the limitation that the minimum value of $M_u = V_u d_v$ does not apply.

This expression can be applied to box sections analyzed and designed with two-dimensional frame or finite element models.

Appendix H – Proposed Ballot Items

The use of springs to represent bedding pressure noted in Article 6A.10.3.1 results in reduced shear and moments. The rating factors for the lower half of box culverts analyzed in this manner may be applied to the locations in the upper half of the culvert provided the following conditions are met:

- The culvert is installed at a depth where live load is not considered.
- The reinforcing in the upper half of the culvert matches that in the lower half.

C6A.10.11.1

Many concrete culverts that have been in service and performed well for many years have rating values less than 1.0 due to computing shear strength by current procedures. There are two primary reasons for this:

- Past editions of AASHTO specifications have allowed designers to assume shear strength is adequate if the section is properly designed for flexure.
- Frame models of box sections are inherently conservative due to the assumption of uniform pressures to model vertical loads.

The equations in this section provide a moderately increased shear capacity to reflect this history. The reduction in negative moment at the critical section is based on:

McGrath, T.J., A.A. Liepins, and J.L Beaver, “Live Load Distribution Widths for Reinforced Concrete Box Sections”, *Transportation Research Record: Journal of the Transportation Research Board, CD 11-S*, Transportation Research Board of the National Academies, Washington, DC, 2005, pp 99-108.

Culvert inspections should evaluate flexural cracking or concrete crushing which could indicate the culvert is carrying more load than considered in design.

C6A.10.12 - Metal Culverts

Metal culverts should only be rated after a field inspection has documented the culvert shape and condition. Metal Culverts should be analyzed for service and factored forces in accordance with the LRFD Design Specifications and appropriate provisions of this Manual. Suitable adjustments should be included to consider the current condition of the culvert.

Metal culverts that are designed using finite element modeling must be rated with the same analysis method. Modeling must consider installation conditions that produce the culvert shape observed in the field.

Appendix H – Proposed Ballot Items

C6.A.10.12

The long-term performance of these culverts is dependent on the performance of the backfill soil around the culvert. The culvert shape is a key indicator of backfill quality and careful measurements in the field are warranted.

National Corrugate Steel Pipe Association (NCSPA) Design Data Sheet No. 19 provides recommended procedures for rating metal culverts and suggested adjustments based on existing conditions. Rating engineers should note that the design methods and load factors for the several types of metal culverts are quite different as they are often empirical or semi-empirical. In addition to loss of section due to corrosion, the field inspection should document the shape of the culvert.

6.A.10.13 -Thermoplastic and Fiberglass Culverts

Thermoplastic and fiberglass culverts should only be rated after a field inspection has documented the culvert shape and condition. Such culverts should be analyzed for service and factored forces in accordance with the LRFD Design Specifications and appropriate provisions of this Manual. Suitable adjustments should be included to consider the current condition of the culvert. The effect of the observed deflected shape on culvert forces must be considered.

C6A.10.13

Thermoplastic and fiberglass culverts are both considered flexible. The long-term performance of these culverts is dependent on the performance of the backfill soil around the culvert. The culvert shape is generally a key indicator of backfill quality and careful measurements in the field are required.

Appendix H – Proposed Ballot Items

Ballot MBE-2**2019 AASHTO BRIDGE COMMITTEE AGENDA ITEM:** [Click here to enter text](#)**SUBJECT:** Rating and Condition Evaluation of Culverts**TECHNICAL COMMITTEE:** T-18 Bridge Management, Evaluation and Rehabilitation, T-13 Culverts

<input type="checkbox"/> REVISION	<input checked="" type="checkbox"/> ADDITION	<input type="checkbox"/> NEW DOCUMENT
<input type="checkbox"/> DESIGN SPEC	<input type="checkbox"/> CONSTRUCTION SPEC	<input type="checkbox"/> MOVABLE SPEC
<input checked="" type="checkbox"/> MANUAL FOR BRIDGE EVALUATION	<input type="checkbox"/> SEISMIC GUIDE SPEC <input type="checkbox"/> OTHER Research	<input type="checkbox"/> MANUAL BRIDGE ELEMENT INSP

DATE PREPARED: 7/3/2019**DATE REVISED:** [Click here to enter a date](#)**AGENDA ITEM:****Item #1****Add New Article 6B.9****Article 6.B.9**

Culverts may be load rated in accordance with the current LRFD Specifications or with the Specifications under which they were originally design. Culvert ratings based on older specifications must be inspected prior to rating and the current conditions must be considered.

C6.B.9

Concrete pipe, metal, thermoplastic, and fiberglass pipe are essentially designed by the same methods as were incorporated into prior bridge design specifications and, thus, most should rate in accordance with the current LRFD Specifications. Reinforced concrete box sections have been designed under AASHTO specifications for many years and the provisions have changed such that many do not meet current standards. This is particularly true for shear strength, as some editions of AASHTO specifications did not require design for shear in slabs, such as the top and bottom slab of box culverts. This article allows rating engineers to take advantage of the less demanding older specifications provided the culvert has demonstrated good performance and the loading has not changed since prior ratings.

Article 6A.10 provides several provisions for analysis and rating that will assist engineers using older specifications for rating.

Appendix I – Improving AASHTO LRFD/LRFR Specs for 2D for Buried Culverts under LL

Appendix I – Improving AASHTO LRFD/LRFR Specifications for 2D
Analysis of Buried Culverts Under Live Load

This appendix provides a white paper prepared by Dr. Katona for Live Load Distribution.

Appendix I – Improving AASHTO LRFD/LRFR Specs for 2D for Buried Culverts under LL

WHITE PAPER

IMPROVING AASHTO LRFD/LRFR SPECIFICATIONS FOR
TWO-DIMENSIONAL ANALYSIS OF BURIED CULVERTS UNDER LIVE LOAD

Dr. Michael Katona

Appendix I – Improving AASHTO LRFD/LRFR Specs for 2D for Buried Culverts under LL

A White Paper
on
Improving AASHTO LRFD/LRFR Specifications
for
Two-dimensional Analysis of Buried Culverts under Live Loads

INTRODUCTION

Background. Buried culverts, due to their long prismatic configuration, are generally designed and analyzed as two-dimensional (2D) systems because the earth pressure acting on the culvert is nearly constant in the longitudinal direction and well represented by 2D models. Comprehensive plane-strain finite element (FEM) programs such as CANDE simulate a representative cross-sectional slice of both soil and culvert to simultaneously determine soil-structure interaction loads and structural responses of the culvert. Design-oriented programs such as BOXCAR and AASHTOWare-BrR use 2D frame models to simulate the culvert without explicitly modeling the soil; rather, approximate methods are used to prescribe the loading on the culvert as specified by AASHTO LRFD Bridge Design Specifications.

Live-load issue. A major difficulty with all 2D models is determining the pressures transmitted to the culvert from live loads acting on the soil surface (wheel footprints). For 2D FEM plane-strain analysis, the live-load pressure automatically spreads in the transverse direction (plane of the culvert span); however, the live-load pressure in the longitudinal direction (out-of-plane) is restrained from spreading due to the limitations of 2D plane-strain geometry. Consequently, longitudinal load-spreading approximations such as recommended by AASHTO are used to avoid overly conservative loading conditions. For 2D frame models, load spreading approximations are required for both transverse and longitudinal directions.

Another, but less understood, problem is that 2D live-load analysis underestimates the culvert's actual stiffness that arises from 3D deformation patterns caused by short-width longitudinal loads. Said another way, 3D deformation patterns caused by short load widths produce additional 3D stiffness effects that are not accounted for by the one-way bending stiffness inherent in 2D analysis. The current AASHTO LRFD specifications recognizes this 3D-stiffness phenomenon for shallow burial of reinforced concrete boxes and arches but not for "general culverts" of other shapes and materials. Specifically, AASHTO provides special equations to account for 3D stiffness effects of r/c boxes and arches under less than 2 feet of fill.

Scope. This white paper focuses on the little-understood 3D stiffness effects that gives rise to the special AASHTO longitudinal distribution widths that are intertwined with the better-understood longitudinal distribution representing load-spreading through the soil. The white paper is divided in two parts. Part I includes a review of AASHTO equations originating from the PennDOT study along with a new conceptual model that explains the 3D stiffness effects using a new parameter called $W_{critical}$. Part II defines a mechanistic model representing the top slab of a box culvert, provides a solution based on the

Appendix I – Improving AASHTO LRFD/LRFR Specs for 2D for Buried Culverts under LL

Ritz Technique, and compares and contrasts results with current AASHTO methods. The paper concludes with a summary of findings and list of recommendations.

PART I -- REVIEWS, CONCEPTS AND ISSUES

REVIEW OF AASHTO DISTRIBUTION WIDTHS

General Culverts. The intuitive AASHTO LRFD model for load-spreading through soil is applicable to all culverts. It assumes the wheel's surface footprint dimensions ($L_0 \times W_0$) spreads with soil depth at a specified angle (typically 30 degrees) in both transverse and longitudinal directions. Further it is assumed the pressure remains uniform so that vertical force equilibrium dictates the pressure decreases in proportion to increased area. Equation 1 is from AASHTO Section 3.6.1.2.6 and represents the expanded footprint length or distribution width in the longitudinal direction for soil depth H .

$$E_{\text{Long}} = W_0 + \text{LLDF} * H \rightarrow \text{for } H < H_{\text{int}} \quad \text{Equation 1}$$

where, E_{Long} = Longitudinal distribution width for 1-wheel load (inches).

H = Soil depth from surface, usually H = cover depth (inches).

W_0 = Wheel longitudinal footprint width on surface (typically 20").

LLDF = Live-load distribution factor = $2 \tan(30^\circ) = 1.15$.

When $H < H_{\text{int}}$, only one wheel ($1/2$ axle load) contributes to the line load magnitude. Thus, the 2D line load for one wheel is given by, $p_1 = 1/2$ axle load/ E_{Long} .

H_{int} is called the 2-wheel interaction soil depth and is dependent on the spacing between the axle's wheels. When $H > H_{\text{int}}$ both wheels (full axle load) contributes to the line load magnitude and the distribution width is redefined as,

$$E_{\text{Long}} = S_{\text{axle}} + W_0 + \text{LLDF} * H \rightarrow \text{for } H > H_{\text{int}} \quad \text{Equation 2}$$

where, E_{Long} = Longitudinal distribution width for 2-wheel load (inches)

S_{axle} = center-to-center wheel spacing on axle (typically 72").

$H_{\text{int}} = (S_{\text{axle}} - W_0) / \text{LLDF}$ (usually computes to 45.2")

Since Equation 2 applies to the full axle load (2 wheels), the 2D line load for two wheels is given by, $p_2 =$ axle load/ E_{Long} . Note that the line-load magnitude is a continuous function of H when transitioning from Equation 1 to Equation 2, i.e.; $p_1 = p_2$ for $H = H_{\text{int}}$.

Reinforced Concrete Box and Arch Culverts. Equations 1 and 2 generally apply to all culverts materials and shapes. However, for reinforced concrete box and arch culverts, AASHTO Section 4.6.2.10 specifies Equation 3 to replace Equation 1 for cover heights less than 2 feet with the understanding this distribution width applies to the full axle load (2 wheels).

$$E_{\text{Long}} = 96" + 1.44 * \text{Span}(\text{ft}) \rightarrow \text{special r/c case, for } H < 2 \text{ feet} \quad \text{Equation 3}$$

where, E_{Long} = Longitudinal distribution width for 2-wheel loading (inches)

Span = Reinforced concrete box or arch span measured in feet.

Appendix I – Improving AASHTO LRFD/LRFR Specs for 2D for Buried Culverts under LL

The reason for the change from Equation 1 to Equation 3 is because analytical studies revealed that Equation 1 is too conservative when H is less than 2 feet particularly for box culverts that are sometimes installed with zero soil cover. For precast boxes and arches, AASHTO sections 12.11.2.1 and 12.14.5.2 infer that E_{Long} should not exceed two lay lengths. Before discussing the origin and implications of Equation 3, it is instructive to compare Equations 3 with Equations 1 & 2 in the context of the reduced-surface-load (RSL) method. RSL is the most common 2D method for reducing the actual longitudinal line load under the wheel(s) to account for longitudinal load spreading at depth H and 3D stiffness effects. The reduction factor r is determined by preserving force equilibrium at the surface and at soil depth H. Given that the surface force is the surface line-load p_0 times the longitudinal width E_0 , and the force at depth H is line-load p_H times E_{Long} , then the reduction factor which is defined as $r = p_H/p_0$ is also given by the geometric ratio,

$$r = \frac{E_0}{E_{Long}} \quad \text{Equation 4}$$

where, r = reduction factor applied to surface line load under wheel(s).

E_0 = distribution width on surface (H=0) dependent 1 or 2 wheels:

- $E_0 = W_0$ for 1 wheel. (Equation 1)
- $E_0 = 2W_0$ for 2 wheels. (Equation 2 or 3)

E_{Long} = distribution width at depth H as defined in Equation 1, 2 or 3.

Figure 1 shows RSL reduction factors versus soil depth for three example culverts:

- (1) general culvert. (Eq. 1 for $0 \leq H < H_{int}$, and Eq. 2 for $H \geq H_{int}$.)
- (2) r/c box culvert with 10-foot span. (Eq. 3 for $0 \leq H < 2'$, and Eqs. 1 & 2 for $H \geq 2'$.)
- (3) r/c arch culvert with 50-foot span. (Eq. 3 for $0 \leq H < 2'$, and Eqs. 1 & 2 for $H \geq 2'$.)

Appendix I – Improving AASHTO LRFD/LRFR Specs for 2D for Buried Culverts under LL

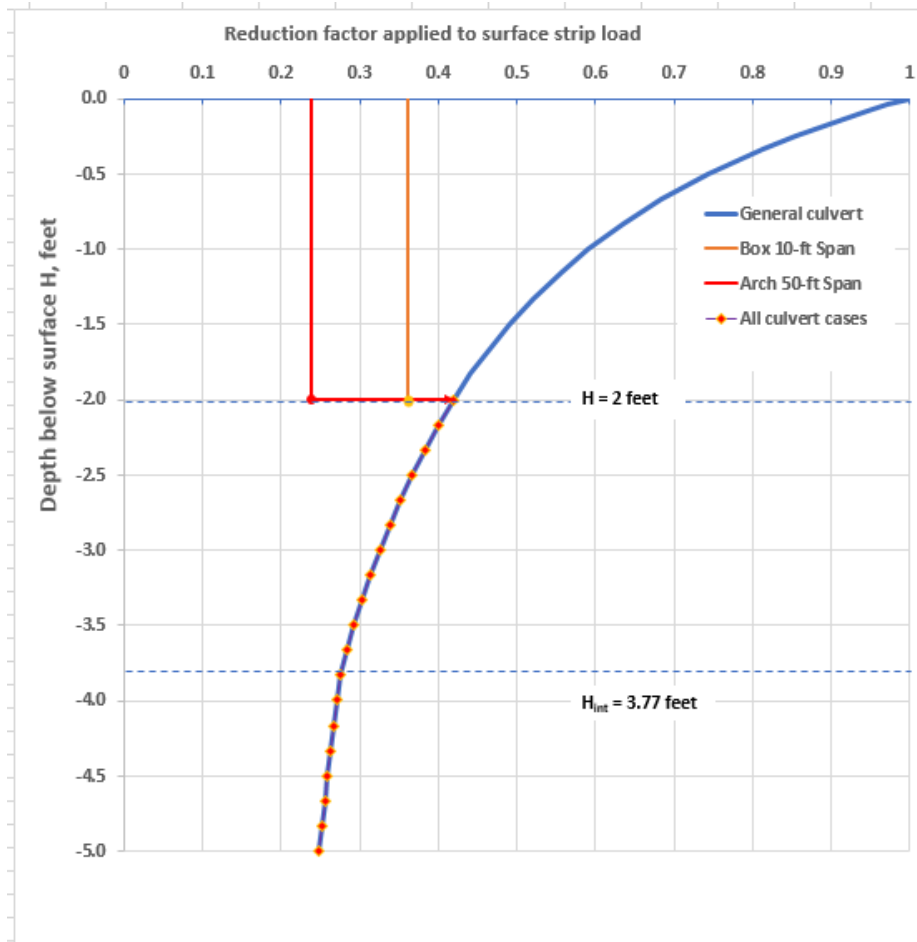


Figure 1. Reduction factor versus soil depth for three example culverts.

Three observations from Figure 1 are worth noting for future reference;

1. For general culverts, the reduction factor is 1.0 at the surface, which is in keeping with Equation 1 because there is no soil depth to spread the load. At 2 feet of fill the reduction factor rapidly but smoothly reduces to 0.42 and continues to smoothly decrease until the 2-wheel interaction depth wherein the slope of reduction factor curve increases, but remains continuous.
2. In contrast, the reinforced concrete box and arch culverts have reduction factors at the surface equal to 0.36 and 0.24, respectively, and remain constant until $H = 2'$. Clearly these reduction factors are not attributed to longitudinal load spreading through soil, rather they are attributed to additional 3D stiffness effects that are not captured in 2D models. A major objective of this report is to fully explain and investigate the meaning behind these 3D stiffness effects.
3. There are obvious discontinuities in the reduction curves for the r/c box and r/c arch when transitioning through $H = 2'$ due to shifting from Equation 3 to Equation 1. Using the r/c arch as an example, we see that $r = 0.24$ at $H = 1.999'$ but jumps to $r = 0.42$ at $H = 2.001'$, a 75% increase over an infinitesimal distance. The consequence of this discontinuity, is that an engineer would design for 75% more load for a cover height $H = 2.001'$ than he would for the same culvert

Appendix I – Improving AASHTO LRFD/LRFR Specs for 2D for Buried Culverts under LL

with $H = 1.999'$. This is a serious problem and needs to be rectified in future AASHTO specifications.

PennDOT Report → AASHTO Equation 3. Equation 3 (i.e., AASHTO LRFD 4.6.2.10.2-1) originates from the well-documented PennDOT study, *Live Load Distributions for Design of Box Culverts (2004)*, conducted by Tim McGrath and engineers from SGH under the sponsorship of Pennsylvania Department of Transportation. The PennDOT study builds upon previous work from NCHRP Project 12-26 *Distribution of Wheel Loads on Highway Bridges* in which the basic assumption is the top slab of shallowly buried box culverts behaves like reinforced concrete bridge-deck slabs.

The PennDOT study used NASTRAN to obtain 3D finite element solutions of reinforced concrete box culverts subject to HS20 two-wheel axle loadings. Overall, 31 linear box and slab model configurations were constructed including a range of haunch dimensions, slab and wall thicknesses, and transverse-traveling HS20 loads applied along the mid-length plane and also along the free-edge plane. Variations of the major system dimensions are listed below:

- Cover height; $H = 0'$ and $2'$.
- Span lengths; $S = 8'$, $16'$ and $24'$.
- Rise height; $R = 0'$ (4 slab models) and $8'$ (27 box models).
- Longitudinal length; $L = 30'$ (fixed for all 31 models).

Longitudinal distribution widths for each r/c box model were computed for maximum positive moment, maximum negative moment, and maximum shear. As inferred in the PennDOT report, the computed distribution widths provide reduction factors (Equation 4) that produce 2D responses equivalent to the 3D NASTRAN solutions. As expected, the controlling distribution widths for maximum shear occurs when the HS20 axle is located near the wall-supported edges of the span, and the controlling distribution widths for maximum moments occurs when the HS20 axle is located in the central region of the span. In all cases the distribution widths tend to increase as the box span increases from $8'$ to $24'$.

Figure 2, as copied from the PennDOT report, shows the distribution widths under 1 wheel for 15 PennDOT box-culvert models that have zero soil cover ($H = 0$) and HS20 axle loads applied symmetrically along the mid-length plane. Also shown are the recommended AASHTO distribution widths for 1-wheel loading as specified in the then-current AASHTO Standard and LRFD Specifications wherein the distribution-width equations are multiplied by $\frac{1}{2}$ to reflect width under 1-wheel.

Appendix I – Improving AASHTO LRFD/LRFR Specs for 2D for Buried Culverts under LL

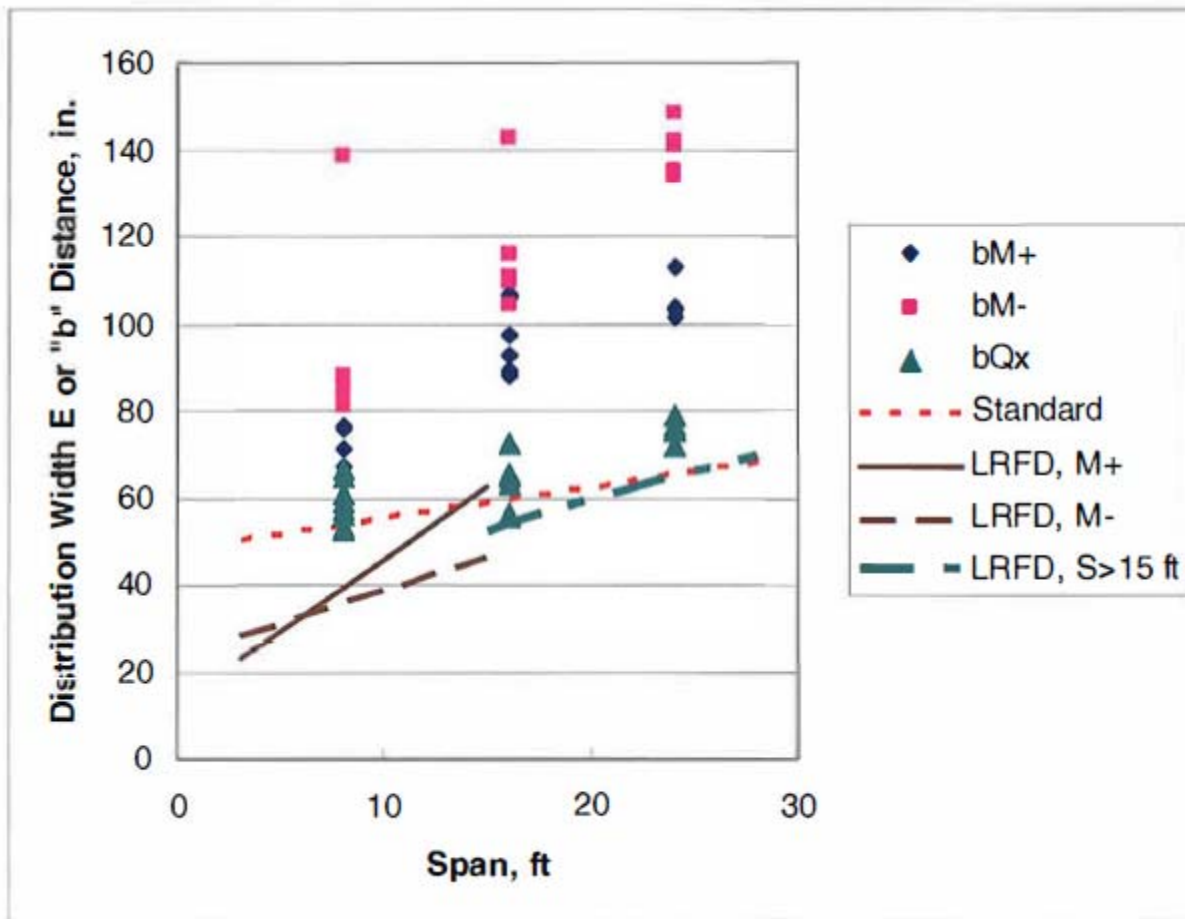


Figure 2. Longitudinal distribution widths for 1-wheel load versus span as tabularized below:

Source of distribution widths	Distribution-width symbols	Relationships/Equations
PennDOT 3D FEM solutions 2004	bM+ = max positive moment bM- = max negative moment bQx = maximum edge shear	Discrete data points for 8', 12' & 24' spans with separate symbols for each maximum force effect.
AASHTO Standard Specifications 2002	----- Standard	$E = \frac{1}{2}(96'' + 1.44\text{Span})$ One equation for all force effects.
AASHTO LRFD Specifications 1998 with 2002 update	M+ = max pos. moment, Span $\leq 15'$ M- = max neg. moment, Span $\leq 15'$ LRFD = all force effects, Span $> 15'$	$E = \frac{1}{2}(26'' + 6.6*\text{Span})$ $E = \frac{1}{2}(48'' + 3*\text{Span})$ $E = \frac{1}{2}(10'' + 5*(\text{Span}*\text{Length})^{\frac{1}{2}})$

Upon inspecting the PennDOT data points in Figure 2, it is seen that the minimum distribution widths (most conservative) are associated the maximum shear criterion. Remarkably, the distribution-width equation from the 2002 Standard AASHTO Specification was observed to provide a reasonable lower bound to PennDOT maximum shear data points. Accordingly, the PennDOT report recommended that the new AASHTO LRFD Specification adopt the equation from the Standard Specification. This provides a brief history behind the origin of Equation 3, but not a meaningful explanation of the physics behind it.

Appendix I – Improving AASHTO LRFD/LRFR Specs for 2D for Buried Culverts under LL

Two other parametric studies from the PennDOT report reveal how distribution widths are influenced by loading along the free edge and by orthotropic properties of the top slab. Not too surprisingly, when the transverse-traveling HS20 load was relocated from the slab center to the free-edge, the computed distribution widths decreased due to less 3D stiffness support. Also, when the longitudinal elastic modulus of the top slab was reduced by 30% in comparison to the transverse modulus, the distribution widths decreased by about 5%.

Review Summary and Issues. Equations 1, 2 and 3 have one common purpose, which is to reduce the magnitude of the surface line so that a 2D solution is not overly conservative, i.e., the RSL method. Said another way, if a 3D solution methodology is being used there is no need for Equations 1, 2 and 3, or the RSL method. Even though the three equations have a common purpose, Equation 3 is fundamentally and physically different than Equations 1 and 2. The latter equations represent an intuitive physical model for an expanding longitudinal distribution width through the soil with cover depth H . In contrast, Equation 3 accounts for a 3D stiffness effect that is missing in 2D analysis. Specifically, the RSL reduction factor as computed from Equation 3 and applied to the surface strip load compensates for the additional longitudinal bending and twisting stiffnesses that are not realized with 2D models.

The PennDOT study resulted in significant improvements in the AASHTO LRFD specifications; however, as listed below, there remain several issues in need of additional research and/or clarification.

- (1) Continuity of distribution widths with soil depth. As was shown in Figure 1, there is a discontinuity in distribution widths at the soil depth $H = 2'$ that is slight or modest for small spans but becomes significant as the span increases. Clearly, a smooth transition methodology needs to be developed.
- (2) Influence of culvert length. The PennDOT study used a fixed culvert length of 30' for all finite element models, which may be appropriate for cast-in-place culverts. However, precast box culverts have lay lengths of 8' or less, and precast arches have lay lengths as small as 4'. Although it has been demonstrated that small depths of soil cover negate the need for shear connectors between adjacent units, the lack of moment continuity between adjacent units reduces the 3D stiffness effects. Therefore, the influence of culvert length on distribution widths need to be investigated. It is interesting to note that the 1998 LRFD AASHTO specifications included lay length in the equations for distribution width for spans $> 15'$.
- (3) Limit on span's linear influence. The PennDOT study investigated box culvert spans of 8', 16' and 24' with the result that distribution widths appear to increase linearly with span as exemplified by Equation 3. However, since precast arches have spans up to 72', it is reasonable to extend the investigation to see if there is a limiting span length beyond which the span does not increase the distribution width.
- (4) Verification of procedure for computing distribution widths. Distribution widths were computed from 3D NASTRAN solutions by numerically integrating the force effect (moment or shear) over the culvert length along the loading line and then dividing the result by the peak value of the force effect. Although the PennDOT report succinctly describes this mathematical procedure, the underlying physics is not clear. Verification of the PennDOT procedure with the procedure proposed in this white paper should be undertaken.

Appendix I – Improving AASHTO LRFD/LRFR Specs for 2D for Buried Culverts under LL

- (5) Justification for applying r/c box culvert results to r/c arches. The PennDOT finite element models simulated r/c box-shaped culverts, not precast arches like Con/Span or Bebo. However, AASHTO LRFD specifications (sections 12.14.5.2 and section 4.6.2.10) assign the distribution width developed for box culverts (Equation 3) to arch culverts as well. Since Equation 3 reflects the maximum shear criterion in a box slab loaded near the supporting wall, it is not likely the arch shape will experience the same level of shear. Additional studies are needed to either verify the validity of Equation 3 for arches or propose new distribution widths.
- (6) Potential 3D-effects for all culvert materials and shapes. Based on the PennDOT study a natural question is, “Why shouldn’t all culvert materials and shapes exhibit some level of 3D effects that could be taken advantage of in 2D analysis?” Perhaps the corrugated nature of steel and aluminum culverts result in orthotropic stiffness properties such that the longitudinal bending stiffness does not provide sufficient 3D-stiffness enhancement. In any event this question should be researched.

OBJECTIVES

This white paper is not intended to provide the final answer to the six issues above. Rather the intent of this paper is to provide a framework of concepts, ideas and mechanistic models that offer guidelines and direction for additional 3D finite element studies like the PennDOT study. To this end, this white paper has the following objectives.

1. Develop a flat plate model that illustrates 3D stiffness effects and explicitly provides the functional influence of culvert length, span and orthotropic bending properties in determining distribution widths applicable to 2D analysis.
2. Show graphs of distribution widths as a function of slab properties and compare results with the PennDOT study for the purpose of guiding future 3D investigations.
3. Present an overall strategy on applying distribution widths for 2D analysis using either the reduced surface load (RSL) technique or the new continuous load scaling (CLS) technique
4. Revisit the six issues listed above and offer suggestions on addressing these problems based on the above findings.

CONCEPTUAL MODEL AND INSIGHTS

Description. Figure 3 portrays a rectangular flat plate representing the top slab of a box culvert with fixed-end boundary conditions along the left and right sides and free to deflect at each end. The x,y,z coordinate system originates from the plate’s center where a variable-length line load of magnitude p is applied symmetrically along the z -axis. Spatial variables are denoted as,

- W^* = width of line load acting on slab (culvert)
- S = Span of slab (culvert)
- L = length of slab (culvert)

Appendix I – Improving AASHTO LRFD/LRFR Specs for 2D for Buried Culverts under LL

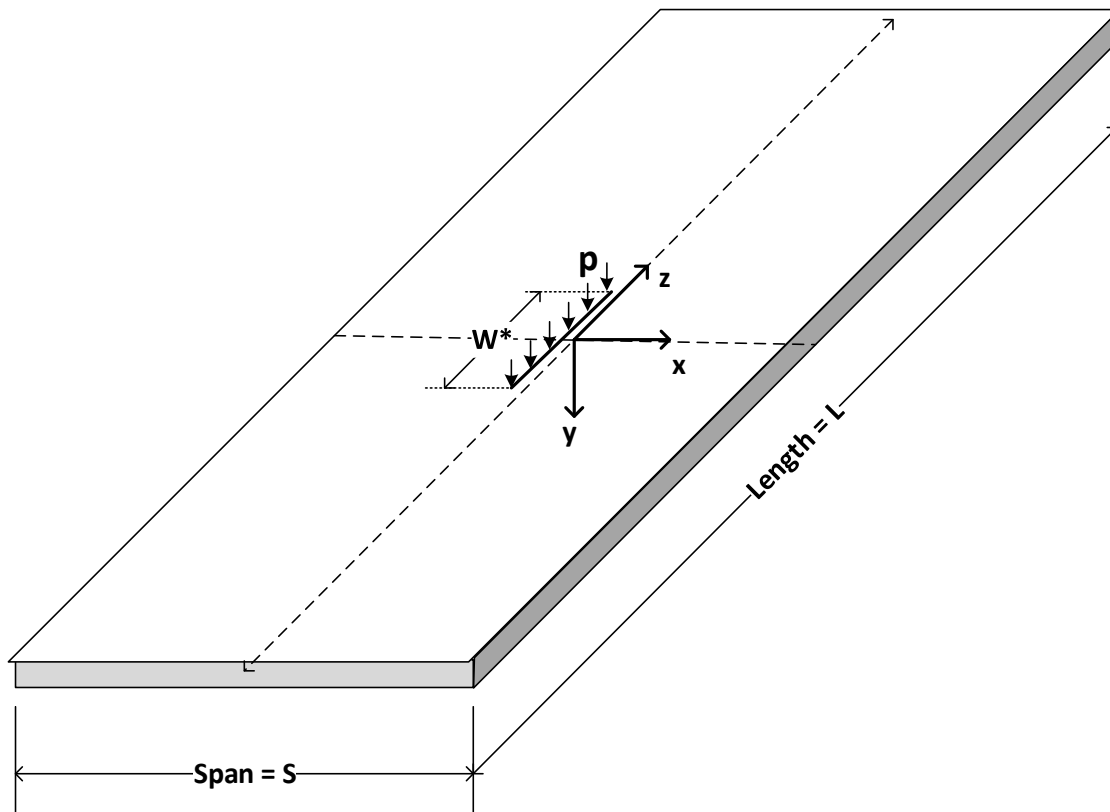


Figure 3. View of rectangular plate model with line-load (lbs./inch).

Big-picture Overview and Concepts. In Part II a closed form solution of the plate model is developed. However, for present purposes, the objective is to illustrate conceptually how this model is useful for shedding light on the special ASSHTO distribution width and providing a clear understanding of the 3D stiffness effects.

To this end, let us temporarily assume that the plate's span, length, line-load magnitude and stiffness properties are fixed, and the only variable parameter is the line-load width W^* . With this understanding, the plate's displacement function is symbolically expressed as,

$$\Delta = f(x, z, W^*) \quad \text{Equation 5}$$

The Δ -function provides a wide range of displaced 3D shapes because W^* may range from 0 to L (or $0 \leq W^*/L \leq 1$). For the special case $W^* = L$, a uniform 2D response is produced because the entire plate deforms in one-way bending like a fixed-end beam. In short, $W^*/L = 1$ produces a uniform, maximum deflected shape independent of z , exactly equivalent to a 2D model using beam theory. Functionally, this maximum displacement profile is denoted by,

$$\Delta_{Max} = f(x, W^* = L) \quad \text{Equation 6}$$

Figure 4 shows the symmetric half of the uniform displacement profile Δ_{Max} from $z = 0$ to $z = L/2$ plotted along the plate centerline through the origin.

Appendix I – Improving AASHTO LRFD/LRFR Specs for 2D for Buried Culverts under LL

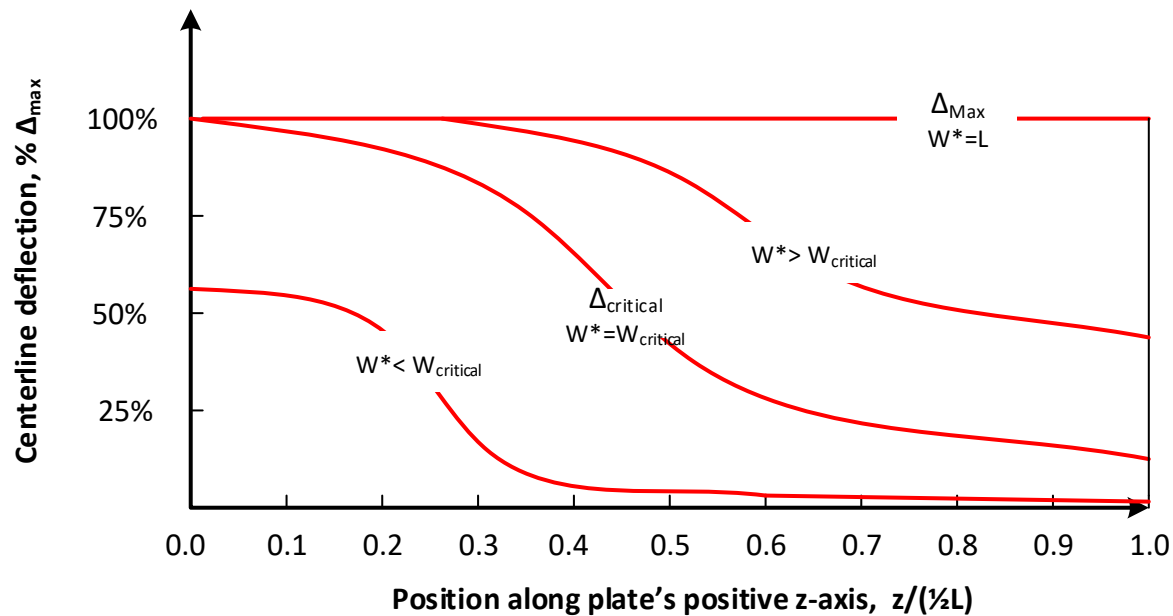


Figure 4. Deflection profiles (symmetric half) for four key choices of W^* .

Also illustrated in Figure 4 is a very special line-load width called the critical distribution width, symbolically expressed as $W_{critical}$. Physically, $W_{critical}$ is the minimum distribution width producing a peak 3D displacement at $z = 0$ that is equal to the uniform maximum 2D displacement, Δ_{Max} . $W_{critical}$ is determined by forming the displacement ratio shown below and incrementally increasing the value of W^* until the ratio is equal to 1.

$$\text{Ratio}(W^*) = \frac{\Delta(W^*)}{\Delta_{Max}} = \frac{f(0,0,W^*)}{f(0,L)} \quad \text{Equation 7}$$

$W_{critical}$ = critical distribution width, i.e., minimum W^* producing $\text{Ratio}(W^*) = 1$

Note that $W_{critical}$ is a physical property of the plate (culvert) irrespective of the soil or burial depth. Moreover, since $W_{critical}$ is determined from the ratio of two solutions, $W_{critical}$ is not influenced by linear plate parameters such as plate stiffness because these parameters cancel out in the ratio. For an isotropic plate, $W_{critical}$ is only dependent on span S and length L .

$W_{critical}$ is used to determine whether or not the actual loading length W^* generates 3D stiffness effects that need to be accounted for in 2D solutions. First consider the case $W^* > W_{critical}$ in which W^* is the line-load width impinging on the slab at soil depth H . As shown in Figure 4, the maximum 3D displacement coincides with maximum 2D displacement in a region about $z = 0$. Within this region both 2D and 3D solutions using the same line-load magnitude produce the same structural distress (i.e., transverse deformations in the plane of the span). Consequently, no adjustment is required for 2D analysis to account for 3D stiffness effects when $W^* > W_{critical}$.

Appendix I – Improving AASHTO LRFD/LRFR Specs for 2D for Buried Culverts under LL

Next consider the 3D deflection profile for the case $W^* < W_{critical}$. As shown in Figure 4 the peak 3D deflection at $z = 0$ is well below the 2D displacement (Δ_{Max}) with the same line-load magnitude. The reduced 3D deflection is due to resistance from longitudinal bending stiffness and plate twisting stiffness in portions of the slab beyond the loading width W^* .

In order to better understand the 3D stiffness effect, imagine the slab (or culvert) to be cut into many beam-like slices parallel to the x-axis, thereby dismantling the 3D stiffness effect by creating 2D slices. If the sliced system is line-loaded over a width W^* , then those loaded slices beneath W^* will deflect to the maximum 2D amount (Δ_{Max}) whereas the unloaded slices remain un-deflected (zero), i.e., no stiffness interaction between loaded and unloaded slices. Hence, it is evident that 2D models lack the additional 3D stiffness that actually exist in contiguous systems. Consequently, some corrective adjustment is required for 2D analysis to account for 3D stiffness effects when $W^* < W_{critical}$.

The traditional and most common method of adjusting the 2D analysis is the reduced surface load (RSL) method previously introduced in the AASHTO review. A second and more accurate method is called continuous load scaling (CLS). Both methods are discussed in the following next two sections to complete the big-picture overview.

Reduced Surface Load (RSL). The RSL method proposed herein is similar to existing AASHTO approach (Equations 1-to-4 and Figure 1) except for two important aspects. First, the discontinuity at $H = 2$ feet is corrected in a logical manner, and second, all distribution widths are referenced to 1-wheel load to avoid the confusion of dealing with axle and 1-wheel loads in the same set of equations. Although the distribution widths are referenced to 1-wheel load, the size of the distribution widths are influenced by both wheel-loads on the axle.

Figure 5 shows a longitudinal view of a culvert shallowly buried at depth H_1 and in deeper burial at depth H_2 . For both burial depths the soil surface is loaded with one wheel so that the longitudinal line-load beneath the wheel on the surface is given by,

$$p_0 = \frac{\text{Wheel-load}}{W_0} \quad \text{Equation 8}$$

where, p_0 = surface line load beneath wheel (lbs./inch)
 Wheel-load = specified weight of 1 wheel (lbs.)
 W_0 = wheel's longitudinal footprint (typically 20 inches)

Shown with red lines is the culvert's critical distribution width $W_{critical}$ that remains constant with soil depth, and shown with green lines the expanding soil-spreading distribution width $W(H)$ representing any valid load-spreading theory. For present purposes, the AASHTO load-spreading theory, as defined in Equations 1 and 2 is adopted, and restated here in terms of 1-wheel load but including the influence of two-wheel axles loads, i.e.,

$$W(H) = \begin{cases} W_0 + LLDF * H & \rightarrow \text{for } H < H_{int} \\ \frac{1}{2}[S_{axle} + W_0 + LLDF * H] & \rightarrow \text{for } H > H_{int} \end{cases} \quad \text{Equation 9}$$

where, $W(H)$ = distribution width under 1-wheel, continuous function of H (inches)
 H = soil depth from surface, usually H = cover depth (inches).
 LLDF = live-load distribution factor = $2\tan(30^\circ) = 1.15$.

Appendix I – Improving AASHTO LRFD/LRFR Specs for 2D for Buried Culverts under LL

S_{axle} = center-to-center wheel spacing on axle (usually 72 inches)

H_{int} = two-wheel interaction soil depth = $(S_{axle} - W_0)/LLDF$ (inches)

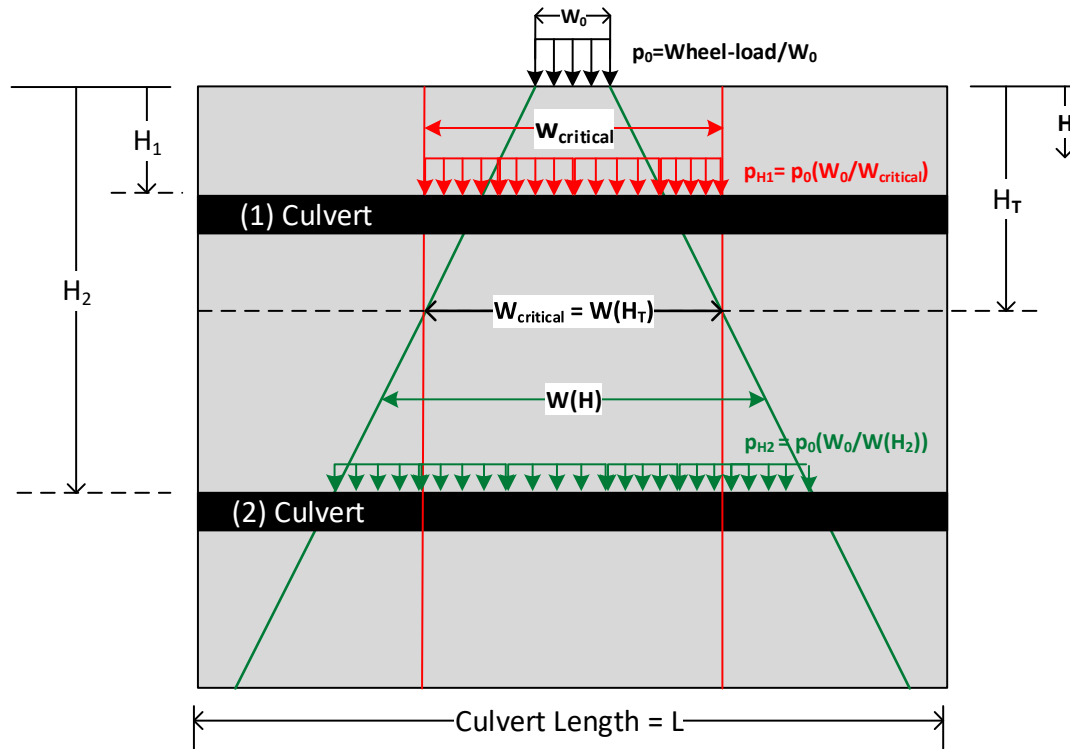


Figure 5. Longitudinal loading on a culvert buried above and below the transition depth, H_T

For shallow burial depth H_1 the above figure indicates that $W_{critical} > W(H_1)$, therefore $W_{critical}$ is the controlling distribution width as explained in the previous section. Preserving the wheel-load force, the reduced surface line load is given by,

$$p_{H1} = r_{H1} p_0 = \text{reduced surface load applicable to } H_1 \quad \text{Equation 10}$$

where, $r_{H1} = \frac{W_0}{W_{critical}}$ = reduction factor for depth H_1

It is worth restating that p_{H1} is not the actual line-load acting on the culvert at depth H_1 ; rather it is a pseudo value to account for the real 3D stiffness effects that are invisible in 2D analysis.

At deeper burial depth H_2 the figure shows $W(H_2) > W_{critical}$; therefore, $W(H_2)$ is the controlling distribution width, and the reduced surface line load is given by,

$$p_{H2} = r_{H2} p_0 = \text{reduced surface load applicable to } H_2 \quad \text{Equation 11}$$

where, $r_{H2} = \frac{W_0}{W(H_2)}$ = reduction factor for depth H_2

Appendix I – Improving AASHTO LRFD/LRFR Specs for 2D for Buried Culverts under LL

The general equation for reduced surface pressure for an arbitrary burial depth H is easily deduced from Equations 10 and 11 as,

$$p_H = r_H p_0 = \text{reduced surface load applicable to any depth H.} \quad \text{Equation 12}$$

where, $r_H = \text{Minimum}\left(\frac{W_0}{W_{\text{critical}}}, \frac{W_0}{W(H)}\right) = \text{reduction factor for any depth H.}$

The above equation for r_H provides a logical and continuous reduction factor for all H; hence, it is recommended as a replacement to the discontinuous AASHTO approach (Equation 4)

As illustrated in Figure 5, the smooth transition occurs at soil depth H_T where red lines intersect the green lines. Simply put, H_T is determined from Equation 9 by setting $W(H_T) = W_{\text{critical}}$; consequently, H_T is not a fixed depth like 2 feet, but rather a variable depth dependent on culvert properties that define W_{critical} .

Although it is not necessary to actually compute H_T , the equation is provided below for reference.

$$H_T = \begin{cases} (W_{\text{critical}} - W_0) / LLDF \rightarrow \text{if } H_T \leq H_{\text{int}} \\ (2W_{\text{critical}} - S_{\text{axle}} - W_0) / LLDF \rightarrow \text{if } H_T > H_{\text{int}} \end{cases} \quad \text{Equation 13}$$

where, H_T = transition soil depth between governing distribution widths (W_{critical} & $W(H)$)

LLDF = live-load distribution factor = $2\tan(30^\circ) = 1.15$.

S_{axle} = center-to-center wheel spacing on axle (usually 72 inches)

H_{int} = two-wheel interaction soil depth = $(S_{\text{axle}} - W_0) / LLDF$ (inches)

In summary the proposed RSL method reduces the surface line load p_0 by the reduction factor r_H as defined by Equation 12 where H is the soil cover depth. Using the reduced line-load on the surface of the 2D model produces structural distress equivalent to 3D analysis.

Continuous Load Scaling (CLS). As presented in the 2017 TRB paper cited below, the CLS method simulates longitudinal load spreading through the soil and structure system by increasing every element's unit thickness by an amplification factor, which is dependent on each element's depth. The amplification factor is simply the inverse of the reduction factor expressed as a variable function of soil depth H, i.e.,

$$\alpha(H_{el}) = \frac{W(H_{el})}{W_0} \quad \text{Equation 14}$$

where, H_{el} = individual cover depth to each soil and culvert element.

$W(H_{el})$ = load spreading width at element level (computed by Equation 9)

$\alpha(H_{el})$ = amplification factor assigned to each individual element.

Equation 14 gives $\alpha(0) = 1.0$ on the surface, and $\alpha(H_{el})$ steadily increases as element depth increases. Thus, unlike RSL that reduces loading based on a single choice of H (usually H= soil cover), CLS reduces the load continuously with soil depth as actually occurs in nature. For details see TRB paper, "Continuous Load Scaling: A New Method to Simulate Longitudinal Live-load Spreading for 2D Finite Element Analysis of Buried Culverts, Transportation Research Record: Journal of the Transportation Research Board, No. 2642, 2017 by M. G. Katona."

Appendix I – Improving AASHTO LRFD/LRFR Specs for 2D for Buried Culverts under LL

As originally presented, the CLS method only corrects for longitudinal load spreading. It did not address the problem of additional 3D stiffness effects in the culvert structure. Fortunately, CLS methodology is well suited to also correct for the missing 3D stiffness effect by modifying the original algorithm as follows. For all culvert elements (not soil elements) whose depths H_{el} are less than the transition depth H_T , the amplification factor is constant and is defined as,

$$\alpha(H_{el}) = \frac{W_{critical}}{W_0} \quad \rightarrow \text{for } H_{el} \leq H_T \text{ (or } W(H_{el}) \leq W_{critical} \text{)} \quad \text{Equation 15a}$$

Otherwise if the culvert element's depth is greater the transition depth, then the original load-spreading amplification factor applies, i.e.,

$$\alpha(H_{el}) = \frac{W(H_{el})}{W_0} \quad \rightarrow \text{for } H_{el} > H_T \text{ (or } W(H_{el}) > W_{critical} \text{)} \quad \text{Equation 15b}$$

Equations 15a&b apply to culvert elements only. All soil elements and other types of elements are amplified by the original CLS procedure (Equation 14).

CRITICAL DISTRIBUTION WIDTH SUMMARY ($W_{CRITICAL}$)

To account for 3D stiffness effects using either RSL or CLS methodology, it is evident that $W_{critical}$ must be known for the particular culvert being analyzed for live loads. To this end, it is useful to summarize essential features of $W_{critical}$ as developed thus far in the white paper.

- $W_{critical}$ is the minimum longitudinal distribution width acting on the surface of a 3D culvert that produces the same in-plane deformation as a 2D culvert with same line-load magnitude.
- By convention $W_{critical}$ is the longitudinal distribution width beneath 1-wheel, not an axle. However, the physical width of $W_{critical}$ is influenced by both wheels on the axle.
- Equation 7 describes how $W_{critical}$ can be determined from 3D culvert models by forming the displacement ratio = $\Delta(W^*)/\Delta(L)$, and then finding the minimum value of W^* such that ratio = 1. Clearly $W_{critical}$ is a culvert property independent of the soil and only dependent on those culvert properties that don't cancel out of the displacement ratio.
- As will be shown, $W_{critical}$ is strongly dependent on culvert span and length (S and L). Other factors influencing $W_{critical}$ include the degree of orthotropic stiffness and the location of the line-load relative to fixed or free edges.
- Currently, the only existing expression representing $W_{critical}$ comes from the PennDOT study, and adopted in the current AASHTO LRFD specifications for r/c boxes and arches. By setting $W_{critical} = \frac{1}{2} \text{ Elong}$ where the $\frac{1}{2}$ factor implies 1-wheel load instead of an axle load, we get,

$$W_{critical} = \frac{1}{2} [96" + 1.44 * \text{Span(ft)}] \quad \text{inches}$$

Appendix I – Improving AASHTO LRFD/LRFR Specs for 2D for Buried Culverts under LL

Using the above expression for $W_{critical}$ in the proposed RSL or CLS methods results in the same 2D analysis prediction as the current AASHTO methodology except soil depths in the range $2' < H < H_T$ wherein the new procedure provides a smooth transition without discontinuities.

The second half of this white paper is devoted to developing a rational framework to quantify $W_{critical}$ based on a plate model representing the top slab of a r/c box culvert. Verification and calibration from 3D finite models are needed to transform the framework into useful equations for AASHTO specifications.

PART II -- PLATE MODEL DEVELOPMENT AND SOLUTION

PLATE MODEL FORMULATION

Configuration. As previously presented in Figure 3, the plate model simulates the top slab of a reinforced concrete box culvert. By taking advantage of double symmetry, the analytical model only requires one quadrant of the full plate as shown in Figure 6. Since the origin of the coordinate system is at the center of the full plate, the quadrant's x and z dimensions are $\frac{1}{2}$ Span and $\frac{1}{2}$ Length, respectively.

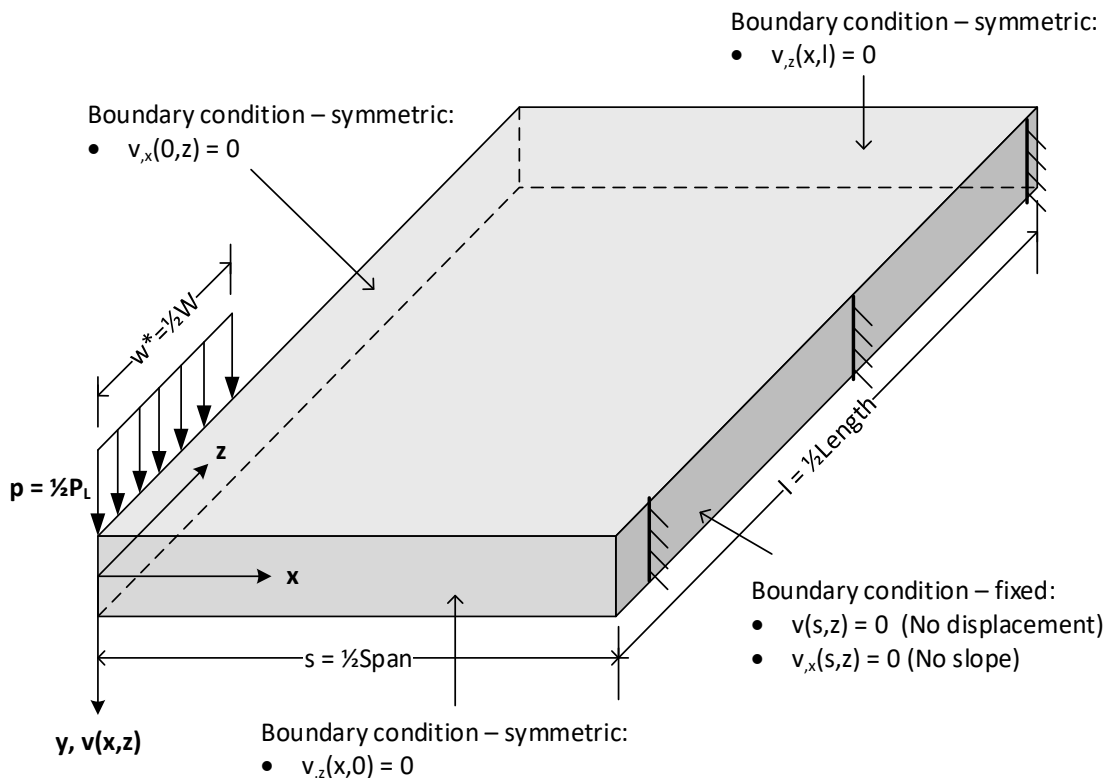


Figure 6. Flat plate model quadrant exploiting double symmetry.

For convenience all half-dimensions are denoted by lower-case letters representing half measures of the full-plate dimensions listed below.

Appendix I – Improving AASHTO LRFD/LRFR Specs for 2D for Buried Culverts under LL

- $s = \frac{1}{2}S =$ half Span of plate (slab)
- $l = \frac{1}{2}L =$ half Length of plate (slab)
- $w^* = \frac{1}{2}W^* =$ half longitudinal load width.

Although Figure 6 appears to be an isotropic plate with uniform thickness h , the following formulation allows for orthotropic moment of inertia values I_x and I_z in the two orthogonal directions.

Formulation. Kirchhoff plate theory is adopted for this study wherein the two basic assumptions are;

(1) lines normal to the mid-surface remain straight and normal upon plate bending, and (2) stress and strain through plate thickness is negligible ($\sigma_{yy} = \epsilon_{yy} = 0$). The above assumptions lead to the following kinematic approximations used in Kirchhoff plate theory (similar to Bernoulli-Euler beam theory),

$$\begin{aligned} v &= v(x, z) \\ u &= u(x, y, z) = -yv_{,x} \\ w &= w(x, y, z) = -yv_{,z} \end{aligned} \quad \text{Equation 16}$$

where, v = vertical displacement of plate, i.e., the primary unknown function.

u, w = in-plate displacement functions, related to gradients of v .

and, $v_{,x} = \frac{\partial v}{\partial x}$ and $v_{,z} = \frac{\partial v}{\partial z}$; higher partial are $v_{,xx} = \frac{\partial^2 v}{\partial x^2}$, $v_{,xz} = \frac{\partial^2 v}{\partial x \partial z}$, $v_{,zz} = \frac{\partial^2 v}{\partial z^2}$, etc.

Shear forces per unit length are defined by integrating the shear stresses over the plate thickness from $y = -\frac{1}{2}h$ to $y = \frac{1}{2}h$.

$$Q_x = \int_{-h/2}^{h/2} \tau_{xy} dy = \text{downward shear force per unit length } dz \text{ acting on the x-face}$$

$$Q_z = \int_{-h/2}^{h/2} \tau_{zy} dy = \text{downward shear force per unit length } dx \text{ acting on the z-face}$$

Moments per unit length are defined by integrating stress components with moment-arm y over the plate thickness from $y = -\frac{1}{2}h$ to $y = \frac{1}{2}h$.

$$M_x = \int_{-h/2}^{h/2} \sigma_{xx} y dy = \text{bending moment per unit length } dz \text{ acting on the x-face (about z-axis)}$$

$$M_z = \int_{-h/2}^{h/2} \sigma_{zz} y dy = \text{bending moment per unit length } dx \text{ acting on the z-face (about x-axis).}$$

$$M_{xz} = \int_{-h/2}^{h/2} \tau_{xz} y dy = \text{twisting moment per unit length } dz \text{ acting on the x-face (about x-axis).}$$

$$M_{zx} = \int_{-h/2}^{h/2} \tau_{zx} y dy = \text{twisting moment per unit length } dx \text{ acting on the z-face (about z-axis).}$$

Appendix I – Improving AASHTO LRFD/LRFR Specs for 2D for Buried Culverts under LL

By expressing stresses in terms of displacement gradients via stress-strain and strain-displacements relationships, the y integrations are performed over the two differential faces $dx dy$ and $dz dy$, wherein different stiffness properties are allowed on the x-face and y-face. This operation results in the following moment-to-curvature equations,

$$M_x = \int_{-h/2}^{h/2} \sigma_{xx} y dy = -\frac{EI_x}{1-\mu^2} (v_{,xx} + \mu v_{,zz})$$

$$M_z = \int_{-h/2}^{h/2} \sigma_{zz} y dy = -\frac{\alpha EI_x}{1-\mu^2} (v_{,zz} + \mu v_{,xx}) \quad \text{Note: } I_z = \alpha I_x \quad \text{Equation 17}$$

$$M_{xz} = M_{zx} = \int_{-h/2}^{h/2} \tau_{xz} y dy = -\frac{\frac{1}{2}(1+\alpha)EI_x}{1-\mu^2} (1-\mu)v_{,xz}$$

where E = Young's modulus of material

μ = Poisson ratio

I_x = 2nd moment of inertia on x-face of plate thickness.

I_z = 2nd moment of inertia on z-face of plate thickness = αI_x

$\alpha = I_z/I_x$ = orthotropic ratio (isotropic if $\alpha = 1$)

Equilibrium of moments about the x and z axis and vertical force equilibrium lead to the following 3 equilibrium equations,

$$Q_x = M_{x,x} + M_{z,x,z} \quad \text{Equation 18}$$

$$Q_z = M_{z,z} + M_{x,z,x} \quad \text{Equation 19}$$

$$M_{x,xx} + 2M_{xz,xz} + M_{z,zz} + q(x,z) = 0 \quad \text{Equation 20}$$

where $q(x,z)$ = applied surface pressure on plate interior.

Finally, inserting the moment-curvature expressions into the governing equilibrium equation leads to the governing partial differential equation for an orthotropic plate,

$$D_X [v_{,xxxx} + (1+\alpha)v_{,xz,xz} + \alpha v_{,zzzz}] = q(x,z) \quad \text{Equation 21}$$

where, $D_X = EI_X/(1-\mu^2)$ = plate bending stiffness for x-face per unit length in z direction.

$D_Z = \alpha D_X$ = plate bending stiffness for z-face per unit length in x direction

$\alpha = I_z/I_X$ = ratio of in-plane to out-of-plane flexural stiffness for orthotropic plates.

$q(x,z) = 0$, No interior surface pressure per Figure 6.

Appendix I – Improving AASHTO LRFD/LRFR Specs for 2D for Buried Culverts under LL

Interior plate pressure loading is zero, $q(x,z) = 0$, because loading is applied through the shear-force boundary condition as discussed next.

Boundary Conditions (BC). Along with the above partial differential, boundary conditions must be specified along the four sides of the plate quadrant as portrayed in Figure 6. Each side of the quadrant requires two valid boundary conditions. A valid boundary condition is called “ridged” if it prescribes displacements or slopes. Alternatively, it is called “natural” if it prescribes shears or moments. Table 1 identifies the two boundary conditions assigned to each of the 4 quadrant sides.

Table 1. Specified boundary conditions as portrayed in Figure 6

B.C. set number	Quadrant side: (x_a, z_a) to (x_b, z_b)	Rigid B.C.	Natural B.C.
1	z-face along front side, $(0,0)$ to $(s,0)$	$v_{,z}(x,0) = 0$ Symmetric condition, no slope	$Q_z = 0$, No shear
2	x-face along left side $(0,0)$ to $(0,l)$	$v_{,x}(0,z) = 0$ Symmetric condition, no slope	$Q_x = p$, shear $0 \leq z \leq w^*$ $Q_x = 0$, No shear $w^* \leq z \leq l$
3	z-face along back side $(0,l)$ to (s,l)	$v_{,z}(x,l) = 0$ Symmetric condition, no slope	$Q_z = 0$, No shear
4	x-face along right side $(s,0)$ to (s,l)	$v(s,z) = 0$ (no displacement) $v_{,x}(s,z) = 0$ (no slope)	None

BC sets #1 and #2 are the double-symmetry assumption, which is enforced by specifying zero slope normal to the boundary side and specifying the value of boundary shear load, zero or otherwise. In particular, BC set #2 prescribes the non-zero shear load p acting over a chosen longitudinal width w^* , where p is the line-load magnitude,

$$p = \frac{1}{2} \frac{\text{Wheel-load}}{W^*} = \frac{1}{2} \frac{\text{Wheel-load}}{2w^*} \quad \text{Equation 22}$$

The above $\frac{1}{2}$ factor implies the full-plate line load P is split into p half-values for each half plate. As a consequence of the BC set #1 the bottom half of the full plate responds as the mirror image of the top half, and BC set #2 the left side of the full plate responds as the mirror image of the right half.

BC set #3 is a special choice that needs explanation. Ordinarily the free end of the culvert would be assigned the natural boundary conditions enforcing shear and moment to be zero ($Q_z = M_z = 0$). However, BC set #3 is assigned a symmetry condition inferring that plate repeats indefinitely in periodic lengths L wherein each periodic length experiences the same shear line-loading defined in BC set #2. For long culvert lengths, say $L \geq 30'$, the periodic longitudinal loading has negligible influence on the deformation in the primary plate, i.e., Saint-Venant's principle. However, for shorter lay lengths, say 4' to 8' lengths typical of precast culverts, the periodic loading causes additional deformation in the primary length, more so for 4' than 8' lengths, but conservative results in either case. Since it is known from the PennDOT study that loading the slab's free end produces more deformation than loading the slab's central region, BC set #3 is intentionally chosen to produce additional deformation in short-length culverts because they are more likely experience free edge loading than longer length culverts. Thus, BC set #3 appears to be a reasonable representation for all lay lengths.

Finally, BC set #4 represents a fixed connection where the top slab is connected to the side walls allowing neither rotation or displacement. This choice is deemed more realistic for a box culvert than a pinned

Appendix I – Improving AASHTO LRFD/LRFR Specs for 2D for Buried Culverts under LL

connection. Moreover, it is postulated that the ratio-forming procedure used to compute the critical distribution width $W_{critical}$ is relatively insensitive to the choice of slab-to-wall connection.

RITZ SOLUTION METHODOLOGY

After an extensive literature search, a closed form solution for the flat palate portrayed in Figure 6 with boundary conditions shown in Table 1 could not be found even for an isotopic plate, let alone an orthotopic case. Accordingly, the author proceeded to develop an approximate closed-form solution based on virtual work together with the Ritz method. Highlights of the development are provided below and detailed developments are presented in the addendum to this report.

Virtual work and Ritz method. Shown below is the virtual work statement that is equivalent to the partial differential equation in Equation 21 and the natural boundary conditions in Table 1.

$$D_x \int_{x=0}^{x=s} \int_{z=0}^{z=l} \{ \delta v_{,xx} (v_{,xx} + \mu v_{,zz}) + \alpha \delta v_{,zz} (v_{,zz} + \mu v_{,xx}) + (1 + \alpha)(1 - \mu) \delta v_{,xz} v_{,xz} \} dx dz - \int_{z=0}^{z=w^*} \delta v(p) dz = 0$$

where δ is the virtual variation symbol and all other symbols are as defined in the previous formulation.

The Ritz method requires choosing a trial function for $v(x,z)$ composed of linearly independent functions in x and z with unknown coefficients. The first requirement is that the trial function must satisfy all rigid boundary conditions, thereby determining values for some of the unknown coefficients. The remaining unknown coefficients are determined by satisfying the virtual work expression, which produces a set of coupled algebraic equations based on the independent virtual variation of each unknown coefficient.

As the number of selected linearly independent functions increases, the Ritz solution is more and more accurate and becomes the exact solution in the limit. For a finite set of linearly independent functions, the Ritz solution is equivalent to minimizing strain energy, but generally reacts a little stiffer than the exact solution.

Ritz trial function. The trial function adopted in this study is separable in x and z as expressed below.

$$v(x, z) = X(x)Z(z) \quad \text{Equation 23}$$

$$\text{where } X(x) = 1 + C_1 \frac{x}{s} + C_2 \frac{x^2}{s^2} + C_3 \frac{x^3}{s^3} \quad \text{Unknown coefficients: } C_1, C_2, \text{ and } C_3$$

$$Z(z) = B_0 + B_1 \frac{z}{l} + B_2 \frac{z^2}{l^2} + B_3 \frac{z^3}{l^3} + B_4 \frac{z^4}{l^4} \quad \text{Unknown coefficients } B_0, B_1, B_2, B_3, \text{ and } B_4.$$

Upon enforcing the 5 rigid boundary conditions listed in Table 1, the Ritz trial function is reduced to the following expression with 3 unknown parameters B_0 , B_2 and B_3 as expressed below,

$$v(x, z) = [1 - 3 \frac{x^2}{s^2} + 2 \frac{x^3}{s^3}] [B_0 + (\frac{z^2}{l^2} - \frac{1}{2} \frac{z^4}{l^4}) B_2 + (\frac{z^3}{l^3} - \frac{3}{4} \frac{z^4}{l^4}) B_3] \quad \text{Equation 24}$$

Finally, introducing the reduced trial function into the virtual work statement provides three algebraic equation for determining B_0 , B_2 and B_3 . This operation is extremely labor-intensive requiring hundreds of

Appendix I – Improving AASHTO LRFD/LRFR Specs for 2D for Buried Culverts under LL

integrations and mathematical manipulations. After several ill-fated attempts, the following results are believed to be accurate.

Ritz solution of plate model. The final Ritz solution for the plate's displacement function due to a single wheel line-load in the middle of the full plate is summarized below:

$$v(x, z) = p \frac{s^3}{D_x} \left[1 - 3 \frac{x^2}{s^2} + 2 \frac{x^3}{s^3} \right] \left[Q_1 + Q_2 \left(\frac{z^2}{l^2} - \frac{1}{2} \frac{z^4}{l^4} \right) + Q_3 \left(\frac{z^3}{l^3} - \frac{3}{4} \frac{z^4}{l^4} \right) \right] \quad \text{Equation 25}$$

where, $v(x, z)$ is plate displacement function

x, z = spatial coordinates with origin at plate center

s = $\frac{1}{2}$ Span of plate in x-direction

l = $\frac{1}{2}$ Length of plate in z-direction.

p = magnitude of line-load over width w^*

D_x = plate stiffness parameter in x-direction

Q_1, Q_2, Q_3 = solution parameters as determined below.

The three Q parameters are dependent on loading components P_1, P_2 and P_3 and system parameters a, b, c and d as shown below:

$$\begin{aligned} Q_3 &= \frac{1}{ad - bc} (-cP_2 + aP_3) \\ Q_2 &= \frac{1}{ad - bc} (dP_2 - bP_3) \\ Q_1 &= P_1 - \frac{7}{30} Q_2 - \frac{1}{10} Q_3 \end{aligned} \quad \text{Equation 26}$$

The three loading components P_1, P_2 and P_3 are dependent on the fraction of culvert length that is loaded by the longitudinal width, w^*/l , as expressed below.

$$\begin{aligned} P_1 &= \frac{1}{12} \left(\frac{w^*}{l} \right) \\ P_2 &= \frac{1}{30} \left(-7 \frac{w^*}{l} + 10 \frac{w^{*3}}{l^3} - 3 \frac{w^{*5}}{l^5} \right) \\ P_3 &= \frac{1}{20} \left(-2 \frac{w^*}{l} + 5 \frac{w^{*4}}{l^4} - 3 \frac{w^{*5}}{l^5} \right) \end{aligned} \quad \text{Equation 27}$$

Finally, the system parameters a, b, c and d are defined below and are dependent on span-to-length ratio s/l and orthotropic stiffness ratio $\alpha = D_z/D_x$,

Appendix I – Improving AASHTO LRFD/LRFR Specs for 2D for Buried Culverts under LL

$$\begin{aligned}
 a &= \frac{64}{175} \left[\left(1 + \frac{s^2}{l^2} \right) + \alpha \frac{s^2}{l^2} \left(1 + \frac{13 s^2}{4 l^2} \right) \right] \\
 b &= \frac{33}{175} \left[\left(\frac{43}{44} + \frac{s^2}{l^2} \right) + \alpha \frac{s^2}{l^2} \left(1 + \frac{39 s^2}{11 l^2} \right) \right] \\
 c &= \frac{33}{175} \left[\left(\frac{43}{44} + \frac{s^2}{l^2} \right) + \alpha \frac{s^2}{l^2} \left(1 + \frac{39 s^2}{11 l^2} \right) \right] \\
 d &= \frac{18}{175} \left[\left(\frac{11}{12} + \frac{s^2}{l^2} \right) + \alpha \frac{s^2}{l^2} \left(1 + \frac{13 s^2}{3 l^2} \right) \right]
 \end{aligned}$$

Equation 28

RITZ 1-WHEEL SOLUTION VERIFICATION AND INSIGHTS

Verification of 1-wheel Ritz solution for one-way bending. When the culvert length is fully loaded so that $W^*/L = 1$, the above equations yield $P_1 = 1/12$ and $P_2 = P_3 = 0$, which in turn dictates that $Q_1 = 1/12$ and $Q_2 = Q_3 = 0$. Consequently, the displacement profile is independent of z , which indicates a 2D response with one-way bending like a beam, i.e.,

$$v(x) = \frac{1}{12} p \frac{s^3}{D_x} \left(1 - 3 \frac{x^2}{s^2} + 2 \frac{x^3}{s^3} \right) \quad \text{Equation 29a}$$

The maximum displacement occurs all along the plate centerline where $x=0.0$, so that the maximum 2D displacement used to normalize the 3D Ritz 1-wheel solutions is given by,

$$\Delta_{Max} = v(0) = \frac{1}{12} p \frac{s^3}{D_x} \quad \text{Equation 29b}$$

As desired, the above equation is identical to the 2D-plane strain displacement profile of a fixed-end beam of length = $2s$ with unit width and central load $2p$. Therefore, the Ritz solution is awarded a degree of confidence that is further bolstered by additional checks that reveal that net shear and moment equilibrium are maintained for all variations of the system parameters. Nonetheless, the Ritz solution is only an approximate solution due to the restricted number of independent Ritz trial functions.

Span and Length Measures for Concrete Culvert Products. The span-to-length ratio (S/L) is a key parameter influencing the longitudinal displacement profile when W^*/L is less than 1. Table 2 lists the span and lay length measures for typical concrete culvert products. Precast r/c products are available in well-defined span and lay-length combinations from manufacturers. On the other hand, cast-in-place products are generally continuous for the entire culvert length. However, 30 feet is considered a reasonable upper limit to retain moment continuity due to cold joints and micro cracking.

Appendix I – Improving AASHTO LRFD/LRFR Specs for 2D for Buried Culverts under LL

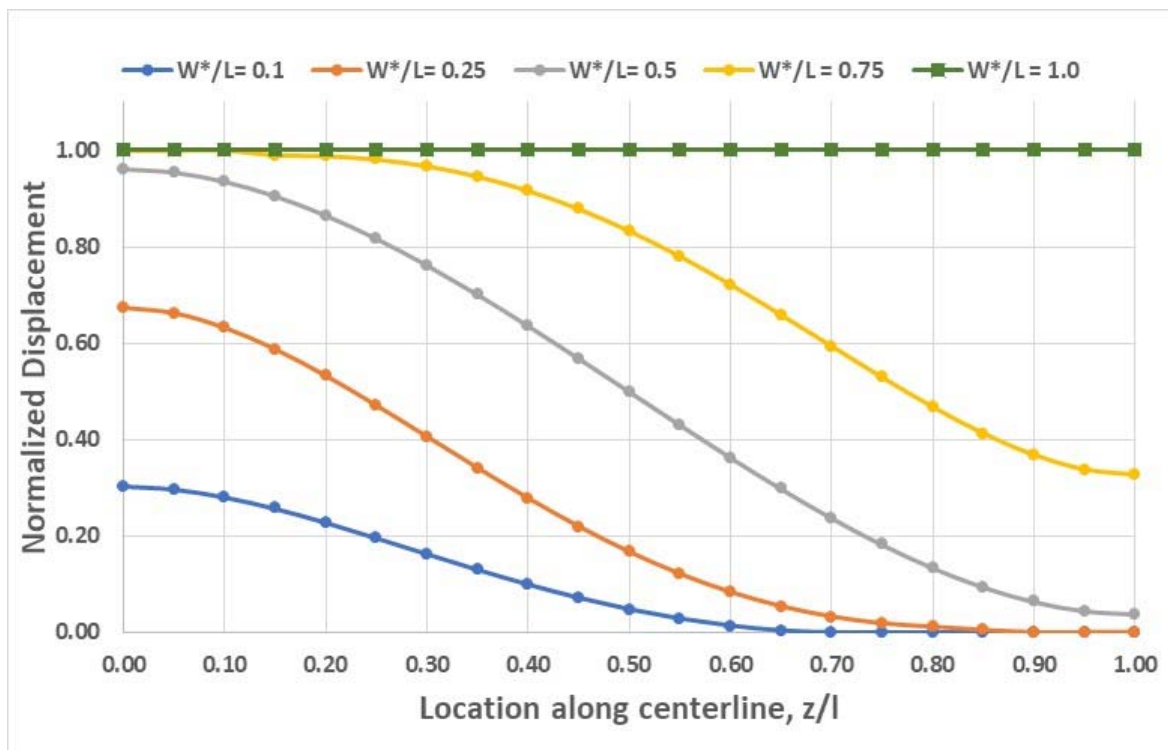
Table 2. Spans and associated lay lengths for R/C culverts.

R/C Culvert Product	Span range 4-10 feet	Span range 12-24 feet	Span range 26-42 feet	Span range 44-72 feet
Precast arch	NA*	L = 8 ft	L = 6 ft	L = 4 ft
Precast box	L = 8 ft	L = 4 ft	NA	NA
Pipes	L = 8 ft	L = 4 ft	NA	NA
Cast-in-place	NA	L = 30 ft	L = 30 ft	L = 30 ft
S/L range	0.5 to 1.3	0.4 to 6.0	0.9 to 7.0	1.5 to 18.0

NA = Generally not available or constructed.

Plots and Insights from 1-wheel loading. The 1-wheel Ritz solution, which is given by Equations 25 to 28, requires graphical plots to gain an understanding of how the displacement profiles are influenced by the parametric ratio S/L . Guided by Table 2, a realistic set of three values are chosen to show how S/L ratios influences displacement patterns.

Figures 7a, b & c show longitudinal displacement profiles for the $S/L = 0.4, 0.8$ and 2.0 , respectively. Each figure shows five displacement profiles representing increased load lengths; $W^*/L = 0.1, 0.25, 0.50, 0.75$ and 1.00 . Each profile starts at the load center ($x = 0, z = 0$) and continues along the centerline to the plate edge ($x = 0, z = l$). Displacements are normalized by dividing by the corresponding 2D solution, i.e., Δ_{Max} in Equation 29b. Isotropic plate properties are assumed in all cases, $\alpha = D_y/D_x = 1$.

**Figure 7a. Normalized displacement profiles for $S/L = 0.4$**

Appendix I – Improving AASHTO LRFD/LRFR Specs for 2D for Buried Culverts under LL

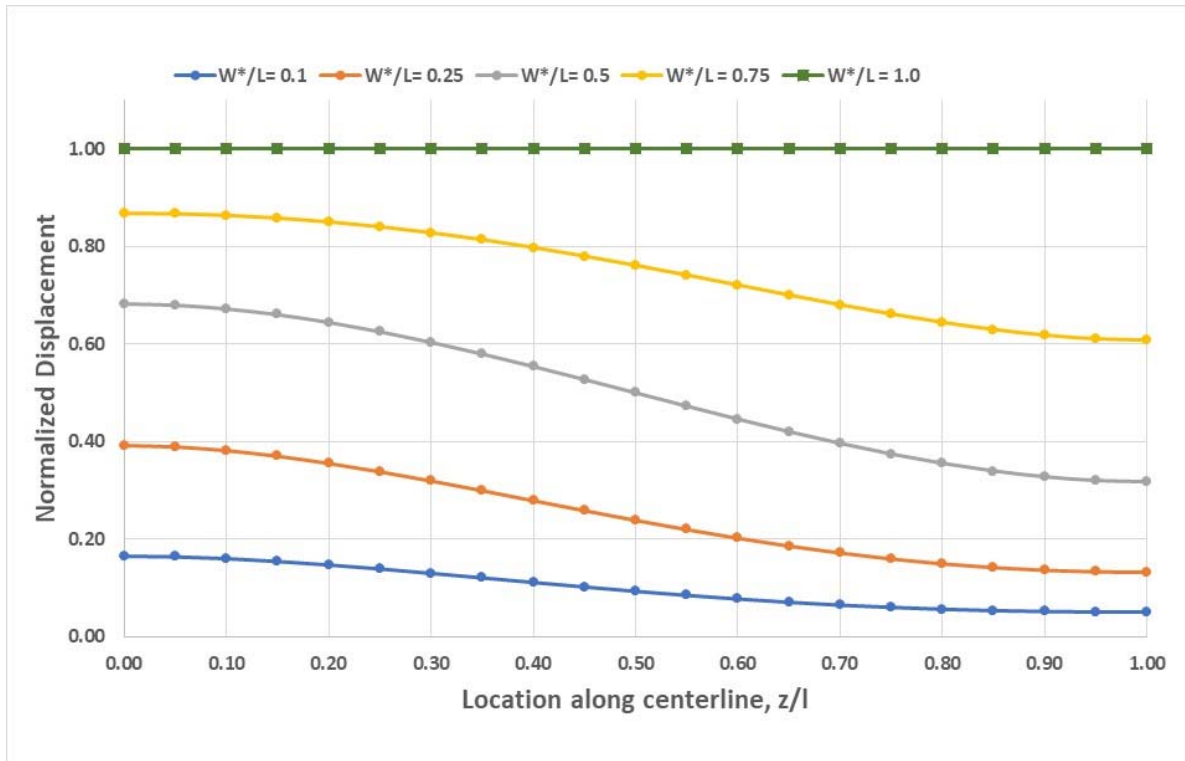
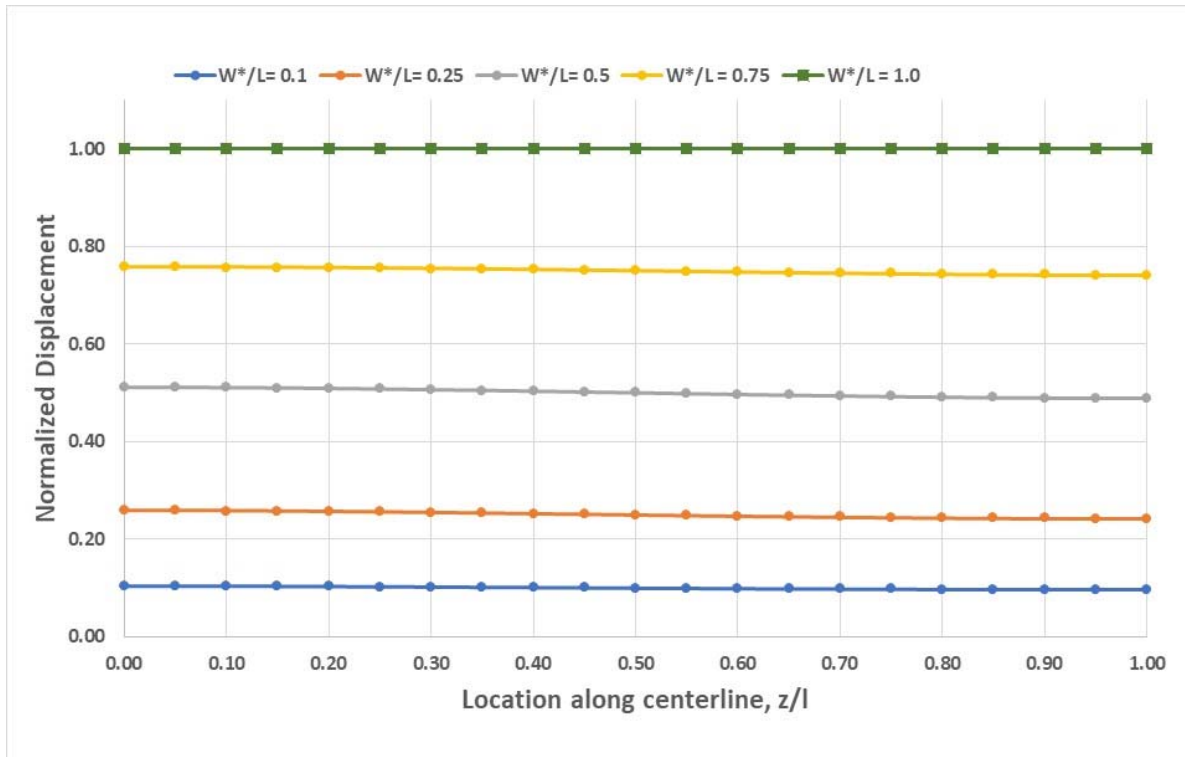


Figure 7b. Normalized displacement profile for $S/L = 0.8$



Appendix I – Improving AASHTO LRFD/LRFR Specs for 2D for Buried Culverts under LL

Figure 7c. Normalized displacement profile for $S/L = 2.0$

Figure 7a shows that when S/L is less than 0.5 the deflection profiles have pronounced peaks under the load, and the value of $W_{critical}/L$ is approximately 0.5 or less. $W_{critical}/L$ is the W^*/L ratio producing the first peak approaching Δ_{Max} . Conversely, Figure 7c illustrates that when S/L is greater than 1.5 the deflection profiles become uniformly flattened and $W_{critical}/L$ is approximately 1.0.

Figure 8 is a useful and pragmatic graph of $W_{critical}/L$ versus S/L with many data points for S/L and W^*/L . $W_{critical}/L$ is determined by special spreadsheet programming to find the first W^*/L value producing a peak displacement equal to 90% of Δ_{Max} . The reduced value of 90% instead of 100% Δ_{Max} was chosen for three reasons; (1) 90% Δ_{Max} produces slightly conservative values for $W_{critical}/L$, (2) 90% Δ_{Max} compensates for inherently over-stiff Ritz solution, and (3) 90% Δ_{Max} mitigates the numerical asymptotic error inherent with 100% Δ_{Max} .

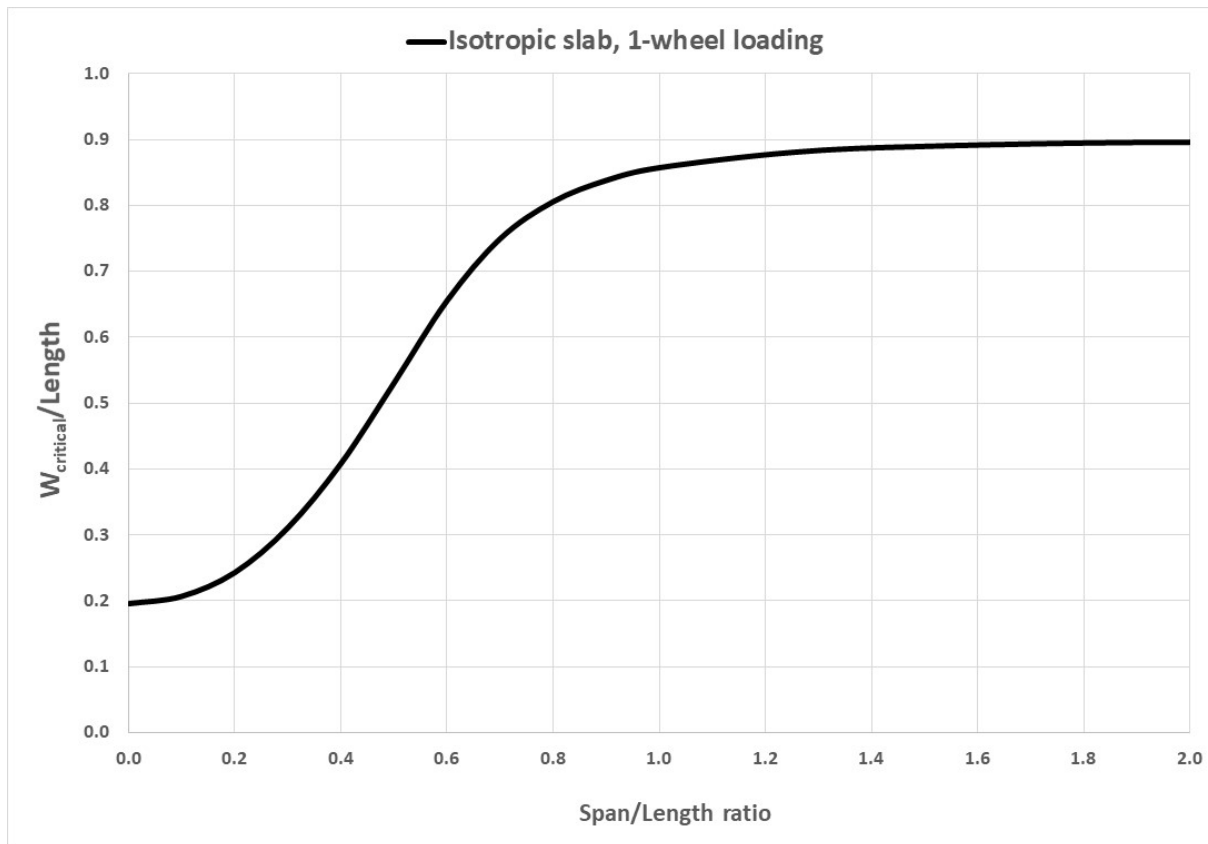


Figure 8. $W_{critical}/Length$ vs $Span/Length$ for 1-wheel loading at slab center (isotropic slab)

The above curve provides a complete solution for $W_{critical}$ for all span and length dimensions assuming the slab is loaded by only 1-wheel at the slab center. Here it is observed that $W_{critical}/L$ increases as S/L increases up to a limit of $S/L \approx 1.5$. Thereafter, $W_{critical}/L$ remains effectively constant at $W_{critical}/L = 0.9$.

Since Figure 8 only applies to 1-wheel load located at the slab center, the curve's pragmatic utility is restricted to lay lengths 6 feet or less because lay lengths greater than 6 feet are subjected to loading from

Appendix I – Improving AASHTO LRFD/LRFR Specs for 2D for Buried Culverts under LL

both wheels on the truck's axle. In the next section, the solution to the 2-wheel problem is approximated by superposition of the 1-wheel R_i

RITZ 2-WHEEL SOLUTION BY SUPERPOSITION

Given that truck axles have two wheels, which are typically spaced at 6 feet, the second wheel may also contribute to the culvert's displacement profile depending on the culvert's lay length. In particular, if the culvert lay length is greater than 6 feet, then the displacement profile induced by the second wheel needs to be added (superimposed) to the deflection profile from first wheel.

In this study the second deflection profile is approximated by rigidly shifting the 1-wheel deflection profile 6 feet (spacing along axle) to the right of the slab center. This approach requires that the culvert must be at least 12 feet long or more in order that the shifted profile makes physically sense for two full wheel loading. To summarize, the 1-wheel Ritz solution applies to culverts 6 feet or less, and the 2-wheel superposition solution applies to culverts 12 feet or more. For lay lengths between 6 and 12 feet, the solutions are interpolated from the 6-foot and 12-foot lay length solutions.

Plots and insights from 2-wheel loading. An illustration of the superposition procedure is shown below for a culvert length $L=15$ feet, span $S = 10$ feet, and loading-length ratio $W^*/L = 0.40$.

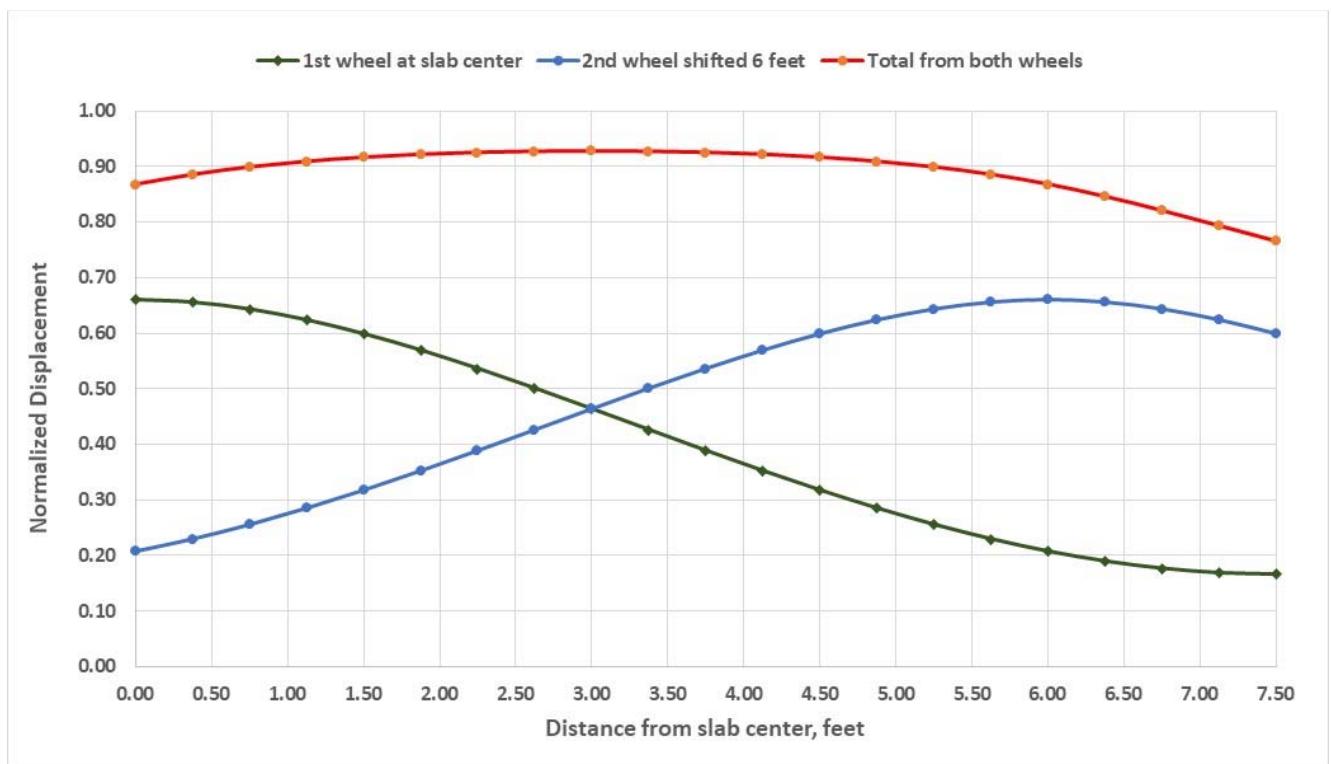


Figure 9. Displacement profiles 2-wheel loading for $L= 15$ ft, $S = 10$ ft and $W^*/L = 0.4$

Since the displacement profile of the first wheel peaks at the origin and is symmetric about the origin, the 2nd wheel displacement profile peaks and is symmetric about the 6-foot offset position due to the ridged shift approximation. Superimposing the two curves to produce the combined 2-wheel deflection profile usually produces a peak displacement midway between the wheels as illustrated by the red curve at the 3-foot mark. In this example $S/L = 0.667$; however, in cases when S/L is smaller, the peak combined displacement may occur at both wheel locations.

Appendix I – Improving AASHTO LRFD/LRFR Specs for 2D for Buried Culverts under LL

One last observation from Figure 9 is the 2-wheel peak displacement happens to be slightly greater than 90% of Δ_{Max} (i.e. 90% of Normalized Displacement), which means $W_{critical}/L$ is slightly less than the chosen ratio $W^*/L = 0.4$. It is important to remember that in this study W^*/L is defined as the loading-length ratio beneath one wheel only. Hence, 2-wheel loading on the slab requires a smaller critical loading-length ratio $W_{critical}/L$ than does just 1-wheel loading.

Similar to Figure 8, Figure 10 presents graphs of $W_{critical}/L$ versus S/L that includes 2-wheel loading for culvert lengths up to 30 feet. As before, $W_{critical}/L$ is determined by special spreadsheet programming to find the first W^*/L value producing a peak displacement equal to 90% of Δ_{Max} . Of course, the superposition procedure is more complex because the 2-wheel peak displacement may occur at the slab center or between the two wheels depending on the S/L ratio and the physical length L . Table 3 summarizes how the parametric-length curves in Figure 10 are generated.

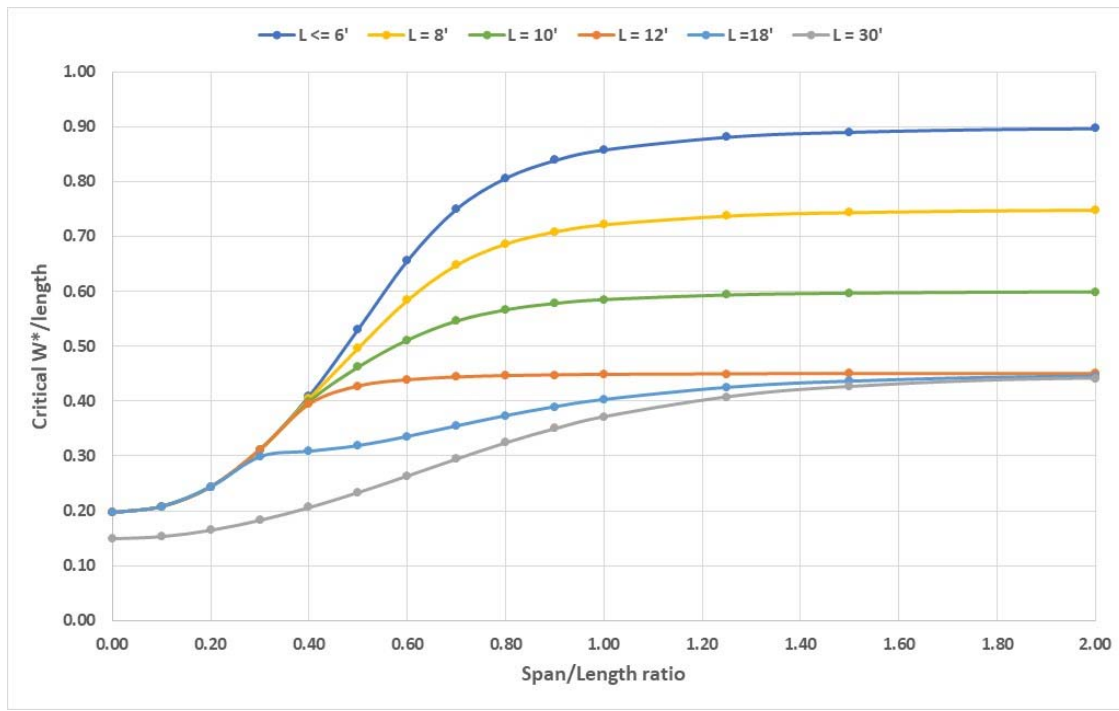


Figure 10. Complete set of graphs for $W_{critical}/L$ versus S/L for parametric slab lengths.

Table 4. Procedure used to generate parametric-length curves in Figure 10.

Culvert length L feet	Procedure to determine $W_{critical}/L$ vs S/L for L-dependent curves
$L \leq 6$ ft	Ritz 1-wheel solution. (Applies to lengths ≤ 6 ft, only 1 wheel fits)
$7 \text{ ft} \leq L \leq 11$ ft	Interpolated between $L = 6'$ & $L = 12'$. (Transition 1 to 2 wheels).
$L \geq 12$ ft	Superposition for 2-wheels. (Applies to lengths ≥ 12 ft, 2 wheels fit)

Appendix I – Improving AASHTO LRFD/LRFR Specs for 2D for Buried Culverts under LL

Given the length and span dimensions for any slab (culvert), Figure 10 provides the means to compute $W_{critical}$ to account for the 3D stiffness effect of that particular culvert. It is interesting to note for culverts with lengths of 12 feet or less, the $W_{critical}/L$ vs S/L curves are identical in the range $0 \leq S/L \leq 0.4$, and thereafter the curves diverge. This is because corresponding displacement profiles for $S/L \leq 0.4$ have pronounced bell shapes such as shown in Figure 7a so the 2nd wheel does not contribute to the peak deflection. As S/L increases all curves approach an asymptotic limit between 0.9 for $L \leq 6$ feet and 0.45 for $L \geq 0.45$.

COMPARE RITZ SOLUTION WITH PENNDOT SOLUTION (L= 30')

Recall the PennDOT study presented “distribution widths” (i.e., $W_{critical}$) for box culverts and slabs for a fixed culvert length = 30 ft and three span dimensions, $S = 8, 16$ and 24 ft. From PennDOT’s set of 31 finite element models, 5 models have loading conditions that conform to the assumptions of the Ritz solution. Specifically, PennDOT box models #1, #9, #17 corresponding to spans of 8, 16, 24 ft and slab models #28 and #30 corresponding to spans of 8 & 16 feet. Like the Ritz model assumptions, these PennDOT models have no soil cover and are loaded with 2 wheels, symmetrically placed about the slab center. Figure 11 compares PennDOT and Ritz predictions for $W_{critical}$ as a function of span.

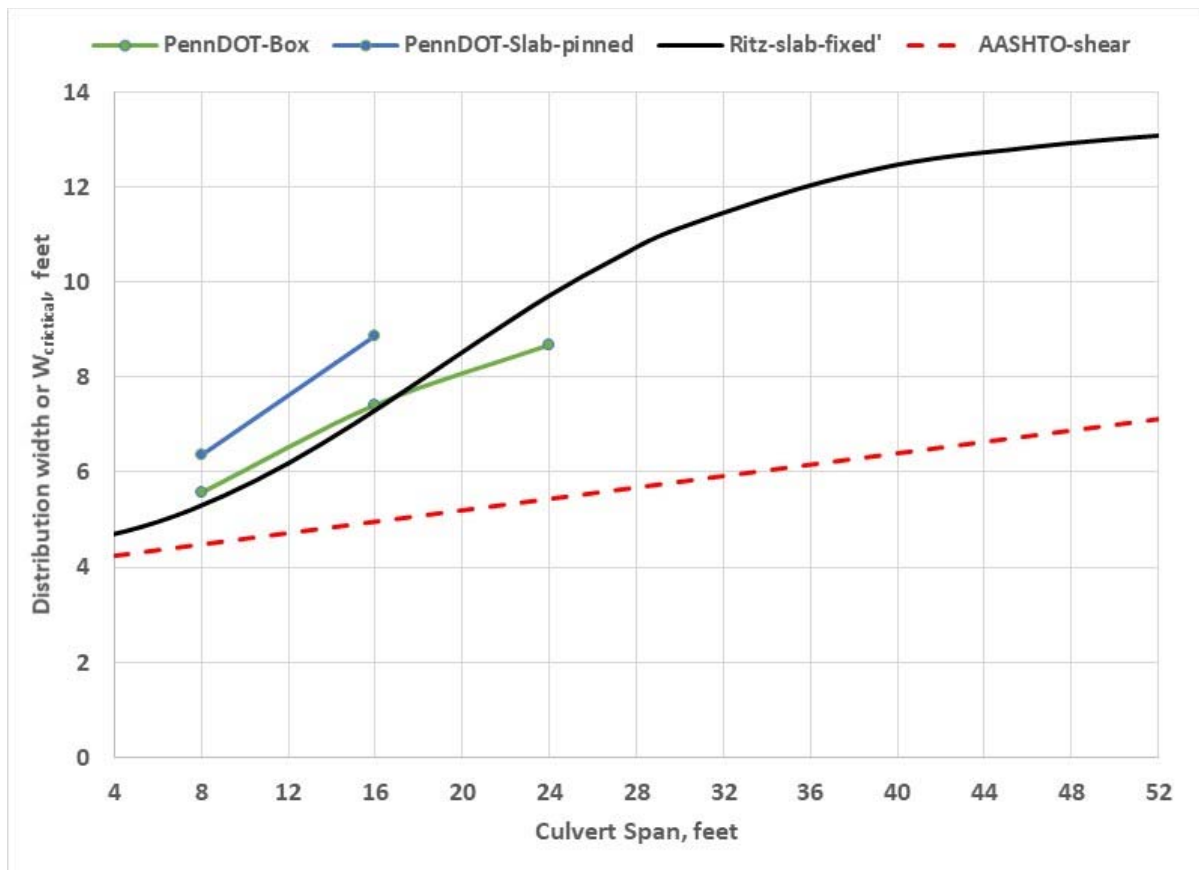


Figure 11. Comparison of compatible PennDOT predictions with Ritz predictions for L = 30 ft.

Remarkably the PennDOT data points for the box culvert are very close to Ritz fixed-slab solution. The PennDOT slab model, which assumes a pinned condition, predicts higher distribution widths than the box model. This indicates that a fixed-slab model better represents the box culvert behavior than does a pinned-slab model. Also shown for reference is the current AASHTO specification for distribution width

Appendix I – Improving AASHTO LRFD/LRFR Specs for 2D for Buried Culverts under LL

based on PennDOT's solution for shear control when the loading location is shifted near the supporting wall of the box. Unfortunately, the Ritz model is only applicable to centrally loaded slabs that produce maximum positive moments and deflections; hence, no direct comparison with the AASHTO specification is meaningful.

The significant finding is that the PennDOT prediction for centrally loaded box culverts is in good agreement with fixed-slab Ritz model for the case when culvert length $L = 30$ feet. In the next section, the Ritz model is used to examine the influence of culvert length, which is not considered in the PennDOT study.

GENERAL RITZ SOLUTION AS FUNCTION OF LENGTH AND SPAN

Figure 12 shows $W_{critical}$ (feet) as a continuous function of culvert span (feet) for a discrete set of practical culvert lengths, $L = 4, 6\text{-to-}12, 18$ and 30 ft. These parametric curves are identical to the general Ritz solutions presented in Figure 10 except the curves are converted to physical units of $W_{critical}$ versus Span instead of the ratios $W_{critical}/L$ versus $Span/L$. As a result of converting to physical units, all culvert lengths between 6 and 12 ft collapse into a single curve as shown by the solid red line below. The collapse into a single curve occurs during the transition from 1-wheel loading to 2-wheel loading wherein the structural benefit of increased slab length is offset by a proportional increase in wheel loading.

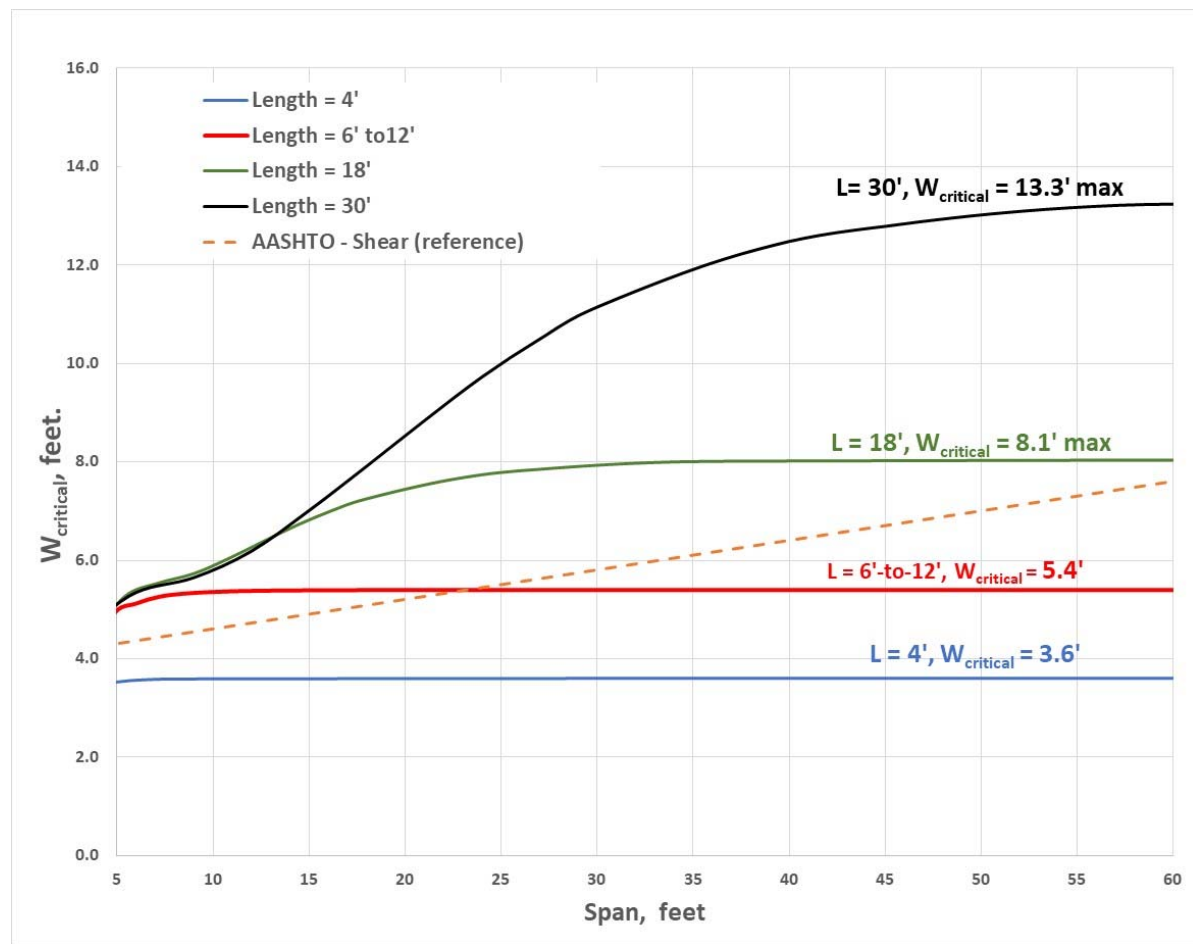


Figure 12. $W_{critical}$ versus span for a set of parametric culvert lengths assuming an isotropic slab.

Appendix I – Improving AASHTO LRFD/LRFR Specs for 2D for Buried Culverts under LL

Figure 12 reveals three significant findings for centrally loaded culverts:

1. Culvert length L has a significant impact on $W_{critical}$ except in the range, $6 \leq L \leq 12$ ft.
2. For culvert lengths $L \leq 12$ feet, $W_{critical}$ is not influenced by the culvert span.
3. For culvert lengths $L > 12$ feet, $W_{critical}$ increases as span and/or length increases.

Recalling from Table 2 that all precast r/c products have lay-lengths less than 12 feet, the consequence of the above findings is that $W_{critical}$ is independent of culvert span and only dependent on culvert length.

Thus for all culvert lengths $L \leq 12$ feet, $W_{critical}$ is given by the following equation.

$$W_{critical} = \begin{cases} 0.9L & \rightarrow \text{if } L \leq 6 \text{ ft} \\ 5.4 \text{ ft} & \rightarrow \text{if } 6 \leq L \leq 12 \text{ ft} \end{cases} \quad \text{Equation 30}$$

where, L = lay length of precast culvert or cast-in-place culvert with $L \leq 12$ ft.

For cast-in-place culverts whose continuous length are greater than 12 feet, the culvert span as well as the culvert length influences $W_{critical}$ as can be observed in Figure 12 for $L = 18$ and 30 ft. For these cases $W_{critical}$ can be approximated by two straight lines. The first line goes from the origin ($S = 5$ ft, $L = 5.4$ ft) to the maximum $W_{critical}$ value on the L -curve where occurs at $S = 2L$. Thereafter, as S increases $W_{critical}$ remains constant at maximum value.

With the above understanding, Equation 31a&b represent straight-line approximations to predict $W_{critical}$ as a function of S and L .

$$W_{critical} = \begin{cases} 5.4' + m(S - 5') & \rightarrow \text{if } 5' \leq S \leq 2L \\ MaxW_{critical} & \rightarrow \text{if } S > 2L \end{cases} \quad \text{Equation 31a}$$

where m is the straight-line slope and $Max-W_{critical}$ is the maximum of value of $W_{critical}$, both dependent L .

$$m = 0.087 \left(\frac{L - 12'}{6'} \right)^{0.46} \quad \text{Equation 31b}$$

$$MaxW_{critical} = 5.4' + m(2L - 5')$$

For reference, Figure 12 also shows the shear-based AASHTO distribution width, which is purportedly applicable to all r/c box and arch culvert lengths even though that the underlying PennDOT study used a fixed length $L = 30$ foot. Given that the Ritz predictions assume central-slab loading and AASHTO predictions assume side-slab loading, there is no expectation of agreement between AASHTO and Ritz predictions even for $L = 30$ ft. Nonetheless, the AASHTO and Ritz predictions are compared and contrasted in the following bullets for the purpose of ultimately improving the AASHTO methodology.

- The main lesson learned from the Ritz solutions is that culvert length L has a pronounced influence on $W_{critical}$, even more so than culvert span S . Clearly, follow-on studies like the PennDOT study need to be undertaken for a range of culvert lengths.

Appendix I – Improving AASHTO LRFD/LRFR Specs for 2D for Buried Culverts under LL

- Because the Ritz and the PennDOT predictions for $W_{critical}$ show good agreement for centrally loaded slabs for the case $L = 30$ feet, it is tentatively concluded that the Ritz slab model is a viable surrogate for all centrally loaded box culverts. However, this conclusion needs to be validated with 3D FEM models with smaller culvert lengths.
- The curved geometry of concrete arches is significantly different from the flat geometry of slabs and box culverts. Consequently, 3D finite element models of typical concrete arches need to be undertaken to assess the influence of curvature on $W_{critical}$, if any.

It is expected that the Ritz predictions for $W_{critical}$ as shown in Figure 12 and quantified by Equations 30 and 31 will need to be adjusted based on future 3D finite element analysis. The true value of Ritz solution is to illustrate the effect of culvert length and span and to establish a template to build upon.

INFLUENCE OF ORTHOTROPIC SLAB PROPERTIES.

Up to this point, all Ritz solutions have assumed the slab is isotropic with the same bending stiffness in the longitudinal plane as the transverse plane, i.e., $D_z = D_x$, where $D_z = EI_z/(1-\mu^2)$ and $D_x = EI_x/(1-\mu^2)$ are the plate stiffness parameters in the longitudinal and transverse planes, respectively. The bold black curve in Figure 13 is $W_{critical}/L$ versus S/L for isotropic case $D_z/D_x = 1$ as previously shown in Figure 8 for 1-wheel loading. Also shown in Figure 13 is a family of curves for $D_z/D_x = 0.01, 0.1, 0.5$ and 2.0 , representing a realistic range of orthotropic properties that may be experienced in rigid or flexible culverts.

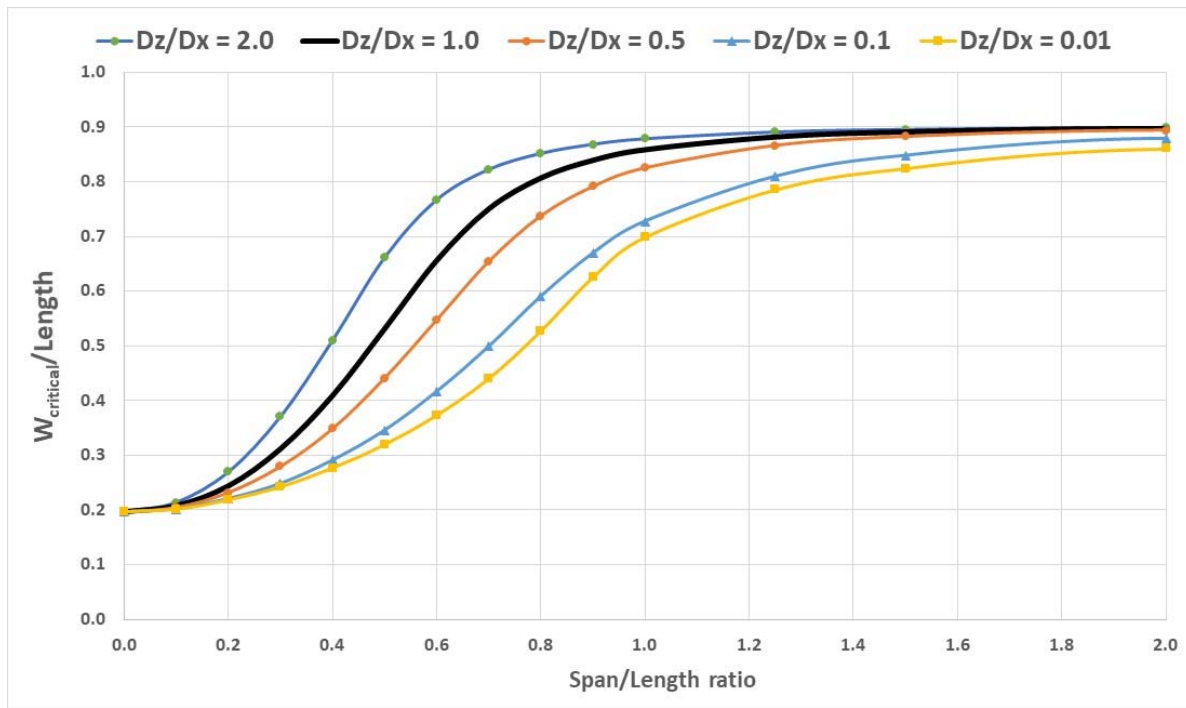


Figure 13. $W_{critical}/L$ versus S/L for several orthotropic stiffness ratios D_z/D_x , (1-wheel loading).

Appendix I – Improving AASHTO LRFD/LRFR Specs for 2D for Buried Culverts under LL

For any particular S/L ratio, the above curves reveal the comparative change in W_{critical}/L when an isotropic slab is compared to an orthotropic slab. The relative change applies to 2-wheel loading as well as 1-wheel loading because 2-wheel loading is achieved by superposition of 1-wheel loading.

To illustrate utilizing the above chart, begin by inspecting Figure 12, which is the general 2-wheel Ritz solutions for W_{critical} for isotropic slabs. Choosing a specific slab dimensions, say $S = 18$ ft and $L = 18$ ft, we find $W_{\text{critical}} \approx 7.2$ ft for the isotropic case. Next, to get the value of W_{critical} for the orthotropic case $D_z/D_x = 0.5$, enter the above chart for $S/L = 18/18 = 1$ and read $W_{\text{critical}}/L \approx 0.82$ from the curve $D_z/D_x = 0.5$ and also read $W_{\text{critical}}/L \approx 0.86$ from the isotropic curve. Forming the ratio $0.82/0.86 = 0.95$ and multiplying it by original isotropic W_{critical} value, we arrive at the orthotropic value for $W_{\text{critical}} = 6.9$ ft.

With regard to reinforced concrete culverts, longitudinal cracks reduce the transverse stiffness D_x , and circumferential cracks reduce longitudinal stiffness D_z as may be predicted from cracked-transformed section properties. If the degree of concrete cracking (or lack of cracking) is relatively the same for longitudinal and circumferential cracks, then an isotropic assumption is reasonable, $D_z/D_x = 1.0$. Field observations of concrete culverts subject to dead and live loads typically show that longitudinal cracks are significantly more prevalent than circumferential cracks so that $D_z/D_x = 2.0$ may be a reasonable orthotropic assumption. However, this assumption results in higher values for W_{critical} and, hence, less conservative. Consequently, it is generally recommended to assume isotropic conditions for r/c culverts, $D_z/D_x = 1.0$.

In contrast to r/c culverts, corrugated metal and corrugated plastic culverts have fixed section properties where D_x is 1 to 2 orders of magnitude larger than D_z dependent on the corrugation geometry. Consequently, the curves for $D_x/D_z = 0.1$ and 0.01 are appropriate for corrugated flexible culverts. Although this white paper is focused on r/c culverts, one of the issues listed at the beginning of this paper asked the question why is the 3D-stiffness effect only applicable to reinforced concrete culverts and not flexible culverts. Figure 13 provides a partial answer because W_{critical} for corrugated culverts are significantly smaller than for isotropic r/c culverts.

A final point of interest is that the curve $D_z/D_x = 0$ (not shown) is indistinguishable from the curve $D_z/D_x = 0.01$. Hence, even if there is no longitudinal stiffness $D_z = 0$ (i.e. $I_z = 0$), there still exists a small 3D stiffness effect due to twisting momenta whose stiffness are a combination of D_x and D_z .

SUMMARY

Part I of this white paper reviewed the AASHTO LRFD distribution-width equations that are used to reduce the magnitude of 2D live loads to account for 3D effects in the longitudinal direction. Equations 1 and 2 are the AASHTO distribution widths that account for the longitudinal load spreading through the soil. These long-standing equations are a function of soil depth H and apply to all culvert sizes, shapes and materials. Equation 3 is a special distribution width that only applies to reinforced concrete box and arch culverts with less than 2 feet of soil cover. This equation originated from the PennDOT study wherein numerous 3D finite element models of r/c box culverts were analyzed to develop a span-dependent, distribution-width equation so that 2D analysis predicts structural responses similar to 3D analysis.

Part I also introduces a conceptual plate model that illustrates the underlying physics behind the special distribution width associated with Equation 3. The physical reason is that there exists a real-world 3D

Appendix I – Improving AASHTO LRFD/LRFR Specs for 2D for Buried Culverts under LL

stiffness effect that is not captured by 2D culvert models subject to live loads at shallow burial depths. More precisely, a 2D model underrepresents the actual 3D stiffness whenever the width of the longitudinal line-load impinging on the plate (culvert) is less than a culvert-specific parameter called the critical distribution width, W_{critical} . Pragmatically, W_{critical} plays the same role as E_{long} in Equation 3, except rather than axle load, W_{critical} applies to one-wheel load, i.e., $W_{\text{critical}} = \frac{1}{2} E_{\text{long}}$.

At the conclusion of Part I, a very useful concept is presented in Figure 5 that illustrates a logical methodology to smoothly transition from the fixed distribution width W_{critical} to the soil-spreading distribution width. In addition, step-by-step procedures are described for 2D live-load analysis based on the Reduced Surface Load (RSL) technique or the Continuous Load Scaling (CLS) technique. In either case W_{critical} plays the pivotal role.

Whereas Part I, deals with concepts and big picture ideas, Part II is focused on obtaining quantifiable insights from a mechanistic model. Specifically, a 3D elastic plate is defined to represent the top slab of an r/c box culvert with a longitudinal strip load placed symmetrically about the slab center as depicted in Figure 6 for a symmetric quadrant of the slab. The associated differential equation and boundary conditions are solved by the Ritz technique to provide an approximate solution for displacements and structural responses. Spread sheet calculations are used to process the Ritz solution to compute W_{critical} for 1- and 2-wheel loading conditions. Solution plots are shown as a function of slab span, length and degree orthotropic stiffness.

Figure 11 compares values of W_{critical} from the Ritz model with the corresponding distribution widths from the PennDOT as a function of slab span with fixed slab length $L = 30$ feet. Remarkably, the correlations are surprisingly close; thereby suggesting the Ritz slab model is a viable surrogate for a centrally loaded r/c box culvert.

Figure 12 portrays the general Ritz solution for W_{critical} as a function of span S and length L assuming isotropic slab stiffness properties. Surprisingly, the culvert length L has a pronounced influence on W_{critical} even more so than the culvert span S . Since the PennDOT study did not vary the box culvert length, this finding has important consequences on the future AASHTO distribution-width equations.

Figure 13 shows that W_{critical} becomes smaller as the orthotropic plate stiffness ratio D_z/D_x becomes smaller. Since corrugated flexible culverts have very small stiffness ratios $D_z/D_x < 0.1$, it is evident that corrugated flexible culverts do not produce 3D stiffness effects as large as rigid r/c culverts whose stiffness ratio are approximately $D_z/D_x \approx 1.0$. Perhaps this explains why AASHTO's special distribution width equations only apply to reinforced concrete and not to other culvert materials.

To conclude this summary, the original six issues listed on page 6 are re-visited in light of the concepts and findings presented in Parts I and II. The six issues are addressed below.

1. **Continuity of distribution widths with soil depth.** As shown in Figure 1, the current AASHTO distribution width equations are discontinuous at the soil depth $H = 2$ ft. In Part I, a logically smooth transition method is illustrated in Figure 5 using a variable transition soil depth H_T , which is dependent on critical distribution width W_{critical} . Said another way, there is no apparent engineering logic behind the current AASHTO stipulation that all transitions occur at $H = 2$ ft whereas the variable transition depth is physically logical.

Appendix I – Improving AASHTO LRFD/LRFR Specs for 2D for Buried Culverts under LL

2. **Influence of culvert length.** The PennDOT study used a fixed culvert length of 30 feet for all finite element models; consequently, Equation 3 is only dependent on culvert span. In sharp contrast, results from Ritz slab model reveals that length L has a pronounced influence on $W_{critical}$ even more so than the culvert span S .
3. **Influence of culvert span.** The PennDOT study investigated box culvert spans of 8, 16 and 24 ft with a fixed length $L = 30$ ft thereby finding that E_{long} is a linearly increasing function of span. In contrast, the Ritz slab model found that $W_{critical}$ is not influenced by the span S if $L \leq 12$ feet, which includes all precast culverts. For cast-in-place culverts with $L > 12$ feet, $W_{critical}$ increases with span but not in a linear fashion. Rather $W_{critical}$ increases on an asymptotic curve as shown in Figure 12.
4. **Verification of procedure for computing distribution widths.** Figure 11 shows remarkably close correlation between the PennDOT and Ritz predictions for distribution widths based on centered 2-wheel loading. Nonetheless, the PennDOT procedure, which is based on integrating force-effect distributions, is significantly different than the Ritz procedure, which is described by Equation 7.
5. **Justification for applying r/c box culvert results to r/c arches.** Neither the PennDOT study nor this white paper considered curved models representative r/c arches. Nonetheless Equation 3 (developed for box culverts) also applies to reinforced concrete arches according to the ASSHTO specifications.
6. **Potential 3D-effects for other culvert materials and shapes.** Both the PennDOT study and Ritz model indicate that 3D stiffness effects are a real phenomenon and potentially applicable to all culvert materials and shapes to some degree. Figure 13 illustrates that orthotropic stiffness ratios representative of corrugated flexible culverts do indeed exhibit 3D stiffness effects but to a lesser degree than isotropic stiffness properties assumed for rigid culverts.

Appendix J – Data Mining BrDR Regression Data

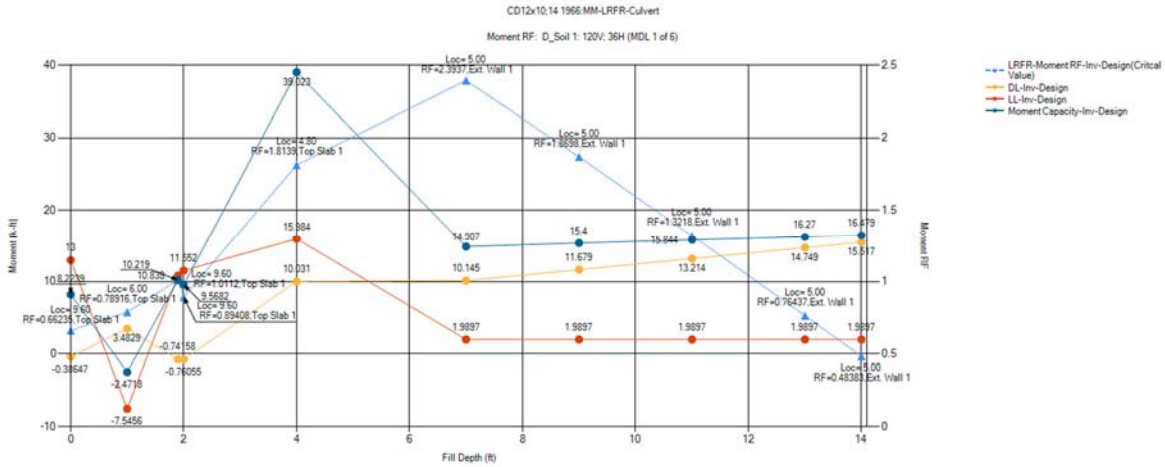
Appendix J – Plots Mined from BrDR Regression Data – Caltrans Double Box

This appendix shows plots mined from BrDR regression data for Caltrans double cell culverts. The plots show the RF and its contributing components.

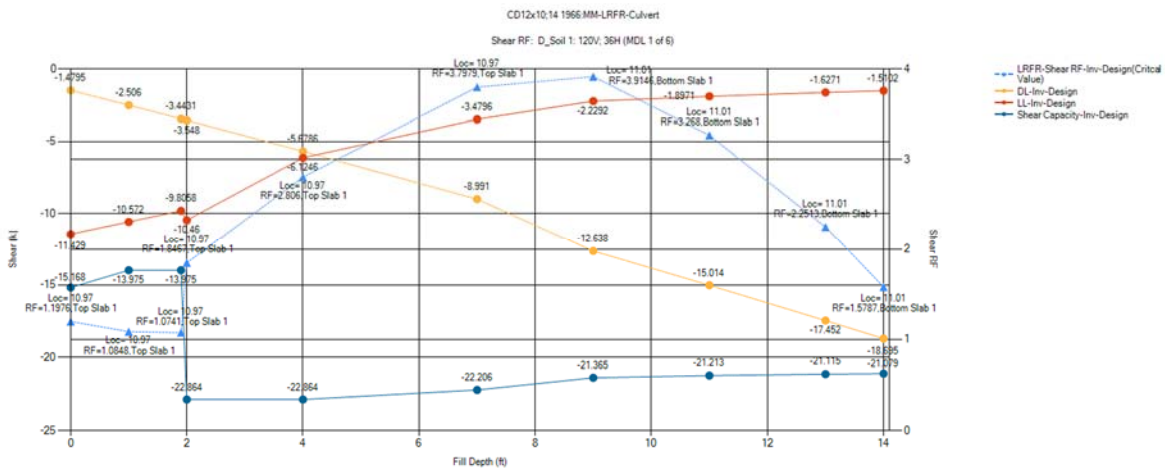


Appendix J – Data Mining BrDR Regression Data

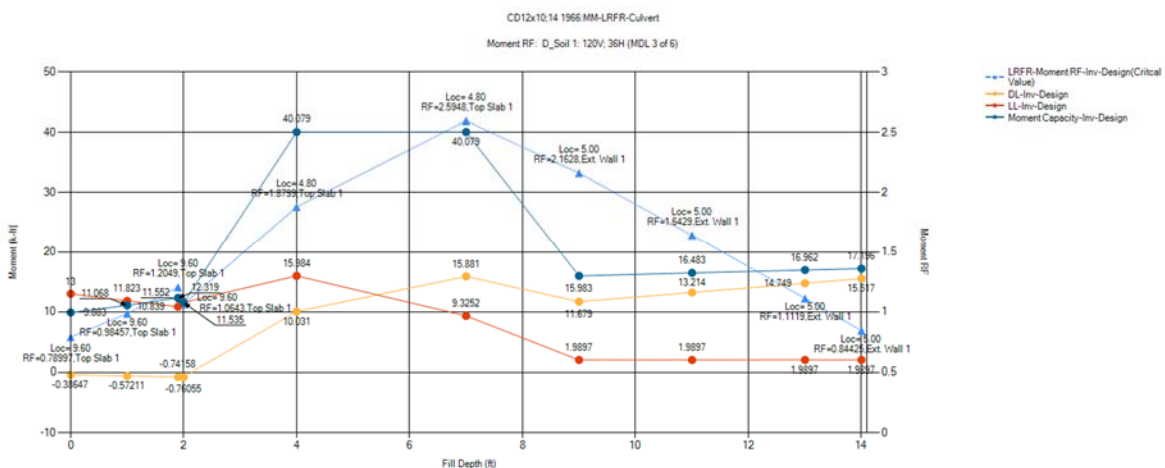
CD12x10;14 1966:MM-LRFR-Culvert: Moment RF: D_Soil 1: 120V; 36H (MDL 1 of 6)



CD12x10;14 1966:MM-LRFR-Culvert: Shear RF: D_Soil 1: 120V; 36H (MDL 1 of 6)

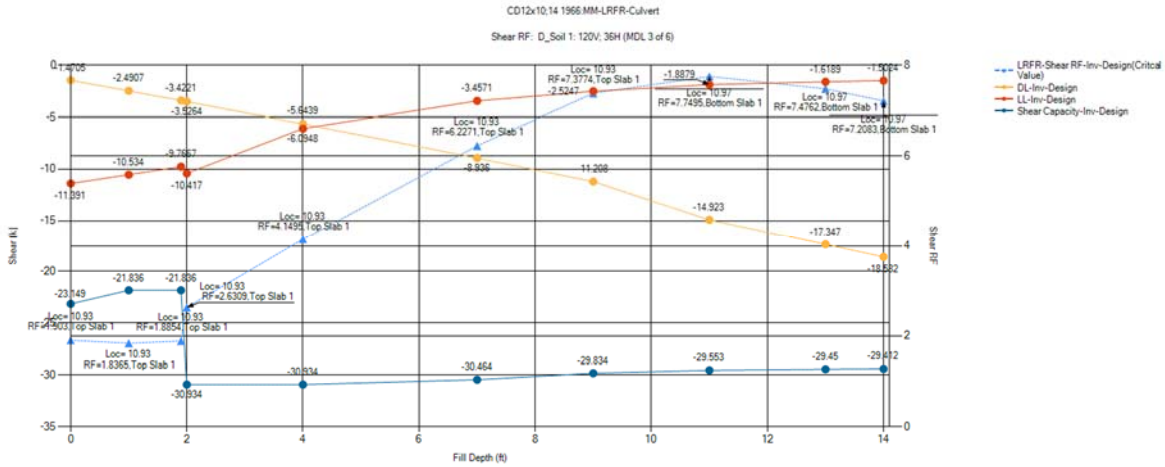


CD12x10;14 1966:MM-LRFR-Culvert: Moment RF: D_Soil 1: 120V; 36H (MDL 3 of 6)

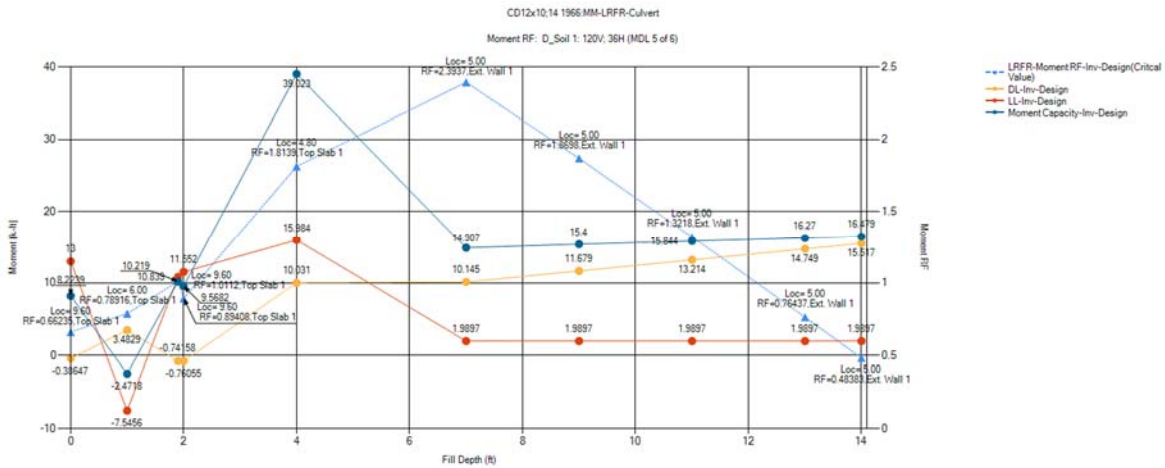


Appendix J – Data Mining BrDR Regression Data

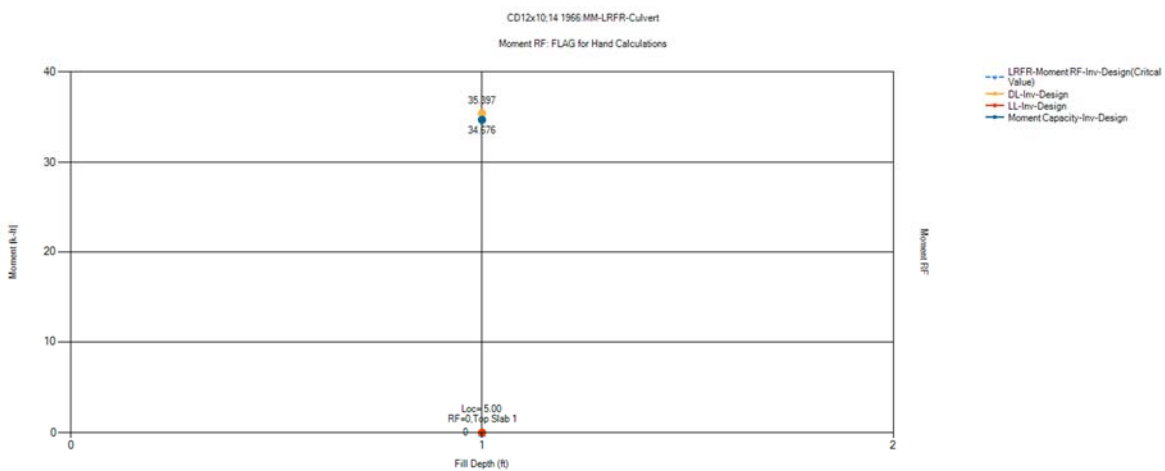
CD12x10;14 1966:MM-LRFR-Culvert: Shear RF: D_Soil 1: 120V; 36H (MDL 3 of 6)



CD12x10;14 1966:MM-LRFR-Culvert: Moment RF: D_Soil 1: 120V; 36H (MDL 5 of 6)

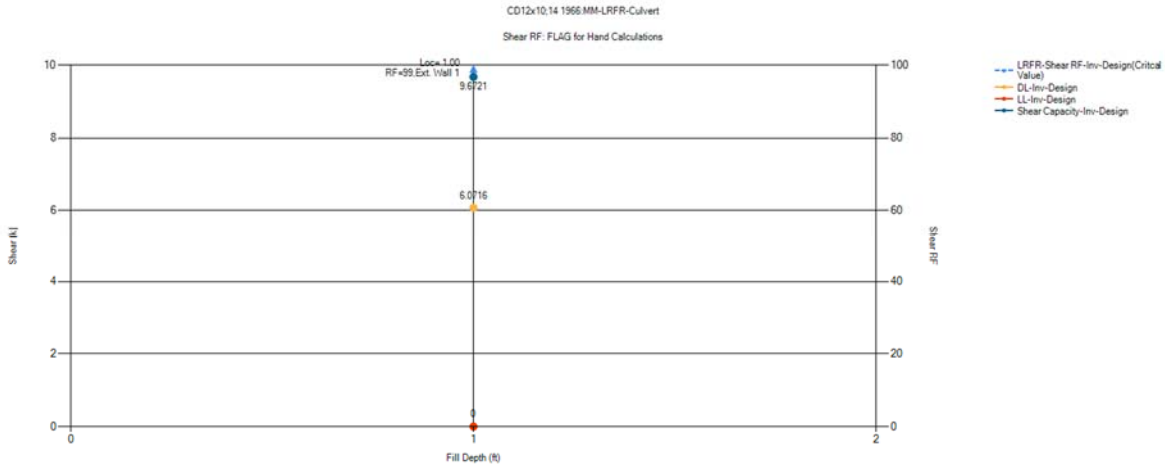


CD12x10;14 1966:MM-LRFR-Culvert: Moment RF: FLAG for Hand Calculations

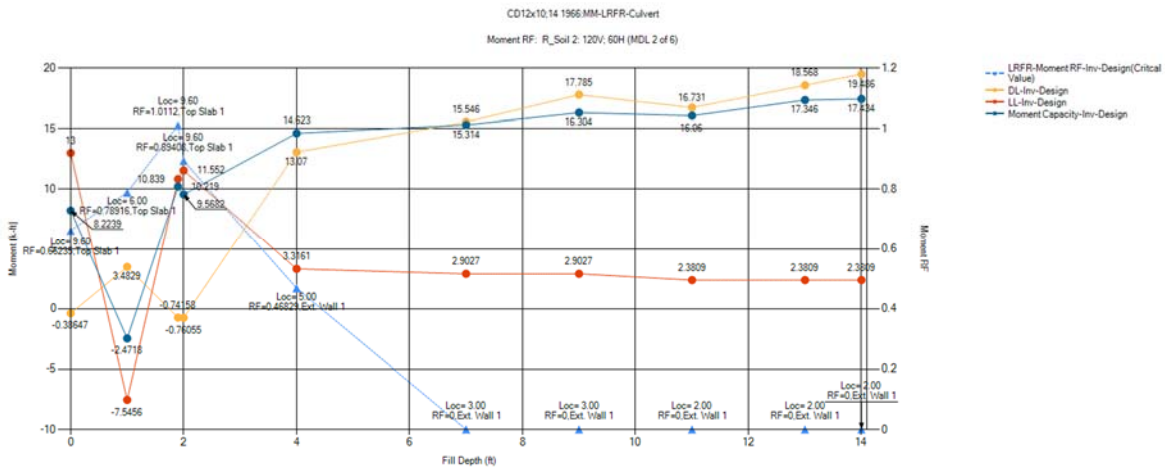


Appendix J – Data Mining BrDR Regression Data

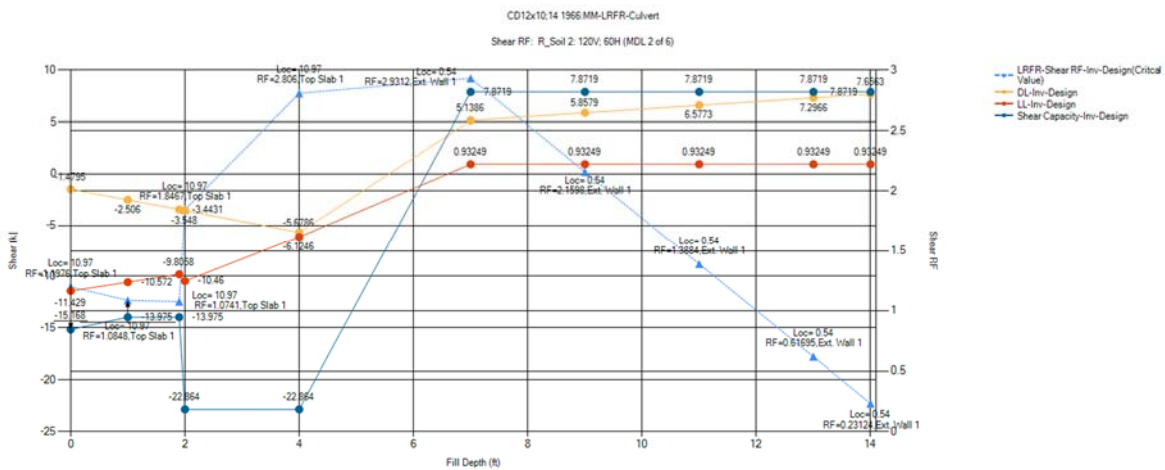
CD12x10;14 1966:MM-LRFR-Culvert: Shear RF: FLAG for Hand Calculations



CD12x10;14 1966:MM-LRFR-Culvert: Moment RF: R_Soil 2: 120V; 60H (MDL 2 of 6)

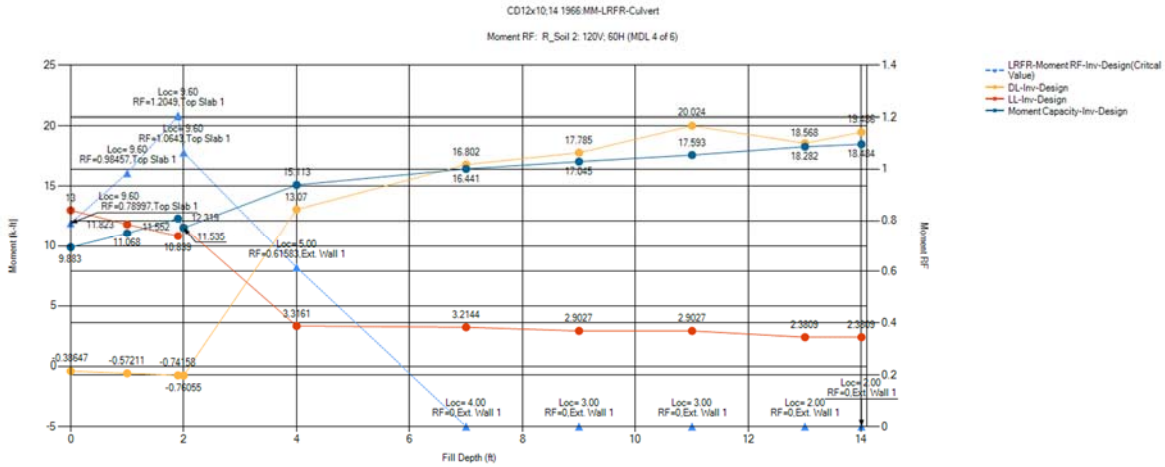


CD12x10;14 1966:MM-LRFR-Culvert: Shear RF: R_Soil 2: 120V; 60H (MDL 2 of 6)

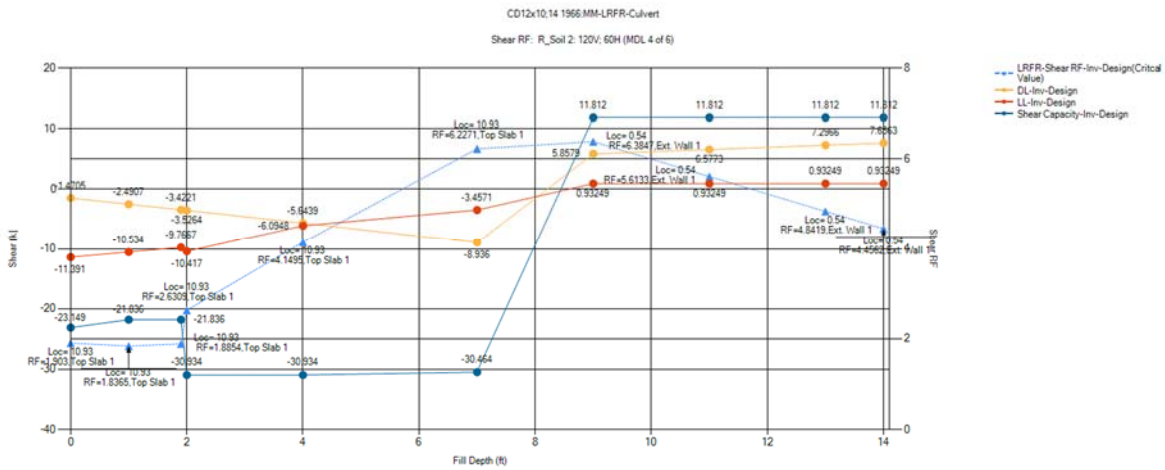


Appendix J – Data Mining BrDR Regression Data

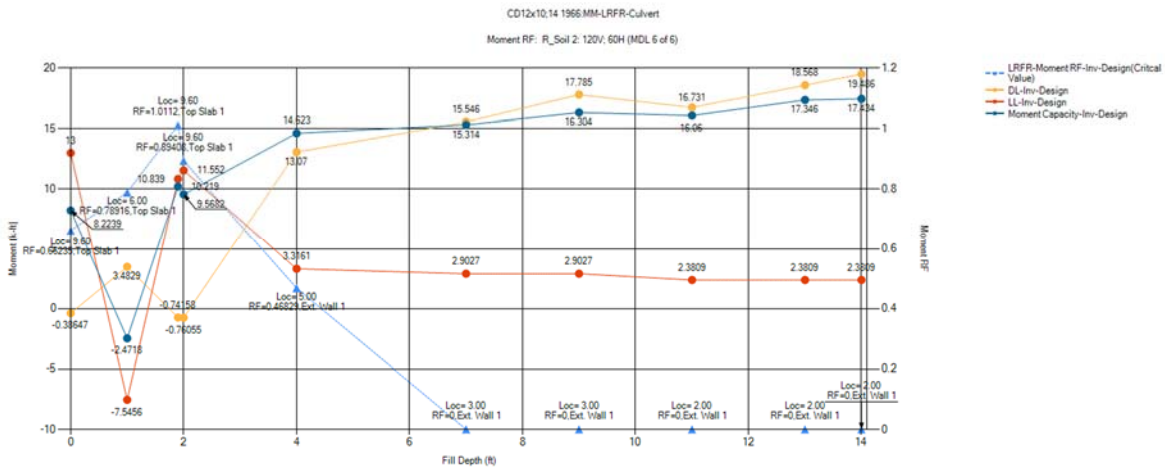
CD12x10;14 1966:MM-LRFR-Culvert: Moment RF: R_Soil 2: 120V; 60H (MDL 4 of 6)



CD12x10;14 1966:MM-LRFR-Culvert: Shear RF: R_Soil 2: 120V; 60H (MDL 4 of 6)

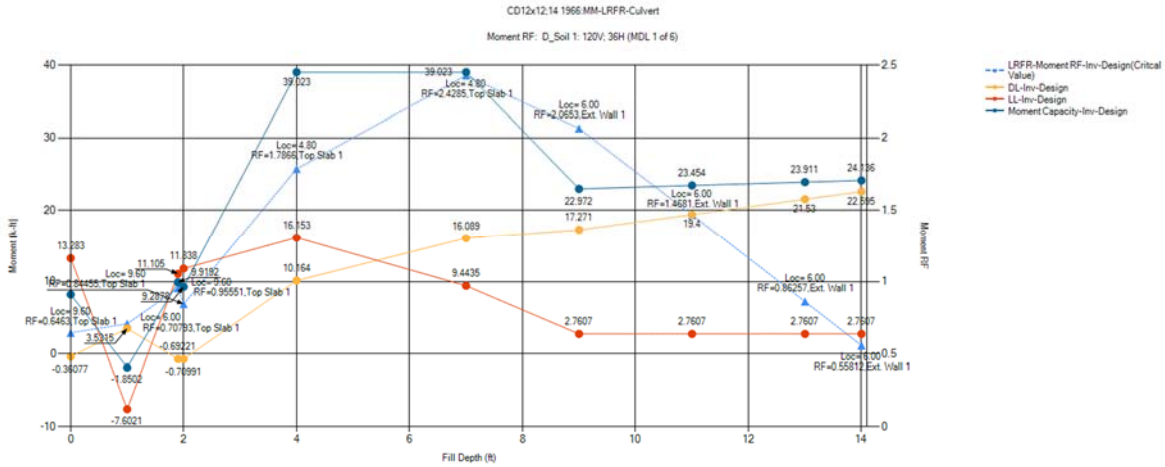


CD12x10;14 1966:MM-LRFR-Culvert: Moment RF: R_Soil 2: 120V; 60H (MDL 6 of 6)

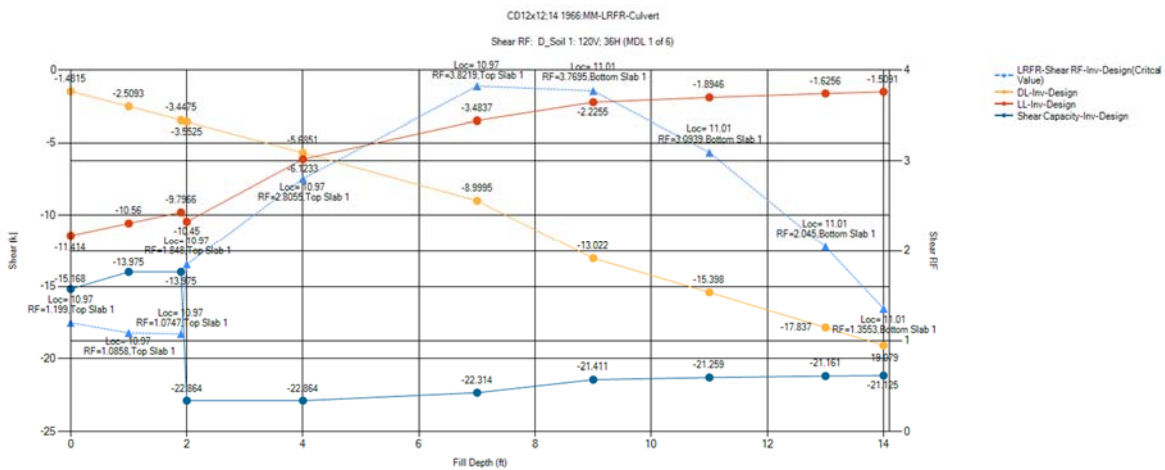


Appendix J – Data Mining BrDR Regression Data

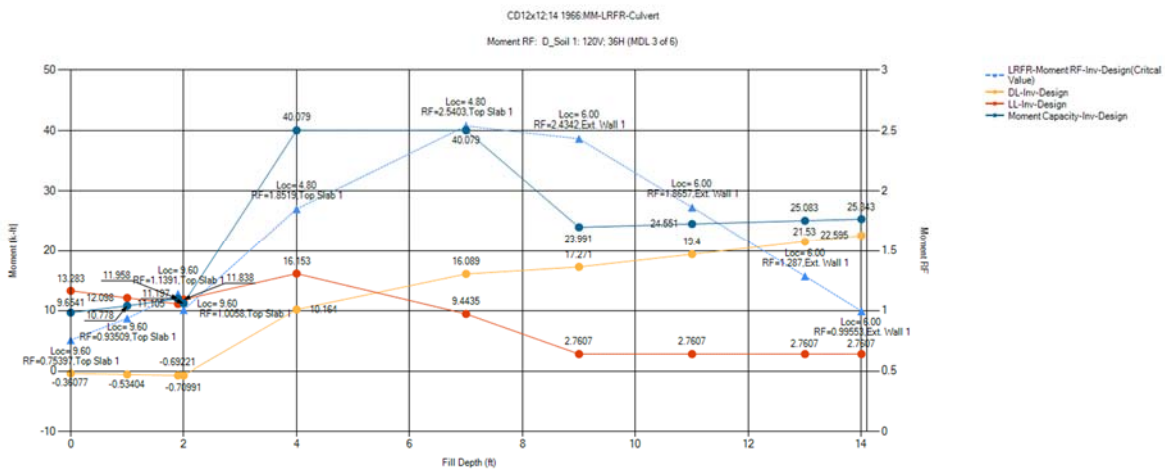
CD12x12;14 1966:MM-LRFR-Culvert: Moment RF: D_Soil 1: 120V; 36H (MDL 1 of 6)



CD12x12;14 1966:MM-LRFR-Culvert: Shear RF: D_Soil 1: 120V; 36H (MDL 1 of 6)

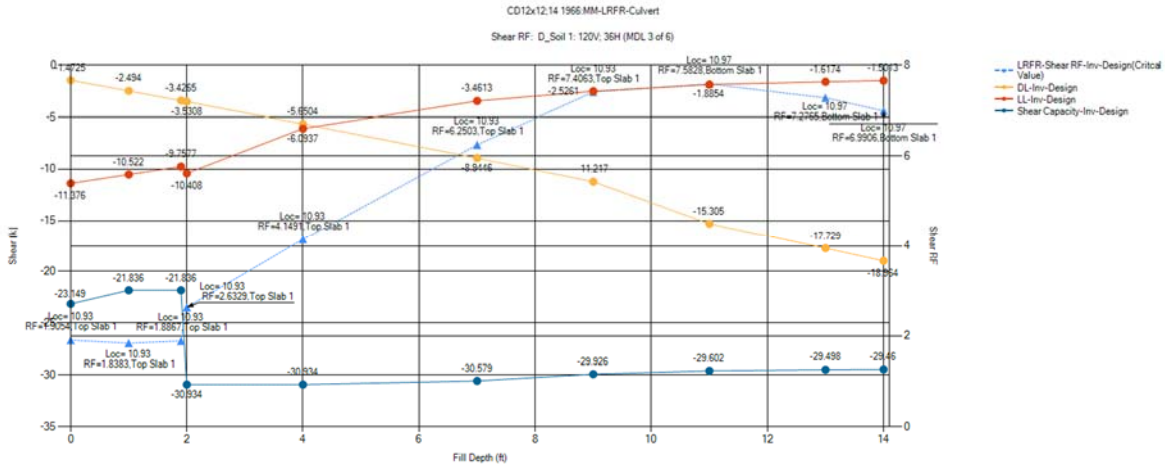


CD12x12;14 1966:MM-LRFR-Culvert: Moment RF: D_Soil 1: 120V; 36H (MDL 3 of 6)

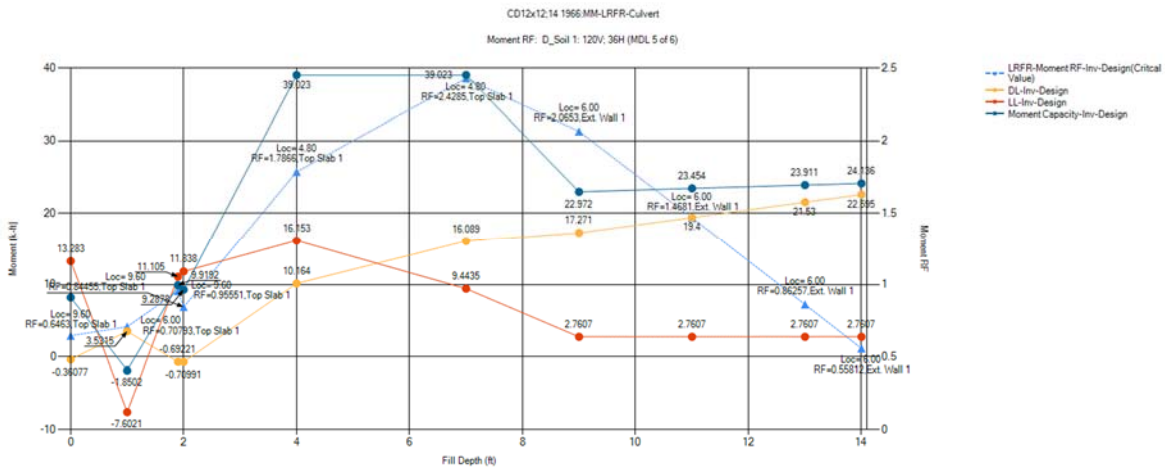


Appendix J – Data Mining BrDR Regression Data

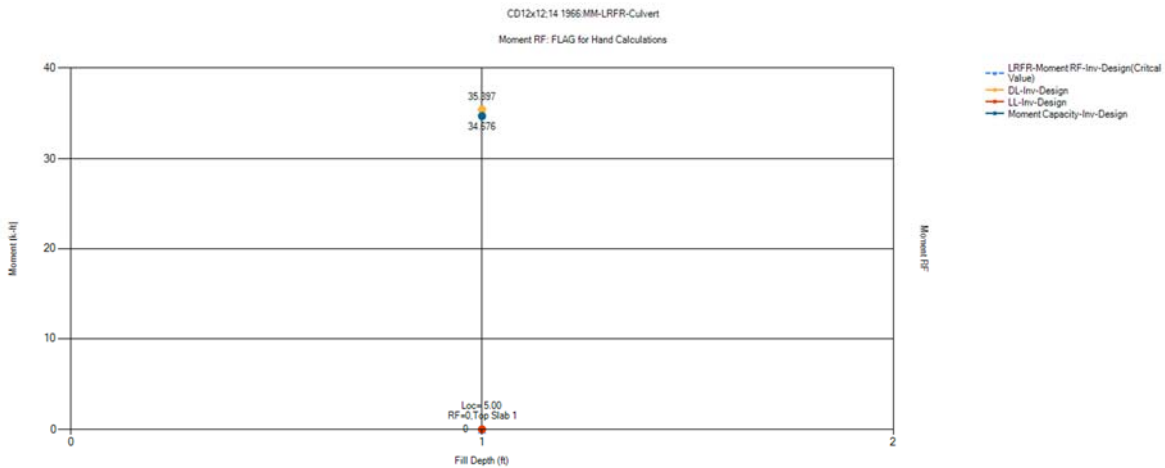
CD12x12;14 1966:MM-LRFR-Culvert: Shear RF: D_Soil 1: 120V; 36H (MDL 3 of 6)



CD12x12;14 1966:MM-LRFR-Culvert: Moment RF: D_Soil 1: 120V; 36H (MDL 5 of 6)

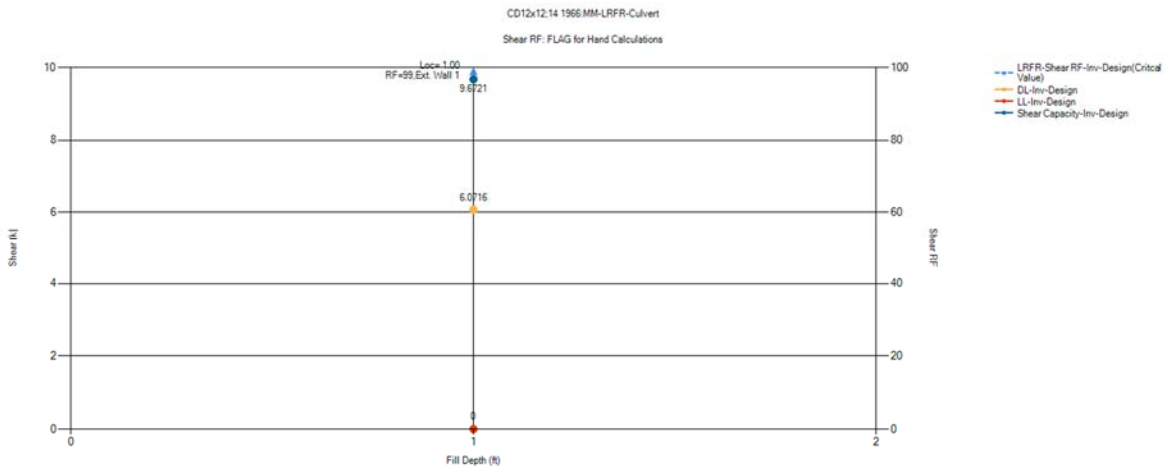


CD12x12;14 1966:MM-LRFR-Culvert: Moment RF: FLAG for Hand Calculations

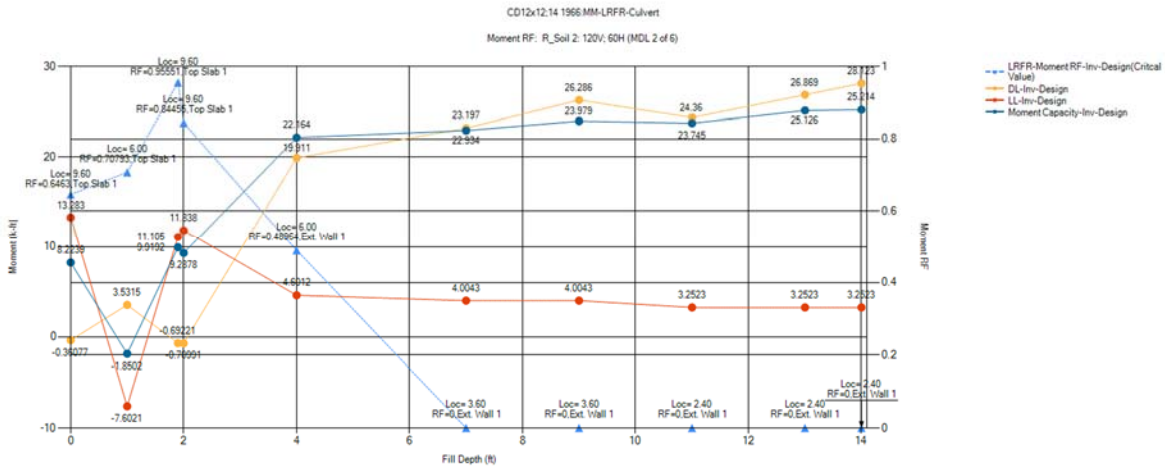


CD12x12;14 1966:MM-LRFR-Culvert: Shear RF: FLAG for Hand Calculations

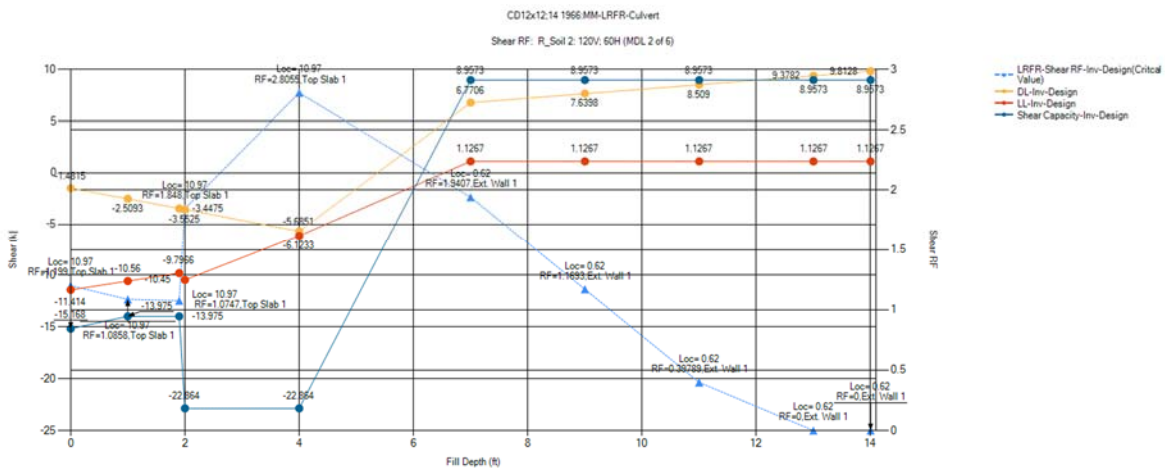
Appendix J – Data Mining BrDR Regression Data



CD12x12;14 1966:MM-LRFR-Culvert: Moment RF: R_Soil 2: 120V; 60H (MDL 2 of 6)

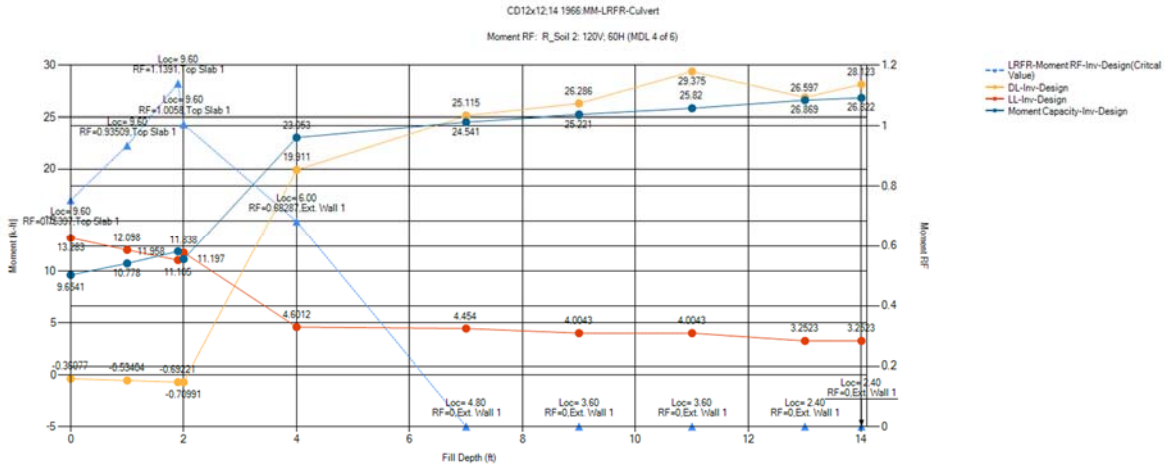


CD12x12;14 1966:MM-LRFR-Culvert: Shear RF: R_Soil 2: 120V; 60H (MDL 2 of 6)

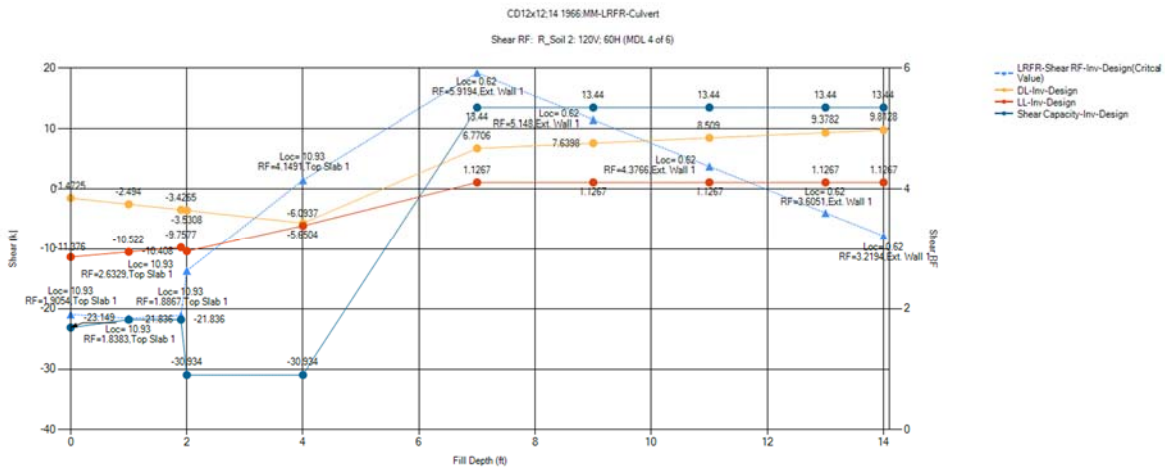


Appendix J – Data Mining BrDR Regression Data

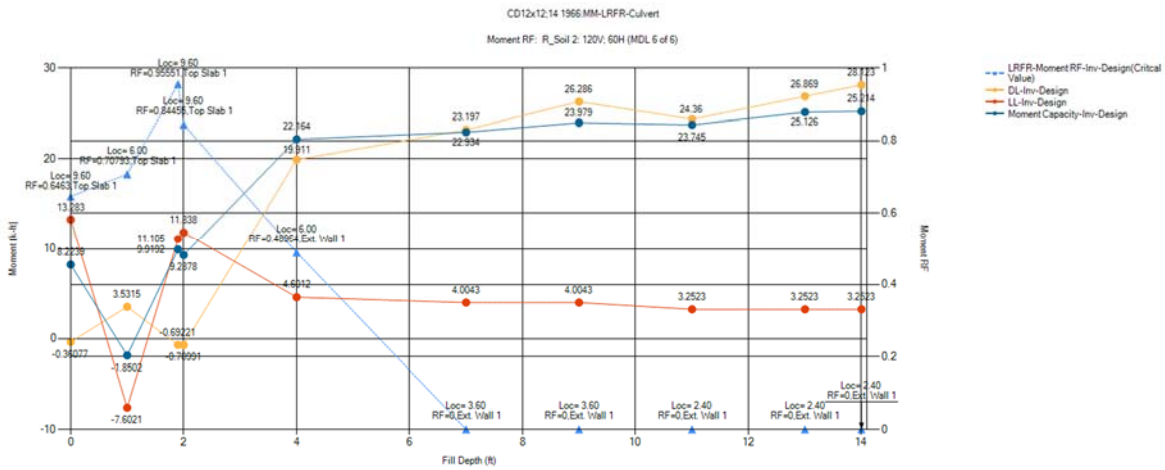
CD12x12;14 1966:MM-LRFR-Culvert: Moment RF: R_Soil 2: 120V; 60H (MDL 4 of 6)



CD12x12;14 1966:MM-LRFR-Culvert: Shear RF: R_Soil 2: 120V; 60H (MDL 4 of 6)

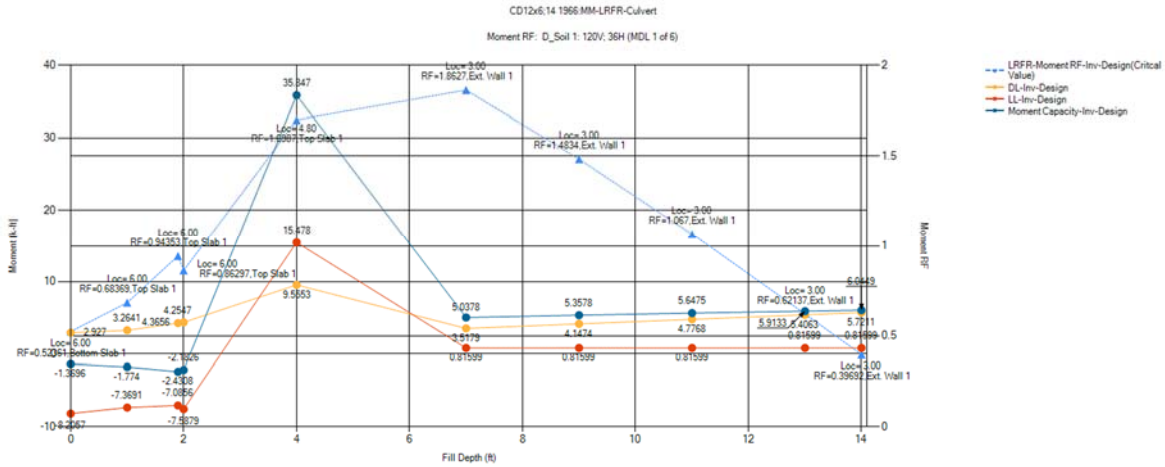


CD12x12;14 1966:MM-LRFR-Culvert: Moment RF: R_Soil 2: 120V; 60H (MDL 6 of 6)

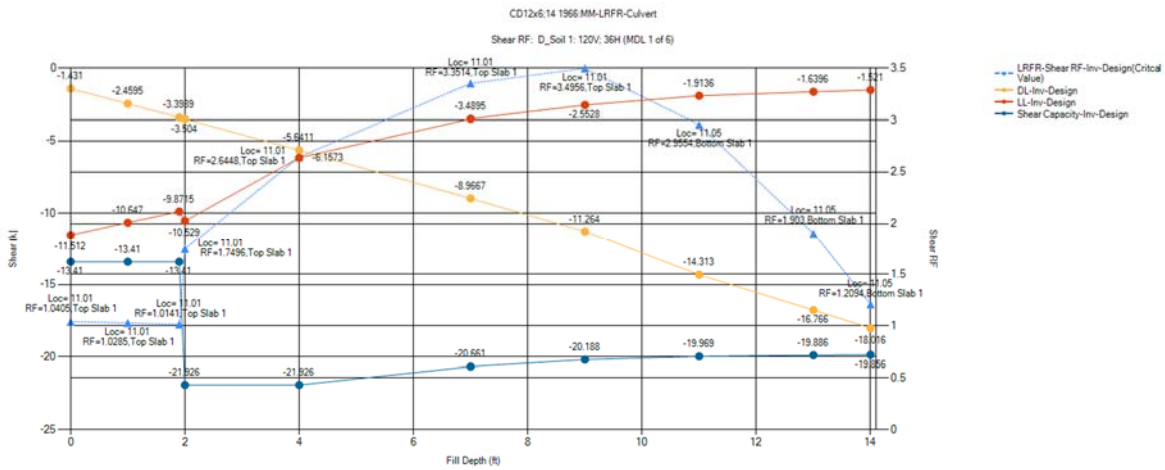


Appendix J – Data Mining BrDR Regression Data

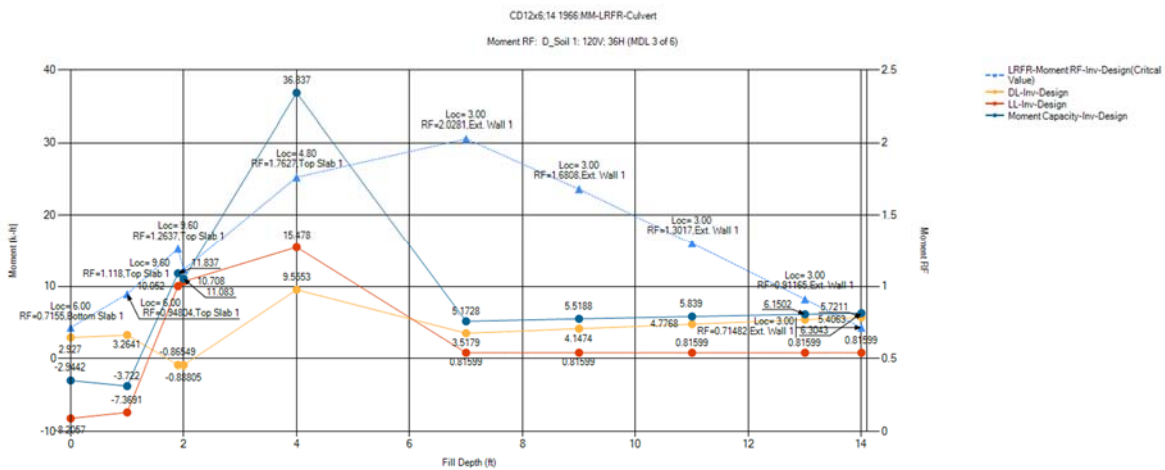
CD12x6;14 1966:MM-LRFR-Culvert: Moment RF: D_Soil 1: 120V; 36H (MDL 1 of 6)



CD12x6;14 1966:MM-LRFR-Culvert: Shear RF: D_Soil 1: 120V; 36H (MDL 1 of 6)

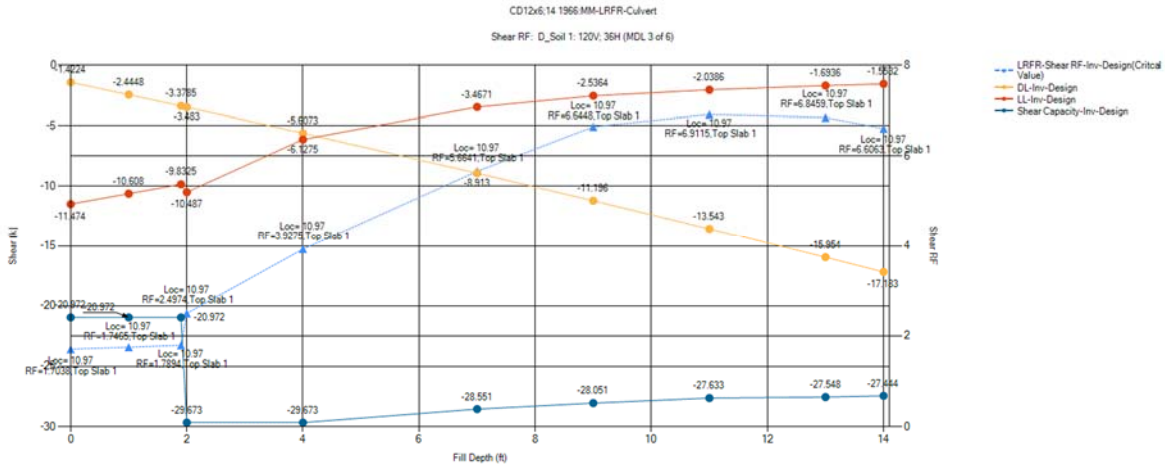


CD12x6;14 1966:MM-LRFR-Culvert: Moment RF: D_Soil 1: 120V; 36H (MDL 3 of 6)

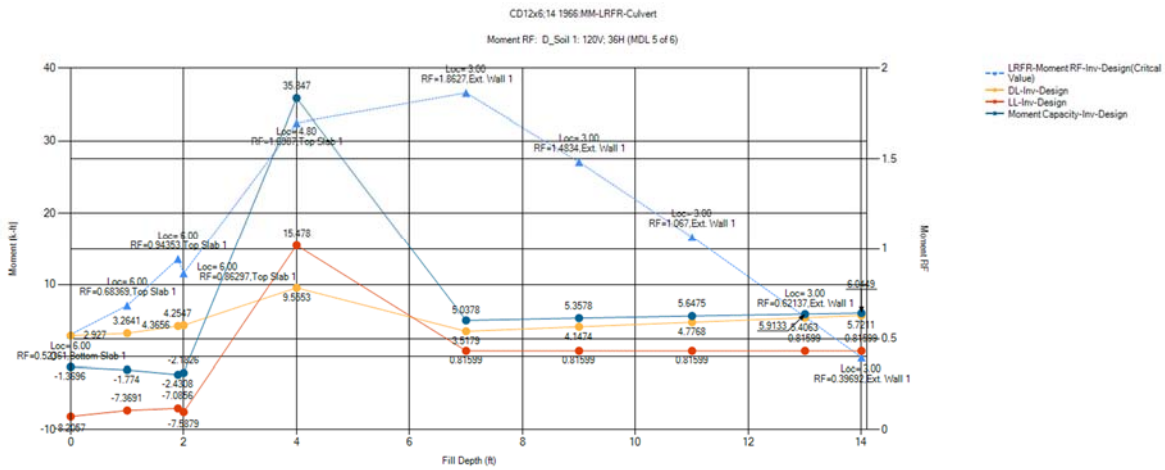


Appendix J – Data Mining BrDR Regression Data

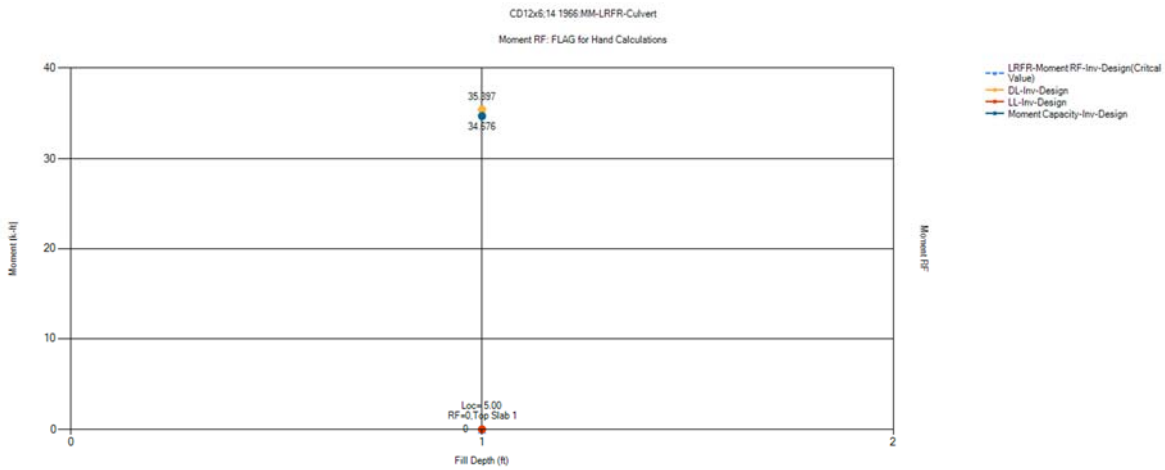
CD12x6;14 1966:MM-LRFR-Culvert: Shear RF: D_Soil 1: 120V; 36H (MDL 3 of 6)



CD12x6;14 1966:MM-LRFR-Culvert: Moment RF: D_Soil 1: 120V; 36H (MDL 5 of 6)

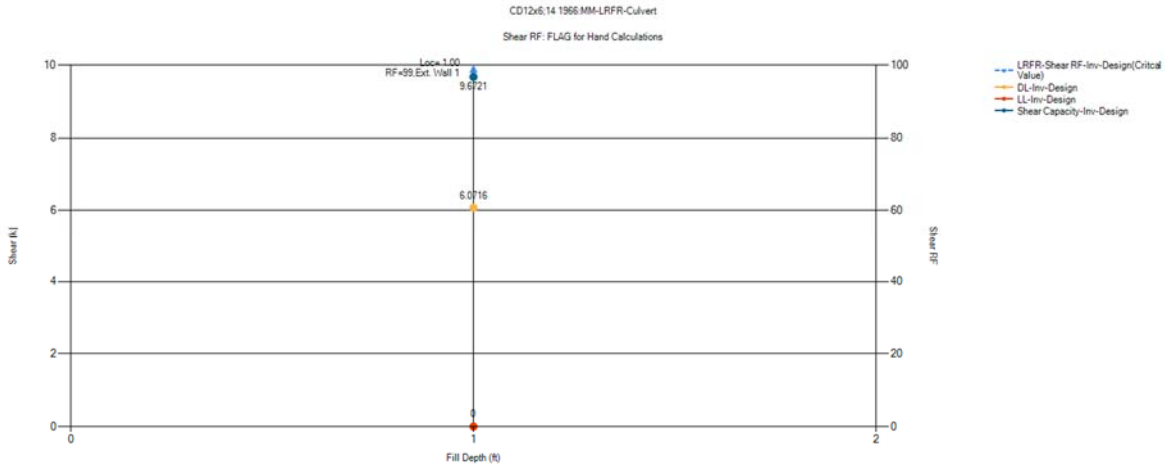


CD12x6;14 1966:MM-LRFR-Culvert: Moment RF: FLAG for Hand Calculations

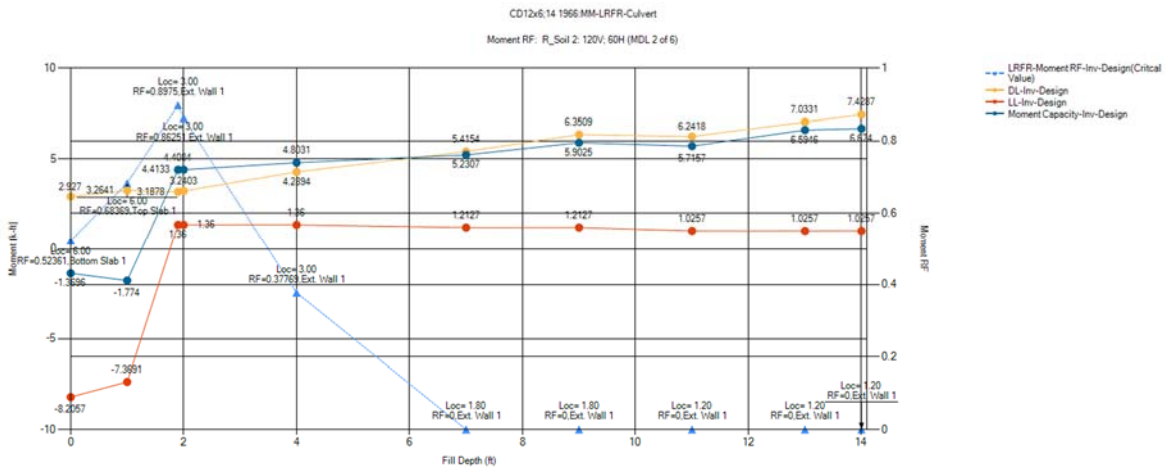


Appendix J – Data Mining BrDR Regression Data

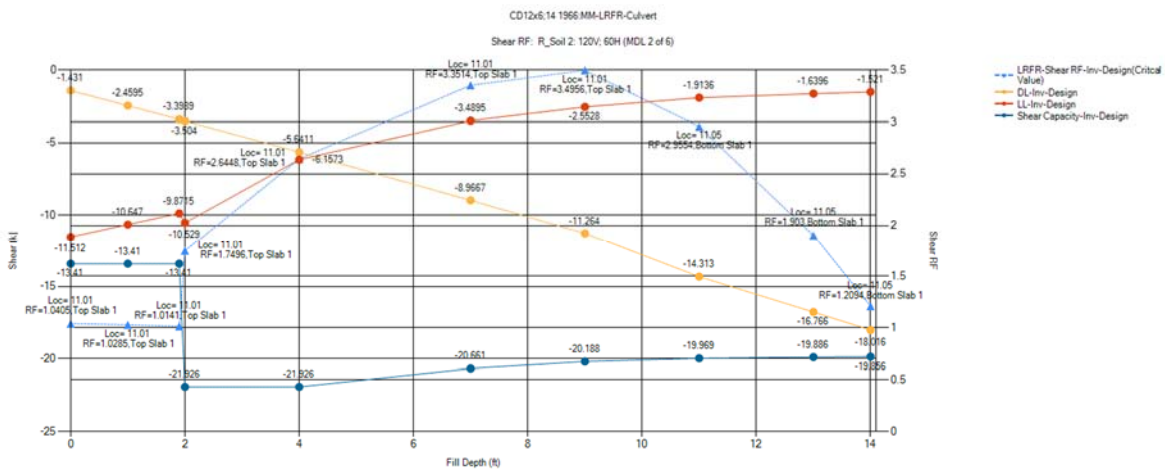
CD12x6;14 1966:MM-LRFR-Culvert: Shear RF: FLAG for Hand Calculations



CD12x6;14 1966:MM-LRFR-Culvert: Moment RF: R_Soil 2: 120V; 60H (MDL 2 of 6)

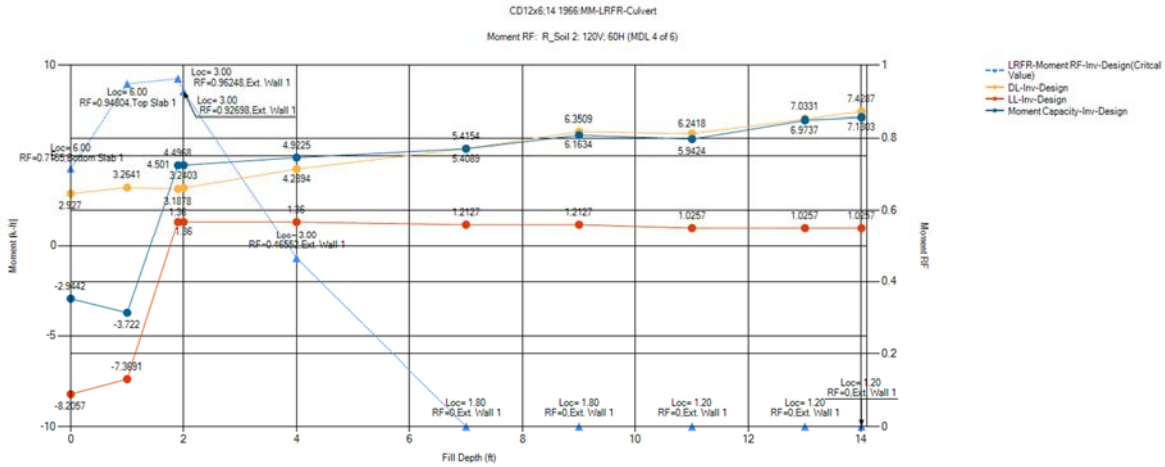


CD12x6;14 1966:MM-LRFR-Culvert: Shear RF: R_Soil 2: 120V; 60H (MDL 2 of 6)

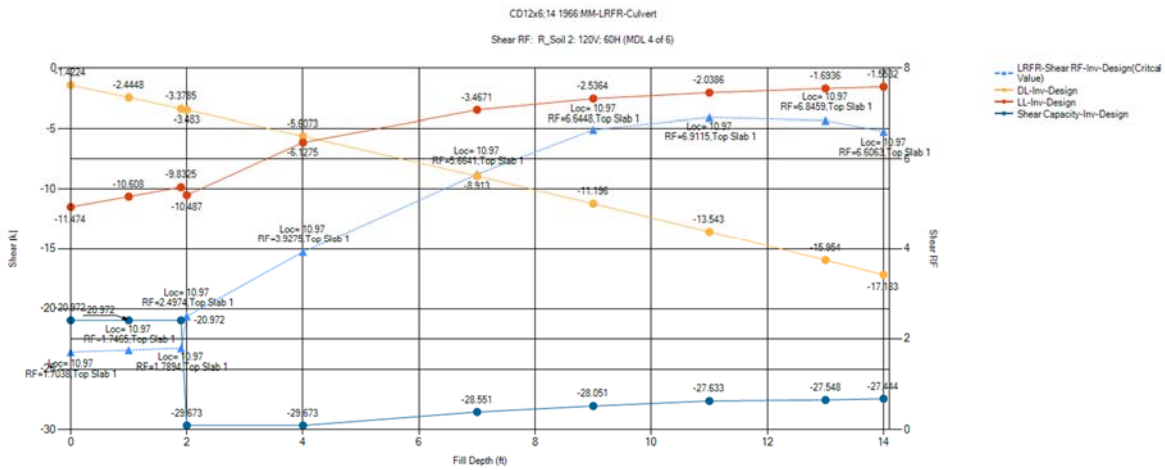


Appendix J – Data Mining BrDR Regression Data

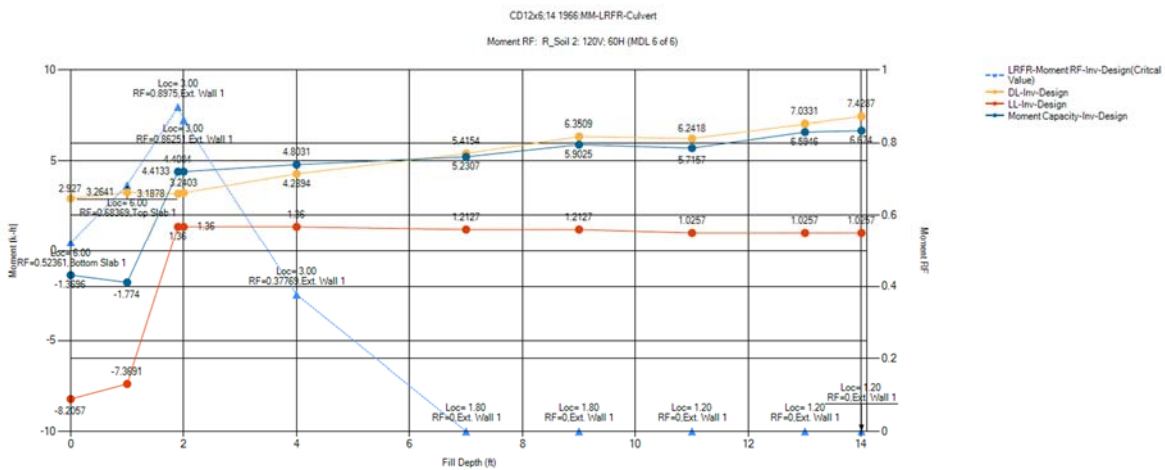
CD12x6;14 1966:MM-LRFR-Culvert: Moment RF: R_Soil 2: 120V; 60H (MDL 4 of 6)



CD12x6;14 1966:MM-LRFR-Culvert: Shear RF: R_Soil 2: 120V; 60H (MDL 4 of 6)

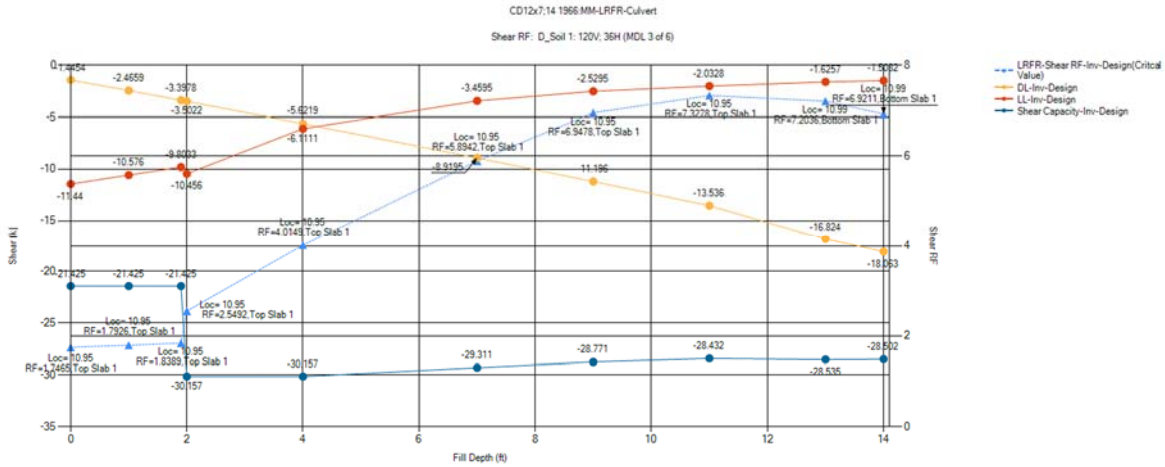


CD12x6;14 1966:MM-LRFR-Culvert: Moment RF: R_Soil 2: 120V; 60H (MDL 6 of 6)

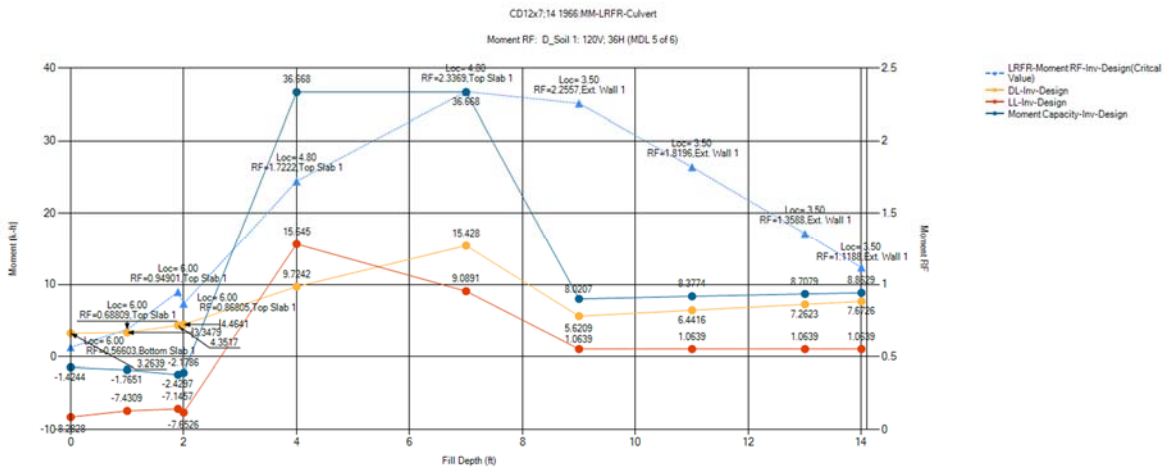


Appendix J – Data Mining BrDR Regression Data

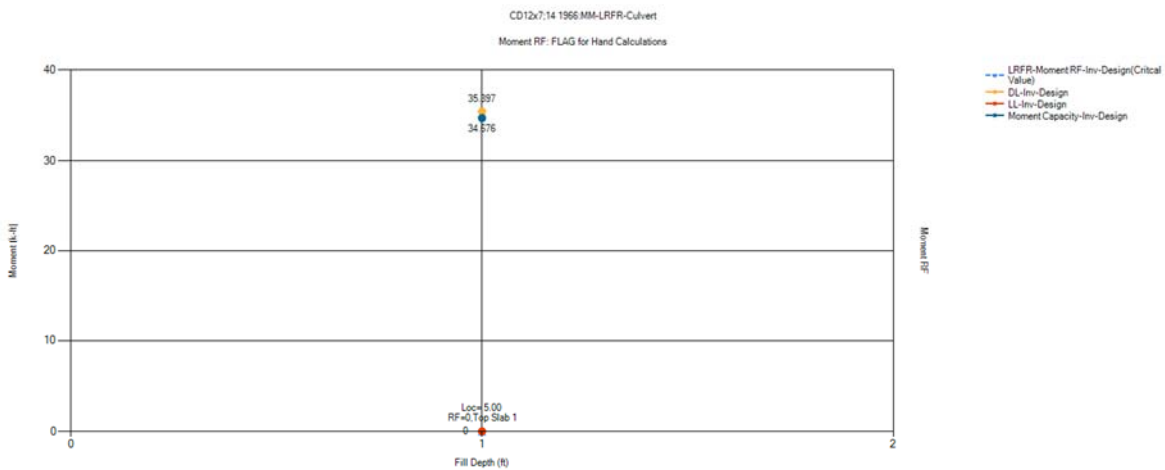
CD12x7;14 1966:MM-LRFR-Culvert: Shear RF: D_Soil 1: 120V; 36H (MDL 3 of 6)



CD12x7;14 1966:MM-LRFR-Culvert: Moment RF: D_Soil 1: 120V; 36H (MDL 5 of 6)

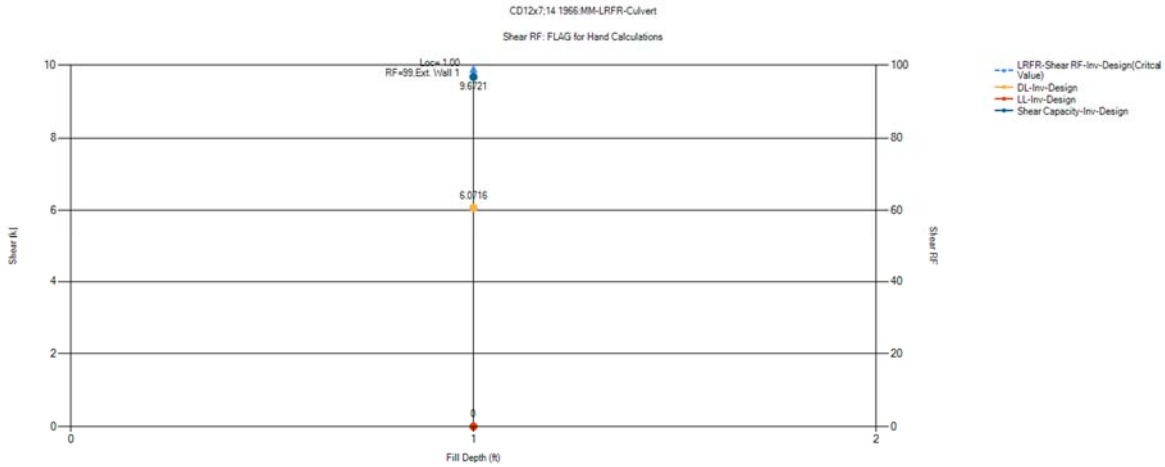


CD12x7;14 1966:MM-LRFR-Culvert: Moment RF: FLAG for Hand Calculations

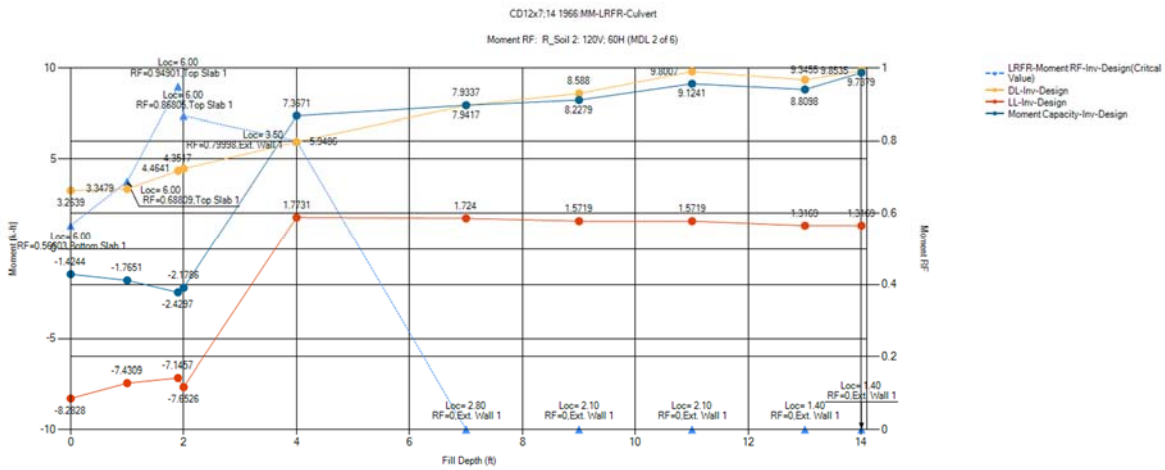


Appendix J – Data Mining BrDR Regression Data

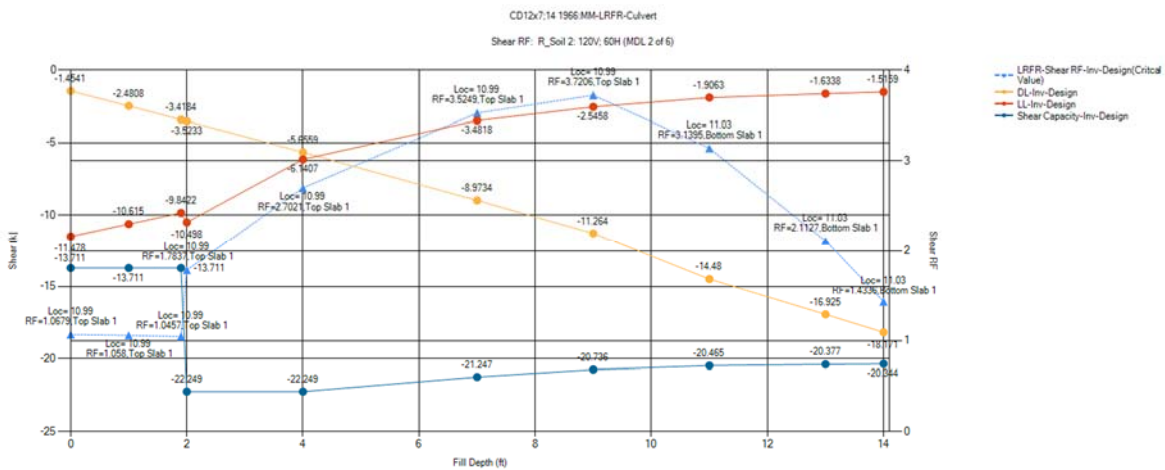
CD12x7;14 1966:MM-LRFR-Culvert: Shear RF: FLAG for Hand Calculations



CD12x7;14 1966:MM-LRFR-Culvert: Moment RF: R_Soil 2: 120V; 60H (MDL 2 of 6)

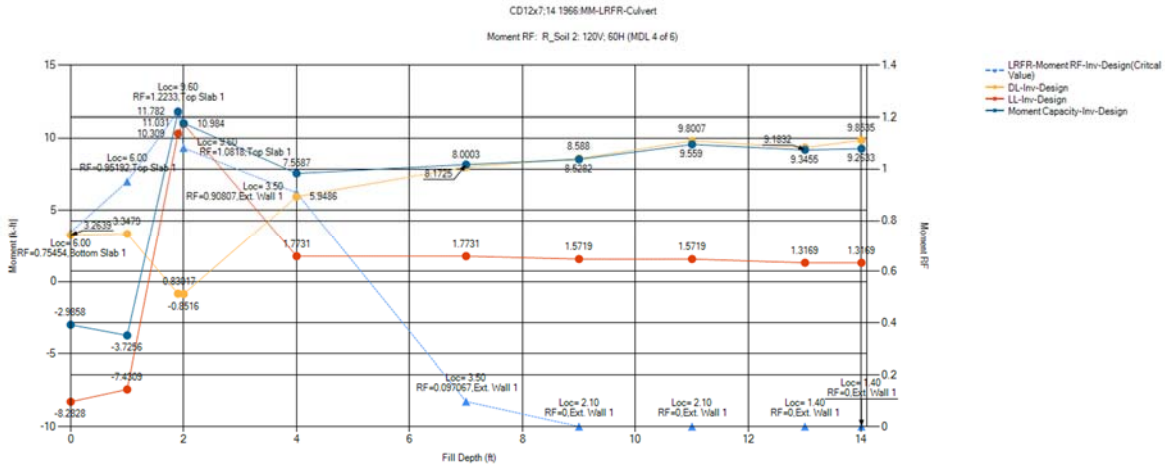


CD12x7;14 1966:MM-LRFR-Culvert: Shear RF: R_Soil 2: 120V; 60H (MDL 2 of 6)

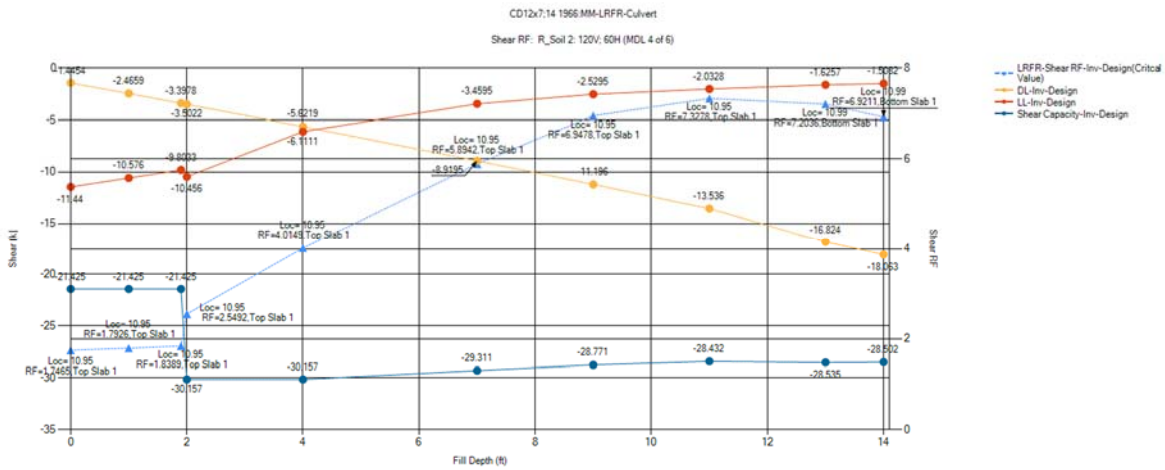


Appendix J – Data Mining BrDR Regression Data

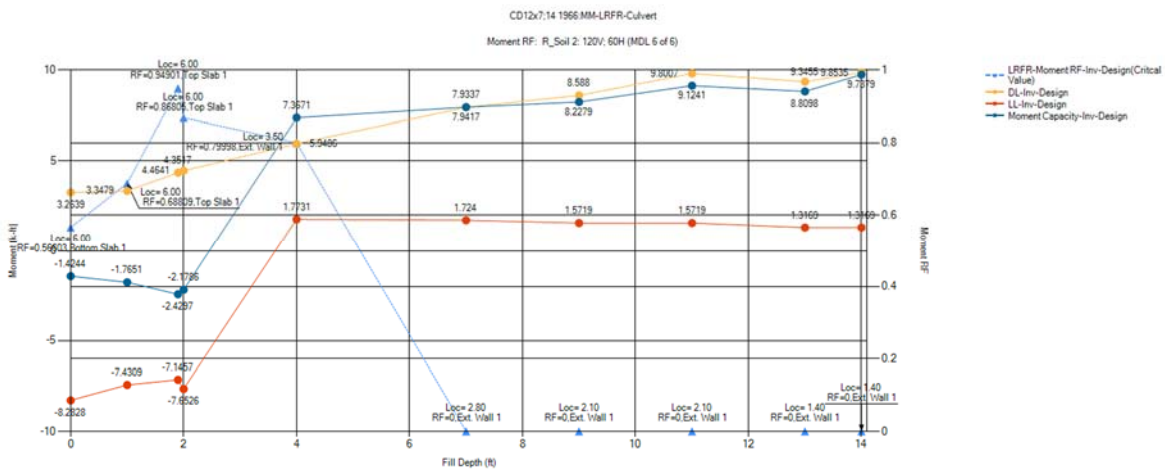
CD12x7;14 1966:MM-LRFR-Culvert: Moment RF: R_Soil 2: 120V; 60H (MDL 4 of 6)



CD12x7;14 1966:MM-LRFR-Culvert: Shear RF: R_Soil 2: 120V; 60H (MDL 4 of 6)

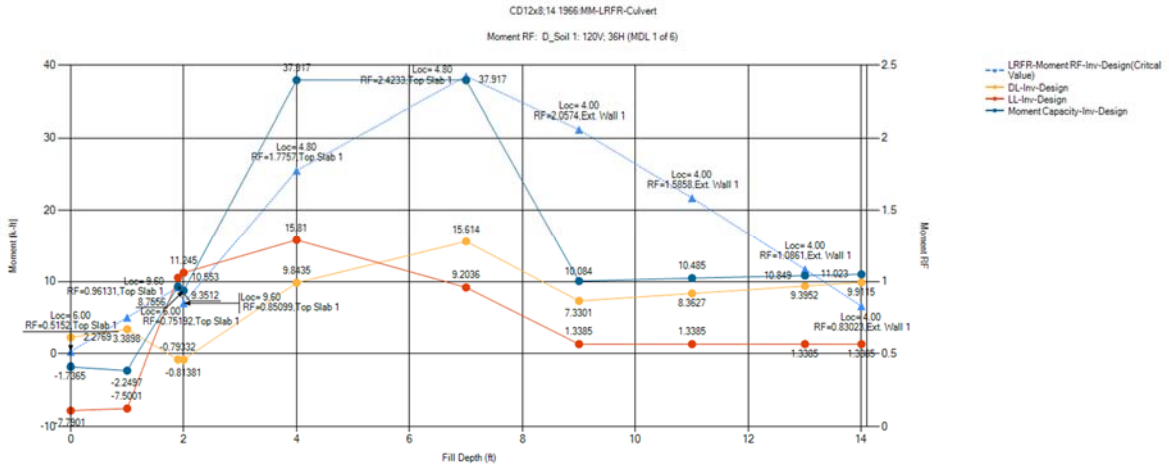


CD12x7;14 1966:MM-LRFR-Culvert: Moment RF: R_Soil 2: 120V; 60H (MDL 6 of 6)

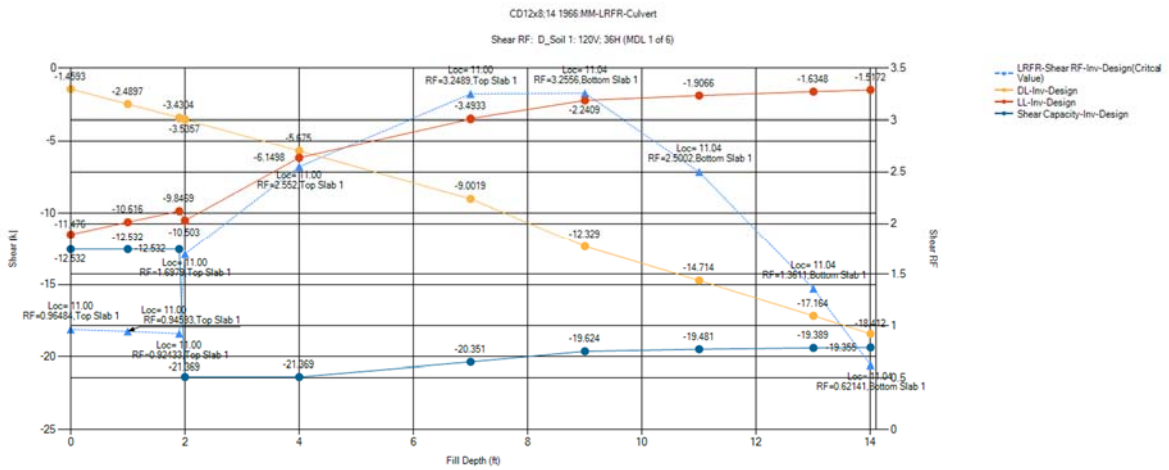


Appendix J – Data Mining BrDR Regression Data

CD12x8;14 1966:MM-LRFR-Culvert: Moment RF: D_Soil 1: 120V; 36H (MDL 1 of 6)



CD12x8;14 1966:MM-LRFR-Culvert: Shear RF: D_Soil 1: 120V; 36H (MDL 1 of 6)



Appendix K – Calibration Information

Appendix K – Calibration Information

Appendix K – Calibration Information

1 Introduction

This appendix contains the calibration summaries for the seven models load tested for this research.

1.1 Calibration Summary – Model 1, Candidate 1

Model 1, Candidate 1 consists of a single-cell precast concrete culvert located in Juniata County, Pennsylvania. Additional details of the testing plan and instrumentation can be found in Appendix F of this document.

The calibration summary herein, presents the LUSAS results (3-D finite element analysis) of Model 1, Candidate 1 under the truck load that was used in the experimental program. The field test loading consisted of two main phases: Phase 1 loading as based on the culvert being loaded with the lift axle of the truck in the up position; and Phase 2 loaded the culvert with the lift axle down. The first phase included four main sets of loading where the marked points are the locations on the slab directly above the line of strain gauge installations:

- U-1: the center of left wheel of Axle 1 of truck over the marked points (see Figure 4).
- U-2: the center of left wheel of Axle 2 of truck over the marked points (see Figure 4).
- U-3: the center of left wheel of Axle 3 of truck over the marked points (see Figure 4).
- U-4: the center of each axle of the truck over the centerline of the line of gauges.

The second phase included five main sets of loading:

- D-1: the center of left wheel of Axle 1 of truck over the marked points (see Figure 4).
- D-2: the center of left wheel of Axle 2 of truck over the marked points (see Figure 4).
- D-3: the center of left wheel of Axle 3 of truck over the marked points (see Figure 4).
- D-4: the center of each axle of the truck over the centerline of the line of gauges.
- D-L: the center of left wheel of Lift Axle of truck over the marked points (see Figure 4).

Experimental Data is recorded and presented in forms of stresses and displacements. The location of the strain gages and the string potentiometers are depicted in Figure 5. The load configuration of the experimental truck for both phases is shown in Figure 6 and Figure 7.

Appendix K – Calibration Information

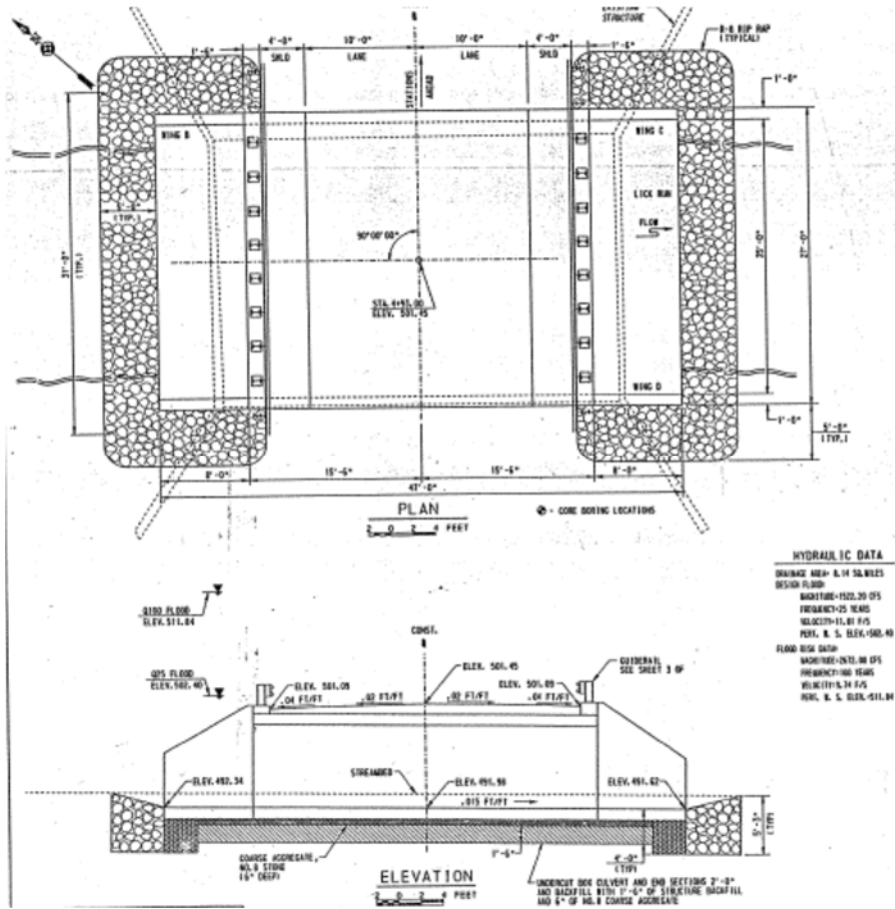


Figure 1 - Culvert Plan and Elevation

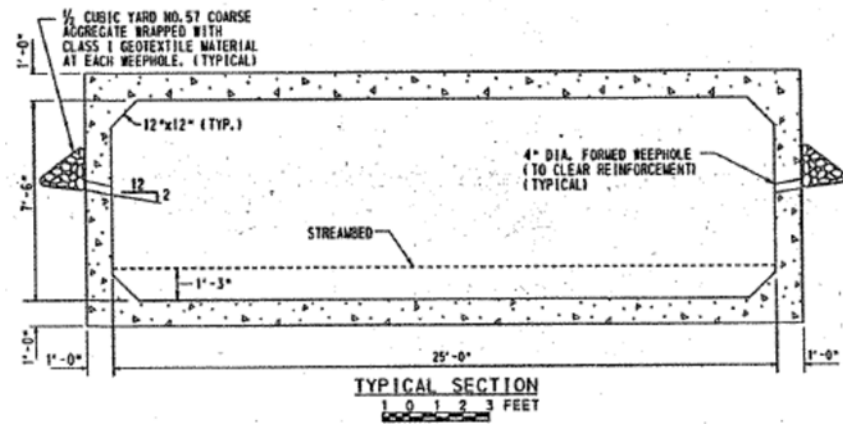


Figure 2 - Culvert Typical Section

Appendix K – Calibration Information

1.1.1 3D LUSAS Model

An isometric view of the 3D LUSAS model is shown in Figure 3 below. In general, the 3D models were developed using the parameters described in Appendix B of this document.

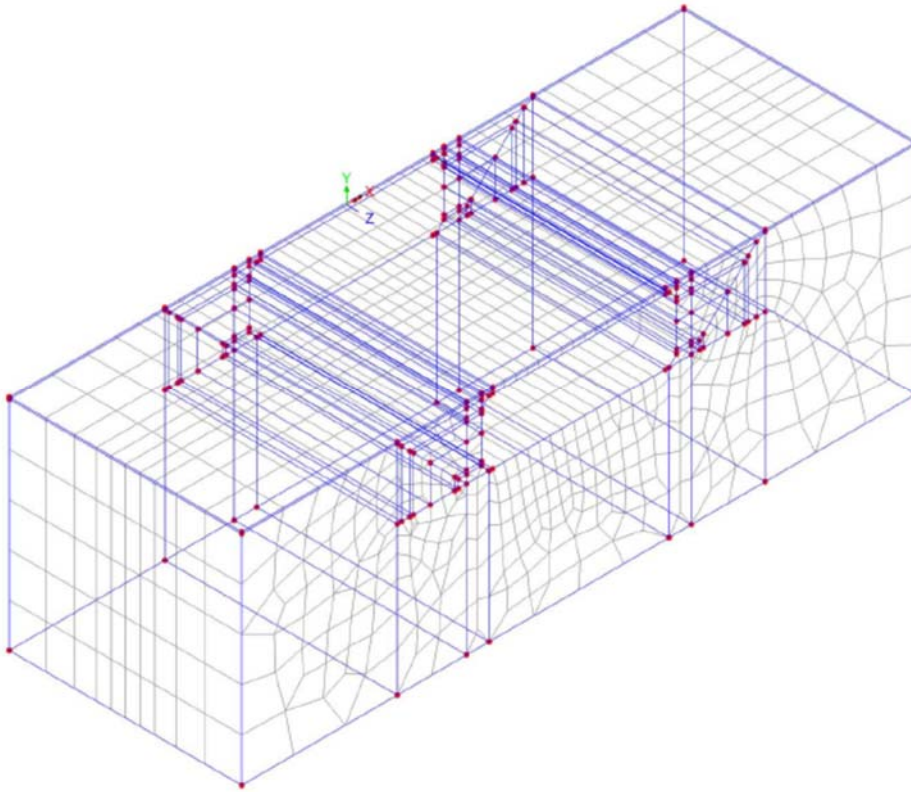


Figure 3 – Model 1 (M1C1) Isometric 3D LUSAS Model

Calibration Results

Comparisons between the field data stresses and displacements as compared to the 3D model predicted values are shown in Figure 8 through Figure 16.

The table below provides a more detailed notation and descriptions of the stress and displacement figures than the abbreviated keys for each these figures. In each of the graphs, the vertical axis represents either the stress (for strain gauge locations) or displacement (for string potentiometer locations). The horizontal axis represents the load locations for each of the five load positions shown in Figure 4. For all gauge locations, see Figure 5.

Appendix K – Calibration Information

Notation	Description
G1	<i>Gage 1 – 3D LUSAS model results</i>
G1 – Data	<i>Gage 1 – Field testing data results</i>
G2	<i>Gage 2 – 3D LUSAS model results</i>
G2 – Data	<i>Gage 2 – Field testing data results</i>
G3	<i>Gage 3 – 3D LUSAS model results</i>
G3 – Data	<i>Gage 3 – Field testing data results</i>
G4	<i>Gage 4 – 3D LUSAS model results</i>
G4 – Data	<i>Gage 4 – Field testing data results</i>
G5	<i>Gage 5 – 3D LUSAS model results</i>
G5 – Data	<i>Gage 5 – Field testing data results</i>
POT-2	<i>String Potentiometer 2 - 3D LUSAS model results</i>
POT-2-Data	<i>String Potentiometer 2 – Field testing data results</i>
POT-3	<i>String Potentiometer 3 - 3D LUSAS model results</i>
POT-3-Data	<i>String Potentiometer 3 – Field testing data results</i>

Figure 8 through Figure 11 are for the lift axle up configuration showing each axle placed over each of the marked points with the left wheel centered on the gauge line and then with the center of the truck centered over the gauge line.

Figure 12 through Figure 16 are for the lift axle down configuration showing each axle placed over each of the marked points with the left wheel centered on the gauge line and then with the center of the truck centered over the gauge line.

As can be seen in Figure 8 through Figure 16, at axle load locations that produce the peak positive and negative moment stresses, good agreement is seen in the negative moment stresses at the corner of the culvert (gauge locations G3 and G4) and at the quarter-point gauge location (G4). Displacement at the midspan of the top slab (Pot 3) also shows good agreement whereas the stresses predicted by the model at that location are significantly less than what was measured in the field.

Appendix K – Calibration Information

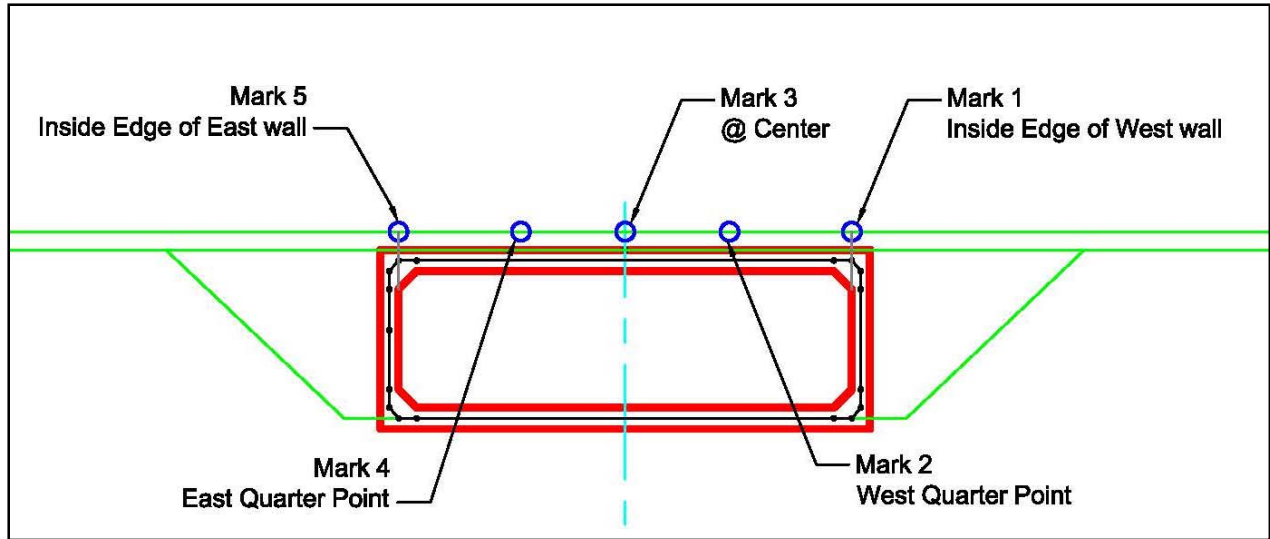


Figure 4 - Location of Marks (Location of Axles for each Load Case) (M1C1)

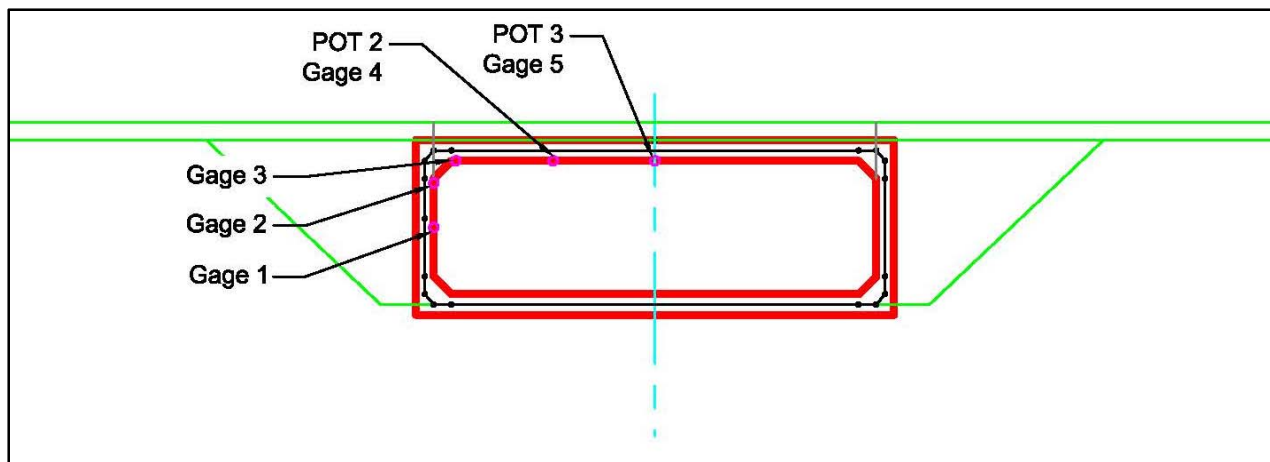


Figure 5 - Location of Strain Gages and String Potentiometers (M1C1)

Appendix K – Calibration Information

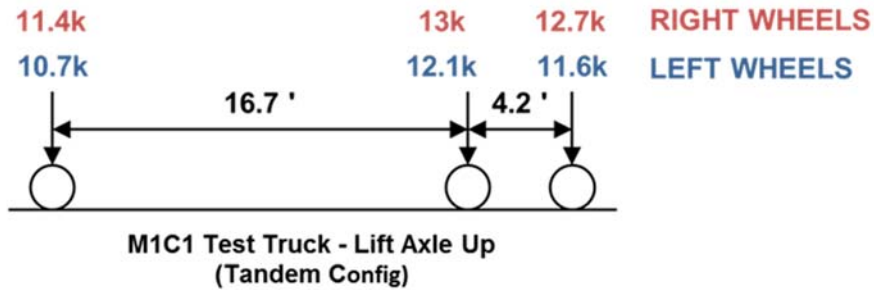


Figure 6 - Load Truck Configuration for Phase 1 (lift axle up) (M1C1)

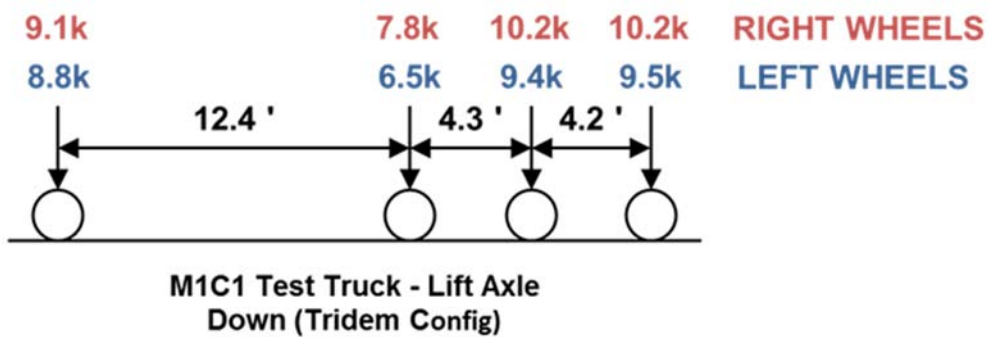


Figure 7 - Load Truck Configuration for Phase 2 (lift axle down)(M1C1)

Appendix K – Calibration Information

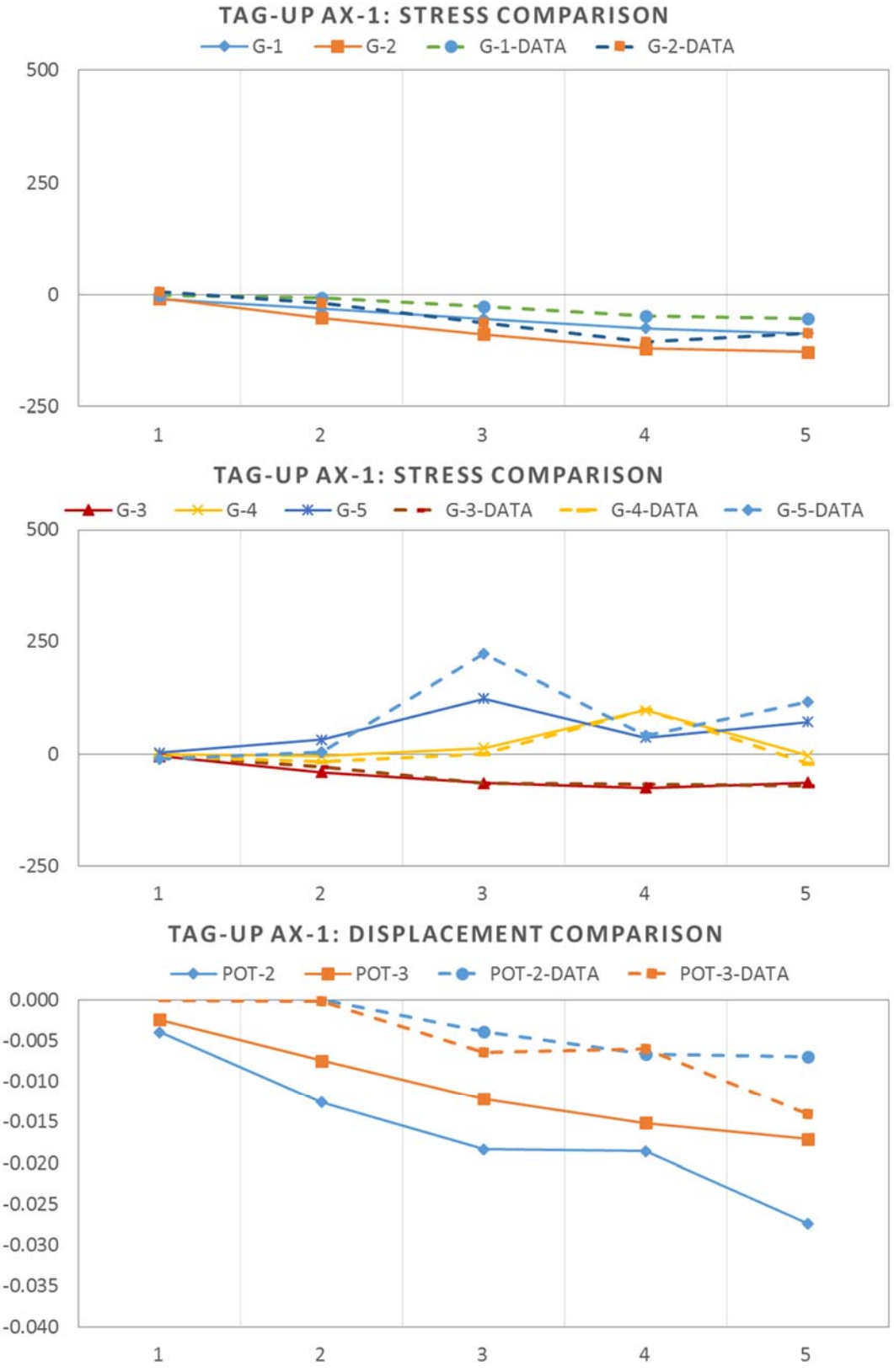


Figure 8 - Load Case U-1: Lift Axle Up and Axle 1 Left Wheel over Marked Points (M1C1)

Appendix K – Calibration Information

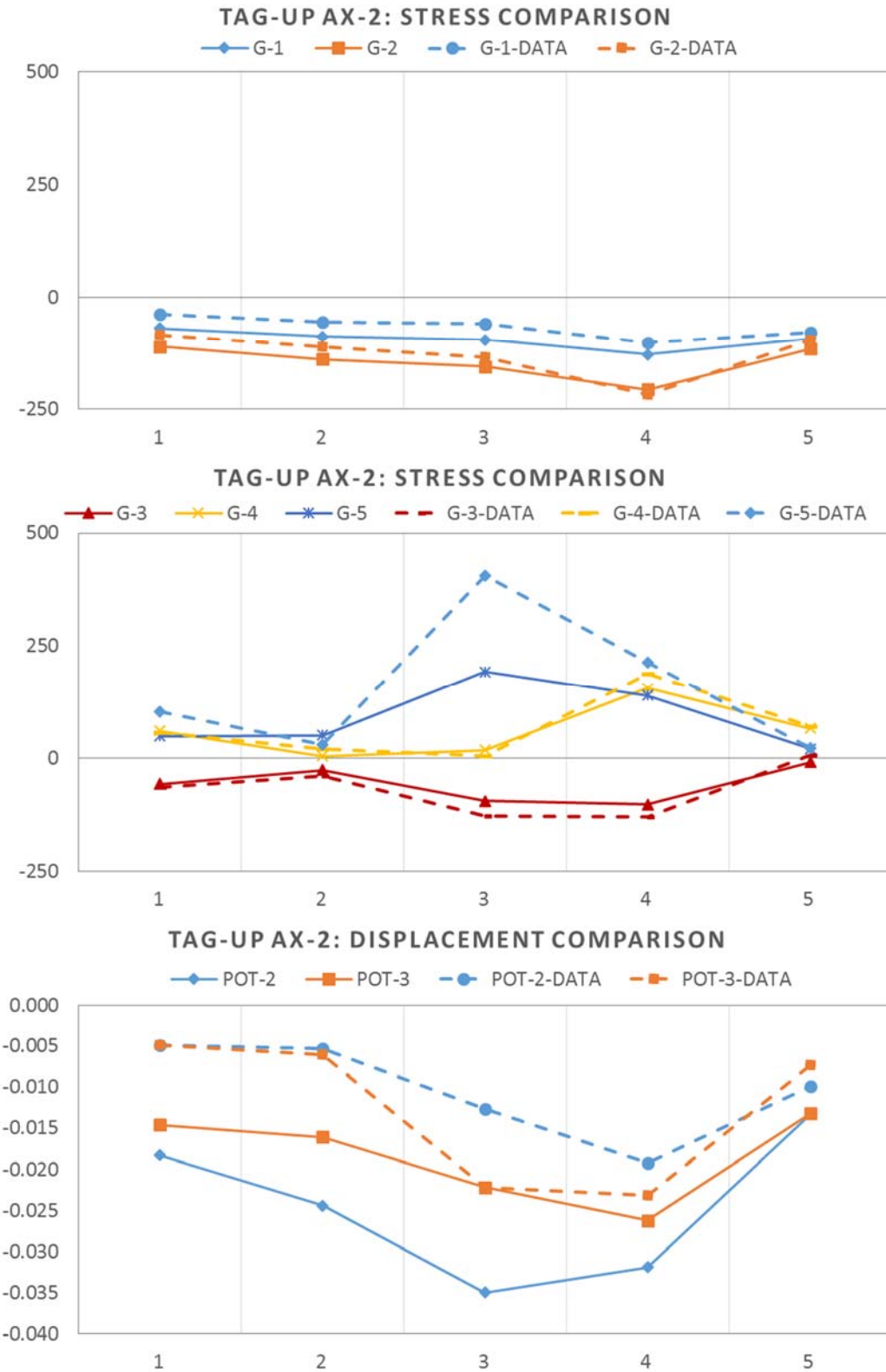


Figure 9 - Load Case U-2: Lift Axle Up and Axle 2 Left Wheel over Marked Points (M1C1)

Appendix K – Calibration Information

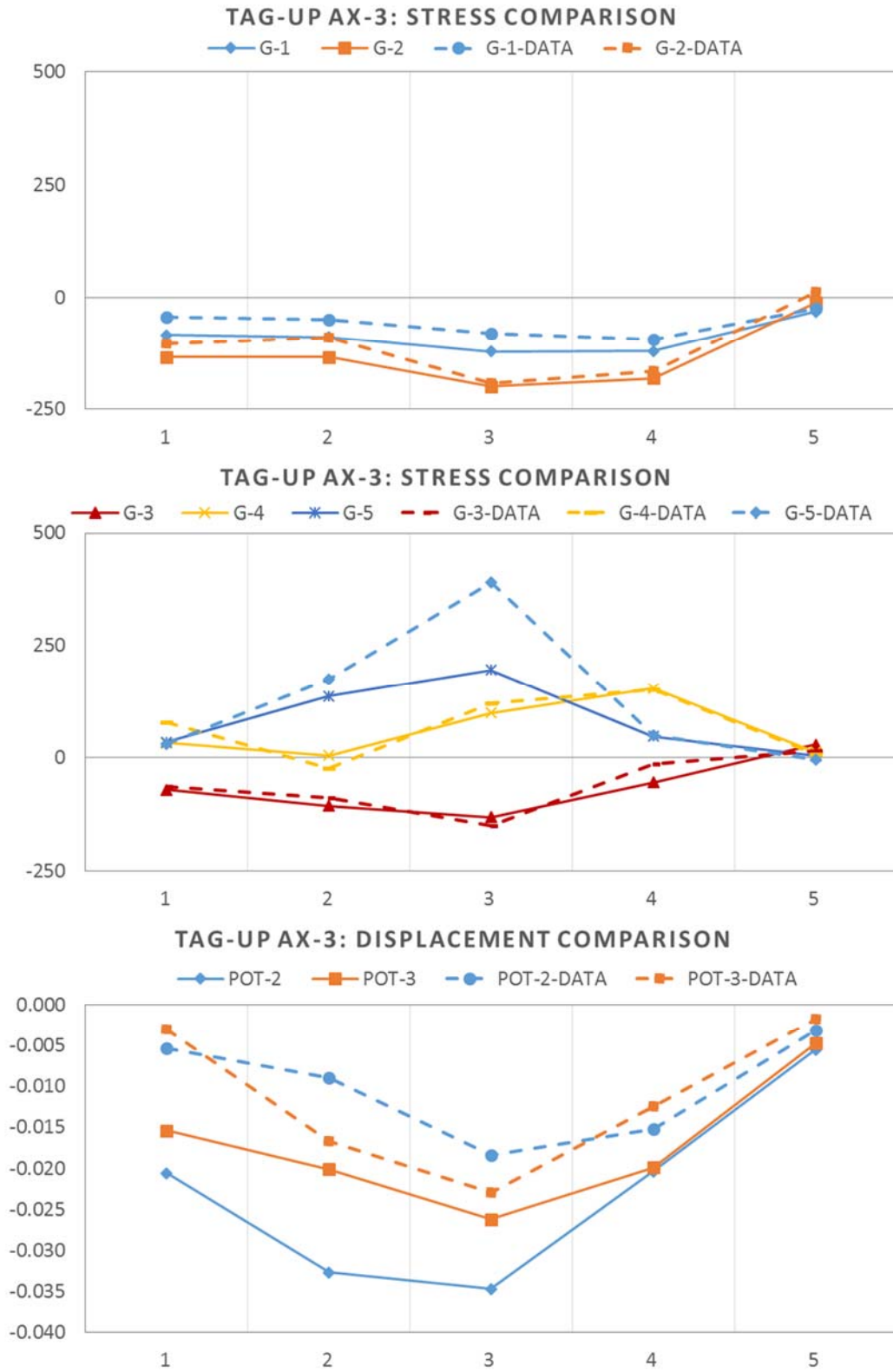


Figure 10 - Load Case U-3: Lift Axle Up and Axle 3 Left Wheel over Marked Points (M1C1)

Appendix K – Calibration Information

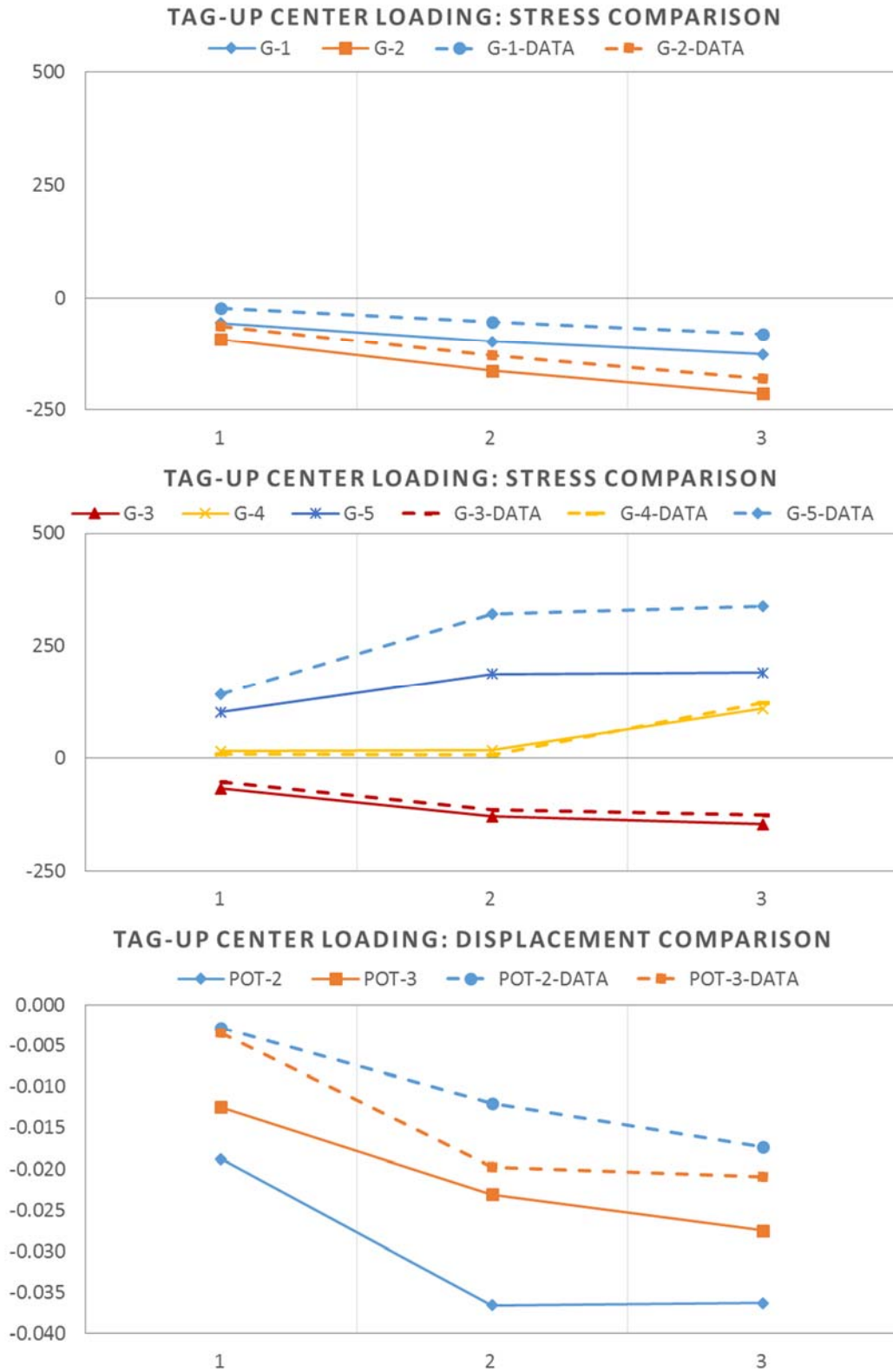


Figure 11 - Load Case U-4: Lift Axle Up and Center of each Axle over Midspan (M1C1)

Appendix K – Calibration Information

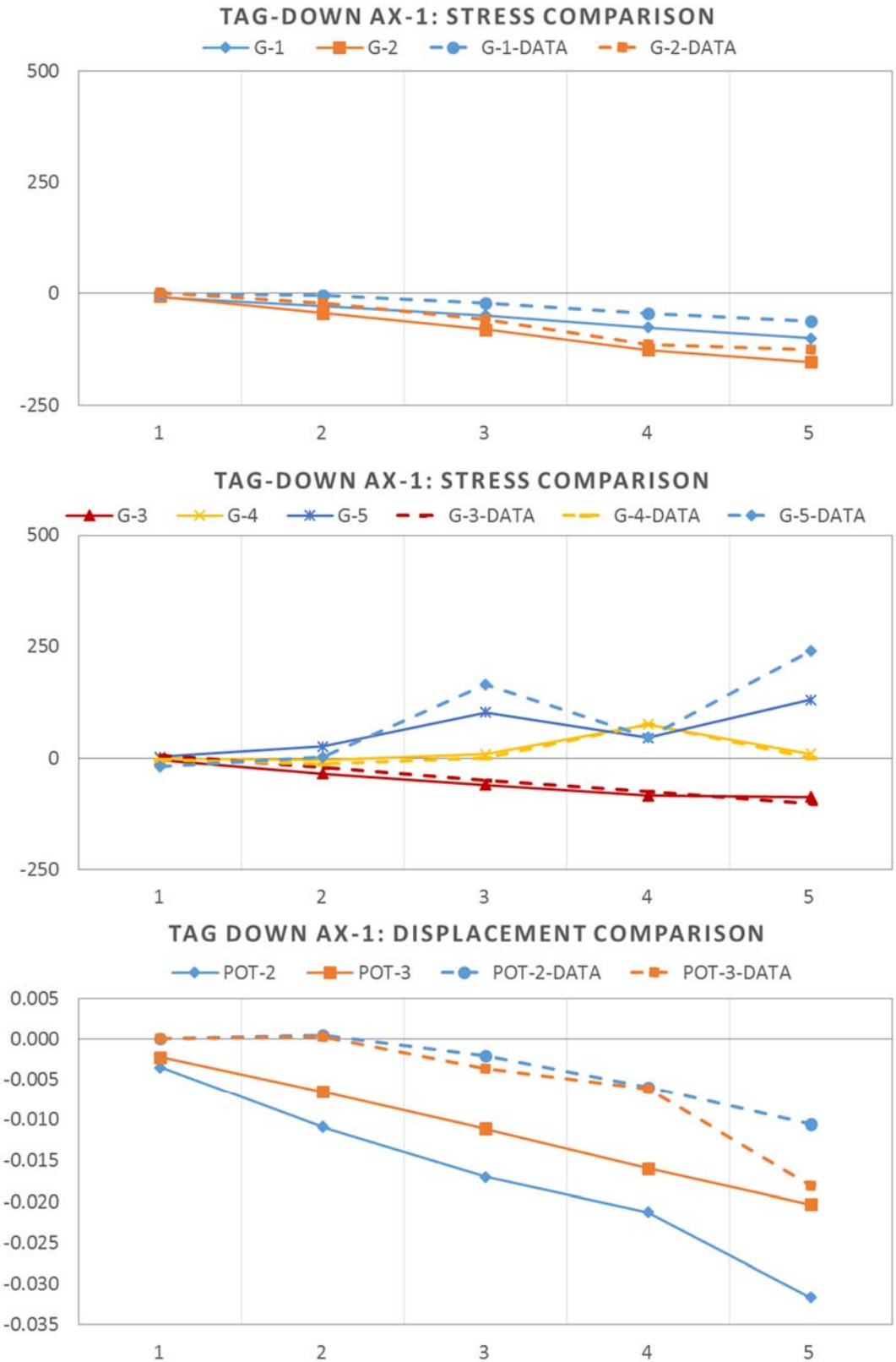


Figure 12 - Load Case D-1: Lift Axle Down and Axle 1 Left Wheel over Marked Points (M1C1)

Appendix K – Calibration Information



Figure 13 - Load Case D-2: Lift Axle Down and Axle 2 Left Wheel over Marked Points (M1C1)

Appendix K – Calibration Information

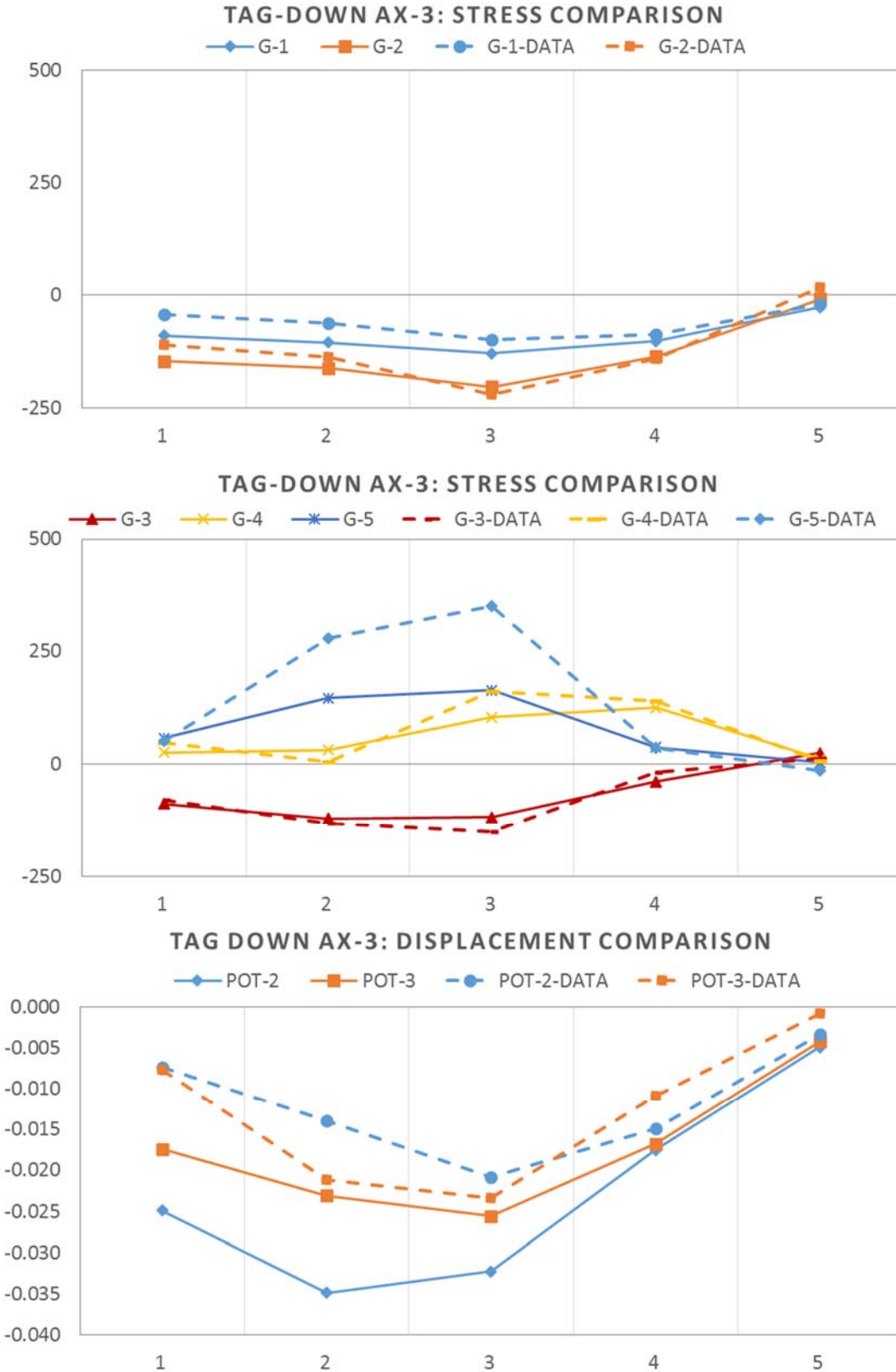


Figure 14 - Load Case D-3: Lift Axle Down and Axle 3 Left Wheel over Marked Points (M1C1)

Appendix K – Calibration Information



Figure 15 - Load Case D-L: Lift Axle Down and Lift Axle Left Wheel over Marked Points (M1C1)

Appendix K – Calibration Information

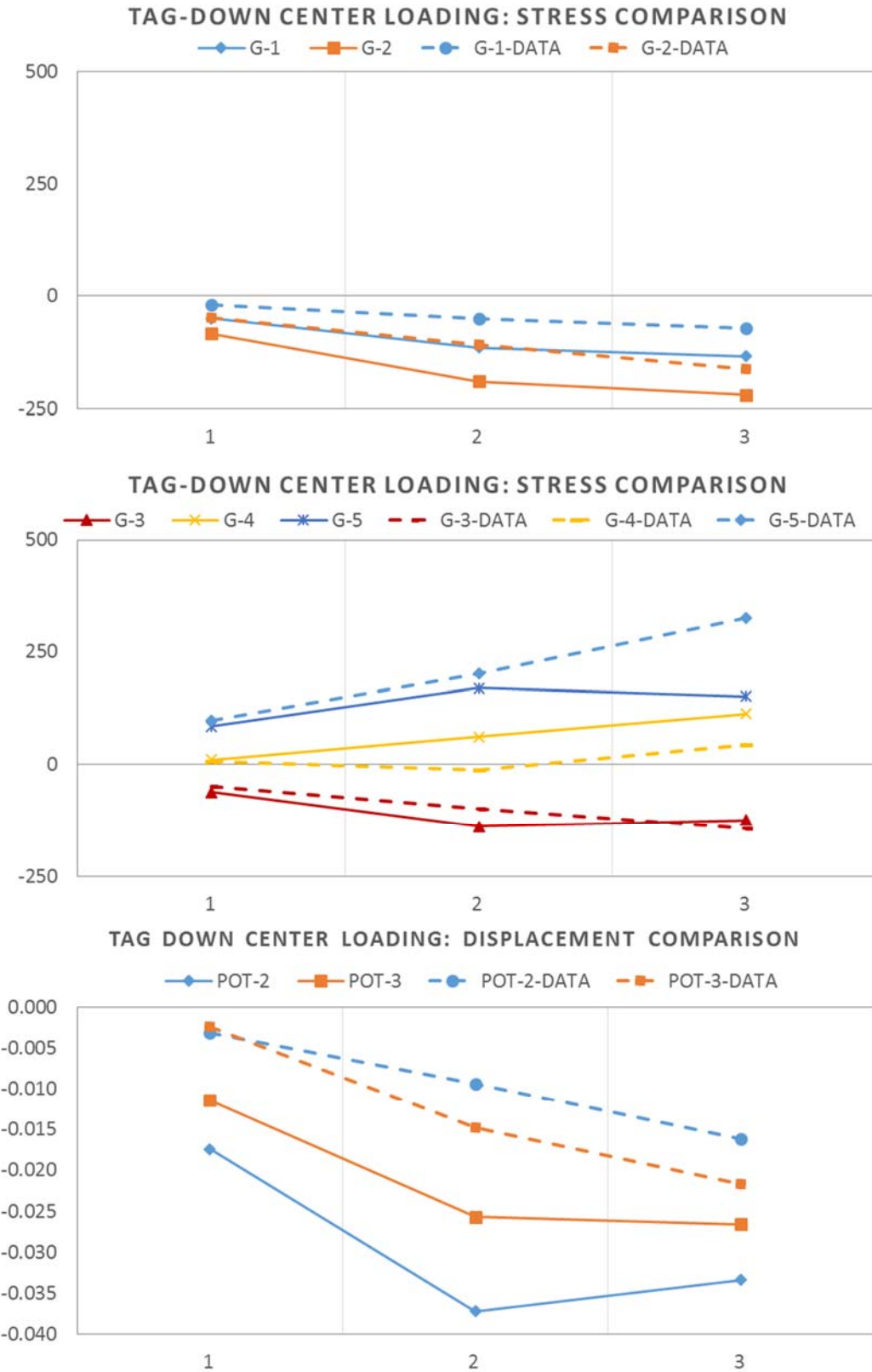


Figure 16 - Load Case D-4: Lift Axle Down and Center of each Axle over Midspan (M1C1)

Appendix K – Calibration Information

1.2 Calibration Summary – Model 2, Candidate 1

Model 2, Candidate 1 consists of a two-cell cast-in-place reinforced concrete culvert located in the state of Maryland and owned by the Maryland DOT (Structure Number 0329500). Additional details of the testing plan and instrumentation can be found in Appendix F of this document.

The calibration summary herein, presents the LUSAS results (3-D finite element analysis) of Model 2, Candidate 1 under the truck load that was used in the experimental program. The field test loading consisted of two main phases: Phase 1 loading as based on the culvert being loaded with the lift axle of the truck in the up position; and Phase 2 loaded the culvert with the lift axle down. The wheel line of the truck was first run over the line of gauges below. Next, the tests in each phase were also repeated for the case where the truck centerline coincided with the line of gauges. The table below summarizes the loading cases.

<i>Test Load Case</i>	<i>Drop Axle Configuration</i>	<i>Axle of Truck Placed on each Load Point*</i>	<i>Wheel Or Truck Centerline Placed Over Line of Gauges</i>
1	Up	1	Wheel
2	Up	3	Wheel
3	Up	4	Wheel
4	Down	1	Wheel
5	Down	2	Wheel
6	Down	3	Wheel
7	Down	4	Wheel
8	Up	1	Truck
9	Up	3	Truck
10	Up	4	Truck
11	Down	1	Truck
12	Down	2	Truck
13	Down	3	Truck
14	Down	4	Truck

*Axles numbered consecutively from steering axle to rear axle

Experimental Data is recorded and presented in forms of stresses and displacements. The location of the strain gages and the string potentiometers are depicted in Figure 21. The load configuration of the experimental truck for both phases is shown in Figure 22 and Figure 23.

Appendix K – Calibration Information

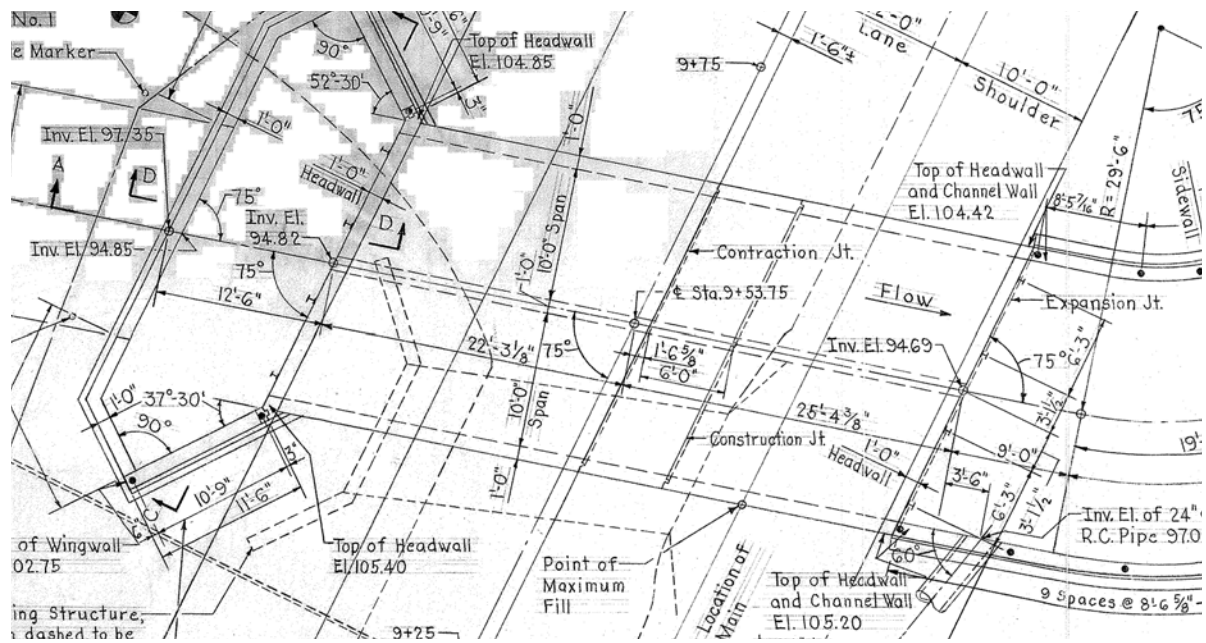


Figure 17 – Culvert Plan View (Skewed)

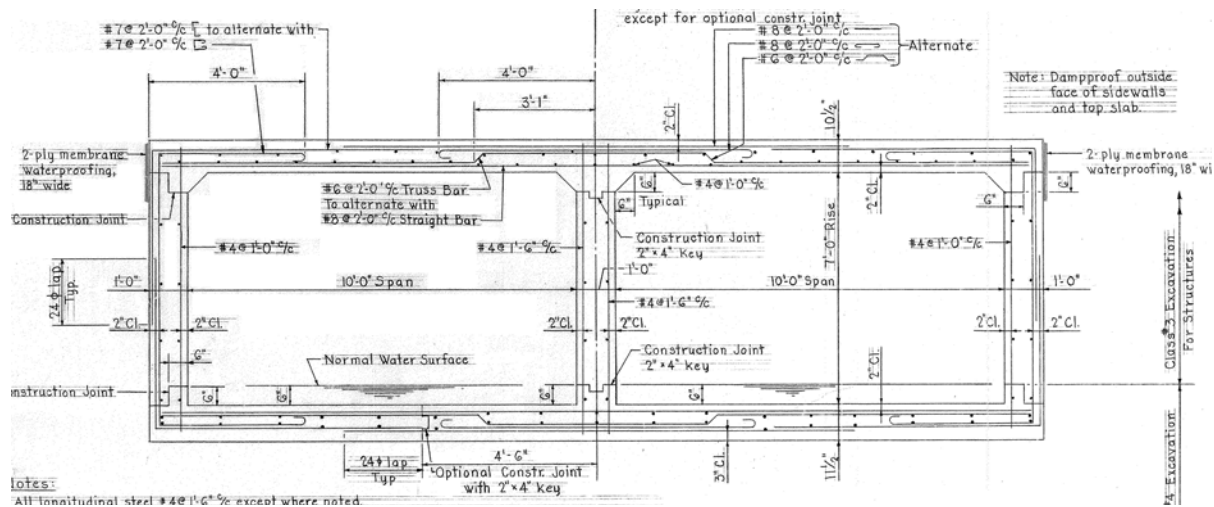


Figure 18 - Culvert Typical Section

Appendix K – Calibration Information

1.2.1 3D LUSAS Model

An isometric view of the 3D LUSAS model is shown in Figure 19 below. In general, the 3D models were developed using the parameters described in Appendix B of this document.

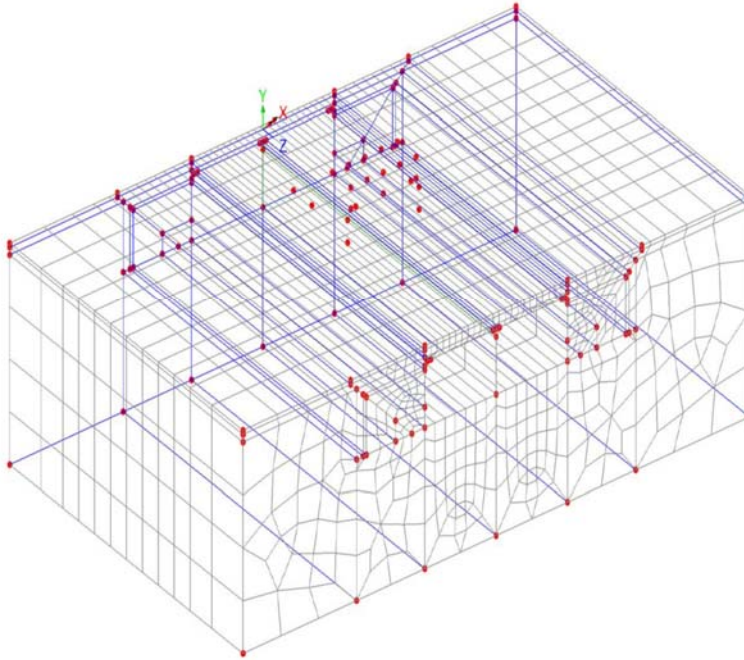


Figure 19 - Isometric View of 3D LUSAS Model (M2C1)

Calibration Results

Comparisons between the field data stresses and displacements as compared to the 3D model predicted values are shown in Figure 24 and Figure 25.

In each of the graphs, the vertical axis represents either the stress at strain gauge locations. The horizontal axis represents the load locations for each of the six load positions shown in Figure 20. For all gauge locations, see Figure 30. In the graphs, the dashed lines represent field-collected data while the solid lines represent the results obtained from the 3D model.

Figure 22 and Figure 23 are for the lift axle up and down configurations, respectively, showing each axle placed over each of the marked points with the centerline of the truck centered on the gauge.

As can be seen in the representative results shown, the 3D model is significantly conservatively overestimating the stresses, particularly for loads placed over the first cell of the culvert. It should be noted that the redundant sets of gauges generally produced similar results to one another.

Appendix K – Calibration Information

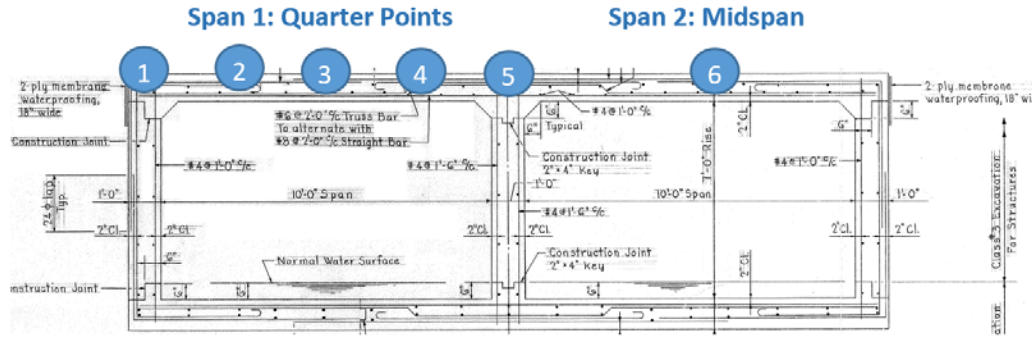


Figure 20 - Location of Marks (Location of Axles for each Load Case) (M2C1)

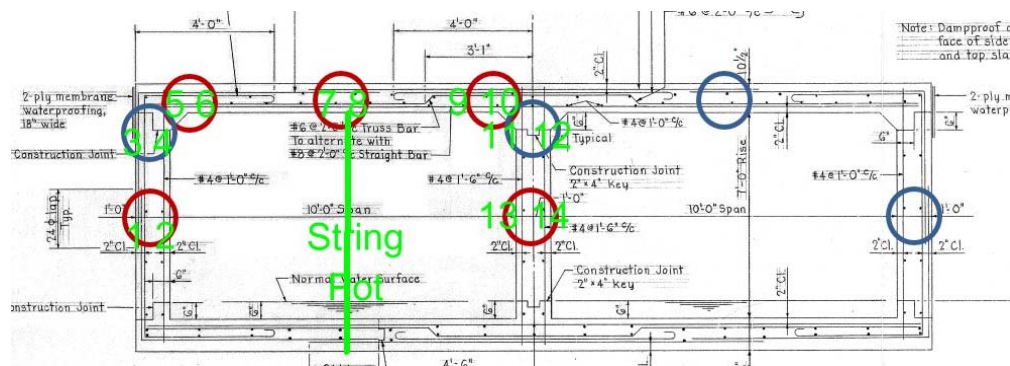
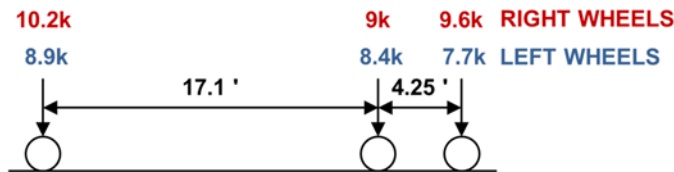
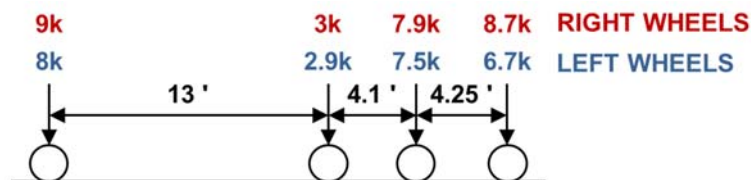


Figure 21 - Location of Strain Gages and String Potentiometers (M2C1)



M2C1 Test Truck - Lift Axle Up
(Tandem Configuration)

Figure 22 - Load Truck Configuration for Phase 1 (lift axle up) (M2C1)



M2C1 Test Truck - Lift Axle Down
(Tridem Configuration)

Figure 23 - Load Truck Configuration for Phase 2 (lift axle down) (M2C1)

Appendix K – Calibration Information

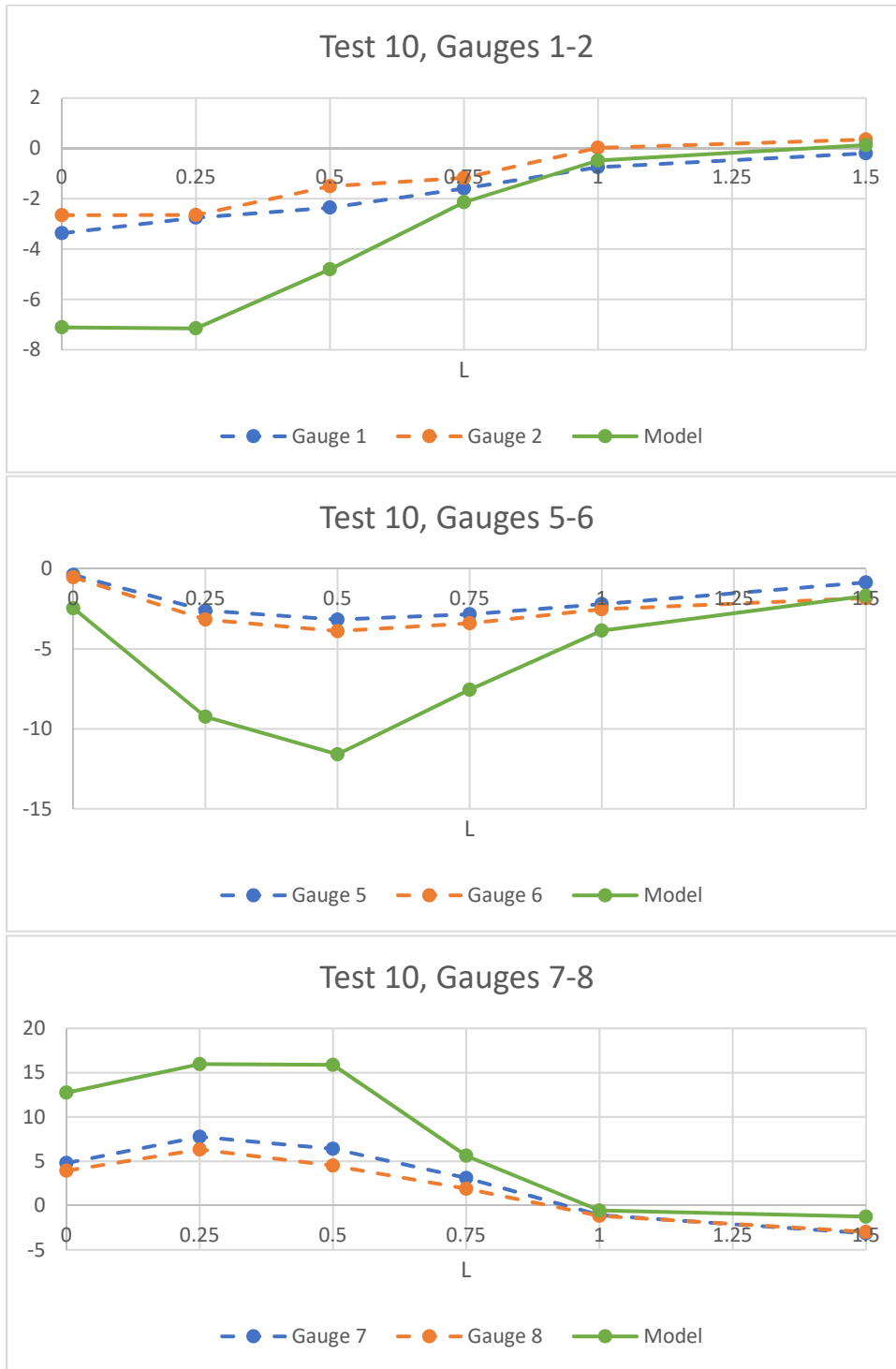


Figure 24 - Load Case 10: Lift Axle Up and Axle 4 Truck Centerline over Marked Points (M2C1)

Appendix K – Calibration Information

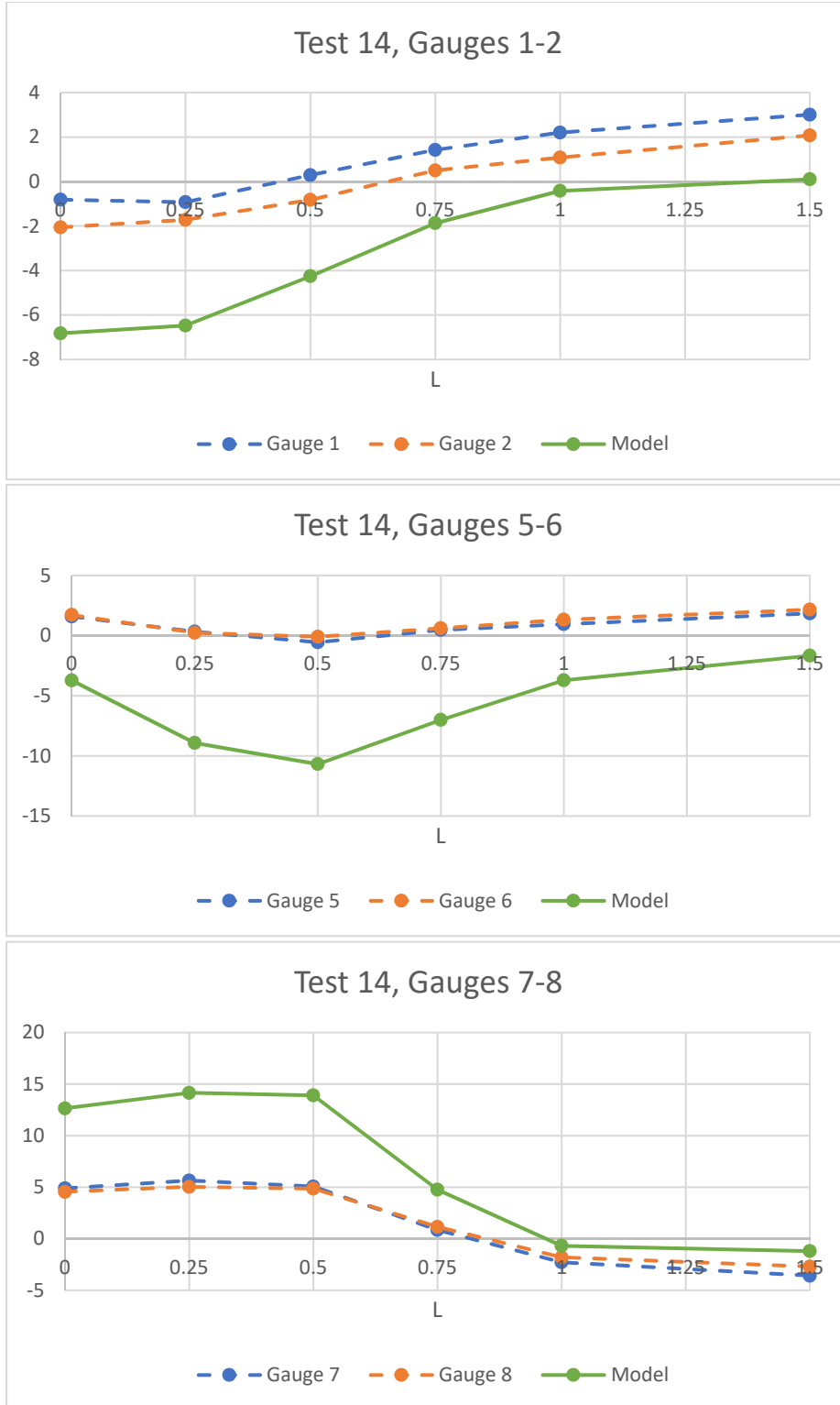


Figure 25 - Load Case 14: Lift Axle Down and Axle 4 Truck Centerline over Marked Points (M2C1)

Appendix K – Calibration Information

1.3 Calibration Summary – Model 3, Candidate 1

Model 3, Candidate 1 consists of a single-cell precast concrete culvert located in Somerset County Pennsylvania and owned by PennDOT (Structure BRKEY 48389). Additional details of the testing plan and instrumentation can be found in the testing plan document. Additional details of the testing plan and instrumentation can be found in Appendix F of this document.

The calibration summary herein, presents the LUSAS results (3-D finite element analysis) of Model 3, Candidate 1 under the truck load that was used in the experimental program. The field test loading consisted of two main phases: Phase 1 loading as based on the culvert being loaded with the lift axle of the truck in the up position; and Phase 2 loaded the culvert with the lift axle down. The wheel line of the truck was first run over the line of gauges below. Next, the tests in each phase were also repeated for the case where the truck centerline coincided with the line of gauges. The table below summarizes the loading cases.

<i>Test Load Case</i>	<i>Drop Axle Configuration</i>	<i>Axle of Truck Placed on each Load Point*</i>	<i>Wheel Or Truck Centerline Placed Over Line of Gauges</i>
1	Up	1	Wheel
2	Up	3	Wheel
3	Up	4	Wheel
4	Down	1	Wheel
5	Down	2	Wheel
6	Down	3	Wheel
7	Down	4	Wheel
8	Down	**	Truck
9	Up	**	Truck

*Axles numbered consecutively from steering axle to rear axle

**Each axle of the truck was placed over the midspan point on the culvert for these tests

Experimental Data is recorded and presented in forms of stresses and displacements. The location of the strain gages and the string potentiometers are depicted in Figure 30. The load configuration of the experimental truck for both phases is shown in Figure 31 and Figure 32.

Appendix K – Calibration Information

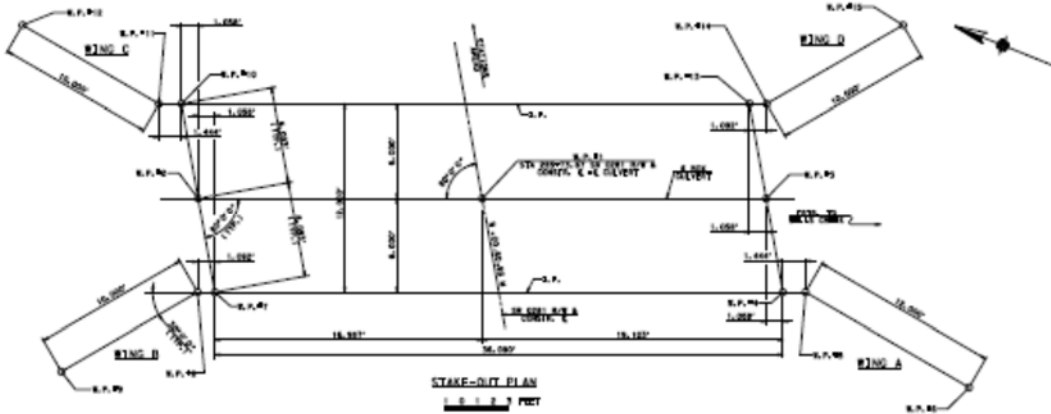


Figure 26 - Culvert Plan View (Skewed) (M3C1)

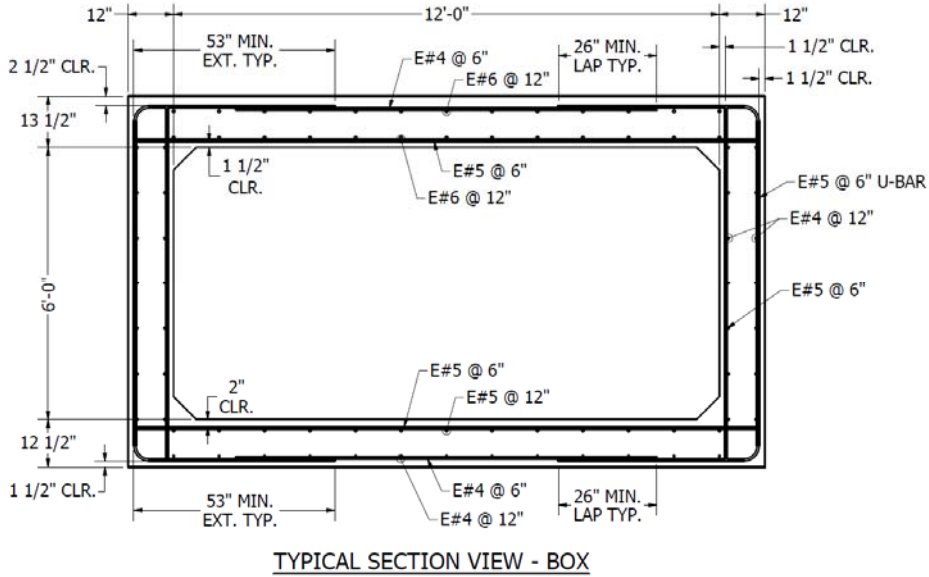


Figure 27 - Culvert Typical Section (M3C1)

Appendix K – Calibration Information

1.3.1 3D LUSAS Model

An isometric view of the 3D LUSAS model is shown in Figure 28 below. In general, the 3D models were developed using the parameters described in Appendix B of this document.

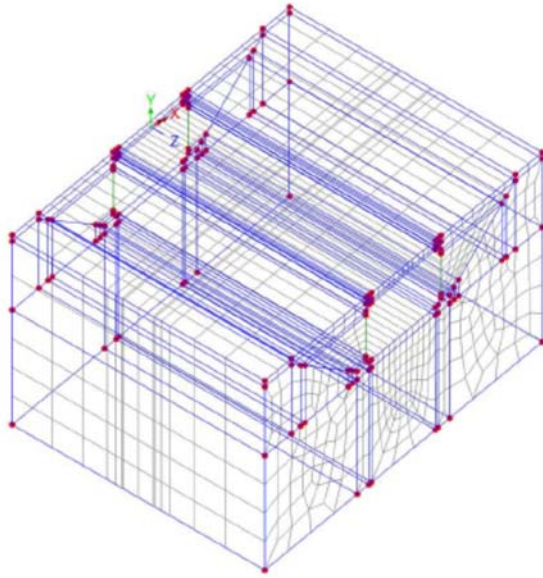


Figure 28 - Isometric View of 3D LUSAS Model

Calibration Results

Comparisons between the field data stresses and displacements as compared to the 3D model predicted values are shown in Figure 33 through Figure 33 .

In each of the graphs, the vertical axis represents either the stress (for strain gauge locations) or displacement (for string potentiometer locations). The horizontal axis represents the load locations for each of the six load positions shown in Figure 29. For all gauge locations, see Figure 30. In the graphs, the dashed lines represent field-collected data while the solid lines represent the results obtained from the 3D model.

Figure 33 shows some representative results for the lift axle up configuration showing each axle placed over each of the marked points with the left wheel centered on the gauge line and then with the center of the truck centered over the gauge line.

Figure 34 shows results for the lift axle down configuration showing each axle placed over each of the marked points with the left wheel centered on the gauge line and then with the center of the truck centered over the gauge line.

As can be seen in Figure 33 and Figure 34, stresses for the gauge clusters at the top slab show fairly good agreement with more disparity seen at the lower gauge of clusters near the bottom slab. At that location, the stresses predicted by the 3D model are conservatively higher than what was observed in the field measurements suggesting that more load spreading is occurring than is predicted by the model.

Appendix K – Calibration Information

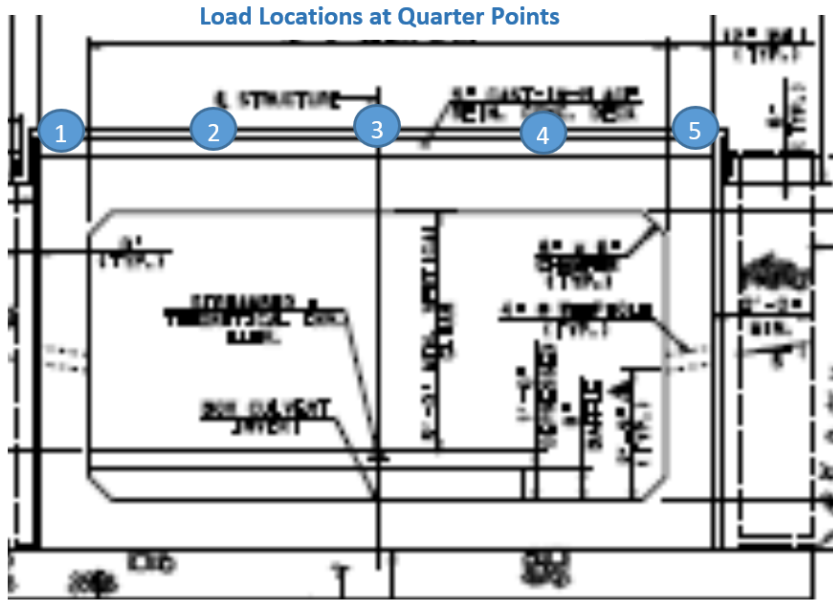


Figure 29 - Location of Marks (Location of Axles for each Load Case) (M3C1)

Instrumentation

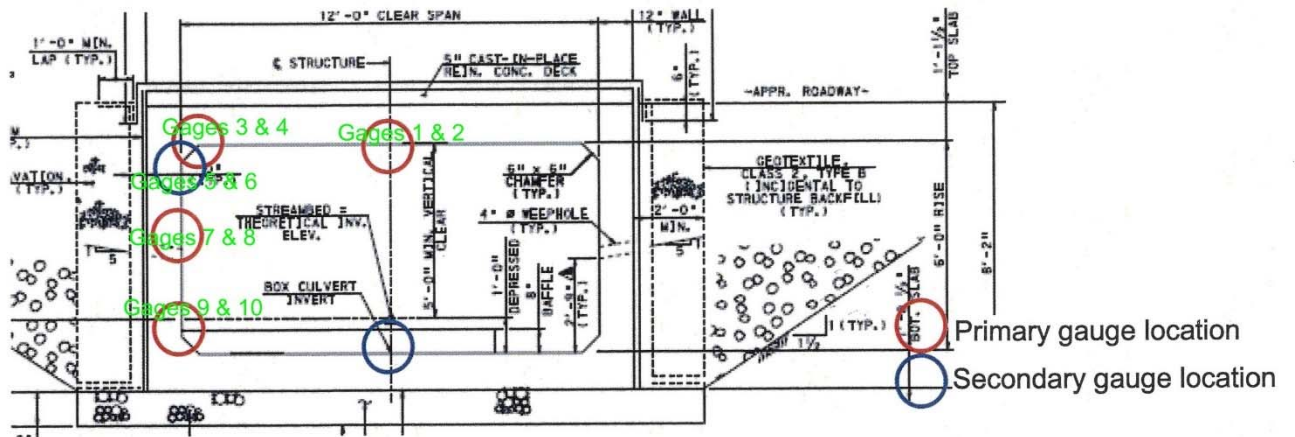


Figure 30 - Location of Strain Gages and String Potentiometers (M3C1)

Appendix K – Calibration Information

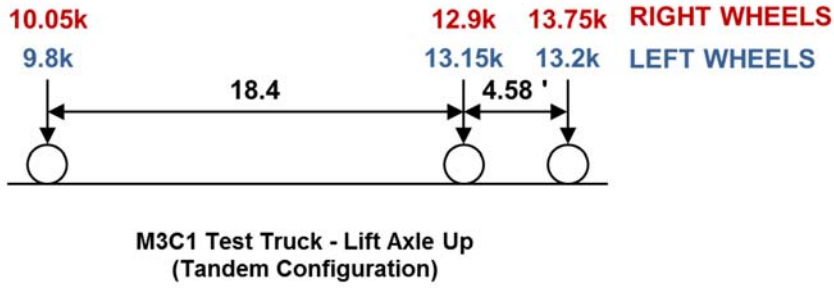


Figure 31 - Load Truck Configuration for Phase 1 (lift axle up) (M3C1)

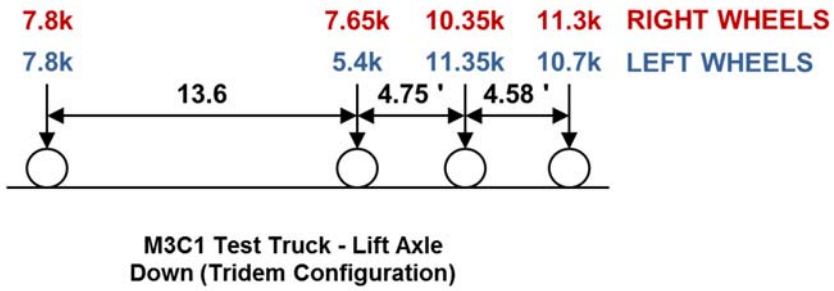


Figure 32 - Load Truck Configuration for Phase 2 (lift axle down) (M3C1)

Appendix K – Calibration Information

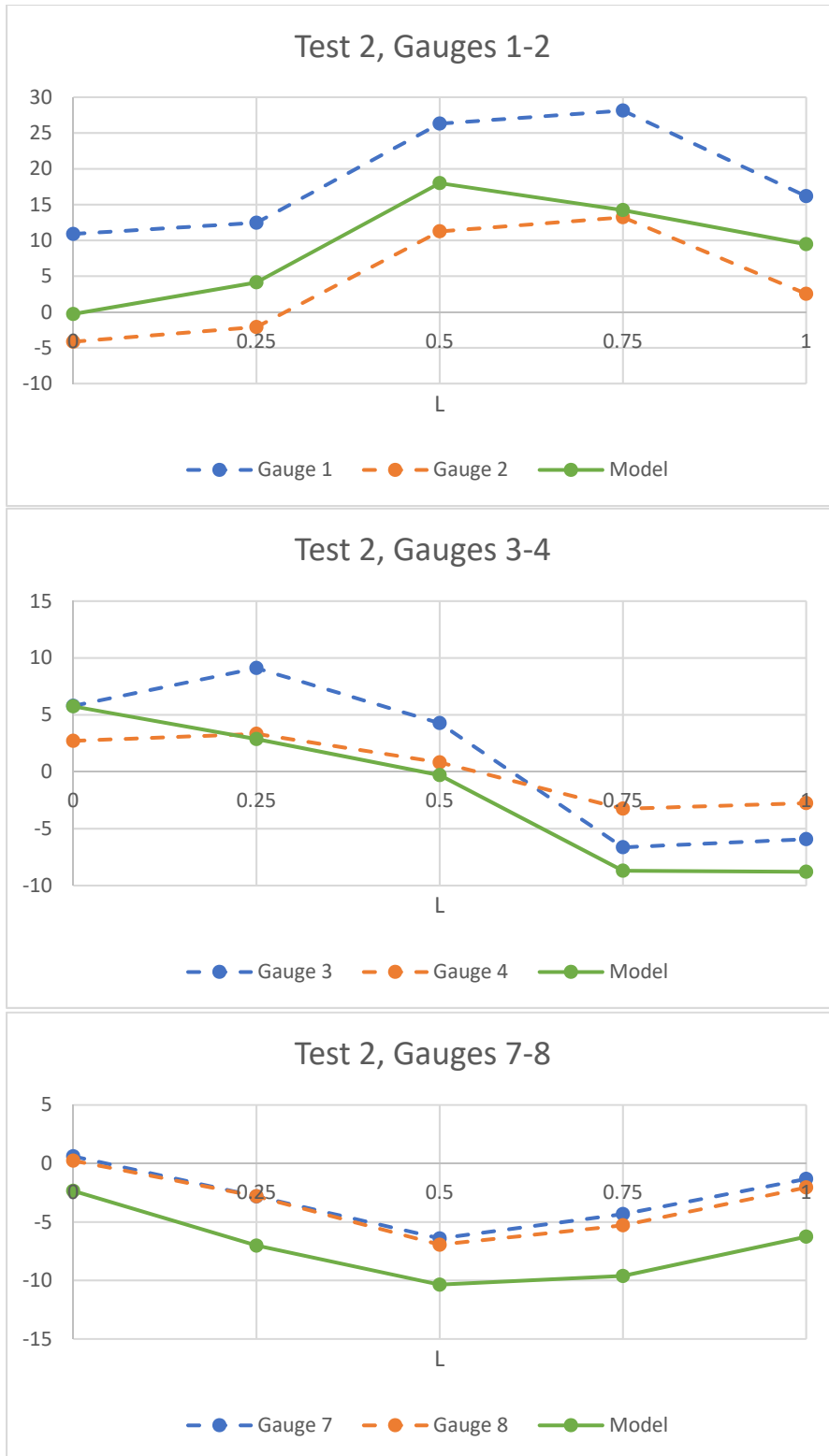


Figure 33 - Model 3 Results for Test 2 (Axle 3), Lift Axle Up (M3C1)

Appendix K – Calibration Information

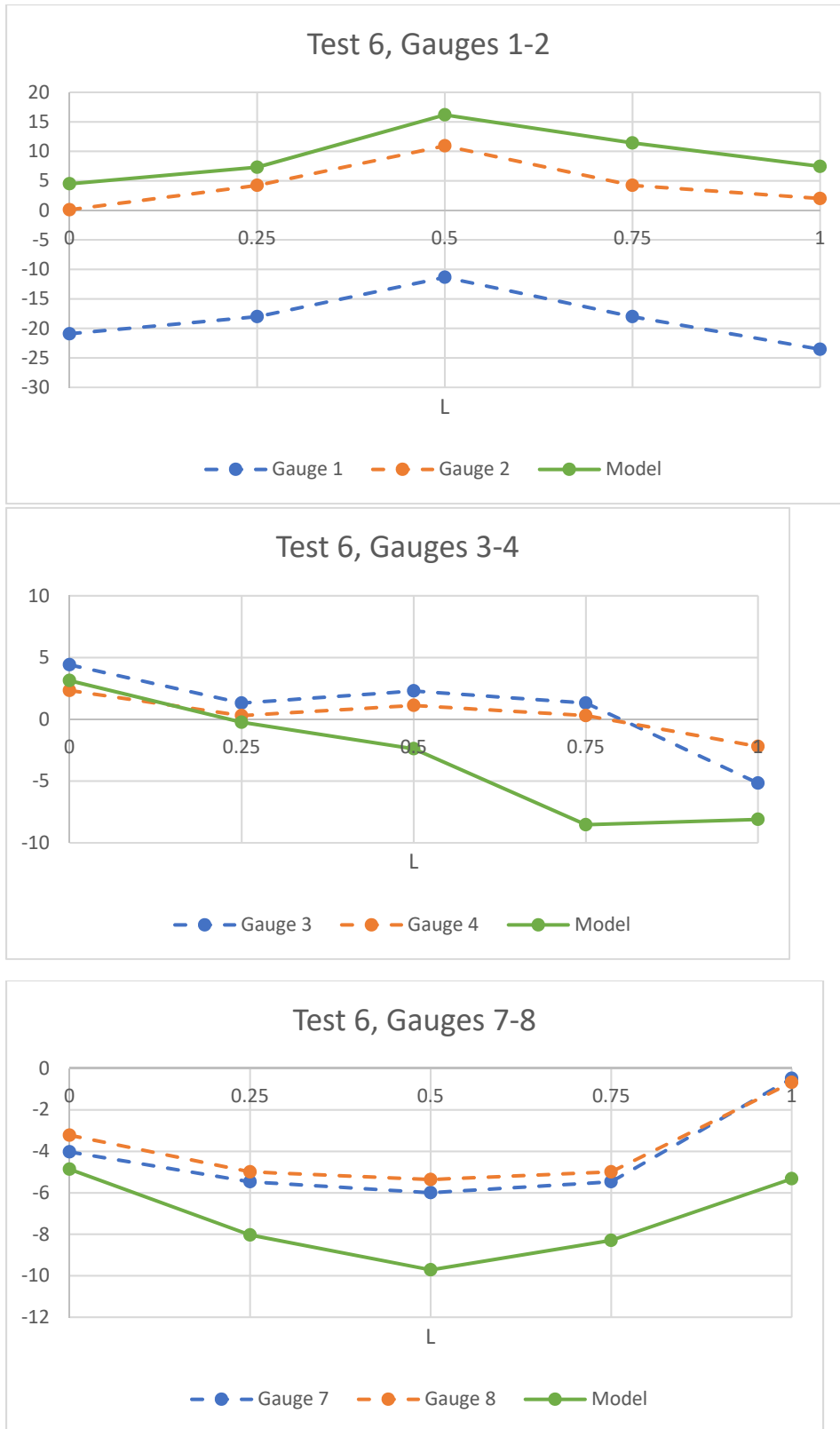


Figure 34 - Model 3 Results for Test 6 (Axle 3), Lift Axle Down (M3C1)

Appendix K – Calibration Information

1.4 Calibration Summary – Model 4, Candidate 1

Model 4, Candidate 1 consists of a *three*-sided precast concrete arch culvert (CONSPAN-type) located in the state of Ohio and owned by the Ohio DOT. Additional details of the testing plan and instrumentation can be found in Appendix F of this document.

The calibration summary herein, presents the LUSAS results (3-D finite element analysis) of Model 4, Candidate 1 under the truck load that was used in the experimental program. The wheel line of the truck was first run over the line of gauges below (Test 1-3). Next, the tests in each phase were also repeated for the case where the truck centerline coincided with the line of gauges (Test Load Cases 4-6). The table below summarizes the loading cases.

<i>Test Load Case</i>	<i>Drop Axle Configuration</i>	<i>Axle of Truck Placed on each Load Point*</i>	<i>Wheel Or Truck Centerline Placed Over Line of Gauges</i>
1	N/A	1	Wheel
2	N/A	2	Wheel
3	N/A	3	Wheel
4	N/A	1	Truck
5	N/A	2	Truck
6	N/A	3	Truck

*Axles numbered consecutively from steering axle to rear axle

Plan and cross-sectional views are shown in Figure 35 and Figure 36, respectively. Experimental Data is recorded and presented in forms of stresses and displacements. The location of the strain gages and the string potentiometers are depicted in Figure 39. The load configuration of the experimental truck for both phases is shown in Figure 40.

Appendix K – Calibration Information

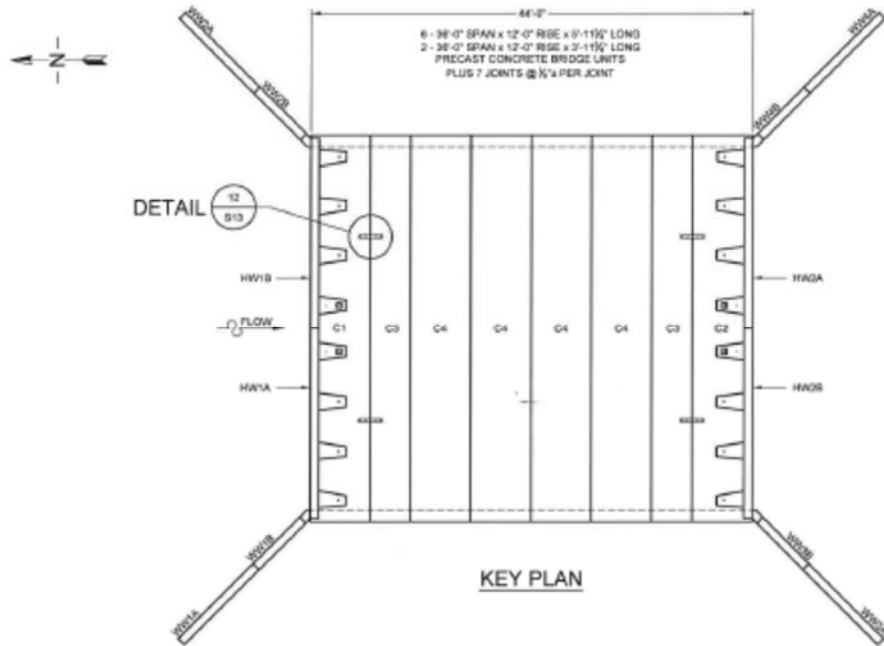
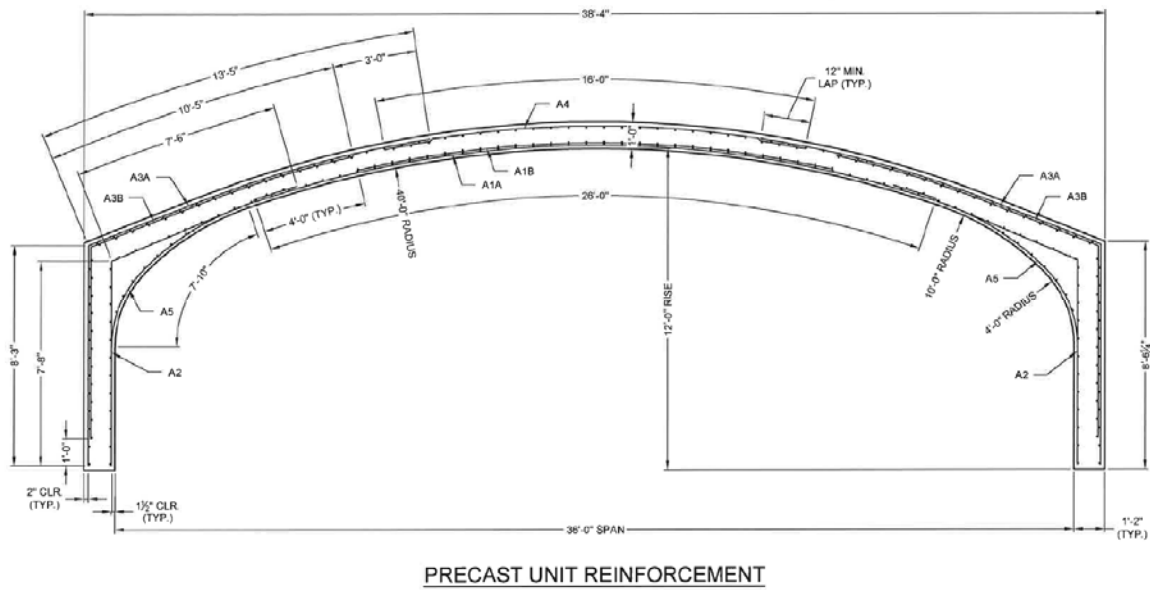


Figure 35 - Culvert Plan View



PRECAST UNIT REINFORCEMENT

Figure 36 - Culvert Typical Section

Appendix K – Calibration Information

1.4.1 3D LUSAS Model

An isometric view of the 3D LUSAS model is shown in Figure 37 below. In general, the 3D models were developed using the parameters described in Appendix B of this document.

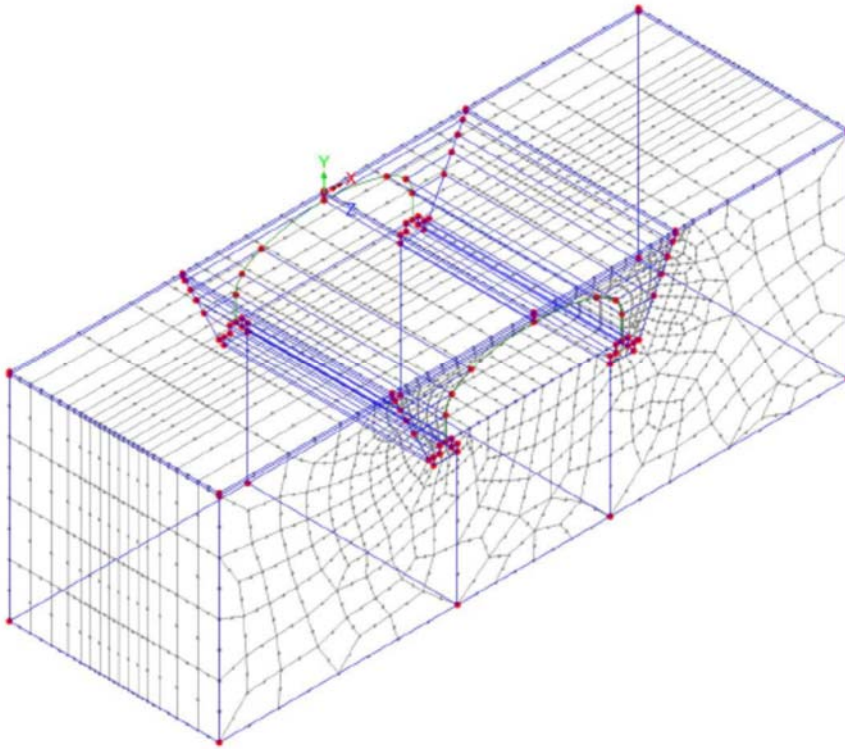


Figure 37 - Isometric View of 3D LUSAS Model (M4C1)

Calibration Results

Comparisons between the field data stresses and displacements as compared to the 3D model predicted values are shown in Figure 41 through Figure 46.

In each of the graphs, the vertical axis represents experimentally measured or modeled stress. The horizontal axis represents the load locations for each of the five load positions shown in Figure 38. For all gauge locations, see Figure 39. In the graphs, the dashed lines represent field-collected data while the solid lines represent the results obtained from the 3D model.

As can be seen, good agreement is seen in the axial gauges (1 & 2) with the axles at midspan although significant differences are seen with the lead axle at the $\frac{3}{4}$ point. At gauges 5 and 6 where a combination of axial and flexural stresses exist, good agreement is observed at all loading points.

Appendix K – Calibration Information

Load Locations at Quarter Points

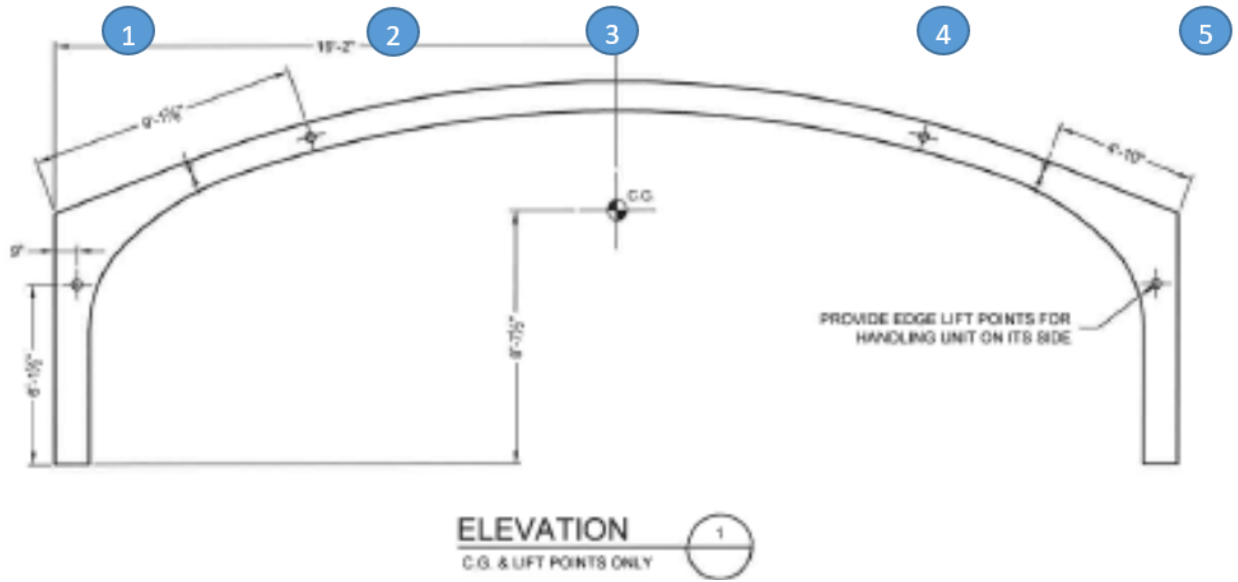


Figure 38 - Location of Marks (Location of Axles for each Load Case) (M4C1)

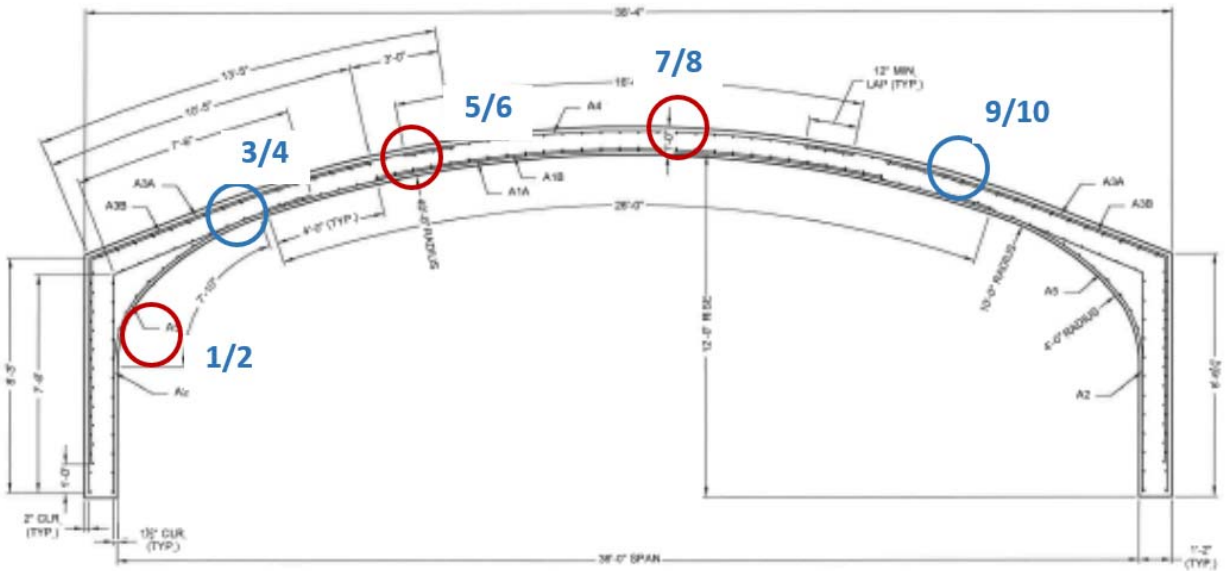


Figure 39 - Location of Strain Gages (M4C1)

Appendix K – Calibration Information

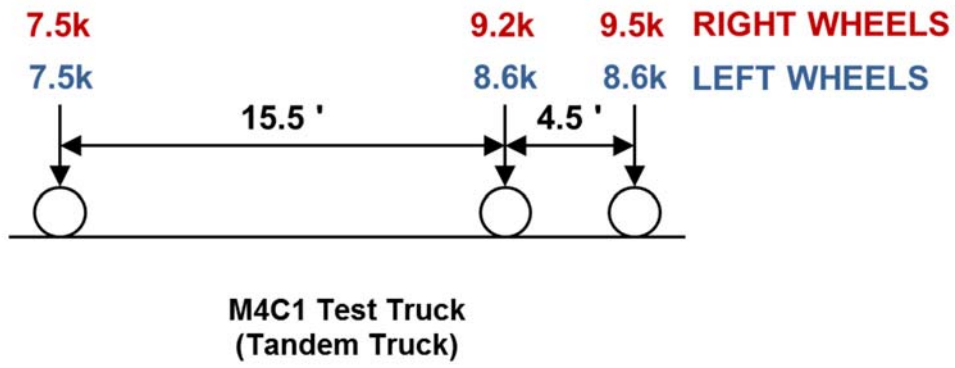


Figure 40 - Load Truck Configuration for Phase 1 (No lift axle) (M4C1)

Appendix K – Calibration Information

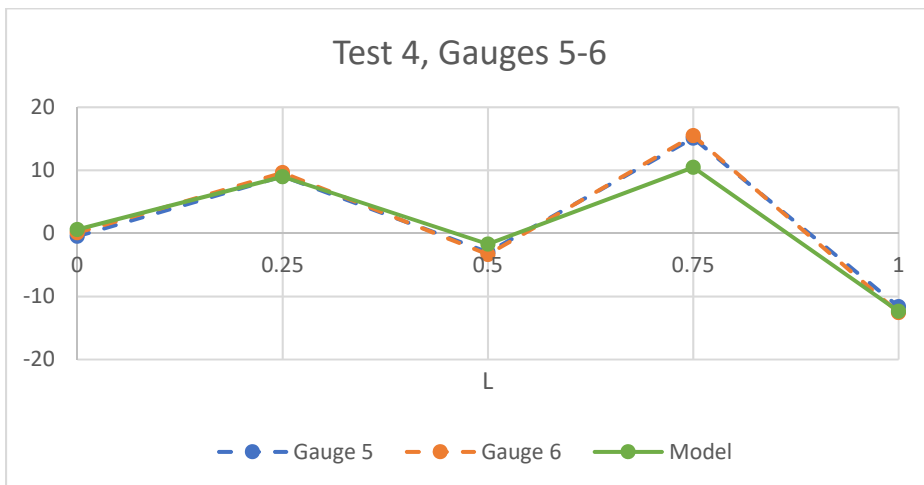
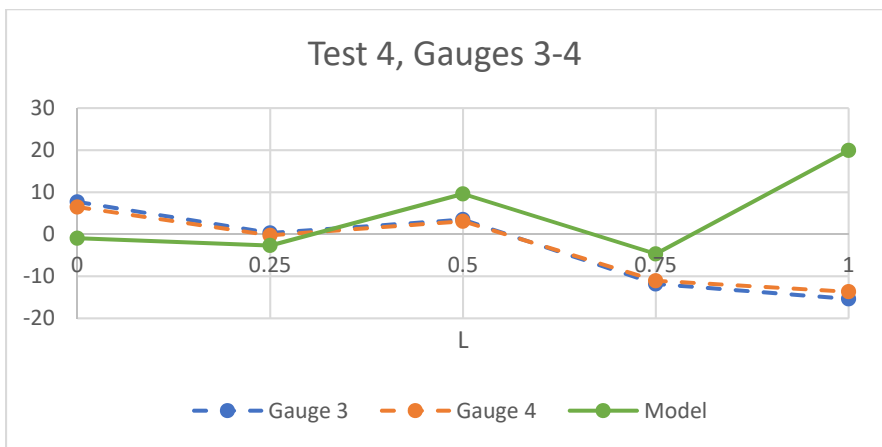
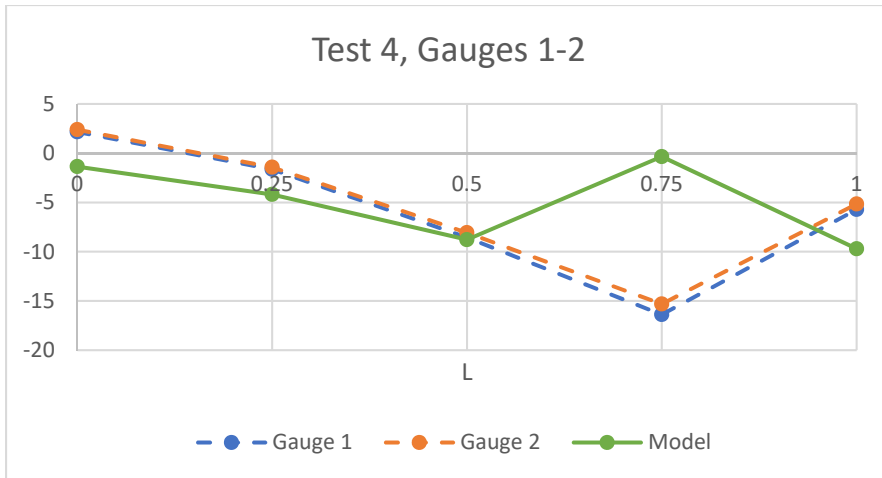


Figure 41 - Load Test 4 (Gauges 1-6) (: Axle 1 over Marked Points (Truck Centered) (M4C1)

Appendix K – Calibration Information



Figure 42 - Load Test 4 (Gauges 7-10) (: Axle 1 over Marked Points (Truck Centered) (M4C1)

Appendix K – Calibration Information

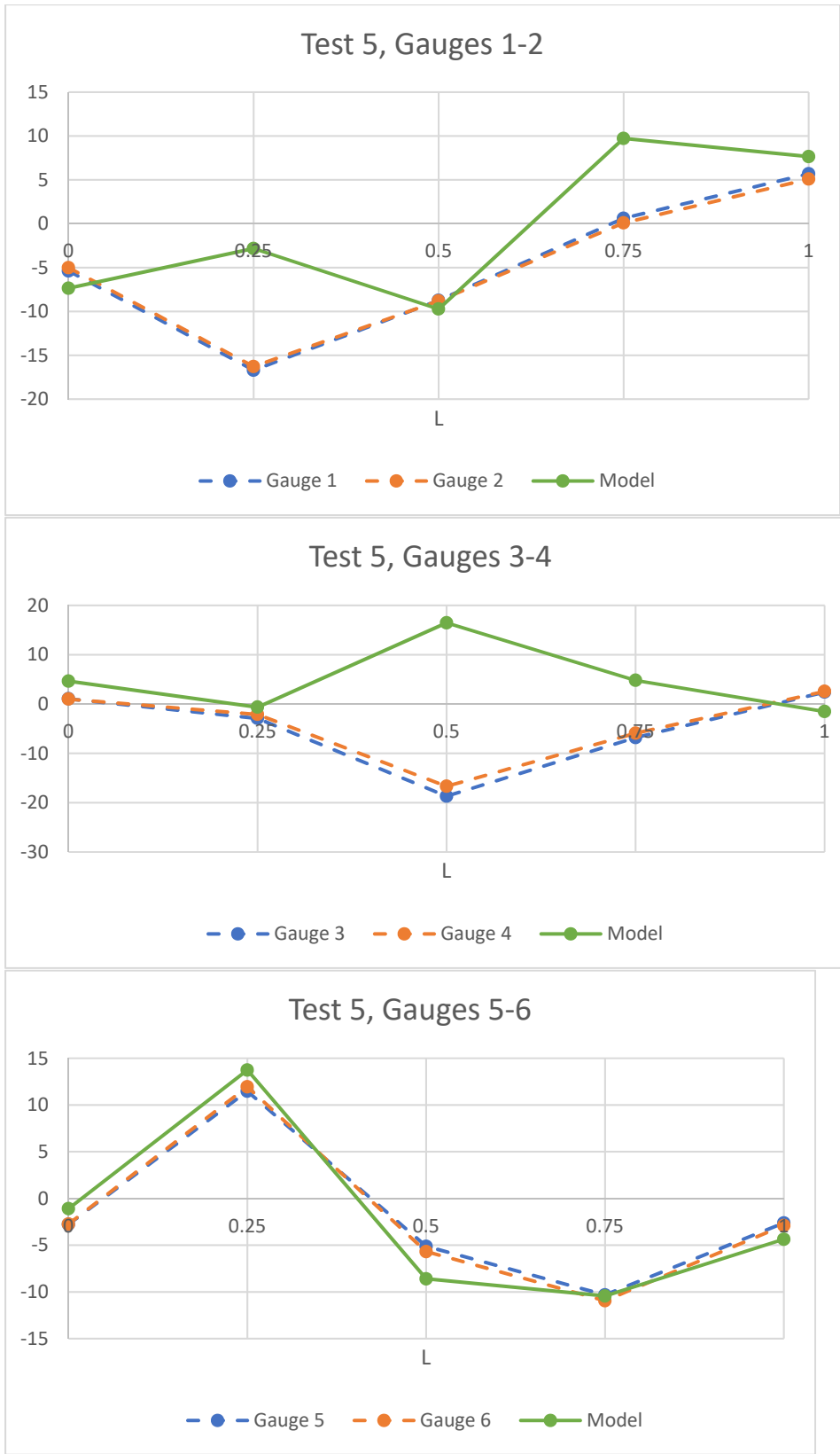


Figure 43 - Load Test 5 (Gauges 1-6): Axle 2 over Marked Points (Truck Centered) (M4C1)

Appendix K – Calibration Information

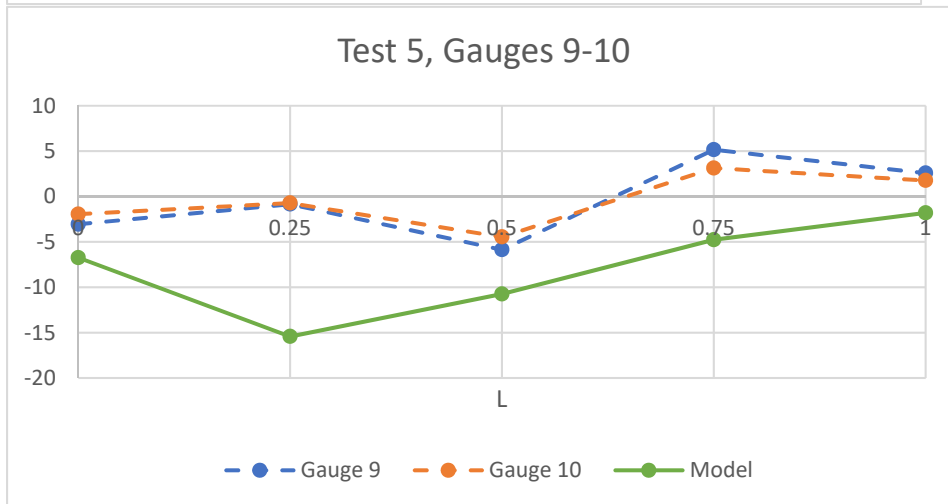
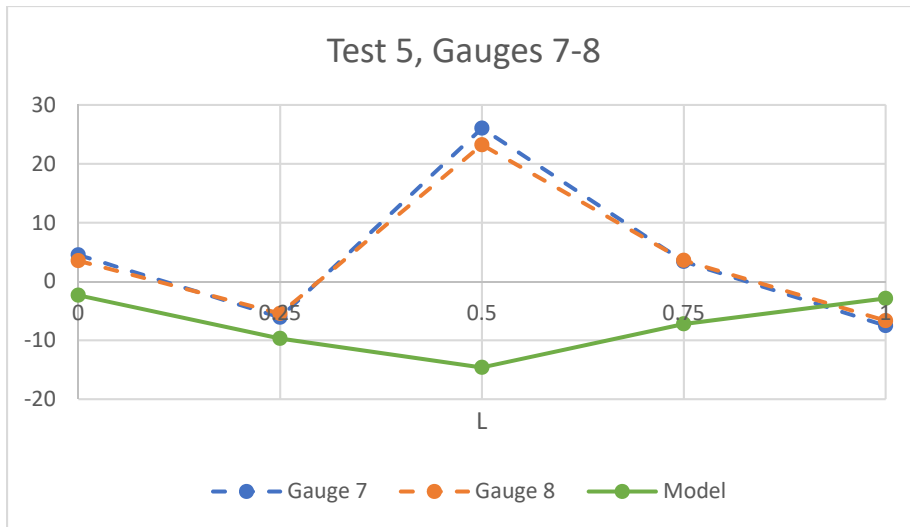


Figure 44 - Load Test 5 (Gauges 7-10): Axle 2 over Marked Points (Truck Centered) (M4C1)

Appendix K – Calibration Information

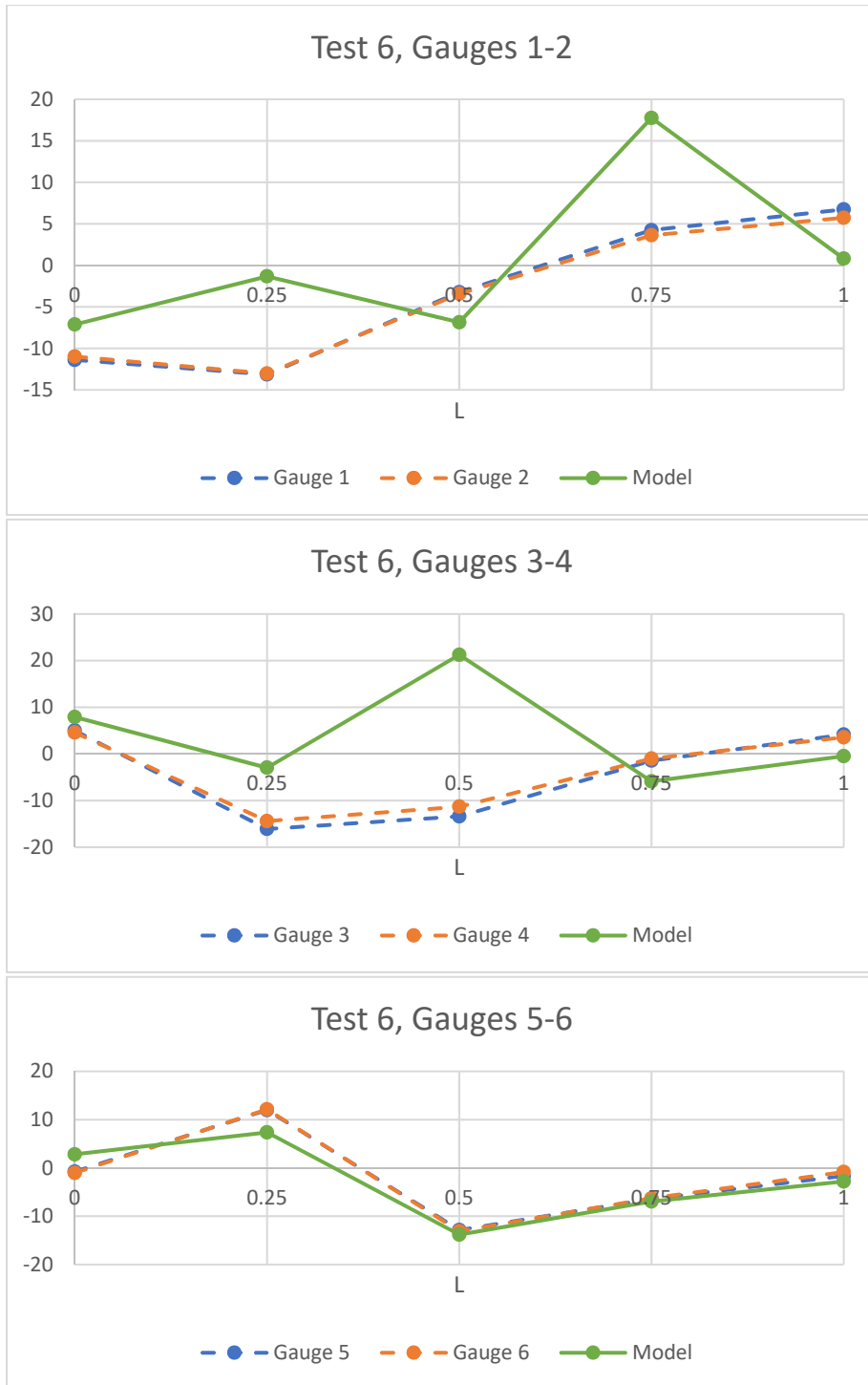


Figure 45 - Load Test 6 (Gauges 1-6): Axle 3 over Marked Points (Truck Centered) (M4C1)

Appendix K – Calibration Information

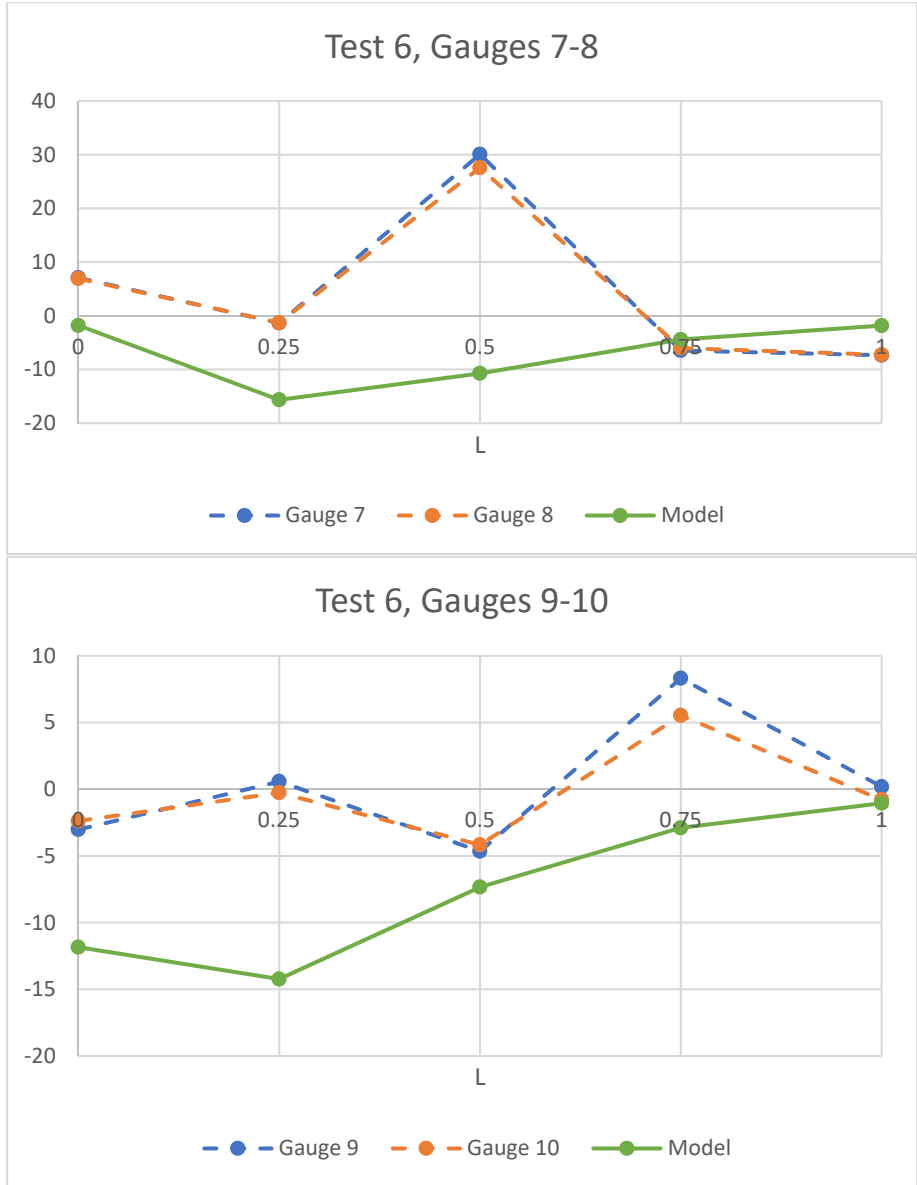


Figure 46 - Load Test 6 (Gauges 7-10): Axle 3 over Marked Points (Truck Centered) (M4C1)

Appendix K – Calibration Information

1.5 Calibration Summary – Model 5, Candidate 1

Model 5, Candidate 1 consists of a corrugated steel arch culvert with a span of 23 feet located in the Lower Paxton Township, Pennsylvania in a private housing development. Additional details of the testing plan and instrumentation can be found in Appendix F of this document.

The calibration summary herein, presents the LUSAS results (3-D finite element analysis) of Model 5, Candidate 1 under the truck load that was used in the experimental program. The wheel line of the truck was first run over the line of gauges below. Next, the tests in each phase were also repeated for the case where the truck centerline coincided with the line of gauges. The table below summarizes the loading cases.

<i>Test Load Case</i>	<i>Drop Axle Configuration</i>	<i>Axle of Truck Placed on each Load Point*</i>	<i>Wheel Or Truck Centerline Placed Over Line of Gauges</i>
1	N/A	1	Wheel
2	N/A	2	Wheel
3	N/A	3	Wheel
4	N/A	1	Truck
5	N/A	2	Truck
6	N/A	3	Truck

*Axles numbered consecutively from steering axle to rear axle

Experimental Data is recorded and presented in forms of stresses and displacements. The location of the strain gages and the string potentiometers are depicted in Figure 62. The load configuration of the experimental truck is shown in Figure 52.

Appendix K – Calibration Information

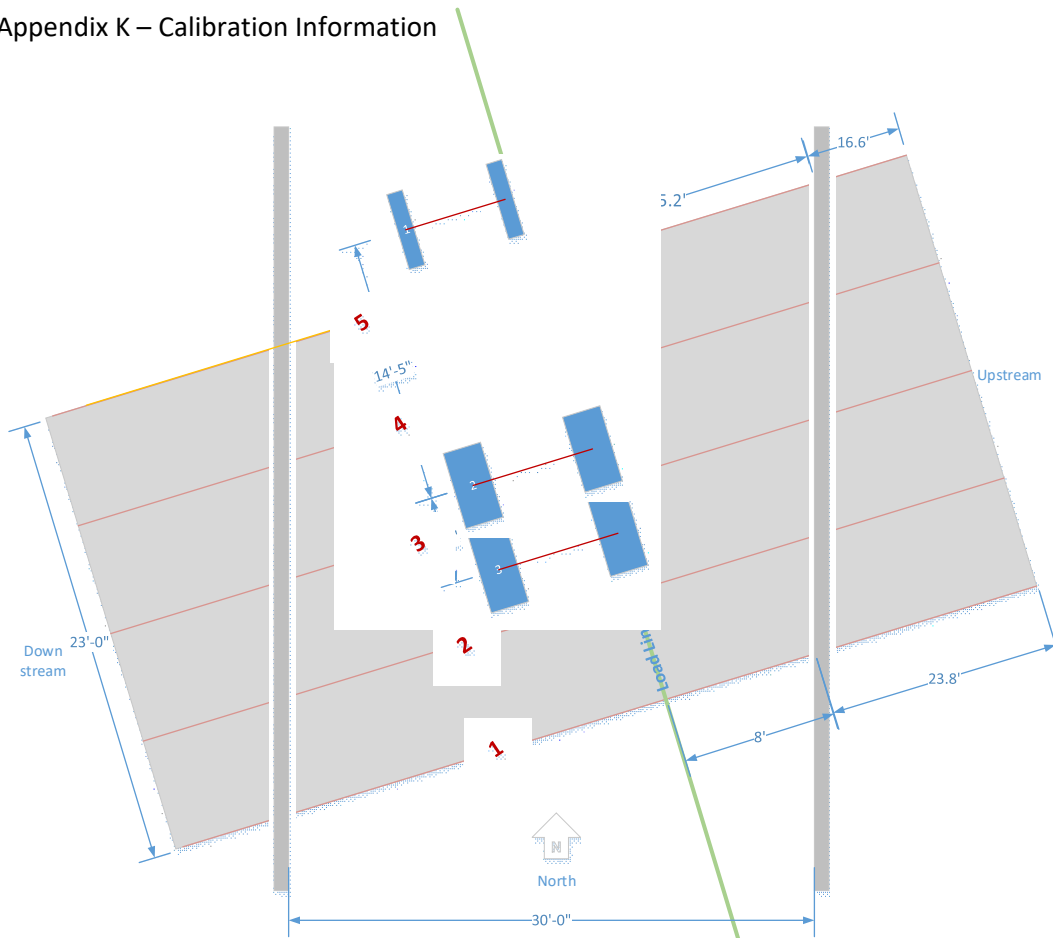


Figure 47 - Culvert Plan View Schematic (Skewed) (M5C1)

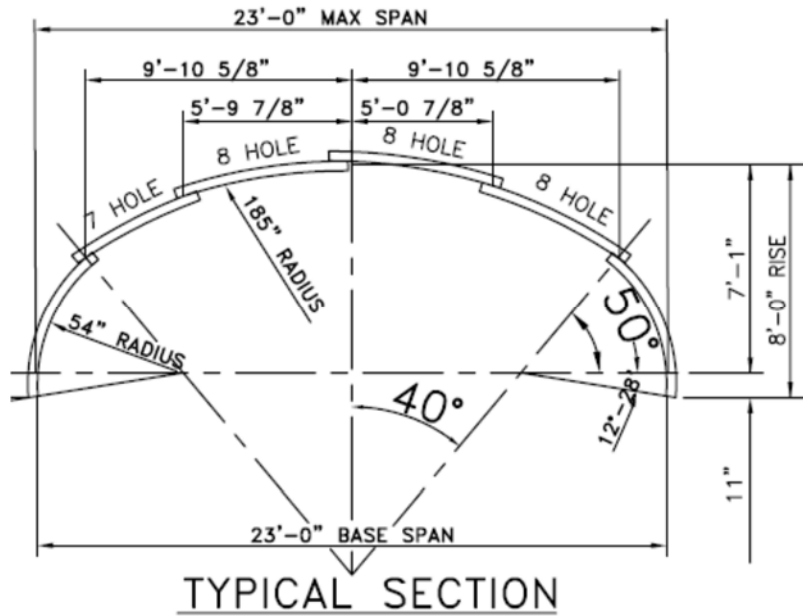


Figure 48 - Culvert Typical Section (M5C1)

Appendix K – Calibration Information

1.5.1 3D LUSAS Model

An isometric view of the 3D LUSAS model is shown in Figure 49 below. In general, the 3D models were developed using the parameters described in Appendix B of this document.

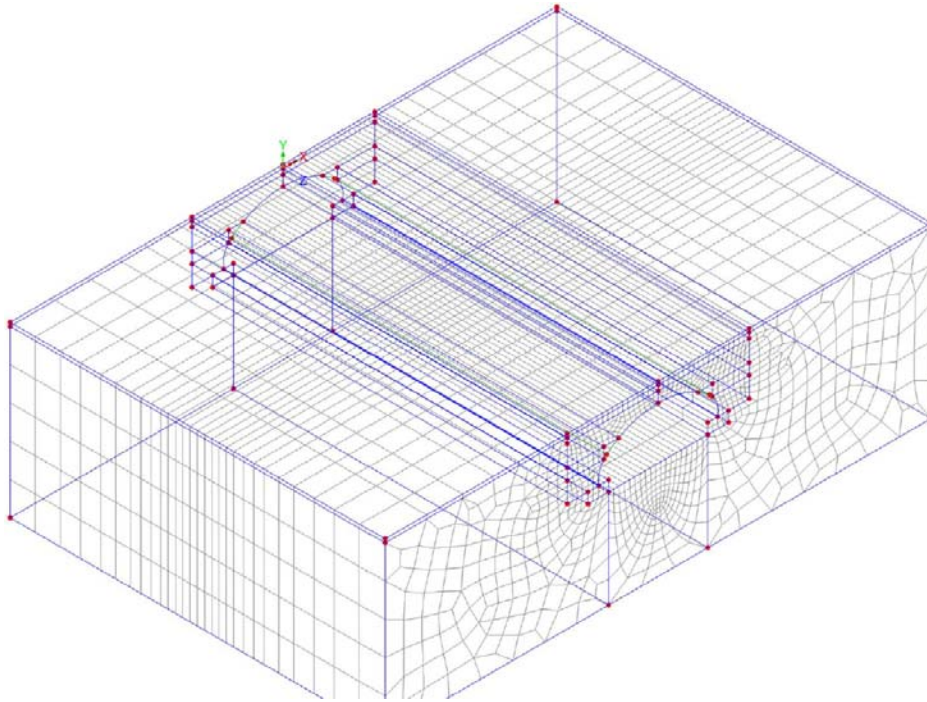


Figure 49 - Isometric View of 3D LUSAS Model (M5C1)

Calibration Results

The results shown in Figure 53 through Figure 54 are for the second series of test loadings for Model 5. The calibration for this model shows good agreement in the shape of the response curves for the various load points. Good agreement was obtained in the displacements between the 3D analyses and the field test results but as discussed herein, greater differences were observed in the stress value comparisons.

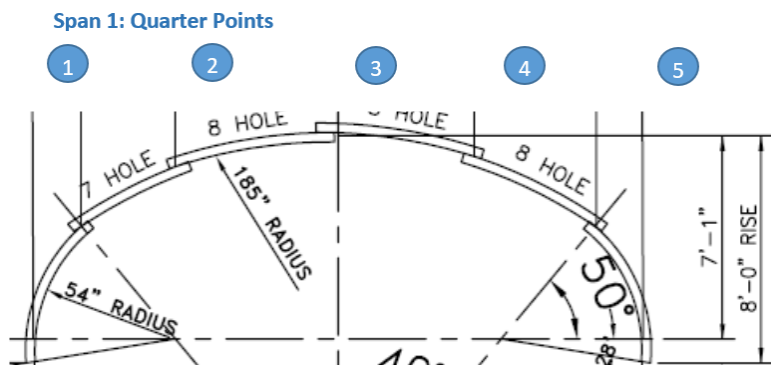


Figure 50 - Location of Marks (Location of Axles for each Load Case) (M5C1)

Appendix K – Calibration Information

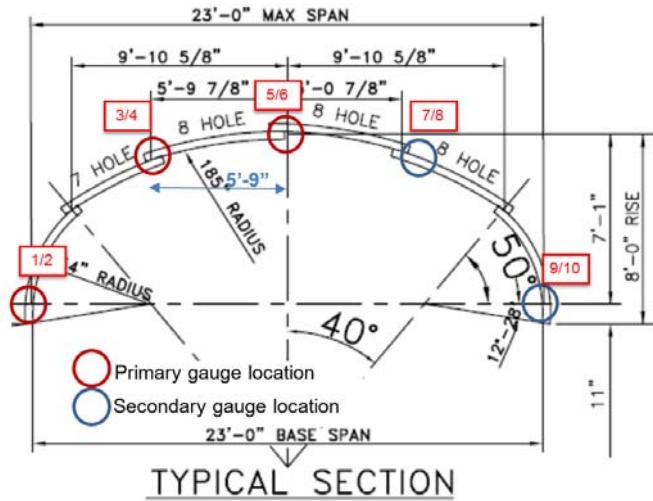


Figure 51 - Location of Strain Gages and String Potentiometers (M5C1)

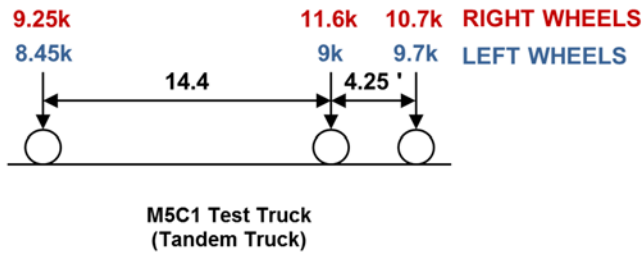


Figure 52 - Load Truck Configuration (M5C1)

Appendix K – Calibration Information

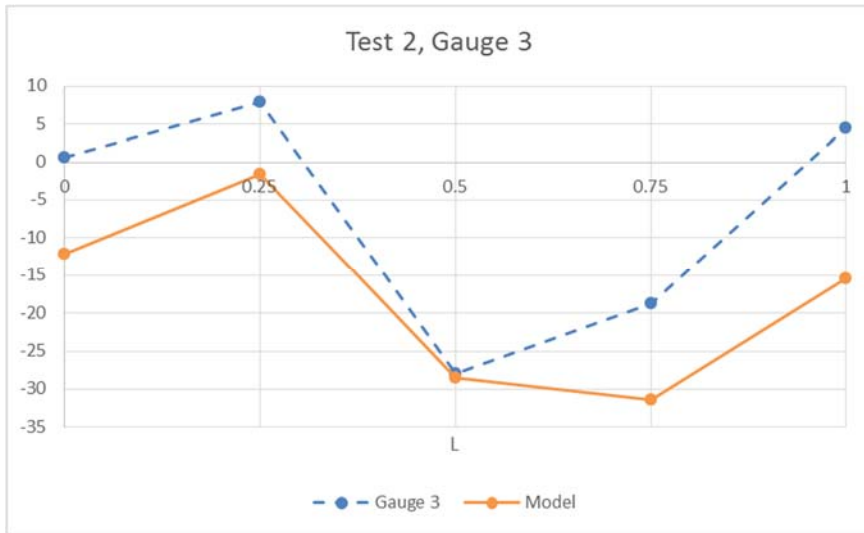
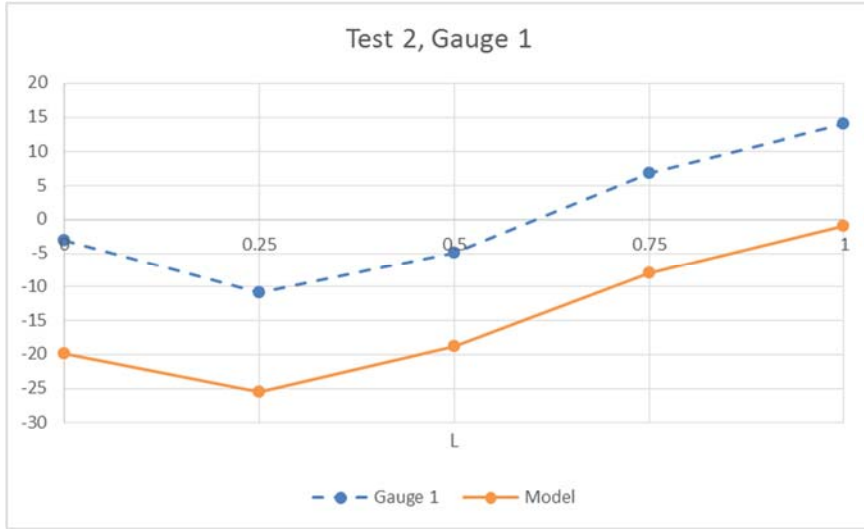


Figure 53 - Load Case 2: Gauges 1 and 3 (M5C1)

Appendix K – Calibration Information

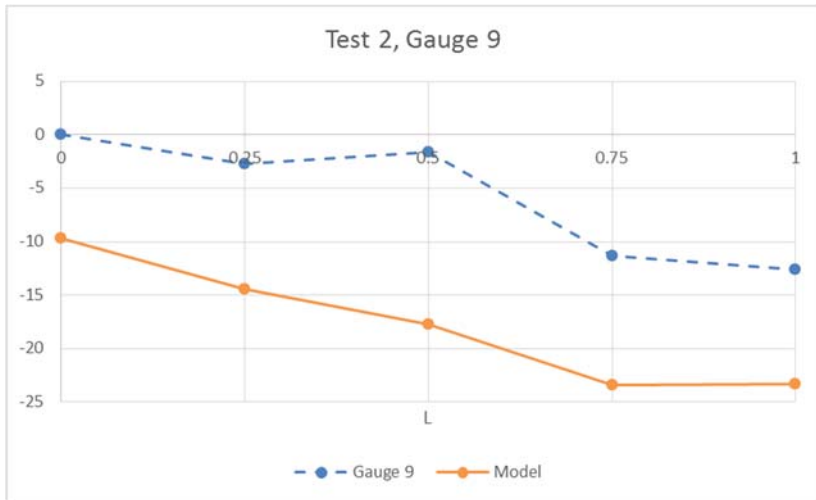
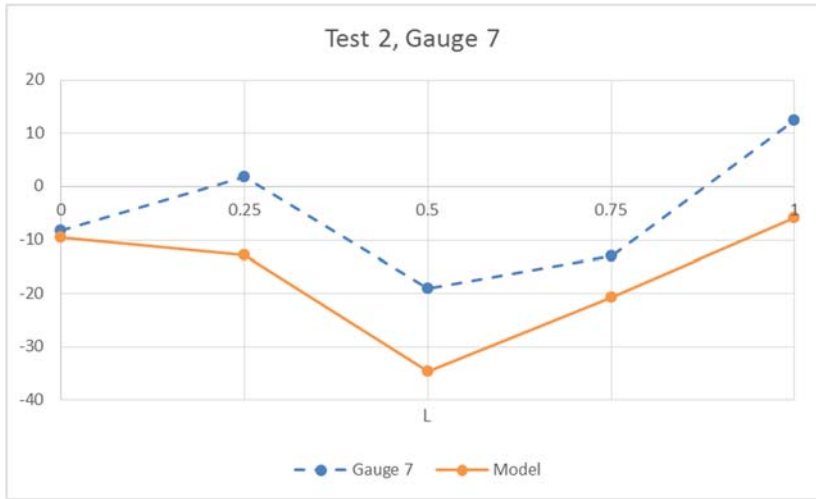
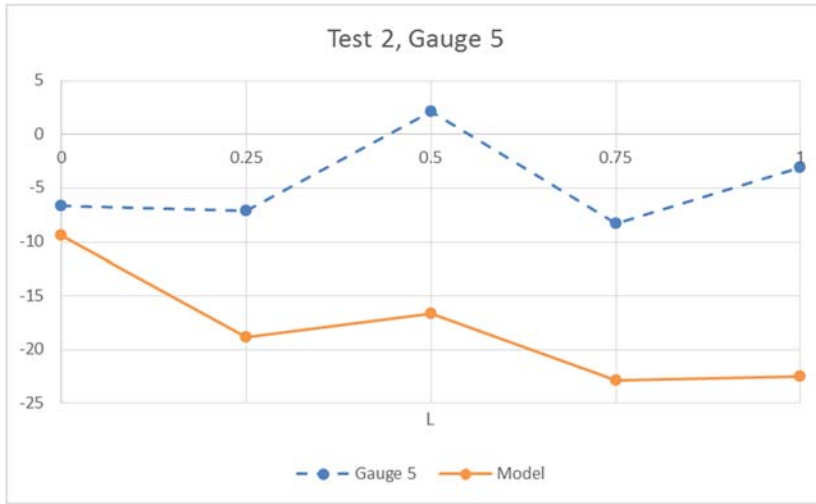


Figure 54 - Load Case 2: Gauges 5, 7, and 9 (M5C1)

Appendix K – Calibration Information

1.6 Calibration Summary – Model 6, Candidate 2

Model 6, Candidate 2 consists of a corrugated aluminum arch culvert Carroll Township, PA. Additional details of the testing plan and instrumentation can be found in Appendix F of this document.

The calibration summary herein, presents the LUSAS results (3-D finite element analysis) of Model 6, Candidate 2 under the truck load that was used in the experimental program. The wheel line of the truck was run over the line of gauges below. Due to the heavy skew and the narrow roadway between guardrails, the load configuration with the centerline of the truck could not be included for this model. Furthermore, only the heavy rear axle could be located over each of the quarter-point loading locations. For a culvert of such a short span, this is expected to be the controlling loading case. Due to the limited number of loadings to be applied in this single load case, the tests were repeated three times.

Test Load Case	Drop Axle Configuration	Axle of Truck Placed on each Load Point*	Wheel Or Truck Centerline Placed Over Line of Gauges
1	N/A	1	Wheel

*Axles numbered consecutively from steering axle to rear axle

Experimental Data is recorded and presented in forms of stresses and displacements. The location of the strain gages and the string potentiometers are depicted in Figure 59. The load configuration of the experimental truck is shown in Figure 60.

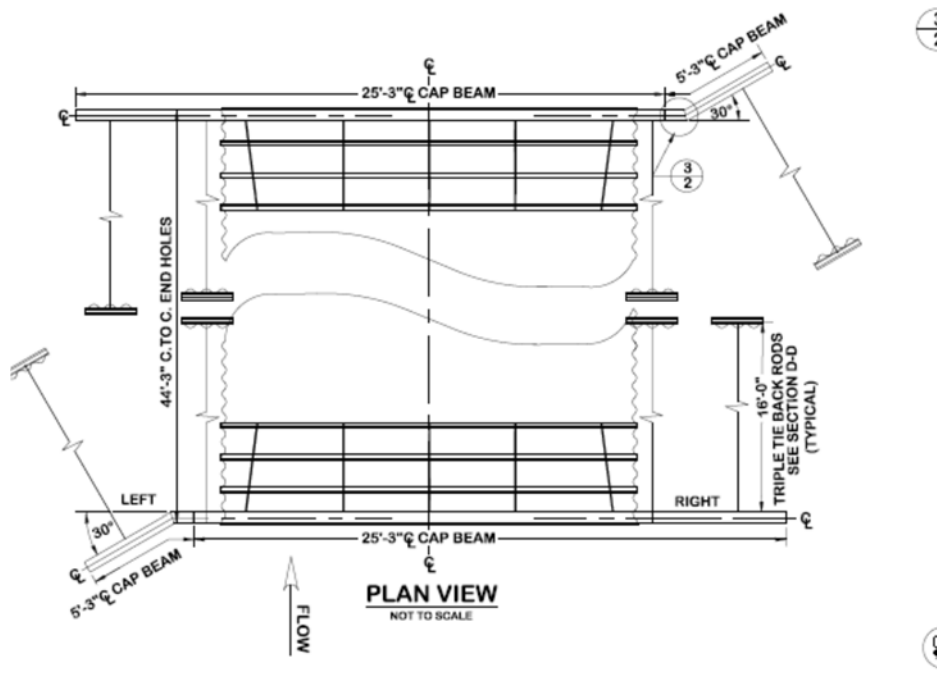


Figure 55 - Culvert Plan View Schematic (Skewed) (M6C2)

Appendix K – Calibration Information

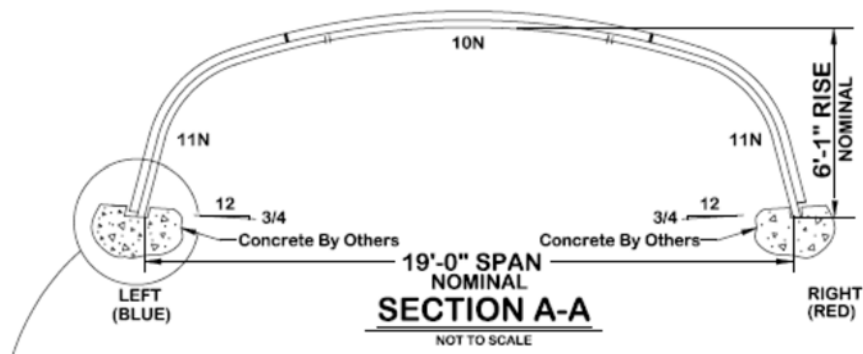


Figure 56 - Culvert Typical Section (M6C2)

1.6.1 3D LUSAS Model

An isometric view of the 3D LUSAS model is shown in Figure 57 below. In general, the 3D models were developed using the parameters described in Appendix B of this document.

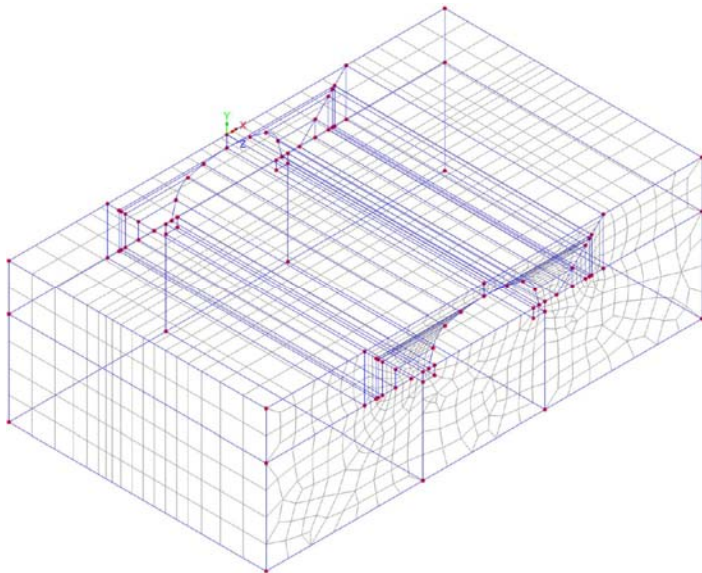


Figure 57 - Isometric View of 3D LUSAS Model (M6C2)

Calibration Results

Comparisons between the field data stresses and displacements as compared to the 3D model predicted values are shown in Figure 61.

In each of the graphs, the vertical axis represents either the stress at strain gauge locations. The horizontal axis represents the load locations for each of the three load positions shown in Figure 58. For all gauge locations, see Figure 59. In the graphs, the dashed lines represent field-collected data while the solid lines represent the results obtained from the 3D model.

The stress comparisons in Figure 61 show similar behavior between the 3D model and the experimental results.

Appendix K – Calibration Information

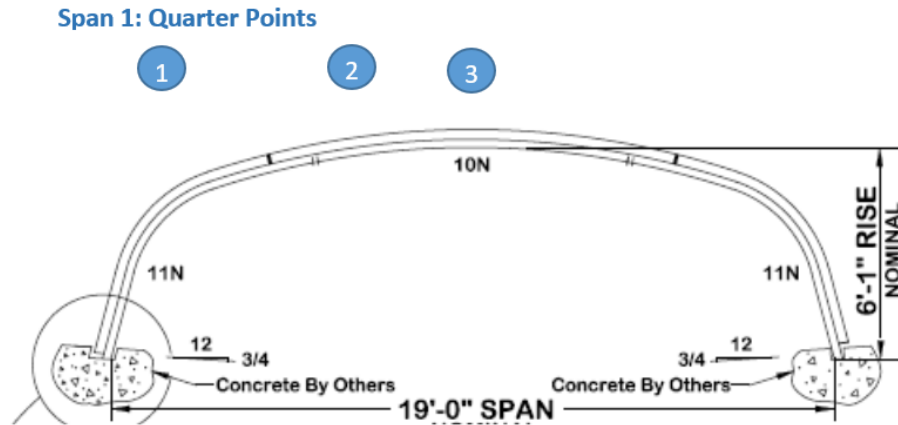


Figure 58 - Location of Marks (Location of Axles for each Load Case) (M6C2)

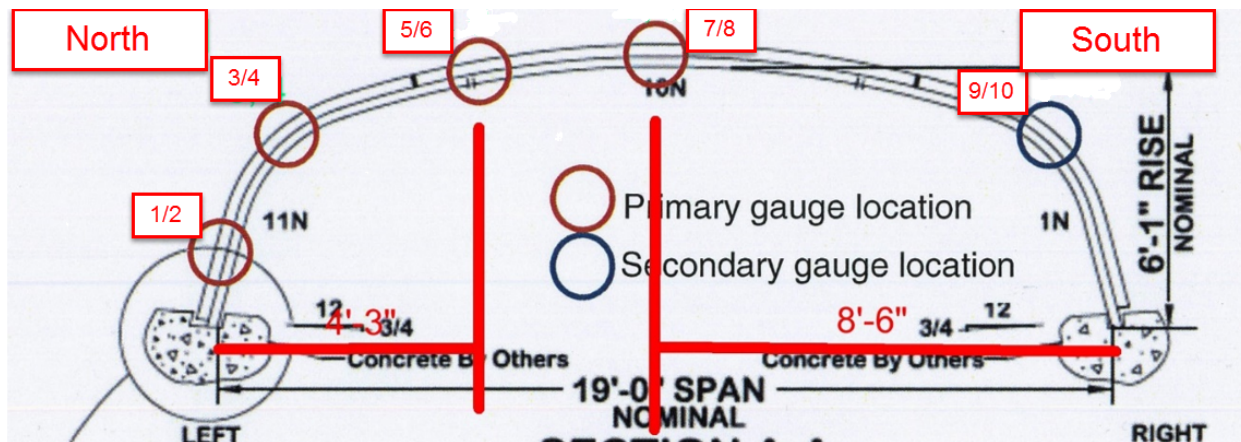
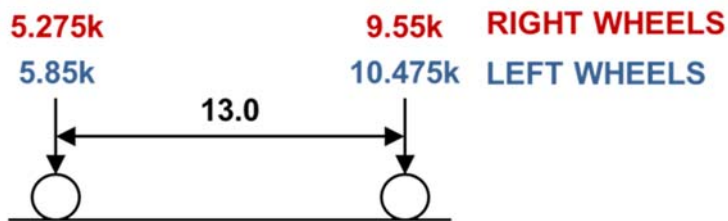


Figure 59 - Location of Strain Gages and String Potentiometers (M6C2)



**M6C2 Test Truck
(Two Axle Dump)**

Figure 60 - Load Truck Configuration (M6C2)

Appendix K – Calibration Information

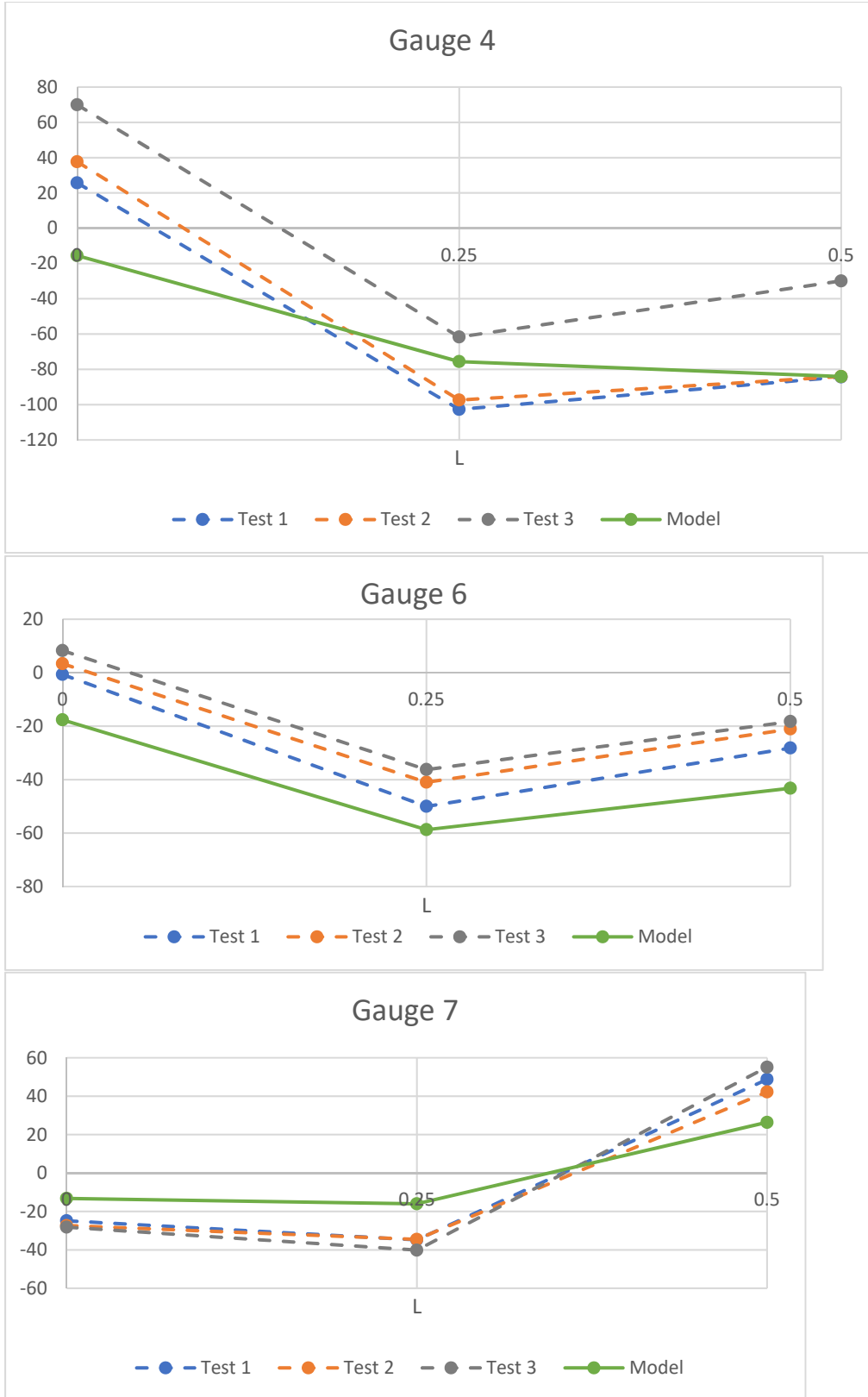


Figure 61 - Load Case 1: Rear Wheel Placed Over Each Loading (Quarter) Point (M6C2)

Appendix K – Calibration Information

1.7 Calibration Summary – Model 7, Candidate 1

Model 7, Candidate 1 consists of a corrugated aluminum arch culvert in Attleboro, Massachusetts. Additional details of the field testing plan and instrumentation can be in Appendix F of this document.

Multiple approaches were taken to determine the best course of modeling the structure in LUSAS and then using the selected approach to carry out the calibration effort. This effort and the lessons learned were then used to shape the approach used to model and calibrate the remaining corrugated metal culverts. A detailed overview of the modeling approach used in the 3D modeling of this culvert is provided following the results along with comparisons between the before and after paving conditions.

Experimental Data is recorded and presented in forms of stresses and displacements. The location of the strain gages and the string potentiometers are depicted in Figure 62. The load configuration of the experimental truck is shown in Figure 63. Phase 1 is the truck configuration for the loading prior to paving and Phase 2 is the configuration for the loading after paving was completed.

The calibration summary herein, presents the LUSAS results (3-D finite element analysis) of Model 7, Candidate 1 under the truck load that was used in the experimental program. The wheel line of the truck was run over the line of gauges below. Because the culvert is composed of corrugated metal rib sections, the gauges were mounted in clusters to capture both the crest and the valley strains in the corrugations. Adjacent ribs were instrumented for redundancy.

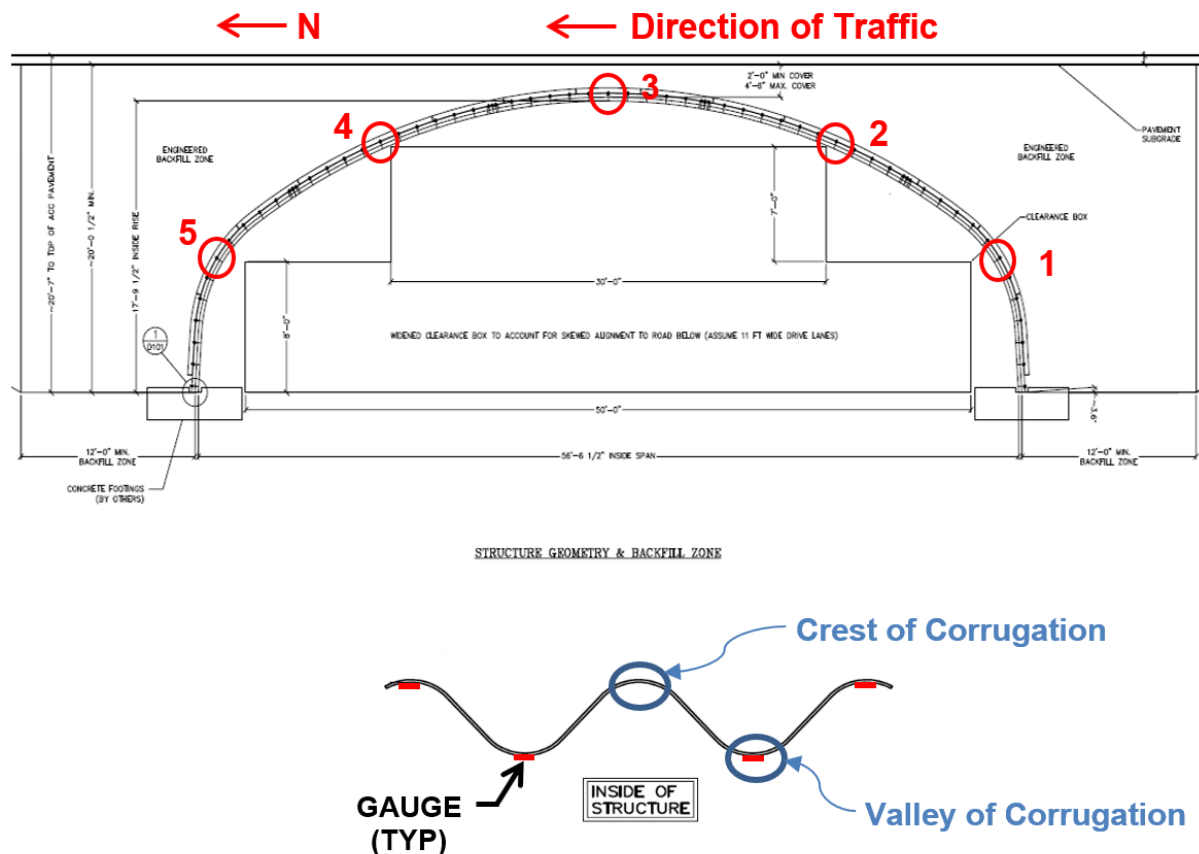


Figure 62 - Location of Strain Gages and String Potentiometers (M7C1)

Appendix K – Calibration Information

1.8 Truck Wheel Load and Spacing Data

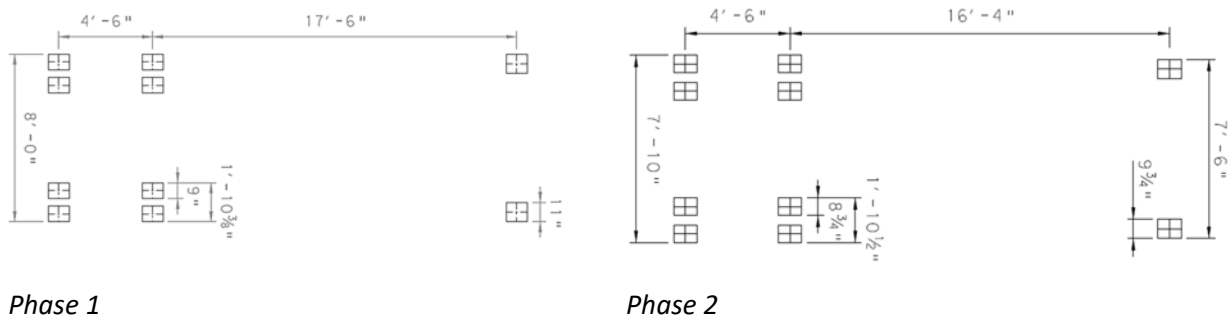


Figure 63 - Truck Loading Configurations for Phases 1 and 2

Appendix K – Calibration Information

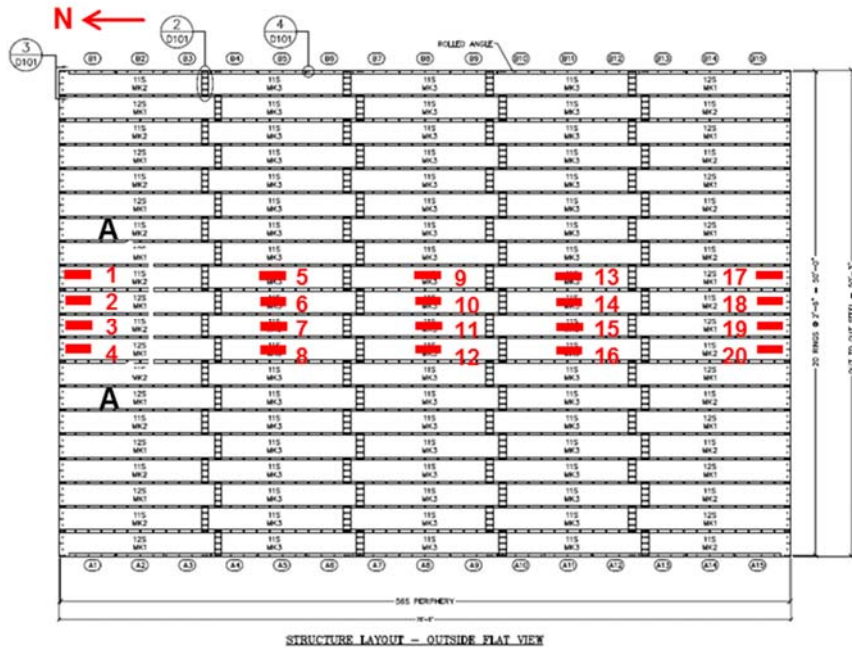
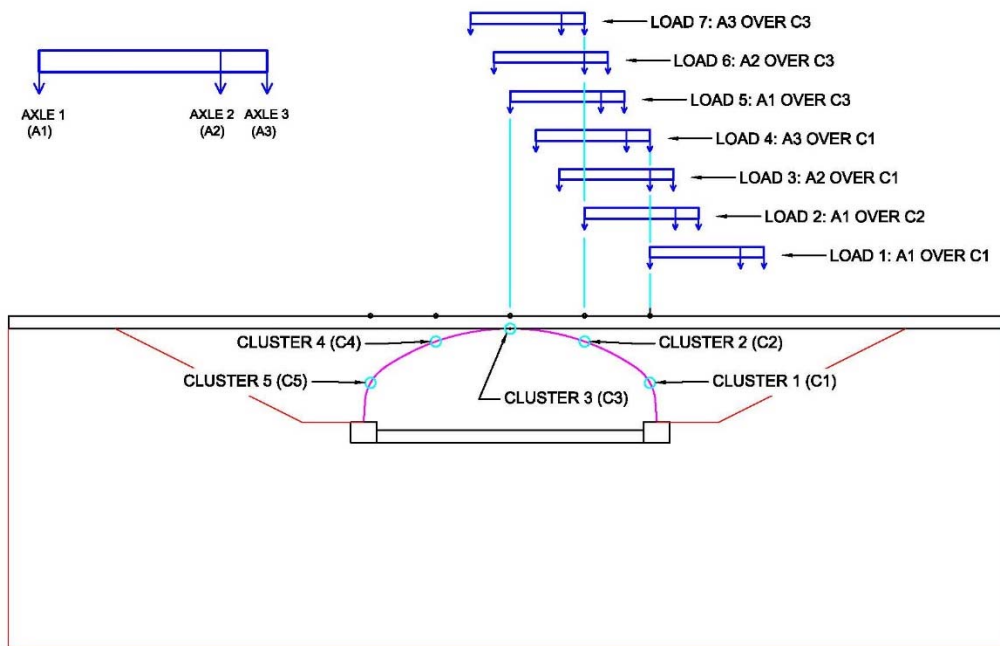
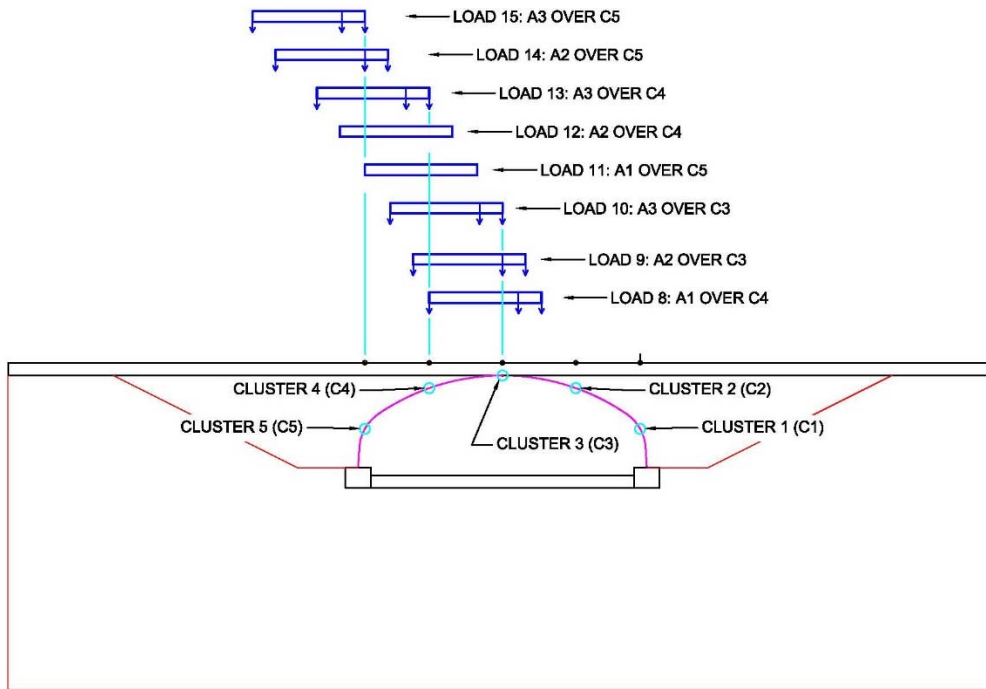


Figure 64 - Culvert Plan View Schematic with Gauge Cluster Locations (M7C1)



Load Set 1 thru 7.

Appendix K – Calibration Information



Load Set 8 thru 15.

Figure 65 - M7C1 Schematics of Loading for Each Load Case

Appendix K – Calibration Information

1.8.1 3D LUSAS Model

An isometric view of the 3D LUSAS model is shown in Figure 57 below. In general, the 3D models were developed using the parameters described in Appendix B of this document.

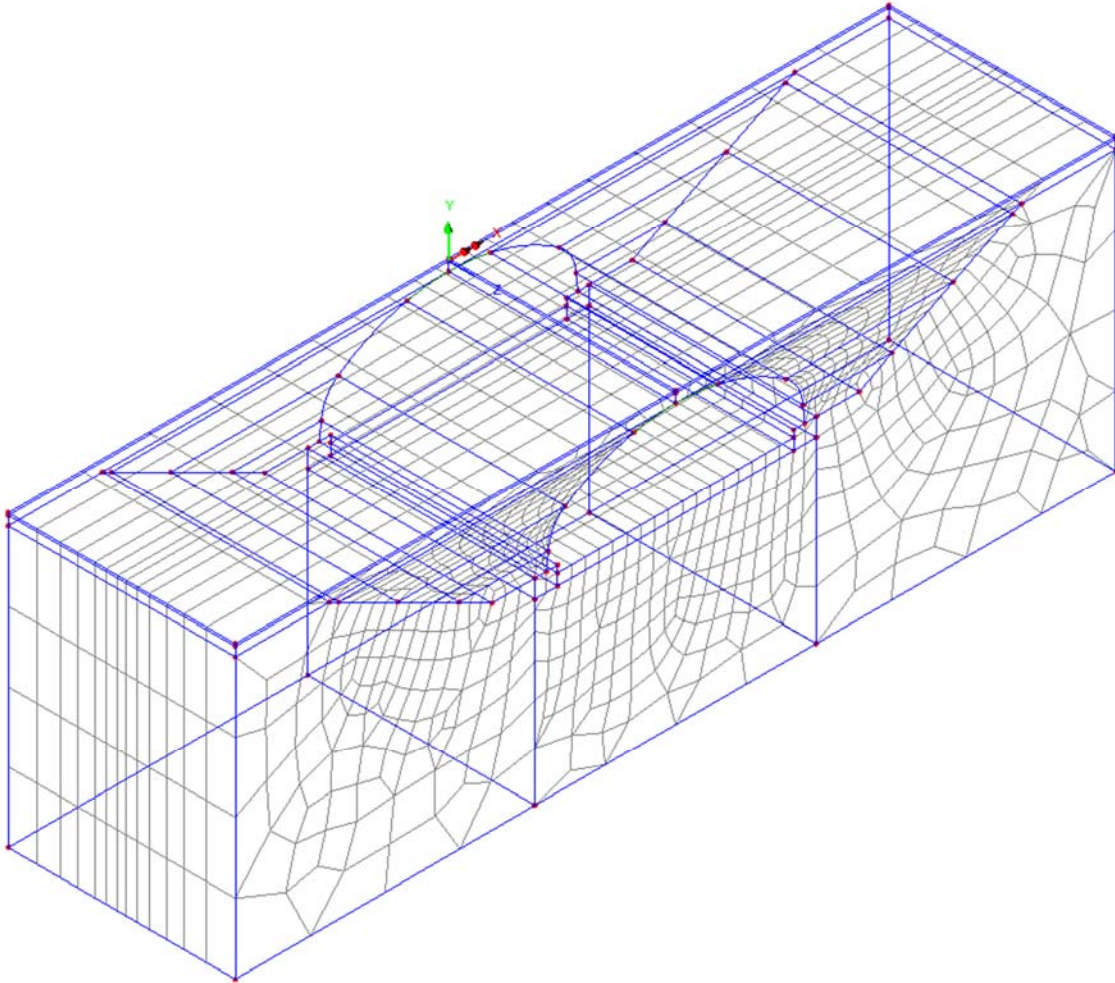


Figure 66 - Isometric View of 3D LUSAS Model (M7C1)

Calibration Results

Comparisons between the field data stresses and displacements as compared to the 3D model predicted values are shown in Figure 67 through Figure 81. A comparison between the Phase 1 and Phase 2 results follows in the next section.

In each of the graphs, the vertical axis represents the stress at strain gauge locations. The horizontal axis represents the load locations for each of the load positions shown in Figure 65. For all gauge locations, see Figure 64 in the graphs, the dashed lines represent field-collected data while the solid lines represent the results obtained from the 3D model.

Appendix K – Calibration Information

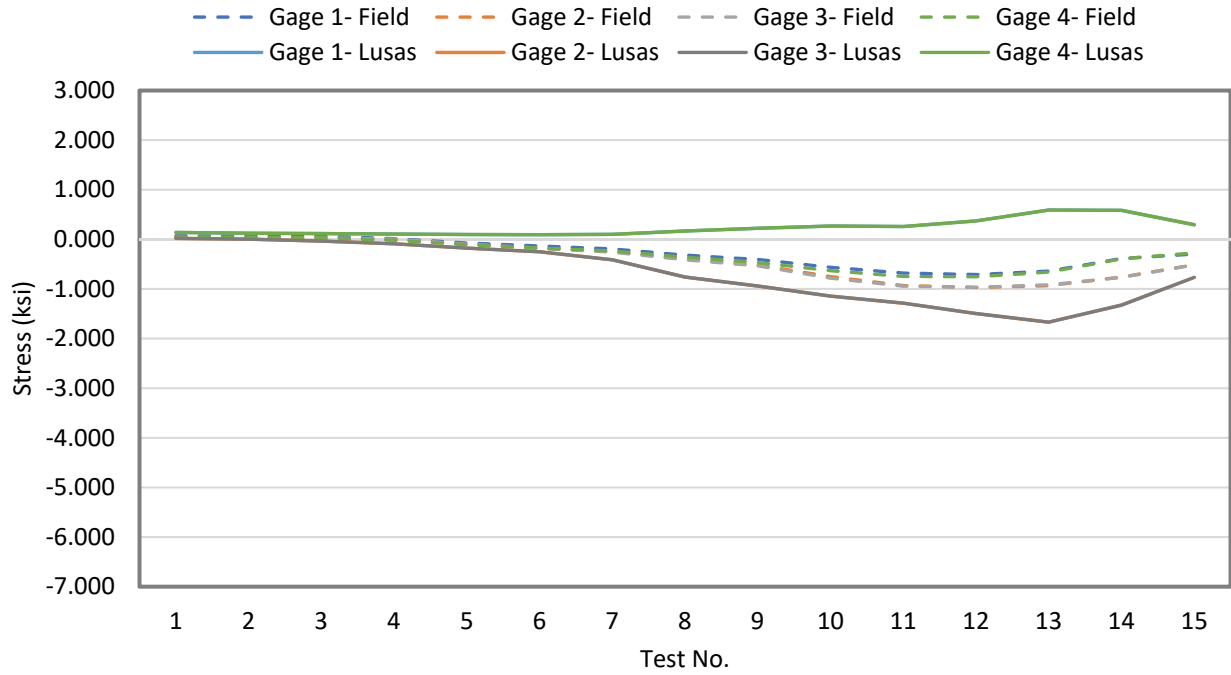


Figure 67 - Results of Test 1-N1 Culvert 7 (15 load-cases) for Gages 1 thru 4 (Gage Cluster 5)

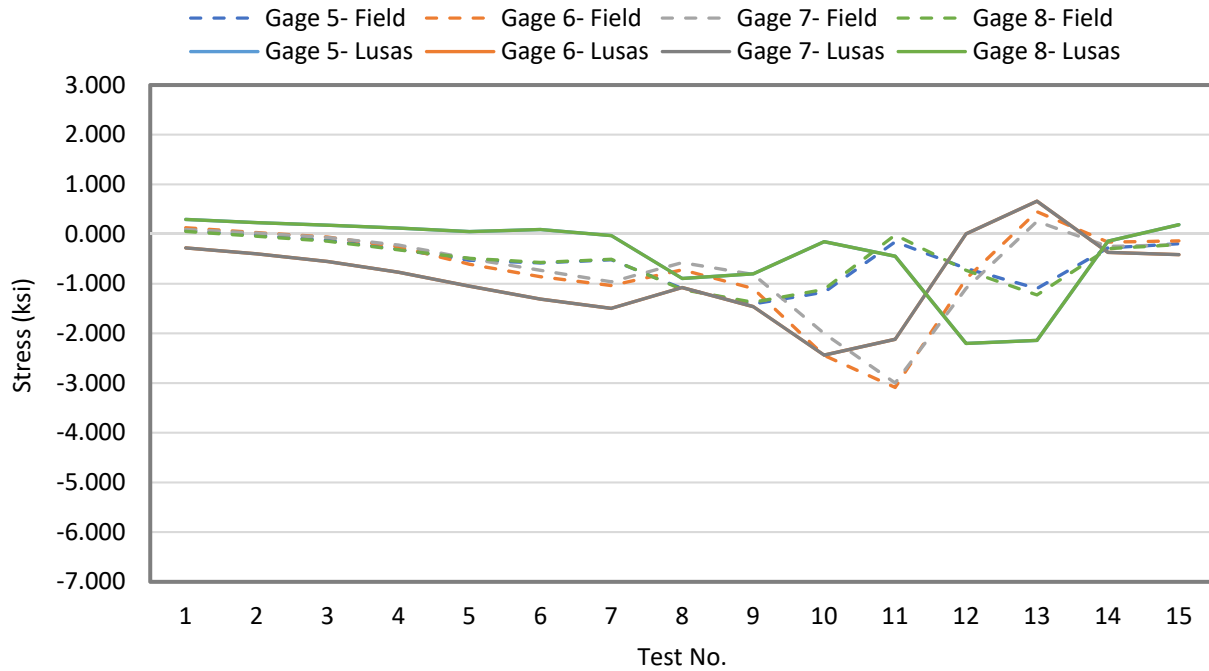


Figure 68 – Results of Test 1-N1 Culvert 7 (15 load-cases) for Gages 5 thru 8 (Gage Cluster 4)

Appendix K – Calibration Information

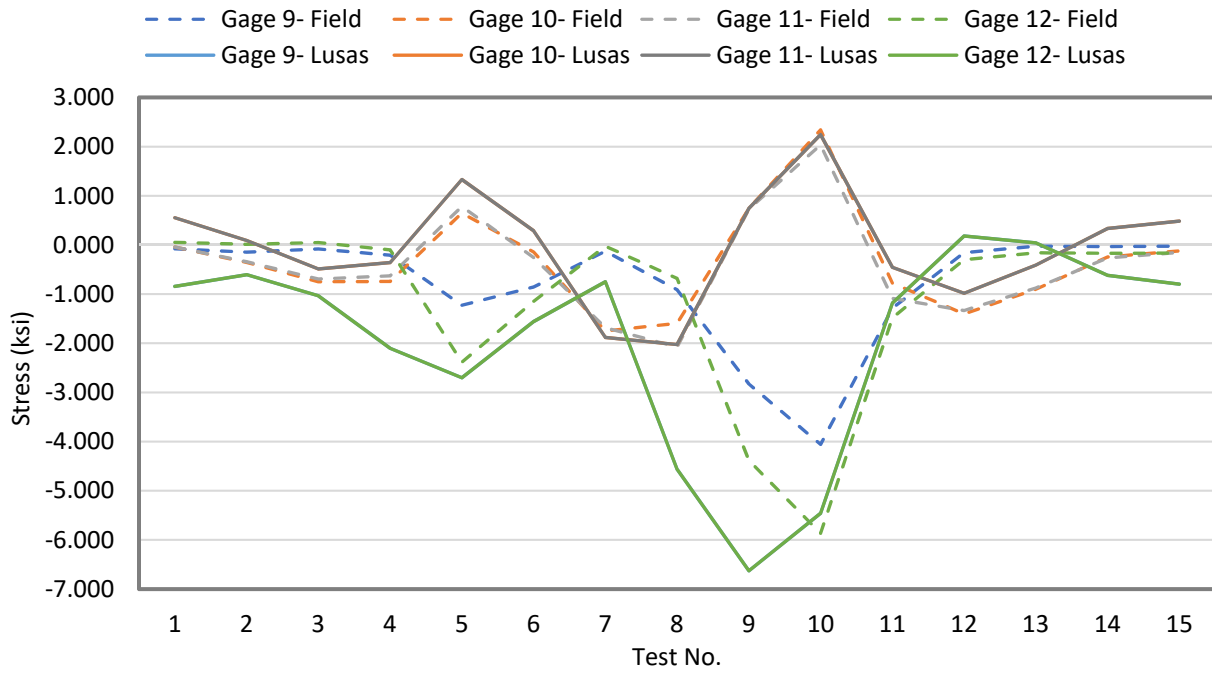


Figure 69 – Results of Test 1-N1 Culvert 7 (15 load-cases) for Gages 9 thru 12 (Gage Cluster 3)

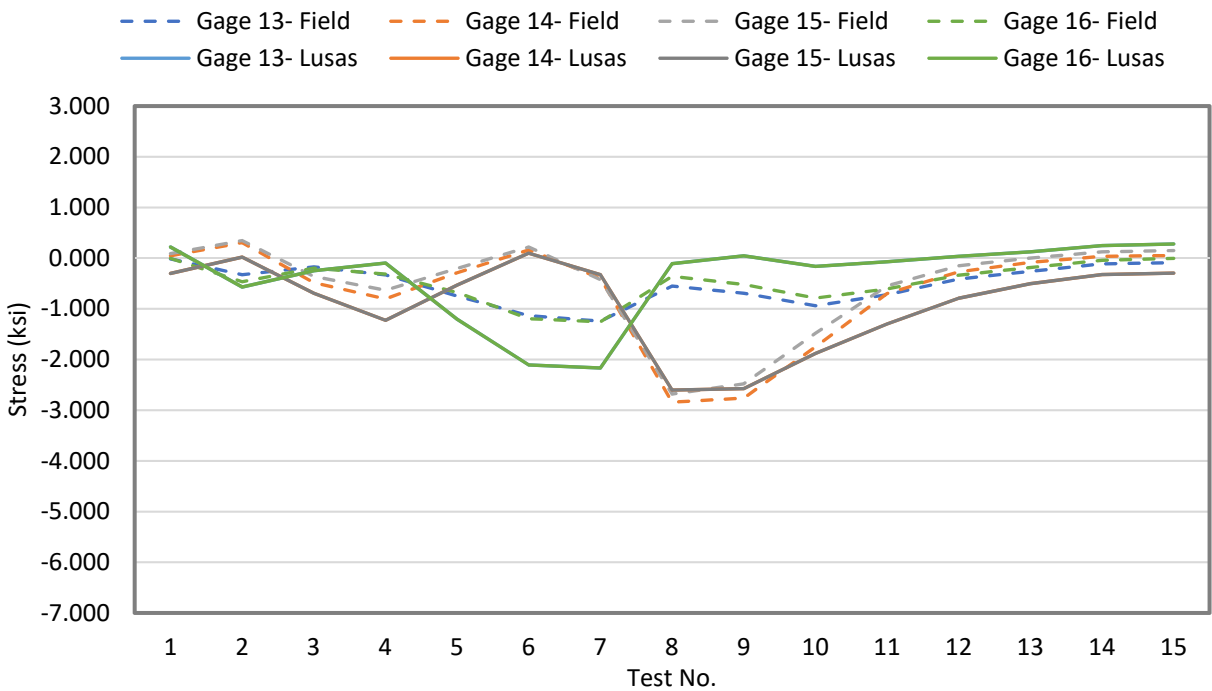


Figure 70 - Results of Test 1-N1 Culvert 7 (15 load-cases) for Gages 13 thru 16 (Gage Cluster 2)

Appendix K – Calibration Information

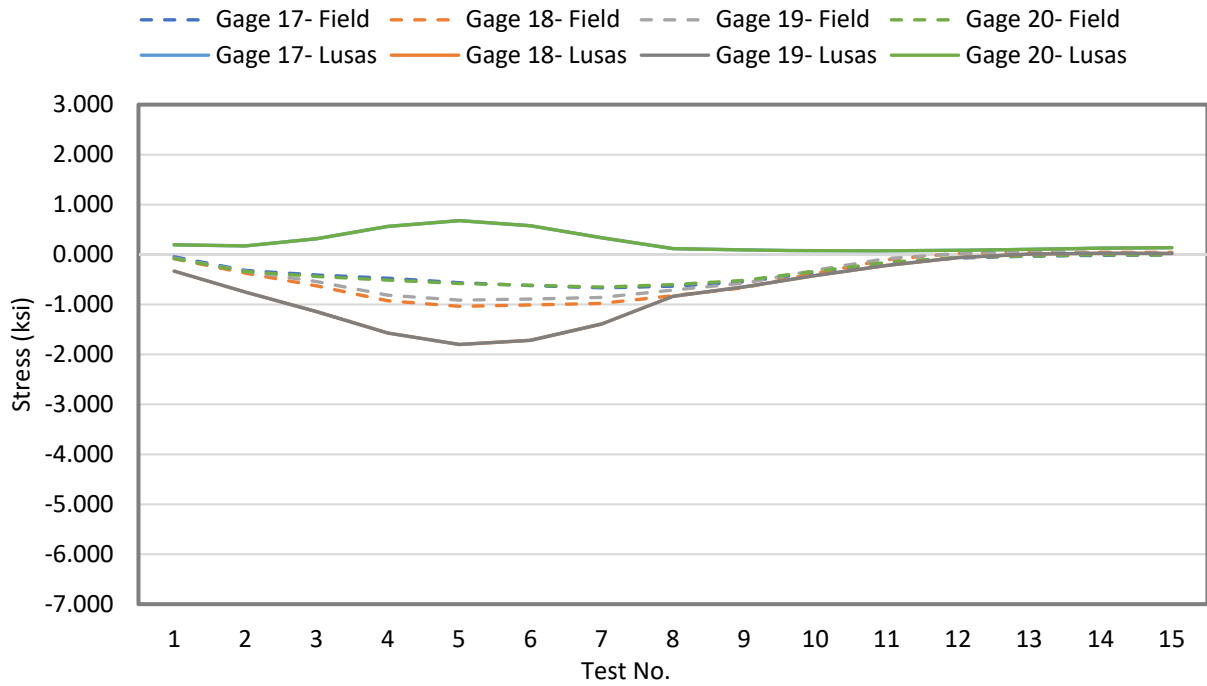


Figure 71 - Results of Test 1-N1 Culvert 7 (15 load-cases) for Gages 17 thru 20 (Gage Cluster 1)

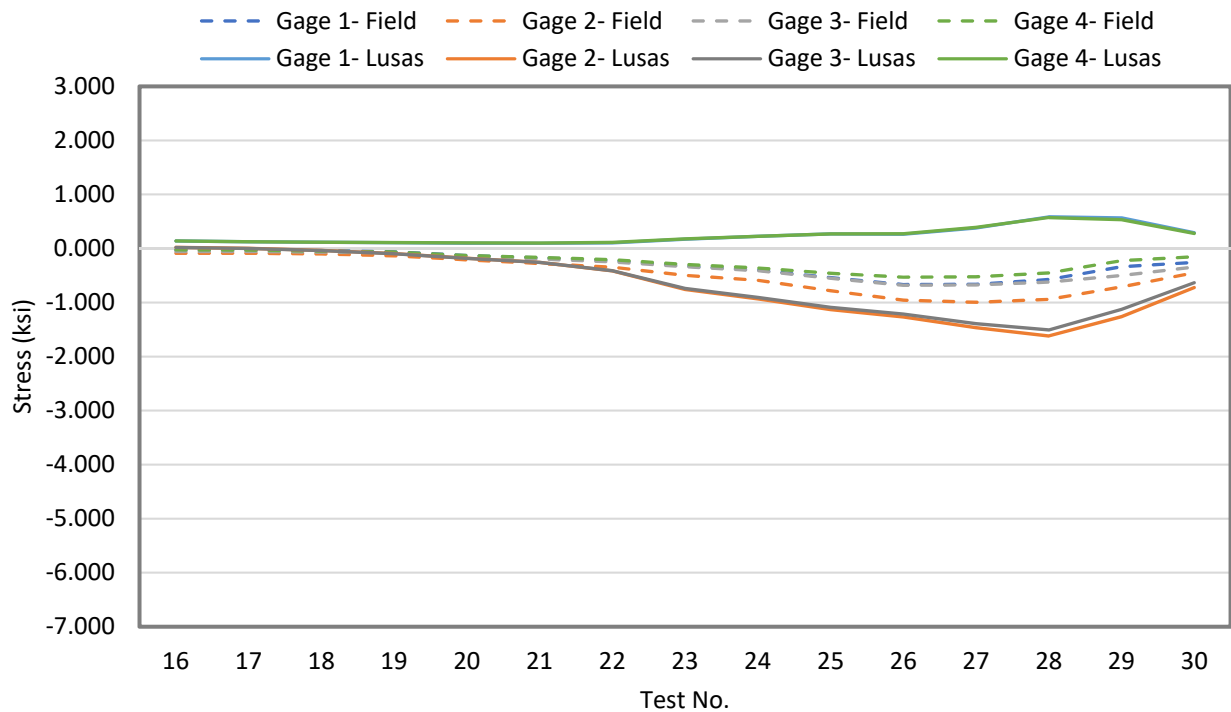


Figure 72 - Results of Test 1-N2 Culvert 7 (15 load-cases) for Gages 1 thru 4 (Gage Cluster 5)

Appendix K – Calibration Information

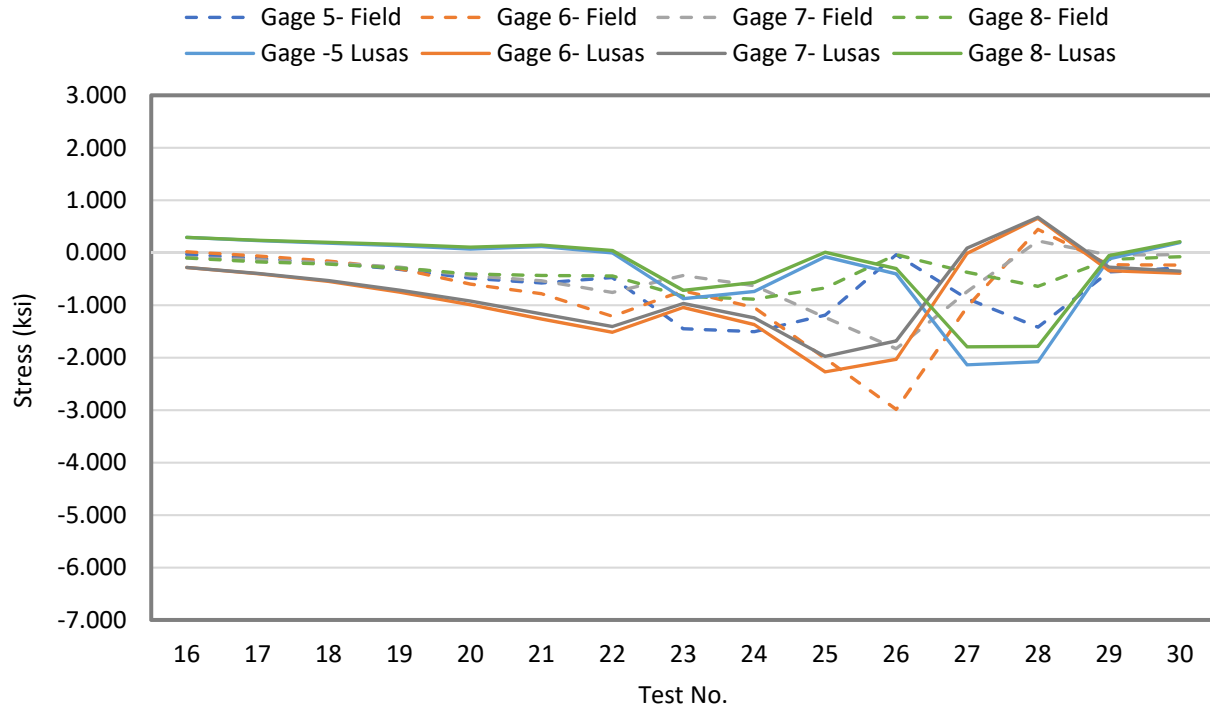


Figure 73 - Results of Test 1-N2 Culvert 7 (15 load-cases) for Gages 5 thru 8 (Gage Cluster 4)

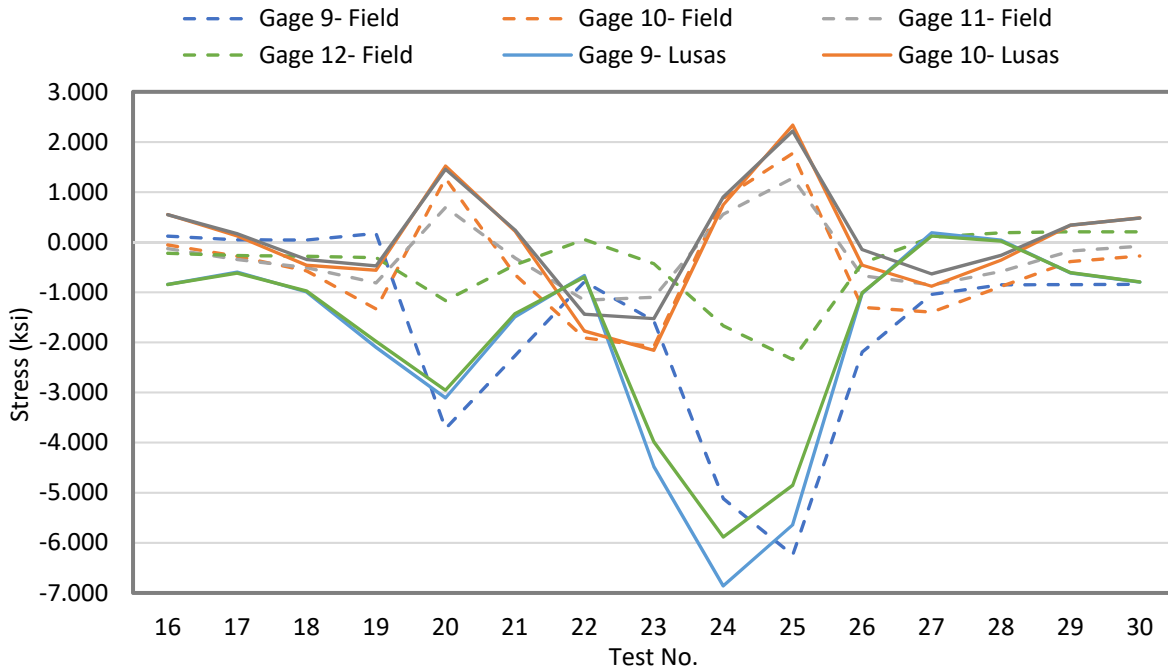


Figure 74 - Results of Test 1-N2 Culvert 7 (15 load-cases) for Gages 9 thru 12 (Gage Cluster 3)

Appendix K – Calibration Information

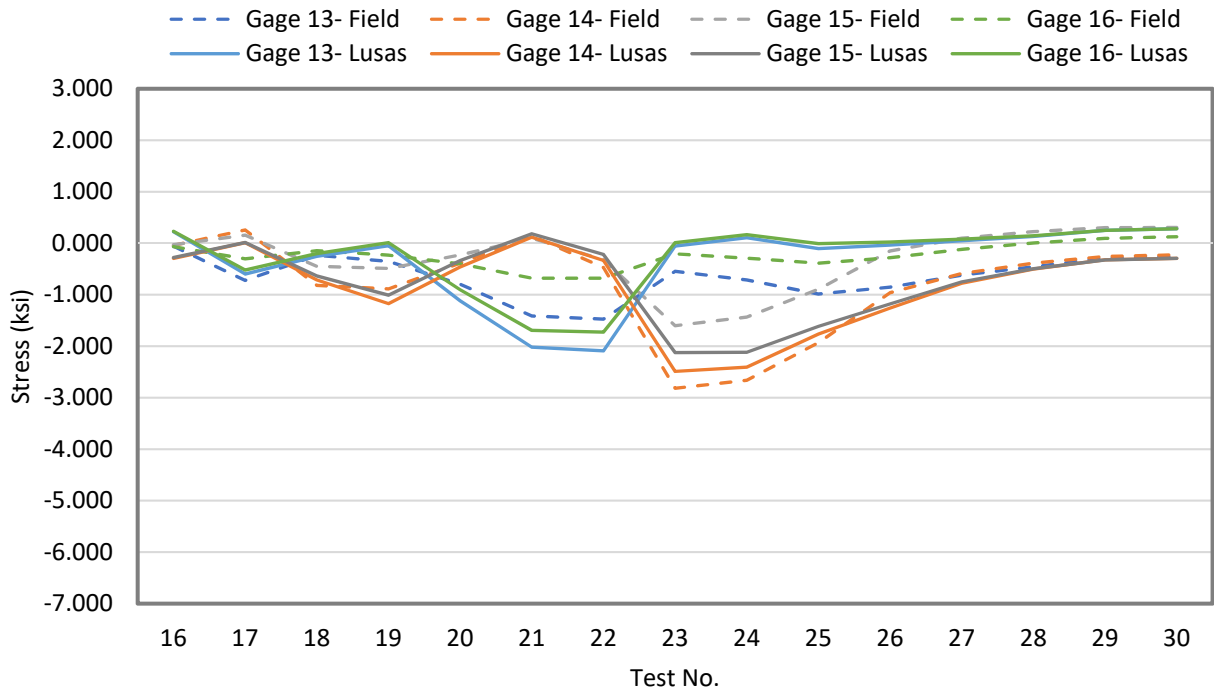


Figure 75 - Results of Test 1-N2 Culvert 7 (15 load-cases) for Gages 13 thru 16 (Gage Cluster 2)

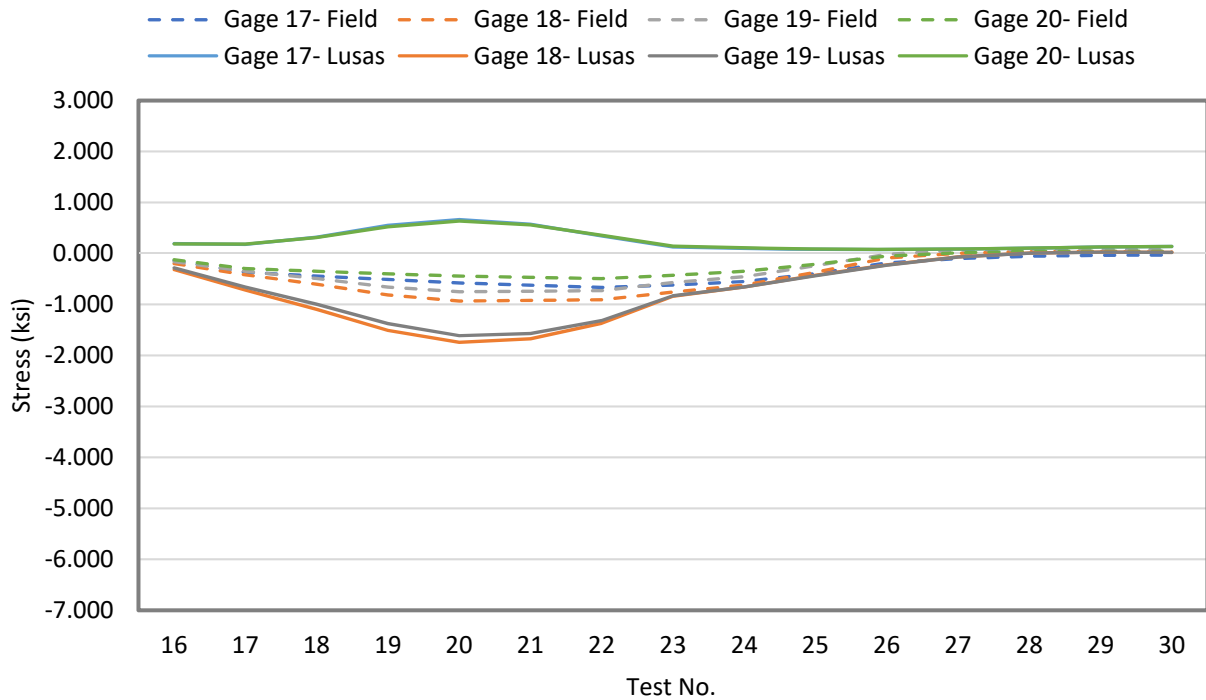


Figure 76 - Results of Test 1-N2 Culvert 7 (15 load-cases) for Gages 17 thru 20 (Gage Cluster 1)

Appendix K – Calibration Information

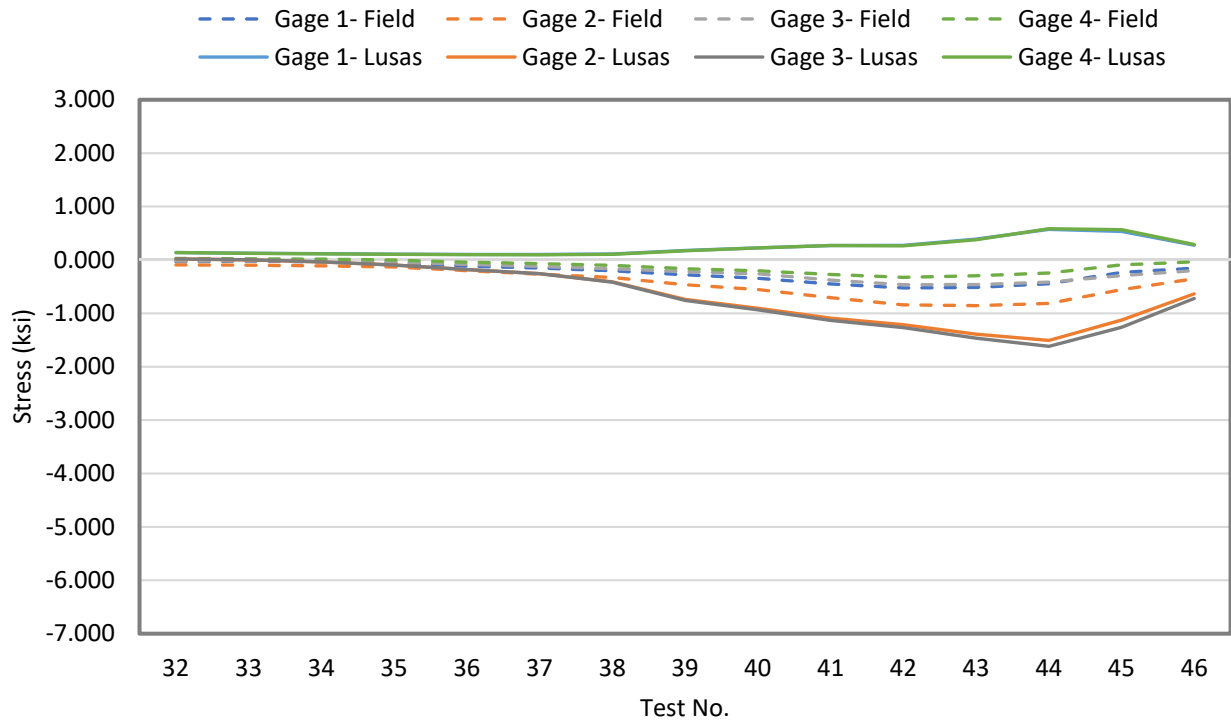


Figure 77 - Results of Test 1-N3 Culvert 7 (15 load-cases) for Gages 1 thru 4 (Gage Cluster 5)

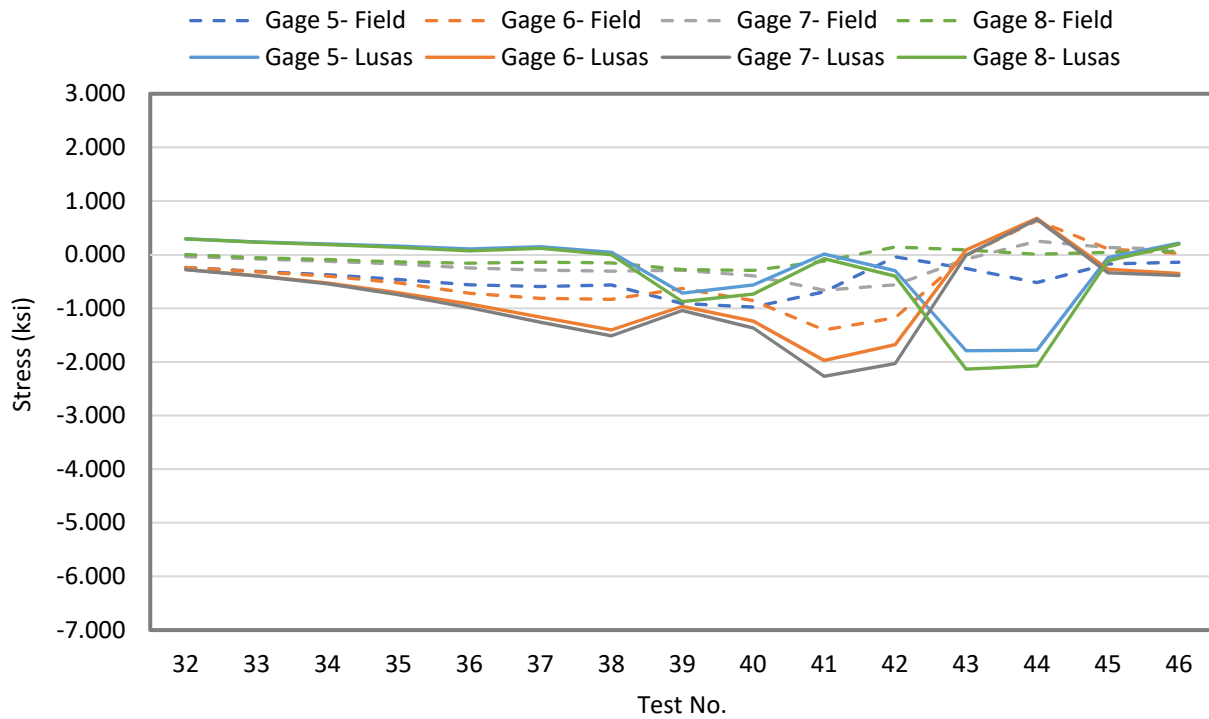


Figure 78 - Results of Test 1-N3 Culvert 7 (15 load-cases) for Gages 5 thru 8 (Gage Cluster 4)

Appendix K – Calibration Information

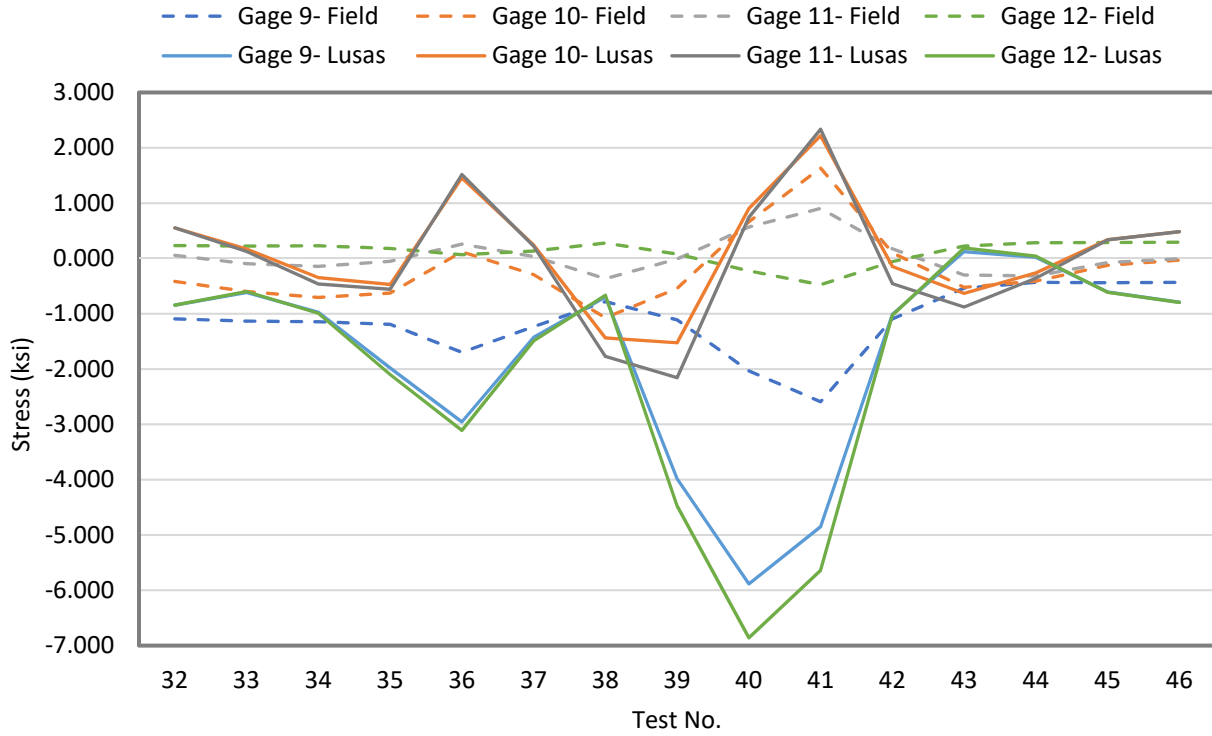


Figure 79 - Results of Test 1-N3 Culvert 7 (15 load-cases) for Gages 9 thru 12 (Gage Cluster 3)

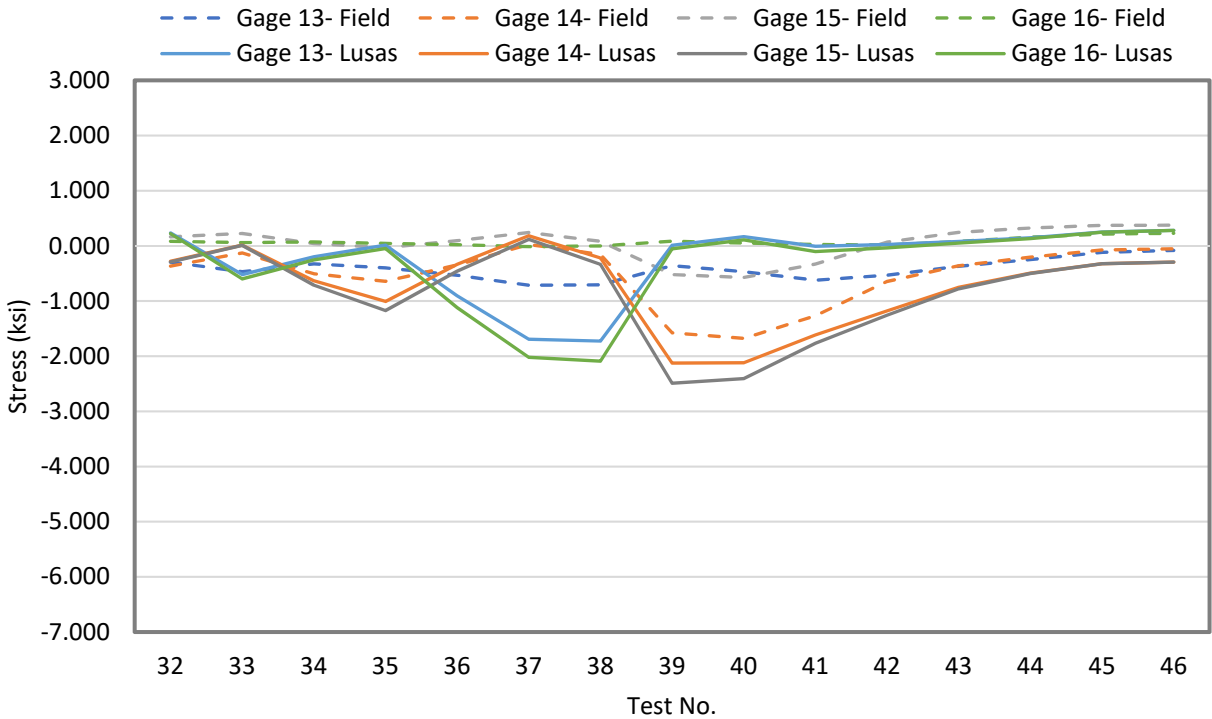


Figure 80 - Results of Test 1-N3 Culvert 7 (15 load-cases) for Gages 13 thru 16 (Gage Cluster 2)

Appendix K – Calibration Information

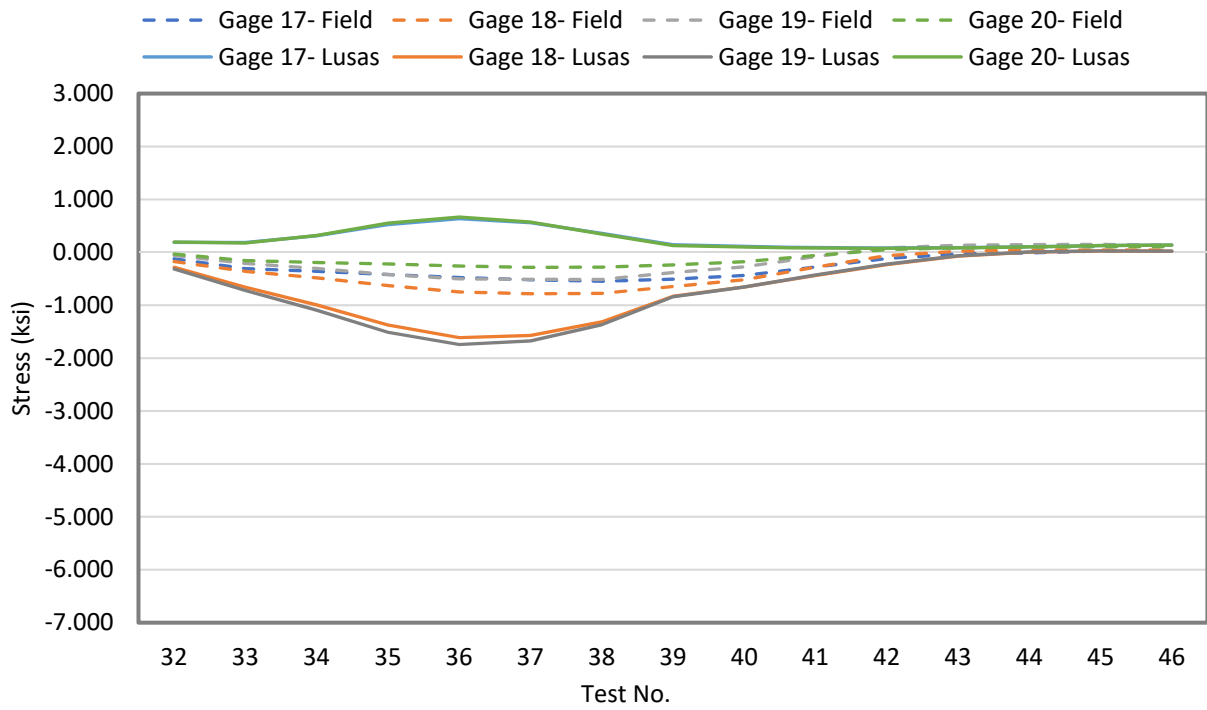


Figure 81 - Results of Test 1-N3 Culvert 7 (15 load-cases) for Gages 17 thru 20 (Gage Cluster 1)

Appendix K – Calibration Information

1.9 Details on Model 7 Calibration

This section documents the process used to model and calibrate Model 7, the long span corrugated metal culvert located in Attleboro, MA. Multiple approaches were taken to determine the best course of modeling the structure in LUSAS and then using the selected approach to carry out the calibration effort. This effort and the lessons learned were then used to shape the approach used to model and calibrate the remaining corrugated metal culverts. These modeling methods can also serve as a guide for further research in the 3D modeling of culverts using FEA.

The experimental program for Culvert 7 consists of two main phases: Phase 1 loading the culvert prior to placement of the pavement; and Phase 2, loading the culvert after the pavement is placed. Each phase included three main sets of loading (Figure 82): N1, with the center of truck over the center of culvert (and gages); N2, with the left wheel line of the truck centered over the centerline of the culvert; and N3, with the right wheel line of the truck centered over the centerline of the culvert.

Five clusters of four gages (20 gages total) are mounted on the lower face of the culvert as shown in Figure 62. For each test, one of the axles of the truck (3 axles) is placed over one of the gage clusters, producing 15 loading configurations for each set of loading

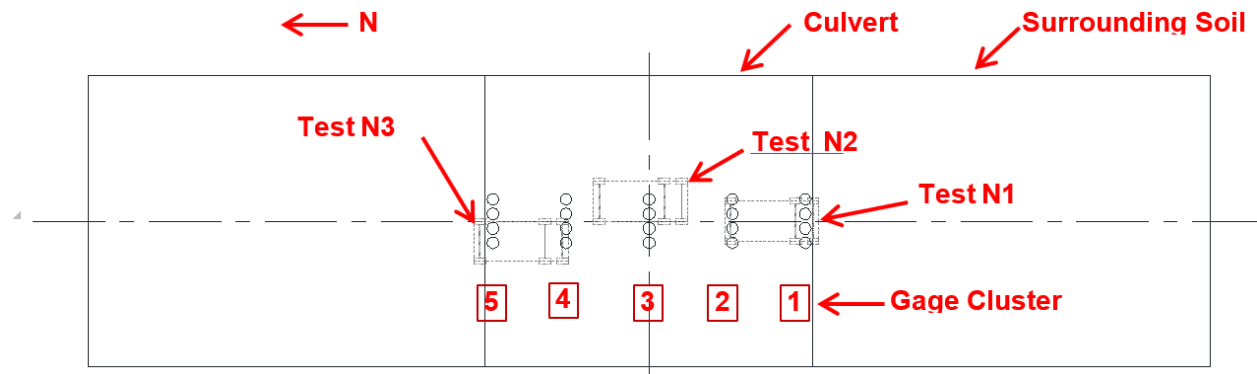


Figure 82 - M7C1 Plan View: Showing Location of Gages and Truck Positioning for Each Set of Test

Model 7 intends to capture the behavior of deep corrugated metal arches. Several approaches are considered to accurately capture the behavior of corrugations including shell elements with orthotropic material properties, shell elements with stiffeners in the direction of corrugations, and double thin shell elements with orthotropic material properties. Table 1 summarizes each approach with assigned material properties. The following is a summary of each model:

- Model 1 is the actual corrugation of Culvert 7.
- Model 2 presents the approach where a stiffener is added to the shell to represent the corrugation.
- Model 3 presents an approach where the thickness and modulus of elasticity in strong axis (E_x) is defined so that both axial rigidity and flexural rigidity in the strong axis match those of the actual corrugation. Modulus of elasticity in weak axis (E_y) is defined based on new thickness to capture the flexural behavior in the weak axis and E_{xy} is defined based on axial adjustment.

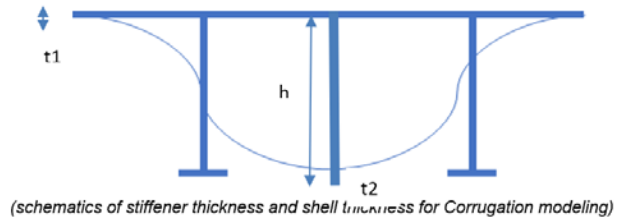
Appendix K – Calibration Information

- Model 4 is similar to Model 3, except that E_y is adjusted based on axial properties and E_{xy} is adjusted based on flexural (warping) properties.
- Model 5 is also similar to Model 3, except that both E_y and E_{xy} are adjusted based on flexural properties.
- Model 6 presents the approach where two overlapping shell elements are defined to capture the behavior of the corrugation. The thickness and moduli of elasticity of each shell element is defined so that the super-imposition of both elements would capture all of the rigidity components of the corrugated metal sheets.

Table 1 - Material and Section Properties of Models for Modeling the Corrugation (M7C1)

CULVERT #	DESCRIPTION	Thickness (in.)	E_x	E_y	E_{xy}	$E_x \cdot t$	$E_y \cdot t$	$E_{xy} \cdot t$	$E_x \cdot t^3$	$E_y \cdot t^3$	$E_{xy} \cdot t^3$
			(strong) (ksi)	(weak) (ksi)	(ksi)	(kip/in)	(kip/in)	(kip/in)	(kip-in)	(kip-in)	(kip-in)
C1	Corrugated Metal Culvert	0.2391	29,000	29,000	11,154	8,951	10.90	2,666.88	382,800	396	12,705
C3	Ex for Flexure and Axial, Ey for Flexure, Exy for Axial	6.5395	1,368.8	1,417	407.81	8,951	9	2,666.88	382,800	396	9,504.0
C4	Ex for Flexure and Axial, Ey for Axial, Exy for Flexure	6.5395	1,368.8	1,667	0.5	8,951	10.9	4	382,800	466	12.7
C5	Ex for Flexure and Axial, Ey for Flexure, Exy for Flexure	6.5395	1,368.8	1,417	0.55	8,951	9	3.57	382,800	396	12.7
C6	X for Flexure and Axial, Y for Flexure t and Exy for Flexure	6.5395	1,368.8	1,417	0.3	8,951	9	1.78	382,800	396	6.353
		0.1691	0.0	0.000	15,758.8	0	0	2,665.13	0	0	6.352
TOTA						8,951	9	2,666.91	382,800	396	12,705

C2	Shell+Stiffener	t1	t2	h
		5.3 in.	2.7 in.	5.5 in.



Appendix K – Calibration Information

The proposed approaches are used to create six culverts (without surrounding soil). Each culvert is loaded with an axial and lateral force and the deformation and stresses at each culvert is compared (Figure 83). Table 2 summarizes the results of each culvert. The green values show close match to actual corrugation, while red or grey values show mismatches.

Results of this study suggest that any of the Model 3, 4, or 5 can adequately capture the behavior of the corrugation. For calibration, Model 3 was selected as the best approach.

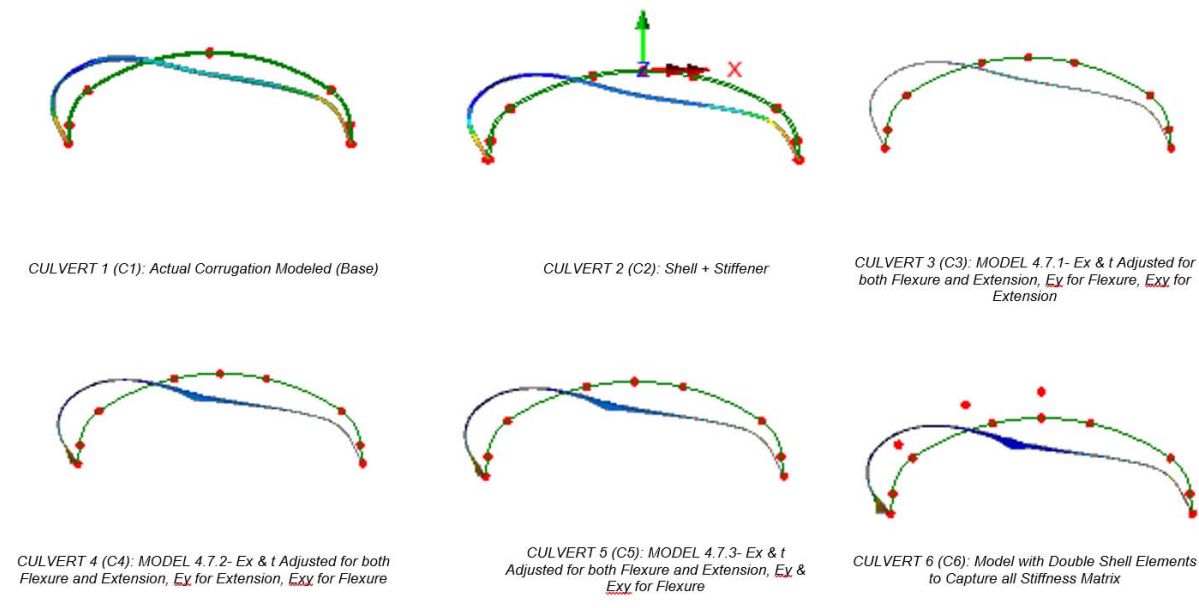


Figure 83 - Deformation Comparison of Six Proposed Models (M7C1)

Calibration and Post-Processing

Using the approach of Model 3, the culvert is modeled using orthotropic material properties. Calibration of the model is carried out by changing the overlay material properties. Given that for Test 1, the culvert was loaded prior to casting the pavement, the loads were transferred to the culvert through compacted overlay. The modulus of elasticity of 7500 ksf is adopted for the overlay material (for well graded coarse material and crushed stone).

In order to make sure that the plastic strains of the soil are not carried to the next load case, each load case is run separately where for each load case, the gravity is applied to model and then the live load is applied to model. Then, the results of the gravity are subtracted from the final results to capture the effect of live load.

Given that shell elements do not have the same section properties as the actual corrugated metal sheet, for post-processing the Force/Moment output is abstracted from the associated nodes and the following equation is used to derive the actual stresses at the location of the strain gages:

Appendix K – Calibration Information

$$\sigma_x = \frac{N_x}{A} + \frac{My}{I_{xx}}$$

where:

σ_x = stress along the direction of strain gages (strong axis);

N_x = Axial force transferred in the direction of the strong axis (kip/in);

A = area of the cross section per unit length = $s/c(t)$;

M = carried moment in the direction of strong axis (k-in/in);

y = half of the depth of corrugation;

I_{xx} = moment of inertia of a unit length of corrugated metal sheet = $\frac{I_{cor}}{c}$;

c = pitch of the corrugation;

s = length of the arch along the corrugation.

Appendix K – Calibration Information

Model 7 Results Before and After Paving

Introduction

Model 7 is a corrugated metal box culvert located in Attleboro, Massachusetts. The Research Team was able to coordinate with MASSDOT and the culvert contractor to instrument and test this culvert under construction with the intent that the effects of paving on the response of the culvert could be captured.

This memorandum presents the LUSAS results (3-D finite element analysis) of Model 7, Candidate 1 under the truck load that was used in the experimental program. For this culvert, the experimental program consisted of two main phases: Phase 1 loading the culvert prior to placement of the pavement; and Phase 2, loading the culvert after the pavement is placed. The results herein show the force effects obtained both prior to and after paving.

The calibration and approach to the 3-D modeling of this culvert in LUSAS is documented in detail in Interim Report No. 3.

Culvert Loading and Instrumentation

Each phase included three main sets of loading (Figure 1): N1, with the center of truck over the center of culvert (and gages); N2, with the left wheel line of the truck centered over the centerline of the culvert; and N3, with the right wheel line of the truck centered over the centerline of the culvert.

Five clusters of four gages (20 gages total) are mounted on the lower face of the culvert as shown in Figure 3. For each test, one of the axles of the truck (3 axles) is placed over one of the gage clusters, producing 15 loading configurations for each set of loading.

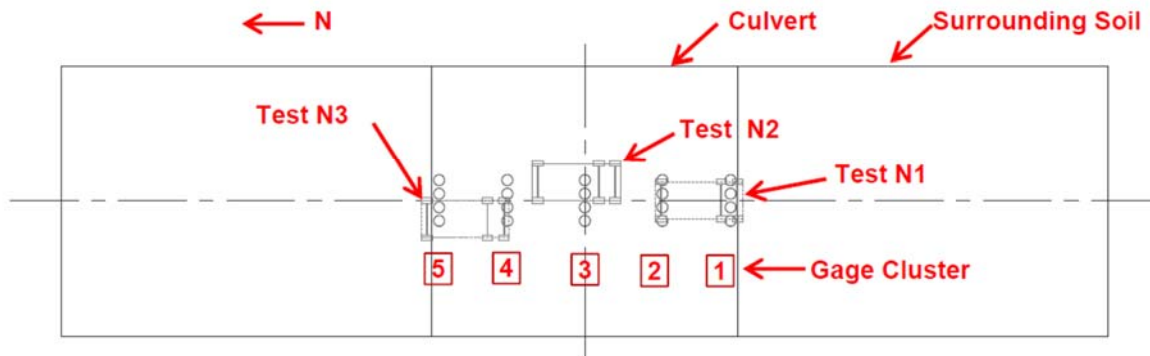


Figure 84 - M7C1 Plan View: Showing Location of Gages and Truck Positioning for Each Set of Test

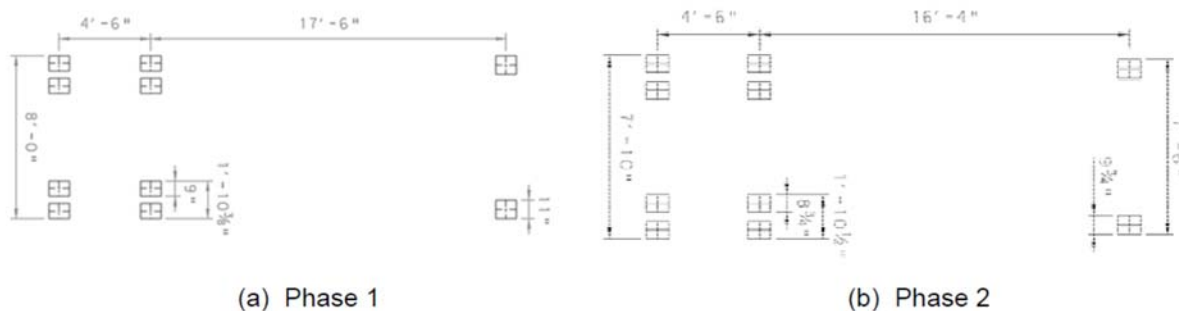


Figure 85 - Truck Dimensions for each Phase of Testing

Appendix K – Calibration Information

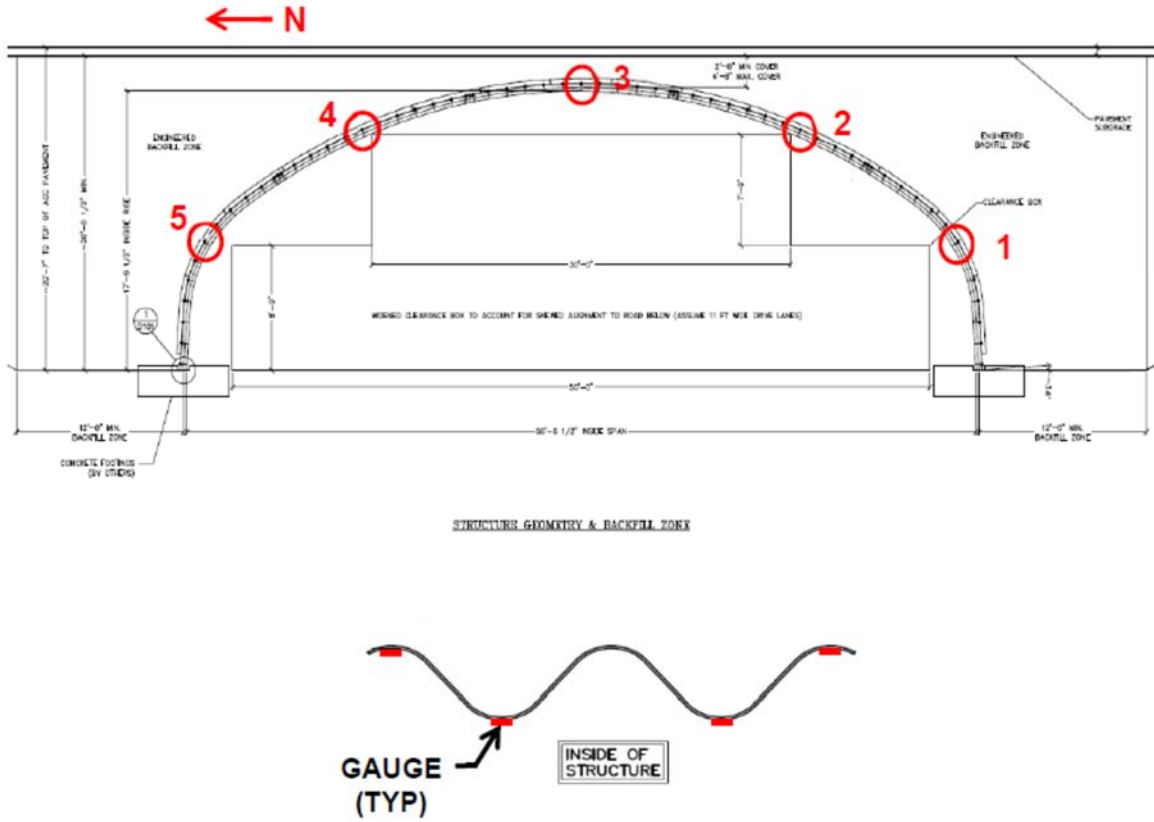
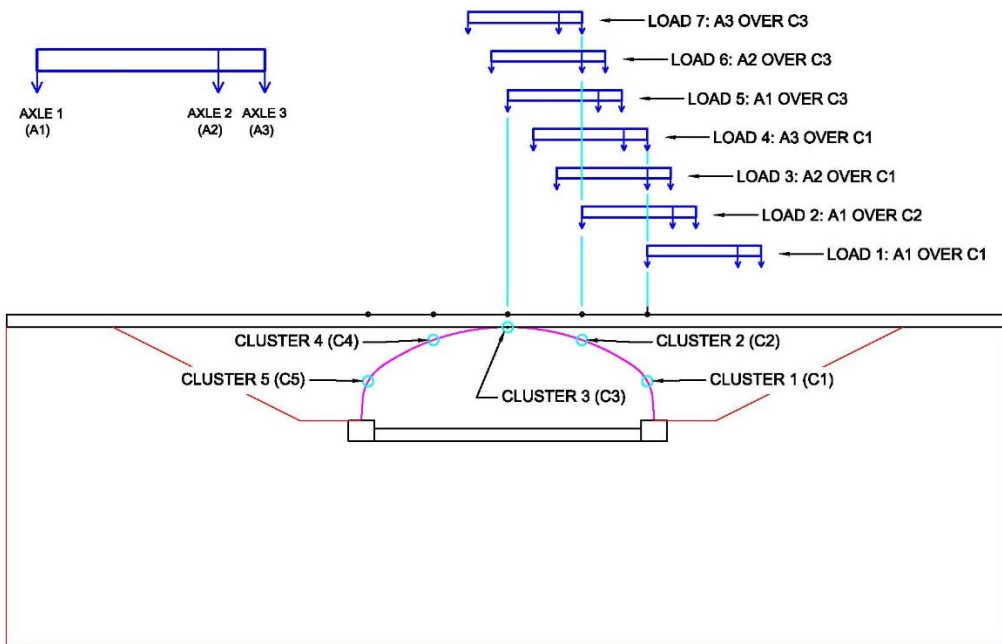
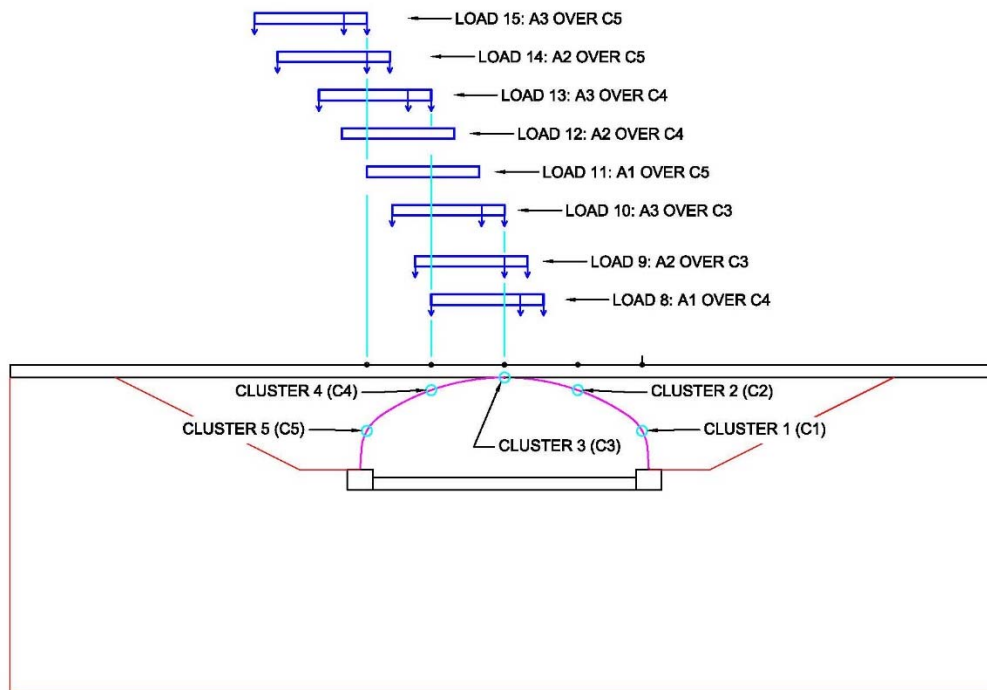


Figure 86 - Instrumentation Locations



Appendix K – Calibration Information

(a) Load Set 1 thru 7.



(b) Load Set 8 thru 15.

Figure 87 - Schematics of Loading for Each Load Case for Culvert 7**Results Before and After Paving**

While the results presented in Interim Report Number 3 document the selection of a 3-D modeling scheme and the corresponding results from Test 1 (prior to paving), the results herein illustrate the differences in the stresses at each of the strain gauge locations as measured in the field. Similar comparisons were made between the stresses at each location as obtained in the 3-D LUSAS models.

In the figures below, Test 1 results are shown in dashed lines and represent the condition without pavement and Test 2 results are shown in solid lines and represent the culvert after paving. The results show a significant reduction in measured strains. Gage Cluster 3 at midspan shows a 33% reduction in peak stress under the live load. Gage Cluster 4 at the shoulder, the other critical location, shows a 50% reduction. These reductions are also notable as the pavement was placed on high quality, highly compacted fill being prepared for interstate traffic. Pavements over softer soils will show a more significant benefit with the same paving.

We conclude that live load ratings can be improved by including the effects of pavement. A 3-D model is not required to analyze live load response associated with a paved surface. The 2-D CANDE software has been modified to allow the user to specify a paved surface (See Interim Report Number 3, Section 5.1.2.2 Updates to the CANDE Toolbox). A parametric study and recommendations on the inclusion of pavement was documented as part of Interim Report Number 2, Section 4.1.2.4.1.

Appendix K – Calibration Information

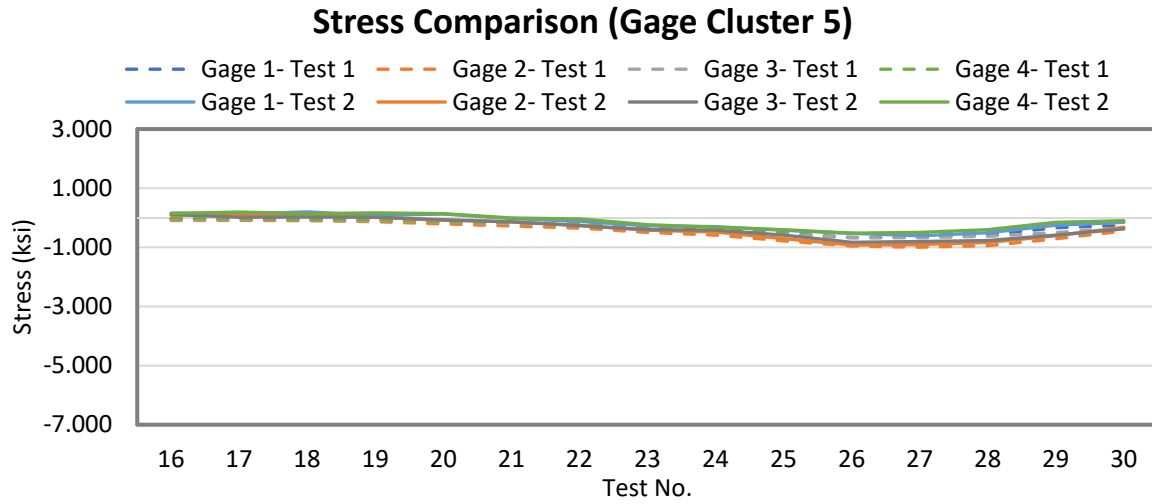


Figure 88 - Model 7 Before and After Paving: Test N1, Gauges 1-4 (Cluster 5)

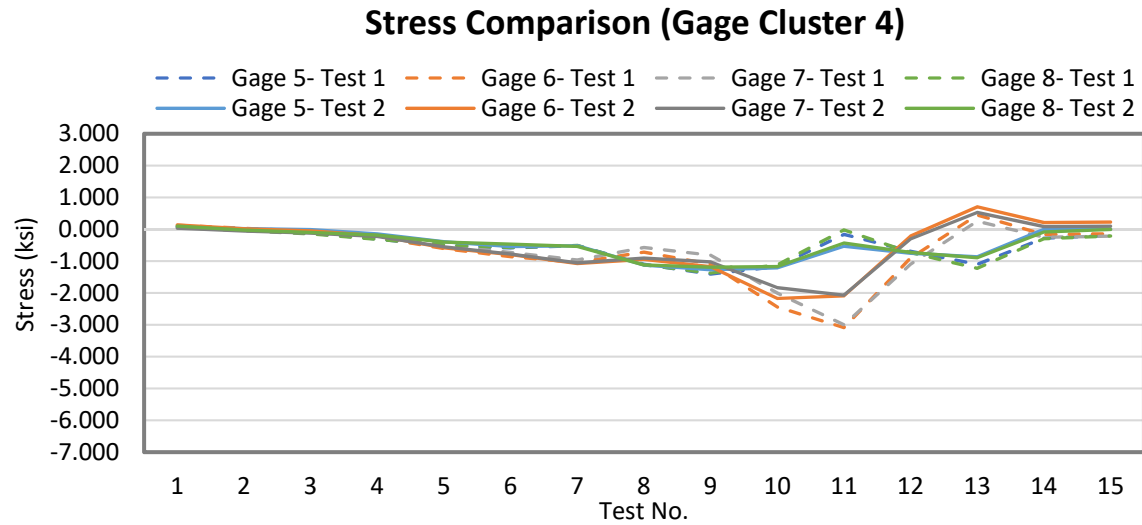


Figure 89 - Model 7 Before and After Paving: Test N1, Gauges 5-8 (Cluster 4)

Appendix K – Calibration Information

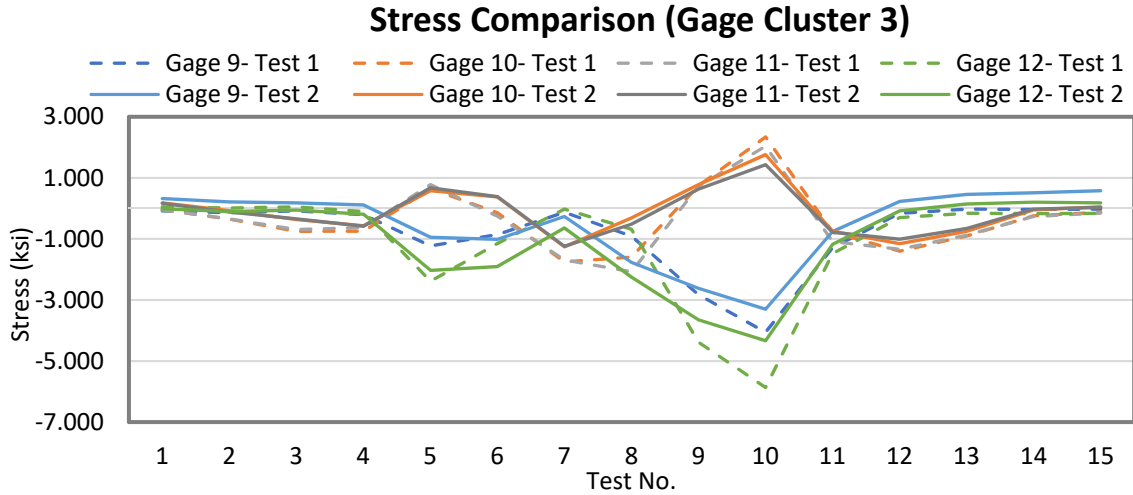


Figure 90 - Model 7 Before and After Paving: Test N1, Gauges 9-12 (Cluster 3)

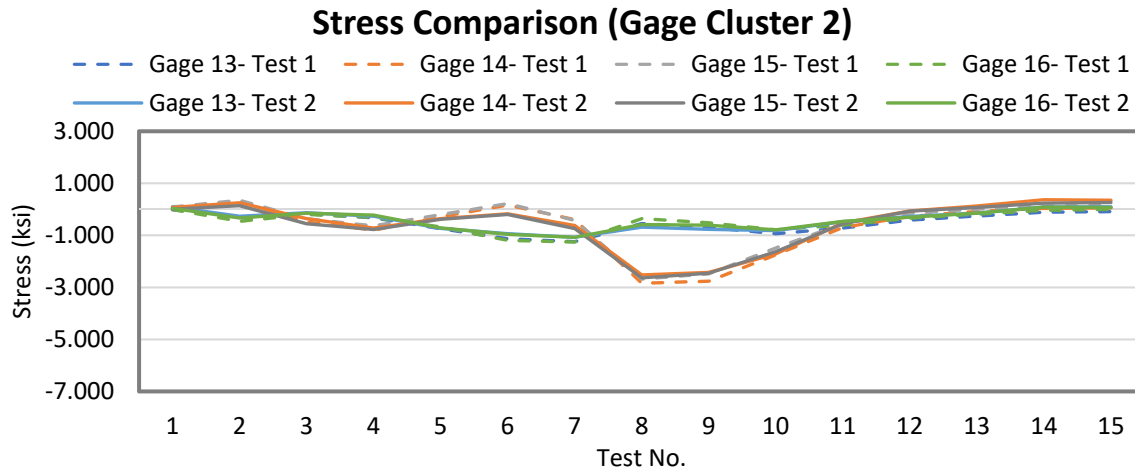


Figure 91 - Model 7 Before and After Paving: Test N1, Gauges 13-16 (Cluster 2)

Appendix K – Calibration Information

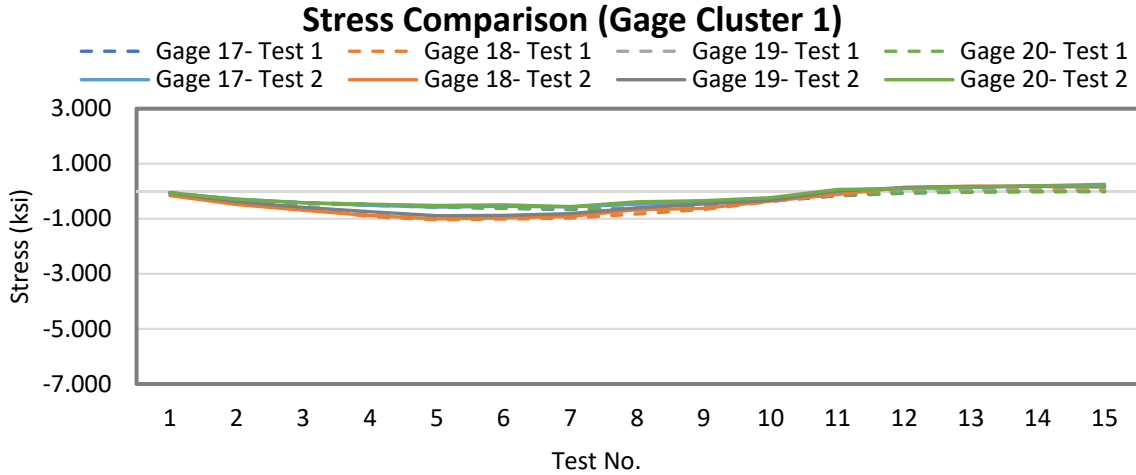


Figure 92 - Model 7 Before and After Paving: Test N1, Gauges 17-20 (Cluster 1)



Figure 93 - Model 7 Before and After Paving: Test N2, Gauges 1-4 (Cluster 5)

Appendix K – Calibration Information

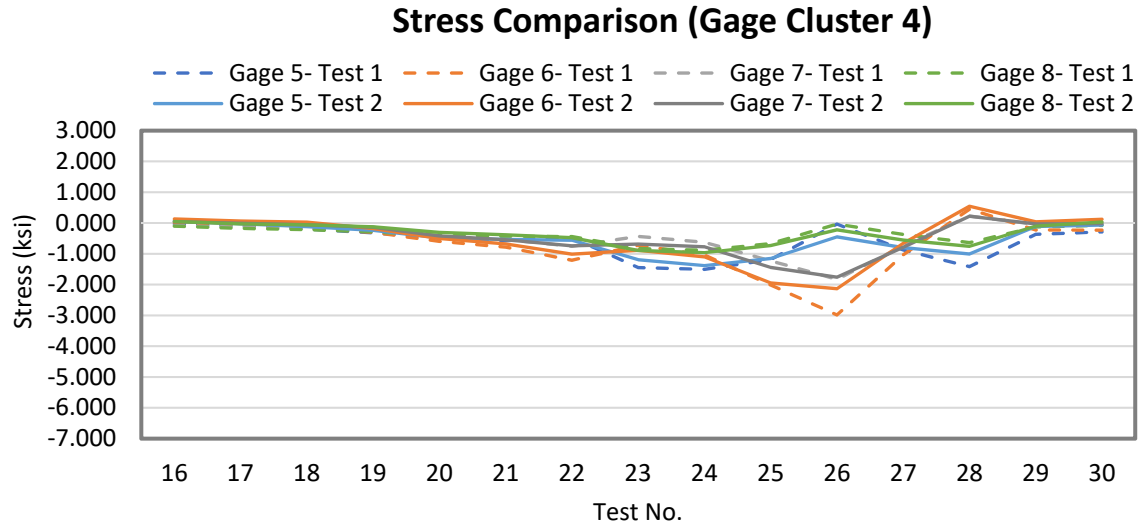


Figure 94 - Model 7 Before and After Paving: Test N2, Gauges 5-8 (Cluster 4)

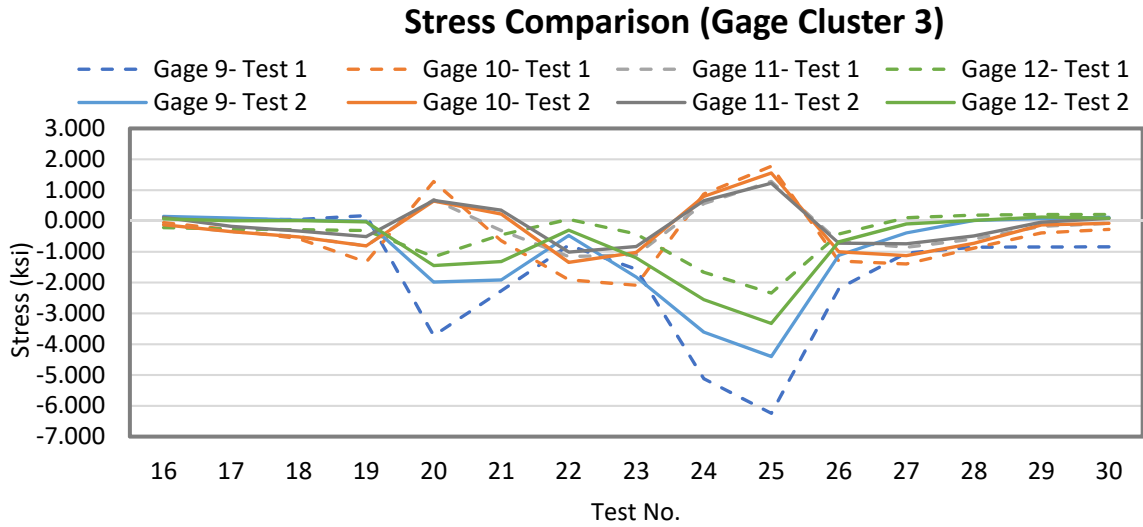


Figure 95 - Model 7 Before and After Paving: Test N2, Gauges 9-2 (Cluster 3)

Appendix K – Calibration Information

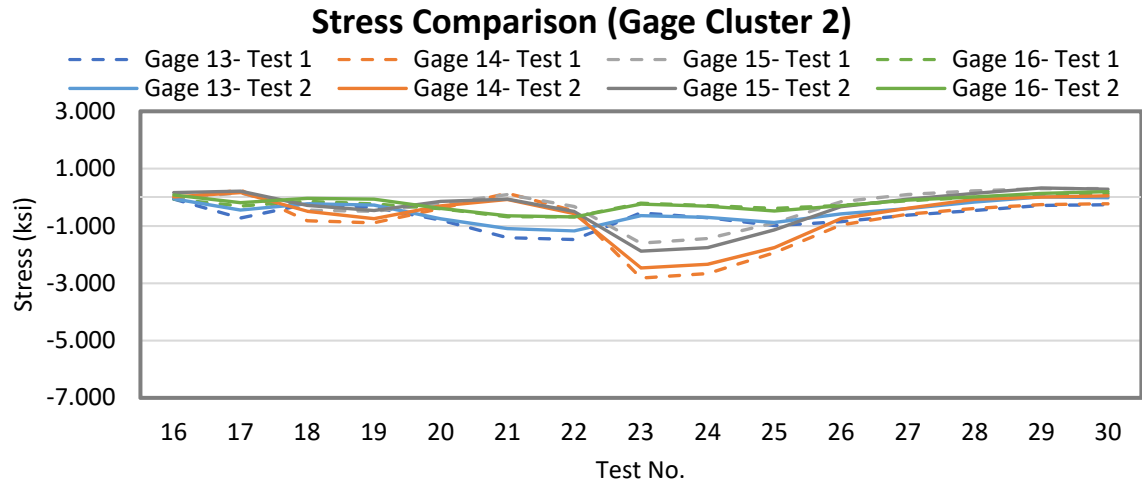


Figure 96 - Model 7 Before and After Paving: Test N2, Gauges 13-16 (Cluster 1)

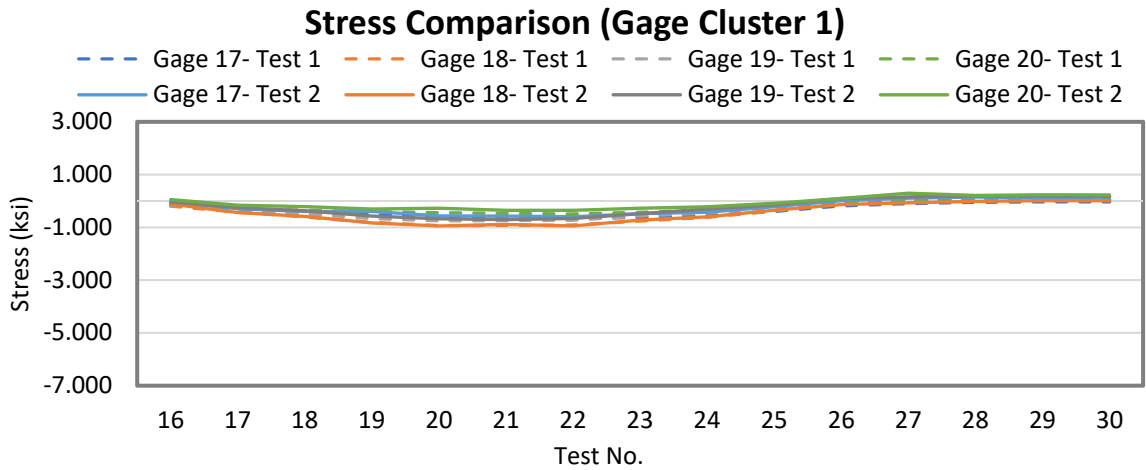


Figure 97 - Model 7 Before and After Paving: Test N2, Gauges 17-20 (Cluster 1)

Appendix K – Calibration Information

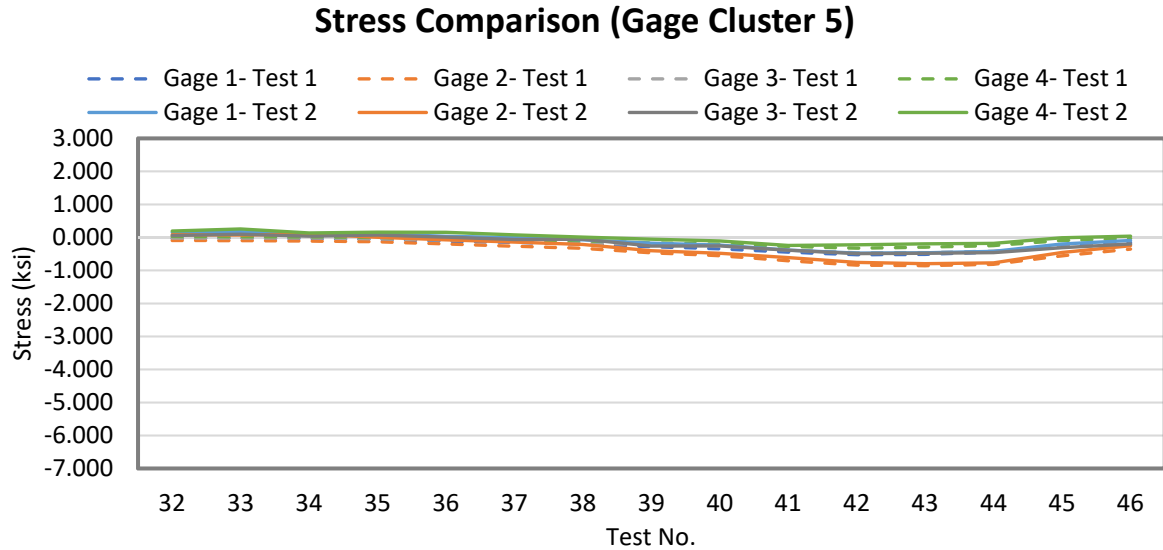


Figure 98 - Model 7 Before and After Paving: Test N3, Gauges 1-4 (Cluster 5)

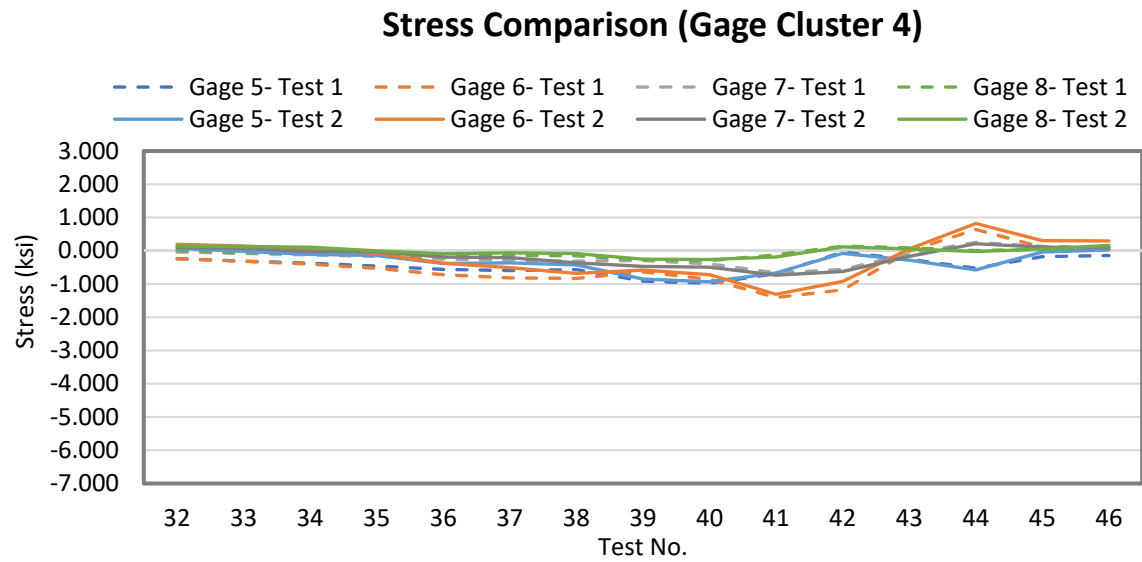


Figure 99 - Model 7 Before and After Paving: Test N3, Gauges 5-8 (Cluster 4)

Appendix K – Calibration Information

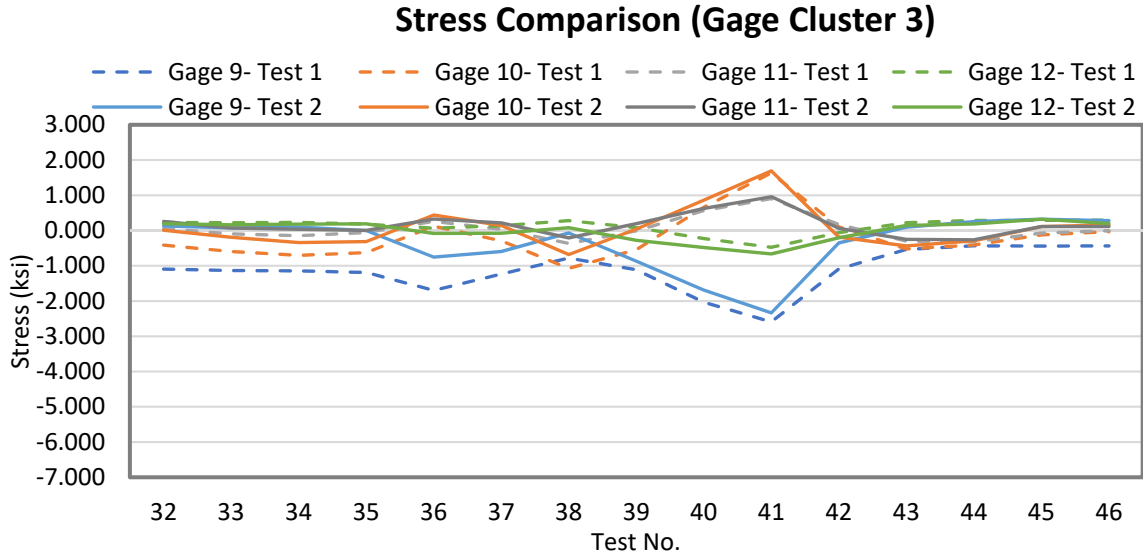


Figure 100 - Model 7 Before and After Paving: Test N3, Gauges 9-12 (Cluster 3)

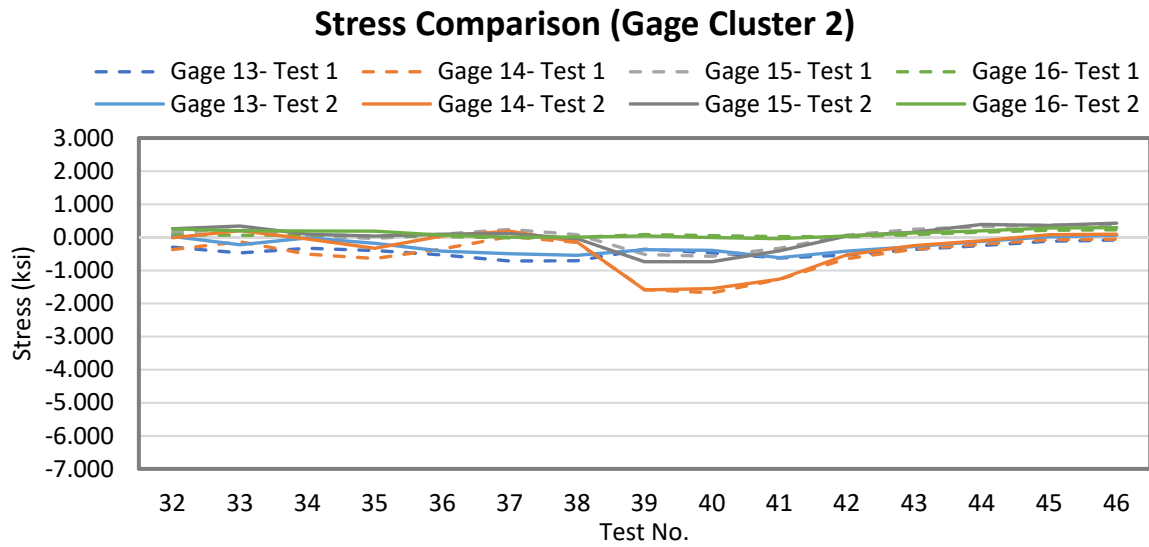


Figure 101 - Model 7 Before and After Paving: Test N3, Gauges 13-16 (Cluster 2)

Appendix K – Calibration Information

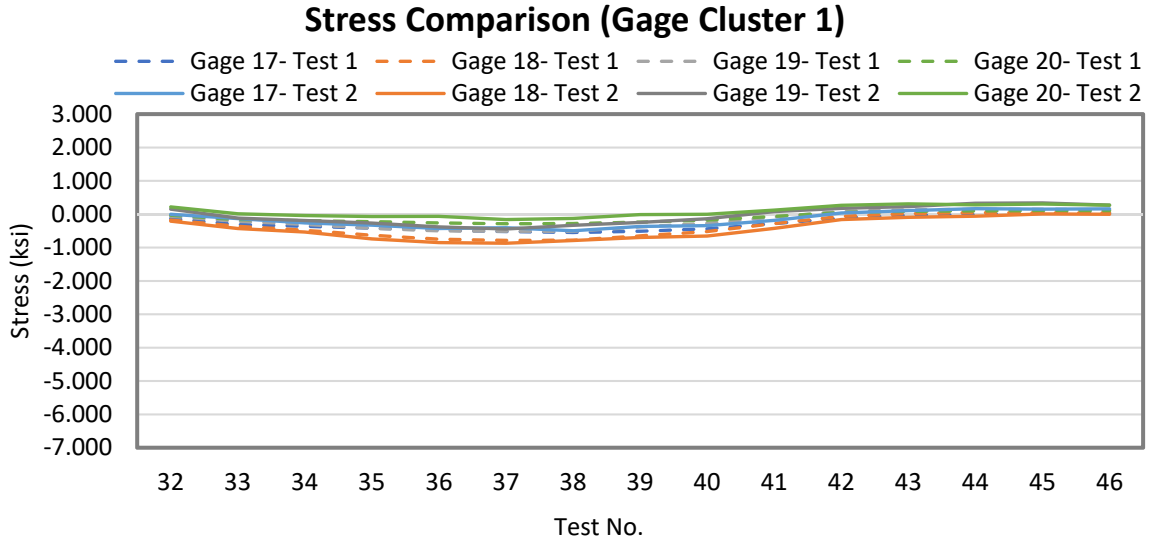


Figure 102 - Model 7 Before and After Paving: Test N3, Gauges 17-20 (Cluster 1)

Appendix L – Caltrans Models-LRFR-LFR Comparisons

Appendix L – LRFR/LFR Rating Comparisons in BrDR Using Caltrans Models

This appendix provides a comparison of a select set of culverts provided by Caltrans in the software package AASHTOWare BrDR. The runs were made in Version 6.8.2 of the software.

Appendix L – Caltrans Models-LRFR-LFR comparisons

Naming convention for ‘Culvert Name’

CX WWxHH; XX DDDD

CS – single cell culvert

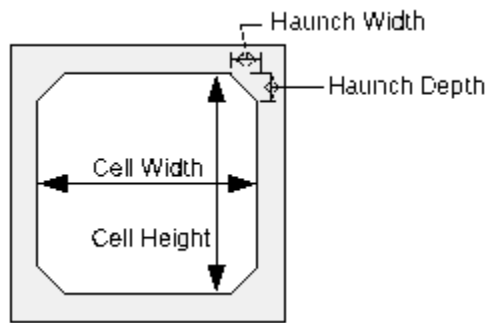
CD – double cell culvert

WW – cell width

HH – Cell height

XX – maximum fill height

DDDD – culvert year



For Example

The culvert name “CS10x8;10 2002”

Is a single cell culvert with a 10’ cell width, 8’ cell height; a maximum fill of 10’ and was designed in 2002.

Notes:

- In the tables on the following pages, the ratio represents the ratio of the LFR rating to the LRFR rating. In cases where the ratio is less than one (i.e. the LFR rating is less than the LRFR rating) the column is highlighted in red.
- The LFR ratings were performed with the HS20-44 vehicle with a scale factor of 1.25

Appendix L – Caltrans Models-LRFR-LFR comparisons

ID	Culvert Name	LRFD Vehicle	Fill Height (ft)	LRFR Inv	LRFR Oper	LFR Vehicle HS20-44 with a 1.25 factor	LFR Inve	LFR Opera	Ratio Inventory LFR/LRFR	Ratio Operating LFR/LRFR
42	CS10x8;10 2002	HL-93 (US)	0	0.609	0.789	HS 20-44	0.544	0.908	0.89	1.15
	CS10x8;10 2002	HL-93 (US)	0.5	0.597	0.774	HS 20-44	0.513	0.856	0.86	1.11
	CS10x8;10 2002	HL-93 (US)	1	0.579	0.75	HS 20-44	0.481	0.804	0.83	1.07
	CS10x8;10 2002	HL-93 (US)	1.5	0.558	0.723	HS 20-44	0.487	0.813	0.87	1.12
	CS10x8;10 2002	HL-93 (US)	1.9	0.539	0.699	HS 20-44	0.459	0.767	0.85	1.10
	CS10x8;10 2002	HL-93 (US)	2	1.002	1.298	HS 20-44	1.023	1.708	1.02	1.32
	CS10x8;10 2002	HL-93 (US)	4	1.472	1.908	HS 20-44	2.109	3.523	1.43	1.85
	CS10x8;10 2002	HL-93 (US)	7	1.752	2.271	HS 20-44	3.188	5.323	1.82	2.34
	CS10x8;10 2002	HL-93 (US)	9	1.615	2.094	HS 20-44	3.421	5.713	2.12	2.73
	CS10x8;10 2002	HL-93 (US)	10	1.413	1.832	HS 20-44	3.297	5.506	2.33	3.01
43	CS10x8;5 1933	HL-93 (US)	0	0.878	1.139	HS 20-44	0.778	1.299	0.89	1.14
	CS10x8;5 1933	HL-93 (US)	0.5	0.847	1.098	HS 20-44	0.743	1.24	0.88	1.13
	CS10x8;5 1933	HL-93 (US)	1	0.813	1.054	HS 20-44	0.707	1.181	0.87	1.12
	CS10x8;5 1933	HL-93 (US)	1.5	0.776	1.006	HS 20-44	0.727	1.213	0.94	1.21
	CS10x8;5 1933	HL-93 (US)	1.9	0.745	0.965	HS 20-44	0.695	1.16	0.93	1.20
	CS10x8;5 1933	HL-93 (US)	2	0.587	0.761	HS 20-44	0.735	1.228	1.25	1.61
	CS10x8;5 1933	HL-93 (US)	3	0.641	0.831	HS 20-44	1.081	1.805	1.69	2.17
	CS10x8;5 1933	HL-93 (US)	4	0.631	0.818	HS 20-44	1.288	2.152	2.04	2.63
	CS10x8;5 1933	HL-93 (US)	5	0.522	0.676	HS 20-44	1.382	2.308	2.65	3.41
44	CS10x8;8 1966	HL-93 (US)	0	0.642	0.833	HS 20-44	0.635	1.06	0.99	1.27
	CS10x8;8 1966	HL-93 (US)	0.5	0.641	0.831	HS 20-44	0.604	1.009	0.94	1.21
	CS10x8;8 1966	HL-93 (US)	1	0.655	0.849	HS 20-44	0.573	0.957	0.87	1.13
	CS10x8;8 1966	HL-93 (US)	1.5	0.653	0.847	HS 20-44	0.587	0.98	0.90	1.16
	CS10x8;8 1966	HL-93 (US)	1.9	0.649	0.842	HS 20-44	0.559	0.934	0.86	1.11
	CS10x8;8 1966	HL-93 (US)	2	0.688	0.892	HS 20-44	0.701	1.17	1.02	1.31
	CS10x8;8 1966	HL-93 (US)	4	0.925	1.199	HS 20-44	1.308	2.185	1.41	1.82
	CS10x8;8 1966	HL-93 (US)	6	0.921	1.194	HS 20-44	1.495	2.496	1.62	2.09
	CS10x8;8 1966	HL-93 (US)	7	0.837	1.085	HS 20-44	1.455	2.43	1.74	2.24

Appendix L – Caltrans Models-LRFR-LFR comparisons

ID	Culvert Name	LRFD Vehicle	Fill Height (ft)	LRFR Inv	LRFR Oper	LFR Vehicle HS20-44 with a 1.25 factor	LFR Inve	LFR Opera	Ratio Inventory LFR/LRFR	Ratio Operating LFR/LRFR
	CS10x8;8 1966	HL-93 (US)	8	0.654	0.848	HS 20-44	1.214	2.028	1.86	2.39
45	CS10x8;10 2010	HL-93 (US)	0	0.737	0.955	HS 20-44	0.708	1.182	0.96	1.24
	CS10x8;10 2010	HL-93 (US)	0.5	0.741	0.96	HS 20-44	0.677	1.131	0.91	1.18
	CS10x8;10 2010	HL-93 (US)	1	0.744	0.965	HS 20-44	0.646	1.079	0.87	1.12
	CS10x8;10 2010	HL-93 (US)	1.5	0.746	0.968	HS 20-44	0.666	1.112	0.89	1.15
	CS10x8;10 2010	HL-93 (US)	1.9	0.747	0.969	HS 20-44	0.638	1.065	0.85	1.10
	CS10x8;10 2010	HL-93 (US)	2	1.306	1.693	HS 20-44	1.331	2.222	1.02	1.31
	CS10x8;10 2010	HL-93 (US)	4	2.023	2.623	HS 20-44	2.845	4.751	1.41	1.81
	CS10x8;10 2010	HL-93 (US)	7	2.862	3.709	HS 20-44	4.754	7.94	1.66	2.14
	CS10x8;10 2010	HL-93 (US)	9	3.151	4.085	HS 20-44	5.816	9.713	1.85	2.38
	CS10x8;10 2010	HL-93 (US)	10	3.162	4.099	HS 20-44	6.174	10.31	1.95	2.52
46	CS10x8;10 1933	HL-93 (US)	0	1.358	1.76	HS 20-44	1.108	1.851	0.82	1.05
	CS10x8;10 1933	HL-93 (US)	0.5	1.346	1.745	HS 20-44	1.073	1.791	0.80	1.03
	CS10x8;10 1933	HL-93 (US)	1	1.346	1.745	HS 20-44	1.036	1.731	0.77	0.99
	CS10x8;10 1933	HL-93 (US)	1.9	1.297	1.681	HS 20-44	1.05	1.754	0.81	1.04
	CS10x8;10 1933	HL-93 (US)	2	1.029	1.334	HS 20-44	1.113	1.858	1.08	1.39
	CS10x8;10 1933	HL-93 (US)	3	1.247	1.616	HS 20-44	1.702	2.842	1.36	1.76
	CS10x8;10 1933	HL-93 (US)	5	1.522	1.973	HS 20-44	2.474	4.131	1.63	2.09
	CS10x8;10 1933	HL-93 (US)	7	1.452	1.882	HS 20-44	3.142	5.247	2.16	2.79
	CS10x8;10 1933	HL-93 (US)	9	1.14	1.478	HS 20-44	3.255	5.436	2.86	3.68
	CS10x8;10 1933	HL-93 (US)	10	0.848	1.1	HS 20-44	3.059	5.108	3.61	4.64
47	CS10x8;5 1952	HL-93 (US)	0	0.593	0.768	HS 20-44	0.547	0.914	0.92	1.19
	CS10x8;5 1952	HL-93 (US)	0.5	0.575	0.746	HS 20-44	0.517	0.864	0.90	1.16
	CS10x8;5 1952	HL-93 (US)	1	0.556	0.72	HS 20-44	0.487	0.813	0.88	1.13
	CS10x8;5 1952	HL-93 (US)	1.5	0.533	0.691	HS 20-44	0.494	0.825	0.93	1.19
	CS10x8;5 1952	HL-93 (US)	1.9	0.513	0.665	HS 20-44	0.466	0.779	0.91	1.17
	CS10x8;5 1952	HL-93 (US)	2	0.511	0.662	HS 20-44	0.52	0.868	1.02	1.31
	CS10x8;5 1952	HL-93 (US)	3	0.564	0.732	HS 20-44	0.758	1.266	1.34	1.73

Appendix L – Caltrans Models-LRFR-LFR comparisons

ID	Culvert Name	LRFD Vehicle	Fill Height (ft)	LRFR Inv	LRFR Oper	LFR Vehicle HS20-44 with a 1.25 factor	LFR Inve	LFR Opera	Ratio Inventory LFR/LRFR	Ratio Operating LFR/LRFR
	CS10x8;5 1952	HL-93 (US)	4	0.612	0.793	HS 20-44	0.869	1.451	1.42	1.83
	CS10x8;5 1952	HL-93 (US)	5	0.581	0.753	HS 20-44	0.861	1.437	1.48	1.91
48	CS10x8;12 1952	HL-93 (US)	0	0.794	1.03	HS 20-44	0.772	1.289	0.97	1.25
	CS10x8;12 1952	HL-93 (US)	0.5	0.806	1.044	HS 20-44	0.744	1.242	0.92	1.19
	CS10x8;12 1952	HL-93 (US)	1	0.817	1.059	HS 20-44	0.715	1.194	0.88	1.13
	CS10x8;12 1952	HL-93 (US)	1.9	0.836	1.084	HS 20-44	0.717	1.198	0.86	1.11
	CS10x8;12 1952	HL-93 (US)	2	0.86	1.115	HS 20-44	0.859	1.434	1.00	1.29
	CS10x8;12 1952	HL-93 (US)	4	1.225	1.588	HS 20-44	1.717	2.867	1.40	1.81
	CS10x8;12 1952	HL-93 (US)	7	1.428	1.851	HS 20-44	2.344	3.914	1.64	2.11
	CS10x8;12 1952	HL-93 (US)	9	1.143	1.482	HS 20-44	2.11	3.523	1.85	2.38
	CS10x8;12 1952	HL-93 (US)	11	12.88	16.696	HS 20-44	13.613	22.734	1.06	1.36
	CS10x8;12 1952	HL-93 (US)	12	13.546	17.56	HS 20-44	0	0	0.00	0.00
49	CS10x8;6 1948	HL-93 (US)	0	0.696	0.902	HS 20-44	0.706	1.178	1.01	1.31
	CS10x8;6 1948	HL-93 (US)	0.5	0.681	0.883	HS 20-44	0.675	1.128	0.99	1.28
	CS10x8;6 1948	HL-93 (US)	1	0.664	0.861	HS 20-44	0.644	1.076	0.97	1.25
	CS10x8;6 1948	HL-93 (US)	1.5	0.645	0.836	HS 20-44	0.664	1.108	1.03	1.33
	CS10x8;6 1948	HL-93 (US)	1.9	0.627	0.813	HS 20-44	0.636	1.062	1.01	1.31
	CS10x8;6 1948	HL-93 (US)	2	0.688	0.892	HS 20-44	0.707	1.181	1.03	1.32
	CS10x8;6 1948	HL-93 (US)	3	0.8	1.037	HS 20-44	1.077	1.798	1.35	1.73
	CS10x8;6 1948	HL-93 (US)	4	0.903	1.17	HS 20-44	1.313	2.192	1.45	1.87
	CS10x8;6 1948	HL-93 (US)	5	0.861	1.115	HS 20-44	1.431	2.39	1.66	2.14
	CS10x8;6 1948	HL-93 (US)	6	0.751	0.973	HS 20-44	1.482	2.474	1.97	2.54
50	CS10x8;5 1922	HL-93 (US)	0	1.018	1.32	HS 20-44	0.765	1.278	0.75	0.97
	CS10x8;5 1922	HL-93 (US)	0.5	1.026	1.33	HS 20-44	0.735	1.228	0.72	0.92
	CS10x8;5 1922	HL-93 (US)	1	1.001	1.298	HS 20-44	0.705	1.177	0.70	0.91
	CS10x8;5 1922	HL-93 (US)	1.5	0.963	1.248	HS 20-44	0.73	1.219	0.76	0.98
	CS10x8;5 1922	HL-93 (US)	1.9	0.931	1.207	HS 20-44	0.702	1.173	0.75	0.97
	CS10x8;5 1922	HL-93 (US)	2	0.735	0.953	HS 20-44	0.791	1.321	1.08	1.39

Appendix L – Caltrans Models-LRFR-LFR comparisons

ID	Culvert Name	LRFD Vehicle	Fill Height (ft)	LRFR Inv	LRFR Oper	LFR Vehicle HS20-44 with a 1.25 factor	LFR Inve	LFR Opera	Ratio Inventory LFR/LRFR	Ratio Operating LFR/LRFR
	CS10x8;5 1922	HL-93 (US)	3	0.848	1.099	HS 20-44	1.225	2.046	1.44	1.86
	CS10x8;5 1922	HL-93 (US)	4	0.912	1.182	HS 20-44	1.529	2.553	1.68	2.16
	CS10x8;5 1922	HL-93 (US)	5	0.871	1.129	HS 20-44	1.717	2.867	1.97	2.54
51	CS10x8;10 1981	HL-93 (US)	0	0.574	0.744	HS 20-44	0.514	0.858	0.90	1.15
	CS10x8;10 1981	HL-93 (US)	0.5	0.556	0.721	HS 20-44	0.483	0.807	0.87	1.12
	CS10x8;10 1981	HL-93 (US)	1	0.537	0.696	HS 20-44	0.452	0.754	0.84	1.08
	CS10x8;10 1981	HL-93 (US)	1.5	0.514	0.666	HS 20-44	0.455	0.76	0.89	1.14
	CS10x8;10 1981	HL-93 (US)	1.9	0.494	0.64	HS 20-44	0.427	0.713	0.86	1.11
	CS10x8;10 1981	HL-93 (US)	2	0.955	1.239	HS 20-44	0.988	1.651	1.03	1.33
	CS10x8;10 1981	HL-93 (US)	4	1.391	1.803	HS 20-44	2.026	3.383	1.46	1.88
	CS10x8;10 1981	HL-93 (US)	7	1.6	2.074	HS 20-44	3.006	5.02	1.88	2.42
	CS10x8;10 1981	HL-93 (US)	9	1.405	1.821	HS 20-44	3.143	5.249	2.24	2.88
	CS10x8;10 1981	HL-93 (US)	10	1.174	1.522	HS 20-44	2.963	4.948	2.52	3.25
52	CS8x8;10 2010	HL-93 (US)	0	0.733	0.95	HS 20-44	0.619	1.034	0.84	1.09
	CS8x8;10 2010	HL-93 (US)	0.5	0.751	0.973	HS 20-44	0.594	0.993	0.79	1.02
	CS8x8;10 2010	HL-93 (US)	1	0.763	0.989	HS 20-44	0.569	0.951	0.75	0.96
	CS8x8;10 2010	HL-93 (US)	1.5	0.756	0.98	HS 20-44	0.589	0.984	0.78	1.00
	CS8x8;10 2010	HL-93 (US)	1.9	0.749	0.97	HS 20-44	0.567	0.946	0.76	0.98
	CS8x8;10 2010	HL-93 (US)	2	0.988	1.28	HS 20-44	1.056	1.761	1.07	1.38
	CS8x8;10 2010	HL-93 (US)	4	1.559	2.021	HS 20-44	2.406	4.004	1.54	1.98
	CS8x8;10 2010	HL-93 (US)	7	2.109	2.733	HS 20-44	4.329	7.23	2.05	2.65
	CS8x8;10 2010	HL-93 (US)	9	12.57	16.294	HS 20-44	10.559	17.634	0.84	1.08
	CS8x8;10 2010	HL-93 (US)	10	12.184	15.794	HS 20-44	10.264	17.141	0.84	1.09
53	CS7x7;10 2010	HL-93 (US)	0	0.793	1.028	HS 20-44	0.625	1.044	0.79	1.02
	CS7x7;10 2010	HL-93 (US)	0.5	0.827	1.072	HS 20-44	0.604	1.009	0.73	0.94
	CS7x7;10 2010	HL-93 (US)	1	0.864	1.12	HS 20-44	0.583	0.973	0.67	0.87
	CS7x7;10 2010	HL-93 (US)	1.5	0.871	1.129	HS 20-44	0.608	1.015	0.70	0.90
	CS7x7;10 2010	HL-93 (US)	1.9	0.872	1.131	HS 20-44	0.588	0.982	0.67	0.87

Appendix L – Caltrans Models-LRFR-LFR comparisons

ID	Culvert Name	LRFD Vehicle	Fill Height (ft)	LRFR Inv	LRFR Oper	LFR Vehicle HS20-44 with a 1.25 factor	LFR Inve	LFR Opera	Ratio Inventory LFR/LRFR	Ratio Operating LFR/LRFR
	CS7x7;10 2010	HL-93 (US)	2	1.11	1.439	HS 20-44	1.145	1.909	1.03	1.33
	CS7x7;10 2010	HL-93 (US)	4	1.953	2.531	HS 20-44	2.845	4.734	1.46	1.87
	CS7x7;10 2010	HL-93 (US)	7	2.879	3.731	HS 20-44	5.489	9.101	1.91	2.44
	CS7x7;10 2010	HL-93 (US)	9	14.511	18.81	HS 20-44	11.776	19.666	0.81	1.05
	CS7x7;10 2010	HL-93 (US)	10	14.125	18.31	HS 20-44	11.481	19.173	0.81	1.05
54	CS6x6;10 2010	HL-93 (US)	0	0.815	1.057	HS 20-44	0.577	0.963	0.71	0.91
	CS6x6;10 2010	HL-93 (US)	0.5	0.844	1.094	HS 20-44	0.559	0.934	0.66	0.85
	CS6x6;10 2010	HL-93 (US)	1	0.874	1.133	HS 20-44	0.541	0.903	0.62	0.80
	CS6x6;10 2010	HL-93 (US)	1.5	0.906	1.174	HS 20-44	0.566	0.945	0.62	0.80
	CS6x6;10 2010	HL-93 (US)	1.9	0.933	1.209	HS 20-44	0.549	0.917	0.59	0.76
	CS6x6;10 2010	HL-93 (US)	2	1.099	1.425	HS 20-44	1.128	1.882	1.03	1.32
	CS6x6;10 2010	HL-93 (US)	4	2.084	2.701	HS 20-44	3.029	5.042	1.45	1.87
	CS6x6;10 2010	HL-93 (US)	7	3.202	4.151	HS 20-44	5.973	9.91	1.87	2.39
	CS6x6;10 2010	HL-93 (US)	9	17.095	22.161	HS 20-44	13.385	22.354	0.78	1.01
	CS6x6;10 2010	HL-93 (US)	10	16.71	21.661	HS 20-44	13.09	21.86	0.78	1.01
	CS5x5;10 2010	HL-93 (US)	0	0.783	1.014	HS 20-44	0.526	0.879	0.67	0.87
Single	CS5x5;10 2010	HL-93 (US)	0.5	0.823	1.066	HS 20-44	0.512	0.855	0.62	0.80
	CS5x5;10 2010	HL-93 (US)	1	0.867	1.124	HS 20-44	0.497	0.83	0.57	0.74
	CS5x5;10 2010	HL-93 (US)	1.5	0.916	1.188	HS 20-44	0.522	0.872	0.57	0.73
	CS5x5;10 2010	HL-93 (US)	1.9	0.96	1.244	HS 20-44	0.508	0.849	0.53	0.68
	CS5x5;10 2010	HL-93 (US)	2	1.065	1.381	HS 20-44	1.13	1.885	1.06	1.36
	CS5x5;10 2010	HL-93 (US)	4	2.189	2.838	HS 20-44	3.299	5.494	1.51	1.94
	CS5x5;10 2010	HL-93 (US)	7	3.724	4.827	HS 20-44	6.679	11.094	1.79	2.30
	CS5x5;10 2010	HL-93 (US)	9	16.684	21.628	HS 20-44	11.593	19.361	0.69	0.90
	CS5x5;10 2010	HL-93 (US)	10	16.299	21.128	HS 20-44	11.298	18.867	0.69	0.89
56	CS4x4;10 2010	HL-93 (US)	0	0.769	0.997	HS 20-44	0.492	0.822	0.64	0.82
	CS4x4;10 2010	HL-93 (US)	0.5	0.826	1.071	HS 20-44	0.481	0.803	0.58	0.75
	CS4x4;10 2010	HL-93 (US)	1	0.893	1.157	HS 20-44	0.469	0.783	0.53	0.68

Appendix L – Caltrans Models-LRFR-LFR comparisons

ID	Culvert Name	LRFD Vehicle	Fill Height (ft)	LRFR Inv	LRFR Oper	LFR Vehicle HS20-44 with a 1.25 factor	LFR Inve	LFR Opera	Ratio Inventory LFR/LRFR	Ratio Operating LFR/LRFR
	CS4x4;10 2010	HL-93 (US)	1.5	0.97	1.258	HS 20-44	0.495	0.827	0.51	0.66
	CS4x4;10 2010	HL-93 (US)	1.9	1.044	1.353	HS 20-44	0.484	0.809	0.46	0.60
	CS4x4;10 2010	HL-93 (US)	2	1.144	1.483	HS 20-44	1.311	2.187	1.15	1.47
	CS4x4;10 2010	HL-93 (US)	4	2.5	3.24	HS 20-44	3.995	6.652	1.60	2.05
	CS4x4;10 2010	HL-93 (US)	7	4.816	6.244	HS 20-44	8.418	13.976	1.75	2.24
	CS4x4;10 2010	HL-93 (US)	9	26.405	34.229	HS 20-44	19.738	32.963	0.75	0.96
	CS4x4;10 2010	HL-93 (US)	10	26.019	33.729	HS 20-44	19.443	32.47	0.75	0.96
57	CD10x8;10 2002	HL-93 (US)	0	0.634	0.822	HS 20-44	0.438	0.731	0.69	0.89
	CD10x8;10 2002	HL-93 (US)	0.5	0.639	0.828	HS 20-44	0.479	0.8	0.75	0.97
	CD10x8;10 2002	HL-93 (US)	1	0.631	0.818	HS 20-44	0.521	0.87	0.83	1.06
	CD10x8;10 2002	HL-93 (US)	1.5	0.621	0.805	HS 20-44	0.567	0.947	0.91	1.18
	CD10x8;10 2002	HL-93 (US)	1.9	0.612	0.793	HS 20-44	0.536	0.895	0.88	1.13
	CD10x8;10 2002	HL-93 (US)	2	0.892	1.156	HS 20-44	1.071	1.733	1.20	1.50
	CD10x8;10 2002	HL-93 (US)	4	1.267	1.643	HS 20-44	1.618	2.664	1.28	1.62
	CD10x8;10 2002	HL-93 (US)	7	1.183	1.534	HS 20-44	1.787	2.979	1.51	1.94
	CD10x8;10 2002	HL-93 (US)	9	0.547	0.709	HS 20-44	1.436	2.369	2.63	3.34
	CD10x8;10 2002	HL-93 (US)	10	0.077	0.1	HS 20-44	0	0	0.00	0.00
58	CD10x8;10 2010	HL-93 (US)	0	0.763	0.99	HS 20-44	0.8	1.336	1.05	1.35
	CD10x8;10 2010	HL-93 (US)	0.5	0.762	0.988	HS 20-44	0.766	1.279	1.01	1.29
	CD10x8;10 2010	HL-93 (US)	1	0.76	0.986	HS 20-44	0.731	1.22	0.96	1.24
	CD10x8;10 2010	HL-93 (US)	1.5	0.757	0.982	HS 20-44	0.753	1.258	0.99	1.28
	CD10x8;10 2010	HL-93 (US)	1.9	0.754	0.978	HS 20-44	0.701	1.171	0.93	1.20
	CD10x8;10 2010	HL-93 (US)	2	1.217	1.577	HS 20-44	1.335	2.229	1.10	1.41
	CD10x8;10 2010	HL-93 (US)	4	1.902	2.465	HS 20-44	2.378	3.898	1.25	1.58
	CD10x8;10 2010	HL-93 (US)	7	2.279	2.954	HS 20-44	3.16	5.27	1.39	1.78
	CD10x8;10 2010	HL-93 (US)	9	1.893	2.454	HS 20-44	3.611	5.987	1.91	2.44
	CD10x8;10 2010	HL-93 (US)	10	1.537	1.993	HS 20-44	3.417	5.669	2.22	2.84
59	CD10x8;2 1966	HL-93 (US)	0	0.257	0.333	HS 20-44	0.532	0.888	2.07	2.67

Appendix L – Caltrans Models-LRFR-LFR comparisons

ID	Culvert Name	LRFD Vehicle	Fill Height (ft)	LRFR Inv	LRFR Oper	LFR Vehicle HS20-44 with a 1.25 factor	LFR Inve	LFR Opera	Ratio Inventory LFR/LRFR	Ratio Operating LFR/LRFR
	CD10x8;2 1966	HL-93 (US)	0.5	0.323	0.418	HS 20-44	0.592	0.988	1.83	2.36
	CD10x8;2 1966	HL-93 (US)	1	0.395	0.512	HS 20-44	0.553	0.923	1.40	1.80
	CD10x8;2 1966	HL-93 (US)	1.5	0.473	0.613	HS 20-44	0.556	0.929	1.18	1.52
	CD10x8;2 1966	HL-93 (US)	1.9	0.509	0.66	HS 20-44	0.522	0.871	1.03	1.32
	CD10x8;2 1966	HL-93 (US)	2	0.436	0.566	HS 20-44	0.689	1.15	1.58	2.03
60	CD10x8;16 1966	HL-93 (US)	0	0.365	0.473	HS 20-44	0.697	1.164	1.91	2.46
	CD10x8;16 1966	HL-93 (US)	1.9	0.751	0.974	HS 20-44	0.79	1.319	1.05	1.35
	CD10x8;16 1966	HL-93 (US)	2	0.556	0.721	HS 20-44	1.039	1.735	1.87	2.41
	CD10x8;16 1966	HL-93 (US)	4	1.83	2.372	HS 20-44	2	3.34	1.09	1.41
	CD10x8;16 1966	HL-93 (US)	7	1.491	1.932	HS 20-44	1.413	2.36	0.95	1.22
	CD10x8;16 1966	HL-93 (US)	9	0.955	1.238	HS 20-44	0.984	1.643	1.03	1.33
	CD10x8;16 1966	HL-93 (US)	11	0.4	0.519	HS 20-44	0.535	0.894	1.34	1.72
	CD10x8;16 1966	HL-93 (US)	13	0	0	HS 20-44	0.087	0.145	#DIV/0!	#DIV/0!
	CD10x8;16 1966	HL-93 (US)	15	0	0	HS 20-44	0	0	#DIV/0!	#DIV/0!
	CD10x8;16 1966	HL-93 (US)	16	0	0	HS 20-44	0	0	#DIV/0!	#DIV/0!
61	CD10x8;3 1952	HL-93 (US)	0	0.259	0.336	HS 20-44	0.504	0.842	1.95	2.51
	CD10x8;3 1952	HL-93 (US)	0.5	0.325	0.422	HS 20-44	0.566	0.945	1.74	2.24
	CD10x8;3 1952	HL-93 (US)	1	0.407	0.528	HS 20-44	0.542	0.905	1.33	1.71
	CD10x8;3 1952	HL-93 (US)	1.5	0.495	0.642	HS 20-44	0.561	0.938	1.13	1.46
	CD10x8;3 1952	HL-93 (US)	1.9	0.573	0.743	HS 20-44	0.541	0.903	0.94	1.22
	CD10x8;3 1952	HL-93 (US)	2	0.439	0.57	HS 20-44	0.596	0.996	1.36	1.75
	CD10x8;3 1952	HL-93 (US)	3	0.678	0.878	HS 20-44	0.752	1.255	1.11	1.43
62	CD10x8;9 1952	HL-93 (US)	0	0.295	0.383	HS 20-44	0.555	0.926	1.88	2.42
	CD10x8;9 1952	HL-93 (US)	0.5	0.373	0.483	HS 20-44	0.646	1.079	1.73	2.23
	CD10x8;9 1952	HL-93 (US)	1	0.461	0.598	HS 20-44	0.739	1.234	1.60	2.06
	CD10x8;9 1952	HL-93 (US)	1.5	0.554	0.719	HS 20-44	0.894	1.494	1.61	2.08
	CD10x8;9 1952	HL-93 (US)	1.9	0.638	0.827	HS 20-44	0.874	1.459	1.37	1.76
	CD10x8;9 1952	HL-93 (US)	2	0.485	0.629	HS 20-44	0.936	1.563	1.93	2.48

Appendix L – Caltrans Models-LRFR-LFR comparisons

ID	Culvert Name	LRFD Vehicle	Fill Height (ft)	LRFR Inv	LRFR Oper	LFR Vehicle HS20-44 with a 1.25 factor	LFR Inve	LFR Opera	Ratio Inventory LFR/LRFR	Ratio Operating LFR/LRFR
	CD10x8;9 1952	HL-93 (US)	4	1.459	1.891	HS 20-44	1.878	3.136	1.29	1.66
	CD10x8;9 1952	HL-93 (US)	6	1.59	2.06	HS 20-44	1.563	2.61	0.98	1.27
	CD10x8;9 1952	HL-93 (US)	8	1.126	1.46	HS 20-44	1.22	2.038	1.08	1.40
	CD10x8;9 1952	HL-93 (US)	9	0.879	1.139	HS 20-44	1.042	1.74	1.19	1.53
63	CD10x8;5 1948	HL-93 (US)	0	0.21	0.272	HS 20-44	0.44	0.734	2.10	2.70
	CD10x8;5 1948	HL-93 (US)	0.5	0.275	0.357	HS 20-44	0.521	0.87	1.89	2.44
	CD10x8;5 1948	HL-93 (US)	1	0.346	0.449	HS 20-44	0.498	0.831	1.44	1.85
	CD10x8;5 1948	HL-93 (US)	1.5	0.425	0.551	HS 20-44	0.514	0.858	1.21	1.56
	CD10x8;5 1948	HL-93 (US)	1.9	0.494	0.641	HS 20-44	0.493	0.823	1.00	1.28
	CD10x8;5 1948	HL-93 (US)	2	0.396	0.513	HS 20-44	0.544	0.908	1.37	1.77
	CD10x8;5 1948	HL-93 (US)	3	0.398	0.516	HS 20-44	0.485	0.811	1.22	1.57
	CD10x8;5 1948	HL-93 (US)	4	0.171	0.221	HS 20-44	0.317	0.53	1.85	2.40
	CD10x8;5 1948	HL-93 (US)	5	0	0	HS 20-44	0.141	0.235	#DIV/0!	#DIV/0!
64	CD10x8;9 1948	HL-93 (US)	0	0.216	0.28	HS 20-44	0.456	0.762	2.11	2.72
	CD10x8;9 1948	HL-93 (US)	0.5	0.281	0.364	HS 20-44	0.547	0.913	1.95	2.51
	CD10x8;9 1948	HL-93 (US)	1	0.358	0.464	HS 20-44	0.633	1.058	1.77	2.28
	CD10x8;9 1948	HL-93 (US)	1.5	0.439	0.569	HS 20-44	0.661	1.103	1.51	1.94
	CD10x8;9 1948	HL-93 (US)	1.9	0.509	0.66	HS 20-44	0.64	1.069	1.26	1.62
	CD10x8;9 1948	HL-93 (US)	2	0.402	0.521	HS 20-44	0.708	1.182	1.76	2.27
	CD10x8;9 1948	HL-93 (US)	4	1.022	1.325	HS 20-44	1.269	2.118	1.24	1.60
	CD10x8;9 1948	HL-93 (US)	6	0.842	1.092	HS 20-44	0.91	1.519	1.08	1.39
	CD10x8;9 1948	HL-93 (US)	8	0.33	0.427	HS 20-44	0.531	0.887	1.61	2.08
	CD10x8;9 1948	HL-93 (US)	9	0.064	0.082	HS 20-44	0.325	0.542	5.08	6.61
65	CD8x8;5 1933	HL-93 (US)	0	0.227	0.294	HS 20-44	0.476	0.796	2.10	2.71
	CD8x8;5 1933	HL-93 (US)	0.5	0.293	0.379	HS 20-44	0.551	0.92	1.88	2.43
	CD8x8;5 1933	HL-93 (US)	1	0.365	0.473	HS 20-44	0.626	1.046	1.72	2.21
	CD8x8;5 1933	HL-93 (US)	1.5	0.447	0.579	HS 20-44	0.756	1.262	1.69	2.18
	CD8x8;5 1933	HL-93 (US)	1.9	0.518	0.672	HS 20-44	0.729	1.218	1.41	1.81

Appendix L – Caltrans Models-LRFR-LFR comparisons

ID	Culvert Name	LRFD Vehicle	Fill Height (ft)	LRFR Inv	LRFR Oper	LFR Vehicle HS20-44 with a 1.25 factor	LFR Inve	LFR Opera	Ratio Inventory LFR/LRFR	Ratio Operating LFR/LRFR
	CD8x8;5 1933	HL-93 (US)	2	0.414	0.537	HS 20-44	0.823	1.374	1.99	2.56
	CD8x8;5 1933	HL-93 (US)	3	0.824	1.068	HS 20-44	1.465	2.447	1.78	2.29
	CD8x8;5 1933	HL-93 (US)	4	1.315	1.705	HS 20-44	1.91	3.19	1.45	1.87
	CD8x8;5 1933	HL-93 (US)	5	1.485	1.925	HS 20-44	1.804	3.013	1.21	1.57
66	CD8x8;10 1933	HL-93 (US)	0	0.318	0.413	HS 20-44	0.615	1.027	1.93	2.49
	CD8x8;10 1933	HL-93 (US)	0.5	0.394	0.511	HS 20-44	0.691	1.154	1.75	2.26
	CD8x8;10 1933	HL-93 (US)	1	0.478	0.62	HS 20-44	0.768	1.283	1.61	2.07
	CD8x8;10 1933	HL-93 (US)	1.9	0.663	0.859	HS 20-44	0.928	1.55	1.40	1.80
	CD8x8;10 1933	HL-93 (US)	2	0.512	0.664	HS 20-44	0.976	1.63	1.91	2.45
	CD8x8;10 1933	HL-93 (US)	3	1.079	1.398	HS 20-44	2.225	3.715	2.06	2.66
	CD8x8;10 1933	HL-93 (US)	5	2.895	3.753	HS 20-44	3.762	6.283	1.30	1.67
	CD8x8;10 1933	HL-93 (US)	7	3.852	4.994	HS 20-44	3.51	5.862	0.91	1.17
	CD8x8;10 1933	HL-93 (US)	9	3.443	4.463	HS 20-44	3.203	5.35	0.93	1.20
	CD8x8;10 1933	HL-93 (US)	10	3.219	4.173	HS 20-44	3.043	5.081	0.95	1.22
67	CD8x8;5 1924	HL-93 (US)	0	0.226	0.293	HS 20-44	0.476	0.795	2.11	2.71
	CD8x8;5 1924	HL-93 (US)	0.5	0.292	0.379	HS 20-44	0.551	0.92	1.89	2.43
	CD8x8;5 1924	HL-93 (US)	1	0.365	0.473	HS 20-44	0.624	1.042	1.71	2.20
	CD8x8;5 1924	HL-93 (US)	1.5	0.447	0.579	HS 20-44	0.655	1.094	1.47	1.89
	CD8x8;5 1924	HL-93 (US)	1.9	0.518	0.671	HS 20-44	0.638	1.066	1.23	1.59
	CD8x8;5 1924	HL-93 (US)	2	0.414	0.536	HS 20-44	0.768	1.282	1.86	2.39
	CD8x8;5 1924	HL-93 (US)	3	0.823	1.067	HS 20-44	1.236	2.064	1.50	1.93
	CD8x8;5 1924	HL-93 (US)	4	1.063	1.378	HS 20-44	1.674	2.795	1.57	2.03
	CD8x8;5 1924	HL-93 (US)	5	1.152	1.494	HS 20-44	2.099	3.506	1.82	2.35
68	CD8x8;10 1924	HL-93 (US)	0	0.269	0.349	HS 20-44	0.526	0.879	1.96	2.52
	CD8x8;10 1924	HL-93 (US)	0.5	0.339	0.439	HS 20-44	0.603	1.006	1.78	2.29
	CD8x8;10 1924	HL-93 (US)	1	0.416	0.539	HS 20-44	0.68	1.135	1.63	2.11
	CD8x8;10 1924	HL-93 (US)	1.9	0.579	0.75	HS 20-44	0.889	1.485	1.54	1.98
	CD8x8;10 1924	HL-93 (US)	2	0.46	0.596	HS 20-44	0.883	1.474	1.92	2.47

Appendix L – Caltrans Models-LRFR-LFR comparisons

ID	Culvert Name	LRFD Vehicle	Fill Height (ft)	LRFR Inv	LRFR Oper	LFR Vehicle HS20-44 with a 1.25 factor	LFR Inve	LFR Opera	Ratio Inventory LFR/LRFR	Ratio Operating LFR/LRFR
	CD8x8;10 1924	HL-93 (US)	3	0.918	1.19	HS 20-44	1.97	3.29	2.15	2.76
	CD8x8;10 1924	HL-93 (US)	5	2.534	3.285	HS 20-44	3.358	5.607	1.33	1.71
	CD8x8;10 1924	HL-93 (US)	7	3.354	4.348	HS 20-44	3.104	5.184	0.93	1.19
	CD8x8;10 1924	HL-93 (US)	9	2.938	3.809	HS 20-44	2.801	4.678	0.95	1.23
	CD8x8;10 1924	HL-93 (US)	10	2.713	3.517	HS 20-44	2.642	4.413	0.97	1.25
69	CS12x8;10 2010	HL-93 (US)	0	0.767	0.995	HS 20-44	0.81	1.353	1.06	1.36
	CS12x8;10 2010	HL-93 (US)	0.5	0.761	0.987	HS 20-44	0.772	1.29	1.01	1.31
	CS12x8;10 2010	HL-93 (US)	1	0.754	0.977	HS 20-44	0.734	1.226	0.97	1.25
	CS12x8;10 2010	HL-93 (US)	1.5	0.744	0.965	HS 20-44	0.754	1.259	1.01	1.30
	CS12x8;10 2010	HL-93 (US)	1.9	0.735	0.953	HS 20-44	0.72	1.202	0.98	1.26
	CS12x8;10 2010	HL-93 (US)	2	1.233	1.598	HS 20-44	1.315	2.197	1.07	1.37
	CS12x8;10 2010	HL-93 (US)	4	1.841	2.386	HS 20-44	2.651	4.427	1.44	1.86
	CS12x8;10 2010	HL-93 (US)	7	2.403	3.115	HS 20-44	3.891	6.498	1.62	2.09
	CS12x8;10 2010	HL-93 (US)	9	2.356	3.054	HS 20-44	4.457	7.444	1.89	2.44
	CS12x8;10 2010	HL-93 (US)	10	2.199	2.85	HS 20-44	4.437	7.41	2.02	2.60
70	CS14x9;10 2010	HL-93 (US)	0	0.849	1.101	HS 20-44	0.958	1.599	1.13	1.45
	CS14x9;10 2010	HL-93 (US)	0.5	0.837	1.085	HS 20-44	0.913	1.525	1.09	1.41
	CS14x9;10 2010	HL-93 (US)	1	0.822	1.066	HS 20-44	0.868	1.45	1.06	1.36
	CS14x9;10 2010	HL-93 (US)	1.5	0.804	1.042	HS 20-44	0.891	1.488	1.11	1.43
	CS14x9;10 2010	HL-93 (US)	1.9	0.789	1.022	HS 20-44	0.851	1.421	1.08	1.39
	CS14x9;10 2010	HL-93 (US)	2	1.167	1.513	HS 20-44	1.489	2.487	1.28	1.64
	CS14x9;10 2010	HL-93 (US)	4	1.842	2.388	HS 20-44	2.684	4.482	1.46	1.88
	CS14x9;10 2010	HL-93 (US)	7	2.357	3.056	HS 20-44	3.772	6.3	1.60	2.06
	CS14x9;10 2010	HL-93 (US)	9	2.236	2.899	HS 20-44	4.25	7.098	1.90	2.45
	CS14x9;10 2010	HL-93 (US)	10	2.001	2.594	HS 20-44	4.192	7	2.09	2.70
71	CS4x3;10 2010	HL-93 (US)	0	0.767	0.994	HS 20-44	0.49	0.819	0.64	0.82
	CS4x3;10 2010	HL-93 (US)	0.5	0.824	1.068	HS 20-44	0.479	0.8	0.58	0.75
	CS4x3;10 2010	HL-93 (US)	1	0.891	1.155	HS 20-44	0.467	0.781	0.52	0.68

Appendix L – Caltrans Models-LRFR-LFR comparisons

ID	Culvert Name	LRFD Vehicle	Fill Height (ft)	LRFR Inv	LRFR Oper	LFR Vehicle HS20-44 with a 1.25 factor	LFR Inve	LFR Opera	Ratio Inventory LFR/LRFR	Ratio Operating LFR/LRFR
	CS4x3;10 2010	HL-93 (US)	1.5	0.969	1.256	HS 20-44	0.493	0.824	0.51	0.66
	CS4x3;10 2010	HL-93 (US)	1.9	1.043	1.352	HS 20-44	0.482	0.806	0.46	0.60
	CS4x3;10 2010	HL-93 (US)	2	1.145	1.484	HS 20-44	1.308	2.182	1.14	1.47
	CS4x3;10 2010	HL-93 (US)	4	2.533	3.283	HS 20-44	3.99	6.644	1.58	2.02
	CS4x3;10 2010	HL-93 (US)	7	4.892	6.342	HS 20-44	8.406	13.959	1.72	2.20
	CS4x3;10 2010	HL-93 (US)	9	36.622	47.472	HS 20-44	26.24	43.821	0.72	0.92
	CS4x3;10 2010	HL-93 (US)	10	36.236	46.972	HS 20-44	25.945	43.327	0.72	0.92
72	CS6x4;10 2010	HL-93 (US)	0	0.812	1.052	HS 20-44	0.574	0.958	0.71	0.91
	CS6x4;10 2010	HL-93 (US)	0.5	0.84	1.089	HS 20-44	0.556	0.929	0.66	0.85
	CS6x4;10 2010	HL-93 (US)	1	0.87	1.128	HS 20-44	0.538	0.899	0.62	0.80
	CS6x4;10 2010	HL-93 (US)	1.5	0.902	1.17	HS 20-44	0.563	0.94	0.62	0.80
	CS6x4;10 2010	HL-93 (US)	1.9	0.93	1.205	HS 20-44	0.547	0.913	0.59	0.76
	CS6x4;10 2010	HL-93 (US)	2	1.075	1.394	HS 20-44	1.096	1.829	1.02	1.31
	CS6x4;10 2010	HL-93 (US)	4	2.037	2.64	HS 20-44	2.952	4.915	1.45	1.86
	CS6x4;10 2010	HL-93 (US)	7	3.239	4.198	HS 20-44	5.791	9.615	1.79	2.29
	CS6x4;10 2010	HL-93 (US)	9	26.381	34.197	HS 20-44	19.409	32.414	0.74	0.95
	CS6x4;10 2010	HL-93 (US)	10	25.995	33.697	HS 20-44	19.114	31.92	0.74	0.95
73	CS8x6;10 2010	HL-93 (US)	0	0.731	0.947	HS 20-44	0.616	1.028	0.84	1.09
	CS8x6;10 2010	HL-93 (US)	0.5	0.749	0.971	HS 20-44	0.591	0.988	0.79	1.02
	CS8x6;10 2010	HL-93 (US)	1	0.768	0.995	HS 20-44	0.567	0.946	0.74	0.95
	CS8x6;10 2010	HL-93 (US)	1.5	0.787	1.02	HS 20-44	0.586	0.979	0.74	0.96
	CS8x6;10 2010	HL-93 (US)	1.9	0.789	1.023	HS 20-44	0.564	0.942	0.71	0.92
	CS8x6;10 2010	HL-93 (US)	2	1	1.296	HS 20-44	1.042	1.738	1.04	1.34
	CS8x6;10 2010	HL-93 (US)	4	1.593	2.066	HS 20-44	2.32	3.875	1.46	1.88
	CS8x6;10 2010	HL-93 (US)	7	2.173	2.817	HS 20-44	4.01	6.697	1.85	2.38
	CS8x6;10 2010	HL-93 (US)	9	15.442	20.017	HS 20-44	11.628	19.419	0.75	0.97
	CS8x6;10 2010	HL-93 (US)	10	15.056	19.517	HS 20-44	11.333	18.925	0.75	0.97
74	CD4x3;10 2010	HL-93 (US)	0	0.685	0.888	HS 20-44	0.45	0.752	0.66	0.85

Appendix L – Caltrans Models-LRFR-LFR comparisons

ID	Culvert Name	LRFD Vehicle	Fill Height (ft)	LRFR Inv	LRFR Oper	LFR Vehicle HS20-44 with a 1.25 factor	LFR Inve	LFR Opera	Ratio Inventory LFR/LRFR	Ratio Operating LFR/LRFR
	CD4x3;10 2010	HL-93 (US)	0.5	0.72	0.933	HS 20-44	0.436	0.728	0.61	0.78
	CD4x3;10 2010	HL-93 (US)	1	0.763	0.989	HS 20-44	0.422	0.704	0.55	0.71
	CD4x3;10 2010	HL-93 (US)	1.5	0.816	1.058	HS 20-44	0.441	0.736	0.54	0.70
	CD4x3;10 2010	HL-93 (US)	1.9	0.867	1.124	HS 20-44	0.428	0.714	0.49	0.64
	CD4x3;10 2010	HL-93 (US)	2	1.282	1.662	HS 20-44	1.457	2.433	1.14	1.46
	CD4x3;10 2010	HL-93 (US)	4	2.994	3.881	HS 20-44	4.089	6.829	1.37	1.76
	CD4x3;10 2010	HL-93 (US)	7	4.798	6.219	HS 20-44	7.743	12.993	1.61	2.09
	CD4x3;10 2010	HL-93 (US)	9	32.975	42.745	HS 20-44	26.682	44.558	0.81	1.04
	CD4x3;10 2010	HL-93 (US)	10	32.806	42.527	HS 20-44	26.386	44.065	0.80	1.04
75	CD6x4;10 2010	HL-93 (US)	0	0.63	0.817	HS 20-44	0.429	0.716	0.68	0.88
	CD6x4;10 2010	HL-93 (US)	0.5	0.641	0.831	HS 20-44	0.407	0.679	0.63	0.82
	CD6x4;10 2010	HL-93 (US)	1	0.644	0.835	HS 20-44	0.384	0.641	0.60	0.77
	CD6x4;10 2010	HL-93 (US)	1.5	0.648	0.84	HS 20-44	0.391	0.653	0.60	0.78
	CD6x4;10 2010	HL-93 (US)	1.9	0.652	0.845	HS 20-44	0.371	0.619	0.57	0.73
	CD6x4;10 2010	HL-93 (US)	2	1.046	1.356	HS 20-44	1.089	1.817	1.04	1.34
	CD6x4;10 2010	HL-93 (US)	4	2.141	2.775	HS 20-44	2.973	4.965	1.39	1.79
	CD6x4;10 2010	HL-93 (US)	7	2.118	2.745	HS 20-44	3	5.013	1.42	1.83
	CD6x4;10 2010	HL-93 (US)	9	2.044	2.649	HS 20-44	3.044	5.098	1.49	1.92
	CD6x4;10 2010	HL-93 (US)	10	1.831	2.374	HS 20-44	2.718	4.557	1.48	1.92
76	CD8x6;10 2010	HL-93 (US)	0	0.64	0.829	HS 20-44	0.58	0.968	0.91	1.17
	CD8x6;10 2010	HL-93 (US)	0.5	0.642	0.832	HS 20-44	0.548	0.915	0.85	1.10
	CD8x6;10 2010	HL-93 (US)	1	0.643	0.834	HS 20-44	0.517	0.864	0.80	1.04
	CD8x6;10 2010	HL-93 (US)	1.5	0.645	0.836	HS 20-44	0.526	0.879	0.82	1.05
	CD8x6;10 2010	HL-93 (US)	1.9	0.646	0.837	HS 20-44	0.499	0.833	0.77	1.00
	CD8x6;10 2010	HL-93 (US)	2	1.253	1.624	HS 20-44	1.29	2.15	1.03	1.32
	CD8x6;10 2010	HL-93 (US)	4	2.09	2.71	HS 20-44	2.655	4.223	1.27	1.56
	CD8x6;10 2010	HL-93 (US)	7	2.124	2.754	HS 20-44	2.765	4.613	1.30	1.68
	CD8x6;10 2010	HL-93 (US)	9	1.807	2.342	HS 20-44	2.749	4.59	1.52	1.96

Appendix L – Caltrans Models-LRFR-LFR comparisons

ID	Culvert Name	LRFD Vehicle	Fill Height (ft)	LRFR Inv	LRFR Oper	LFR Vehicle HS20-44 with a 1.25 factor	LFR Inve	LFR Opera	Ratio Inventory LFR/LRFR	Ratio Operating LFR/LRFR
	CD8x6;10 2010	HL-93 (US)	10	1.52	1.97	HS 20-44	2.361	3.954	1.55	2.01
77	CD12x8;10 2010	HL-93 (US)	0	0.784	1.016	HS 20-44	0.886	1.479	1.13	1.46
	CD12x8;10 2010	HL-93 (US)	0.5	0.771	0.999	HS 20-44	0.823	1.374	1.07	1.38
	CD12x8;10 2010	HL-93 (US)	1	0.756	0.98	HS 20-44	0.78	1.302	1.03	1.33
	CD12x8;10 2010	HL-93 (US)	1.5	0.74	0.959	HS 20-44	0.798	1.333	1.08	1.39
	CD12x8;10 2010	HL-93 (US)	1.9	0.725	0.94	HS 20-44	0.76	1.269	1.05	1.35
	CD12x8;10 2010	HL-93 (US)	2	1.263	1.637	HS 20-44	1.43	2.327	1.13	1.42
	CD12x8;10 2010	HL-93 (US)	4	1.732	2.245	HS 20-44	2.178	3.584	1.26	1.60
	CD12x8;10 2010	HL-93 (US)	7	2.022	2.621	HS 20-44	2.622	4.374	1.30	1.67
	CD12x8;10 2010	HL-93 (US)	9	1.82	2.359	HS 20-44	2.887	4.755	1.59	2.02
	CD12x8;10 2010	HL-93 (US)	10	1.521	1.971	HS 20-44	2.542	4.184	1.67	2.12
78	CD14x9;10 2010	HL-93 (US)	0	0.866	1.123	HS 20-44	0.991	1.655	1.14	1.47
	CD14x9;10 2010	HL-93 (US)	0.5	0.845	1.096	HS 20-44	0.941	1.571	1.11	1.43
	CD14x9;10 2010	HL-93 (US)	1	0.823	1.066	HS 20-44	0.891	1.487	1.08	1.39
	CD14x9;10 2010	HL-93 (US)	1.5	0.798	1.034	HS 20-44	0.91	1.519	1.14	1.47
	CD14x9;10 2010	HL-93 (US)	1.9	0.776	1.006	HS 20-44	0.865	1.445	1.11	1.44
	CD14x9;10 2010	HL-93 (US)	2	1.327	1.72	HS 20-44	1.393	2.322	1.05	1.35
	CD14x9;10 2010	HL-93 (US)	4	1.757	2.278	HS 20-44	2.204	3.631	1.25	1.59
	CD14x9;10 2010	HL-93 (US)	7	1.895	2.456	HS 20-44	2.486	4.144	1.31	1.69
	CD14x9;10 2010	HL-93 (US)	9	1.649	2.138	HS 20-44	2.666	4.37	1.62	2.04
	CD14x9;10 2010	HL-93 (US)	10	1.278	1.656	HS 20-44	2.293	3.751	1.79	2.27
79	CS4x3;10 2002	HL-93 (US)	0	0.764	0.991	HS 20-44	0.488	0.816	0.64	0.82
	CS4x3;10 2002	HL-93 (US)	0.5	0.822	1.066	HS 20-44	0.477	0.797	0.58	0.75
	CS4x3;10 2002	HL-93 (US)	1	0.889	1.153	HS 20-44	0.466	0.778	0.52	0.67
	CS4x3;10 2002	HL-93 (US)	1.5	0.968	1.255	HS 20-44	0.491	0.821	0.51	0.65
	CS4x3;10 2002	HL-93 (US)	1.9	1.033	1.339	HS 20-44	0.481	0.803	0.47	0.60
	CS4x3;10 2002	HL-93 (US)	2	0.974	1.262	HS 20-44	1.304	2.176	1.34	1.72
	CS4x3;10 2002	HL-93 (US)	4	1.761	2.282	HS 20-44	3.984	6.635	2.26	2.91

Appendix L – Caltrans Models-LRFR-LFR comparisons

ID	Culvert Name	LRFD Vehicle	Fill Height (ft)	LRFR Inv	LRFR Oper	LFR Vehicle HS20-44 with a 1.25 factor	LFR Inve	LFR Opera	Ratio Inventory LFR/LRFR	Ratio Operating LFR/LRFR
	CS4x3;10 2002	HL-93 (US)	7	3.14	4.071	HS 20-44	8.391	13.938	2.67	3.42
	CS4x3;10 2002	HL-93 (US)	9	25.714	33.334	HS 20-44	21.136	35.297	0.82	1.06
	CS4x3;10 2002	HL-93 (US)	10	25.603	33.19	HS 20-44	21.095	35.229	0.82	1.06
80	CS6x4;10 2002	HL-93 (US)	0	0.754	0.977	HS 20-44	0.571	0.953	0.76	0.98
	CS6x4;10 2002	HL-93 (US)	0.5	0.767	0.994	HS 20-44	0.553	0.924	0.72	0.93
	CS6x4;10 2002	HL-93 (US)	1	0.779	1.01	HS 20-44	0.535	0.894	0.69	0.89
	CS6x4;10 2002	HL-93 (US)	1.5	0.792	1.026	HS 20-44	0.56	0.935	0.71	0.91
	CS6x4;10 2002	HL-93 (US)	1.9	0.815	1.057	HS 20-44	0.544	0.908	0.67	0.86
	CS6x4;10 2002	HL-93 (US)	2	0.874	1.133	HS 20-44	1.084	1.809	1.24	1.60
	CS6x4;10 2002	HL-93 (US)	4	1.566	2.03	HS 20-44	2.932	4.884	1.87	2.41
	CS6x4;10 2002	HL-93 (US)	7	2.143	2.777	HS 20-44	5.749	9.548	2.68	3.44
	CS6x4;10 2002	HL-93 (US)	9	19.44	25.2	HS 20-44	13.853	23.134	0.71	0.92
	CS6x4;10 2002	HL-93 (US)	10	19.262	24.969	HS 20-44	13.557	22.64	0.70	0.91
81	CS8x6;10 2002	HL-93 (US)	0	0.73	0.946	HS 20-44	0.614	1.026	0.84	1.08
	CS8x6;10 2002	HL-93 (US)	0.5	0.73	0.946	HS 20-44	0.59	0.985	0.81	1.04
	CS8x6;10 2002	HL-93 (US)	1	0.727	0.942	HS 20-44	0.565	0.944	0.78	1.00
	CS8x6;10 2002	HL-93 (US)	1.5	0.721	0.935	HS 20-44	0.585	0.977	0.81	1.04
	CS8x6;10 2002	HL-93 (US)	1.9	0.715	0.927	HS 20-44	0.563	0.94	0.79	1.01
	CS8x6;10 2002	HL-93 (US)	2	0.882	1.144	HS 20-44	1.045	1.743	1.18	1.52
	CS8x6;10 2002	HL-93 (US)	4	1.339	1.736	HS 20-44	2.347	3.92	1.75	2.26
	CS8x6;10 2002	HL-93 (US)	7	1.681	2.179	HS 20-44	4.084	6.821	2.43	3.13
	CS8x6;10 2002	HL-93 (US)	9	13.761	17.839	HS 20-44	10.054	16.79	0.73	0.94
	CS8x6;10 2002	HL-93 (US)	10	13.376	17.339	HS 20-44	9.758	16.296	0.73	0.94
82	CS12x8;10 2002	HL-93 (US)	0	0.608	0.788	HS 20-44	0.592	0.989	0.97	1.26
	CS12x8;10 2002	HL-93 (US)	0.5	0.595	0.771	HS 20-44	0.554	0.925	0.93	1.20
	CS12x8;10 2002	HL-93 (US)	1	0.579	0.751	HS 20-44	0.516	0.861	0.89	1.15
	CS12x8;10 2002	HL-93 (US)	1.5	0.561	0.728	HS 20-44	0.515	0.86	0.92	1.18
	CS12x8;10 2002	HL-93 (US)	1.9	0.545	0.707	HS 20-44	0.481	0.803	0.88	1.14

Appendix L – Caltrans Models-LRFR-LFR comparisons

ID	Culvert Name	LRFD Vehicle	Fill Height (ft)	LRFR Inv	LRFR Oper	LFR Vehicle HS20-44 with a 1.25 factor	LFR Inve	LFR Opera	Ratio Inventory LFR/LRFR	Ratio Operating LFR/LRFR
	CS12x8;10 2002	HL-93 (US)	2	0.93	1.206	HS 20-44	0.982	1.64	1.06	1.36
	CS12x8;10 2002	HL-93 (US)	4	1.318	1.709	HS 20-44	1.897	3.168	1.44	1.85
	CS12x8;10 2002	HL-93 (US)	7	1.493	1.935	HS 20-44	2.44	4.074	1.63	2.11
	CS12x8;10 2002	HL-93 (US)	9	1.191	1.544	HS 20-44	2.245	3.748	1.88	2.43
	CS12x8;10 2002	HL-93 (US)	10	0.872	1.13	HS 20-44	1.776	2.966	2.04	2.62
83	CS14x9;10 2002	HL-93 (US)	0	0.655	0.849	HS 20-44	0.684	1.143	1.04	1.35
	CS14x9;10 2002	HL-93 (US)	0.5	0.635	0.823	HS 20-44	0.639	1.067	1.01	1.30
	CS14x9;10 2002	HL-93 (US)	1	0.612	0.793	HS 20-44	0.594	0.991	0.97	1.25
	CS14x9;10 2002	HL-93 (US)	1.5	0.582	0.755	HS 20-44	0.591	0.986	1.02	1.31
	CS14x9;10 2002	HL-93 (US)	1.9	0.549	0.712	HS 20-44	0.55	0.918	1.00	1.29
	CS14x9;10 2002	HL-93 (US)	2	0.917	1.189	HS 20-44	1.096	1.83	1.20	1.54
	CS14x9;10 2002	HL-93 (US)	4	1.231	1.595	HS 20-44	2.006	3.349	1.63	2.10
	CS14x9;10 2002	HL-93 (US)	7	1.153	1.495	HS 20-44	2.222	3.982	1.93	2.66
	CS14x9;10 2002	HL-93 (US)	9	0.742	0.961	HS 20-44	2.091	3.771	2.82	3.92
	CS14x9;10 2002	HL-93 (US)	10	0.339	0.44	HS 20-44	1.531	2.321	4.52	5.28
84	CD4x3;10 2002	HL-93 (US)	0	0.686	0.889	HS 20-44	0.451	0.753	0.66	0.85
	CD4x3;10 2002	HL-93 (US)	0.5	0.722	0.935	HS 20-44	0.437	0.73	0.61	0.78
	CD4x3;10 2002	HL-93 (US)	1	0.765	0.992	HS 20-44	0.423	0.706	0.55	0.71
	CD4x3;10 2002	HL-93 (US)	1.5	0.819	1.062	HS 20-44	0.442	0.738	0.54	0.69
	CD4x3;10 2002	HL-93 (US)	1.9	0.871	1.13	HS 20-44	0.429	0.716	0.49	0.63
	CD4x3;10 2002	HL-93 (US)	2	1.155	1.497	HS 20-44	1.319	2.202	1.14	1.47
	CD4x3;10 2002	HL-93 (US)	4	2.675	3.468	HS 20-44	3.662	6.115	1.37	1.76
	CD4x3;10 2002	HL-93 (US)	7	4.214	5.462	HS 20-44	6.905	11.582	1.64	2.12
	CD4x3;10 2002	HL-93 (US)	9	21.358	27.686	HS 20-44	17.621	29.427	0.83	1.06
	CD4x3;10 2002	HL-93 (US)	10	21.181	27.457	HS 20-44	17.525	29.267	0.83	1.07
85	CD6x4;10 2002	HL-93 (US)	0	0.634	0.822	HS 20-44	0.429	0.717	0.68	0.87
	CD6x4;10 2002	HL-93 (US)	0.5	0.642	0.832	HS 20-44	0.407	0.68	0.63	0.82
	CD6x4;10 2002	HL-93 (US)	1	0.646	0.837	HS 20-44	0.384	0.642	0.59	0.77

Appendix L – Caltrans Models-LRFR-LFR comparisons

ID	Culvert Name	LRFD Vehicle	Fill Height (ft)	LRFR Inv	LRFR Oper	LFR Vehicle HS20-44 with a 1.25 factor	LFR Inve	LFR Opera	Ratio Inventory LFR/LRFR	Ratio Operating LFR/LRFR
	CD6x4;10 2002	HL-93 (US)	1.5	0.651	0.843	HS 20-44	0.392	0.654	0.60	0.78
	CD6x4;10 2002	HL-93 (US)	1.9	0.655	0.849	HS 20-44	0.372	0.621	0.57	0.73
	CD6x4;10 2002	HL-93 (US)	2	1.026	1.329	HS 20-44	1.068	1.781	1.04	1.34
	CD6x4;10 2002	HL-93 (US)	4	1.773	2.298	HS 20-44	3	5.01	1.69	2.18
	CD6x4;10 2002	HL-93 (US)	7	1.884	2.443	HS 20-44	3.056	5.107	1.62	2.09
	CD6x4;10 2002	HL-93 (US)	9	1.648	2.136	HS 20-44	3.132	5.244	1.90	2.46
	CD6x4;10 2002	HL-93 (US)	10	1.374	1.781	HS 20-44	2.821	4.729	2.05	2.66
86	CD8x6;10 2002	HL-93 (US)	0	0.602	0.78	HS 20-44	0.529	0.883	0.88	1.13
	CD8x6;10 2002	HL-93 (US)	0.5	0.602	0.78	HS 20-44	0.498	0.831	0.83	1.07
	CD8x6;10 2002	HL-93 (US)	1	0.601	0.779	HS 20-44	0.467	0.78	0.78	1.00
	CD8x6;10 2002	HL-93 (US)	1.5	0.6	0.778	HS 20-44	0.472	0.788	0.79	1.01
	CD8x6;10 2002	HL-93 (US)	1.9	0.599	0.777	HS 20-44	0.445	0.742	0.74	0.95
	CD8x6;10 2002	HL-93 (US)	2	1.158	1.501	HS 20-44	1.165	1.943	1.01	1.29
	CD8x6;10 2002	HL-93 (US)	4	1.627	2.109	HS 20-44	2.331	3.715	1.43	1.76
	CD8x6;10 2002	HL-93 (US)	7	1.473	1.91	HS 20-44	2.249	3.75	1.53	1.96
	CD8x6;10 2002	HL-93 (US)	9	0.963	1.249	HS 20-44	1.948	3.252	2.02	2.60
	CD8x6;10 2002	HL-93 (US)	10	0.553	0.717	HS 20-44	1.183	1.975	2.14	2.75
87	CD12x8;10 2002	HL-93 (US)	0	0.669	0.867	HS 20-44	0.471	0.786	0.70	0.91
	CD12x8;10 2002	HL-93 (US)	0.5	0.659	0.854	HS 20-44	0.516	0.861	0.78	1.01
	CD12x8;10 2002	HL-93 (US)	1	0.64	0.829	HS 20-44	0.561	0.937	0.88	1.13
	CD12x8;10 2002	HL-93 (US)	1.5	0.618	0.802	HS 20-44	0.636	1.062	1.03	1.32
	CD12x8;10 2002	HL-93 (US)	1.9	0.6	0.777	HS 20-44	0.598	0.998	1.00	1.28
	CD12x8;10 2002	HL-93 (US)	2	0.918	1.19	HS 20-44	1.04	1.715	1.13	1.44
	CD12x8;10 2002	HL-93 (US)	4	1.211	1.569	HS 20-44	1.55	2.555	1.28	1.63
	CD12x8;10 2002	HL-93 (US)	7	1.095	1.42	HS 20-44	1.507	2.512	1.38	1.77
	CD12x8;10 2002	HL-93 (US)	9	0.368	0.477	HS 20-44	0.938	1.572	2.55	3.30
	CD12x8;10 2002	HL-93 (US)	10	0	0	HS 20-44	0	0	#DIV/0!	#DIV/0!
88	CD14x9;10 2002	HL-93 (US)	0	0.747	0.969	HS 20-44	0.627	1.047	0.84	1.08

Appendix L – Caltrans Models-LRFR-LFR comparisons

ID	Culvert Name	LRFD Vehicle	Fill Height (ft)	LRFR Inv	LRFR Oper	LFR Vehicle HS20-44 with a 1.25 factor	LFR Inve	LFR Opera	Ratio Inventory LFR/LRFR	Ratio Operating LFR/LRFR
	CD14x9;10 2002	HL-93 (US)	0.5	0.722	0.936	HS 20-44	0.679	1.134	0.94	1.21
	CD14x9;10 2002	HL-93 (US)	1	0.694	0.9	HS 20-44	0.731	1.22	1.05	1.36
	CD14x9;10 2002	HL-93 (US)	1.5	0.664	0.861	HS 20-44	0.748	1.249	1.13	1.45
	CD14x9;10 2002	HL-93 (US)	1.9	0.638	0.827	HS 20-44	0.703	1.174	1.10	1.42
	CD14x9;10 2002	HL-93 (US)	2	0.951	1.233	HS 20-44	1.05	1.754	1.10	1.42
	CD14x9;10 2002	HL-93 (US)	4	1.278	1.656	HS 20-44	1.635	2.697	1.28	1.63
	CD14x9;10 2002	HL-93 (US)	7	1.115	1.445	HS 20-44	1.506	2.51	1.35	1.74
	CD14x9;10 2002	HL-93 (US)	9	0.304	0.394	HS 20-44	0.967	1.619	3.18	4.11
	CD14x9;10 2002	HL-93 (US)	10	0	0	HS 20-44	0	0	#DIV/0!	#DIV/0!
89	CS2x1_;66 1966	HL-93 (US)	0	0.779	1.01	HS 20-44	0.53	0.884	0.68	0.88
	CS2x1_;66 1966	HL-93 (US)	1.9	1.833	2.376	HS 20-44	0.553	0.923	0.30	0.39
	CS2x1_;66 1966	HL-93 (US)	2	2.521	3.268	HS 20-44	3.255	5.425	1.29	1.66
	CS2x1_;66 1966	HL-93 (US)	4	6.838	8.865	HS 20-44	10.538	17.495	1.54	1.97
	CS2x1_;66 1966	HL-93 (US)	10	33.031	42.818	HS 20-44	28.849	48.178	0.87	1.13
	CS2x1_;66 1966	HL-93 (US)	25	37.175	48.19	HS 20-44	34.455	57.539	0.93	1.19
	CS2x1_;66 1966	HL-93 (US)	40	40.402	52.374	HS 20-44	38.91	64.979	0.96	1.24
	CS2x1_;66 1966	HL-93 (US)	50	42.24	54.756	HS 20-44	41.137	68.698	0.97	1.25
	CS2x1_;66 1966	HL-93 (US)	60	0	0	HS 20-44	0	0	#DIV/0!	#DIV/0!
	CS2x1_;66 1966	HL-93 (US)	66	0	0	HS 20-44	0	0	#DIV/0!	#DIV/0!
90	CS4x3;28 1966	HL-93 (US)	0	0.723	0.937	HS 20-44	0.562	0.939	0.78	1.00
	CS4x3;28 1966	HL-93 (US)	1.9	0.984	1.275	HS 20-44	0.562	0.938	0.57	0.74
	CS4x3;28 1966	HL-93 (US)	2	1.188	1.54	HS 20-44	1.302	2.174	1.10	1.41
	CS4x3;28 1966	HL-93 (US)	4	2.522	3.27	HS 20-44	3.93	6.562	1.56	2.01
	CS4x3;28 1966	HL-93 (US)	7	4.868	6.311	HS 20-44	8.268	13.808	1.70	2.19
	CS4x3;28 1966	HL-93 (US)	10	12.768	16.552	HS 20-44	11.111	18.556	0.87	1.12
	CS4x3;28 1966	HL-93 (US)	15	12.351	16.011	HS 20-44	11.089	18.519	0.90	1.16
	CS4x3;28 1966	HL-93 (US)	20	11.911	15.44	HS 20-44	10.991	18.355	0.92	1.19
	CS4x3;28 1966	HL-93 (US)	25	0	0	HS 20-44	0	0	#DIV/0!	#DIV/0!

Appendix L – Caltrans Models-LRFR-LFR comparisons

ID	Culvert Name	LRFD Vehicle	Fill Height (ft)	LRFR Inv	LRFR Oper	LFR Vehicle HS20-44 with a 1.25 factor	LFR Inve	LFR Opera	Ratio Inventory LFR/LRFR	Ratio Operating LFR/LRFR
	CS4x3;28 1966	HL-93 (US)	28	0	0	HS 20-44	0	0	#DIV/0!	#DIV/0!
91	CS6x4;10 1966	HL-93 (US)	0	0.654	0.848	HS 20-44	0.665	1.11	1.02	1.31
	CS6x4;10 1966	HL-93 (US)	0.5	0.661	0.857	HS 20-44	0.648	1.082	0.98	1.26
	CS6x4;10 1966	HL-93 (US)	1	0.668	0.866	HS 20-44	0.63	1.052	0.94	1.21
	CS6x4;10 1966	HL-93 (US)	1.5	0.674	0.873	HS 20-44	0.663	1.108	0.98	1.27
	CS6x4;10 1966	HL-93 (US)	1.9	0.689	0.894	HS 20-44	0.647	1.081	0.94	1.21
	CS6x4;10 1966	HL-93 (US)	2	0.758	0.982	HS 20-44	1.049	1.752	1.38	1.78
	CS6x4;10 1966	HL-93 (US)	4	1.304	1.691	HS 20-44	2.635	4.4	2.02	2.60
	CS6x4;10 1966	HL-93 (US)	7	1.641	2.127	HS 20-44	5.03	8.4	3.07	3.95
	CS6x4;10 1966	HL-93 (US)	9	6.654	8.626	HS 20-44	5.997	10.015	0.90	1.16
	CS6x4;10 1966	HL-93 (US)	10	6.531	8.466	HS 20-44	5.94	9.92	0.91	1.17
92	CS8x6;13 1966	HL-93 (US)	0	0.59	0.764	HS 20-44	0.536	0.894	0.91	1.17
	CS8x6;13 1966	HL-93 (US)	0.5	0.599	0.777	HS 20-44	0.512	0.855	0.85	1.10
	CS8x6;13 1966	HL-93 (US)	1	0.607	0.787	HS 20-44	0.488	0.815	0.80	1.04
	CS8x6;13 1966	HL-93 (US)	1.5	0.577	0.748	HS 20-44	0.502	0.838	0.87	1.12
	CS8x6;13 1966	HL-93 (US)	1.9	0.568	0.736	HS 20-44	0.48	0.802	0.85	1.09
	CS8x6;13 1966	HL-93 (US)	2	0.757	0.981	HS 20-44	0.738	1.232	0.97	1.26
	CS8x6;13 1966	HL-93 (US)	4	1.103	1.43	HS 20-44	1.541	2.574	1.40	1.80
	CS8x6;13 1966	HL-93 (US)	6	1.286	1.668	HS 20-44	2.081	3.475	1.62	2.08
	CS8x6;13 1966	HL-93 (US)	7	1.272	1.649	HS 20-44	2.201	3.675	1.73	2.23
	CS8x6;13 1966	HL-93 (US)	8	1.21	1.569	HS 20-44	2.204	3.68	1.82	2.35
93	CS12x8;5 1966	HL-93 (US)	0	0.567	0.734	HS 20-44	0.615	1.027	1.08	1.40
	CS12x8;5 1966	HL-93 (US)	0.5	0.54	0.701	HS 20-44	0.578	0.966	1.07	1.38
	CS12x8;5 1966	HL-93 (US)	1	0.511	0.663	HS 20-44	0.541	0.903	1.06	1.36
	CS12x8;5 1966	HL-93 (US)	1.5	0.479	0.621	HS 20-44	0.545	0.91	1.14	1.47
	CS12x8;5 1966	HL-93 (US)	1.9	0.451	0.584	HS 20-44	0.512	0.854	1.14	1.46
	CS12x8;5 1966	HL-93 (US)	2	0.496	0.642	HS 20-44	0.531	0.887	1.07	1.38
	CS12x8;5 1966	HL-93 (US)	3	0.538	0.698	HS 20-44	0.748	1.249	1.39	1.79

Appendix L – Caltrans Models-LRFR-LFR comparisons

ID	Culvert Name	LRFD Vehicle	Fill Height (ft)	LRFR Inv	LRFR Oper	LFR Vehicle HS20-44 with a 1.25 factor	LFR Inve	LFR Opera	Ratio Inventory LFR/LRFR	Ratio Operating LFR/LRFR
	CS12x8;5 1966	HL-93 (US)	4	0.561	0.727	HS 20-44	0.813	1.358	1.45	1.87
	CS12x8;5 1966	HL-93 (US)	5	0.485	0.628	HS 20-44	0.748	1.249	1.54	1.99
94	CD4x3;11 1966	HL-93 (US)	0	0.405	0.525	HS 20-44	0	0	0.00	0.00
	CD4x3;11 1966	HL-93 (US)	0.5	0.48	0.622	HS 20-44	0	0	0.00	0.00
	CD4x3;11 1966	HL-93 (US)	1	0.576	0.747	HS 20-44	0	0	0.00	0.00
	CD4x3;11 1966	HL-93 (US)	1.9	0.725	0.939	HS 20-44	0	0	0.00	0.00
	CD4x3;11 1966	HL-93 (US)	2	0.666	0.863	HS 20-44	0	0	0.00	0.00
	CD4x3;11 1966	HL-93 (US)	4	1.822	2.361	HS 20-44	4.163	6.952	2.28	2.94
	CD4x3;11 1966	HL-93 (US)	6	2.37	3.072	HS 20-44	6.623	11.061	2.79	3.60
	CD4x3;11 1966	HL-93 (US)	8	2.754	3.57	HS 20-44	6.995	11.682	2.54	3.27
	CD4x3;11 1966	HL-93 (US)	10	13.535	17.546	HS 20-44	11.551	19.291	0.85	1.10
	CD4x3;11 1966	HL-93 (US)	11	13.385	17.351	HS 20-44	11.494	19.195	0.86	1.11
95	CD6x4;4 1966	HL-93 (US)	0	0.28	0.363	HS 20-44	0	0	0.00	0.00
	CD6x4;4 1966	HL-93 (US)	0.5	0.351	0.455	HS 20-44	0	0	0.00	0.00
	CD6x4;4 1966	HL-93 (US)	1	0.432	0.56	HS 20-44	0	0	0.00	0.00
	CD6x4;4 1966	HL-93 (US)	1.5	0.527	0.683	HS 20-44	0.496	0.828	0.94	1.21
	CD6x4;4 1966	HL-93 (US)	1.9	0.618	0.801	HS 20-44	0.476	0.796	0.77	0.99
	CD6x4;4 1966	HL-93 (US)	2	0.484	0.628	HS 20-44	0.847	1.415	1.75	2.25
	CD6x4;4 1966	HL-93 (US)	3	1.118	1.449	HS 20-44	1.653	2.761	1.48	1.91
	CD6x4;4 1966	HL-93 (US)	4	1.362	1.765	HS 20-44	2.564	4.282	1.88	2.43
96	CD8x6;3 1966	HL-93 (US)	0	0.274	0.355	HS 20-44	0	0	0.00	0.00
	CD8x6;3 1966	HL-93 (US)	0.5	0.337	0.437	HS 20-44	0.583	0.974	1.73	2.23
	CD8x6;3 1966	HL-93 (US)	1	0.418	0.542	HS 20-44	0.553	0.924	1.32	1.70
	CD8x6;3 1966	HL-93 (US)	1.5	0.51	0.661	HS 20-44	0.567	0.946	1.11	1.43
	CD8x6;3 1966	HL-93 (US)	1.9	0.572	0.742	HS 20-44	0.54	0.902	0.94	1.22
	CD8x6;3 1966	HL-93 (US)	2	0.457	0.592	HS 20-44	0.691	1.155	1.51	1.95
	CD8x6;3 1966	HL-93 (US)	3	0.521	0.675	HS 20-44	0.609	1.017	1.17	1.51
97	CD12x8;2 1966	HL-93 (US)	0	0.29	0.376	HS 20-44	0.554	0.926	1.91	2.46

Appendix L – Caltrans Models-LRFR-LFR comparisons

ID	Culvert Name	LRFD Vehicle	Fill Height (ft)	LRFR Inv	LRFR Oper	LFR Vehicle HS20-44 with a 1.25 factor	LFR Inve	LFR Opera	Ratio Inventory LFR/LRFR	Ratio Operating LFR/LRFR
	CD12x8;2 1966	HL-93 (US)	0.5	0.367	0.475	HS 20-44	0.665	1.11	1.81	2.34
	CD12x8;2 1966	HL-93 (US)	1	0.455	0.59	HS 20-44	0.677	1.131	1.49	1.92
	CD12x8;2 1966	HL-93 (US)	1.5	0.555	0.72	HS 20-44	0.682	1.138	1.23	1.58
	CD12x8;2 1966	HL-93 (US)	1.9	0.578	0.749	HS 20-44	0.64	1.068	1.11	1.43
	CD12x8;2 1966	HL-93 (US)	2	0.481	0.624	HS 20-44	0.655	1.094	1.36	1.75
98	CD12x8;14 1966	HL-93 (US)	0	0.515	0.668	HS 20-44	0.684	1.143	1.33	1.71
	CD12x8;14 1966	HL-93 (US)	1	0.752	0.975	HS 20-44	0.702	1.172	0.93	1.20
	CD12x8;14 1966	HL-93 (US)	1.9	0.924	1.198	HS 20-44	0.777	1.298	0.84	1.08
	CD12x8;14 1966	HL-93 (US)	2	0.666	0.863	HS 20-44	0.932	1.556	1.40	1.80
	CD12x8;14 1966	HL-93 (US)	4	1.625	2.106	HS 20-44	2.324	3.881	1.43	1.84
	CD12x8;14 1966	HL-93 (US)	7	2.31	2.994	HS 20-44	2.312	3.861	1.00	1.29
	CD12x8;14 1966	HL-93 (US)	9	2.052	2.66	HS 20-44	1.954	3.263	0.95	1.23
	CD12x8;14 1966	HL-93 (US)	11	1.583	2.052	HS 20-44	1.57	2.622	0.99	1.28
	CD12x8;14 1966	HL-93 (US)	13	1.085	1.406	HS 20-44	1.183	1.976	1.09	1.41
	CD12x8;14 1966	HL-93 (US)	14	0.604	0.783	HS 20-44	0.99	1.653	1.64	2.11
99	CS2x1_;32 1952	HL-93 (US)	0	0.995	1.29	HS 20-44	0.641	1.07	0.64	0.83
	CS2x1_;32 1952	HL-93 (US)	1.9	2.341	3.035	HS 20-44	0.677	1.131	0.29	0.37
	CS2x1_;32 1952	HL-93 (US)	2	2.335	3.027	HS 20-44	2.983	4.982	1.28	1.65
	CS2x1_;32 1952	HL-93 (US)	4	6.337	8.215	HS 20-44	9.647	16.111	1.52	1.96
	CS2x1_;32 1952	HL-93 (US)	7	13.523	17.53	HS 20-44	22.315	37.266	1.65	2.13
	CS2x1_;32 1952	HL-93 (US)	12	30.496	39.531	HS 20-44	26.513	44.276	0.87	1.12
	CS2x1_;32 1952	HL-93 (US)	18	31.4	40.703	HS 20-44	28.209	47.108	0.90	1.16
	CS2x1_;32 1952	HL-93 (US)	24	32.303	41.875	HS 20-44	29.822	49.803	0.92	1.19
	CS2x1_;32 1952	HL-93 (US)	30	33.207	43.047	HS 20-44	31.186	52.081	0.94	1.21
	CS2x1_;32 1952	HL-93 (US)	32	33.509	43.437	HS 20-44	31.641	52.84	0.94	1.22
100	CS4x3;13 1952	HL-93 (US)	0	0.773	1.002	HS 20-44	0.587	0.981	0.76	0.98
	CS4x3;13 1952	HL-93 (US)	1	0.908	1.177	HS 20-44	0.566	0.946	0.62	0.80
	CS4x3;13 1952	HL-93 (US)	1.9	1.077	1.396	HS 20-44	0.591	0.988	0.55	0.71

Appendix L – Caltrans Models-LRFR-LFR comparisons

ID	Culvert Name	LRFD Vehicle	Fill Height (ft)	LRFR Inv	LRFR Oper	LFR Vehicle HS20-44 with a 1.25 factor	LFR Inve	LFR Opera	Ratio Inventory LFR/LRFR	Ratio Operating LFR/LRFR
	CS4x3;13 1952	HL-93 (US)	2	0.966	1.253	HS 20-44	1.059	1.768	1.10	1.41
	CS4x3;13 1952	HL-93 (US)	4	1.983	2.57	HS 20-44	3.122	5.213	1.57	2.03
	CS4x3;13 1952	HL-93 (US)	7	3.644	4.724	HS 20-44	6.283	10.493	1.72	2.22
	CS4x3;13 1952	HL-93 (US)	9	8.235	10.675	HS 20-44	7.542	12.595	0.92	1.18
	CS4x3;13 1952	HL-93 (US)	11	8.091	10.488	HS 20-44	7.623	12.731	0.94	1.21
	CS4x3;13 1952	HL-93 (US)	12	8.018	10.394	HS 20-44	7.664	12.799	0.96	1.23
	CS4x3;13 1952	HL-93 (US)	13	7.946	10.301	HS 20-44	7.673	12.814	0.97	1.24

Appendix M – 3D Culvert Approach

Appendix M – 3D Culvert Analysis Approach

MEMORANDUM

DATE: January 4, 2017
TO: Mark Mlynarski
FROM: Thomas Murphy
RE: NCHRP 15-54 – 3D Culvert Analysis PN3471

This memo documents M&M's planned approach to modeling the 6 test culverts using three dimensional FEA. The intent is to communicate to the research team our approach, and resolve any concerns prior to beginning model development.

Soil Constitutive Model: linearly-elastic, perfectly-plastic model with a Mohr-Coulomb failure criterion for backfill soils and a linear-elastic model for in-situ soils

- LUSAS Mohr-Coulomb material model will be used for backfill soils. (See attached description) It is applicable where there is no volumetric strain during shear but allows volumetric plastic strain.
 - Mohr-Coulomb models require the following information:
 - Initial Cohesion
 - Initial Friction Angle
 - Final Friction Angle
 - Dilation Angle
- We were not planning on getting into two phase material modeling, but rather adjusting the properties as appropriate when below the ground water table.
- Modulus will vary depending on depth; use values shown in table below from Selig (1990) for backfill soil. Use initial Maximum Principal Stress Level to determine which values to use based on compaction level. Likely will bound the modulus.
- For in-situ soils, use a linear elastic material with an elastic modulus in the range of 6-20 ksi. Modulus should be high enough to limit settlement of in-situ soil in model.

Appendix M – 3D Culvert Approach

Table 1 – Elastic soil properties for Backfill (Selig, 1990)

Gravelly Sand (SW)						
Maximum Principal Stress Level (psi)	95% Standard Compaction			85% Standard Compaction		
	E (psi)	B (psi)	v	E (psi)	B (psi)	v
0 to 1	1,600	2,800	0.40	1,300	900	0.26
1 to 5	4,100	3,300	0.29	2,100	1,200	0.21
5 to 10	6,000	3,900	0.24	2,600	1,400	0.19
10 to 20	8,600	5,300	0.23	3,300	1,800	0.19
20 to 40	13,000	8,700	0.25	4,100	2,500	0.23
40 to 60	16,000	13,000	0.29	4,700	3,500	0.28
Sandy Silt (ML)						
Maximum Principal Stress Level (psi)	95% Standard Compaction			85% Standard Compaction		
	E (psi)	B (psi)	v	E (psi)	B (psi)	v
0 to 1	1,800	1,900	0.34	600	400	0.25
1 to 5	2,500	2,000	0.29	700	450	0.24
5 to 10	2,900	2,100	0.27	800	500	0.23
10 to 20	3,200	2,500	0.29	850	700	0.30
20 to 40	3,700	3,400	0.32	900	1,200	0.38
40 to 60	4,100	4,500	0.35	1,000	1,800	0.41
Silty Clay (CL)						
Maximum Principal Stress Level (psi)	95% Standard Compaction			85% Standard Compaction		
	E (psi)	B (psi)	v	E (psi)	B (psi)	v
0 to 1	400	800	0.42	100	100	0.33
1 to 5	800	900	0.35	250	200	0.29
5 to 10	1,100	1,000	0.32	400	300	0.28
10 to 20	1,300	1,100	0.30	600	400	0.25
20 to 40	1,400	1,600	0.35	700	800	0.35
60	1,500	2,100	0.38	800	1,300	0.40

Pavement Constitutive Model: assume pavement behaves in linear-elastic fashion.

- elastic pavement properties based on material (concrete or asphalt)
 - Asphalt pavement modulus varies based on temperature and individual materials; values increase with decreased temperatures
 - Range from 70 ksi to 434 ksi in (Little, Crockford, & Gaddam 1992).
 - Report provides the following equation for modulus based on temperature but is may only be useful for that particular combination of materials:
 $E = e^{-12.211195 + 0.056374F - 0.000619F^2}$ where F is in degrees Fahrenheit (note that this equation is only valid for a range of temperatures). May be able to use other data in report to develop other equations.
 - Asphalt pavement Poisson's ratio varies based on temperature and individual materials; values decrease with decreased temperature
 - Deteriorated pavement will be modeled using either reduced thickness or reduced modulus. Upper and lower limits will be bounded in the analyses.

3D FEA

Element Usage

- Culvert Structure Elements - use shell elements with linear elastic material properties

Appendix M – 3D Culvert Approach

- Use isotropic material properties/elements for concrete and smooth metal culverts. For concrete, an effective moment of inertia will be utilized in those areas where preliminary analysis indicates cracking is likely.
- Use orthotropic material properties/elements for corrugated metal and profile wall culverts. With orthotropic material properties, the bending stiffness in both directions will be correct, and the axial stiffness in one direction will be correct, but not in the other. This approach will be validated with a more detailed model.
- Culvert-Soil Interface – The interface will not be explicitly modeled.
- Soil – use hexahedra solid elements to represent soil, using material properties from Selig. We will define different materials to be used throughout the depth of the trench to account for the variation in principal stress.
- Pavement – use solid elements to represent pavement
 - select reasonable values for required material properties
 - Use of solid elements will allow modeling of the load spreading through the pavement in both horizontal directions.
- Refine mesh based on initial results; increase density in areas of large strains.
- Choice of linear or quadratic elements (mid-side nodes) left to designer based on speed and accuracy of results.

MODELING TECHNIQUES:

- Extents of soil to be included in analysis
 - The width of the model will be approximately 3 times the culvert span
 - Model full length of culvert
 - Include 2×culvert rise of soil under bottom of trench surface where culvert is placed, may reduce to 1×culvert rise due to load spreading through the pavement and soil above the culvert.
- Do not model stages of construction and back-fill, but assume a soil density and in-situ stress state.
- In-situ stresses
 - Assumed based on depth of culvert and type of soils
 - Vertical pressure will depend on the material – take as $\gamma \times h$ where γ is the unit weight of the overburden soil and h is the depth to the location of interest.
 - Horizontal pressure will depend on the vertical pressure and K_o as well as the amount of water present.
 - K_o can range from 0.3 to 1.1 depending on the type of soil. Will use one of the common equations for concrete culverts. Use of equations for metal culverts will have to be evaluated. A panel member asked how K_o is computed. In finite element analysis the lateral pressures develop as soil is placed in increments. The lateral pressures are variable as a function of the soil properties input by the user. This can result in some discrepancies from frame analysis results where specific lateral pressures are input. We will assess whether these discrepancies are acceptable or need to be addressed.
 - γ ranges from 70-150 lb/ft³
 - accounted for using initial stress loadings
- Live loads
 - Wheel loads and areas need to be measured during field testing to be used in LUSAS

Appendix M – 3D Culvert Approach

- Wheel loads will be modeled using patch loads
- Wheel loads will be marched across the structure in each analysis – use non-linear analysis
- Nonlinear & Transient Analysis
 - We will not consider consolidation, or other time-related effects.
- Support conditions
 - Restraints
 - Horizontal restraint provided on vertical faces of soil
 - Provide vertical restraint at bottom surface of model
 - Restrain rotation about the X- (along direction of travel) and Y- (vertical) axes at the culvert edges at the extents of the model.
 - Rigid restraints or springs
 - Will use rigid restraints with the model boundaries a relatively large distance away from the culvert such that their effect is minimized.

REFERENCES

Selig, E.T. (1990), "Soil Properties for Plastic Pipe Installations," *Buried Plastic Pipe Technology*, STP1093, G.S. Buczala and M.J. Cassady, Eds., ASTM, Philadelphia, PA, pp. 141-158.

Little, D.N., W.W. Crockford, and V.K.R. Gaddam. (1992), "Resilient Modulus of Asphalt Concrete." Texas Transportation Institute, The Texas A&M University System, College Station, TX, 168 pp, Report No. FHWA/TX-93-1177-1F.